



IFM-GEOMAR

Leibniz-Institut für Meereswissenschaften
an der Universität Kiel

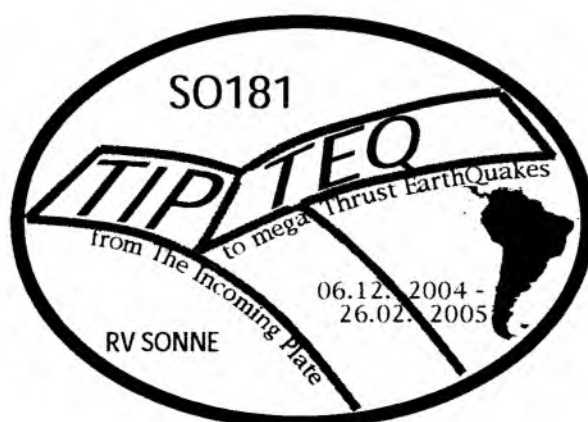
FS Sonne

Fahrtbericht / Cruise Report SO 181

TIPTEQ

from The Incoming Plate to mega Thrust EarthQuakes

Valparaiso - Talcahuano
06.12.2004 - 26.02.2005



Edited by
Ernst R. Flueh & Ingo Grevemeyer

Berichte aus dem Leibniz-Institut
für Meereswissenschaften an der
Christian-Albrechts-Universität zu Kiel

Nr. 2, März 2005

ISSN Nr.: 1614-6298



Das Leibniz-Institut für Meereswissenschaften
ist ein Institut der Wissenschaftsgemeinschaft
Gottfried Wilhelm Leibniz (WGL)

The Leibniz-Institute of Marine Sciences is a
member of the Leibniz Association
(Wissenschaftsgemeinschaft Gottfried
Wilhelm Leibniz).

Herausgeber / Editor:
Ernst R. Flueh & Ingo Grevermeyer

IFM-GEOMAR Report
ISSN Nr.: 1614-6298

Leibniz-Institut für Meereswissenschaften / Leibniz-Institute of Marine Sciences
IFM-GEOMAR
Dienstgebäude Westufer / West Shore Building
Düsternbrooker Weg 20
D-24105 Kiel
Germany

Leibniz-Institut für Meereswissenschaften / Leibniz-Institute of Marine Sciences
IFM-GEOMAR
Dienstgebäude Ostufer / East Shore Building
Wischhofstr. 1-3
D-24148 Kiel
Germany

Tel.: ++49 431 600-0
Fax: ++49 431 600-2805
www.ifm-geomar.de

Table of Contents

1.1	Summary	1
1.2	Zusammenfassung	2
2.	Introduction	4
2.1	The objectives of the cruise SO181 Leg 1&2	4
2.2	Regional geologic-tectonic setting	11
2.3	Previous Investigations	14
2.4	Seismology in Chile	17
3.	Participants	20
3.1	Scientists	20
3.2	Crew	21
3.3	Addresses of participating institutions	23
4.	Agenda of the cruise	28
4.1	Agenda of the cruise SO-181-1a	28
4.2	Agenda of the cruise SO-181-1b	28
4.3	Agenda of the cruise SO-181-2	32
5.	Scientific Equipment	35
5.1	Shipboard equipment	35
5.1.1	Navigation	35
5.1.2	Simrad EM-120 swathmapping bathymetry system	35
5.1.3	Parasound	36
5.1.4	CTD	37
5.2.	Hard and Software	40
5.2.1	Computer facilities for bathymetry, magnetic, and seismic data processing	40
5.2.2	Seismic processing of OBH/OBS wide-angle data	41
5.2.3	Processing of earthquake data	54
5.3	Seismic Instrumentation	59
5.4	Magnetometer	78
5.5	Magnetotellurics	78
5.6	Heatflow instruments	80
5.7	Coring device	86
6.	Work completed and first results	87
6.1	Hydroacoustic Work	87
6.2	Discussion of heat flow results	96
6.3	Geological Sampling	101
6.4	Magnetotellurics	104
6.5	Magnetic data	106
6.5.1	SO181-1a	106
6.5.2	SO181-1b	106
6.5.3	SO181-2	110

6.6	Seismic and seismological investigations	112
6.6.1	The Outer Rise networks	112
6.6.2	Seismic reflection data – first results	168
6.6.3	Profile 05	176
6.6.4	Profile 07	229
6.6.5	Profile 08	289
6.6.6	Profile 06	339
6.6.7	Profile 09	407
6.6.7	Test of the SEND prototype long period seismometer	448
7.	Acknowledgements	457
8.	References	457
9.	Appendices	460
9.1	Magnetic profiles	460
9.2	Ocean Bottom Recorders	462
9.3	Airgun Shots	469
9.4	Heatflow Stations	472
9.5	Magnetotellurics	483
9.6	Gravity Core Stations	484
9.7	Captain's report	488
9.7.1	Captain's report SO181-1a	488
9.7.2	Captain's report SO181-1b	495
9.7.3	Captain's report SO181-2	510
9.8	Press clippings	538

1.1 Summary

From December 2004 to February 2005 the RV *SONNE* cruise SO181 took place as part of the TIPTEQ (from The Incoming Plate to mega-Thrust EarthQuake processes) project in southern Chile to acquire various geophysical and geological datasets across the subduction zone between 35° S and 48° S. Here, the oceanic Nazca plate, the oceanic Antarctic plate and the continental South American plate join at the Chile Triple Junction, south of which the active spreading centre is subducting. To the north of the triple junction, the Nazca plate is segmented by several fracture zones across our survey area, allowing us to study subduction of differently aged oceanic crust and thus different thermal regimes. In addition, a simple plate motion environment exists with a constant convergence rate between the Nazca and the South American plate, constant spreading rates at the spreading centres, and a homogeneous motion vector, turning this area into a favourable natural laboratory for subduction zone process studies. We have chosen five major east-west oriented corridors as transects for the data acquisition, with crustal ages ranging from 25 Ma down to 3 Ma, four of the lines north and one line south of the triple junction. All transects were covered with seismic wide-angle refraction and vertical incidence reflection data, and the northern four transects also with heat flow and sediment probing either on or near the transects. The northern line had seven ocean bottom magnetotelluric stations deployed as an extension of a magnetotelluric land line. Furthermore, two short-term and two long-term seismological networks of ocean bottom seismometers and hydrophones were deployed. The short-term arrays were located on top of the outer rise and recorded for about six weeks, and four short streamer profiles were shot across them, firstly to re-locate the ocean bottom receivers and secondly to obtain structural images. The long-term seismological arrays were deployed towards the end of this cruise to be recovered in October 2005. During the entire survey bathymetric profiling took place and several long magnetic profiles were collected. In total, 260 ocean bottom seismometer and hydrophone stations were deployed, with 30 instruments remaining on the seafloor for the long-term seismological networks, one instrument being lost, two stations recovered by dredging after unfruitful attempts of acoustic releases, and 227 totally successful recoveries. The data quality overall is good to excellent, with only few components being weak or without data. Three types of airguns were used for shooting the seismic lines; for wide-angle refraction shooting these were two simultaneous bolt guns of 32 l each, and a cluster of 8 G-guns of 8 l each, i.e. nominally 64 l capacity for each wide-angle shot; for shallow reflection shooting into a seismic streamer only, we used two 1.72 l GI-guns. A total number of 45180 shots were fired during this cruise at an overall excellent performance rate.

Initial results from onboard data analyses exhibited a high data quality, and superb results are to be expected. For example, the outer rise networks recorded several thousand earthquakes, almost 600 of which have been located during the cruise, and it appears that this pilot study exhibits a clear potential for analysing plate-bending related earthquakes at outer rise areas. Furthermore, the combined 1440 km of seismic wide-angle coverage along the five TIPTEQ corridors illuminate well the different stages of the subduction. Strong seismic anisotropy of about 7% was detected in the upper mantle, with the fast orientation matching the direction of spreading. Seismic reflection profiling produced clear images of the sedimentary cover. Remarkably, only small differences exist in the sedimentary thicknesses between the lines, despite the difference in ages of the oceanic crust. The sedimentation rate appears high except around 41° S. The reflection data also confirm a pervasive existence of the bottom simulating reflector, indicating gas hydrates, and this reflector will allow heat flow estimates. However, from our in-situ heat flow probing, we directly measured values of 100-200 mW/m² in the trench, 230-450 mW/m² towards the outer bulge, and around 35-70 mW/m² landwards of the

trench. Anomalously low heat flow values around 20 mW/m^2 in the trench seem to be influenced strongly by sedimentation effects, and extremely low values of 7 mW/m^2 correlate with apparent sea-water inflow into the oceanic crust. A large variety of sedimentary cores were sampled at 16 locations. Recovered sediments comprise hemipelagic muds, clayey to silty and sandy deep-sea trench deposits, and deep-sea trench fan deposits. Detailed mechanical and chemical analyses of these cores will be carried out on land. High resolution bathymetry data across a large part of these sediments were collected along about 17600 km of ship track, complementing existing multibeam data. These bathymetric images show a well developed sedimentary cover, however no surface-cutting faults from plate bending were identified in the new areas. As for the magnetotelluric stations, of the seven ocean bottom instruments deployed, five were recovered successfully, with all electric, magnetic and temperature channels continuously recorded. Combined with land data, these will be looking specifically at fluids in the subduction thrust. Finally, the magnetic field measurements successfully detected the magnetic field reversals imprinted in the oceanic crust and allow an accurate age determination of the incoming plate. Profiles along these anomalies, roughly north-south oriented, did not detect possible magnetite from serpentinisation, however anomalies from fracture zones could be measured.

1.2 Zusammenfassung

Von Dezember 2004 bis Februar 2005 fand die Fahrt SO181 der FS *SONNE* als Teil des TIPTEQ- (from The Incoming Plate to mega-Thrust EarthQuake processes) -Projektes in Südchile statt, um diverse geophysikalische and geologische Daten von der Subduktionszone zwischen 35° S und 48° S zu sammeln. Hier treffen die ozeanische Nazca-Platte, die ozeanische Antarktische Platte und die kontinentale Südamerikanische Platte an der Chile Triple Junction aufeinander, wo südlich davon das aktive Spreizungszentrum subduziert. Nördlich der Triple Junction ist die Nazca-Platte durch Bruchzonen in unserem Arbeitsgebiet so aufgeteilt, dass Subduktion von unterschiedlich alter Kruste und somit von unterschiedlichen thermalen Zuständen erforscht werden kann. Zusätzlich existiert ein einfaches Plattenbewegungsumfeld mit konstanter Konvergenzrate zwischen Nazca- und Südamerikanischer Platte, konstanter Spreizungsrate an den Spreizungszentren, und einem homogenen Bewegungsvektor, womit dieses Gebiet zu einem bevorzugten natürlichem Labor für die Studie von Subduktionsprozessen wird. Wir haben fünf Ost-West orientierte Hauptkorridore als Transekte für die Datenakquisition ausgewählt, mit Krustenaltersstufen von 3-25 Ma, vier dieser Linien nördlich und eine Linie südlich der Triple Junction. Alle Transekte wurden mit seismischen Weitwinkel-Refraktions- und vertikal einfallenden Reflexionsprofilen abgedeckt, die nördlichen vier Transekte zudem mit Wärmestrom und Sedimentproben auf oder in der Nähe von den Transekten. Auf der nördlichen Linie wurden sieben magnetotellurische Ozeanbodenstationen eingesetzt als Verlängerung einer magnetotellurischen Landlinie. Desweiteren wurden je zwei seismologische Kurzzeit- und Langzeit-Netze mit Ozeanbodenseismometern und -hydrophonen ausgesetzt. Die Kurzzeitnetze befanden sich auf dem Outer Rise und zeichneten ungefähr sechs Wochen lang auf, und vier kurze seismische Profile wurden über sie geschossen, erstens zur Relokalisation der Ozeanbodeninstrumente und zweitens für strukturelle Abbildungen. Die seismologischen Langzeitnetze wurden gegen Ende der Fahrt ausgesetzt, um im Oktober 2005 wieder eingeholt zu werden. Während der gesamten Fahrt fanden bathymetrische Messungen statt, und mehrere lange magnetische Profile wurden aufgenommen. Insgesamt wurden 260 Ozeanbodenseismometer- und -hydrophonstationen ausgelegt, wovon 30 Instrumente für das

seismologische Langzeitnetz auf dem Meeresboden blieben, ein Instrument verloren wurde, zwei Stationen nach erfolglosen akustischen Auslöseversuchen schliesslich durch Dredgen eingeholt wurden, und 227 Stationen problemlos geborgen wurden. Insgesamt ist die Datenqualität gut bis sehr gut, mit nur wenigen schwachen oder nicht vorhandenen Datenkomponenten. Für die Seismik wurden drei verschiedene Airguntypen eingesetzt; für Weitwinkelseismik waren dies zwei simultane Boltguns mit je 32 l, und ein Cluster von 8 G-guns mit je 8 l, d.h. nominell eine Kapazität von 64 l pro Weitwinkel-Schuss; für flache Reflexionsseismik nur mit Streamer wurden zwei 1.72 l GI-guns benutzt. Eine Gesamtzahl von 45180 Schüssen wurde während der Fahrt abgegeben mit einem insgesamt exzellentem Durchhaltevermögen.

Erste Ergebnisse der Datenbearbeitung an Bord zeigen eine hohe Datenqualität auf, und hochwertige Ergebnisse sind zu erwarten. Zum Beispiel haben die Outer Rise Erdbebennetze mehrere tausend Erdbeben aufgezeichnet, wovon fast 600 während der Fahrt lokalisiert wurden, und somit weist dieses Pilotprojekt ein eindeutiges Potential für Studien von Plattenbiegungsbeben an anderen Outer Rise Gebieten auf. Desweiteren illuminierte die insgesamt 1440 km umfassende Abdeckung der fünf TIPTEQ-Korridore mit seismischen Weitwinkeldaten deutlich die unterschiedlichen Stadien der Subduktion. Hohe seismische Anisotropie von ungefähr 7% wurde im oberen Mantel festgestellt, wobei die schnelle Komponente mit der Spreizungsrichtung überein stimmt. Seismische Reflexionsprofile ergaben klare Abbildungen der Sedimentschicht. Bemerkenswerterweise existieren nur geringe Unterschiede in den Sedimentmächtigkeiten zwischen den Linien, trotz der unterschiedlichen Alter der ozeanischen Kruste. Die Sedimentationsrate erscheint hoch außer um 41° S. Die Reflexionsdaten bestätigen zudem eine verbreitete Existenz des bodensimulierenden Reflektors, der Gashydrate anzeigt und Wärmestromabschätzungen ermöglicht. Jedoch haben wir von unseren in-situ Wärmestromuntersuchungen direkt Werte gemessen, und zwar 100-200 mW/m² im Tiefseegraben, 230-450 mW/m² Richtung Outer Bulge, und 35-70 mW/m² auf der Landseite vom Tiefseegraben. Niedrige Wärmestromanomalien um die 20 mW/m² am Tiefseegraben sind anscheinend stark von Sedimentationseffekten beeinflusst, und extrem niedrige Werte von 7 mW/m² entsprechen scheinbarem Meerwasserzufluss in die ozeanische Kruste. Eine große Vielfalt von Sedimentkernen wurden an 16 Lokationen gezogen. Die Sedimentproben umfassen hemipelagische Schlamme, lehmig bis siltige und sandige Tiefseegrabenablagerungen, und Tiefseegrabenfächerablagerungen. Detaillierte mechanische und chemische Analysen der Kerne werden an Land durchgeführt. Hochauflösende Bathymetriedaten über einen Großteil dieser Sedimente wurden entlang einer Strecke von ungefähr 17600 km gesammelt, was existierende Multibeamdaten komplementiert. Diese Bathymetrieabbildungen zeigen eine gut entwickelte Sedimentablagerung, allerdings wurden keine Oberflächenverwerfungen in den neu erschlossenen Gebieten festgestellt. Was die Magnetotellurikstationen angeht, so sind von den sieben ausgesetzten Ozeanbodeninstrumenten fünf erfolgreich wieder aufgesammelt worden, und alle Kanäle für elektrische, magnetische und Temperatur-Daten haben kontinuierlich aufgezeichnet. Mit diesen Daten werden, zusammen mit den Landdaten, speziell die Fluide des Subduktionskeils untersucht werden. Schließlich haben noch die magnetischen Messungen erfolgreich die eingeprägte Umkehrung des Erdmagnetfeldes in der ozeanischen Kruste erfasst, was eine genaue Altersbestimmung der abtauchenden Platte ermöglicht. Profile entlang dieser Anomalien, grob Nord-Süd orientiert, haben keine möglichen Magnetite von Serpentinisation aufgedeckt, jedoch konnten Anomalien der Bruchzonen gemessen werden.

2. Introduction

2.1 The objectives of the cruise SO181 Legs 1 & 2

A long-term goal of continental margin research is to study the “subduction factory”, i.e. the processes by which oceanic plate subduction drives arc magmatism, continental accretion or erosion, and earthquake processes. One key first-order parameter shaping the subduction factory is the thermal structure (i.e. age) of the subducting slab. Cruise SO181 as part of the TIPTEQ (from **T**he **I**ncoming **P**late to mega**T**hrust **E**arth**Q**uake processes) initiative chose the area around the Chile Triple Junction for investigating subduction at various thermal regimes.

The TIPTEQ project is a multidisciplinary study that aims at the quantification of:

- 1) Material fluxes (mass and fluids) along and across the forearc area,
- 2) Thermal structure of the oceanic plate and subduction zone,
- 3) Rheological behaviour of the subducting sediment along the interplate megathrust,
- 4) Seismic activity and generation of large subduction-related earthquakes, and
- 5) Relationship between material fluxes and volcanic arc products, including thermal modelling of the entire subduction zone system.

The results to these goals will yield a detailed view of the entire subduction system. A comprehensive data set was to be collected along five corridors with geophysical data and sediment cores at key locations during SO181 (Figure 2.1.1). Each corridor provides wide-angle seismic data, multichannel seismic data (either existing or new high-resolution data), heat flux measurements, multibeam bathymetry and potential field data. The corridors were complemented by a broader mapping with multibeam bathymetry and potential field data. Additionally, two short-term (1 month) and two long-term (9 months) seismological networks were planned offshore to obtain a robust data set in this little studied area. Furthermore a combined on-offshore magnetotelluric experiment was carried out along a profile extending from the oceanic plate to the volcanic arc. The recovered sediment cores will be used to conduct geotechnical tests on the frictional properties of the trench sediment in order to simulate failure and earthquake rupture.

Growing evidence indicates that the oceanic lithosphere undergoes profound changes as it flexes at the outer rise and plunges into the trench. Multibeam bathymetry at different margins shows that the ocean plate can be pervasively broken by flexural normal faults (e.g. Masson, 1993; von Huene et al., 1999, 2000). In addition, some outer rise earthquakes document that normal faults can in some cases cut to > 20 km depth. The consequence is that water can penetrate along permeable faults to mantle depths so that the oceanic mantle is serpentinised and the ocean lithosphere may be dramatically cooled by water circulation along the faults. Recent modelling and geochemical studies suggest that water circulation and serpentinisation of the ocean mantle may play a major role in the thermal structure of the plates and in magma generation at volcanic arcs (Peacock, 2001). A major goal of this project was to collect a comprehensive data set as well as material (gravity coring) from the ocean plate immediately seaward of the trench in order to understand the material input into the subduction system. Multibeam bathymetry will show the response of the different oceanic crust segments to flexure and the variations in normal faulting. Magnetic data will provide detailed information on lithospheric age and the nature of tectonic boundaries. Wide-angle seismic data (P and S waves) will map the changes in crustal and/or mantle velocities and Poisson ratios along and across the ocean plate yielding an estimate of the amount of serpentinisation and thus on the amount of water added to the ocean plate. Seabottom magnetotellurics in conjunction with onshore data will provide estimates of the fluid content in the plate interface. Heat flux

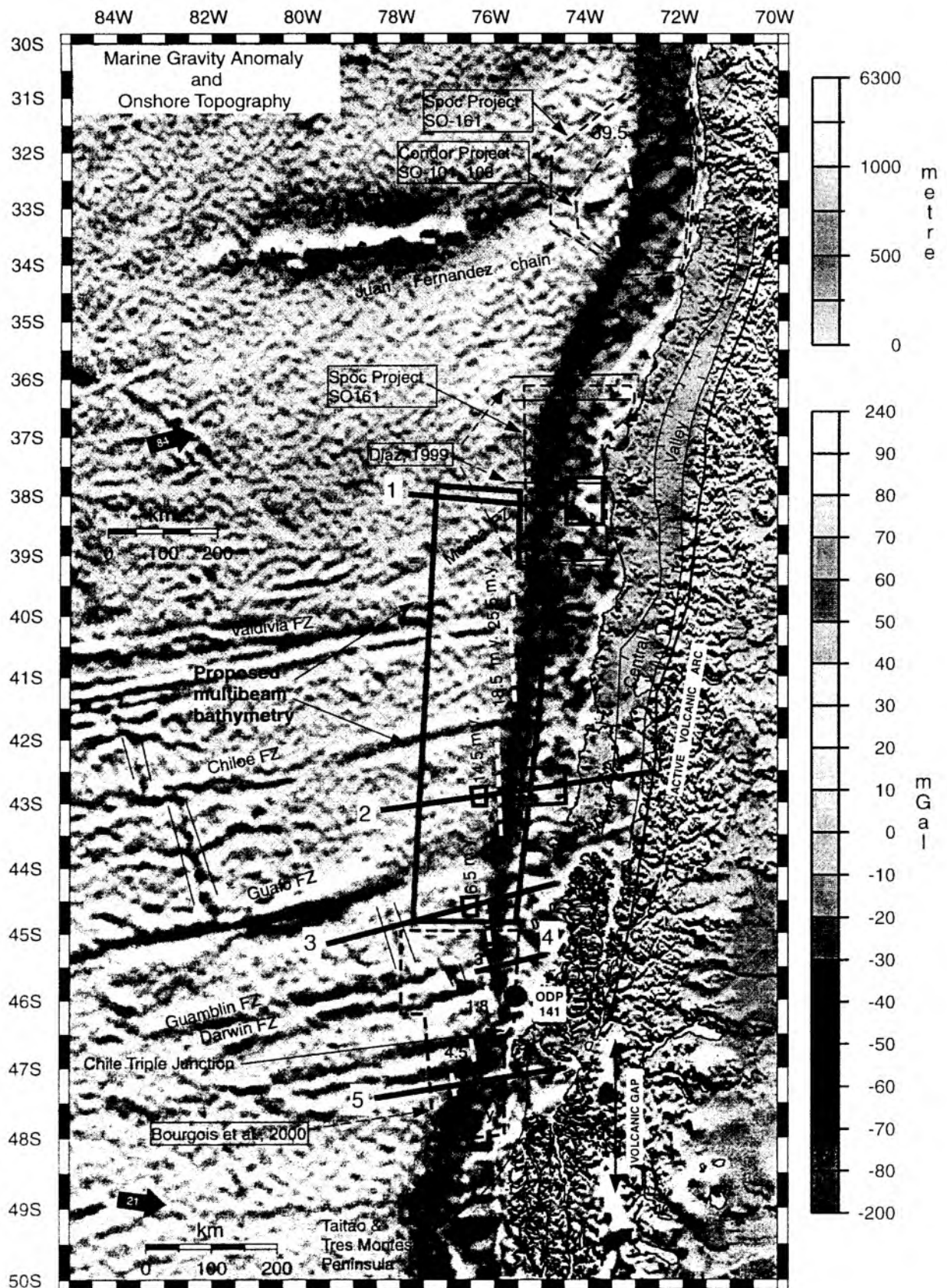


Figure 2.1.1: TIPTEQ main profiles 1-5 (thick black lines), overlying marine gravity anomalies and land topography. They provide information on lateral changes in subduction structures of different ages. Small black rectangles indicate locations of seismological ocean bottom networks. Grey box marks area for detailed bathymetric and magnetic surveys of the TIPTEQ projects. Dashed boxes show areas of previous investigations. Thick black arrows show plate motion vectors with convergence rates in mm/a.

measurements will show the changes in thermal structure related to age and to water circulation.

The subduction of laterally heterogeneous ocean plate segments influences the evolution of the arc-forearc system. The processes, however, can only be understood by collecting data that yield information on the entire thickness of the overriding plate and on volumes of different types of rocks along and across the forearc area. The geophysical corridors collected across the ocean plate were extended into the margin to evaluate the material flux variation related to changes in structure of the subducting ocean plate and trench sediment supply. Such data allow to quantitatively estimate material fluxes of accreted sediment and continental framework rock. Detailed velocities from prestack depth migrated seismic reflection profiles will yield information on the location and amount of fluid flow at the front of the margin. Geotechnical testing of the trench sediment, heat flux measurements and thermal modelling of the subduction system constrain the depths of metamorphic reactions and dehydration. Heat flux data also provide the observations necessary to estimate the temperature at the plate boundary at depth.

Seismological observations are crucial to relate long term deformation observed to other methods and to the short term response of the structures. Earthquake depths, distribution and focal mechanisms determine the depth of faulting in the ocean lithosphere at the outer rise. Furthermore they inform on the evolution of subducted structures of the ocean plate showing whether structures like fracture zones and normal faults remain active and their topographic expression continues to grow beneath the continental plate. It is of particular interest to find out if the subducted part of the Chile Ridge continues spreading beneath the forearc and volcanic arc, as the limited data of Murdie et al. (1993) seem to indicate. This is crucial for the attempt to locate the subducted ridge and understand the relationship between spreading centre subduction, the gap in arc volcanism and slab window processes. The combination of seismicity, heat flux measurement and data from frictional properties of the subducting sediment helps to understand whether the updip limit of seismic rupture (seismogenic zone) is controlled by the 100-150°C isotherm at the megathrust related to the illite - smectite phase change (Hyndman et al., 1993) or to other processes and other temperatures (Saffer et al., 2001).

The ocean plate north of the Valdivia Fracture Zone system where the oceanic plate is older and the age changes gradually to the north will be a reference area for normal subduction away from the influence of the spreading centre. Previous and ongoing studies provide a good knowledge of the structure of the continental margin: The Condor Project (von Huene et al., 1997; Flueh et al., 1998; Yanez et al., 2001), a PhD with multichannel seismic reflection lines carried out at GEOMAR (Diaz, 1999) and the SPOC project (BGR-GEOMAR) with R/V Sonne in autumn 2001 (Kopp et al., 2004; see also Figure 2.1.1). In addition, an initial assessment of the thermal regime of the margin between Valparaíso and Valdivia has been derived from the occurrence of Bottom Simulating Reflectors (BSR) and from temperature data obtained during Ocean Drilling Program leg 202 in the sites 1233, 1234 and 1235 (Grevemeyer et al., 2003). BSRs mark the base of the gas hydrate stability field and represent an isotherm-like feature and can therefore be used to yield heat flow anomalies (Grevemeyer and Villinger, 2001). Additional heat flow data to the north of Talcahuano were obtained in March 2004 aboard the Chilean navy research vessel Vidal Gormaz (Grevemeyer et al., 2005) and can be used as reference base for the data acquired during this cruise.

The first corridor of the present cruise (# 1 in Figure 2.1.1) is an extension of a wide-angle seismic profile collected during the SPOC project (autumn 2001) across the continental

margin and the trench. The new transect extends for about 200 km across the outer bulge to the area where pristine ocean lithosphere not deformed by flexure can be found. This section will give the reference structure for old oceanic lithosphere. Additionally, long-period off- and onshore MT soundings were planned along this transect. The heat flow survey in the corridor #1 area, however, was carried out to the north of the seismic refraction line to benefit from existing data obtained on the continental slope with Vidal Gormaz in early 2004.

The second corridor (# 2 in Figure 2.1.1) is located across much younger oceanic plate (< 14.5 Ma). A temporarily deployed seismological network on the Island of Chiloe with stations in-line of this profile enables the acquisition of onshore-offshore data and extends the profile into the margin to obtain the continental plate structure.

The third corridor (# 3 in Figure 2.1.1) is located on a still younger segment of subducting oceanic crust (6.5 Ma). It crosses the spreading centre and provides the structure of the zero-age lithosphere. This geophysical transect overlies a previously acquired multichannel seismic reflection line from the Lamont-Doherty Earth Observatory, line 734 collected in 1988 by the R/V Condor (Figure 2.1.2).

The fourth corridor (# 4 in Figure 2.1.1) is a shorter transect near the triple junction running across the shelf and slope into the oceanic plate and will be shot coincident with the existing multichannel seismic reflection line 743 (Figure 2.1.3). This line, in addition to several multichannel reflection profiles in the ODP 141 area (Figure 2.1.1), provides the reference to deep structures in the area of spreading centre axis collision.

The fifth corridor (# 5 in Figure 2.1.1) is situated south of the triple junction across continental shelf and slope, and shows the structure of the continental plate healing from the spreading-centre subduction tectonics by high-rate subduction accretion (Behrmann & Kopf, 2001). Data from this corridor also yield new information on the plate structure seaward of the northern section of the gap in the modern volcanic arc. This structure is presumably very similar to that of the plate currently beneath the extinct volcanic arc to the south. The seismic wide-angle data are shot coincident with the existing multichannel seismic reflection line 769 (Figure 2.1.4). Several of the multichannel seismic reflection lines will be reprocessed and pre-stack depth migrated as part of the TIPTEQ project.

The observations made in the ocean plate along the five corridors are linked to existing multibeam and potential field data in the area of the triple junction (Bourgois et al., 2000) and new multibeam bathymetry and potential field data collected from the outer rise to the trench during SO181. These data show the variations in the tectonic fabric of the oceanic plate (e.g. amount of normal faulting) related to changes in age and the lithospheric bending response to flexure. By providing the lateral variability and the precise location of the boundaries, these data allow to extrapolate the results of the two-dimensional corridors along strike into three dimensions.

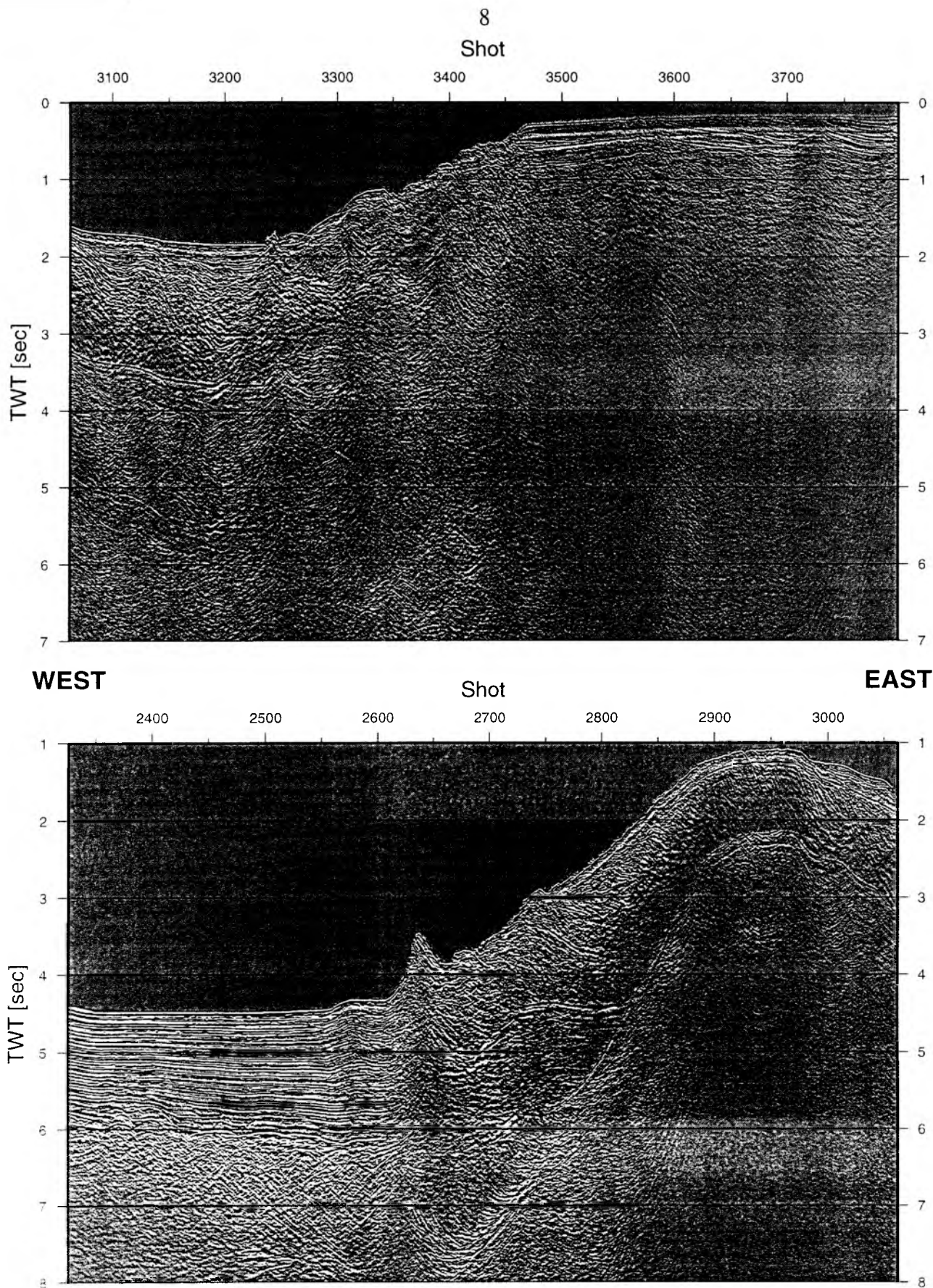


Figure 2.1.2: Line 734 of Lamont-Doherty Earth Observatory's Conrad cruise in 1988. This finite-difference migrated section is located on TIPTEQ corridor 3, imaging the structures from the undisturbed thick trench sediments and the underlying oceanic crust to the accreted sediments of the shelf.

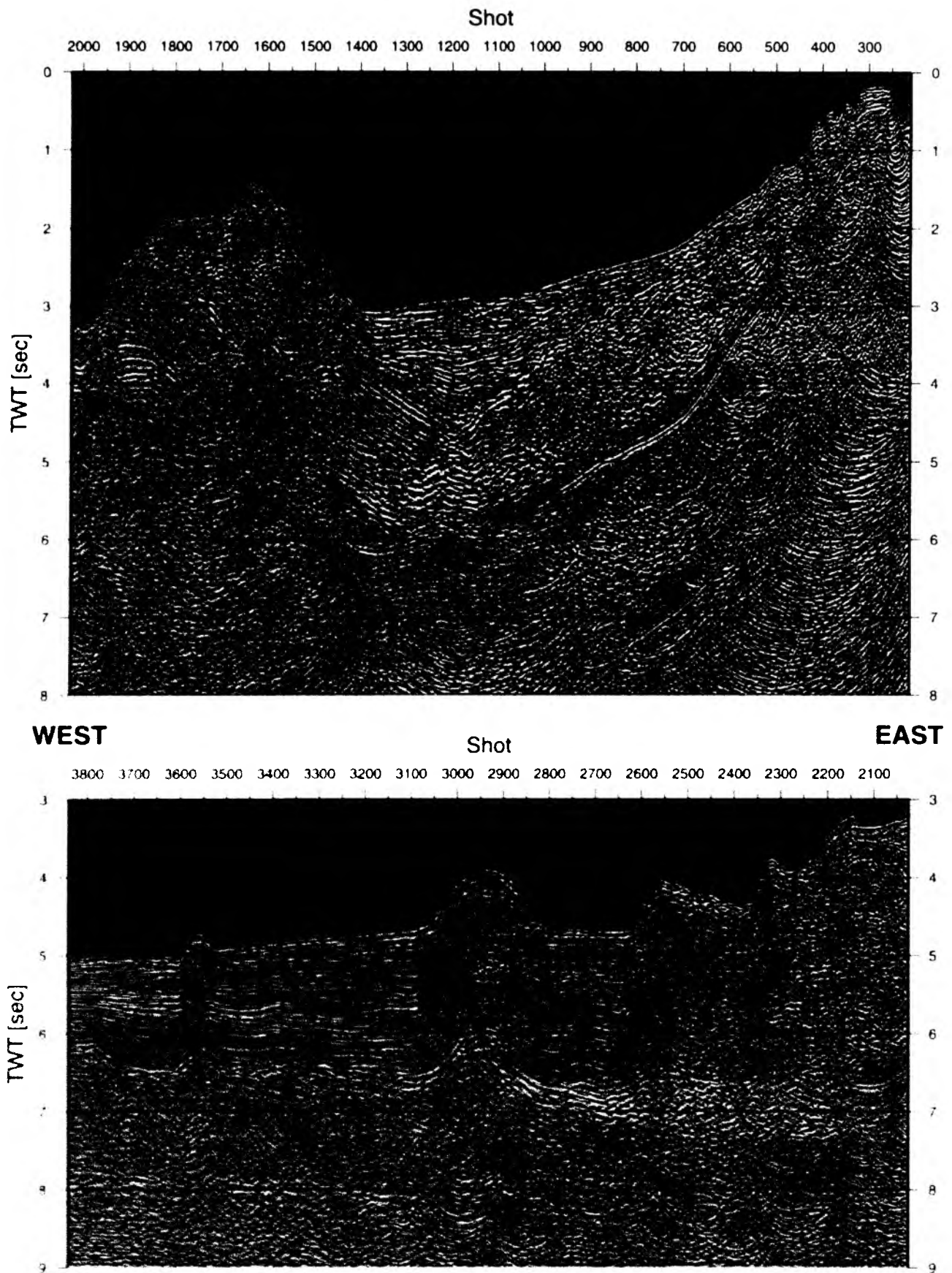


Figure 2.1.4: Line 769 of Lamont-Doherty Earth Observatory's Conrad cruise in 1988. This finite-difference migrated section is located on TIPTEQ corridor 5, imaging the deformation front and the accretionary wedge south of the Chile Triple Junction.

2.2 Regional geological-tectonic setting

Within a region along the Chile Trench surrounding the Chile Triple Junction, there exists a unique natural laboratory isolating subduction zone processes for detailed geophysical investigation. Here natural right-stepping offsets of the Chile (Nazca-Antarctic) Ridge have created a situation in which neighbouring sections of oceanic lithosphere, formed along the same spreading centre, are subducting at ages ranging from 0-20 Ma. There are obvious slab-age-dependent effects on the tectonics and volcanism of the overriding South American plate. Anomalously high regional forearc subsidence due to tectonic erosion (e.g. Behrmann et al., 1994) strongly correlates with younging ages of the subducting plate (Figure 2.2.1) producing up to several kilometres of along-forearc subsidence in the region just north of the subducting ridge. Where the ridge itself is actively subducting, there is a focussed pulse of local forearc uplift and subsidence (Behrmann et al., 1994; Behrmann & Kopf, 2001) (Figure 2.2.1). Furthermore, a gap in arc magmatism exists just to the south of the region of active ridge subduction, in the region between 47°-49° S, where subducted slab of age ~ 10 Ma is underlying the 'normal location' for arc magmatism. This ~ 900 -km-long region of southwards increasing regional forearc subsidence is also the site of the 1960 Great Chile Earthquake, the world's largest recorded earthquake, during which more than 800 km of plate boundary rupture occurred.

The Geologic Record of Past Ridge Subduction

The geological record along a large portion of the circum-Pacific region includes abundant evidence of the singular effects of subducting young oceanic seafloor, which is commonly called Spreading Centre Subduction. Spreading centre subduction during the Cenozoic has occurred at the Japan Trench (Uyeda and Miyashiro, 1974), Aleutian Trench (Grow and Atwater, 1970), western North America (Atwater, 1970), South America (Herron et al., 1981), and the Antarctic peninsula (Herron and Tucholke, 1976). The overriding plate records spreading centre subduction with a combination of structural and petrological signatures spanning from the backarc region to the front of the margin, some of the previously noted effects are: rapid uplift followed by subsidence of the forearc area (DeLong et al., 1979; Cande and Leslie, 1986), tectonic erosion at the front of the margin (Herron et al., 1981; Baker, 1982; Behrmann et al., 1992), anomalous near trench magmatism (Marshak and Karig, 1977; Lagrabielle et al., 1994), anomalous backarc volcanism and a gap in arc volcanism (Ramos and Kay, 1992), ophiolite emplacement (Forsythe and Nelson, 1985), hydrothermal activity and associated mineralisation (Haeussler et al., 1995). Currently there are few locations where active spreading centres are subducting; examples are: the Juan de Fuca Ridge subducting offshore North America, the Woodlark spreading centre, and the Chile Ridge subducting beneath South America. The collision of the Woodlark spreading centre and the Juan de Fuca Ridge with the trench is geometrically and thus tectonically more complex than the collision of the Chile Ridge with the Chile Trench (Cande and Leslie, 1986). The latter involves relatively simpler kinematics because the spreading centre segments bounded by fracture zones are roughly parallel to the trench strike (Figure 2.1.1). Therefore, the Chile Triple Junction has previously attracted in the past a large number of studies.

The large scale structure of the Chilean margin

Relevant for this project is the large scale structure of the ocean plate and the continent. The Chile Ridge is offset by fracture zones in a series of left-stepping segments so that the age of the ocean lithosphere being subducted changes suddenly across the fracture zones (Figure

2.1.1). The largest ridge offset occurs across the Valdivia fracture zone system (Figure 2.2.1) north of

which the subducting plate is older than 25 Ma (Tebbens et al. 1997) progressively reaching 39.5 Ma offshore Valparaíso in the Condor study area (Figure 2.1.1; Yanez et al., 2001). To the south of the Valdivia Fracture Zone system sudden changes in age occur across a number of fracture zones from 18.5 Ma to age zero at the triple junction (Tebbens et al 1997). South of the triple junction the plate increases in age.

The changes in lithospheric age coincide with changes in ocean plate depth (Figure 2.2.1) and marine gravity anomalies (Figure 2.1.1). The differences in elastic thickness of the segments of the incoming plate are prominent. North of the Valdivia Fracture Zone system, the seafloor approaching the trench is deeper than 4 km, but bulges up to slightly less than 4 km at the outer rise. South of the Valdivia Fracture Zone system the seafloor is shallower than 3.5 km reaching locally 3 km depth at the outer rise. Near the triple junction the ocean floor lies ~3 km deep and does not show an outer rise bulge (Cande and Leslie, 1986). South of the triple junction the water depth increases again.

The continent displays a number of structures that parallel the ocean plate segmentation, indicating a probable influence of the ocean plate segmentation on the tectonics over the entire width of the forearc. The central valley first develops at ~33° S, i.e. to the south of the area of subduction of the buoyant Juan Fernandez Ridge (Figure 2.1.1). Its topography becomes shallower towards the south, and in the area of the projection of the Valdivia Fracture Zone system there exist several large lakes. Further south a large bay gives way to a marine basin at ~42° S. Across the projection of the Guafo Fracture Zone the basin seems to disappear or at least narrows to a confined fiord, and the land topography of the peninsulas and islands rises. Surprisingly the central valley widens and deepens between the Valdivia and Guafo Fracture Zones because the adjacent ocean plate is much shallower than to the north. A possible explanation is that extensional continental tectonics plays a more important role here than to the north. Another plausible explanation is that a younger, hotter and therefore shallower dipping subducting plate is eroding the underside of the continental plate across the entire forearc. If the area is under regional isostatic equilibrium, as could be expected, the topography indicates a thinner overriding plate. To the south of the projection of the Guafo Fracture Zone, the margin topography becomes more elevated probably because the spreading centre is much closer to the margin. In contrast, the narrower shelf area north of 40° S cannot be explained by the deeper ocean plate subducting at a steeper angle and may instead be due to a thicker continental plate.

All these observations indicate that the impact of the Chile Ridge on the forearc tectonics has two different wavelengths. A short wavelength effect occurs at the locus of the subduction of the spreading centre axis where most previous studies have concentrated. A second, longer wavelength is the effect produced over the margin due to the segmentation of the spreading centre. The segmentation causes the ocean plate from the triple junction to the lithosphere north of Valdivia Fracture Zone system to be markedly heterogeneous with a variable thermo-mechanical structure and thus to respond differently to the subduction process.

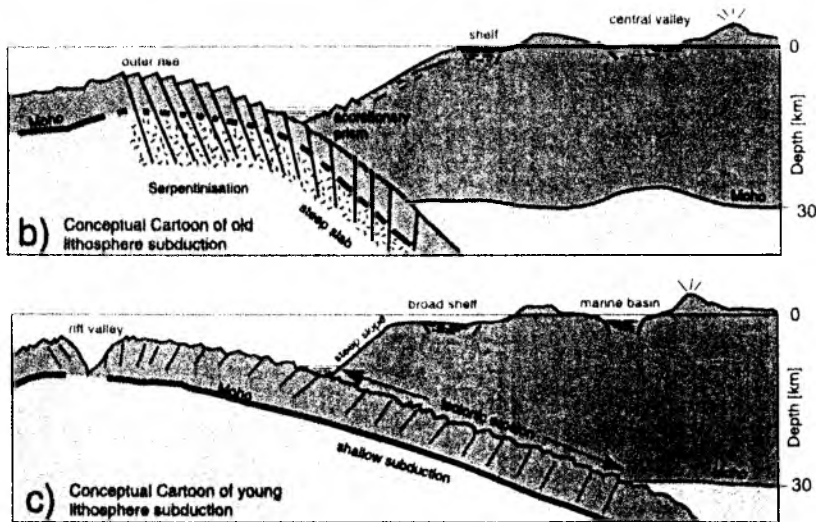
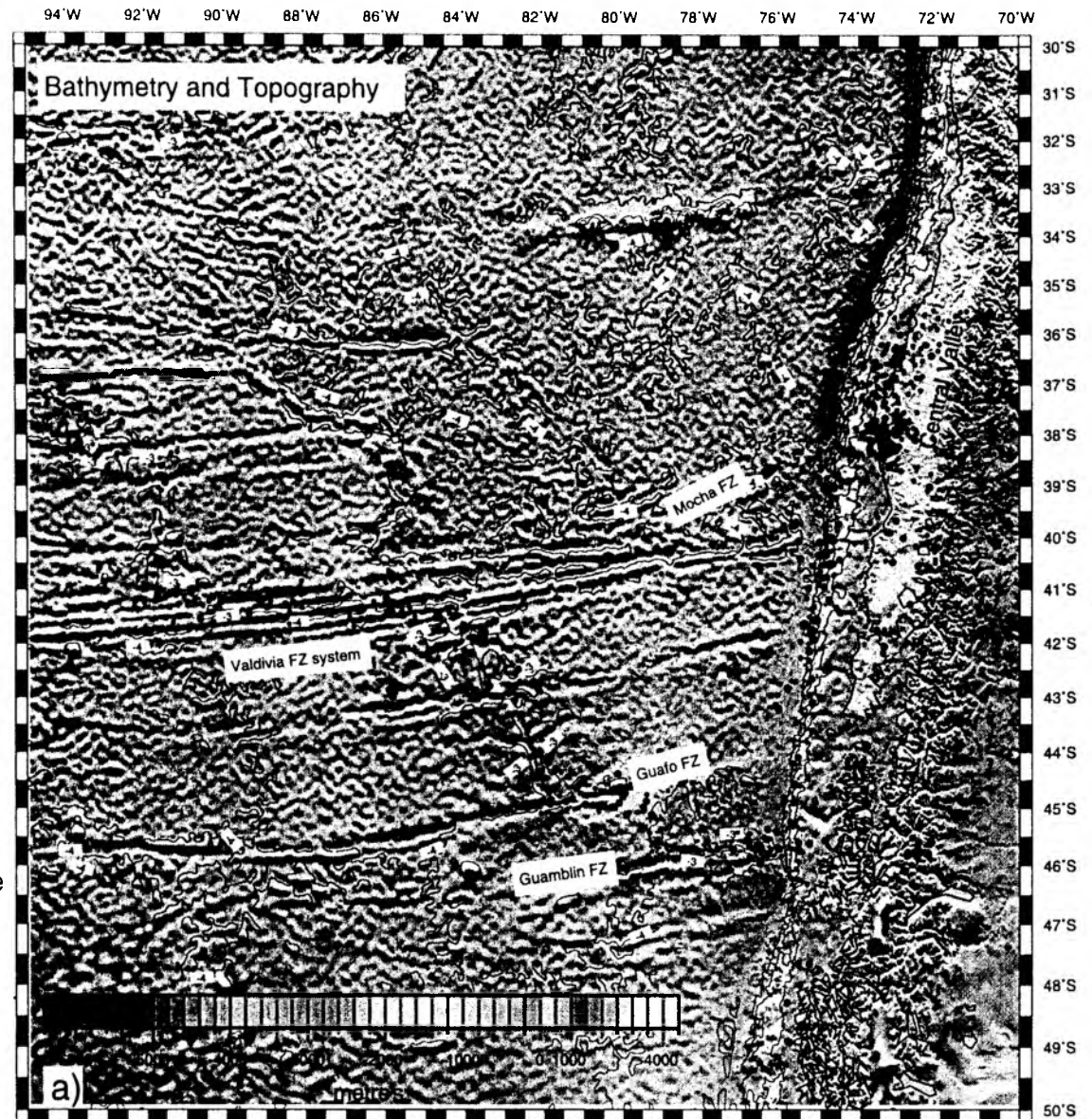


Figure 2.2.1 a) Bathymetry and topography: Outer rise, continental margin and onshore Chile. Fracture zones cut the spreading centre into several segments, resulting in abrupt changes in age of the subducting oceanic plate, as illustrated in the bathymetry. North of the Guafo Fracture Zone (FZ) the oceanic plate bulges upwards at the outer rise, however near the Chile Triple Junction the bulge is absent. Bathymetry contours are every kilometre. Black dots mark earthquakes shallower than 40 km; only events south of 35° are shown.

b) Sketch of subduction of old lithosphere (34°-35° S). Oceanic plate forms outer rise, and deeply penetrating faults develop. Faulting allows large scale serpentinization in the upper mantle. The forearc dips gently and consists of a well developed accretionary wedge. The continental shelf is narrow and the basin of the central valley lies above sea-level

c) Subduction of young lithosphere (43°-46° S). Oceanic plate is young and of little elastic thickness. Outer rise is small or absent. Faults abut above the Moho and thus prevent serpentinization. The dip of the subducting slab is shallow, causing distributed subduction erosion, leading to a broad shelf and a steep slope; the central valley is a marine basin.



2.3 Previous investigations

Much of the work to study the effects of spreading centre subduction along the Chilean margin has concentrated on the near vicinity of the area where the spreading centre axis is currently underthrusting the continental plate (Figure 2.1.1). Onshore, field work in the Tres Montes and Taitao Peninsula (Figure 2.1.1) found recent anomalous near trench magmatism and ophiolites, probably related to the spreading centre subduction (Lagabriele et al., 1994, 2000). Offshore, early seismic reflection, single beam echosounder, magnetics and a few heat flux measurements established a basic understanding of the geological consequences of the subduction of the Chile Ridge (Herron et al., 1981; Cande and Leslie, 1986, Cande et al., 1987). Tectonic erosion of the overriding plate narrows and steepens the continental slope where the ridge is subducting. In contrast, sediment accretion is active to the south of the Triple Junction in the area where the ridge has already been subducting. Side-scan sonar data from the GLORIA project of 1988 (G. Westbrook, pers. comm. 2004) further document this change in subduction style across the Chile Triple Junction (Figure 2.3.1). Heat flux measurements in the lower continental slope document a large pulse of heat in the area where the spreading centre is subducting.

These studies were the basis for ODP 141 (Behrmann et al., 1992) and a pre-site survey with acquisition of multichannel seismic reflection data and limited multibeam bathymetry across the continental slope and the ocean trench (Bangs et al., 1992; Behrmann et al., 1992). See Figures 2.1.2 to 2.1.4 for examples of the multichannel seismic reflection data. Recently, Bourgois et al. (2000) revisited the area and mapped a large strand of the triple junction with multibeam bathymetry and shallow seismic reflection data. Those studies demonstrate the complex interplay between the subducting spreading centre topography, the front of the margin and the supply of sediment at the trench. The results from drilling confirmed tectonic erosion at the area of ridge subduction. In combination with the seismic reflection data have been used for mass balance calculations. Estimates based on depth conversion of time sections yielded a $20\text{--}30 \text{ km}^3/\text{km trench} \times \text{Ma}$. (Behrmann and Kopf, 2001). In contrast, calculations based on the depth of magma generation for near trench magmatism yielded $230\text{--}440 \text{ km}^3/\text{km trench} \times \text{Ma}$ for the same area (Bourgois et al., 1996). A major shortcoming in that type of analysis is that little is known about the structure of the plates and the dip of the slab at a depth $> 3\text{--}5 \text{ km}$ below seafloor. A number of multichannel seismic reflection profiles collected near the triple junction were only preliminary processed and only one of them was preliminary pre-stack depth migrated at GEOMAR (Bangs et al., 1992), and they do not provide a well constrained structure of the front of the margin. In addition, the only earthquake seismology study in the area does not provide depth control of the slab geometry due to the lack of available velocity information (Murdie et al., 1993).

The subduction of the spreading centre is also the locus of a major boundary segmenting the seismicity along the convergent margin. To the north, seismicity is characterized by numerous subduction thrust earthquakes and deeper Wadati-Benioff events. South of the triple junction, seismicity is almost absent (Barazangi and Issacks, 1976; Murdie et al., 1993). At large scale, seismicity is further segmented in areas of flat subduction and steep subduction (Barazangi and Issacks, 1976). At smaller scale, topographic features of the ocean plate like the Guafo and Chiloe fracture zones produce swaths of seismic events that can be followed for 100s of km into the continent (Murdie et al., 1993). Thus, the seismicity indicates that ocean plate topography of different scales (e.g. spreading centre segments, fracture zones) must have an observable tectonic impact on the continents.

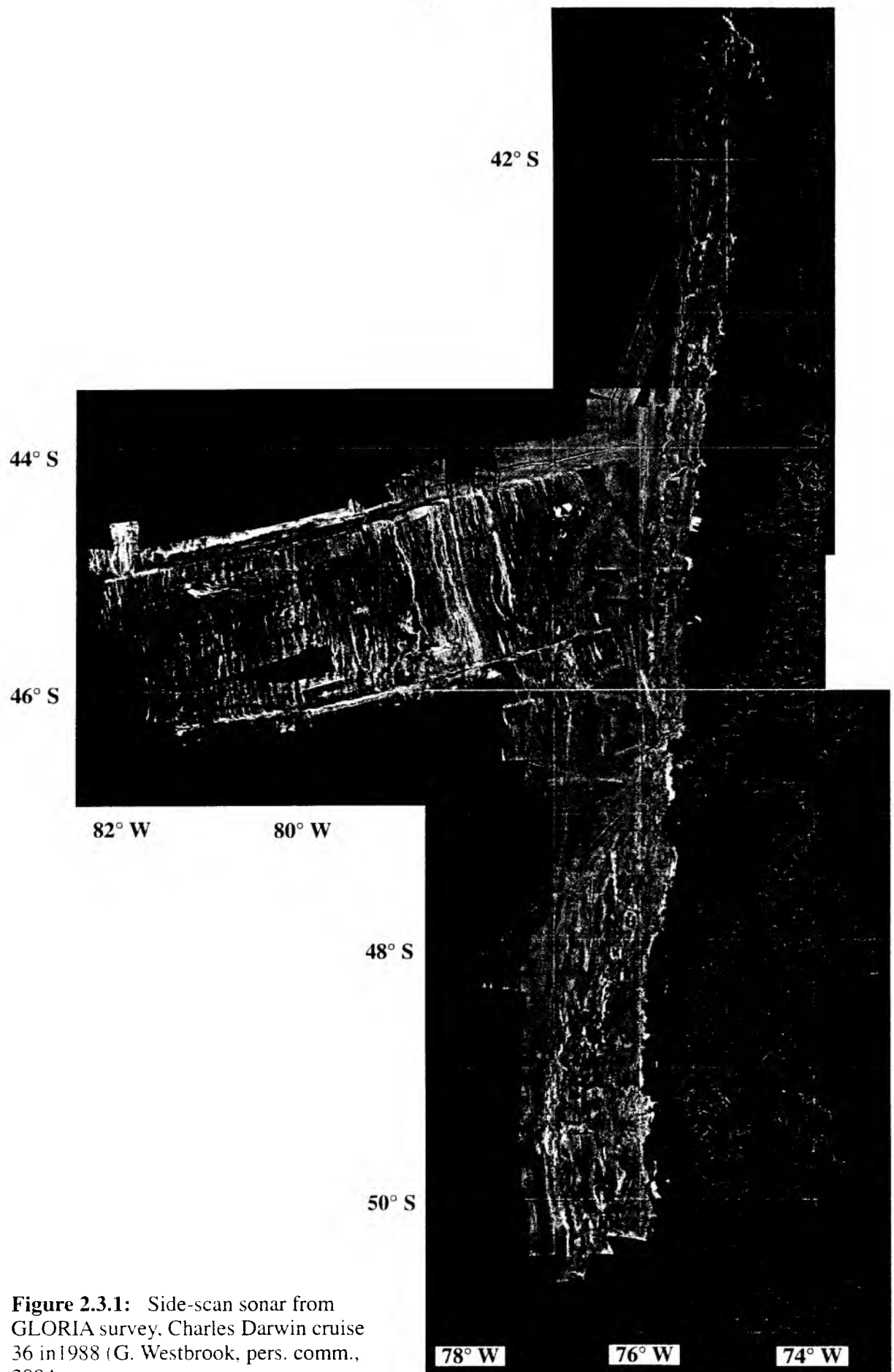


Figure 2.3.1: Side-scan sonar from GLORIA survey, Charles Darwin cruise 36 in 1988 (G. Westbrook, pers. comm., 2004)

The world's largest historically recorded earthquake, the 1960 Chile event ($M_w=9.5$), nucleated on the projection of the Mocha Fracture Zone (Figure 2.2.1) and ruptured ~800 km of the plate to about 45.5° S, just north of the Chile Triple Junction. The earthquake ruptured across an area where the subducting oceanic plate has a wide range of ages and thus a variable thermal structure and dip angle.

Extensive geological information on the structure and dynamics of the South American forearc in the vicinity of the Chile Triple Junction was provided by Leg 141 of the Ocean Drilling Program (Behrmann et al., 1992; Behrmann et al., 1994; contributions in Lewis et al., 1995). The combination of high-resolution swath bathymetric maps, seismic reflection profiles, drillhole and core data from five sites (ODP Sites 859-863) provides important data that define the tectonic, structural and stratigraphic effects of this unique modern example of spreading ridge subduction. A change from subduction accretion to subduction erosion occurs along strike of the South American forearc near 46° S. This change is prominently expressed by normal faulting, up to 2 km of forearc subsidence, oversteepening of topographic slopes, and intensive sedimentary mass wasting, overprinted on older signatures of sediment accretion, overthrusting and uplift processes in the forearc. Data from drillsites north of the Triple Junction (Sites 859-861) show that after an important phase of forearc building in the lower to upper Pliocene, subduction accretion had ceased in the upper Pliocene. Since that time sediment on the downgoing oceanic Nazca plate has been subducted. Site 863 was drilled into the forearc in the immediate vicinity of the triple junction above the subducted spreading ridge axis. Here, thick and intensely folded and faulted trench-slope sediments of Pleistocene age are currently involved in the frontal deformation of the forearc. Early faults with thrust and reverse kinematics are overprinted by later normal faults. The Chile Triple Junction is also the site of apparent ophiolite emplacement into the South American forearc. Drilling at Site 862 on the Taitao Ridge revealed an offshore volcanic sequence of Plio-Pleistocene age associated with the Taitao Fracture Zone, adjacent to exposures of the Pliocene-aged Taitao ophiolite onshore. Despite the large-scale loss of material from the forearc at the triple junction, ophiolite emplacement produces a large topographic promontory in the forearc immediately following ridge subduction, and represents the first stage of forearc rebuilding.

Arc volcanism displays a segmentation that parallels the oceanic plate structure. North of the triple junction there is an active Holocene arc, whereas south of the triple junction a ~200 km long segment of the arc has been inactive at least in the Holocene (Figure 2.1.1). Historical lavas from the active arc show Uranium and ^{10}Be enrichment that has been interpreted as indicating subduction of the youngest trench sediment infill to mantle wedge depths (Sigmarsson et al., 1990). The enrichment in those elements is higher south of 39° S, i.e. south of the land projection of the Valdivia Fracture Zone system. The gradient in the chemistry of the lavas is explained by a more efficient sediment subduction south of 39° S (Sigmarsson et al., 1990). Results of a recent study investigating the contribution of subducted trench sediment to arc melts in the Southern Andes (Kilian and Behrmann, 2003) indicates that mantle sources of basalts from the Southern Andes Volcanic Zone (41° - 47° S) were contaminated by 3-5 vol.% of a terrigenous sediment melt with variable amounts of Ba-rich pelagic sediments, but were not contaminated by slab-derived fluids. Adakites of the Austral Andes Volcanic Zone (49° - 55° S) formed by melting of a relatively hot subducted slab, and contain a variable amount of subducted terrigenous sediment (0-20 vol.% sediment melt).

2.4 Seismology in Chile

The Chilean margin presents one of the largest rates of seismic activity in the world and in 1960 was the locus of the largest earthquake instrumentally recorded so far. Although the largest frequency and intensity of seismicity is concentrated between its northern most point (Arica) and the Taitao Peninsula, seismic activity in Chile can be observed throughout its territory from Arica to Cape Horn.

The "Servicio Sismológico Nacional" based in the Geophysics Department, University of Chile, Santiago, is the main institution where observation and analysis of seismicity is carried out in Chile. Instrumental seismology in Chile can be traced back to 1849 when I.M. Gillis, leading an USA astronomical expedition in the southern hemisphere, installed a "simoscope" in Santiago, which on 2 April 1851 recorded a seismic event for the first time in Chile.

After the 1906 great earthquake that destroyed Valparaíso and seriously affected Central Chile, Mr. Valentin Letelier, Universidad de Chile's Rector, pointed out the importance of seismological observations in Chile. Under his proposition and during the government of President Pedro Montt, the National Seismological Service was founded on May 1st, 1908. The Seismological Service's first director was Mr. Ferdinand Montessus de Ballore, a well known scientist from l'Ecole Polytechnique de Paris.

In 1908, Montessus de Ballore installed a first station in "Cerro Santa Lucía", downtown Santiago. Stations were also installed in Tacna, Copiapo, Osorno and Punta Arenas. In few years a total of 29 stations were in operation throughout Chile, configuring at that time one of the most modern seismological networks of the world. After Montessus de Ballore's death in 1923, however, Chilean seismology was limited almost exclusively to the gathering of data, losing its national dynamics and the presence gained in the previous 15 years.

A new impulse to Chilean seismology came with the engineer Federico Greeve, Servicio Sismológico's Director between 1941 and 1958. He built mechanical seismographs and was able to repair the already old equipment. Greeve compiled and complemented the information on intensities of historical earthquakes started by Montessus de Ballore.

Around 1980, the first analog seismological network with telemetric support was installed in Central Chile. A total of 7 sensors were acquired with United Nation's funds, through the Chilean Nuclear Energy Commission. These instruments together with the already working Peldehue and Santiago stations formed the first relatively dense seismological network around Santiago Metropolitan Region. Funds provided by CODELCO (Corporación del Cobre) allowed to expand this network up to San Fernando, about 150 km south of Santiago.

Since the late nineties, the Servicio Sismológico has received dedicated public funds that have allowed to update the network with digital stations, and expanded it to regions north and south of Santiago.

The following Figure 2.4.1 present the Servicio Sismológico Nacional stations south of Santiago, most relevant to the TIPTEQ project. Figure 2.4.2 exhibits tentative locations for stations to be installed jointly by the Northwestern University, USA, and the Geophysics Department, Universidad de Chile.

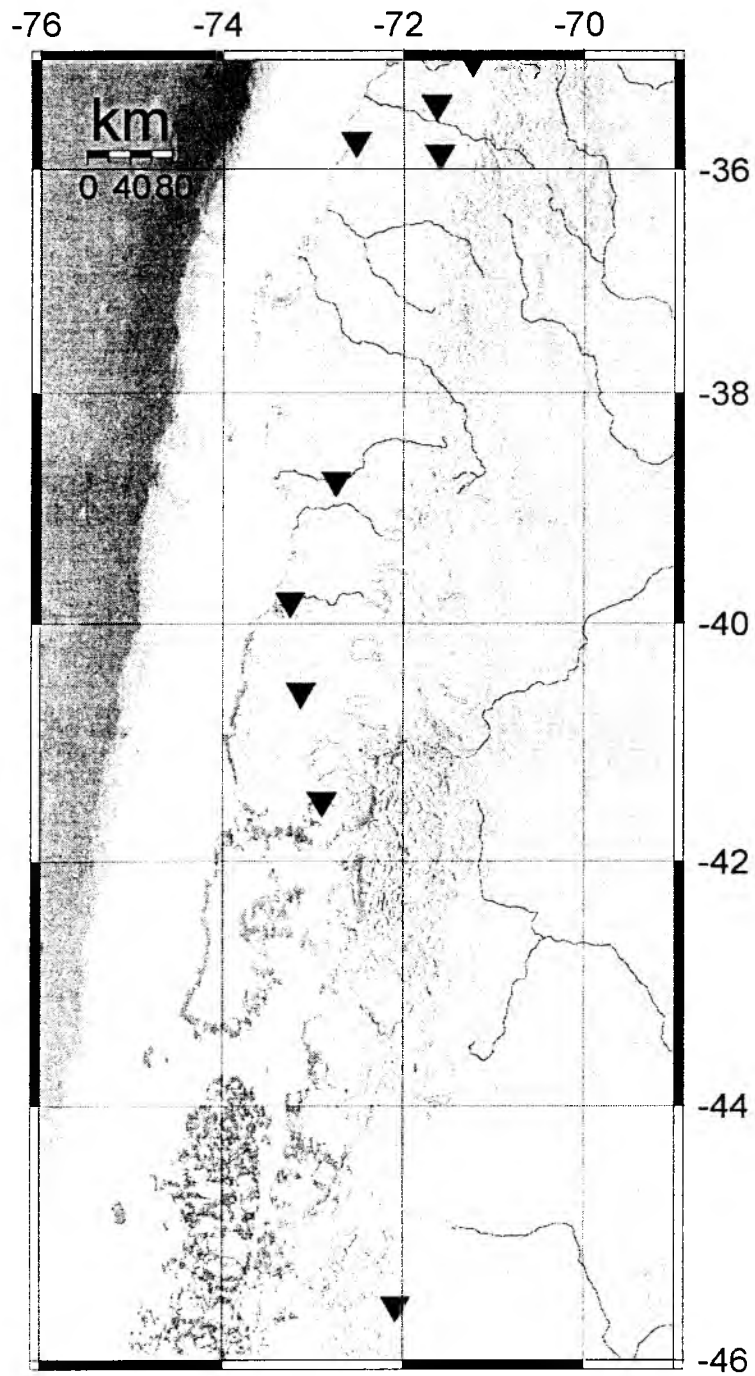


Figure 2.4.1: Seismological network in southern Chile.

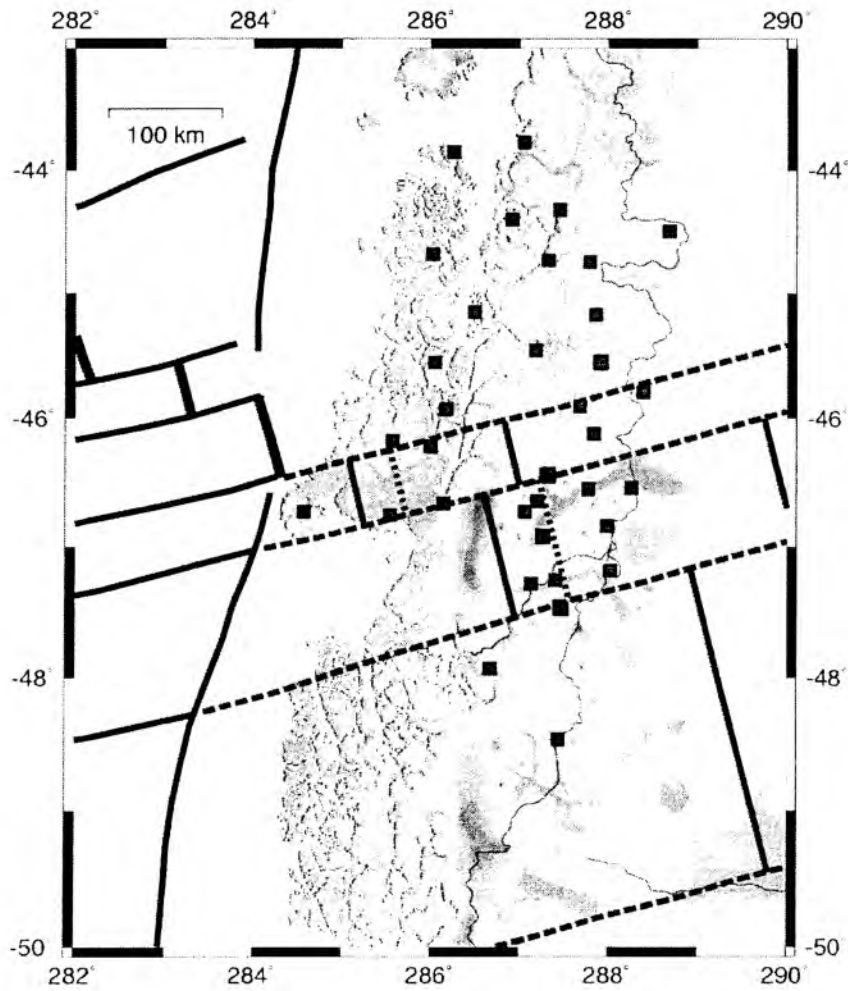


Figure 2.4.2: Proposed seismometer deployment sites for stations to be installed by the Northwestern University, USA, and the Geophysics Department, Universidad de Chile. The trench is marked as the curved NS-oriented line. Other lines represent actual and projected locations of fracture zones and spreading centres.

3. Participants

3.1 Scientists

3.1.1 Scientists - SO 181-1a

Prof. Dr. Flüh, Ernst	IFM-GEOMAR, chief scientist
Anh, Mai Hoàng	GeoB
Bailey, John William	WHOI
Prof. Dr. Behrmann, Jan-Hinrich	GI - Freiburg
Beitz, Manuel	IFG – Hamburg
Dr. Brasse, Heinrich	FU Berlin
del Pilar, Alejandra Flores Arabach	DGF U. de Chile
Gardner, Allan Thompson	WHOI
Hensch, Martin	IFG – Hamburg
Hofmann, Sonja Dorothea	IFG – Hamburg
Prof. Dr. Kopf, Achim	RCOM Bremen
Moeller, Helmuth Hinrich	Moeller
Dr. Petersen, Jörg	SFB574, University of Kiel
Röser, Georg	GI - Freiburg
Schäfer, Raphael Andreas	GeoB
Dr. Scherwath, Martin	IFM-GEOMAR
Schnese, Michael	IFG – Hamburg
Steffen, Klaus-Peter	IFM-GEOMAR
Dr. Vera, Emilio Eduardo	DGF U. de Chile
Villar-Muñoz, Lucía Alejandra	PUCV

3.1.2 Scientists - SO 181-1b

PD Dr. Grevemeyer, Ingo	IFM-GEOMAR, chief scientist
Buddensiek, Maïke	IFM-GEOMAR
Egana Erazo, Matias J.	DGF U. de Chile
Dr. Fabian, Marcus	GeoB
Dr. Gennerich, Hans-Hermann	GeoB
Haase, Claudia	CAU
Heesemann, Bernd	GeoB
Heesemann, Martin	GeoB
Dr. Kaul, Norbert	GeoB
Nehniz, Wiebke	GeoB
Röser, Georg	GI - Freiburg
Schlesinger, Angela	CAU
Schwarz, Michael	GI - Freiburg
Trümper, Monika	GeoB
Prof. Dr. Villinger, Heinrich	GeoB

3.1.3 Scientists - SO 181-2a

Prof. Dr. Flüh, Ernst	IFM-GEOMAR, chief scientist
Arroyo, Ivonne	IFM-GEOMAR
Barroso, Eleonora	PUCV
Becel, Anne	IPGP
Dr. Bialas, Jörg	IFM-GEOMAR

Buddensiek, Maike	IFM-GEOMAR
Dannowski, Anke	IFM-GEOMAR
Diaz, Daniel	DGF U. de Chile
Fromm, Tanja	IFM-GEOMAR
Dr. Gossler, Jürgen	KUM
Heimann, Sebastian	IFG – Hamburg
Herber, Rolf	IFG – Hamburg
Hofmann, Barbara	IFG – Hamburg
Kahle, Richard	BULLARD
Dr. Krabbenhöft, Anne	IFM-GEOMAR
Miensopust, Marion	IFG – Hamburg
Dr. Papenberg, Cord	IFM-GEOMAR
Dr. Petersen, Jörg	SFB574, University of Kiel
Redenz, Rodrigo	PUCV
Dr. Scherwath, Martin	IFM-GEOMAR
Steffen, Klaus-Peter	IFM-GEOMAR
Villar-Muñoz, Lucía Alejandra	PUCV
Zamora, Natalia	ECG, Universidad de Costa Rica

3.1.4 Scientists - SO 181-2b

Prof. Dr. Flüh, Ernst	IFM-GEOMAR, chief scientist
Arroyo, Ivonne	IFM-GEOMAR
Barroso, Elenora	PUCV
Becel, Anne	IPGP
Prof. Dr. Dahm, Torsten	IFG – Hamburg
Diaz, Daniel	DGF U. de Chile
Fromm, Tanja	IFM-GEOMAR
Gardner, Allan Thompson	WHOI
Dr. Gossler, Jürgen	KUM
Heimann, Sebastian	IFG – Hamburg
Herber, Rolf	IFG – Hamburg
Hofmann, Barbara	IFG – Hamburg
Kapinos, Gerhard Antonius	FU Berlin
Miensopust, Marion	IFG – Hamburg
Dr. Papenberg, Cord	IFM-GEOMAR
Dr. Petersen, Jörg	SFB574, University of Kiel
Redenz, Rodrigo	PUCV
Dr. Scherwath, Martin	IFM-GEOMAR
Steffen, Klaus-Peter	IFM-GEOMAR
Dr. Weinrebe, Wilhelm	IFM-GEOMAR
Villar-Muñoz, Lucía Alejandra	PUCV
Zamora, Natalia	ECG, Universidad de Costa Rica

3.2 Crew

3.2.1 Crew - SO 181-1

Kull, Martin	Master
Korte, Detlef Peter	Chief Mate
Meyer, Oliver	1st Offc.

Büchele, Heinz-Ulrich	2nd Offc.
Guzman-Navarrete, Werner	Ch/Eng
Grund, Helmuth	2nd Engineer
Klinder, Klaus-Dieter	2nd Engineer
Zebrowski, Dariusz Marek	Electrician
Heuser, Sabine	Doctor
Hoffmann, Wolf Hilmar	Chief Electrician
Borchert, Wolfgang (only leg 1a)	System Operator
Leppin, Jörg	System Operator
Blohm, Volker	Fitter
Golabowski, Daniel	Motorman
Zeitz, Holger	Motorman
Tiemann, Frank	Chief Cook
Pytlik, Franciszek	2nd Cook
Slota, Werner	Chief Steward
Krzesowski, Artur	2nd Steward
Jahns, Winfried	Bosun
Schrapel, Max Karol Andreas	A. B.
Kraft, Jürgen	A. B.
Vor, Hans-Jürgen	A. B.
Dehne, Dirk Wolfgang	A. B.
Bierstedt, Torsten	A. B.
Faber, Florian	Trainee
Föster, Tino	Trainee

3.2.2 Crew - SO 181-2

Lutz, Mallon	Master
Meyer, Oliver	Chief Mate
Aden, Nils	1st Offc.
Büchele, Heinz-Ulrich	2nd Offc.
Guzman-Navarrete, Werner	Ch/Eng
Grund, Helmuth	2nd Engineer
Lindhorst, Norman	2nd Engineer
Ulbricht, Martin	Electrician
Heuser, Sabine	Doctor
Hoffmann, Wolf Hilmar	Chief Electrician
Borchert, Wolfgang	System Operator
Leppin, Jörg	System Operator
Blohm, Volker	Fitter
Golabowski, Daniel	Motorman
Saathoff, Maurice	Motorman
Tiemann, Frank (only leg 2a)	Chief Cook
Wieden, Wilhelm (only leg 2b)	Chief Cook
Pytlik, Franciszek	2nd Cook
Slota, Werner	Chief Steward
Krzesowski, Artur	2nd Steward
Jahns, Winfried	Bosun
Hödl, Werner	A. B.
Kraft, Jürgen	A. B.

Vor, Hans-Jürgen	A. B.
Etzdorf, Detlef	A. B.
Bierstedt, Torsten	A. B.
Föster, Tino	Trainee

3.3 Addresses of Participating Institutions

IFM-GEOMAR Leibniz-Institut für Meeresforschung
 an der Christian-Albrechts-Universität zu Kiel
 Wischhofstr. 1-3
 24148 Kiel
 Germany
 Tel.: +49 – 431 – 600 – 2971
 Fax: +49 – 431 – 600 – 2922
 e-mail: Iname@ifm-geomar.de
 Internet: www.ifm-geomar.de

BULLARD Bullard Laboratories, Madingley Rise House
 Dept. Of Earth Sciences, Madingley Road
 University of Cambridge
 Cambridge
 CB30EZ
 Tel: +44-1223-337-191
 e-mail: kahle@esc.cam.ac.uk
 Internet: www.esc.cam.ac.uk

CAU Institut für Geowissenschaften
 Christian-Albrechts-Universität zu Kiel
 Otto Hahn Platz 1
 24118 Kiel
 Germany
 Email: Iname@geophysik.uni-kiel.de
 Tel: +49-431-880-3913
 Fax +49-431-880-3900
 Internet: www.uni-kiel.de

DGF Universidad de Chile
 Departamento de Geofísica.
 Facultad de Ciencias Básicas y Matemáticas
 Blanco Encalada 2002, Santiago
 Chile
 Tel: +56-02-6784565
 Fax: +56-02-6968686
 e-mail: evera@dgf.uchile.cl
 Internet: www.dgf.uchile.cl

FU FU Berlin
 Fachrichtung Geophysik
 Malteserstr. 74-100
 D-12249 Berlin
 Germany
 Tel.: +49-30-83870434
 Fax.: +49-30-83870729
 e-mail: h.brasse@geophysik.fu-berlin.de
 Internet: www.fu-berlin.de/geophysik

GeoB

Fachbereich 5 – Geowissenschaften
 Universität Bremen
 Klagenfurter Str.
 28359 Bremen
 Postfach 33 04 40
 28334 Bremen
 Germany
 Tel: +421-218 4509
 Fax: +421-218 7163
 e-mail: vill@uni-bremen.de
 Internet: www.uni-bremen.de

GI

Geologisches Institut
 Albert-Ludwig-Universität
 Albertstr. 23-B
 79104 Freiburg
 Germany
 Tel: +49-761-203495
 Fax: +49-761-2036496
 Email: jan.Behrmann@geologie.uni-freiburg.de
 Internet: www.uni-freiburg.de

IFG

Institut für Geophysik
 University of Hamburg
 Bundesstr. 55
 20146 Hamburg
 Germany
 Tel.: +49-40-428382973
 Fax: +49-40-428385441
 e-mail: sonja.hofmann@dkrz.de
 Internet: www.geophysics.dkrz.de

IPGP

Institut de Physique du Globe de Paris
 Laboratoire de Sismologie Experimentale
 T24-14 4eme Etage
 4, Place Jussieu
 75252 Paris Cedex05
 France
 Tel: +33-144-274-781
 e-mail: becel@ipgp.jussieu.fr
 Internet: www.ipgp.jussieu.fr

KUM

K.U.M. Umwelt- und Meerestechnik Kiel GmbH
 Wischhofstraße 1-3, Geb. D5
 24148 Kiel
 Germany
 Tel.: 0049 – 431 – 7209 – 220
 Fax: 0049 – 431 – 7209 – 244
 e-mail: KUM.Umweltsmeerestechnik@t-online.de

- Moeller** Helmut Moeller
5393 Belardo Dr. San Diego Calif. 92124
USA
Tel: +1-858-4679145
e-mail: horusmoeller@yahoo.com
- PUCV** Pontificia Universidad Católica de Valparaíso
Laboratorio de Geofísica Marina, Escuela de Ciencias del Mar
Av. Altamirano 1480 of. 119, Valparaíso
Chile
Tel: +56-32-274255
Fax: +56-32-274242
e-mail: jdiaz@ucv.cl
Internet: www.ucv.cl
- RCOM** Research Center Ocean Margins
Am Fallturn 1 TAB
28359 Bremen
Postfach 330440
28334 Bremen
Germany
Tel: +421-218-8782
Fax: +421-2188783
e-mail: akopf@uni-bremen.de
Internet: www.rcom-bremen.de
- RF** RF Forschungsschiffahrt GmbH
Blumenthalstr. 15
28023 Bremen
Germany
Tel.: + 49 – 421 – 20 76 60
Fax: + 49 – 421 – 20 76 670
e-mail: info@rf-bremen.de
Internet: www.rf-bremen.com
- SFB574** Sonderforschungsbereich 574
University of Kiel
Wischhofstr. 1-3, 24148 Kiel
Germany
e-mail: jpetersen@ifm-geomar.de
Internet: www.ifm-geomar.sfb574.de
- WHOI** Woods Hole Oceanographic Institution
98 Water Street, Biselow G-7
Woods Hole, MA 07543
USA
Tel: +1-508-789-7890
Fax: +1-508-457-2194
e-mail: jbailey@whoi.edu
Internet: www.whoi.edu



Figure 3.1.1.1: Participants of cruise SO181-1a.



Figure 3.1.2.1: Participants of cruise SO181-1b.



Figure 3.1.3.1: Participants of cruise SO181-2a.



Figure 3.1.4.1: Participants of cruise SO181-2b.

4. Agenda of the cruises

4.1 Agenda of the cruise SO181-1a

Cruise SO181-1a started upon departure of RV Sonne at 10:00 on 7 December 2005 in Valparaiso heading southwards. On 8 Dec. two gravity cores were taken in the Chile trench, and two more on 9 Dec., when also the first four magnetotelluric (MT) stations were deployed. The remaining three MT stations were deployed during the night of 9/10 Dec., and after taking gravity core SL-181-05, the acoustic release systems for the ocean-bottom seismic instruments were tested at a depth of 4000m. Since the core SL-181-05 was empty, another core was tried, and about 2 m of sediments could be recovered. Two more cores were taken further south, before the deployment of the first seismic network was started at 02:30 on 12. Dec. Altogether 17 stations were deployed, at an average spacing of 8.1 nm. This was completed at 17:00, and subsequently three seismic profiles were shot with two 32 litre airguns. A short streamer was also deployed, which however was lost at the beginning of profile P03. Apparently, it had been bitten by sharks. Along profile P03 also the magnetometer was deployed. Shooting was terminated at 22:00 on 13 Dec., and another gravity core was taken in the area, before a transit of about 80 nm to the southern outer rise seismological network was started. Here another 12 instruments were deployed, and one seismic line was shot across this array. During shooting, also the magnetometer was deployed. Shooting was terminated at 05:00 on 15 Dec., and during the transit to Valdivia two more gravity cores were taken. In addition, a number of lines were included to increase the existing bathymetric database. RV Sonne met the pilot off Corral/Valdivia on 17 Dec. at 13:00, terminating cruise SO181-1a after 10 days at sea and cruising for 1930 nm. The cruise track is shown in Figure 4.1.1.

4.2 Agenda of the cruise SO181-1b

On Friday 18 Dec. at 10:48 local time RV Sonne cruise SO181-1b commenced after a vessel safety exercise, departing from the harbour of Corral. Immediately after leaving the bay of Corral, the magnetometer was deployed and for the first three days a magnetic and SIMRAD EM120 swathmapping survey (Survey1b-1) was run on the continental slope between the town of Corral/Valdivia and the southern terminus of the Isla Chiloe, with the main emphasise on the slope offshore Chiloe. At 13:30 UTC on 20 Dec. the first 170 nm long high resolution seismic reflection line SCS01 was shot along corridor #2. As the seismic source a 2.5-litre GI-airgun was operated at 140 bar in Harmonic mode, and seismic shots were recorded on a 16-channel Teledyne streamer. On 21 Dec. at 23:30 UTC the equipment was recovered and the first heat flow measurement, station H0401 with ten successful penetrations, was carried out on 9 Ma old seafloor, at a distance roughly 250 km from the trench axis. After running an additional survey line (Survey1b-2) parallel to SCS01, on 22 December at 22:50 UTC, the second heat flow station H0402 was placed on 14 Ma old crust about 100 km from the trench. A short magnetic and EM120 profile led us to H0403 on the continental slope, where 12 heat flow determinations over gas hydrate bearing sediments were planned. However, only at four stations the heat probe was able to penetrate the sediments. All other stations failed. On 24 Dec. at 7:30 local time the instrument was back on deck and a 700 nm long magnetic and EM120 survey (Survey1b-4) was conducted over the Christmas weekend to survey the slope area and incoming plate between 45°10'S and 40°10'S.

On 27 Dec. at 10:10 UTC heat flow station H0404 was placed seaward of the deformation front offshore Chiloe. After six successful penetrations, Sonne headed (Survey1b-5) for corridor #3, located between Guafo and Guamblin fracture zones. On 28 Dec. at 17:30 UTC we deployed the streamer and airgun for the second seismic line SCS02. However, due to problems with the GI-gun, we had to stop the seismic line at 22:26 UTC. While repairing the gun, we sailed south (Survey1b-6) to collect two cores along corridor #4 (SL-1b-01 + SL-1b-02) and to obtain heat flow data (H0405) from the lower slope and at the deformation front in corridor #4. Nine penetrations

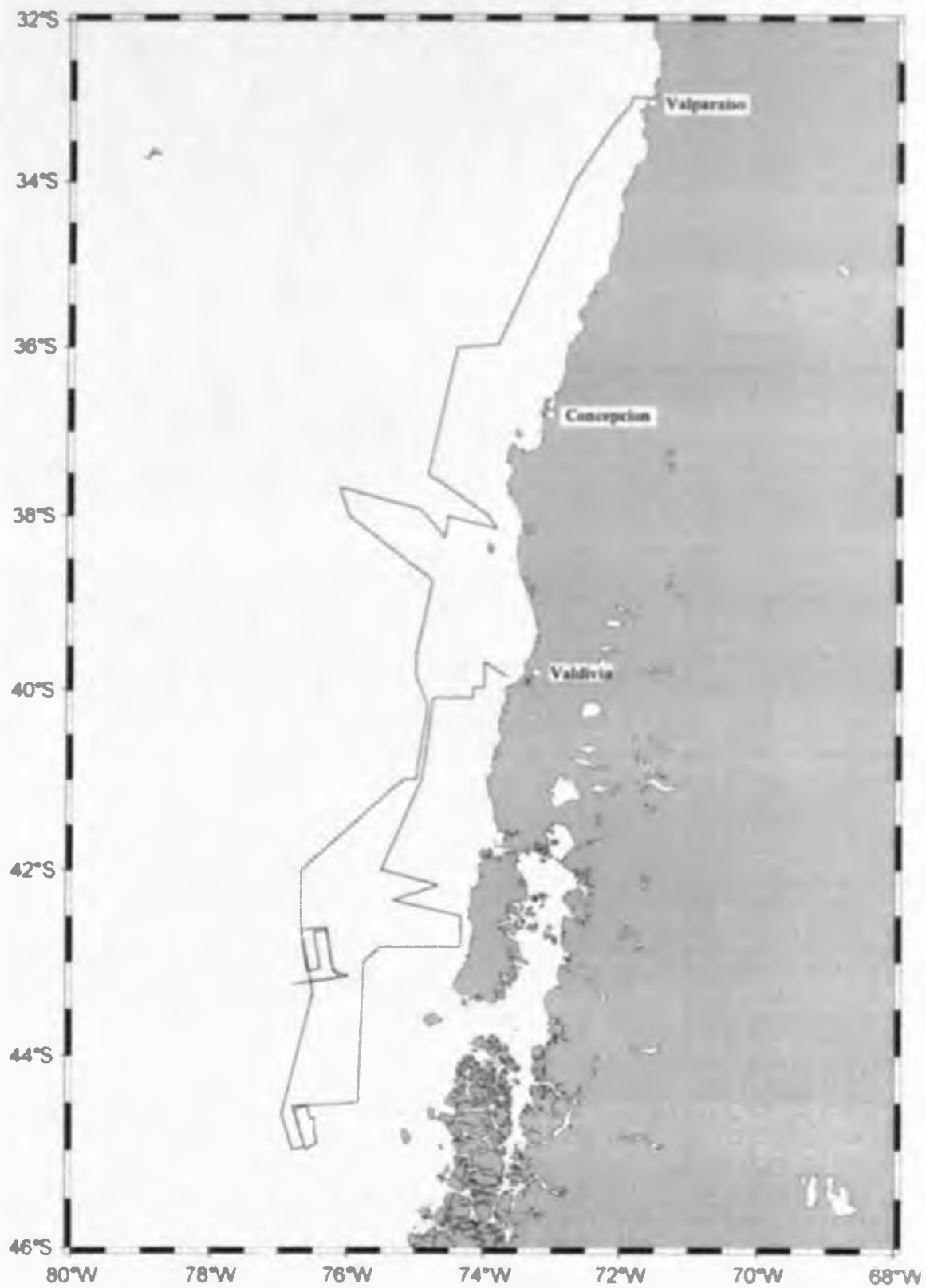


Fig. 4.1.1: Track chart of SO181-1a Valparaiso – Corral/Valdivia

were made. At 07:00 local time the heat probe was back on deck and Sonne sailed to the southernmost location of Leg 1b to obtain a gravity core (SL1b-03) at South Canyon south of the Chile Triple Junction. Three additional cores were planned to be taken at a fault scar on the continental slope to the northeast of Ocean Drilling Program site 863. However, only one core (SL1b-04) on the hanging wall was successfully taken. Since the core SL1b-05 was empty, another core was tried. Both SL1b-06 and SL1b-07 were empty and we stopped the coring at 23:45 local time on 30 December 2004. Until 3 January 2005 a 3.5 days EM120 survey was run on the continental slope between $46^{\circ}40'S$ and $\sim 43^{\circ}S$, and on the incoming plate between $43^{\circ}S$ and $40^{\circ}10'S$ (Survey1b-7). In the morning of 31 Dec., the survey was stopped for a test of the repaired GI-gun. The airgun was ready for the next profile. The 838 nm long survey was finished on 3 Jan. at 10:50 UTC.

At 08:00 local time on 3 January, the streamer, airgun and the magnetometer were deployed again to survey corridor #3 with high-resolution seismics along profile SCS02-2. After roughly 24 hours of operation, the electrical trigger cable to the airgun was damaged due to bad weather conditions at night. It was decided to stop the survey. A short EM120 and magnetic survey (Survey1b-8) was run parallel to SCS02-2 and heat flow measurements on station H0406 – consisting of 12 penetrations – were conducted along corridor #3 on 7 Ma old seafloor. After a short transit, H0407 was placed on the lower continental slope, at the deformation front and on the incoming plate. Perhaps related to thin layers of sand, the penetration was not always successful. However, the probe penetrated five times out of ten. On 6 Jan. at 0:00 UTC a 610 nm long EM120 Survey1b-9 was started. Between 18:00 UTC and 22:00 UTC on 7 Jan. a portion of the survey, a 40 nm long E-W profile, was run with the magnetometer deployed. At 08:15 local time the heat probe was lowered into the water. HF0408 was a short station on seismic line SCS01 offshore Chiloe with only three penetrations to get the heat flow in an area roughly 70 km from the trench axis where the sedimentary blanket was not affected by turbiditic sedimentation to provide an unbiased crustal heat flow. After roughly 6 hours the probe was back on deck and Sonne sailed to a second station on the slope offshore Chiloe. At 07:30 local time the heat probe hit the seafloor for the first time. However, except for a single penetration, HF0409 was a failure. We believe that sand layers stopped the probe to penetrate three times out of four. Survey1b-10 closed gaps in the bathymetric coverage between $42^{\circ}S$ and $40^{\circ}40'S$. At 15:00 UTC on 9 Jan. the third high resolution seismic line SCS03 was shot across the continental slope into the incoming plate where the Harvard catalogue indicated an increased activity of outer rise earthquakes.

On 10 January line SCS03 terminated roughly 110 km from the trench axis. To fill in gaps in the coverage and to obtain an additional magnetic line perpendicular to the margin Survey1b-11 was conducted and provided 220 line kilometres of multibeam bathymetry and 155 km of magnetic data. At 08:10 local time HF0410 was collected on the lower continental slope along SCS03. Six successful penetrations were obtained. At 17:00 local time the heat probe was back on deck and a 2 days bathymetric survey was started to extend the existing bathymetric coverage to the north of Valdivia. The existing data had been acquired during RV Sonne cruise SO161, where large areas of the incoming plate and of the continental had been surveyed with the EM120 multibeam sonar. On 12 Jan. at 16:10 UTC the magnetometer was deployed to survey along a profile magnetic seafloor spreading anomalies to the north of the Mocha fracture zone. At 17:30 local time Sonne was on the continental shelf and airgun and streamer were deployed to survey SCS04. At $\sim 18:30$ Sonne crossed ODP site 1234. The profile terminated at 8:40 on 14 January. After a short transit to the last heat flow station, HF0411 was collected over roughly 30 Ma old crust. At 0:00 UTC on 15 January, after 8 successful penetrations, the heat probe was back on deck. For the remaining 1.5 days a EM120 and magnetic survey (Survey1b-13) was conducted offshore Concepcion to look for proposed anomalies in the magnetic field which should form when fluids penetrate down to mantle depth and form serpentinites. On 16 January at 2:50 UTC the magnetometer was recovered and

Sonne headed for the port of San Vicente. At 08:00 local time the ship met the pilot, terminating the cruise after 30 days at sea. Figure 4.2.1 shows the track of the cruise SO181-1b.

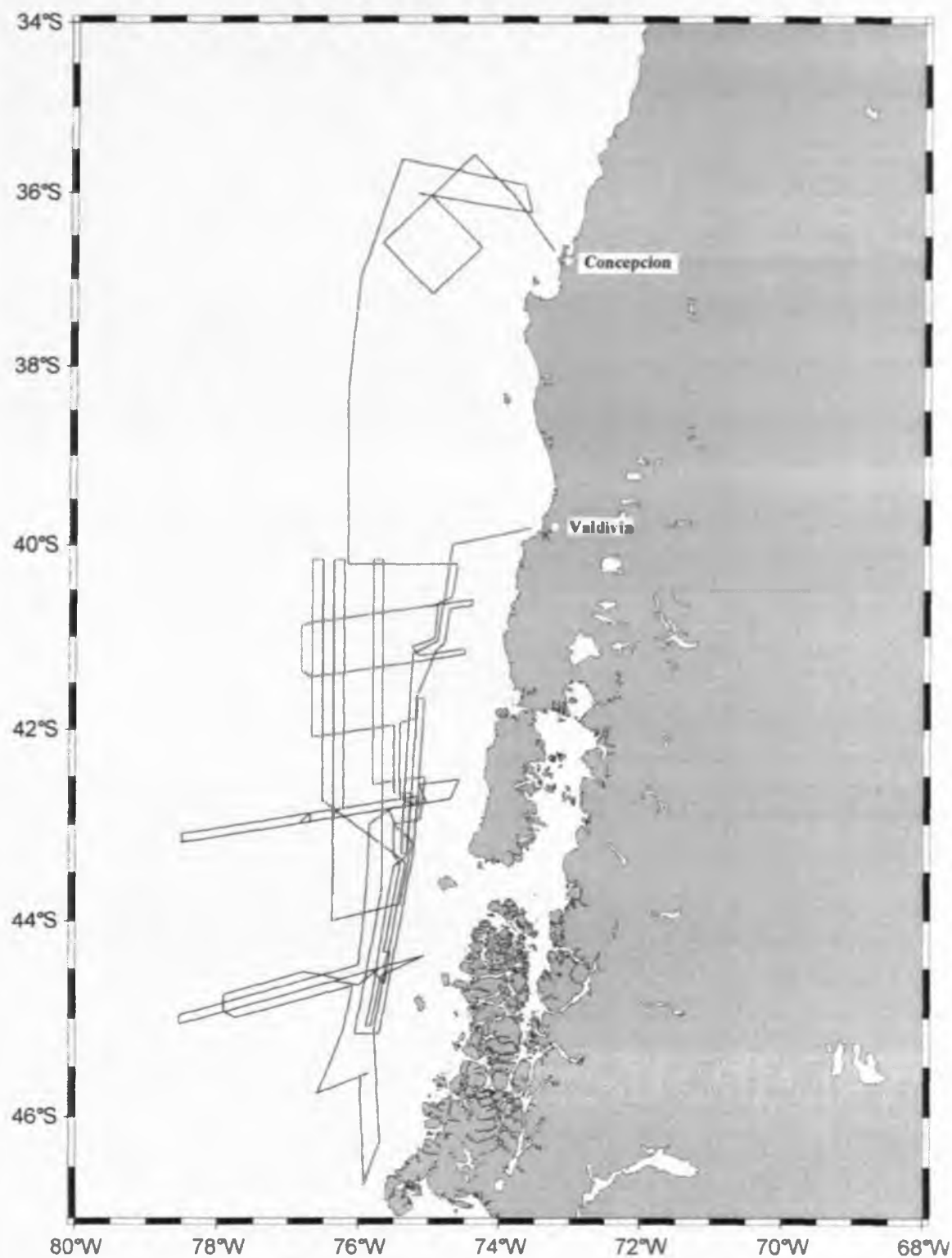


Fig. 4.2.1: Track chart of SO181-1b Corral/Valdivia – San Vicente/Concepcion

4.3 Agenda of the cruise SO181-2

Cruise SO181-2 started after the port call in San Vicente, where scientific equipment was unloaded and new equipment and supplies were taken on board, at 06:30 on 19 Jan. 2005. Twentythree scientists from Argentina, Chile, Costa Rica, Germany, Great Britain and France made up the scientific party. Force 7 winds made installation of equipment onboard impossible, therefore for the afternoon of 19 Jan. Sonne was seeking shelter near the northeast coast of Sta. Maria Island. Along the ca. 450 nm transit to the first working area at 42:30S instrumentation was prepared. In the morning of 20 Jan. altogether 27 acoustic releases were tested using the W6 winch to a depth of 4000 m. A CTD was also attached to the cable. All releasers worked fine, and in the evening of 21 Jan. we reached the working area. The transit was planned such that gaps in the bathymetric coverage could be filled. Strong winds and swell sometimes reduced the transit speed considerably.

Along Profile P05 a total of 40 OBH/S were deployed, and three instruments of the seismological array deployed in December 2004 during leg SO181-1a were left to record the airgun shots. During deployment, 14 instruments of seismological array were recovered and redeployed at the western end of the line. Deployment and recovery went smoothly and lasted from 20:00 on 21 Jan. to 16:00 on 23 Jan. The first shot along the 190 nm line P05 (coincident with SCS01 of Leg SO181-1b) was fired at 21:30 on 23 Jan. During shooting the so far prevailing strong winds calmed down for the first time. One gun array failed after a short time, but otherwise no problems were encountered and the profile was finished by 18:00 on 25 Jan. Recovery of the 43 instruments started immediately after retrieval of the guns and went smoothly, and all instruments were back on board at 04:00 on 27 Jan.

We then headed south to recover the second seismological array; all 12 instruments were retrieved by 04:30 on 28 Jan.

The next seismic profile to be shot was the southernmost line. We reached Golfo de Penas at 20:00 the same day; 45 instruments were deployed at an average spacing of 2.7 nm. Shooting along this ca 120 nm long profile was done at 3 kn and lasted from 16:30 on 29 Jan. to 09:30 on 31 Jan. At this time there was very little swell and practically no wind, thus conditions were perfect. A short 100 m long streamer was also deployed, and 7 out of 8 guns worked continuously throughout the line. Unfortunately, the first OBS (112) to be released did not surface. Since it replied, we attempted to dredge it. This was successfully accomplished by 15:00 on 31 Jan. Another OBS (118) also refused to return to the surface. Since we expected additional instruments to fail, we decided to continue the recovery, which was successfully completed at 17:00 on 01 February. On the transit back to OBS118 the magnetometer was deployed. We first tried to locate the instrument in 140 m water depth using the new camera system of Hamburg University, however failed to find it despite 3 hours of search. We then used the dredge again and recovered the instrument soon after.

On 03 February we deployed 37 instruments (OBS157 to 193) along Profile P08, between the coast and the Chile Rise. Shooting along this line was terminated at 09:00 on 05 Feb., the shots were also recorded by the 100 m long streamer. All guns worked perfectly throughout the profile, and weather conditions were favourable. Instrument recovery was finished at 10:30 on 06 February, and two magnetic profiles were recorded before the next seismic profile was started.

Along profile P06 a total of 50 instruments (OBS70 to 111, OBS194 to 201) were deployed on 07 and 08 February, and shooting along this 160nm long line from the Chile Rise to the coast lasted for 48 hours, and terminated at 18:00 10 February. Recovery of instruments was completed early in the morning of 12 February, except for OBH92, which confirmed release commands and was found

in a vertical position. Therefore an attempt to dredge this instrument was made later that day, unfortunately without success.

On 13 February a seismological network, comprising 20 stations, separated by about 12 nm each, was deployed offshore Chiloe. Together with a land network, these instruments shall be in operation until October 2005.

Following a 320 nm transit with the magnetometer deployed, Sonne reached the northernmost line, where seismic data were to be collected. In absolutely calm seas 29 instruments were deployed along Profile P09, which is the seaward continuation of a seismic profile collected during Sonne cruise SO161. Shooting started soon after midnight on 16 February and lasted until midday 17 February. Instruments were all recovered a day later, and with the magnetometer deployed a few survey lines were acquired before Sonne reached Corral, where an exchange of personnel was made between 10:00 and 12:15 on 19 February.

In the remaining days a seismological network comprising 10 instruments (OBS/H 251 to 260) were deployed seaward from Isla Mocha, and the magnetotelluric stations (MT01 to MT07), deployed at the very beginning of SO181, were recovered. From the 10 instruments in the seismological network, four were Hamburg-type OBS and were deployed using the video-guided deployment frame. The first OBS was deployed at 23:00 on 19 February. The MT-Stations were not equipped with a flashlight, and moreover surfaced upside down, so that the radio signal was not detectable. It was therefore decided to pick up these stations during daytime only. Unfortunately MT02 did not reply to any release command, and could not be spotted, either, despite an intensive search. MT03 and 04 were recovered on 20 February. All seismic instruments were deployed by 21 February, and MT05 and 06 were also recovered 21 February. On 22 February an attempt to recover station MT07 was made. The instrument replied to the release commands sent, but after four hours it had only risen by 800 m. After another visit eight hours later it had risen another 600 m, but was still at 2700 m. At this speed there was not enough time left to wait for a possible surfacing of the instrument. It was thus given up, and with the magnetometer deployed Sonne headed towards Talcahuano. She berthed at 09:00 on 24 February 2005, terminating a very successful cruise. Figure 4.1.3 shows the track of the cruise SO181-2.

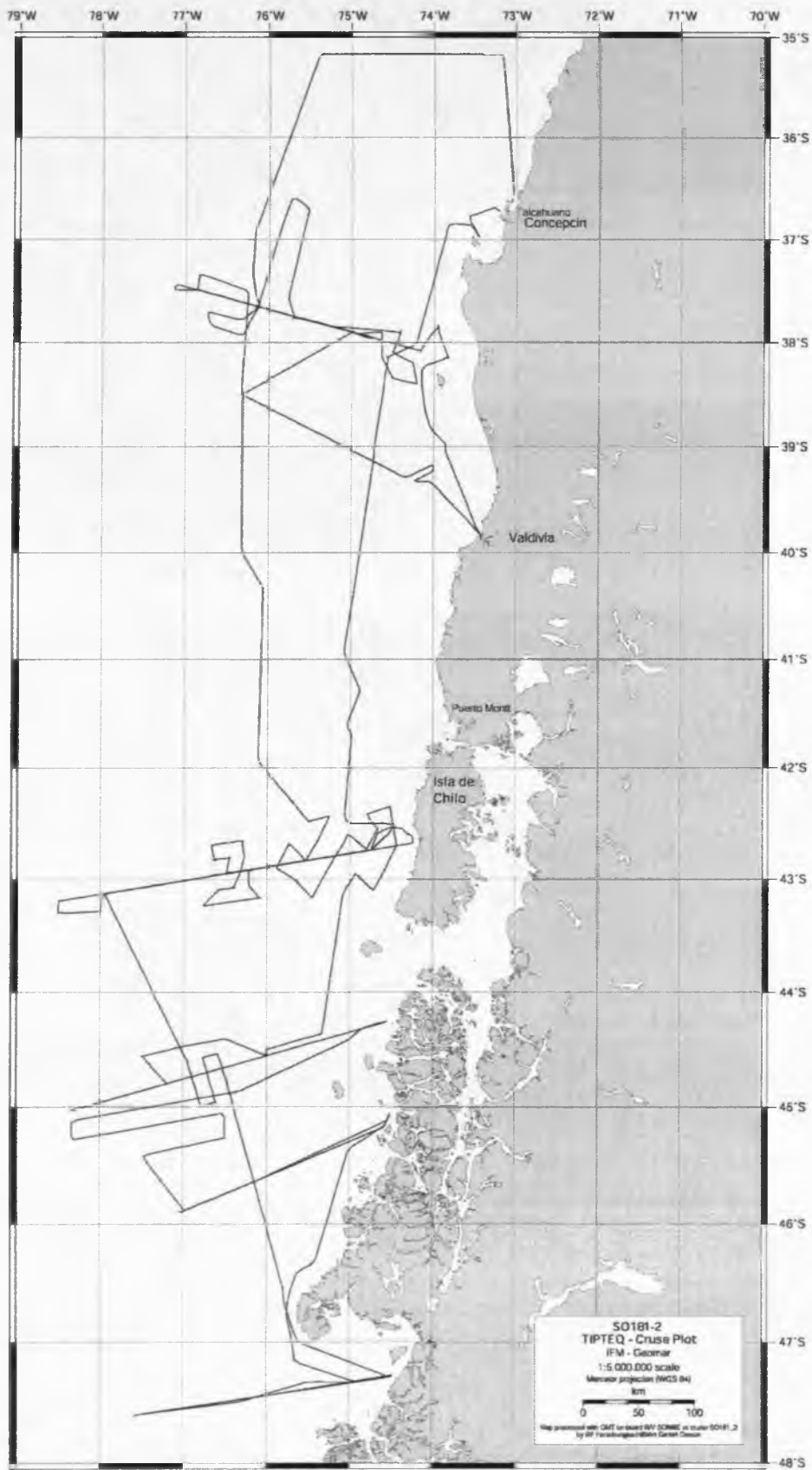


Fig. 4.3.1: Track chart of SO181-2 San Vicente – Talcahuano

5. Scientific equipment

5.1 Shipboard equipment

5.1.1 Navigation

A crucial prerequisite for all kinds of marine surveys is the precise knowledge of position information (latitude, longitude, altitude above/below a reference level). Since 1993 the global positioning system (GPS) has been commercially available and widely used for marine surveys. It operates 24 satellites in synchronous orbits, thus at least 3 satellites are visible anywhere at any moment (Seeber, 1996). The full precision of this originally military service yields positioning accuracies of a few metres. In the past its use was restricted to military forces and inaccessible to commercial users (Blondel and Murton, 1997). Since about 2000 the full resolution has been generally available. During the cruise SO181 the operation of the differential (DGPS) option was not requested as standard precision coordinates were precise enough for the work planned.

GPS-values as well as most other cruise parameters are continuously stored in the navigation database, and are distributed via the DVS- ("data distribution system") on the ship's network.

5.1.2 Simrad EM120 swathmapping bathymetry system

The EM120 system is a multibeam echosounder (with 191 beams) providing accurate bathymetric mapping up to depths exceeding 11000 m. This system is composed of two transducer arrays fixed on the hull of the ship, which send successive frequency coded acoustic signals (11.25 to 12.6 kHz). Data acquisition is based on successive emission-reception cycles of this signal. The emission beam is 150° wide across track, and 2° along track direction (Fig. 5.1.2.1). The reception is obtained from 191 overlapping beams, with widths of 2° across track and 20° along it (Fig. 5.1.2.1). The beam spacing can be defined as equidistant or equiangular, and the maximum seafloor coverage may be set to a fixed value. The echoes from the intersection area (2°x2°) between transmission and reception patterns (Fig. 5.1.2.1), produce a signal from which depth and reflectivity are extracted.

For depth measurements, 191 isolated depth values are obtained perpendicular to the track for each signal. Using the 2-way-travel-time and the beam angle known for each beam, and taking into account the ray bending due to refraction in the water column by sound speed variations, depth is estimated for each beam. A combination of phase (for the central beams) and amplitude (lateral beams) is used to provide a measurement accuracy practically independent of the beam pointing angle. The raw depth data need then to be processed to obtain depth-contour maps. In the first step, the data are merged with navigation files to compute their geographic position, and the depth values are plotted on a regular grid to obtain a digital terrain model (DTM). In the last stage, the grid is interpolated, and finally smoothed to obtain a better graphic representation.

Together with depth measurements, the acoustic signal is sampled every 3.2ms and processed to obtain a cartographic representation, commonly named mosaic, where grey levels are representative of backscatter amplitudes. These data provide thus information on the sea-floor nature and texture: it can be simply said that a smooth and soft seabed will backscatter little energy, whereas a rough and hard relief will return a stronger echo.

The EM120 swathmapping system was used continuously during all legs. Bathymetric data were processed routinely onboard during the survey, using the NEPTUNE software from Simrad, available on board and the academic software MB-System from Lamont-Doherty Earth Observatory. Data collected during all legs were merged and maps were generated.

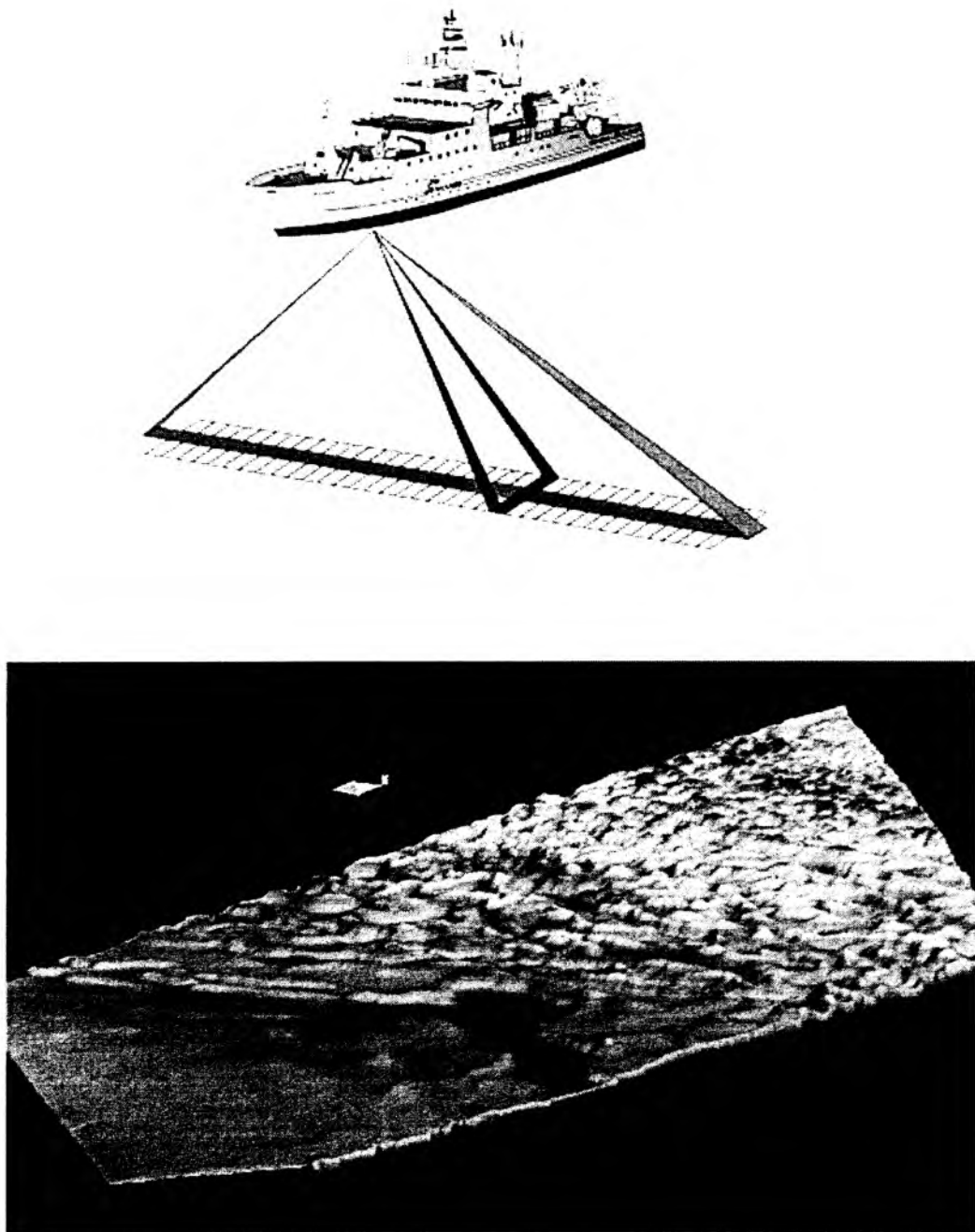


Figure 5.1.2.1: Acquisition method for bathymetric and backscatter data from the Simrad EM120 system (crossed beams technique).

5.1.3 Parasound

The PARASOUND system works both as a low-frequency sediment echosounder and as a high-frequency narrow beam sounder to determine the water depth. It utilizes the parametric effect, which produces additional frequencies through nonlinear acoustic interaction of finite amplitude waves. If two sound waves of similar frequencies (here 18 kHz and e.g. 22 kHz) are emitted

simultaneously, a signal of the difference frequency (e.g. 4 kHz) is generated for sufficiently high primary amplitudes. The new component travels within the emission cone of the original high frequency waves, which are limited to an angle of only 4° for the equipment used. Therefore, the footprint size of 7% of the water depth is much smaller than for conventional systems and both vertical and lateral resolution are significantly improved.

The PARASOUND system is permanently installed on the ship. The hull-mounted transducer array has 128 elements within an area of 1 m^2 . It requires up to 70 kW of electric power due to the low degree of efficiency of the parametric effect. In 2 electronic cabinets, beam formation, signal generation and the separation of the primary (18, 22 kHz) and secondary frequencies (4 kHz) is carried out. Using the third electronic cabinet located in the echosounder control room, the system is operated on a 24 hour watch schedule.

Since the two-way travel time in the deep sea is long compared to the length of the reception window of up to 266 ms, the PARASOUND System sends out a burst of pulses at 400 ms intervals, until the first echo returns. The coverage in this discontinuous mode is dependent on the water depth and also produces non-equidistant shot distances between bursts.

The main tasks of the operators are system and quality control and to adjust the start of the reception window. Because of the limited penetration of the echosounding signal into the sediment, only a short time window close to the sea floor is recorded.

In addition to the analogue recording features with the b/w DESO 25 device, the PARASOUND System is equipped with the digital data acquisition system ParaDigMA, developed at the University of Bremen. The data is stored on removable hard disks using the standard, industry-compatible SEG-Y-format. The 486-processor based PC allows for buffering, transfer and storage of the digital seismograms at very high repetition rates. Of the emitted series of pulses, usually only every second pulse can be digitized and stored, resulting in recording intervals of 800 ms for a given pulse sequence. The seismograms were sampled at a frequency of 40 kHz, with a typical registration length of 266 ms for a depth window of $\sim 200 \text{ m}$. The source signal was a band limited, 2-6 kHz sinusoidal wavelet with a dominant frequency of 4 kHz and duration of 1 period (250 μs total length).

During the cruises SO181 the Parasound signals were visually inspected, but only recorded in digital form along the high resolution seismic reflection lines of leg 1b.

5.1.4 CTD data

The CTD rosette onboard RV Sonne was deployed during cruise SO181-1a and during SO181-2 to measure physical oceanographic parameters (Fig. 5.1.4.1.). The CTD station was run to a water depth of 4000 m at a velocity of 1 m/s measuring the sound speed in-situ continuously. The sound velocity profiles are shown in Figure 5.1.4.2.

Accurate sound velocity profiles are needed for calibration of the water sound velocity to transfer the echo times of the bathymetric swathmapping into water depth. The velocity profiles exhibit the typical curvature with similar characteristics of measurements conducted elsewhere. Sound velocity in shallow water shows a very high negative gradient in the upper 500 m of the water column, decreasing to approx. 1480 m/s. Below 500 m water depth, the sound velocity remains nearly constant down to $\sim 1000 \text{ m}$. Below, the deeper water column is characterized by an increase in sound velocity and a positive well defined gradient. A second CTD taken during SO181-1a provided nearly the same velocity-depth profile.

During Leg 2 of S0181 another CTD measurement was made on 20.01.05. these results are shown in the lower panel of Figure 5.1.4.2. they compare well with those shown in the top panel.

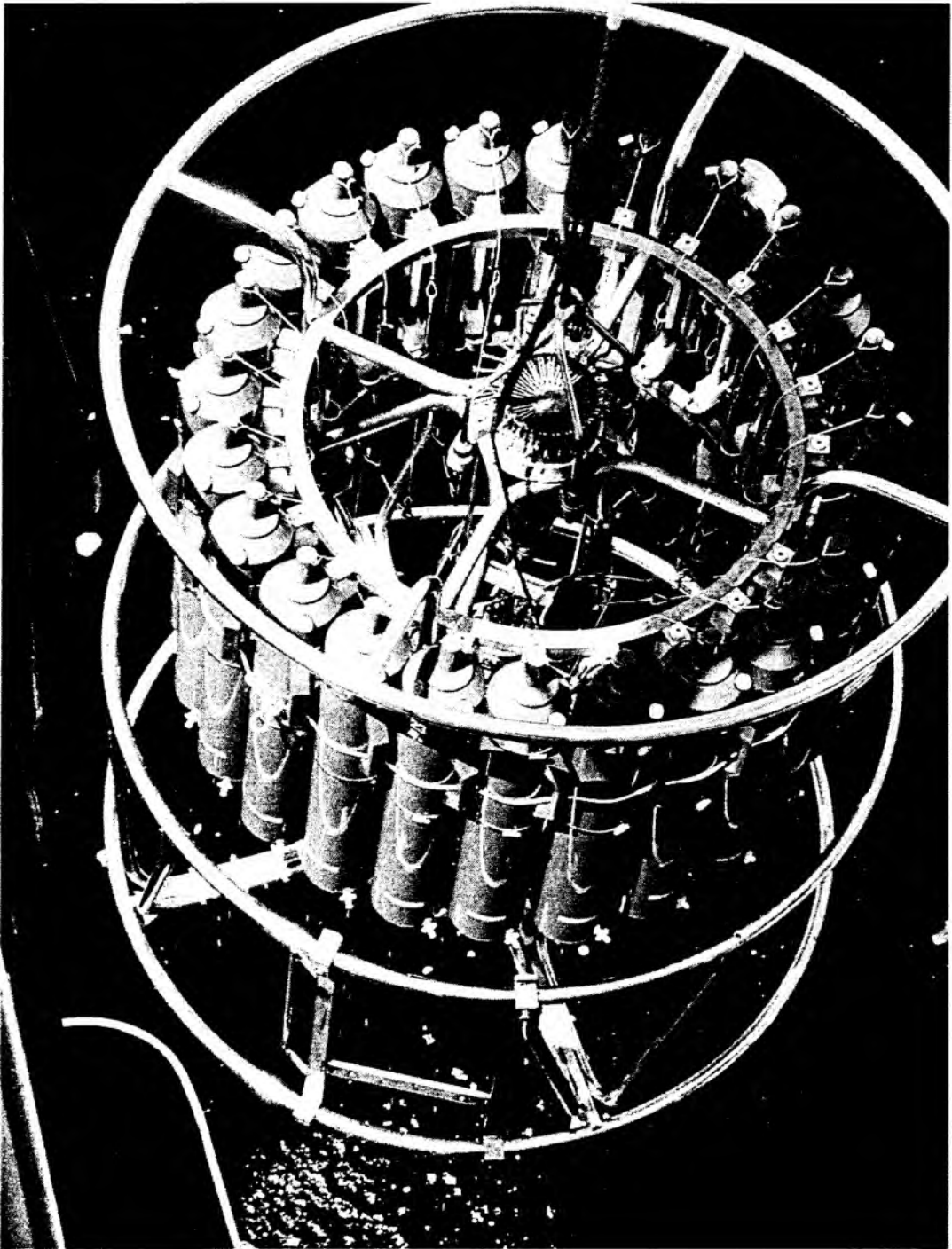


Figure 5.1.4.1: RV SONNE's onboard CTD rosette upon deployment.

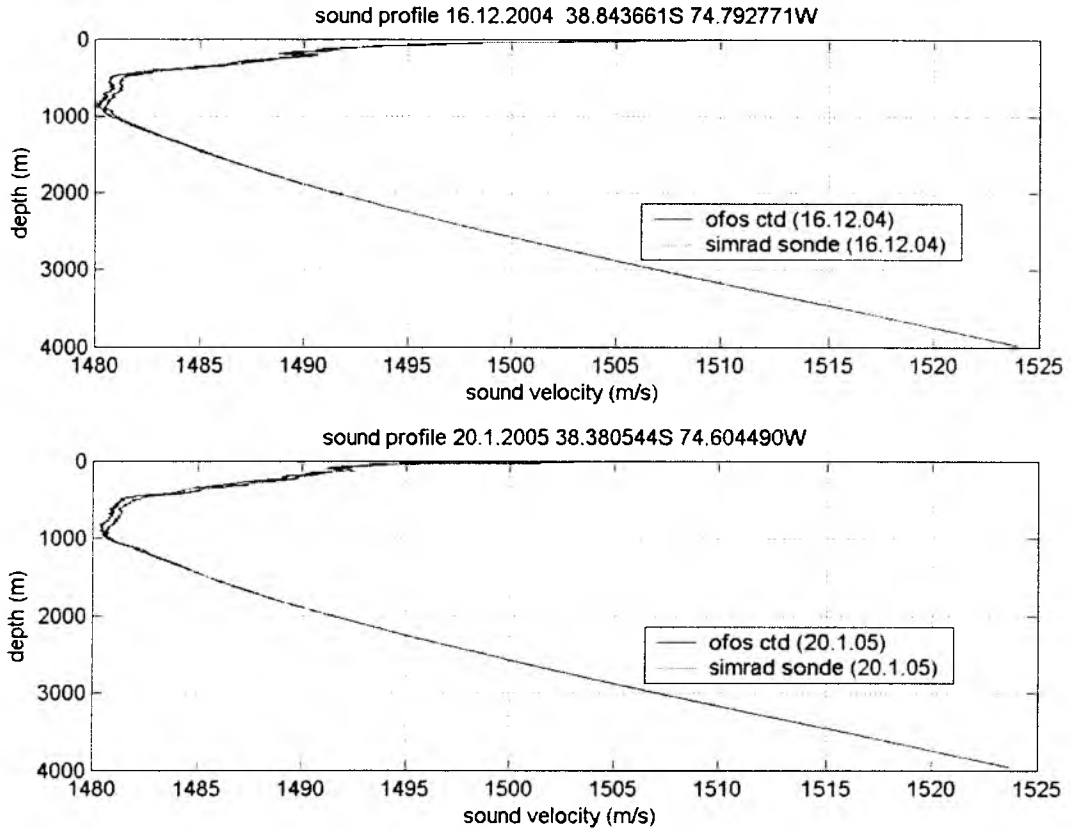


Figure 5.1.4.2: Sound velocity profiles obtained from CTD measurement during SO181-1a (top panel) and SO181-2 (bottom panel).

5.2 Hard and Software

5.2.1 Computer facilities for bathymetry, magnetic, and seismic data processing

The experiments and investigations during SO181 required special computing facilities in addition to the existing shipboard systems. For programming of ocean bottom stations, processing, analysis and interpretation of seismic, bathymetric and magnetic data, several workstations and PCs were installed by the wide angle and seismology groups of IFM-GEOMAR. Due to the large amount of data transfer IFM-GEOMAR installed two workstation clusters onboard comprising the following systems:

1	"moho" (server)	SUN Sparc 20	2 CPU, 192 MB memory	20 GB disks, DAT, DLT, CD	Sun Solaris 2.8
2	"devonia"	SUN Ultra 60	2 CPU 1 GB memory	150 GB disks, DLT, DAT, CD	Sun Solaris 2.6
3	"crimea"	AMD Duron 700 MHz	1 CPU, 128 MB memory	150 GB disks, 6x PCMCIA	WinXP/ Linux

1	"aurinacien" (server)	SUN Ultra 1	2 CPU 768 MB memory	150 GB disks, CD	Sun Solaris 2.6
2	"hotblack"	SUN Ultra 1	1 CPU, 320 MB memory	4 GB disks, DLT, DAT	Sun Solaris 2.8
3	"roorise"	AMD Athlon 1.8 GHz	1 CPU, 512 MB memory	80 GB disks, DVD	WinXP/ Linux
4	"pinta"	AMD Duron 700 MHz	1 CPU, 128 MB memory	150 GB disks, 6x PCMCIA	WinXP/ Linux

For seismic modelling two Macintosh computers were installed:

- 1 PowerMacintosh G3/300 MHz
- 2 PowerBook G4

In addition to these computers, two X-Windows-Terminal NCD-15r and several laptops were used. For plotting and printing one Kyocera Postscript Laserprinter (papersize A3 and A4) as well as the shipboard color plotters were available.

The raw and processed data were stored onto two 8 harddrive-systems (Raid "STOR3 Triple Stor"/Oxygen v3.34A) with a total capacity of 1080 GB, each connected to the "devonia" and to the "aurinacien". An additional backup device is installed within the Raid system to restore lost data after a possible harddisk failure. For external backup three Tandberg DLT 8000 tape drives and two DAT tape drives were used.

To preserve power supply in case of a ships internal power breakdown, the Raid system, harddrives and "devonia" were secured by an UPS (uninterruptible power supply) to maintain network operation and to avoid a complete system crash, which could lead to a loss of data.

The workstation clusters were placed in the "Magnetik-" and "Reinlabor" where they were set up according to a "client-server" model, with "moho" and "aurinacien", respectively, being the server. One Macintosh computer was located in the "Chemie (Nass)-Labor", the other in the "Reinlabor", both being connected to the ships network. All important file systems from the main server at IFM-GEOMAR were duplicated onto the two servers "moho" and "aurinacien". Using NFS-, NIS-, and automounter services the computing environment was identical to that at IFM-GEOMAR, so every user found his/her familiar user interface. The convenience of network mounted file systems has to be paid for with a heavy network load, particularly during transfer of OBH-data from the PC hard disks to the RAID system. This required a high-performance network, which was accomplished by a switched twisted-pair ethernet. A 12-port ethernet switching-hub (3COM-SuperstackII 1000) with an uplink connection of 100 Mbps to the servers and dedicated 10 Mbps ports for the client workstations maintained the necessary network performance. In order to keep the shipboard network undisturbed by the workstation cluster, but to allow for communication between them, the servers "moho" and "aurinacien" were equipped with two network interfaces and served as router. This provided the additional benefit of a simplified network configuration. Considerable setup work was dedicated to "moho" and "aurinacien", while the other workstations used the same IP-addresses and network configuration as at IFM-GEOMAR. This network setup showed a reliable and stable performance, and no breakdowns were observed.

5.2.2 Seismic Processing of OBH/OBS wide-angle data

The processing scheme

The OBH/S data recorded in continuous mode on the MLS, MBS and MES units have to be converted into standard trace-based SEG-Y format for further processing. The necessary program structure was mainly taken from the existing REFTEK routines and modified for the OBH requirements and IFM-GEOMAR's hardware platforms.

The flow chart shown in Figure 5.2.2.1 illustrates the processing scheme applied to the raw data. A detailed description of the main programs follows below:

send2pas

For the PC-cards used with the MBS and MLS recorders, data expansion and format conversion into REFTEK data format is performed using a DOS/Windows based PC. The program send2pas reads data from the flashcards used during recording. Decompressed data are written onto the PC's hard disk using PASSCAL data format. Either 16 or 32 bit storage is available. After ftp transmission to a SUN workstation, ref2segy and all other software can be used to handle and process the data files and store them as SEG-Y traces.

While processing the MLS recordings many time slips of one sampling interval were detected by the send2pas software, typically at a rate of one time slip every 1-2 hours. The time slips are caused by mismatch of the actual sampling rate of the MLS recorder compared to the desired sampling rate. This mismatch arises because the clock rate of the crystal oscillator in

the MLS recorder is temperature dependent (Klaus Schleisiek, SEND GmbH, pers. comm.). The temperature dependence is known and corrected for in the determination of the system time, but for performance reasons the sampling pulses are directly generated from the oscillator signal without any time correction. The send2pas routine detects when the accumulated inaccuracies of the sample rate cause an effective timing error of one sample, but it only reports and does not correct the “time slip”.

The resulting total time error was on average 200 to 400 ms for the wide-angle profiles and up to several tens of seconds for the seismology network, showing clearly the necessity of a special time slip correction for the MLS data. A correction for the time slips is applied with the “unslip” routine.

ref2segy

The ref2segy program converts the output of send2pas to a pseudo SEG-Y trace consisting of one header and a continuous data trace containing all samples, as used by the PASSCAL suite of seismic utility programs. For each channel (normally pressure, vertical velocity, and velocity along two mutually perpendicular horizontal directions for OBS; pressure for OBH) one file is created with the name derived from the start time, the serial number of the Methusalem system, and the channel number. The file size of the pseudo-SEG-Y file is directly related to the recording time. For instance, a recording time of one hour sampled at 200 Hz (16 Bit) will produce a file size of 1.44 MB per channel. A record with two channels and a recording time of two days will produce a total data volume of 70 MB.

send2x

The program library SEND2X converts the compressed recordings of GEOLON-MES into different formats. Send2x is available for the operating system Linux. The current version allows the conversion of raw data into a binary file, an audio-wave file, or into the SEG-Y format if an appropriate shot file is available. Furthermore, the log data includes the parameter settings such as the sample rate and the amplifier gain for each channel. The internal temperature and humidity as well as the battery voltage will be stored together with the recorded seismic data on the internal disk.

- **meslog**

All control, status, and identification information of the current experiment are stored on GEOLON's harddisk. Furthermore, the log data includes the parameter settings such as the sample rate and the amplifier gain for each channel. Normally the program meslog displays these data on the screen. Through the assignment of the standard output to the harddisk on the connected external PC, these data can alternatively be stored in a text-file.

- **mescopy**

Via an IEEE-1394 Firewire interface the raw data is copied to a Linux-PC.

- **mesread**

The program mesread converts the raw and compressed data to a s2x-format and provides the extraction of the engineering data out of the recorded data stream.

- **seg-ywrite**

seg-ywrite converts the data stored in s2x format to standard SEG-Y format. The option --reftek is used for a pseudo SEG-Y output format.

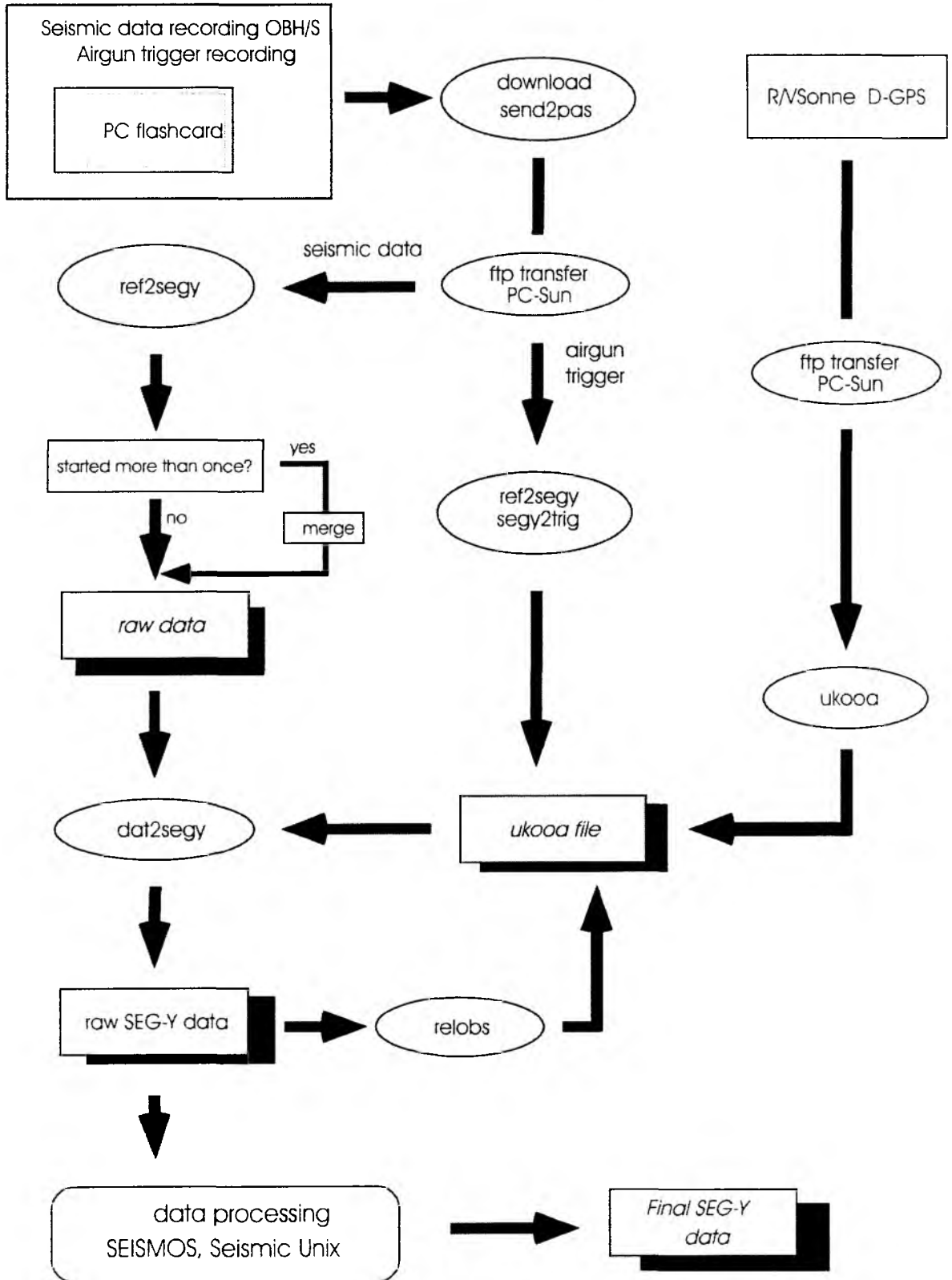


Figure 5.2.2.1: Processing flow of seismic refraction data (OBS/OBH) from raw data to SEG-Y records.

merge

If an error occurs during the download process, the ref2segy program has to be restarted. This may lead to several data files with different start times. Merging these files into a single file is performed by the merge program. Gaps between the last sample and the first sample of the consecutive data traces are filled with zeros. Overlapping parts are cut out.

pql

pql (Passcal Quick Look) is a simple display program for continuous seismic data. Its interactive zooming capability allows a rapid inspection of data quality.

segy2trig

The trigger signal, provided by the airgun control system, is recorded on an additional MBS unit during the shooting period. The trigger data are treated similarly to regular seismic data and downloaded to the hard disk via the send2pas and ref2segy programs. Then, the segy2trig program detects the shot times in the data stream by identifying the trigger signal through a given slope steepness, duration and threshold of the trigger pulse. The output is an ASCII table consisting of the shot number and the shot time. Accuracy of the shot time is one of the most crucial matters in seismic wide-angle work, and must be reproduced with a precision of a few ms. Due to this demand the shot times have to be corrected with the shift of the internal recorder clock. Additionally, the trigger file contains the profile number, the start/end time of the profile and the trigger recording. The shot times are part of the ukooa file, which links them with the source coordinates. Since a time shift between the external trigger pulse (Ofos) and the actual airgun firing was observed in the seismic data, a delay of 135 ms was incorporated when determining the shot times (see trigger description in Chapter 5.3 for more details).

ukooa

The ukooa program is used to establish the geometric database by calculating the positions of sources at any given shot time and offset from the ship. The source is placed on the ship track using simple degree/meter conversions and then written to a file in UKOOA-P84/1 format. Corrections for offsets between antenna and airguns as well as consistency checks are included. This file will be used when creating a SEG-Y section via the dat2segy program. The program requires the trigger file to contain the shot times, the ship's navigation, and a Parameter file containing information for the UKOOA file header as basic input information.

dat2segy

The dat2segy program produces standard SEG-Y records either in a 16 or 32 bit integer format by cutting the single SEG-Y trace (the ref2segy output) into traces with a defined time length based on the geometry and shooting time information in the ukooa file. In addition, the user can set several parameters for controlling the output. These parameters are information about the profile and the receiver station, number of shots to be used, trace length, time offset of the trace and reduction velocity (to determine the time of the first sample within a record). Also the clock drift of the recorder (skew) is taken into account and corrected for. For the MLS data the total time error resulting from the observed time slips described above was subtracted from the clock drift value. The final SEG-Y format consists of the file header followed by the traces. Each trace is built up by a trace header followed by the data samples. The output of the dat2segy program can be used as input for further processing with GEOSYS, SEISMOS or Seismic Unix (SU).

relobs

Because of drifting of the OBH and OBS instruments during deployment and inaccuracies in the ship's GPS navigation system, the OBH positions may be mislocated by up to several 100 m. Since this error leads to asymmetry and incorrect traveltimes in the record section, it has to be corrected. This is accomplished with the program *relobs*.

For input, the assumed OBH location, shot locations and the picked traveltimes of the direct wave near to its apex are needed. To simplify the picking a static correction with a hyperbolic equation was performed to flatten the direct wave. This yields a much more coherent direct arrival which would normally suffer from strong spatial aliasing in the uncorrected section making it difficult to track. By shifting the OBH position, *relobs* minimizes the deviation between computed and real travel times using a least mean square fitting algorithm (assuming a constant water velocity). The source offset, i.e. the distance from the research vessel's GPS position to the center of the airgun array, was determined to 100 m.

Besides these main programs for the regular processing sometimes additional features are needed for special handling of the raw data:

divide

The program *divide* cuts the raw data stream into traces of a given length without offset and time information, storing the output in SEG-Y format. The routine is useful for a quick scan of the raw data or if a timing error has occurred.

segynhdr

The routine *segynhdr* prints all the header values of the raw data on the screen.

segyshift

Segyshift modifies the time of the first sample, allowing the whole raw data trace to be shifted by a given value. This is very useful when shifting the time base from Middle European Time to Greenwich Mean Time or any local time. Because of recording problems, the data sometimes show a constant time shift, which can be corrected with *segyshift*, too.

castout

The program *castout* allows the user to remove a specified time window from the raw data stream. When the shooting window is much smaller than the recording time, one can reduce the data volume by cutting out only the useful information. This will reduce the required disk space.

OBH/OBS data analysis and processing with source signals of 64 l G-Gun Cluster

Raw data: As an example, the record section of OBH89 for profile 06 after crude frequency filtering with SU software is shown in Figure 5.2.2.2 (a). For the analysis, the offset range between 7-16 km west of the instrument is presented in detail.

Frequency filter analysis: To determine the frequencies of the seismic energy, filter panels with narrow frequency band passes for the offset range of 7-16 km are shown in Figure 5.2.2.3. In the lower section of the figure the amplitude spectra of the corresponding panels are appended. The amplitude spectra of the used Ormsby frequency filter operators are

characterized by linear slopes. The filter is described by four corner frequencies, i.e. lower stop/pass band boundary and upper pass/stop boundary.

The main energy of the phase between 4 and 4.5 s is between 3-43 Hz and for the direct wave it reaches up to over 70 Hz. As a broad frequency range is contained in the data, time and offset dependent filtering was applied (see below).

Deconvolution analysis: To improve the temporal resolution of the seismic data a deconvolution is applied to compress the basic seismic wavelet. The recorded wavelet has many components, including the source signature, recording filter, and hydrophone/geophone response. Ideally, deconvolution should compress the wavelet components, leaving only the earth's reflectivity in the seismic trace.

We applied Wiener deconvolution in successive trace segments, based on the following assumptions:

1. The earth's reflectivity is 'white'.
2. The wavelet shows the minimum-delay phase behavior.

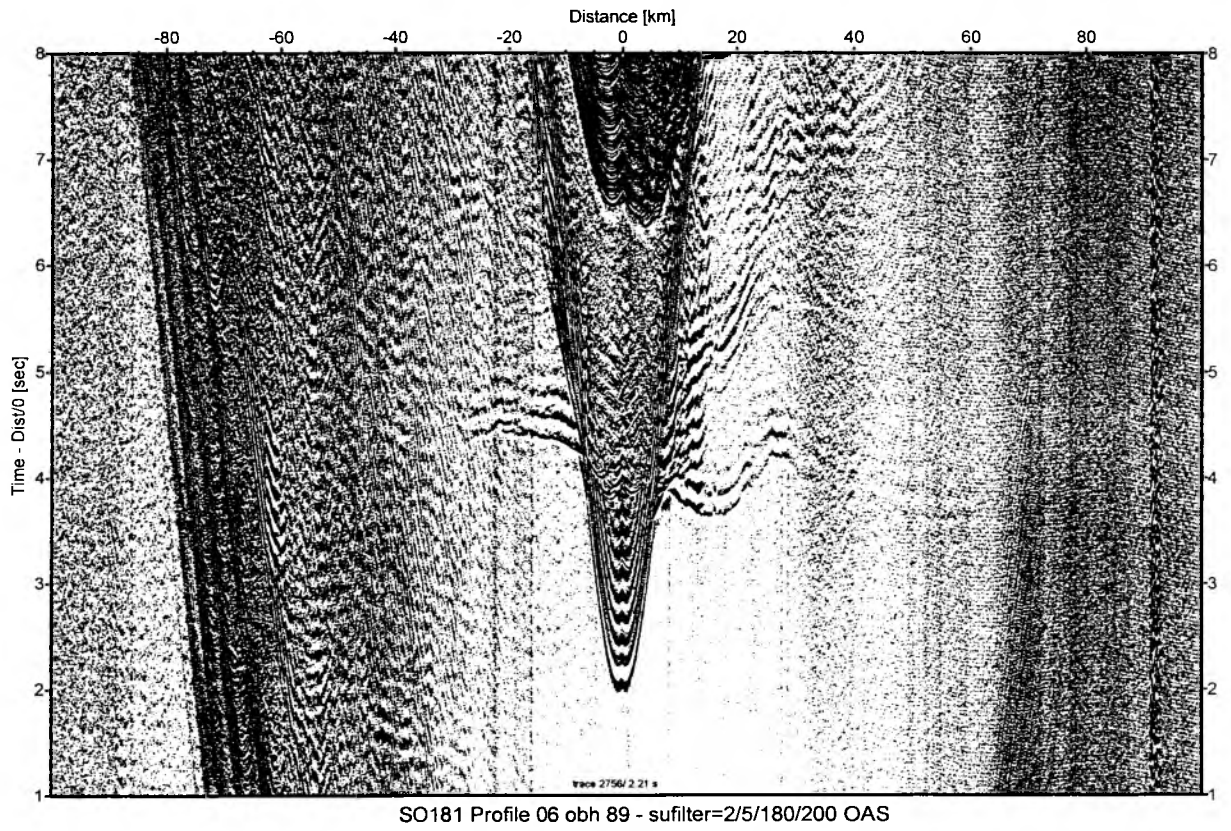
As in this wide-angle data the amplitude spectra of the seismic traces vary with time and offset (e.g. reflected refracted PP phases and reflected PS and SS phases), the deconvolution must be able to follow these time and offset variations. To improve especially the spatial resolution of the seismic data a multi-trace deconvolution also called rollalong deconvolution which uses autocorrelograms averaged over a number of traces is performed to compress the basic seismic wavelet. Here, each trace is divided into 3-s data gates with 1-s overlaps, in which time invariant deconvolution operators are computed from the average autocorrelation function of 51 traces. The operator is recalculated for every trace in each data segment and applied. The overall deconvolved trace results from a weighted merging of the independently deconvolved gates.

Input for the deconvolution process is raw data. As several recordings were influenced by a DC shift, a 1-3-Hz high-pass minimum delay Kaiser frequency filter with 60 dB attenuation between the pass and reject zone was applied prior to deconvolution in order to centre the amplitudes around zero.

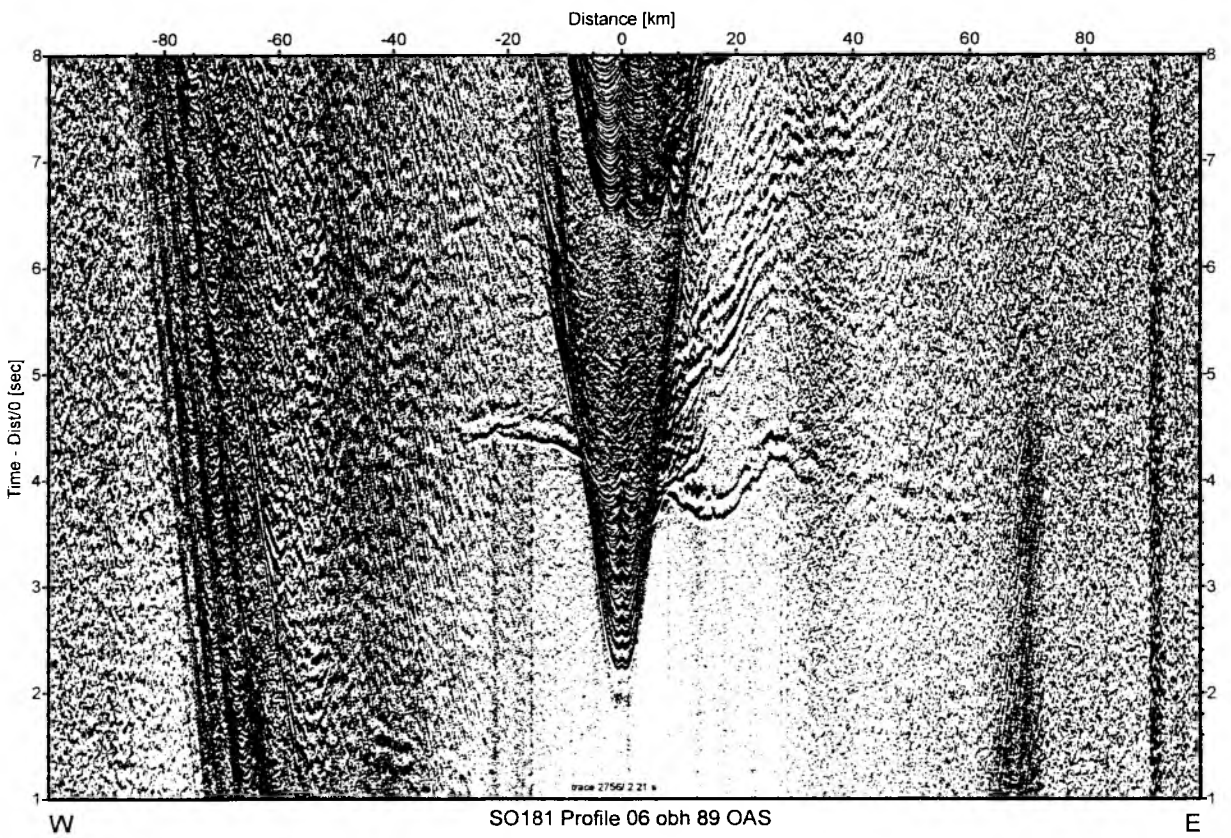
The deconvolution test panels are shown in Figures 5.2.2.4 for the offset ranges 7-16 km. In the lower section of the figure the autocorrelation function is appended. Constant operator lengths of 400 ms and 800 ms (predictive lag excluded) with a variation of the prediction lag from 4 to 240 ms are displayed for a multi-trace deconvolution (average=51).

The undeconvolved data in the leftmost panel of Figure 5.2.2.4 show a strong energy of up to 400 ms behind the zero lag. The best compromise between temporal resolution and signal-to-noise ratio is obtained for an operator length of 520 ms including a predictive length of 120 ms which was chosen for the processing of the data sets of this cruise.

After deconvolution an offset- and time-variant Ormsby filter with zero-phase characteristic was applied. As the seafloor depth changes along the seismic lines, each trace was statically corrected to a fixed seafloor travel time of 11 s based on the water depth before filtering. This information is available in the trace headers. After this filter was applied, the data were shifted back to their original travel times.



(a)



(b)

Figure 5.2.2.2: Record sections of OBH89, profile 06: (a) after crude frequency filtering, (b) after deconvolution and time- and offset-dependent frequency filtering

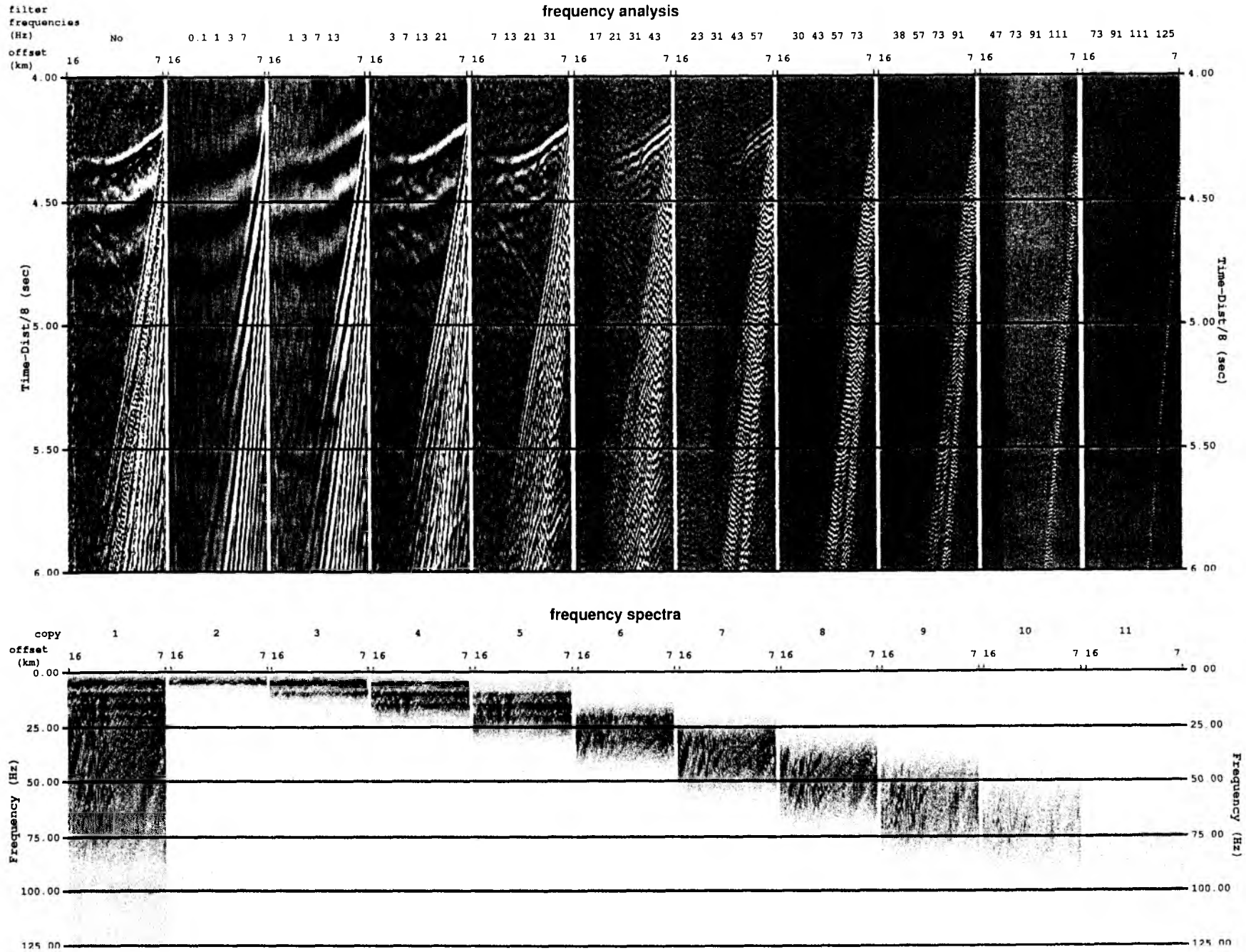


Figure 5.2.2.3: Frequency analysis from record section obh 89 for offset range 7-16 km, Profile 06.

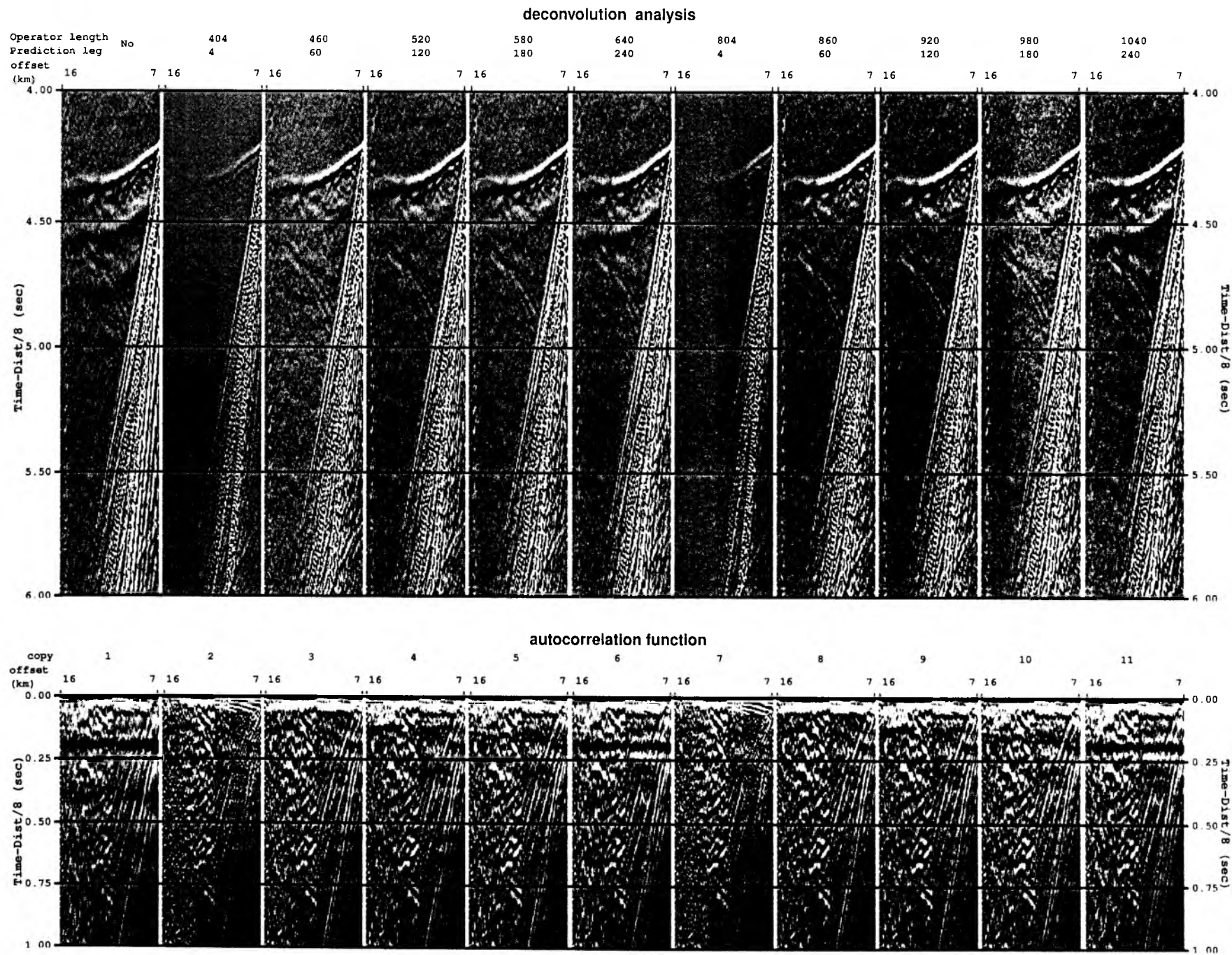


Figure 5.2.2.4: Deconvolution test with autokorrelation functions from record section obh 89 for offset range 7-16 km, Profile 06.

Processed data: Comparison of the preprocessed data in Figure 5.2.2.2 (b) to the unprocessed data in Figure 5.2.2.2 (a) shows a clear compression of the wavelet signal and an increase in signal-to-noise ratio, especially in the far offset range. For the picking of events and model building by raytracing both sections were used to keep all available seismic information.

Final processing sequence

- Input: SEG-Y-data, 4 ms or 5ms sampling rate with complete geometry information.
- Tapering the first 0.5 s to zero to reduce the response of the debias filter operator.
- Kaiser highpass (debias).
- Gated Wiener deconvolution: gate length 3 s, overlap 1 s, length of merge region 1 s, operator length 520 ms (prediction interval included), prediction interval 120 ms.
- Static correction to a fixed seafloor traveltime of 11 s.
- Time and offset-dependent Ormsby frequency filter.

On time-shifted traces with a reduced time scale of 6 km/s the following filter parameters were used:

lower stop/pass	upper pass/stop (Hz)	offset(m)	beginfull(s)	endfull(s)
3/5	65/85	0	0	12.8
		8000	0	12.6
		48000	0	0
2/4	45/60	0	13.7	14.3
		8800	13.5	14.4
		13200	13.0	13.9
		52000	2.0	4.7
		107000	0.5	1.0
1/3	30/40	0	15.3	16.8
		11700	15.1	16.6
		19200	14.8	16.3
		61700	7.0	10.1
		114000	2.0	3.0
1/3	20/30	152000	1.5	2.4
		0	19.0	trace length
		20000	18.4	trace length
		130000	3.5	trace length

• **Data archiving**

Data recorded with the MBS/MLS recorder on flash discs were transferred via a PC to a SUN workstation. On the workstation they were transformed into a so-called PSEUDO-SEG-Y format.

After navigation data had been merged and SEG-Y formatted traces with the appropriate header words had been created, the data were also archived. Finally, a third set was stored and archived after the shipboard processing, as described above, had been applied. All final processed SEG-Y data were archived on tapes.

• **Data exchange**

For the exchange of the OBH/OBS data, the SEG-Y-format on disk with a Sun tar-format was chosen. The raw segy data is in Integer2 format with trailer bytes between the record structure

of SEGYY. The processed data is in IBM-floating point without trailer bytes between the records.

For UTM transformation into Cartesian coordinates use: WGS84 spheroid, central meridian 76 0. 0. W, southern hemisphere.

The following is the definition of the segy trace header for the IFM-GEOMAR OBS wide-angle reflection data. The extension of the standard SEGYY header from byte 181 to 240 is a layout in order to process the data on the GEOSYS/SEISMOS software system. Reading bytes directly into this header will allow access to all of the fields.

BytePos	Bytes	Information	Comments (note: not all headers available in processed data)
1-8	(2x4)	lineSeq, reelSeq;	/* Sequence numbers within line and reel, resp.*/ /* here station and shot number Def: 1, 1 */
9-12	(4)	profNumber;	/* Original field record number */ /* Here profile number */
13-16	(4)	traceNumber;	/* Trace number within the original field record.*/ /* Here station (receiver) Number */
17-20	(4)	energySourcePt;	/* Energy source (shot) point numbe */ /* Def: 0 */
21-24	(4)	cdpEns;	/* CDP ensemble number: shot number */ /* Def: 0 */
25-28	(4)	traceInEnsemble;	/* Trace number within CDP ensemble */ /* Here azimuth in seconds of arc for unprocessed data*/
29-30	(2)	traceID;	/* Trace identification code: 1=seismic data (Def) 4=time break 7=timing 2=dead 5=uphole 8=water break 3=dummy 6=sweep 9..., optional use */
31-34	(2x2)	vertSum, horSum;	/* Def: 1, 1 */
35-36	(2)	dataUse;	/* 1=production (Def), 2=test */
37-40	(4)	sourceToRecDist;	/* Distance in (m) */
41-44	(4)	recElevation;	/* Elevation in (m), Def: 0 */
45-48	(4)	sourceSurfaceElevation;	/* Def: 0 (m) */
49-52	(4)	sourceDepth;	/* Def: 0 (m) */
53-60	(2x4)	datumElevRec, datumElemSource;	/* Def: 0, 0 (m) */
61-68	(2x4)	sourceWaterDepth, recWaterDepth;	/* Def: 0, 0 (m) */
69-70	(2)	elevationScale;	/* Scale elevations Def: 0 (10**0) */
71-72	(2)	coordScale;	/* Scale coordinates Def: -2, means coordinates multiplied by 10**(-2) to get real value for unprocessed data. NOTE: for processed data -100 means to divide by 100 to get the real value */
73-80	(2x4)	sourceLongOrX, sourceLatOrY;	/* Either Cartesian or geographic */
81-88	(2x4)	recLongOrX, recLatOrY;	
89-90	(2)	coordUnits;	/* 1= meter or feet; 2=sec of arc */
91-92	(2)	weatheringVelocity;	/* Def: 0 (m/s) */
93-94	(2)	subWeatheringVelocity;	/* Reduction velocity, Def: 6000 (m/s) */
95-96	(2)	sourceUpholeTime;	/* Def: 0 (ms) */
97-98	(2)	recUpholeTime;	/* Def: 0 (ms) */

```

99-102 (2x2) sourceStaticCor, recStaticCor; /* Def: 0, 0 (ms) */
103-104      (2)    totalStatic;           /* Def: 0 (ms) */
105-106      (2)    lagTimeA;              /* T(shottime) - T(first sample) */
107-108      (2)    lagTimeB;              /* Def: 0 (ms) */
109-110      (2)    delay;                  /* Def: 0 (ms) */
111-114      (2x2)  muteStart, muteEnd;    /* Def: 0, 0 (ms) */
115-116      (2)    sampleLength;          /* Number of samples in this trace */
                                           /* ( > 32767 )? = 32767
                                           set long samp_rate in 185-188 byte */
117-118      (2)    deltaSample;           /* Sampling interval in microseconds. */
119-120      (2)    gainType;              /* 1=fixed (Def), 2=binary,
                                           3=floating, 4... opt.*/
121-122      (2)    gainConst;              /* Gain of recording channel */
123-124      (2)    initialGain;           /* Gain of preamplifier in db */
125-126      (2)    correlated;            /* 1=no (Def), 2=yes */
127-130      (2x2)  sweepStart, sweepEnd;  /* min. and max. amplitude of trace */

131-132      (2)    sweepLength;           /* Here defined as
                                           fraction of second of shot time */
133-134      (29)   sweepType;             /* Source type:
                                           1=linear, 2=parabolic, 3=exponential, 4=others
                                           5=bohrhole explosive, 6=water explosive, 7=airgun (Def)
                                           or fraction of microsecond of shot time for high resolution data */

135-138      (2x2)  sweepTaperAtStart, sweepTaperAtEnd; /* Start and end of trace (ms)
                                           relative to Tred(0) */
139-140      (2)    taperType;              /* scaling factor for last two values Def: 1 (x10) */
141-144      (2x2)  aliasFreq, aliasSlope; /* Def: 0, 0 */
145-148      (2x2)  notchFreq, notchSlope; /* Def: 0, 0 */
149-152      (2x2)  lowCutFreq, hiCutFreq; /* Def: 0, 0 */
153-156      (2x2)  lowCutSlope, hiCutSlope; /* Def: 0, 0 */
157-166      (5x2)  year, day, hour,      /* Source (shot) time, the fraction of sec */
minute, second; /* is set in millisec between 131-132 byte
is set in microsec between 133-134 */

167-168      (2)    timeBasisCode;        /* 1=local, 2=GMT, 3=MET (GMT+1 hour) (Def) */
169-170      (2)    traceWeightingFactor; /* */
171-172      (2)    phoneRollPos1;        /* Component: 1=time code, 2=radial, 3=transverse
                                           4=vertical, 5=hydrophone (Def) */
173-174      (2)    phoneFirstTrace;       /* Methusalem instrument number in YYNN */
175-176      (2)    phoneLastTrace;        /* Channel number */
177-178      (2)    gapSize;               /* Source charge in cubic inches (airgun)
                                           or kg (explosives) */

179-180      (2)    taperOvertravel;       /* Def: 0=meaningless 1=up, 2=down */

/* !!! Following is extension !!! */

181-182      (2)    compNo;                /* 1=time code, 2=radial, 3=transverse
                                           4=vertical, 5=hydrophone (Def) */
183-184      (2)    samplingRate;          /* samples/sec */
185-188      (4)    numberSamples;         /* ( <= 32767 ) ? sampleLength | ( > 32767 ) */

```

189-190	(2)	shotPointNo;	
191-192	(2)	ADCCoeff;	/* Coefficient of A/D converter in mv/digit */
193-194	(2)	receiverCoeff;	/* Conversion coefficient of receiver, pascal/cm2 for hydrophone, velocity(m/s)/volt for geophone */
195-196	(2)	receiverType;	/* 1=hydrophone (Def), 2=geophone, 3...*/
197-200	(4)	lengthData;	/* Def: 0 (ms), not used here */
201-204	(4)	distance;	/* Source to receiver distance in (m) */
205-208	(4)	(float) scaleFactor;	/* Scale factor same as in <seg.y.h> Here azimuth in second of arc for processed data */
209-210	(2)	azimuth;	/* Orientation of the component in min */
211-212	(2)	eigenperiod;	/* Eigenperiod of geo- or hydrophone in (ms) */
213-216	(4)	minAmpl;	/* Min. peak amplitude within trace */
217-220	(4)	maxAmpl;	/* Max. peak amplitude within trace */
221-222	(2)	stationNo;	/* Station number */
223-224	(2)	channelNo;	/* Channel number (Default: 1) */
225-228	(4)	sourceCharge;	/* Charge in kg (explosive) or cc (airgun) */
229-230	(2)	redVelocity;	/* reduction velocity in (m/s); Def: 0 if no reduction velocity se */
231-232	(2)	timeOffset;	/* Time offset in (ms) of first sample relative to reduced source time: positive if earlier than reduced time */
233-236	(4)	redTime;	/* Reduced time in (ms) = distance/redVel */
237-238	(2)	unused2;	
239-240	(2)	instNo;	/* Methusalem instrument number */

5.2.3 Processing of earthquake data

The initial data processing of earthquake data is identical to the processing sequence for wide angle data described in Section 5.2.2 (i.e., reading of the flashcards, conversion into the PASSCAL Reftek format, and further on into a pseudo SEGY format (PASSCAL SEGY)). The routines for all above mentioned processing steps are *transfer* (DOS batch file, running *send2pas* and *FTP*) and *ref2segy*.

After conversion the raw data files are compressed and backed up on magnetic DLT tapes.

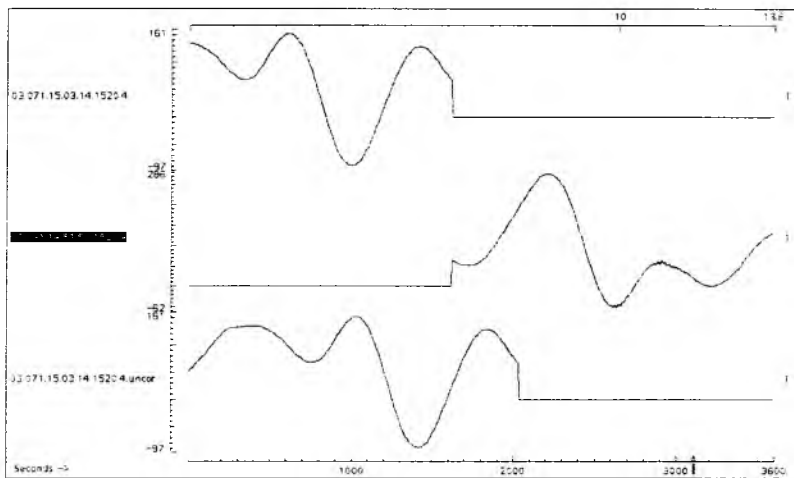


Figure 5.2.3.1: Seismogram example that shows how the unslip process works. While the uncorrected trace (bottom) does not fit to the adjacent trace (centre), the unslipped trace (top) fits exactly. Missing samples are filled up by zeros (straight lines).

The occurrence of time slips (extra or missing samples) due to a mismatch of the desired and actual sample rates (see Section 5.2.2 for a more detailed discussion of time slips) has to be corrected. The occurrence time of all time slips is read out from the SEND2PAS log and the PASSCAL error file. If multiple PASSCAL Reftek files were directly produced by *send2pas* because of large file sizes the time slips before the beginning of the record are disregarded because the start time of these files is correct (Figure 5.2.3.1). For time slips during the record a sample is added (positive time slips) or removed (negative time slips) at the appropriate time. This procedure is only approximate (a correct treatment would require resampling of the whole record, fraught with its own difficulties), and in general the apparent time of a sample can be off by up to half a sample length due to this approximation. Relative times within the same record can be off by up to one sample length if the time span straddles a time slip. The routine for time slip correction is *unslip_all.csh*.

After unslipping, the PASSCAL SEGY files have to be cut into 25 hours records with one hour overlap between adjacent records, such that each record begins at 0:00:01 (except on the first day of recording, of course). This cutting makes files sizes smaller (more manageable) and enables time corrections to be applied on a daily basis. The routine for cutting is *split_segy.pl*.

The recording period of the short term arrays stretches over New Years Eve which causes problems with the splitting routine. In the SEGY data the days are simply counted forward ignoring the change of year. We fix this bug by splitting the primary PASSCAL SEGY file at midnight of December 31, and modifying header entries for year and day of the resulting SEGY file. The routine to fix New Year problem is *fix_newyear.sh*

Another step is to merge SEGY files for days where the original PASSCAL Refttek files were split due to large file sizes. The routine for merging these files is *merge_splitfiles.sh*.

Next, the timing of each 25 hours SEGY record has to be corrected. Timing errors occur because of the slow drift of the internal clock relative to GPS time. The system time is compared with GPS time at the beginning and the end of the deployment, and a linear drift rate is inferred from the observed difference (skew). The time of each 25 hour record is corrected by applying the shift appropriate for the time 12.5 hours after the beginning of the record. The underlying assumption is that the system clock does indeed drift linearly, and that the drift over any given 24 hour period is negligible (i.e. much less than one sample length) which is usually the case. The routine for linear clock drift correction is *clock_cor.pl*.

The daily data is quality controlled using the *pql* (PASSCAL Quick Look) seismogram viewer. A quality status protocol is also prepared.

A short-term-average versus a long-term-average (STA/LTA) trigger algorithm is then applied to the data to search for seismic events. A 5-20 Hz bandpass filter must be applied prior to triggering, because of strong long-period noise around 0.2-0.5 Hz that shows up not only on broad-band sensors like DPG pressure sensors and Spahr-Webb seismometers, but also on many hydrophone channels (Figure 5.2.3.2). Because the filter cannot directly be applied to the SEGY data files, these files must be converted first into SAC format. The trigger parameters are length of the short term (s) and long term (l) time window, the mean removal window length (m), the trigger (t) and dettrigger ratio (d), minimum number of stations (S) and the network trigger time window length (M). The trigger parameters must be defined for each data set. The trigger parameters used for shipboard processing are shown in Table 5.2.3.1. For each network a continuous 24 hours data stream of all stations is visually checked to test the trigger results. Applying these trigger parameters we obtain less than 5% false triggers and lose only those events that were recorded on a few stations only, while all major events are triggered. Shots from active seismics are sorted out due to their regular occurrence. The routine for triggering is *trig_all.csh* (uses PASSCAL reft trig trigger algorithm).

Table 5.2.3.1: Trigger parameters as defined in the text to search the continuous recordings for seismic events.

Parameter	s	l	m	t	d	S	M
Value	0.5 s	60 s	500 s	2.8	0.8	4	20 s

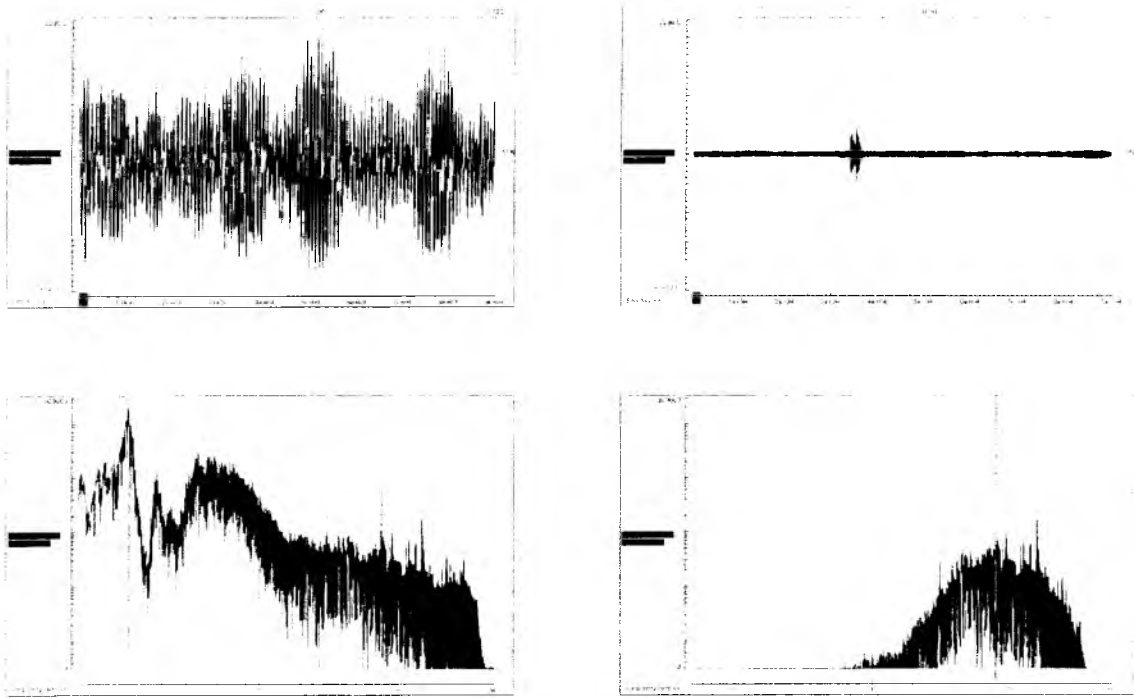


Figure 5.2.3.2: Seismogram example recorded by a hydrophone. The raw seismogram (top left) contains strong long-period noise covering all higher frequency details. The noise frequency of ~ 0.1 Hz produces a large dominating peak in the raw spectrum (bottom left). On the 5–20 Hz bandpass filtered seismogram (top right) a small earthquake can be identified, that can only be detected by the trigger routine if a prefilter is applied. The filtered seismogram spectrum (bottom right) does not contain low frequencies any more.

After finding event triggers the events are cut from the 25 hours files and stored into subdirectories, one per event. Because we are investigating local earthquakes the appropriate time window length for the events is 3 minutes, starting 60 s prior to trigger time. Usually the events have to be quality checked again, bad triggers sorted out. We do this later together with picking the first arrivals of the earthquakes. The routine for event cutting is *collate_ev.pl*.

The SEG-Y traces in the event directories are converted first into SAC, and then into SEISAN waveform format, which makes it possible to store all traces associated with an event into a single waveform file. After conversion the data are registered into the SEISAN database (Havskov and Ottemöller, 2001). The routines for conversion are *segy2sac_all.csh*, *sac2sei.sh*, *seisei.sh*, and *autoreg*.

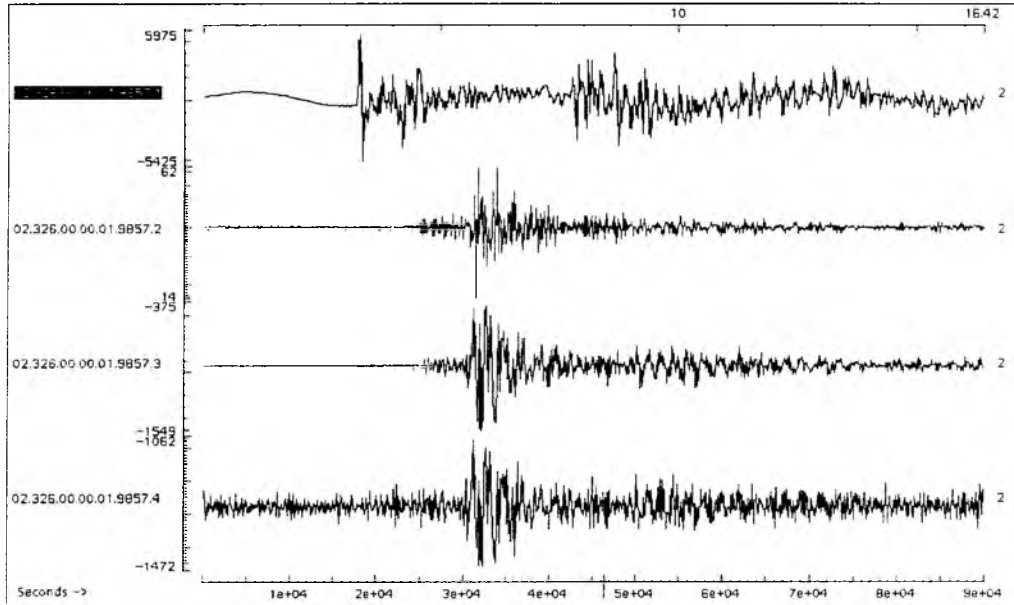


Figure 5.2.3.3: Seismogram example of an OBS that shows the water multiple on the hydrophone channel (top) at about 8 seconds (top scale). The S phase can be clearly identified on the seismometer channels (2-4) at about 5.5 seconds .

At last, P and where possible S phases are picked and events are preliminarily located with the program HYP, which employs an iterative solution to the nonlinear localisation problem (Lienert and Havskov, 1995). A 1-D velocity model is used. When picking S phases on hydrophone channels it must be carefully figured out not to pick the water multiple (Figure 5.2.3.3).

Figure 5.2.3.4 gives an overview of the earthquake data processing

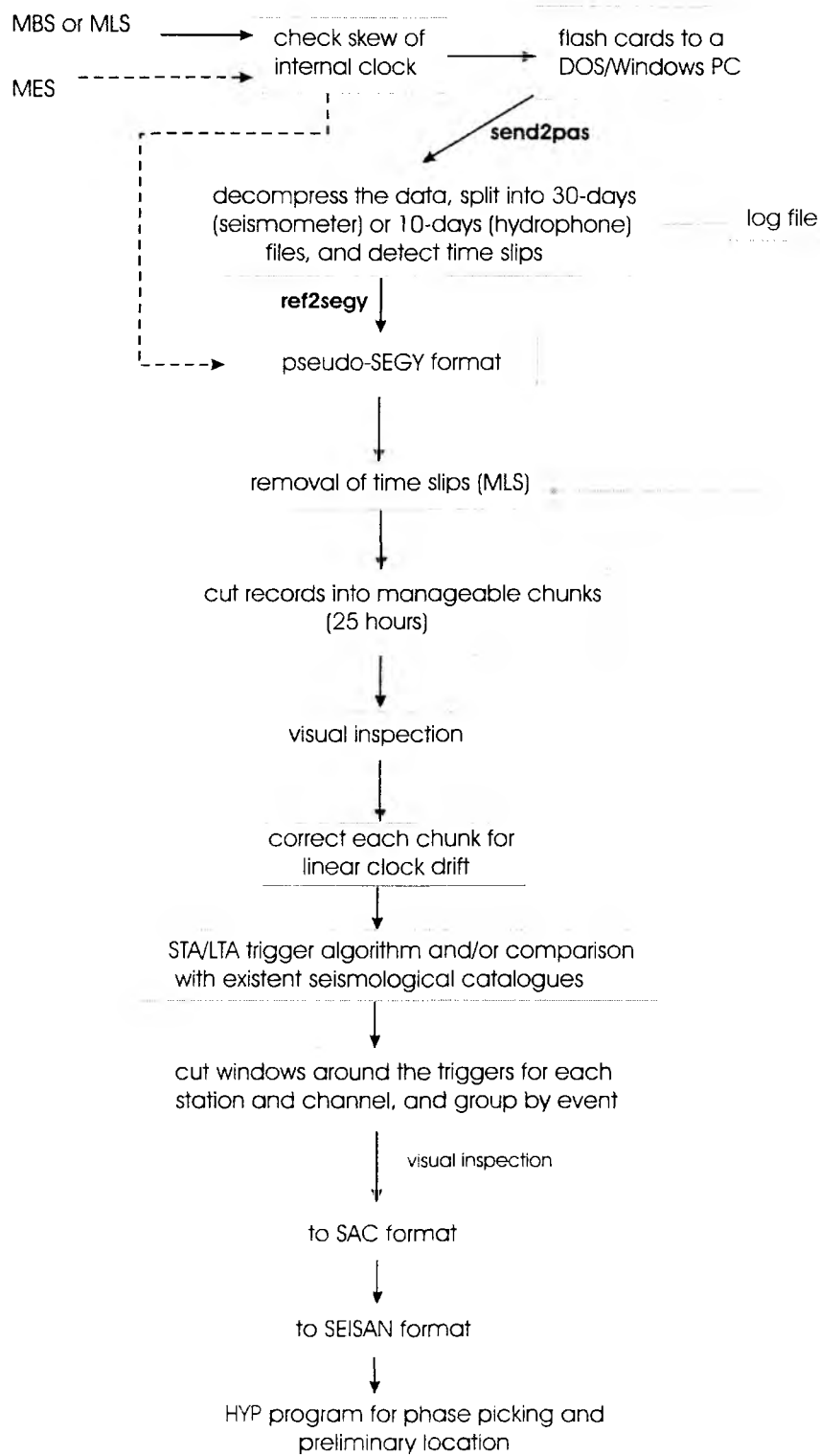


Figure 5.2.3.4: Flow diagram of the earthquake data processing.

5.3 Seismic instrumentation

The Ocean Bottom Hydrophone

The first GEOMAR Ocean Bottom Hydrophone was built in 1991 and tested at sea in January 1992. This type of instrument has proved to have a high reliability; more than 3000 successful deployments were conducted since 1991. A total of 20 OBH and 30 OBS instruments were available for SO181. Altogether 260 sites were engaged during the SO181 cruise.

The principle design and a photograph showing the instrument upon deployment are shown in Figure 5.3.1. The design is described in detail by Flueh and Bialas (1996).

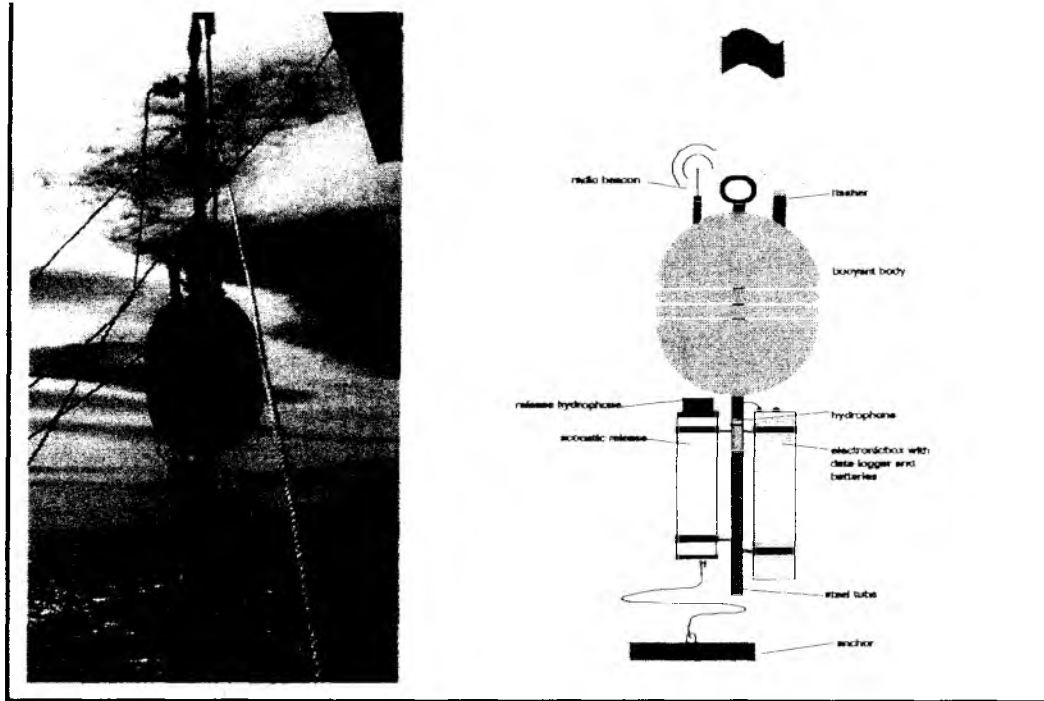


Figure 5.3.1: Principle design of the GEOMAR OBH (right panel, after Flueh and Bialas, 1996) and the instrument upon deployment (left panel).

The system components are mounted on a steel pipe which holds the buoyancy body on its top. The buoyancy is made of syntactic foam and is rated, as are all other components of the system, for a water depth of 6000 m. Attached to the buoyant body are a radio beacon, a flash light, a flag and a swimming line for retrieving from aboard the vessel. The hydrophone for the acoustic release is also mounted here. The release transponder is a model *RT661CE* or *RT861* made by *MORS Technology* which recently became *IXSea*, or alternatively a *K/MT562* made by *KUM GmbH*. Communication with the instrument is possible through the ship's transducer system, and even at maximum speed and ranges of 4 to 5 miles release and range commands are successful. For anchors, we use pieces of railway tracks weighing about 40 kg each. The anchors are suspended 2 to 3 m below the instrument. The sensor is an *E-2PD*

hydrophone from *OAS Inc.*, or the *HTI-01-PCA* hydrophone from *HIGH TECH INC.* and the recording device is a *MBS*, *MLS* or *MES* recorder of *SEND GmbH*, which is contained in its own pressure tube and mounted below the buoyant body opposite the release transponder (see Figure 5.3.1).

The Ocean Bottom Seismometer

The Ocean Bottom Seismometer (OBS) construction (Bialas and Flueh, 1999; Figure 5.3.2) is based on the experiences with the GEOMAR OBH. For system compatibility the acoustic release, pressure tubes, and the hydrophone are identical to those used for the OBH. Syntactic foam is used as floatation again but of larger diameter due to the increased payload. In contrast to the OBH the OBS has three legs around a centre post to which the anchor weight is attached (Figure 5.3.2). While the OBH is floating about 1 m above the sea bottom, the OBS is positioned on the sea bottom to avoid collisions between the seismometer cable and the anchor.

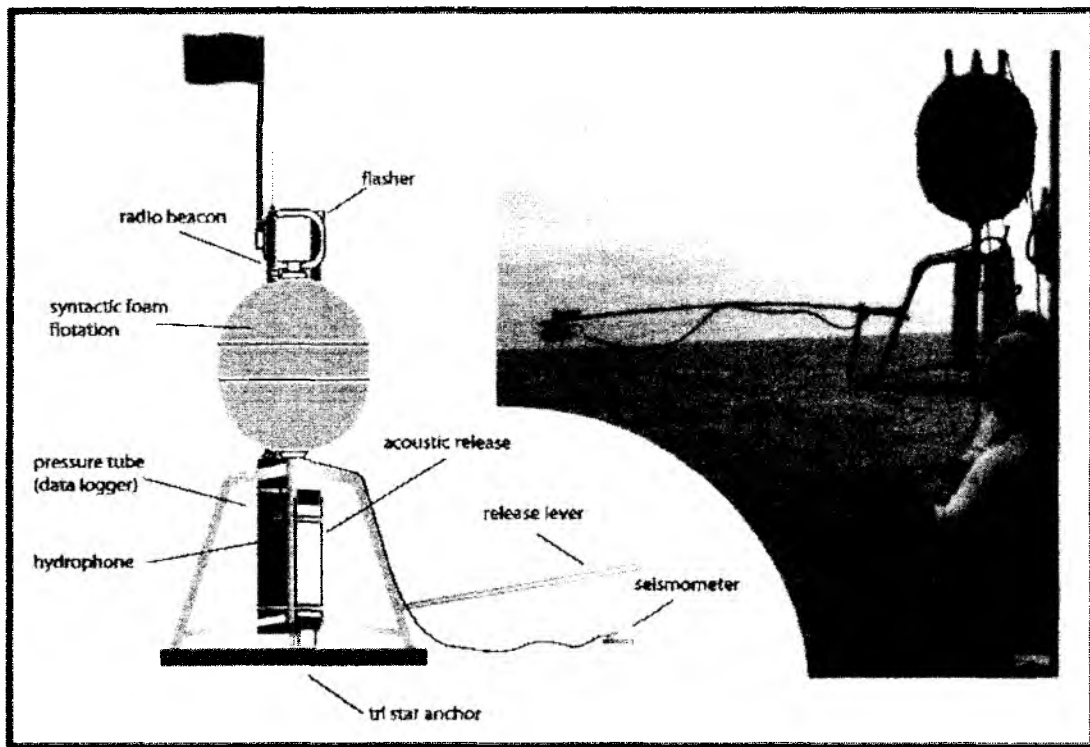


Figure 5.3.2: Drawing and Photograph of the IFM-GEOMAR Ocean-Bottom-Seismometer. The instrument rests on its anchor weight on the seafloor, while the seismometer is deployed from the release lever avoiding any fixed connection to the system carrier.

The sensitive seismometer is deployed about 1 m to the side of the system once the OBS lands on the sea floor. An electrolytic burn wire releases the seismometer two or five hours after deployment. At this time the only connection from the seismometer to the instrument is a cable and an attached wire which retracts the seismometer during ascent to the sea surface. An

oscillation of the instrument caused by possible currents is therefore not transmitted mechanically to the seismometer. All three channels are recorded by the standard recorders as used in the OBH units. During cruise SO181, 4.5 Hz sensors from SENSOR were used with the seismometers (s.b.). Parallel to these three channels the standard hydrophone is recorded on the fourth channel.

The GEOMAR Ocean Bottom Seismometer 2002

The GEOMAR Ocean Bottom Seismometer 2002 (OBS-2002; Figure 5.3.3) is a new design based on experiences gained with the GEOMAR Ocean Bottom Hydrophone (OBH; Flueh and Bialas, 1996) and the GEOMAR Ocean Bottom Seismometer (OBS, Bialas and Flueh, 1999). For system compatibility the acoustic release, pressure tubes, and the hydrophone are identical to those used for the OBH and OBS. Syntactic foam was used as floatation again but this time in less expensive cylinder shape. The entire frame can be dismounted for transportation, which allows storage of more than 50 instruments in one 20" container. Upon cruise preparation onboard all parts are screwed together within a very short time. Four main floatation cylinders are fixed within the system frame, while additional disks can be added to the sides without changes. The basic system is designed to carry a hydrophone and a small seismometer for higher frequency active seismic profiling. The sensitive seismometer is deployed about 1 m to the side of the system once the OBS lands on the sea floor. At this time the only connection from the seismometer to the instrument is a cable and an attached wire, which retracts the seismometer during ascent to the sea surface. An oscillation of the instrument caused by possible currents is therefore not transmitted mechanically to the seismometer. Alternatively, the seismometer can be clamped to the anchor. The three component seismometer (*KUM*) is housed in a titanium tube, modified from a package built by Tim Owen (Cambridge) earlier. Geophones of 4.5, 15, or 30 Hz natural frequency are available. In addition, a 4.5 Hz self gimbaled geophone from *Geospace* was used as a prototype during the cruise. By changing the frontal third of the frame (opening four screws) a broadband seismometer can be attached to the system carrier. The "Spahr Webb" type seismometer is based on *Mark-L4* sensors, which are operated with a feedback loop to enable recordings of frequencies as low as about 60 sec. As the sensors are sensitive to horizontal or vertical adjustment the complete construction is fully gimbaled. Tilt is measured at selected intervals and two electric motors are used to adjust and fix for a proper positioning. The system is mounted within a 17" glass sphere. The sensor is recorded by use of the *Marine Longtime Recorder (MLS)*, which is manufactured by *SEND GmbH* and specially designed for long-time recordings of low frequency bands. The hydrophone can be replaced by a differential pressure gauge (DPG) as described by Cox et al. (1984). While deployed to the seafloor the system rests horizontally on the anchor frame. After releasing its anchor weight the instrument turns 90° into the vertical and ascends to the surface with the floatation on top. This ensures maximal reduced system height and water current sensibility at the ground (during measurement). On the other hand the sensors are well protected against damage during recovery and the transponder is kept under water, allowing permanent ranging, while the instrument floats at the surface.

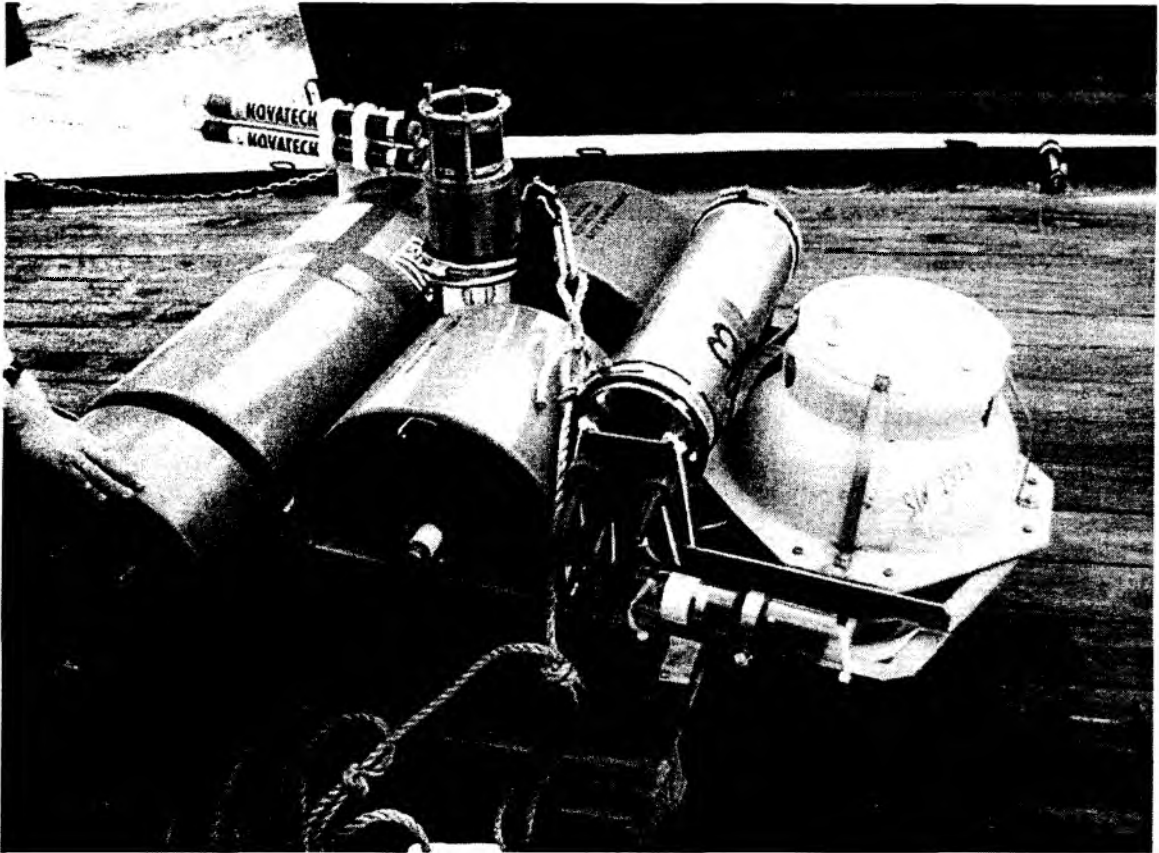


Figure 5.3.3: *Instrument setup of the Ocean Bottom Seismometer 2002.
Here configured with Webb type broadband seismometer and HTI hydrophone.*

The Hamburg Ocean Bottom Hydrophone

The ocean bottom hydrophone (OBH) of the University of Hamburg is built in a epoxy (GFK) frame and consists of two glass floatation spheres, an acoustic release of type *RT6xx* by *IXSea* and a pressure tube (either titanium or aluminium). Figure 5.3.4 shows the construction of the Hamburg OBH. The glass floatation spheres are fixed on a frame with 6 steel screws which also fix the orange plastic mantle of the spheres. On its top flasher and radio beacons are placed for recovery, as well as a hydrophone transponder that is directly connected with the releaser to open the anchor hook (anchor: rail, rope and ring at the under side of the OBH). The pressure tube is fixed between floatations and releaser, the hydrophone (type OAS) is lying horizontally between the floatations. The data logger unit, a SEND Geolon MLS (see below), powered by 48 size D 1.5V batteries, is placed inside the pressure tube. With an anchor weight of 40kg it descends with 2m/sec and raises after releasing with about 1-1.5m/sec. Glass spheres, pressure tube and releaser are built for measurements down to 6000m.

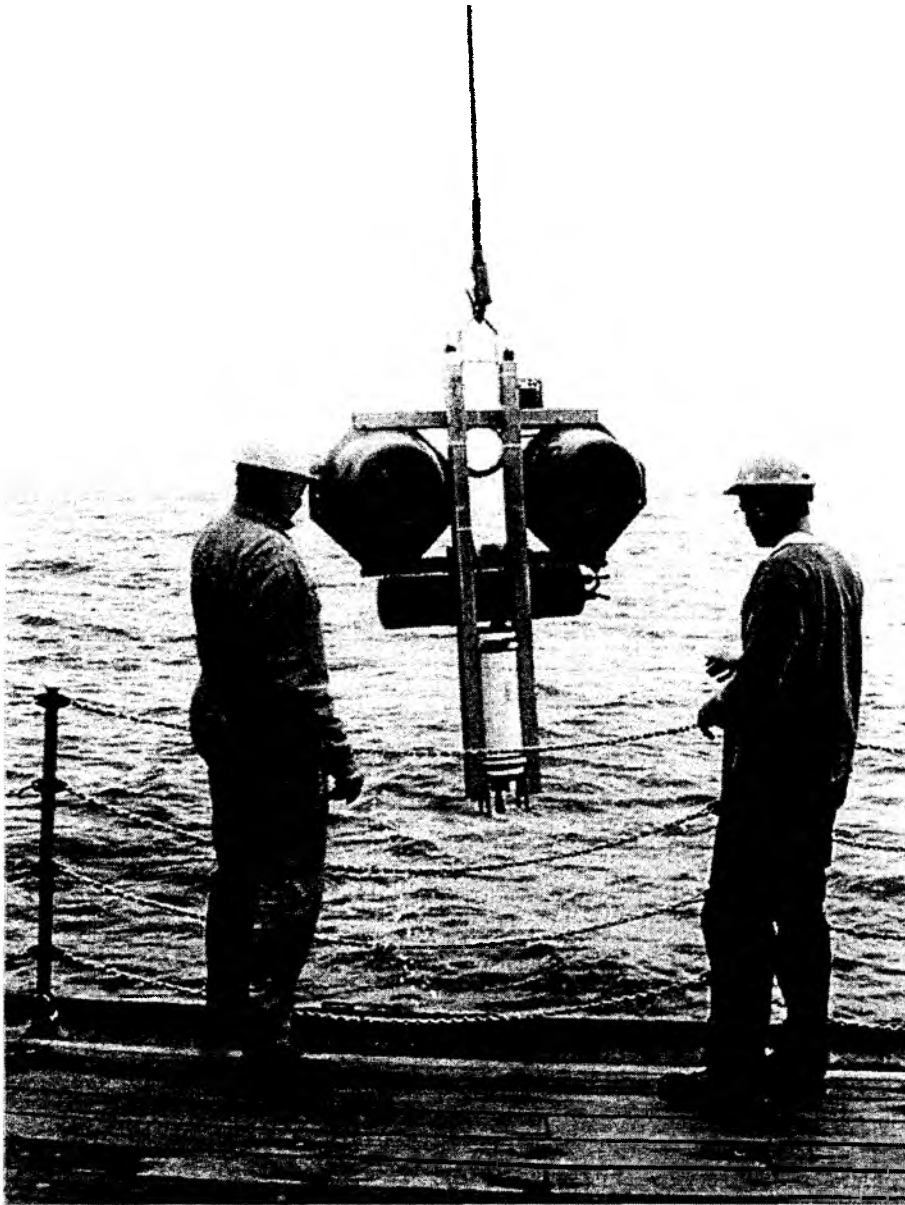


Figure 5.3.4: *The Hamburg OBH upon recovery*

The instrument consists of glass sphere floatations in orange hard casse at top left and right, pressure cylinder with recording electronics in the centre with a horizontally mounted hydrophone above, acoustic release transponder in the lower centre

The Hamburg Ocean Bottom Seismometer and the video-controlled deployment frame

The ocean bottom seismometer (OBS) needs four glass-spheres for buoyancy (red hard cases). The seismic wide-band sensor (flat from 0.03 – 30 Hz, PMD 117) is passively gimbaled within one of the buoyancy spheres. The lower part of the sensor is surrounded by

a highly viscous oil so that a possible differential movement between the sensor and the frame (ground) is not present at frequencies above 0.04 Hz. The releaser (Mors-Oceano) is mounted horizontally in the middle of the frame between the flotation spheres. An iron anchor of about 100 kg ensures that the station falls down and couples to the ground. Two pressure tubes (red tubes) hold the electronics (data logger MLS, pre-amplifiers, etc.) and three battery packs (3 x 48 size D 1.5 V). The longest possible deployment time is one year, but only a half year deployment has been realized before in the Tyrrhenian Sea. Thus, TIPTEQ will use the long-term capability of the station for the first time. The same recovery tools as for the OBH are used (flash-light, radio beacon). The station design was developed to minimize the station height and thus flow resistance causing current-induced noise at low frequencies. The relatively large dimension of the frame and anchor (about 1.2 x 1.2 x 0.6 m) should minimize tilt-induced noise.

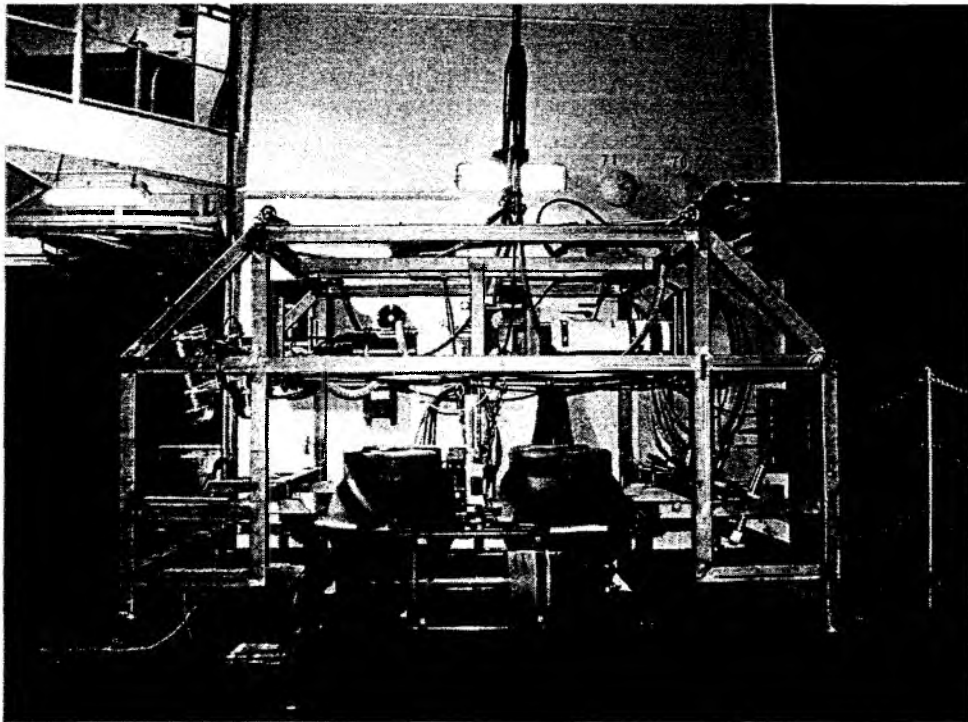


Figure 5.3.5: The Hamburg OBS mounted on the new camera-controlled (video) deployment frame.

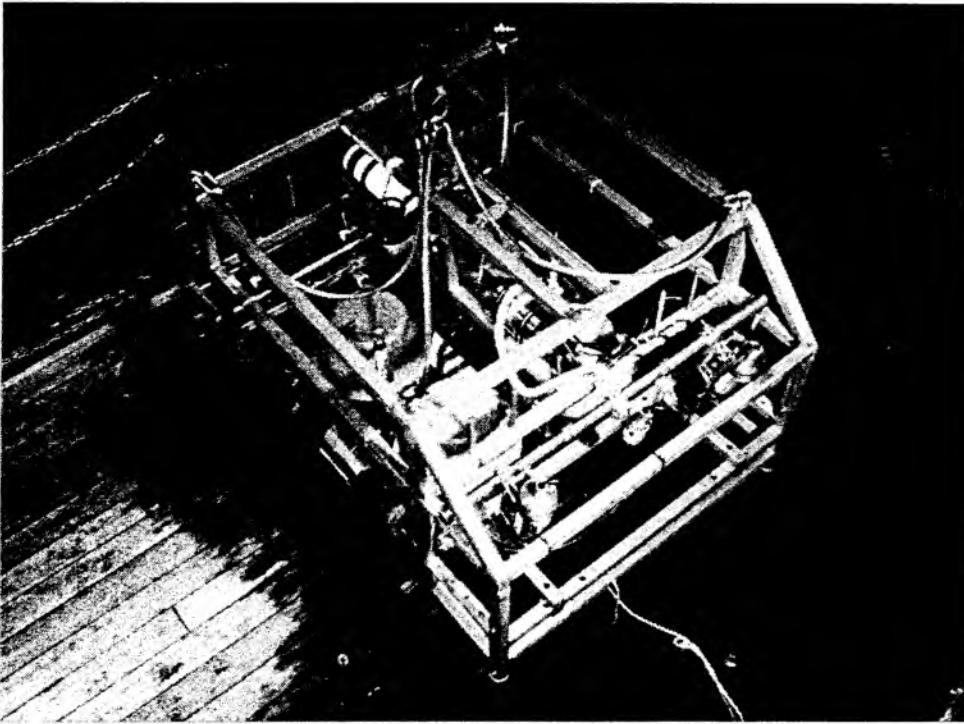


Figure 5.3.6: *Another perspective of the Hamburg OBS*

Four OBS stations have been deployed in the northern long-term array off-coast Concepcion. For the first time a newly developed video-camera controlled deployment frame (Figure 5.3.5 and 5.3.6) has been used to place the stations on the seafloor. The deployment system is equipped with an underwater camera, two spot lights, three laser pointers to estimate the distance to the ground a few metre above the seafloor, and an electric device in a steel pressure tube. A current meter including a tilt-meter and a magnetic compass is available but has not been installed on this cruise. The video control unit is on board. The station is mounted to the deployment frame with an iron chain that can be released from the ship on command by means of an acoustic releaser. The test of the system was successful and highly satisfactory. No technical problems occurred and handling was easy. The video telemetry system enabled us to investigate the seafloor prior to deployment. In this case sandy seafloor was present. Different deployment approaches had been tested. Firstly, putting the station and deployment frame on the seafloor, waiting until the dust-cloud disappeared (about 3 minutes) and releasing after optically checking the station position, it was possible to observe dust flow and to identify a strong water current at the bottom around station. Therefore, using the current meter in the future appears useful. The second deployment test was to stop the cable when the frame was 1 to 2 m above the seafloor and then let the station fall to the ground. A third test was to re-deploy the station from one place to another nearby, when the first location seemed unsuitable. The deployment and frame recovery in 3000 m depth took about 2.5 hours. This extra time seems acceptable when planning long-term deployments.

Several improvements might be discussed. E.g. the orientation and direction of camera, spot lights and laser pointed are not yet optimised. The deployment approach may be extended in

the future to check the tilt angle of the station on the seafloor before a final release is performed. It may also be possible to generate a mechanical calibration sweep (pulse) and checking the coupling conditions prior to final release. In summary, we have been quite enthusiastic about this experiment. A summarising film sequence (DVD) will be prepared when back in Hamburg.

Marine Broadband Seismic Recorder (MBS)

The so-called *Marine Broadband Seismic recorder (MBS)* (Bialas and Flueh, 1999), manufactured by *SEND GmbH*, was developed based upon experience with the DAT based recording unit *Methusalem* (Flueh and Bialas, 1996) over previous years. This new recorder avoids a mechanically driven recording media, and the PCMCIA technology enables static flash memory cards to be used as unpowered storage media. Read/write errors due to failure in tape handling operations should not occur with this system. In addition, a data compression algorithm is implemented to increase data capacity. Redesign of the electronic layout enables a decreased power consumption (1.5 W) of about 25% compared to the *Methusalem* system. Depending on the sampling rate, data output could be in 16 to 18 bit signed data. Based on digital decimation filtering, the system was developed to serve a variety of seismic recording requirements. Therefore, the bandwidth reaches from 0.1 Hz for seismological observations to the 50 Hz range for refraction seismic experiments and up to 10 kHz for high resolution seismic surveys. The basic system is adapted to the required frequency range by setting up the appropriate analogue front module. Alternatively, 1, 2, 3 or 4 analogue input channels may be processed. Operational handling of the recording unit is similar to the *Methusalem* system or by loading a file via command or automatically after power-on. The time base is based on a DTCXO with a 0.05 ppm accuracy over temperature. Setting and synchronising the time as well as monitoring the drift is carried out automatically by synchronisation signals (DCF77 format) from a GPS-based coded time signal generator. Clock synchronisation and drift are checked after recovery and compared with the original GPS units. After software preamplification the signals are low-pass filtered using a 5-pole Bessel filter with a -3 dB corner frequency of 10 kHz. Then each channel is digitised using a sigma-delta A/D converter at a resolution of 22 bits producing 32-bit signed digital data. After delta modulation and Huffman coding the samples are saved on PCMCIA storage cards together with timing information. Up to 4 storage cards may be used. Data compression allows increase of this capacity. Recently technical specifications of microdrives (disk drives of PCMCIA type II technology) have been modified to operate below 10 °C, therefore 2 GB drives are now available for data storage. After recording the flashcards need to be copied to a PC workstation. During this transcription the data are decompressed and data files from a maximum of four flash memory cards are combined into one data set and formatted according to the PASSCAL data scheme used by the *Methusalem* system. This enables full compatibility with the established processing system. While the *Methusalem* system did provide 16 bit integer data, the 18 bit data resolution of the *MBS* can be fully utilised using a 32 bit data format.

The Marine Exploration Seismic Recorder (MES)

This data logger is based on the experiences with the MBS and MLS devices. It has been developed by *SEND GmbH* and is supposed to replace the MBS system in the future. New features are a 24 bit A/D converter which provides a signal to noise ratio above 120 dB. The internal time system is based on the same high precision clock, which has proved its high reliability for the MBS devices. In case the time deviations show large offsets the clock can

now be calibrated in the field using GPS time service. As the development of PC cards did not allow the use of high capacity cards (above 2 GB) in low-temperature surroundings like the ocean floor the new data logger uses an internal hard disk. From developments in laptop technology, drives are available that withstand a harsh working environment and need only a small amount of power. High data transfer through a firewire (5 GB < 10 min) ensures that the entire 20 GB disk drive can be copied within 40 min. Further features are similar to the MBS. Together with the data logger a new set of Linux-based programs allows to run the complete data transformation up to SEG-Y formatted trace segmentation without switching between different operating systems or computing platforms. Seven recorders were available for SO 181 and worked well.

The Marine Longtime Seismograph (MLS)

For the purpose of low-frequency recordings such as seismological observations of earthquakes during long term deployments of about one year time a new data logger, the Marine Longtime Seismograph (MLS) was developed by *SEND GmbH* with support from IFM-GEOMAR.

The MLS is a four channel data logger whose input channels have been optimised for 3-component seismometers and one hydrophone channel. The modular design of the analogue front end allows to adapt different seismometers and hydrophones or pressure sensors. Currently front ends for the Spahr Webb, PMD and Guralp seismometers as well as for a differential pressure gauge (DPG), a pressure sensor of high sensitivity and the OAS/HTI hydrophone are available. With these sensors we are able to record events between 50 Hz and 120 s. The very low power consumption of 250 mW during recording together with a high precision internal clock (0.05 ppm drift) allows data acquisition for one year. Data storage is done on up to 12 PCMCIA type II flashcards or microdrives, now available with up to 2 GB capacity. The instrument can be parameterised and programmed via a RS232 interface. After low pass filtering the signals of the input channels are digitised using Sigma-Delta A/D converters. A final decimating sharp digital low-pass filter is realised in software by a Digital Signal Processor. The effective signal resolution depends on the sample rate and varies between 18.5 bit at 20 ms and 22 bits at 1 s. Playback of the data is done under the same scheme as described for the MBS above. After playback and decompression the data is provided in PASSCAL format from where it can be easily transformed into standard seismological data formats.

Seismic sources

32 I BOLT Airgun

Three airguns Model 800 CT *BOLT* were used during the cruise; a photo of one gun is shown in Figure 5.3.7. The guns have a volume of 32 litres (2000 inch³), and generate a signal with a main frequency centred around 6 to 8 Hz and higher harmonics. The guns were deployed and towed by the assistant winch and beam normally used for the piston corer recovery on starboard side while the outer hook of the A-frame is used for the portside gun. Trigger cables and airhoses were deployed manually. The guns were suspended on two floats with an additional float attached to the supply lines to prevent contact between the guns and the towing wire. They were towed 60 m behind the vessel and operated at 145 bar in 7 to 8 m depth. Due to good weather conditions the handling of the guns was smooth all the time. During cruise SO181-1a more than 9100 shots

were fired, at a 30 or 60 s shot interval. The ship's compressor system worked smoothly and caused no delays or interruptions.

G-gun Cluster

As the main seismic source G-gun clusters manufactured by *Sercel Marine Sources Division* (former *SODERA*) and *Seismograph Services Inc.* were operated in two arrays. Five guns owned by IFM-GEOMAR and three guns loaned from AWI, Bremerhaven, were set up in four clusters, carried by two 5 m long frames (Figure 5.3.8). All guns were fired through the IFM-GEOMAR LongShot airgun source controller manufactured by *RealTime* using the shipboard photo trigger of the *Preussag* telemetry system (see External Trigger below).



Figure 5.3.7: 32 l Bolt gun upon deployment onboard RV SONNE.

Each cluster comprises two 520 cubic-inch (8 l) G-guns (Figure 5.3.9). Compared to the large volume *Bolt* guns the cluster technology provides a better primary to bubble signal ratio. Operating eight guns provides a total volume of 64 litres, i.e. the same as the two 32 l Bolt

guns, but they should be preferable to the two Bolt guns because they radiate energy from more guns and use a higher working pressure. Instead of the 140 bar pressure used with the *Bolt* guns the G-guns were operated at 210 bar. For this purpose a second compressor was set up by RF onboard SONNE for the first time to increase the 140 bar pressure from the onboard *Leobersdorfer* unit to 210 bar. During test runs it turned out that for overpressure prevention a spring controlled valve was built into the circuit. This valve releases pressure above 210 bar but does not close until the system pressure has dropped down to 190 bar. This valve needs to be replaced by a different unit to ensure constant pressure of 210 bar with less alteration when overpressure is released. Due to the significant variations of working pressure from shot to shot the true shot time of each gun, measured by a sensor signal, varies from shot to shot by several milliseconds. Alternatively the shot interval was shortened to 40 seconds to find a compromise between desired interval of 60 seconds and variations in the working pressure due to over-pressure release. Using this interval the pressure could be kept between 205 and 210 bar with rare pressure drops due to the opening of the safety valve. The single delay times of the guns kept constant during this time and hence should provide a consistent shape of the source signal.

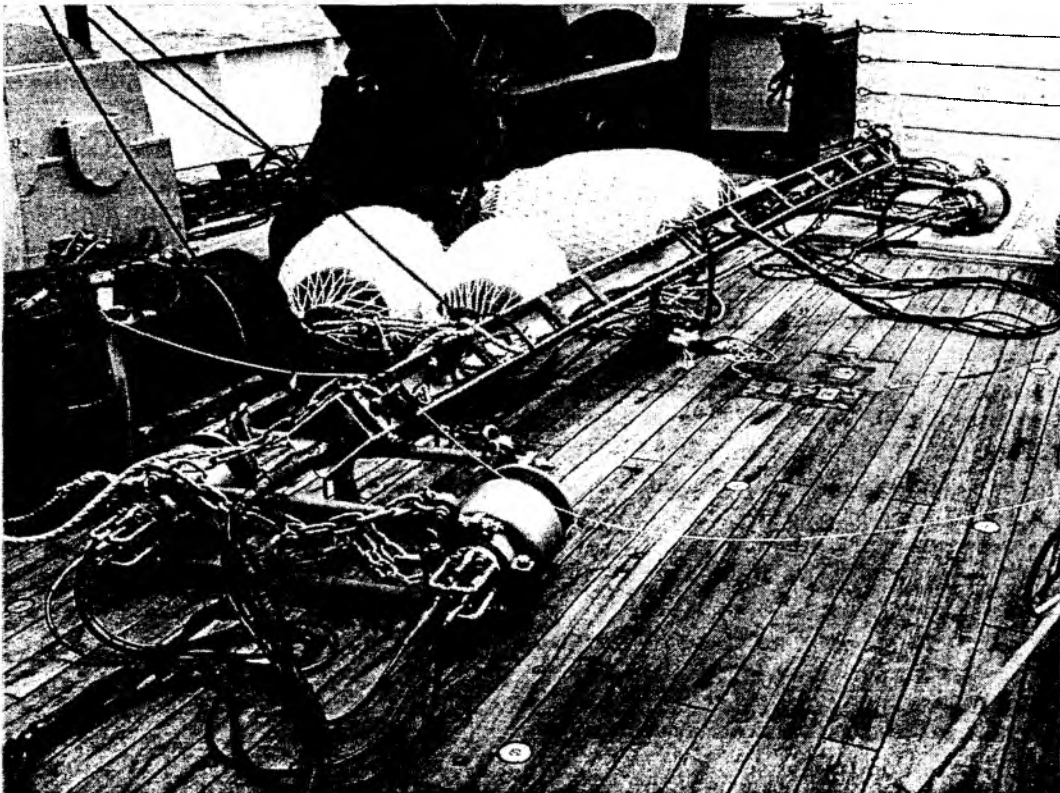


Figure 5.3.8: Picture of a 5 m long G-gun Cluster carrier
Two G-gun clusters are mounted below the carrier, while four Polyform floatations are visible on the left hand side.

The gun carriers (each 5 m long) were deployed through the inside of the A-frame, while towing was done by the aft mooring winches, with the cables being guided through blocks on the outside ends of the A-frame. For lifting purposes a triangle shaped hoisting rope was attached to the ends of the carrier, while the towing cable was attached to the front end where the support hoses of the guns were lead in as well. First the assistance winch of the A-frame lifted one gun carrier, which was then guided behind the aft of the vessel. Here, the towing winch took the weight while the back of the carrier already dipped into the water. Now the hoisting rope was attached to the towing rope and finally the entire carrier was lowered into the water. Meanwhile four F11 size *Polyform* buoys were pushed into the water, acting as flotation for the frame. During the first deployment operation it turned out that the assistant winches of the A-frame were too slow and hence lowering of the gun into water took too much time. During this time the gun carrier started moving as the vessels rolled due to swell. Work around the boson provided a steel wire which was led through the centre block of the A-frame and guided through mobile blocks on the deck to the outer drum of the mooring winch by an eye in the ships rail. This steel wire needs to be shifted to that winch currently not involved in the deploying operation. The hoisting rope of the gun frame was extended with a rope, long enough to be attached to the towing wire before the gun frame was deployed into the water, where it was released by a slip-hook. This procedure allowed to deploy the guns and frame in horizontal position, which minimises the danger of destroying pipes and cables. As the mooring winch operates much faster than the assistant winch of the A-frame, danger caused by the moving frame for people and equipment was reduced further. The two pairs of F11 size floatations on each carrier had been fixed at front, middle and middle, end in the first design. This was changed to single point fixing at the front and end of the carrier. Now the end float could be dropped into water prior to lowering of the carrier while it floated away from the vessel. The front buoy was kept on slip on the back post of the A-frame. It was dropped into water when the carrier started floating and hence cross cuts with ropes and floats was avoided. Furthermore, danger to the crew working within the A-frame space was avoided. The entire procedure now allows deployment by lifting the front of the gun carrier out of the water by only about 2 metres. Figure 5.3.11 shows a drawing with the setup of the used wires and ropes. During the recovery procedure the extended hoisting rope allowed to keep the gun carrier in horizontal position all the time as well. After that, the second carrier was deployed/recovered in the same manner.

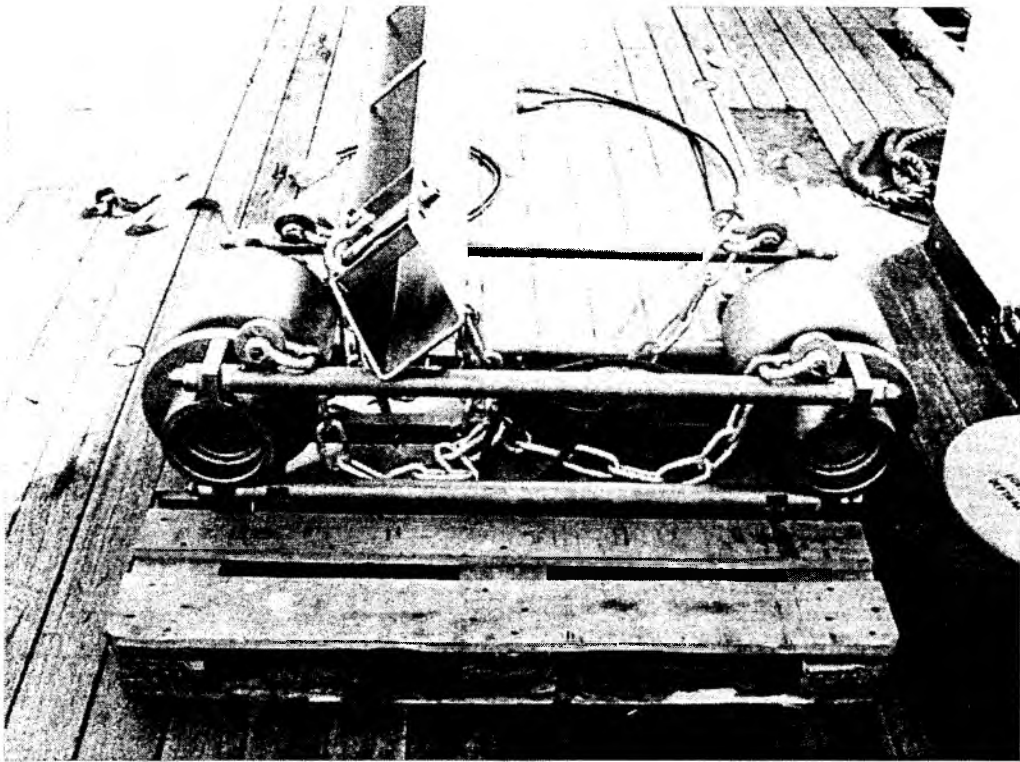


Figure 5.3.9: Photograph of a G-gun cluster

Two 520 cubic-inch G-guns separated by 1m long rods. Chains fix the cluster 1 m below the 5 m long gun carrier.

External trigger during SO181-2

Since the replacement of the old *Atlas* ANP navigation system on the bridge by the new DSHIP system from *Werum* GPS, controlled seismic trigger signals are no longer available. Therefore the control device of the digital camera used with the *Preussag* OFOS telemetry system was used to provide a trigger signal for the airgun shots. The impulse was delivered to the *LongShot* trigger box. The trigger pulses from the OFOS system, necessary for subsequent data processing and instrument location, were stored on an MBS recorder and displayed in real time for quality checks. For this process the same time basis was used as for the OBH. A test of the timing reliability of the *LongShot* trigger box was performed, consisting of a synchronous recording of the OFOS trigger signal and the Clock Time Break (CTB) of the *Longshot* device, i.e. a TTL pulse that is 5 ms wide and represents the aim-point or the time when the guns are firing. This aim-point was set to be 60 ms after the OFOS trigger pulse, but the test resulted in a delay of 155 ms indicating an additional internal delay of the *Longshot* trigger box. After careful analysis of the direct arrivals and multiples in the seismic data, a delay of 135 ms with respect to the OFOS trigger pulse was determined, thus indicating a time shift of 20 ms of the airgun firing time given by the CTB pulse.

Exact calculation of the ship's position at shot time should be done by later post-processing using shot time and UTC time values stored with GPS coordinates in the ship's data base.



Figure 5.3.10: Starboard side G-gun carrier during recovery

The gun frame is lifted by the hoisting rope with its extension operated by the port side mooring winch through the centre block in the A-frame. Starboard towing wire can be seen towards the top left where it passes through a roll on the outside part of the A-frame

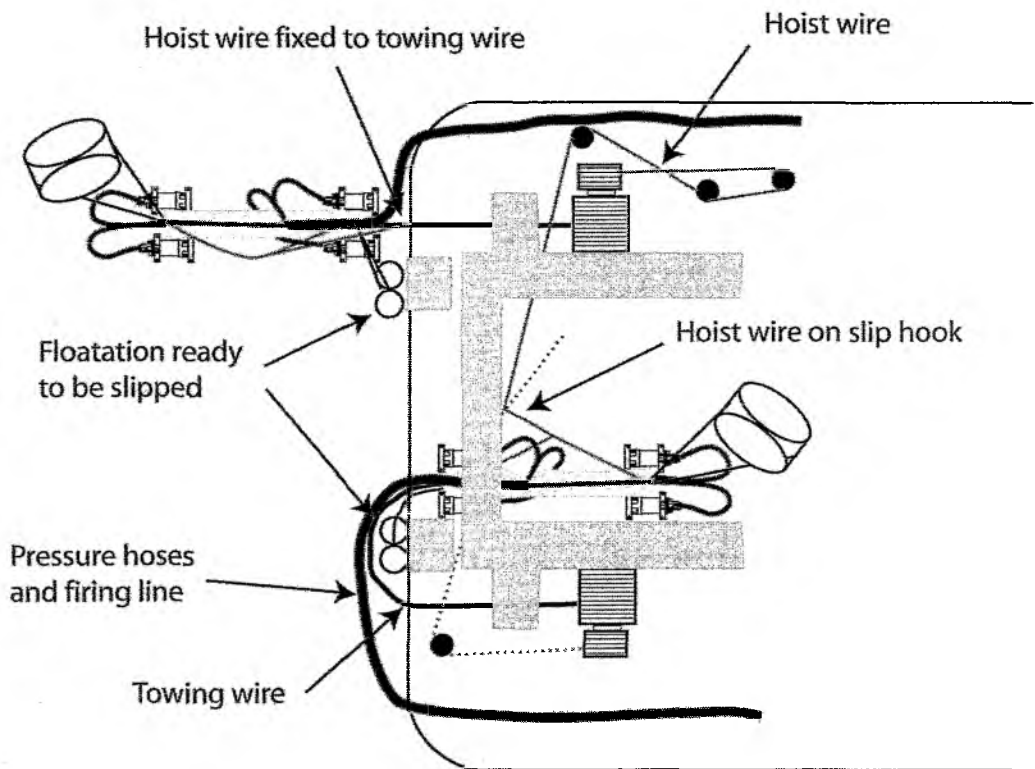


Figure 5.3.11: Drawing of the setup wires and ropes used during deployment and recovery. The front of the portside frame is lifted about 2 m out of the water to attach the hoisting wire to the towing wire. The starboard frame is configured to be deployed next.

Reflection seismic data acquisition

SO-181/1a

In addition to the ocean bottom seismic recorders, a mini-streamer was used during seismic profiling. This streamer was borrowed from the University of Gent, Belgium, and manufactured by SIG (*Service et Instruments de Geophysique, France*). The system comprises several parts: four 12.5 m long active sections with 25 hydrophones spaced at 0.5 m. The lead-in cable is 150 m long and directly connected to the lab. The individual hydrophones are omnidirectional and have a flat frequency response from 10 to 1000 Hz. The sensitivity is -90 dB, re $1 \text{ V}/\mu\text{bar}$, ± 1 dB. The hydrophones are mounted in an oilfilled polyurethane pipe of 34 mm diameter, with a nominal density of 1.12 gr/cm^3 . The tow depth had to be controlled by visual inspection. The streamer had to be deployed and recovered manually.

The signals recorded by the streamer were stored on a four-channel MBS / MES recorder, identical to those used in the ocean bottom seismic recorders. The streamer winch was placed amidships about 8 m away from aft of the vessel. Unfortunately, the streamer was lost due to fish-bite on profile P03 during Leg SO181-1a.

SO-181/1b

Seismic recording equipment during SO181_1b consists of a 16 channel, 100 m long hydrophone array, one SSI GI® seismic source and a Geometrics Strataview® Seismograph. Trigger signal is generated in time dependent mode by a stand alone PC and a SORCUS® interface card. Separate trigger signals are supplied for generator and injector guns and the Geometrics seismograph. Power amplification of the trigger pulse is necessary for the GI valve solenoids. Occasional misfires could be overcome by ensuring an electrical trigger signal width of more than 30 ms. As the seismic lines reach from the shallow shelf area across the trench up to the ridge crest, a water delay is favourable for data recording. This water delay is applied externally to the seismograph. For source generation one GI gun is towed at starboard side, tuned at 40 – 50 ms delay according to source depth and available compressed air of 140 bar. A source hydrophone allows quality control of the source signal by an oscilloscope display. Optimal tuning is achieved when the signal strength, detected by the source hydrophone exceeds 14 V_{pp}. The receiver array, towed amidships, is intended to deliver single channel data after stacking. Velocity analysis or CMP stacking is not reasonable due minor length of the array and huge water depth. Trace editing is required since channels 6 and 7 dropped out. Data format of recorded shot files is SEG-2. Conversion to tape format SEG-Y is possible with built-in programs or on an external processing system.

Seismic surveys are carried out at a speed of 5 kn and a firing interval of 10 s, yielding a shot spacing of approximately 25 m.

Technical parameters are as follows:

Source: SSI GI gun, 2 x 1.72 litre (2 x 105 in³) in Harmonic Mode
 Delay: 40 ms (SCS01), 50 ms (SCS02)
 Source depth: 5 m
 Position: approx. 5 m behind aft deck
 Operation pressure: 14 x 10⁶ Pascal (140 bar)

Receiver: Teledyne Streamer, 16 channels @ 6,25 m
 Lead in: 125 + 25 m
 Position of first channel: approx. 140 m behind aft deck

Seismograph: Geometrics Strataview®, 60 channels
 Filter: 10 – 250 Hz
 Sampling rate: 1 ms
 Record length: 4000 ms
 Gain: +48 dB
 Delay: 0. 3000 ms externally applied

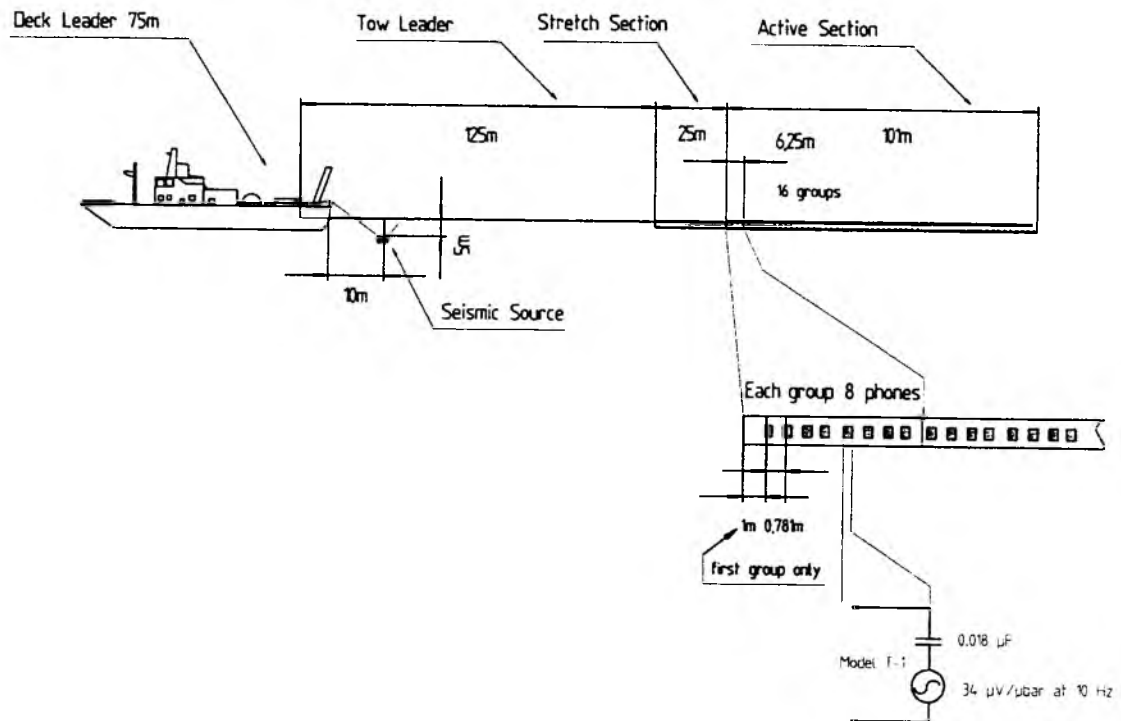


Figure 5.3.12: Configuration of 16 channel receiver array during SO181_1b.

SO181-2

For cruise SO181-2, a 16 channel streamer was provided from the group of Prof. Villinger from University of Bremen. It is the same unit used during cruise SO181-1b described above. Unlike the Villinger group, we used a four channel MBS data logger (s.a.) to record the seismic signals of the G-gun clusters. As the frequency band covered by the source signal of the 64 l G-gun cluster does not exceed about 80 Hz, we added two neighbouring channels prior to recording. Direct water wave arrival and reflection signals could be well observed using the online display capabilities of the MBS device (s.a.). Due to the close distance between the two G-gun arrays at the stern of SONNE it was decided not to deploy the streamer madcap through the guns but to use the portside magnetometer boom on the Backdeck. The streamer was entirely taken off its drum and deployed through the large diameter rolls of the IFM-GEOMAR magnetometer to avoid strong bending. With 7 m offset to the side vessel the streamer was guided in save distance to the port gun array.

Prototype Broadband Seismometer SEISMO-001

For cruise SO181-2 the prototype SEISMO-001 of a new broadband seismometer was available from *SEND GmbH*. The sensor is designed to record signals within a range of 0.03 Hz to 50 Hz. The seismic signal (airgun shots, natural seismicity) is recorded by three standard 4.5 Hz sensors, which have been modified by the manufacturer to be orientation independent (Figure 5.3.13). An electro-mechanic back coupling circuit developed by SEND modifies the sensitivity of the sensors to the range given above. For the back coupling the principle of “Force-Balance” from Prof. Wielandt has been applied.

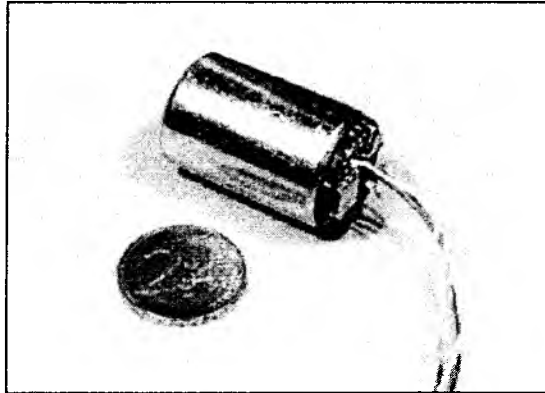


Figure 5.3.13: Photograph showing one of the three standard 4.5 Hz sensors used within the SEISMO-001. For scale, a 2 EURO-Cent coin is placed in front.

In contrast to a standard seismometer, the shaking is not measured by the relative motion between a fixed magnet and moving coil, but instead an electric circuit forces the coil to follow the movement of the magnet and hence housing of the seismometer. Consequently the force of momentum is measured. To allow such measurement, a capacitor is mounted within each sensor. One side is fixed to the housing the other side connected to the moving coil. Hence movement of the coil changes the capacity, which causes the electric circuit to initiate an electric current through the coil large enough to build up magnetic forces that suppress the relative motion of coil and magnet. Due to this principle the mechanical effects caused by the springs which hold the coil in place become negligible, and hence the function of transmission depends only on the electric circuit. Tests on a shaking table at the University of Jena were undertaken up to a frequency of 8 Hz. These tests verified a constant transmission from 0.06 Hz up to 6 Hz.

Table 5.3.1: Table of technical details for the SEISMO-001 prototype

Frequency range:	0.03 Hz – 50 Hz
Sensitivity:	500 Vs/m
Max. tilt:	90°
Power consumption:	approx. 180 mW (with three components)
Weight on air:	98 g (single sensor)
	390 g (three components with electric circuit)

An upgraded version of the circuit should now provide a flat curve of transmission between 0.03 Hz and 50 Hz. Table 5.3.1 gives the technical details of the three component sensor (Figure 5.3.14). With 88 Lithium batteries such a sensor could be operated with an MLS recording device for up to 365 days.

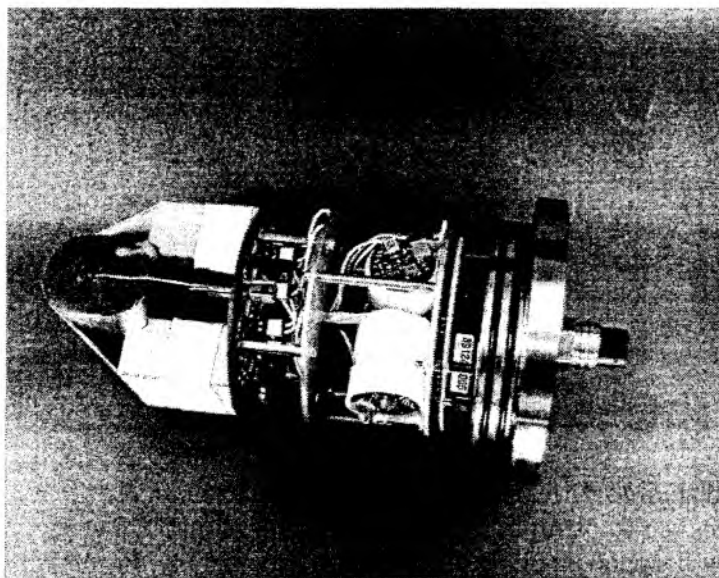


Figure 5.3.14: *Photograph of the SEISMO-001 prototype mounted to the top plate of a 6000 m depth rated pressure housing. In the centre the three coils of the three single component sensors are visible*

During cruise SO181-2 two test deployments were undertaken when Ocean-Bottom-Seismometers were deployed for active seismic recording. For this purpose the sensor was mounted on one of the three leg type OBS from IFM-GEOMAR. Results from these recordings are discussed within Section 6.6.8.

5.4 Magnetometer

A GeoMetrics G801/3 Marine Proton Magnetometer was deployed during all three legs of the cruise SO181 to record the Earth's magnetic field in the area, with the main aim to get magnetic reversals. The seafloor had inherited those reversals during its creation at the Chile spreading centre some millions of years ago. These magnetic reversals will allow us to reveal the age of the seafloor.

The G801/3 magnetometer consists of a gasoline-filled sensor attached to a 250-m-long marine cable and a control unit. The sensor essentially consists of two coils. During the polarisation cycle an electric current generates a strong magnetic field in one of the coils and forces the magnetic moments of the protons of the gasoline for a short time to be aligned parallel to the applied field. During the following measuring cycle, i.e. when the electric current is turned off, the protons start realigning themselves with the Earth's magnetic field. According to the moment preservation law, this happens by precession of the protons with a frequency proportional to the intensity of the geomagnetic field. The AC electric current induced by the precession of the protons is picked up by the second coil, then amplified, counted and transformed into magnetic field intensity values (measuring unit: 10^{-9} Tesla = 1 nT).

In order to minimise the influence of the ship's hull, the sensor of the Magnetometer is towed ~180 m behind the ship. This distance between the ship and the sensor is sufficient to minimise the magnetic influence of the vessel resulting in a resolution of about 5 nT. On board RV Sonne, the winch was placed on the port back deck and the sensor was towed to the port side of the vessel. A boom held the cable about 7 m away from the side of the ship in order to prevent it from colliding with the ship.

Before data acquisition, the tow fish was disassembled and the membrane condition checked, and after that the gasoline was filled in. The measured values of the total intensity magnetic field were displayed on a console and written as digital output coded in BCD values. The system was set to deliver one data value every 3 seconds via digital multiport interface to a PC, where the data are stored as a function of UTC time in ASCII tables. After data backup the files were transferred to a SUN workstation. GPS coordinates and time were taken from the ship's navigation system and assigned to each magnetic stamp on the basis of the recorded time. The magnetic and the navigation data were resampled to a 10-s interval. After optional median filtering they were displayed using GMT plot routines (Wessel and Smith, 1995).

5.5 Magnetotellurics

For the seafloor magnetotelluric measurements on cruise SO-181 a newly designed HEFMAG system (Woods Hole Oceanographic Institution) was employed. The instrument measures the natural temporal geomagnetic and geoelectric (telluric) field variations in a period range from $T = 80\text{s} - \text{DC}$. While fluxgate magnetometers are sensing the three components of the magnetic field, a short-span device incorporating a saltwater bridge and unpolarizable Ag/AgCl electrodes is used for probing the electric field (cf. Filloux 1973, 1974; see also Figure 5.5.1). Since the electromagnetic variations are severely attenuated by the overlying, well conducting seawater layer, special care has to be taken with respect to signal-to-noise ratio; for an overview of current techniques see, e.g., Chave et al. (1991). Details concerning the individual instruments are given in Table A.5.1 in the appendix. Mainly due to the tubes for

the telluric field the descend speed is relatively low (20m/min), the rise speed is unknown for the time being but expected to be even lower.

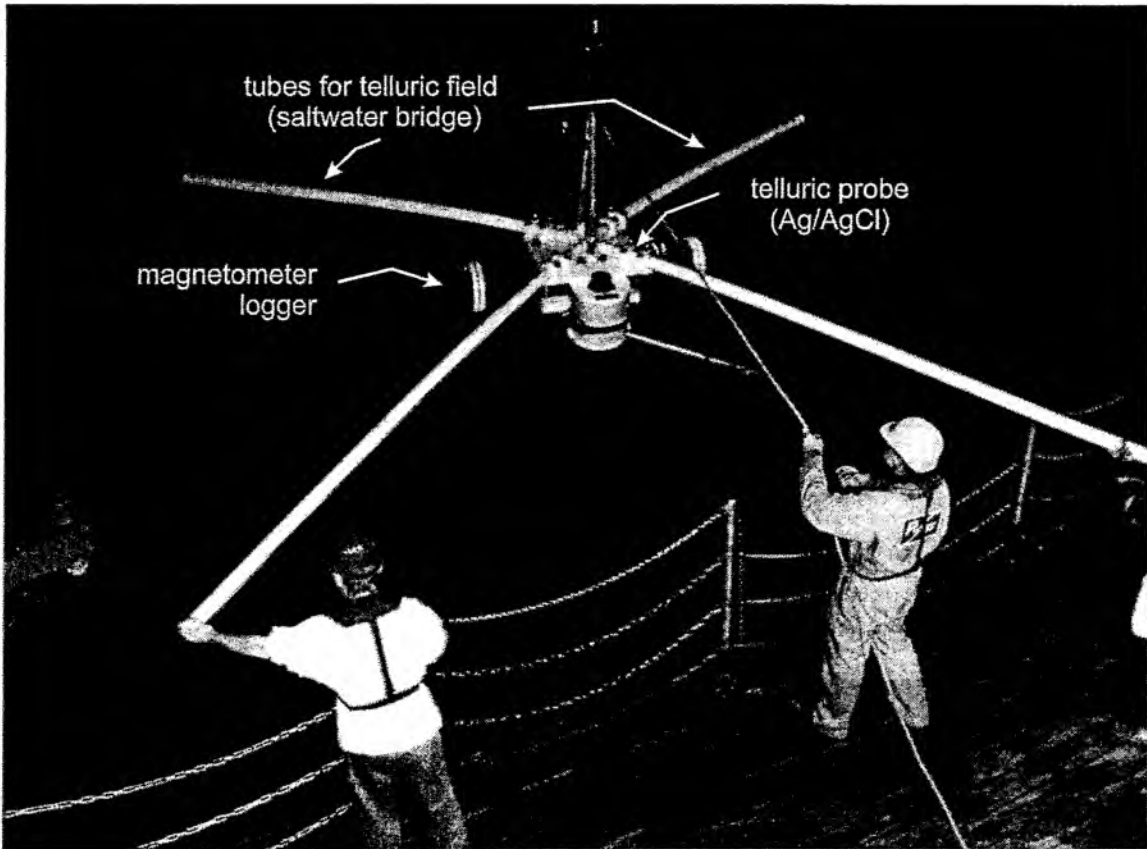


Figure 5.5.1: Deployment of the HEFMAG seafloor magnetotelluric system.

A total of 8 instruments were available on this cruise; 7 of these were deployed along a profile centred at 38°S, 75°W (unfortunately the mainboard of the 8th system was destroyed due to a grounding fault of the ship's power supply). This offshore profile reaches from the oceanic plate over the trench close to the coast (for deployment and recovery information see appendix 5.5), where it is due to be continued on-land at the end of 2004 – beginning of 2005. Water depths range from 560m – 4.600m. The stations will be recovered during cruise SO182b in February 2005. Preliminary information (e.g., time series) will only be available thereafter. For subsequent modelling and inversion the ocean has to be incorporated as an a-priori structure in the finite difference mesh and therefore the knowledge of water conductivity is essential. A CTD log to depths of 4.000m was performed close to the measuring area. A plot of conductivity, resistivity, temperature and salinity is shown in Appendix 9.5.

5.6 Heat flow instruments

Two different heat flow probes of violin bow type were employed during SO 181-1b. The smaller one is capable of 3 m penetration into the sea floor, thus abbreviated as 3 m-HF while the second has a length of 6 m and hence is named Giant Heat Flow probe (GHF). The intention of getting longer temperature gradients within the sediments is to gain reliable values of undisturbed heat flow in case of the presence of transient temperature disturbances due to mobility of water bodies. This is likely to occur on the continental slope in water depths less than 2000 m.

Heat flow stations are clustered locations of measurements, consisting of usually 10 positions with a spacing of 1 km. Multi penetration mode (pogo style) is the most effective way of advancing along a station while the probe is lifted above sea floor some hundred metres. Both instruments are equipped with online data transmission for operation control and independent data storage inside the instrument for double data security (Figure 5.6.1).

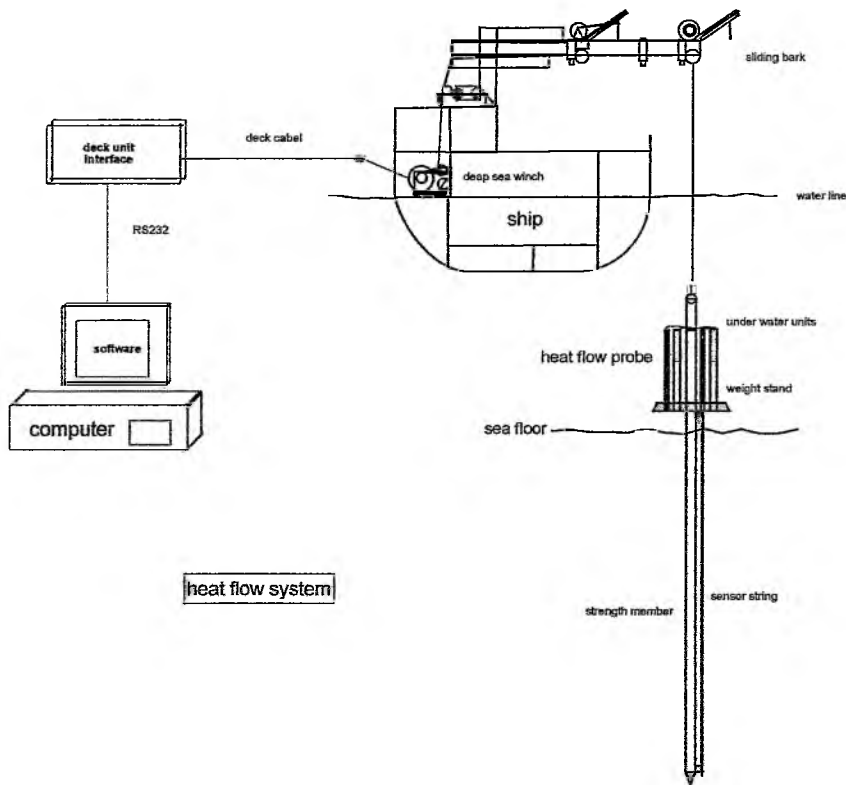


Figure 5.6.1: Operation of HF probes on RV Sonne

3 m HF Probe

The 3m HF probe was normally used in deep sea environments where transient disturbances of temperatures are unlikely to occur and the nature of the sediments likely permits easy penetration to full depth of 3 m.

 Technical specifications of 3 m HF probe:

Probe #:	6845
Heat pulse	600 J/m
Pulse duration	20 sec
Sample rate:	10 sec
Online transmission:	2400 Baud via coax cable

Winch speed during payout and retrieval is 1.0 m/s which generally guarantees full penetration in this working area. Time to equilibrate is assumed to be 7 minutes, time for heat pulse decay observation takes another 7 minutes. Mean time consumption including transit and measurement is 1 – 1 ½ h per single point of measurement.

6 m GHF probe

The 6m Heat Flow probe used during the TIPTEQ Sonne cruise 181-1b was developed in the BmBF funded INGGAS project (BmBF grant 03G0564C) in GEOTECHNOLOGIEN in 2001/2002 at the University of Bremen by Dr. Hans-Hermann Gennerich in the working group of Prof. Dr. H. Villinger as a tool for gas hydrate research.

The mechanically robust up to 6 m deep penetrating heat probe is designed for the operation in a pogo-style mode with a wide application range from 6000 m deep sea trenches with mostly soft sediments to the upper continental slope where sediments are often sandy and difficult to penetrate. Due to the 6 m length of its temperature sensor string undisturbed temperature gradients can be determined even in shallow water where seasonal bottom water temperature variations are superimposed on the undisturbed temperature field close to the sea floor.

The heat probe (Figure 5.6.2) is constructed in the classical "violin bow" design (Hyndman et al., 1979), with 22 thermistors distributed over a total length of 6 m in 0.27 m intervals mounted inside an oil filled hydraulic tube (O.D. 14 mm) which is attached to the strength member (O.D. 130 mm). The sensor tube also contains a heater wire for the generation of high energy heat pulses of typically more than 300 watts for in situ thermal conductivity measurements (Lister, 1979). Only non-corrosive steel was used for the heat probe, with a special high strength non corrosive steel for the strength member and the fins attaching the sensor tube to it.

The complete data acquisition unit including power supply is housed in a single 110 mm O.D. x 300 mm long titanium pressure case and mounted inside the probe's weight stand, whose weight can be adjusted with additional steel plates of up to 2000 kg total weight to allow enough penetration in the case of stiff sediments. A second pressure case of the same size houses the energy for heat pulses and echo sounder.

The signal of the temperature sensors is measured with a resolution of 20-bit at a sample rate of 1 sec, resulting in a final temperature resolution of better than 1 mK at ambient sea floor temperatures. A carefully calibrated PT-100 seawater sensor on top of the weight stand allows to measure the absolute bottom water temperature and to check the calibration of the sensor string in deep water with high accuracy. Inclination and acceleration of the probe is measured

also with a 1 sec sample rate to monitor the penetration process into the sediments and potential disturbances during the measurement period while the probe sits in the sediment. Data from a pressure sensor in conjunction with an acoustic altimeter allow the exact absolute measurement of the final penetration depth of the probe.

The complete data set is stored in the probe but also transmitted via coax cable on board in real time where the data are visualized and stored with a PC. The operator always has complete control of the instrument which allows operational decisions during long term deployments.

In addition the heat probe can be operated in a completely autonomous mode with internal data storage and automated heat pulses if a coax cable is not available. The battery capacity allows for 3 days continuous operation in a pogo-style mode.

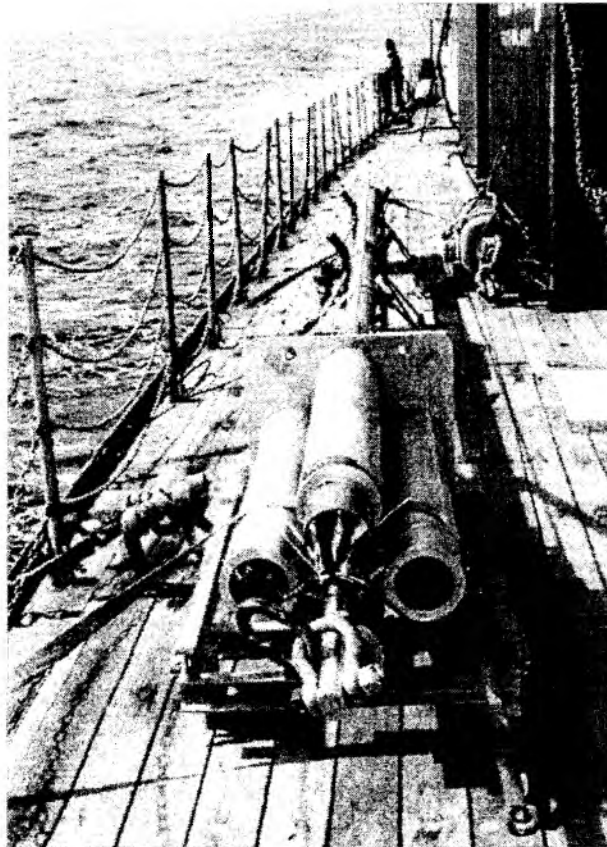


Figure 5.6.2: The 6 m GHF Heat Flow Probe on Deck of RV Sonne during cruise 181-1b

Processing of heat flow measurements

In order to illustrate the steps involved to process a heat flow measurement, Fig. 5.6.3 shows a typical unprocessed data set of the GHF probe. Determination of undisturbed sediment temperature and in situ thermal conductivity follow the pulsed needle probe method (Lister, 1970). When the sensor string penetrates the sediment the friction between sensor tube and sediment creates heat resulting in a temperature rise. The following temperature decay is recorded for a preset time span (7 or 10 minutes, depending on the probe used), after which a

heat pulse of known energy is fired. The heat pulse decay is monitored for at least 7 to 10 minutes until the probe is pulled out of the sediment.

The processing of the raw measurements requires three steps:

1. determine undisturbed sediment temperatures from frictional decay
2. correct heat pulse decay for the remaining effect of the frictional decay
3. calculate in situ thermal conductivities from heat pulse decay.

The basic design of the processing of heat flow measurements is outlined in Hyndman *et al.* (1979) which was basically a manual procedure based on the work of Lister (1970) and Lister (1979). The steps described here are the same for both probes.

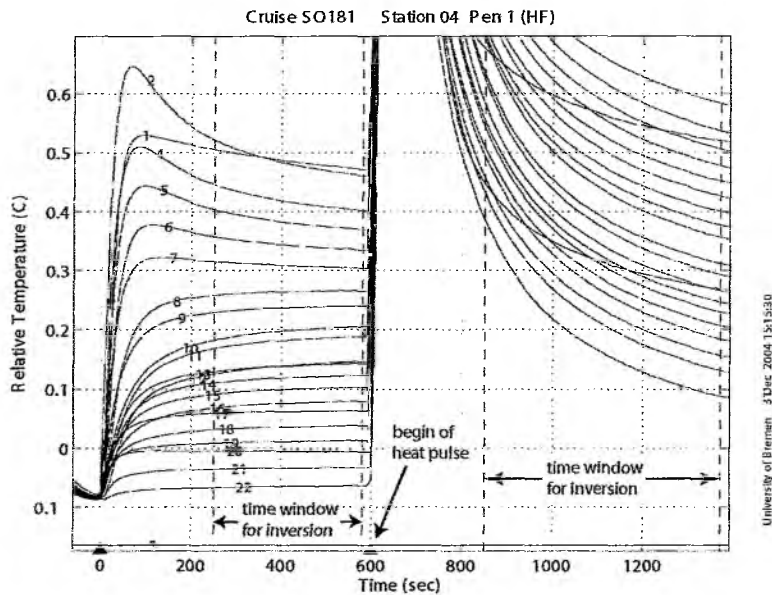


Figure 5.6.3: Unprocessed temperature record of a heat flow measurement with the 6m-long, 22 channel heat probe (GHF). Sensor '1' is the lowermost, sensor '22' the uppermost sensor; spacing between sensors is 0.27 cm. Sensor '3' is not functional and set to a preset value.

The theoretical background for the analysis of heat flow measurements is discussed in Bullard (1954), Lister (1970), Hyndman *et al.* (1979), Villinger & Davis (1987) and Hartmann & Villinger (2002). The following simplified model for the sensor string is used: a cylinder of radius a and infinite extent in the z -direction is situated in a homogenous infinite material. Whereas the material surrounding the cylinder has a finite thermal conductivity k and thermal diffusivity κ , the cylinder itself is of infinite conductivity and diffusivity, with the constraint that $(\rho c)_c$, the product of specific heat c and density ρ of the cylinder, remains finite. At time $t = 0$, the cylinder is at temperature T_0 and the ambient space at T_a . The temperature at the centre $r = 0$ of the cylinder can then be described by the thermal decay curve of the cylinder, described in detail in the literature cited above.

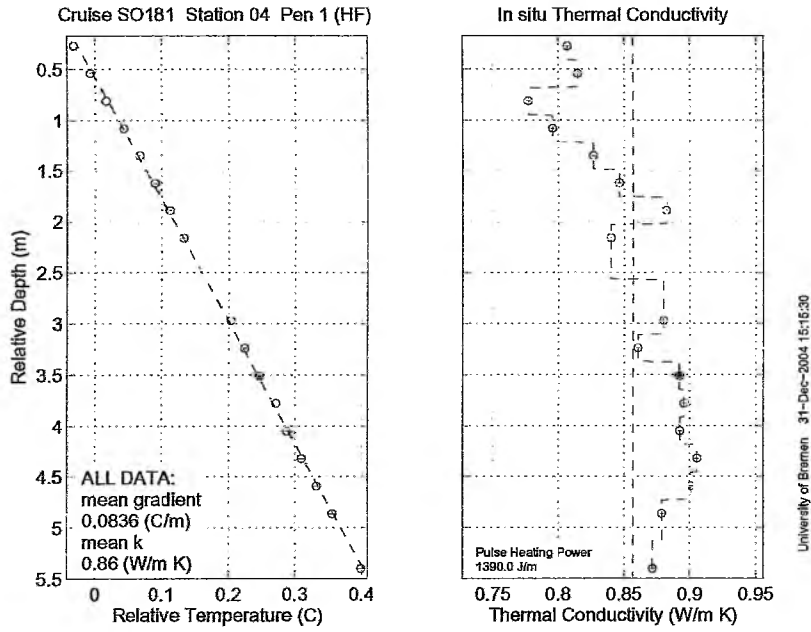


Figure 5.6.4: Estimates of in situ temperatures (left) and in situ thermal conductivity (right) vs. depth, derived from the temperature measurements shown in Figure 5.6.3.

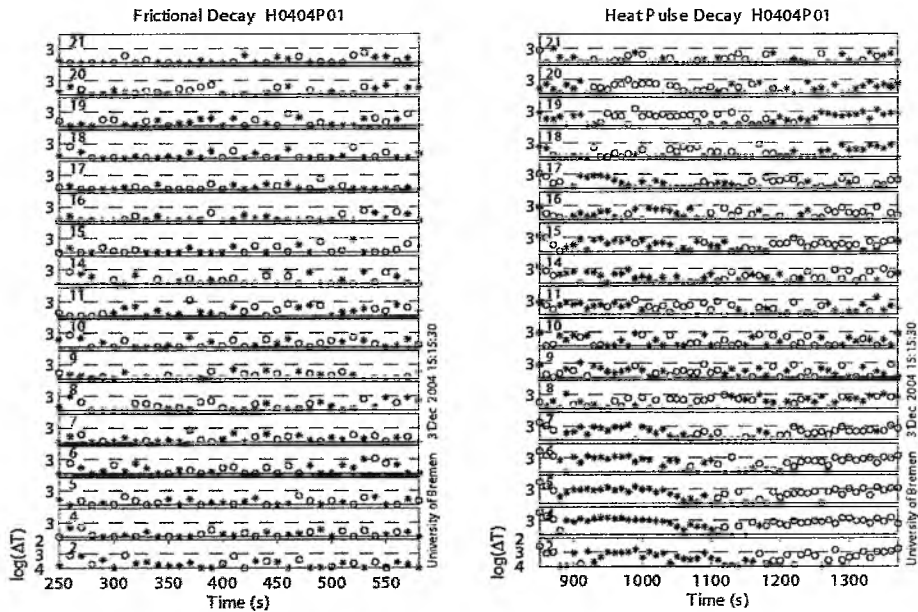


Figure 5.6.5: Temperature difference between measurements and the assumed temperature decay model as quality control for the inversion process (left: penetration decay; right: heat pulse decay).

Measurements of the temperature decay immediately after penetration or immediately after firing of the heat pulse will be inherently affected by geometric deviations from the one-dimensional model with radial symmetry and a Dirac-type temperature disturbance. Therefore, these records have to be excluded from analysis. However, temperatures within the analysed time range still show slight deviations from the ideal behaviour. This deviation can

be best modelled by introducing a new parameter, the time-shift t_s . The measured time origin is always the onset of the penetration or heat-pulse. Introduction of the parameter t_s approximates the heating of finite length by an instantaneous temperature rise, shifted relative to the onset of the heating. Although mathematically not rigorously proven, this concept is reasonable from a physical point of view and has been shown to provide reliable results (Hyndman *et al.*, 1979; Villinger & Davis, 1987; Hartmann & Villinger, 2002).

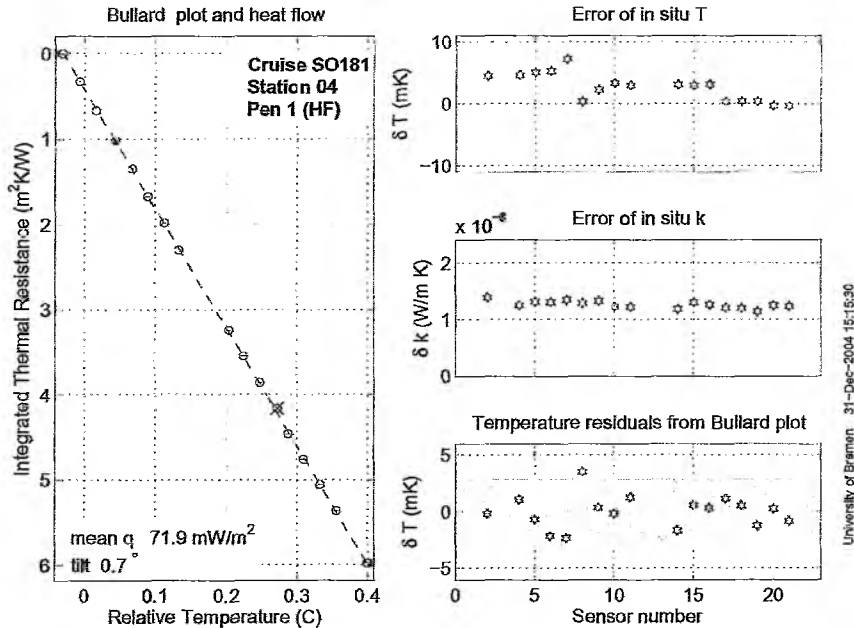


Figure 5.6.6: Bullard plot (left) and errors of in situ temperature and thermal conductivity (right), calculated on the basis of the temperature and thermal conductivity profiles shown in Figure 5.6.4.

To overcome deficiencies of the processing routine described in Villinger & Davis (1987) and to incorporate platform independent plotting routines, a mathematically sound inversion scheme of observed temperature decays was implemented in a program called T2C, using Matlab®, a widely used software package for numerical analysis. This allows creation of a very compact code for the inversion, on-screen graphics and plots. In addition, automated processing or reprocessing of a large number of individual measurements is possible. The inversion of the integral describing the decay of a temperature pulse allows the use of the same algorithm for the calculation of undisturbed sediment temperatures (using the frictional decay) and thermal conductivities of the sediment (using the heat-pulse decay). Inversion theory allows the calculation of realistic errors in a well-defined and mathematically rigorous way based on the sample rate and temperature resolution used.

Before the data can be processed, the complete temperature-time record of one station has to be separated into individual penetration data files which contain only the temperature measurements while the probe has penetrated the seafloor. A plot of the raw data (Figure 5.6.3) helps to identify bad temperature records or sensors which did not penetrate and therefore record only bottom water temperatures. These channels which will not be used for analysis are tabled in a file which is read by T2C. In addition, a table is set up which contains assumed conductivities for penetrations with no in situ measurements. These assumed conductivities are based on nearby in situ thermal conductivity measurements.

Figures 5.6.3 to 5.6.6 show a typical example of a temperature measurement and its inversion. In Figure 5.6.3, the temperature rise just after the probe enters the sediment ($t=0$ sec) is caused by frictional heating, which is more pronounced at the lowermost sensors (sensors 1 and 2). The magnitude of this rise depends mostly on the nature of the sediments and can vary substantially. After about 10 minutes a calibrated, 30 sec long heat pulse heats up the sensor string with 1390 J/m. The rate of decay after the heat pulse stops is a measure of the thermal conductivity of the sediments (Lister, 1979). The time window between the dashed vertical lines is used in the inversion with T2C. Figure 5.6.4 shows the basic data set which is needed to calculate the heat flow: temperature vs. depth (left) allows to calculate the temperature gradient which is combined with the in situ thermal conductivity (right, obtained from the inversion of the heat pulse decay) to get the heat flow. The quality of the inversion can be checked by inspecting the differences between model and measured temperatures (Figure 5.6.5), as systematic differences would easily be identifiable in these plots. In the case of varying thermal conductivities with depth, the so called Bullard-Plot (Bullard, 1939) is used to calculate the heat flow by a linear regression of integrated thermal resistance vs. in situ temperatures (Figure 5.6.6, left). The right-hand side of Figure 5.6.6 shows calculated errors of the in situ temperatures and thermal conductivities, based on the inversion algorithm. For the thermal conductivities, these errors are results of the inversion and not an absolute calibration of the whole sensor string. Therefore conservative estimates of the errors of the in situ thermal conductivities are on the order of 1 to 3 %.

5.7 Coring devices

Gravity corer

During SO181-1a and -1b, a gravity corer with tube lengths of alternatively 5 m, 7 m, or 8 m and a weight of approx. 1.5 tons was used to recover sediment mostly from the incoming plate. Before using the coring tools, the plastic liners inside the steel tubes were marked lengthwise with a straight line in order to retain the orientation of the core for subsequent paleomagnetic analysis. Once on board, the sediment core was cut into 1 m sections, closed with caps on both ends and labelled. Cores have been marked SL-xx, where xx is the station number. The one metre sections were consecutively numbered -1, -2, etc., from top to bottom.

6 Work completed and first results

6.1 Hydroacoustic work

SO181-1a

During the first leg, the main focus was to deploy the ocean bottom magnetotelluric stations on the margin wedge and the seismological stations on the incoming oceanic plate. However, the SIMRAD EM120 swathmapping system collected continuously bathymetric data, in total 1780 nm. The data were merged with the data from leg 1b.

SO181-1b

Roughly two weeks of the programme of SO181-1b have been used to map the seafloor offshore southern central Chile. Track lines with a length of 4570 nm have been mapped during 13 surveys. In addition, 484 nm have been collected along four seismic lines, providing in total 5054 nm or 9360 line kilometres of swath mapping bathymetry.

A major aim of the second TIPTEQ leg was to map the continental slope and the incoming ocean plate in the area between the Valdivia fracture zone (named after the town of Valdivia, which is immediately to the north of the fracture zone trace) and the Guamblin fracture zone near 45°20'S. Figure 6.1.1 has a grey scale illuminated image of the seafloor bathymetry in this area. Three major domains can easily be classified: (i) the incoming plate with a well developed abyssal hill fabric of horst and grabens striking roughly NNW-SSE; (ii) a well sedimented deep sea trench without any prominent features, except some mass wasting deposits at the foot of some major canyons cutting through the slope; and (iii) the continental slope with several canyons cutting through this slope. These canyons are more frequent to the south of Chiloe, suggesting that the sediment transport in the south is more vigorous than to the north of Chiloe. However, the trench is well filled along the whole study area, suggesting that sediments are redistributed from south to north along the trench axis. A major topographic gradient may drive this process: the seafloor in the south is roughly 2.5 to 3 km deep, while it is approximately 5000 m offshore Concepcion. In addition, the slope is faulted and little evidence for accretionary ridges is found. However, the deformation front is generally well defined by small folds.

A major target of the mapping campaign was the study of so called bending related normal faults. These faults are believed to be path ways for fluids into the lithosphere. The very thick sedimentary cover in the trench, however, covers these faults in the survey area. Figure 6.1.1 indicates earthquakes that are related to faulting in the incoming plate (white and black dots) and the corresponding fault plane solutions from the Harvard earthquake catalogue for the larger events. Most earthquakes occur in the sediment covered area. In the high resolution seismic reflection data (Section 6.6.2), however, these fault are well resolved in both basement topography and sedimentary record.

The abyssal hill fabric inherently related to the formation process of the oceanic lithosphere at a mid-ocean ridge is well imaged in the western region of the mapped area. These hills reach closer to the trench in the south than in the north. This observation is related to the much younger lithosphere entering the trench in the south. At 45°S / 78°20'W the median valley of the spreading centre was mapped. In addition, the abyssal hill fabric nicely confirms the segmentation of the incoming oceanic plate. Fracture zones clearly cut through the NNW-SSE

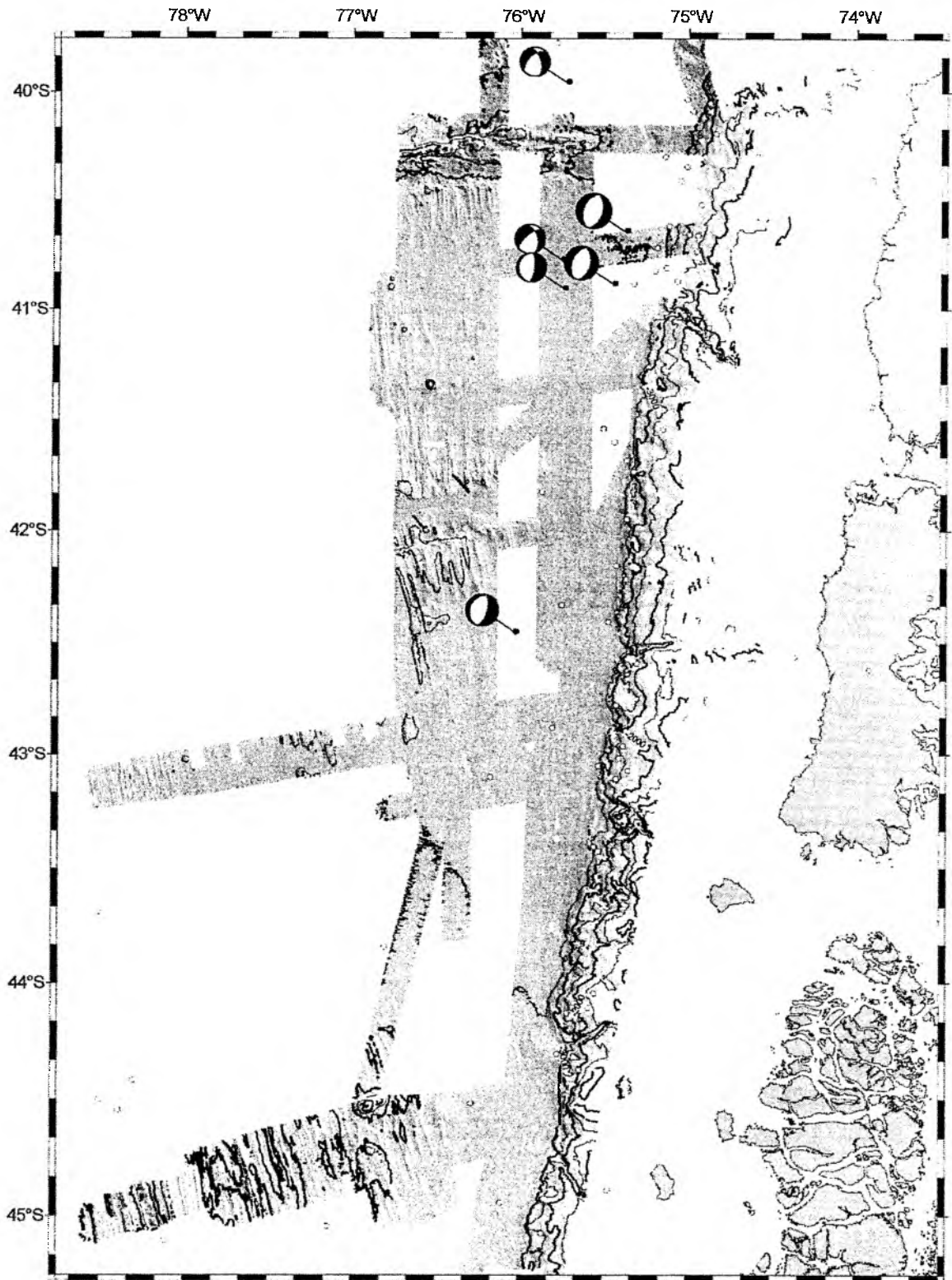


Figure 6.1.1: Grey scale illuminated EM120 bathymetry collected during SO181-1. Circles mark earthquake epicentres; filled circles are larger events with fault plane solutions.

trend of the hills. Moreover, major fracture zones have an impact on the structure of the adjacent continent. Chiloe, for example, is bounded to the north and south by fracture zones, suggesting that the fracture zones entering the subduction channel erode much more effectively the continental margin than the adjacent normal crustal segments.

SO181-2

Bathymetric mapping with the Simrad EM120 multibeam system was continued during SO181-2 in order to extend the bathymetric coverage of the area. In total, some 5000 km of track lines have been surveyed with 632000 pings. The complete bathymetric coverage from all legs of SO181 is shown in Figure 6.1.2. Figure 6.1.3 shows this data merged with all available bathymetric data from other cruises.

Bathymetric data now cover most of the Chilean continental margin between 48°S and 32°S, leaving two gaps, 44°30'S – 43°30'S and 35°30'S – 33°30'S, where only a stripe of the lower slope and the trench have been mapped so far. The results are shown in Figures 6.1.4 to 6.1.7 in more detail. The Southern area between 48°S and 40°S is shown in Figures 6.1.4 and 6.1.5. Figure 6.1.4 is based on bathymetric data from SO181 whereas Figure 6.1.5 shows these data merged with available bathymetric data from other cruises. Figures 6.1.6 and 6.1.7 show the Northern area between 40°S and 32°S accordingly.

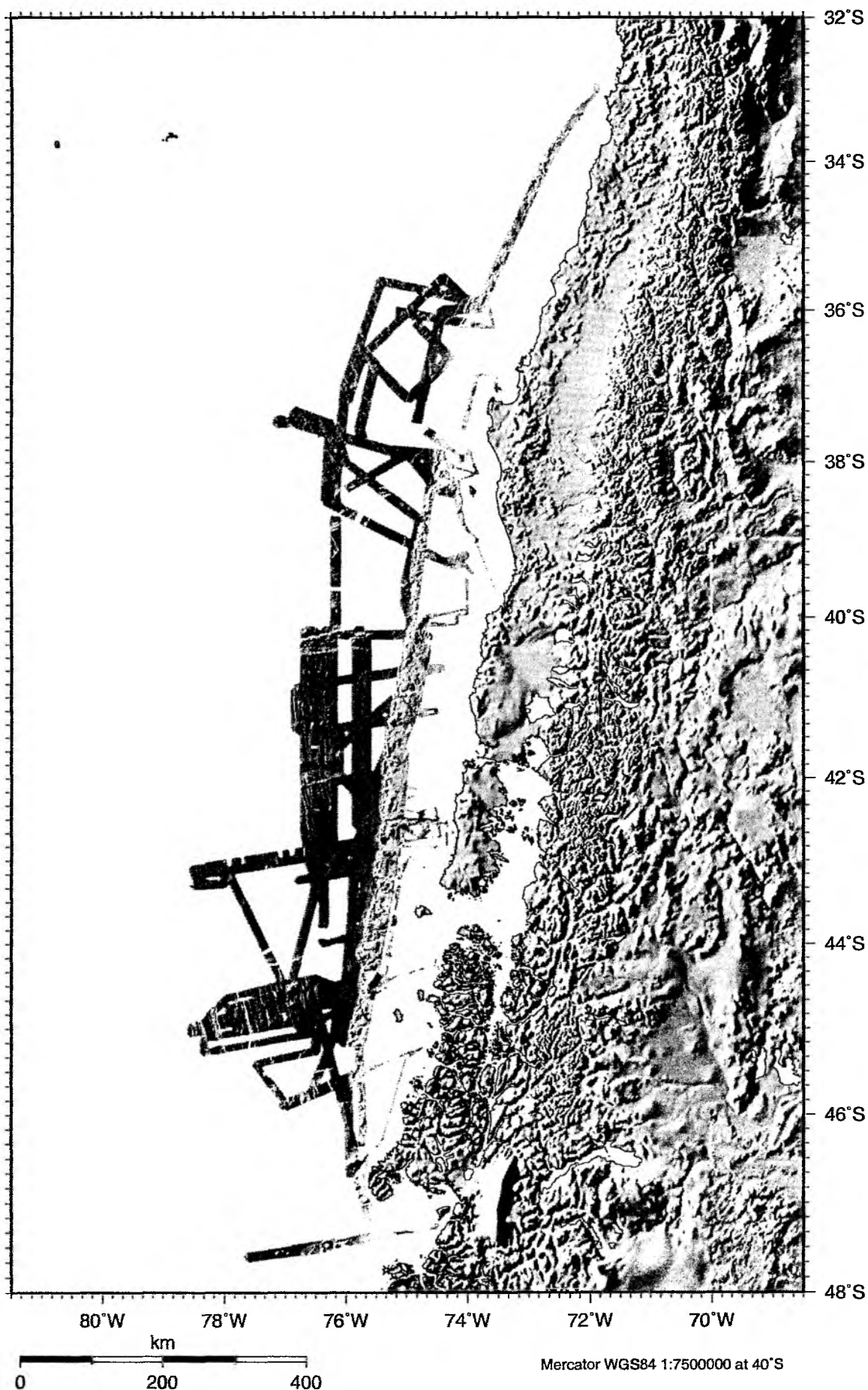


Figure 6.1.2: Grey scale illuminated EM120 bathymetry collected during SO181-1&2

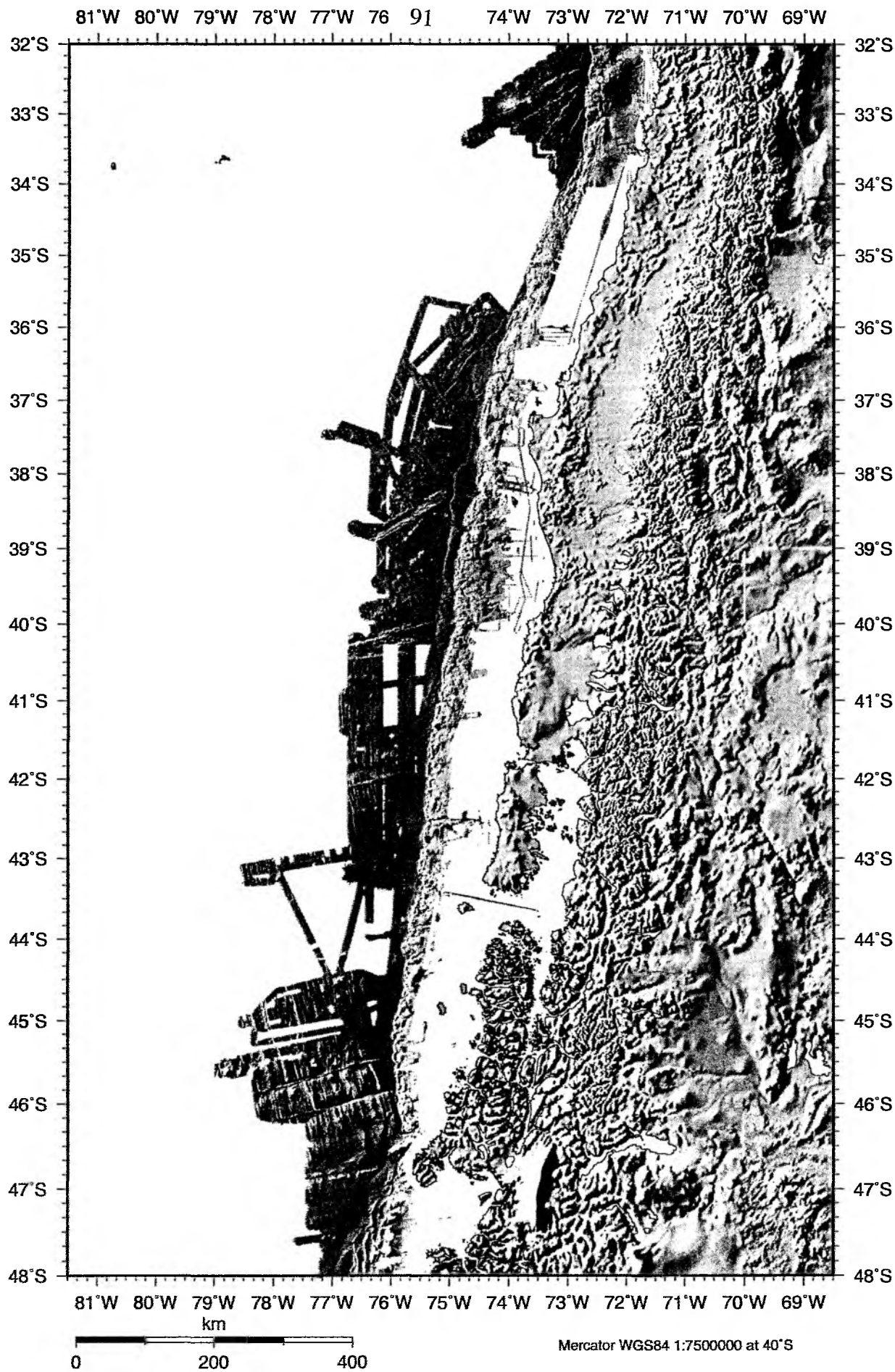


Figure 6.1.3: SO181 bathymetry merged with data from other cruises

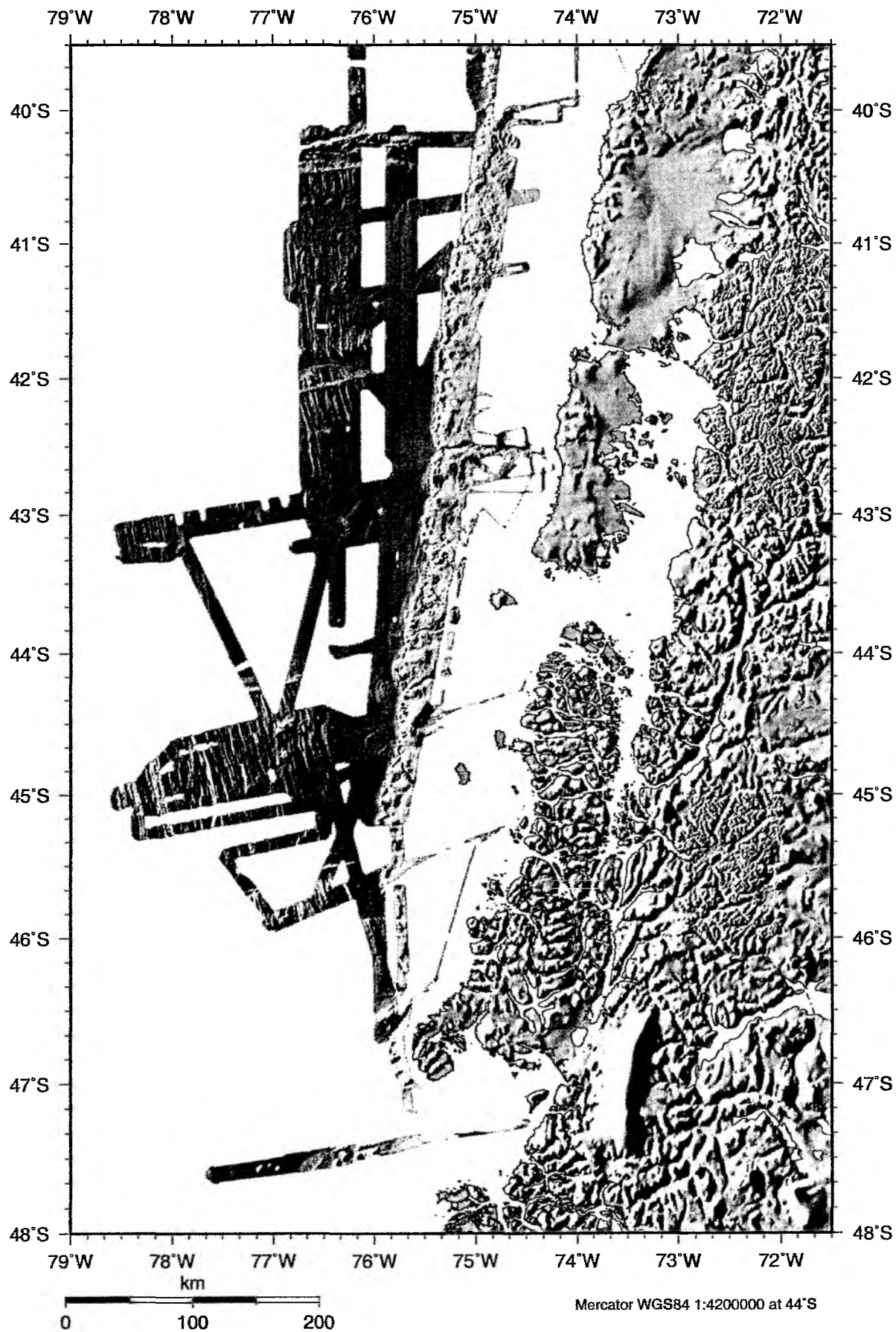


Figure 6.1.4: Grey scale illuminated bathymetry in the Southern Area collected during SO181

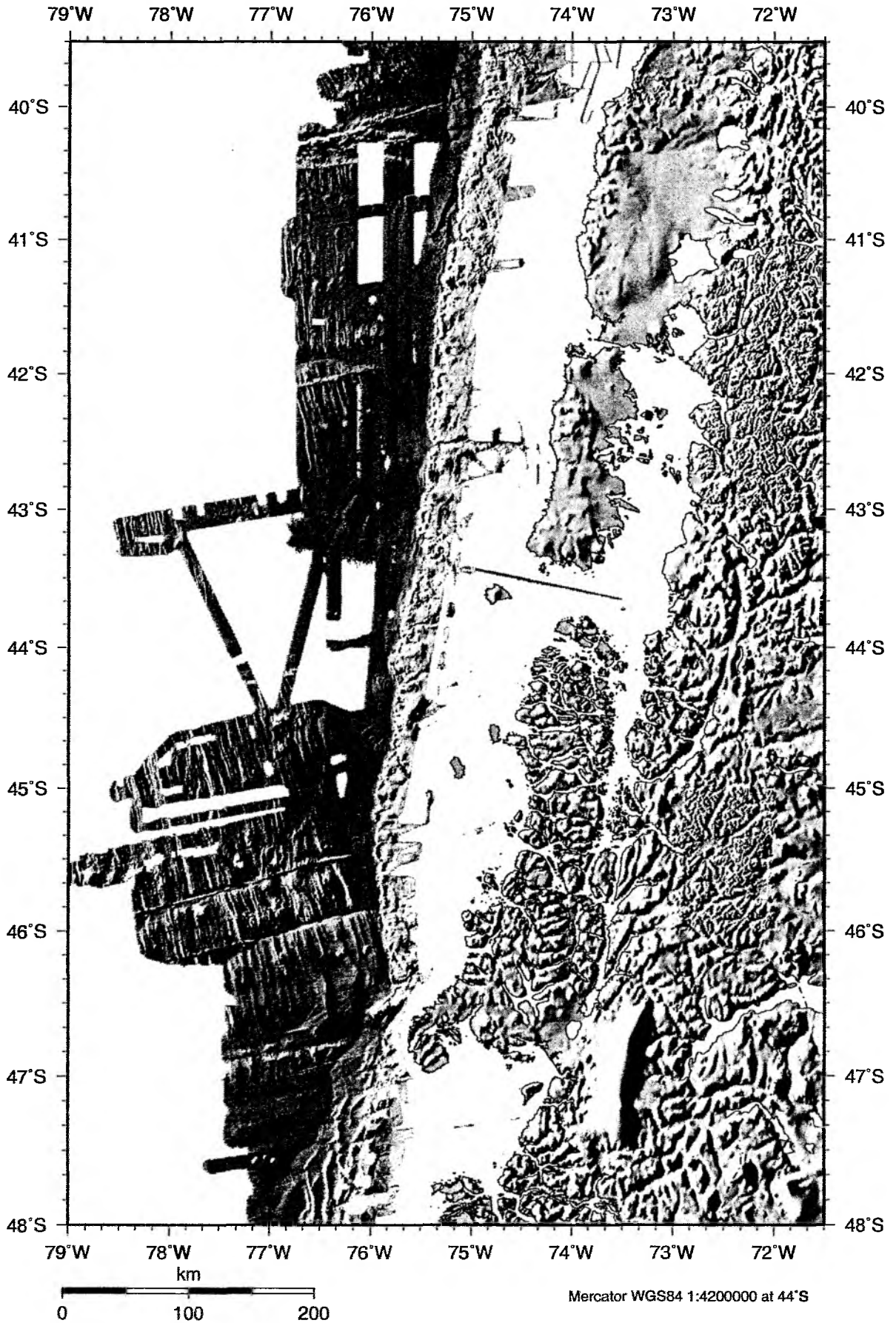


Figure 6.1.5: SO181 bathymetry merged with data from other cruises / Southern Area

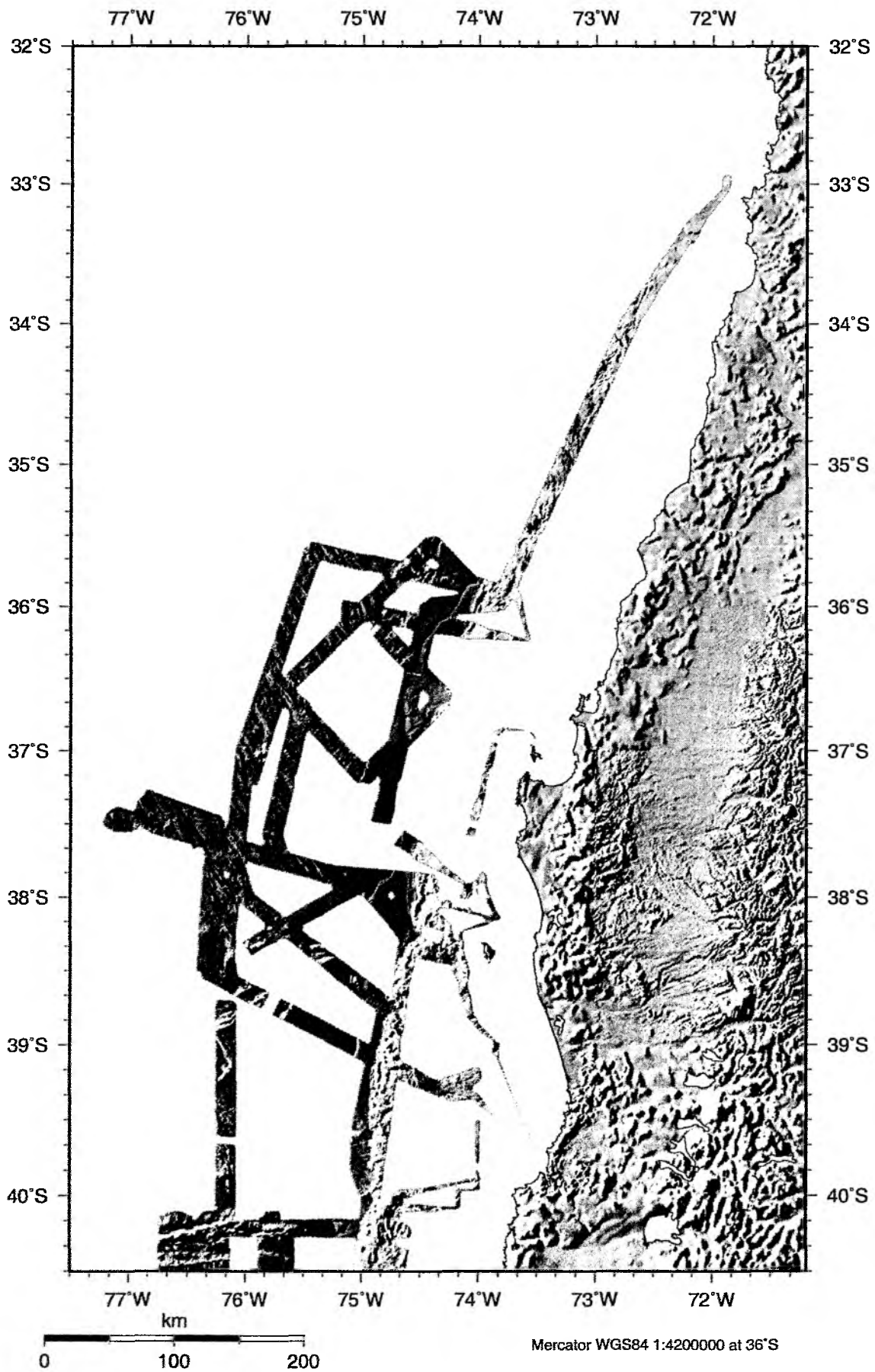


Figure 6.1.6: Grey scale illuminated bathymetry in the Northern Area collected during SO181

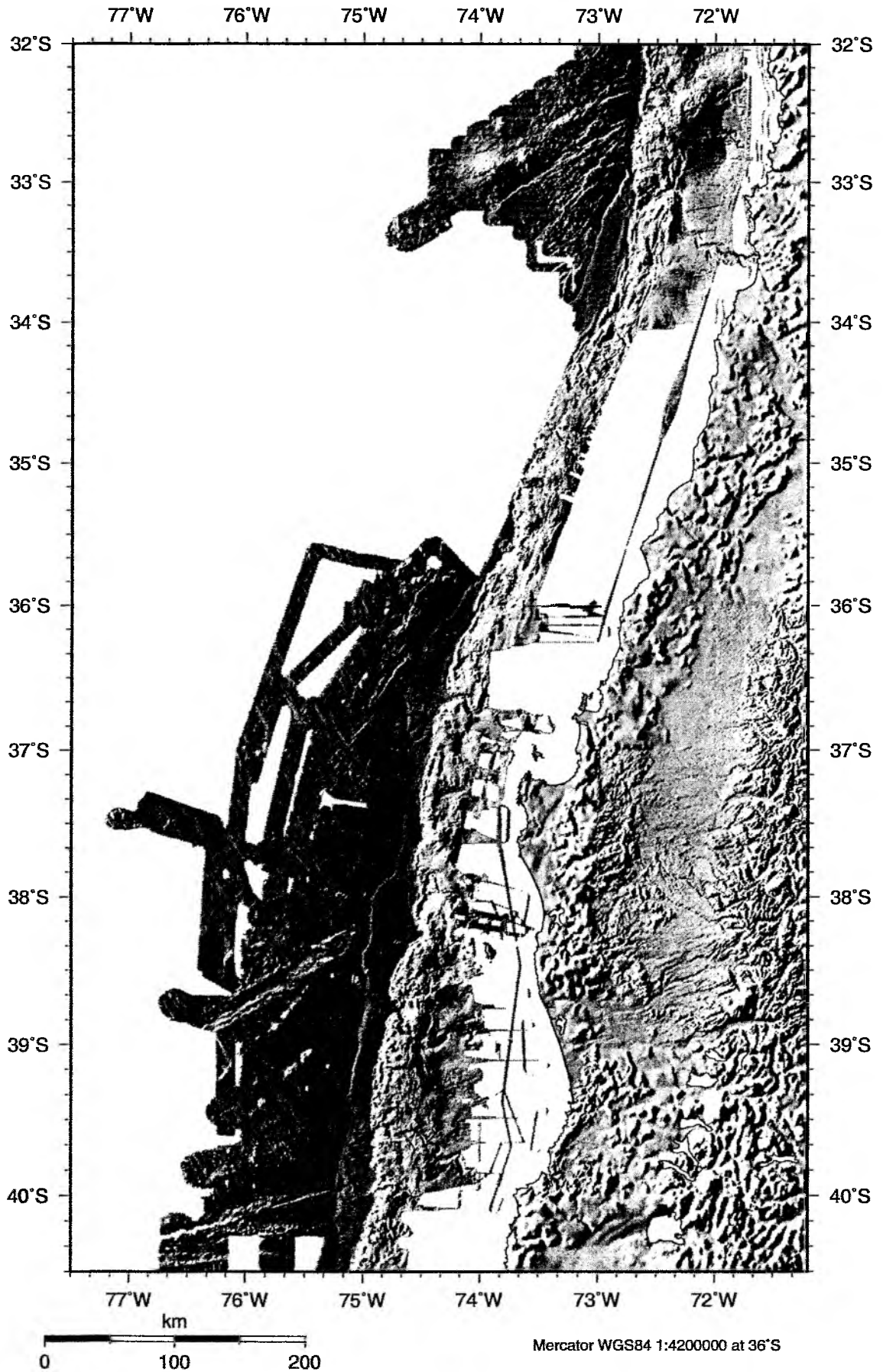


Figure 6.1.7: SO181 bathymetry merged with data from other cruises / Northern Area

6.2 Discussion of heat flow results

Oceanic heat flow decreases with increasing crustal age as described by the Parson-Sclater model of a conductively cooling lithosphere. The agreement between model and observations is best for crustal ages over about 40 to 60 Mio years. The heat flow pattern on young to middle-aged oceanic crust is generally characterized by hydrothermal exchange processes between ocean and upper crust which lead to a large scatter of high and low heat flow values over comparatively small distances. The pathways for the exchange are small seamounts or outcrops along basement ridges where cold seawater penetrates the upper crust and cools it efficiently. In a situation like north of the Chile Triple Junction or at the eastern flank of the Juan de Fuca Ridge, the situation is somewhat different as the proximity to the continental margin provides a large sedimentary influx which covers even basement highs and small seamounts with impermeable sediments and confines the circulation mostly to the upper basement levels. This will in general smooth the large scatter in heat flow observed elsewhere on crust of comparable age. Rapid sedimentation in the trench will lower the measured surface heat flow, and so undisturbed heat flow will be higher depending on the sedimentation rate. Measurements on the accretionary prism will be compared to BSR-derived heat flow (e.g., Grevenmeyer and Villinger, 2001), which in turn will then be used to calculate heat flow at shallower depth levels where stiff sediments either prevented the heat probe from penetration or where large observed transient temperature disturbances in the upper sedimentary layers do not allow to determine a steady-state heat flow. The overall goal of the heat flow measurements was to constrain the thermal structure of the downgoing slab and the subduction zone.

For the thermal work, the corridor #1 was shifted by some tens of kilometres to the north (Figure 6.2.1) to benefit from thermal data obtained in ODP sites 1234 and 1235 (Grevenmeyer et al., 2003) and from three heat flow stations which have been obtained in 2003 on the Chilean Navy research vessel Vidal Gormaz as joint work between the University of Bremen, IFM-GEOMAR, and the University of Valparaiso. The rest of the main study area was to the south of Valdivia and offshore Chiloe. Heat flow data have also been collected along corridors #2 to #4 (Figure 6.2.2).

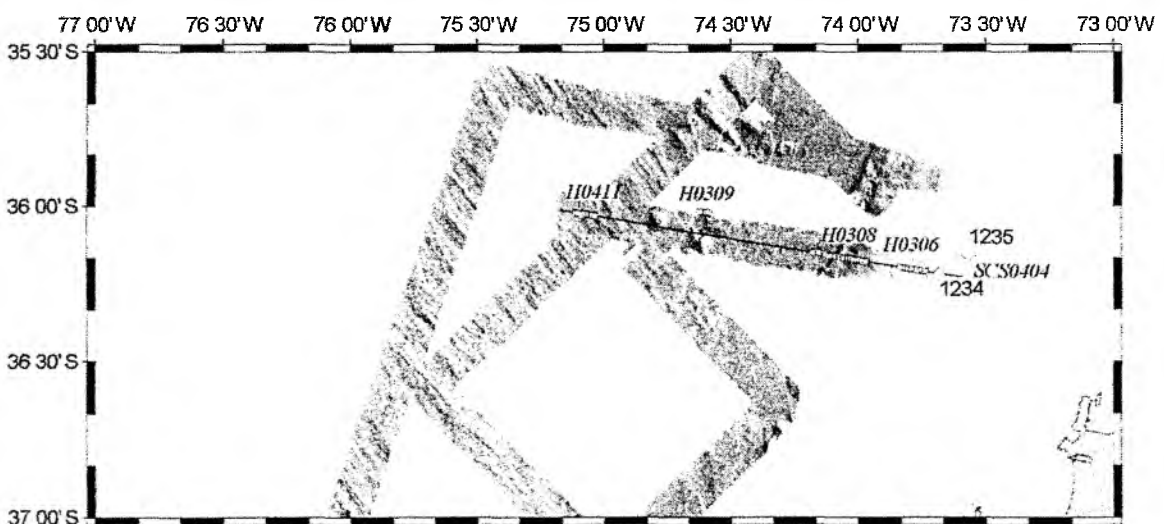


Figure 6.2.1.: Heat flow stations offshore Concepcion. Stations H0306, H0308 and H0309 have been obtained in 2003 aboard the Chilean Navy research vessel Vidal Gormaz; 1234 and 1235 mark ODP drill holes with temperature measurements.

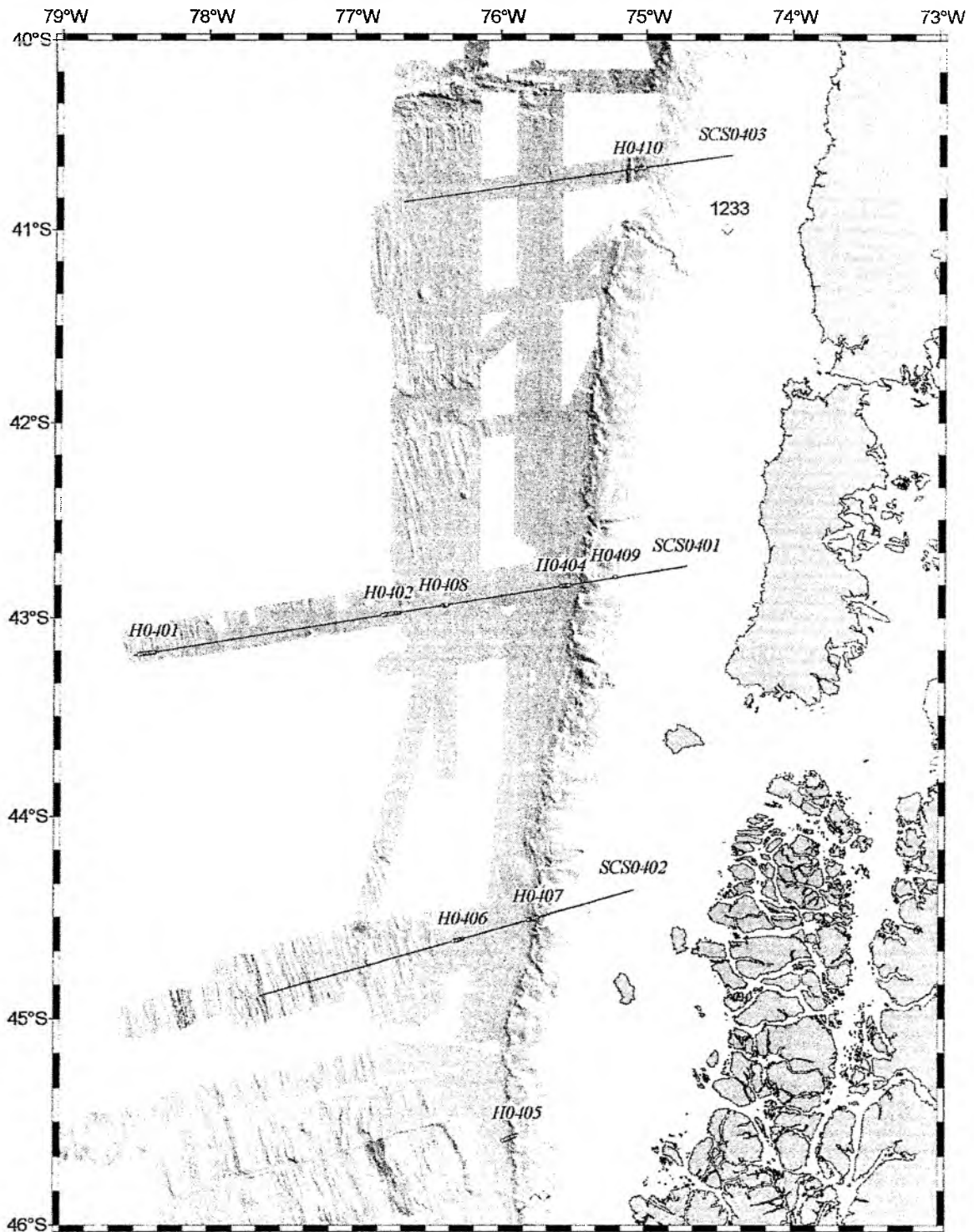


Figure 6.2.2: Main study area: heat flow stations to the south of Valdivia. Diamonds represent ODP drill sites.

Heat flow station H0405

Heat flow station H0405 (Figure 6.2.3) is located just north of the ODP drill sites of Leg 141 and extends from the trench upslope to a water depth of about 2500m . Values in the trench of

around 200 mW/m^2 are fairly uniform and decrease to values around $50\text{--}70 \text{ mW/m}^2$ landward of the deformation front. The low values in the trench which are far too small for a crustal age of about 1.5 Mio years can be explained by sedimentation effects. Values on the slope are in the same range as the ones measured further south at ODP site 859 (Leg 141).

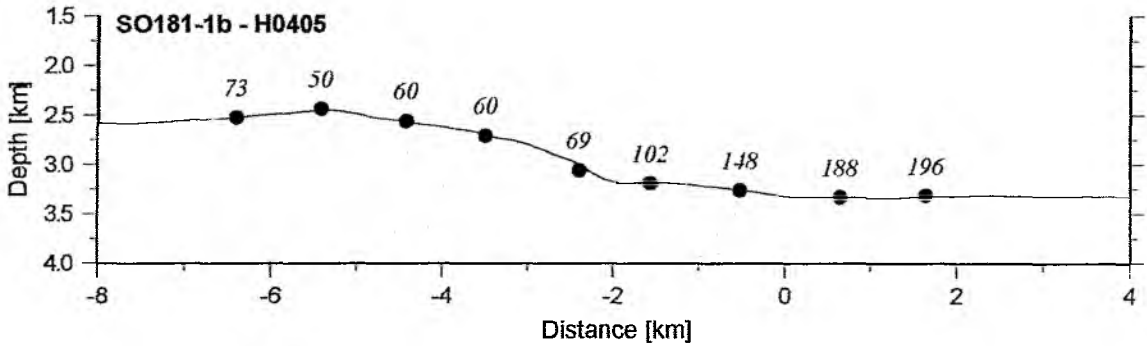


Figure 6.2.3: Heat flow stations along RV Conrad line 743 – corridor #4.

Heat flow stations H0407, H0406 on SCS02-2

Heat flow station H0407 (Figure 6.2.4) on SCS02-2 covers the accretionary prism and the deformation front. Values at the prism are uniform around 70 mW/m^2 and then increase towards the deformation front. The last two measurements right at the deformation front failed as the probe did not penetrate the sediments. The seismic section shows clear indications of a large scale slump in this area.

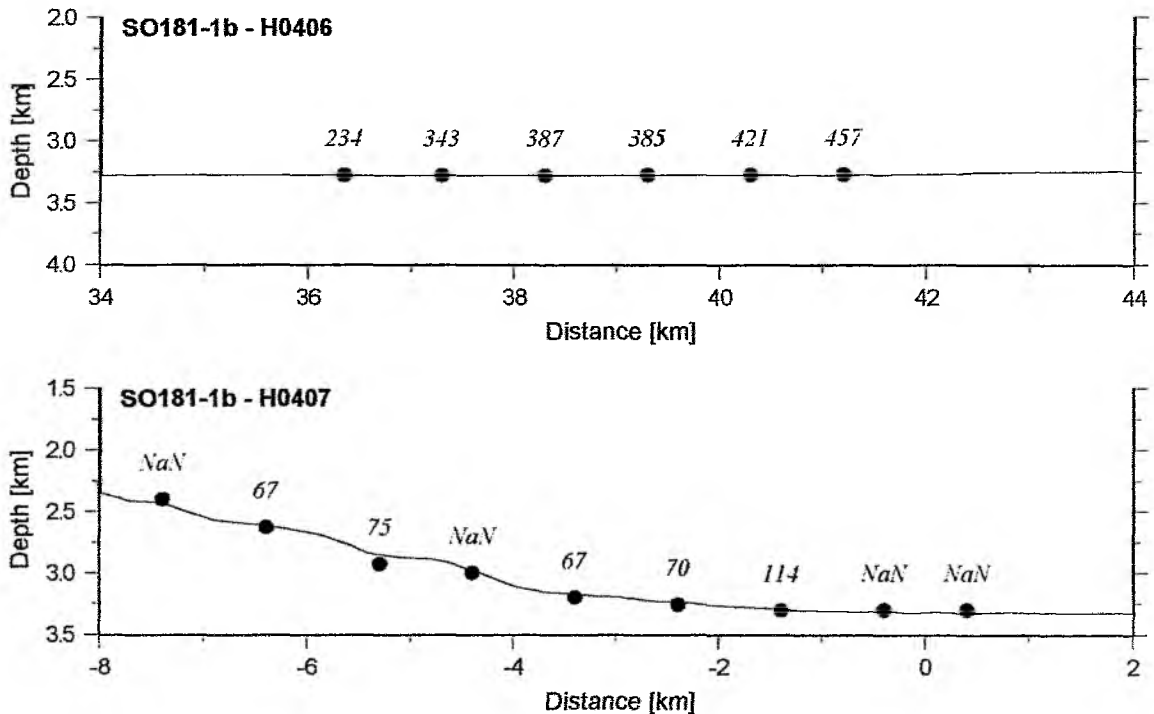


Figure 6.2.4: Heat flow stations along SCS02-2 – corridor #3.

Heat flow station H0406 (Figure 6.2.4) runs from the trench up the outer bulge. Values here are very high increasing steadily from about 230 mW/m^2 to 450 mW/m^2 over a distance of only about 5 km. Unfortunately only 5 measurements were successful due to malfunction of the heat probe.

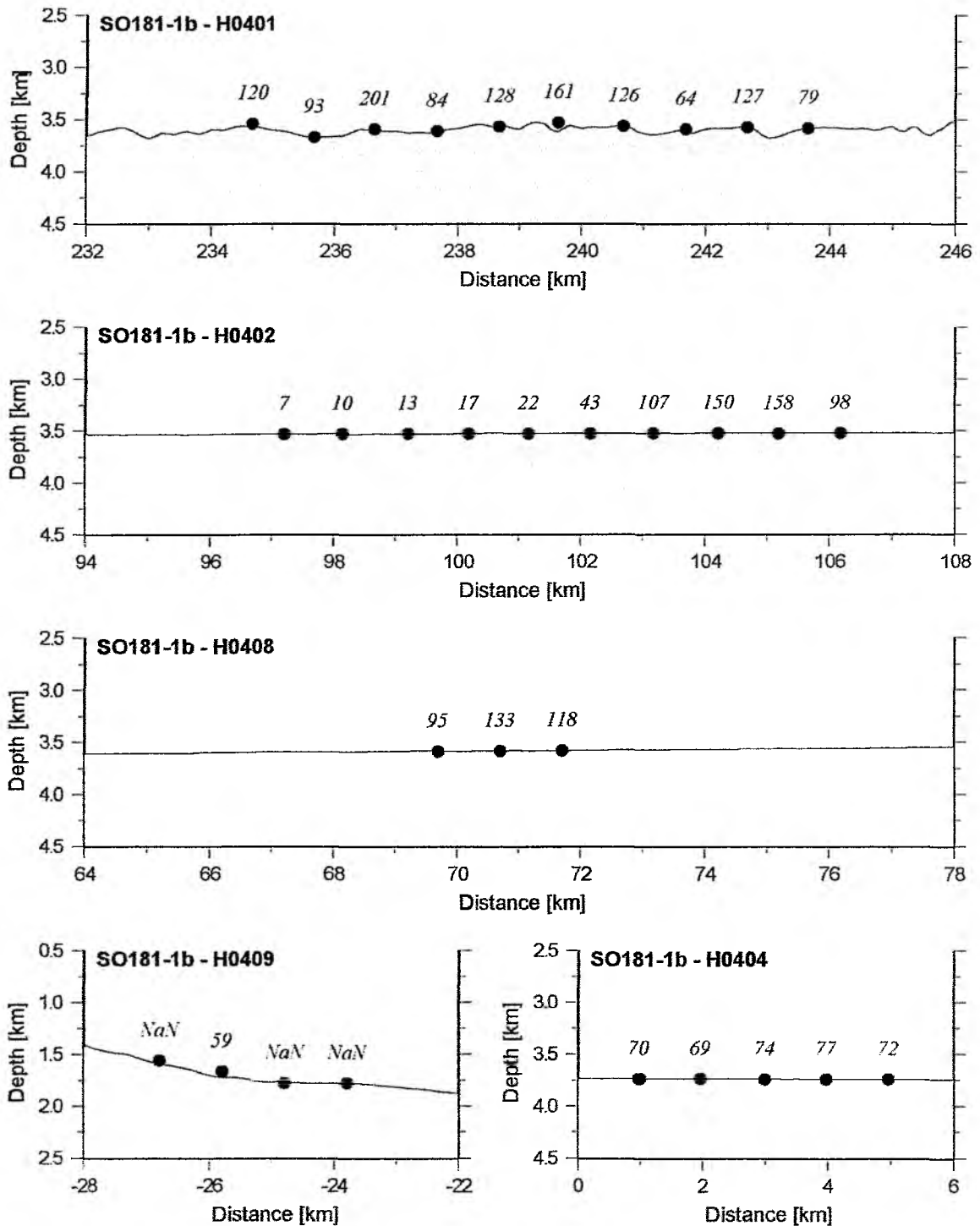


Figure 6.2.5: Heat flow stations along SCS01 – corridor #2.

Heat flow stations H0409, H0404, H0408, H0402 and H0401 on SCS01

Heat flow station H0401 at the westerly end of SCS01 (Figure 6.2.5) on 14 Ma old crust reflects the exchange processes between ocean and upper crust with its varying heat flow although a continuous sediment cover smoothes this variations substantially. Heat flow on H0402 is as low as 7 mW/m^2 and increases rapidly by almost a factor of 20 within less than 10 km. These low values can only be explained by a very efficient inflow of cold seawater into the oceanic crust through a basement outcrop located about 5 km north of the profile. Heat flow scatters around 100 to 150 mW/m^2 towards the trench where it becomes more uniform but substantially lower with about 70 mW/m^2 . Measurements upslope landward of the deformation front were not successful due to stiff sediments except in one place where the probe barely penetrated but gave a reliable measurement of 59 mW/m^2 .

Heat flow station H0410 on SCS03

Heat flow station H0410 on the accretionary prism (Figure 6.2.6) shows values which increase from about 35 mW/m^2 close to the deformation front to values of close to 50 mW/m^2 higher up slope. These values will be used in conjunction with the observed BSR to calibrate BSR-derived heat flow estimates.

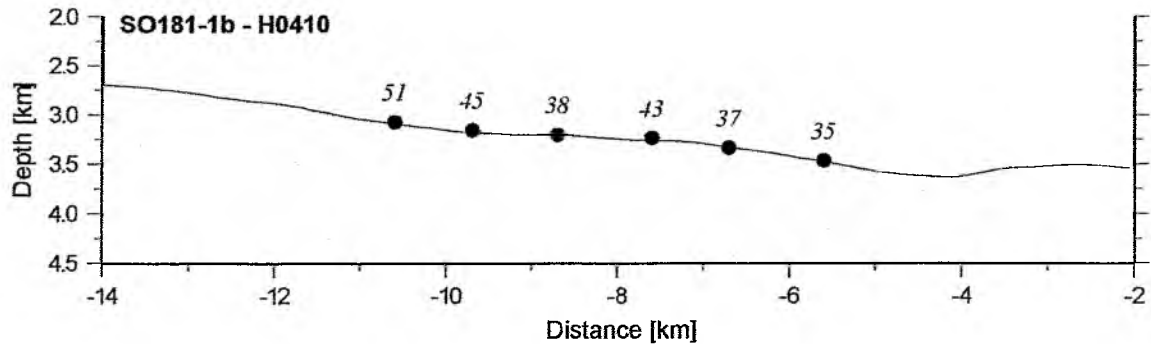


Figure 6.2.6: Heat flow stations along SCS03.

Heat flow station H0411 on SCS04

Heat flow station H0411 (Figure 6.2.7) on ~30 Ma old crust shows surprisingly low values of around 20 mW/m^2 with one exception where heat flow is over 70 mW/m^2 . The low values compare very well with measurements in the trench made during a Chilean-German heat flow survey in 2003 on the same profile but with measurements located much closer to the trench and in the trench itself. One explanation for these low values would be efficient cooling due to exchange processes far away from the trench and significant sedimentation effects on heat flow in the trench itself. However, in order to test this hypothesis one would have to observe other areas with higher heat flow far from the trench as well. Lack of time prevented us from additional survey along SCS04.

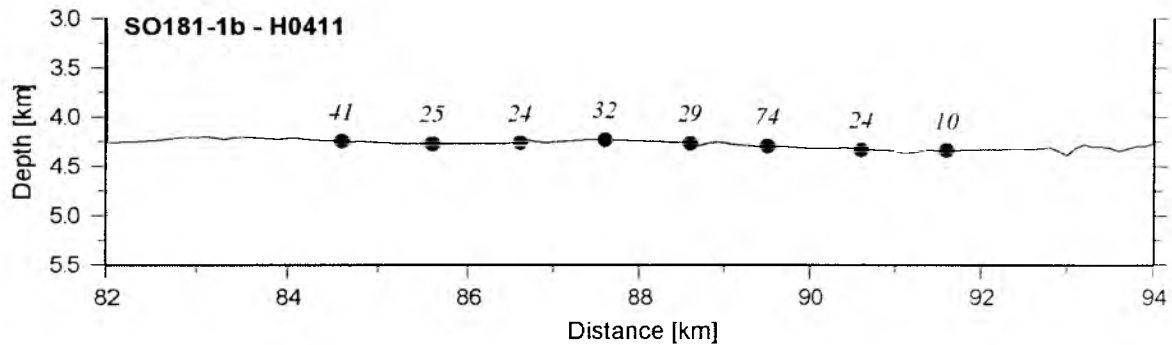


Figure 6.2.6: Heat flow stations along SCS03.

6.3 Geological sampling

Leg 181-1a

During Leg SO181-1a, a total of 12 gravity cores were taken in the northern and central parts of the study area. This included samples from the area north of TIPTEQ corridor #1 to the latitude where corridor #3 is located. Recovery depended largely on grain size and strength of the sediment. In most places, clayey muds with silt and fine sand were recovered. In some of the deep sea fans sampled, however, coarser-grained sandy turbidite interlayers prevented recovery of long cores. A list of cores taken is provided in Appendix 9.6, where the exact locations, water depths, and lengths of recovered cores are given. For more convenient reference, the coring locations are also plotted on a map (Figure 6.3.1).

All cores were cut into 1 m segments immediately after recovery, and stored in the refrigerated core store aboard RV Sonne at 4°C. The core catcher materials were used for initial sediment description before being preserved in sample bags in the freezer (-32 °C) for shore-based analyses such as pore water geochemistry.

The sediments recovered during Leg 1a can be divided into three categories:

- i) hemipelagic muds,
- ii) clayey to silty and sandy deep-sea trench deposits, and
- iii) deep-sea trench fan deposits, mostly silty or sandy.

Hemipelagic muds were recovered in cores SL-181-09 and SL-181-10, both located some 50nm seaward of the trench along corridors #2 and #3, respectively. The dark grey to dark olive grey fine-grained deposits appear homogeneous, however, a detailed description will be carried out onshore.

Trench sediments were cored at stations SL-181-01, SL-181-03, SL-181-11, and SL-181-12. The material is characterized by fine- to medium grained muds and turbidites.

Similarly, the trench fan deposits consist of fine- to medium-grained turbidites (stations SL-181-02, SL-181-04, SL-181-05, SL-181-6, SL-181-07 and SL-181-08); rarely, dark grey to very dark grey coarse-grained sand layers (cm-thickness) were observed. Detailed analyses and dating will follow onshore.

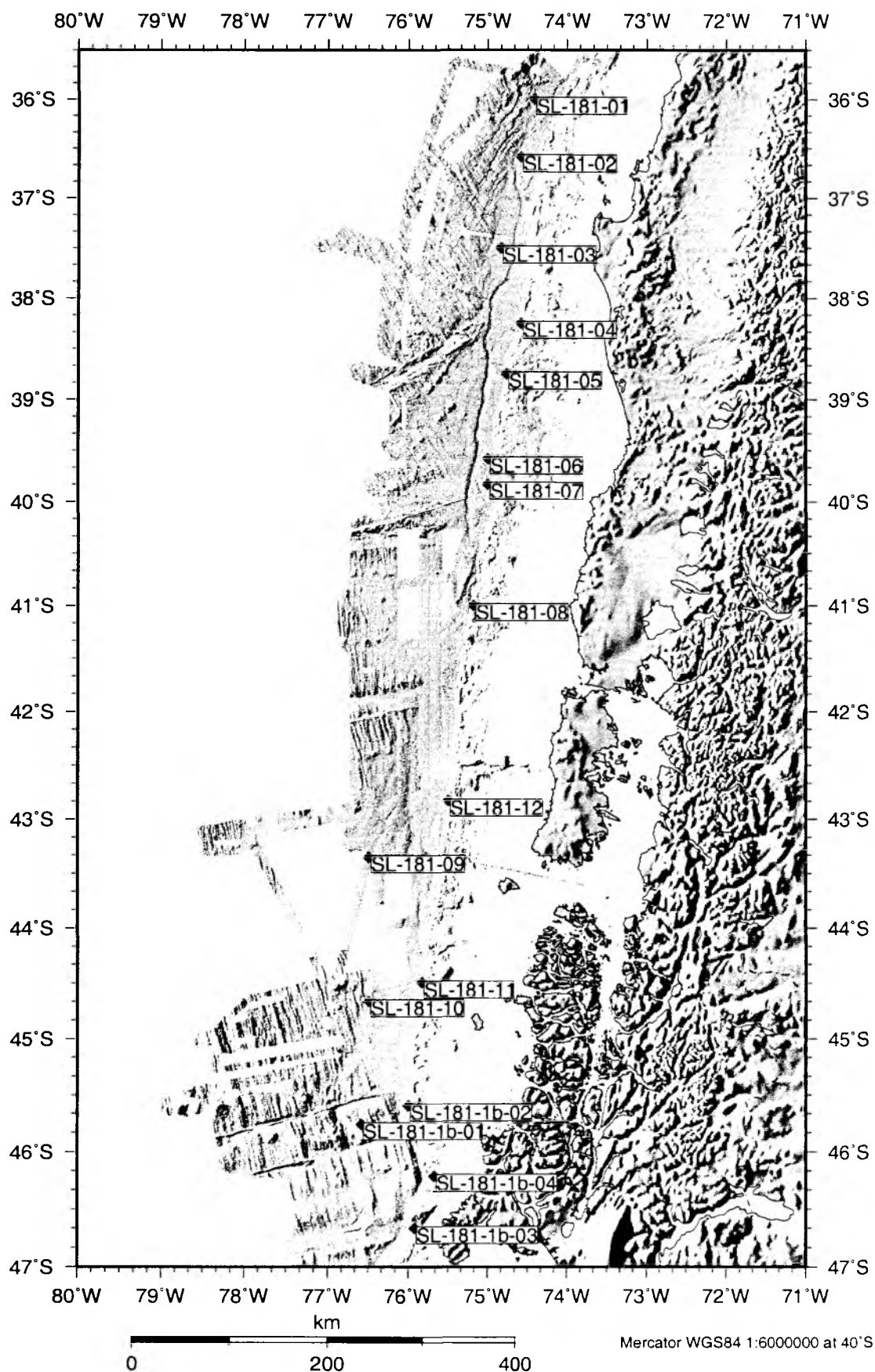


Figure 6.3.1: SO181 gravity core locations.

Leg 181-1b

During SO181-1b, a total of 4 gravity cores were taken in the southern part of the study area. This includes two cores in the area of corridor #4, one slightly south of this corridor and one of three planned cores over a normal fault scarp. Unfortunately only the core at the uppermost part of the normal fault was sampled successfully. Further information about all recovered cores, including exact location, water depth and core length, is provided in Appendix 9.6. and Figure 6.3.1 shows the stations on a map.

Recovery depended largely on the topography of the seafloor, grain size and strength of the sediment. Clayey mud with layers of silt and fine sand dominated most of the recovered sediment at stations SL-181-1b-1 and SL-181-1b-2. The longest cores of Leg 1b with up to 5 m were recovered here.

At station SL-181-1b-3, coarser grained sandy turbidite interlayers prevented a sediment penetration of more than 2.4 m.

Station SL-181-1b-4 is located above the upper part of a normal fault scarp. At this station the water depth of approximately 1500 m was the least of all stations during Legs 1a and 1b. The recovered sediment was silty and sandy clay of dark grey to black colour. Pieces of wood with diameters of centimetres occurred and the sediment had a foul smell. A sediment penetration of more than 2.7 m was not possible.

The two stations above the lower parts of the normal fault scarp could not be sampled successfully. After several tries, the liner stayed empty except for some small rock fragments which indicated a surface too hard for gravity core penetration. The steep topography of the seafloor might have prevented penetration as well.

All cores were cut into 1 m segments immediately after recovery and stored aboard R/V SONNE in a refrigerated core store at 4° C. Material from the core catcher was sampled in sample bags and preserved in the freezer at -32° C for shore-based analyses such as pore water geochemistry.

Detailed geotechnical analyses and dating of all taken sediment cores will take place onshore.

6.4 Magnetotellurics

Previous long-period magnetotelluric studies in the Southern Chilean Andes revealed a modest high conductivity zone (HCZ) in the lower crust beneath the active volcanic arc and an additional HCZ associated with the Lanahue fault in the forearc, running obliquely to the main morpho-structural units. Another previous finding was based on the anomalous behaviour of geomagnetic induction vectors, which point consistently NE over the whole study area instead of the expected E direction due to the presence of the highly conducting Pacific Ocean. This spectacular effect is (and can only be) explained by anisotropy of the lower crust.

To corroborate these unexpected results, a combined on-/offshore magnetotelluric experiment was carried out in southern hemisphere summer 2004/2005 along a profile running perpendicularly to the trench and the volcanic arc from the incoming plate to the Argentinean border between 37.5°S and 39°S (Figure 6.4.1). As part of the multi-disciplinary TIPTEQ program, it aims especially at imaging fluids in the interface between the downgoing Nazca and the overriding South American plate (Figure 6.4.2).

The offshore part of the profile that runs from the oceanic plate beyond the trench to close to the coast was carried out during the cruise SO181. A total of 7 ocean bottom instruments (HEFMAG) developed at the Woods Hole Oceanographic Institution were deployed on the ocean bottom in December 2004 along the profile with a station spacing of approximately 30-35 km and a depth range between 560 m (for the station above the continental slope) and about 4600m (for the stations above the oceanic plate).

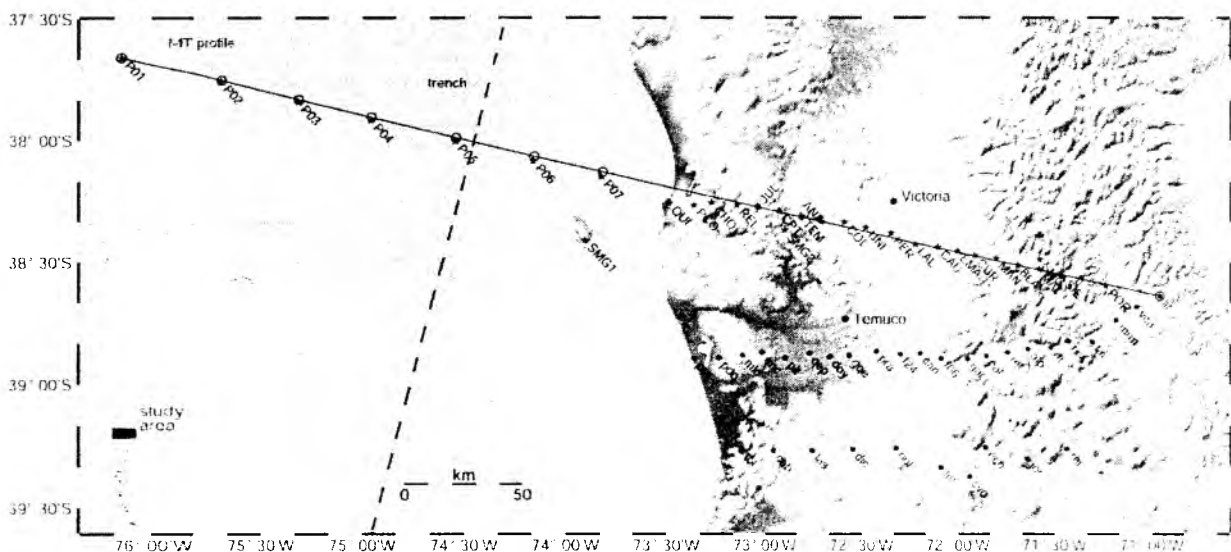


Figure 6.4.1: Northern part of the survey area of the TIPTEQ projects from December 2004 until February 2005 with locations of on-/offshore long period electromagnetic sites.

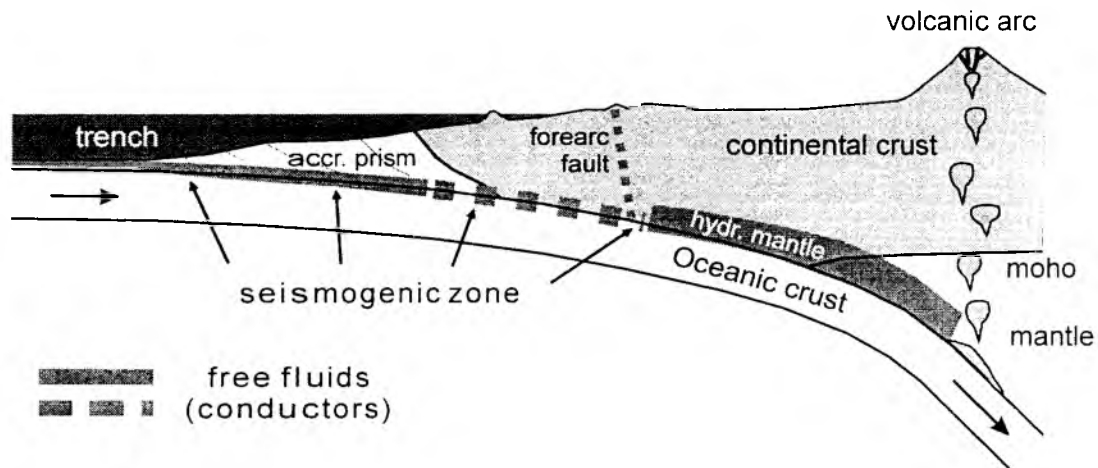


Figure 6.4.2: Model of ocean-continent subduction system with fluids in the interface between the plates.

The five recovered MT stations (two stations could not be recovered) logged data from their programmed turn-on time at 1200 UTC on 13 December 2004 until their recoveries on 20/21 February 2005. All electric field, magnetic field, and temperature channels appeared to have been recorded correctly. The built-in compass recorded headings and coarse pitch and roll readings. The fine scale tilt sensors worked correctly with only one exception. Station 3 landed at a 25.3 degree roll according to the on board compass. This exceeds the maximum limit of the fine scale tilt sensor, and thus the tilt data from this instrument are unusable. Otherwise, all data look suitable for further analysis.

For subsequent modelling and inversion, the ocean has to be incorporated as an a-priori structure in the finite difference mesh and therefore the knowledge of water conductivity is essential. A CTD log to depths of 4km was performed close to the measuring area (Appendix 9.5).

6.5. Magnetic Data

6.5.1 SO181-1a

During R/V SONNE cruise SO 181-1a the magnetometer was set up and tested along the seismic profiles while the airguns were operating, however no usable data were recorded.

6.5.2 SO181-1b

The Earth's magnetic field was measured during SO181-1b along 4490 line kilometres (Figure 6.5.2.1). The main aim of magnetic surveying was to explore the age of the incoming plate by using the magnetic reversals imprinted on the crust while it was formed at a mid-ocean ridge millions of years ago. Therefore, the magnetometer was primarily towed along lines running roughly in seafloor spreading direction and hence perpendicular to the margin in the area south of the Valdivia fracture zone, i.e., south of latitude 40°S. In addition, during the first surveys additional data were obtained on the continental slope to yield the fracture zone traces running into the margin.

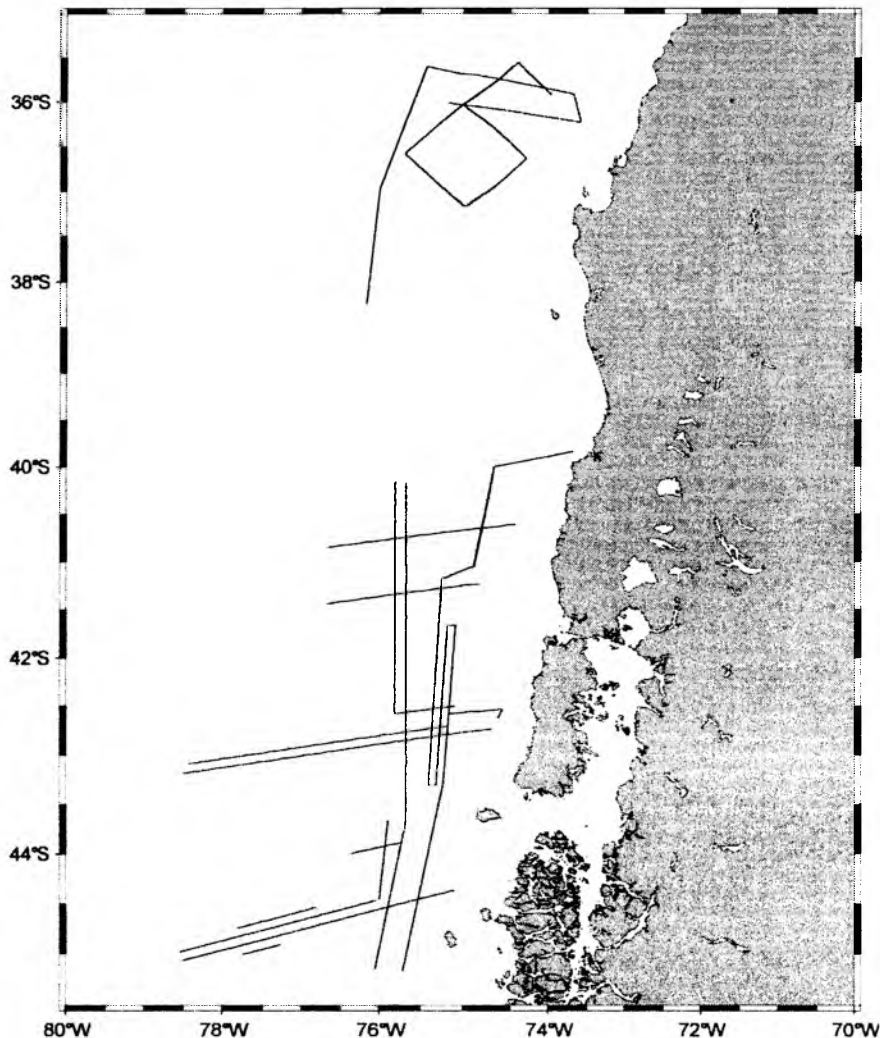


Figure 6.5.2.1: Magnetic track lines of SO181-1b.

The magnetic data transmitted from the magnetometer to the ship are stored as simple time series as a function of UTC time. Later, the ship's navigation was merged with the magnetic field data by using the UTC time as a common basis. In addition, to obtain the magnetic field anomaly, the appropriate 2005 International Geomagnetic Reference Field (IGRF) was removed from the measured field data. Figure 6.5.2.2 shows the measured field data, the IGRF field and the magnetic anomaly obtained during a north-south trending line of Survey1b-2. The profile illustrates the change in the Earth magnetic field in the survey area. At 40°S the main field is ~27000 nT and increases to the south to values of >30000 nT. Magnetic anomalies are generally between -300 to 300 nT.

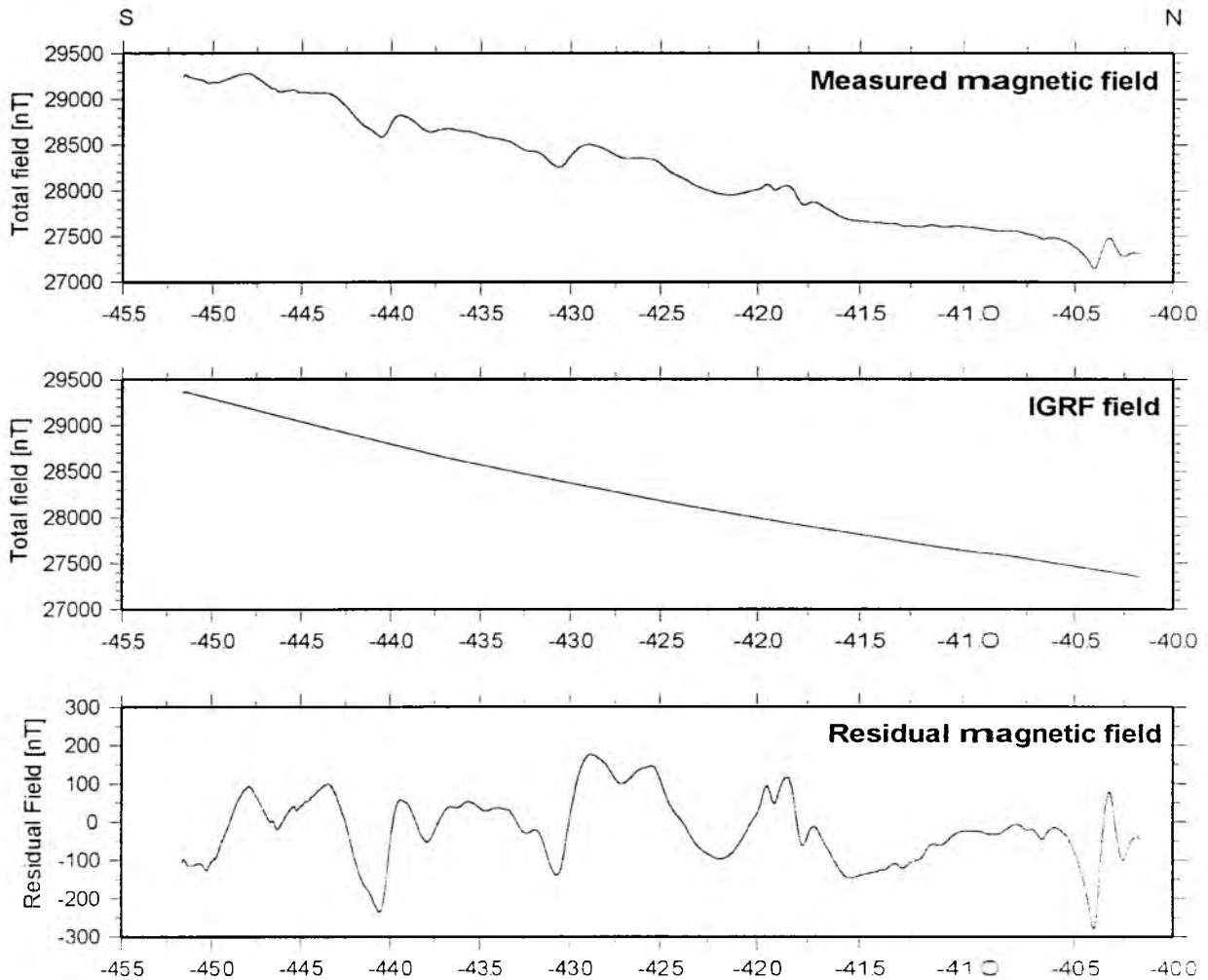


Figure 6.5.2.2: Magnetic field along a N-S trending line of Survey1b-2.

In the areas between the Valdivia fracture zone and the Guambin fracture zone, an area between 40°S to 45°S and 79°W to 74°W, the main focus of the magnetic surveying was to detect magnetic reversals to obtain the age of the ocean floor. Figure 6.5.2.3 shows all profiles running along plate flow line direction. Magnetic reversals are well resolved in the data and will allow us to gain the age of the plate at the trench. This information is important to assess

the thermal state of the plate entering the subduction zone. In addition, the seafloor age is important to derive sedimentation rates from the seismic records.

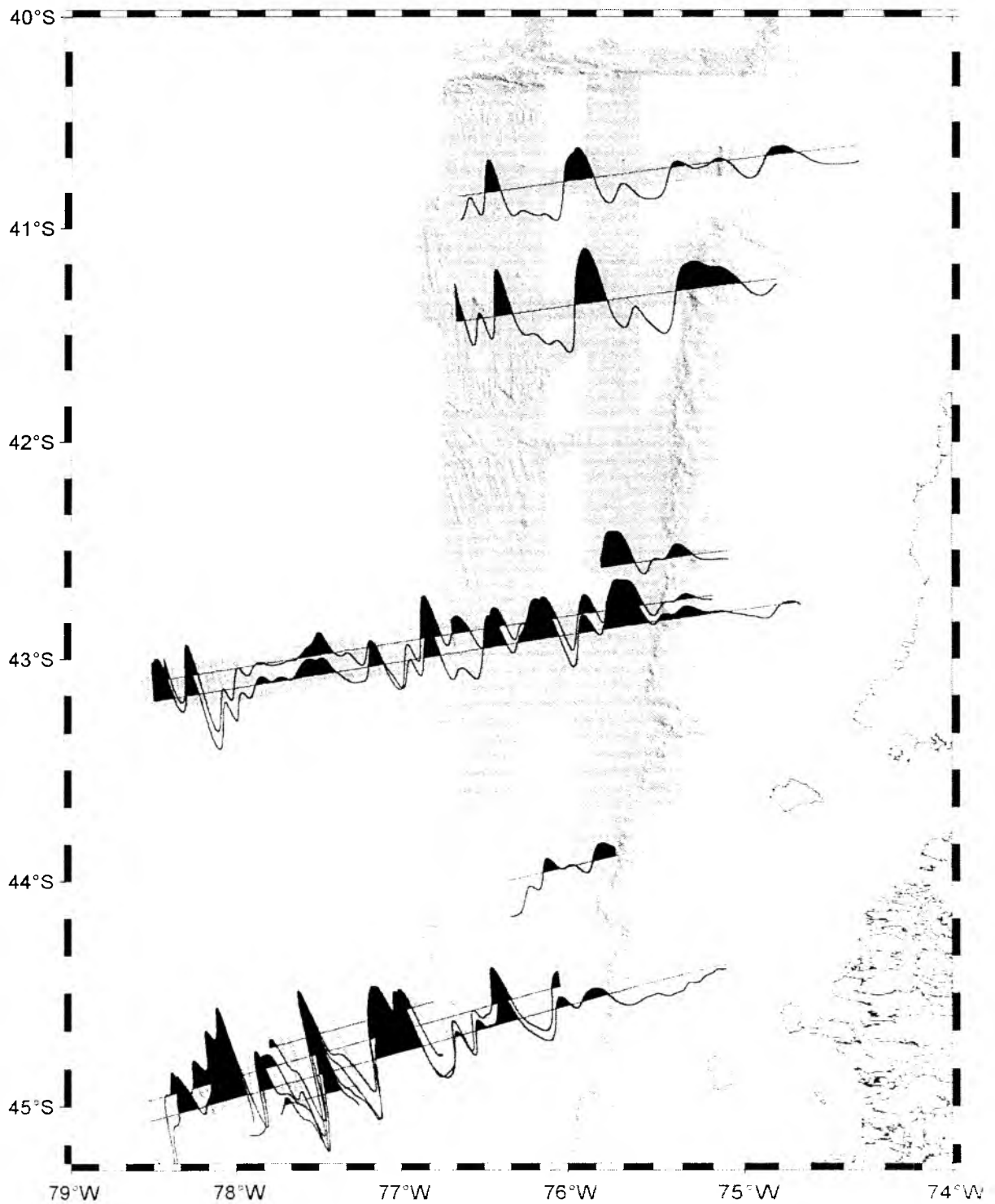


Figure 6.5.2.3: Magnetic flow line profiles between Valdivia and Guambin fracture zone showing magnetic reversals and hence crustal age.

During the last two days of Leg SO181-1b additional magnetic data were acquired offshore Concepcion between $35^{\circ}30'S$ and $37^{\circ}10'S$. The survey in this area was focussing on the idea that normal faulting seaward of the deep sea trench provides path ways for fluids to reach the mantle and alter the mantle peridotites and hence form serpentinite. Serpentinites generally contain magnetite and are therefore expected to produce profound anomalies in the magnetic field. Offshore Concepcion, faulting in the outer rise area is well imaged by multibeam bathymetry obtained during SO161 cruises and during SO181-1b. To the north of the Mocha fracture zone ($\sim 38-39^{\circ}S$), the normal faults run roughly normal to the strike of the paleo-spreading centre. Thus, if serpentinization occurs the magnetic field along isochrons should change. We therefore obtained magnetic data along profiles orientated along isochrons (Figure 6.5.2.4). Isochrons were defined by magnetic track lines running roughly in flow line direction and the seafloor morphology from the EM120 survey showing the abyssal hill fabric. However, the magnetic field changes very little along isochrons. Therefore, it appears that serpentinisation is only a minor issue offshore Central Chile.

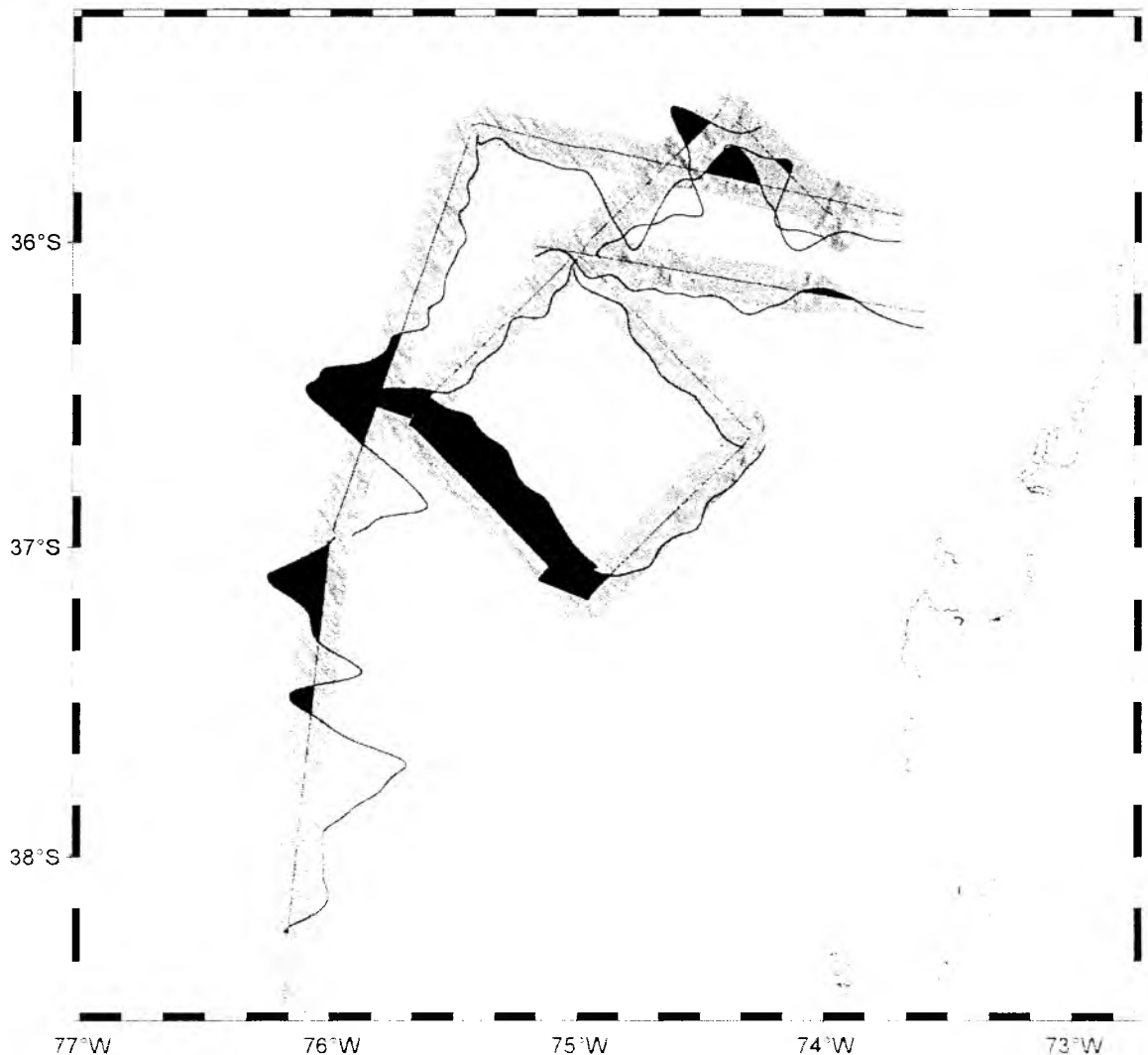


Figure 6.5.2.4: Magnetic field survey offshore Concepcion to study the relationship between outer rise normal faulting and serpentinisation.

6.5.3 SO181-2

Additional magnetic field measurements were carried out during the last and longest leg of this cruise. Central focus again was the detection of the earth's magnetic field reversals that allow the determination of the age of the ocean floor.

A large part of Leg 2 was the seismic data acquisition of the five TIPTEQ corridors, during which frequent hovering of the ship during deployment and recovery of the seismic instruments or the use of the seismic streamer during the shooting prevented the use of the magnetometer. However, in between the transects, several east-west as well as north-south profiles were covered with the magnetometer. This complemented the magnetic data already collected during Leg SO181-1.

Figure 6.5.3.1 exhibits the magnetic anomalies along the southern magnetic profiles of Leg 2. Similar to Figure 6.5.2.3, these east-west profiles show the correlation between these lines, and with subsequent identification of these anomalies thus enabling the determination of crustal ages. The northern magnetic profiles are shown in Figure 6.5.3.2. The north-south profiles exhibit some correlation with the Valdivia fracture zone as well as the Mocha fault zone, and remain for possible magnetic modelling.



Figure 6.5.3.1: Magnetic anomalies from SO181-2 in the southern area.

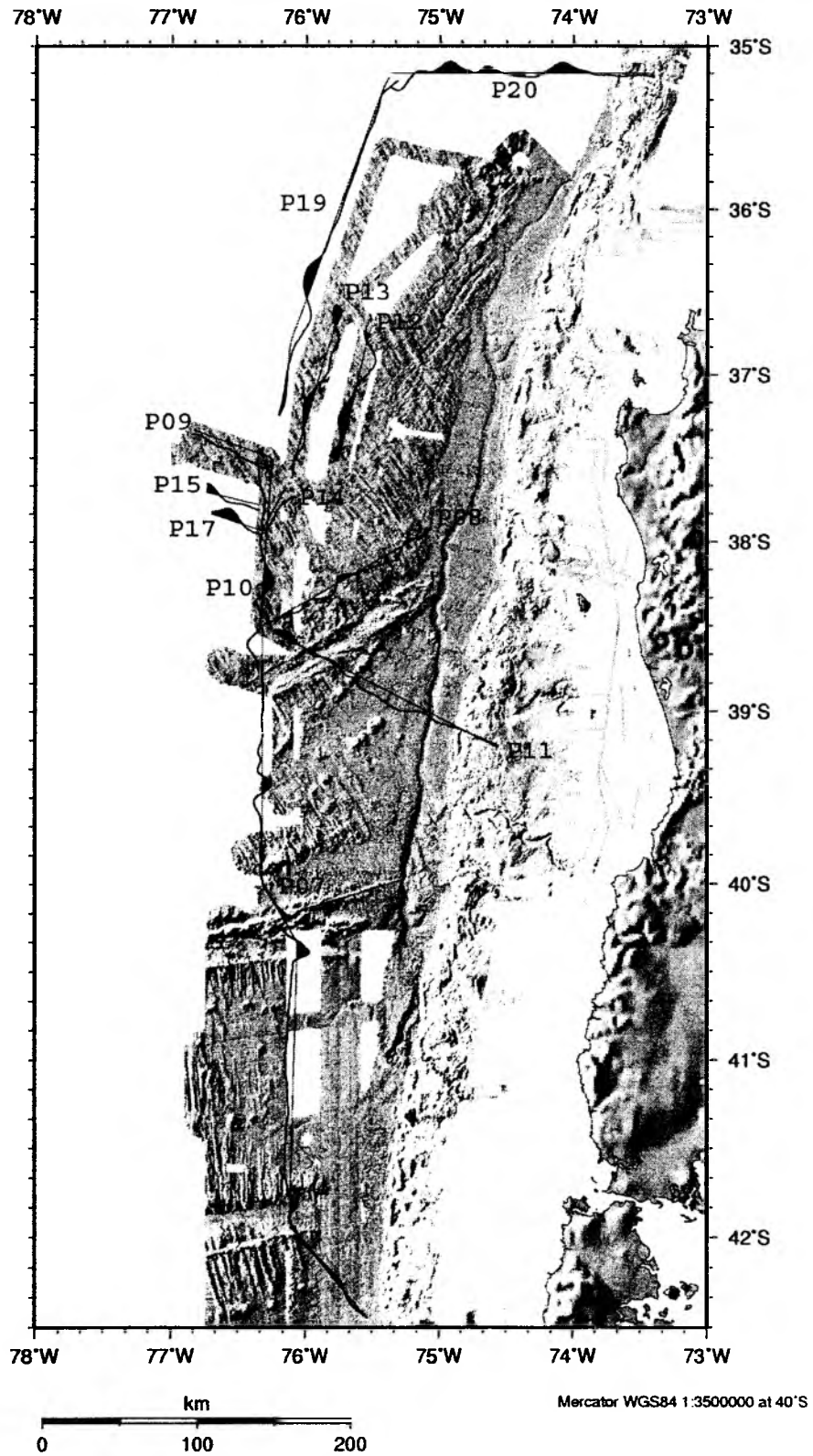


Figure 6.5.3.2: Magnetic anomalies from SO181-2 in the northern area.

6.6 Seismic and seismological investigations

During cruise SO181 numerous seismic investigations dominated the work program. First, two seismological networks were deployed on the outer rise to record possible bend faulting of the incoming plate. These networks recorded for ca. 45 days, and are discussed in Section 6.6.1. High resolution multichannel seismic reflection data were acquired at four locations covering the incoming plate from the outer rise, crossing the trench and reaching up to the shelf break (Section 6.6.2). Along the same lines and additional lines several high density seismic wide angle profiles were shot, discussed in Sections 6.6.3 to 6.6.7. Finally, towards the end of the cruise two seismological networks were deployed on the margin, reaching into the trench. These networks shall be recovered on a cruise in October 2005. An overview of all seismic profiles and all OBH/S positions is given in Figure 6.6.1.

6.6.1 The Outer Rise networks

Two networks to observe possible outer rise seismicity were installed during leg SO181-1a. The northern array centred around 43°S consisted of 17 instruments, spaced at 8 nm distance (OBS/H 01 to 17), including five long-period Webb seismometers. Across and into this array several seismic lines (P01 to P03) were shot with two Bolt airguns. A short four channel streamer was also deployed, but unfortunately lost at the beginning of line P03 due to shark bite. In Figure 6.6.1.1 the location of the instruments and the shooting lines are shown, details on instrumentation can be found in Appendices 9.2 and 9.3. On 22/23 January altogether 14 of these instruments were recovered after a deployment time of 43 days, and three instruments (OBS03, 06, and 11) remained at the seafloor to also record shots along profile P05 (see chapter 6.6.3). These instruments were then recovered 26 January. The reflection seismic data recorded along Profiles P01a to P02b are shown in Figure 6.1.1.3.

The southern array comprised 12 instruments, also spaced in a regular grid of 8 nm. Across this array a seismic line (P04) was shot using one Bolt airgun. The locations of the instruments are shown in Figure 6.6.1.2. These instruments were recovered 27/28 January. Details on instruments and shots can be found in Appendices 9.2 and 9.3.

Examples of record sections from the active source profiling from the two arrays are shown in Figures 6.6.1.4 to 6.6.1.24. In Figure 6.6.1.16 a marked change in quality of the recording on the three-component seismometer is seen at a distance of 25 km. This is a result of the levelling command executed at this time. An onboard analysis of the velocity fields was attempted, and preliminary results are discussed below.

Profile 01

Profile 01, comprising 5 OBH/S, is a 33 nm East-West profile across the outer rise. A forward modelling technique was used to reveal the structure of the oceanic crust in this area. The record sections from the OBH/S are of good quality (Figures 6.6.1.5 to 6.6.1.9). All of these sections exhibit clear refracted waves from the oceanic crust (Pg waves), and also clear Moho wide-angle reflections (PmP) and refracted waves from the oceanic mantle (Pn waves). These different phases were picked and used to establish a preliminary layered model for the oceanic crust. The software “MacRay” (Luetgert, 1992) was used to trace rays in a 2-D model. On the record section from the OBH 14, a time shift was observed for the far offsets in the western part and has not been resolved yet. We hence decided not to consider this OBH for the forward modelling.

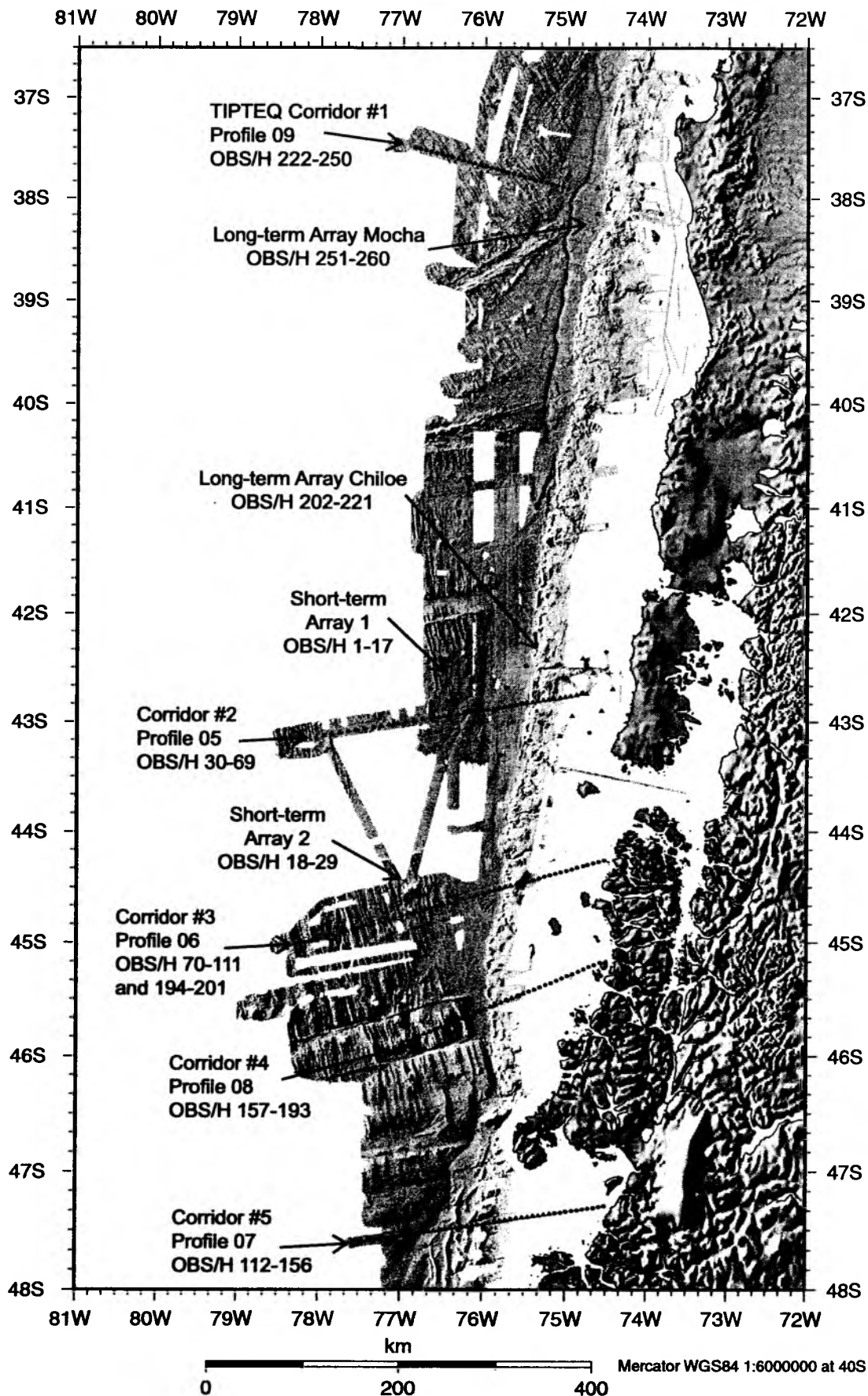


Figure 6.6.1: All OBS and OBH locations of SO181. Triangles represent OBH and circles represent OBS stations.

Short term array (STA) 1

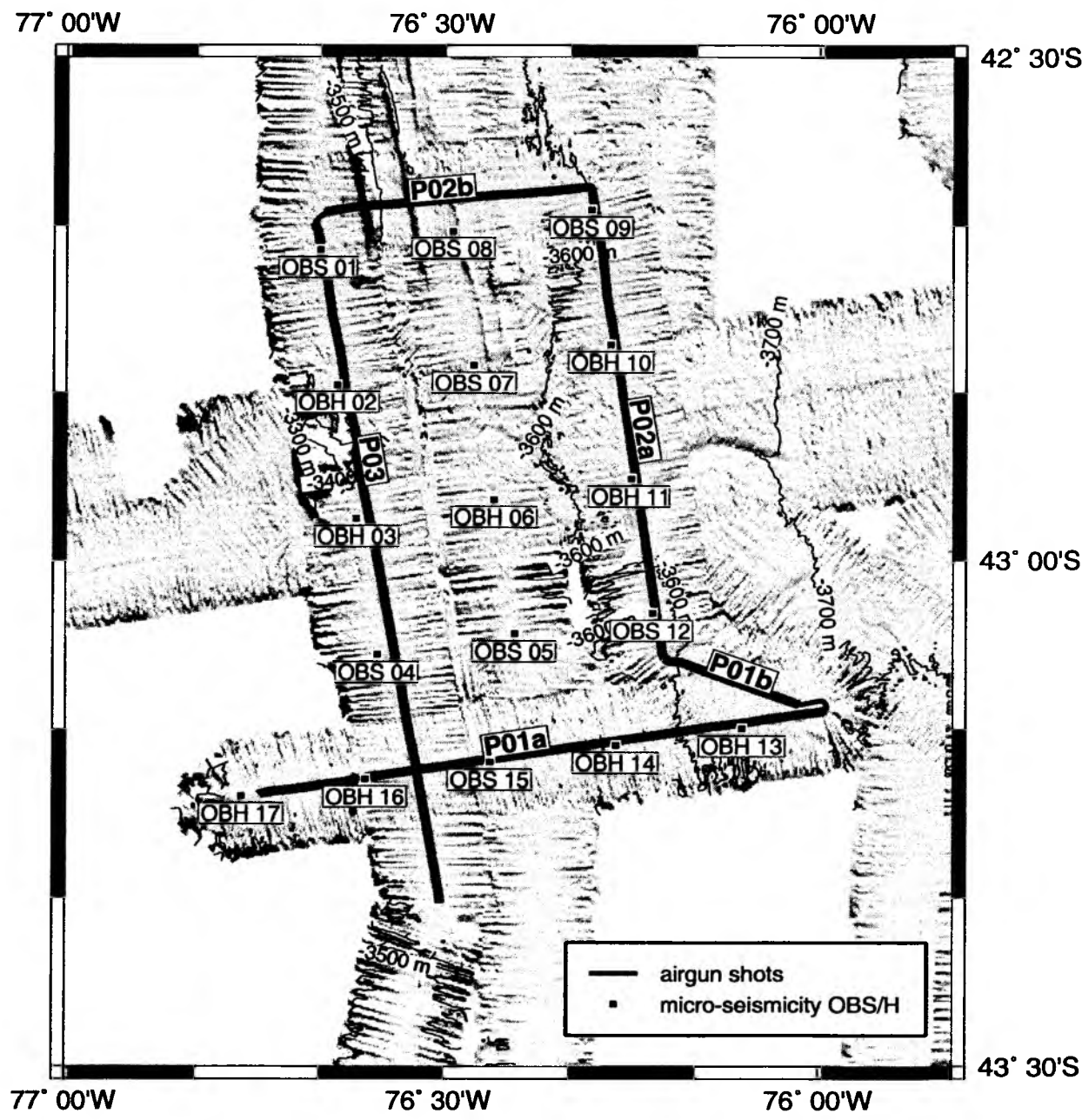


Figure 6.6.1.1: Basemap of short-term array (STA) 1 of ocean bottom seismometer and hydrophone array to study outer rise micro-seismicity. Also shown are airgun profiles. Thicker grey lines mark streamer profiles. Bathymetry contours every 100m.

Short term array (STA) 2

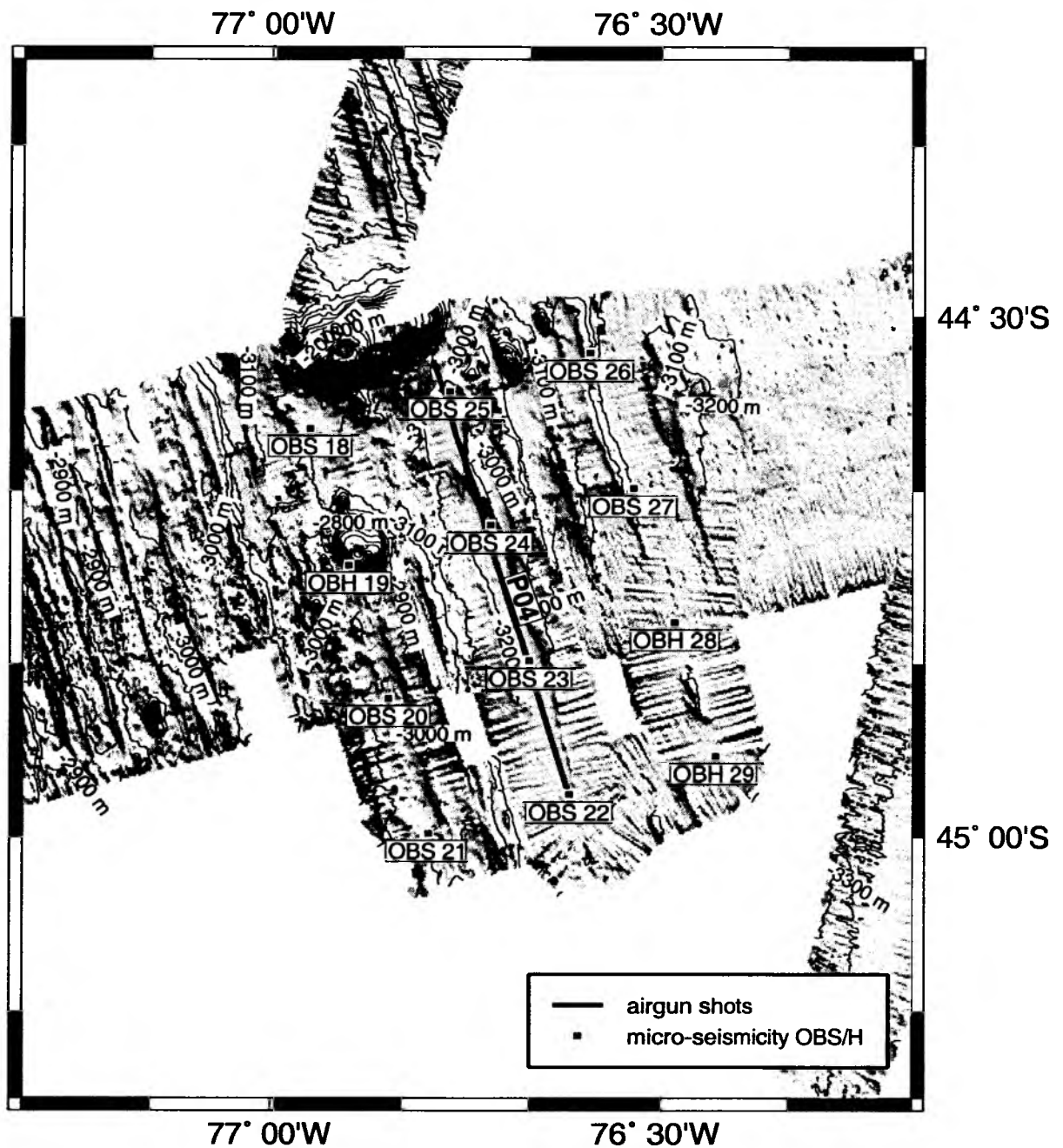


Figure 6.6.1.2: Basemap of short-term array (STA) 2 of ocean bottom seismometer and hydrophone array to study outer rise micro-seismicity. Also shown are airgun profiles. Bathymetry contours every 100m.

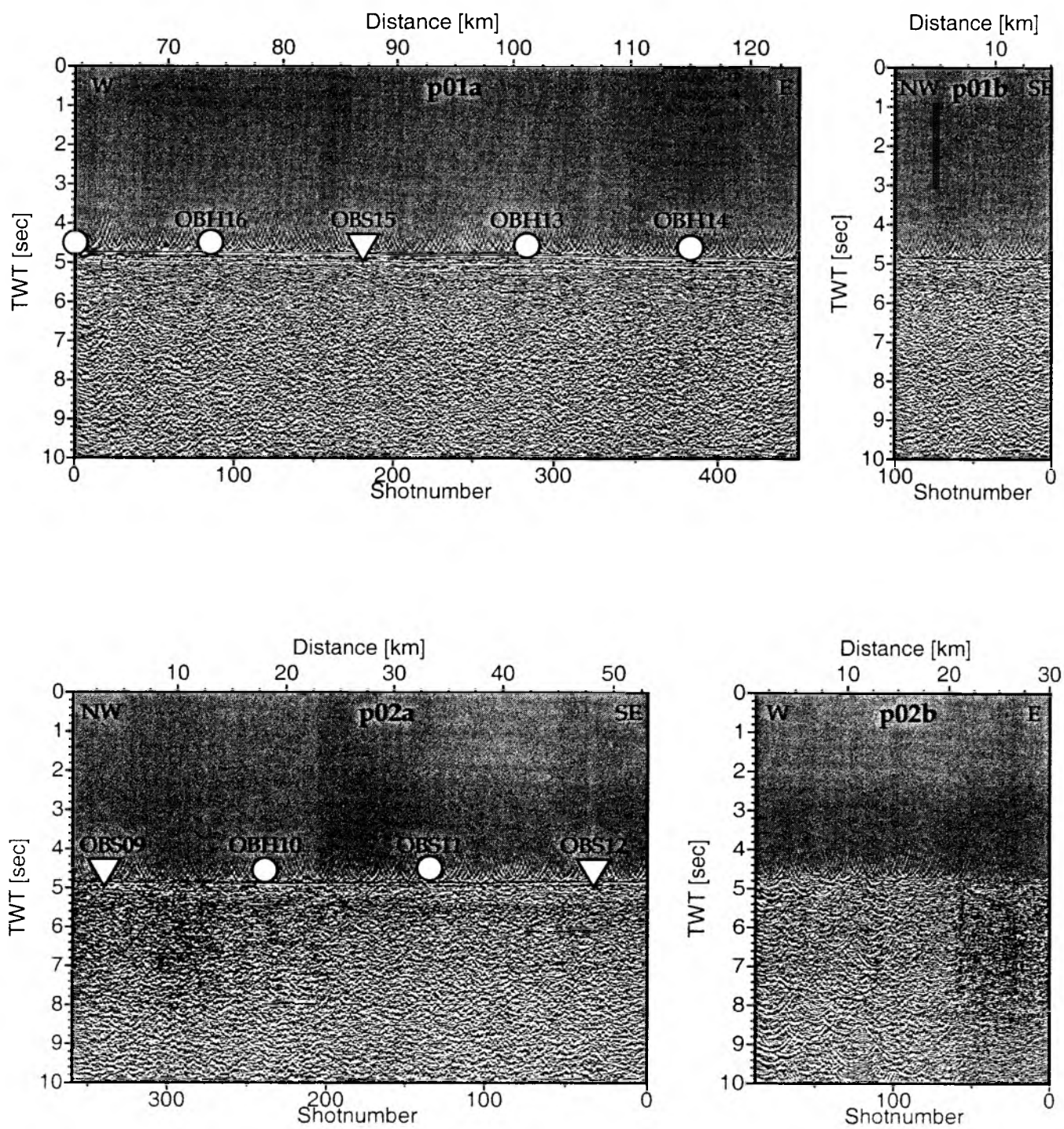


Figure 6.6.1.3: Record sections from MCS after water migration.

Time X-T/6

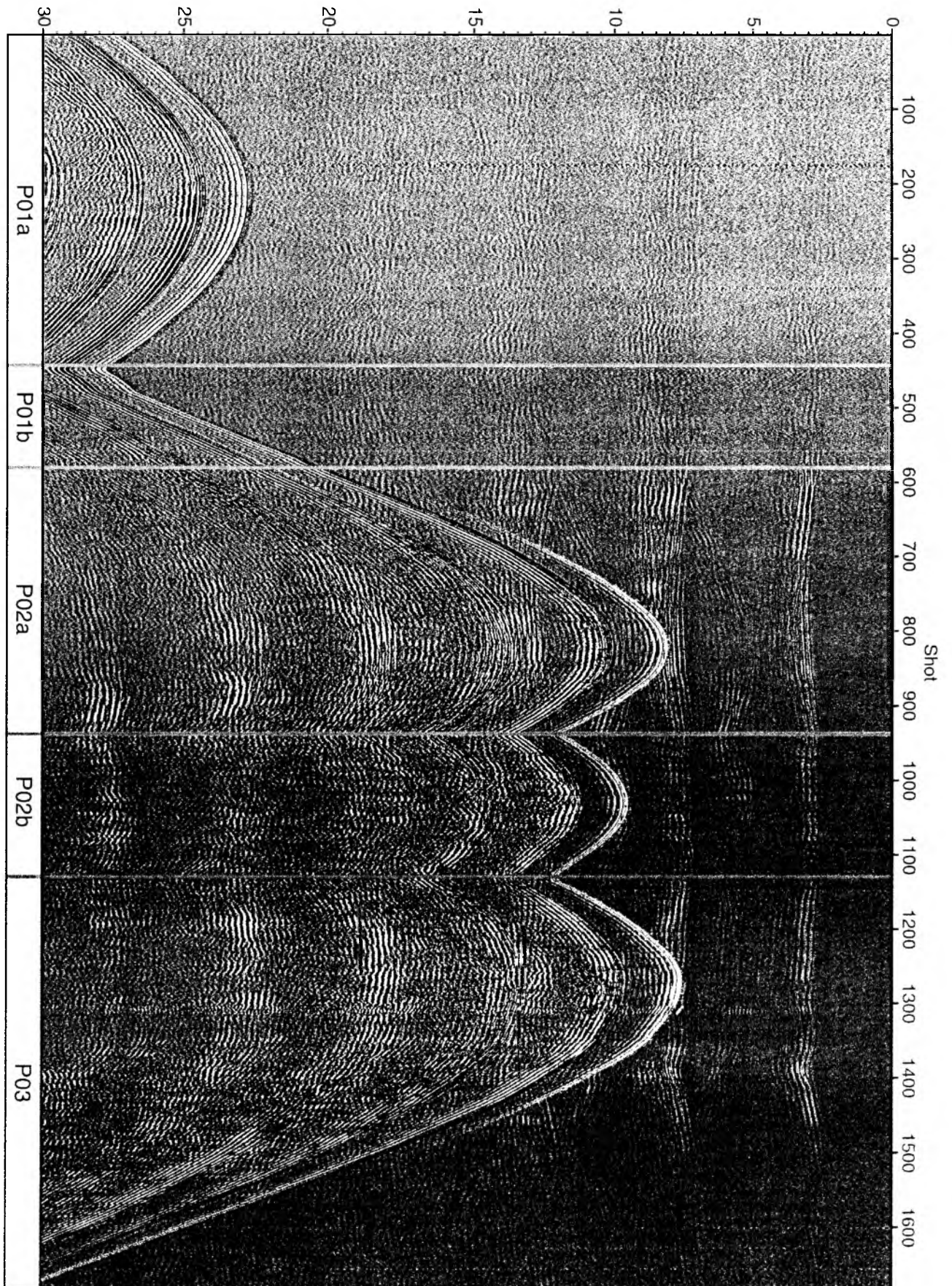


Fig. 6.6.1.4: Record section of OBH 07, Profiles 01a to 03

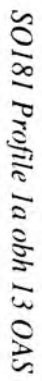


Figure 6.6.1.5: Record section from obh 13 OAS, Profile 1a.

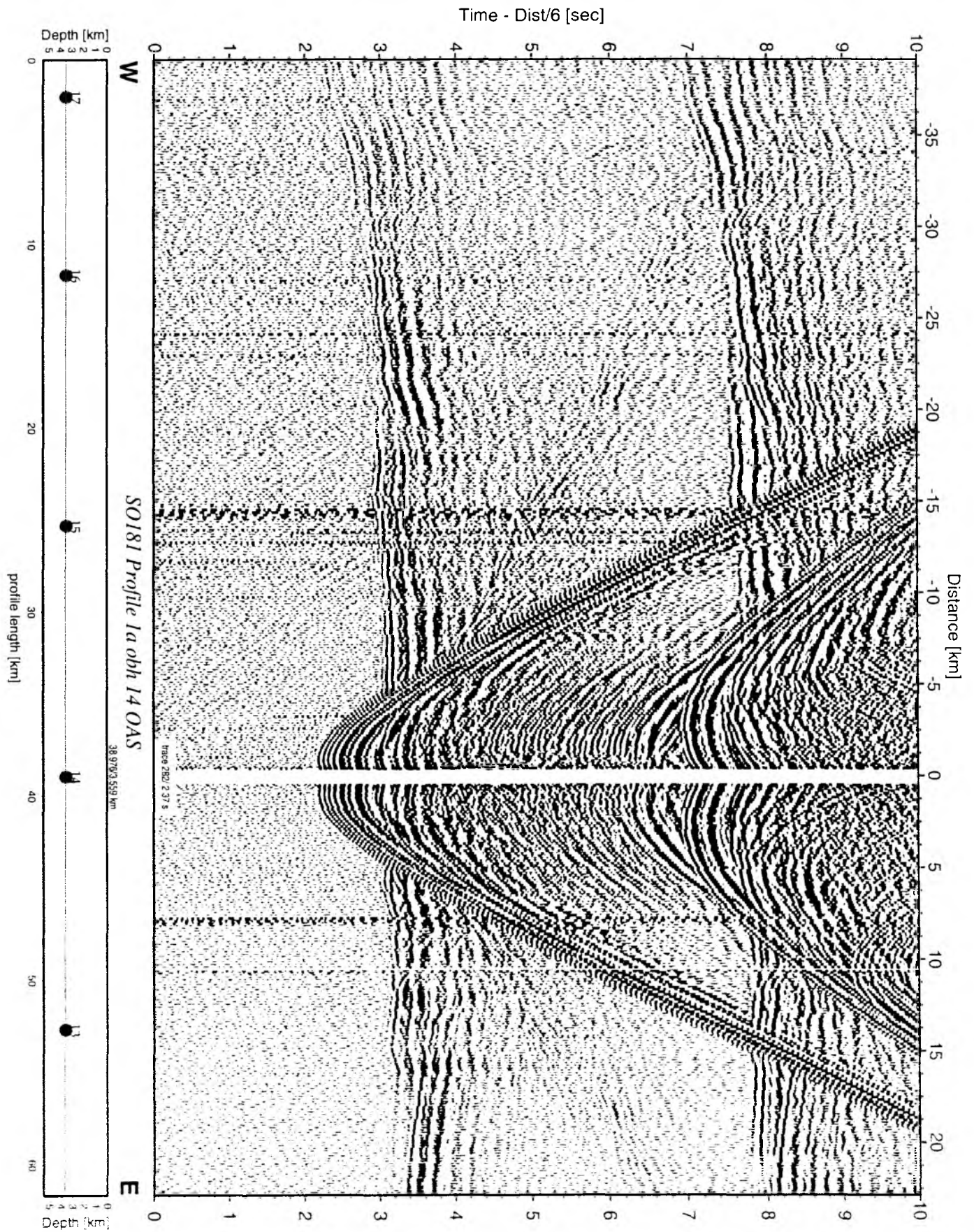


Figure 6.6.1.6: Record section from obh 14 OAS, Profile 1a.

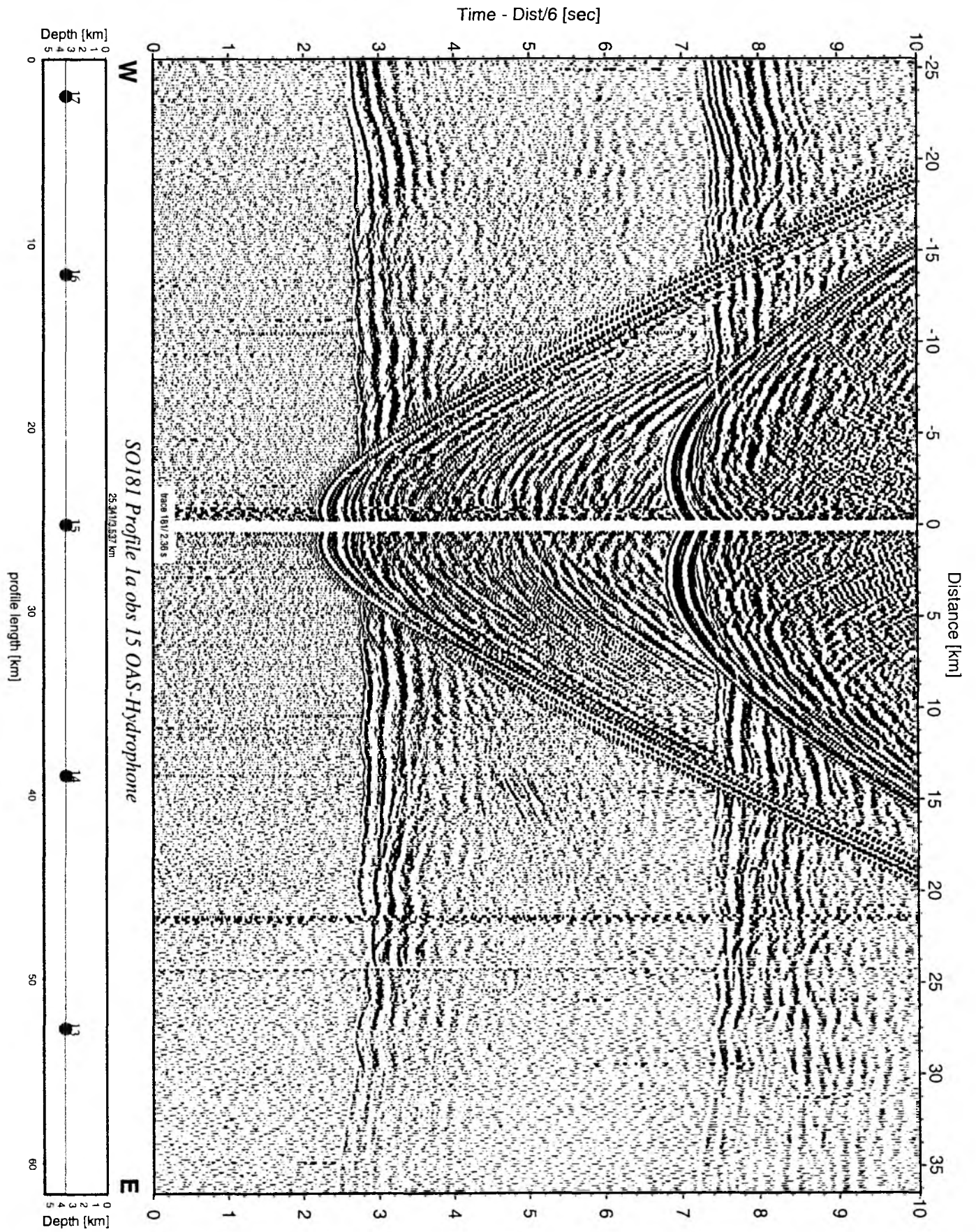


Figure 6.6.1.7: Record section from obs 15 OAS-Hydrophone, Profile 1a.

Time - Dist/6 [sec]

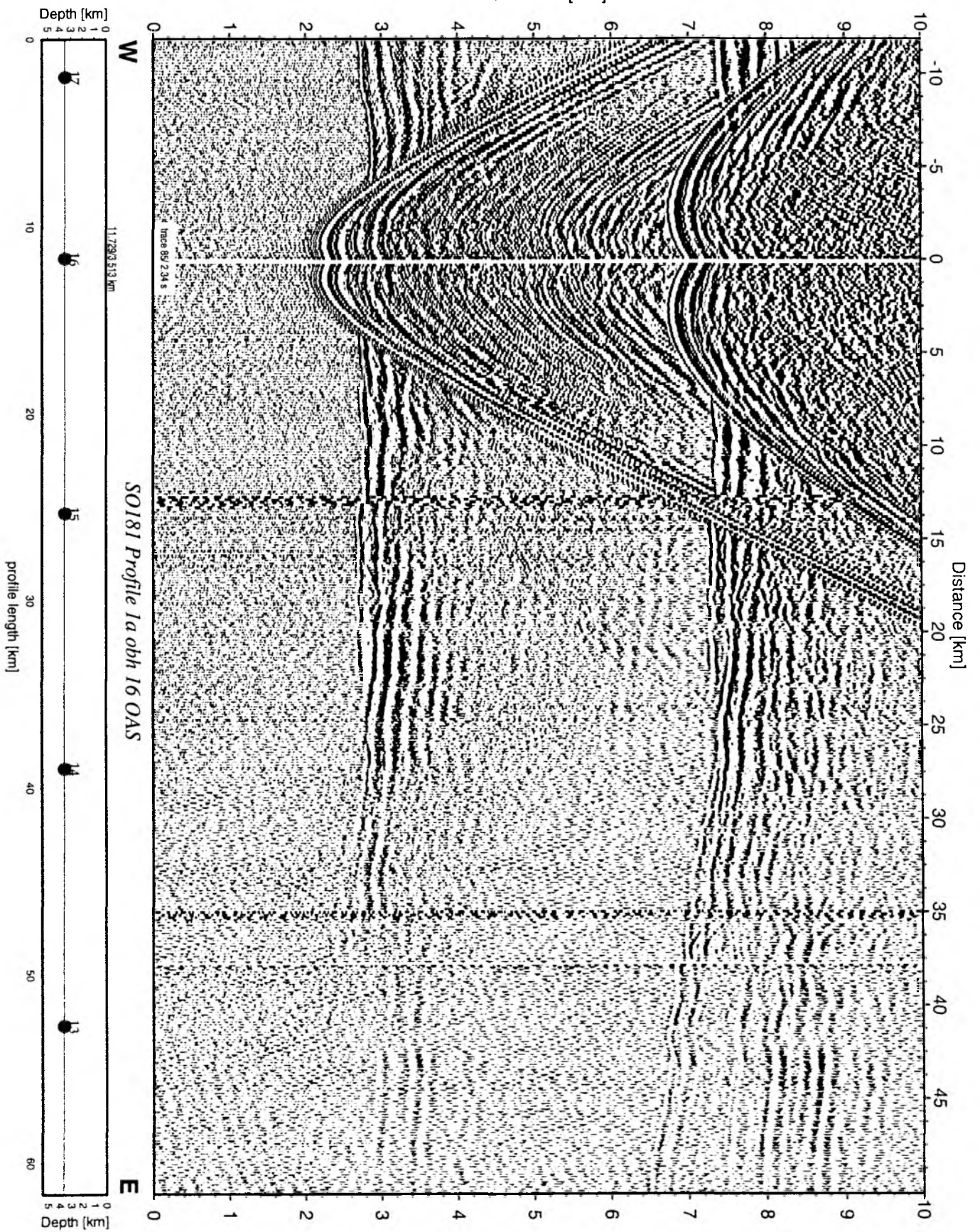


Figure 6.6.1.8: Record section from obh 16 OAS, Profile 1a.

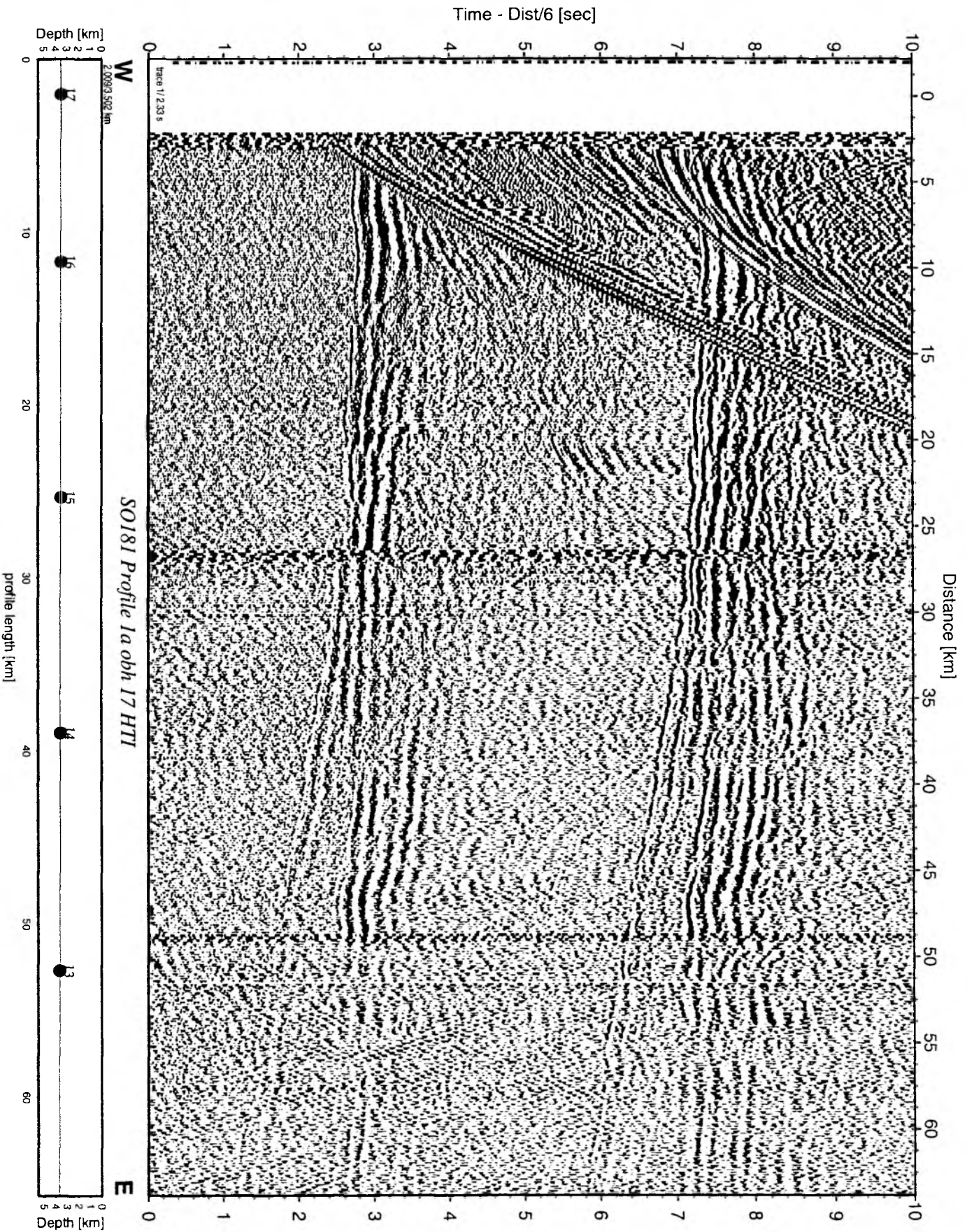


Figure 6.6.1.9: Record section from obh 17 HTI, Profile 1a.

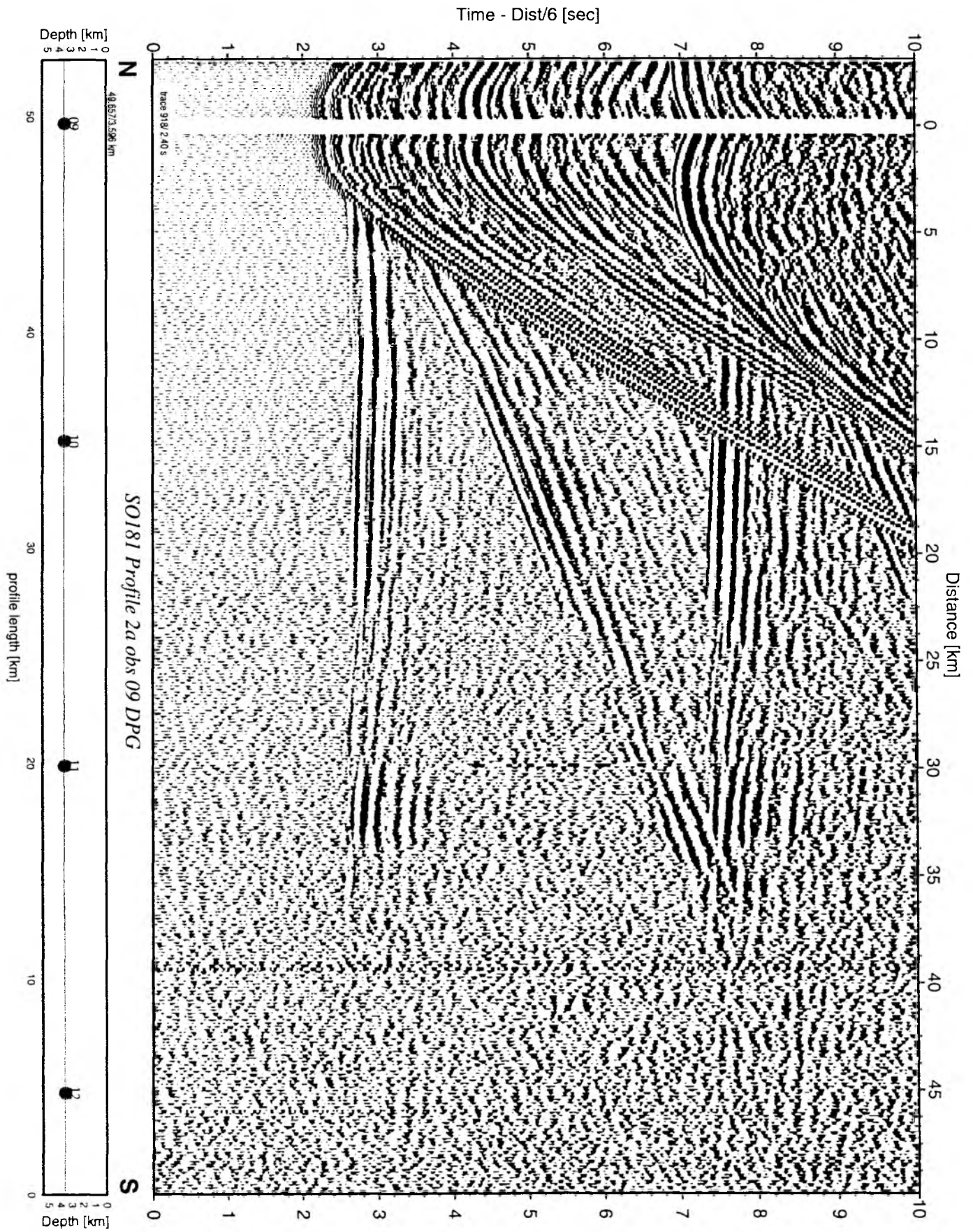


Figure 6.6.1.10: Record section from obs 09 DPG, Profile 2a.

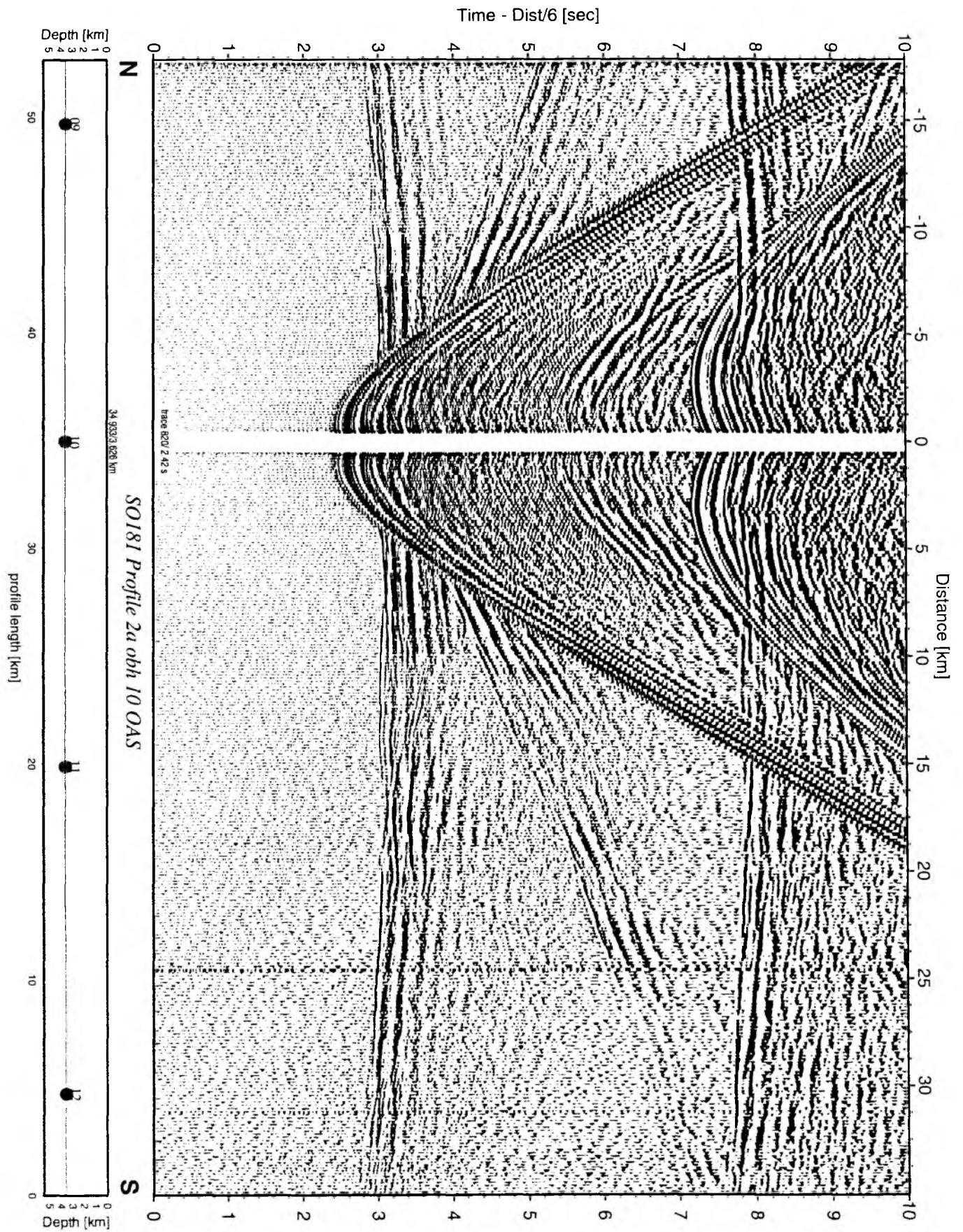


Figure 6.6.1.11: Record section from obh 10 OAS, Profile 2a.

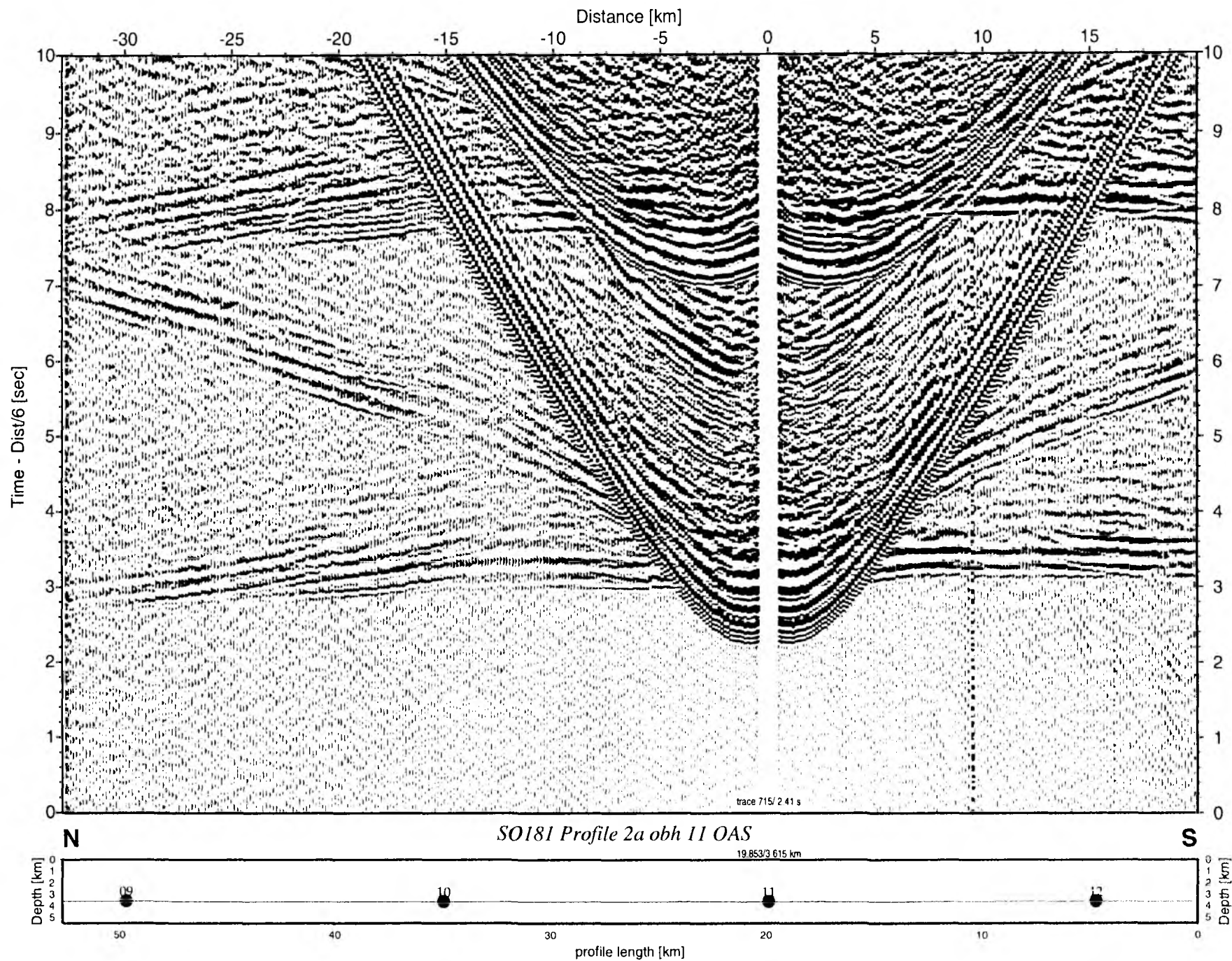


Figure 6.6.1.12: Record section from obh 11 OAS, Profile 2a.

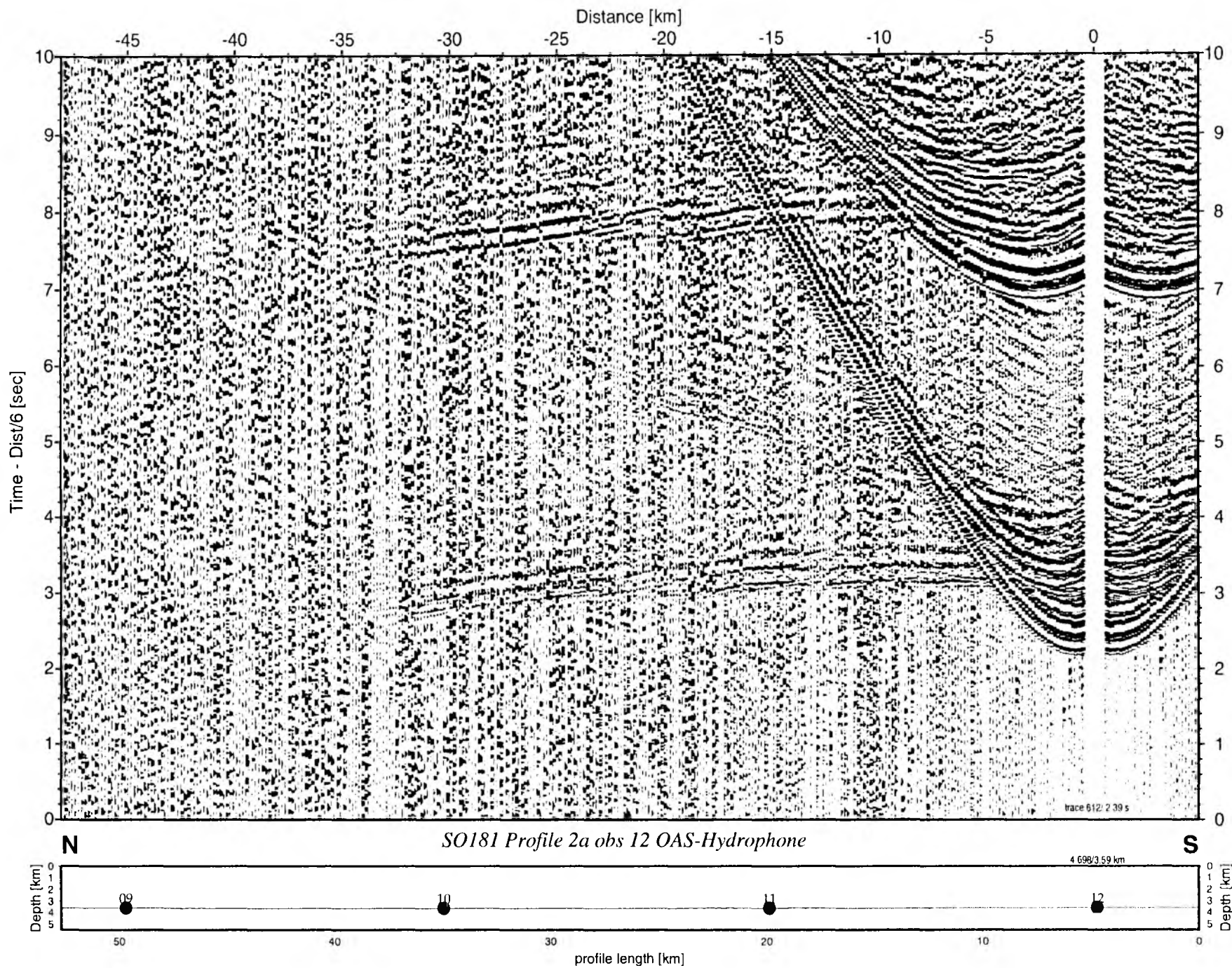


Figure 6.6.1.13: Record section from obs 12 OAS-Hydrophone, Profile 2a.

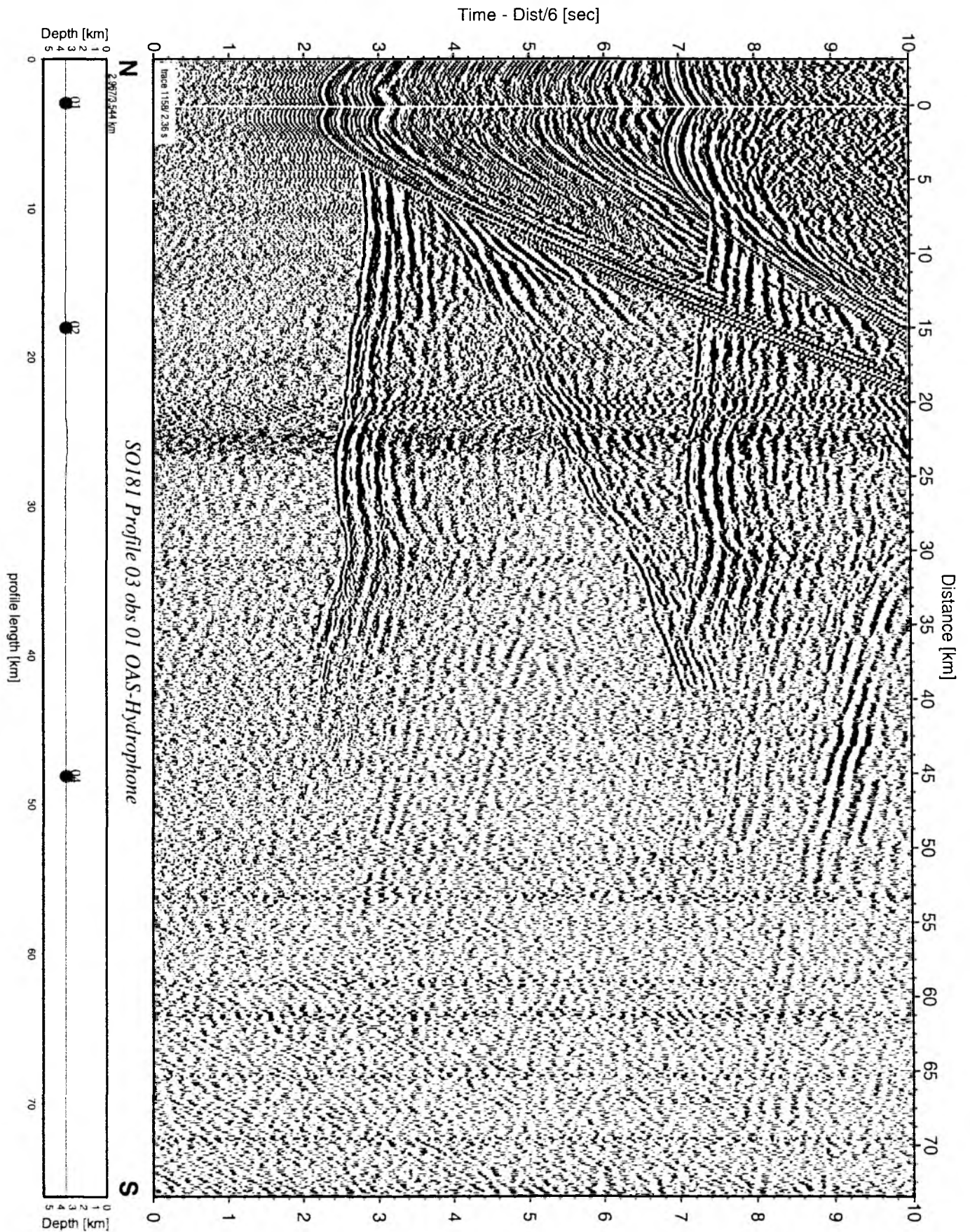


Figure 6.6.1.14: Record section from obs 01 OAS-Hydrophone, Profile 03.

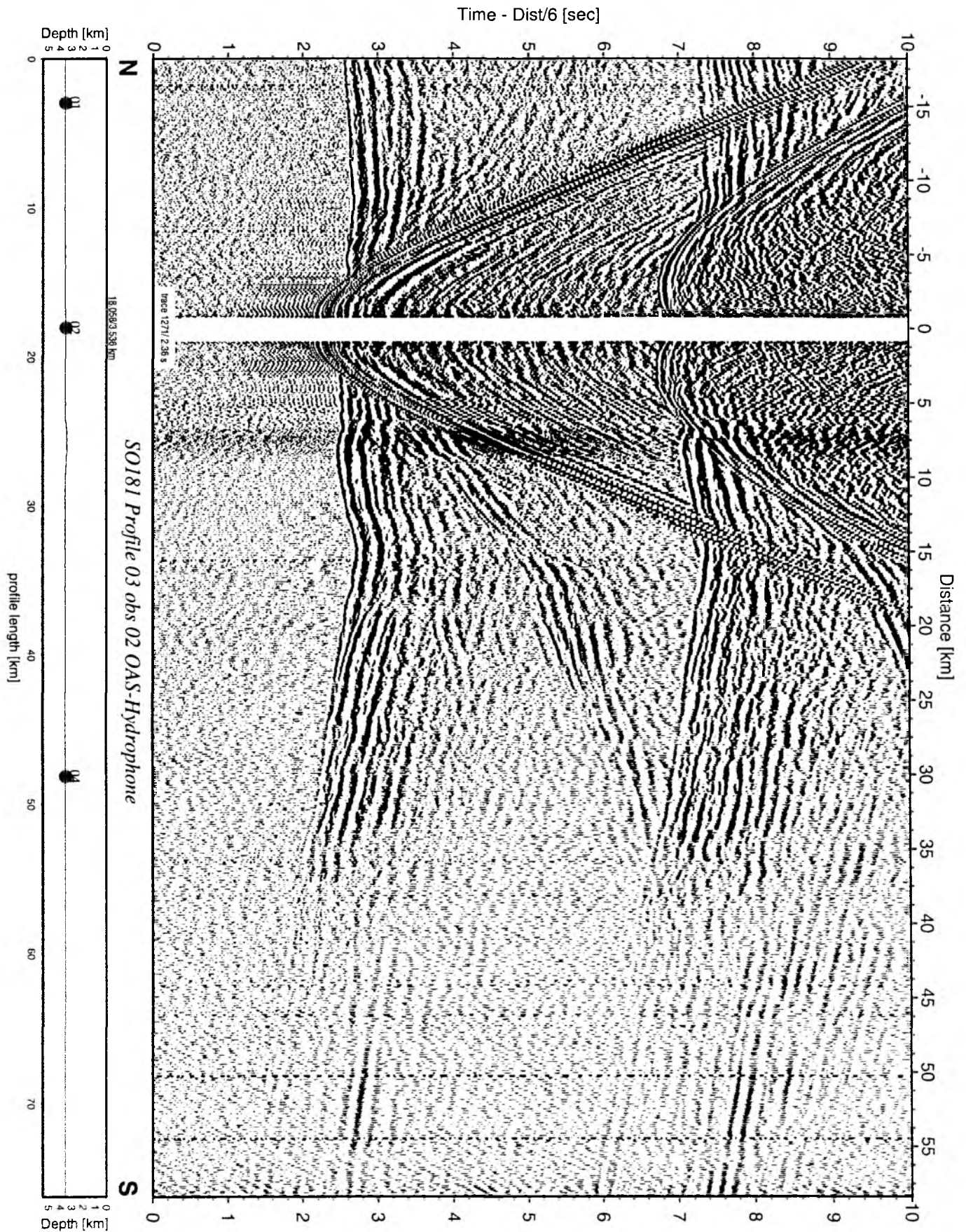


Figure 6.6.1.15: Record section from obs 02 OAS-Hydrophone, Profile 03.

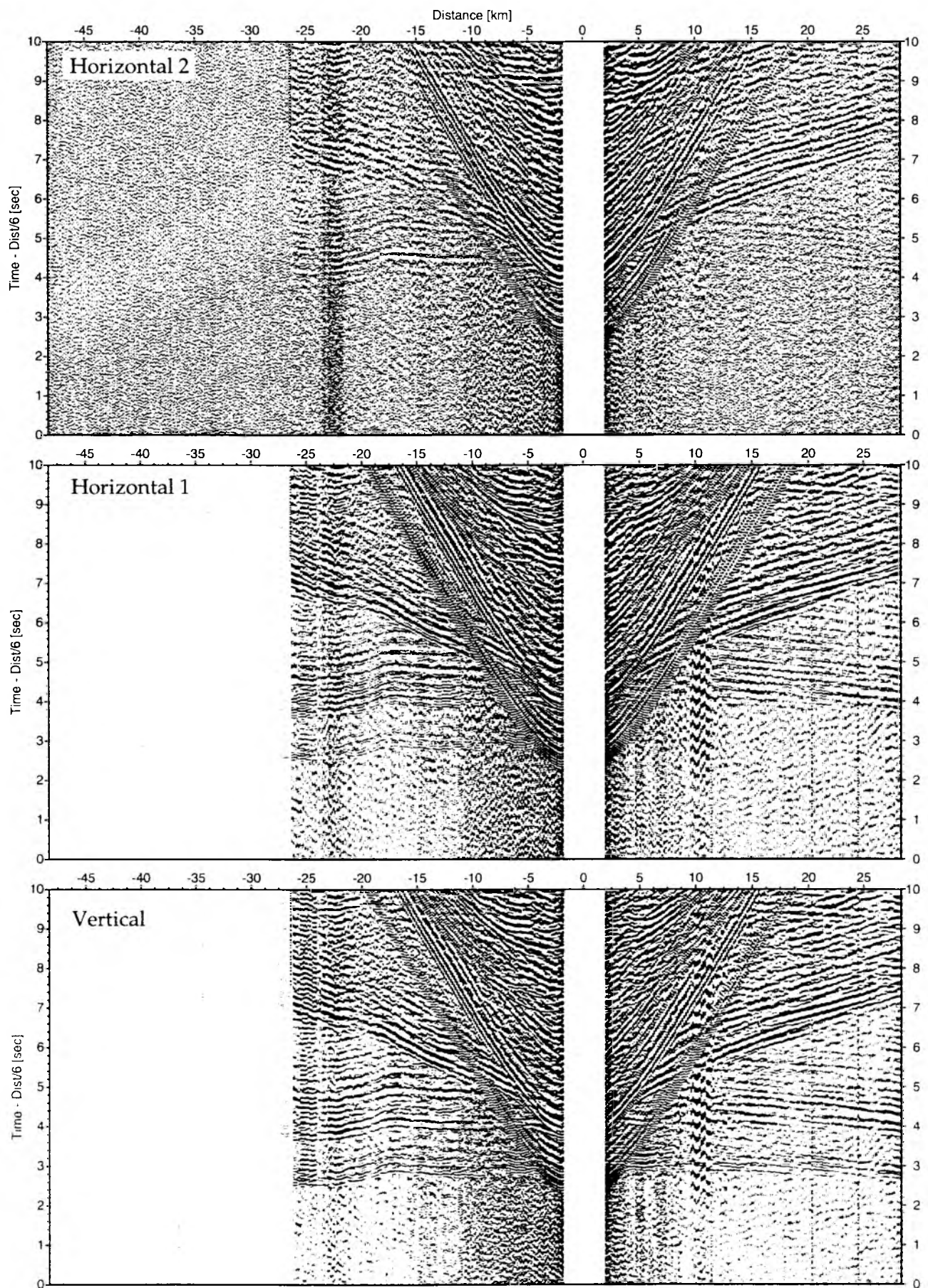


Figure 6.6.1.16: Record sections from obs 04 DPG/WEBB, SO181 Profile 03.

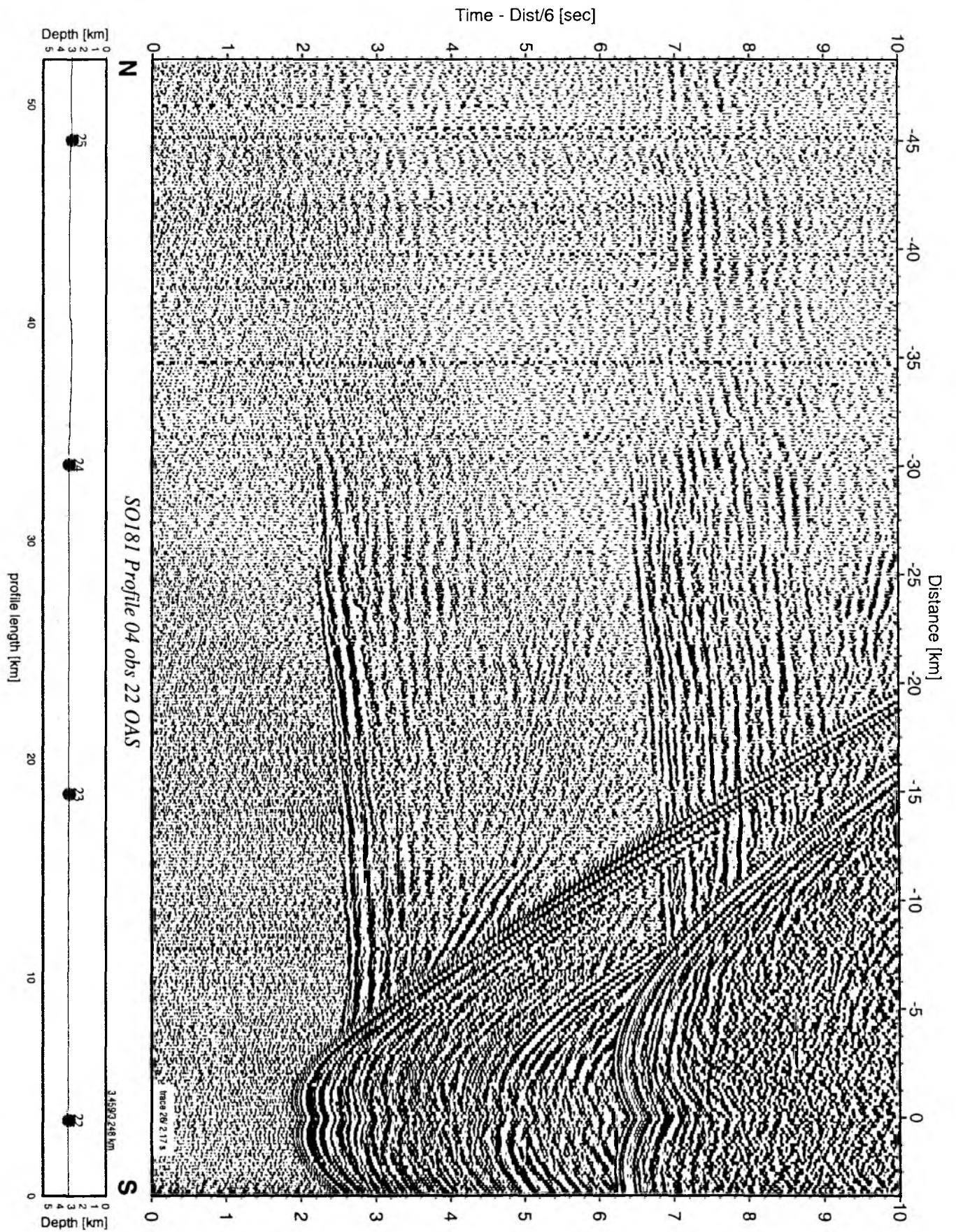


Figure 6.6.1.17: Record section from obs 22 OAS, Profile 04.

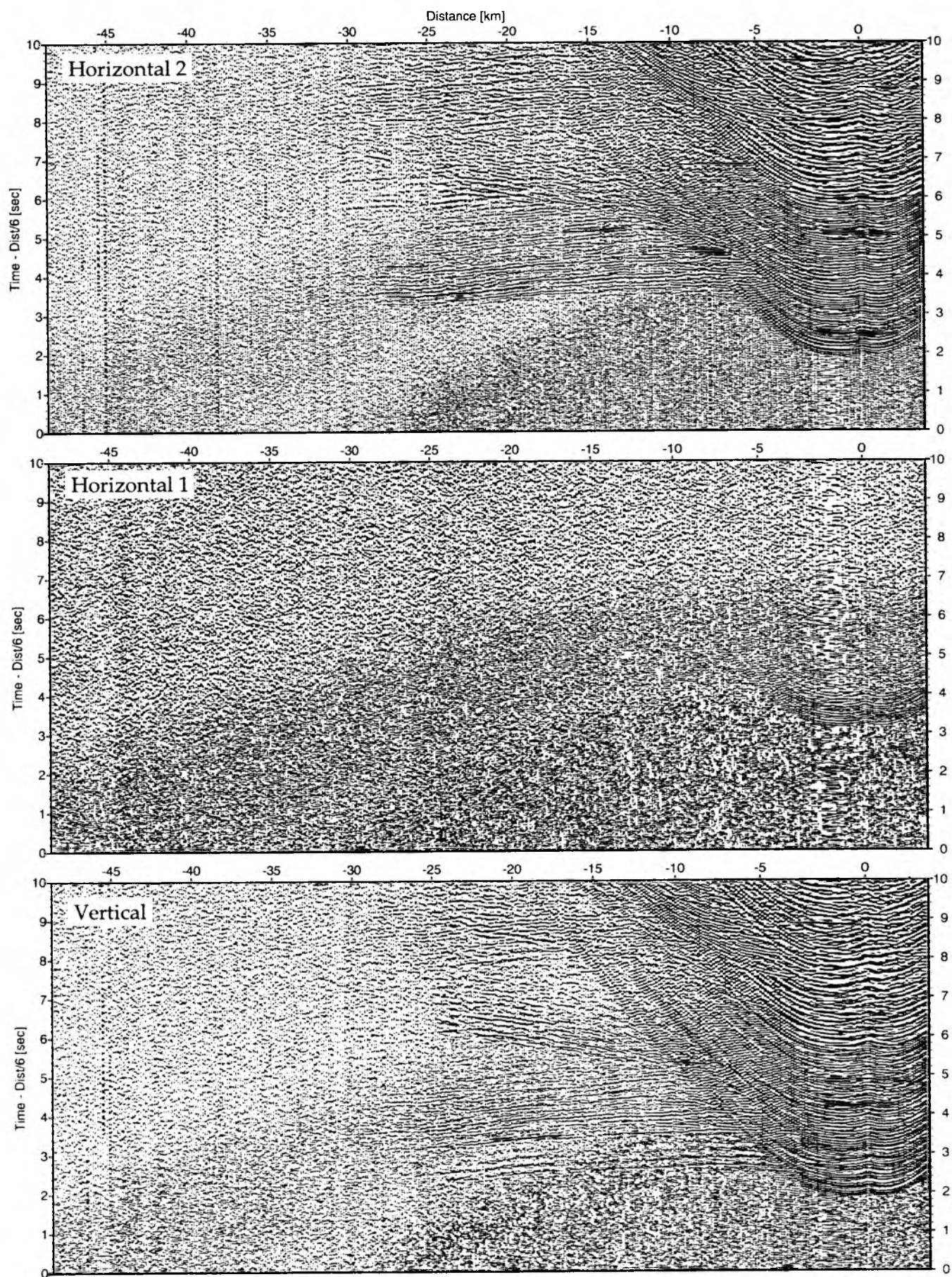


Figure 6.6.1.18: Record sections from obs 22 OAS/Owen-4.5Hz, SO181 Pro file 04.

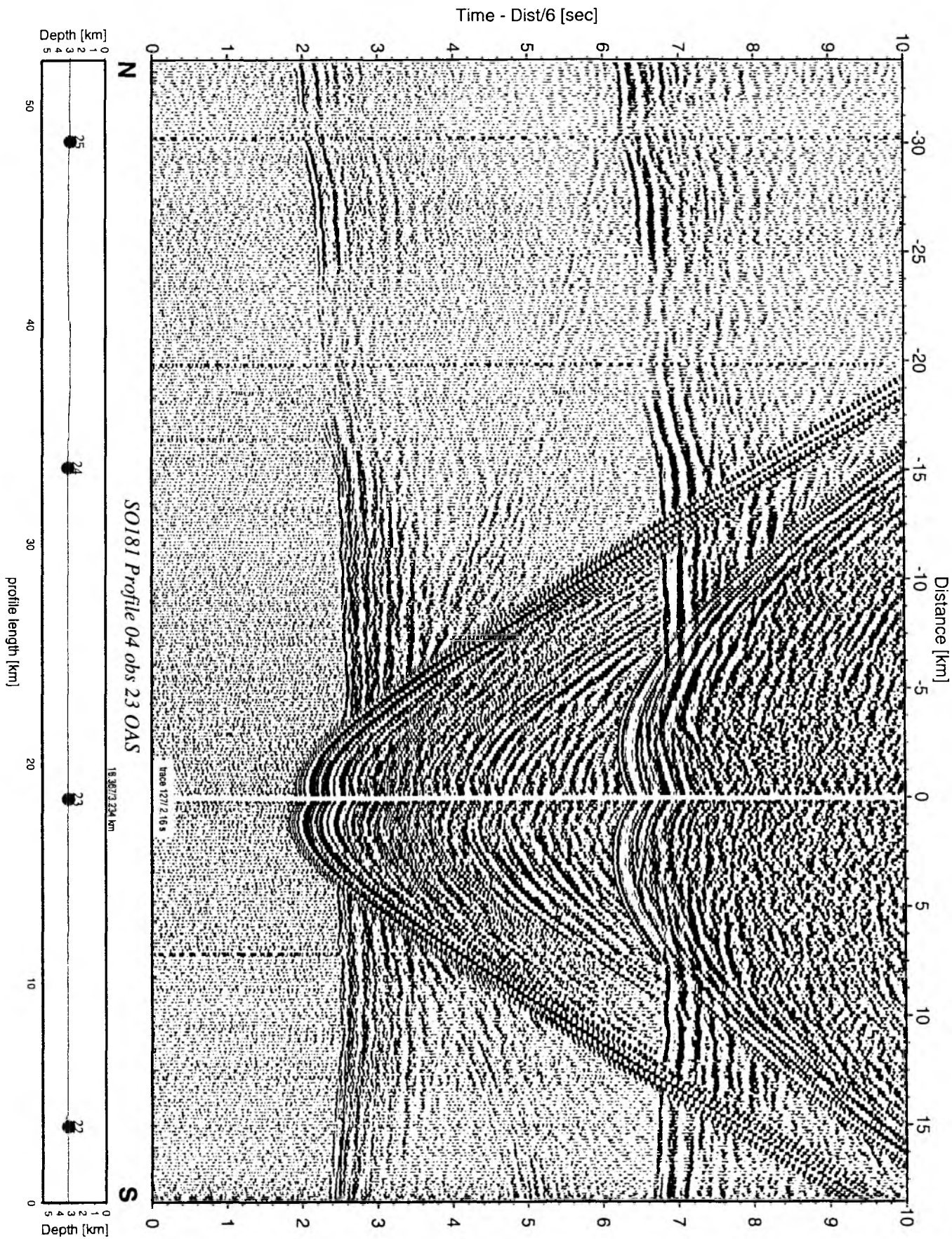


Figure 6.6.1.19: Record section from obs 23 OAS, Profile 04.

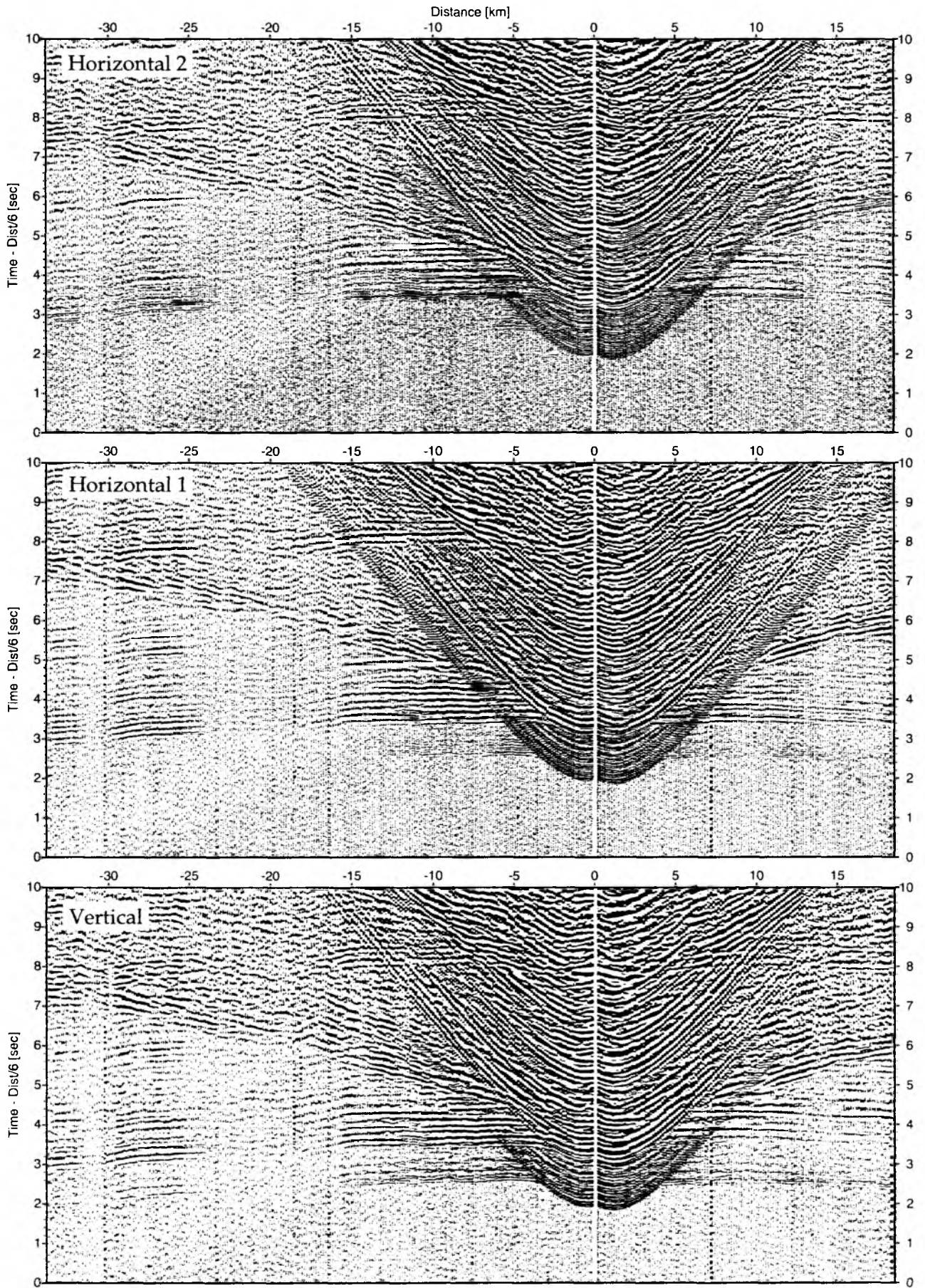


Figure 6.6.1.20: Record sections from obs 23 OAS/Owen-4.5Hz, SO181 Profile 04.

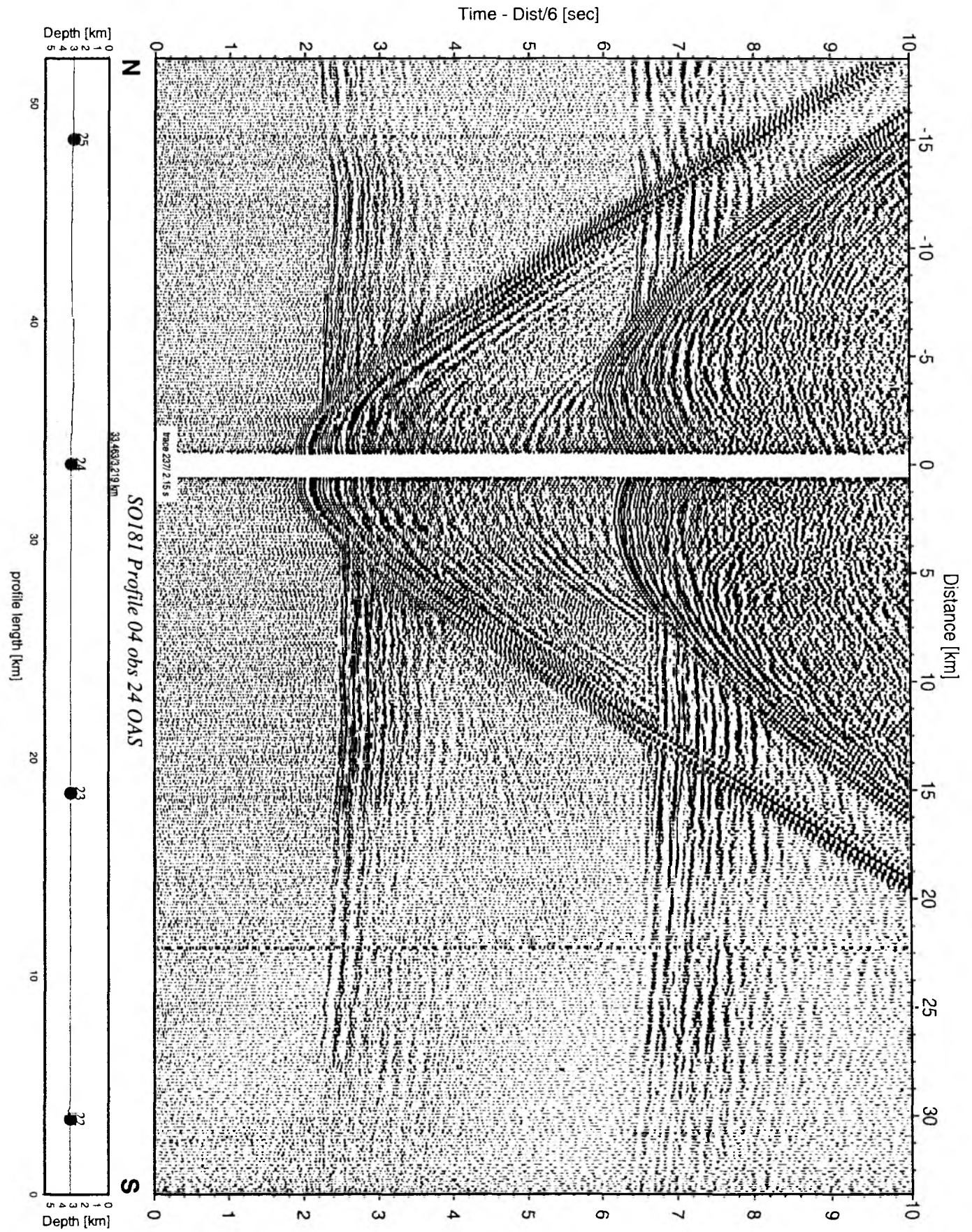


Figure 6.6.1.21: Record section from obs 24 OAS, Profile 04.

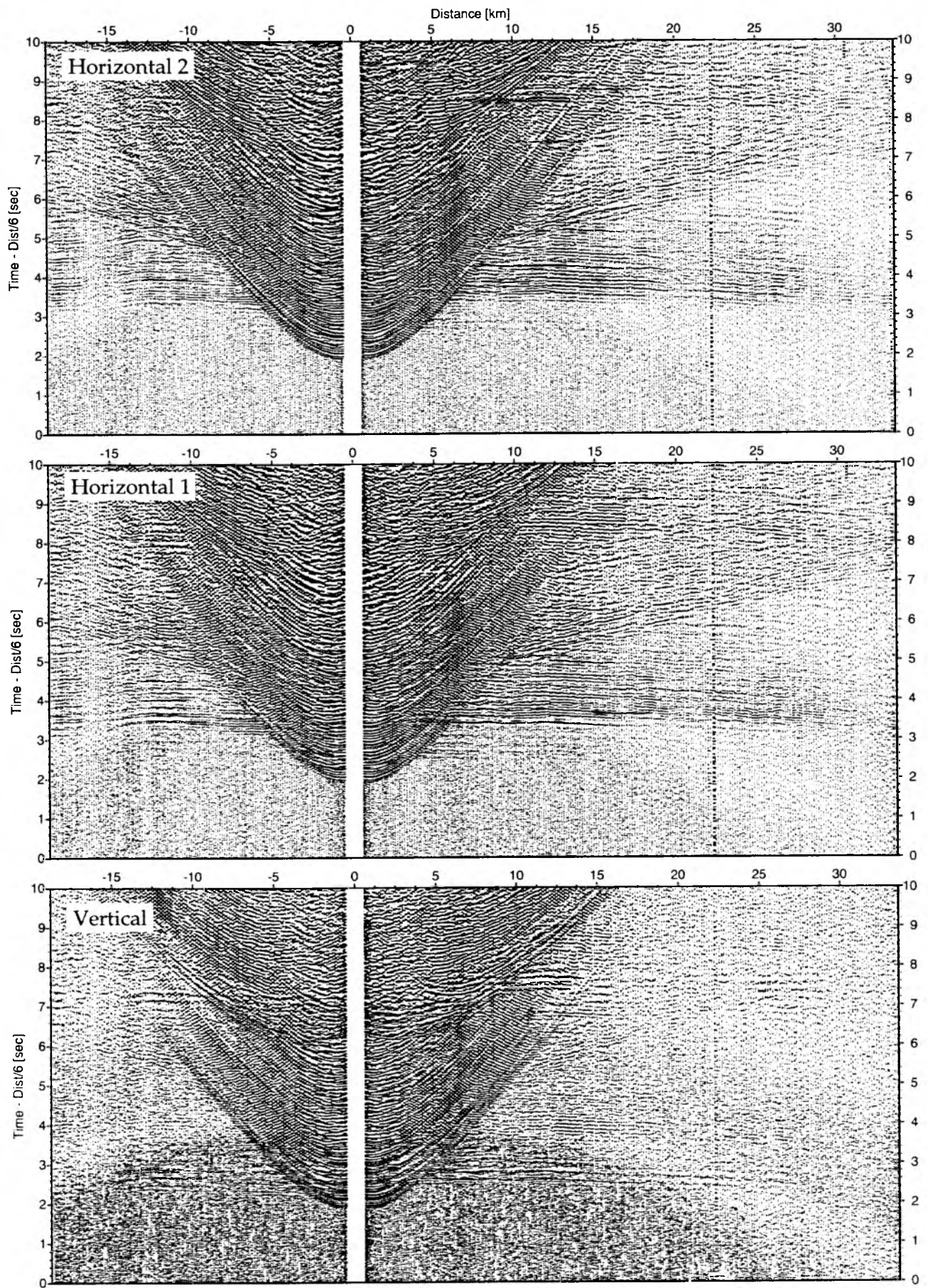


Figure 6.6.1.22: Record sections from obs 24 OAS/Owen-4.5Hz, SO181 Profile 04.

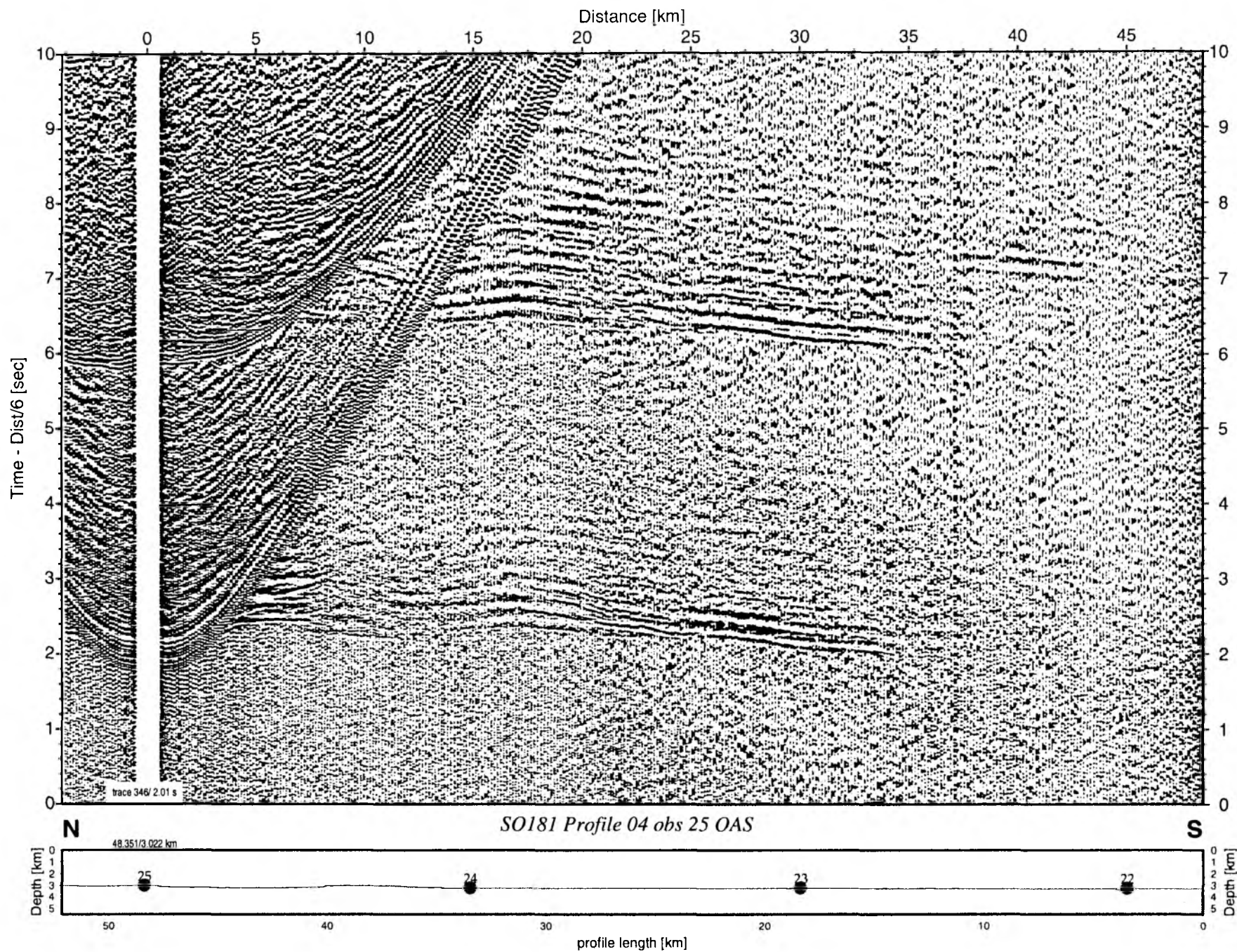


Figure 6.6.1.23: Record section from obs 25 OAS, Profile 04.

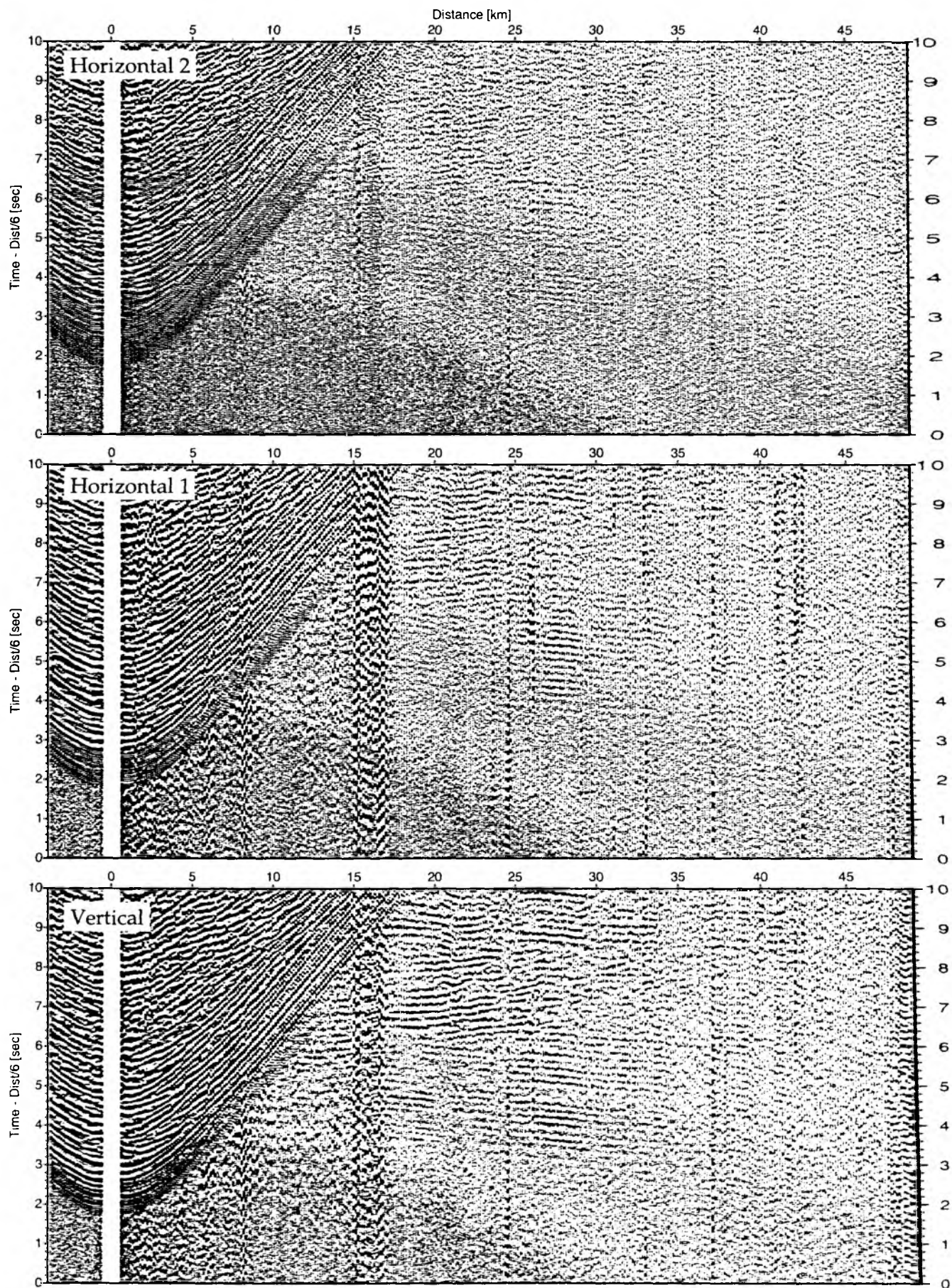


Figure 6.6.1.24: Record sections from obs 25 OAS/Owen-4.5Hz, SO181 Profile 04.

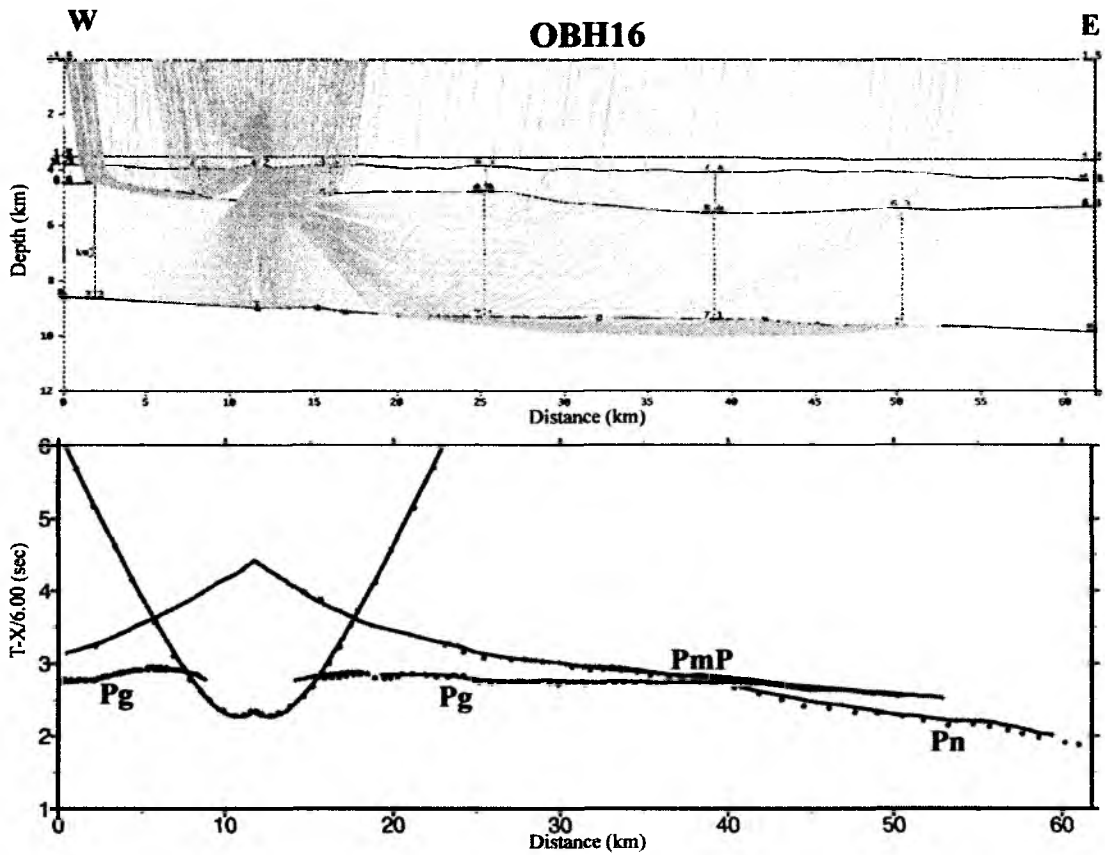


Fig 6.6.1.27: raypaths (solid lines) and travel times picks (circles) of OBH16

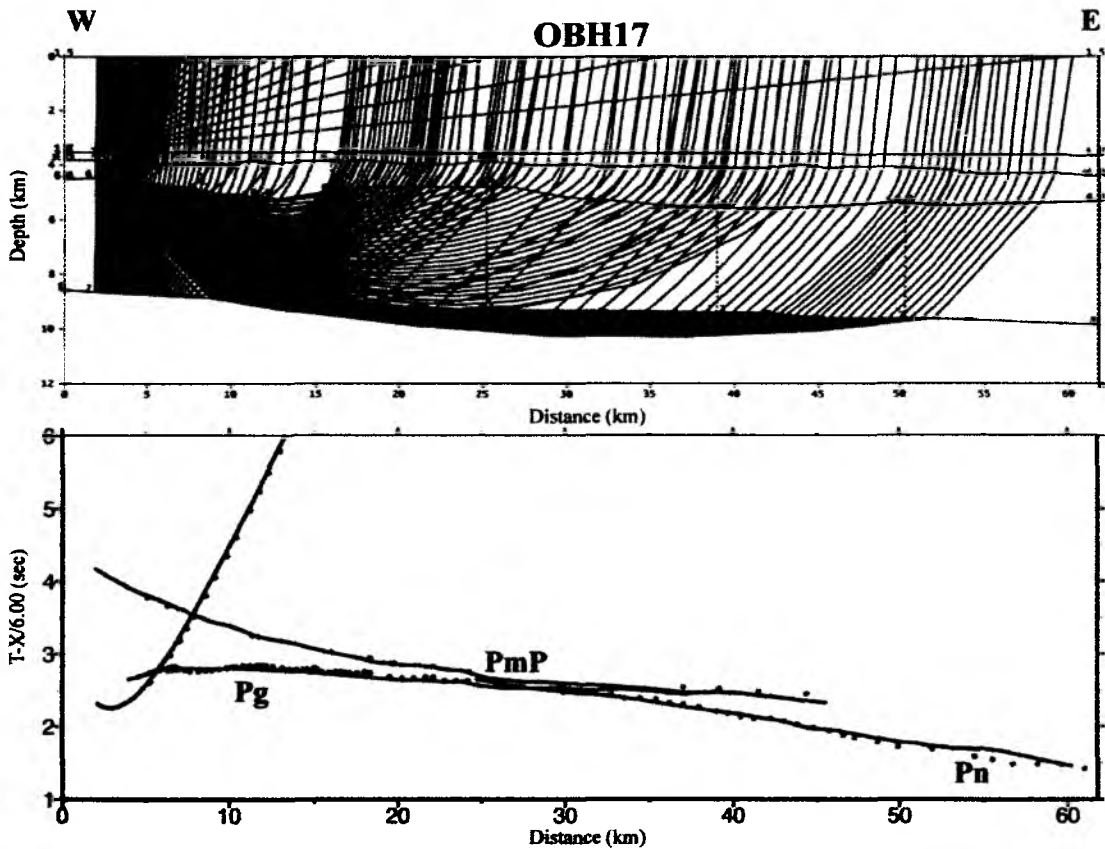


Fig 6.6.1.28: raypaths (solid lines) and travel times picks (circles) of OBH17

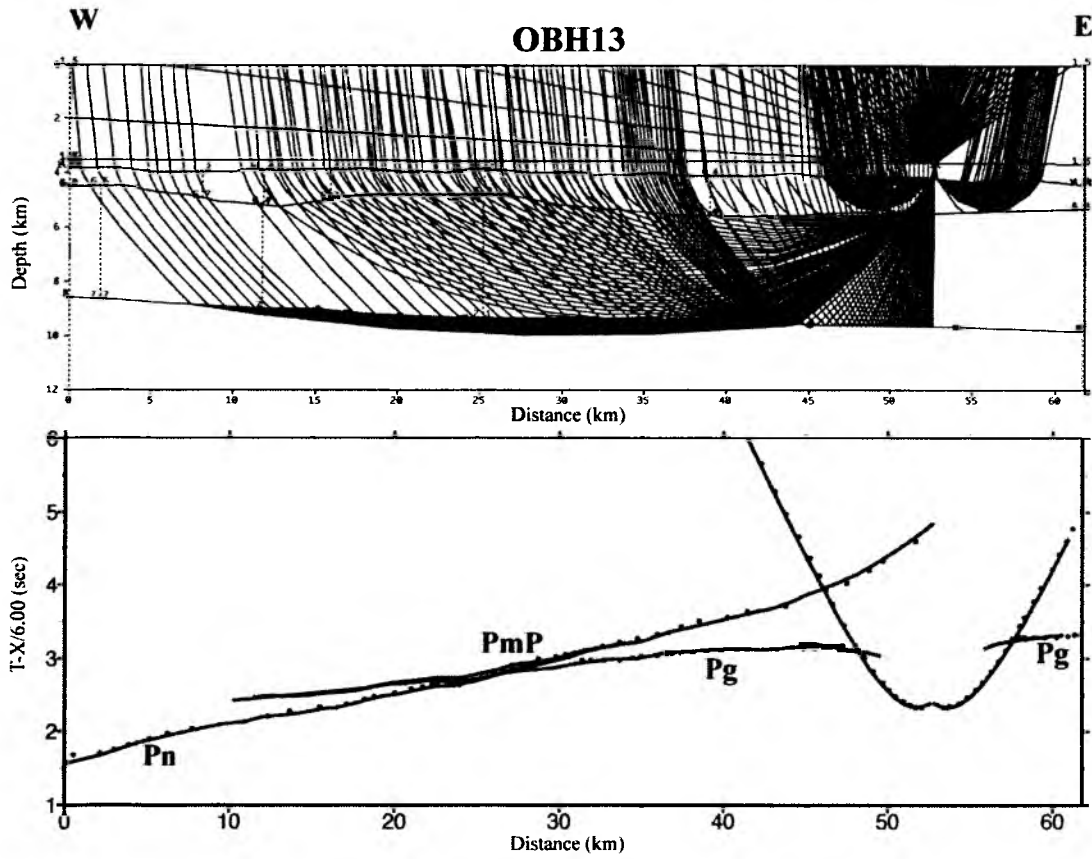


Fig 6.6.1.25: raypaths (solid lines) and traveltimes picks (circles) of OBH13

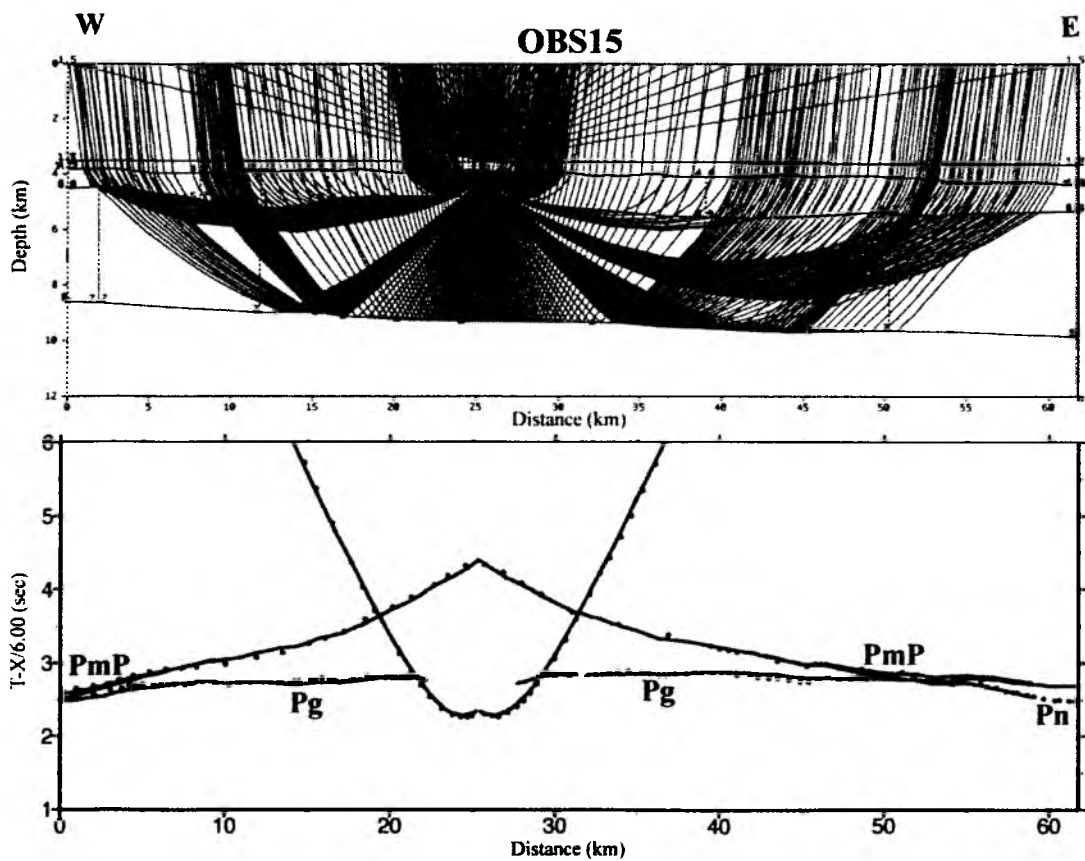


Fig 6.6.1.26: raypaths (solid lines) and traveltimes picks (circles) of OBS15

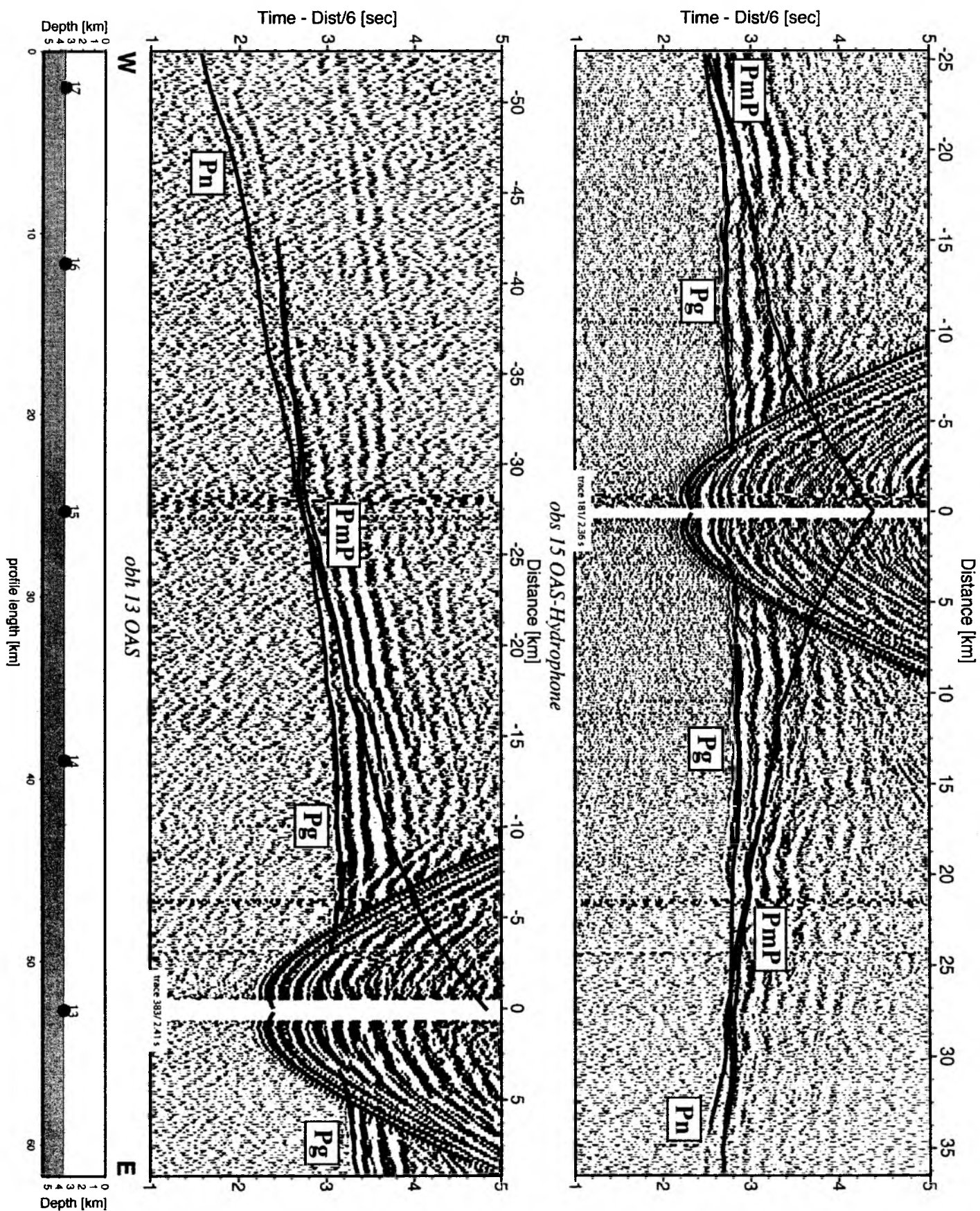


Figure 6.6.1.29: Record sections from obh 13 OAS and obs 15 OAS-Hydrophone with calculated travel times surimposed

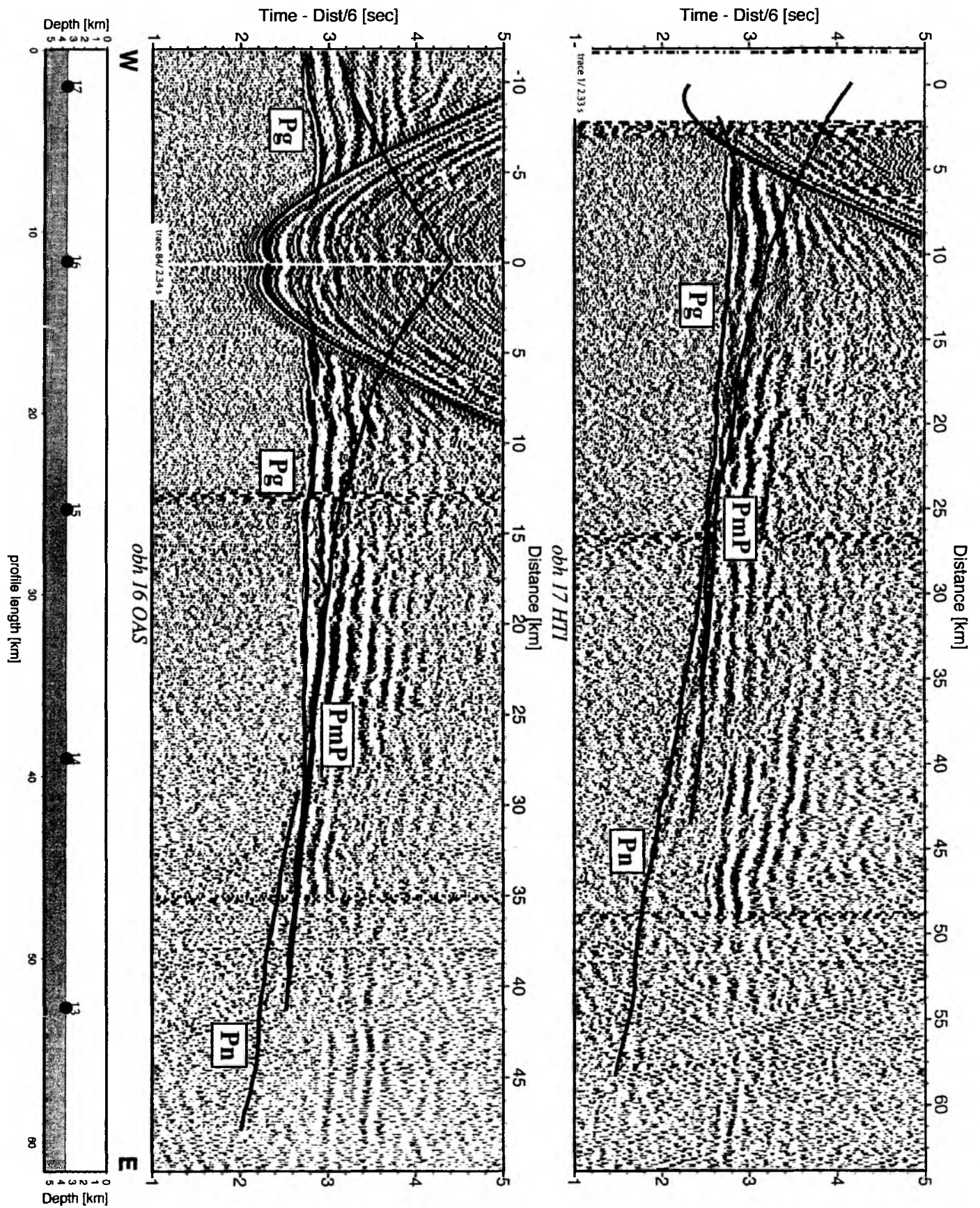


Figure 6.6.1.30: Record sections from obh 16 OAS and obh 17 HTI with calculated travel times surimposed

The ray paths and the results of the modelling for OBH 13, 16, 17 and for the OBS 15 are shown in Figures 6.6.1.25 to 6.6.1.28. Figures 6.6.1.29 and 6.6.1.30 show the record sections with calculated travel times superimposed. The calculated travel times do not fit accurately the picks extracted from the record sections but are sufficient to discuss the structure of the oceanic crust. The preliminary velocity depth model obtained from the forward modelling is shown in Figure 6.6.1.31.

To establish the velocity depth model, the water depths were taken from the bathymetry files. The vertical incidence reflections on MCS data helped to extract the thickness of the sedimentary sequence (see Figure 6.6.1.3). The basement was picked and converted to depth using a constant velocity of 1700 m/s. However the refracted waves in this sedimentary cover cannot be observed in OBH/S data due to its low velocity and its thickness of only about 300 m. Next, the oceanic crust was modelled with an upper (layer 2) and lower (layer 3) oceanic crust. The refracted waves in these both layers are difficult to distinguish on the sections. The upper oceanic crust of 1 to 2 km thickness was modelled with a velocity depth gradient from 4.2 to 6.3 km/s. The lower oceanic crust is about 4 to 4.5 km thick with a velocity increasing from 6.4 to 7.1 km/s. The top of the oceanic mantle is at about 9 km depth and was modelled using a velocity of 8 km/s. The modelling process leads us to conclude that we observe in this area a normal oceanic crust with a thickness of about 5 km which is reasonable with respect to its age of about 15 My. However, this preliminary model does not yet allow discussing the bend faulting expected in this area.

Profiles 02/03

Four OBH/S stations along profile P02a was used for the forward modelling of this profile. It has a length of about 50 km and is directed from N-NW to S-SE, orthogonal to P01 and P05. The record sections of the stations show a good quality in data with clear refracted and reflected P and S wave signals from the oceanic crust and the Moho. Using the bathymetry and the streamer data the sediment thickness could be estimated and a velocity model was created.

There are no large changes in the interfaces along this profile. The sediment thickness decreases from 500 m in the south-east to 100 m in the north-west. For the sediments a constant velocity of 1700 m/s was used in the model (Figure 6.6.1.32). Layers 2 and 3 were modelled with velocities of 4.3 to 5.8 km/s and 6.1 to 7.1 km/s, respectively. The upper oceanic crust has a thickness between 1 and 1.2 km and modelling the PmP arrivals results in a thickness of 3.4 to 4 km of the lower crust which has a lower gradient compared to the upper crust. Total crustal thickness is thus 5 km, and the Moho lies at a depth near 9 km below sea level.

Also the OBH/S stations in profile P03 show strong shear waves. P03 has a length of 75 km and is situated parallel to P02a in the western part of the array. No streamer data are available to establish the thickness of the sedimentary sequence. The basement depth was estimated from the seismic sections at each station, taking the multiples into account where the basement is relatively clearly seen. A constant velocity of 1700 m/s was again used for the sediments.

Between 43°00 S and 43°10 S a small seamount exists without sedimentary cover. In the northern part the sediment thickness increases to 500 m. Velocity and crustal thickness seem to P02.

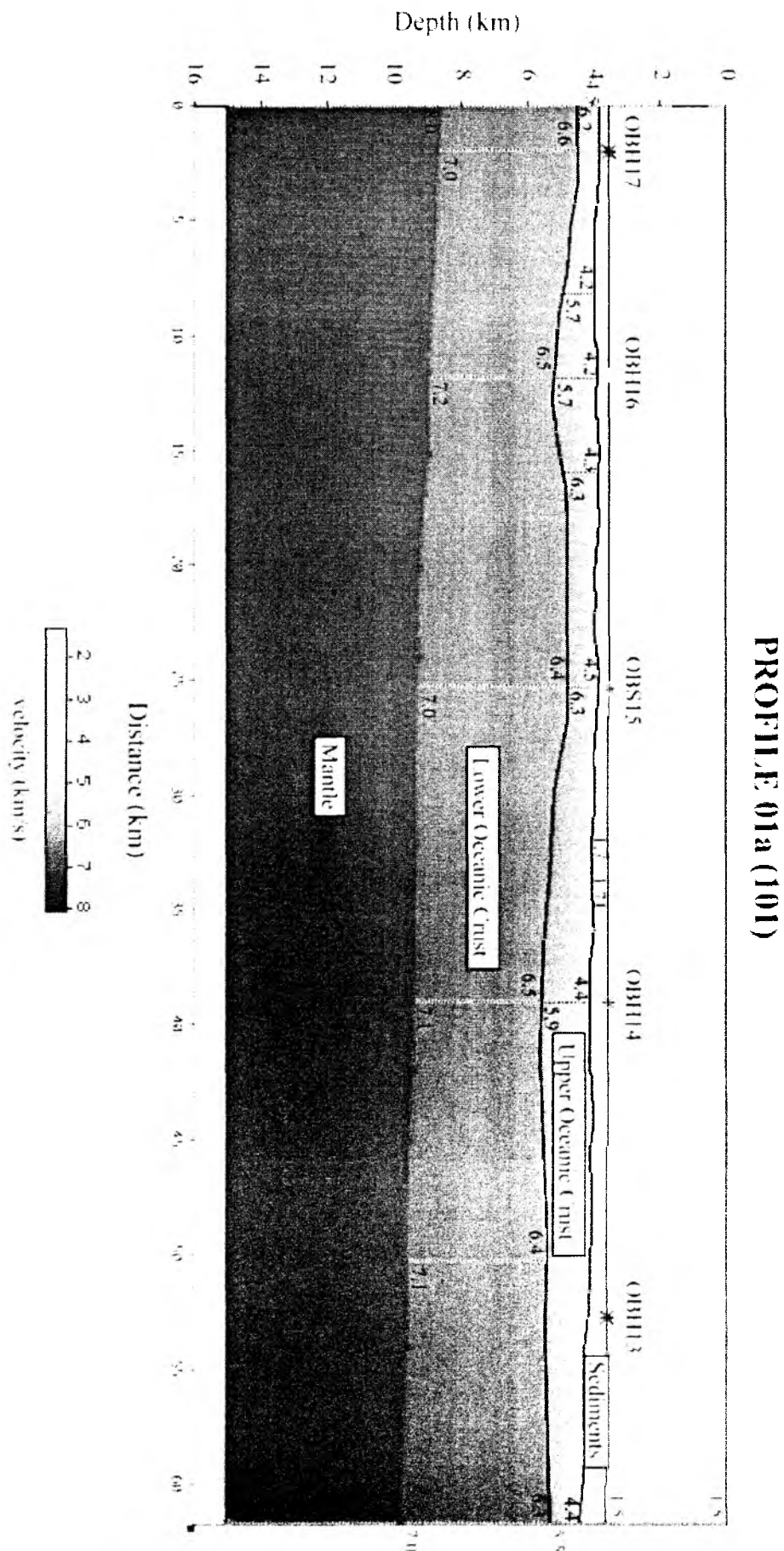


Fig 6.6.1.31 : Velocity Depth Model for Profile 01a

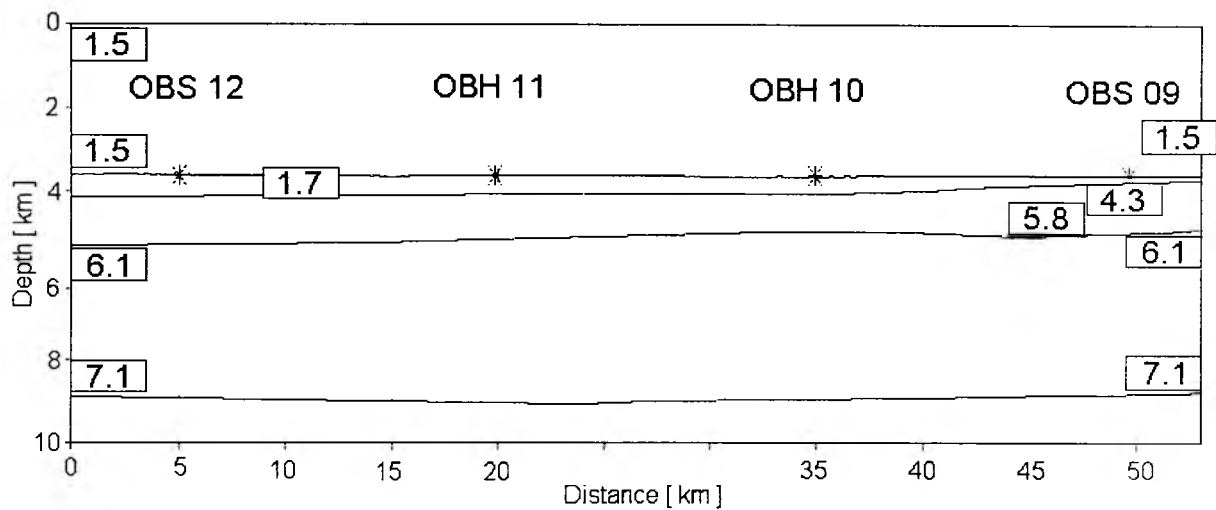


Figure 6.6.1.32: Velocity model for profile P02.

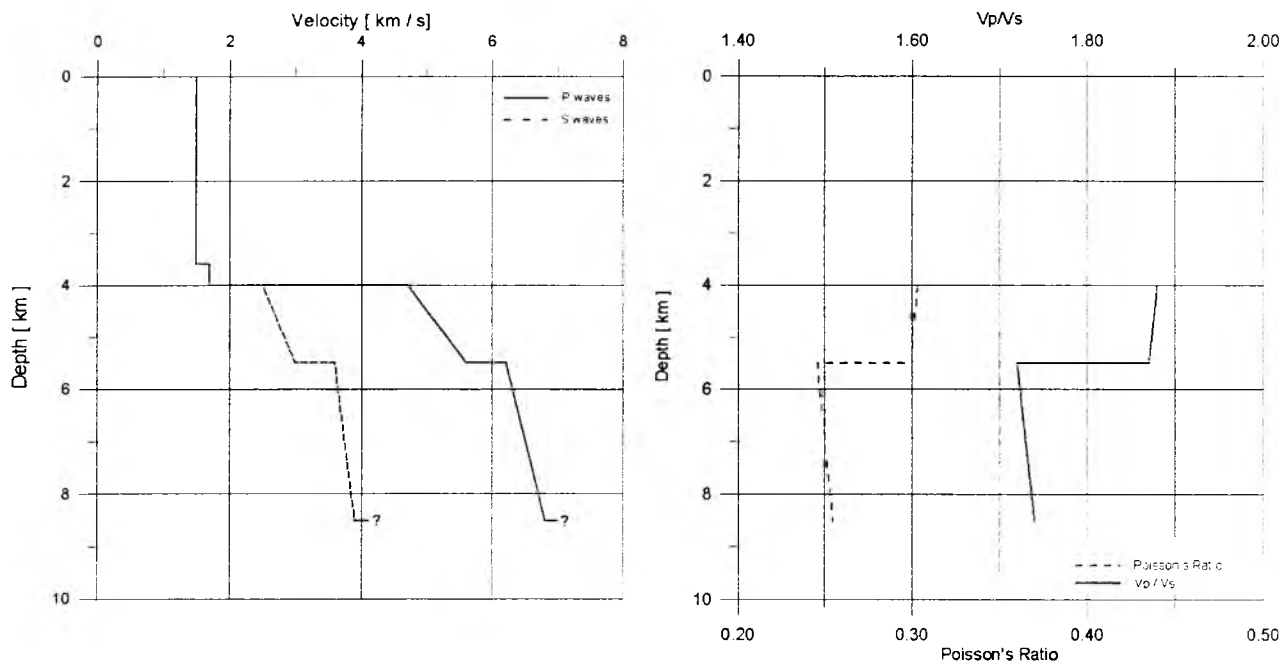


Figure 6.6.1.33: Velocity-depth model for OBH 11 on profile P02.

The data in the whole network are of a good quality. There is a pronounced difference in the appearance, depending on the direction of the profiles. In the E-W profiles one can see the clear refractions from the oceanic crust and wide-angle PmP reflections from the Moho starting around 22 km offset and continuing to larger offset. No shear waves can be seen in contrast to the N-S profiles P02a and P03 where one can detect very good shear wave signals. On the N-S profile the PmP critical distance is greater (28 km on average versus 22 km from P02), and the PmP is much shorter. Pn phases are only seen along P01, thus mantle velocities for P02 and P03 can only be estimated based on the critical distance of PmP.

To investigate Poisson's ratio a 1-D model has been derived for OBH11, after travel time correction for the sediment thickness and water depth. The P-S conversion is expected to be at the basement.

Poisson's ratio is determined by the following relation between P and S wave velocities:

$$\nu = \frac{2v_p^2 - 2v_s^2}{2(v_p^2 + v_s^2)}$$

The following table shows the v_p , v_s , their ratio, and the Poisson's ratio:

Depth in km	v_p in km/s	v_s in km/s	v_p / v_s	ν	Layer
0.0	1.5				Water
3.6	1.5				
3.6	1.7				Sediment
4.1	1.7				
4.1	4.91	2.7	1.82	0.283	Upper Oceanic Crust
5.5	5.868	3.0	1.96	0.323	
5.5	6.15	3.4	1.81	0.280	Lower Oceanic Crust
8.5	6.8	4.0	1.7	0.235	

Figure 6.6.1.33 shows the 1-D depth-velocity model of the OBH 11. With no observed Pn or Sn phases, it is not determined for the mantle.

Profile P04

Profile 04 belongs to the short-term array 2 (STA2) and consists of four OBS (22 to 25, see Figure 6.6.1.17 to Figure 6.6.1.23). The 52km long north-south line is located along 77° W (Figure 6.6.1.2). Data of a streamer were only available for OBS 24 from the crossline P06.

Comparing the calculated direct wave with the recorded data a different time shift for each OBS was observed. OBS 22 and OBS 23 have both a shift of 30ms. For OBS 24 the direct wave fits exactly. OBS 25 did not have a clear first arrival of the direct wave in the data records. Based on refractions of this station and taking into account all stations, a time shift of 30ms appeared necessary for OBS 25, too. The reasons for these time shift are not yet explained.

The record sections are of good quality. On the two outermost stations the refracted wave from the mantle can be observed. The mantle reflections are recorded at all stations.

For creating a preliminary model of the subsurface structure a forward modelling method was used. The water depths were taken from the bathymetry measurements. The resulting model is shown in Figure 6.6.1.34. Between kilometres 34 and 40 a small seamount without a sedimentary cover appears. It has a pronounced effect on all refractions. The thickness of the sediments varies between 0 and 500m. A velocity of 1.7km/s was assigned to the sediments. Because of the missing streamer data the structure of the sediments was mostly modelled to fit small undulations in the refractions from the oceanic crust. The upper crust has a thickness between 1.0 and 1.5 km with a velocity increasing with depth from 4.3 to 6 km/s. The lower oceanic crust is 2.9 to 3.8km thick with a velocity between 6.5 and 7 km/s. Underneath the seamount the lower crust is markedly thickened. The mantle is placed at a depth of 7.7 to 8km with a small dip southward, and its velocity is 7.5km/s. This velocity is unusually slow and a comparison with P06 indicates a pronounced anisotropy in the upper mantle, observed in oceanic mantle near spreading centres as well.

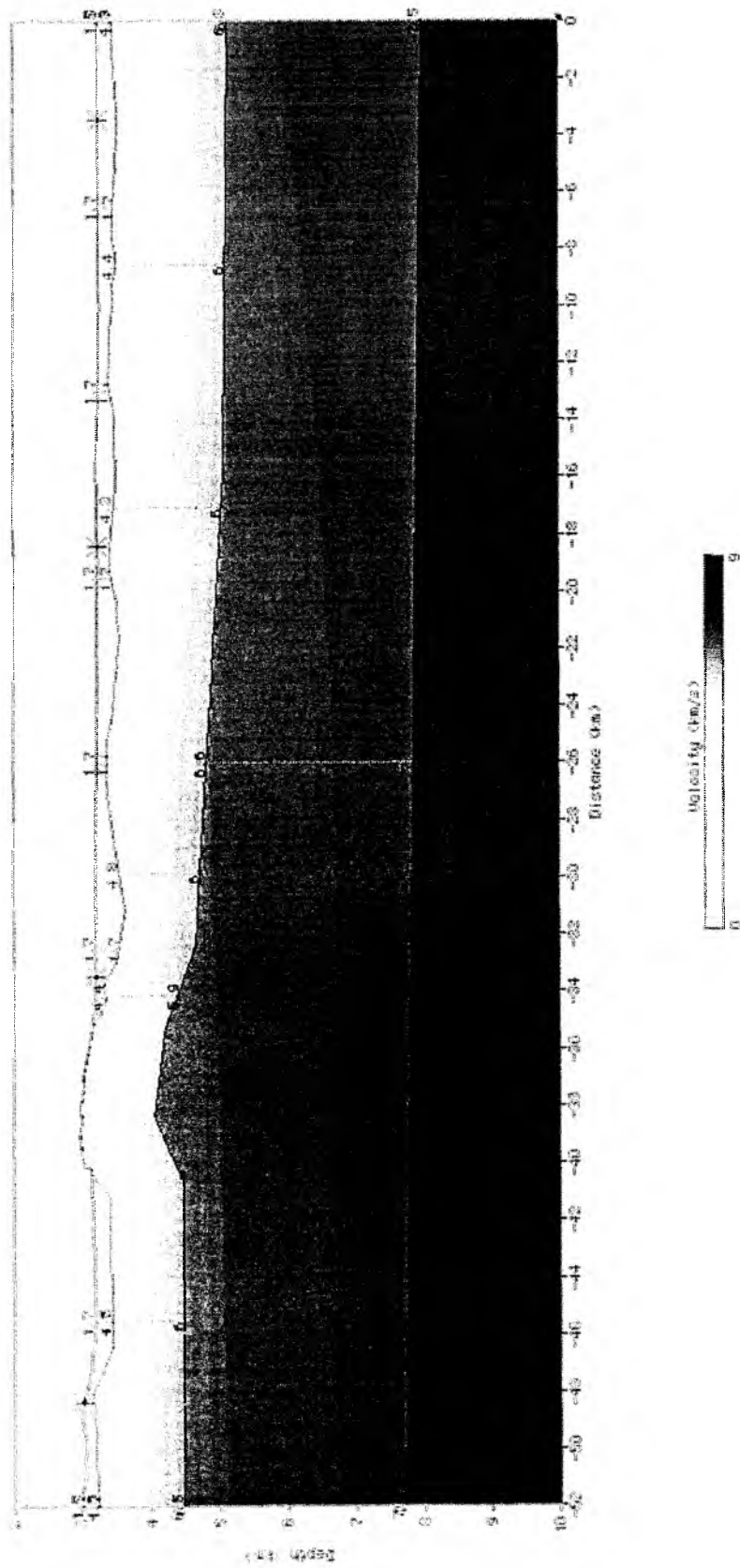


Figure 6.6.1.34: Velocity depth model for P04.

The northern outer rise earthquake network at 43°S – short term array (STA) 1

Two short-term seismic networks were deployed on the outer rise offshore southern Chile to record microseismicity generated by the bending of the subducting Nazca plate. Situated directly above most curved ocean floor, the networks were aimed at recording the seismic activity of the normal faults, extending through most of the crust and possibly reaching the uppermost mantle. Knowledge about the local earthquake activity at the outer rise is rare, and so recording microseismicity here should result in fundamental information on the activity, distribution and energy release of local earthquakes of bending incoming plates. Furthermore, accurately determined hypocentres of the local earthquakes should yield structural information as well as depth distribution. Together with airgun shots recorded in these networks, a tomographic inversion of all recorded active and passive seismic arrivals could result in a detailed structural model resolving fine structures such as fault zones. Moreover, placing the two networks on top of differently aged oceanic crust will allow establishing a relationship between thermal structure and bending related intraplate seismicity.

The northern network termed short term array 1 was positioned on corridor #2 of the TIPTEQ main transects at about 43° S (Figure 6.6.1.1), off the coast of Chiloe. Here, the age of the subducting crust is around 14.5 Ma.

Table 6.6.1.1: The station locations and sensor types of STA 1.

Station	Latitude (N)	Longitude (W)	Depth (m)	Sensors
OBS 01	42 41.54	76 39.68	3543	OAS 28 + Webb 2329
OBS 02	42 49.55	76 38.34	3526	OAS 75 + Owen (4.5 Hz) 61
OBS 03	42 57.54	76 36.71	3537	OAS 05 + Owen (4.5 Hz) 63
OBS 04	43 5.45	76 35.08	3524	DPG 87 + Webb 2352
OBS 05	43 4.39	76 24.15	3566	OAS 2 + Owen (4.5 Hz) 62
OBH 06	42 56.33	76 25.73	3559	Hydr. 5 (Univ. Hamburg)
OBS 07	42 48.31	76 27.34	3555	OAS 30 + Owen (4.5 Hz) 59
OBS 08	42 40.38	76 29.02	3553	OAS 44 + Owen (4.5 Hz) 26
OBS 09	42 39.32	76 18.01	3590	DPG + Webb 2353
OBH 10	42 47.18	76 16.46	3627	OAS 10
OBH 11	42 55.22	76 14.80	3616	Hydr. 2 (Univ. Hamburg)
OBS 12	43 3.32	76 13.16	3590	OAS 15 + Webb 1625
OBH 13	43 10.01	76 5.96	3613	Hydr. 4 (Univ. Hamburg)
OBH 14	43 10.97	76 16.03	3559	Hydr. 7 (Univ. Hamburg)
OBS 15	43 12.00	76 25.98	3530	OAS 3 + Webb 2328
OBH 16	43 12.99	76 35.92	3511	OAS 32
OBH 17	43 14.00	76 45.95	3504	HTI 63

The network of 17 stations operated 42 days starting 11 Dec 2004 until 23 Jan 2005. OBS 03, OBH 06 and 11 were recovered later, on 26 Jan, because they were part of profile 05 (see Section 6.6.3). Station locations and instrumentation of STA 1 are described in Table 6.6.1.1. In general, the data quality of the recordings of STA 1 was good. A major problem was that the seismometer channels of the Owen sensors had low gain, so that small earthquakes are often under-amplified to allow phase picking (Figure 6.6.1.35), especially the vertical components. We suggest using an additional signal amplifier for Owen type seismometers

operated together with MLS recorders (amplification factor ~100). The differential gauge sensor (DPG) of OBS 04 failed completely. The hydrophone of OBH 13 went offscale after

Table 6.6.1.2: Data quality of individual stations of STA 1. Channel 1 denotes the hydrophone record, 2-4 the seismometer records. DOY is the day of the year, earthquakes means that individual earthquakes are visible on the raw data. The vertical channel is indicated by Z.

Station	Data quality	Instrument
OBS 01	DOY 347 - 022 chan. 1 (hydr.) ok, 3 noisy, shots DOY 348 ok, earthquakes. Chan. 2,4 no (too low) gain, do not use!	OAS 28 Webb 2329
OBS 02	DOY 347 - 022 chan. 1 (hydr.) ok, 3 low, shots DOY 348 ok, earthquakes. Chan. 2,4 no (too low) gain, do not use!	OAS 75 Owen 61
OBS 03	DOY 347 - 007 ok, Z=4, shots DOY 347/348 and 356 ok, earthquakes. Chan. 1 (Hydr.) spiky since DOY 364, 2-4 low gain 2nd flash card damaged, data not readable!	OAS 05 Owen 63
OBS 04	DOY 347 - 022 chan. 2 (Z)-4 ok, shots DOY 348 ok, earthquakes. Chan. 1 (DPG) only noise, do not use!	DPG 87 Webb 2352
OBS 05	DOY 347 - 022 fairly ok, Z=4, shots DOY 347/348 ok, earthquakes. Chan. 4 (Z) low gain, chan. 1 often spiky	OAS 2 Owen 62
OBH 06	DOY 347 - 026 ok, shots DOY 347/348 (filter) and 024 ok, earthquakes. Sometimes spiky	Hydr. 5 (HH)
OBS 07	DOY 347 - 023 ok, Z=4, shots DOY 347/348 ok, earthquakes. Chan. 2,3 (Hor) low, 4 (Z) very low gain	OAS 30 Owen(4.5) 59
OBS 08	DOY 347 - 022 fairly ok, Z=4, shots DOY 348 ok, earthquakes. Chan. 2-4 very low gain, chan. 1 some spikes	OAS 44 Owen(4.5) 26
OBS 09	DOY 347 - 022 chan. 1, 2 (Z?), 3 ok, shots DOY 347/348 ok, earthquakes. Chan. 4 bad signal, do not use! DPG often clipped!	DPG Webb 2353
OBH 10	DOY 347 - 022 ok, shots DOY 348 ok, earthquakes, sometimes strange 6 s signal every ~5 h	OAS 06
OBH 11	DOY 347 - 026 ok, shots DOY 348 and 024 ok, earthquakes, shots DOY 347 and 356 only with filter	Hydr. 2 (HH)
OBS 12	DOY 347 - 022 fairly ok, Z=2, shots DOY 348 fairly ok, clipped signals, chan. 1 (Hydr.) very noisy, high gain!	OAS 15 Webb 1625
OBH 13	DOY 347/348 ok, shots DOY 348 ok, earthquakes. Offscale since DOY 348 07:00	Hydr. 4 (HH)
OBH 14	DOY 347 - 022 ok, shots DOY 347/348 ok, earthquakes. Very good station!	Hydr. 7 (HH)
OBS 15	DOY 347 - 022 chan. 1 (Hydr.) fairly ok, 4 poor, shots ok. Chan. 2, 3 (seism.) do not use! Everything gets worse since D. 357	OAS 3 Webb 2328
OBH 16	DOY 347 - 022 ok, shots DOY 347/348 ok, earthquakes	OAS 32
OBH 17	DOY 347 - 022 ok, shots DOY 347/348 ok, earthquakes. Some spikes	HTI 63

two days, so that this station recorded only the shots of the wide angle seismics. On OBS 15 we assume that the recorder did not work properly because all channels are affected. A summary about the individual stations is given in Table 6.6.1.2.

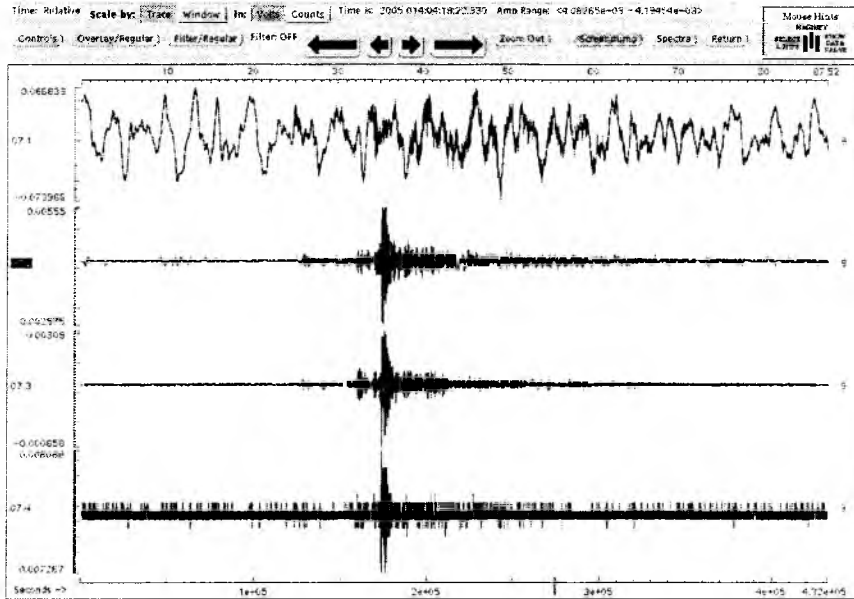


Figure 6.6.1.35: Small local earthquake recorded by OBS 07 on 14 Jan 2005. Traces are normalised individually. While the S-phase is visible on all seismometer components (trace 2-4), the P-arrival cannot be identified. The gain of the seismometer channels is smaller than on the hydrophone, by a factor ~ 100 .

In Section 5.2.3 we described the LTA/STA trigger algorithm to search the data for seismic events. Before triggering, a 5–20 Hz bandpass filter is applied to reduce the long-period noise between 0.03 and 0.5 Hz that often prevents the seismic events from being detected (Figure 5.2.3.2).

Initially, for triggering we selected 14 channels from 12 stations that produced good data (Table 6.6.1.3). Four horizontal components were included because of the high signal-to-noise ratio of S-arrivals on seismometer records. Trigger parameters are described in chapter 5.2.3. OBH 10 and the horizontal components from OBS 04 and 12 produced 5–10 times higher trigger numbers than the other stations. Checking 24 hours of data exhibited that 26 larger earthquakes were recorded on many stations, 21 smaller earthquakes were recorded on less than 3 stations. Furthermore, 14 T-waves and 17 false triggers (22%) were detected. 32 very poor events with no clear first arrivals were not detected. Excluding the three channels with extremely high trigger numbers yielded better results: 26 earthquakes, 12 T-waves and only 6 false triggers (14%). The trigger numbers of each component are shown in Table 6.6.1.3.

T-waves (tertiary waves) are sound waves trapped in the oceanic water layer, travelling at very low velocities compared to earthquakes. The normal salinity and temperature profile of the ocean decrease the compressional wave velocity of seawater from 1.7 km/s at the surface to about 1.5 km/s at a depth of 800–1300 m. Below this depth the velocity increases. This low-

velocity channel also called SOFAR (Sound fixing and ranging channel) traps sounds waves, which are bounced back and forth between the top and the bottom of the channel. The T-waves do not have sharp onsets, consist of high frequencies and are usually monochromatic (Lay and Wallace, 1995). See Figure 6.6.1.42 for an example.

Table 6.6.1.3: Numbers of STA/LTA triggers from selected STA 1 stations. (1) denotes the hydrophone, (2) the horizontal seismometer channel. OBS 04, 12 and OBH 10 detection rates are extremely high. After checking that most of that triggers are noise events, these stations were excluded for the network triggering.

Station	No. of triggers	Days	Triggers/day
OBS 01 (1)	3835	42	91
OBS 02 (1)	6479	42	154
OBS 04 (2)	25730	42	613
OBH 06	9747	42	232
OBS 07 (1)	4398	42	105
OBS 07 (2)	7392	42	176
OBS 08 (1)	14597	42	348
OBS 08 (2)	1841	42	44
OBH 10	52321	42	1246
OBH 11	6526	42	155
OBS 12 (2)	27954	42	666
OBH 14	7700	42	183
OBH 16	4996	42	129
OBH 17	6880	42	119

With a minimum number of 4 traces (i.e. an event must trigger on 2-4 stations) and a coincidence interval of 20 seconds to define a network trigger we found 3512 events with, and 1976 events without the detections of OBS 04, 12 and OBH 10 during the deployment time from 12 Dec 2004 until 22 Jan 2005. Because all major events were detected in the 24 hours test, we decided to use the latter trigger result, giving a daily trigger rate of 48 events on average.

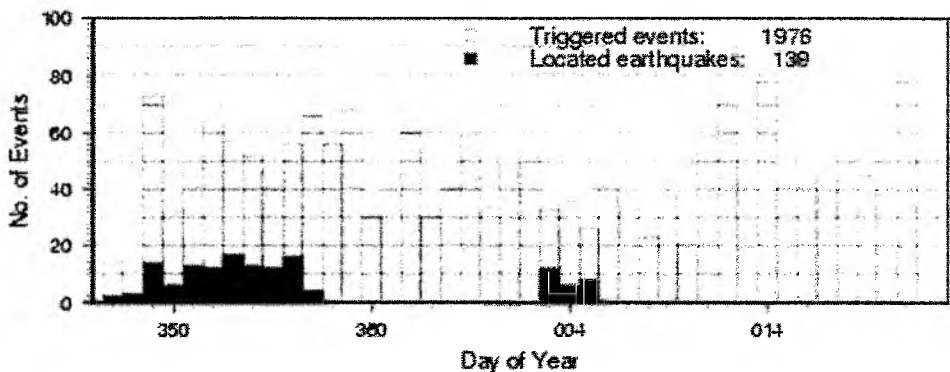


Figure 6.6.1.36: Daily number of triggered events (grey bars) and located earthquakes (black). From 12 Dec 2004 (DOY 347) until 22 Jan 2005 (DOY 022) a total of 1976 events were detected, and 139 earthquakes were already located on board.

Figure 6.6.1.36 shows the daily network trigger frequency and distribution of the 139 events already located onboard. The detection rate is changing significantly during the deployment interval between 21 and 78 events per day. This may be caused either by changes in natural seismicity (a possible earthquake swarm has been detected southeast of the network) or by a change of the false trigger rate caused by instrument failures (see Table 6.6.1.2). In the first two days when the instruments were deployed and active shooting took place only few events were detected.

After picking P- and S-arrivals the events were located using the following 1D velocity model which is a simplified version of the 2-D model from profile P01a (Figure 6.6.1.31):

Vp (km/s)	Depth (km)
1.8	0.0
4.4	0.3
5.8	1.5
6.6	2.0
6.9	3.5
8.1	6.0
8.2	11.0

In Figure 6.6.1.37 the seismicity recorded from STA 1 is shown. Most of the 139 already located earthquakes seem to belong to an earthquake swarm centred about 18 km south of OBH 14. We do not know if they are aftershocks of a larger event taking place just before the deployment, or if this is a permanent small scale seismicity pattern. The focal depths of the located earthquakes vary between 0 km at the sea floor and 30 km in the mantle, however insufficient receiver coverage and yet unknown 3D velocity structures prevent accurate hypocentre determination.

The epicentre distribution in Figure 6.6.1.37 shows that by using small scale networks like STA 1, it may happen that the major zone of seismicity is not fully covered by the network, which implies less accuracy in hypocentre determination. Adding at least 3 or 4 stations in the vicinity of the network in a 1-2 array diameter distance away from the centre may solve this problem in the future.

On 26 Dec 2004 the catastrophic $M_w = 9.0$ earthquake happened in Sumatra, Indonesia, killing more than 150,000 people. It was the strongest earthquake for the last 40 years, the 4th largest ever recorded. The stations of STA 1 and 2 recorded this event though they are not designed for recording teleseismic earthquakes. The hydrophones, however, recording frequencies down to ~ 0.02 Hz, produced records of good quality. Using a bandpass filter from 0.001 to 0.05 Hz with a sharp cutoff (8 poles) we were able to identify the first arrival of this event at 01:16:38 UTC. Signals of that event were received for about 3 hours. Figure 6.6.1.38 and 6.6.1.39 show the records from OBS 12 and OBH 16, respectively.

Seismogram examples are shown in Figures 6.6.1.40 and 41. The first earthquake presented from 15 Dec 2004 took place half way between OBS 12 and OBH 14 inside the network. The second example shows a swarm earthquake from 06 Jan 2005 located 33 km south from OBH 14 with $M_c = 2.9$.

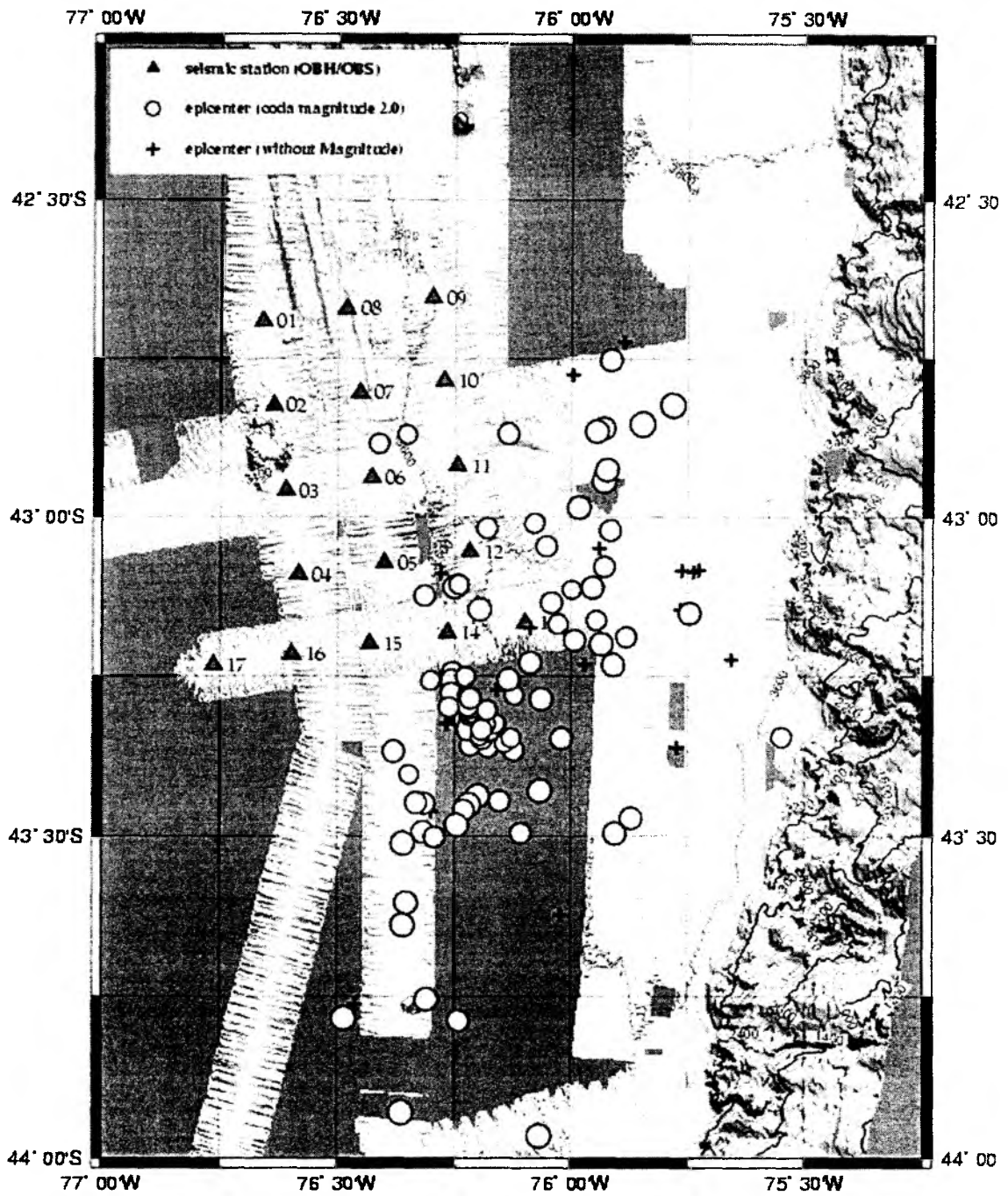


Figure 6.6.1.37: Epicentres from earthquakes located so far by STA 1 network. Most of the seismicity happened outside the network close to its southeast corner. Coda magnitudes are indicated when available.

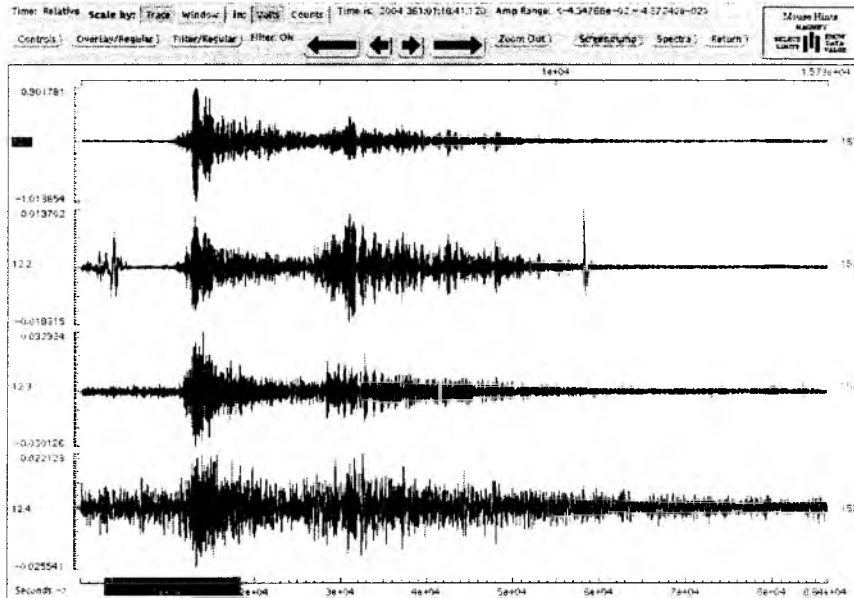


Figure 6.6.1.38: Seismogram of the $M_W = 9.0$ Sumatra earthquake from 26 Dec 2004 recorded from OBS 12 and 0.01-0.1 Hz bandpass filtered. The OAS-hydrophone (top) shows the best recording quality, while the Webb seismometer with an Eigenfrequency of 1 Hz has a lower signal-to-noise ratio. Ground displacement on site OBS 12 lasted for more than 3 hours.

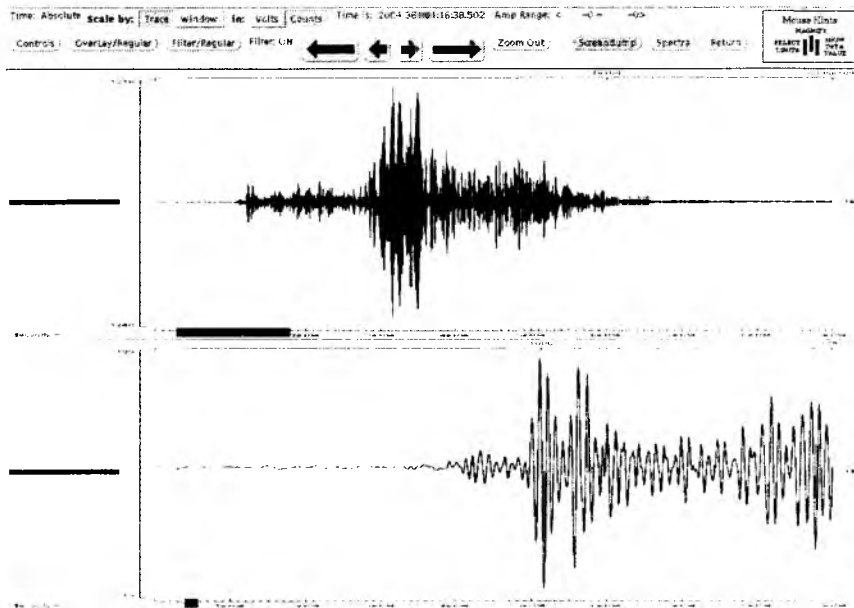


Figure 6.6.1.39: A 0.001-0.05 Hz bandpass filtered seismogram of the Sumatra earthquake from 26 Dec 2004 recorded from OBH 16 (OAS Hydrophone). The top panel shows the entire earthquake whose ground displacement lasted for about 3 hours at the receiver site. In the bottom panel the P-wavelet is zoomed in to demonstrate that the teleseismic P-arrival can be accurately determined when using a very long period filter.

STA1 2004-12-15-1048-48S STA1_038

Plotstart time: 2004-12-15 10:49 36.717

2004-12-15-1049-46.0 L -43.111 -76.252 16.7 TIP 150.4 2.8CTIP

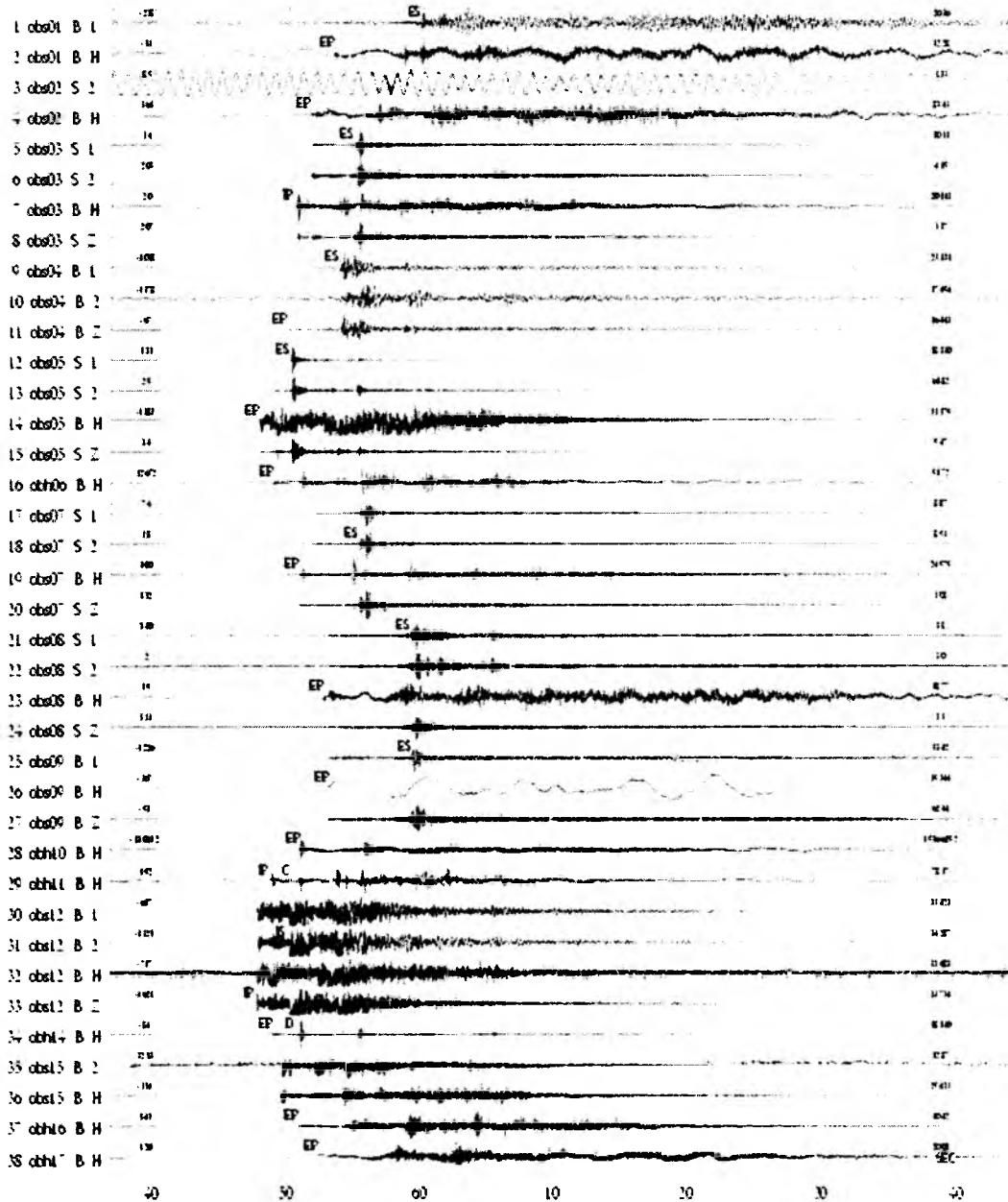


Figure 6.6.1.40: Deep focus earthquake from 15 Dec 2004, 10:49 UTC located by the STA 1 network at 43.111° S, 76.252° W within the network with a focal depth of 17 km. Where it was possible, P and S first arrivals are indicated as well as polarities.

Figure 6.6.1.41: Another deep focus event from 06 Jan 2005, 21:48 UTC located outside the network 33 km south of OBH 14. This earthquake may belong to the swarm detected in the area south of OBH 14.

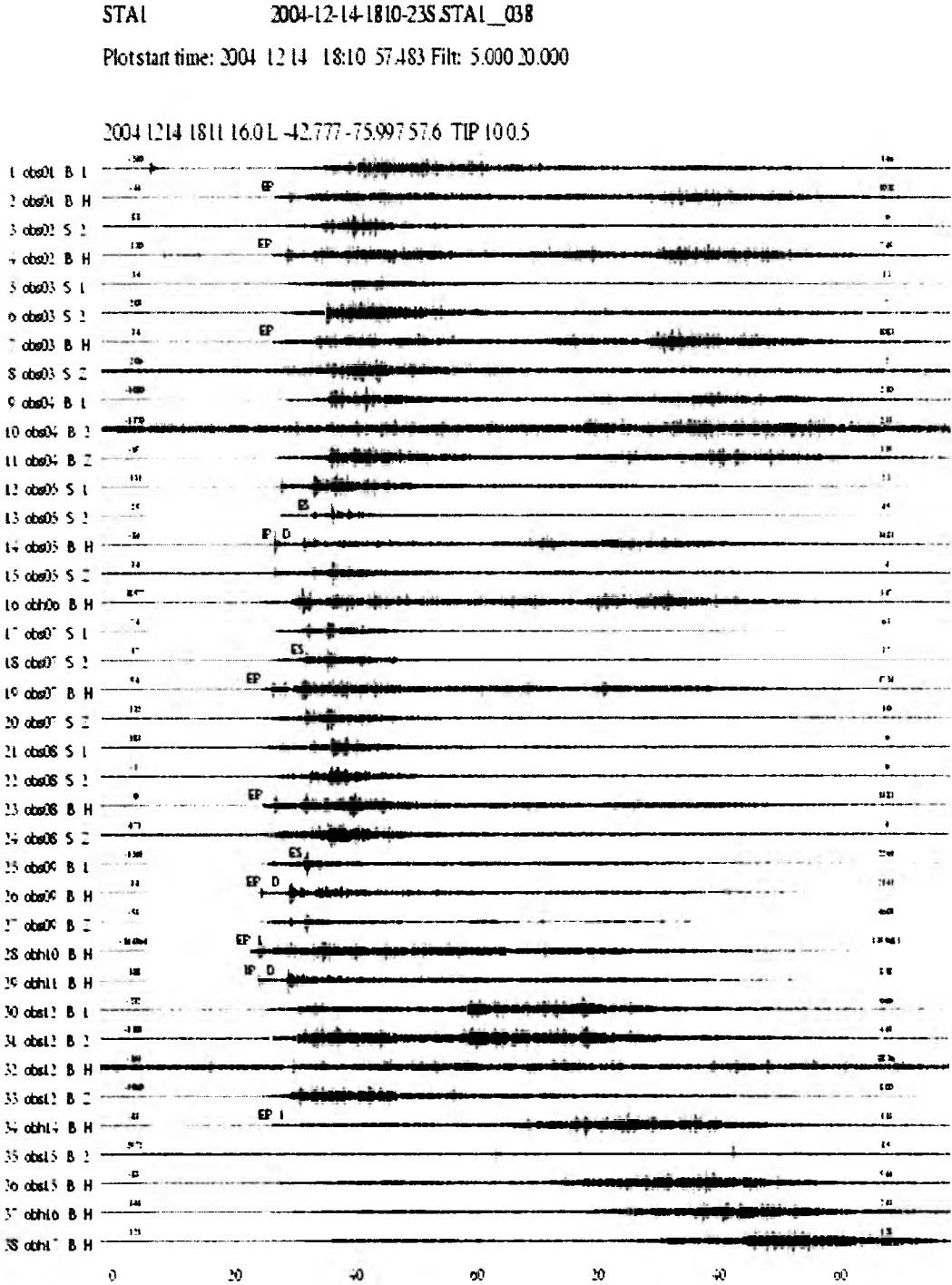


Figure 6.6.1.42: Earthquake from 14 Dec 2004, 18:11 UTC accompanied by T-waves. The event was located 23 km east of OBH 10 at 42.777° S, 75.997° W.

The southern outer rise earthquake network at 45°S - short term array (STA) 2

The main objectives of the passive seismological experiment here is to detect and record the local seismicity induced by outer rise bending of the oceanic plate prior to its subduction to understand the mechanism of plate bending and find possible fluid paths through the crust into the uppermost mantle which are bounding conditions for serpentinization models. The spatial dimensions of the passive seismic networks are designed to register local tectonic events associated with plate bending.

The southern network (STA 2) was located 200 km south of STA 1, on the other side of the Guafo Fracture Zone, where the subducting crust is only 6.5 Ma old.

Our preliminary earthquake locations within STA 2 let us assume that the lateral coverage with hypocentres should be sufficient for a detailed seismic tomographic study of the outer rise area. Furthermore, a combined tomographic inversion including earthquake and shots from the seismic lines should be achieved. Detailed initial velocity models are available from the active seismic experiments carried out during this cruise (P04 and P06).

Table 6.6.1.4: *The station locations and sensor types of STA 2 array.*

Station	Latitude (N)	Longitude (W)	Depth (m)	Sensors
OBS 18	44 36.48	76 56.95	3074	HTI 61 + Owen (4.5 Hz) 19
OBH 19	44 44.35	76 53.89	2787	HTI 45
OBS 20	44 52.05	76 50.73	3025	OAS 45 + Owen (4.5 Hz) 27
OBS 21	44 59.83	76 47.59	3106	OAS 37 + Owen (4.5 Hz) 24
OBS 22	44 57.58	76 36.68	3262	OAS 35 + Owen (4.5 Hz) 41
OBS 23	44 49.99	76 39.65	3237	OAS 29 + Owen (4.5 Hz) 29
OBS 24	44 42.03	76 42.78	3221	OAS 17 + Owen (4.5 Hz) 20
OBS 25	44 34.33	76 45.93	3029	HTI 28 + Owen (4.5 Hz) 60
OBS 26	44 32.09	76 35.07	3017	HTI 43 + Owen (4.5 Hz) 40
OBS 27	44 39.92	76 31.79	3240	HTI 37 + Owen (4.5 Hz) 10
OBH 28	44 47.65	76 28.63	3255	Hydr. 6 (Univ. Hamburg)
OBS 29	44 53.37	76 25.56	3263	OAS 4 + Owen (4.5 Hz) 57

Twelve ocean bottom instruments operated from 14 Dec 2004 until 28 Jan 2005 in the outer rise short term array 2 centred about 44° 50' S, 76° 40' W on the outer rise of the south Chilean subduction zone (Table 6.6.1.4). All stations consisted of a hydrophone and a 3-D short period seismometer, except OBH 19 and 28 which are hydrophones only. A location map is shown in Figure 6.6.1.2.

All stations operated well throughout the deployment interval except OBS 26 which produced no usable data due to a recorder failure. The hydrophones of OBS 21 and 25 had no gain or went offscale. On OBS 18, 24, 25 and 27 the polarity of the HTI-hydrophone channels are flipped (Figure 6.6.1.43). This may be common for HTI hydrophones! The OAS hydrophones seemed to have correct polarity. In general, the gain of the seismometer channels was too low, so that only the shots from the active seismic experiments and the first arrivals of stronger earthquakes are well recorded. However, the seismometer data are still useful, because the S

Table 6.6.1.5: Data quality of individual stations. Channel 1 is the hydrophone record, 2-4 the seismometer records. DOY denotes day of the year, earthquakes means that individual earthquakes are visible onto the traces. The vertical component is indicated by Z.

Station	Data quality	Sensor
OBS 18	DOY 349-020 chan. 1 ok, 2-4 low gain, shots DOY 350 ok, earthquakes, Z=2 (!)	HTI 61 Owen(4.5) 19
OBH 19	DOY 349-027 ok, shots DOY 350 (filter) and 004 ok, earthquakes	HTI 45
OBS 20	DOY 349-027 chan. 1-3 ok, 4 (Z) low gain, shots D. 350 ok, Earthquakes. Timing error of ~7 sec since start (→skew!).	OAS 45 Owen(4.5) 27
OBS 21	DOY 349-022 chan. 2-4 (Z) low gain, shots very poor, earthquakes. Chan. 1 (Hydr.) no gain, do not use!	OAS 37 Owen(4.5) 24
OBS 22	DOY 349-027 chan. 1 ok, 4 (Z) low gain, shots DOY 350 ok, earthquakes. Chan. 2 (002-021), 3 (all) no gain, do not use!	OAS 35 Owen(4.5) 41
OBS 23	DOY 349-027 ok, Z=4, shots DOY 350 ok, earthquakes	OAS 29 Owen(4.5) 29
OBS 24	DOY 349-027 ok, Z=4, shots DOY 350 ok, earthquakes	OAS 17 Owen(4.5) 20
OBS 25	DOY 349-027 chan. 3 and 4 (Z) low gain, shots ok, earthquakes. Chan. 1 (Hydr.) offscale since DOY 350 13:34, chan. 2 no gain	HTI 28 Owen(4.5) 60
OBS 26	No usable data ! (recorder problem > MLS 040101)	HTI 43 Owen(4.5) 40
OBS 27	DOY 349-027 ok, Z=4, shots DOY 350 and 003 ok, earthquakes	HTI 37 Owen(4.5) 10
OBH 28	DOY 350-028 ok, shots DOY 350 (filter) ok, earthquakes	Hydr. 6 (HH)
OBS 29	DOY 350-028 ok, Z=4, shots DOY 350 chan. 1 (Hydr.) ok, chans. 2-4 low gain, earthquakes	OAS 4 Owen(4.5) 57

arrivals have higher amplitudes and can be picked, and so the S-P time interval constrains the source-receiver distance very well. Because of the short operating interval no timing problems occurred due to power outages. A more detailed overview about individual stations is given in Table 6.6.1.5.

As described in Section 5.2.3, an LTA/STA trigger algorithm was applied to the data to search for seismic events. Prior to the trigger a 5–20 Hz bandpass filter had to be applied to reduce the long-period noise between 0.03 and 0.5 Hz that often prevents the seismic events from being triggered (Figure 5.2.3.2). Using the trigger parameters from Table 5.2.3.1 we obtained less than 5% false triggers and loose only minor events which are visible on less than

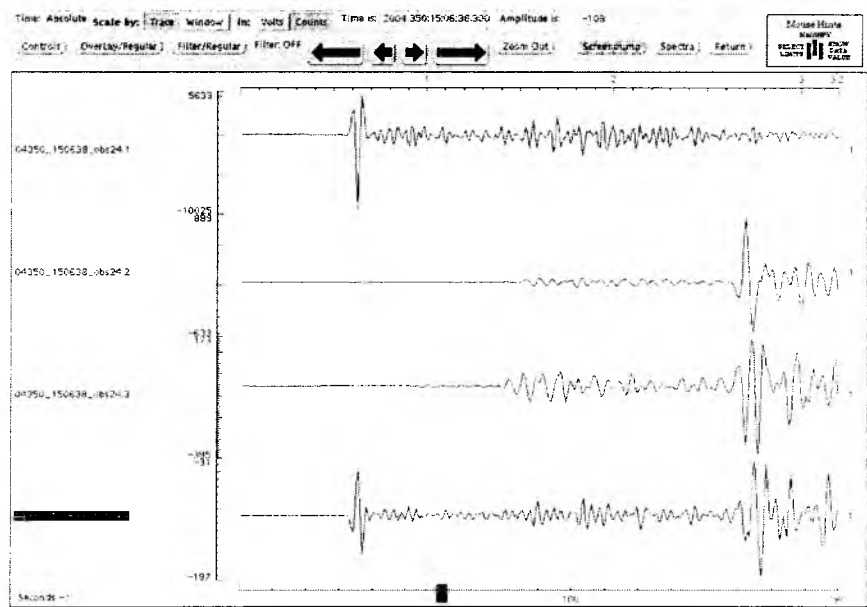


Figure 6.6.1.43: Flipped polarities of the P-arrival of an earthquake from 15 Dec 2004 recorded on OBS 24. Usually P-polarities of hydrophone (top) and vertical seismometer component (bottom) should be identical. The other HTI hydrophones show the same behaviour, so that it seems a systematic failure.

3 stations. For each day we obtained a trigger file that contained the valid network trigger times, on which the event cutting was based. We selected 8 stations for triggering that produced good data. Because of the high signal-to-noise ratio of S-arrivals on the seismometer records we included trace 2 from the selected OBS. The trigger numbers of each component selected are shown in Table 6.6.1.6. There are no extreme deviations from the

Table 6.6.1.6: STA/LTA triggers numbers from selected STA 2 stations. (1) means hydrophone, (2) horizontal seismometer channel. Detection rates are very similar except OBS 24 (2), OBS 27 (1) and OBS 29 (2). The average trigger rate per day is 142.

Station	No. of triggers	Days	Triggers/day
OBH 19	4648	45	103
OBS 20 (1)	5502	45	122
OBS 20 (2)	4304	45	96
OBS 22 (1)	4935	45	110
OBS 22 (2)	3536	25	141
OBS 23 (1)	5561	45	124
OBS 23 (2)	6657	45	148
OBS 24 (1)	5428	45	121
OBS 24 (2)	14625	45	325
OBS 27 (1)	11079	44	252
OBS 27 (2)	5761	44	131
OBH 28	5115	44	116
OBS 29 (1)	5677	44	129
OBS 29 (2)	3066	44	70

daily average, which means that the recording performance of the selected stations are comparable. With a minimum number of 4 traces (i.e. an event must trigger on at least 2 stations) and a coincidence interval of 20 seconds to define a network trigger we found 3868 events during the deployment time, i.e. 86 triggers per day on average. Checking a full day of data, we found 3% false triggers. Undetected events were either small earthquakes with an unclear shape on most records, or T-waves.

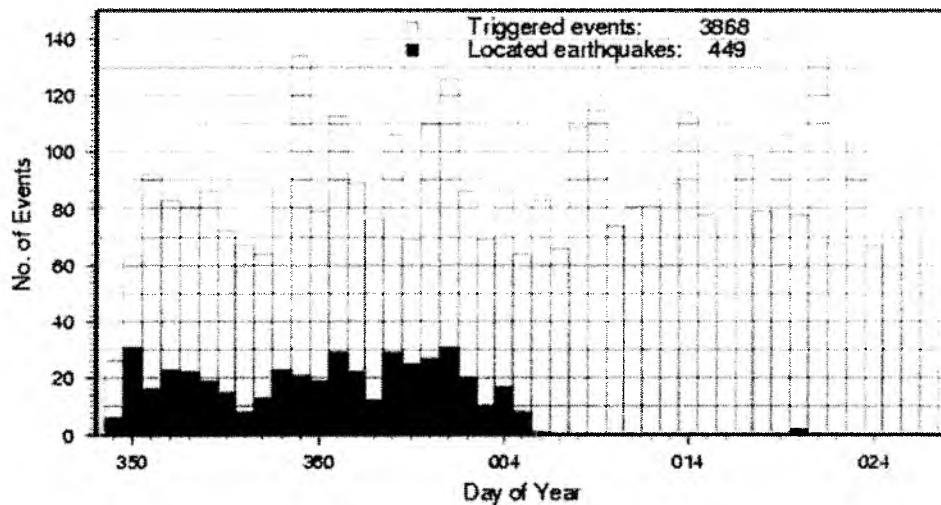


Figure 6.6.1.44: Daily number of triggered events (grey bars) and earthquakes already located (black). A total of 3868 events were triggered from 14 Dec 2004 (DOY 349) until 27 Jan 2005 (DOY 027). 449 earthquakes were already located on board.

Figure 6.6.1.44 shows the daily amount of network triggers and the number of earthquakes already located onboard (in total 449). The daily trigger frequency lies between 64 and 114 with three outliers larger than 126. Its distribution did not change significantly during the recording time. Also no stronger earthquake occurred prior or within the deployment interval which may have induced higher seismic activity. Therefore, we may assume that the observed seismicity is representative for the normal local seismicity in this area. A crude test of the trigger times yielded that about 15% of the events detected by STA 2 coincide with events triggered from STA 1.

After picking P- and S-arrivals the events were located using the following 1D velocity model which is a simplified version of the 2-D model from profile P04 (Figure 6.6.1.34).

Vp (km/s)	Depth (km)
1.8	0.0
4.3	0.3
5.2	1.0
6.6	2.0
7.0	3.0
8.0	5.0
8.2	11.0

Most of the 449 earthquake epicentres located so far are within or nearby the network and are concentrating in the eastern part. Figure 6.6.1.45 shows the epicentre distribution of the located events. Coda magnitudes are indicated if available. No local magnitudes based on amplitudes (Gutenberg and Richter, 1954) were determined due to the lack of instrument response functions. Coda magnitudes are calculated using parameters obtained from onshore stations in California (Lee et al., 1972) which may not be valid for this area and for OBS stations, especially. We suggest that the coda magnitudes should be calibrated by using earthquakes recorded by both, the OBS network and the temporary land stations of the TIPTEQ project. The magnitudes presented here can only be used to obtain relationships between earthquakes from the STA 2 catalogue only. Figure 6.6.1.46 shows the magnitude distribution of STA 2 events already analysed.

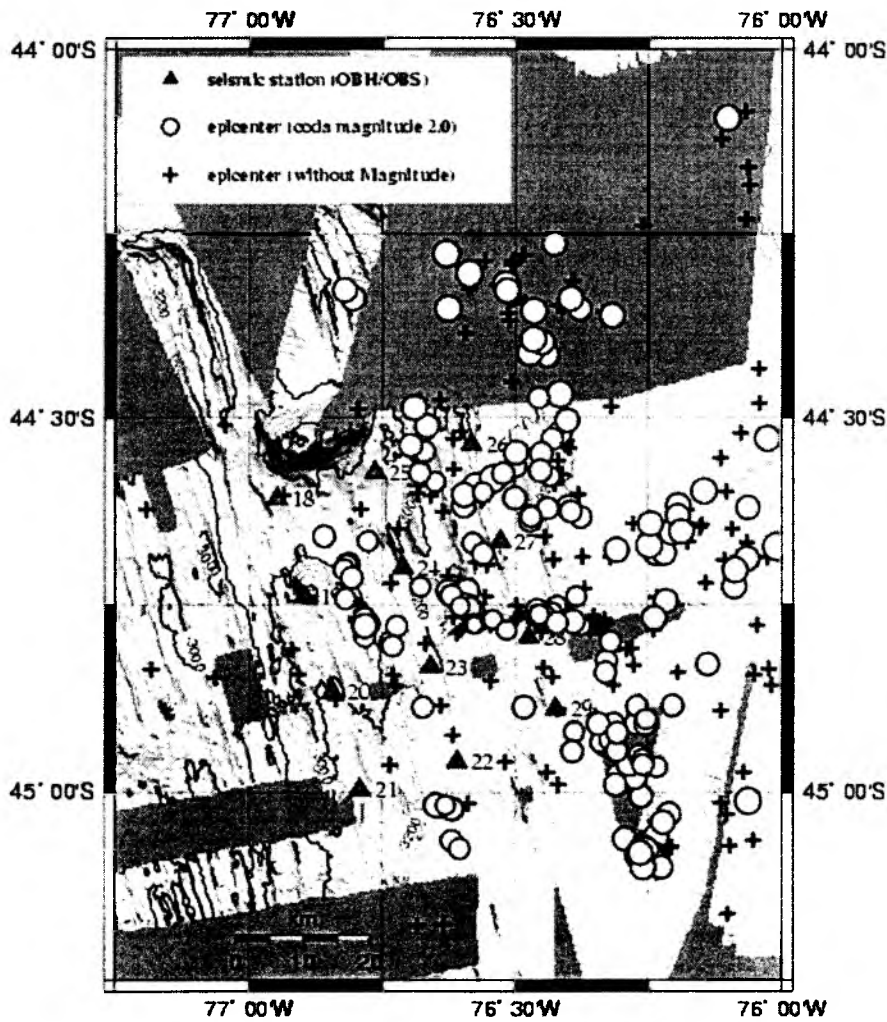


Figure 6.6.1.45: The epicentre distribution of 449 located earthquakes in the STA 2 area with bathymetric information where it is available. Seismicity clusters parallel to the main structures (spreading ridges) of the oceanic plate.

The epicentres appear as linear clusters that follow the main tectonic features (i.e. the spreading ridges), with an increase of seismicity towards the trench. This seems to imply that

when the oceanic plate starts bending faults are opened along the instability zones of the spreading ridges. How deep these faults are and if they extend into the mantle is subject to further investigation.

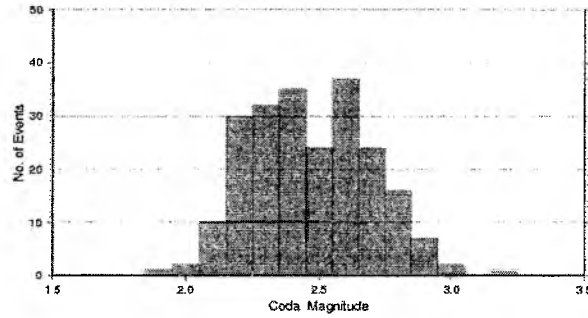


Figure 6.6.1.46: Coda magnitudes of 221 earthquakes located with the STA 2 network.

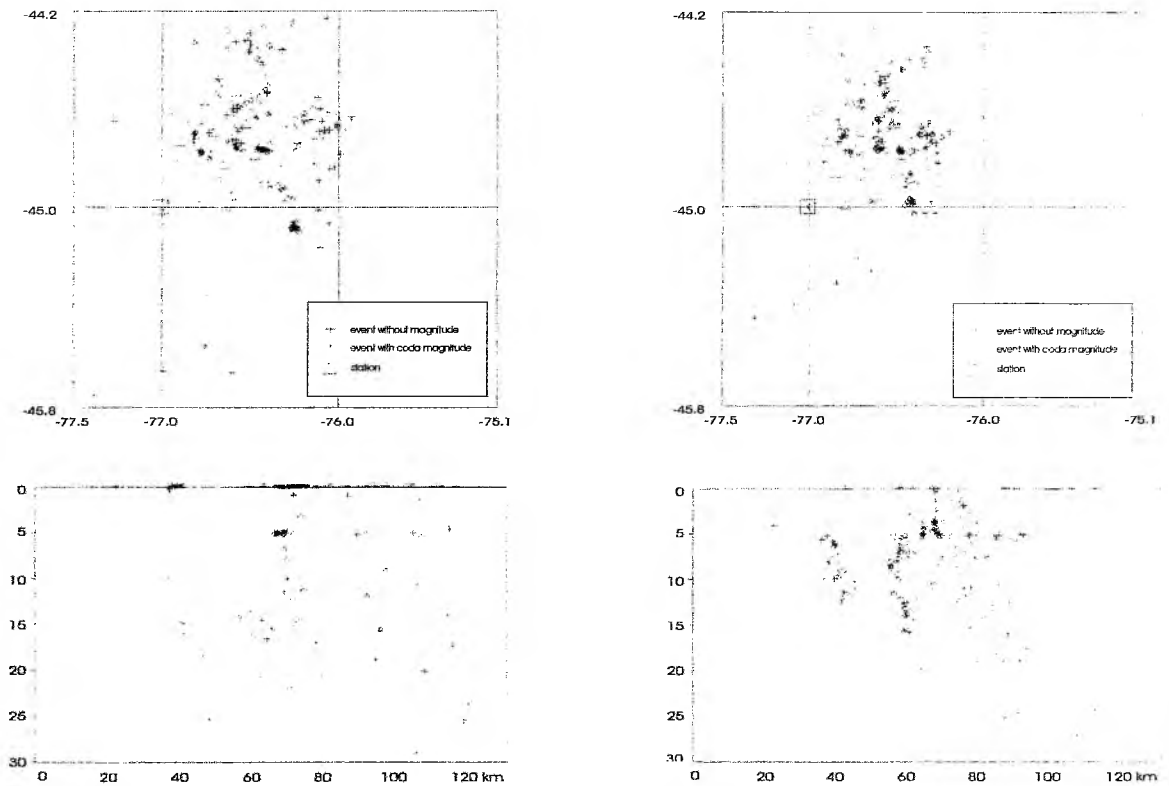


Figure 6.6.1.47: Hypocentres of 210 earthquakes recorded from the STA 2 array with 6 or more stations providing valid phases for localisation. Depth sections (bottom) show hypocentres projected onto the lines in the centre of the squares. Hypocentres determined with a V_P/V_S ratio of 1.85 are shown on the left whereas a V_P/V_S ratio of 2.30 was used for calculating hypocentres shown on the right. In the left panel most hypocentres are pinned to the zero level of the model at the ocean bottom, all others are distributed within a diffuse cloud. Increasing the V_P/V_S ratio to 2.30 the hypocentres leave the ocean bottom and form linear structures stretching downward into the uppermost mantle to 25 km depth.

The depth extent of the earthquakes located is less certain. With the velocity model of P04 many earthquakes were located directly at the ocean bottom (zero level) which is the starting depth of the location algorithm. Because of the very low velocities obtained from wide angle profile P04, which is characteristic for layers containing deep water, we assumed that the V_p/V_s ratio, which usually is about 1.74, must be increased. The average V_p/V_s ratio obtained from Wadati diagrams (i.e. S-P time over P traveltime plots) of earthquakes with 6 or more stations contributing phases is 1.8. This is another hint that the V_p/V_s ratio is higher than usual. Figure 6.6.1.47 (a) shows the hypocentres of 210 earthquakes with valid phases from 6 or more stations projected onto a profile perpendicular to the spreading ridges, employing a V_p/V_s ratio of 1.85 which we also used to determine the epicentres shown in Figure 6.6.1.45. The depths in Figure 6.6.1.47 (b) were calculated with $V_p/V_s = 2.30$. The high V_p/V_s ratio pushes the hypocentres away from the ocean bottom into deeper regions where they form focussed linear structures, which may represent fault zones. However, the 1D model employed here may not be accurate enough to calculate hypocentre distribution of the earthquakes in the outer rise area.

The epicentre distribution in Figure 6.6.1.45 shows again, that placing 3-4 additional stations at 1-2 array diameter distance around the network may significantly enhance its locating accuracy due to a better azimuthal coverage of the source region.

Three seismogram examples recorded by STA 2 network are presented. Figure 6.6.1.48 shows an earthquake from 15 Dec 2004 that happened beneath the network. Most stations have good records except OBS 25 due to the relative strength ($M_C = 2.5$) and the short focal distance. A deep focus event from 26 Dec 2004 is presented in Figure 6.6.1.49. It is located 32 km east of OBH 28. This earthquake occurred closest to the trench. All stations delivered good signals.

Earthquakes that come from >30 km distance and show T-wave arrivals were often recorded in both networks (see subsection of STA 1). The lack of clear onsets made only few of these earthquakes locatable. Most of them originated south of the network, at distances from 30 to 70 km. In many cases only the T-waves were recorded because of their characteristically high amplitudes. In the case of this experiment, these wave sets had durations from 20 to 50 s. Figure 6.6.1.50 presents another example of T-waves accompanying an event located approximately 70 km south from OBS 21.

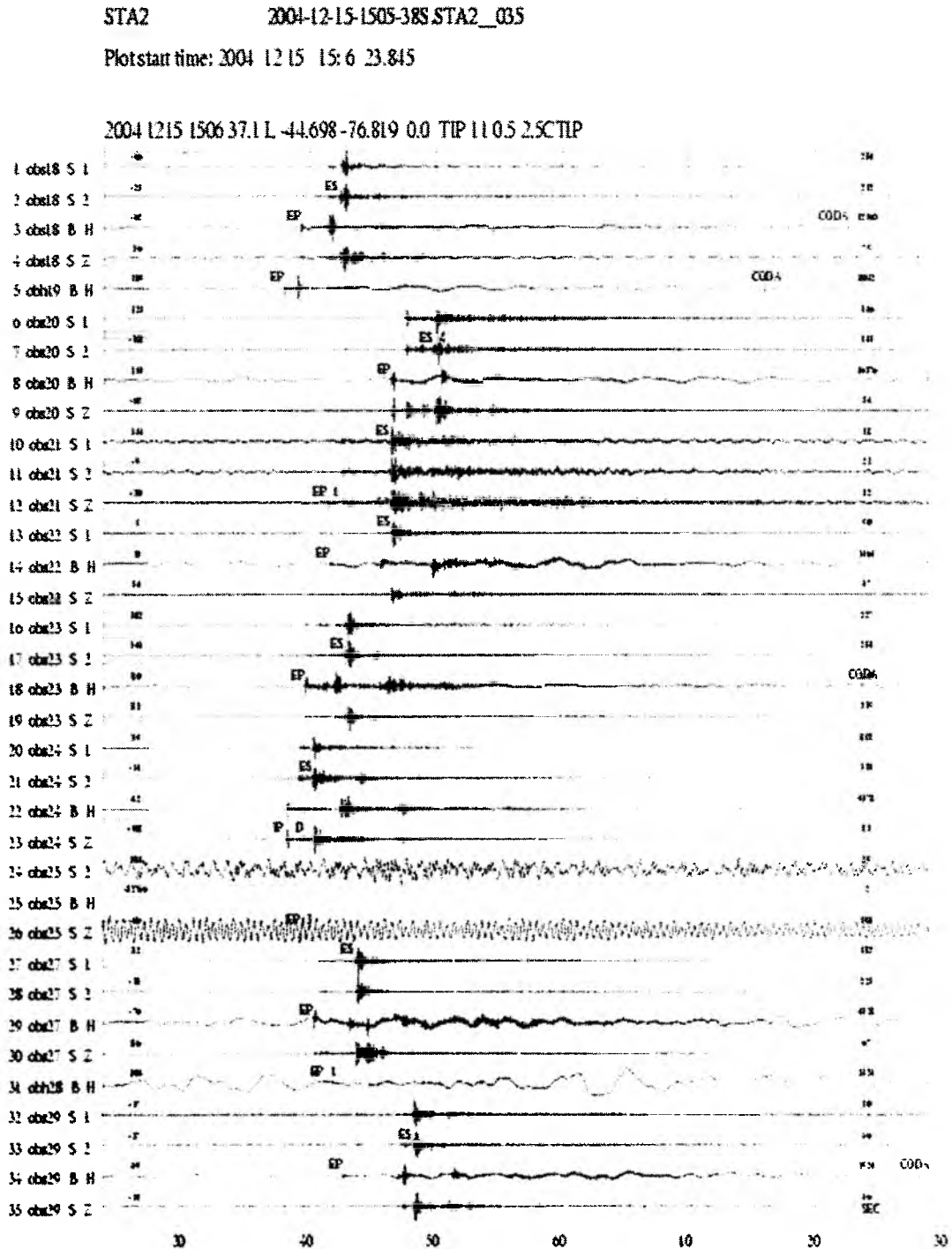


Figure 6.6.1.48: Inner network earthquake from 15 Dec 2004, 15:06 UTC located at 44.698°S, 76.819°W at the ocean bottom. See the previous subsection for the reliability of the depths of these shallow earthquakes.

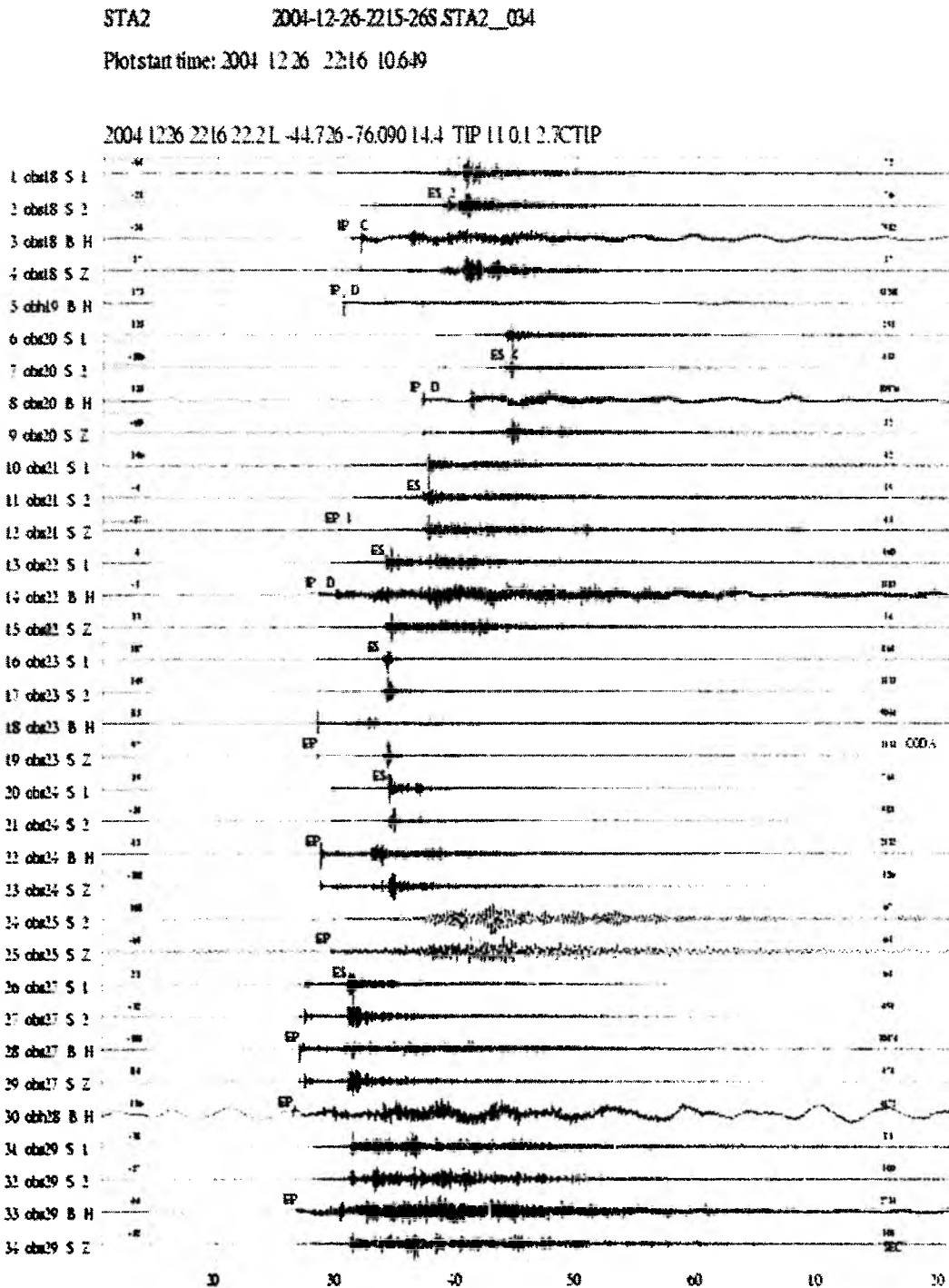


Figure 6.6.1.49: Magnitude 2.7 deep focus (14.4 km) event from 26 Dec 2004, 22:16 UTC, located 32 km east of OBH 28 at 44.726° S, 76.090° W. This is the closest earthquake to the trench recorded from STA 2.

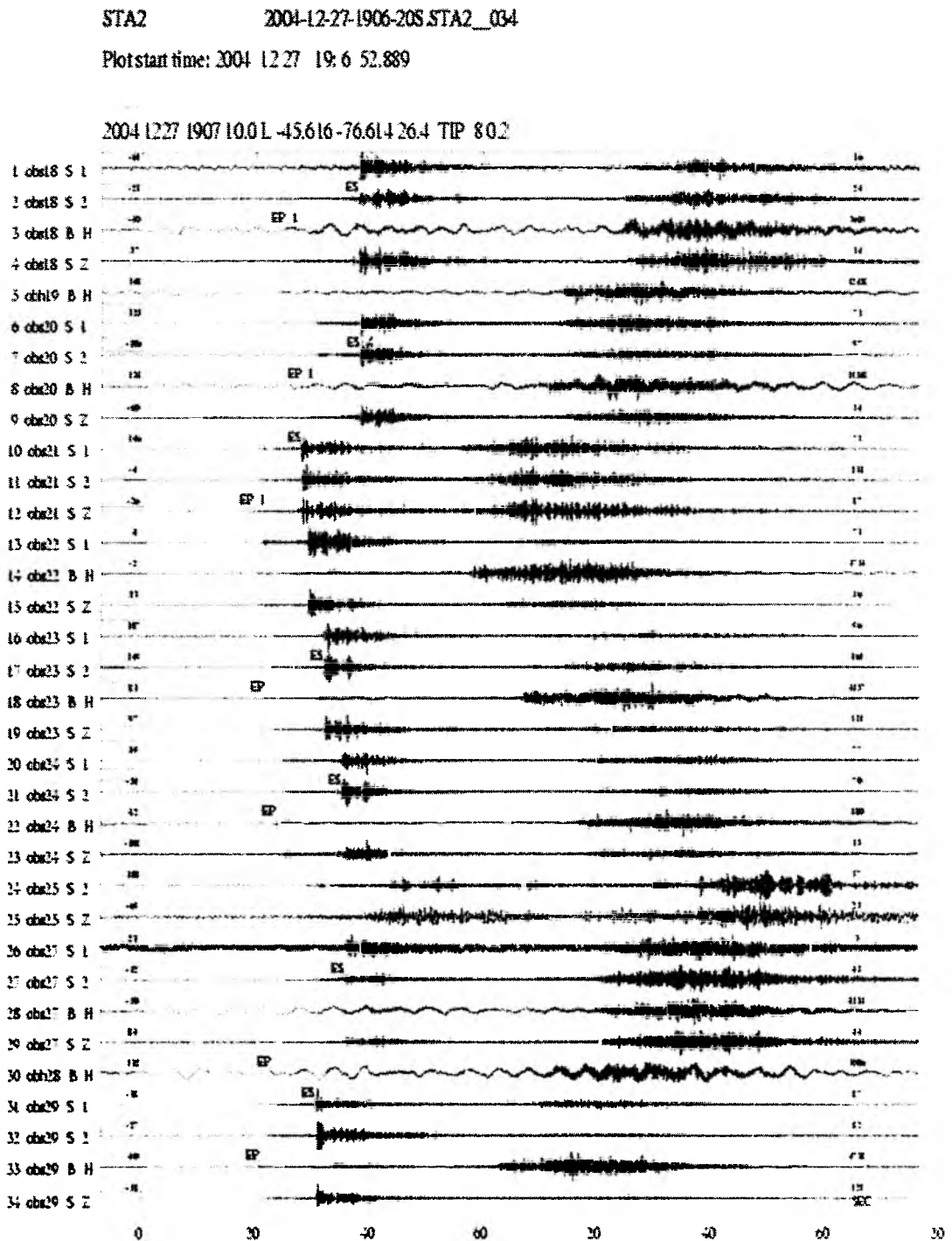


Figure 6.6.1.50: Local earthquake causing T-waves from 27 Dec 2004, 19:07 UTC. The strong tremor-like signals following the earthquake travel in the water column with seawater P-wave velocity and therefore are slower than the P- and S-waves of the earthquake.

6.6.2 Seismic reflection data – first results

Four high resolution seismic reflection lines were shot during cruise SO181-1b (Figure 6.6.2.1). All profiles studied the stratigraphy of sediments on the ocean plate seaward of the trench and the sedimentary apron on the continental slope and were between 170 and 80 nm long. The lines SCS01 and SCS02 were shot along the TIPTEQ corridors #2 and #3, respectively. The data will be used to provide constraints on the sedimentary cover on the incoming plate for both heat flow work and seismic refraction work of SO181-2a. Moreover, the fault pattern resolved in both the sediments and the basement provide important constraints on the tectonic activity in the outer rise area caused by bending of the plate prior to subduction. An additional line – profile SCS03 – was placed to the north of latitude 41°S. In this area several major (outer rise) normal faulting earthquakes have been reported in the seismological catalogue of the Harvard University. The fourth line SCS04 was shot offshore Concepcion and crosses ODP site 1234 (Grevemeyer et al., 2003) and three heat flow stations obtained in 2003 on the Chilean Navy research vessel Vidal Gormaz as joint work between the University of Bremen, IFM-GEOMAR, and the University of Valparaiso. The northernmost line was chosen to benefit from an extensive geothermal dataset and replaces the geothermal stations along corridor #1.

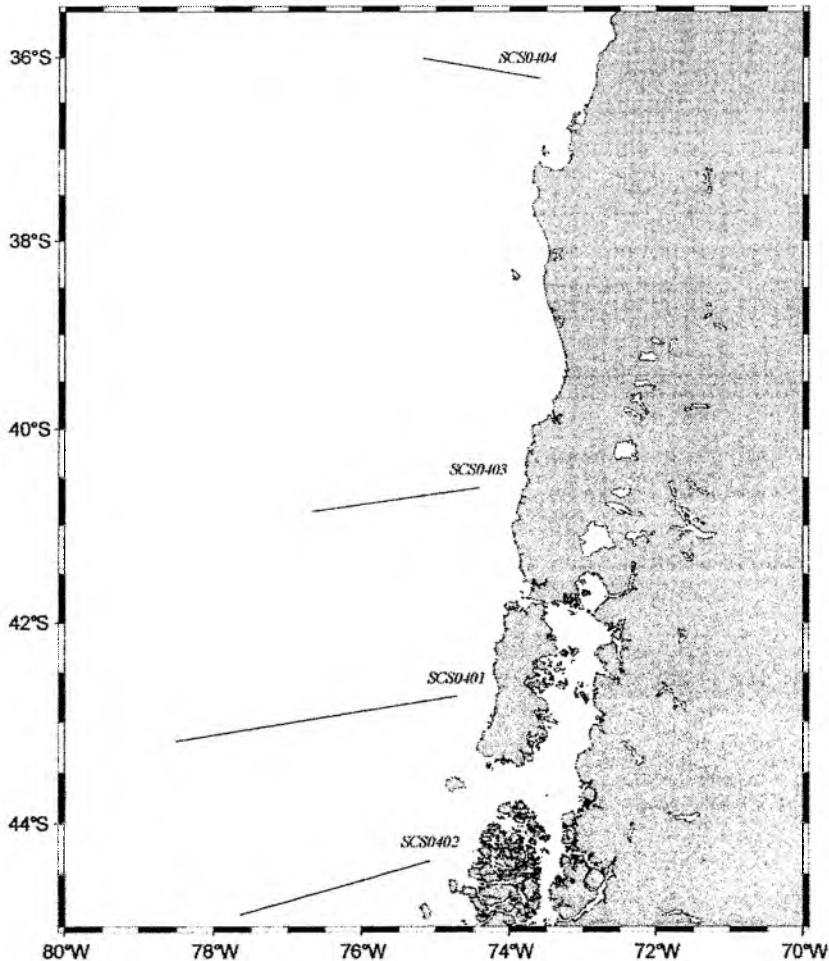


Figure 6.6.2.1: High resolution seismic lines shot during SO181-1b.

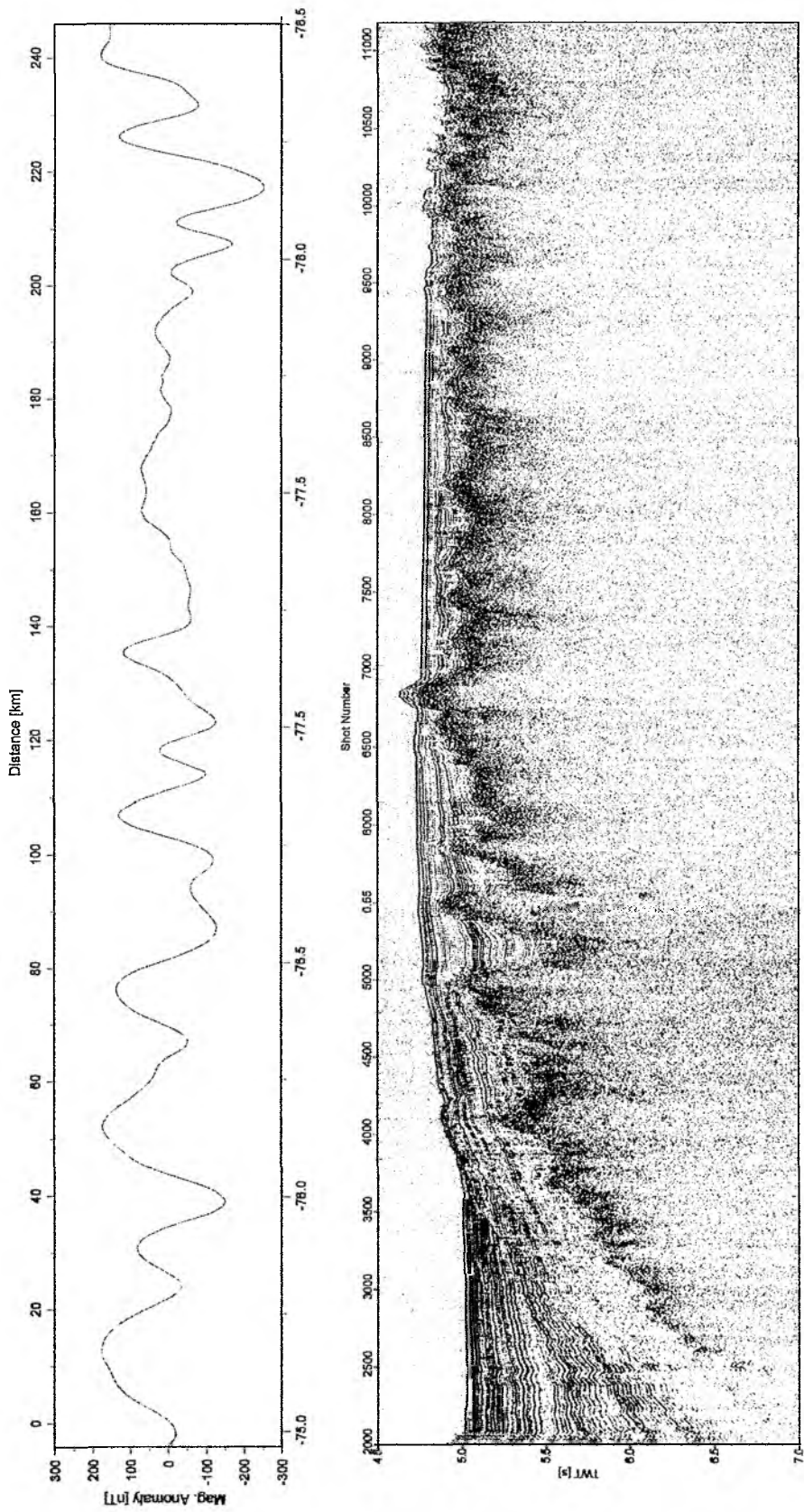


Figure 6.6.2.2: High resolution seismic line SCS01 and magnetic anomaly.

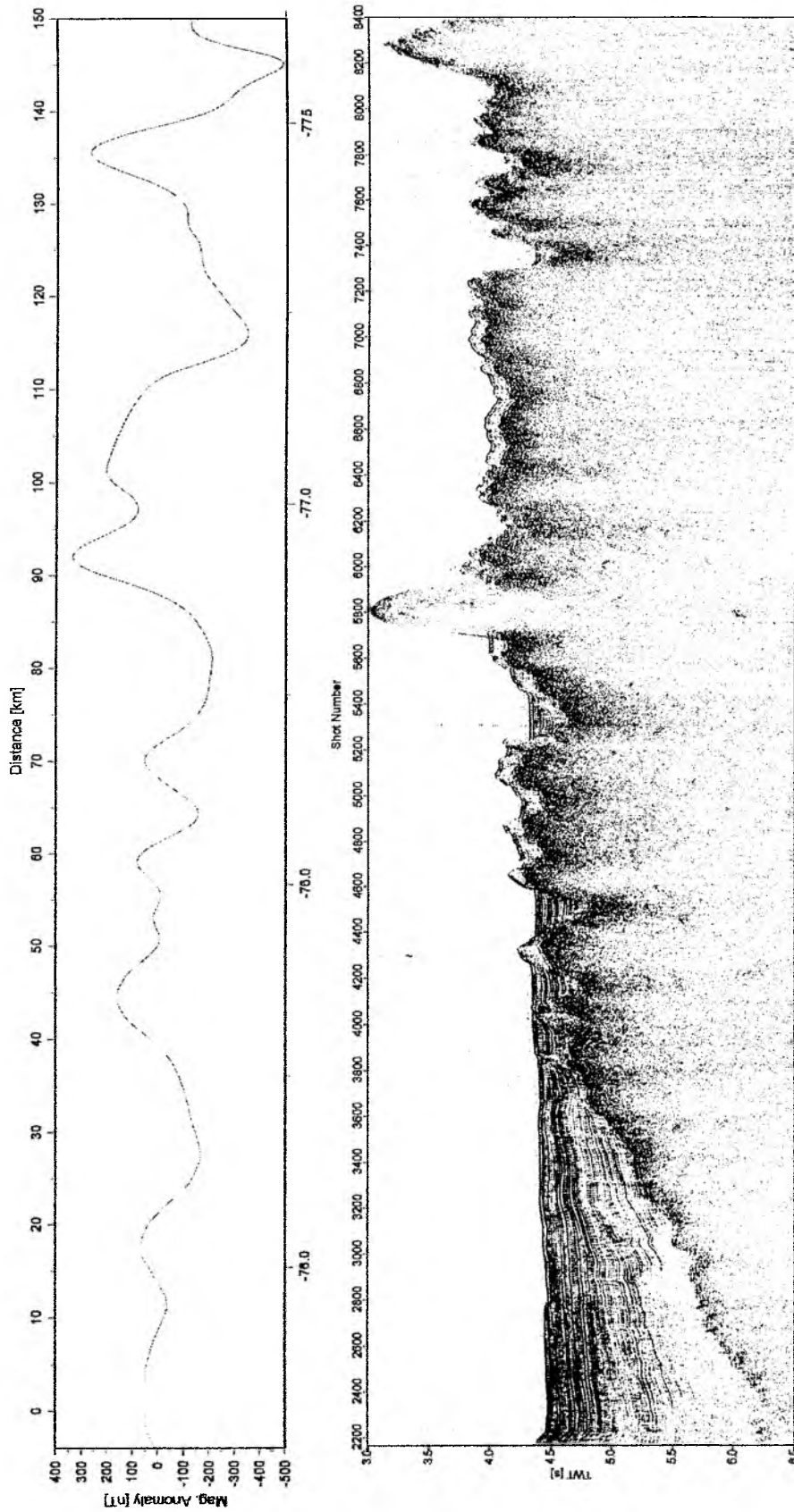


Figure 6.6.2.3: High resolution seismic line SCS02 and magnetic anomaly.

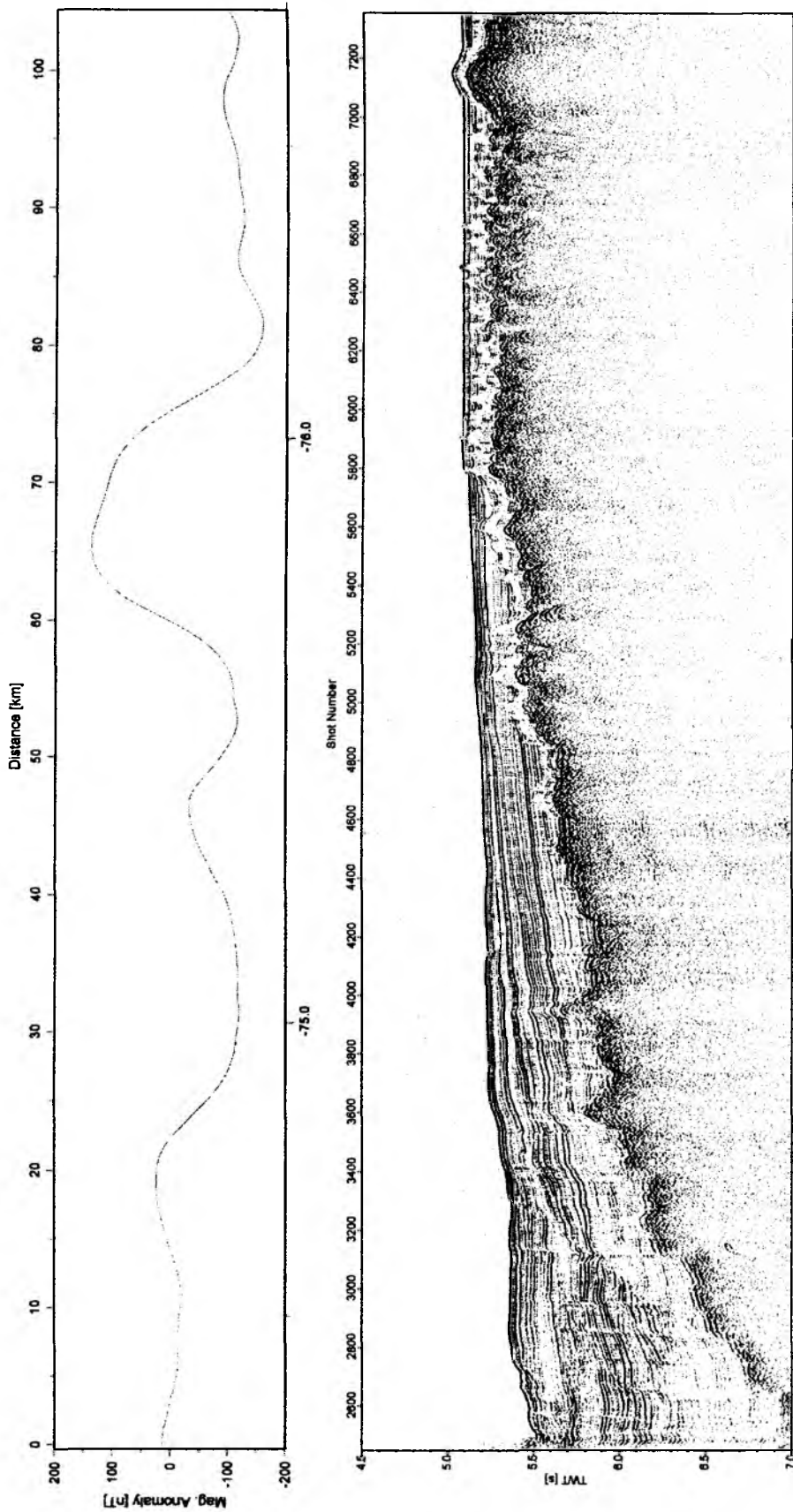


Figure 6.6.2.4: High resolution seismic line SCS03 and magnetic anomaly.

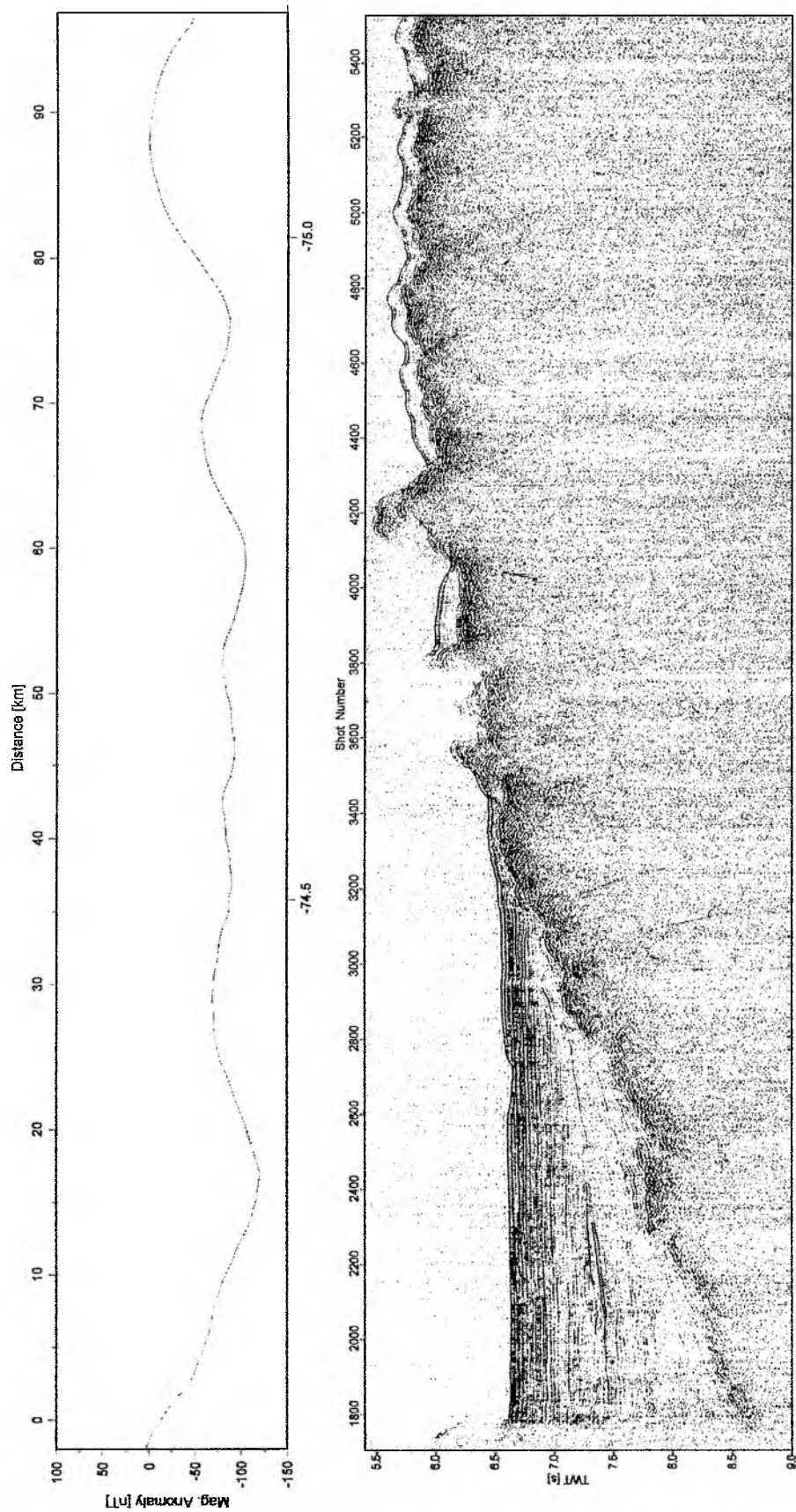


Figure 6.6.2.5: High resolution seismic line SCS04 and magnetic anomaly.

The seismic data from the 16-channel streamer were quality checked before stacking the channels to a single channel record. Bad channels were rejected. In addition, the shots in shallow water on the shelf and upper slope produced a move out on the streamer. Thus, before stacking the normal moveout was corrected. Final on board data processing included a bandpass filter of 30 to 80 Hz.

For the presentation of first results, we discuss first the data from the incoming plate. Figure 6.6.2.2 to 6.6.2.5 show seismic sections for SCS01, SCS02, SCS03, and SCS04 from ~3 km landward of the deformation front out to 240 km, 150 km, 100 km, and 96 km, respectively. The oceanic plate becomes older from south to north. At the trench axis the age is ~6.5 Ma, 14.5 Ma, 18.5 Ma, and 30 Ma for SCS02, SCS01, SCS03, and SCS04, respectively. Though the age is changing, the thickness of sediment in the trench changes very little. Profiles SCS01, SCS02, and SCS04 have about 2 s TWT of sediments (roughly 2 km) and SCS03 1.5 s TWT. Except for line SCS03, the trench fill produces a flat and nearly horizontal seafloor, suggesting a vigorous supply of sediment from the Andes. Along line SCS03, however, the seafloor decreases towards the trench and sediments and basement show very prominent normal faults and may therefore indicate an increased tectonic activity at 40°S, which is supported by the larger number of earthquakes in this area. Drape-like sedimentation on the incoming plate and a seafloor topography that mimics the abyssal hill fabric occurs ~60 km from the trench on line SCS02 (youngest crust studied, ~3-4 Ma), at ~210 km on line SCS01 (on ~9 Ma old crust), at 80 km on line SCS03 (on ~12 Ma old crust) and at 50 km on line SCS04 (oldest crust studied, ~30 Ma) suggesting a much higher sediment input to the south of Puerto Montt (~42°S).

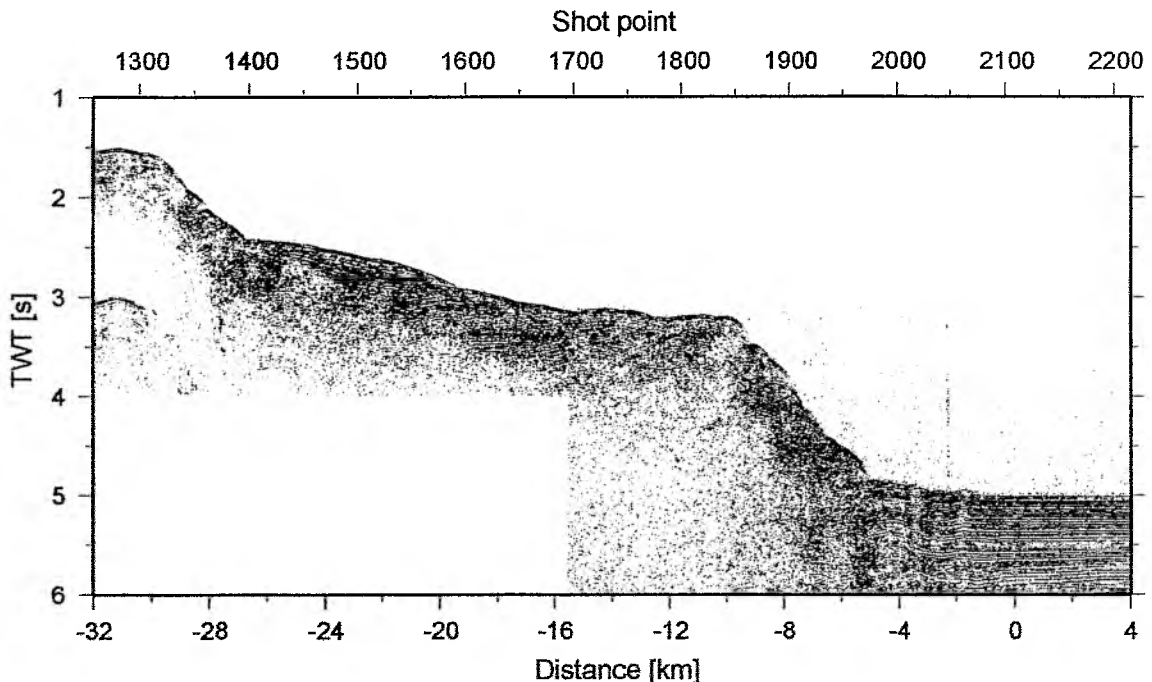


Figure 6.6.2.6: Deformation front and lower slope on SCS01.

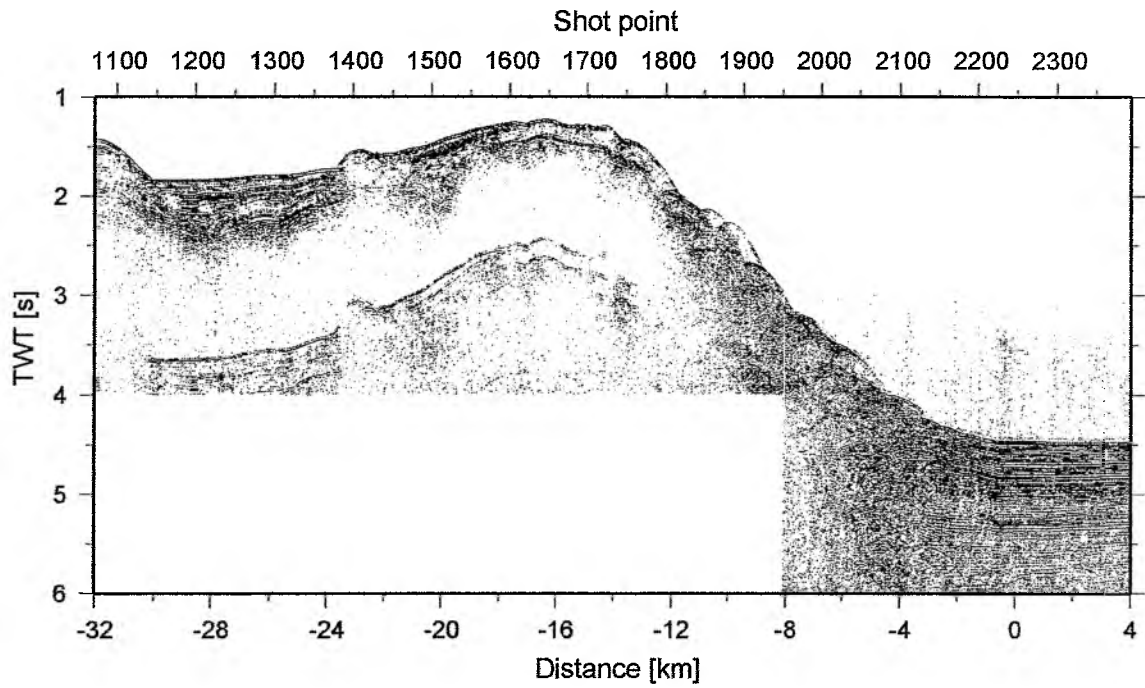


Figure 6.6.2.7: Deformation front and lower slope on SCS02.

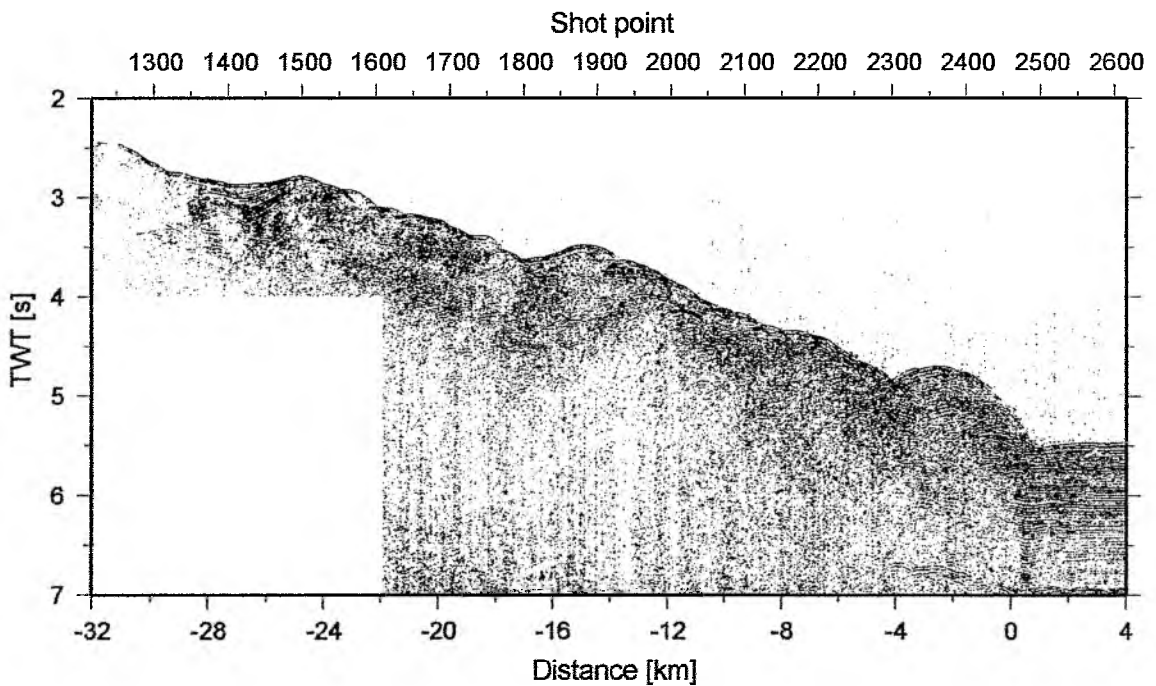


Figure 6.6.2.8: Deformation front and lower slope on SCS03.

A second aim of the reflection seismic survey was to study the slope apron and the deformation at the toe. On all lines the existence of gas hydrates was confirmed by imaging bottom simulating reflectors (BSRs). In addition, profound changes in the structure of the lower slope could be observed (Figures 6.6.2.6 to 6.6.2.9). On line SCS02 the features of the slope and thick deposits/slides in the deep sea trench suggest that mass wasting and slope failure occur. Features that may present accretionary ridges could only be observed along lines SCS03 and SCS04.

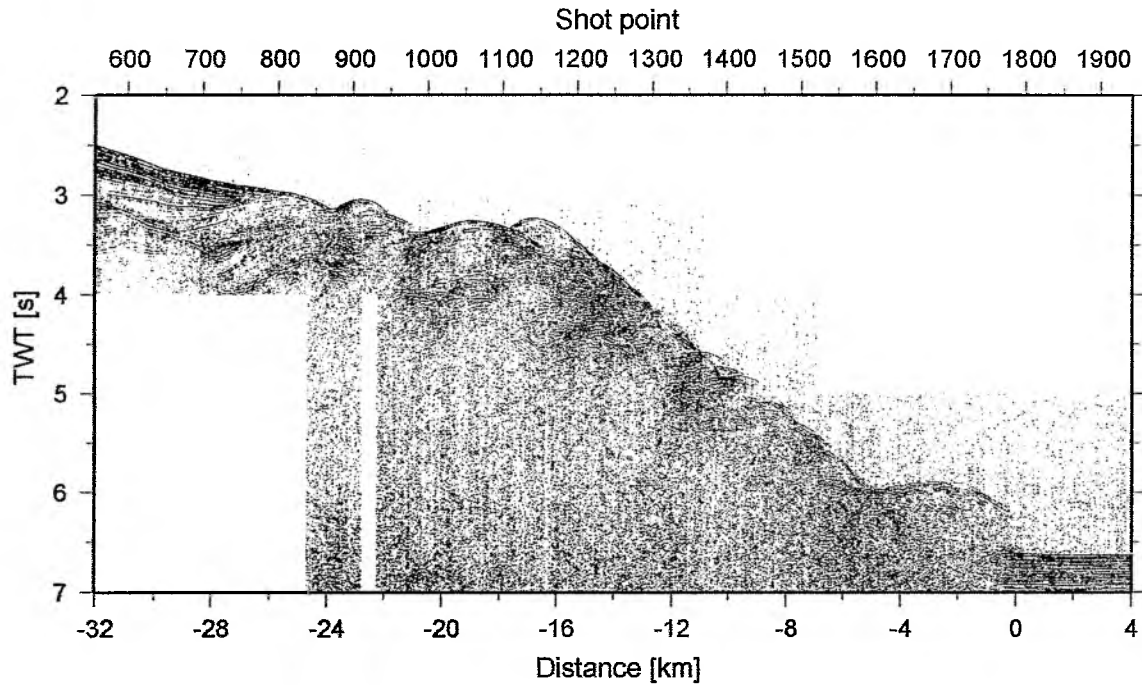


Figure 6.6.2.9: Deformation front and lower slope on SCS04.

6.6.3 Profile P05

Along this profile altogether 43 instruments were deployed between 21 Jan. and 23 Jan. Three of these instruments (OBH03, 06, and 11) were also part of the outer rise network (see Section 6.6.1). Shooting was done in almost perfect conditions from 21:30 on 23 Jan to 18:00 on 25 Jan. Throughout most of the time three G-Gun cluster were in operation, the fourth one failed soon after the start of the profile. Instruments were picked up once shooting was terminated, and they were all back onboard by 04:00 on 27 Jan. Details of instruments and shots can be found in Appendices 9.2 and 9.3. Most instruments recorded well. Along most of this line, a high resolution reflection profile was recorded on the previous leg; see Section 6.6.2 and Figures therein. A location map is shown in Figure 6.6.3.1, and record sections are shown in Figures 6.6.3.2 to 6.6.3.51. A preliminary onboard analysis was attempted, taking also the results (sediment thickness) from the seismic reflection data into account.

Preliminary interpretation of profile P05

The 350 km long profile extends over the subduction zone covering oceanic crust and continental shelf in E-W direction. P-wave arrivals from all receiver gathers were picked but only five gathers (OBH/S 06, 51, 42, 36, and 31) were used to create a velocity model. A starting velocity model based on the sediment thickness was estimated from the streamer data of profile SCS01 which was shot during leg 1 of this cruise. The model itself was created with the ray-tracing program MacRay (Luetgert, 1992). Modelling concentrated on the upper section as long offset arrivals are not yet interpreted. Therefore structure and velocity of lower crust and upper mantle are only rough features in the model.

The model, shown in Figure 6.6.3.52, consists of six layers. Below a water layer with a velocity of 1.5 km/s, sediments appeared as a thin layer with a velocity from 1.8-1.9 km/s on the oceanic plate and increasing in thickness towards the shelf reaching up to 2 km at the subduction zone. The sediment velocity is increasing up to 2.3 km/s on the continental shelf. As a result of focusing mainly on the upper structures, the oceanic basement merges with the upper continental crust, leaving the model simple. Starting as a thin layer with a velocity of 4.4 km/s it is increasing on the continental shelf to about 4 km and a velocity from 4.5-5.0 km/s. Similarly, a combined layer of mid oceanic crust and lower continental crust exist. In this simple model these two different crusts appear as one layer with increasing thickness and velocity, up to 4.6-6.5 km/s, at the continental shelf. The lower oceanic crust starts as a thick layer with a velocity of 6.8-7.1 km/s and decreases in thickness underneath the continental shelf. This observation is again due to the focus on the upper structures and probably does not resemble the real structure. Upper mantle is placed at a depth of 11 km and subducts as expected underneath the shelf with a velocity from 8.0-8.2 km/s.

Time - Dist/8 [sec]

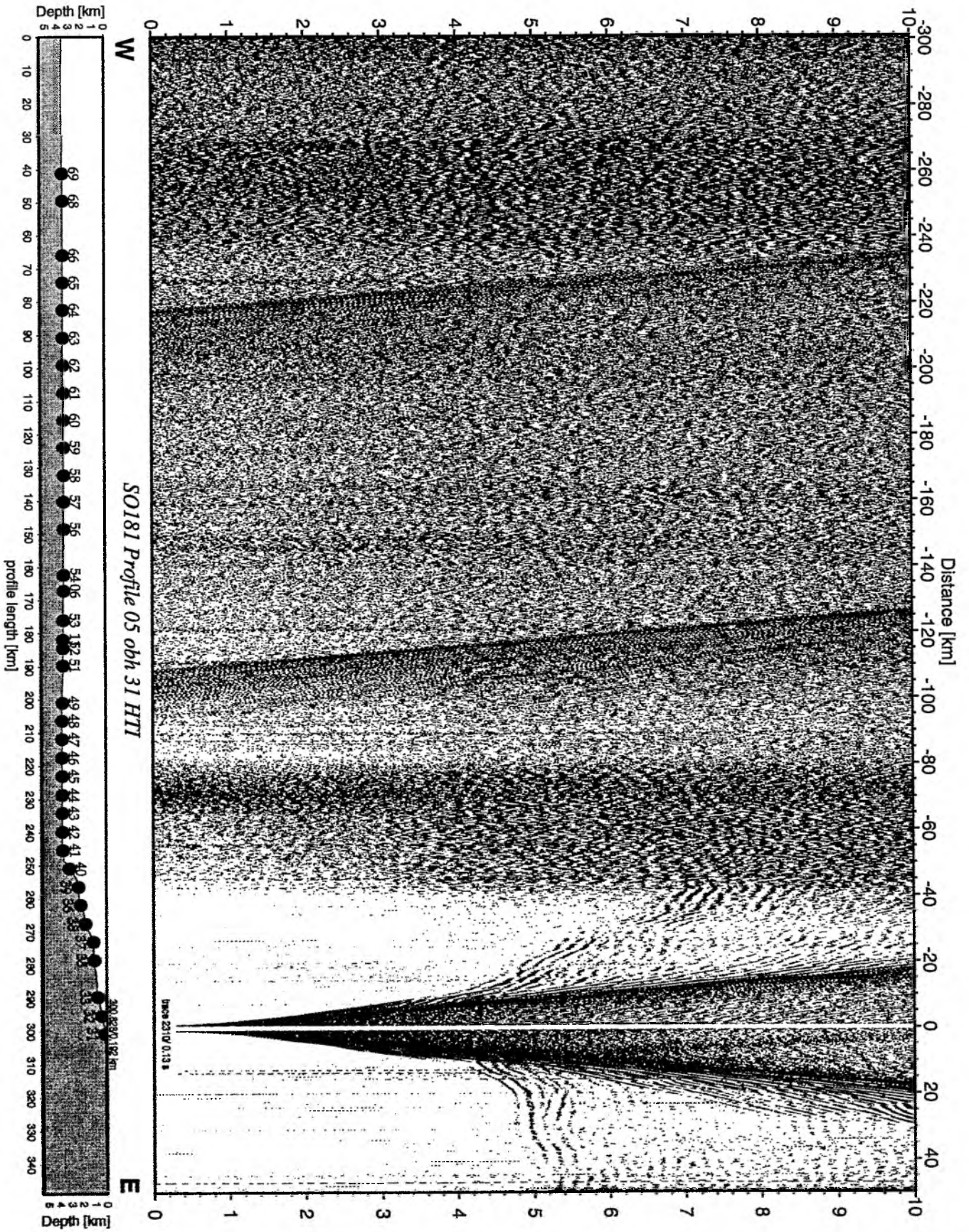


Figure 6.6.3.2:

Record section from obh 31 HTI, Profile 05.

Time - Dist/8 [sec]

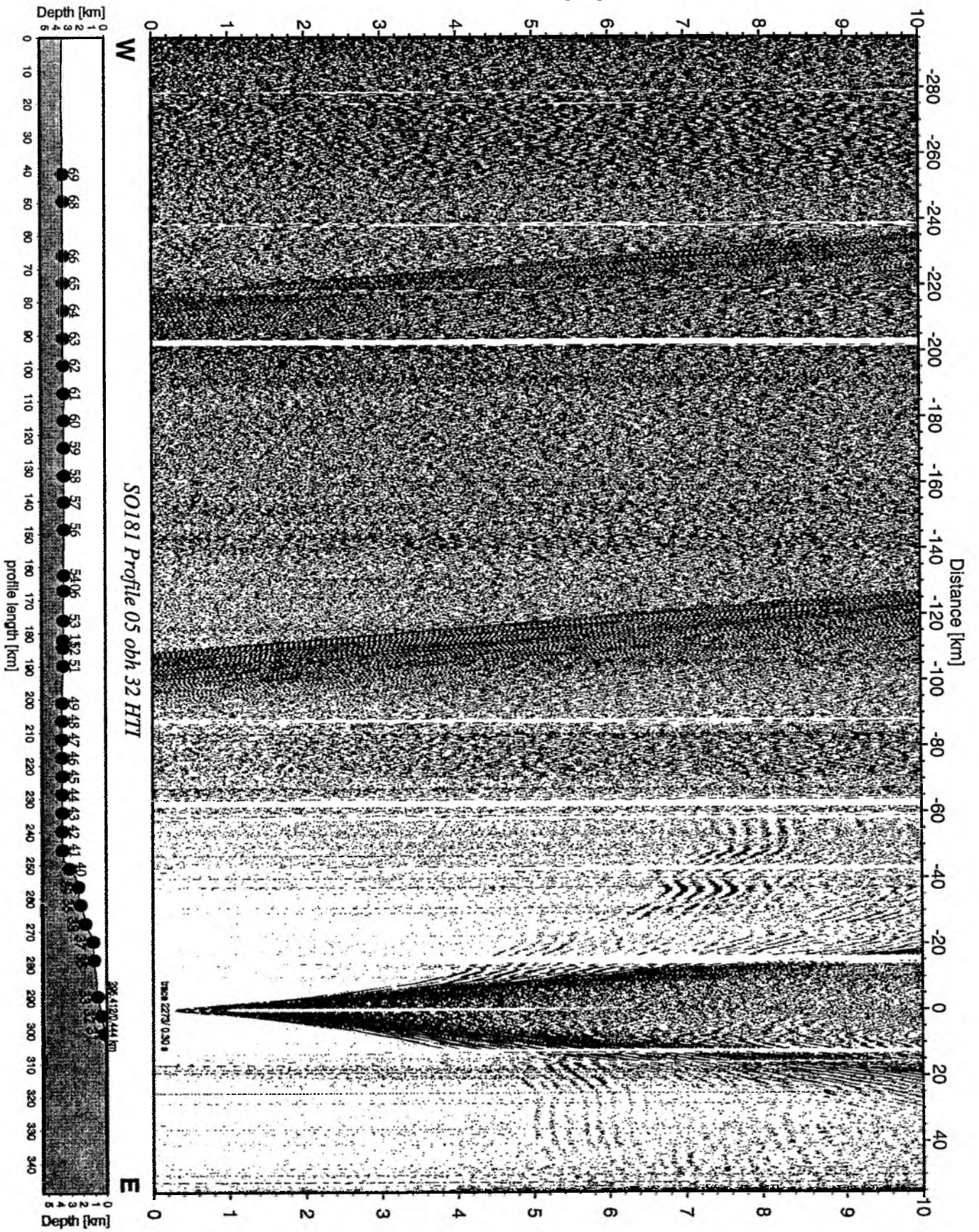
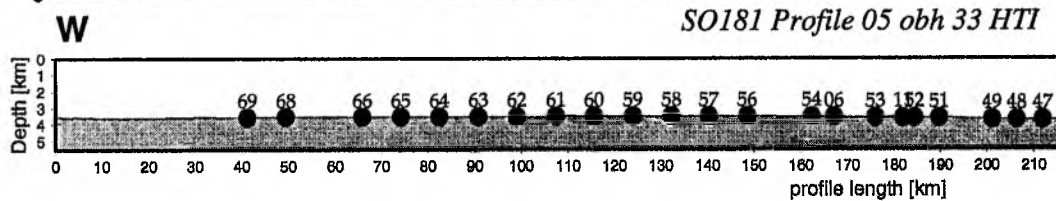
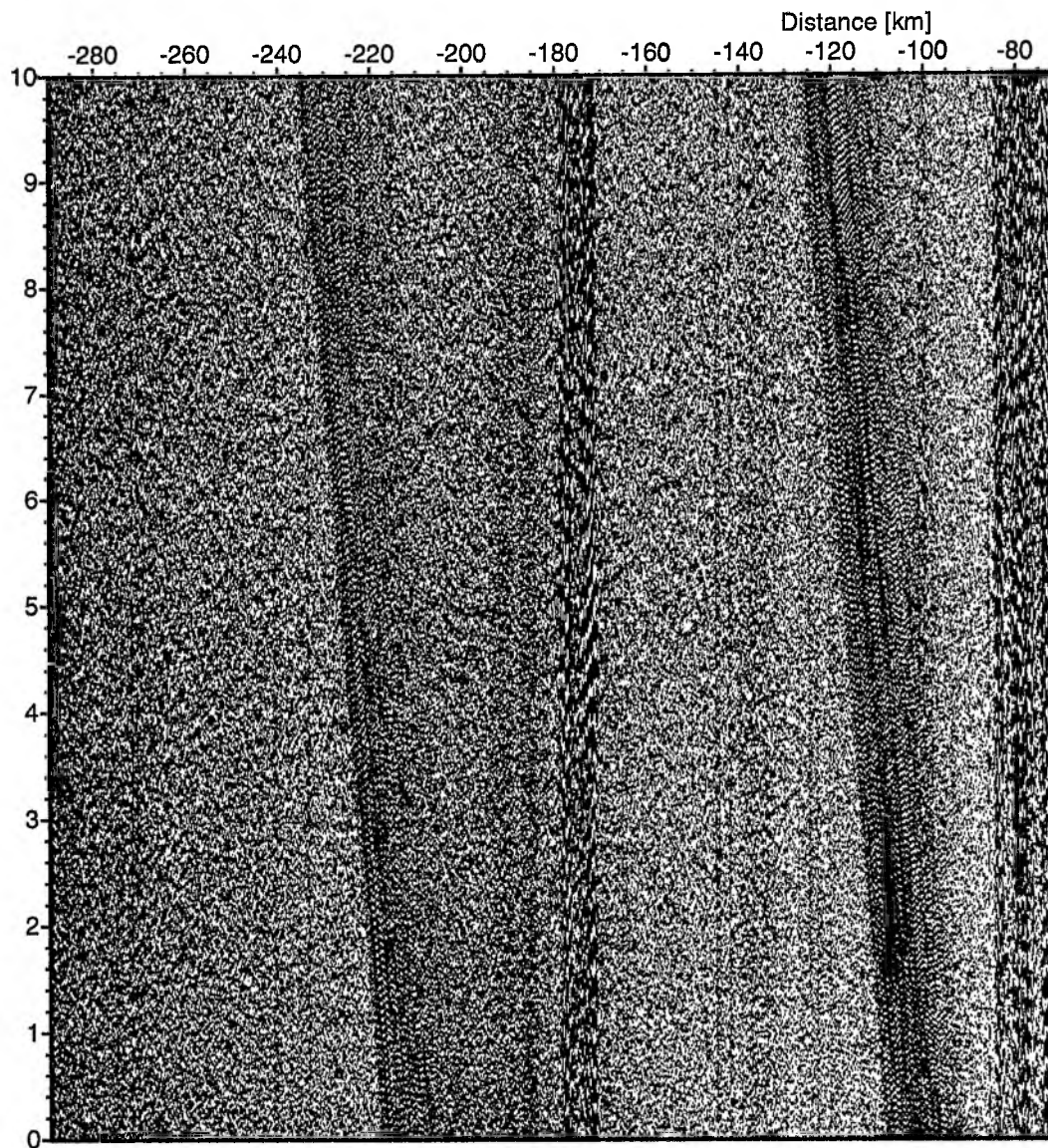


Figure 6.6.3.3: Record section from obh 32 HTI, Profile 05.

180

Time - Dist/8 [sec]



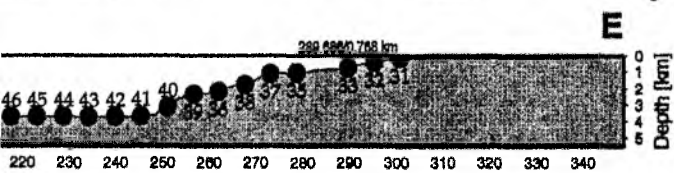
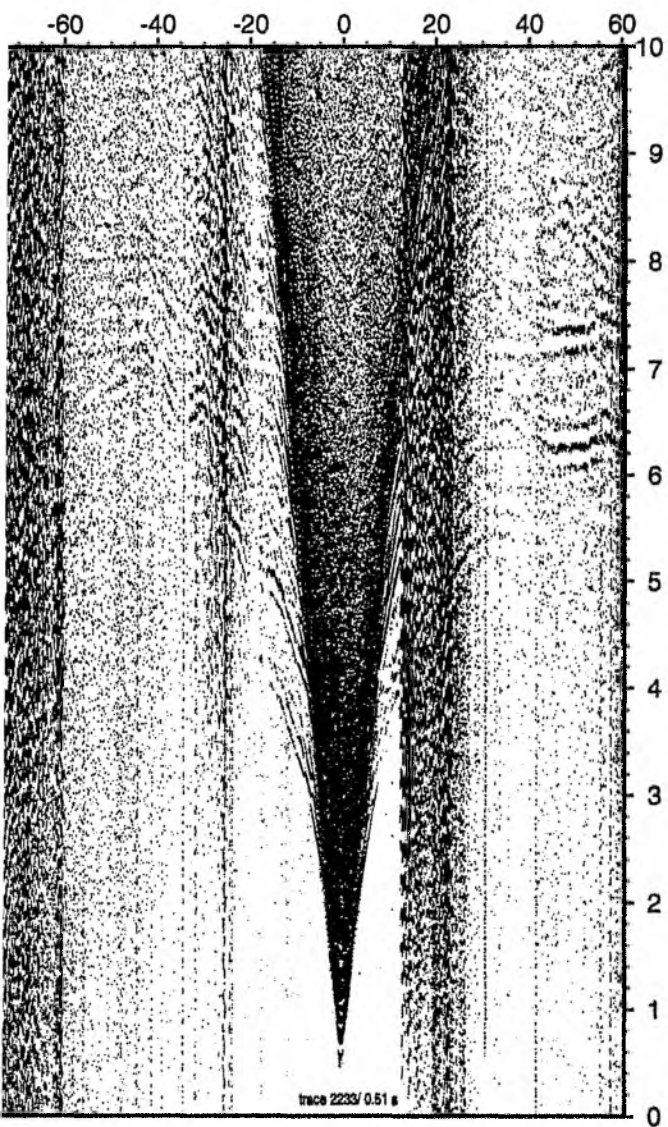


Figure 6.6.3.4: Record section from obh 33 HTL, Profile 05.

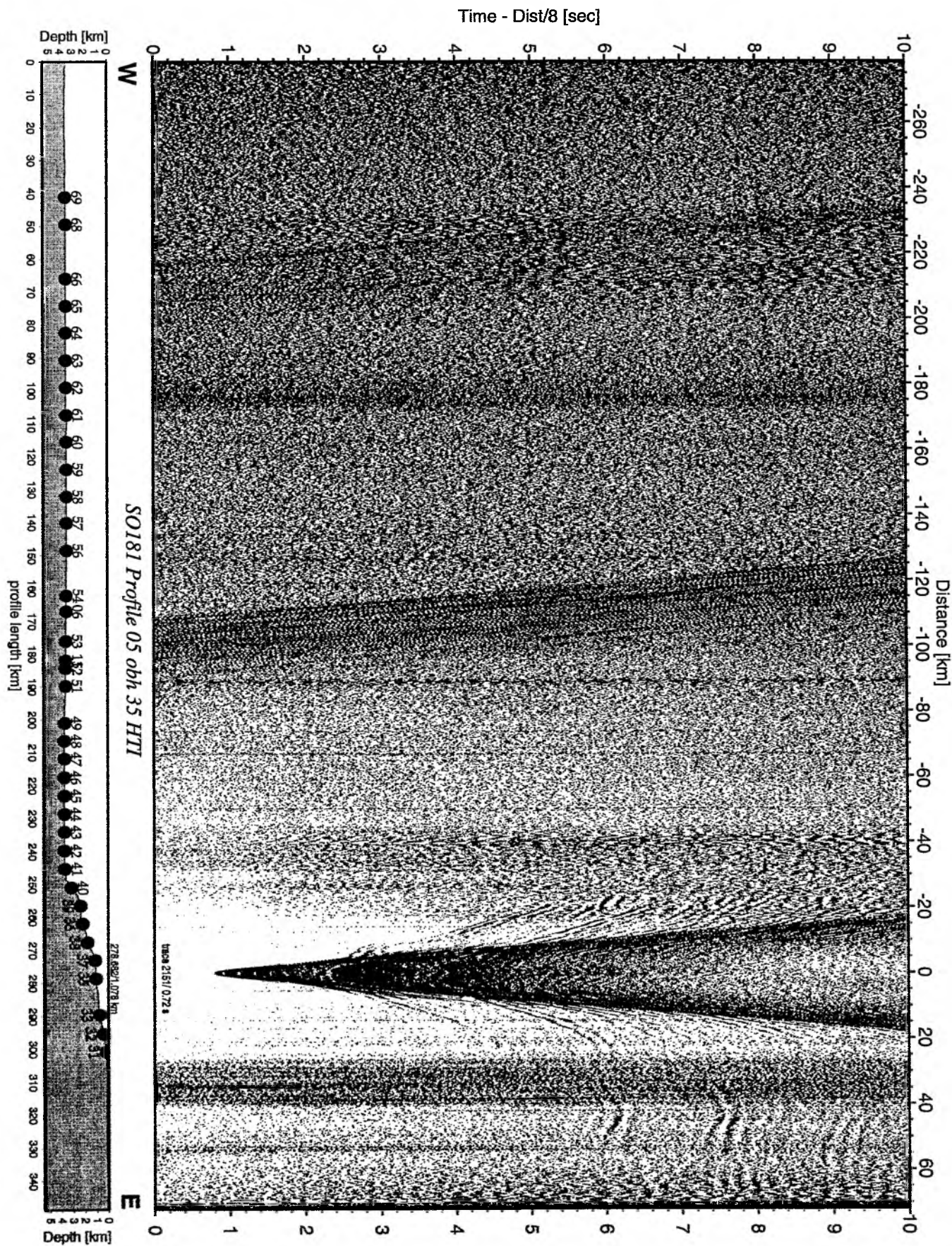


Figure 6.6.3.5: Record section from obh 35 HTI, Profile 05.

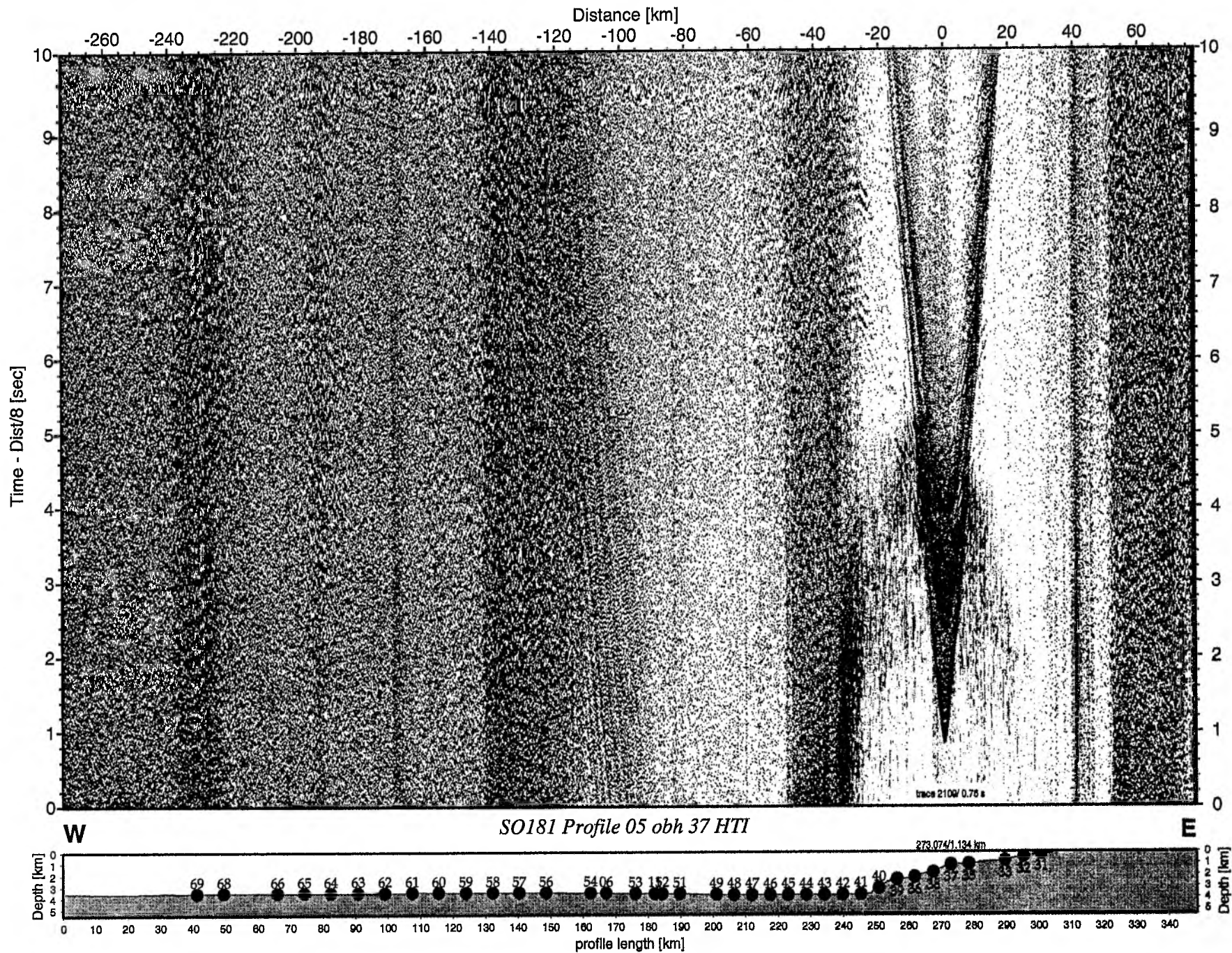


Figure 6.6.3.6: Record section from obh 37 HTI, Profile 05.

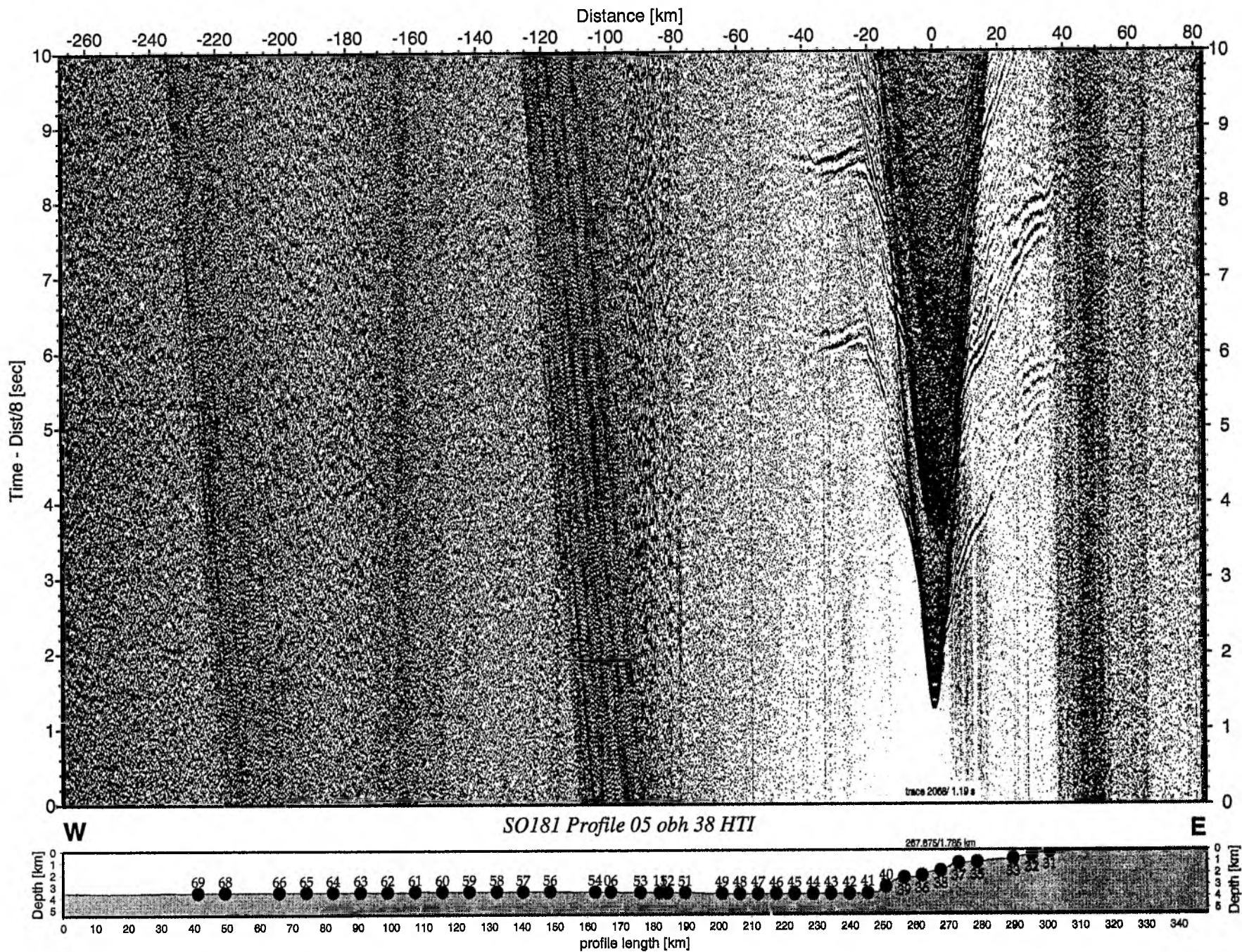


Figure 6.6.3.7: Record section from obh 38 HTI, Profile 05.

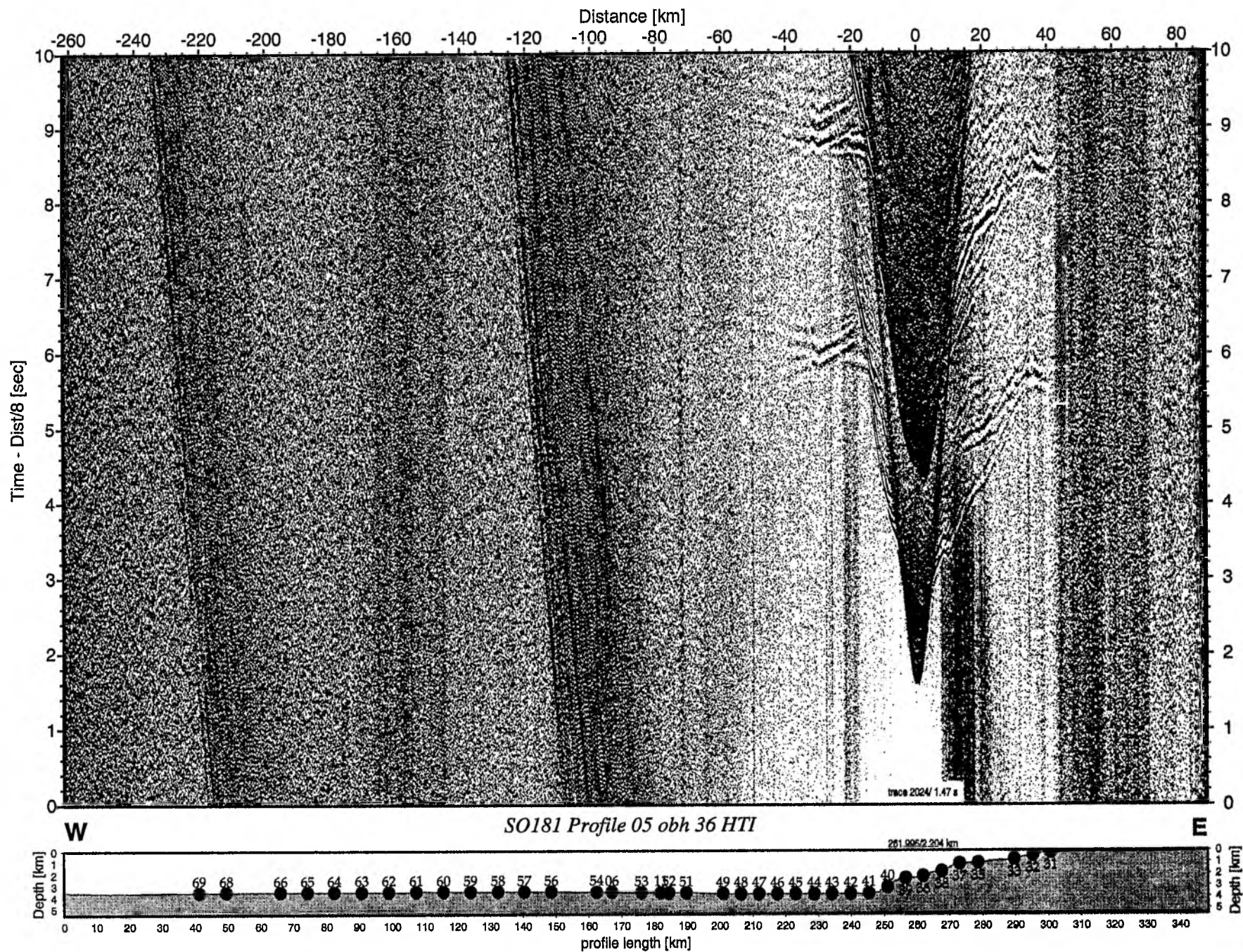


Figure 6.6.3.8: Record section from obh 36 HTI, Profile 05.

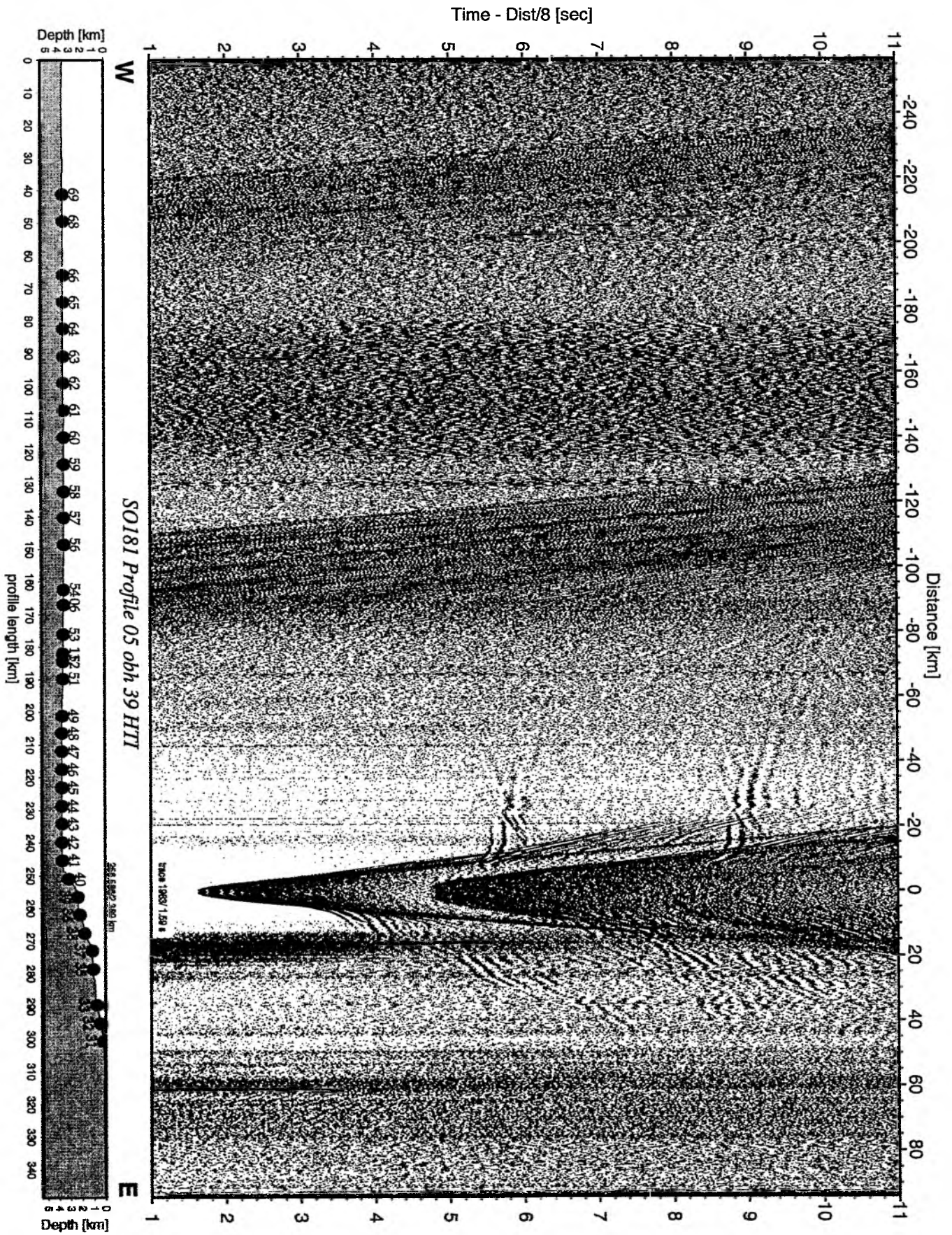


Figure 6.6.3.9: Record section from obh 39 HTI, Profile 05.

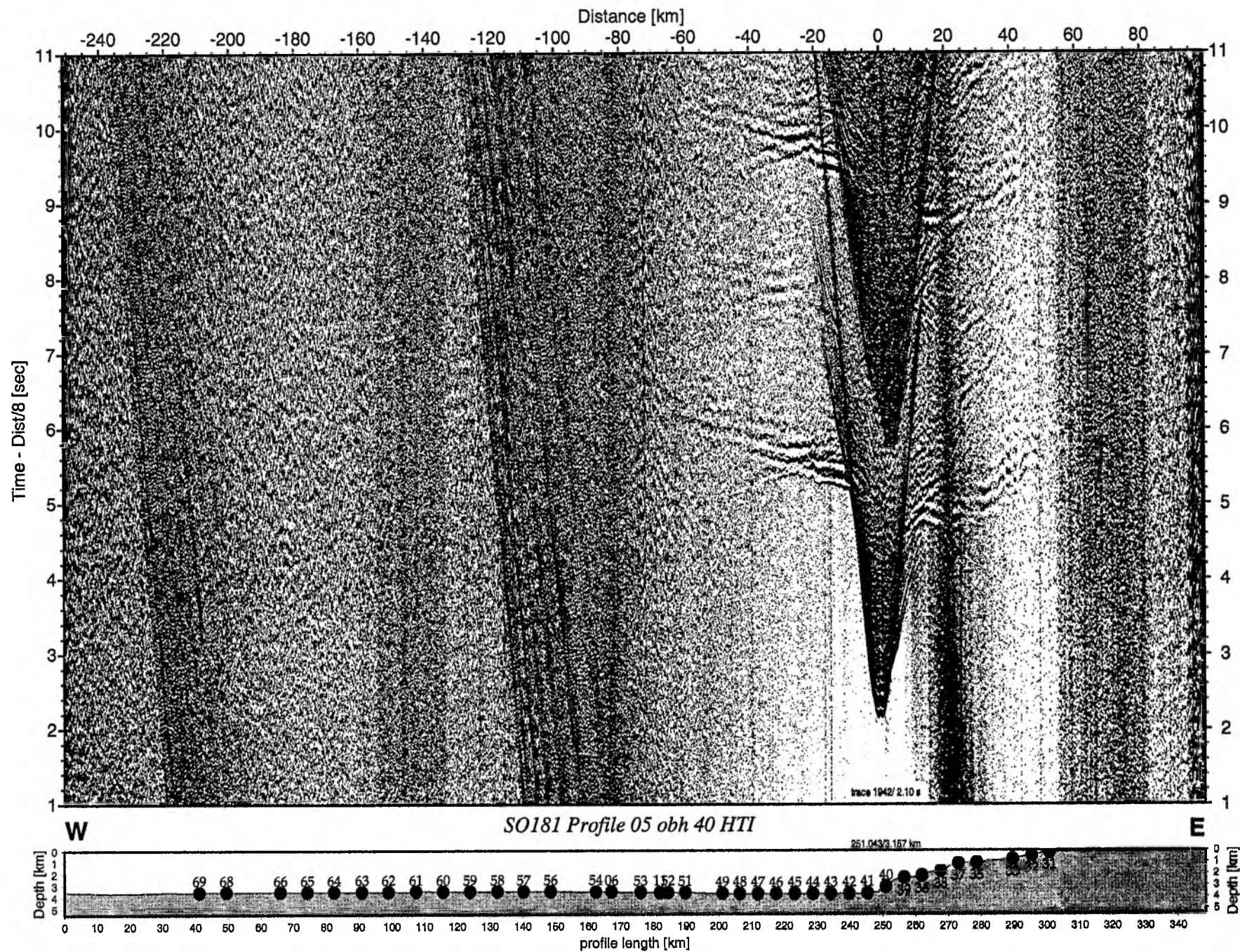


Figure 6.6.3.10: Record section from obh 40 HTI, Profile 05.

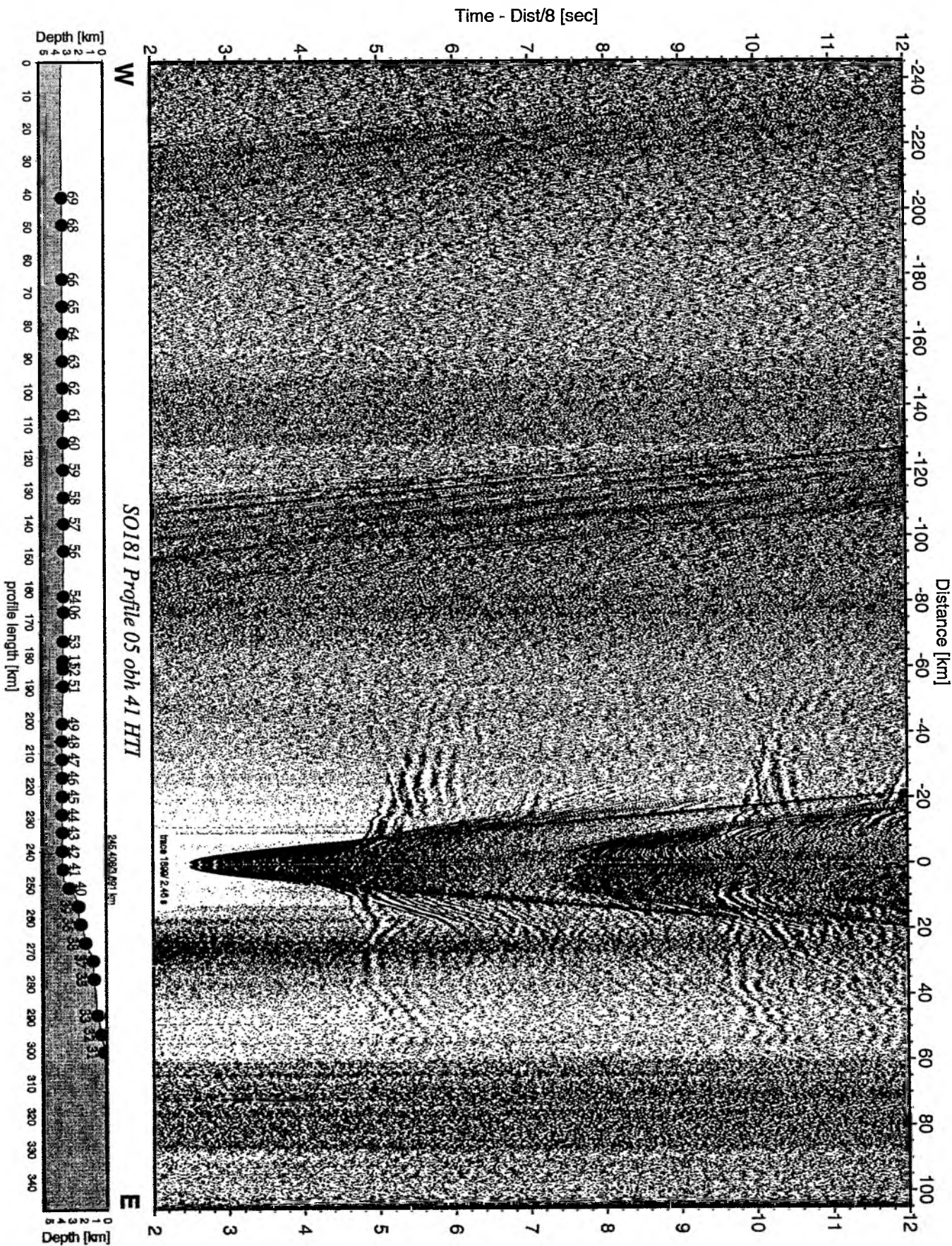


Figure 6.6.3.11: Record section from obh 41 HTI, Profile 05.

Time - Dist/8 [sec]

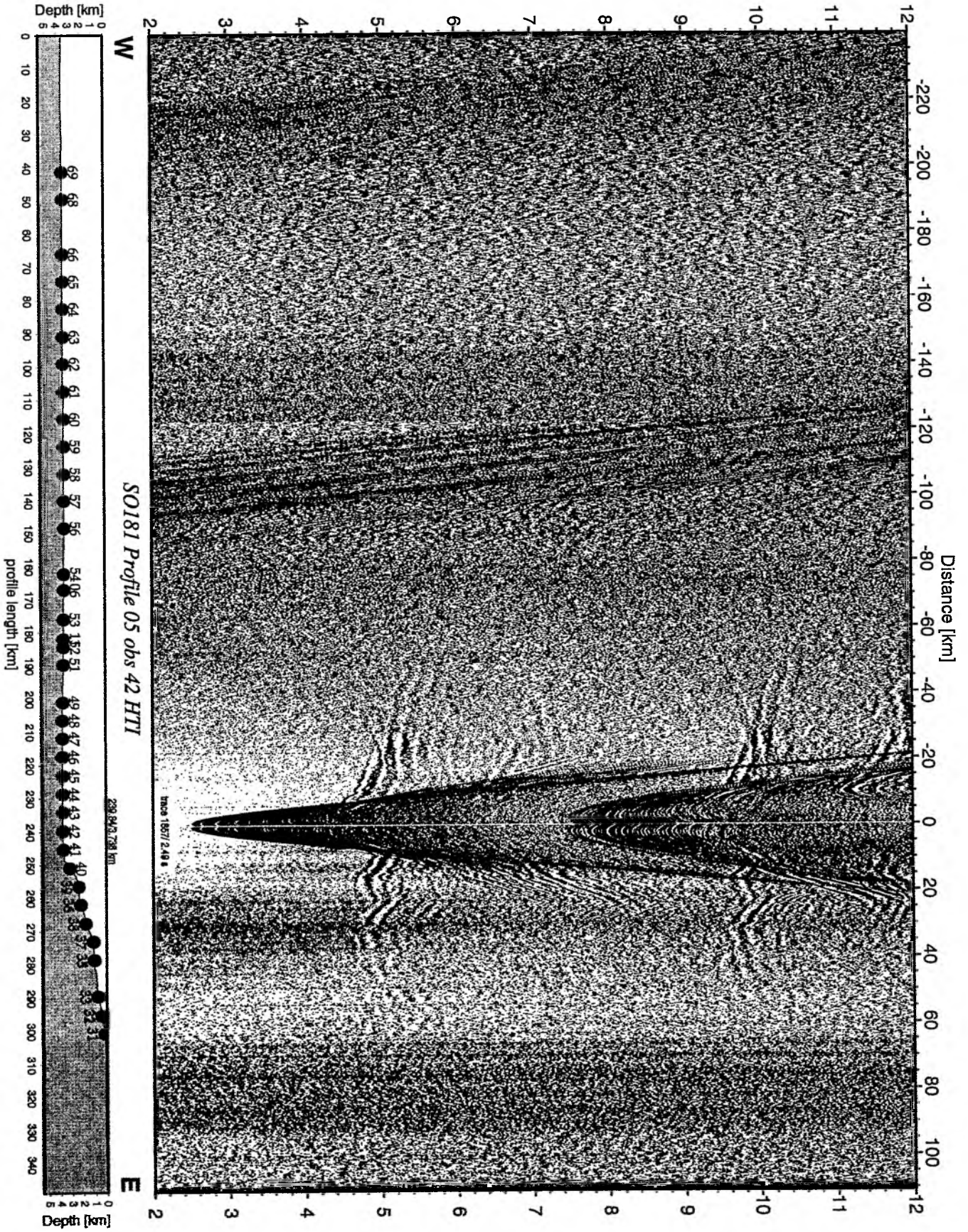


Figure 6.6.3.12: Record section from obs 42 HTI, Profile 05.

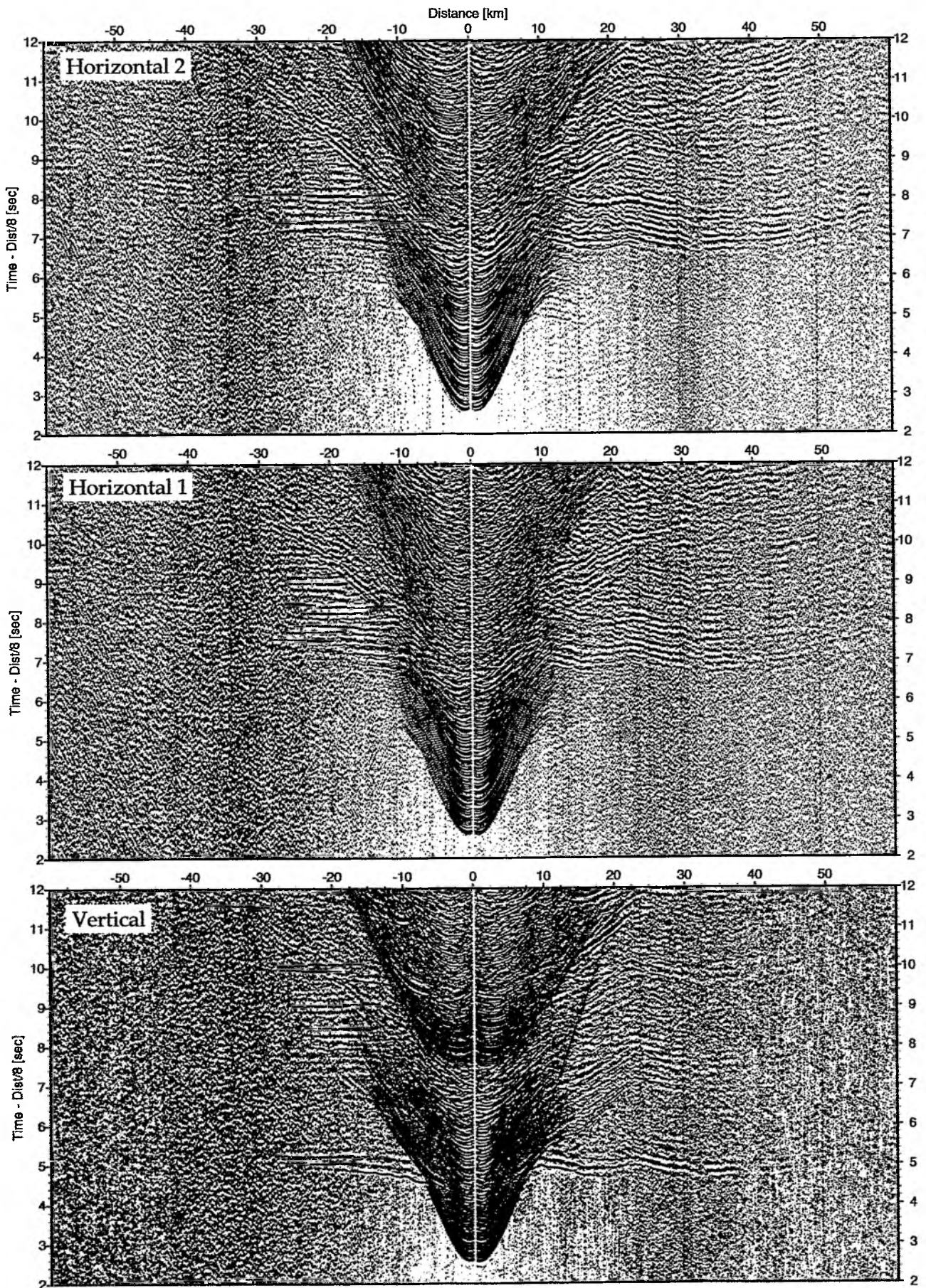


Figure 6.6.3.13: Record sections from obs 42 HTI/Owen-4.5Hz, SO181 Profile 05.

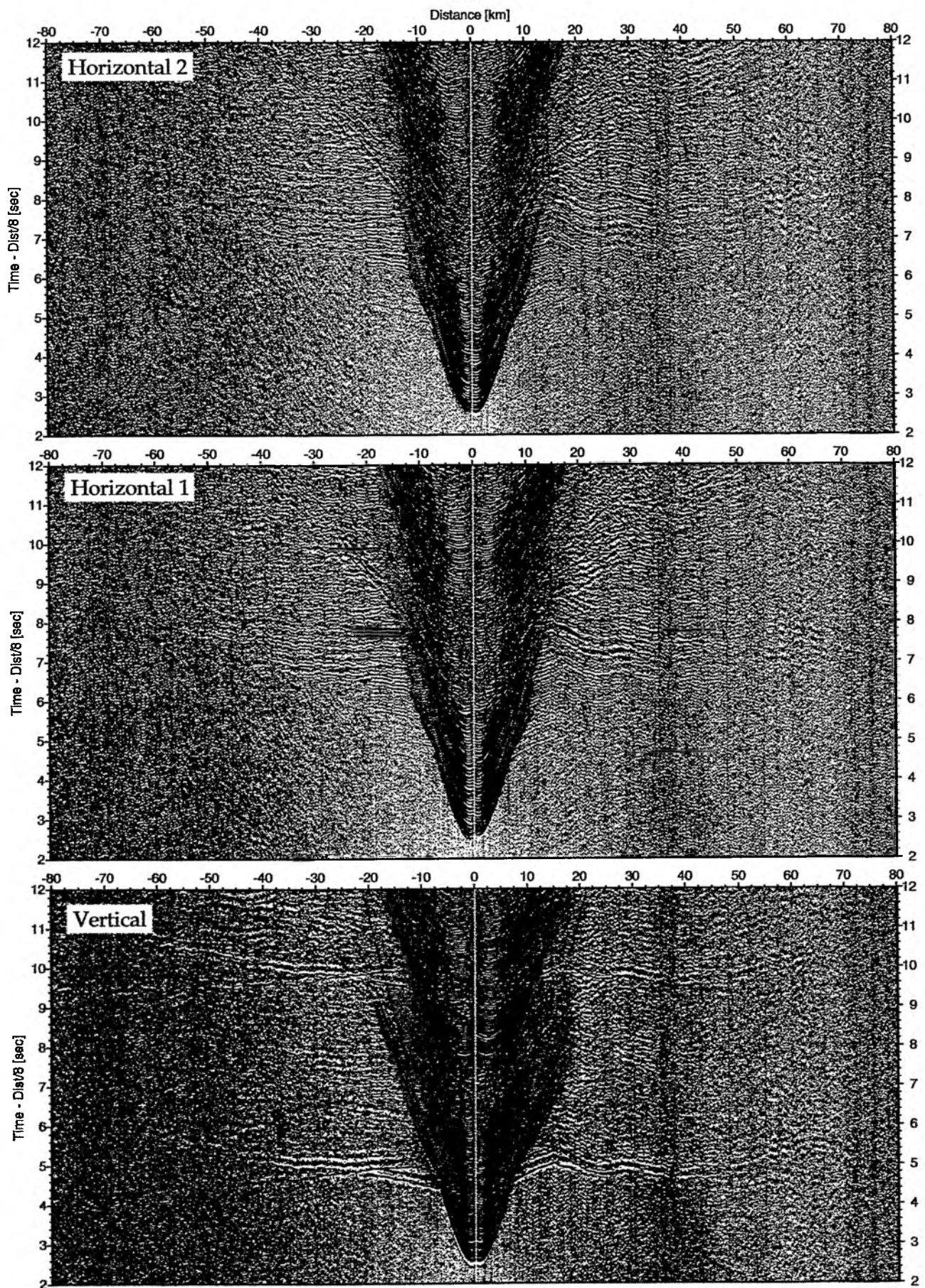


Figure 6.6.3.14: Record sections from obs 43 OAS/Owen-4.5Hz, SO181 Profile 05.

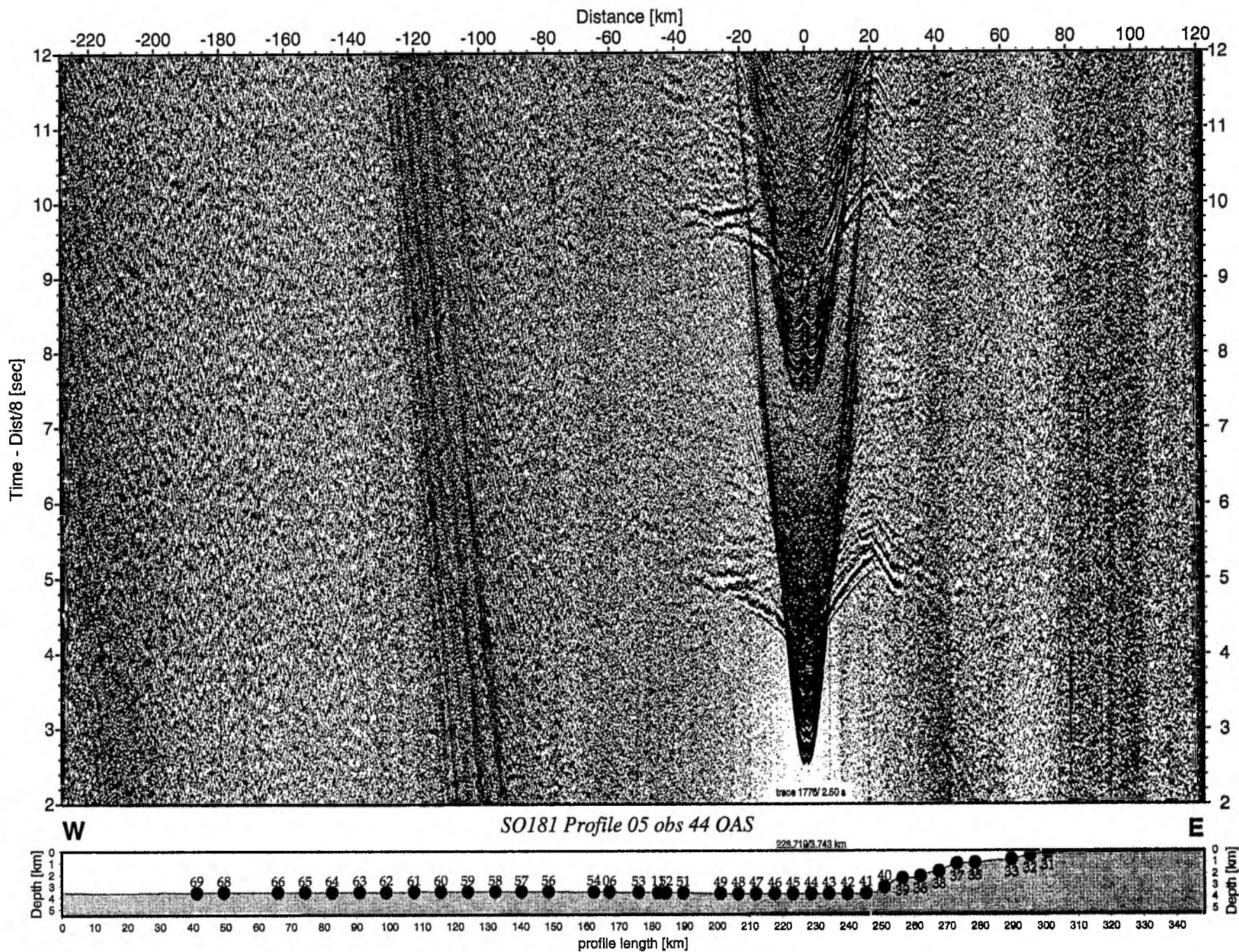


Figure 6.6.3.15: Record section from obs 44 OAS, Profile 05.

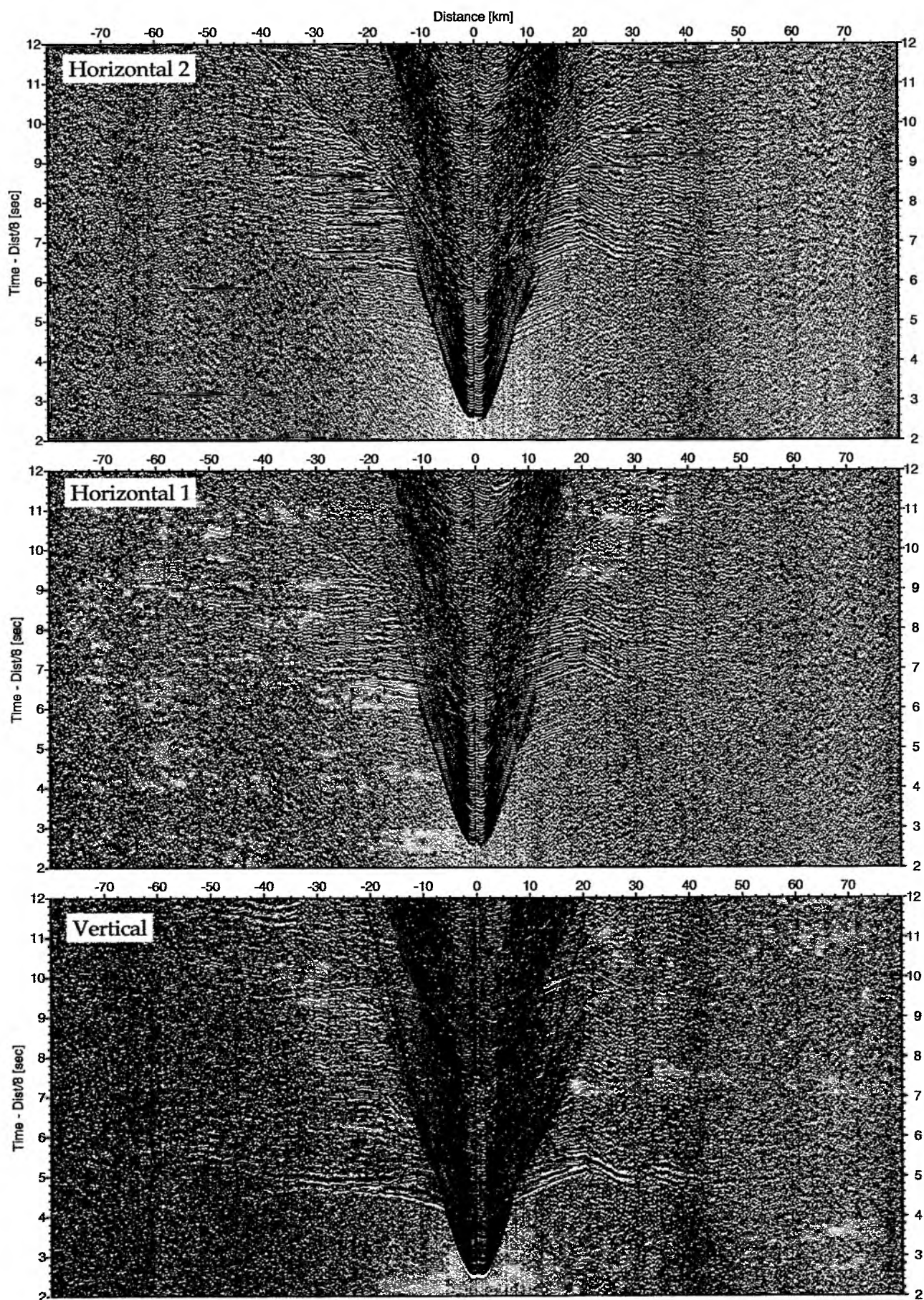


Figure 6.6.3.16: Record sections from obs 44 OAS/Owen-4.5Hz, SO181 Profile 05.

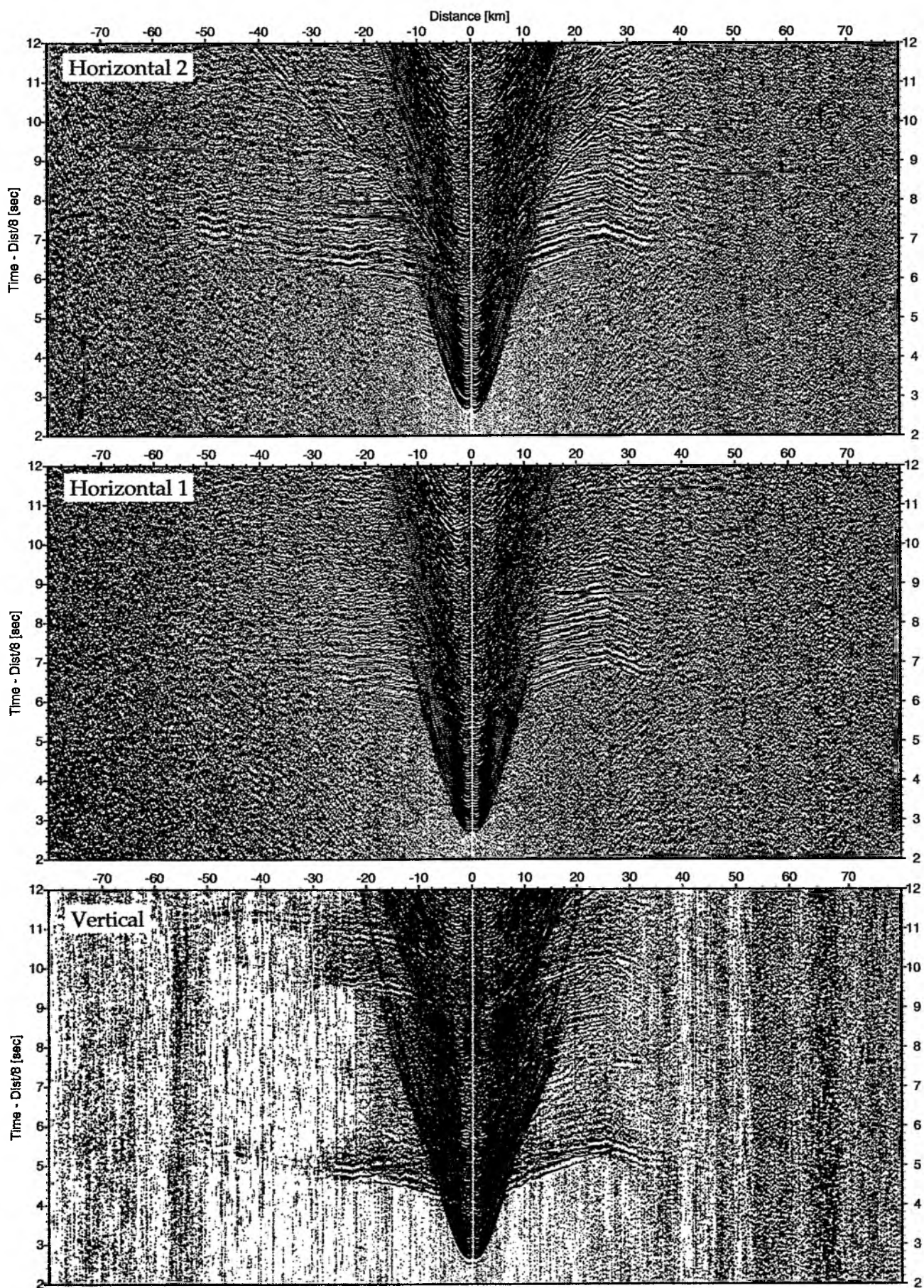


Figure 6.6.3.17: Record sections from obs 45 OAS/Owen-4.5Hz, SO181 Profile 05.

Time - Dist/8 [sec]

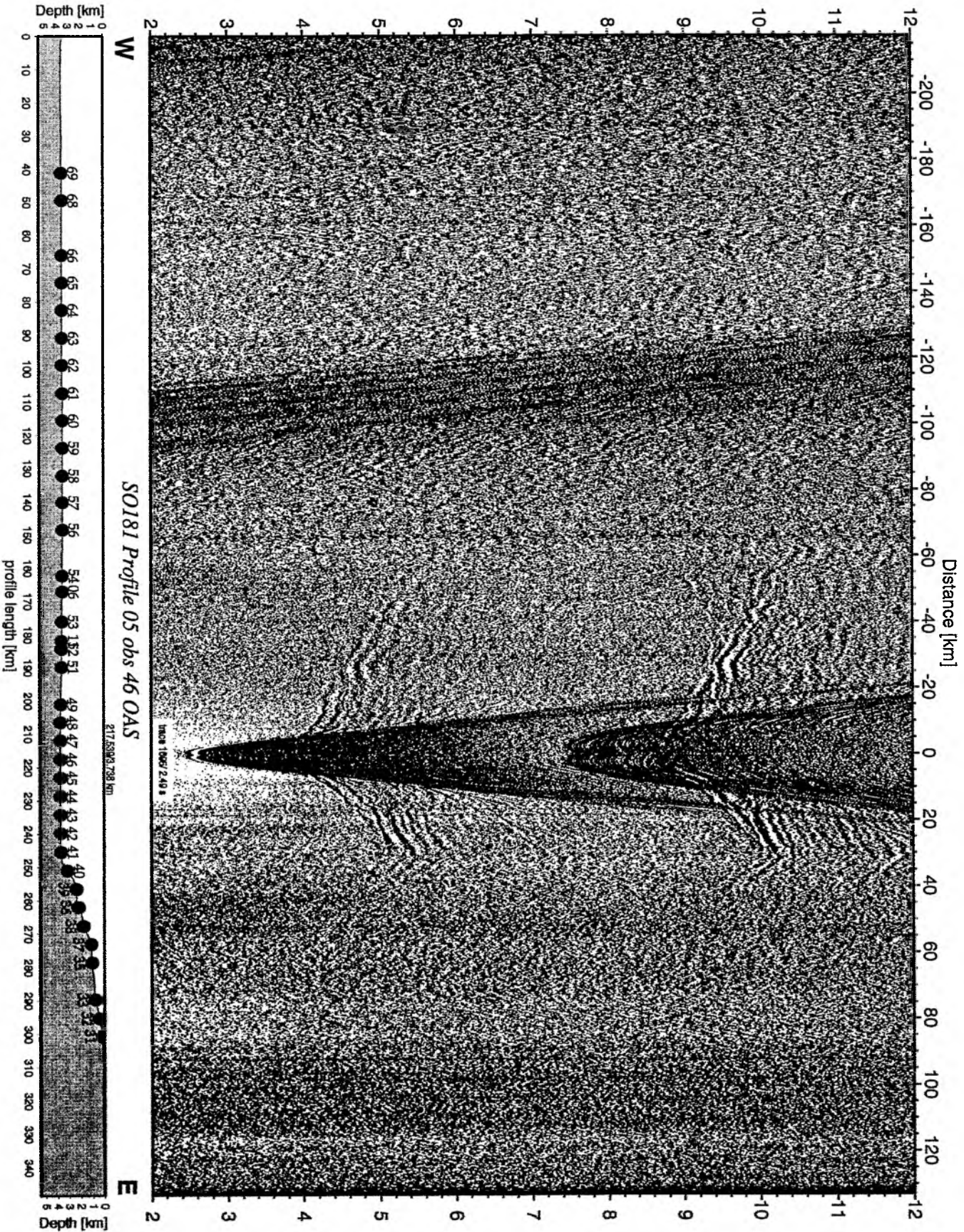


Figure 6.6.3.18: Record section from obs 46 OAS, Profile 05.

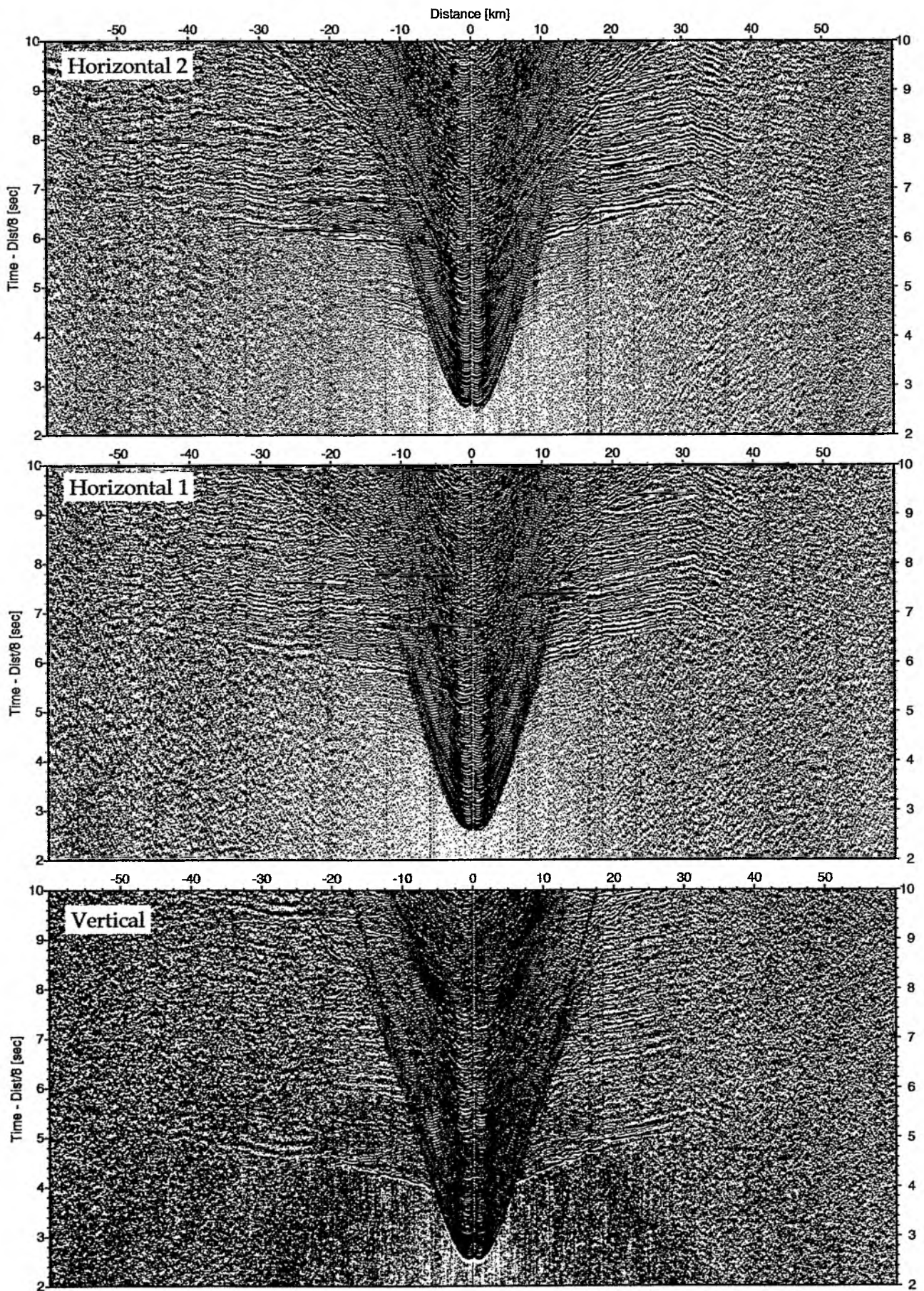


Figure 6.6.3.19: Record sections from obs 46 OAS/Owen-4.5Hz, SO181 Profile 05.

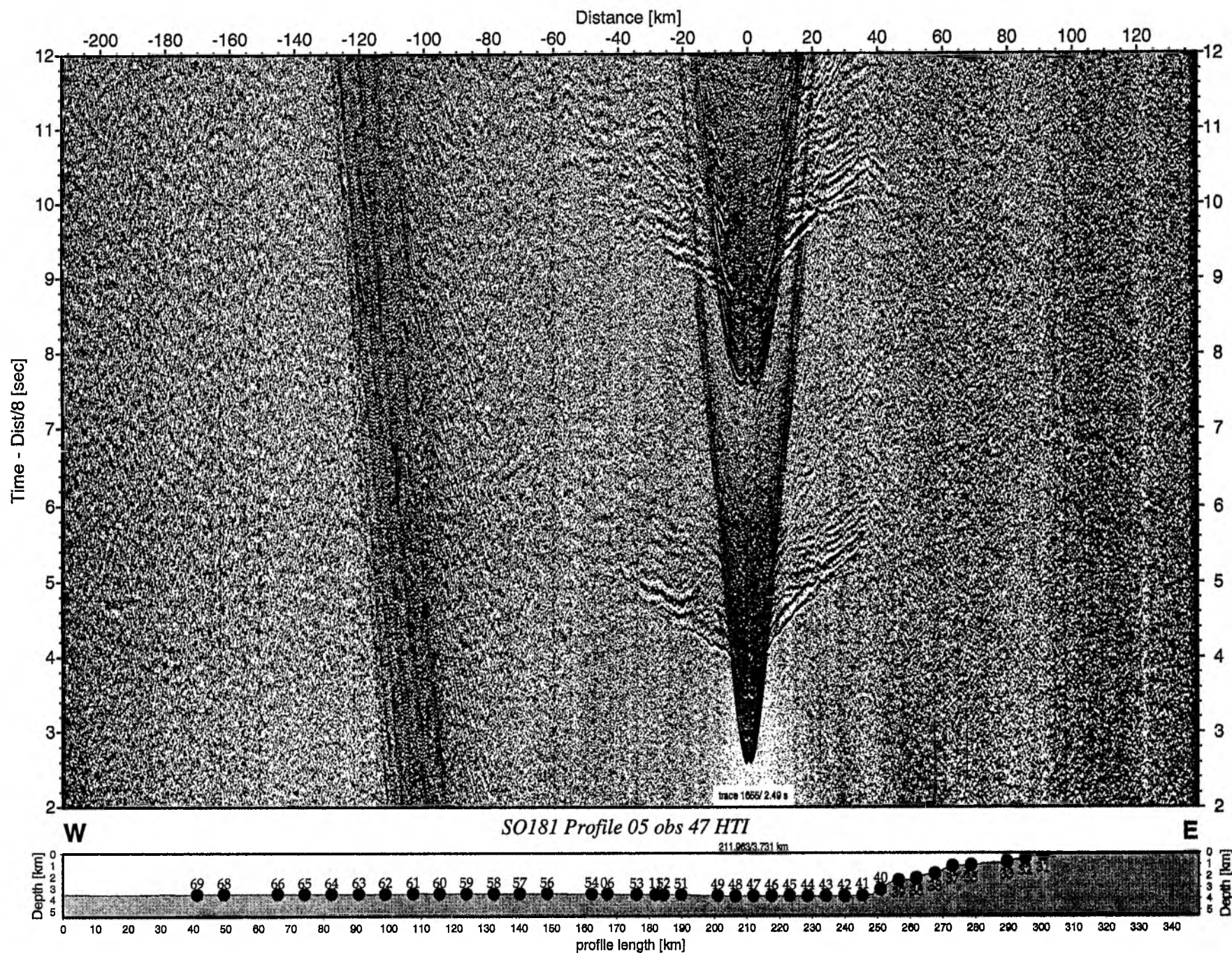


Figure 6.6.3.20: Record section from obs 47 HTI, Profile 05.

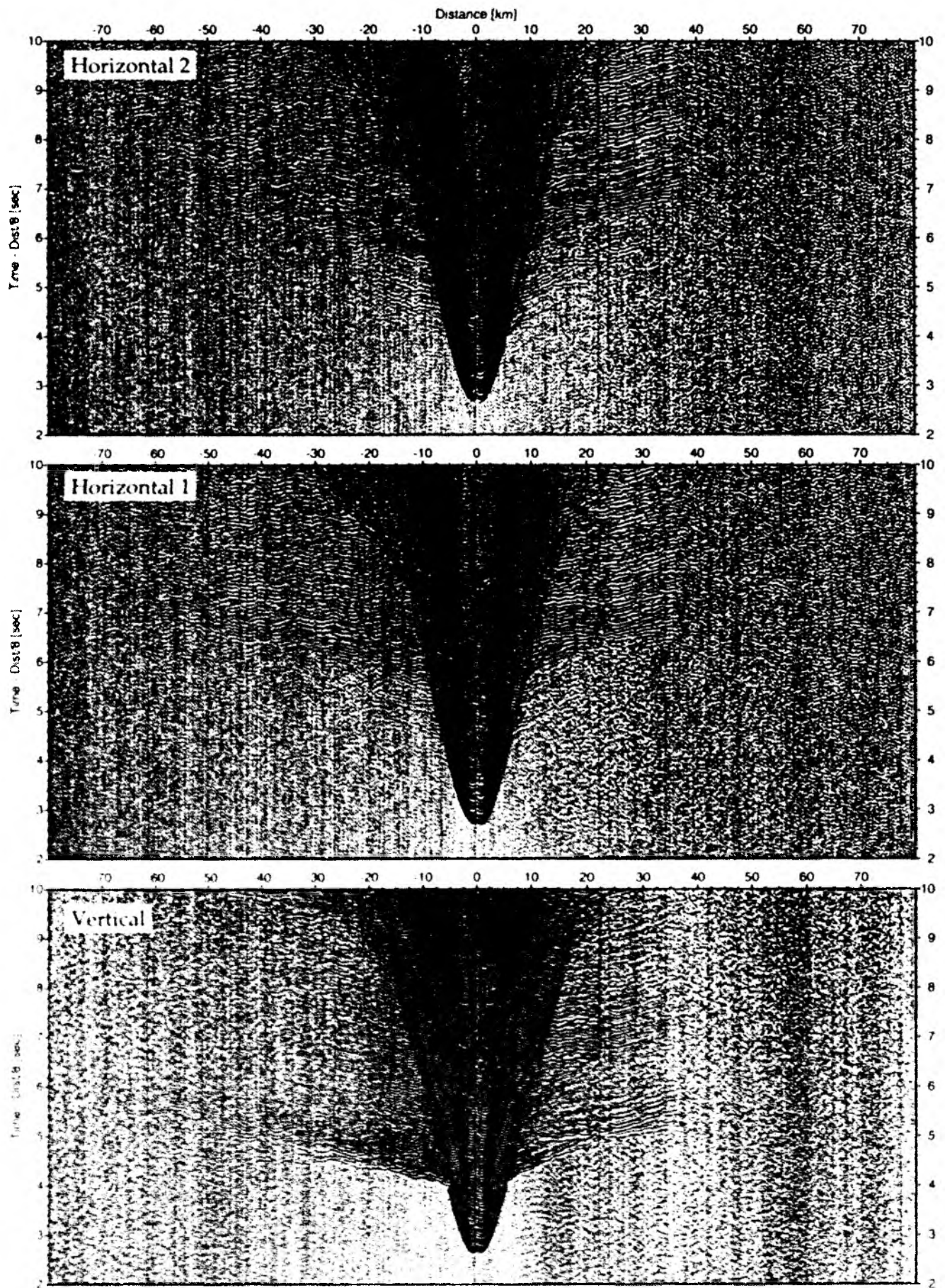


Figure 6.6.3.21: Record sections from obs 47 HTI/Owen-15Hz, SO181 Profile 05.

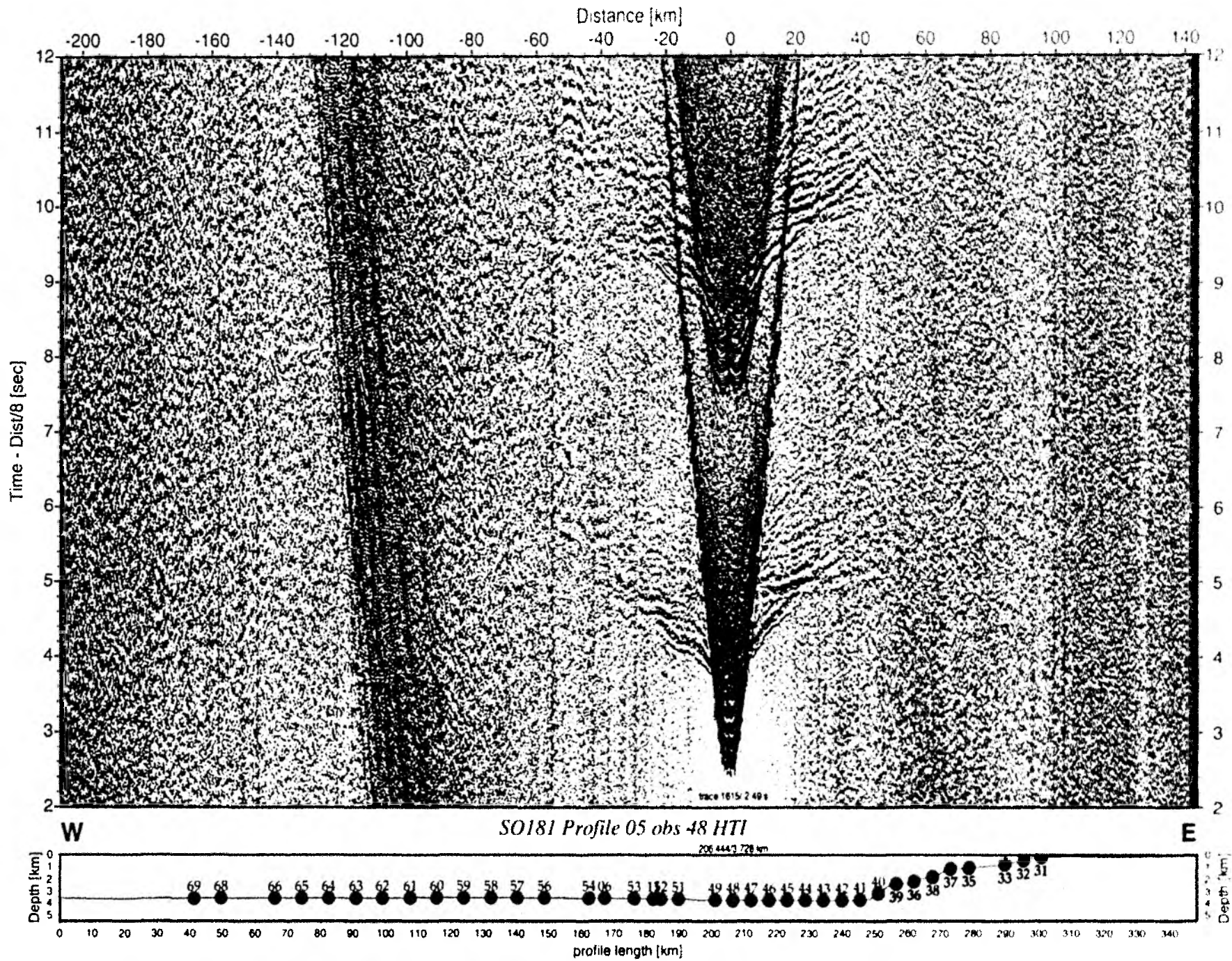


Figure 6.6.3.22: Record section from obs 48 HTI, Profile 05.

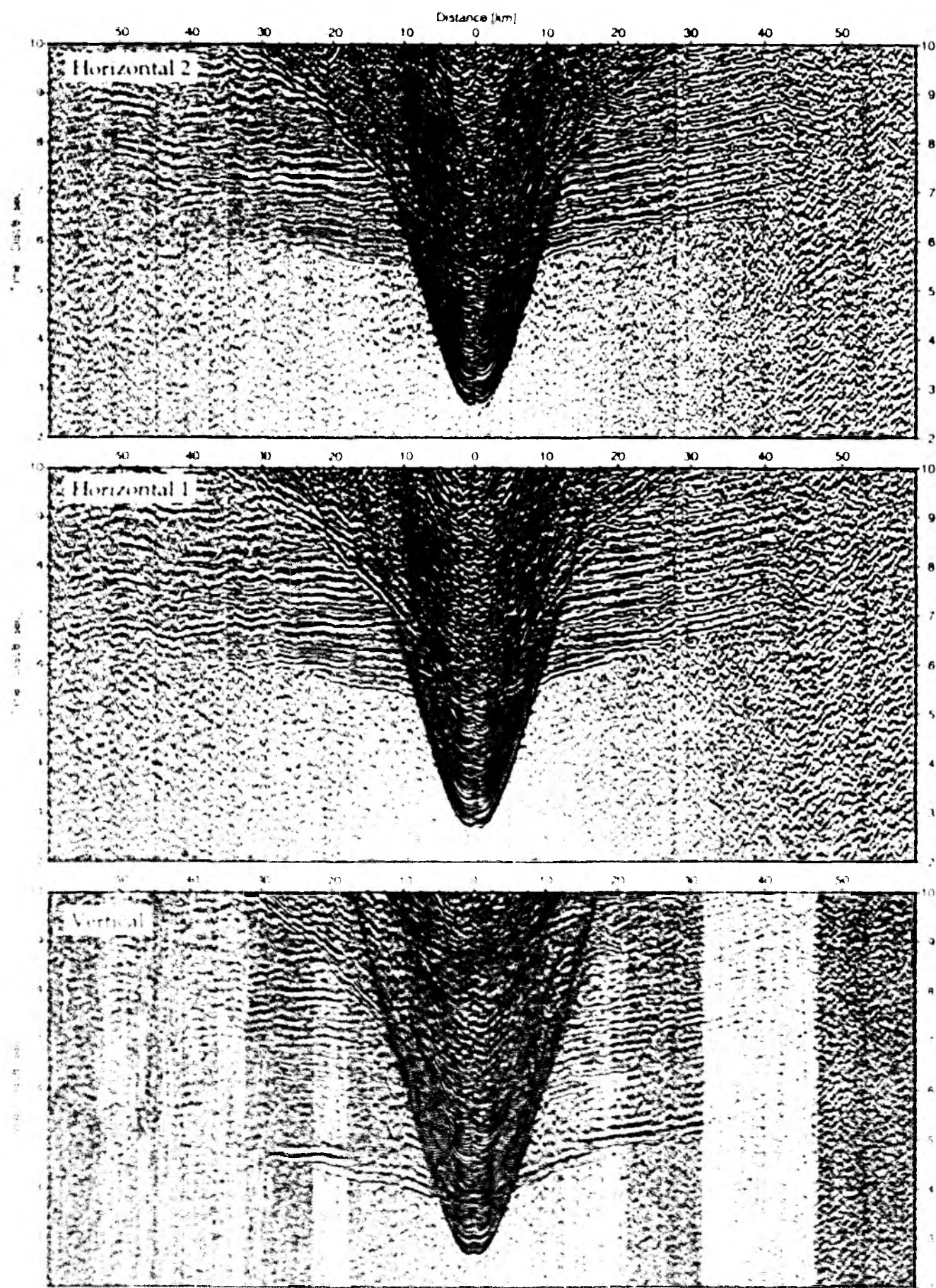


Figure 6.6.3.23. Record sections from obs 48 HPL Owen-4.5Hz & OLS1 Profile 05.

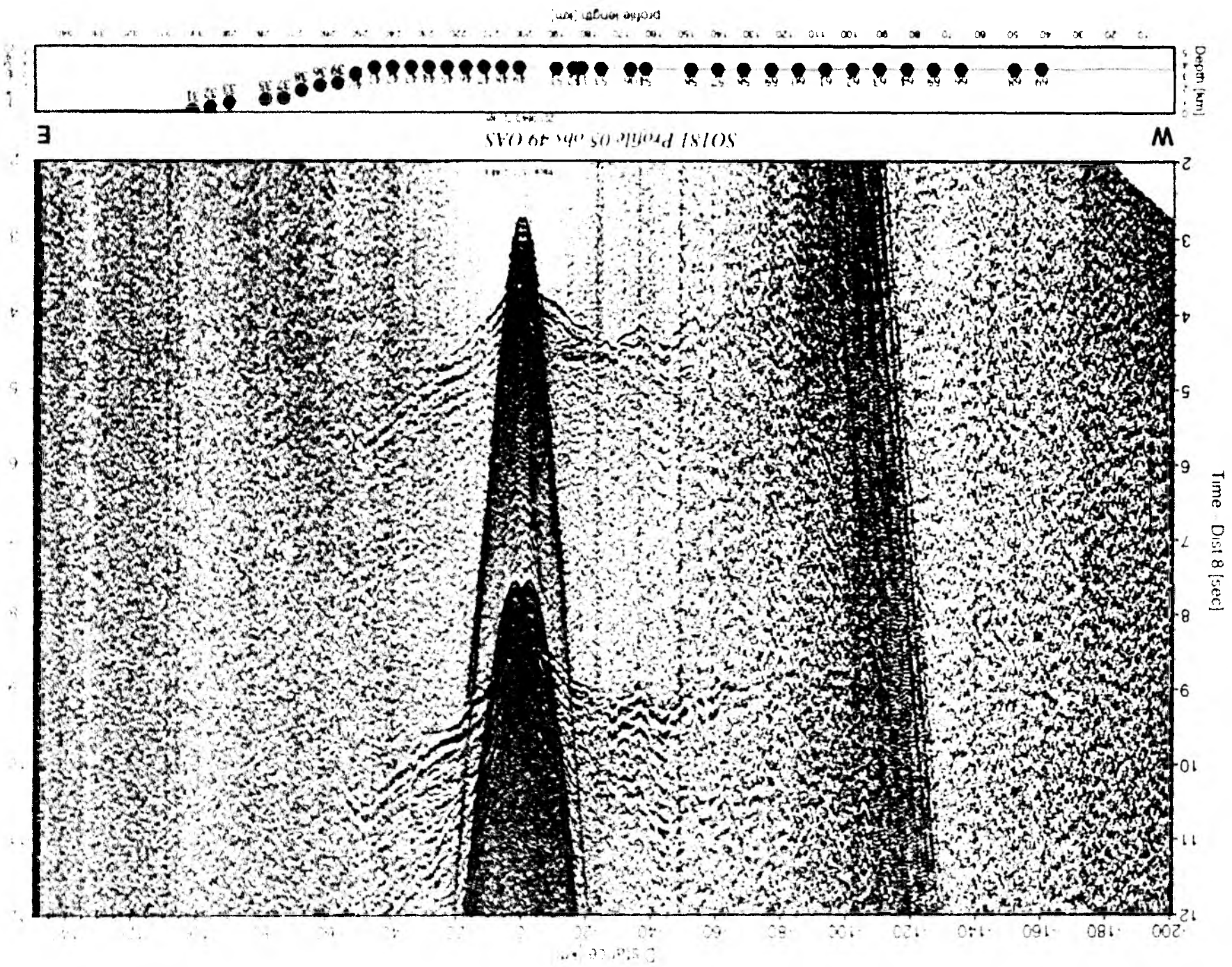


Figure 6.6.3.24: Reverted section from obs 49 OAS Profile 05

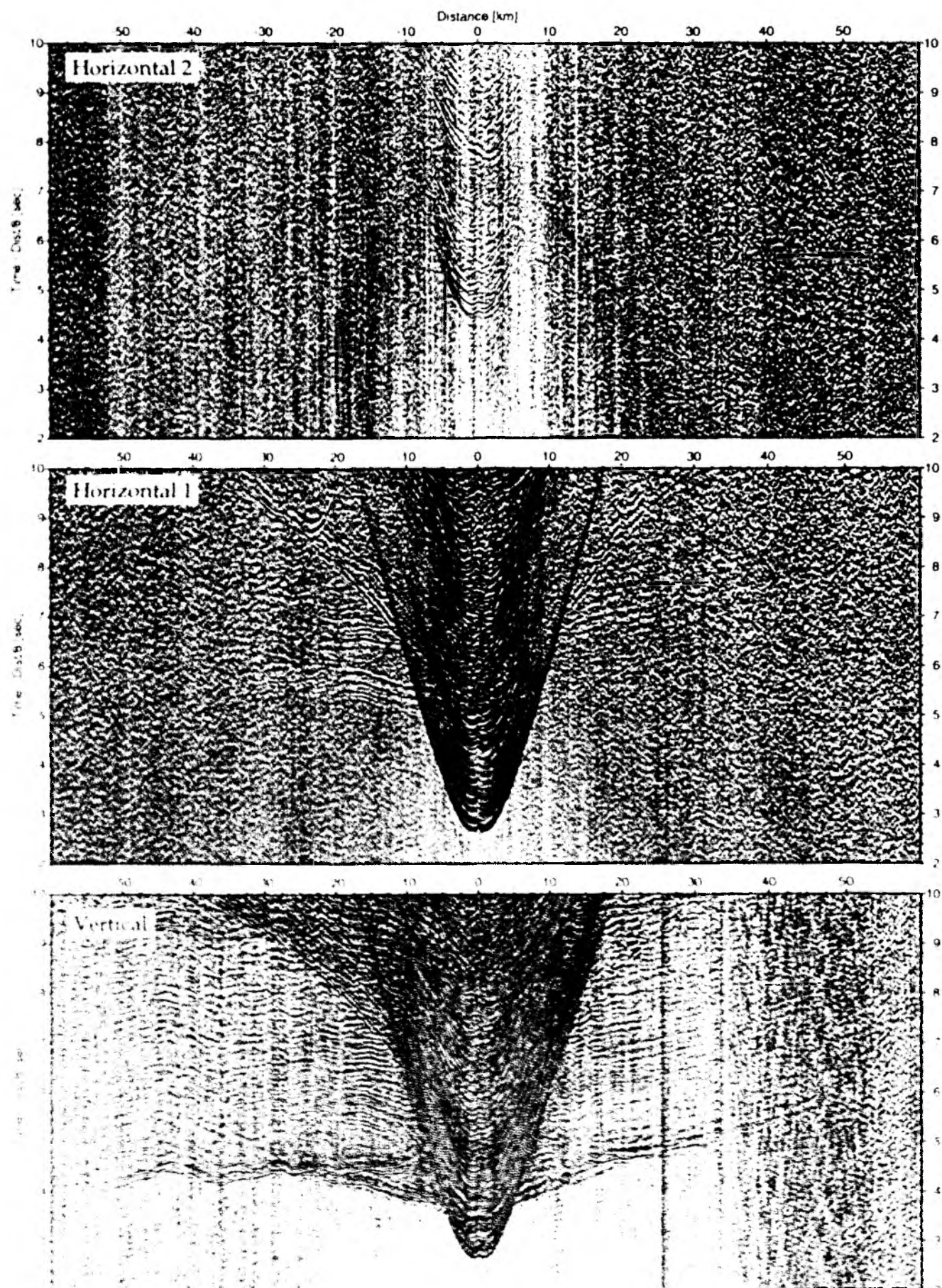


Figure 6.6.3.25: Record sections from obs 49 QAS, Owen-4 5Hz, S01S1 Profile 05

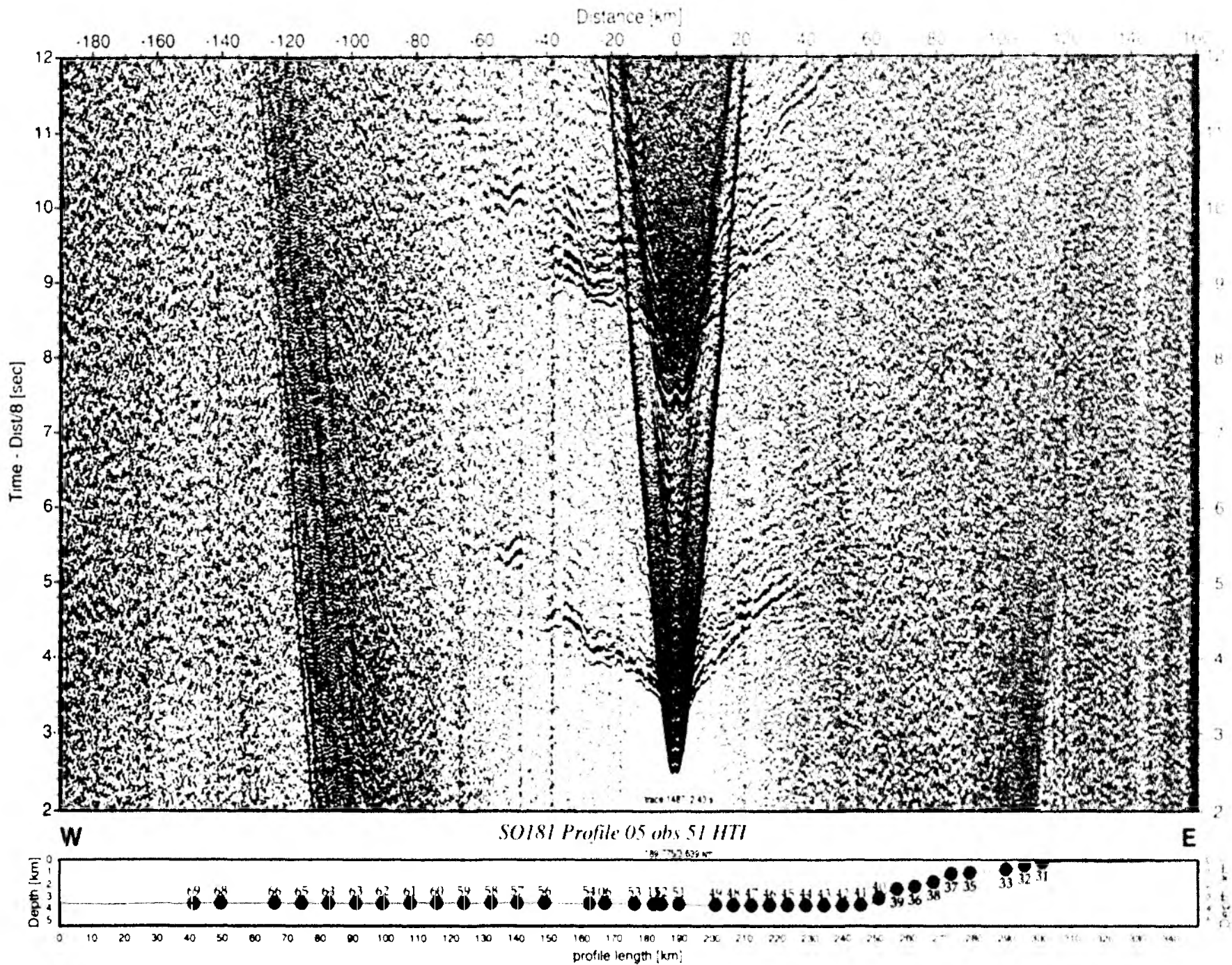


Figure 6.6.3.26: Record section from obs 51 HTI, Profile 05

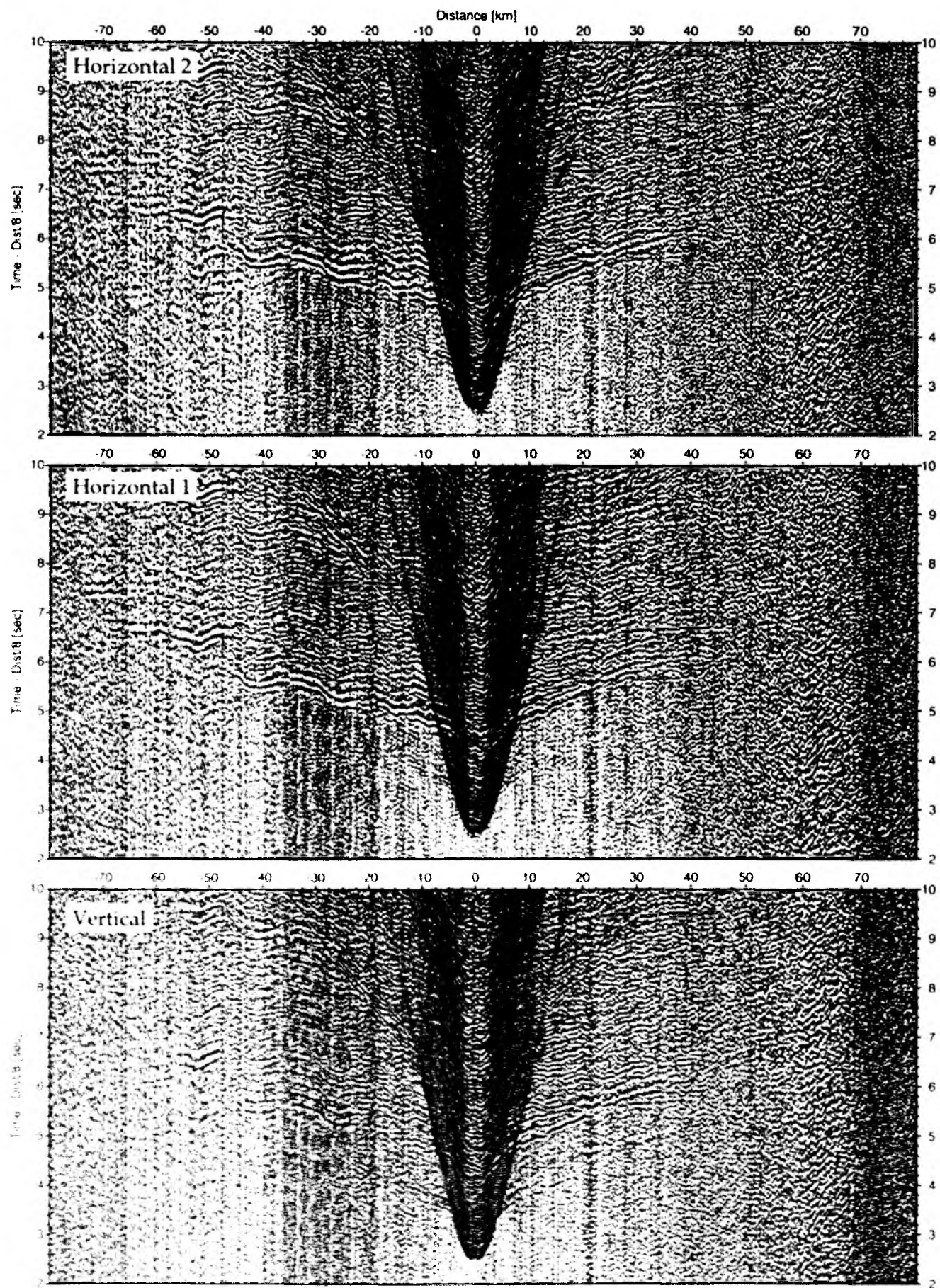


Figure 6.6.3.27: Record sections from obs 51 HTU/Owen-4.5Hz, SO181 Profile 05.

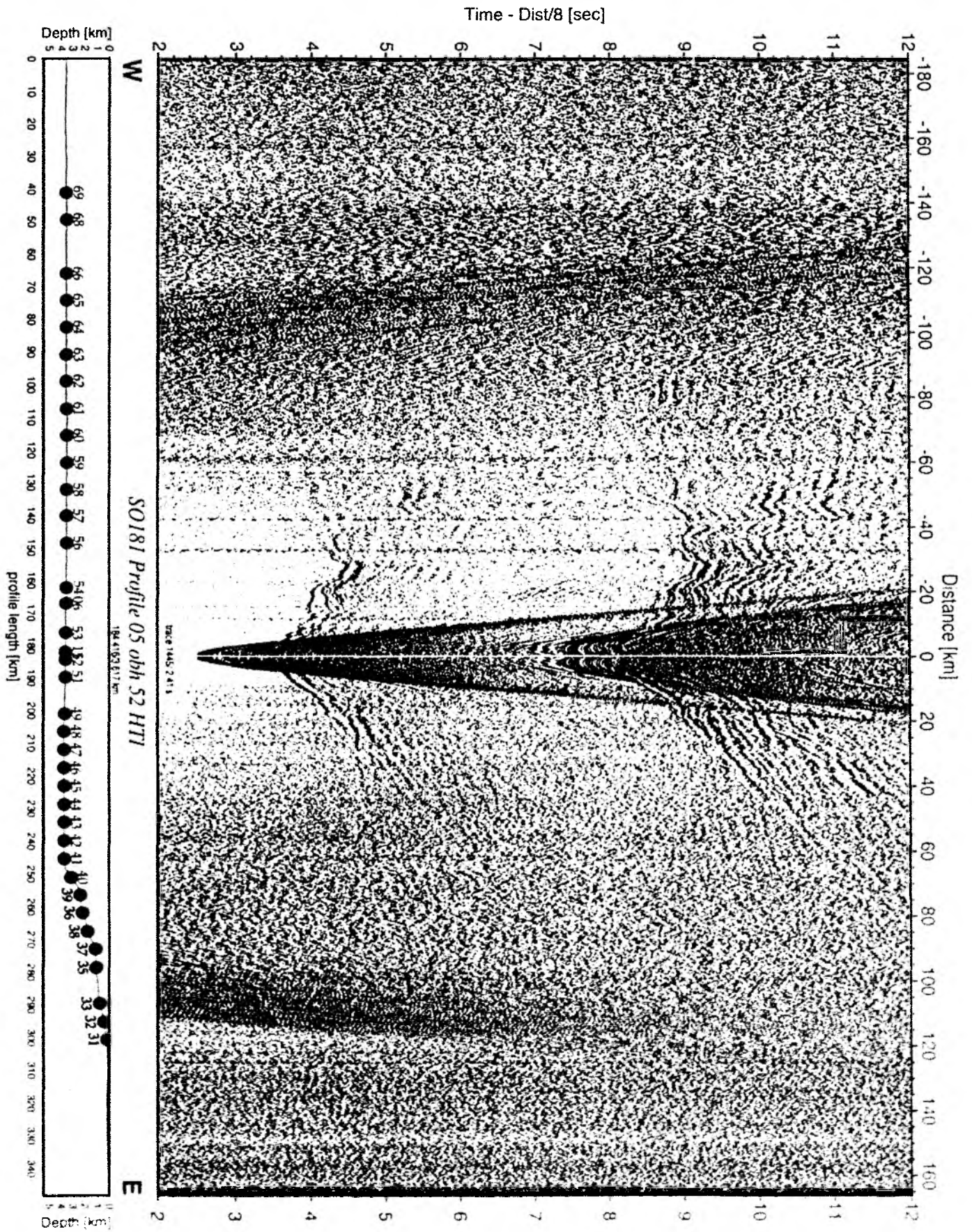
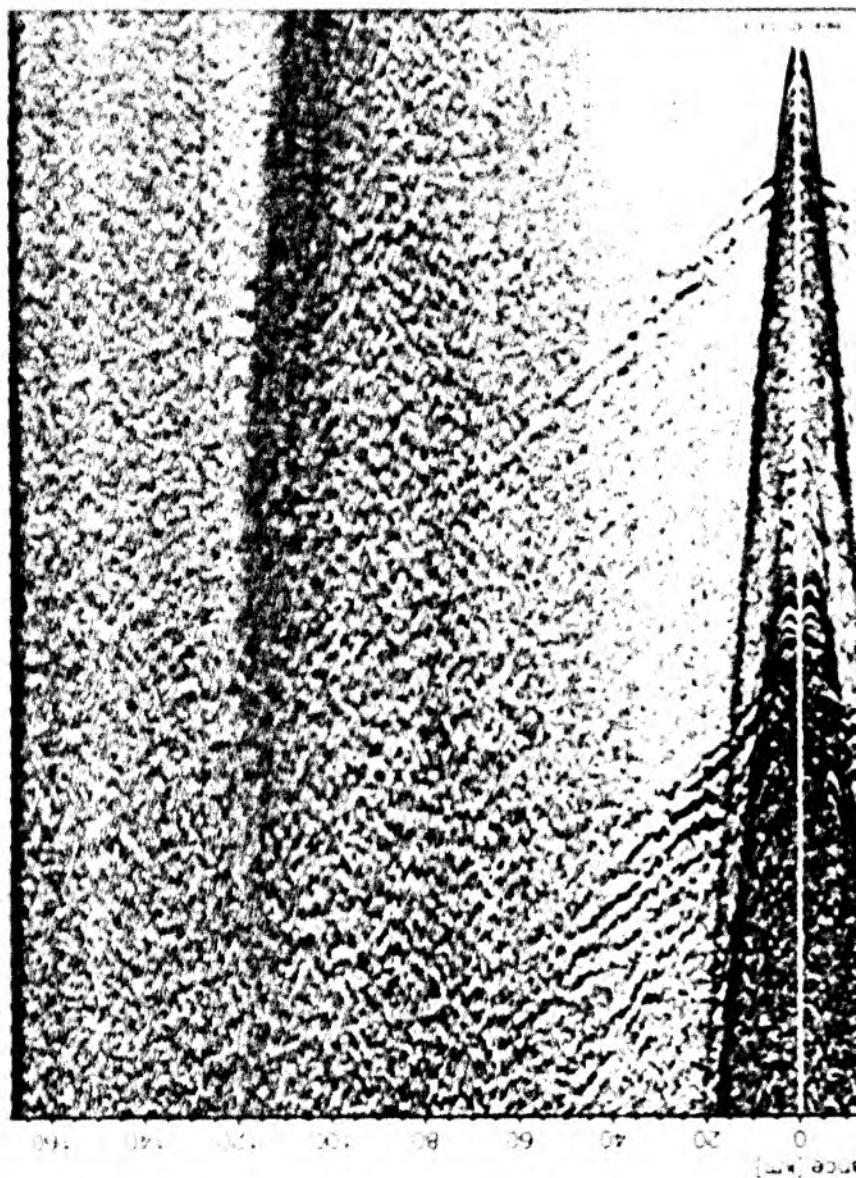
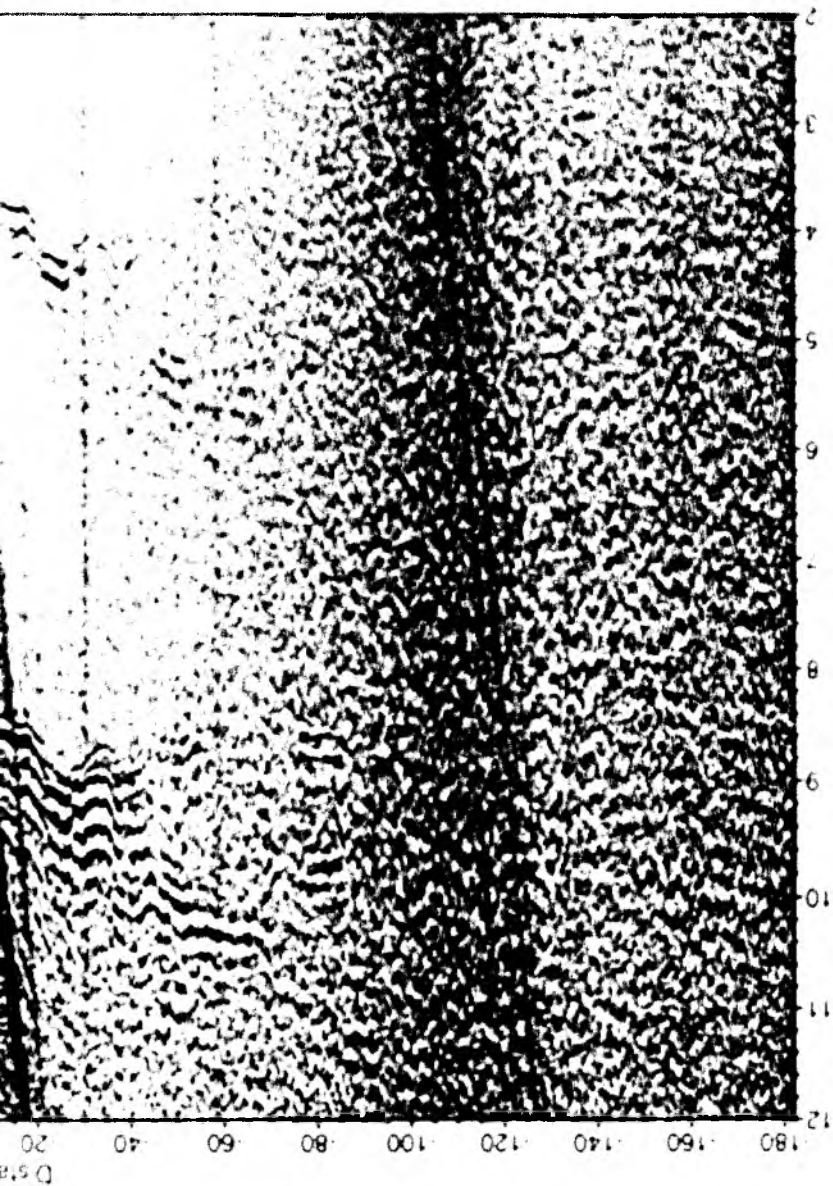


Figure 6.6.3.28: Record section from obh 52 HTI, Profile 05.

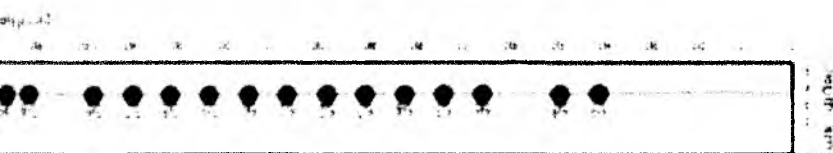


Time Dist [sec]



M

S0181 Dist [sec]



Time Dist B (sec)

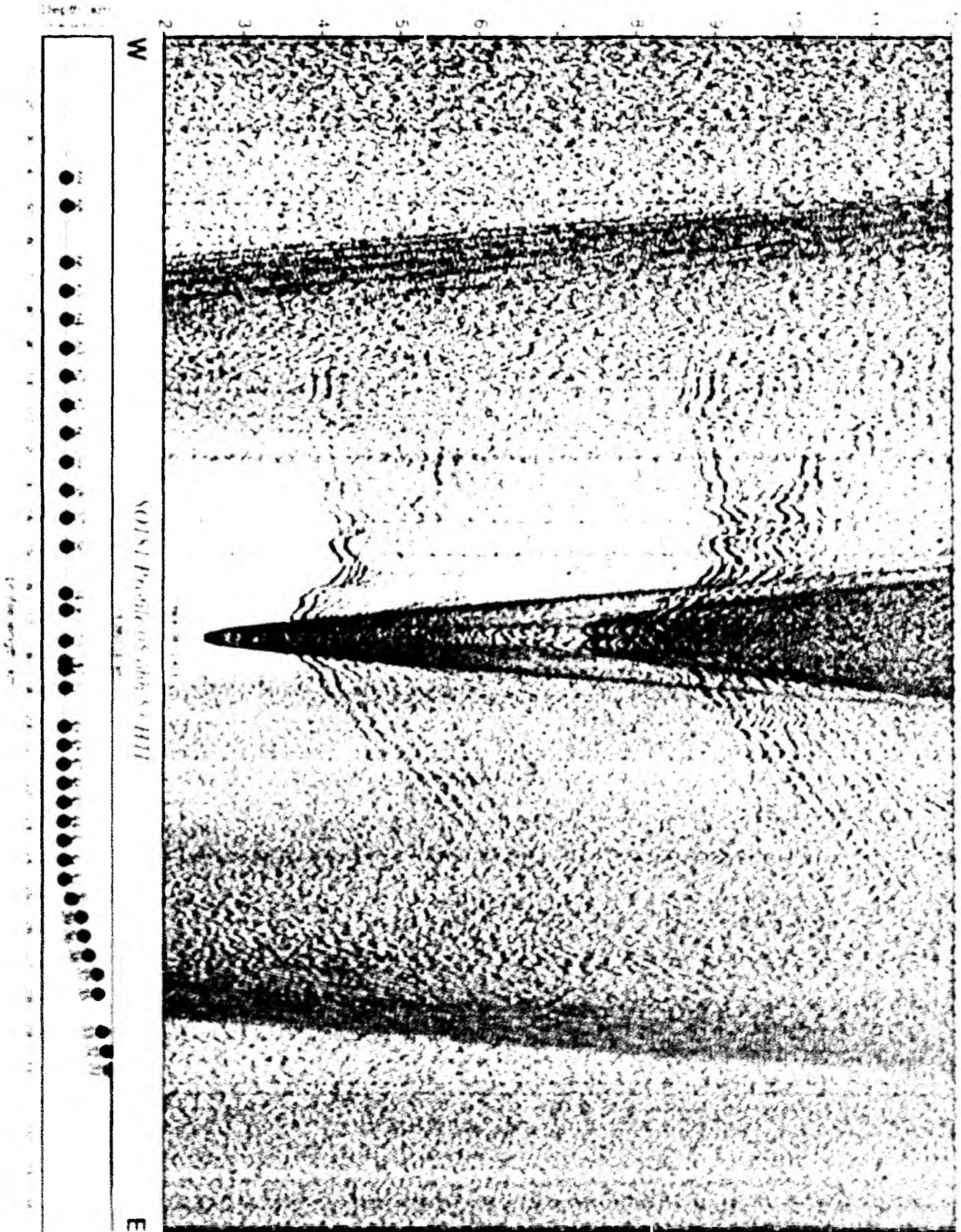


Figure 6.3.30

S. 40th S. 11th

S. 40th S. 11th

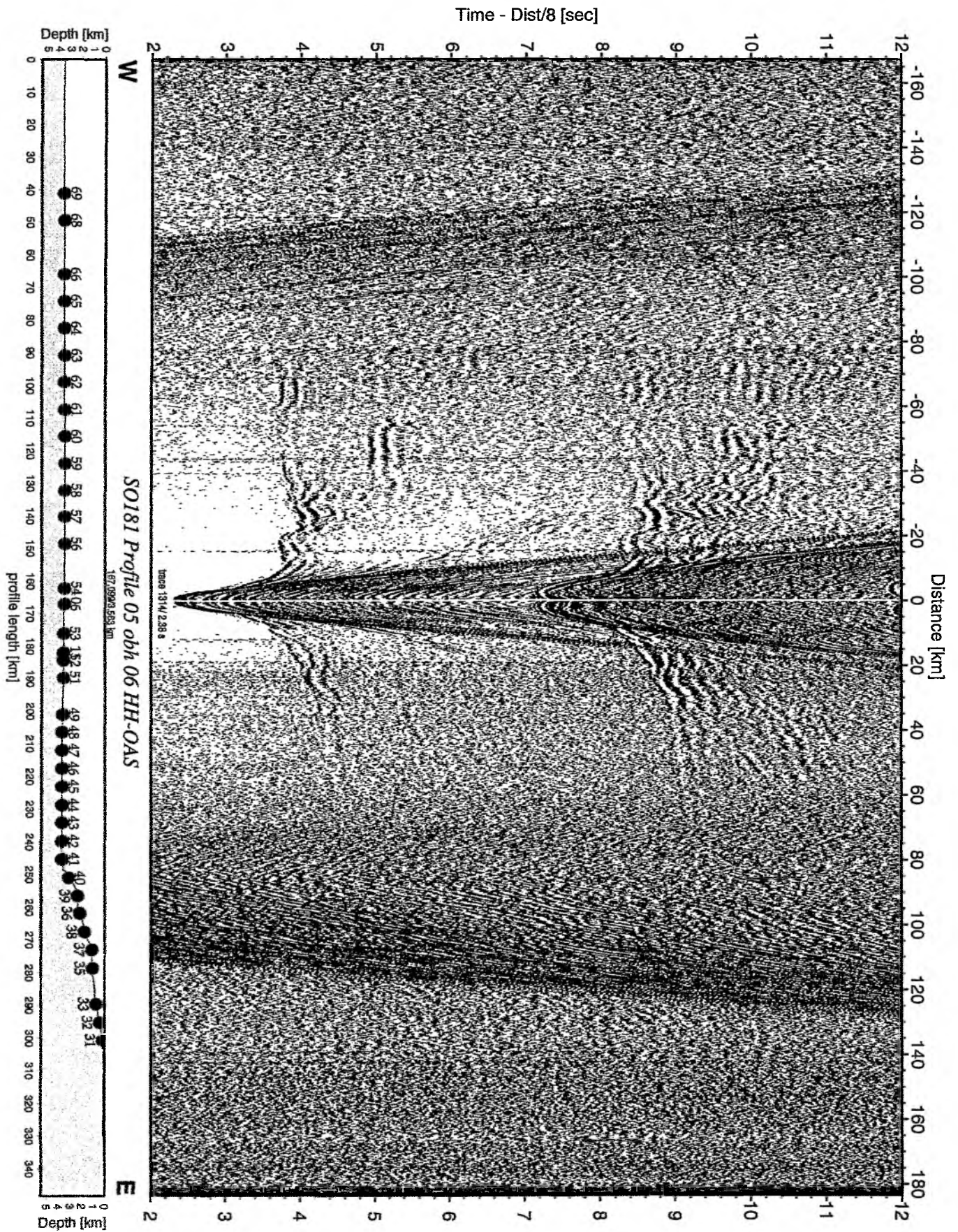


Figure 6.6.3.31: Record section from obh 06 HH-OAS, Profile 05.

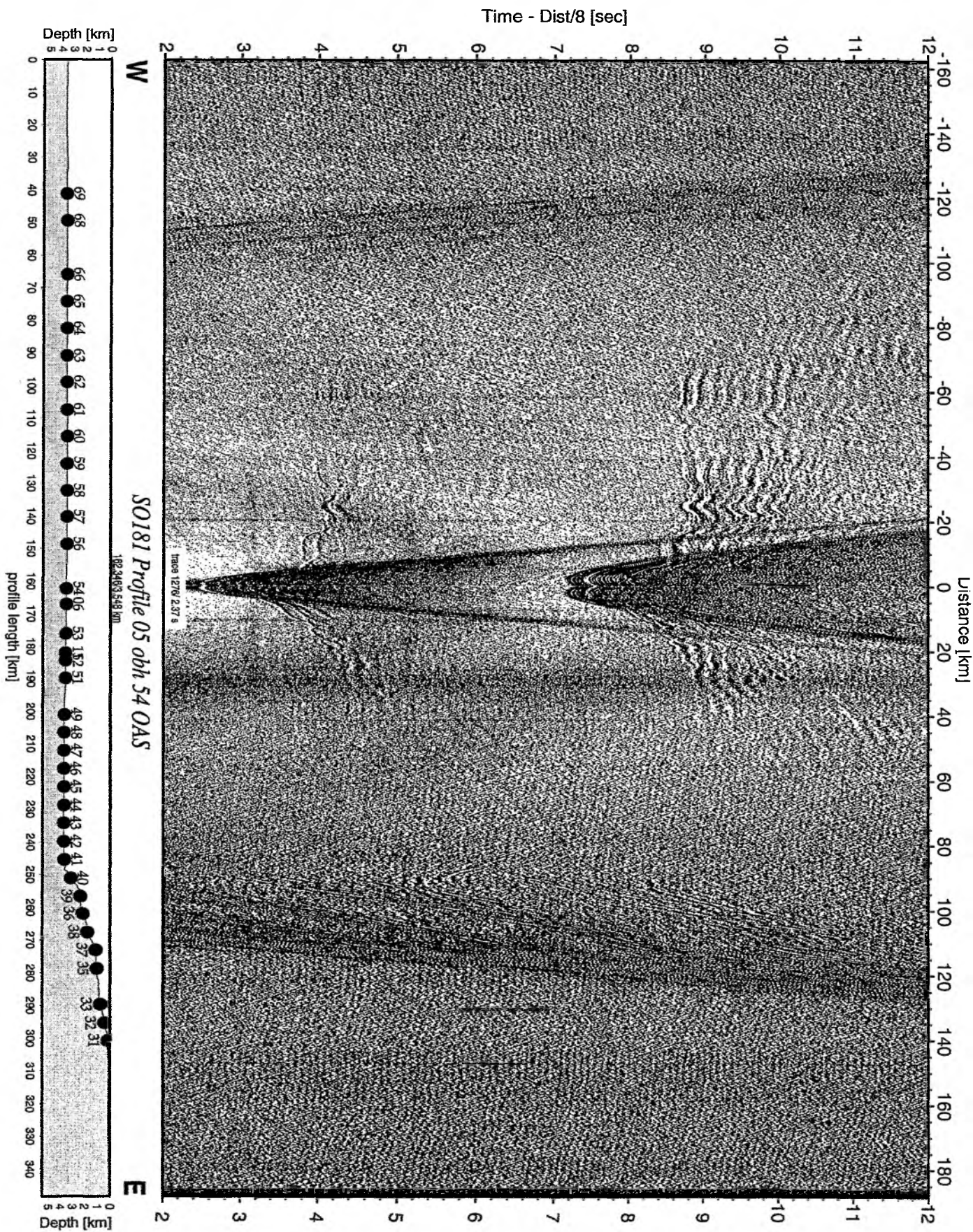


Figure 6.6.332: Record section from obh 54 OAS, Profile 05.

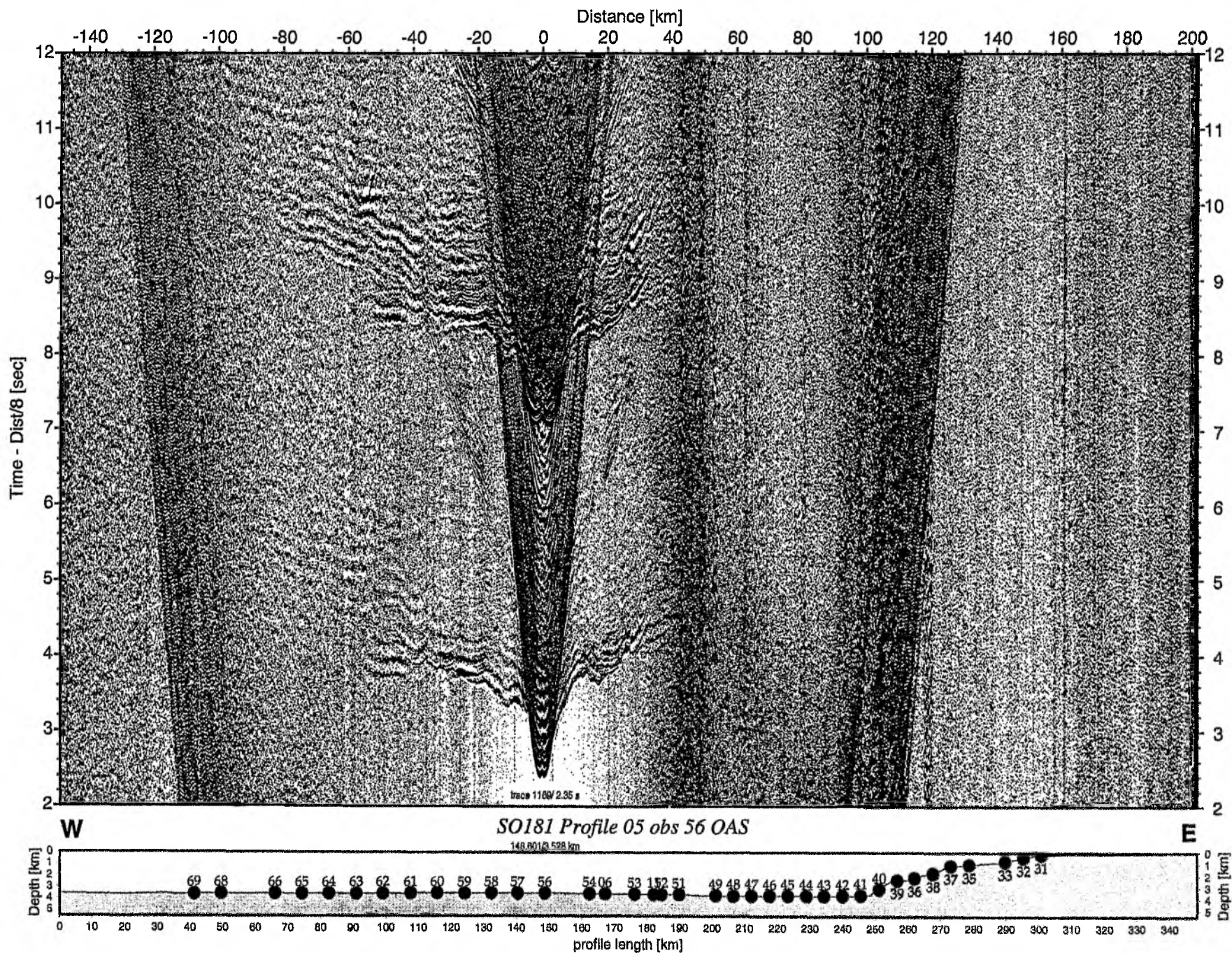


Figure 6.6.3.33: Record section from obs 56 OAS, Profile 05.

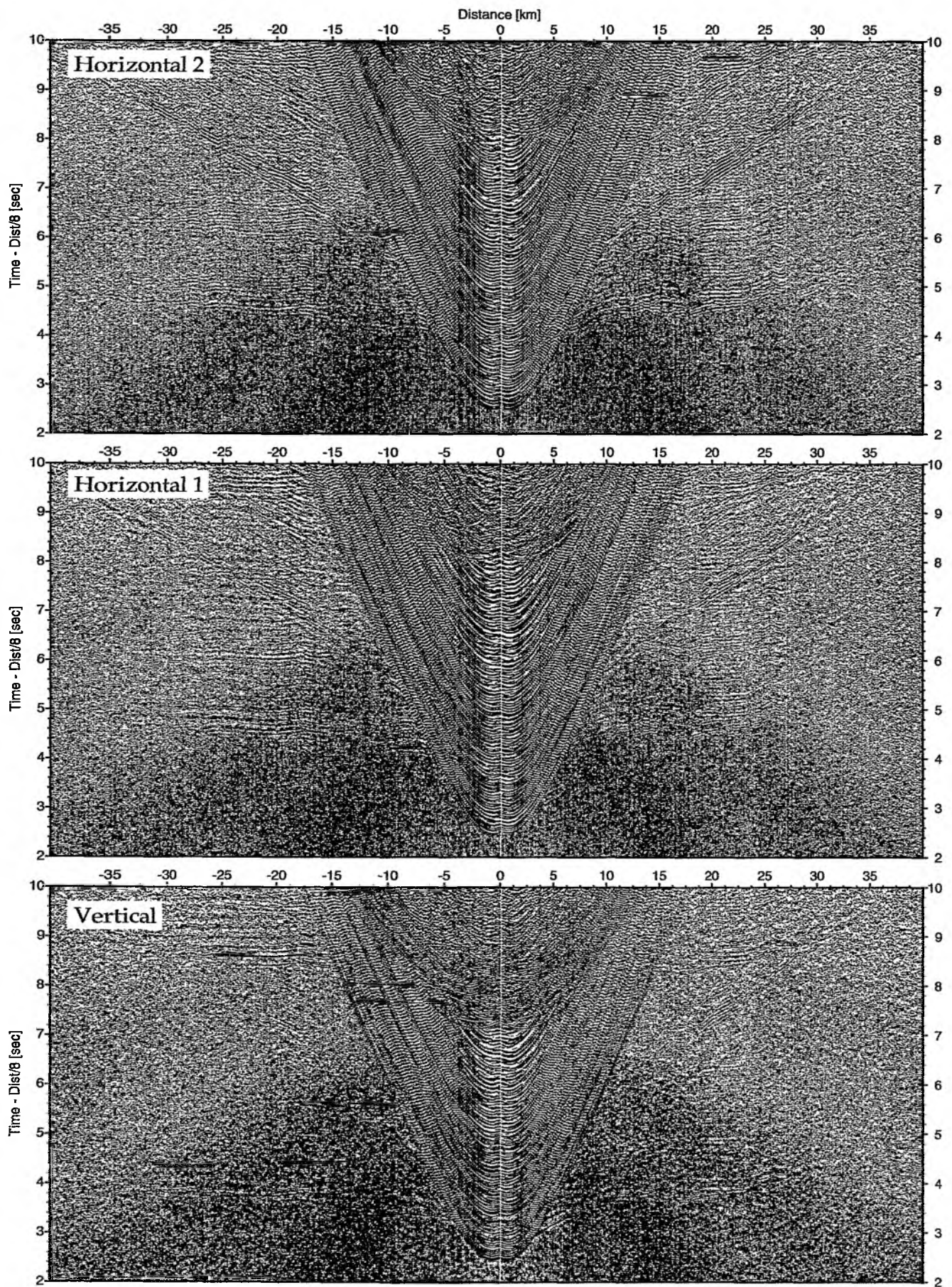


Figure 6.6.3.34: Record sections from obs 56 OAS/Owen-4.5Hz, SO181 Profile 05.

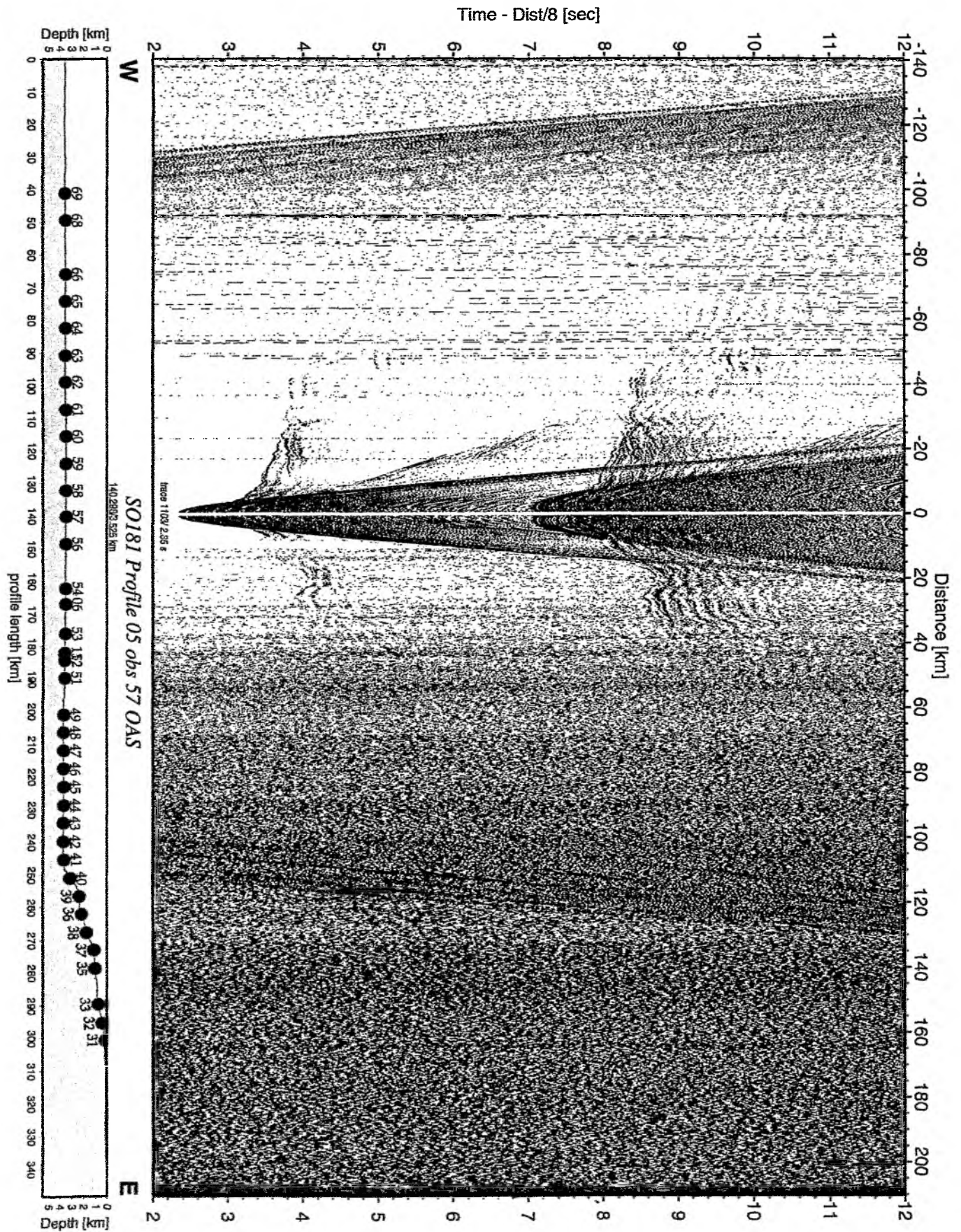


Figure 6.6.3.35: Record section from obs 57 OAS, Profile 05.

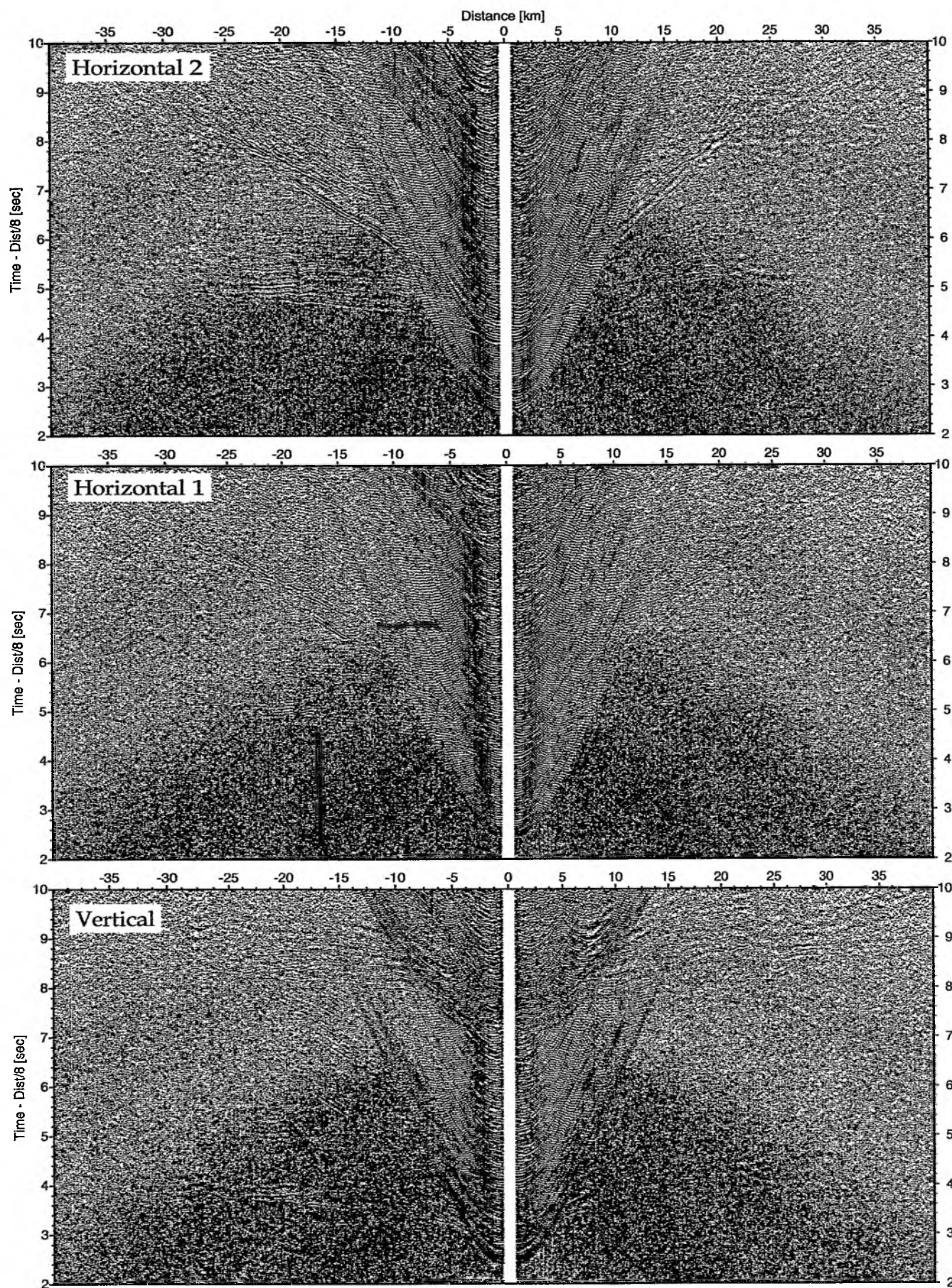


Figure 6.6.3.36: Record sections from obs 57 OAS/Owen-4.5Hz, SO181 Profile 05.

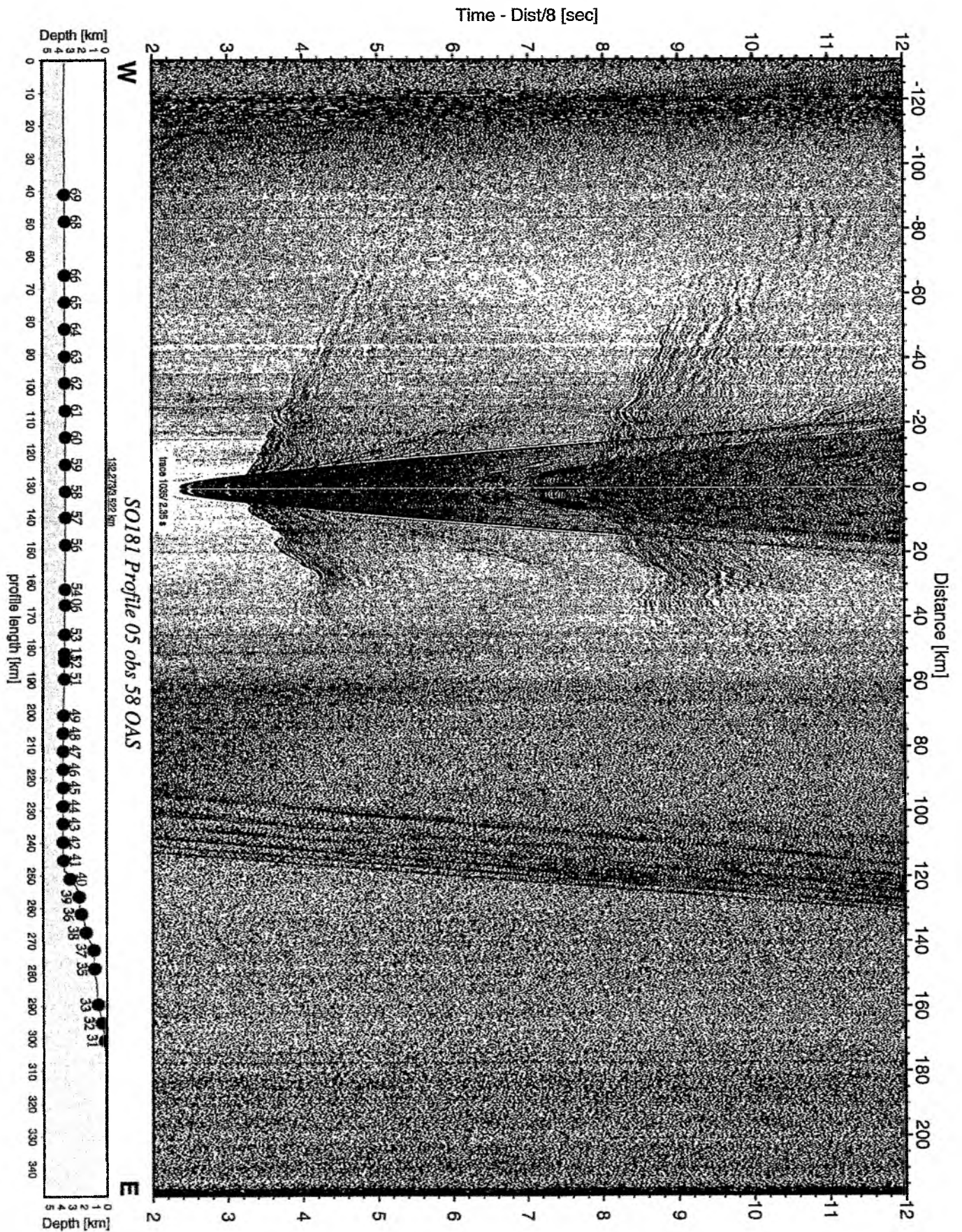


Figure 6.6.3.37: Record section from obs 58 OAS, Profile 05.

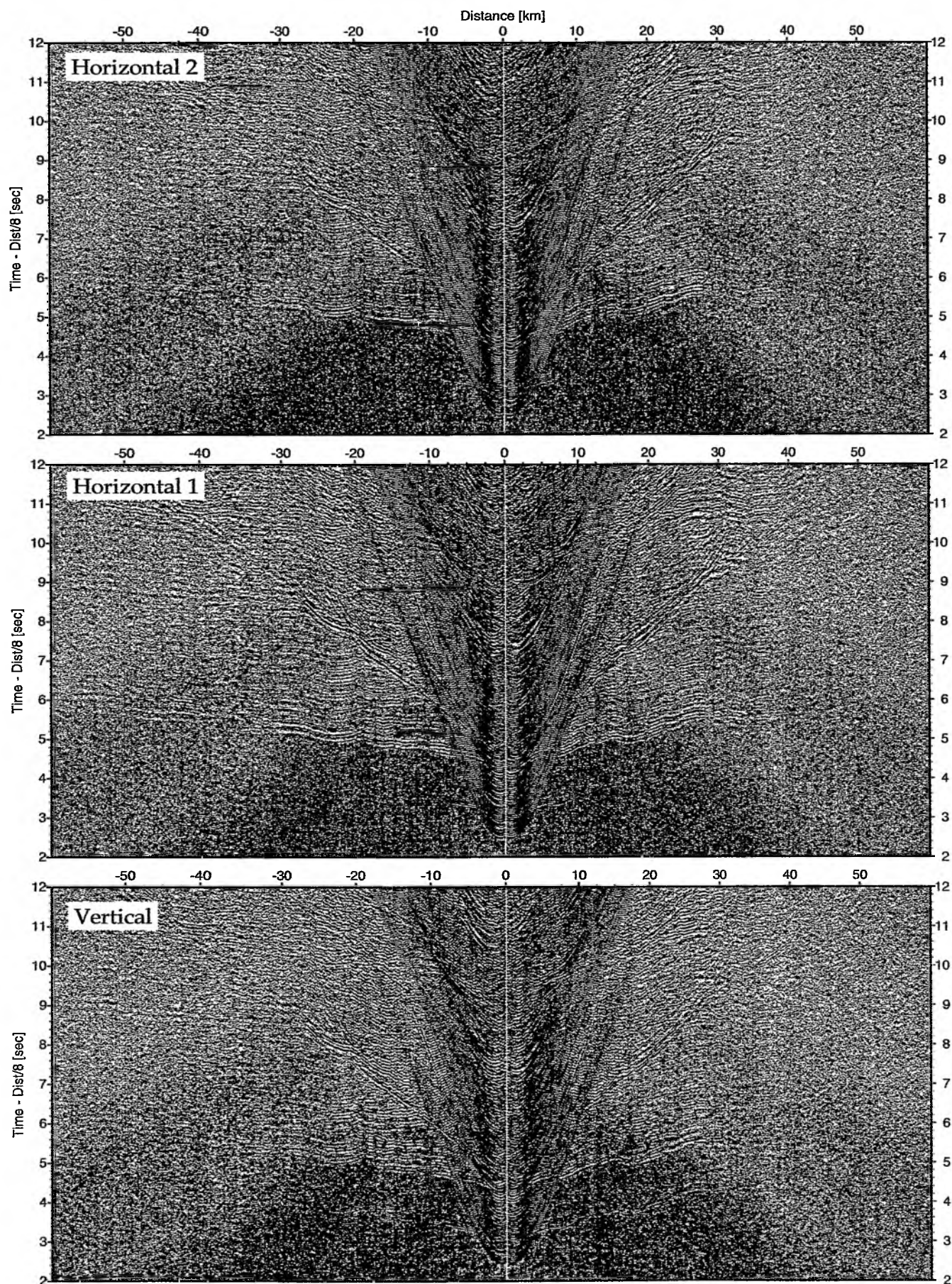


Figure 6.6.3.38: Record sections from obs 58 OAS/Owen-4.5Hz, SO181 Profile 05.

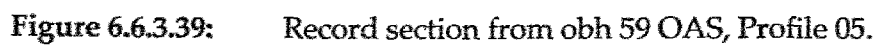


Figure 6.6.3.39: Record section from obh 59 OAS, Profile 05.

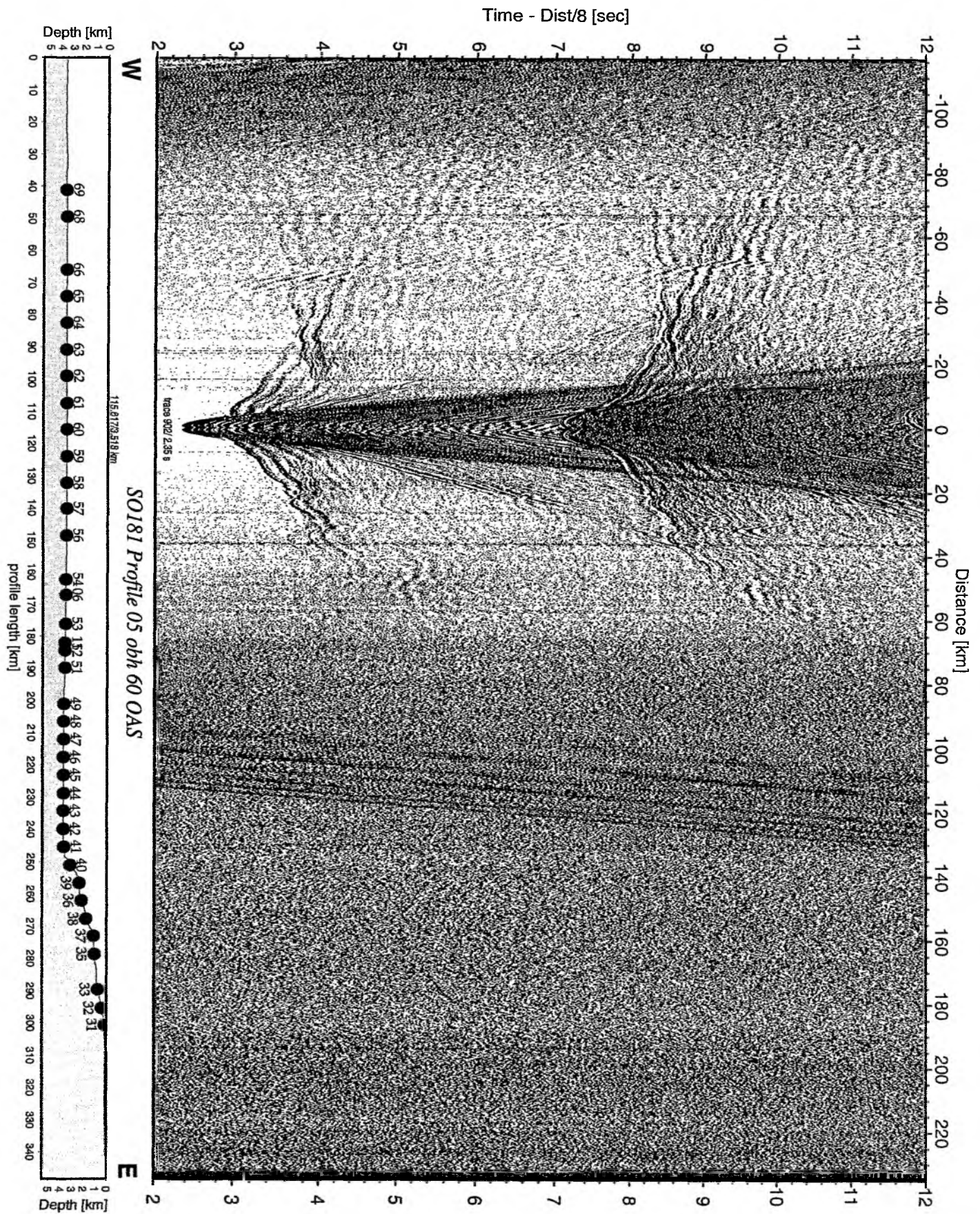


Figure 6.6.3.40: Record section from obh 60 OAS, Profile 05.

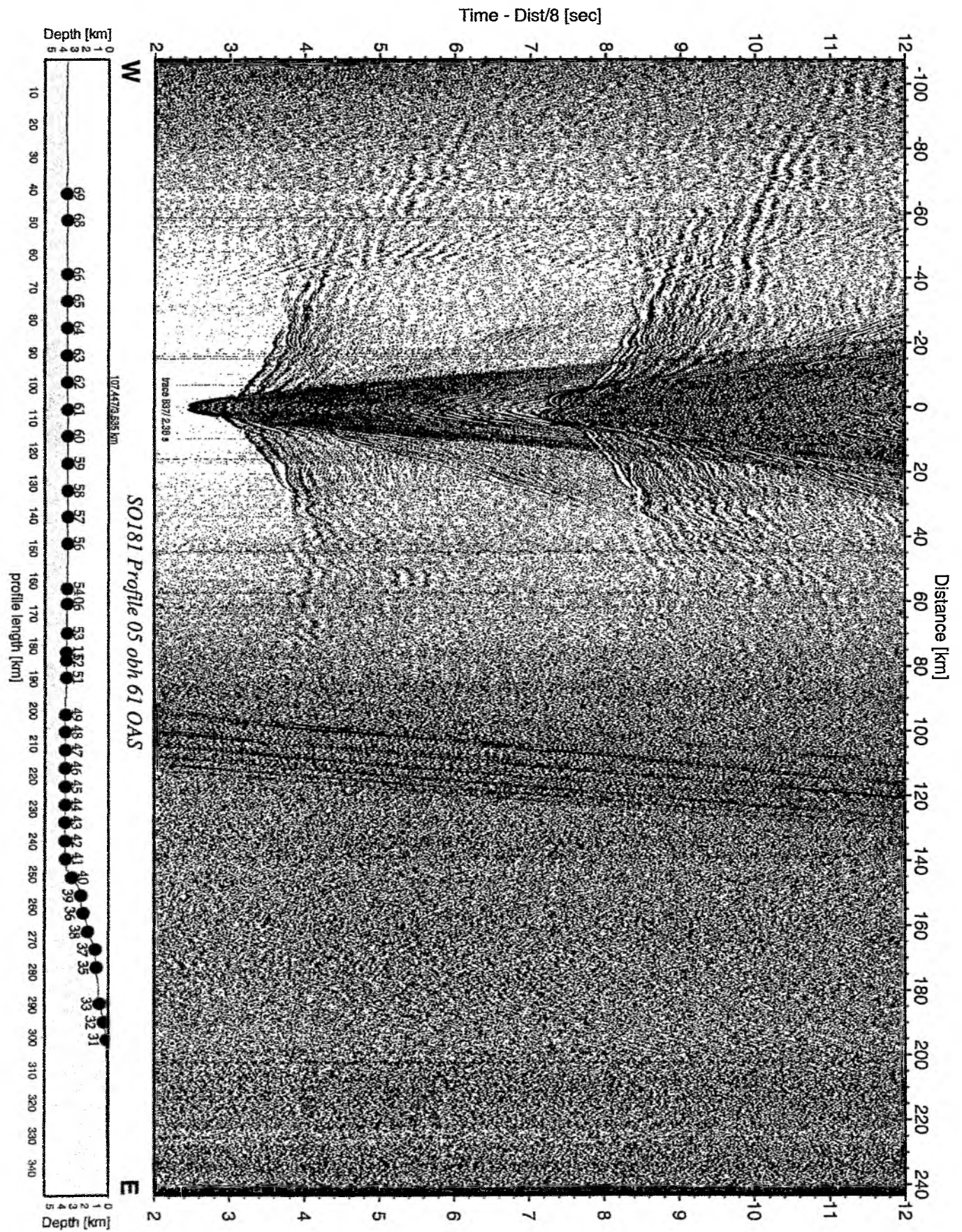


Figure 6.6.3.41: Record section from obh 61 OAS, Profile 05.

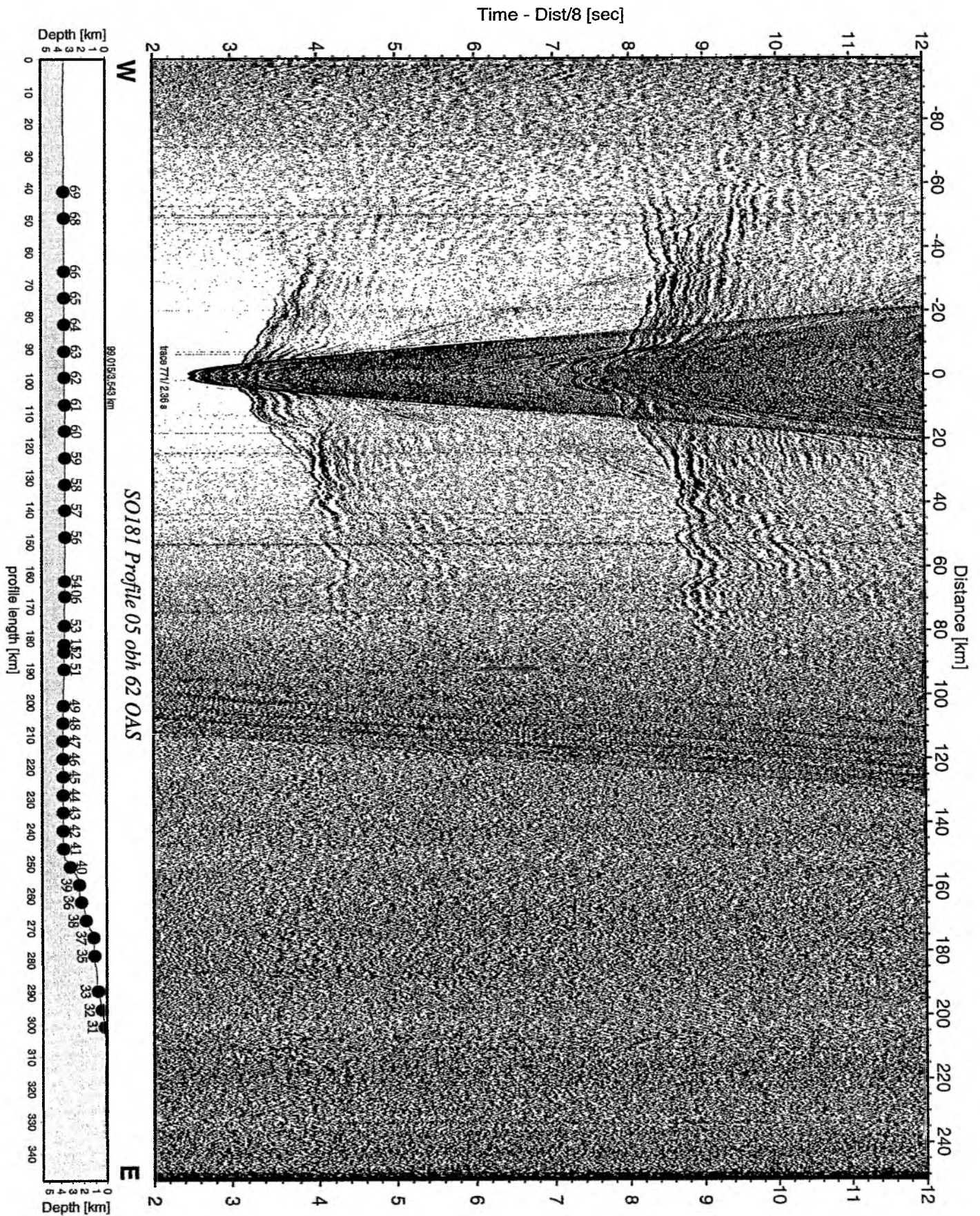


Figure 6.6.3.42: Record section from obh 62 OAS, Profile 05.

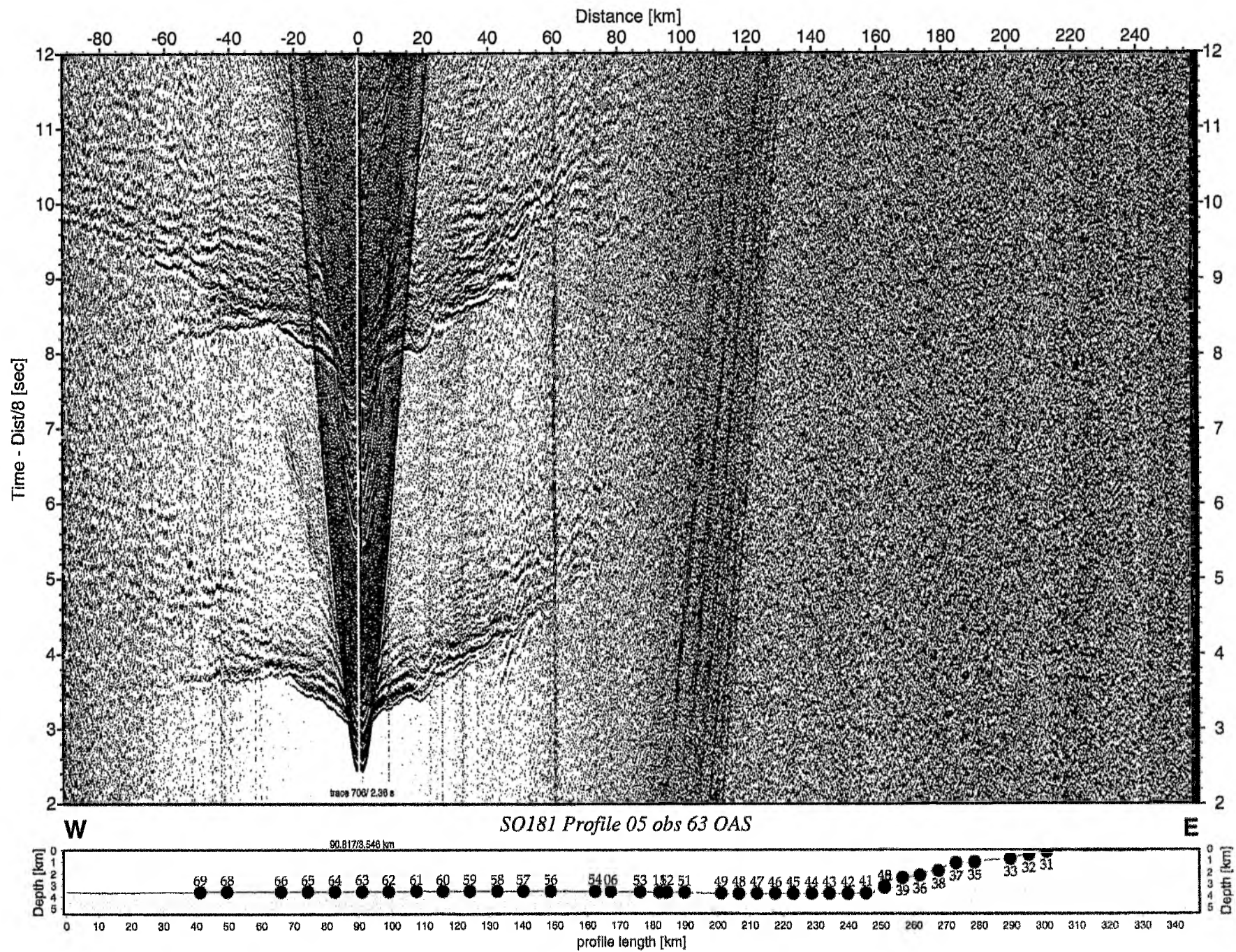


Figure 6.6.3.43: Record section from obs 63 OAS, Profile 05.

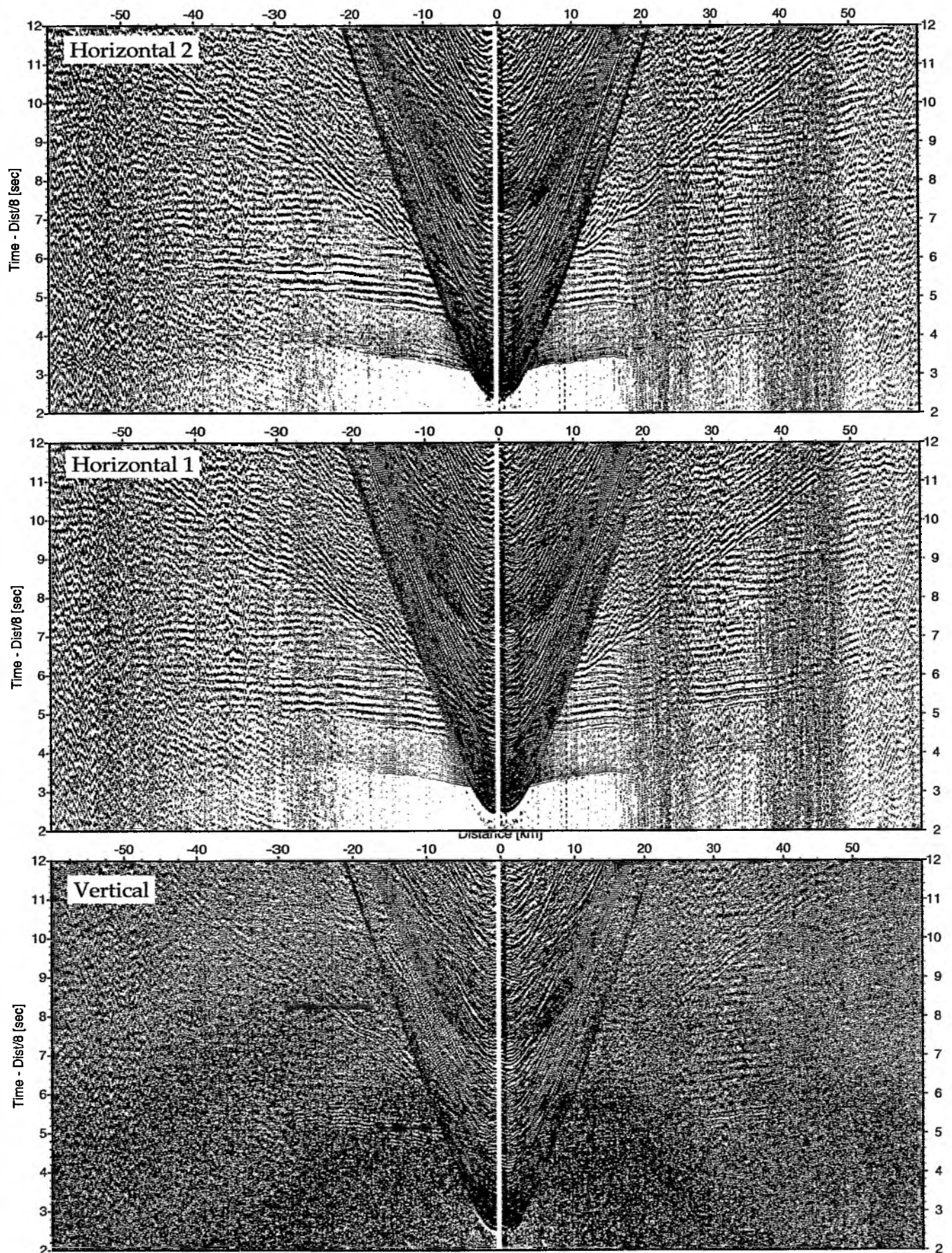


Figure 6.6.3.44: Record sections from obs 63 OAS/WEBB, SO181 Profile 05.

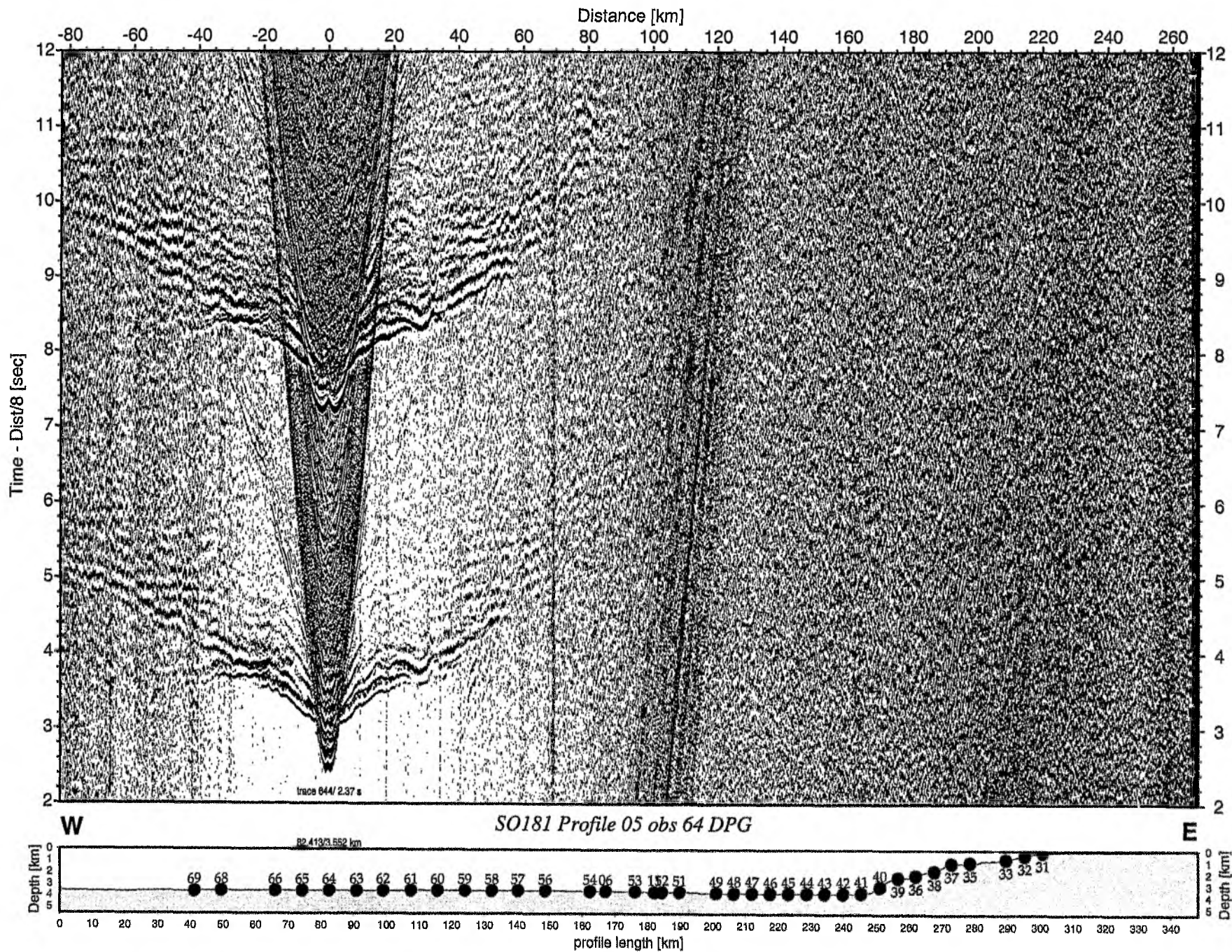


Figure 6.6.3.45: Record section from obs 64 DPG, Profile 05.

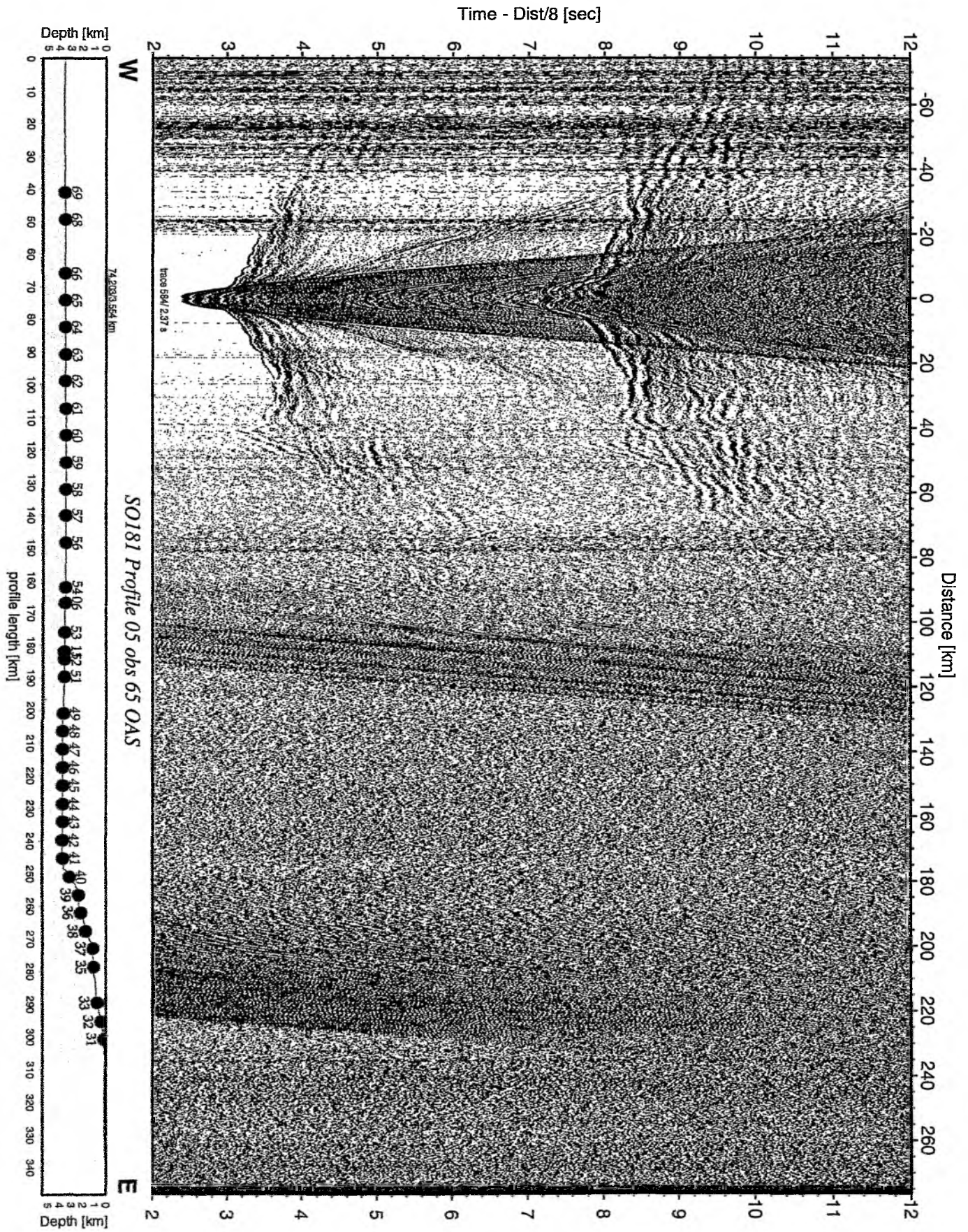


Figure 6.6.3.46: Record section from obs 65 OAS, Profile 05.

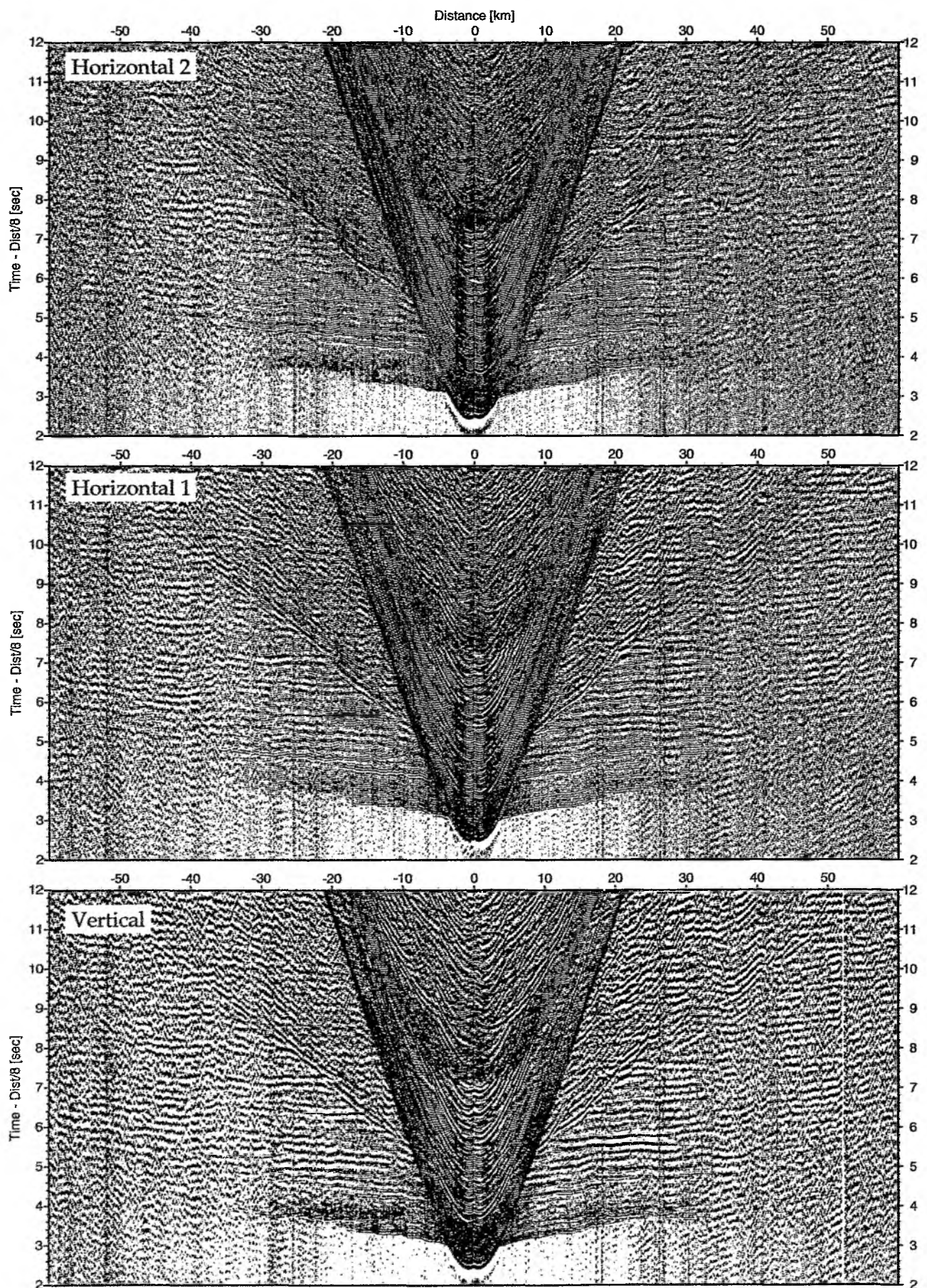


Figure 6.6.3.47: Record sections from obs 65 OAS/WEBB, SO181 Profile 05.

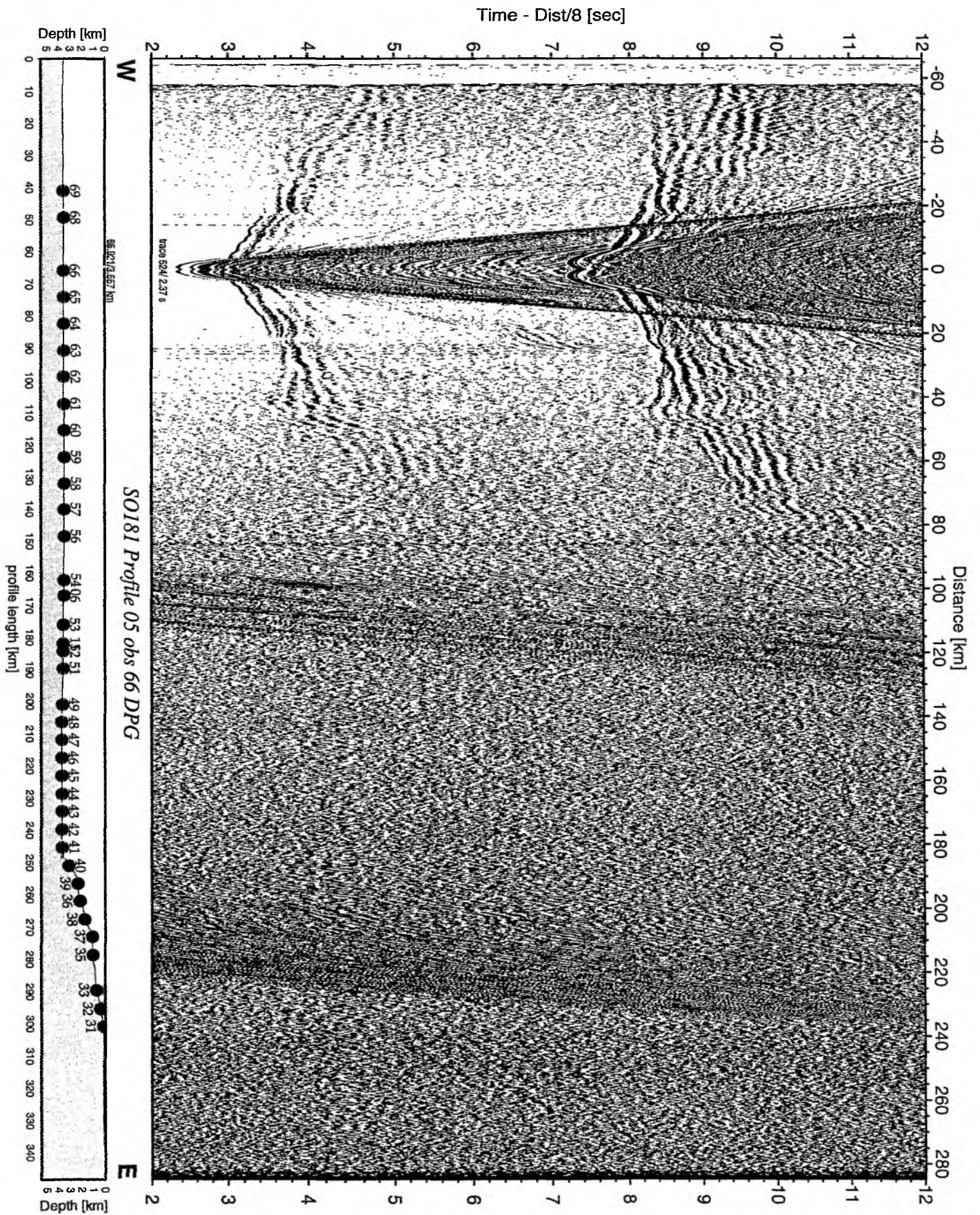


Figure 6.6.3.48: Record section from obs 66 DPG, Profile 05.

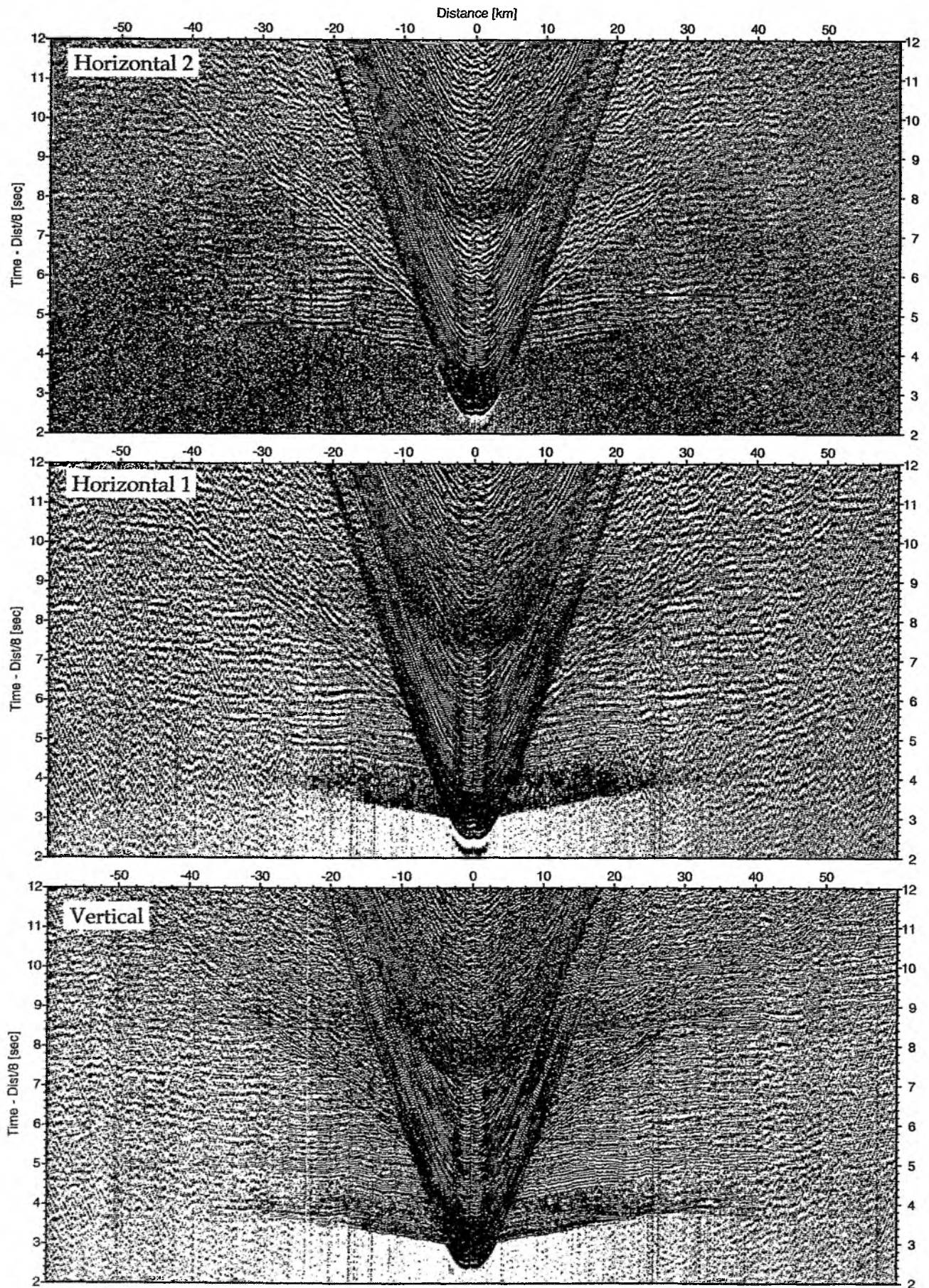


Figure 6.6.3.49: Record sections from obs 66 DPG/WEBB, SO181 Profile 05.

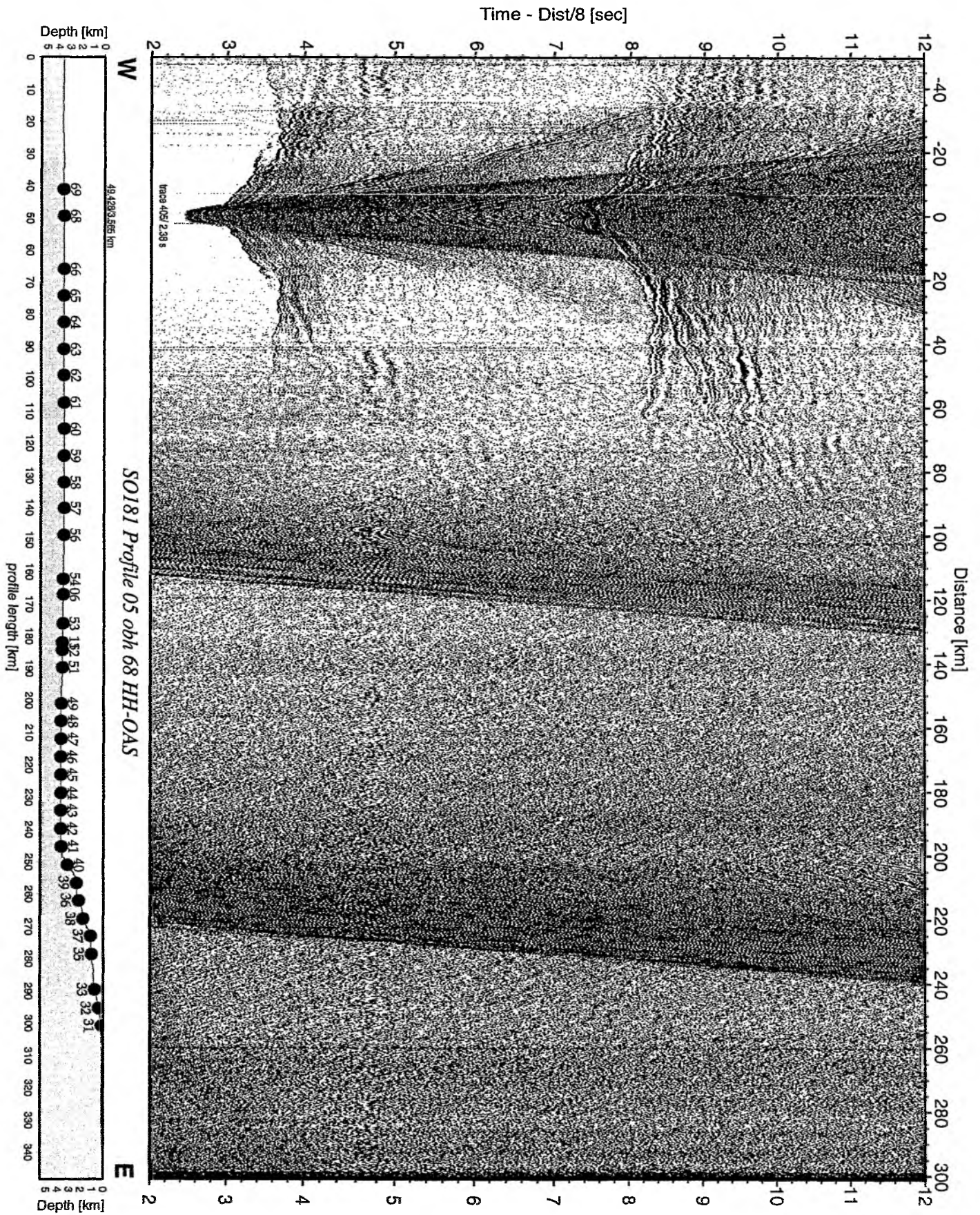


Figure 6.6.3.50: Record section from obh 68 HH-OAS, Profile 05.

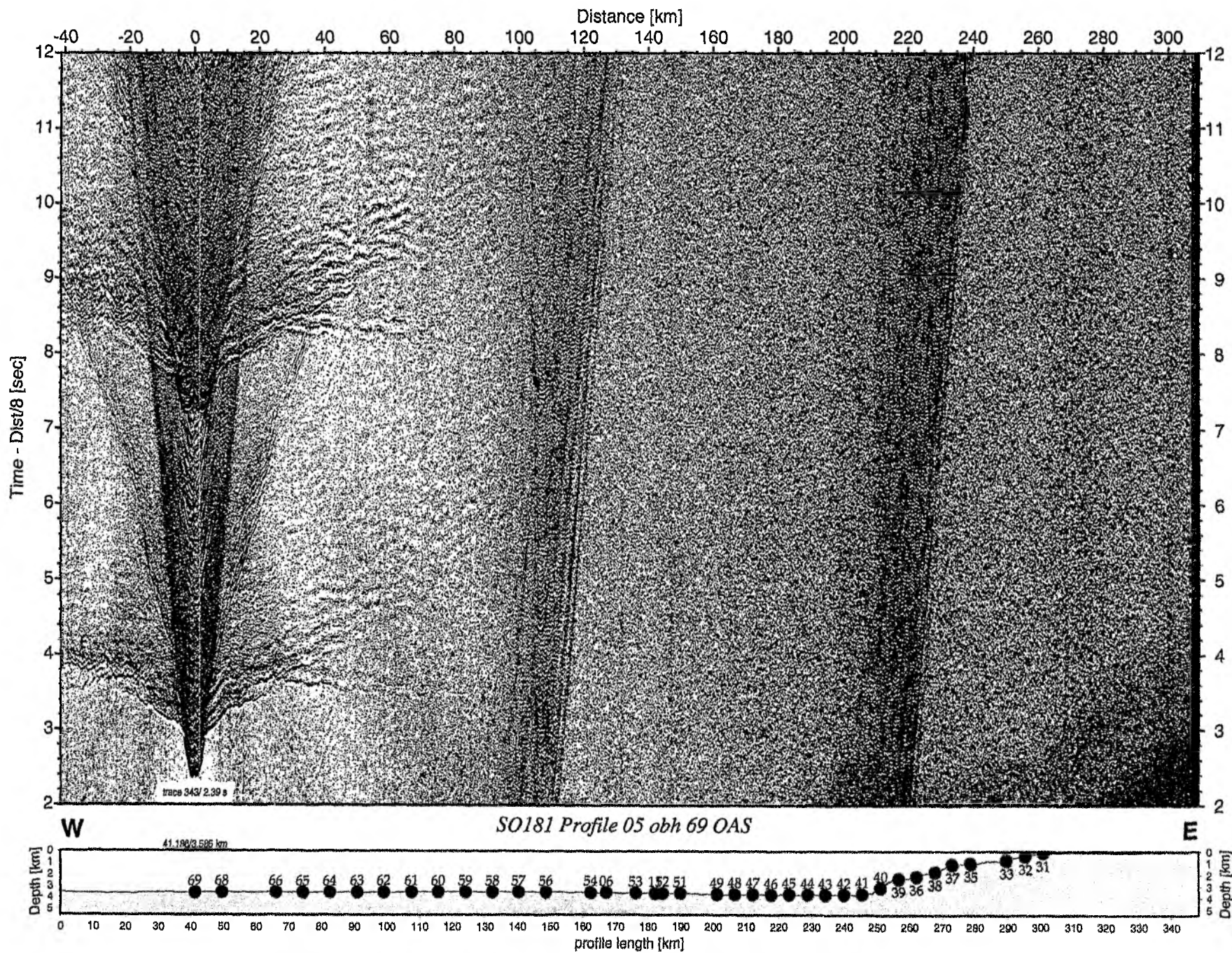


Figure 6.6.3.51: Record section from obh 69 OAS, Profile 05.

6.6.4 Profile P07

For profile 07 a total of 45 instruments were deployed between 28 and 29 January. Shooting was done in almost perfect conditions from 16:30 on 29 Jan to 09:30 on 31 Jan. During most of the time all four G-Gun cluster were in operation. A four channel streamer was deployed throughout the profile, augmenting existing MCS data for parts of the profile. Instruments were picked up once shooting was terminated, and were all back onboard by 09:00 on 02 Feb. Two instruments did not rise after release command had been issued. The first instrument (OBS 112) was successfully dredged on 31 Jan. For OBS 118 we first attempted a visual inspection using the new Hamburg deployment aid equipped with a camera, but after three hours without sighting the instrument in about 150 m of water a dredge was deployed and the instrument could be recovered safely. We believe that a poor anchor design was responsible for the release failure. Details of instruments and shots can be found in Appendices 9.2 and 9.3. Most instruments recorded well. A location map is shown in Figure 6.6.4.1, and record sections are shown in Figures 6.6.4.2 to 6.6.4.58. A first onboard analysis was attempted, taking into account the results (sediment thickness) from the seismic reflection data.

Preliminary interpretation of profile P07

As shown in the streamer section of Figure 6.6.4.2, the 236 km long, E-W oriented profile extended over the subduction zone covering oceanic crust as well as the continental shelf. Most record sections of the stations show a good data quality with clear refracted and reflected P- and S-wave signals from the sediments, the oceanic and continental crust, and the upper mantle. All receiver gathers were interpreted and picked, however for the preliminary on-board analysis, only the sections of OBH/S 112, 121, 127, 129, 134, 143, 147 and 156 were used to create a velocity model of the profile. A starting velocity model based on the sediment thickness estimated from the streamer section of P07 was created, and then traveltimes were calculated using the ray-tracing program MacRay (Luetgert, 1992). In an iterative process, the velocity model was changed to match the calculated (predicted) with the observed traveltimes (forward modelling). The preliminary velocity model P07 is shown in Figure 6.6.4.59. The velocity model consists of 7 layers, resembling the data coarsely:

- I. The water layer (1.5 km/s),
- II. a slow sediment layer (1.7 - 2.1 km/s) ,
- III. a fast sediment layer (3.6 - 3.7 km/s),
- IV. a continental crust (5.2 - 5.9 - 6 km/s),
- V. an upper (5.7 - 5.9 km/s) and
- VI. lower (6.8 - 7.1 km/s) oceanic crust, and
- VII. the upper mantle (8.0 - 8.1 km/s).

The bathymetric high at offset 117 km is interpreted as an accretionary ridge of the subduction zone. Below this ridge, the MCS stacked section (Figure 2.1.4) shows a thrust fault in the upper layer IV. The triangular feature of the upper boundary of layer IV resembles this thrust fault.

The thickness of the slow sediment layer II ranges from 400 m to 2.8 km just before the accretionary wedge. A faster sediment layer was modeled on the continental shelf with a thickness of 900 m, so that the total thickness of sediments measures 1.3 km on the shelf. In the data, we distinguished the upper (1.2 km thick) and the lower (3.3 km thick) oceanic crust, which results in a thickness of 4.5 km for the oceanic crust. The continental crust of layer IV reaches a thickness up to approximately 6 km within the profile. The Moho is located 5.3 km below sea level on the oceanic plate and 12.3 km on the continental shelf, respectively.

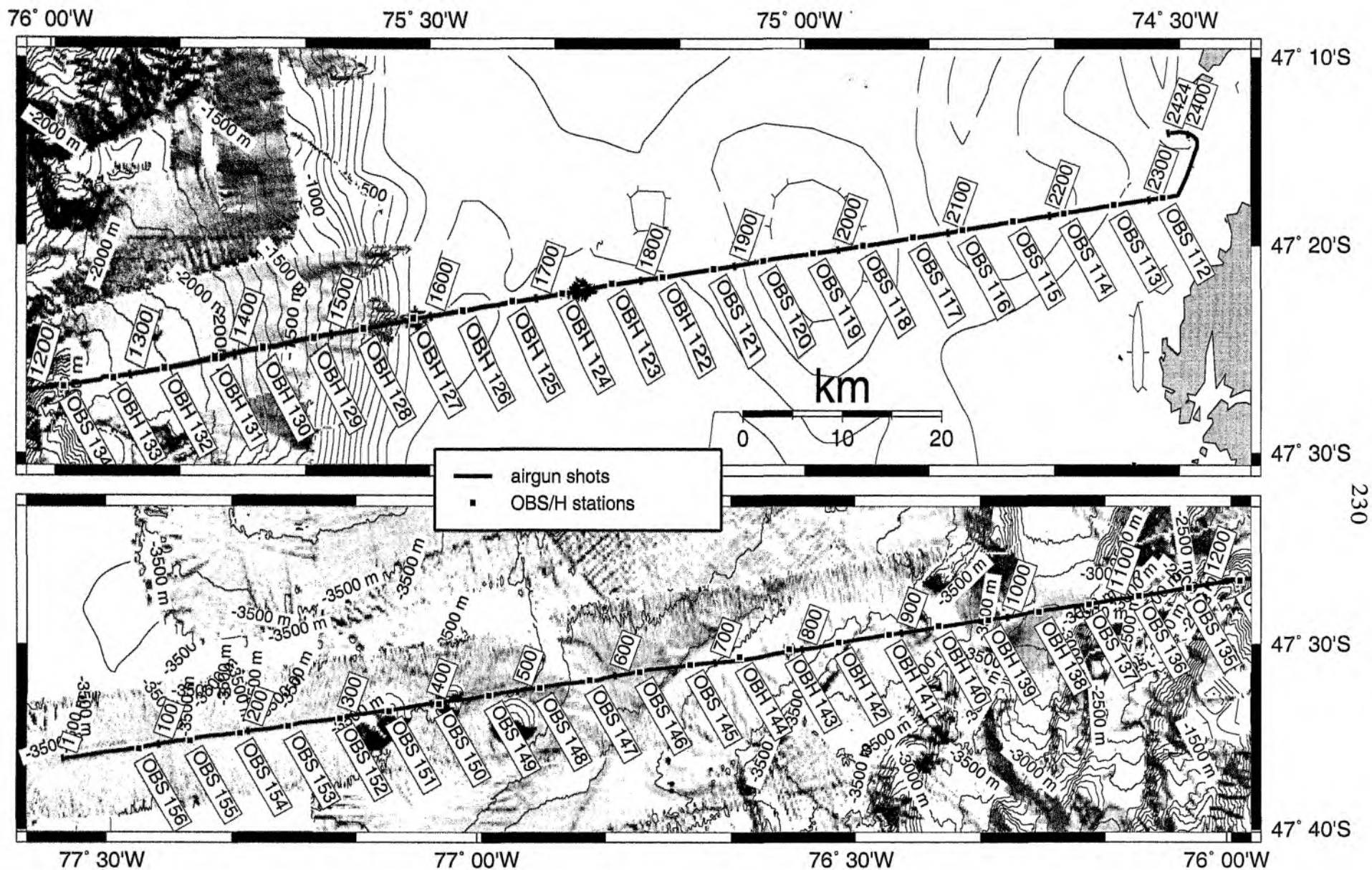


Figure 6.6.4.1: Basemap of P07; transect of ocean bottom seismometer and hydrophone stations and line of airgun shots. Bathymetry contours every 100m.

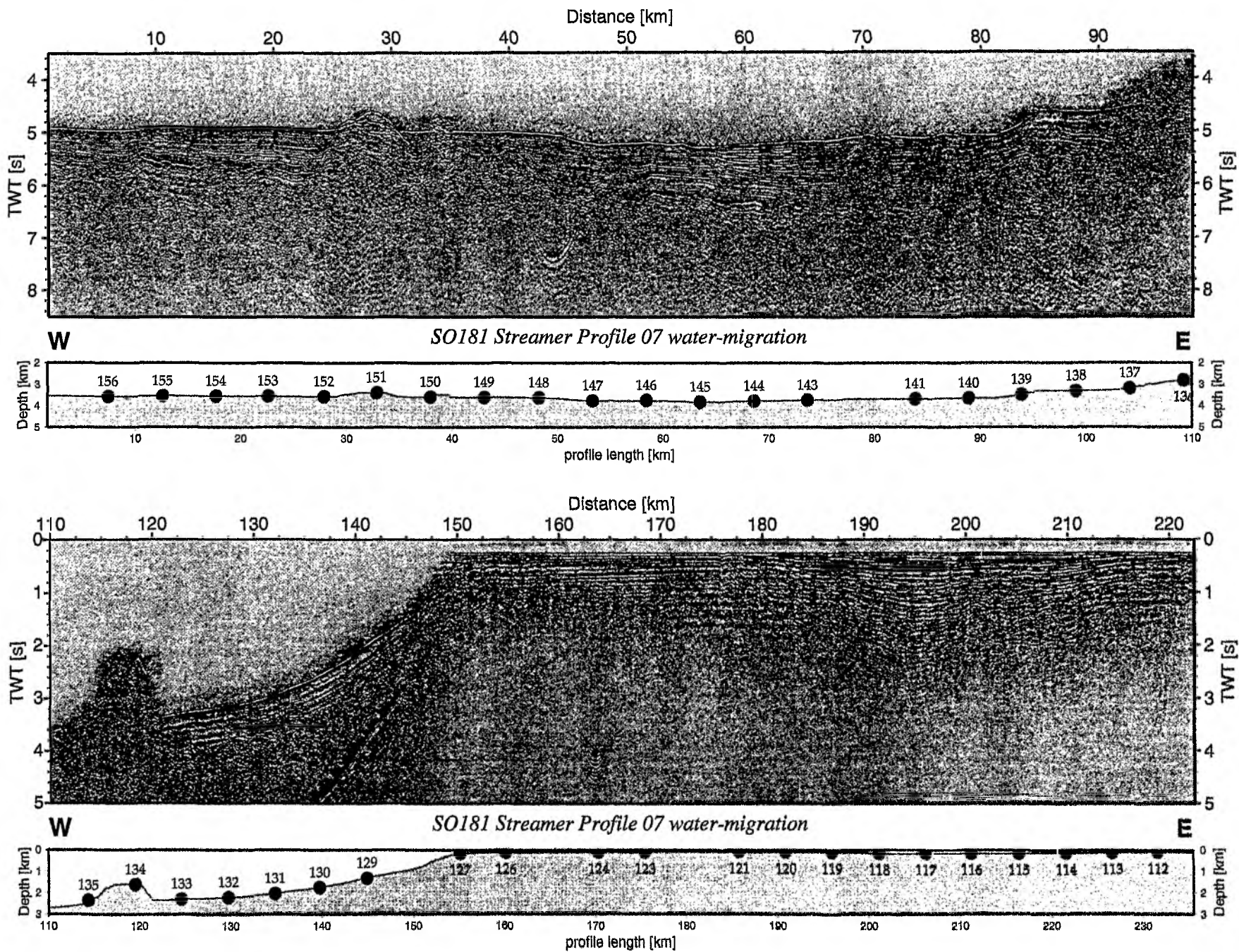


Figure 6.6.4.2: Record section from Streamer Profile 07 water-migration.

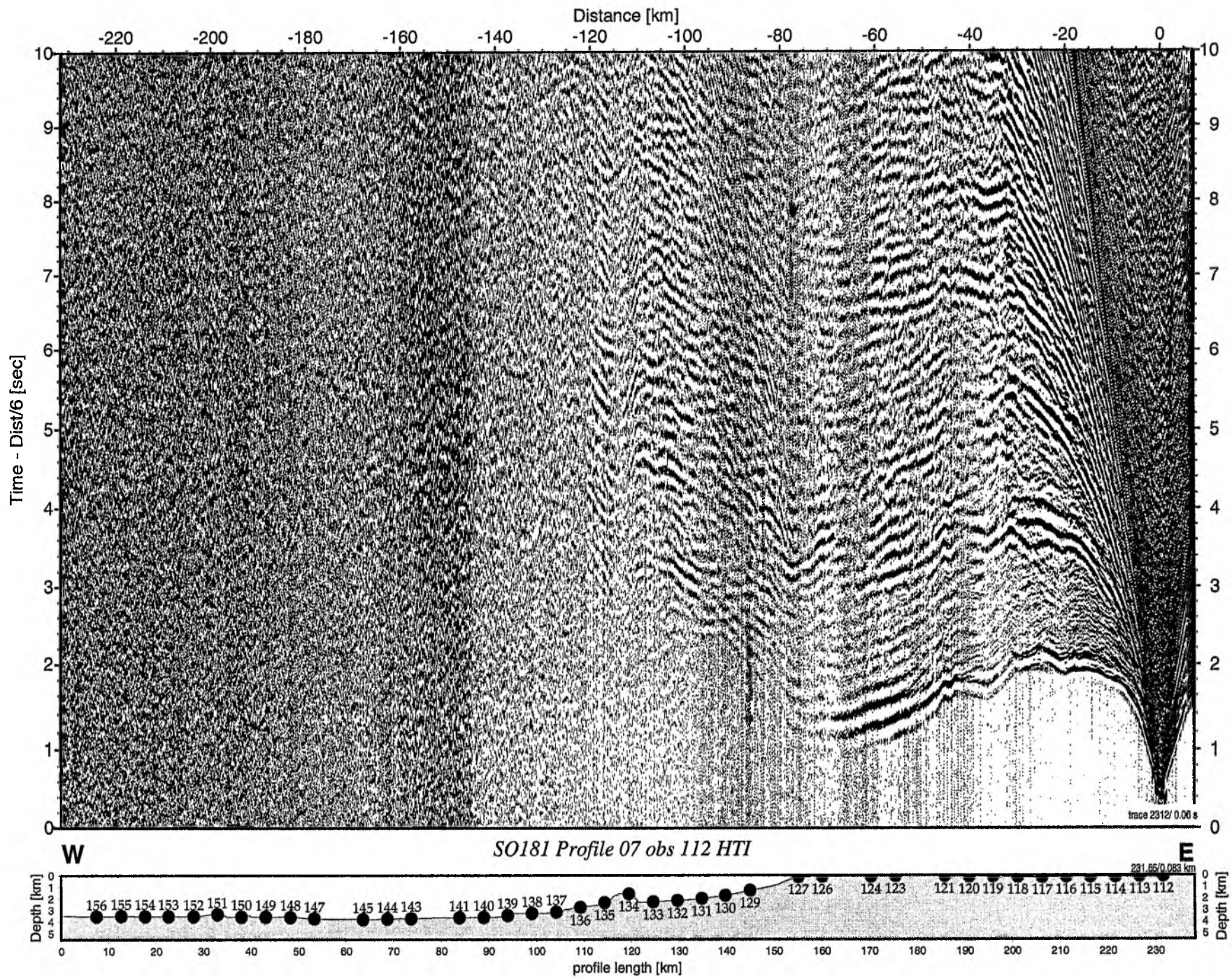


Figure 6.6.4.3: Record section from obs 112 HTI, Profile 07.

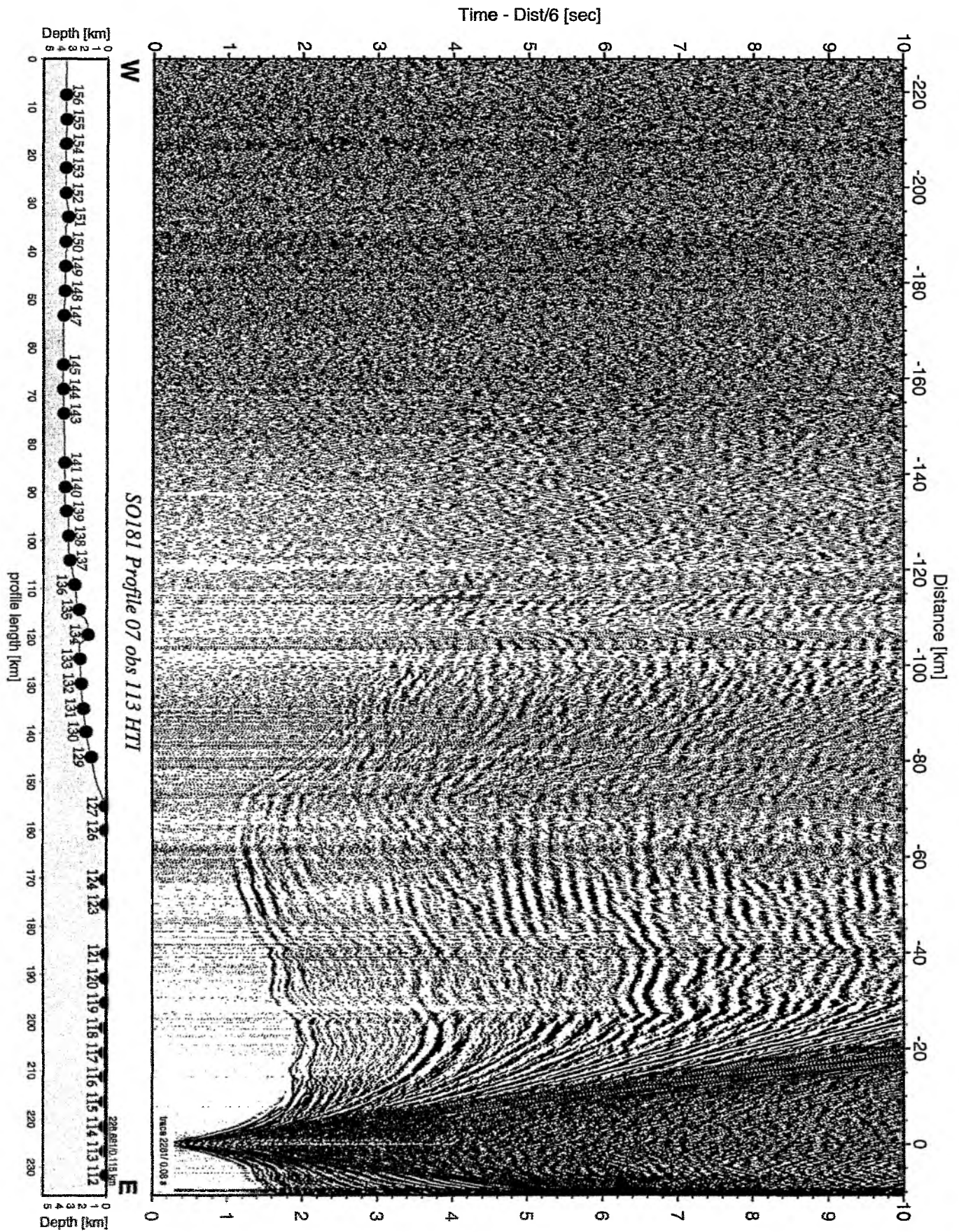


Figure 6.6.4.4: Record section from obs 113 HTI, Profile 07.

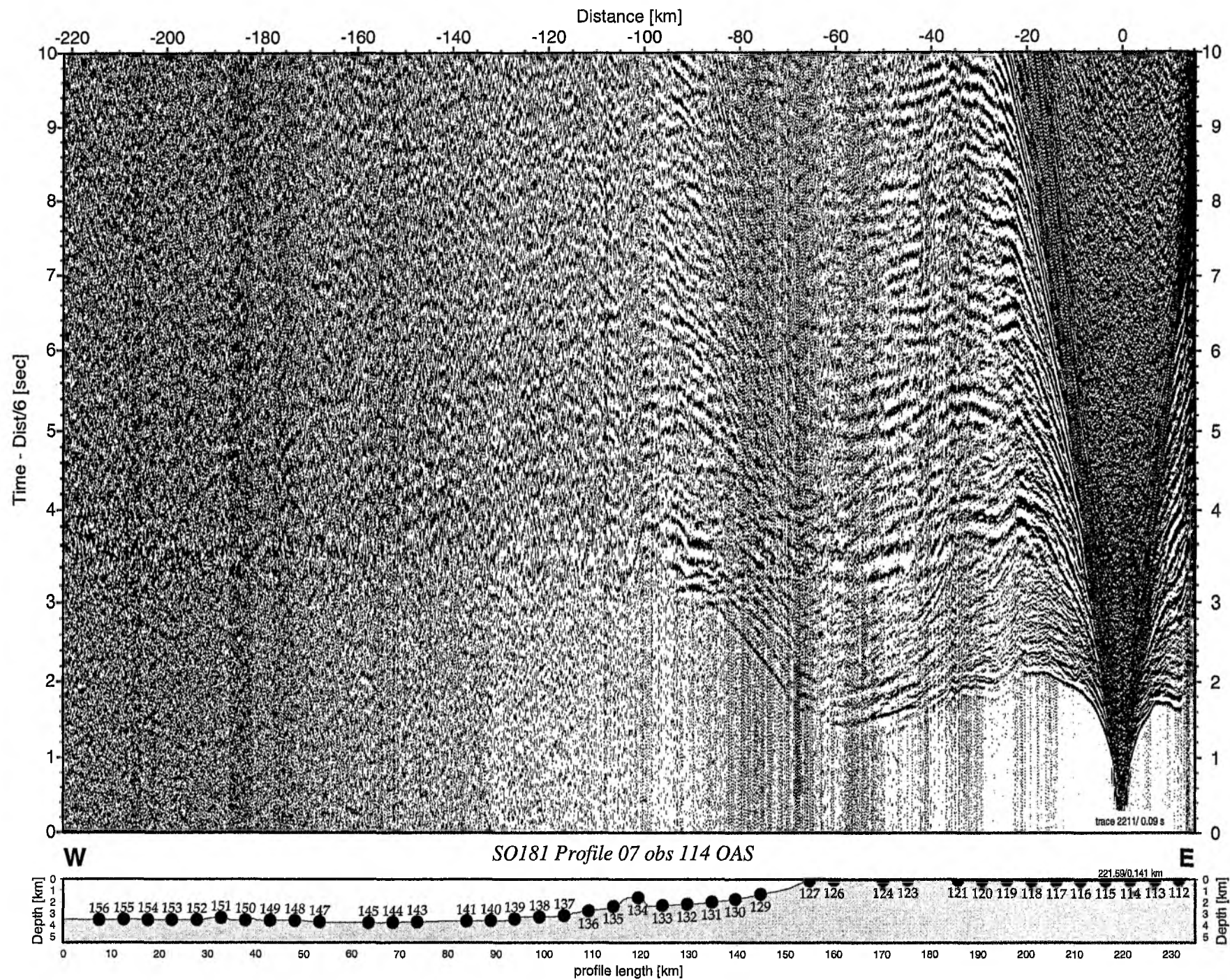


Figure 6.6.4.5: Record section from obs 114 OAS, Profile 07.

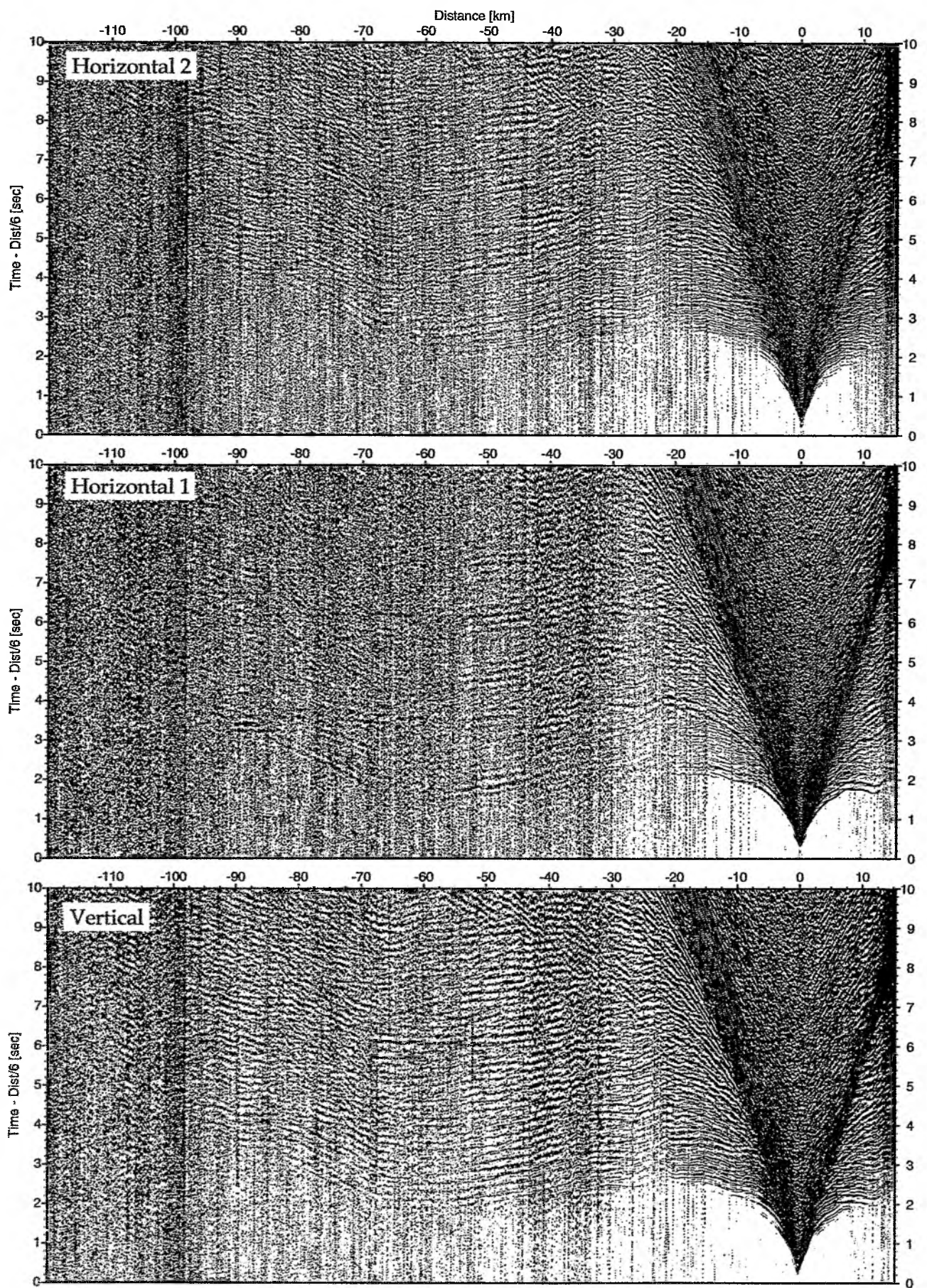


Figure 6.6.4.6: Record sections from obs 114 OAS/Owen-4.5Hz, SO181 Profile 07.

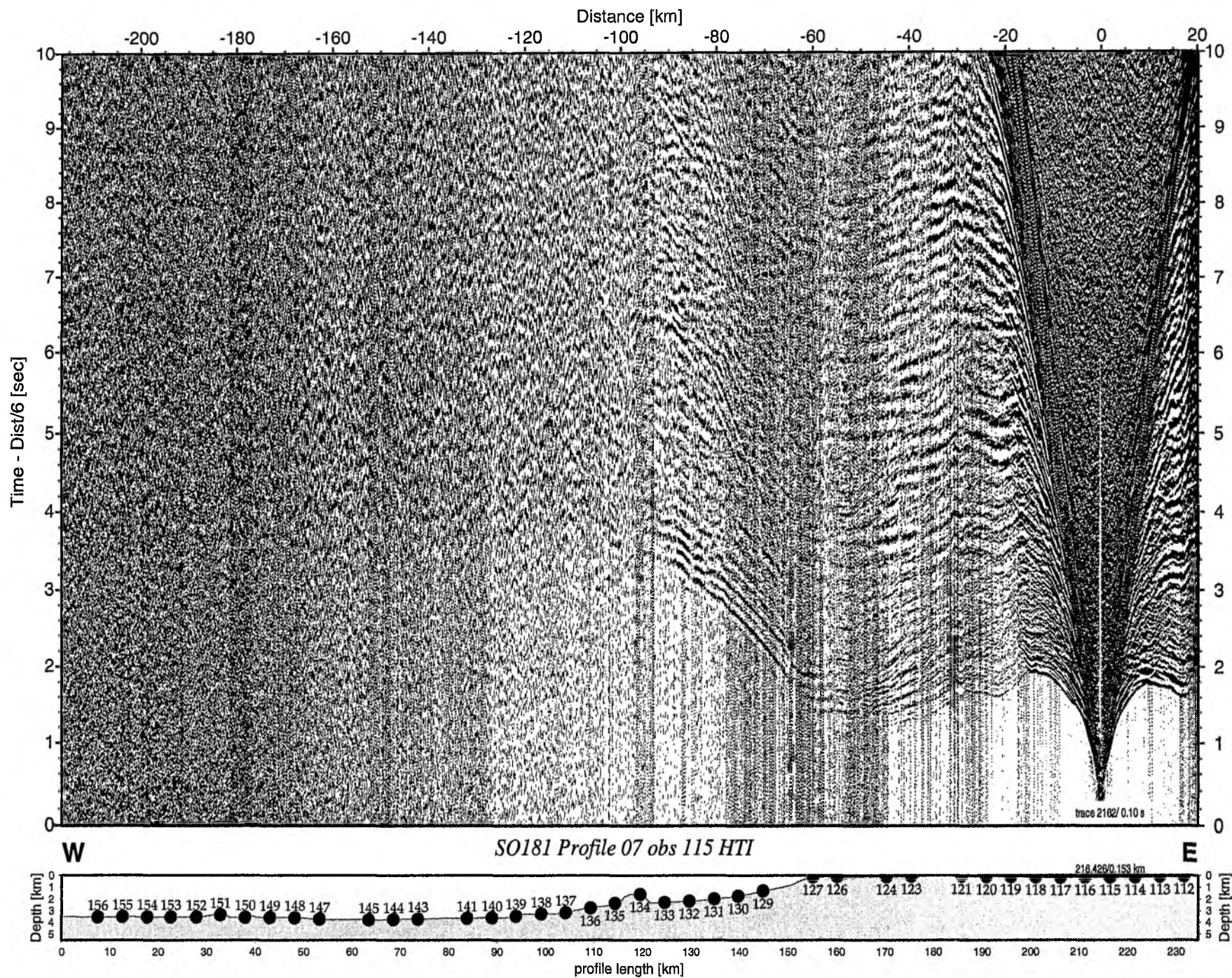


Figure 6.6.4.7: Record section from obs 115 HTI, Profile 07.

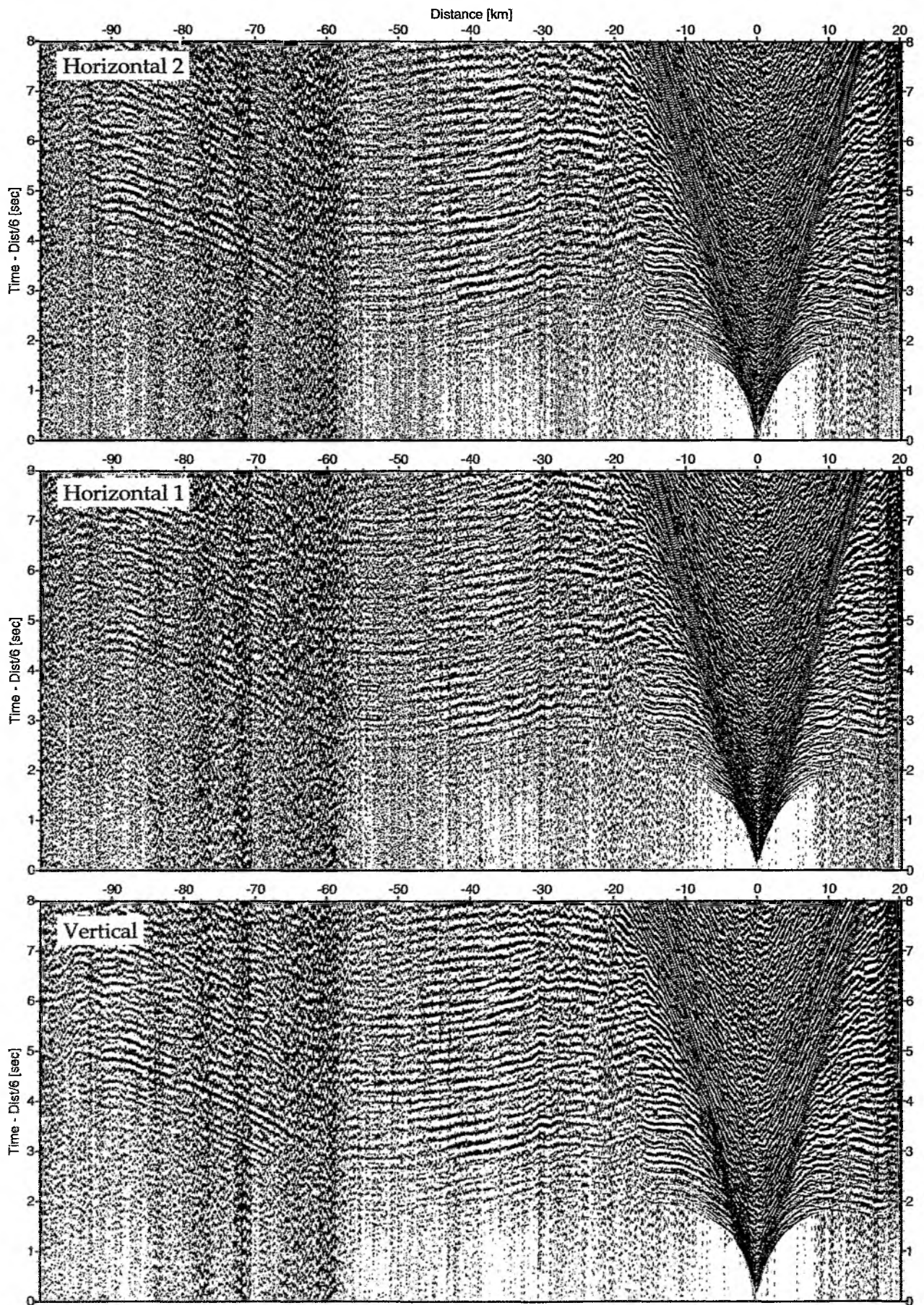


Figure 6.6.4.8: Record sections from obs 115 HTI/Owen-4.5Hz, SO181 Profile 07.

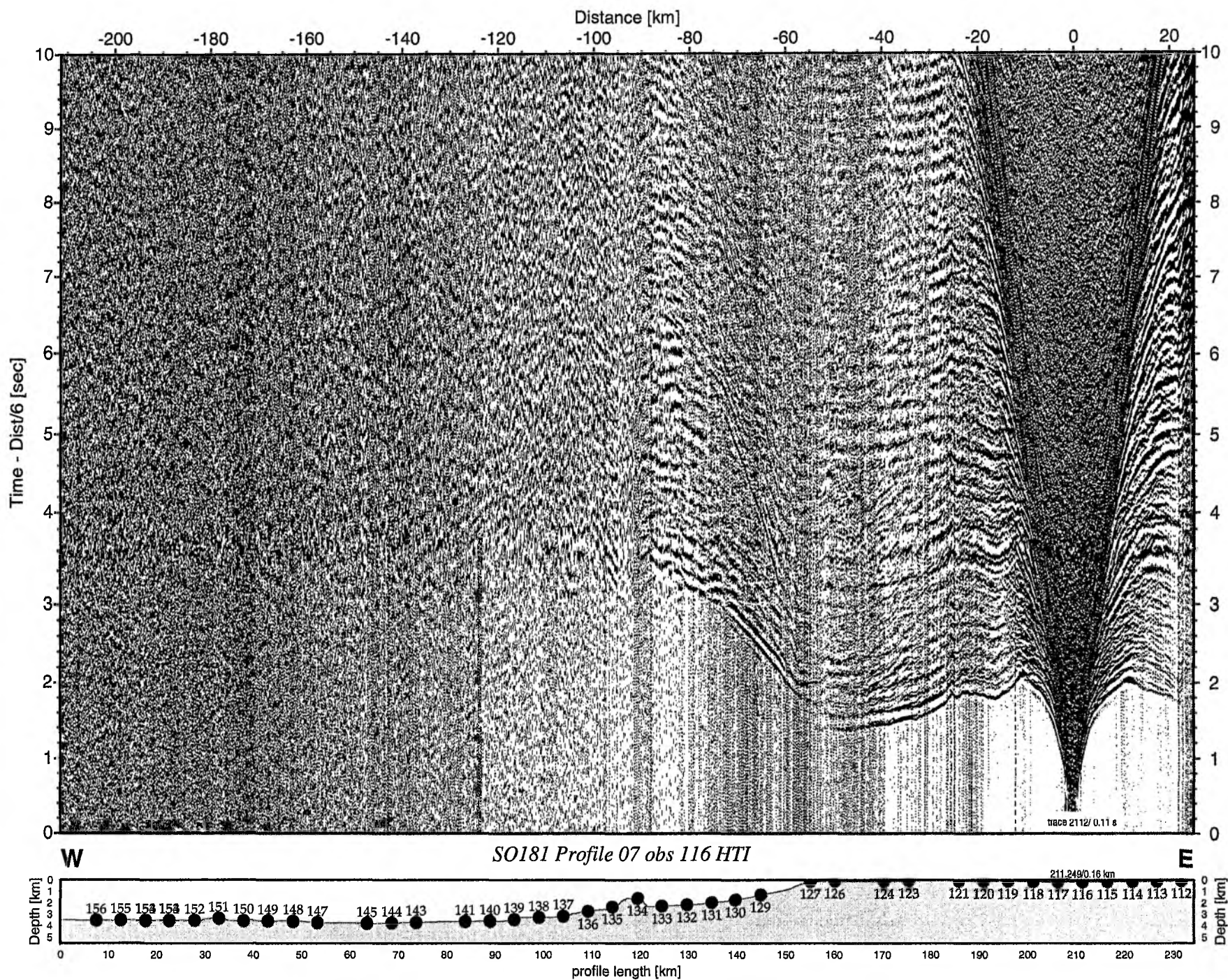


Figure 6.6.4.9: Record section from obs 116 HTI, Profile 07.

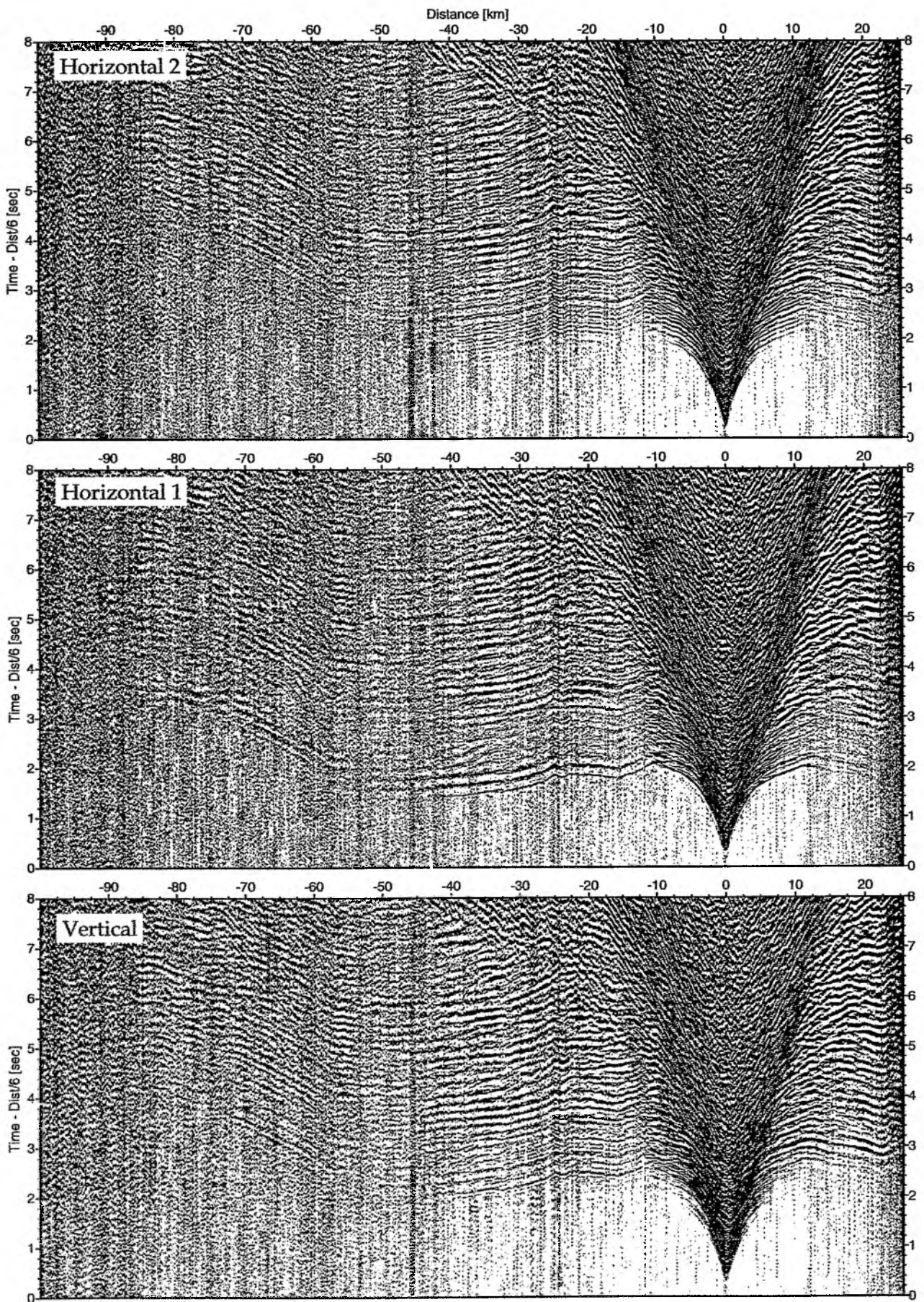


Figure 6.6.4.10: Record sections from obs 116 HTI/Owen-4.5Hz, SO181 Profile 07.

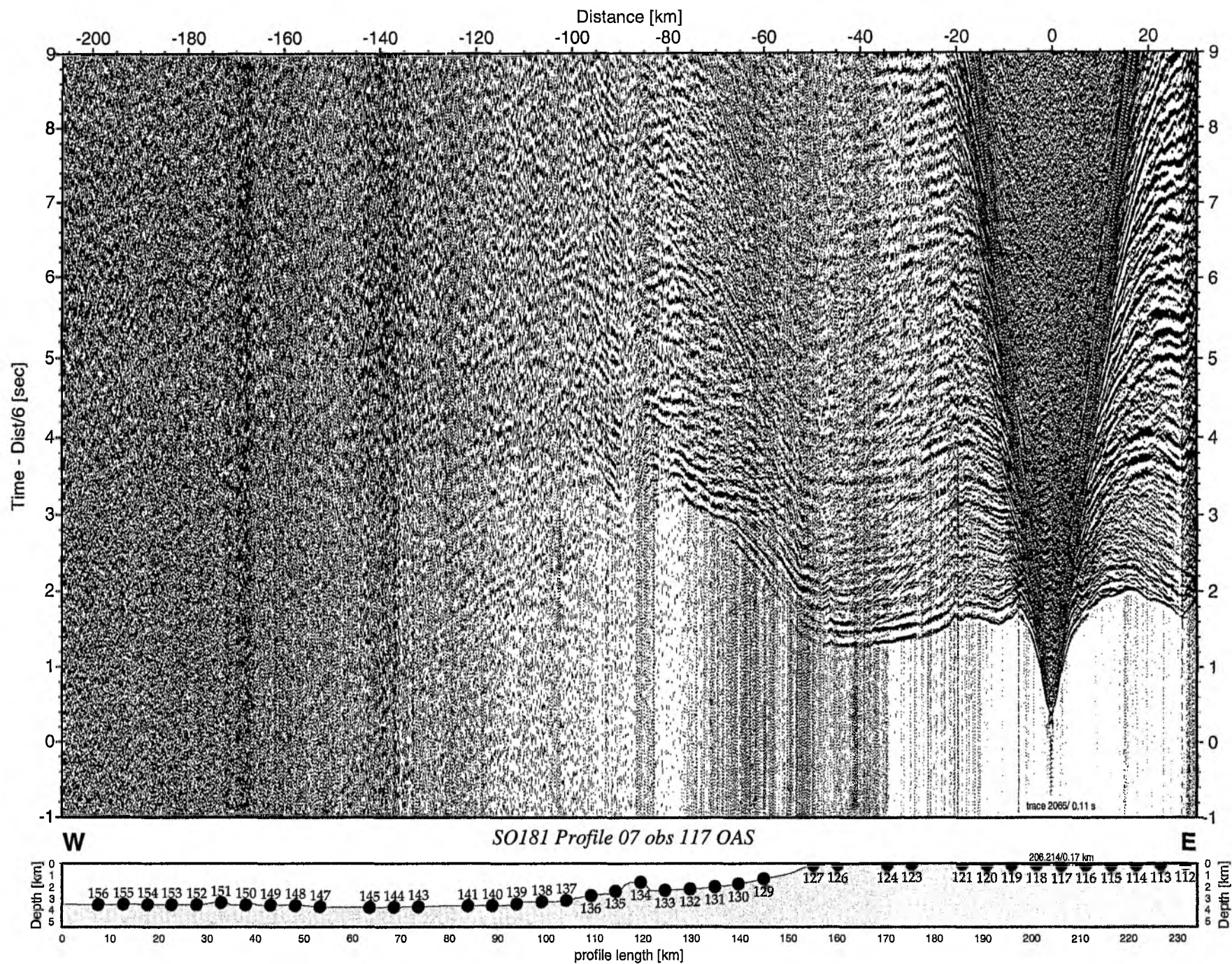


Figure 6.6.4.11: Record section from obs 117 OAS, Profile 07.

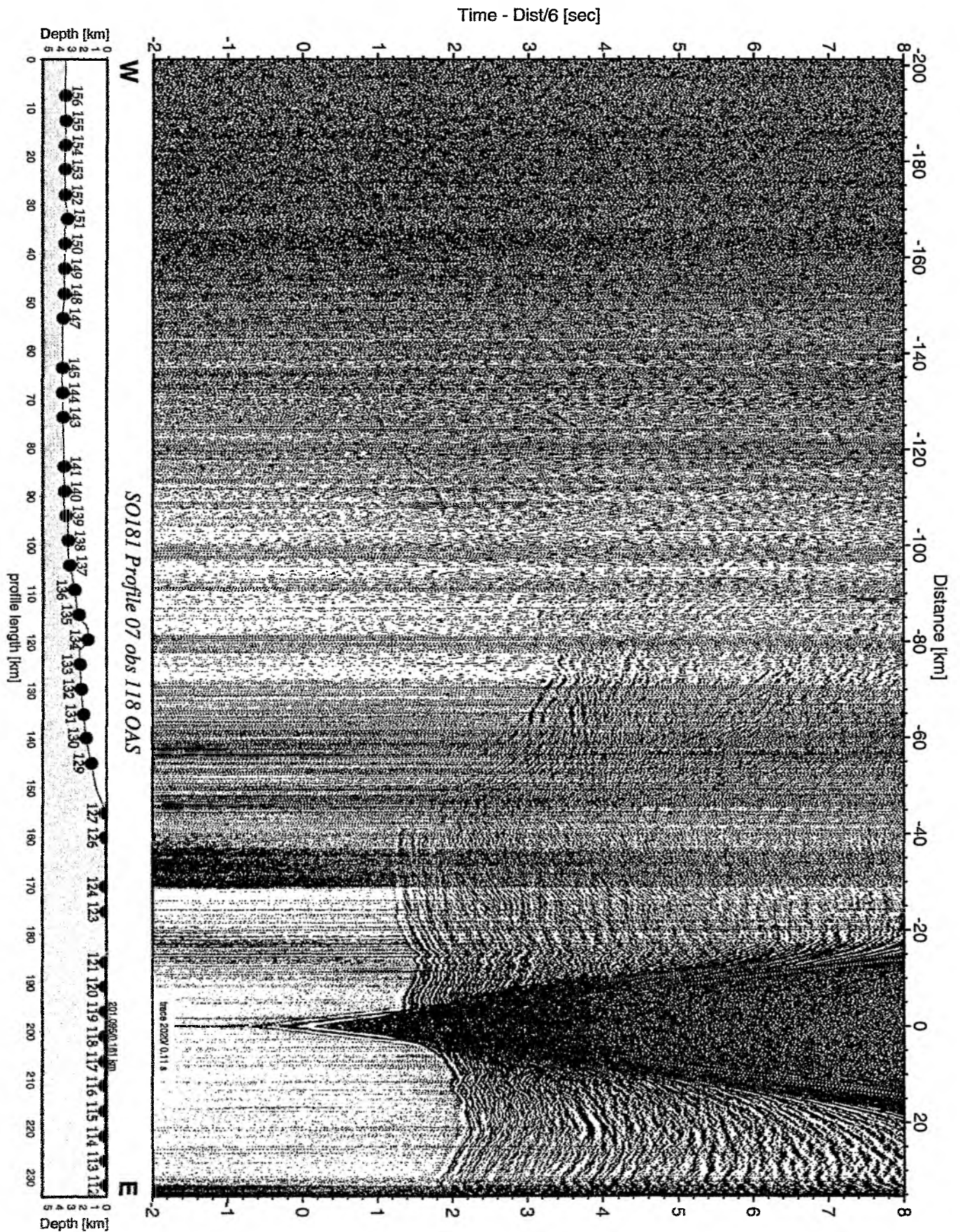


Figure 6.6.4.12: Record section from obs 118 OAS, Profile 07.

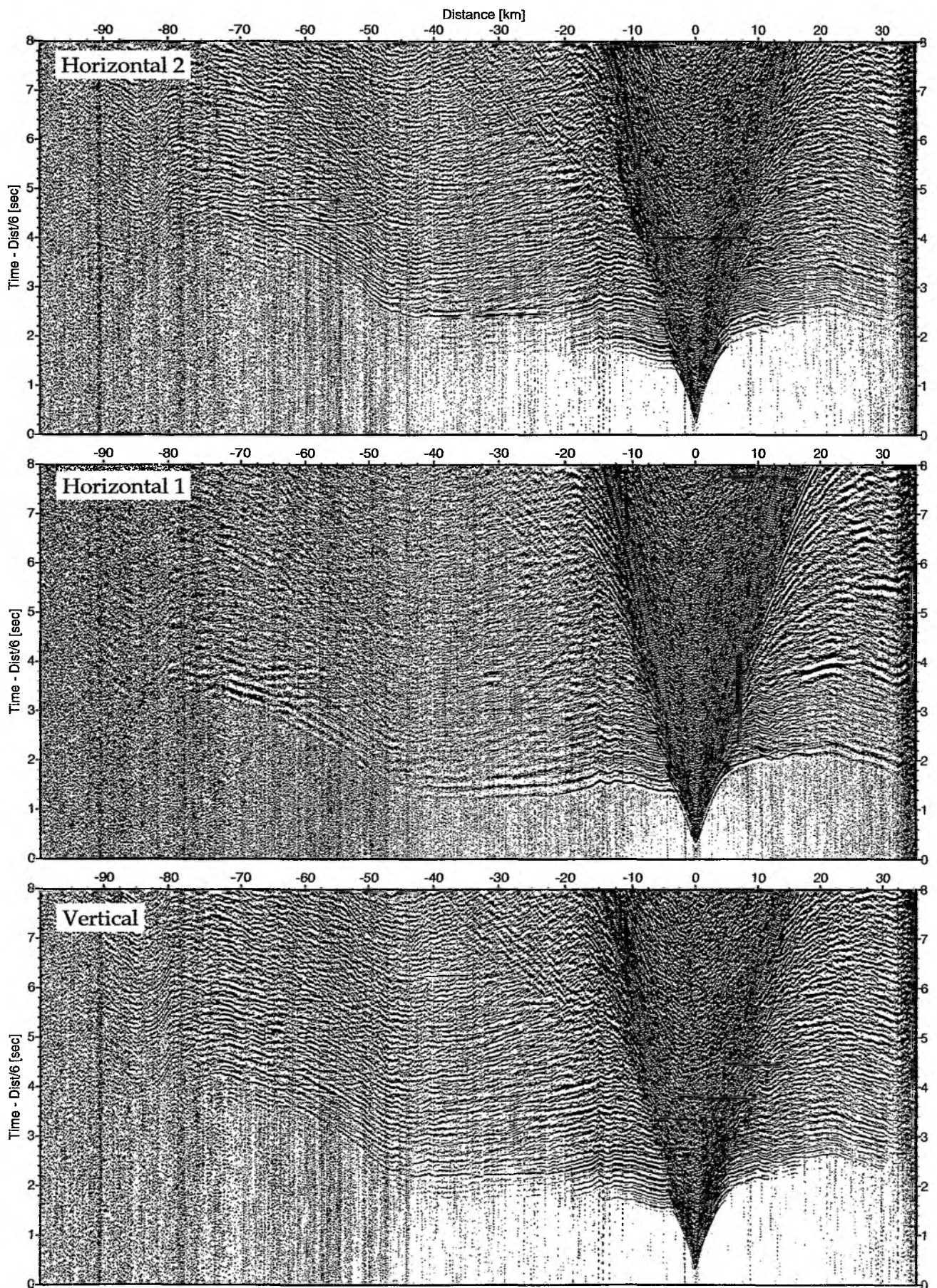


Figure 6.6.4.13: Record sections from obs 118 OAS/Owen-4.5Hz, SO181 Profile 07.

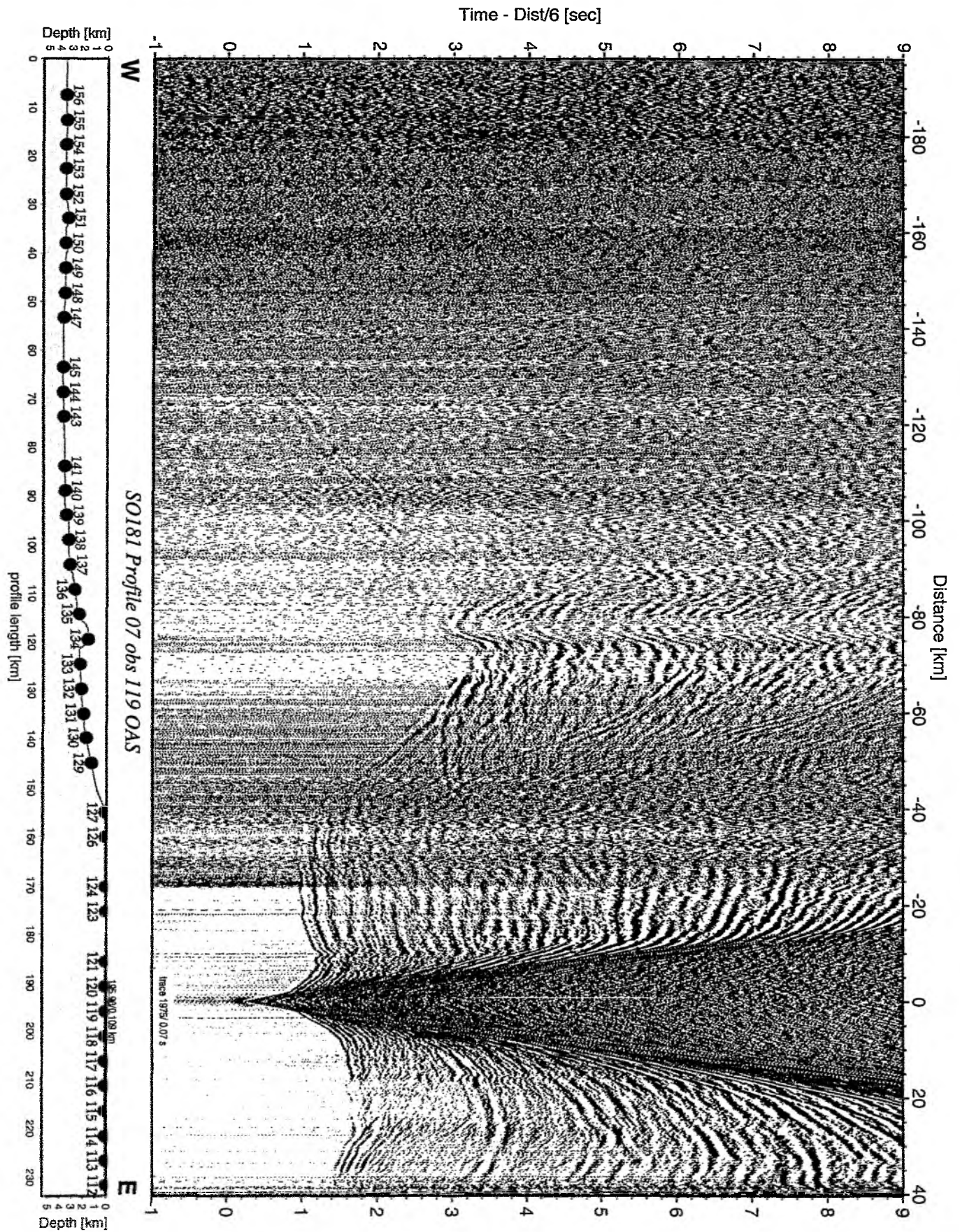


Figure 6.6.4.14: Record section from obs 119 OAS, Profile 07.

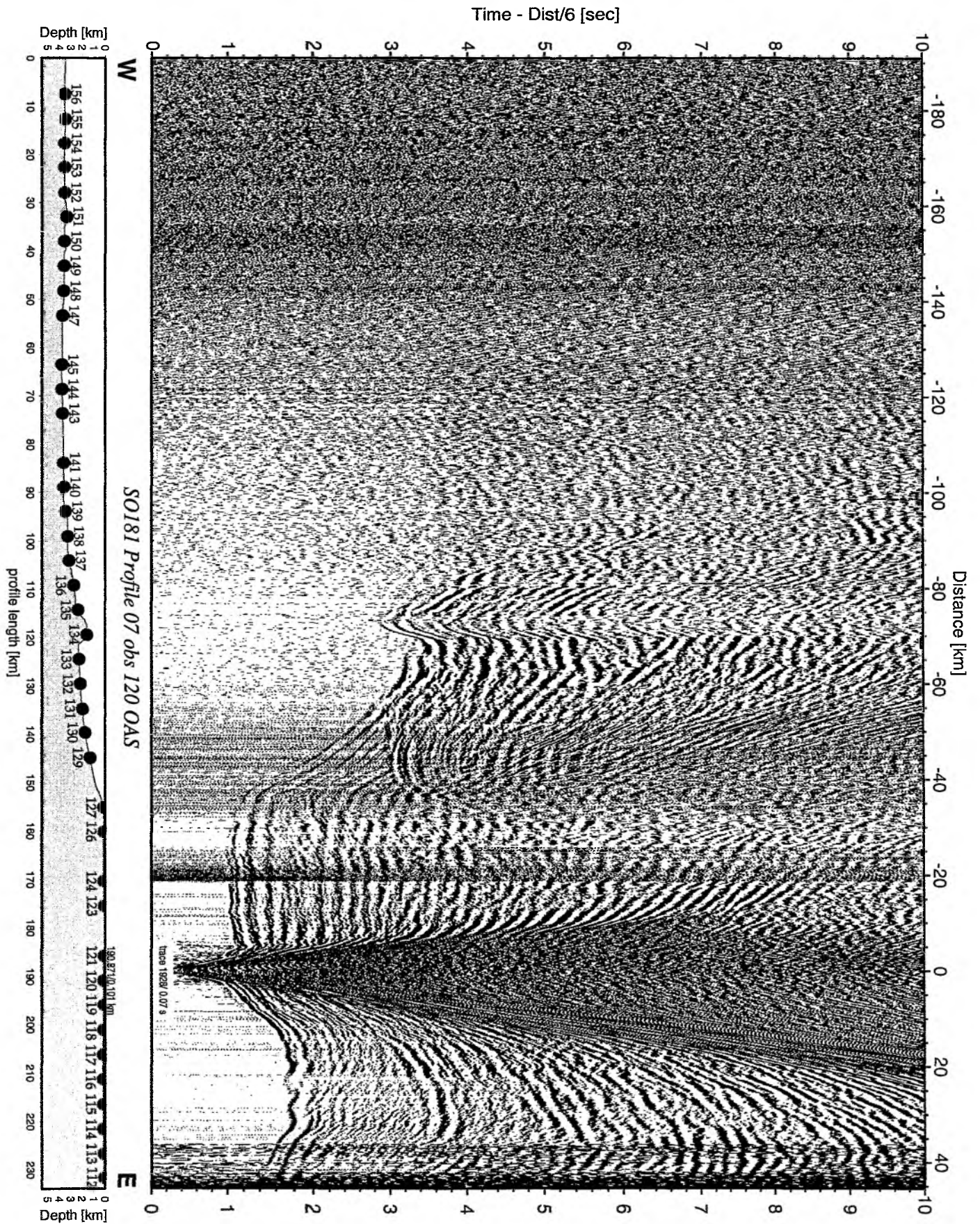


Figure 6.6.4.15: Record section from obs 120 OAS, Profile 07.

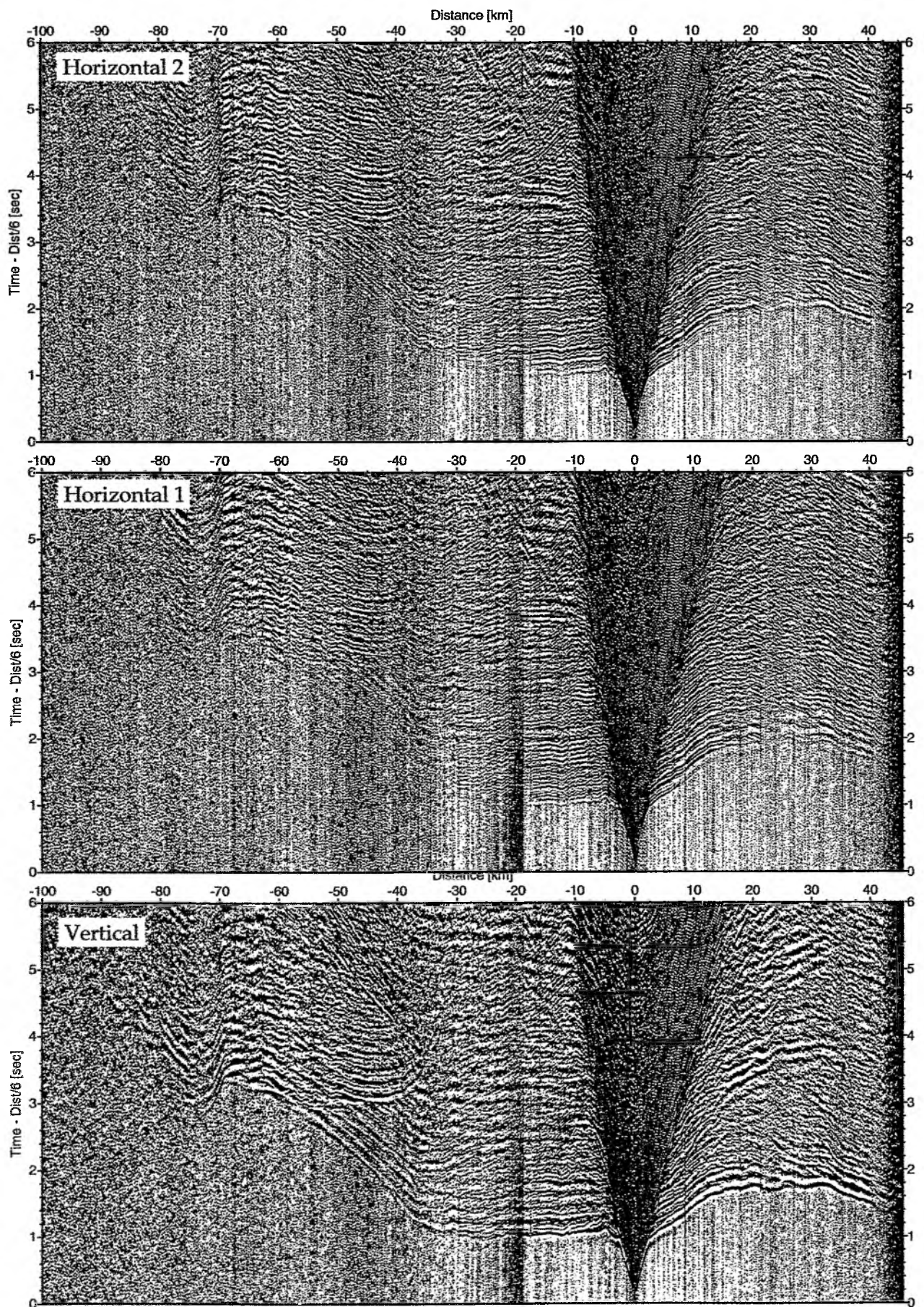


Figure 6.6.4.16: Record sections from obs 120 OAS/Owen-4.5Hz, SO181 Profile 07.

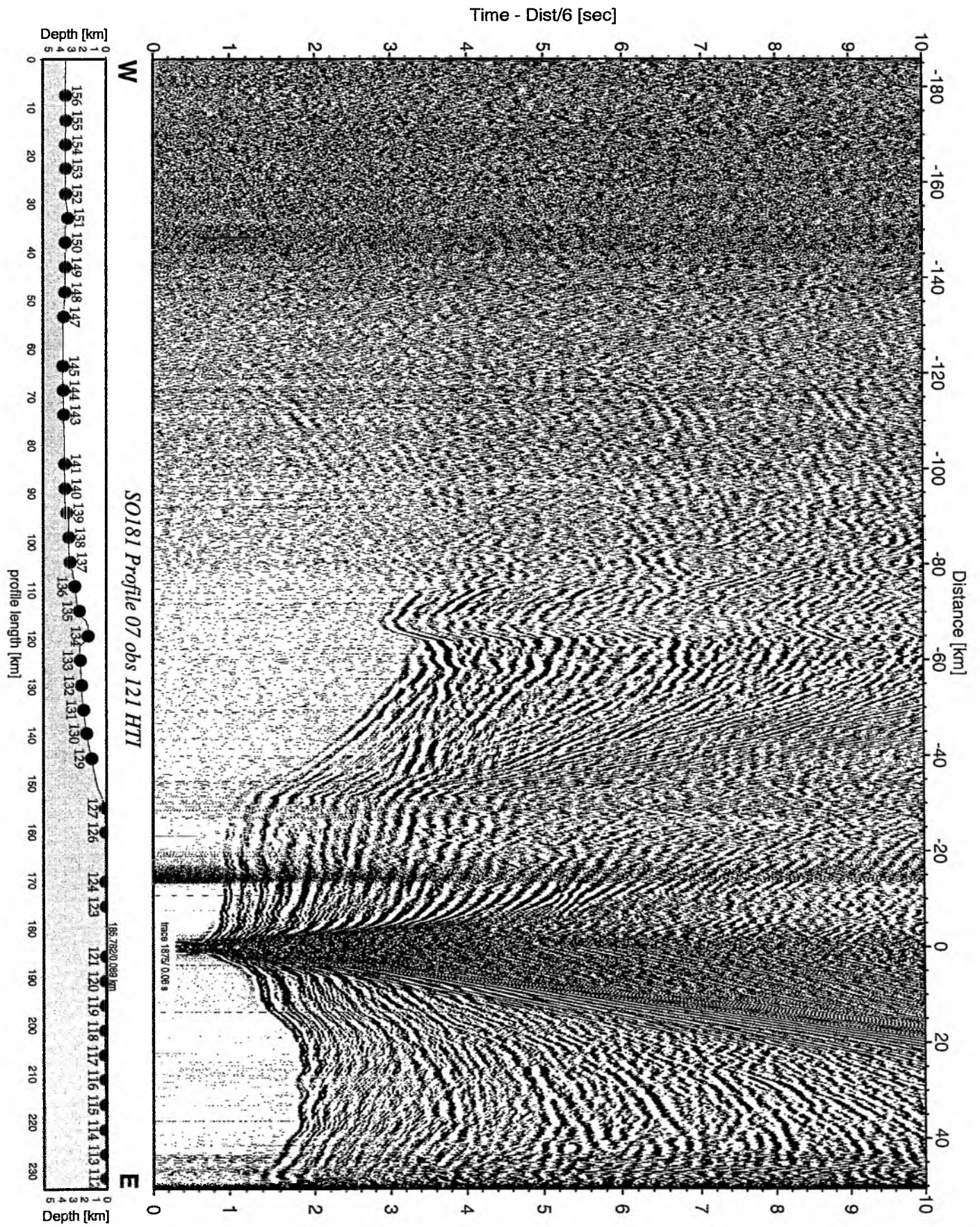


Figure 6.6.4.17: Record section from obs 121 HTI, Profile 07.

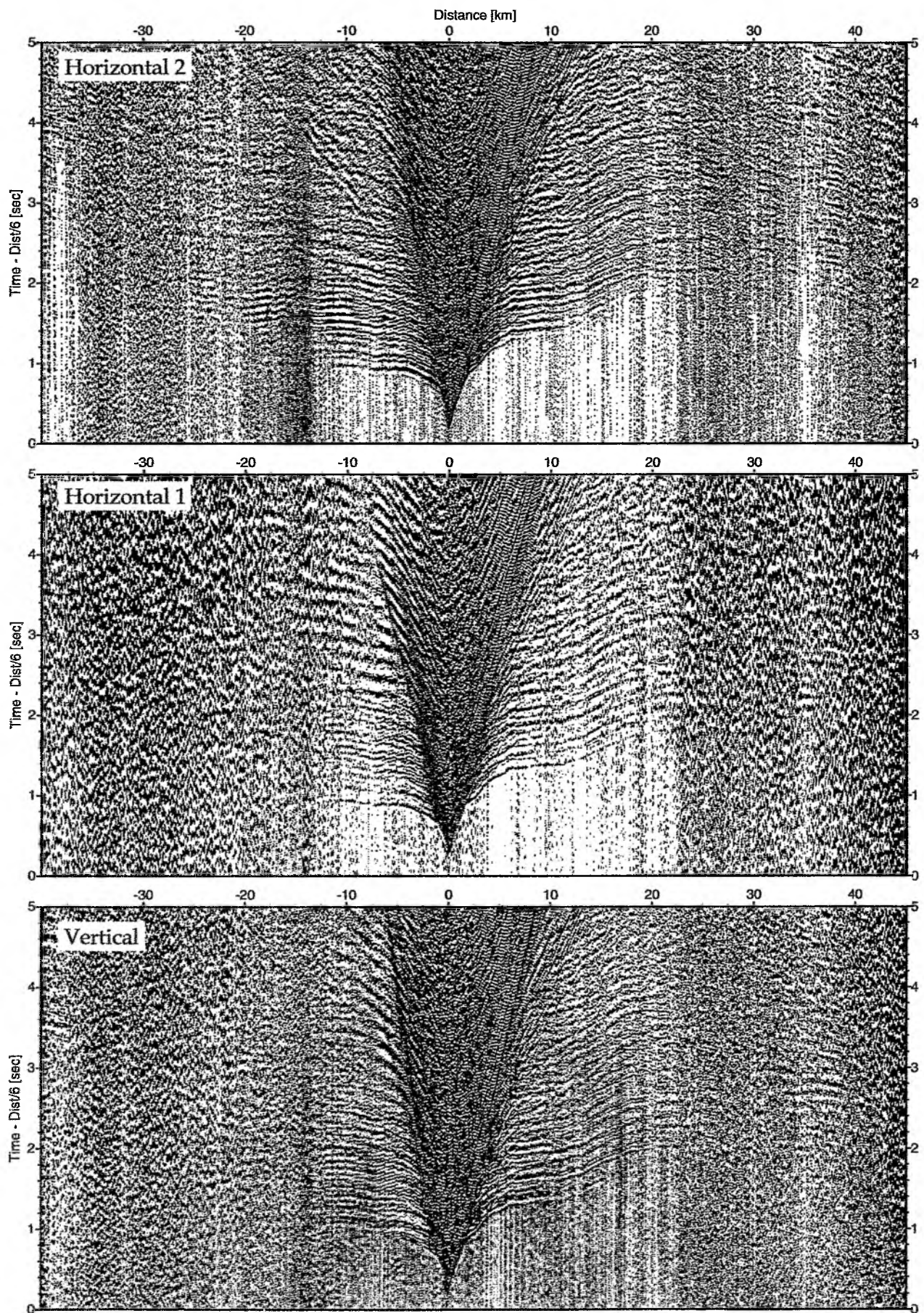


Figure 6.6.4.18: Record sections from obs 121 HTI/Owen-4.5Hz, SO181 Profile 07.

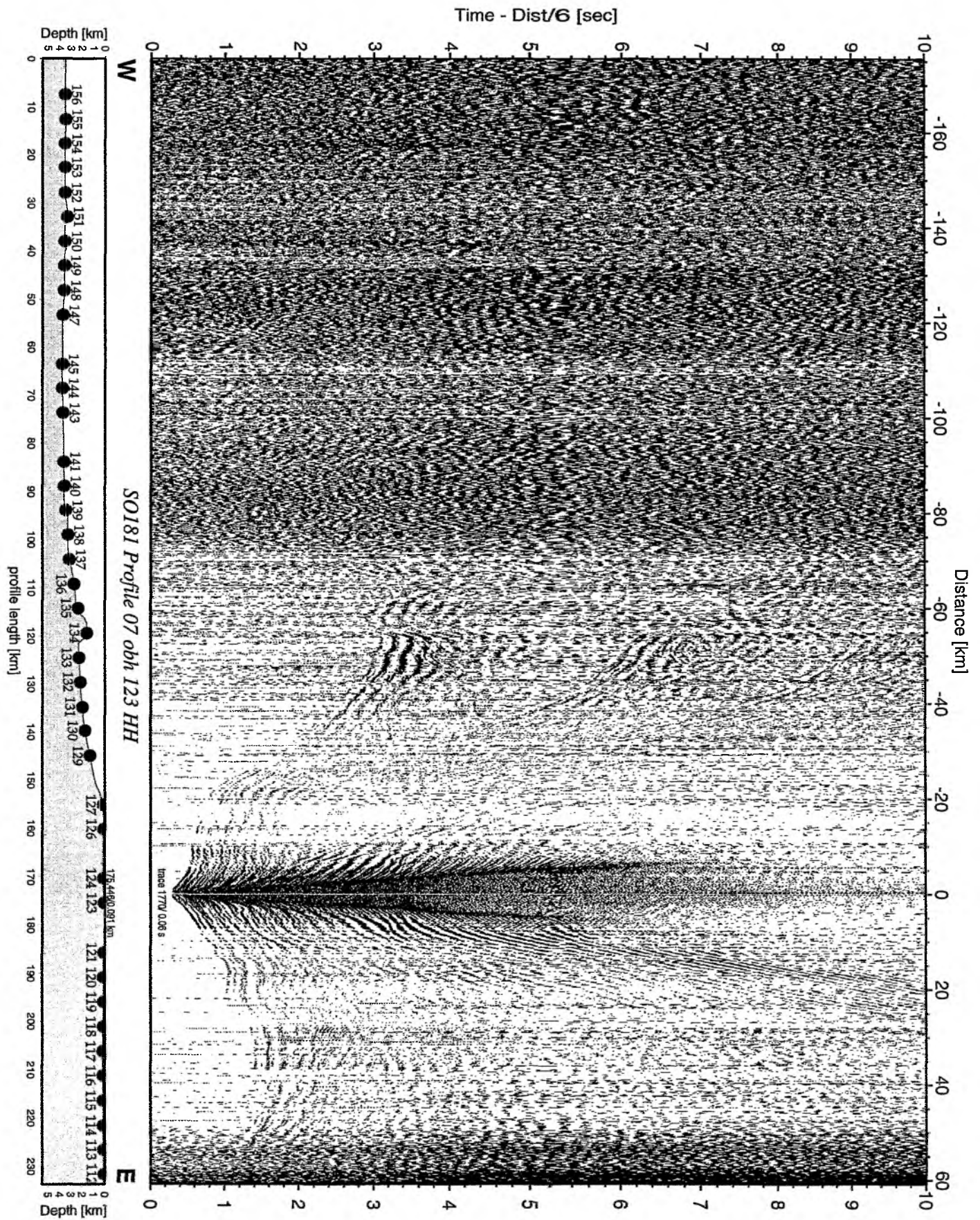


Figure 6.6.4.19: Record section from obh 123 HH, Profile 07.

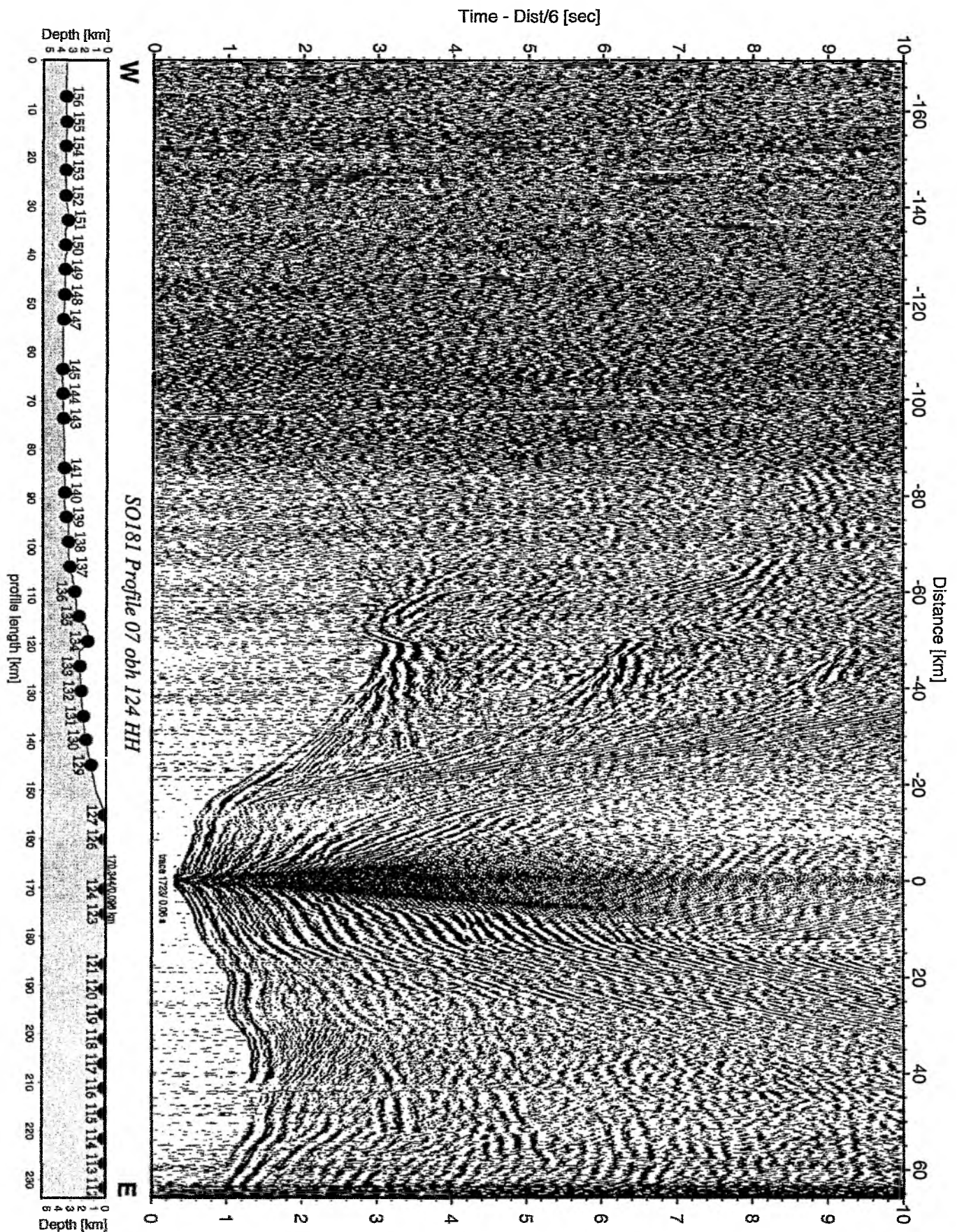


Figure 6.6.4.20: Record section from obh 124 HH, Profile 07.

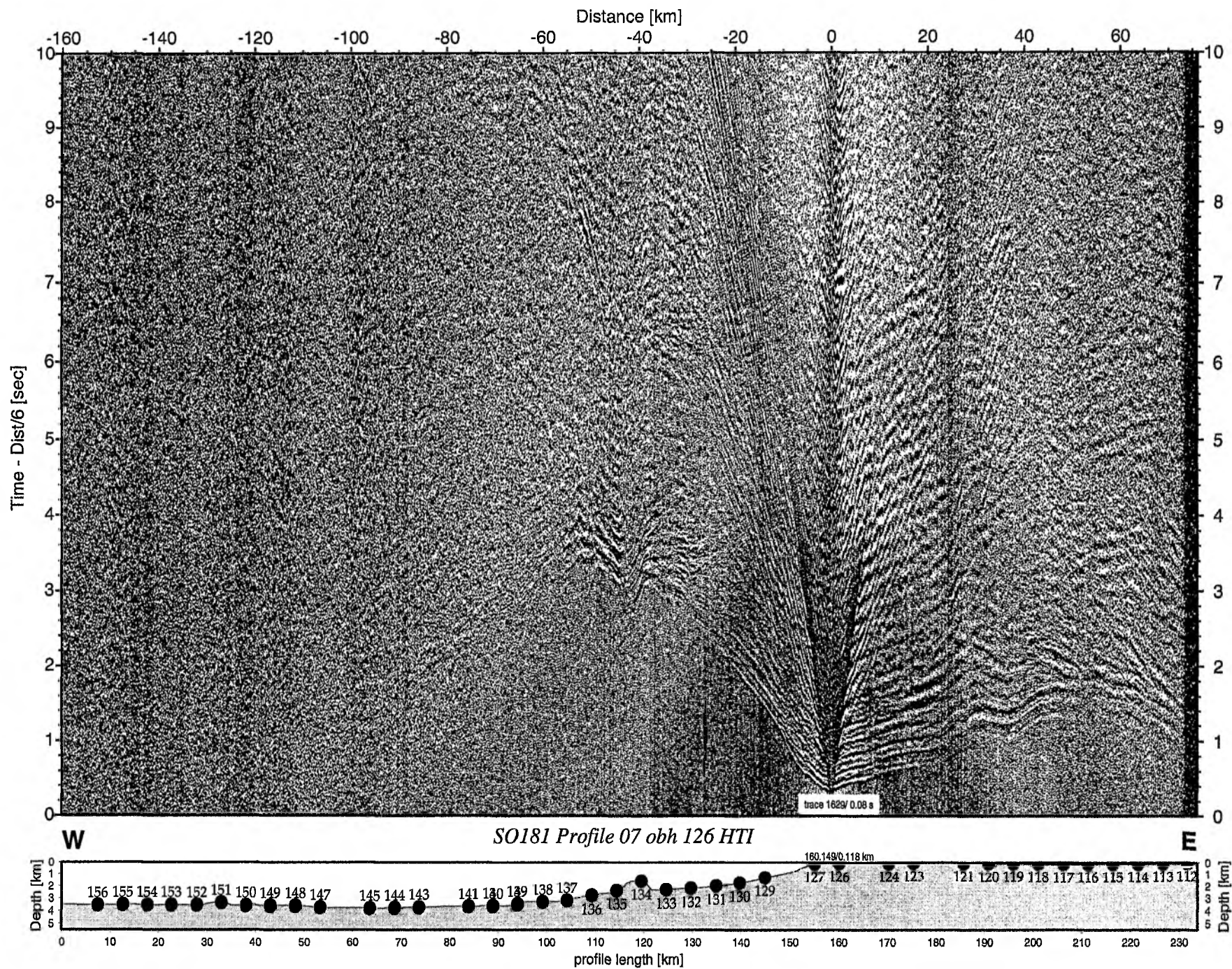


Figure 6.6.4.21: Record section from obh 126 HTI, Profile 07.

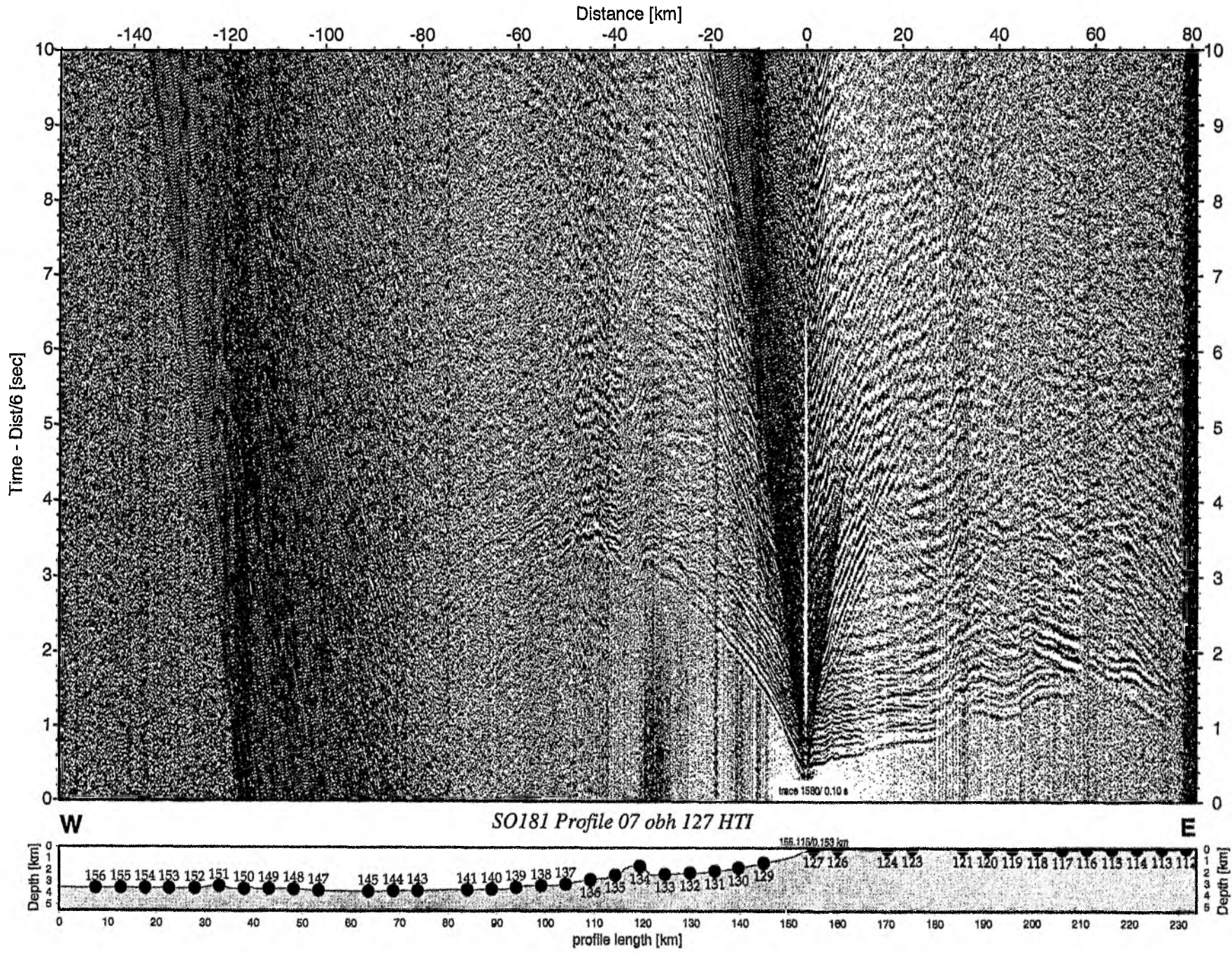


Figure 6.6.4.22: Record section from obh 127 HTI, Profile 07.

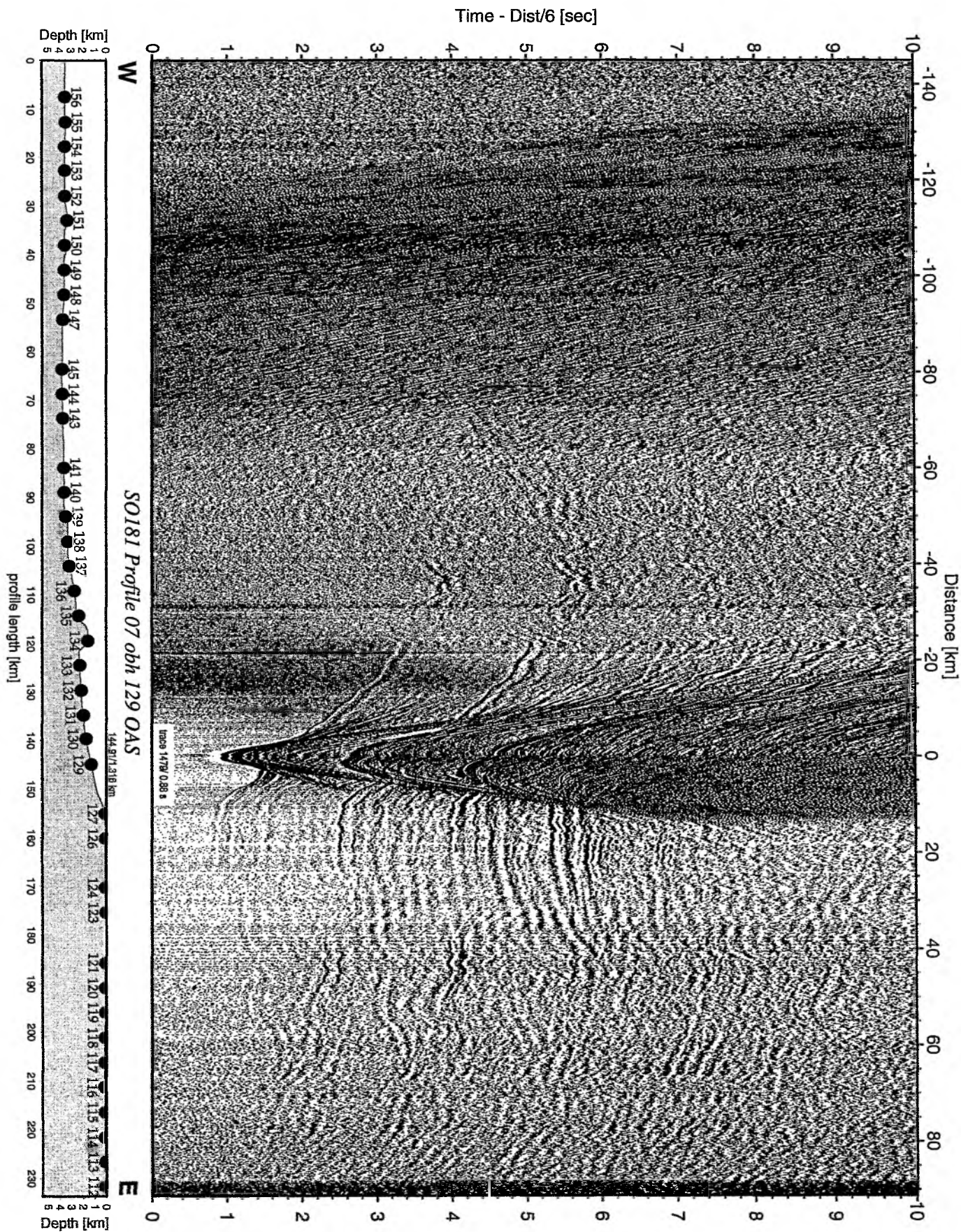


Figure 6.6.4.23: Record section from obh 129 OAS, Profile 07.

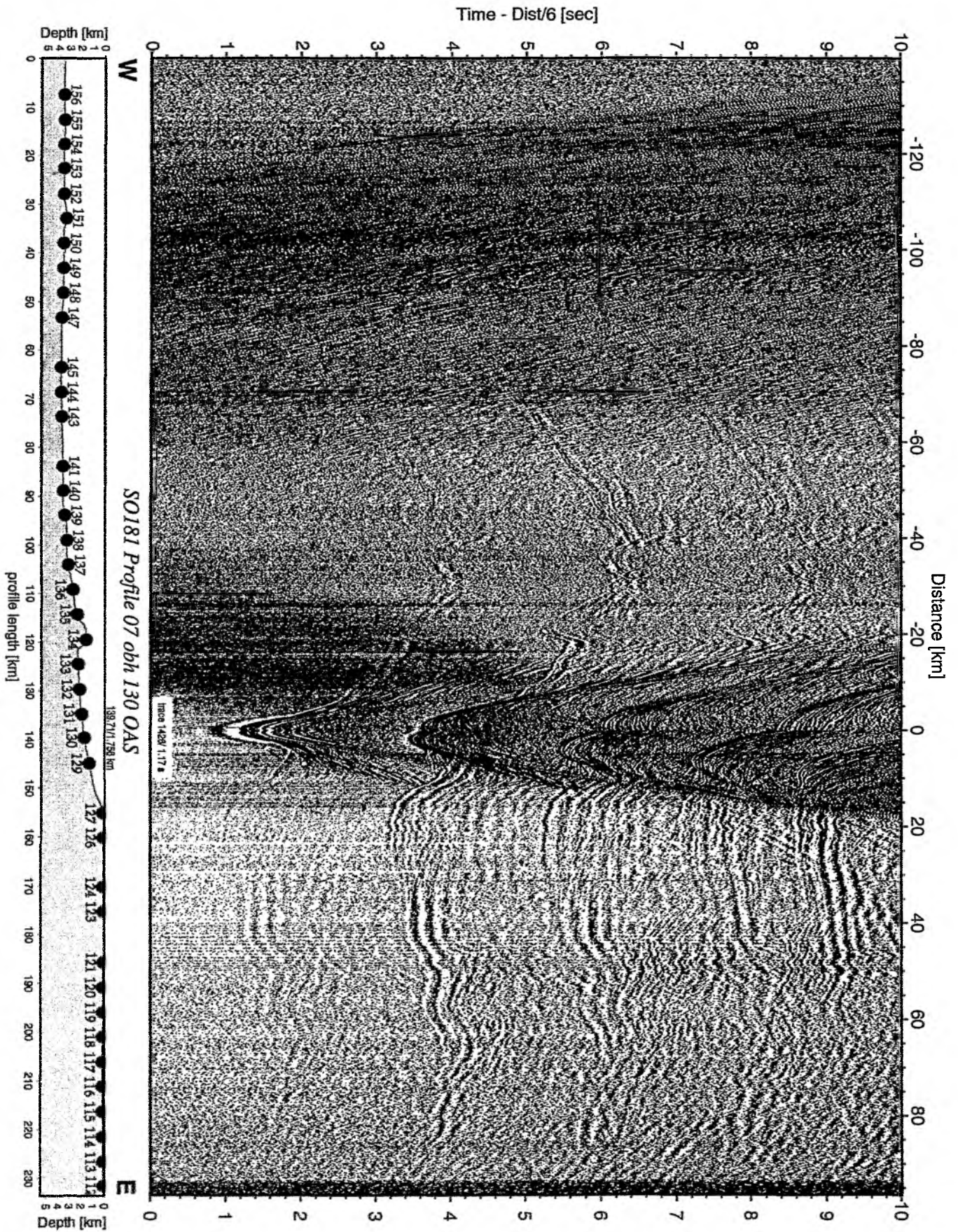


Figure 6.6.4.24: Record section from obh 130 OAS, Profile 07.

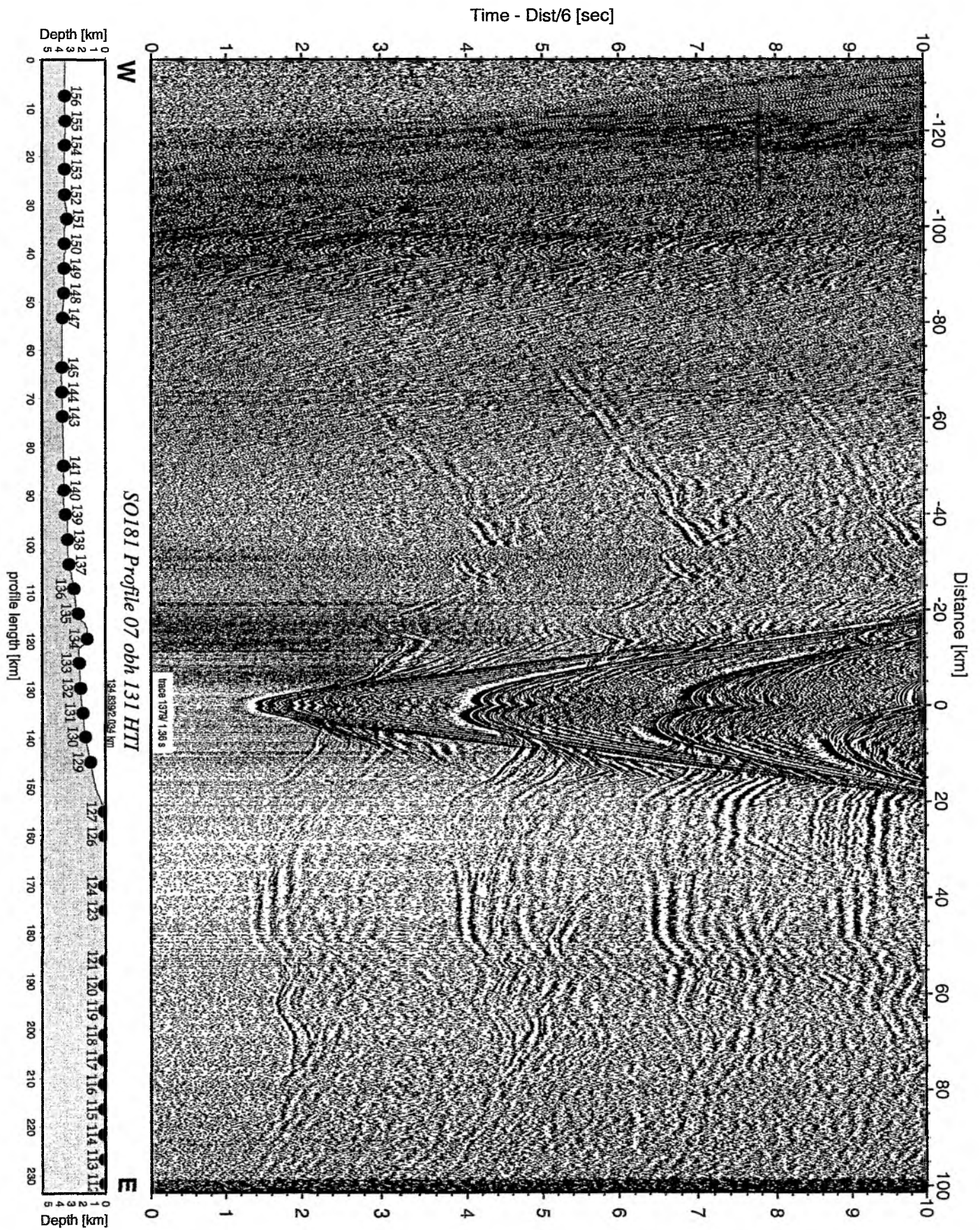


Figure 6.6.4.25: Record section from obh 131 HTI, Profile 07.

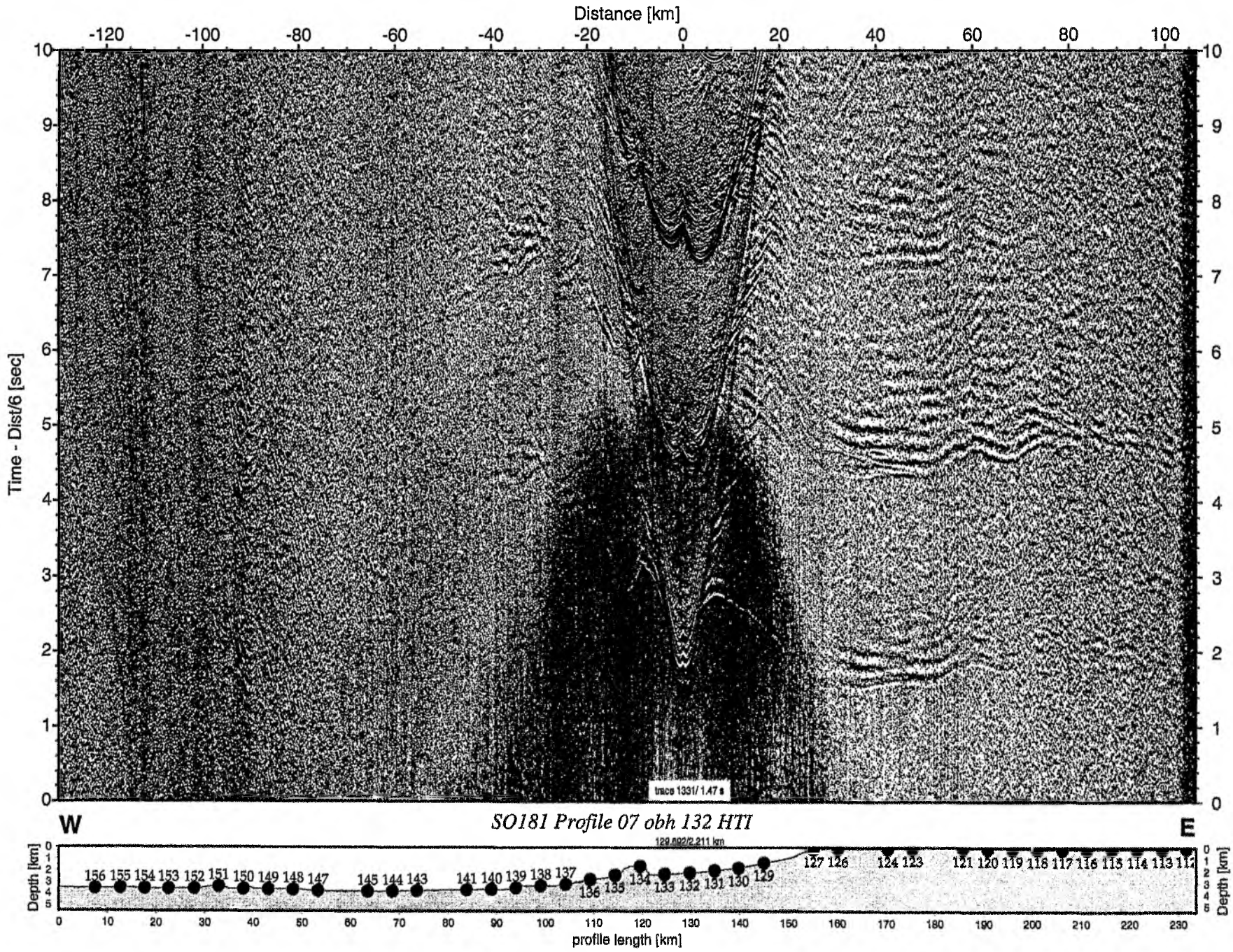


Figure 6.6.4.26: Record section from obh 132 HTI, Profile 07.

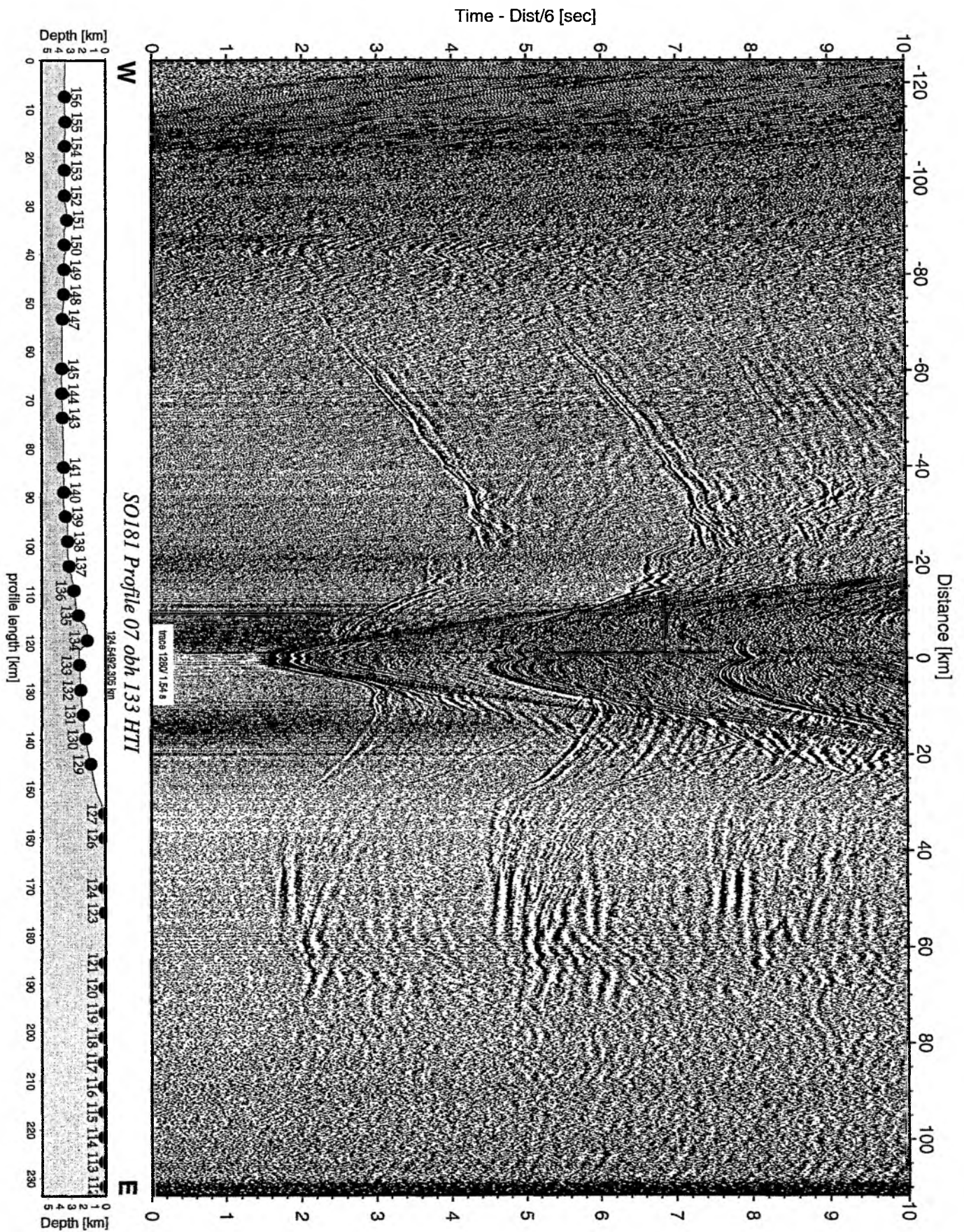


Figure 6.6.4.27: Record section from obh 133 HTI, Profile 07.

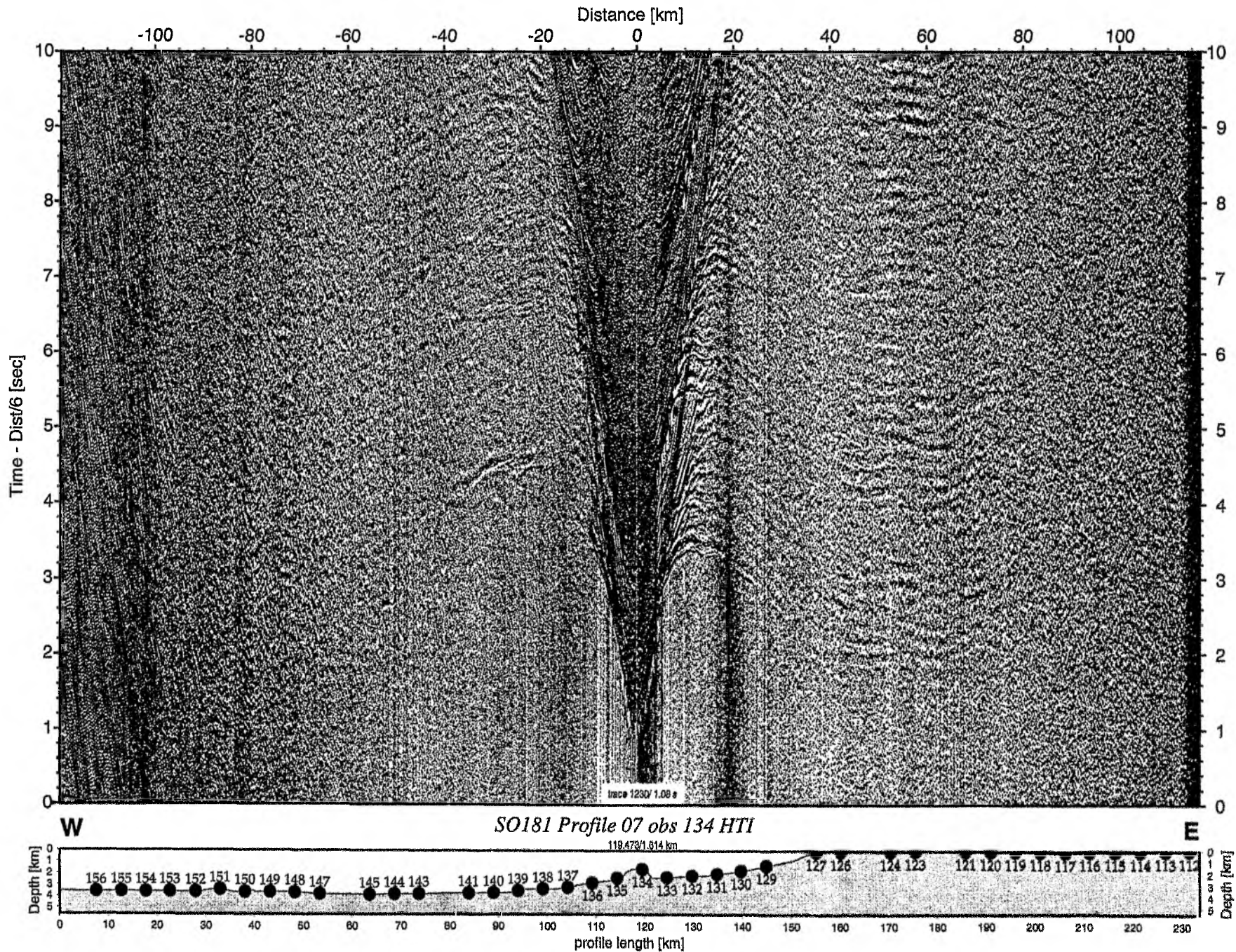


Figure 6.6.4.28: Record section from obs 134 HTI, Profile 07.

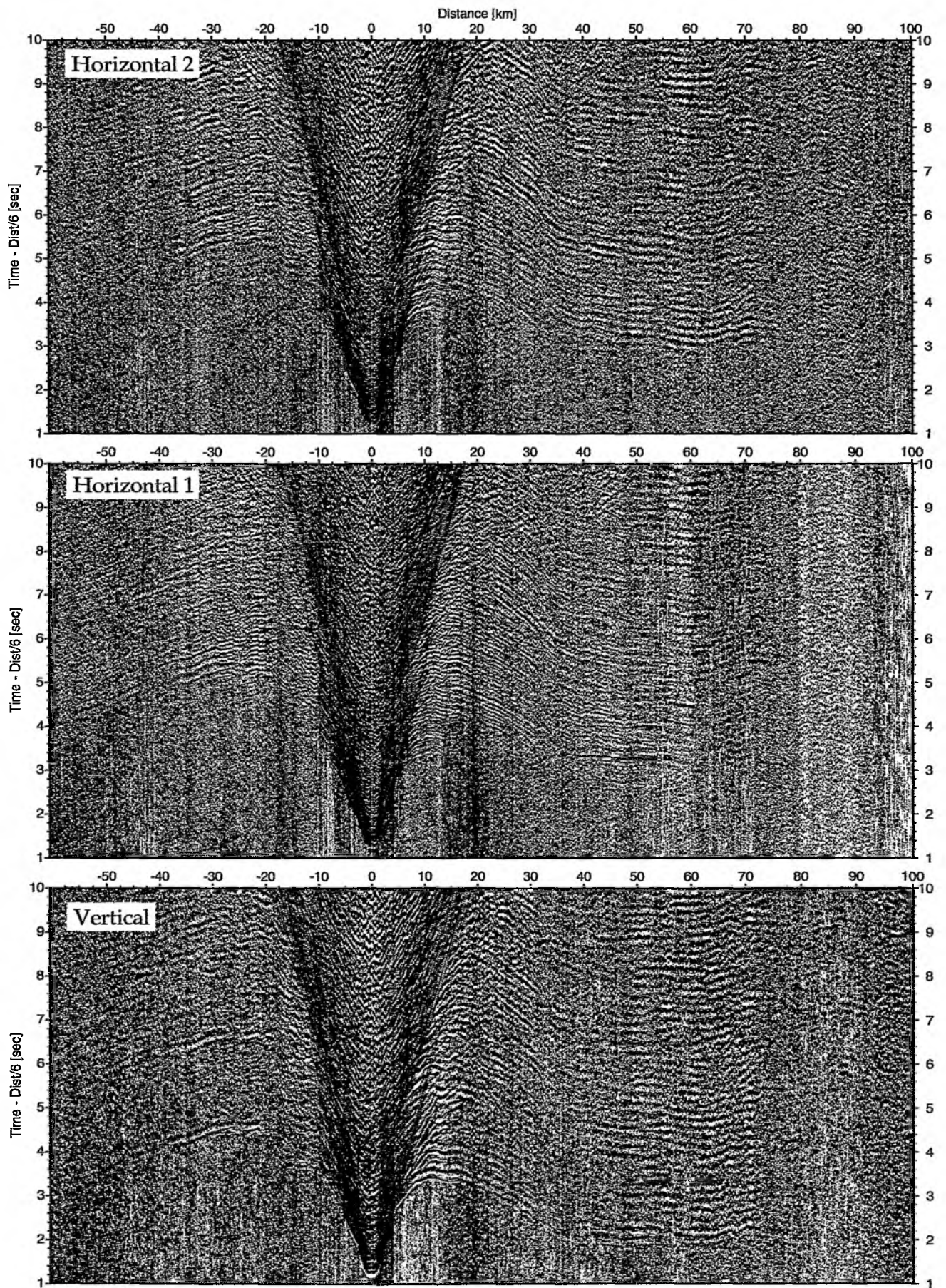


Figure 6.6.4.29: Record sections from obs 134 HTI/Owen-4.5Hz, SO181 Profile 07.

Time - Dist/6 [sec]

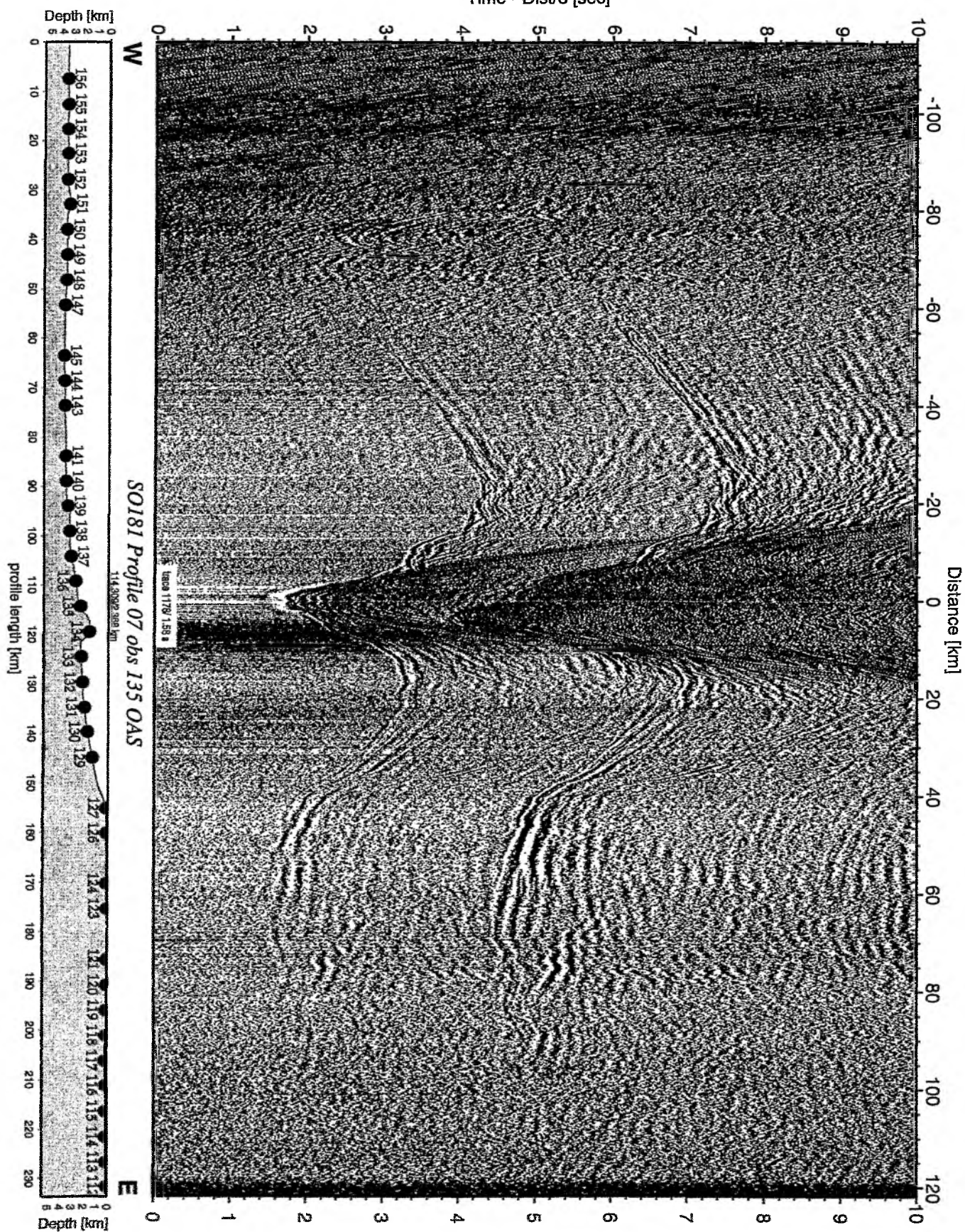


Figure 6.6.4.30: Record section from obs 135 OAS, Profile 07.

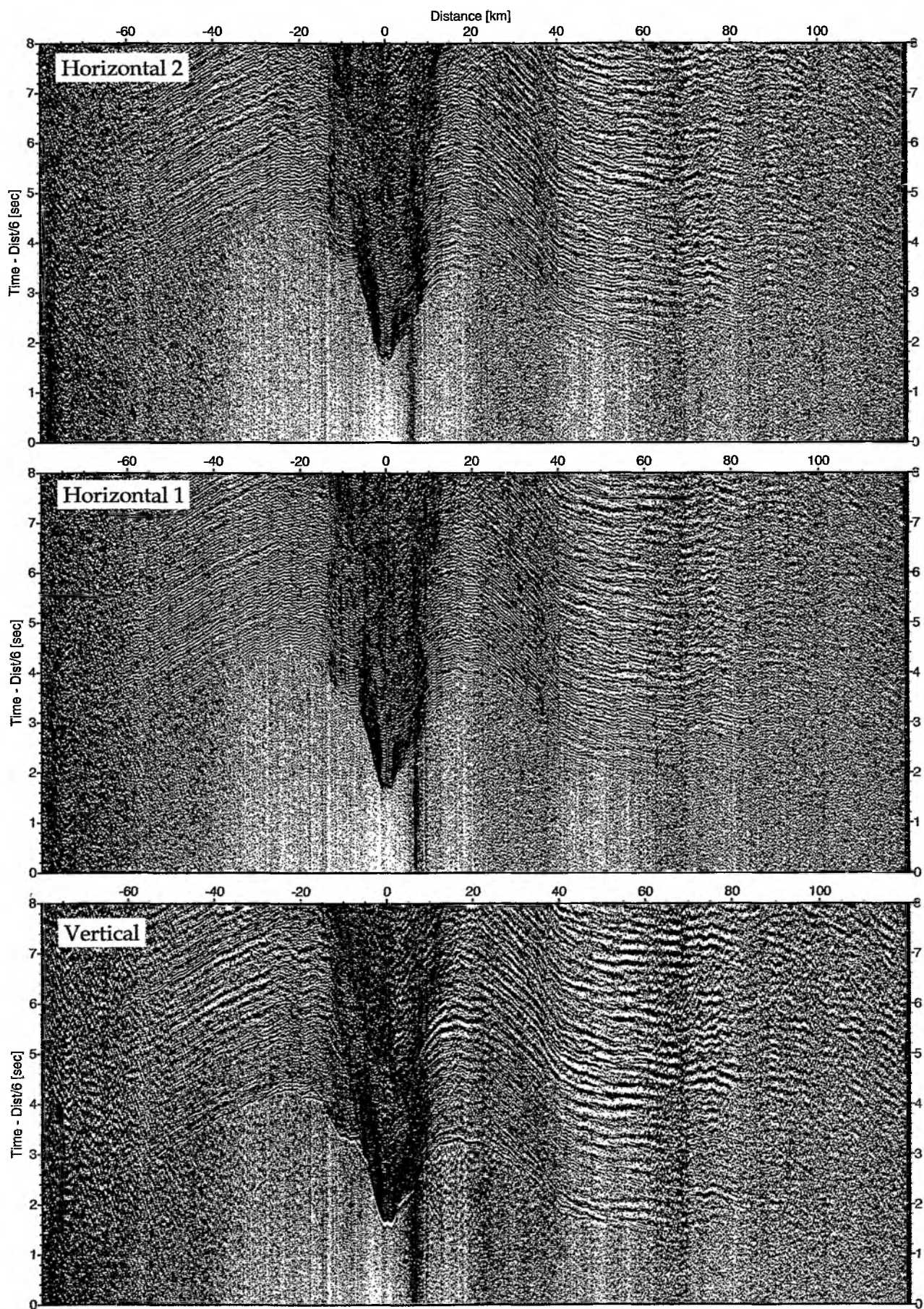


Figure 6.6.4.31: Record sections from obs 135 OAS/Owen-4.5Hz, SO181 Profile 07.

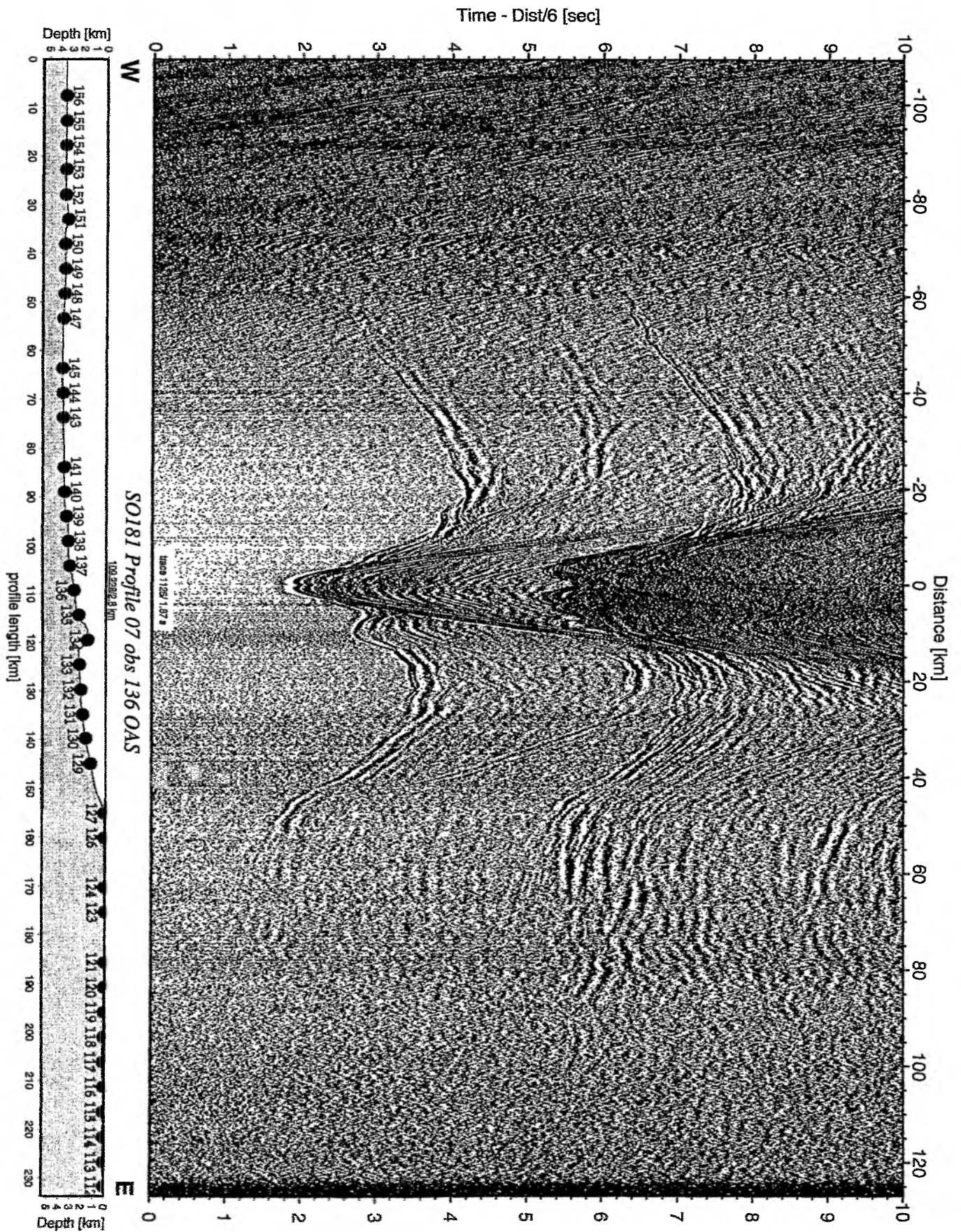


Figure 6.6.4.32: Record section from obs 136 OAS, Profile 07.

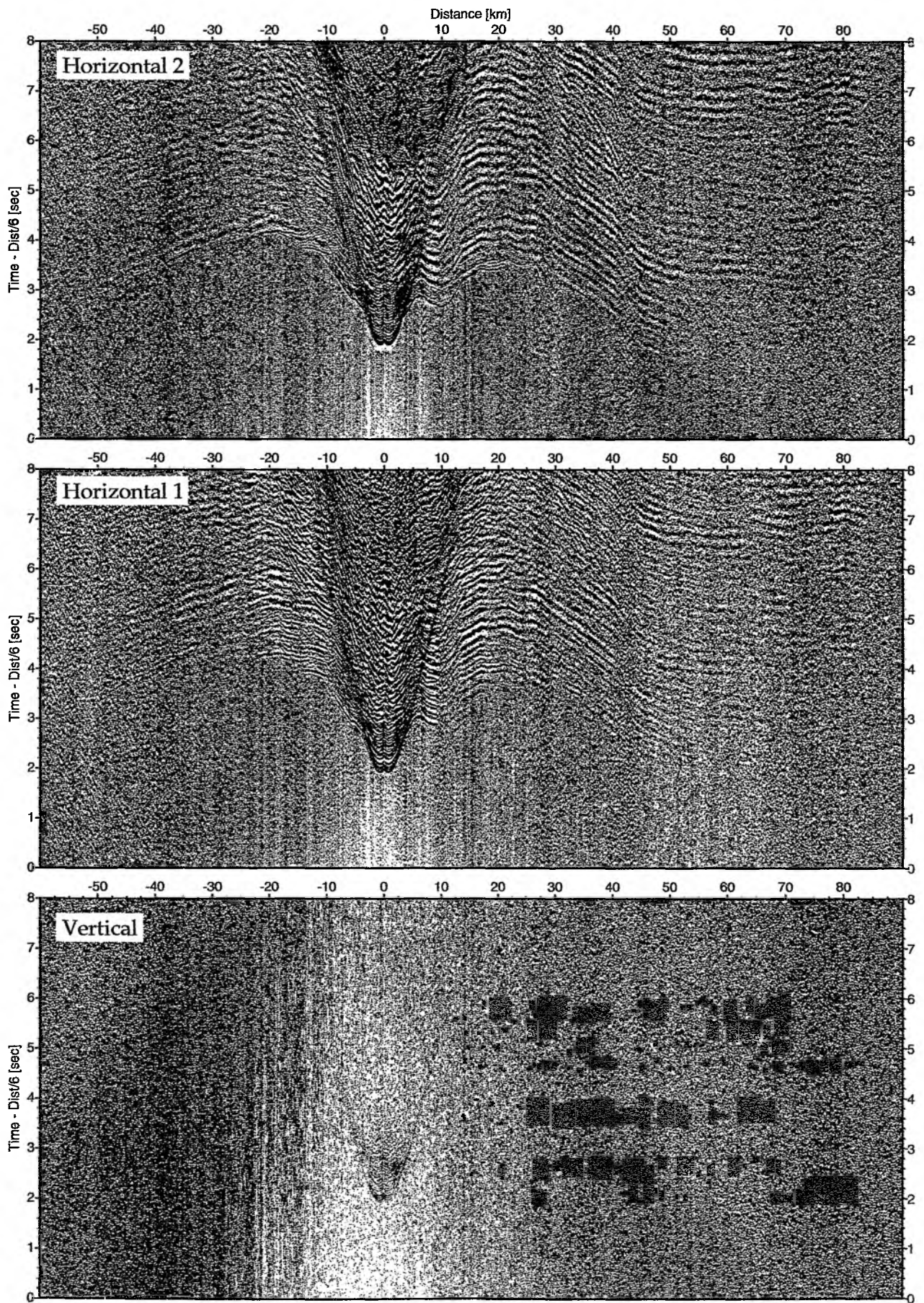


Figure 6.6.4.33: Record sections from obs 136 OAS/Owen-4.5Hz, SO181 Profile 07.

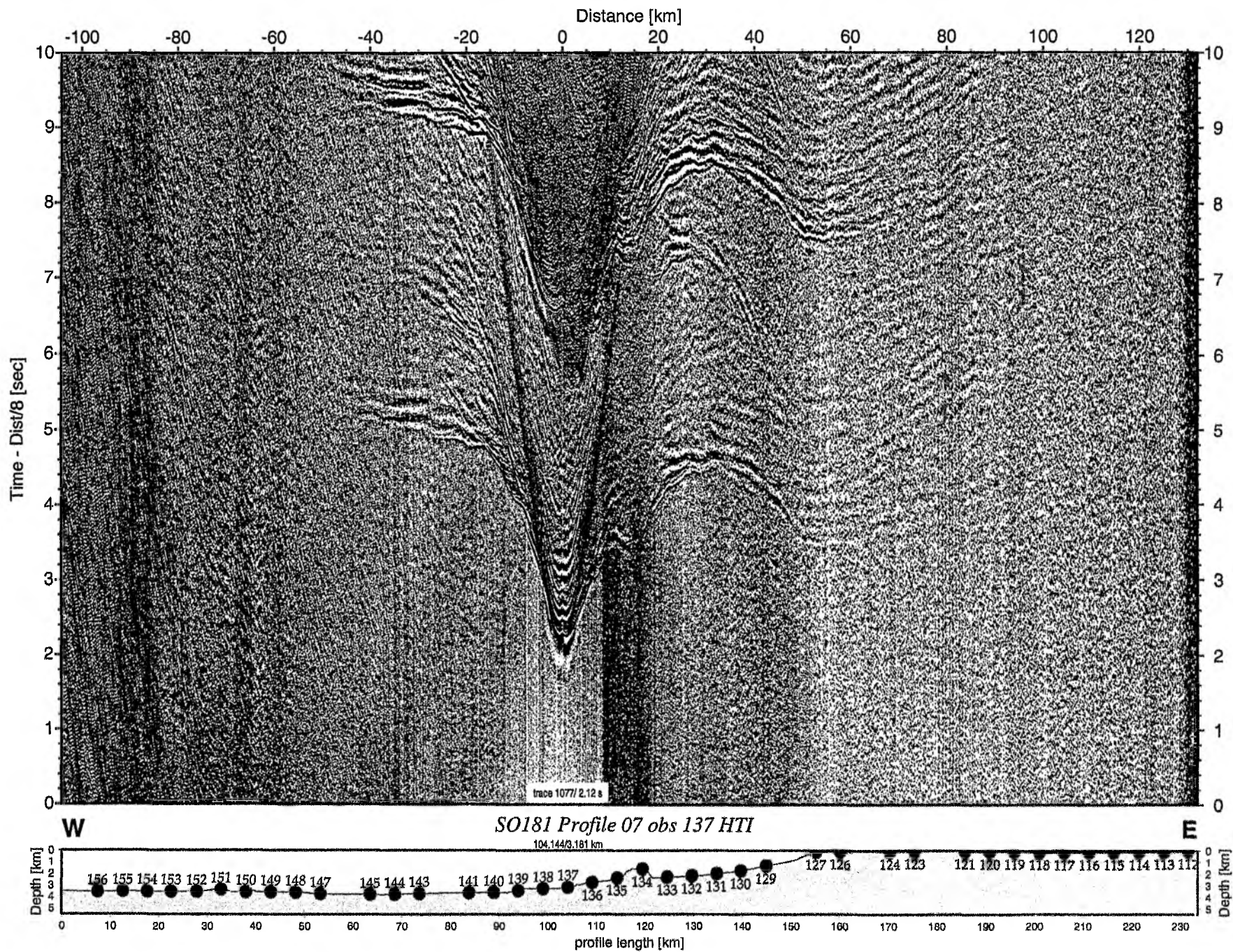


Figure 6.6.4.34: Record section from obs 137 HTI, Profile 07.

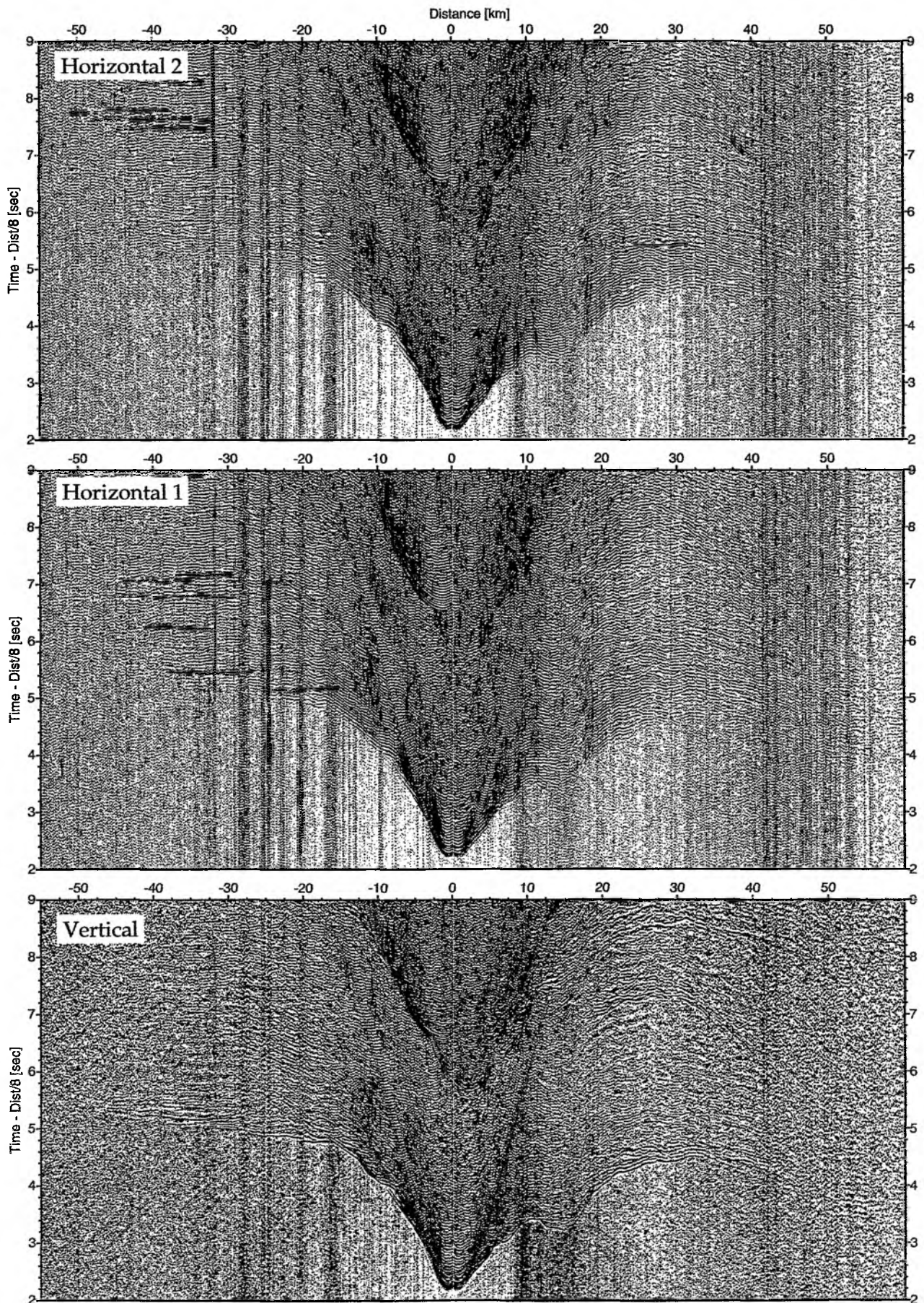


Figure 6.6.4.35: Record sections from obs 137 HTI/Owen-15Hz, SO181 Profile 07.

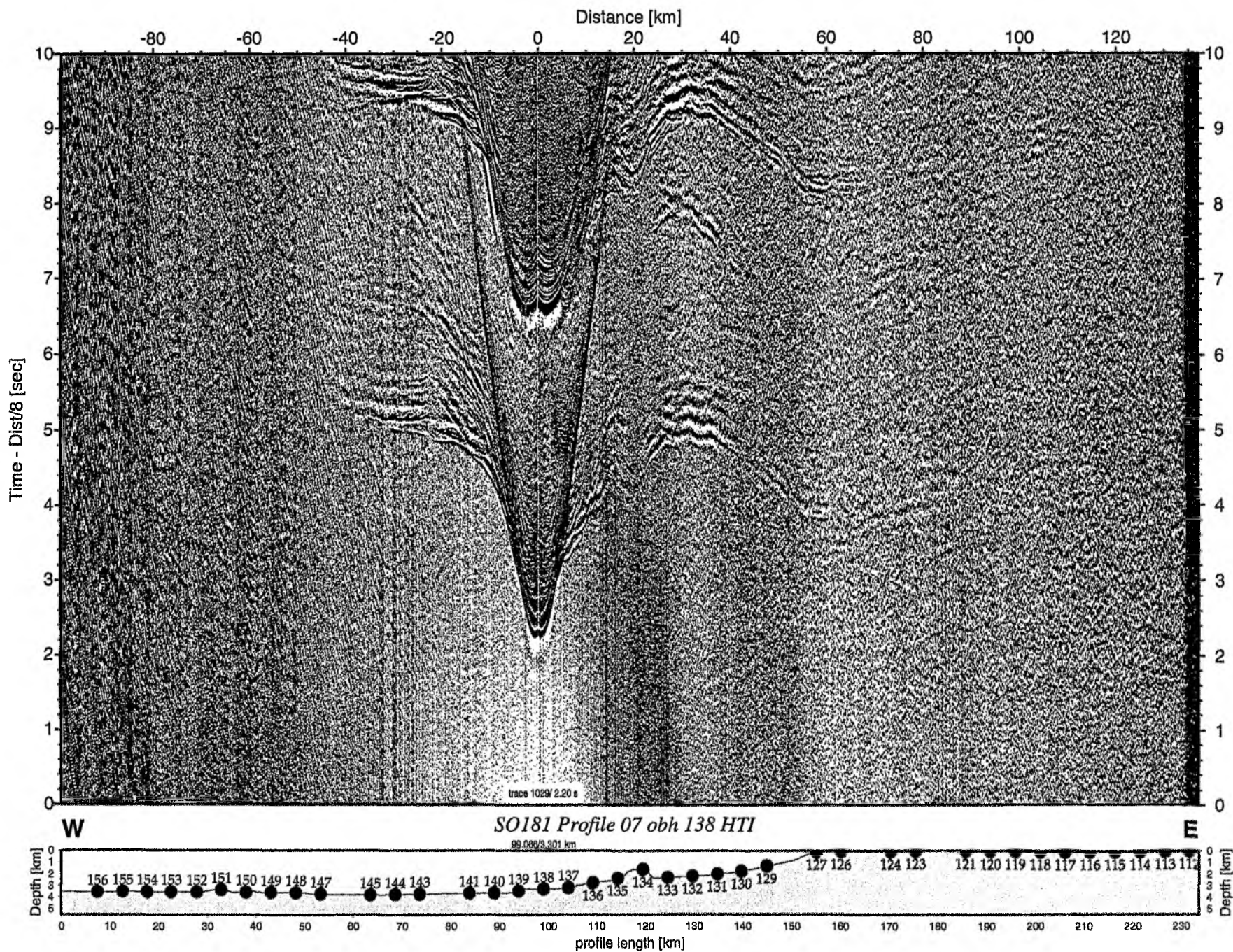


Figure 6.6.4.36: Record section from obh 138 HTI, Profile 07.

Time - Dist/8 [sec]

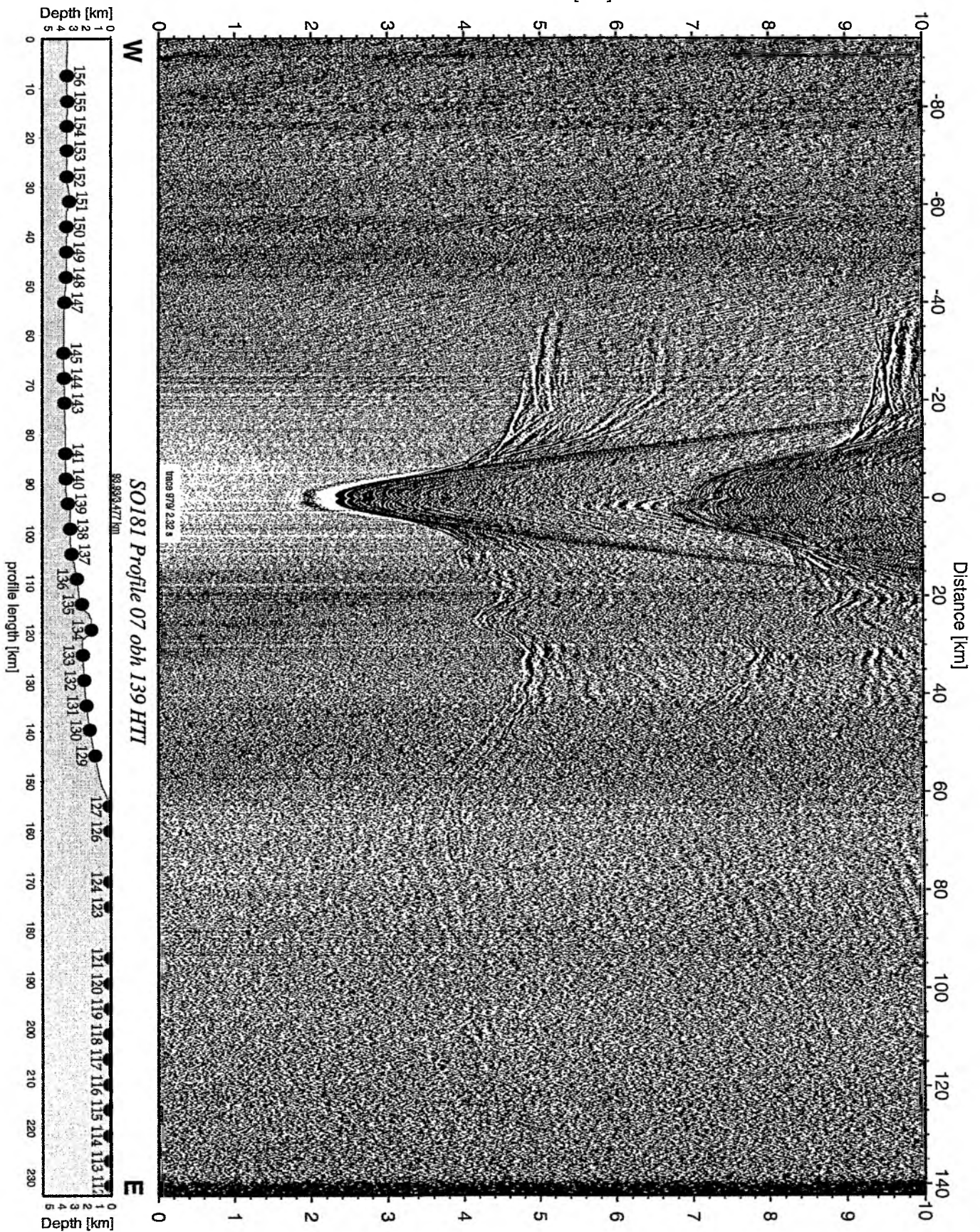


Figure 6.6.4.37: Record section from obh 139 HTI, Profile 07.

Time - Dist/8 [sec]

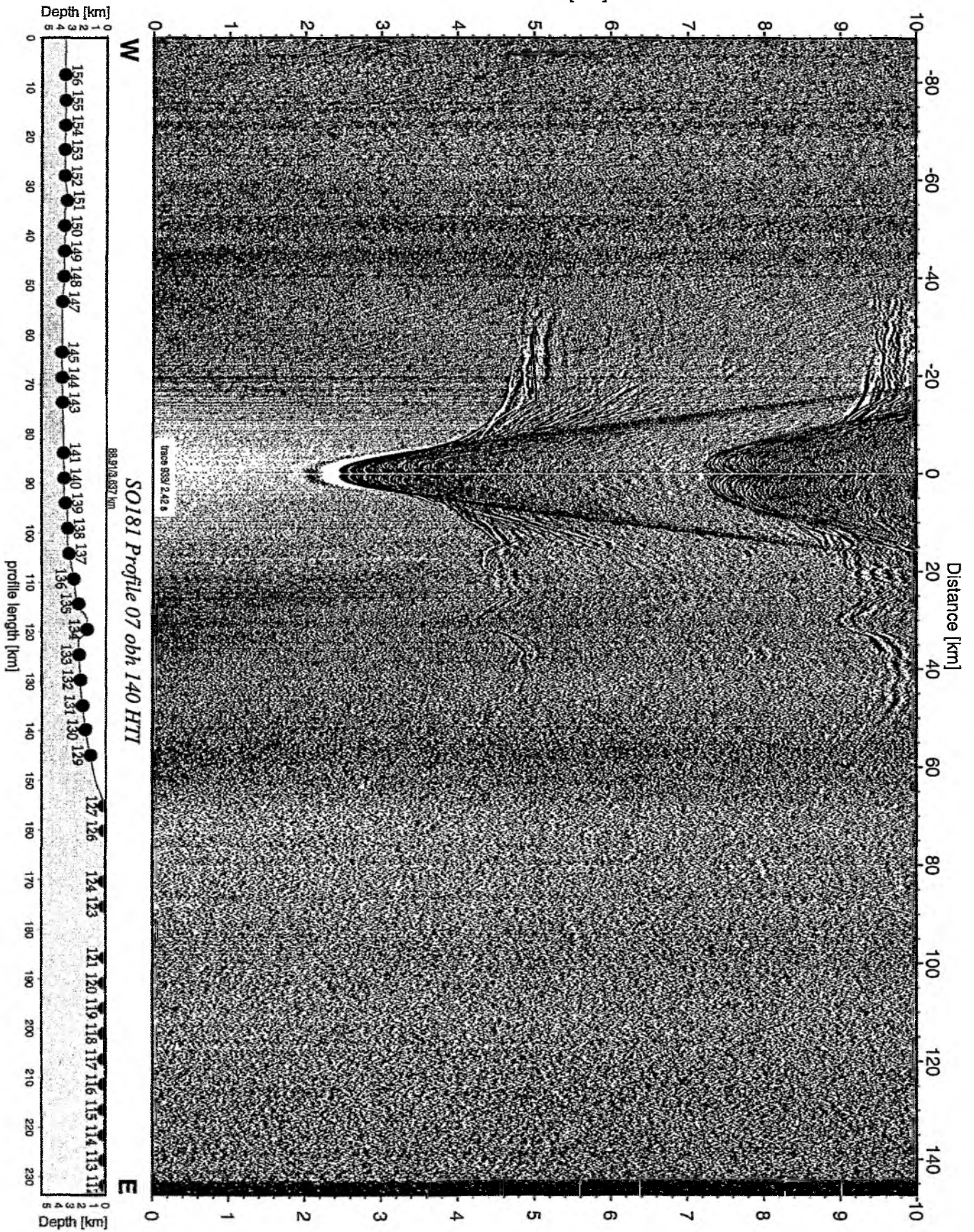


Figure 6.6.4.38: Record section from obh 140 HTL, Profile 07.

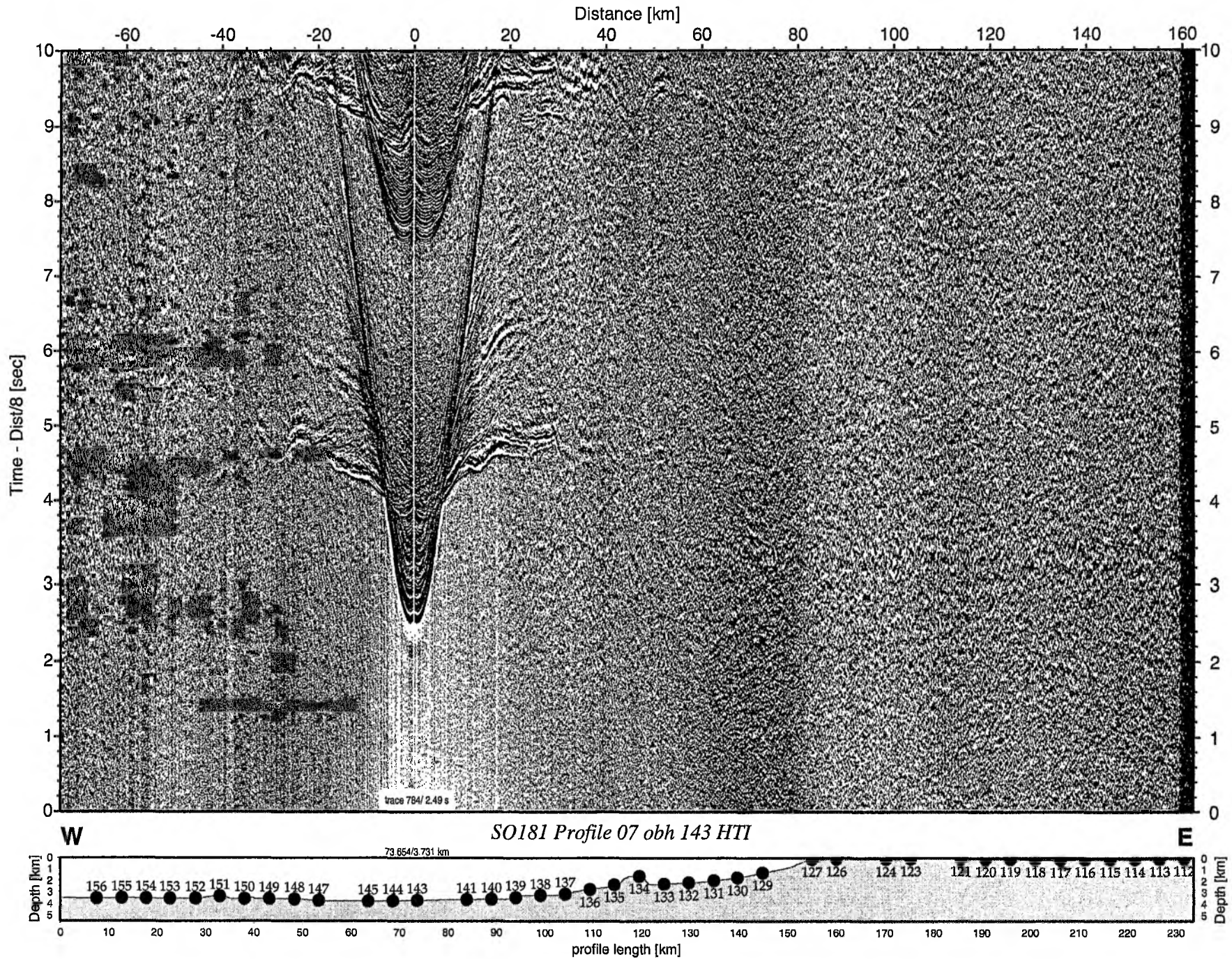


Figure 6.6.4.39: Record section from obh 143 HTI, Profile 07.

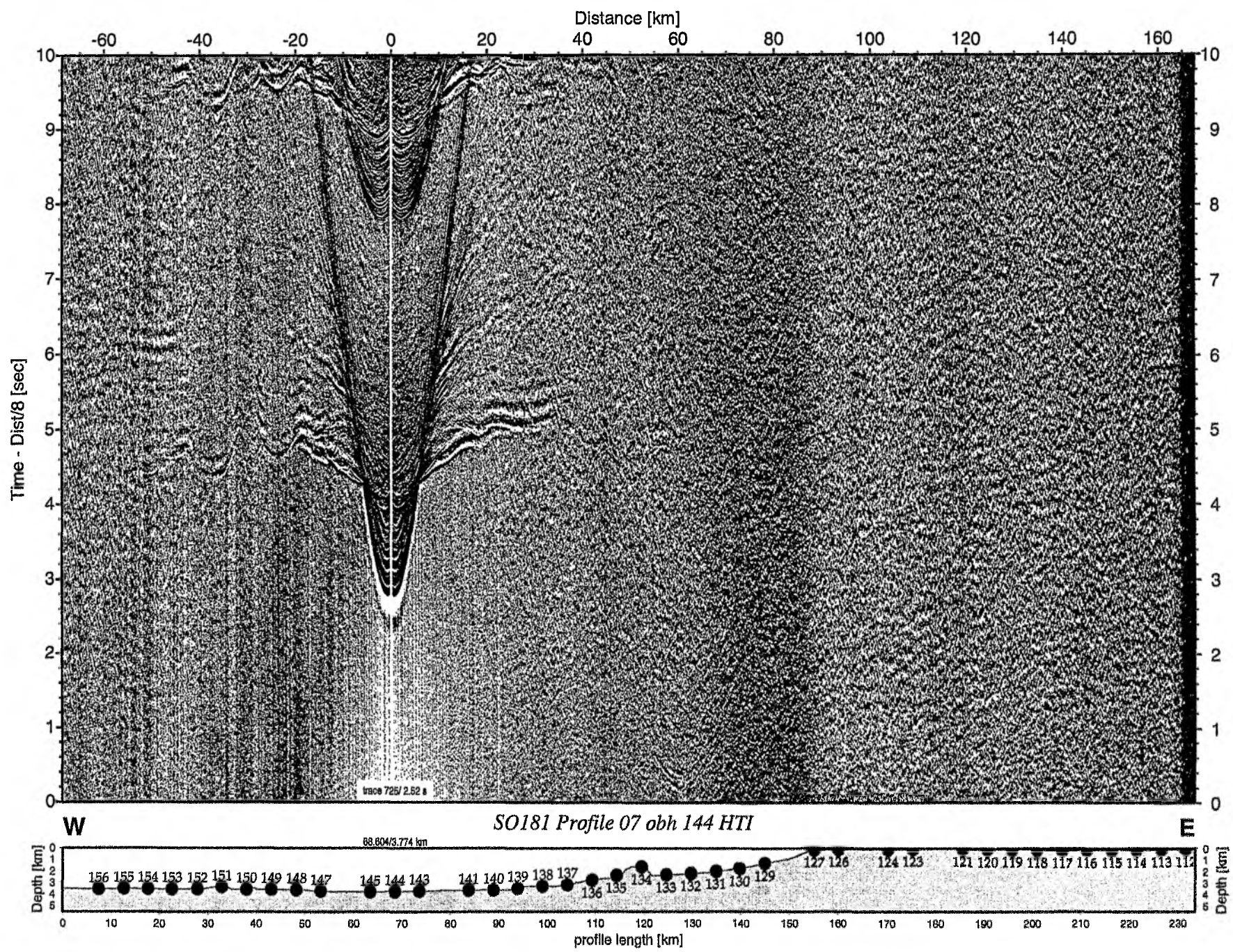


Figure 6.6.4.40: Record section from obh 144 HTI, Profile 07.

Time - Dist/8 [sec]

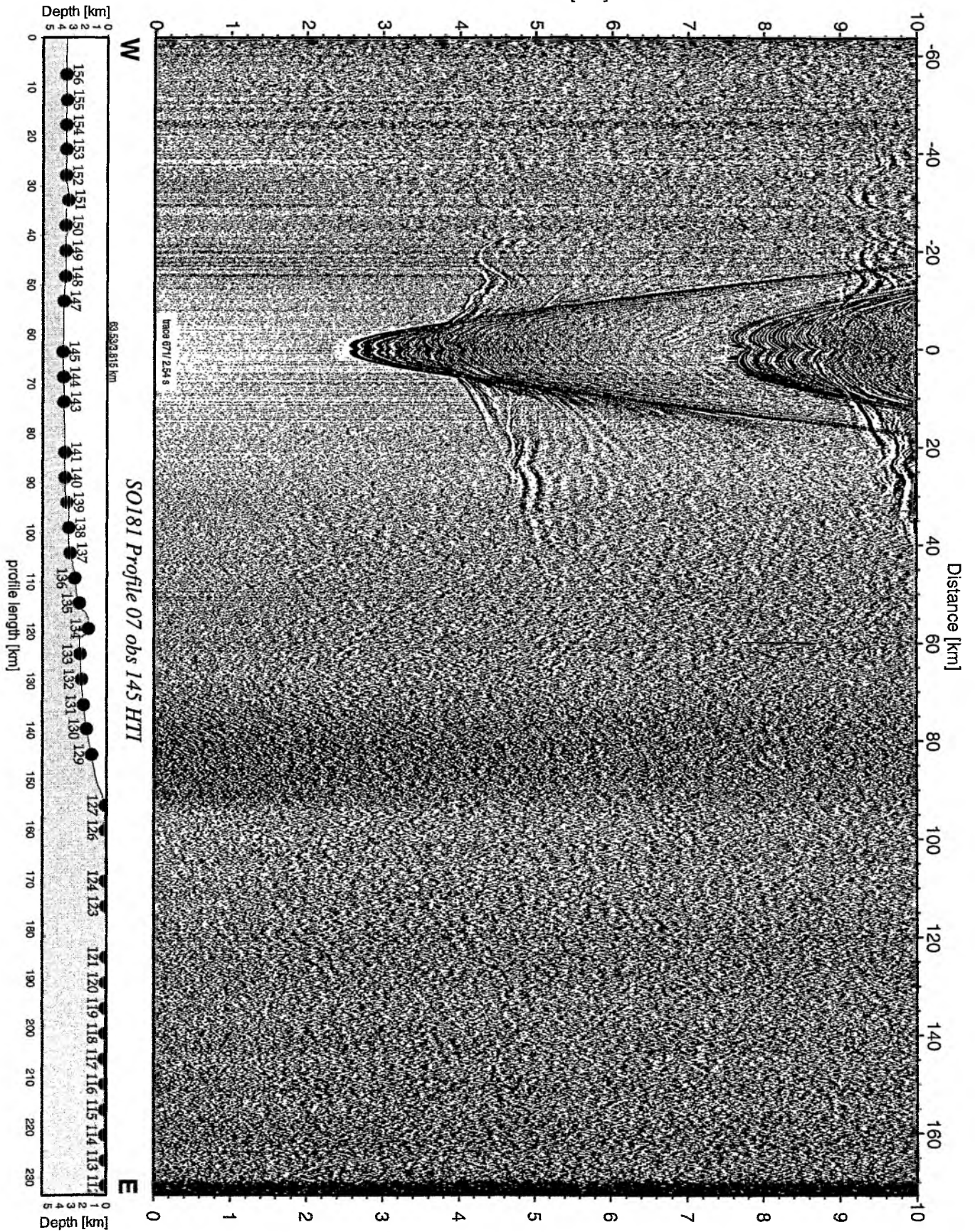


Figure 6.6.4.41: Record section from obs 145 HTI, Profile 07.

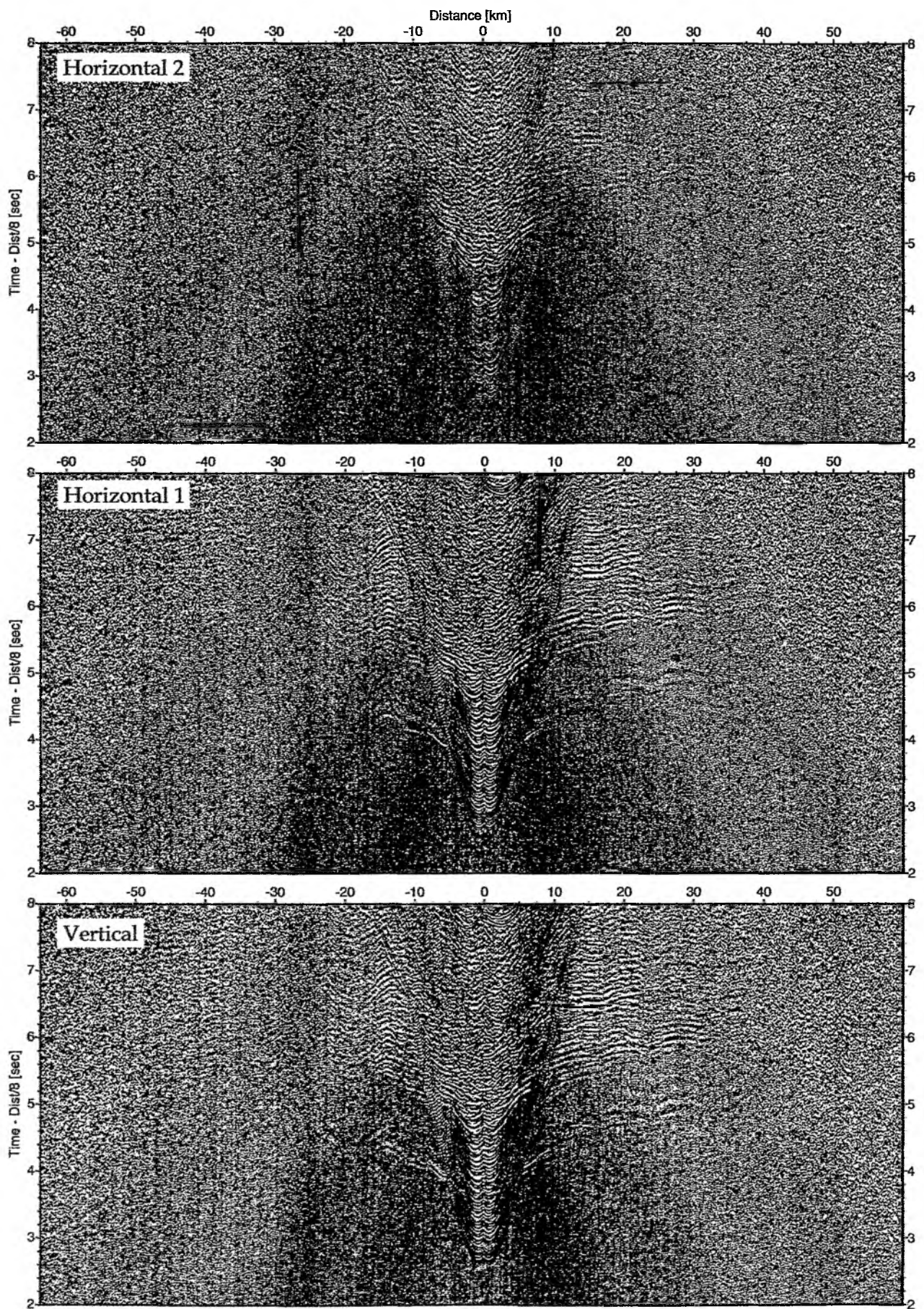


Figure 6.6.4.42: Record sections from obs 145 HTI/Owen-4.5Hz, SO181 Profile 07.

Time - Dist/8 [sec]

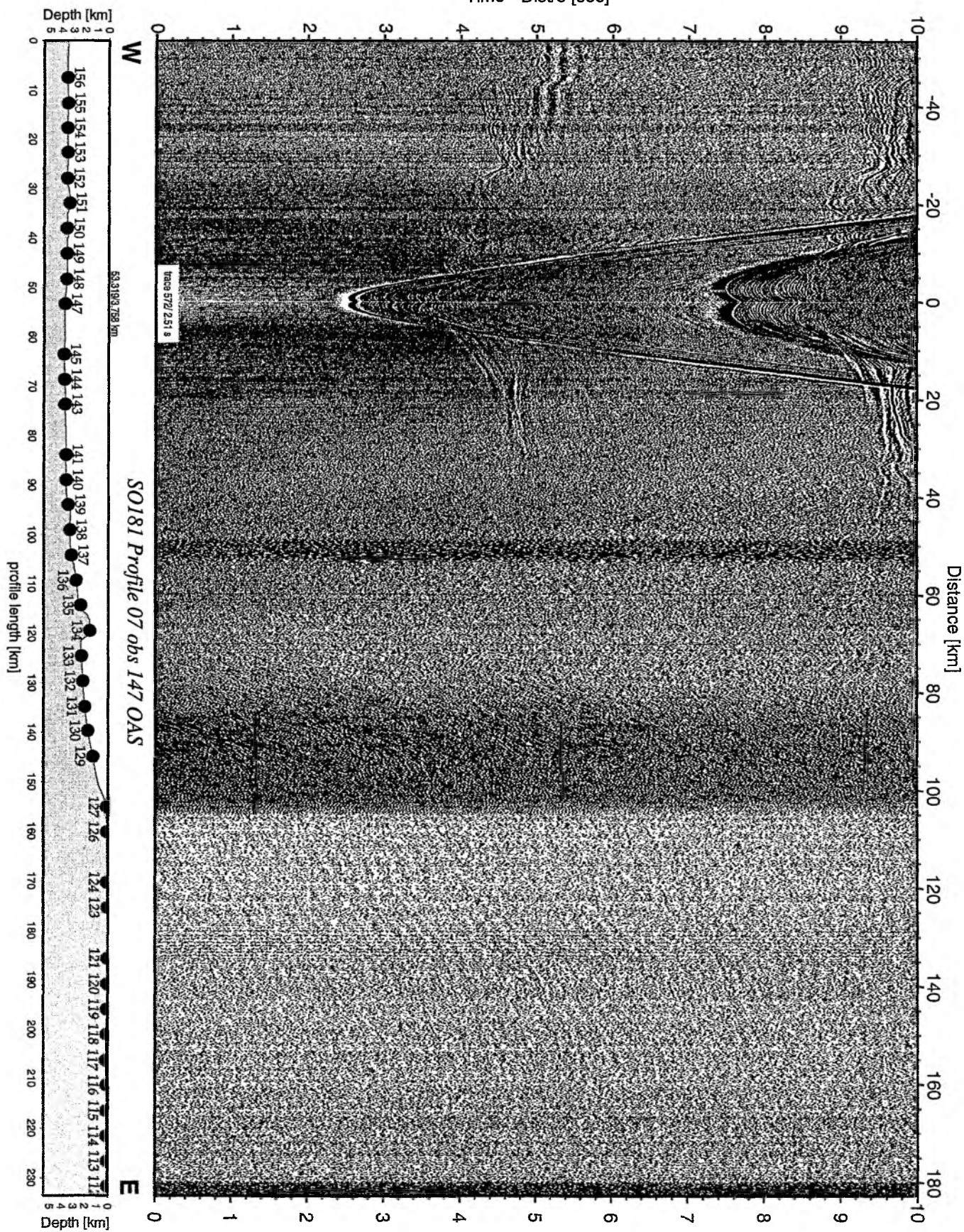


Figure 6.6.4.43: Record section from obs 147 OAS, Profile 07.

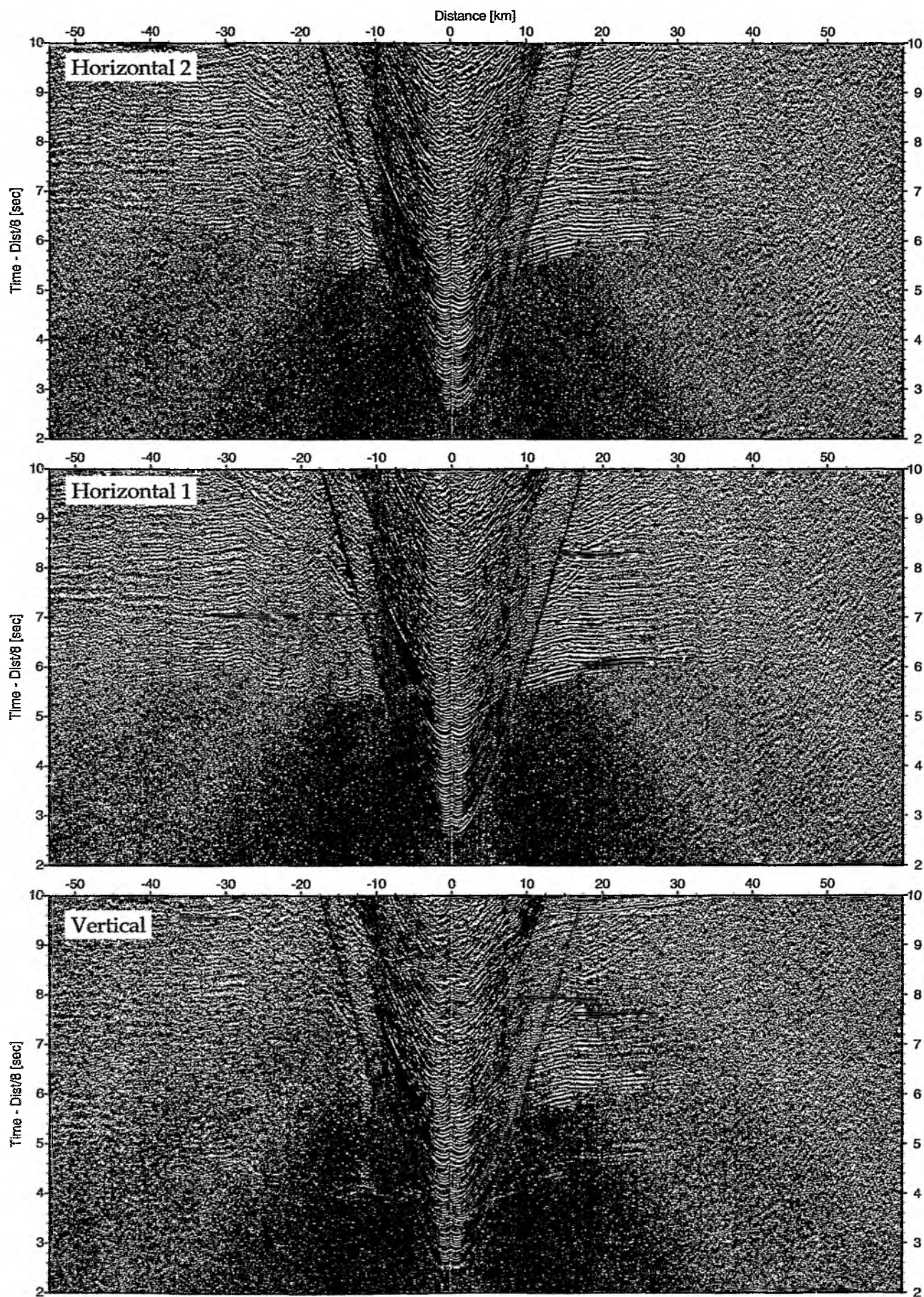


Figure 6.6.4.44: Record sections from obs 147 OAS/Owen-4.5Hz, SO181 Profile 07.

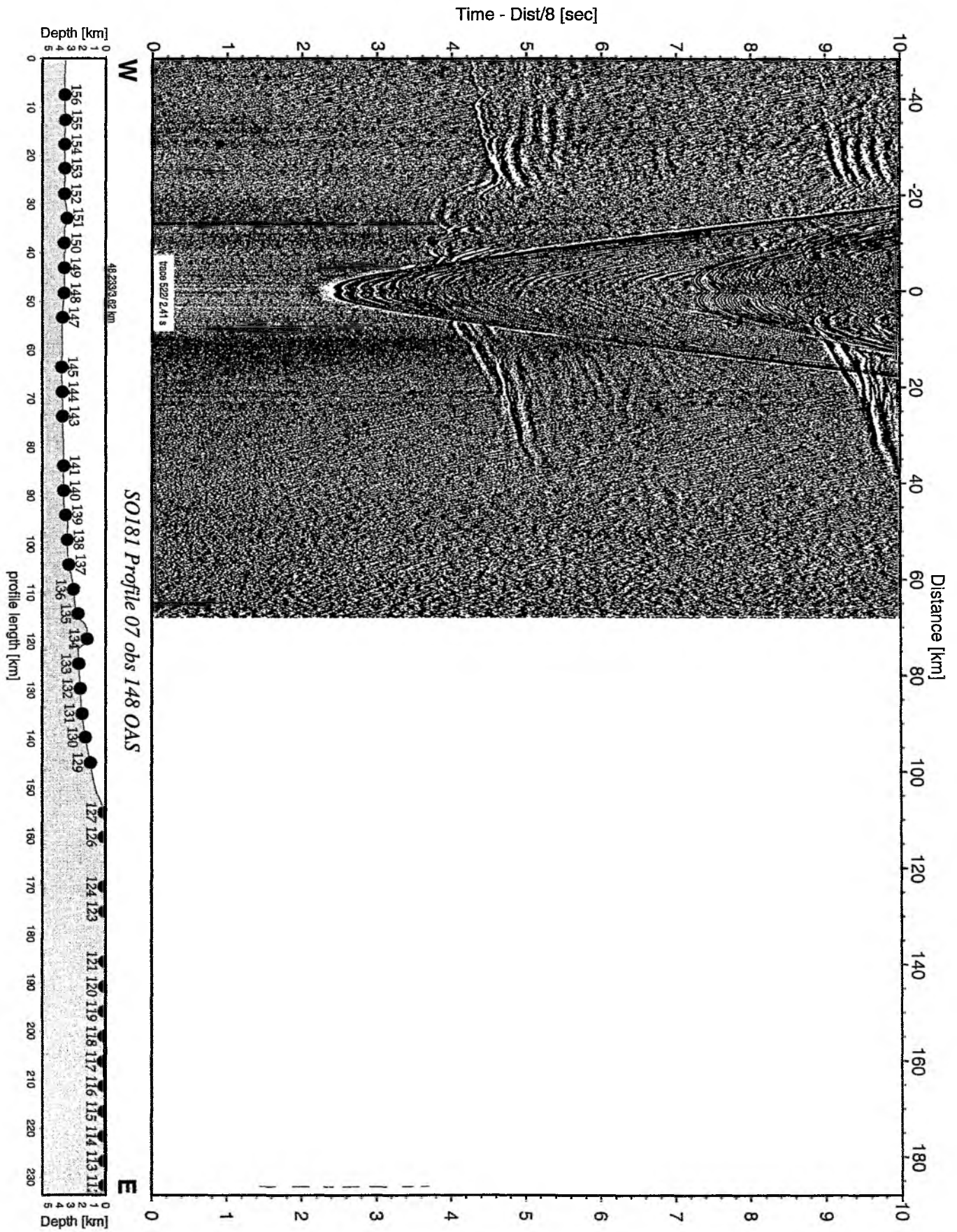


Figure 6.6.4.45: Record section from obs 148 OAS, Profile 07.

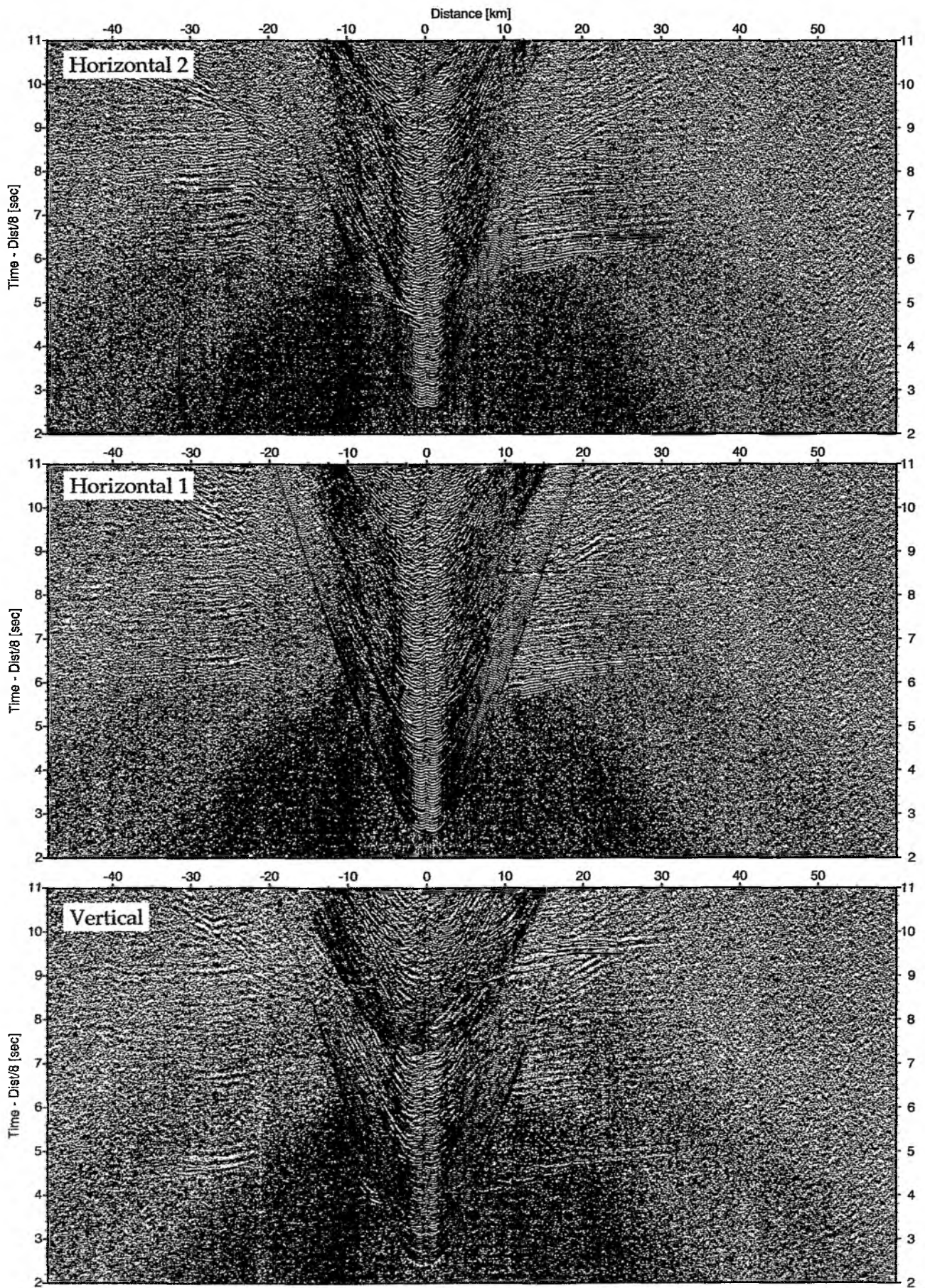


Figure 6.6.4.46: Record sections from obs 148 OAS/Owen-4.5Hz, SO181 Profile 07.

Time - Dist/8 [sec]

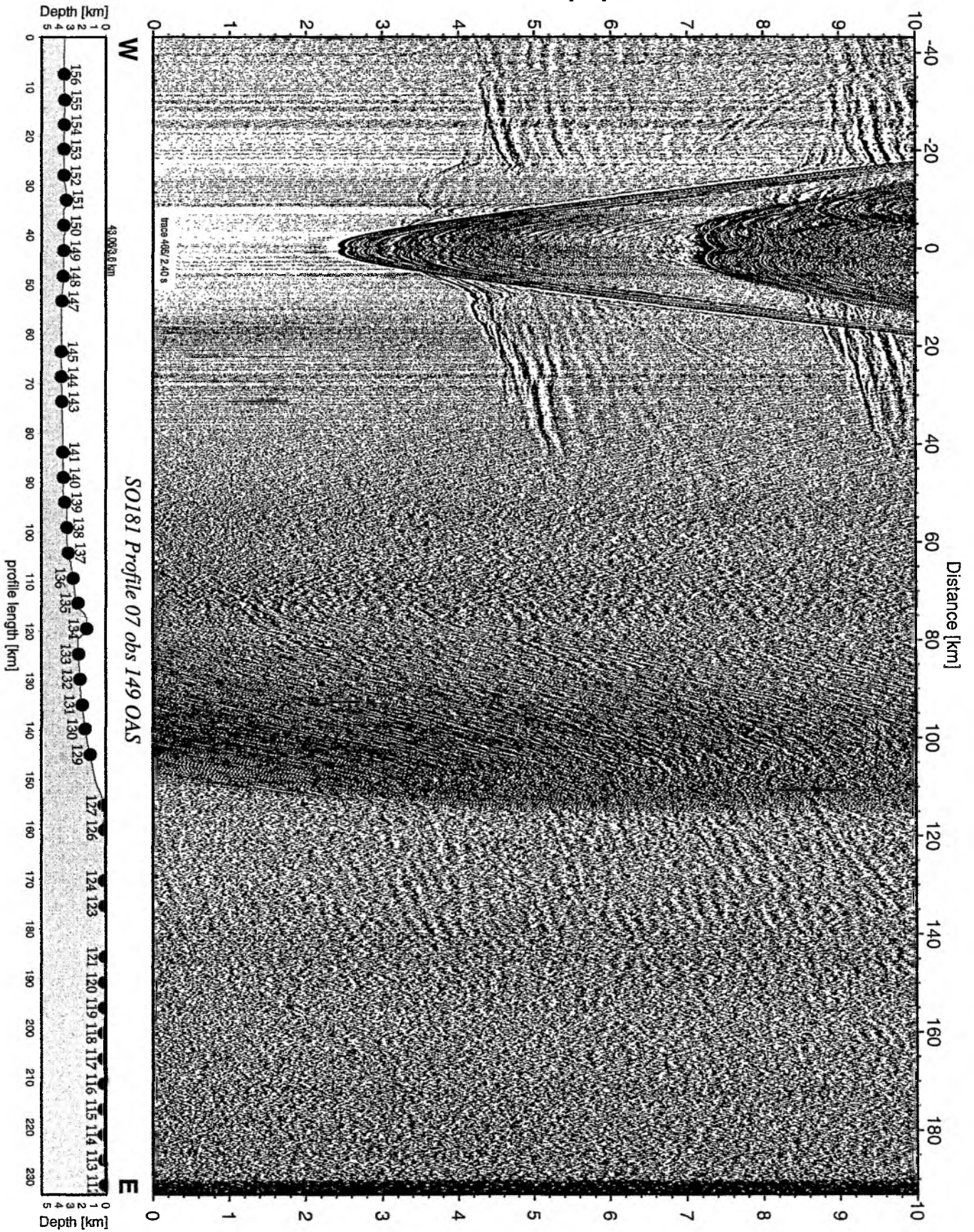


Figure 6.6.4.47: Record section from obs 149 OAS, Profile 07.

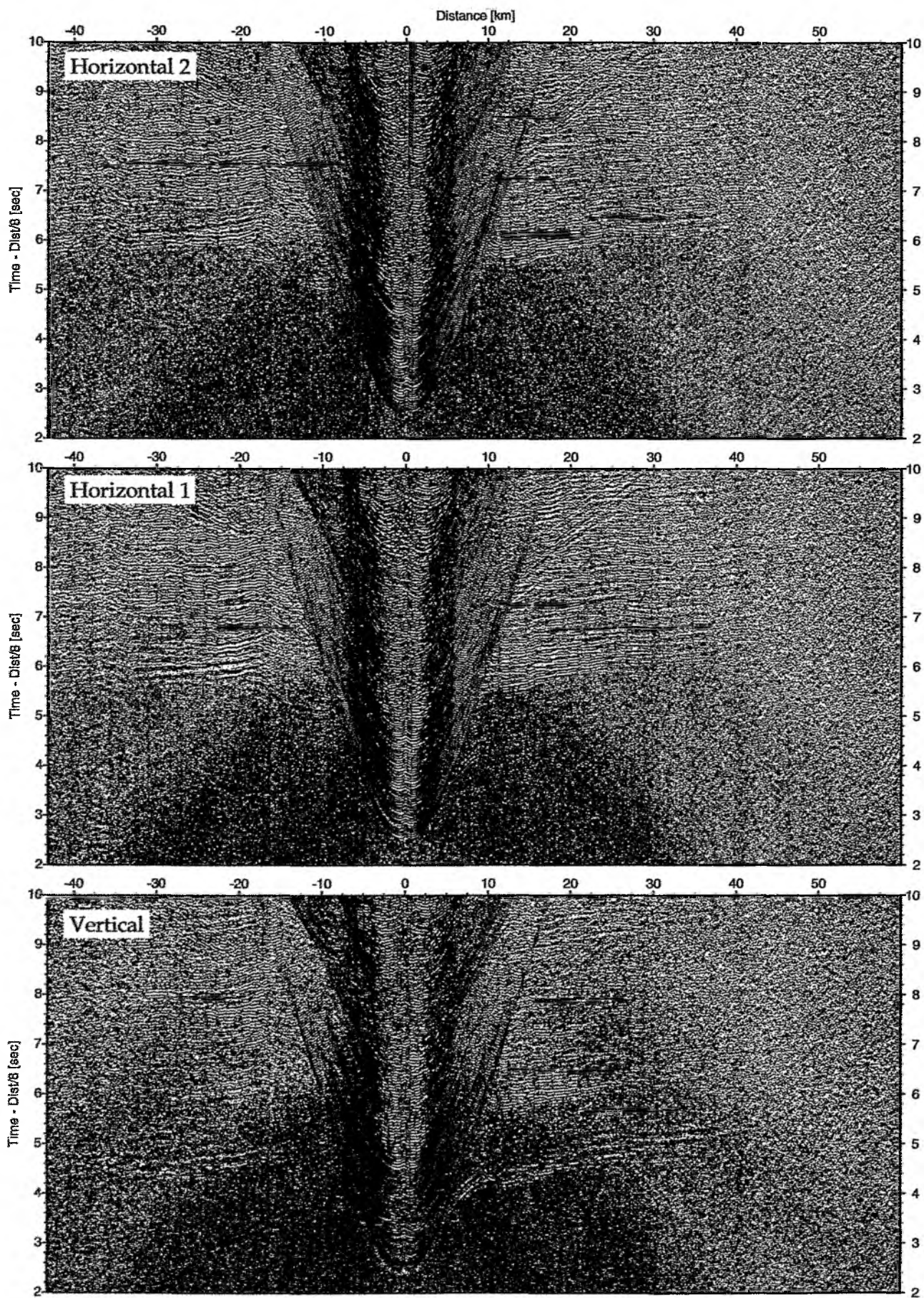


Figure 6.6.4.48: Record sections from obs 149 OAS/Owen-4.5Hz, SO181 Profile 07.

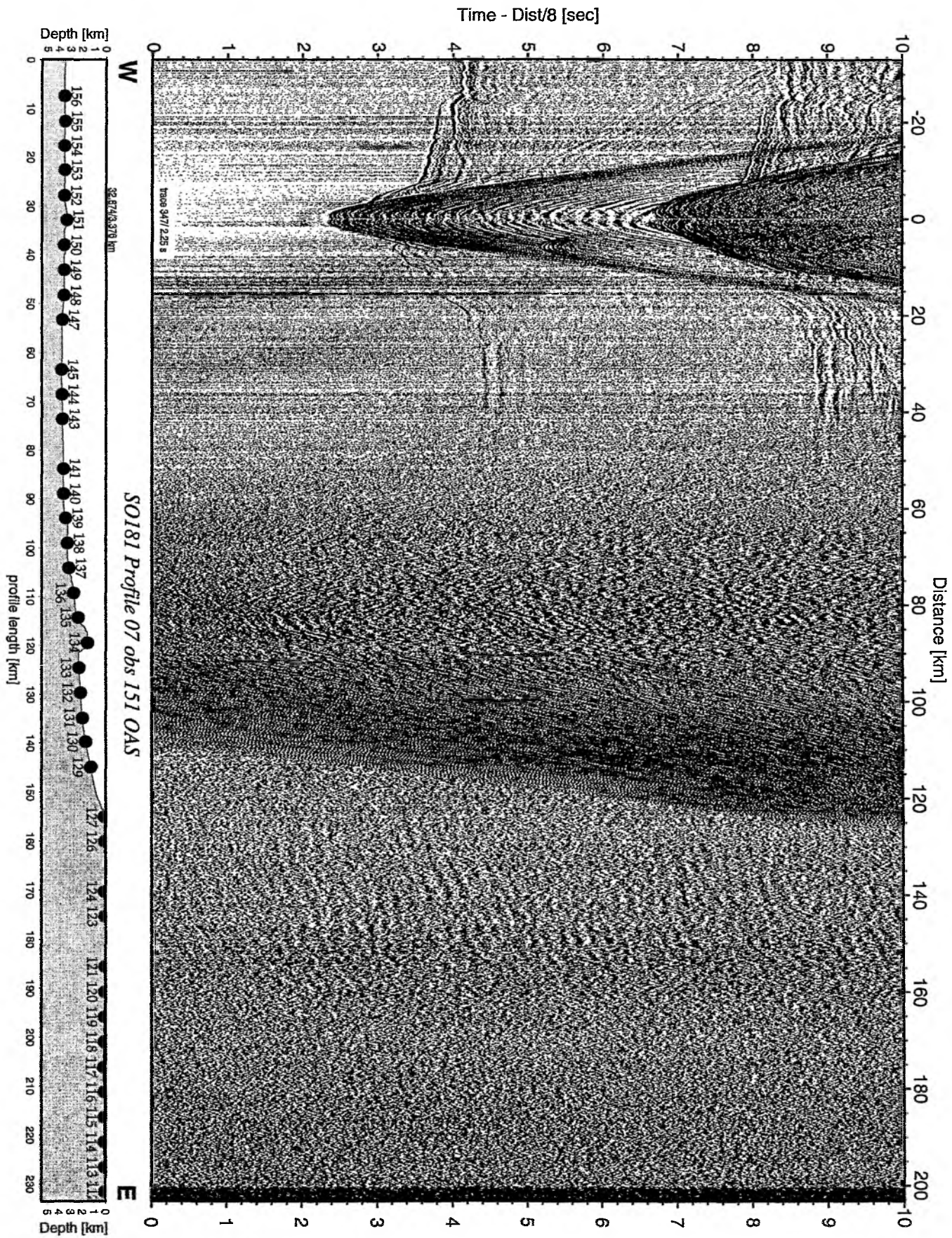


Figure 6.6.4.49: Record section from obs 151 OAS, Profile 07.

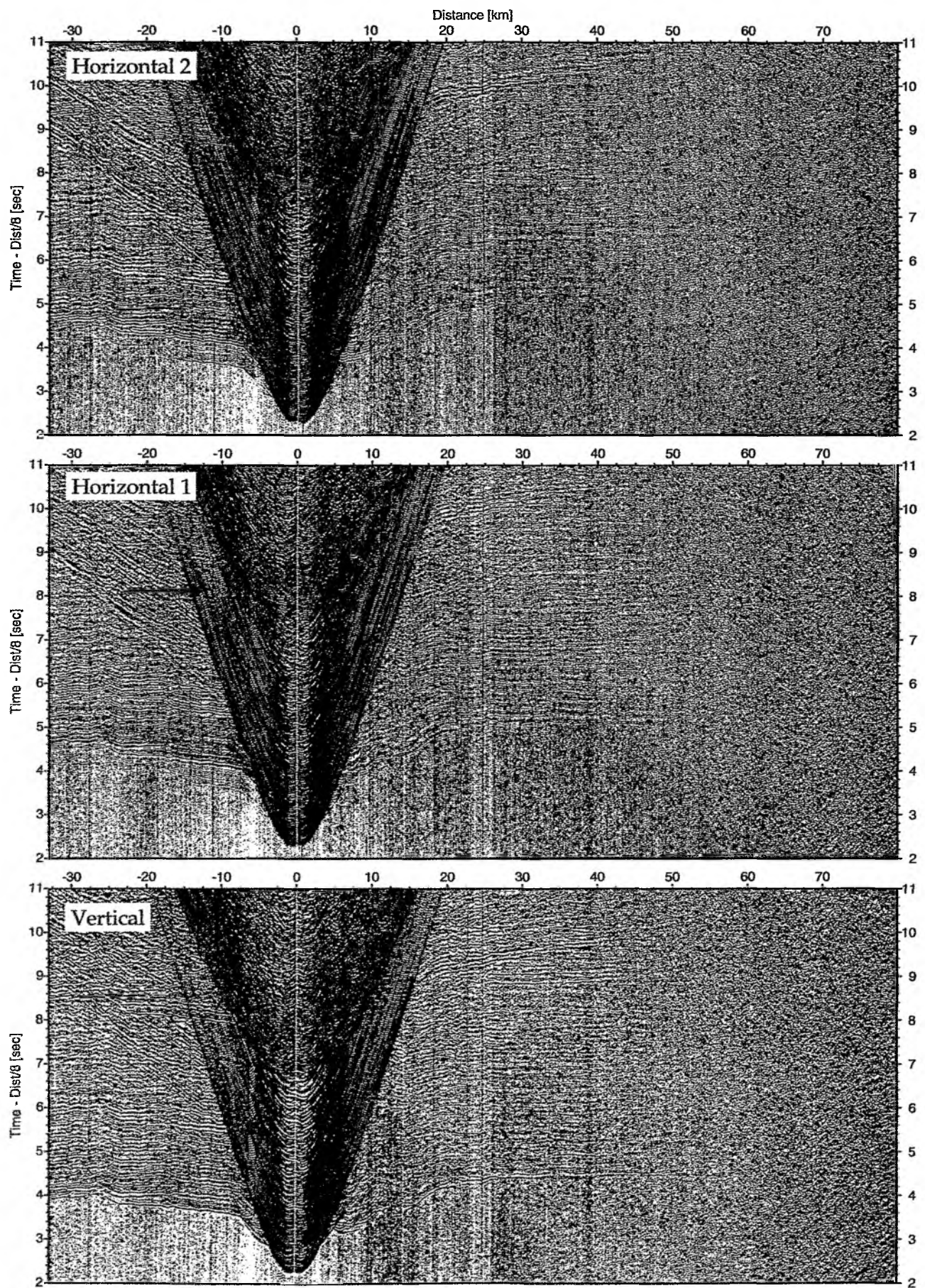


Figure 6.6.4.50: Record sections from obs 151 OAS/Owen-4.5Hz, SO181 Profile 07.

Time - Dist/8 [sec]

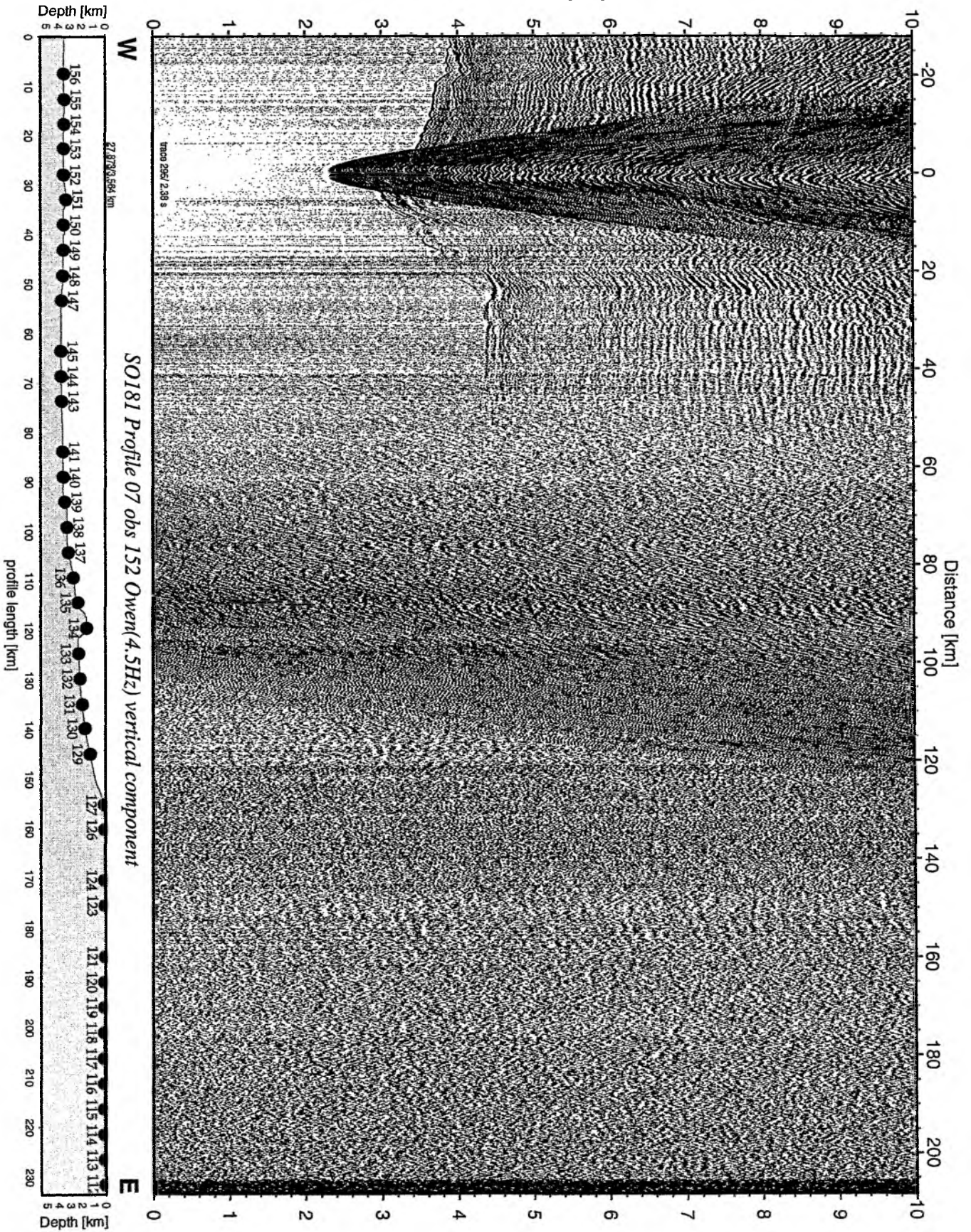


Figure 6.6.451: Record section from obs 152 Owen(4.5Hz) vertical component, Profil

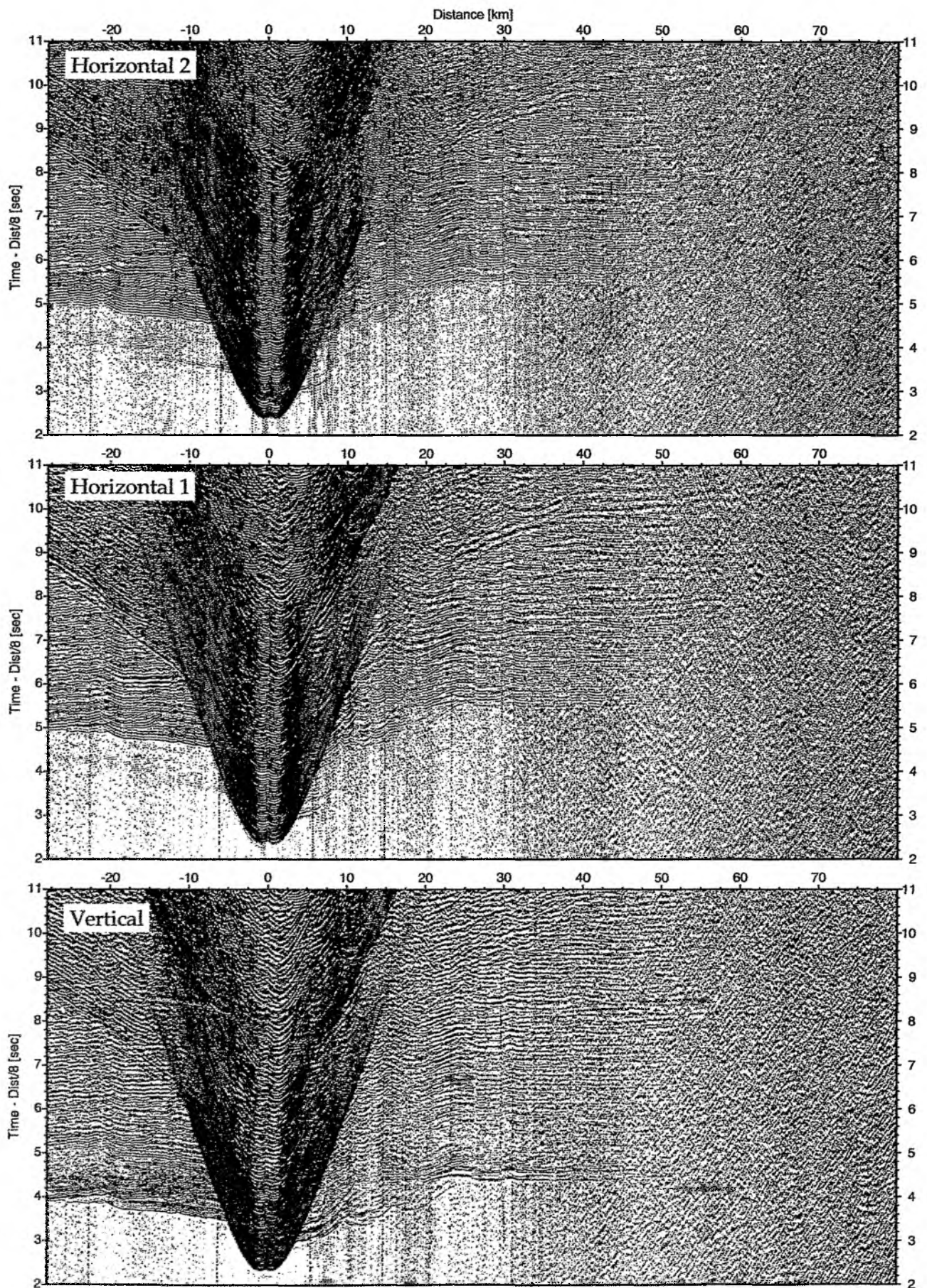


Figure 6.6.4.52: Record sections from obs 152 OAS/Owen-4.5Hz, SO181 Profile 07.

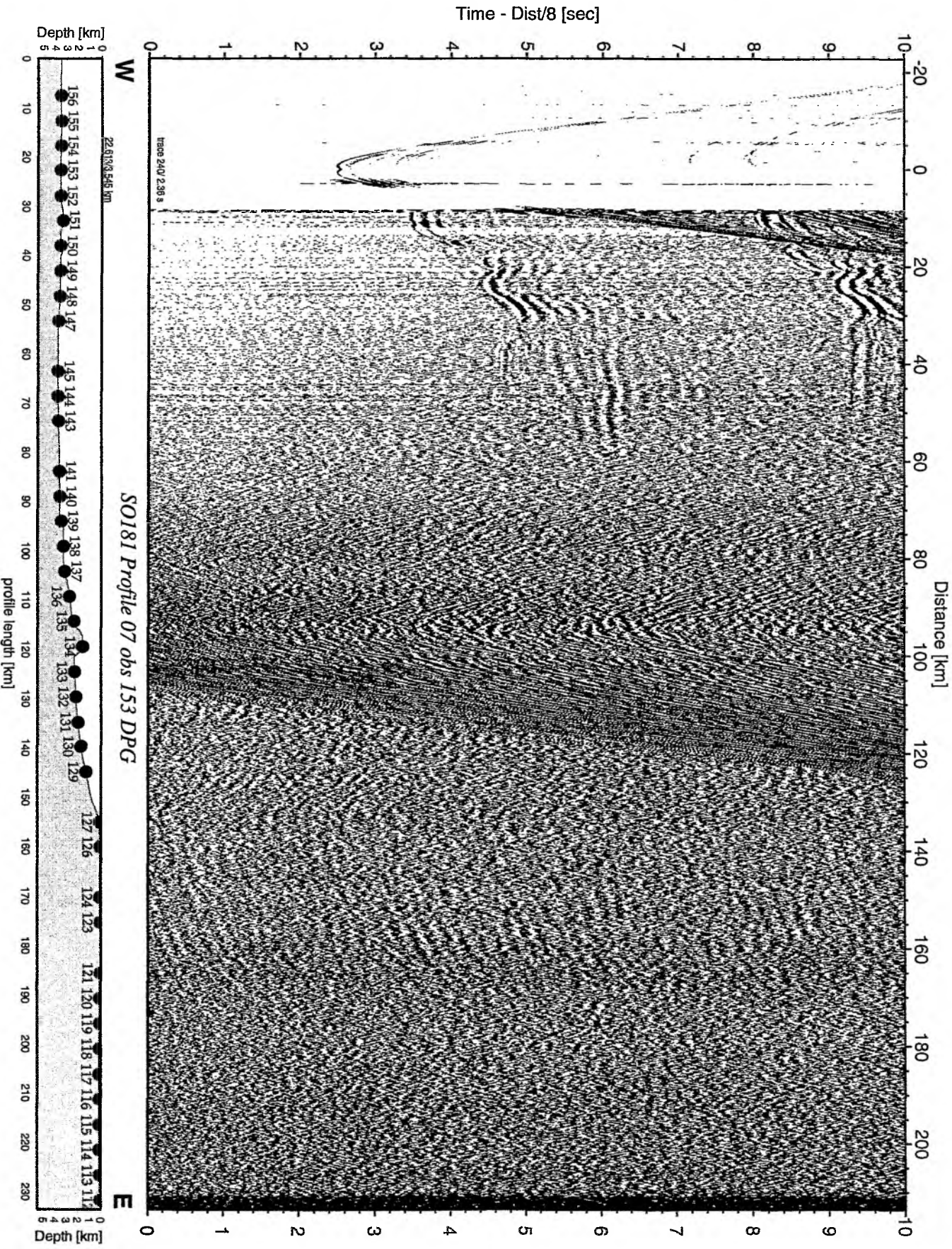


Figure 6.6.4.53: Record section from obs 153 DPG, Profile 07.

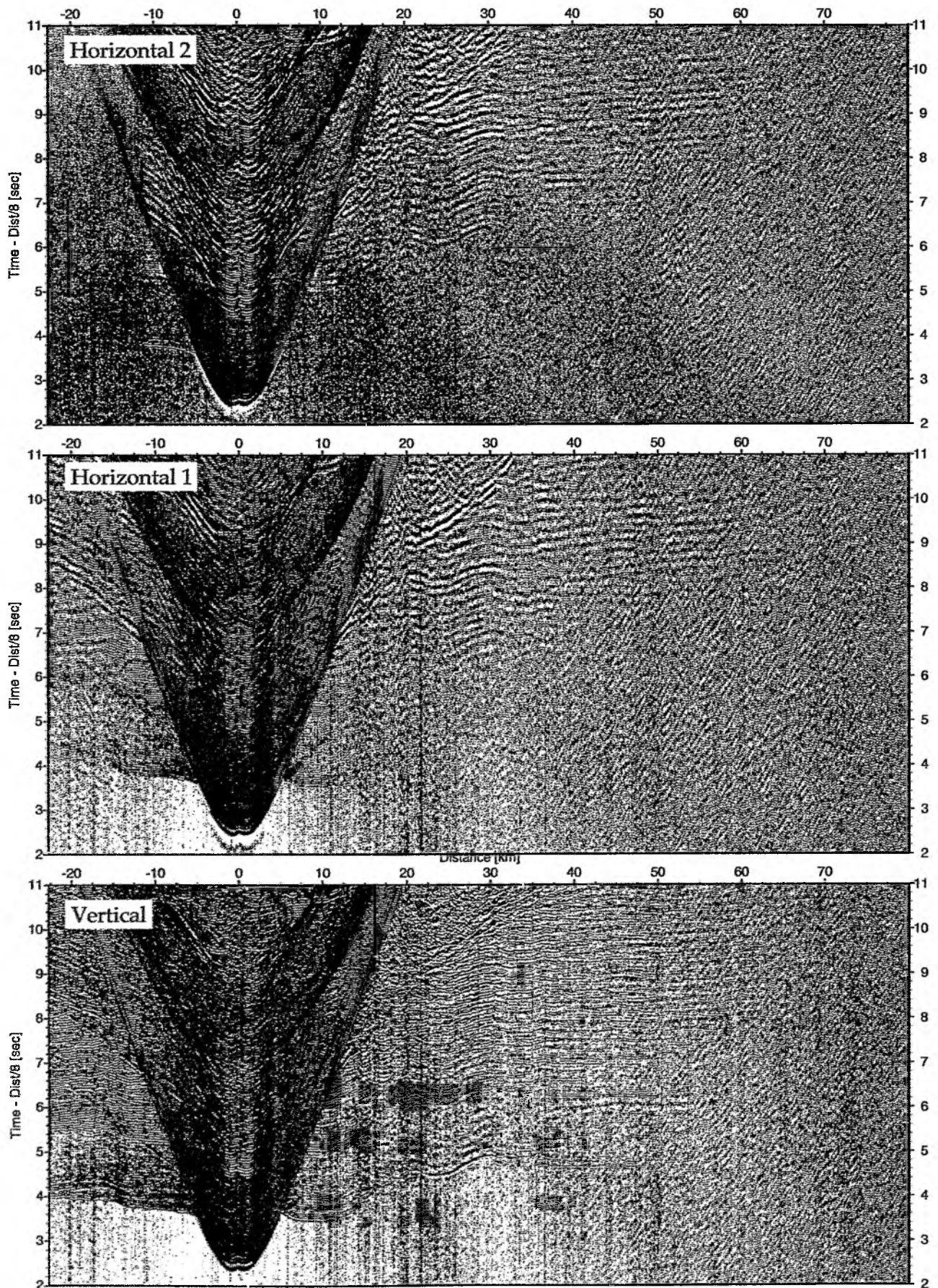


Figure 6.6.4.54: Record sections from obs 153 DPG/WEBB, SO181 Profile 07.

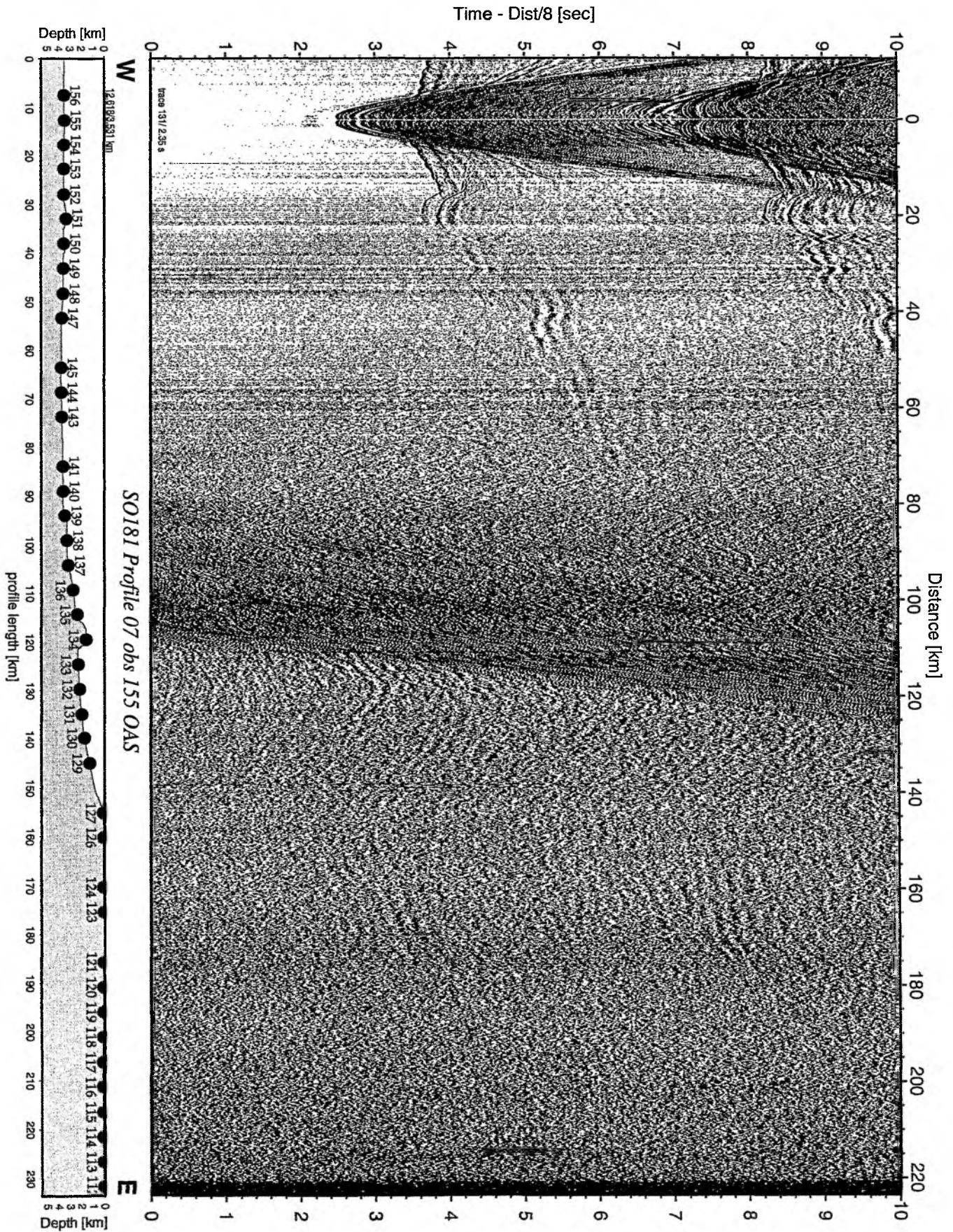


Figure 6.6.4.55: Record section from obs 155 OAS, Profile 07.

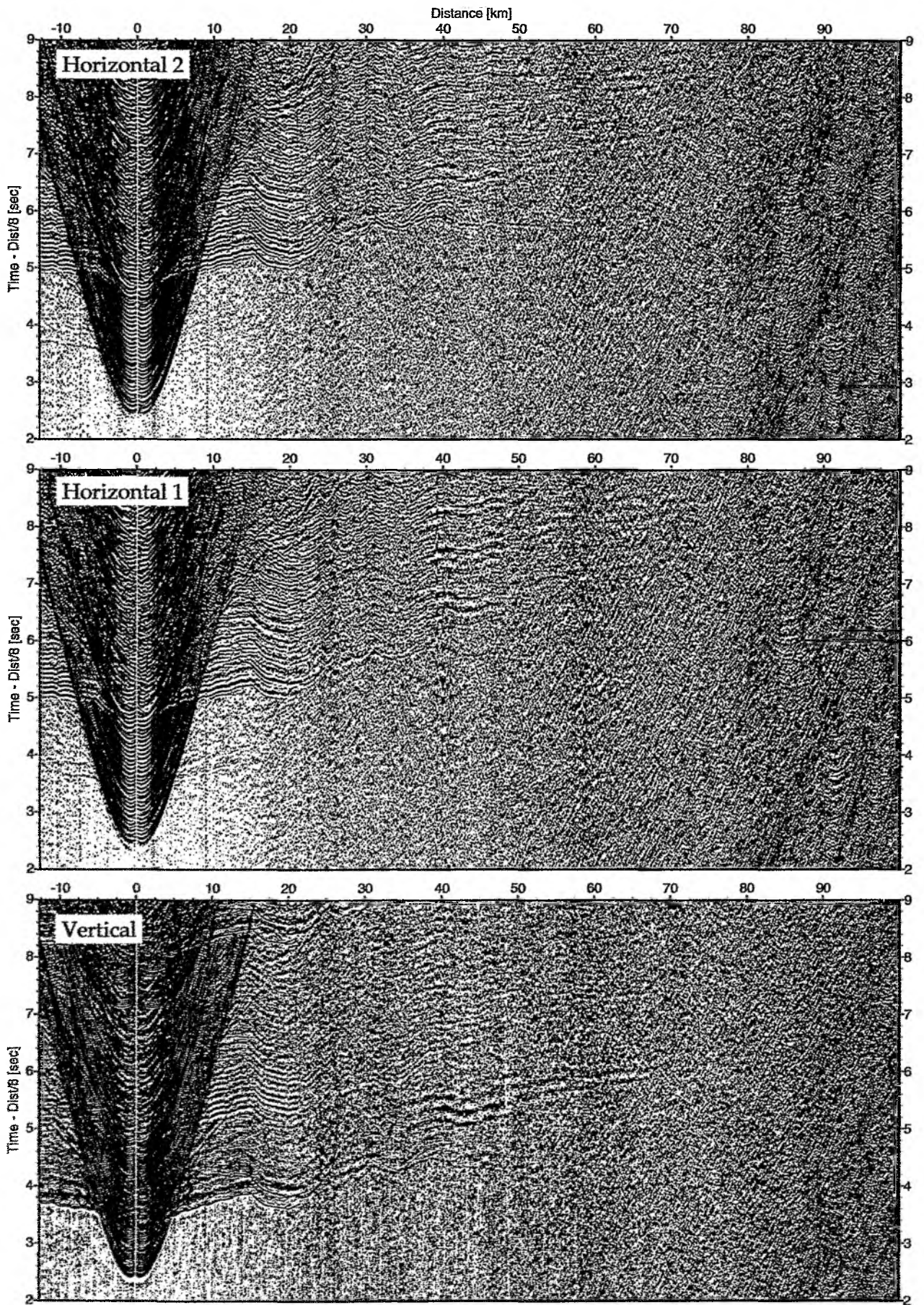


Figure 6.6.4.56: Record sections from obs 155 OAS/Owen-4.5Hz, SO181 Profile 07.

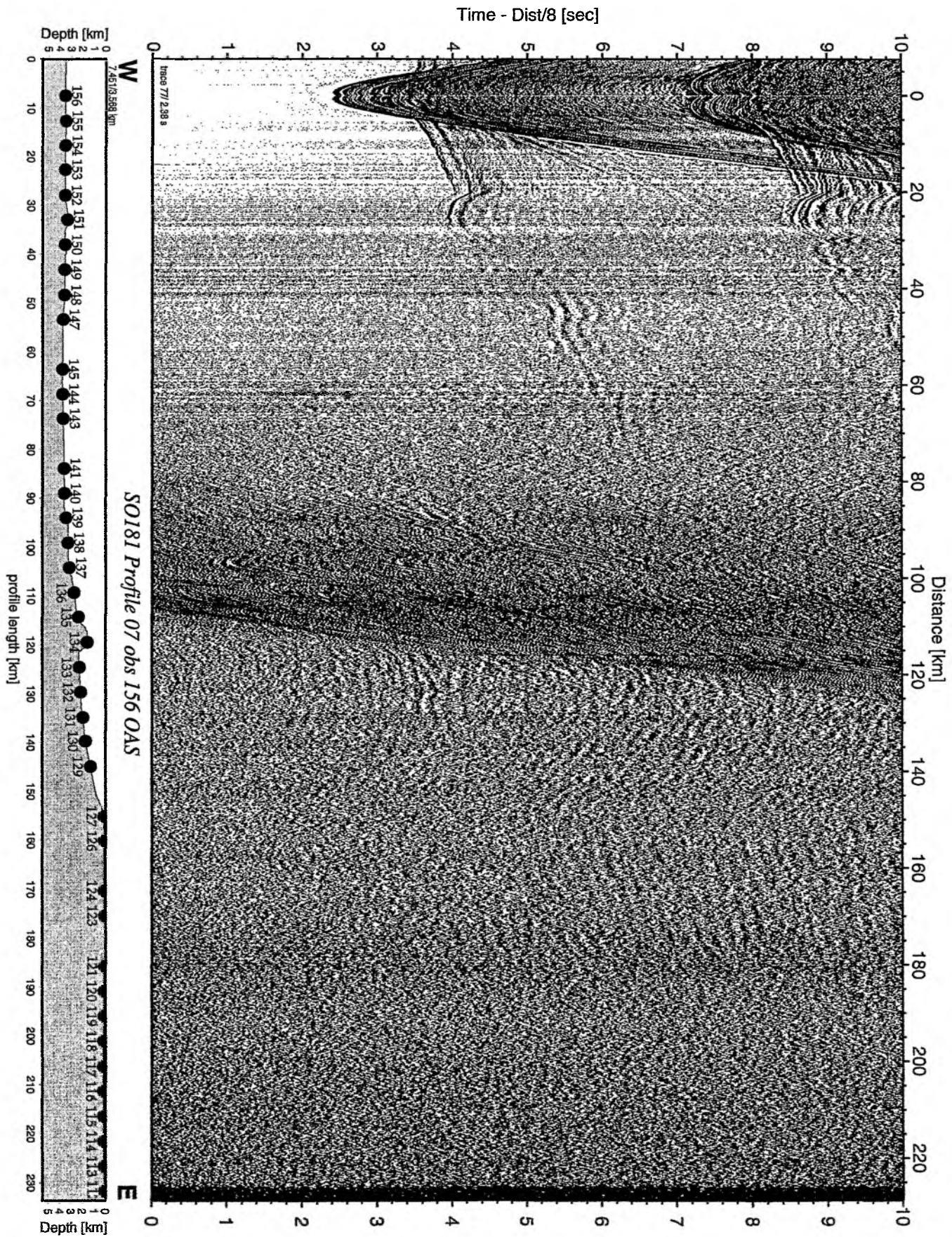


Figure 6.6.4.57: Record section from obs 156 OAS, Profile 07.

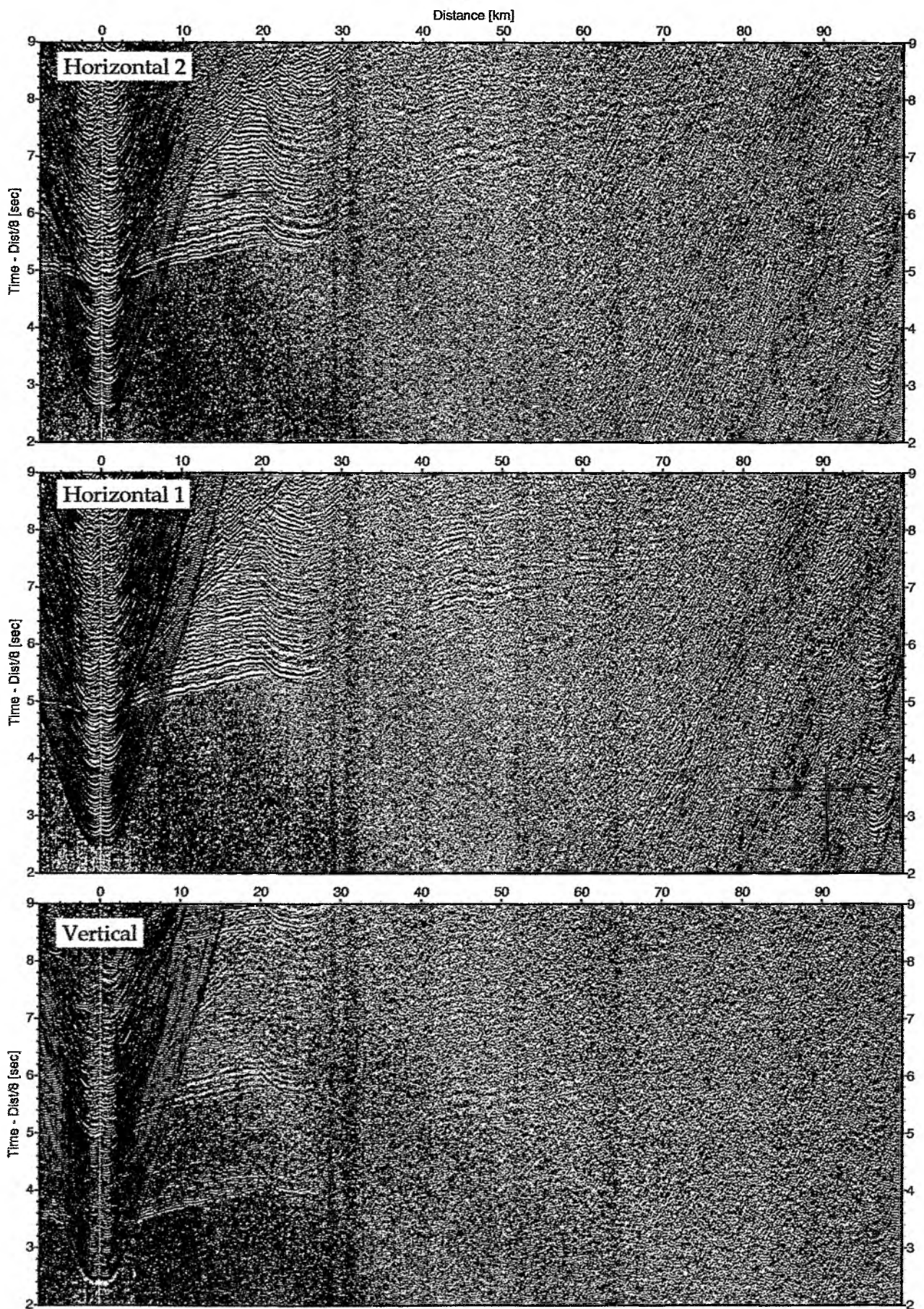


Figure 6.6.4.58: Record sections from obs 156 OAS/Owen-4.5Hz, SO181 Profile 07.

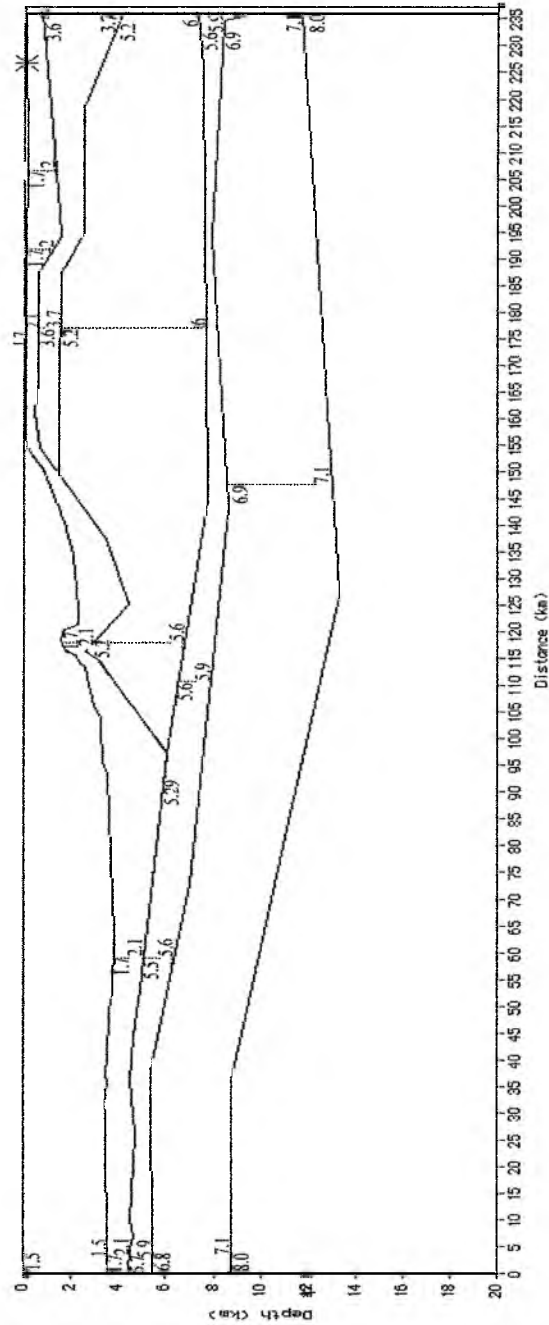


Figure 6.6.4.59: Preliminary model of Profile P07. The western, oceanic part of the model consists of a water and one sedimentary layer, an upper and a lower oceanic crust, whereas the eastern, continental part across the shelf has a two sedimentary layers below the water, plus thicker, continental crust. No phase from the continental mantle has been identified, therefore the entire model is underlain only by oceanic mantle.

6.6.5 Profile P08

This profile was shot between $45^{\circ} 10' \text{ S}$ and $45^{\circ} 53' \text{ S}$, about 200 km from the coastline out to sea. The line is parallel to fracture zones surrounding the subducting spreading ridge system and lies about one degree north of the triple junction. Along this profile 37 instruments were deployed from the Chile Rise to the coast between 02 and 03 Feb. Shooting was done in almost perfect conditions from 17:00 on 03 Feb to 09:00 on 05 Feb. All four G-gun cluster remained in operation during the shooting. For a short period of time a Bolt gun was fired in addition to the G-guns to investigate a possible improvement of the signal strength. A four channel streamer was deployed throughout the profile, augmenting existing MCS data for parts of the profile. Instruments were picked up once shooting was terminated. They were all back onboard by 10:30 on 06 Feb. Details of instruments and shots can be found in Appendices 9.2 and 9.3; most instruments recorded well. A location map is shown in Figure 6.6.5.1, and record sections are shown in Figures 6.6.5.2 to 6.6.5.47.

A preliminary onboard analysis was attempted, taking also the results (sediment thickness) from the seismic reflection data into account. The high quality data exhibit reflections off the subducting, recorded on instruments as far out as the continental margin (OBS 157). For a distance of about twenty kilometres in the centre of the profile, however, a trigger error resulted in double shots and hence less clear arrival times. A triggering time delay of about 135 ms was factored into the modelling process. Some stations, however, showed anomalous time shifts of up to five seconds in one extreme example; these were individually edited to allow for sensible arrival times.

The Oceanic Plate

A sedimentary layer, upper and lower crust have been modelled to fit the observed refraction and in a few cases also reflection arrivals from the hydrophones of 13 stations in the outermost 100 km of the profile. A rough model has been assembled for this part of the profile, exhibiting some noteworthy features Figure 6.5.48.

For the sedimentary layer a slow p-wave velocity of 1.6 to 1.7 km/s in the western part of the model and 1.7 to 1.8 km/s for the sediments above the older crust in the eastern part of the plate was fixed and the thickness of the layer adjusted to fit the observed data. As already proposed by multi-channel streamer data, the oceanic crust between the spreading centre and the subduction zone seems to show several undulations filled with sediments.

In the upper crust velocities of about 4.6 to 5.5 km/s, in the lower crust 6.5 to 7.7 km/s have been estimated. Though no clear evidence can be given yet, the data seem to support a lower velocity for the crust in the spreading centre.

The subduction zone has not been modelled accurately so far, but the data from station 177 at km 92 of the profile, showing very good near offset reflections supposedly from the upper and lower boundary of the subducting oceanic sediments should in combination with stations from the eastern part of the profile offer quite some potential for further studies.

The Continental Margin

The analysis of the continental margin was focused on the structure of the uppermost five kilometres. Although in places strong reflections are present, priority was given to refracted arrivals, with reflections being used only as a rough guide, leading to the preliminary model shown here (Figure 6.6.5.49).

The shallow structure of the continental margin consists of sedimentary layers upon basement rock. At the easternmost edge of the profile, the basement is particularly shallow, however this seems reasonable because of the adjacent land exhibits fiorded mountains rising steeply out of the ocean. The basement dips westwards to around three kilometres below the uppermost sediments, effecting rather asymmetric first arrivals about nearby stations. Following this dip, there is a small trough before a sudden rise to about 2 km depth, and then a gradual dipping towards the subduction interface.

The sharp rise after the trough could be due to a large fault or series of faults. Evidence to support this proposition is threefold: there is a corresponding sudden contrast in bathymetry directly above the basement rise; the sediments show a similar steep ascent; finally, there is a marked basement velocity shift across this line, with values around 5.3 km/s to the east and 4.4 km/s to the west. The lower velocities in the west are likely the result of large-scale fracturing caused by stresses from the subducting plate. A fault such as this, however, cannot be clearly seen in the streamer data.

Above the basement are at least two distinct layers of slower velocity material. The lower layer could possibly be divided yet again, particularly in the west but has been treated as a single entity for reasons of simplicity. Its velocities range between 2.4 km/s and 2.7 km/s at its upper surface, increasing to 3.0-3.2 km/s just above the basement rock. It is thin to non-existent as the basement rises the surface in the east, but quickly settles on a thickness of around 2 km once the basement is sufficiently deep. Just to the west of the proposed fault mentioned above, the basement once more becomes shallow and the top of the lower sedimentary layer has been eroded to a flat surface just below sea level.

The upper sedimentary layer has slow velocities between 1.7 km/s and 1.8 km/s and corresponds to recent depositions. Its thickness is mostly around 0.5 km, except where the layer below is too shallow for this. The velocity and thickness of this uppermost layer, however, is not particularly well constrained since its refracted arrivals for most stations lie behind the water wave. These values are thus generally inferred by the delay in refracted arrivals from the second layer, but there is scope for the trade off between velocity and depth.

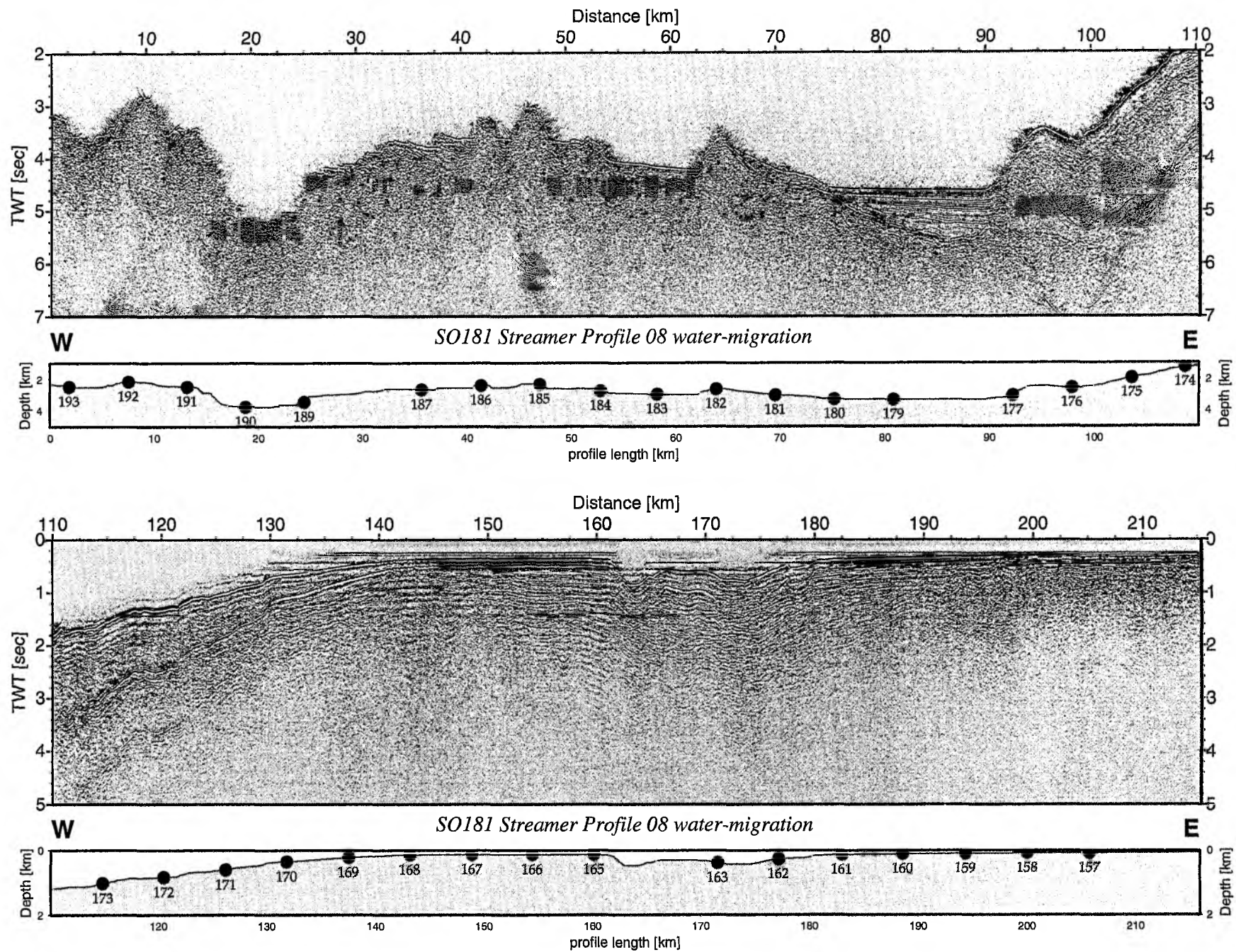


Figure 6.6.5.2: Record section from Streamer Profile 08 water-migration.

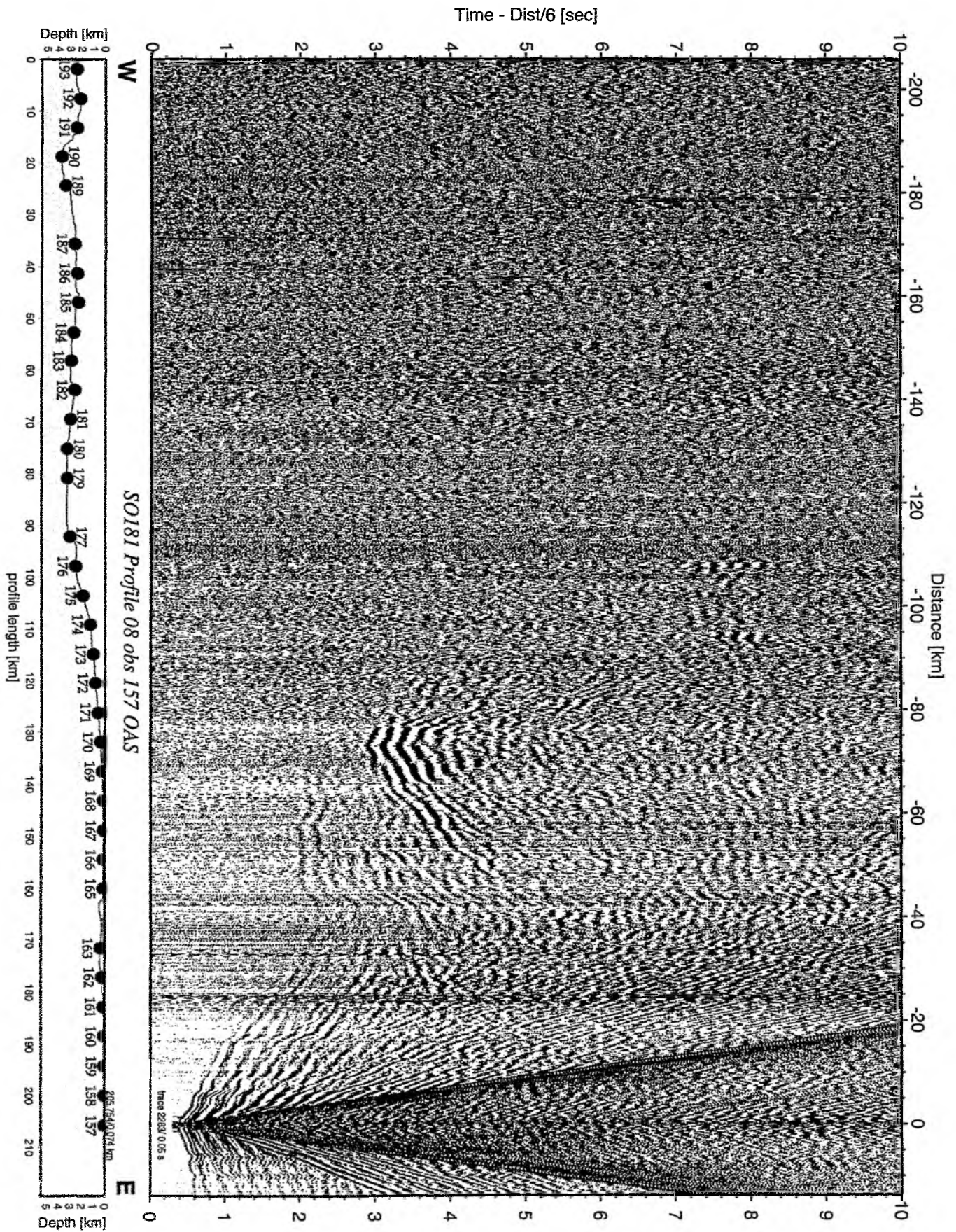


Figure 6.6.5.3: Record section from obs 157 OAS, Profile 08.

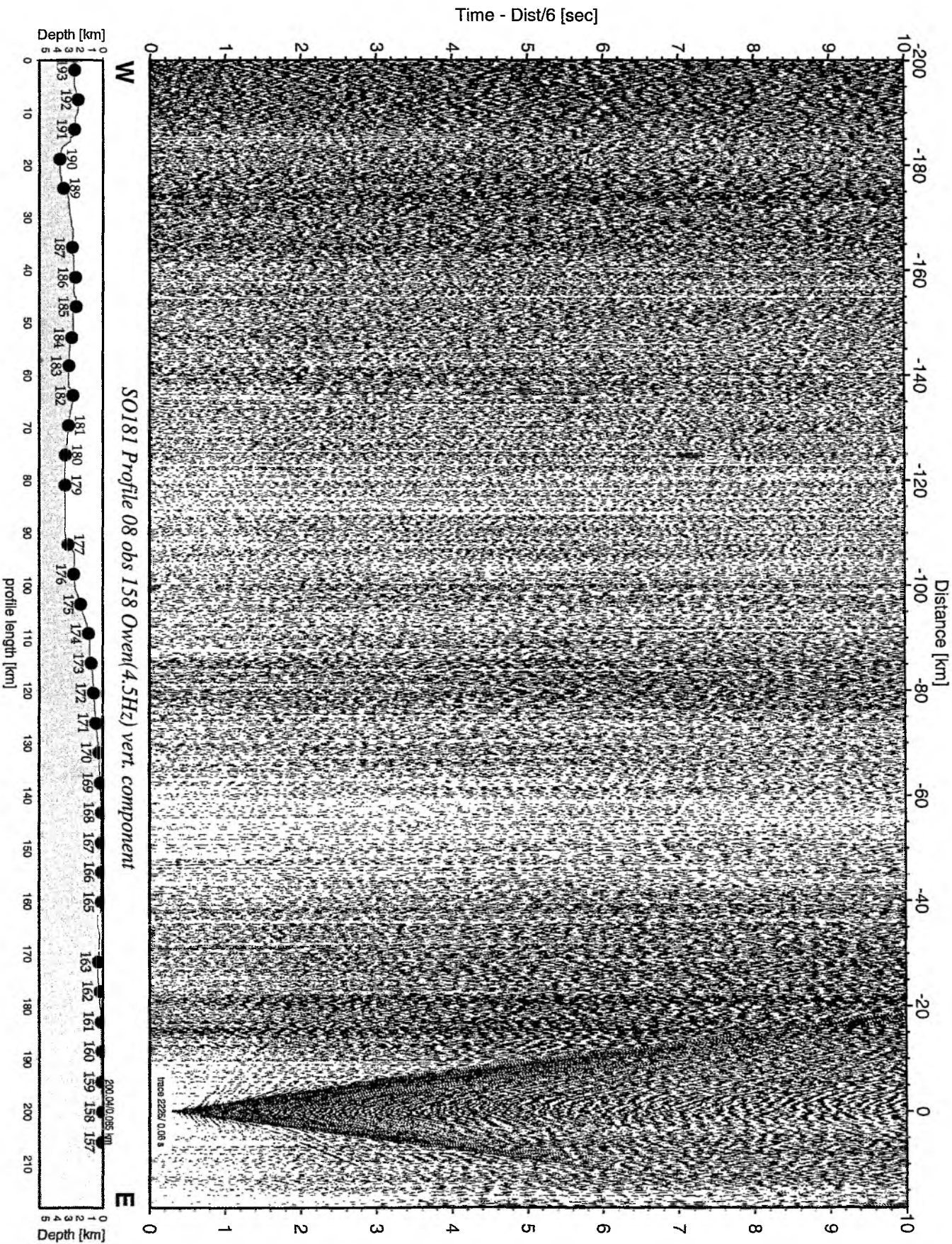


Figure 6.6.5.4: Record section from obs 158 Owen(4.5Hz) vert. component, P08.

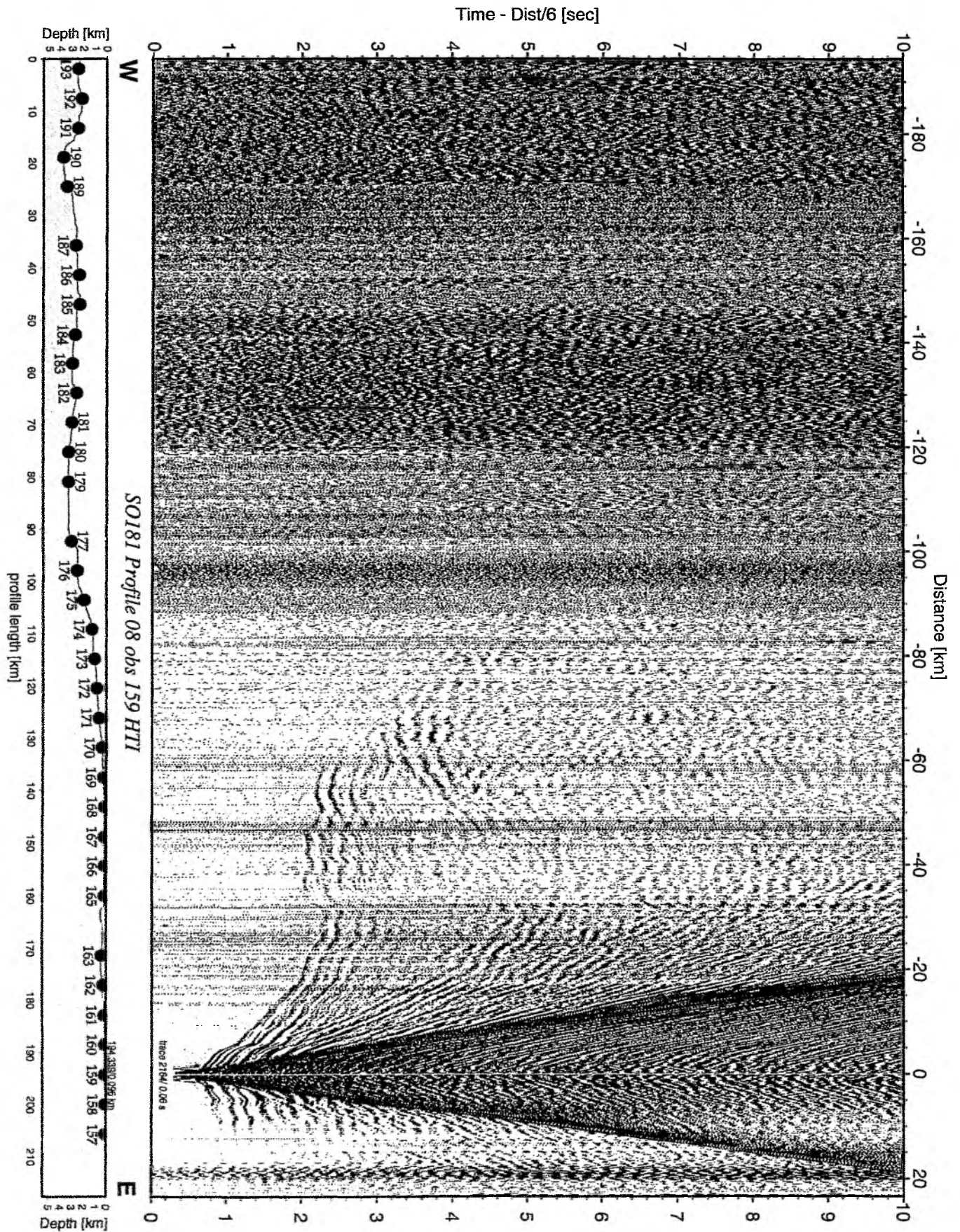


Figure 6.6.5.5: Record section from obs 159 HTI, Profile 08.

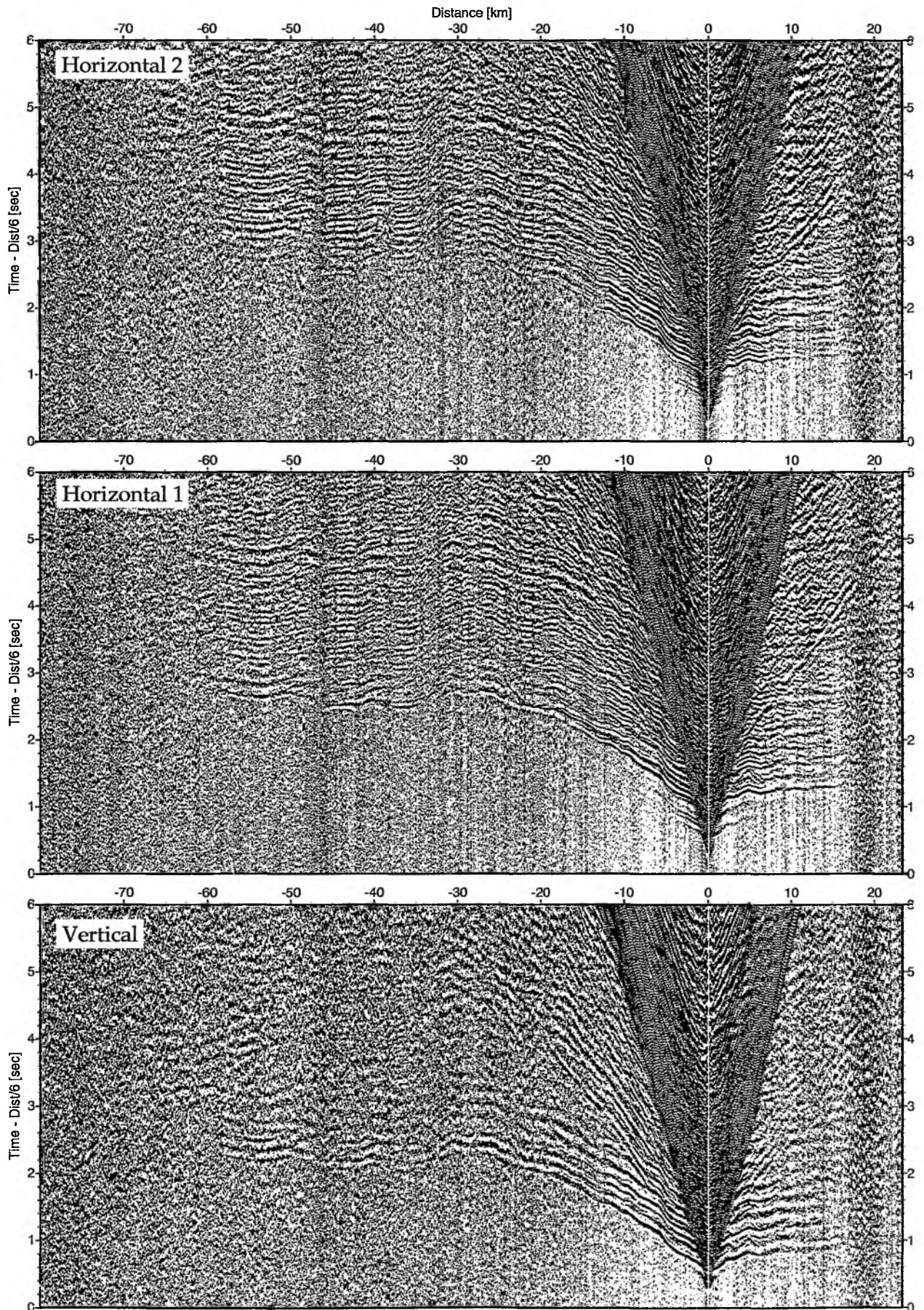


Figure 6.6.5.6: Record sections from obs 159 HTI/Owen-4.5Hz, SO181 Profile 08.

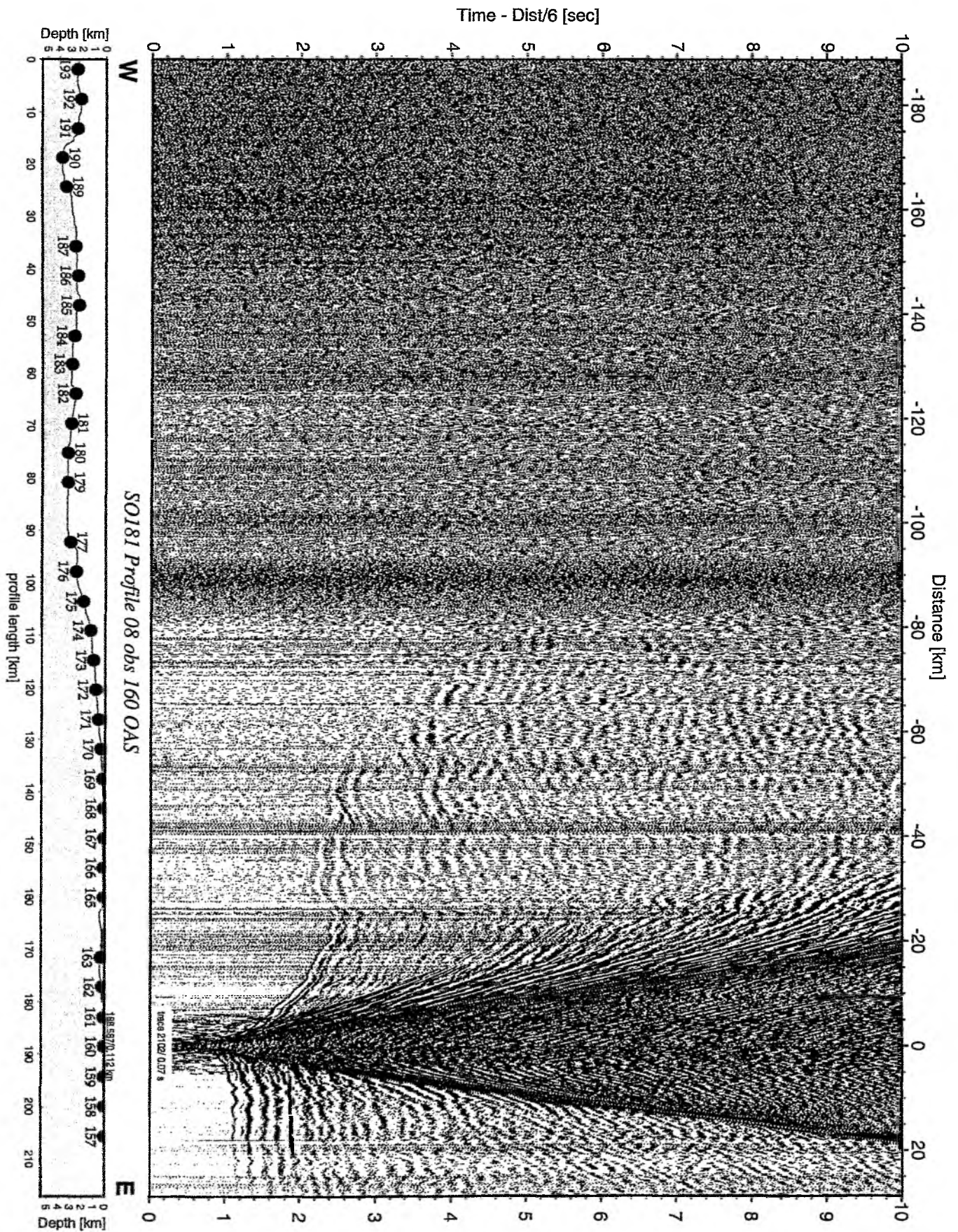


Figure 6.6.5.7: Record section from obs 160 OAS, Profile 08.

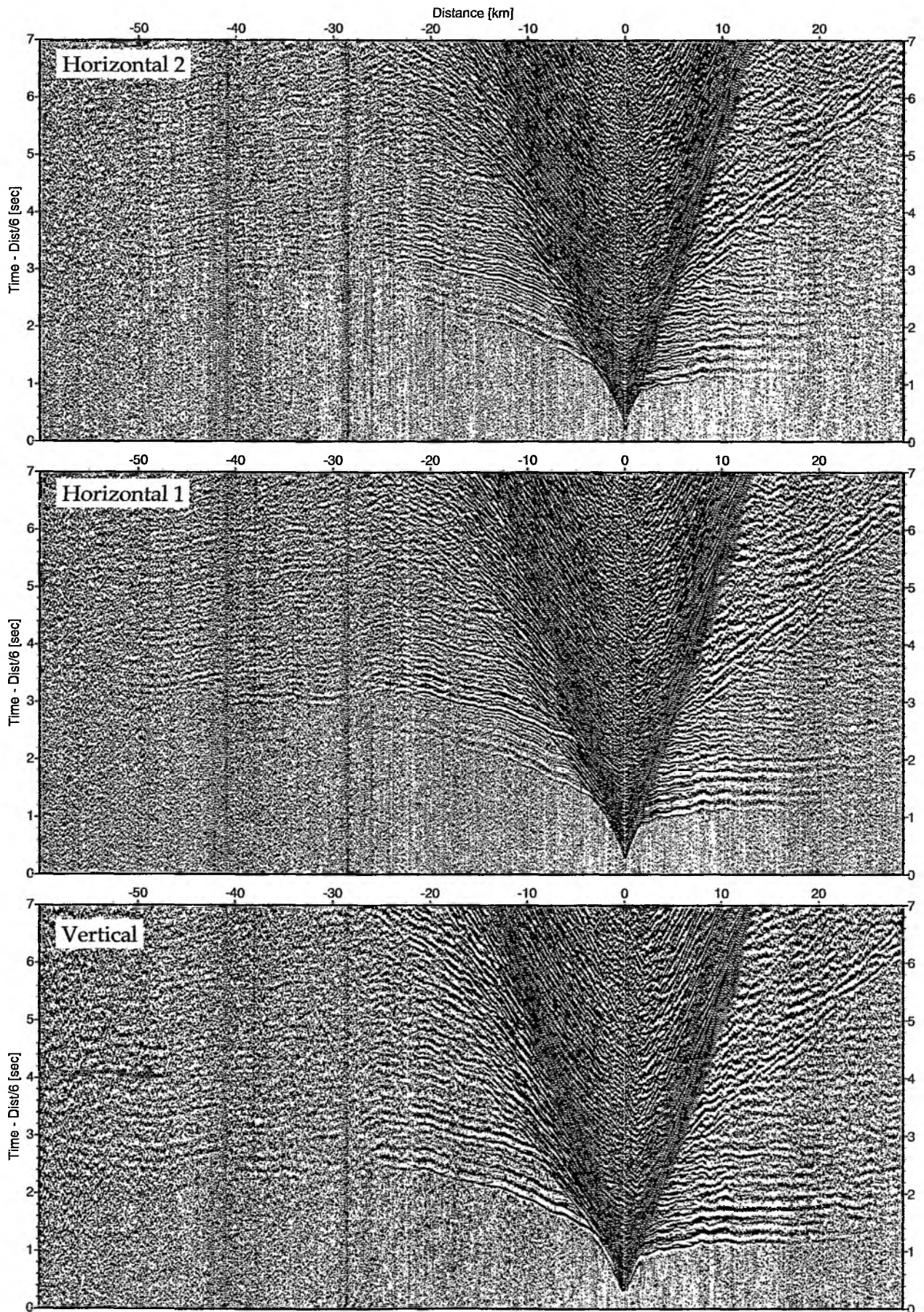


Figure 6.6.5.8: Record sections from obs 160 OAS/Owen-4.5Hz, SO181 Profile 08.

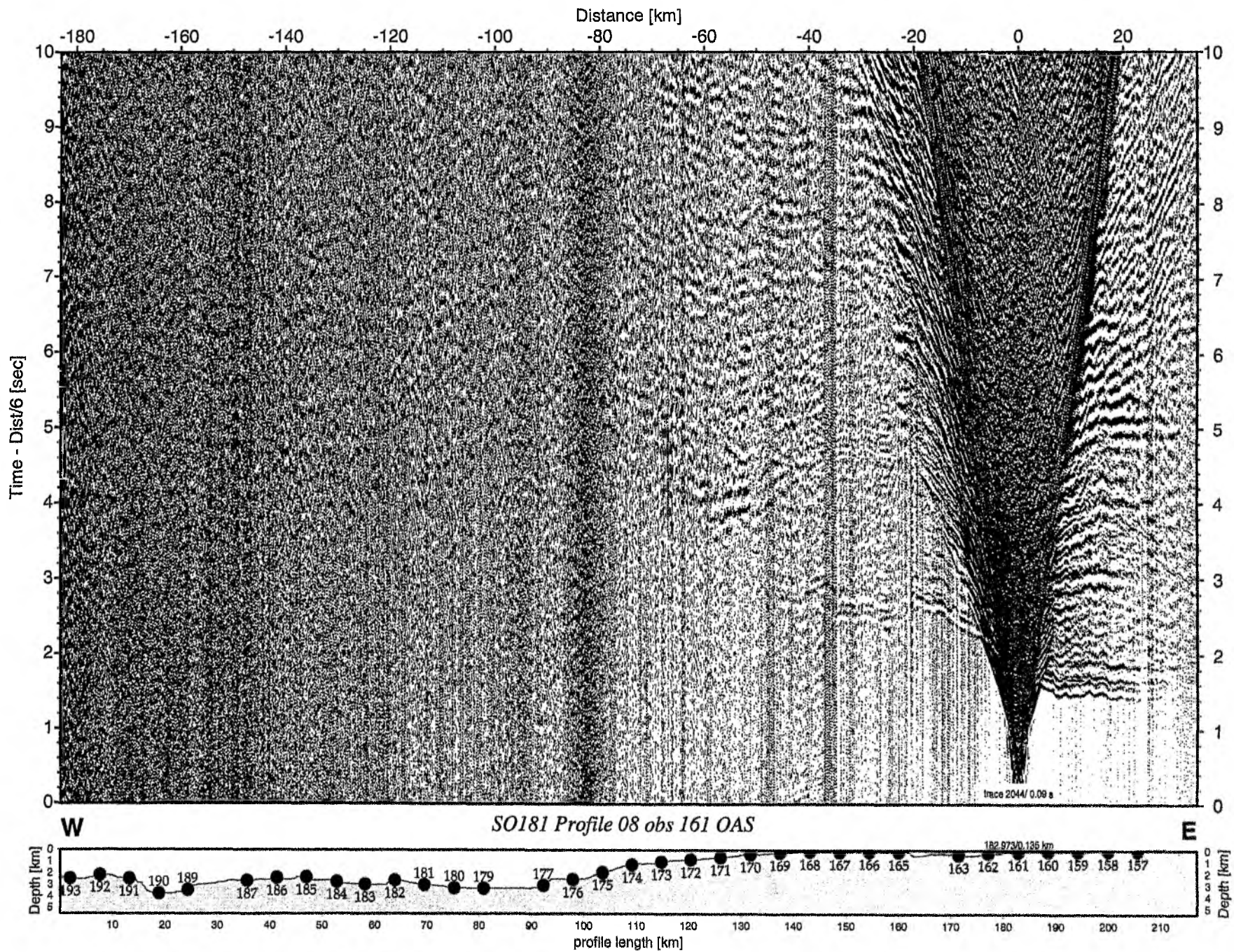


Figure 6.6.5.9: Record section from obs 161 OAS, Profile 08.

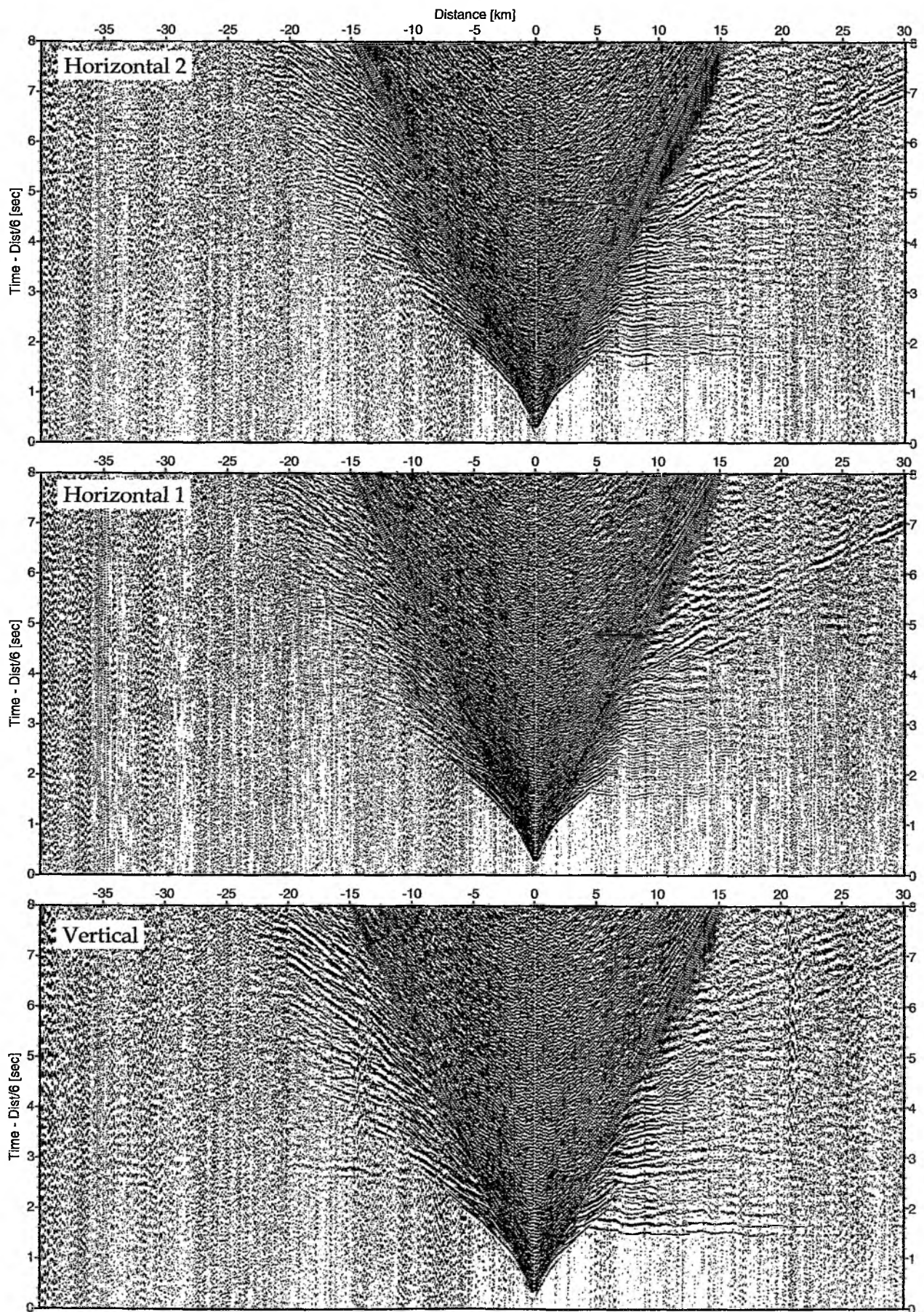


Figure 6.6.5.10: Record sections from obs 161 OAS/Owen-4.5Hz, SO181 Profile 08.

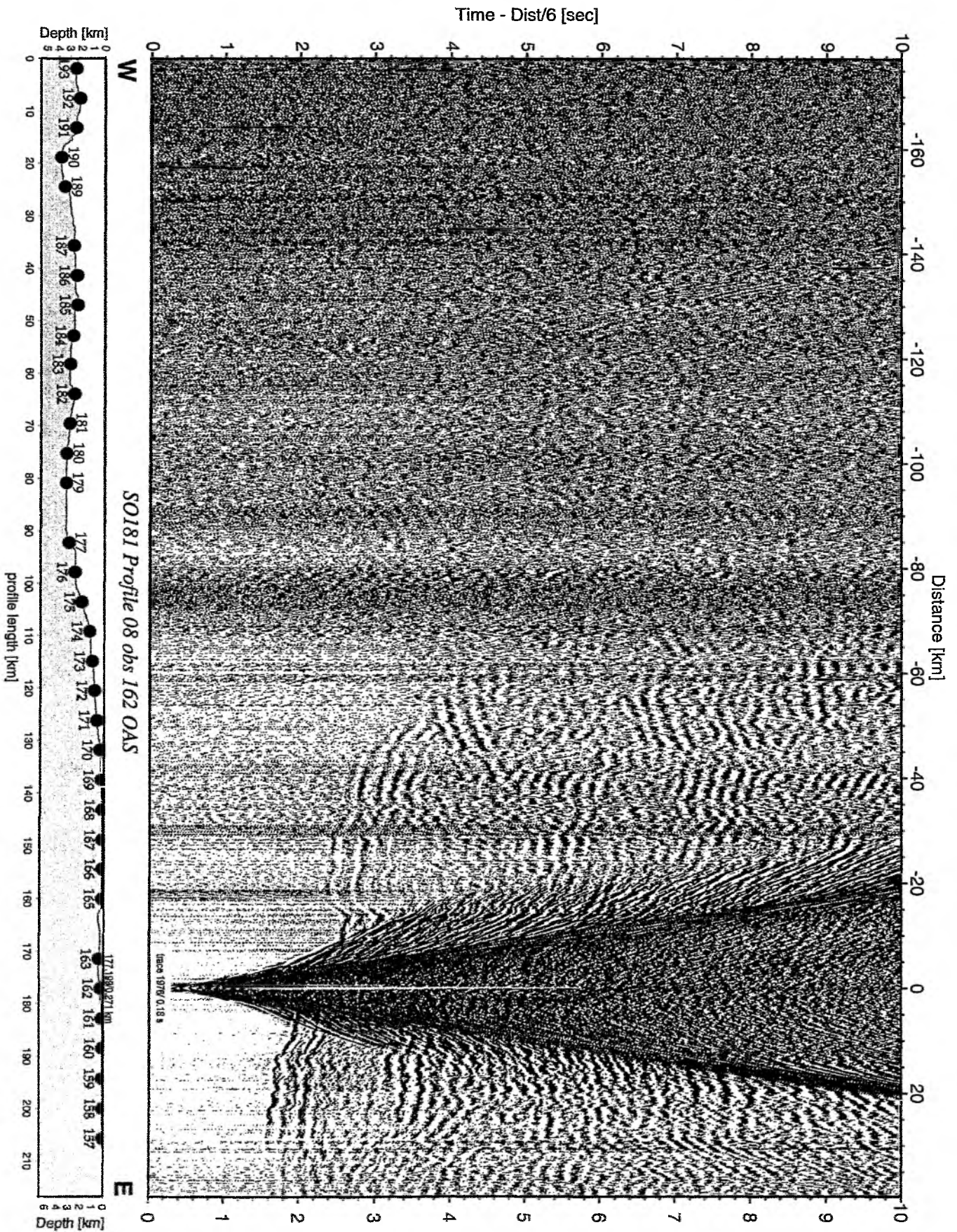


Figure 6.6.5.11: Record section from obs 162 OAS, Profile 08.

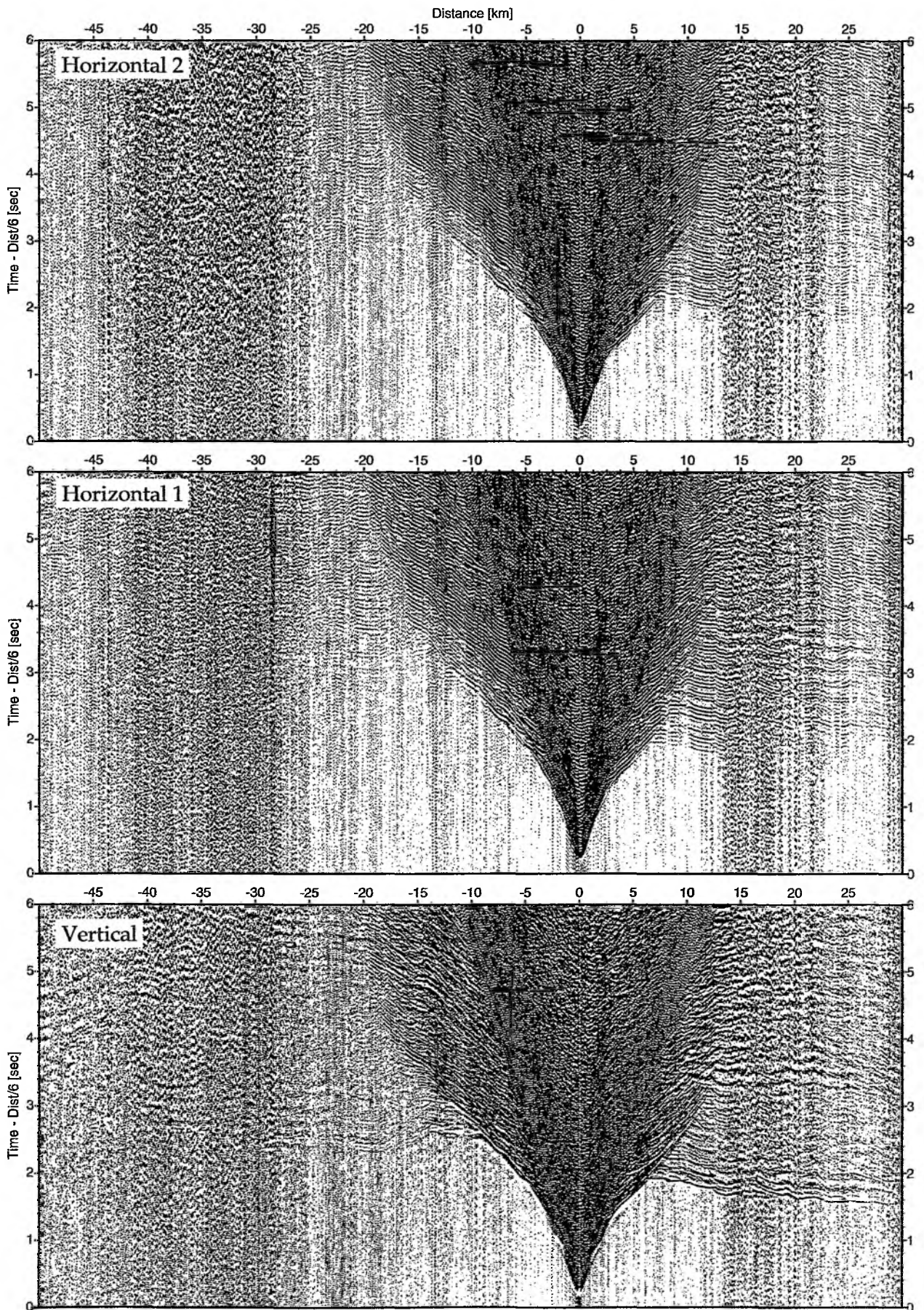


Figure 6.6.5.12: Record sections from obs 162 OAS/Owen-4.5Hz, SO181 Profile 08.

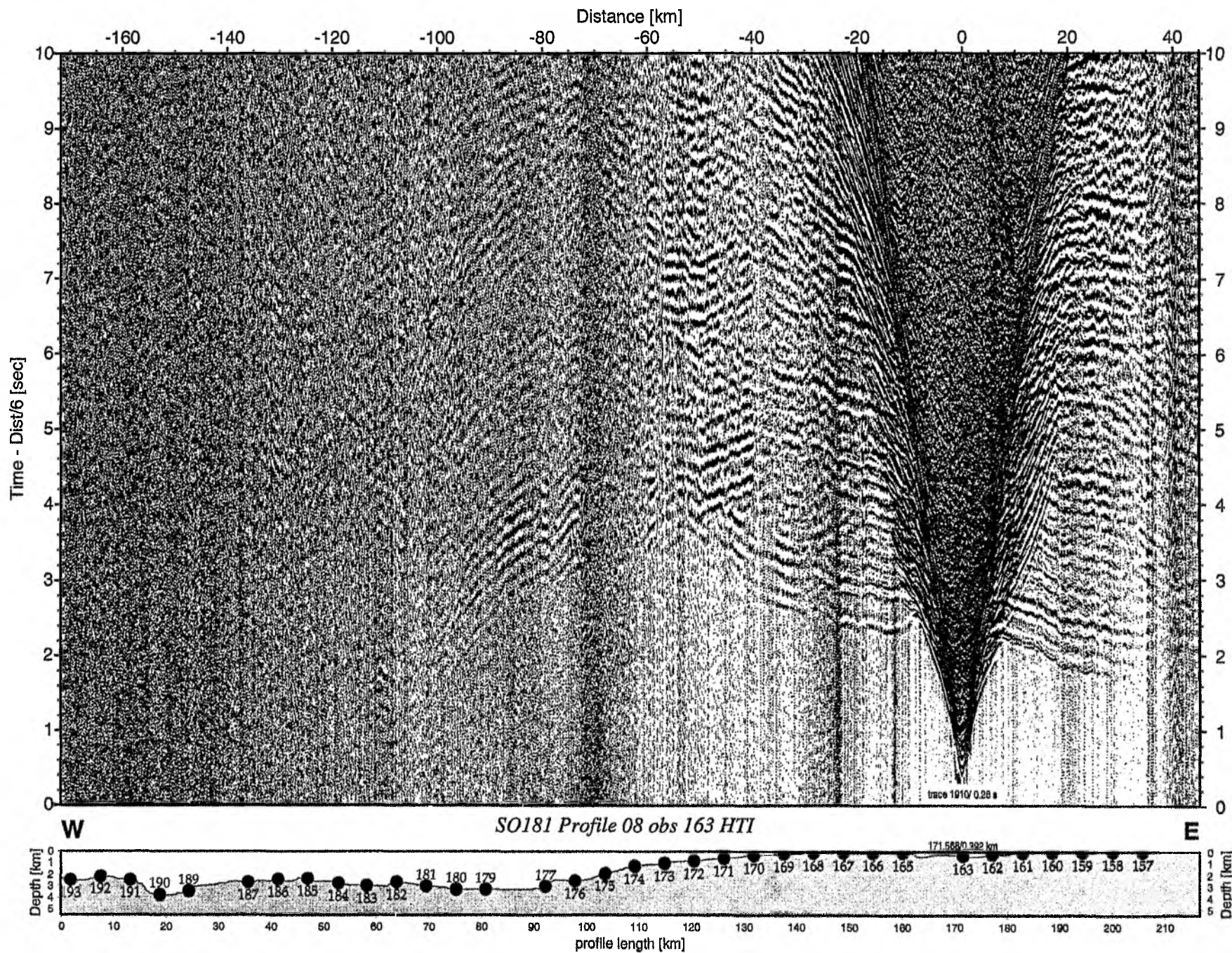


Figure 6.6.5.13: Record section from obs 163 HTI, Profile 08.

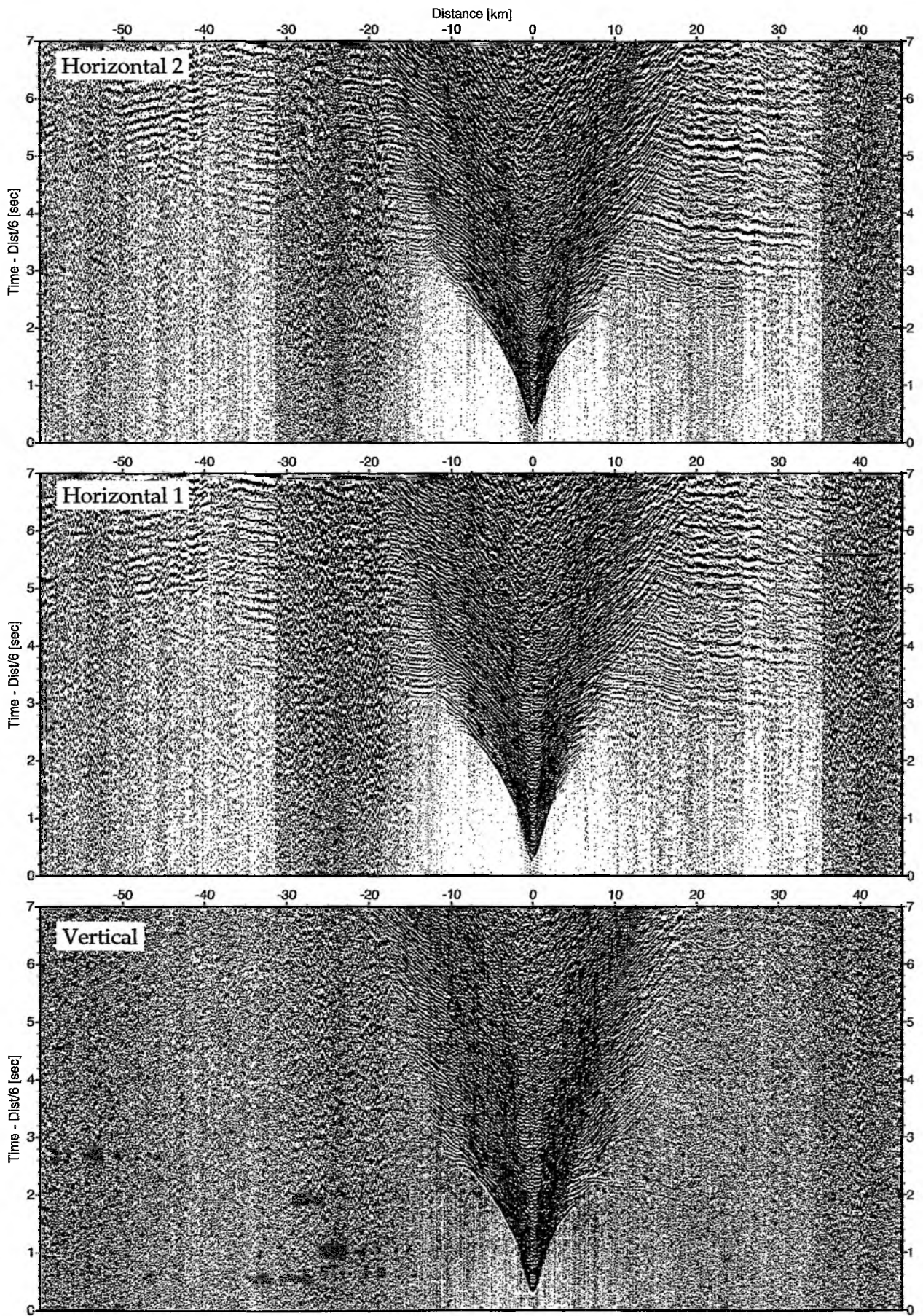


Figure 6.6.5.14: Record sections from obs 163 HTI/Owen-4.5Hz, SO181 Profile 08.

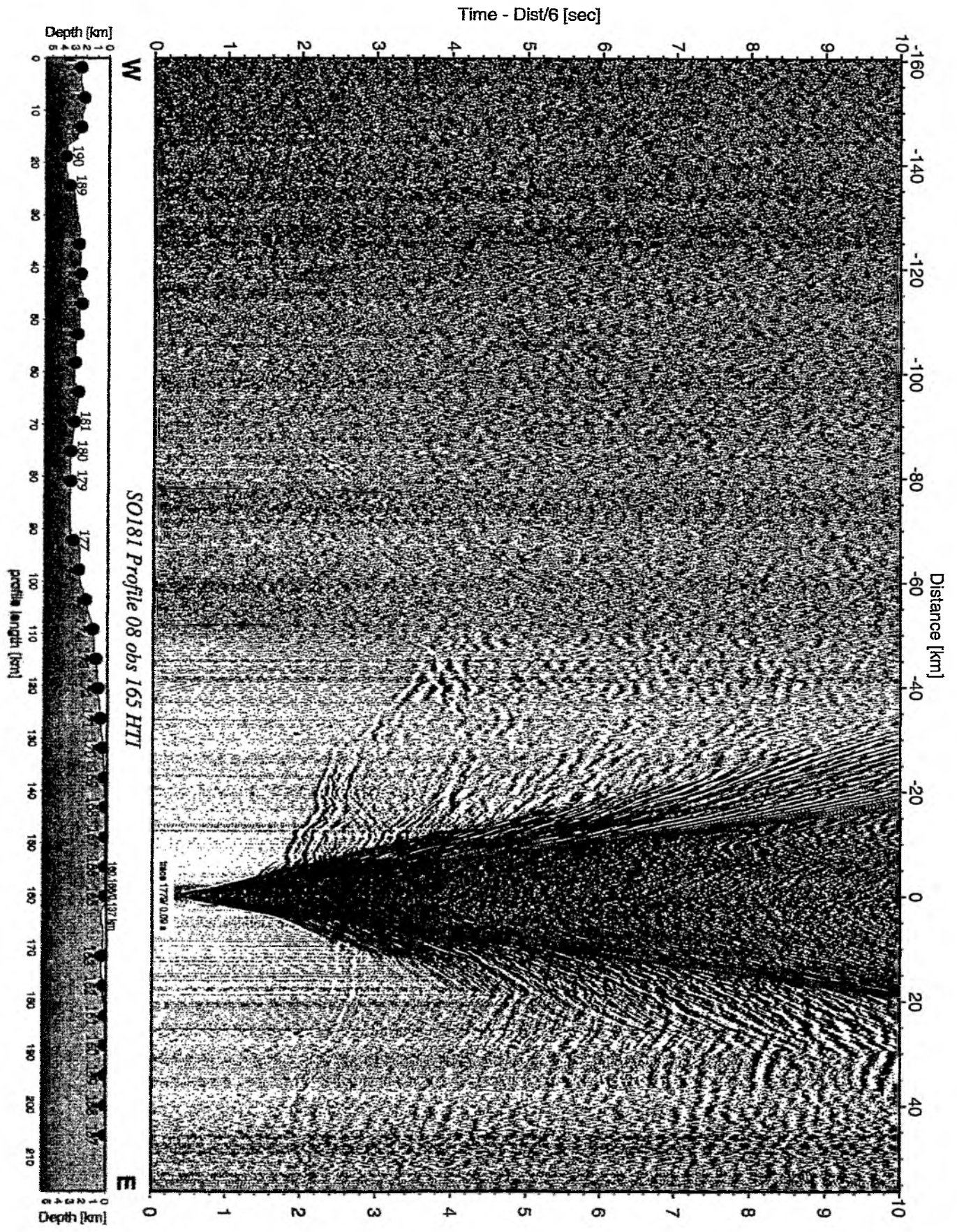


Figure 6.6.5.15: Record section from obs 165 HTI, Profile 08.

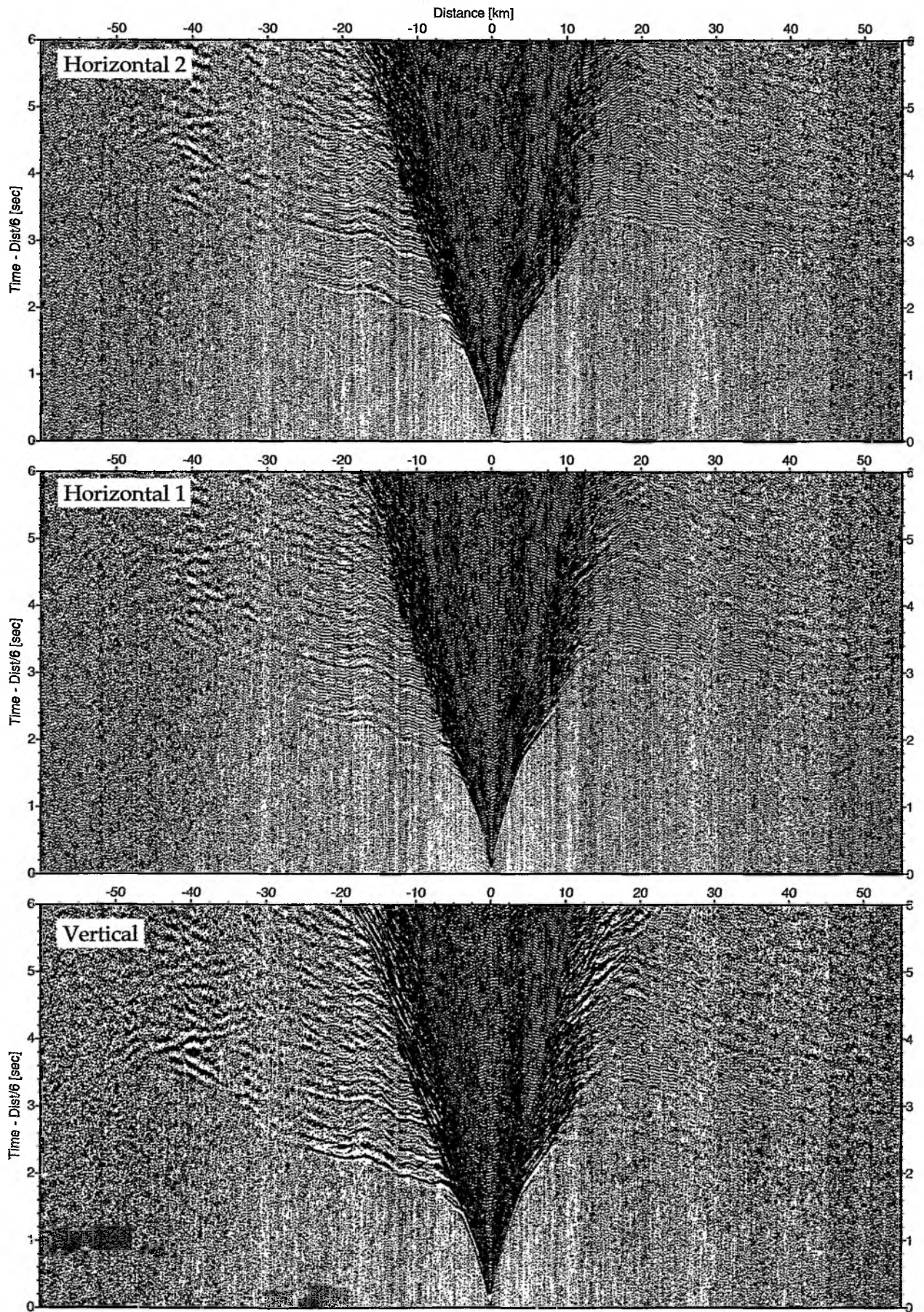


Figure 6.6.5.16: Record sections from obs 165 HTI/Owen-4.5Hz, SO181 Profile 08.

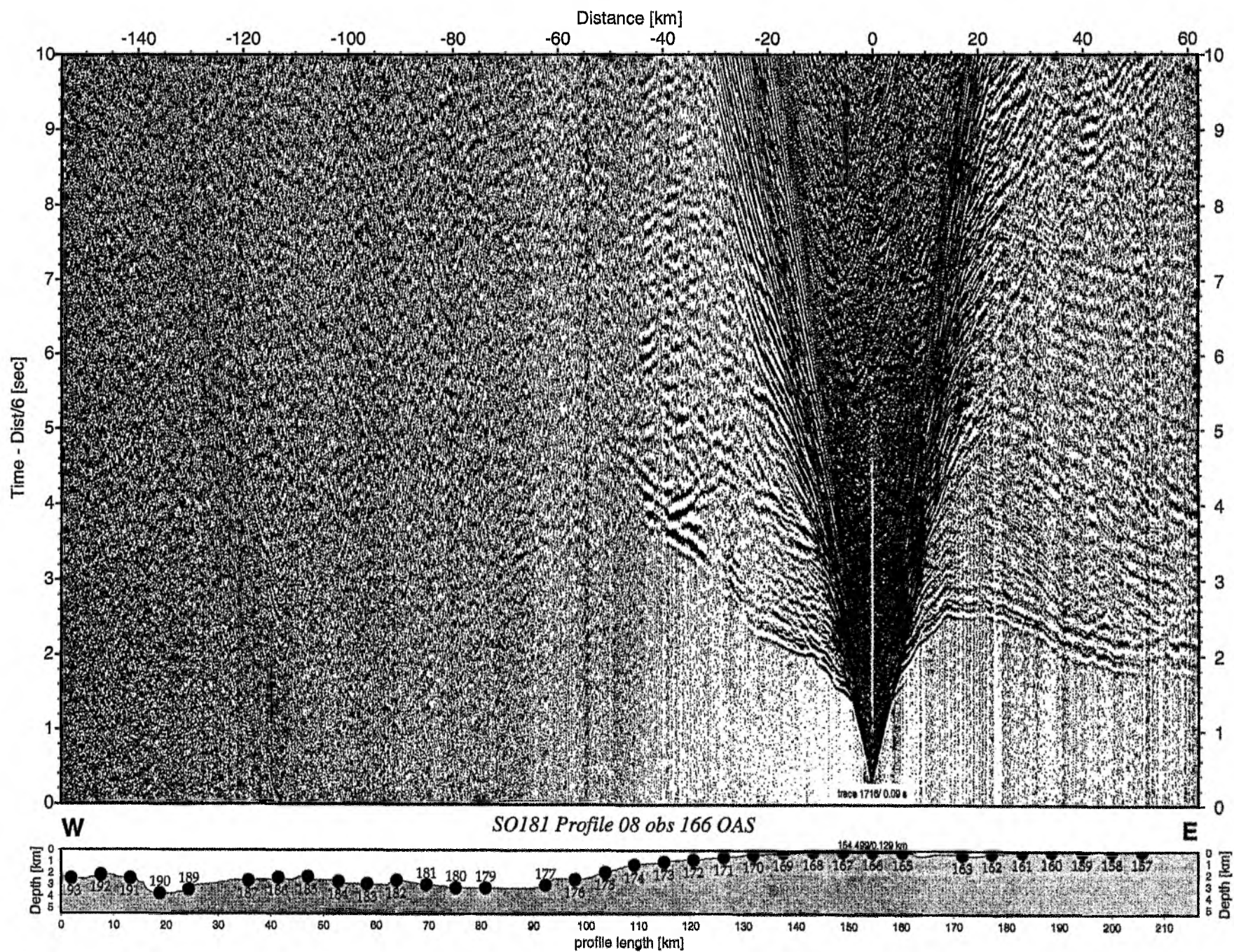


Figure 6.6.5.17: Record section from obs 166 OAS, Profile 08.

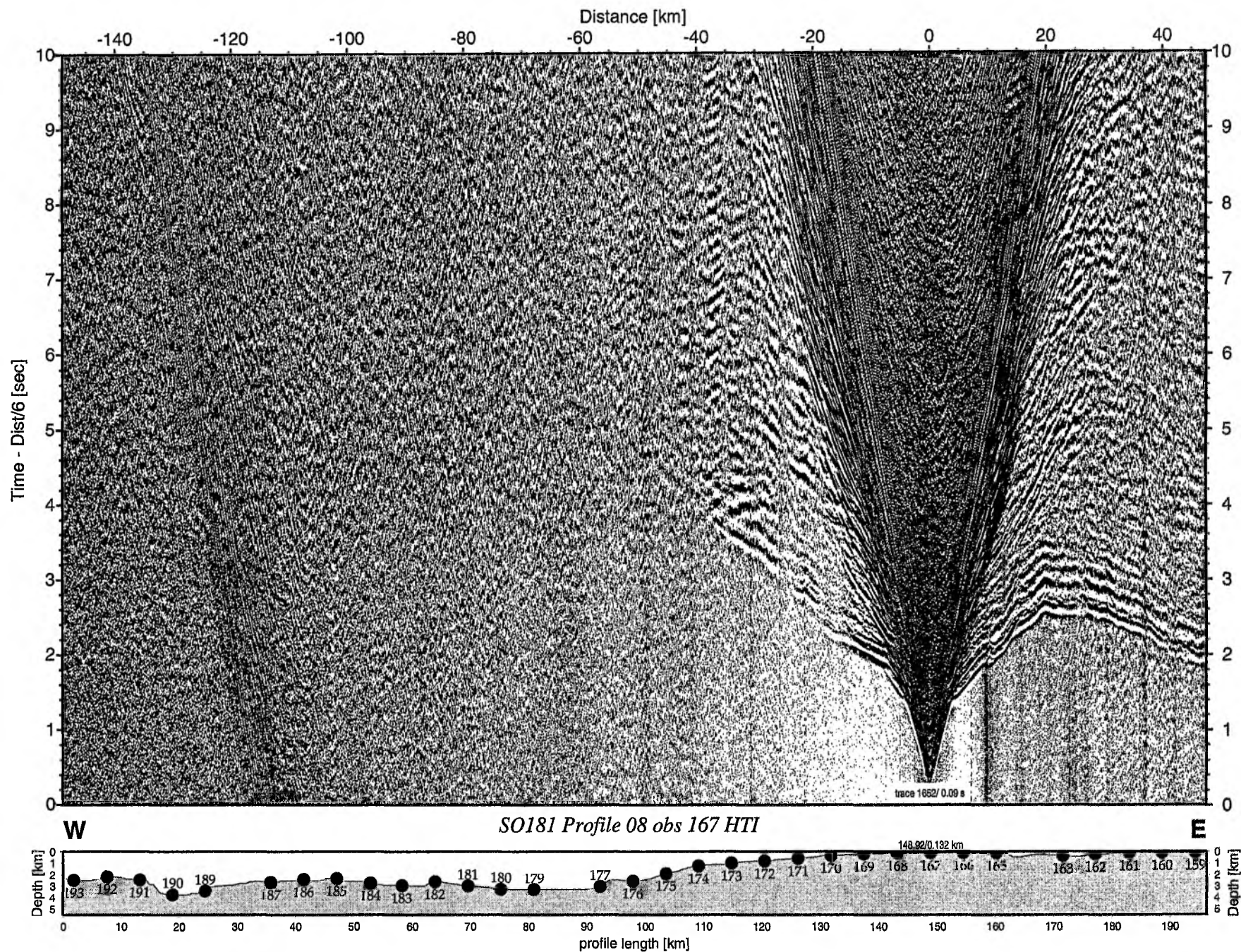


Figure 6.6.5.18: Record section from obs 167 HTI, Profile 08.

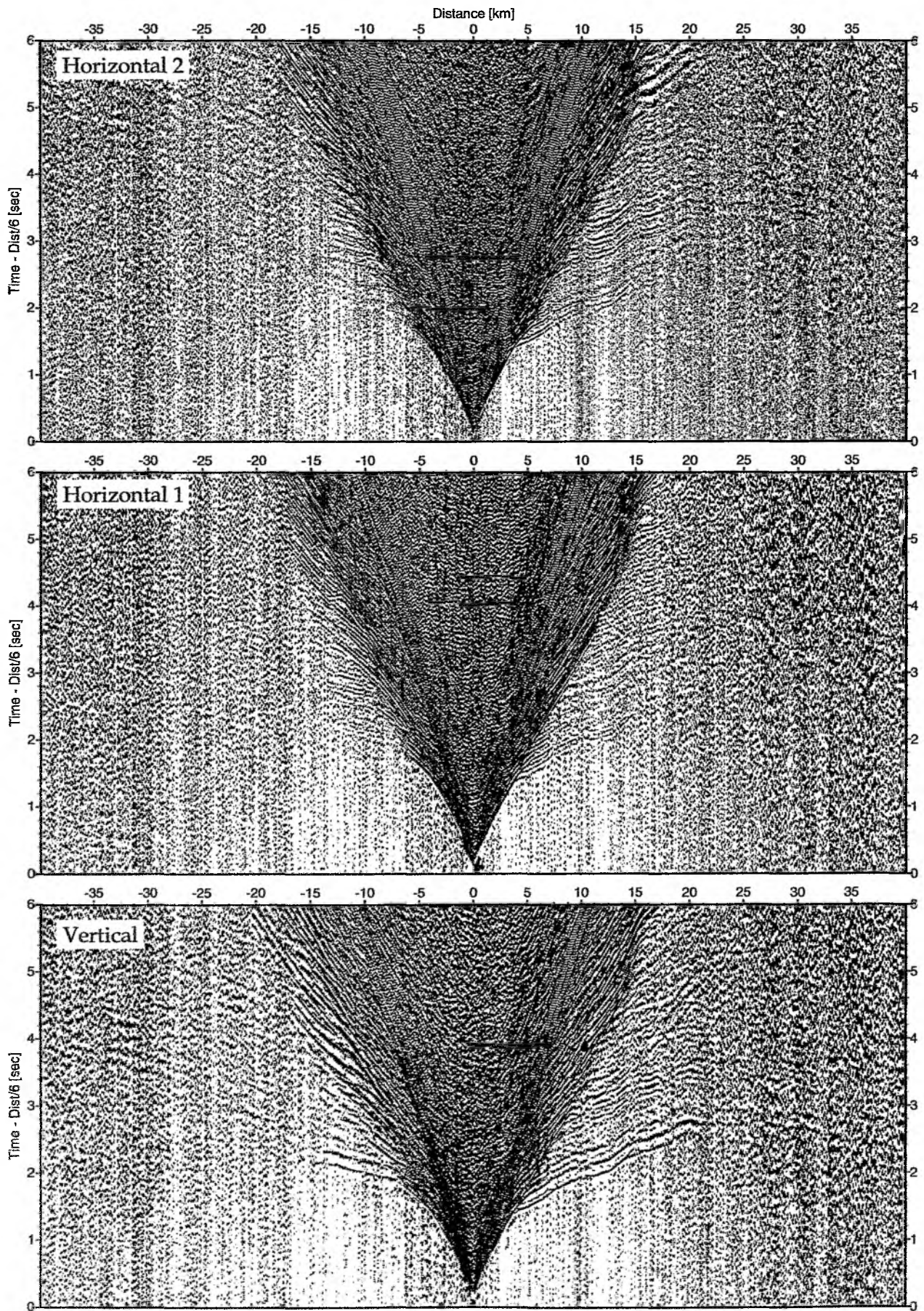


Figure 6.6.5.19: Record sections from obs 167 HTI/Owen-4.5Hz, SO181 Profile 08.

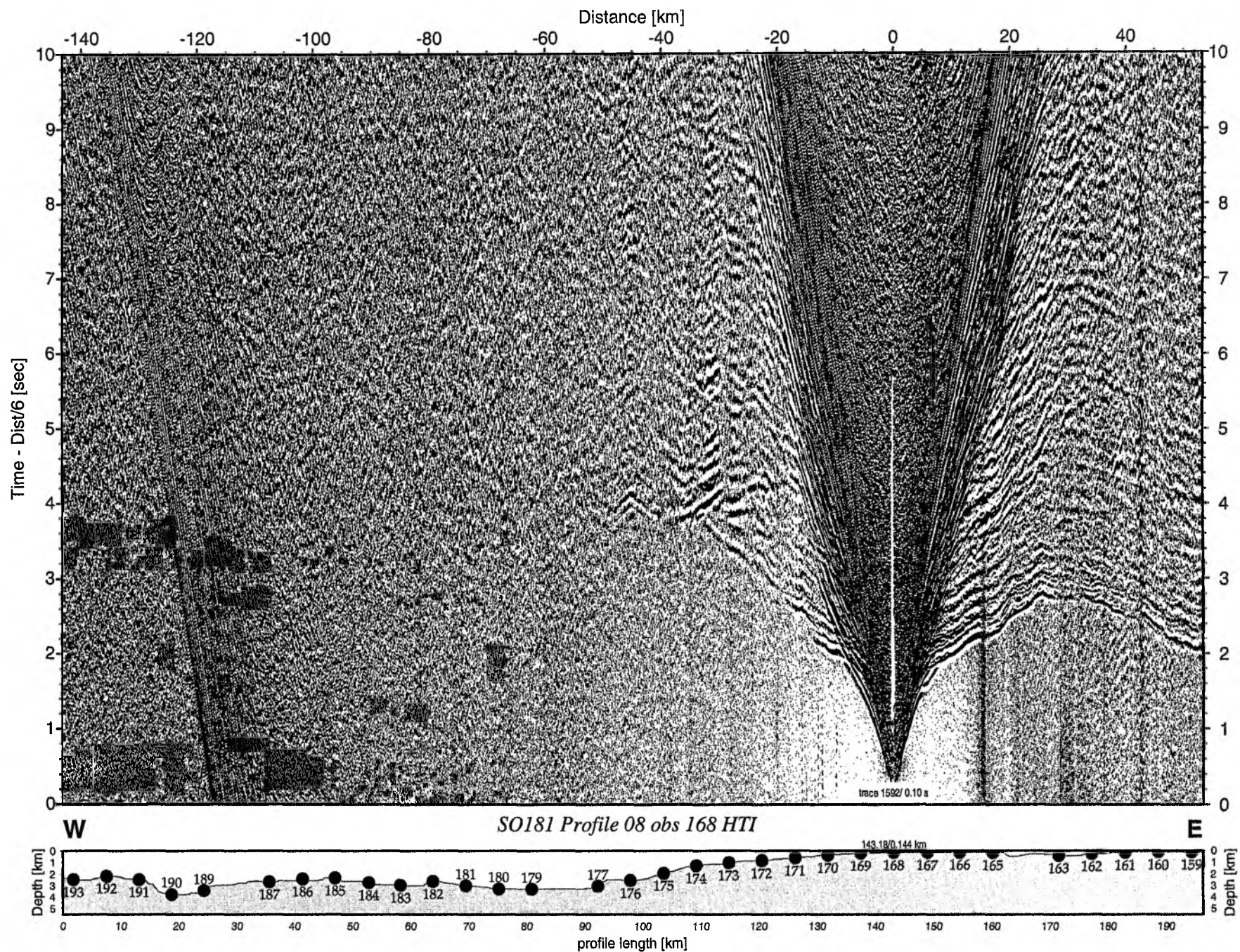


Figure 6.6.5.20: Record section from obs 168 HTI, Profile 08.

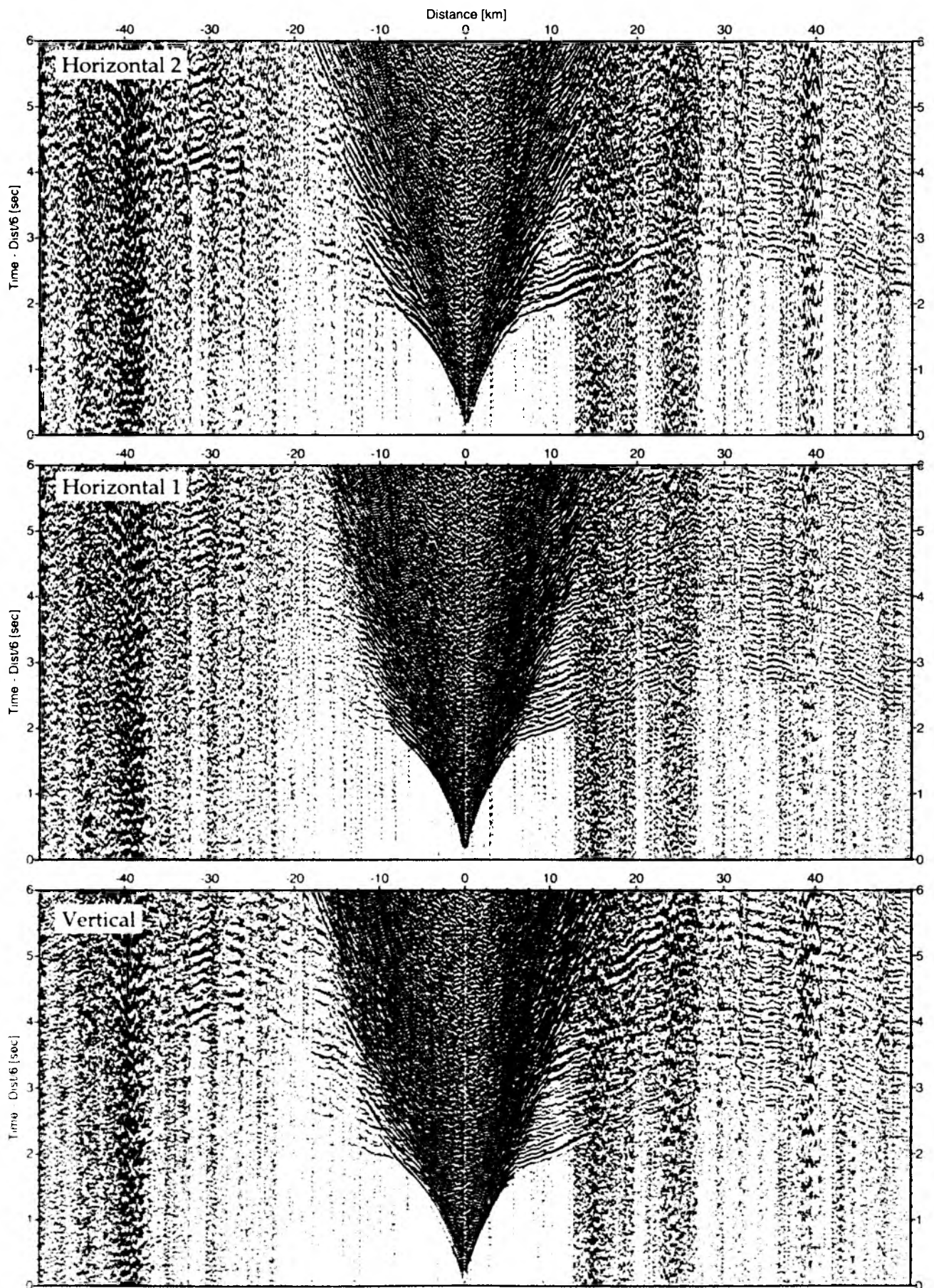


Figure 6.6.5.21: Record sections from obs 168 HTI/Owen-4.5Hz, SO181 Profile 08.

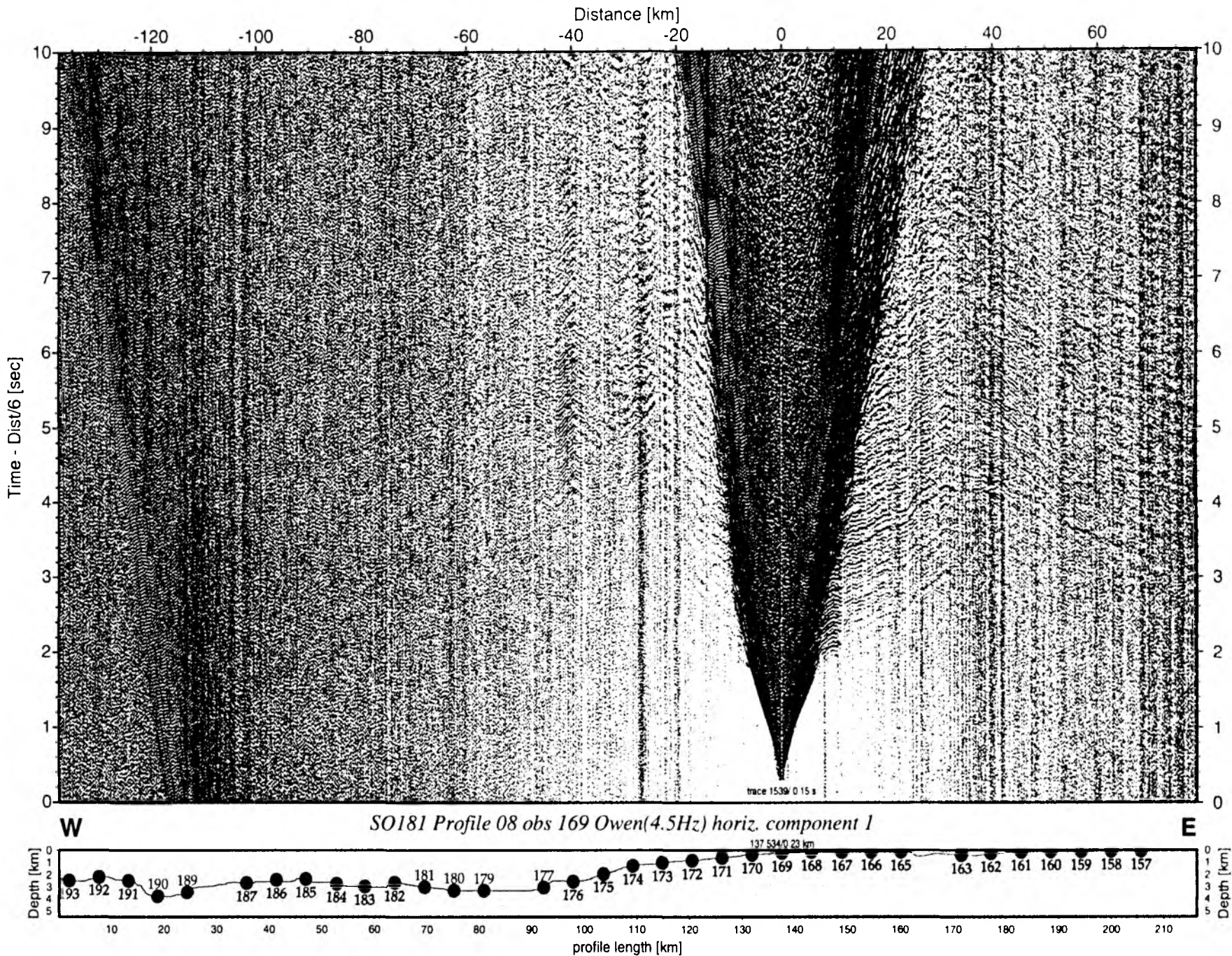


Figure 6.6.5.22: Record section from obs 169 Owen(4.5Hz) horiz. component 1, P08.

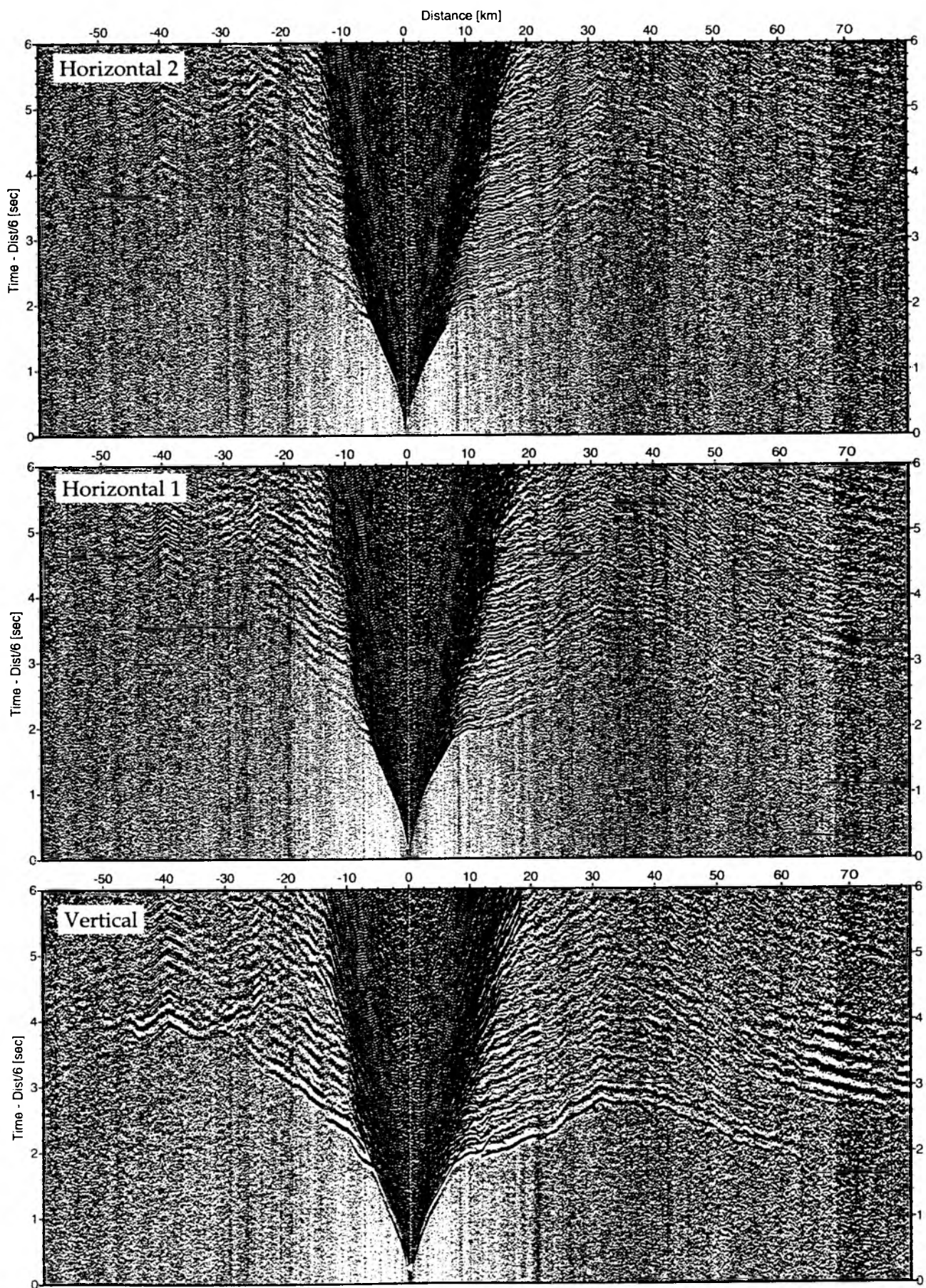


Figure 6.6.5.23: Record sections from obs 169 OAS/Owen-4.5Hz, SO181 Profile 08.

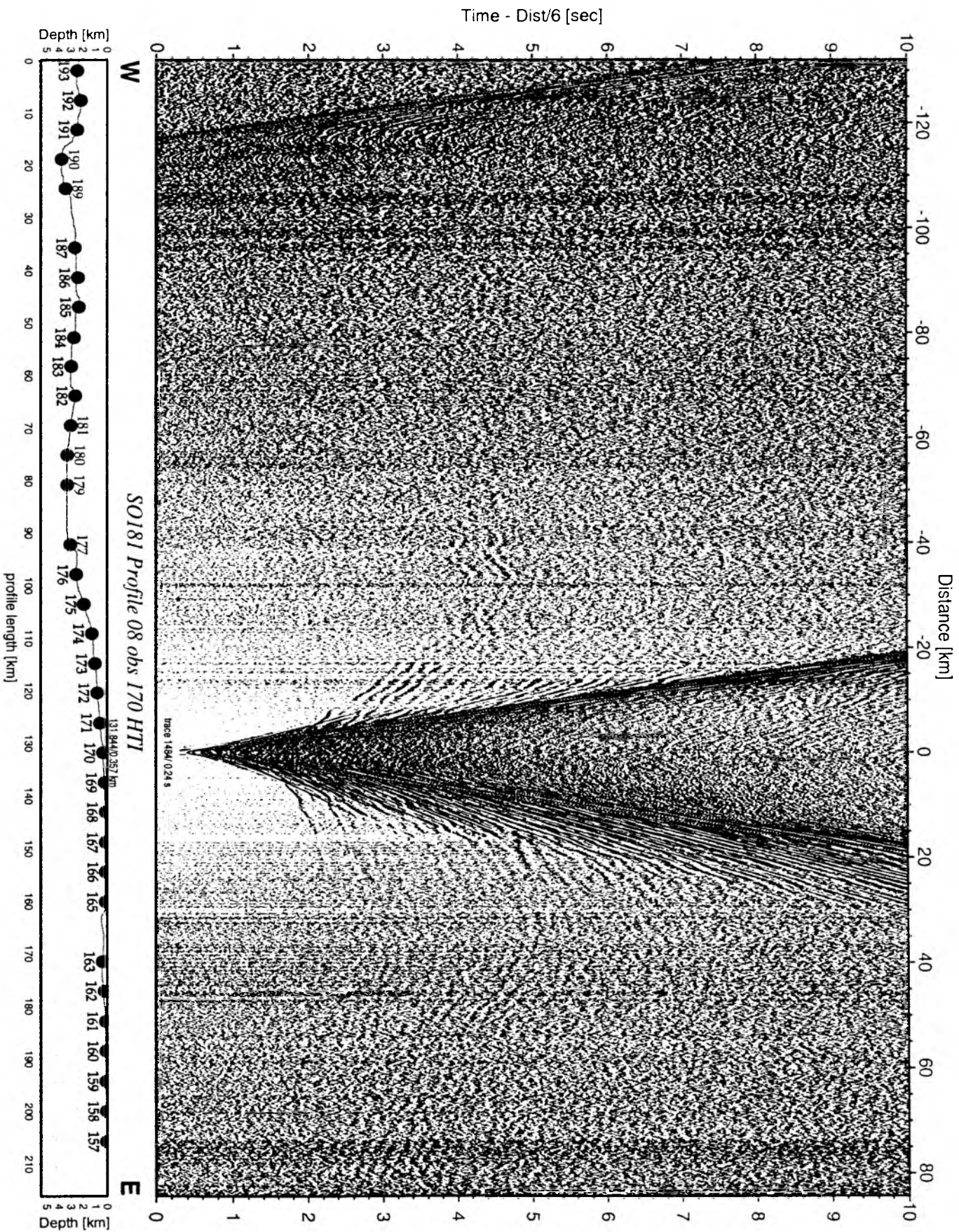


Figure 6.6.5.24: Record section from obs 170 HTI, Profile 08.

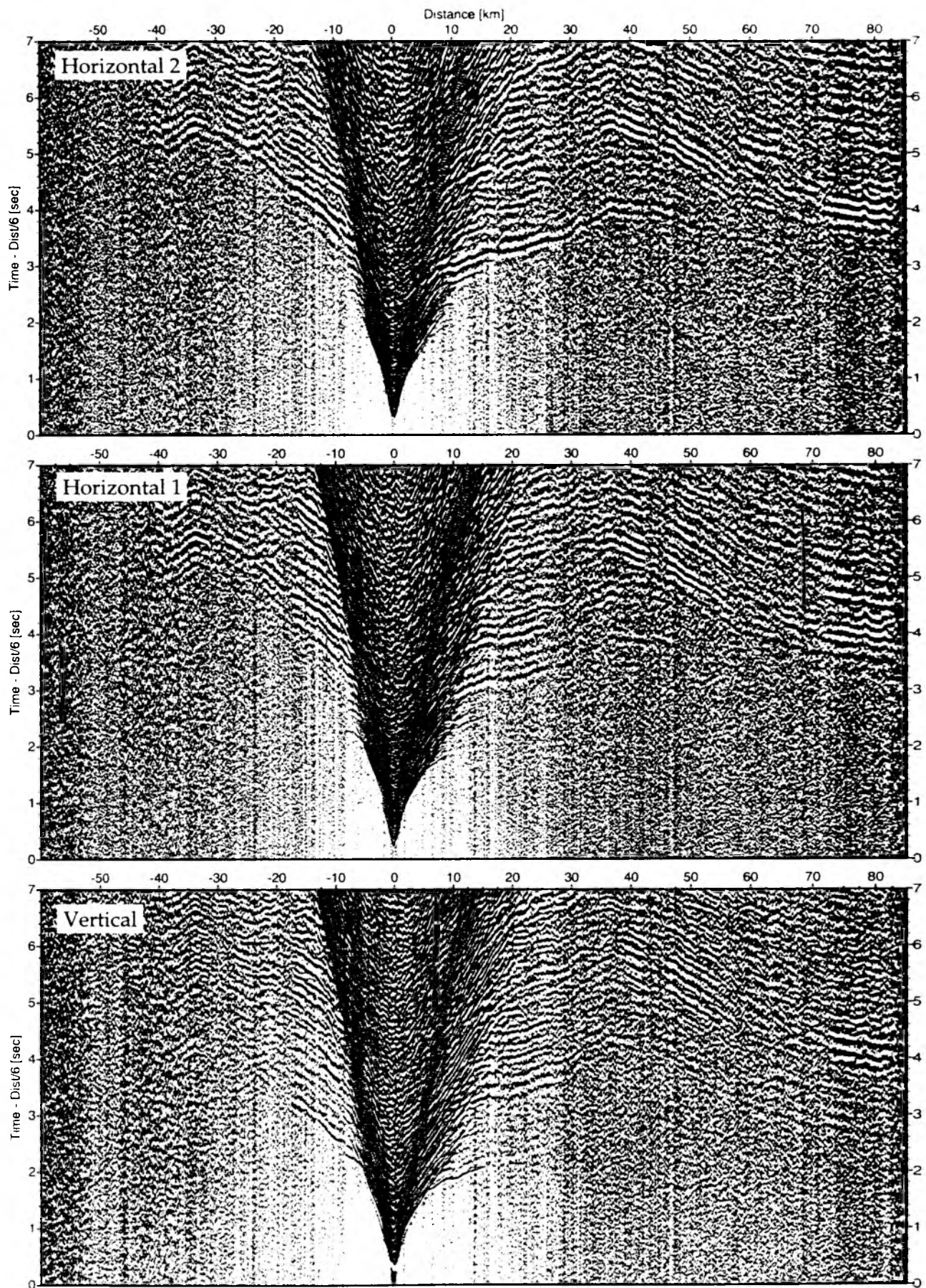


Figure 6.6.5.25: Record sections from obs 170 HTI/Owen-4.5Hz, SO181 Profile 08.

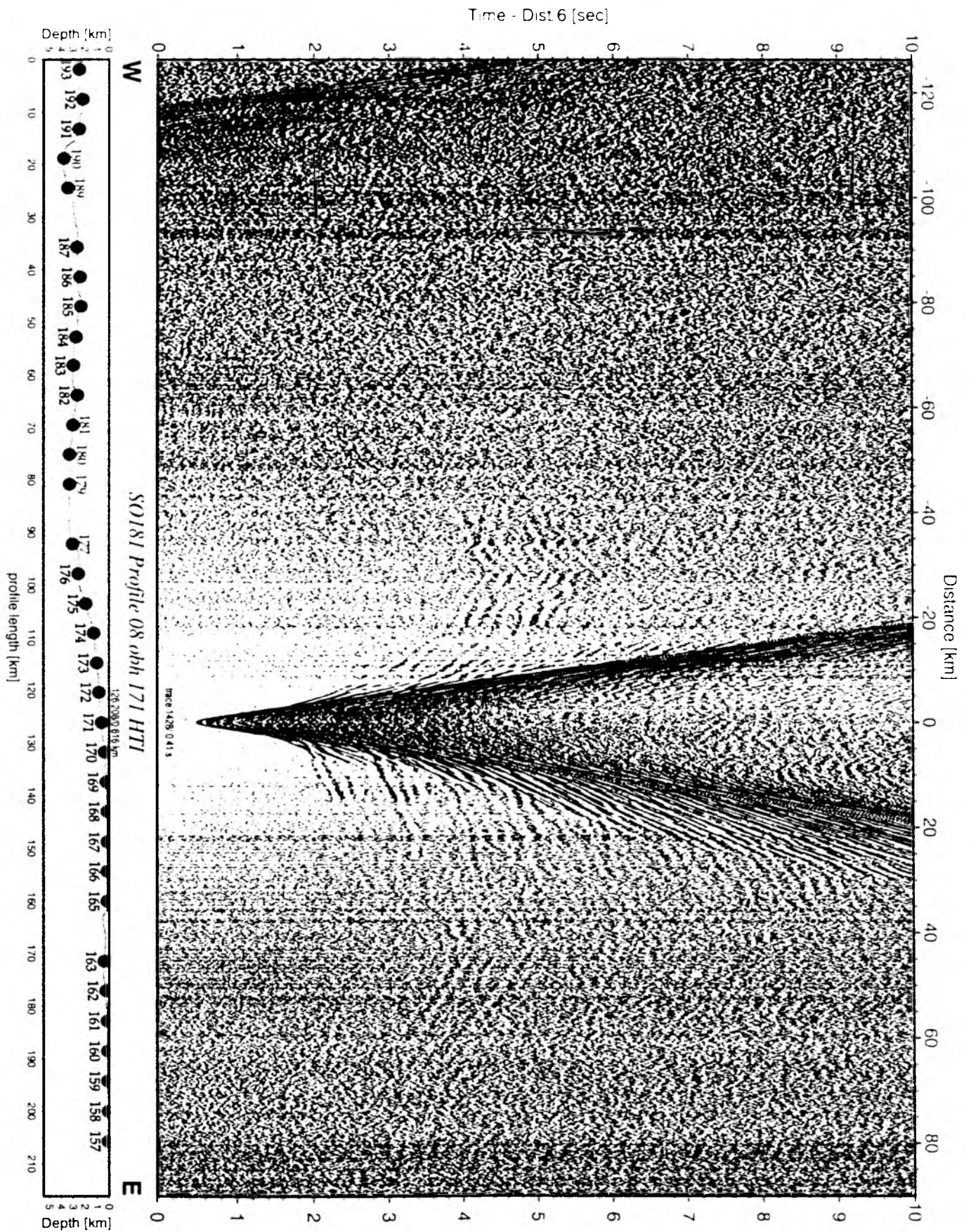


Figure 6.6.5.26: Record section from obh 171 HTI, Profile 08.

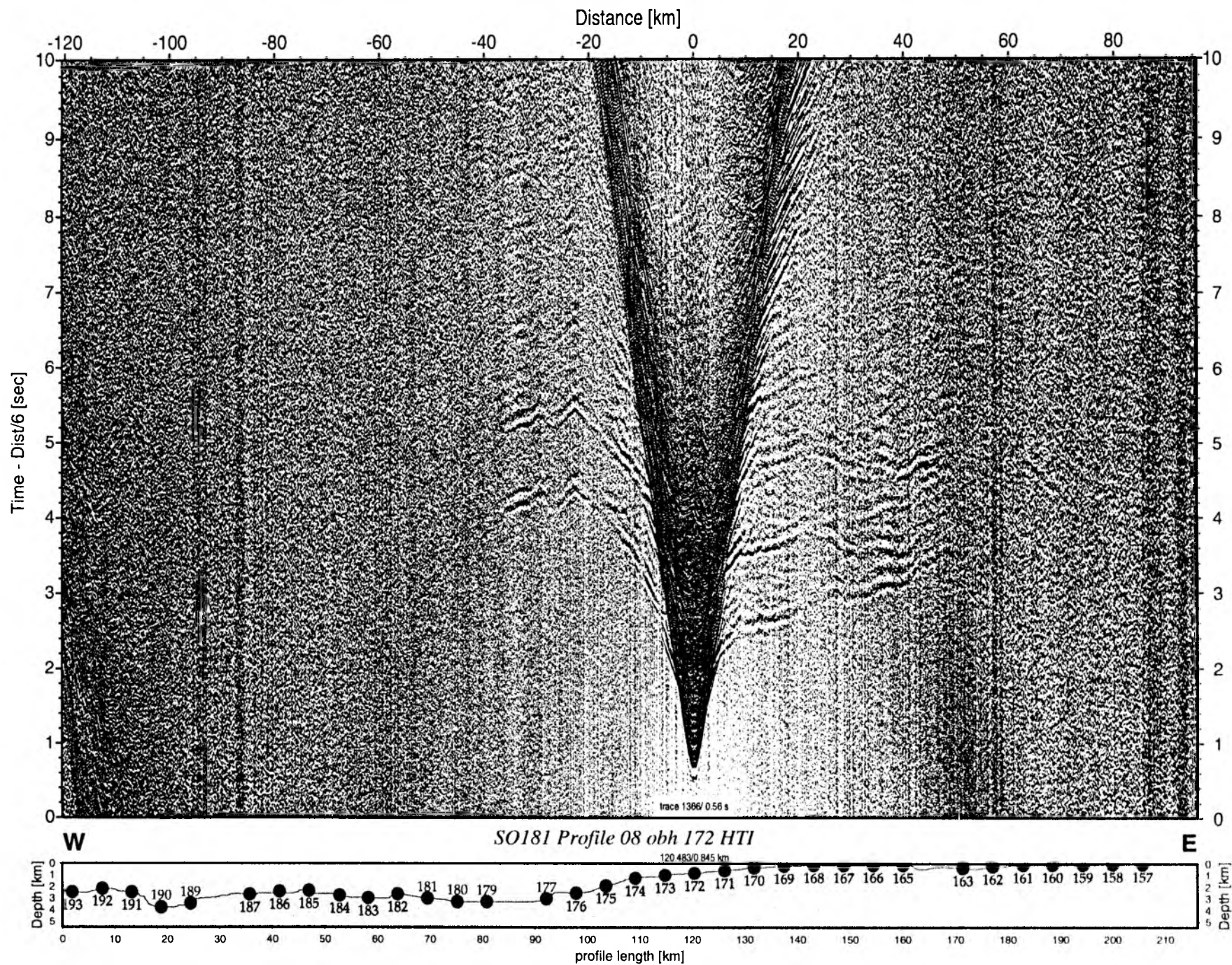


Figure 6.6.5.27: Record section from obh 172 HTI, Profile 08.

Time - Dist/8 [sec]

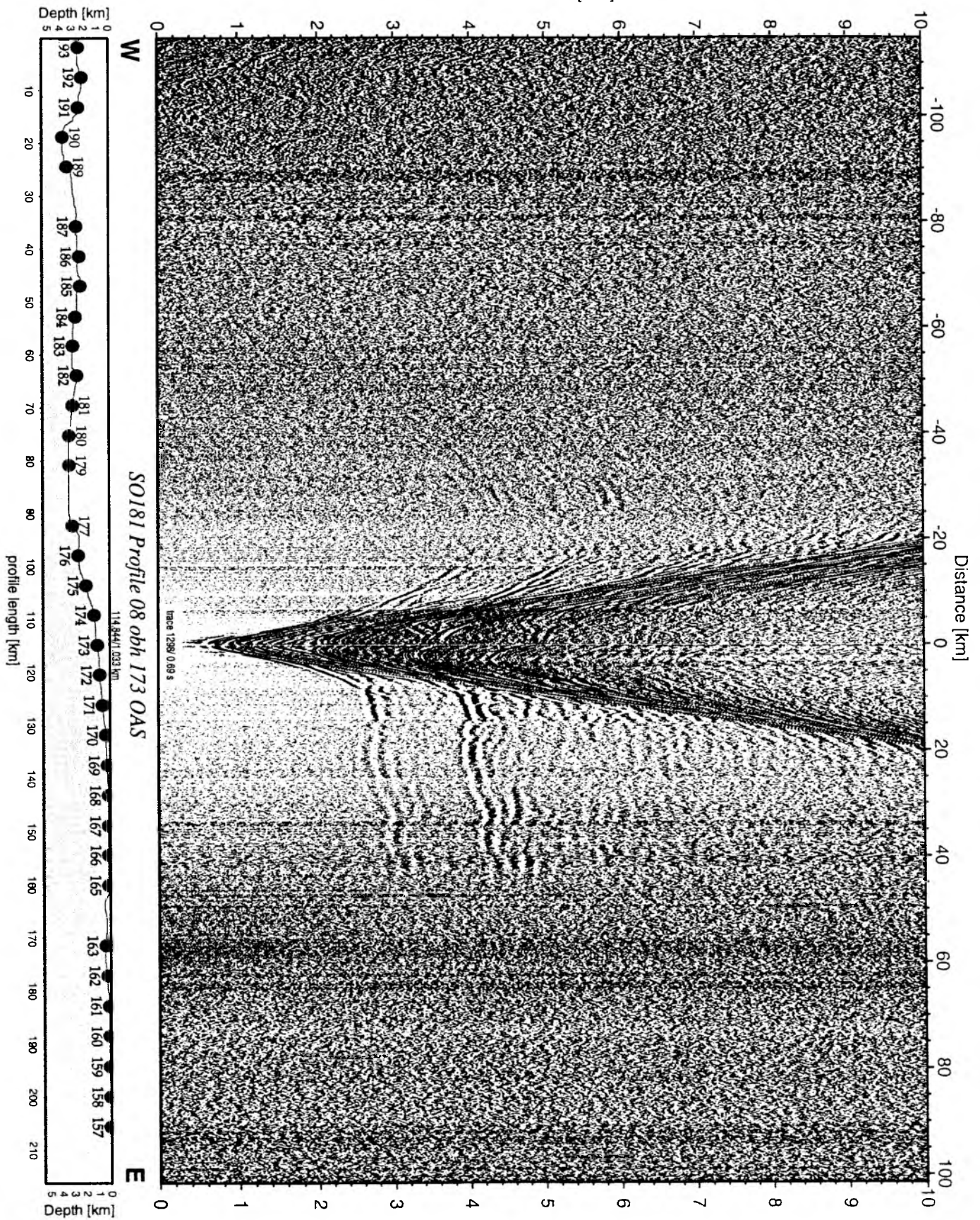


Figure 6.6.5.28: Record section from obh 173 OAS, Profile 08.

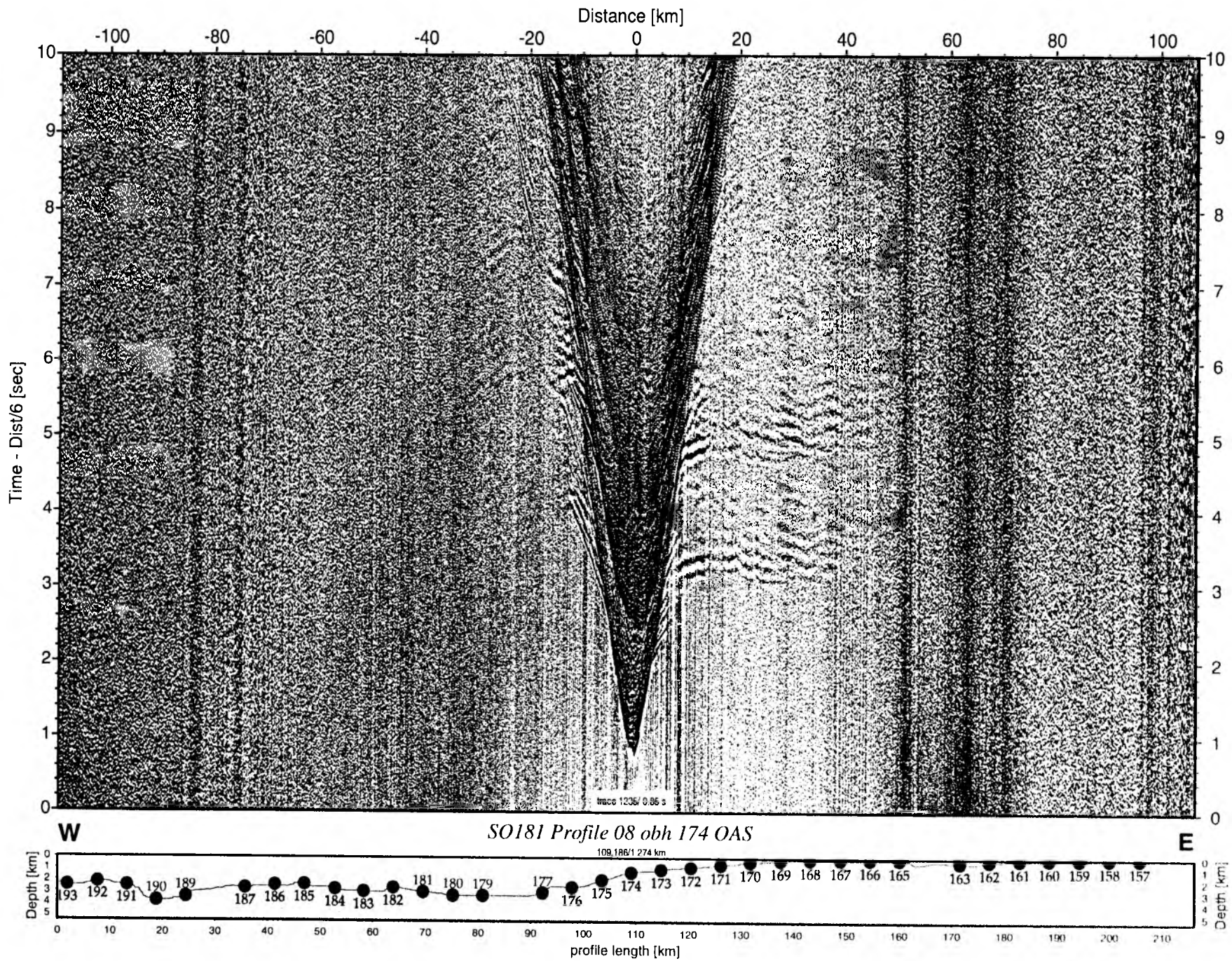


Figure 6.6.5.29: Record section from obh 174 OAS, Profile 08.

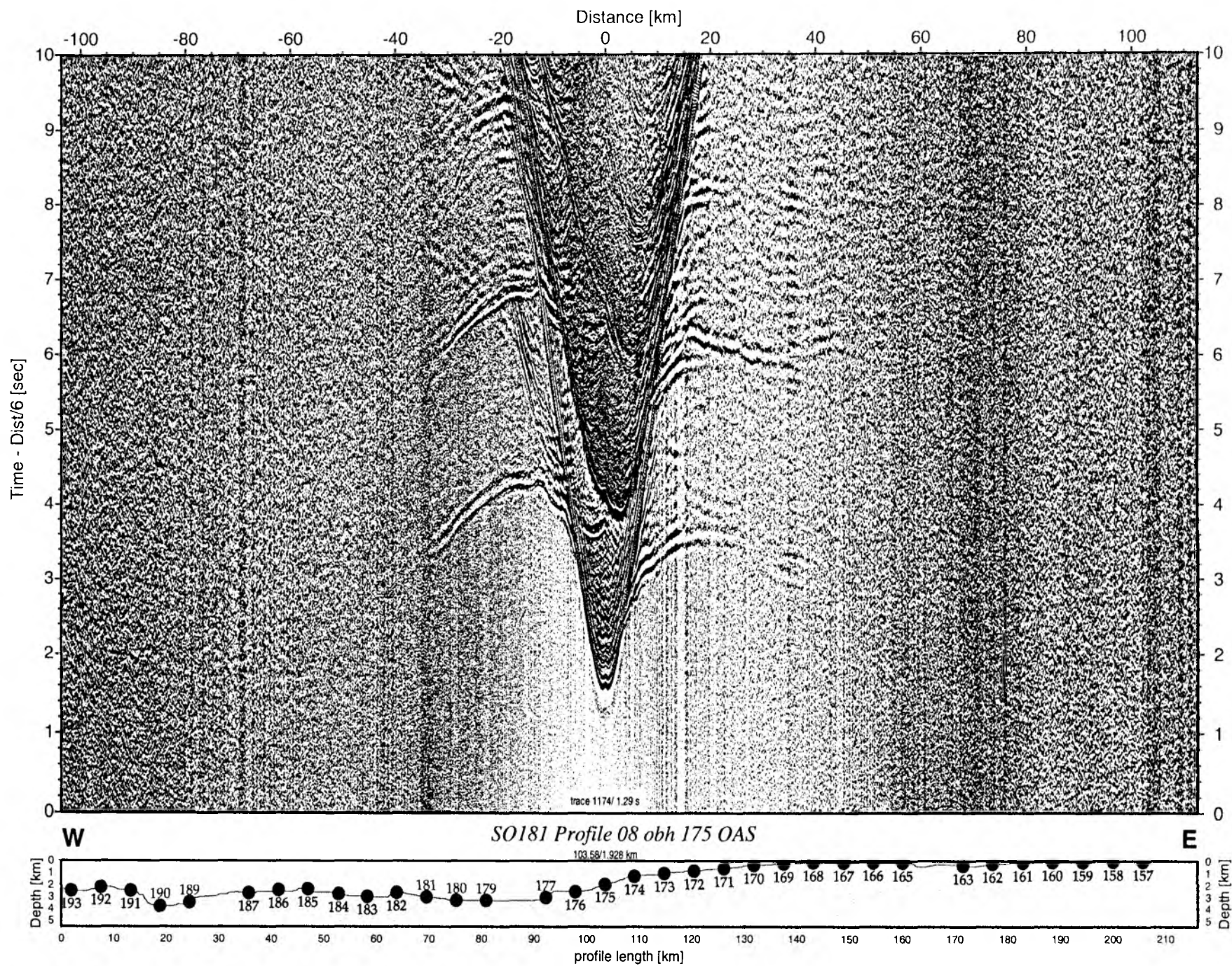


Figure 6.6.5.30: Record section from obh 175 OAS, Profile 08.

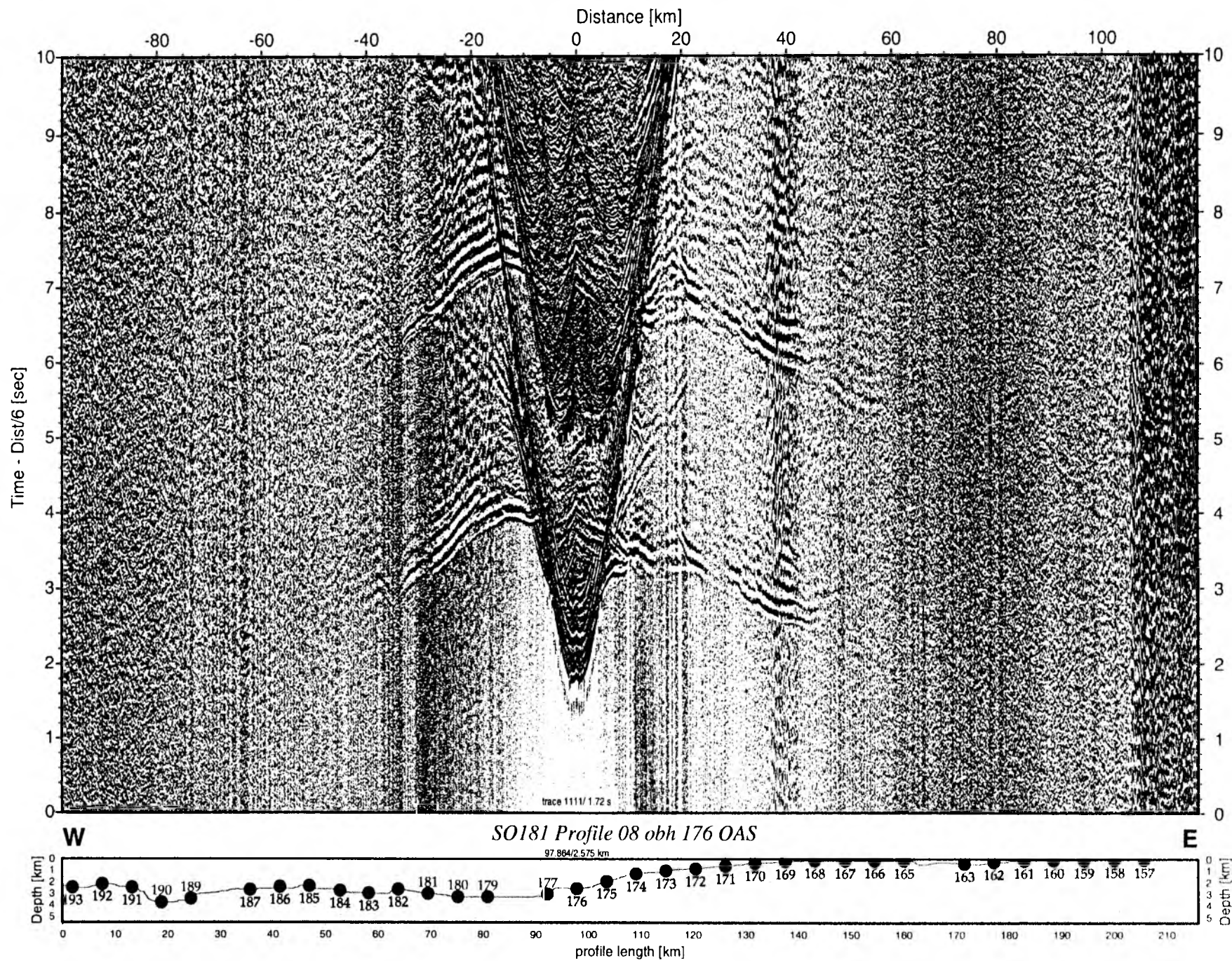


Figure 6.6.5.31: Record section from obh 176 OAS, Profile 08.

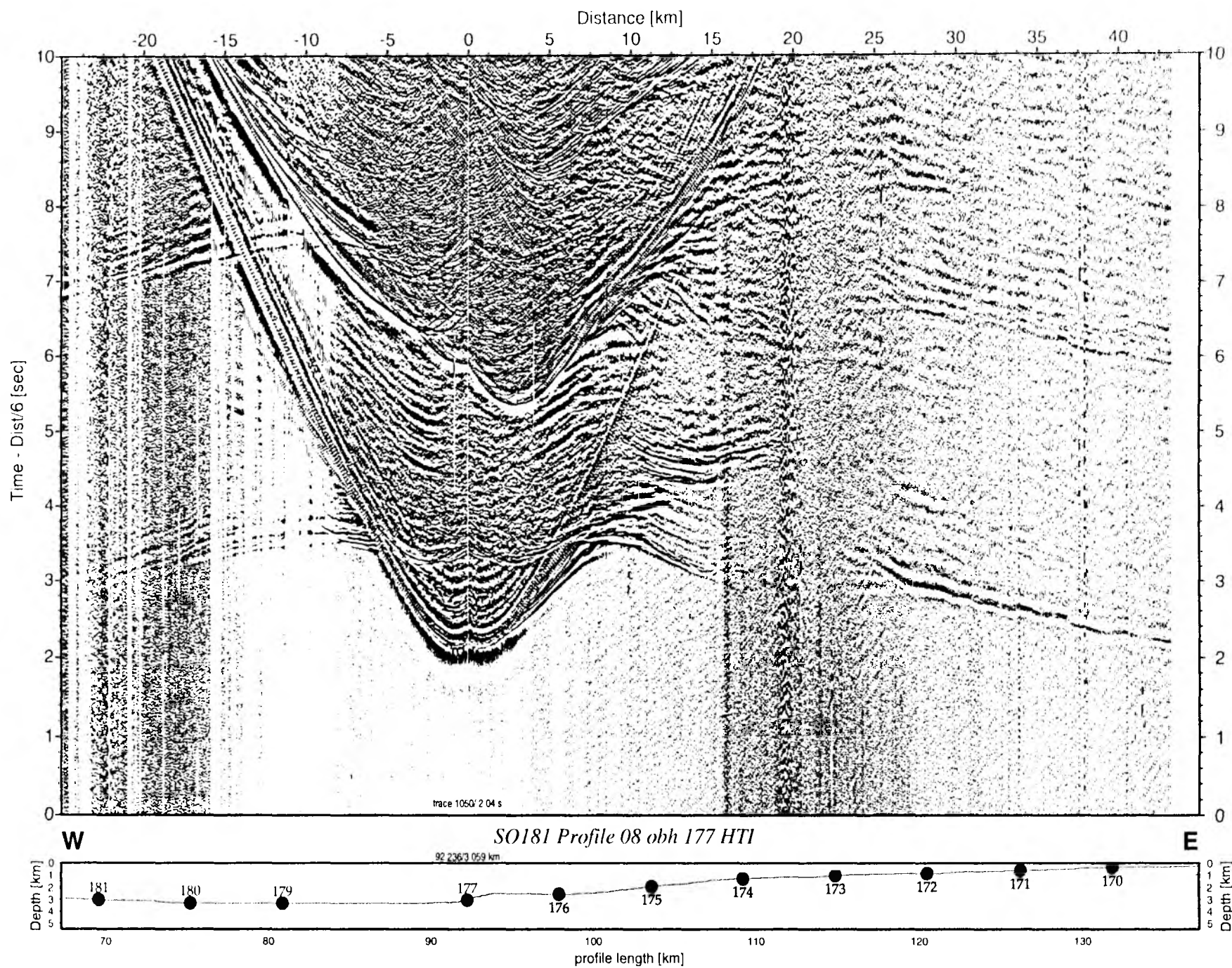


Figure 6.6.5.32: Record section from obh 177 HTI, Profile 08.

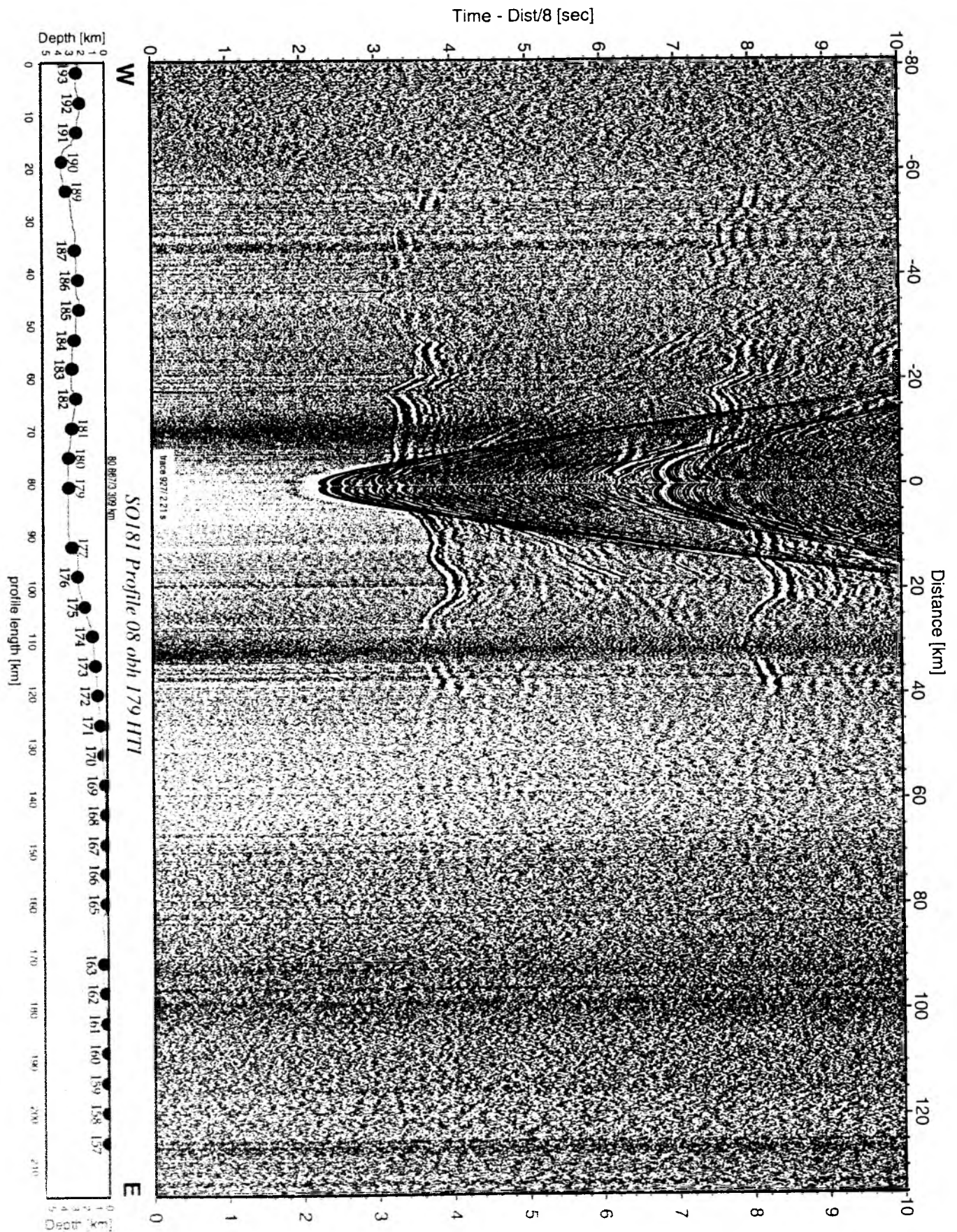


Figure 6.6.5.33: Record section from obh 179 HTI, Profile 08.

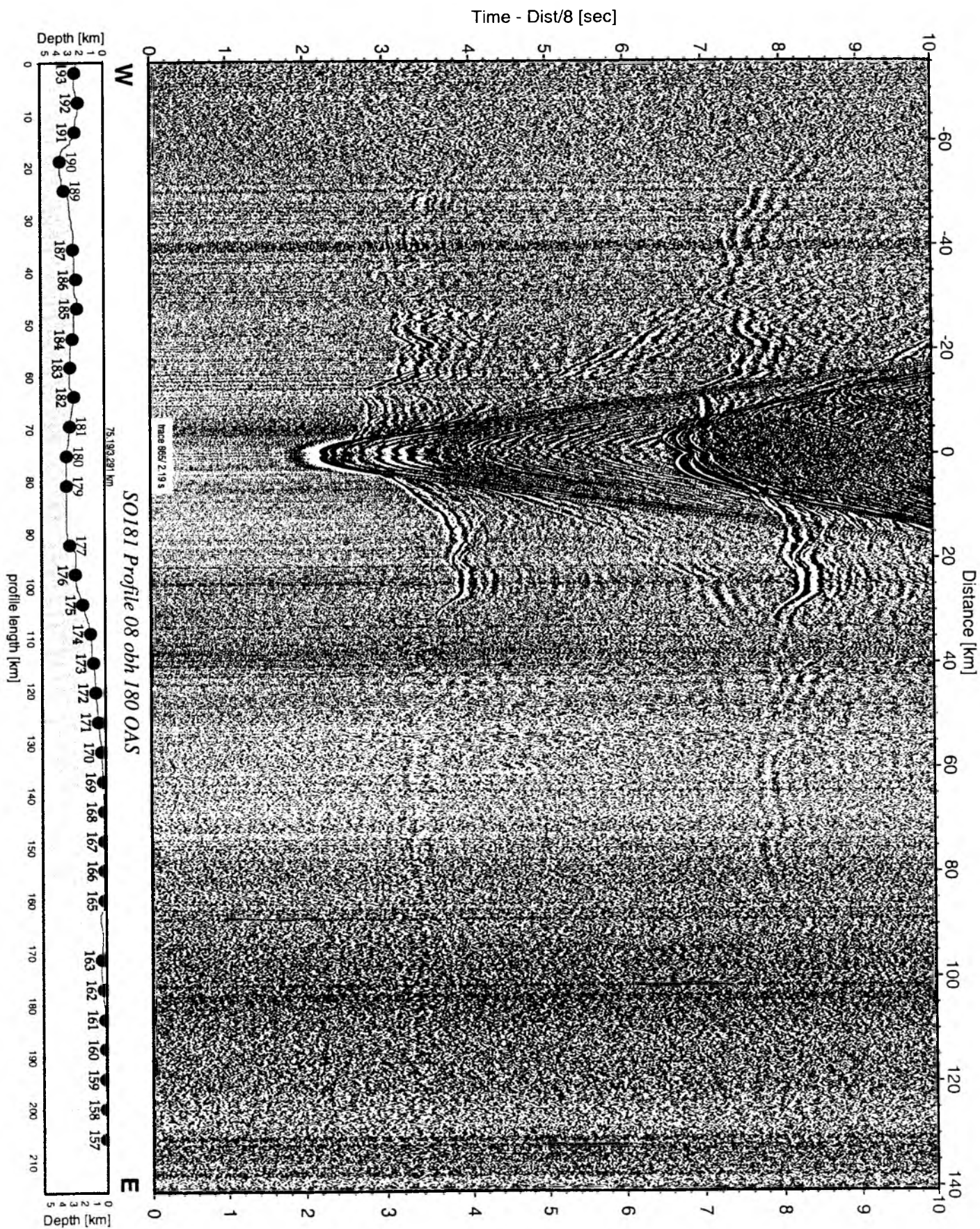


Figure 6.6.5.34: Record section from obh 180 OAS, Profile 08.

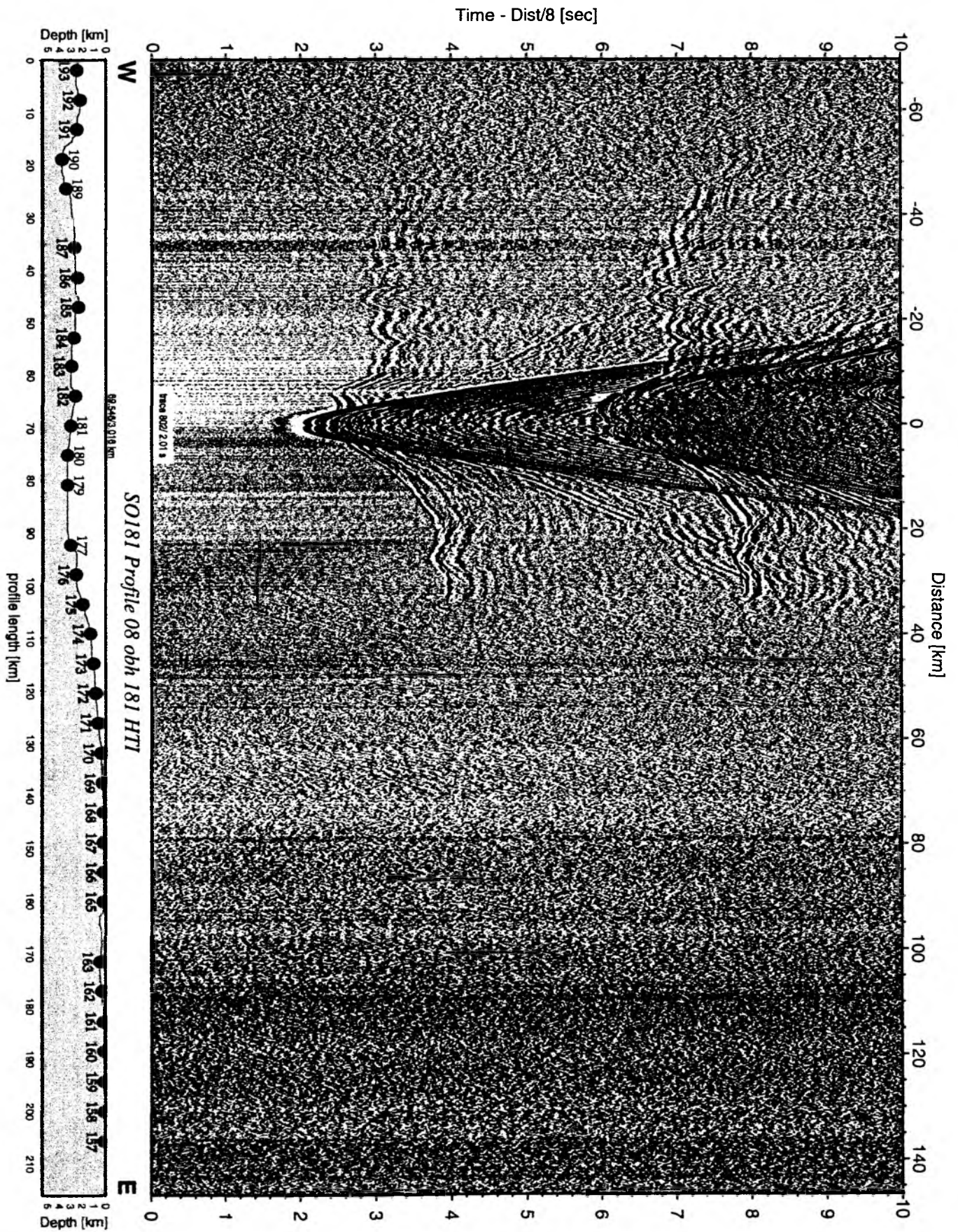


Figure 6.6.5.35: Record section from obh 181 HTI, Profile 08.

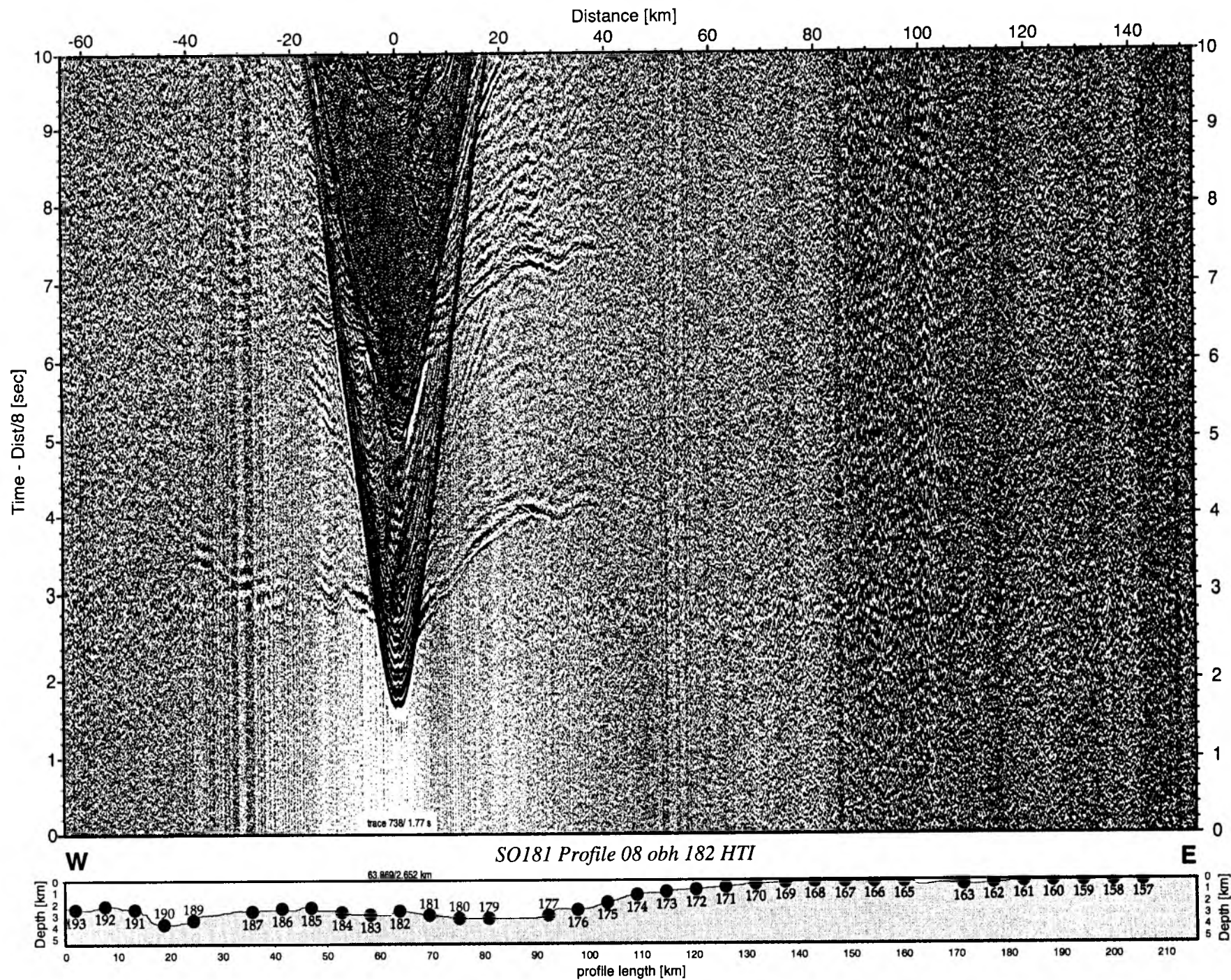


Figure 6.6.5.36: Record section from obh 182 HTI, Profile 08.

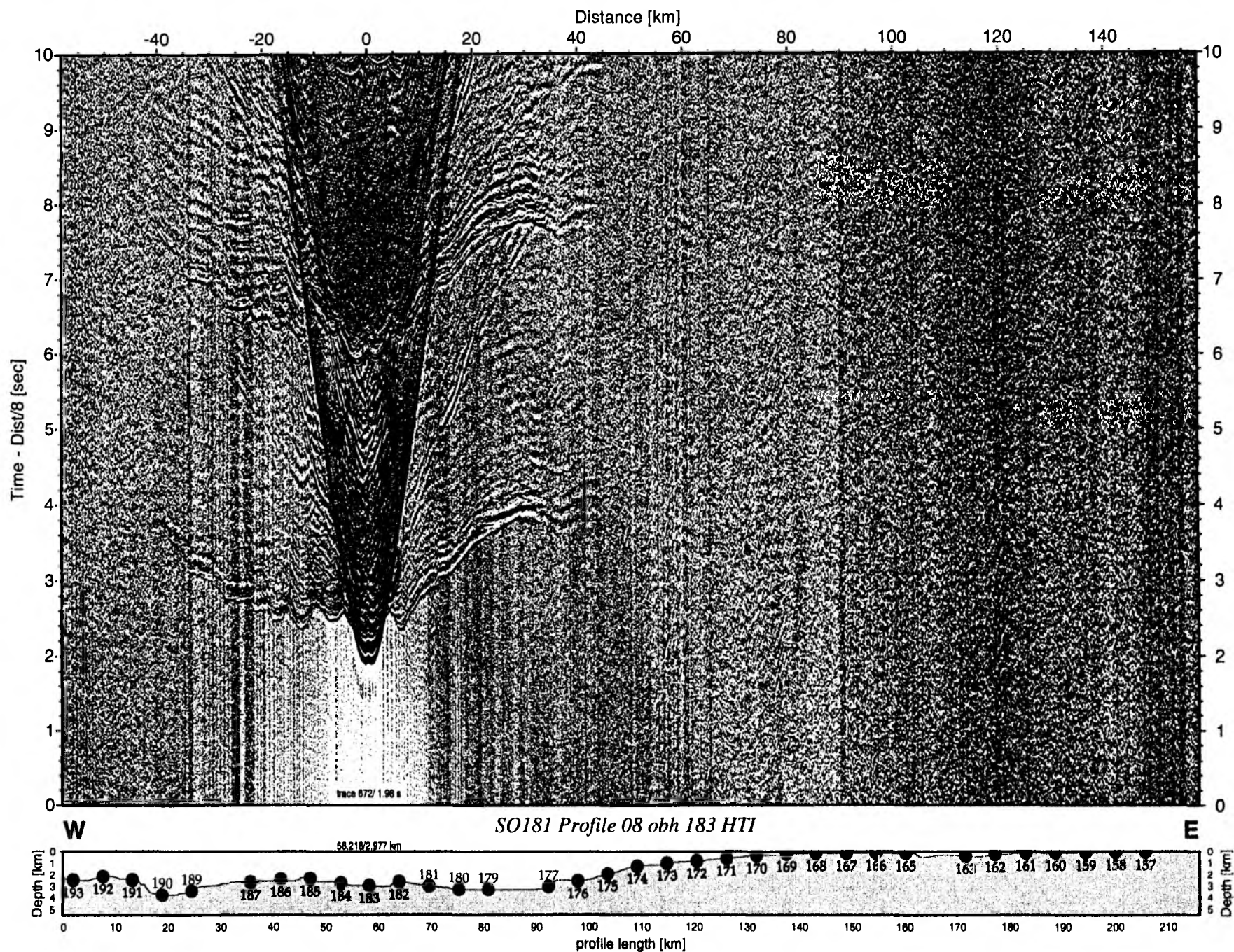


Figure 6.6.5.37: Record section from obh 183 HTI, Profile 08.

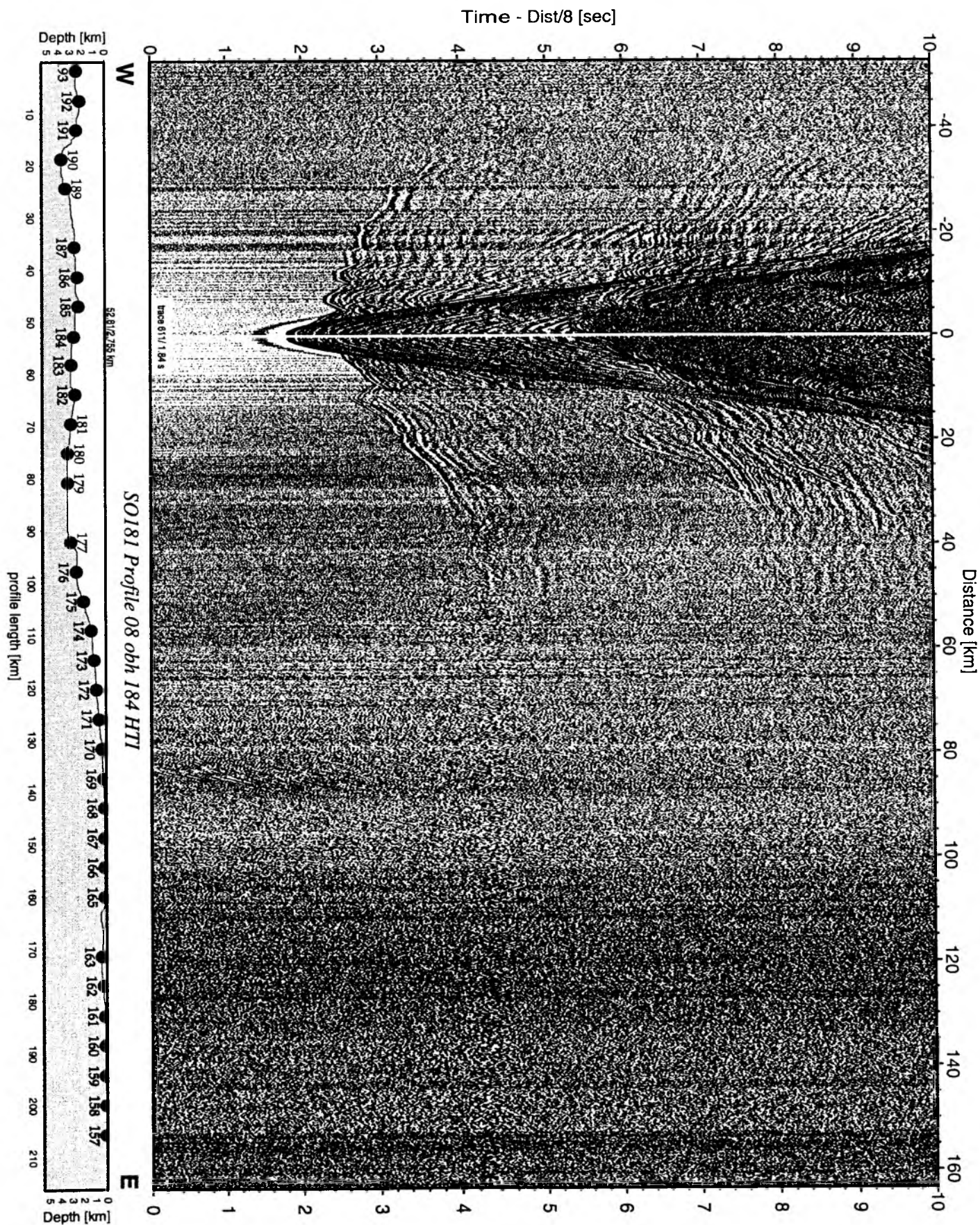


Figure 6.6.5.38: Record section from obh 184 HTI, Profile 08.

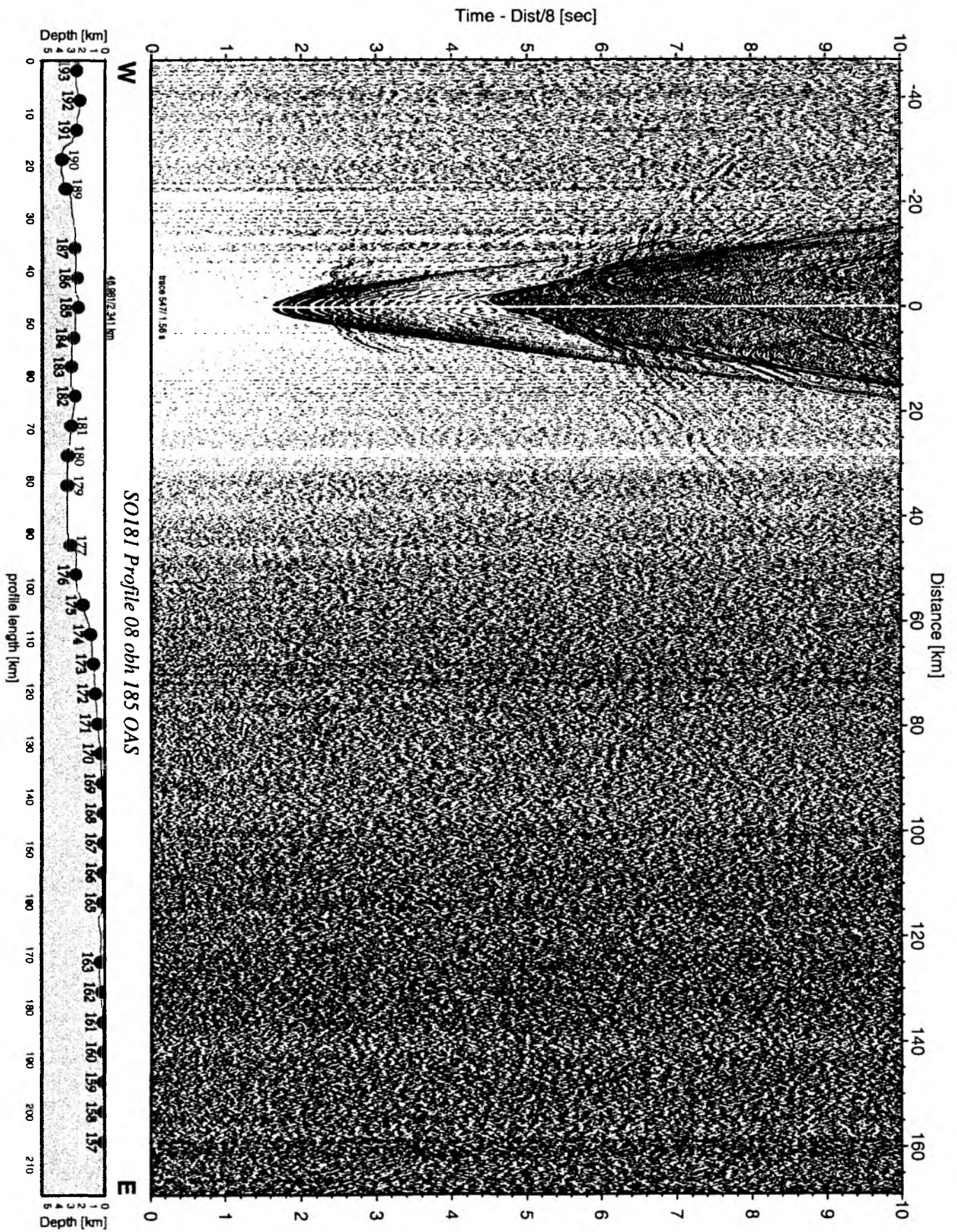


Figure 6.6.5.39: Record section from obh 185 OAS, Profile 08.

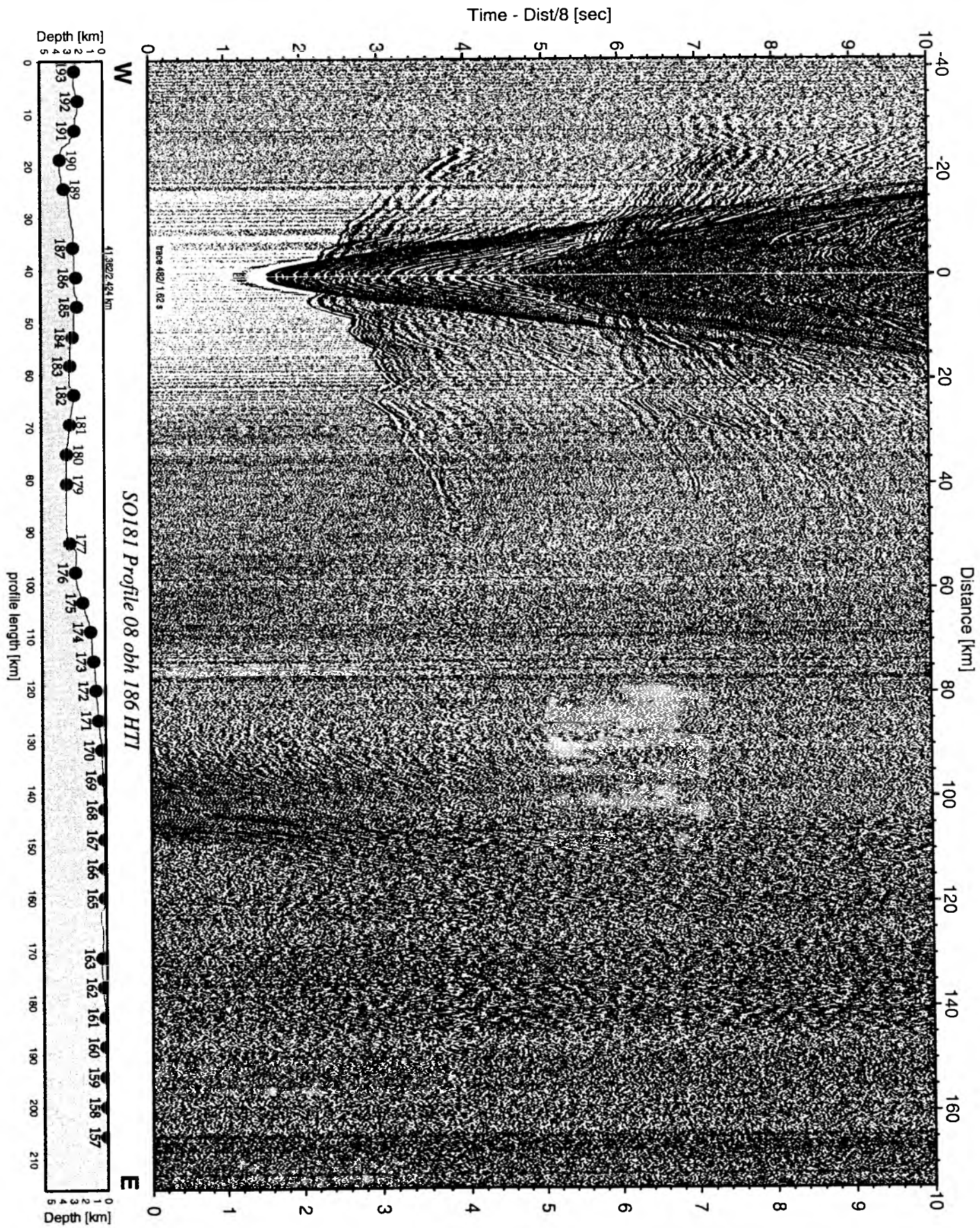


Figure 6.6.5.40: Record section from obh 186 HTI, Profile 08.

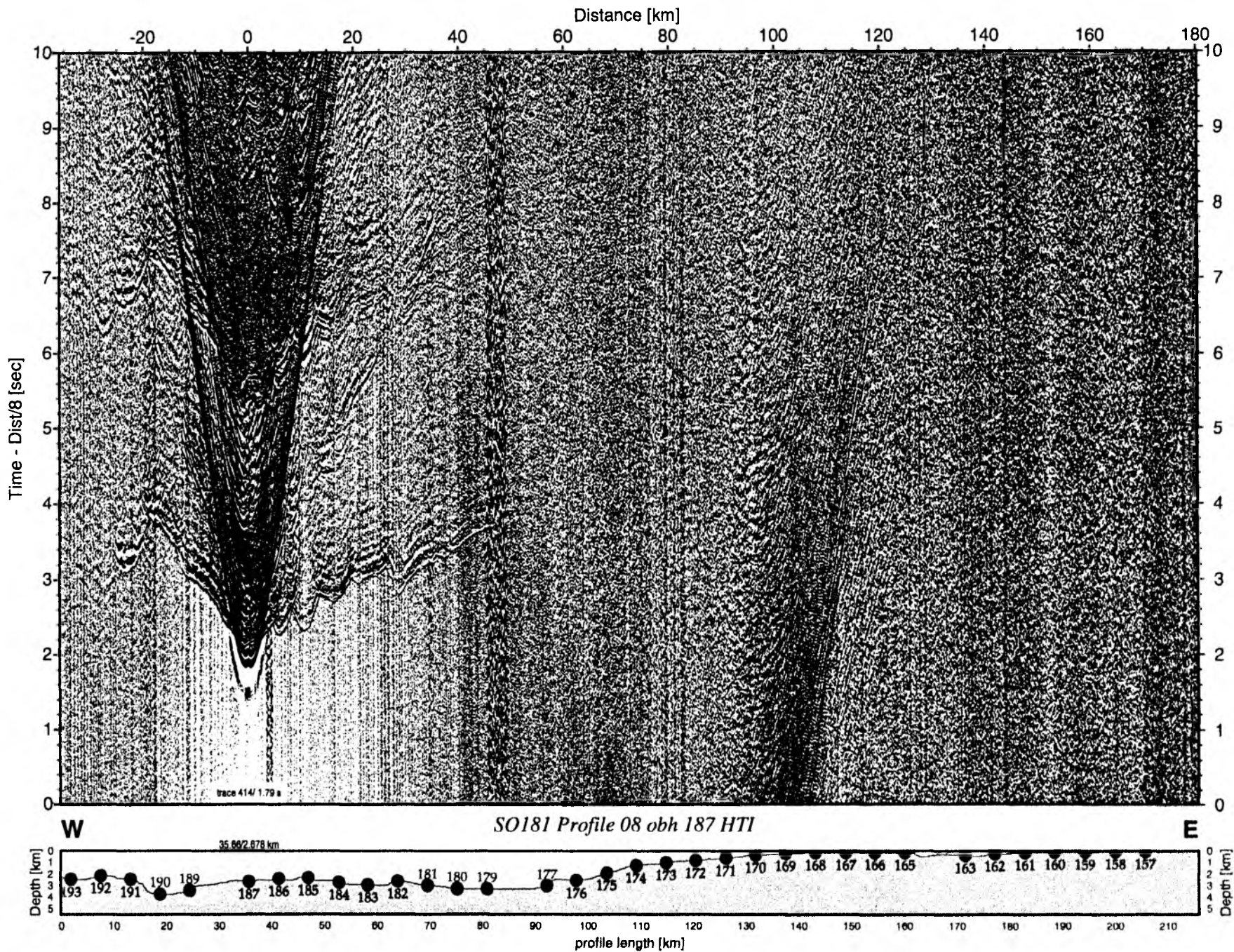


Figure 6.6.5.41: Record section from obh 187 HTI, Profile 08.

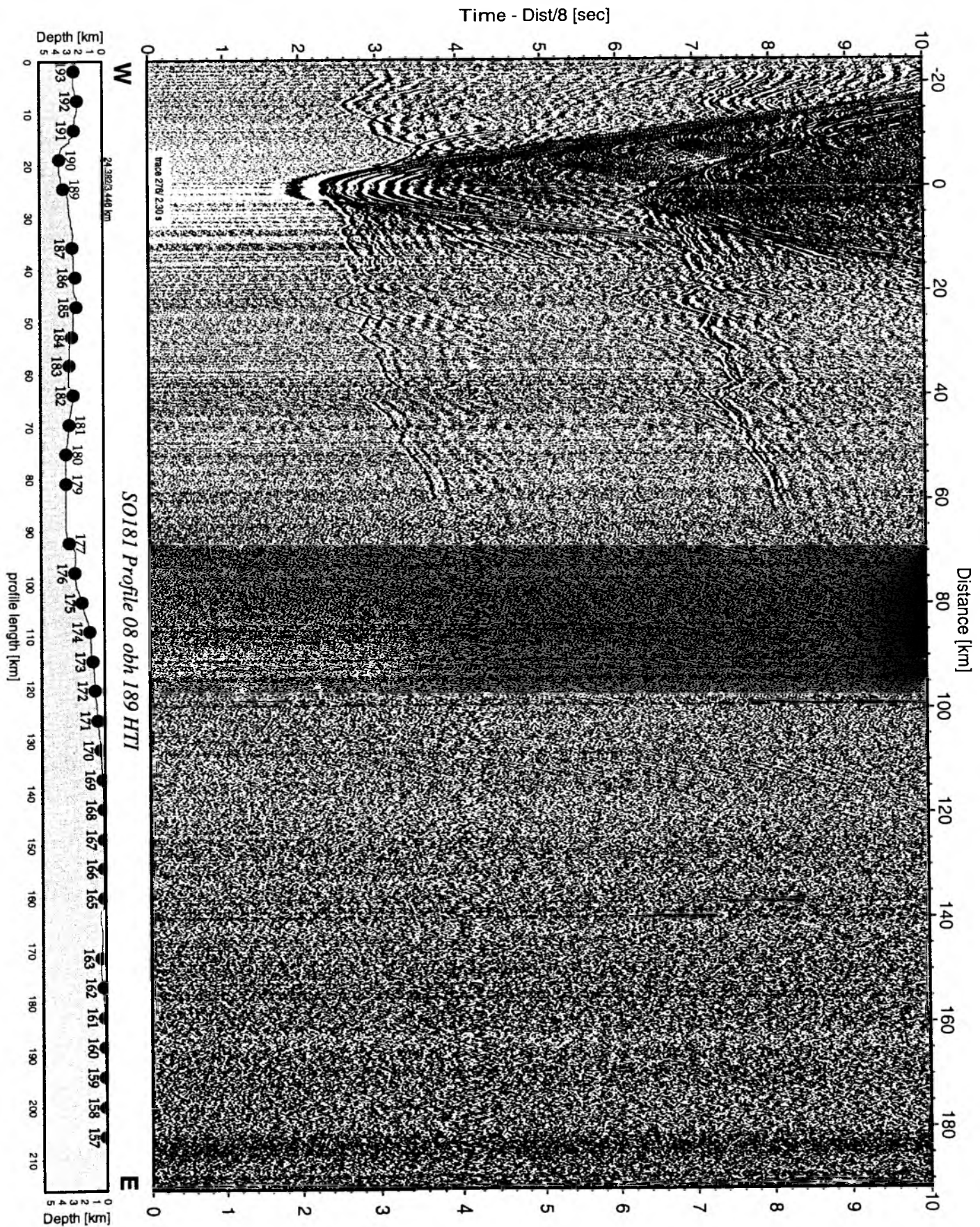


Figure 6.6.5.42: Record section from obh 189 HTI, Profile 08.

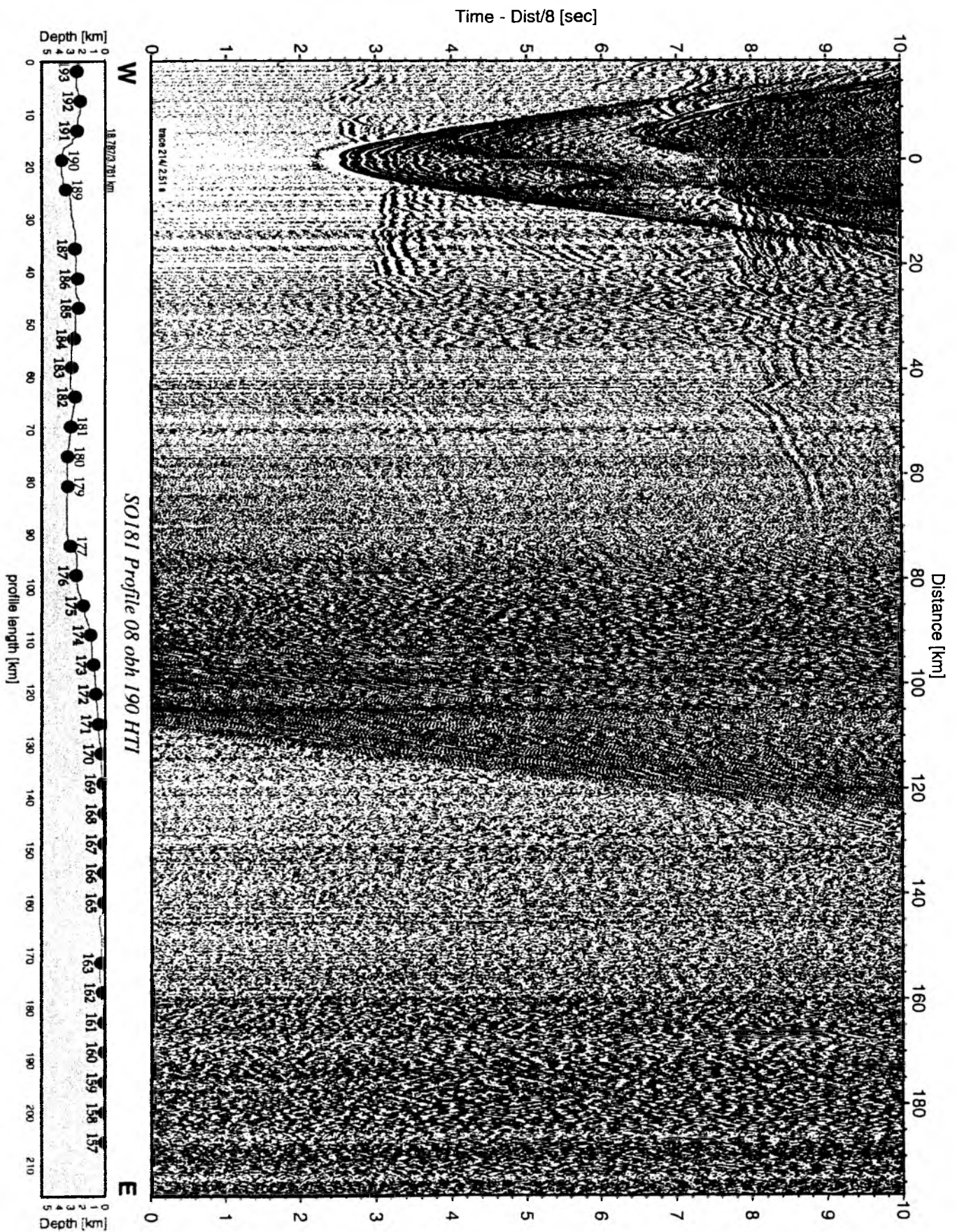


Figure 6.6.5.43: Record section from obh 190 HTI, Profile 08.

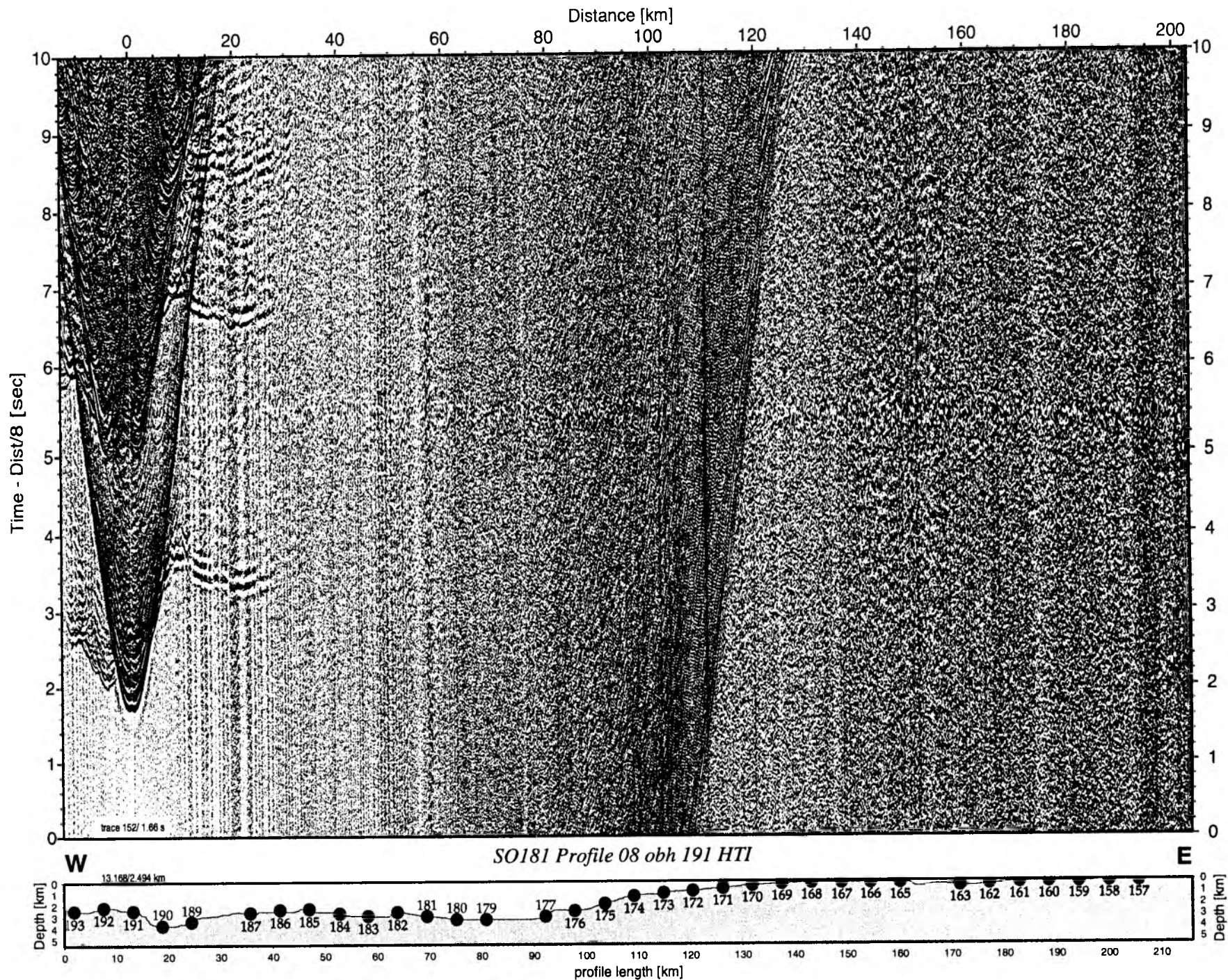


Figure 6.6.5.44: Record section from obh 191 HTI, Profile 08.

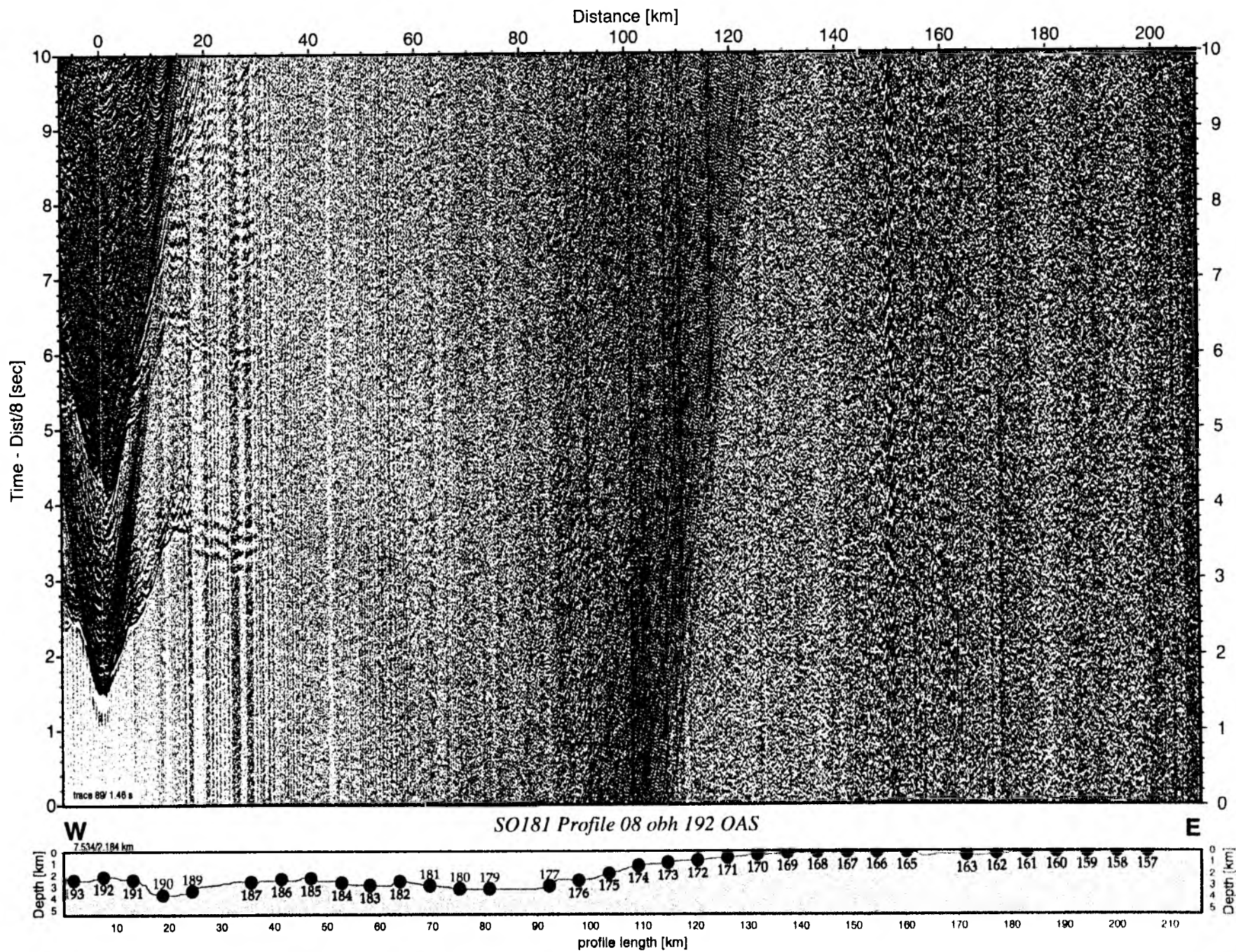


Figure 6.6.5.45: Record section from obh 192 OAS, Profile 08.

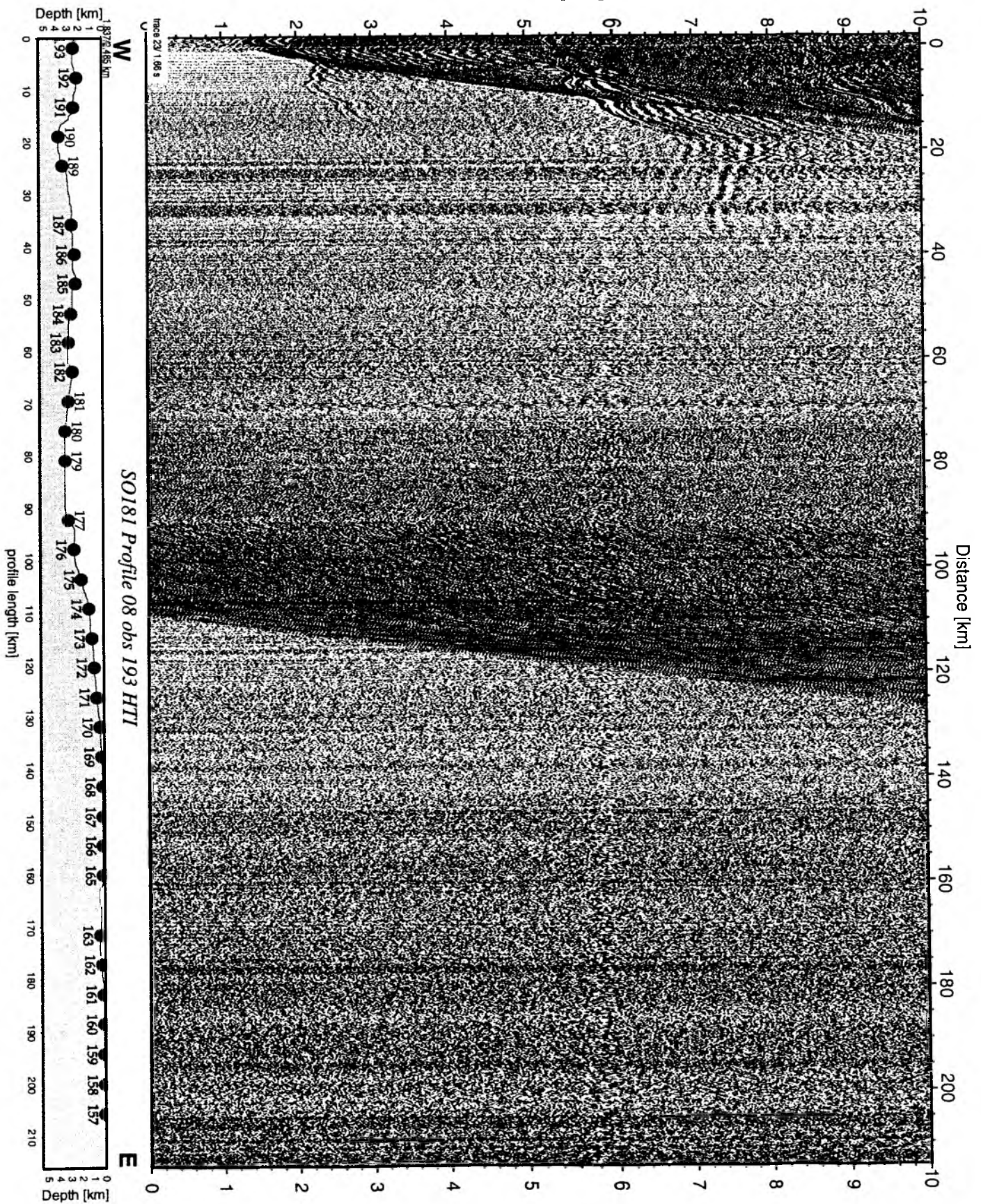


Figure 6.6.5.46: Record section from obs 193 HTI, Profile 08.

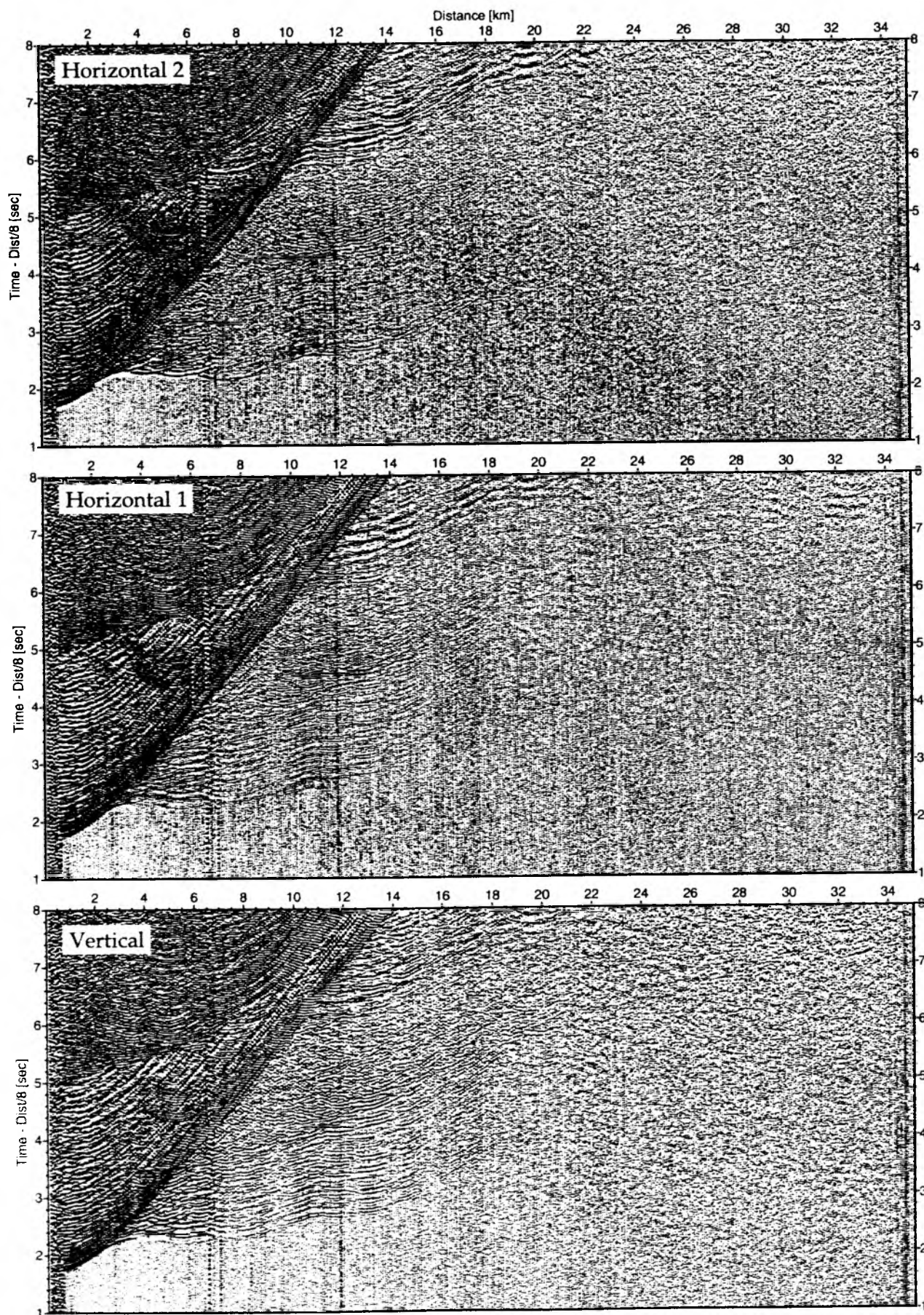


Figure 6.6.5.47: Record sections from obs 193 HTI/Owen-15Hz, SO181 Profile 08.

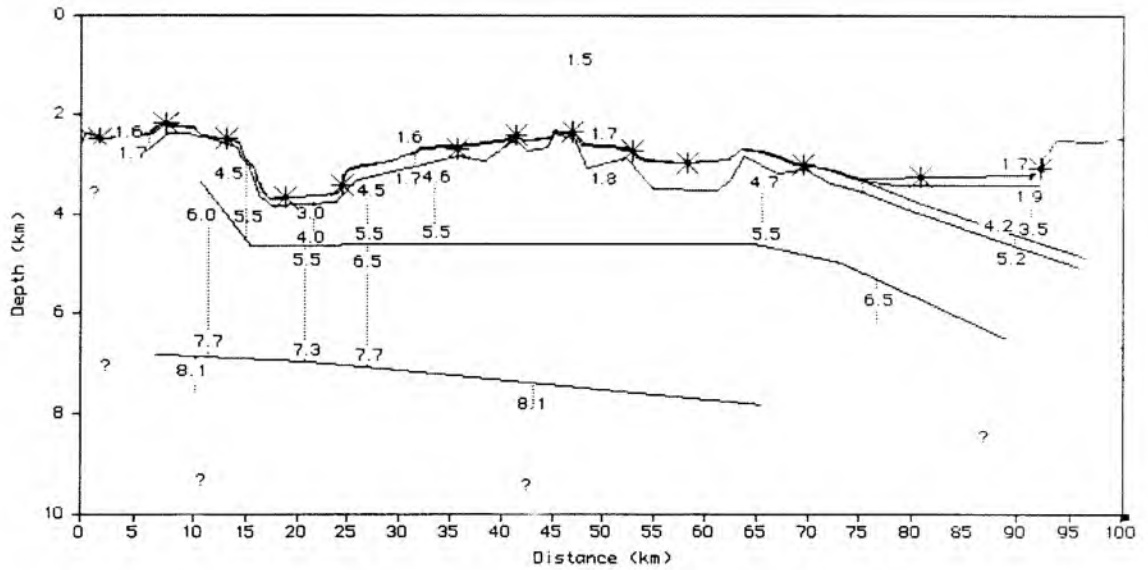


Figure 6.6.5.48: Preliminary velocity model for the oceanic plate of P08

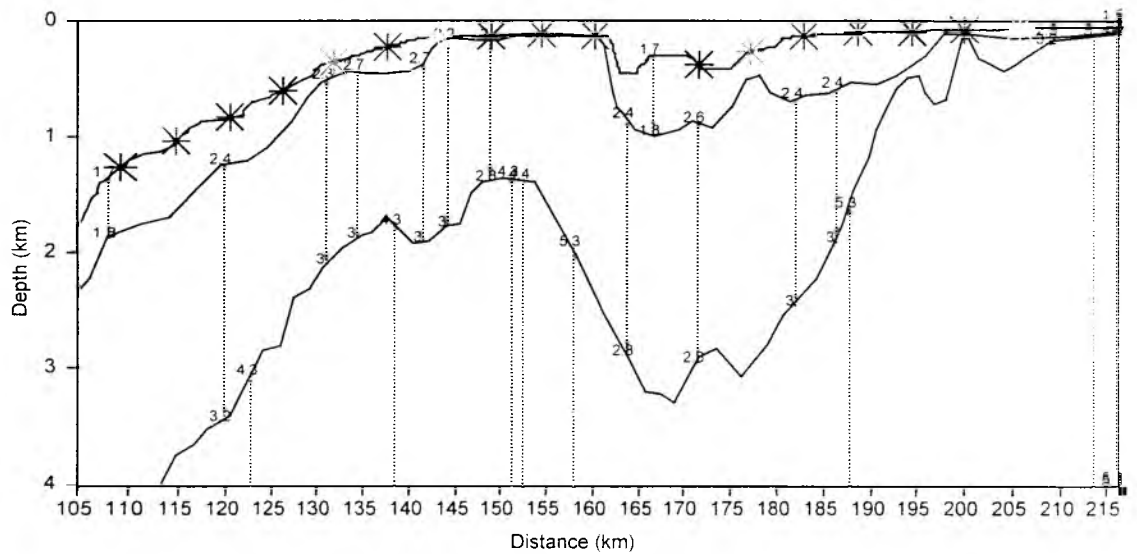


Figure 6.6.5.49: Preliminary velocity model for the continental margin of P08.

6.6.6 Profile P06

In total, 50 instruments were deployed along this profile from the Chile Rise to the coast between 07.02 and 08.02. Shooting was done in almost perfect conditions from 17:30 on 08 Feb to 18:00 on 10 Feb. During the entire shooting all four G-Gun cluster were in operation. The shooting interval was reduced to 40 sec. A four channel streamer was deployed throughout the profile, augmenting existing MCS data for parts of the profile. Instruments were picked up once shooting was terminated, they were all back onboard on 12 Feb. Details of instruments and shots can be found in Appendices 9.2 and 9.3; most instruments recorded well. A location map is shown in Figure 6.6.6.1, and record sections are shown in Figures 6.6.6.2 to 6.6.6.62. A preliminary onboard analysis was attempted, taking also the results (sediment thickness) from the seismic reflection data into account.

The data are of good quality. Most of the data exhibit clear refracted waves in the oceanic and continental crust, clear Moho wide-angle reflections from the oceanic crust which become less clear when the Moho becomes deeper. Also some refracted waves from the mantle are observed.

The preliminary velocity depth model obtained has been built using data from the bathymetry files, the seismic reflection data as well as refraction data. The bottom of the sedimentary layer has been picked on the streamer section and converted to depth for the oceanic crust up to the trench. In the zone of the accretionary prism, the thickness of sediments becomes too large to observe the basement on the reflection data. However, these data show that the shallow sedimentary layers exhibit undulations that are most likely due to basement topography.

The preliminary velocity depth model is shown in Figure 6.6.1.63. The different phases observed on all the record sections from the OBS/H have been picked but only 8 OBS/H (OBS 73, 78, 82, 84, 109, 195, and OBH 93) have been taken into account for the forward modelling for lack of time.

The raypaths and the results of the modelling for these 8 OBS/H are shown in Figures 6.6.6.64 to 6.6.6.67. Some misfit still exists between the calculated and the observed traveltimes.

The oceanic crust consists of a thin sedimentary layer with a velocity of about 1.8 km/s, an upper crust which is about 1 to 2 km thin with a velocity increasing from 4.2 to 5.9 km/s, and a lower oceanic crust of about 4 km thickness with a velocity increasing from 6.3 to 6.9 km/s. The oceanic mantle has been modelled using a velocity of 8 km/s. The westernmost part of this profile transgresses the ridge but the data in this area have not been studied sufficiently to draw conclusions.

The trench sediments are about 2 km thick for the deepest part and are well imaged on the seismic reflection profile. The bending and dipping of the subducting oceanic crust is mostly constrained by the data from the OBS99 and 93 (Figure 6.6.6.66).

The accretionary prism and the "shelf" consist of a thick sedimentary sequence with a velocity of 1.8 to 2.2 km/s. The basement exhibits a strong topography, affected probably by faults. The velocity at the top of the basement is about 4.2 km/s. An intra-crustal interface has been added to fit the data. This interface has a strong topography which may be dubious. A laterally strongly varying velocity structure in the crust can be suspected in this region.

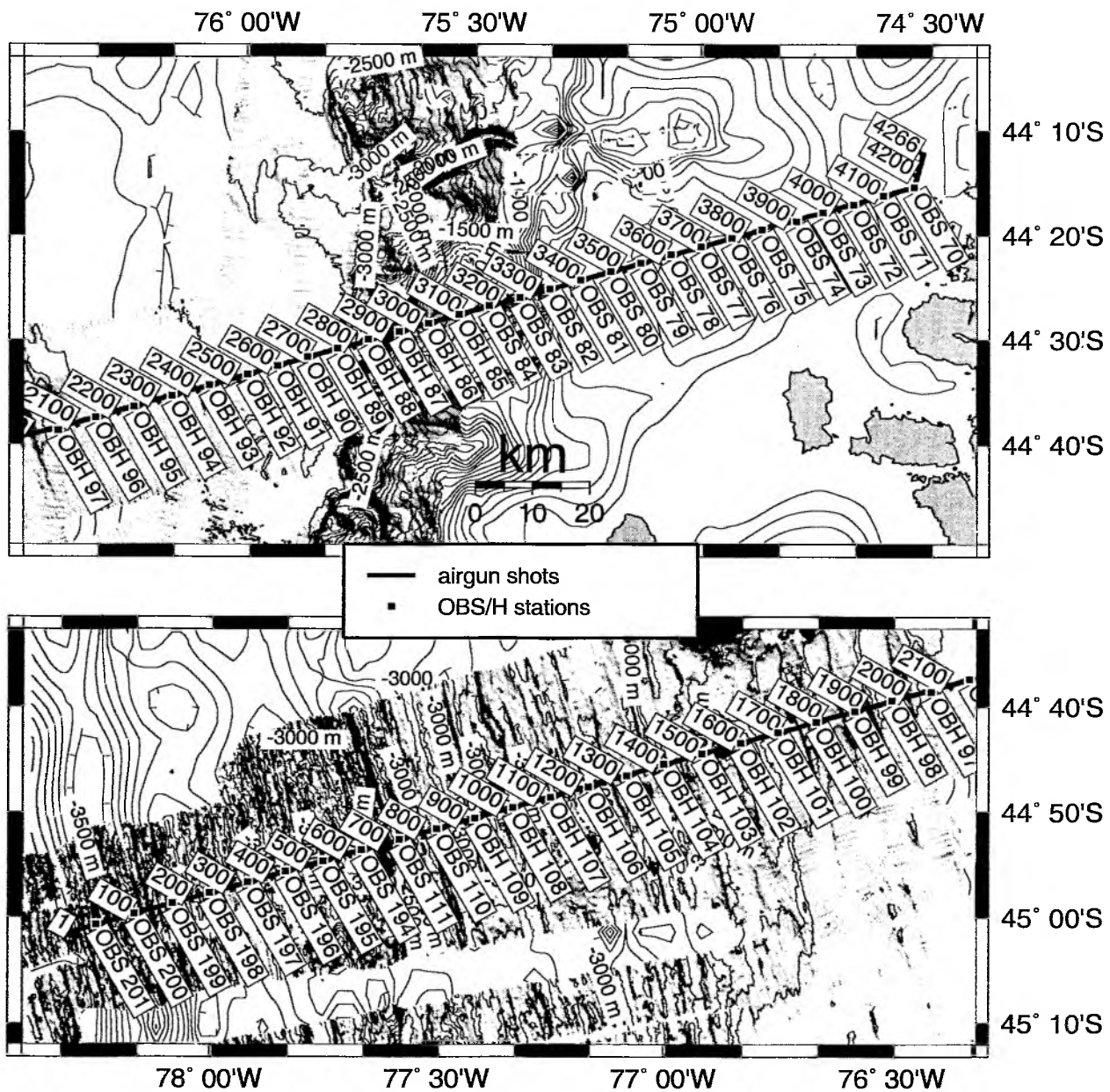


Figure 6.6.6.1: Basemap of P06; transect of ocean bottom seismometer and hydrophone stations and line of airgun shots. Bathymetry contours every 200m.

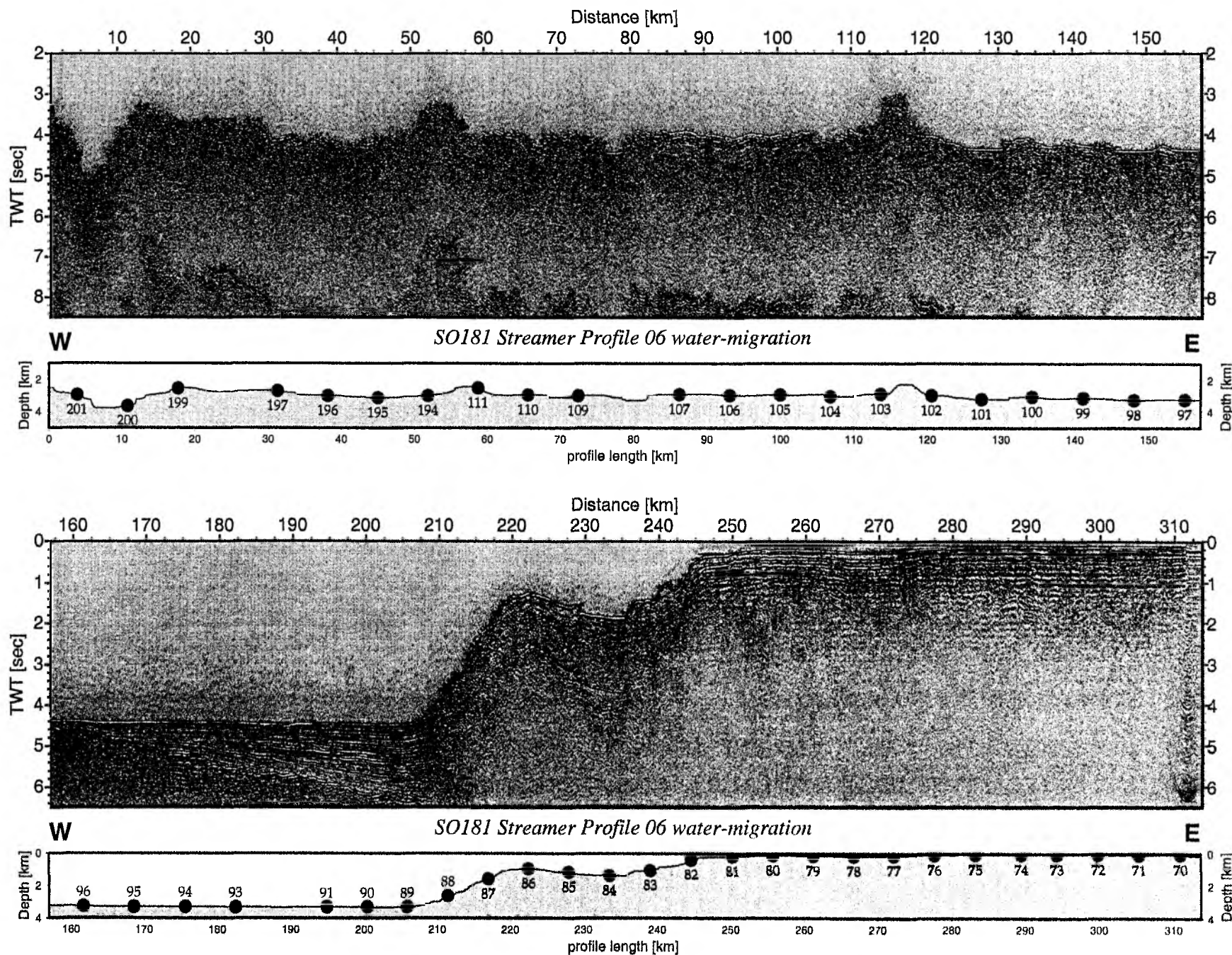


Figure 6.6.6.2: Record section from Streamer Profile 06 water-migration.

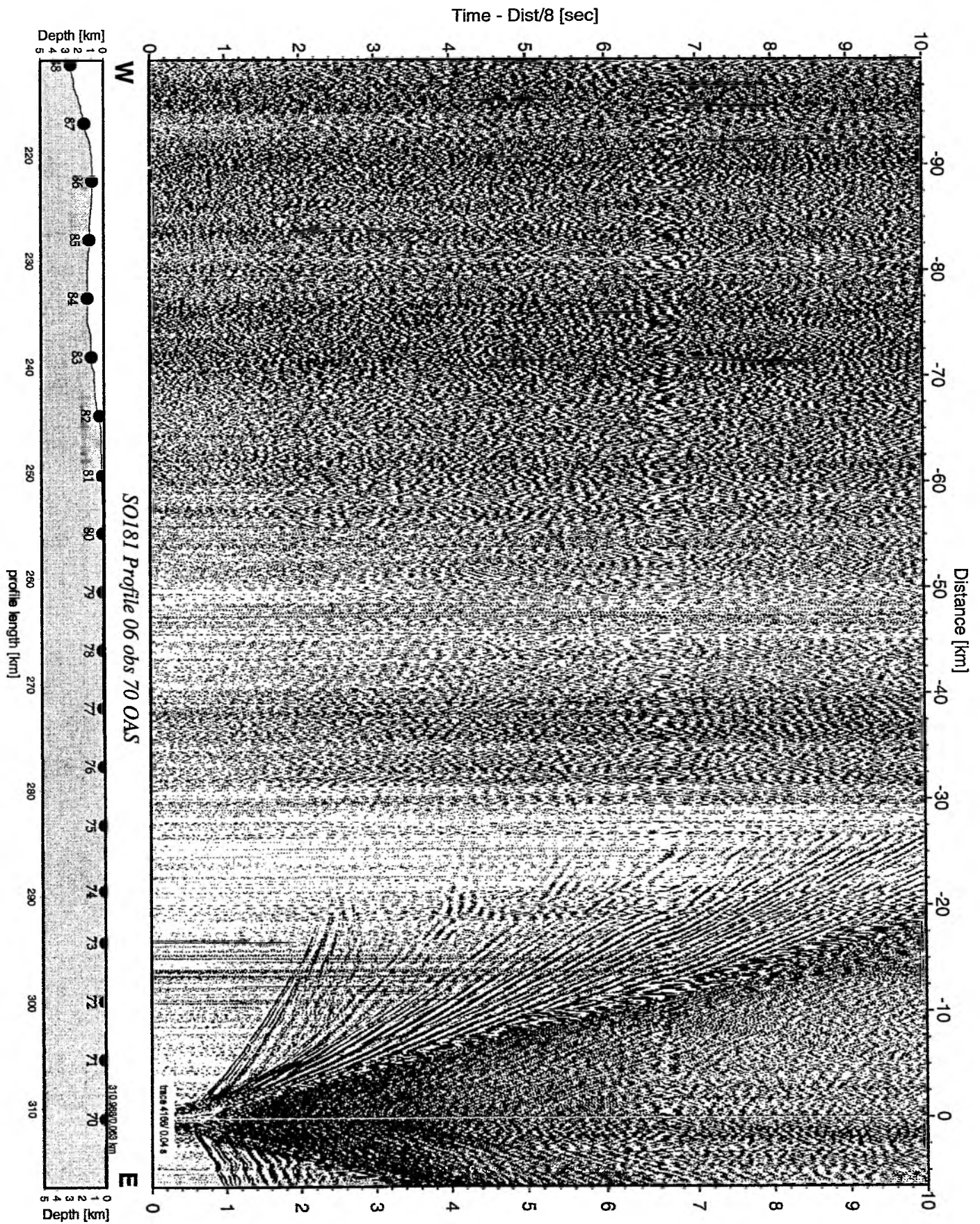


Figure 6.6.6.3: Record section from obs 70 OAS, Profile 06.

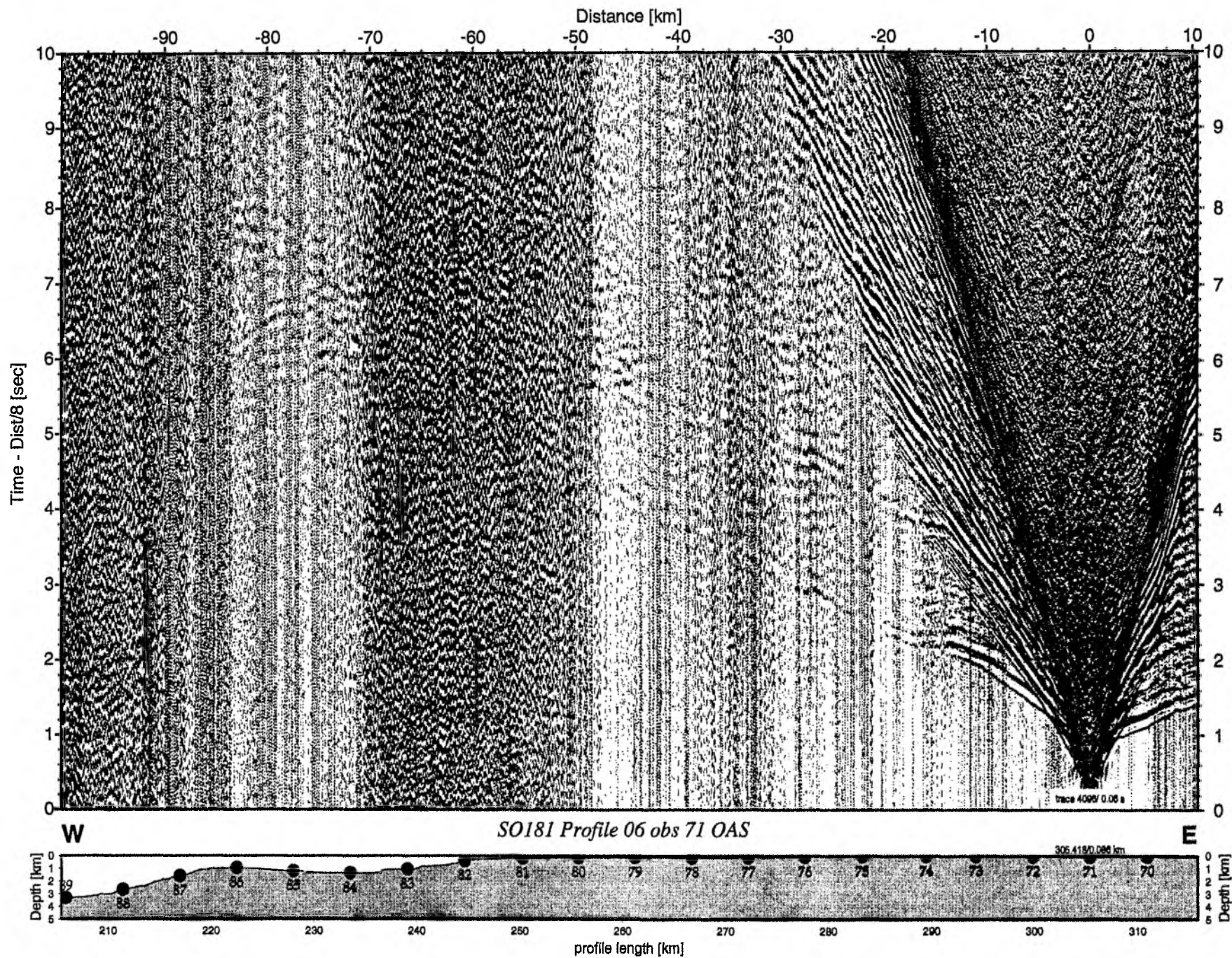


Figure 6.6.6.4: Record section from obs 71 OAS, Profile 06.

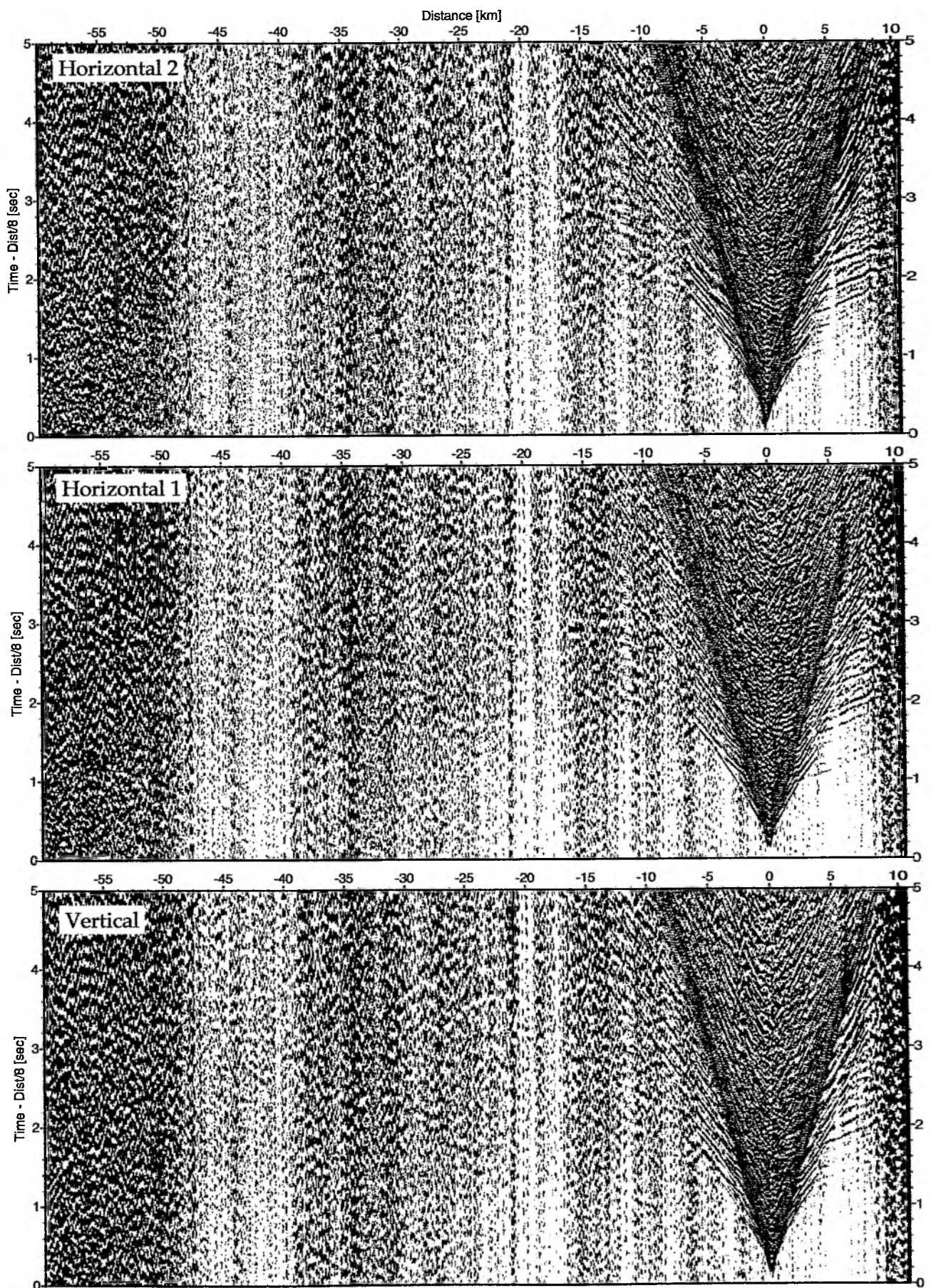


Figure 6.6.6.5: Record sections from obs 71 OAS/Owen-4.5Hz, SO181 Profile 06.

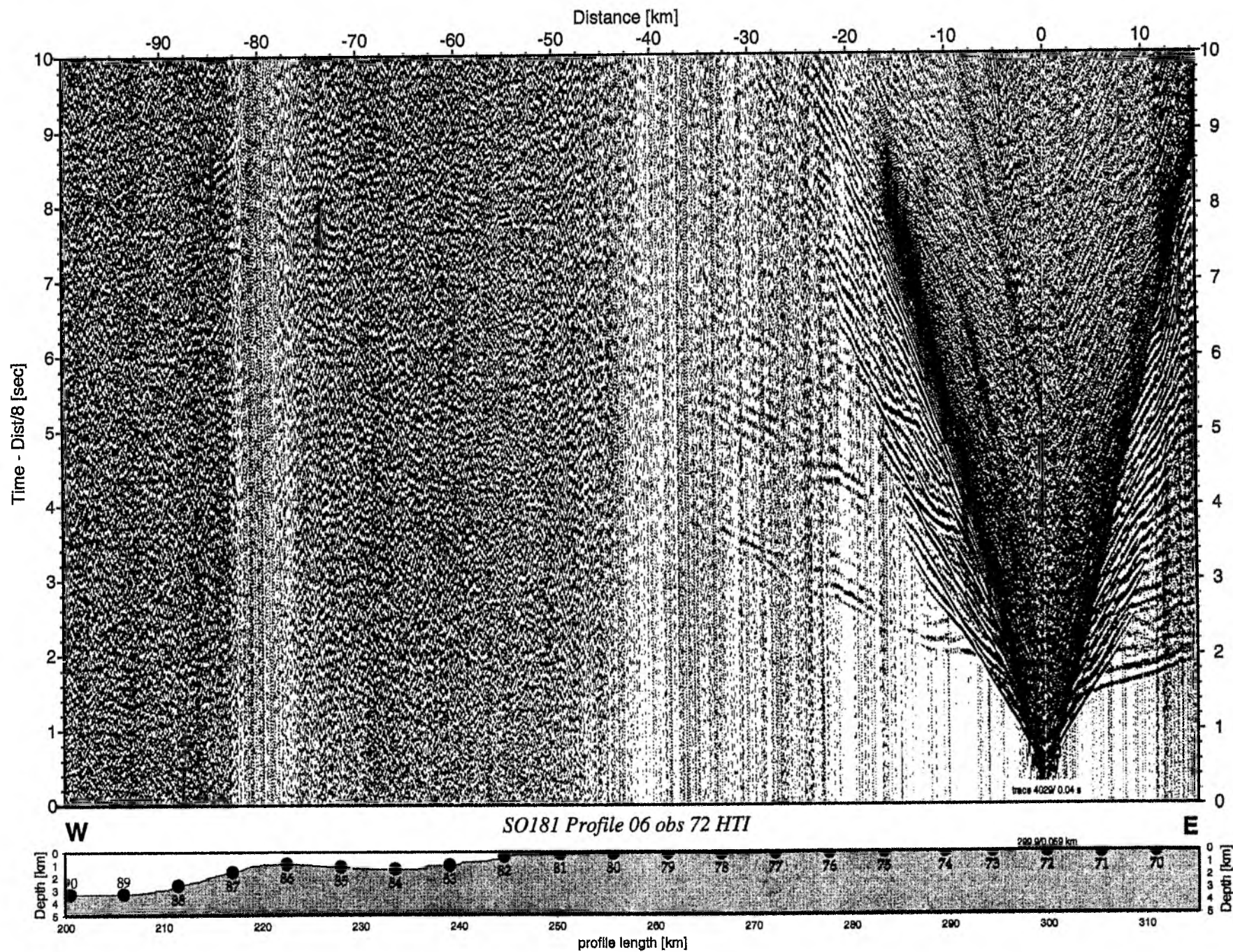


Figure 6.6.6.6:

Record section from obs 72 HTI, Profile 06.

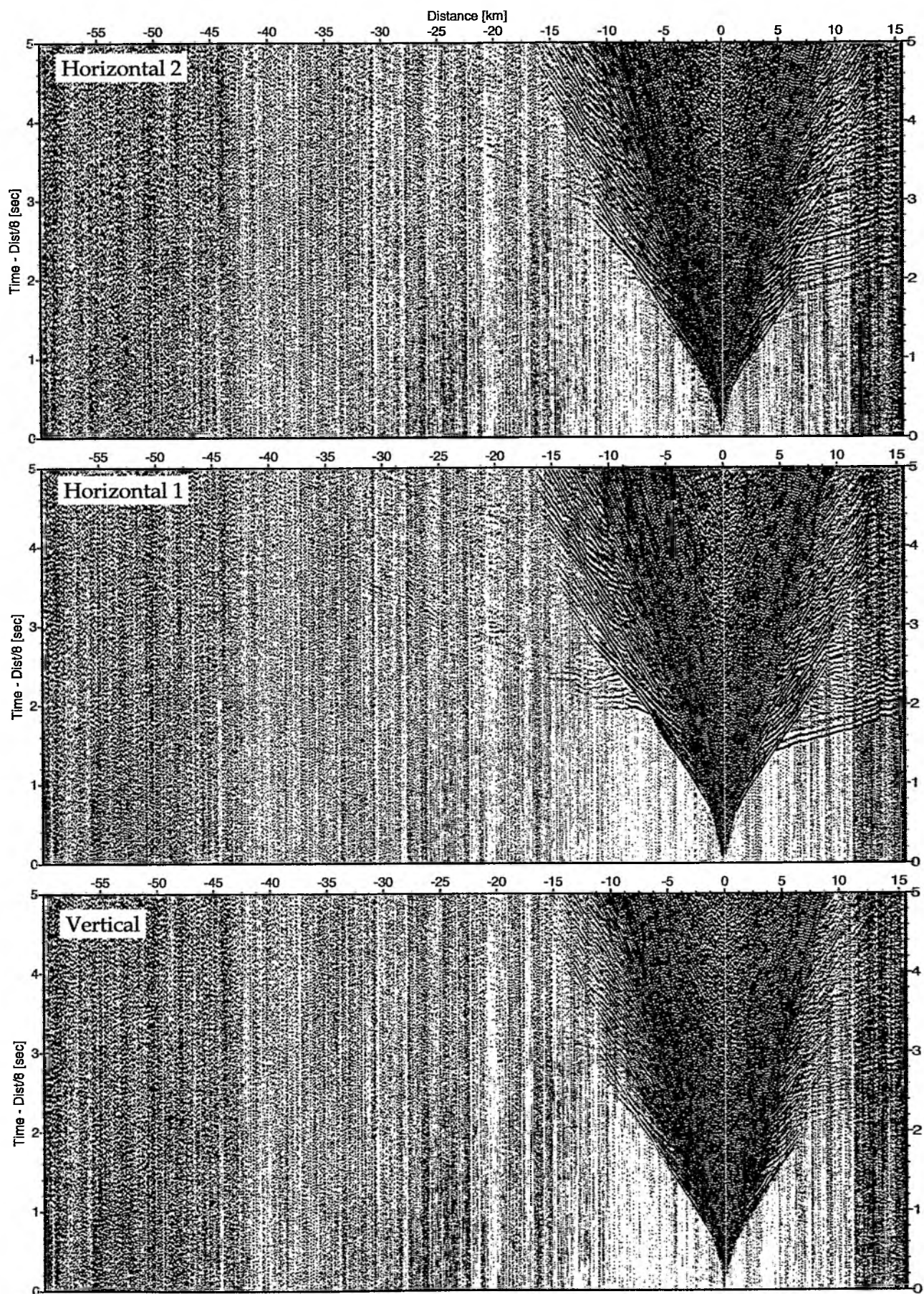


Figure 6.6.6.7: Record sections from obs 72 HTI/Owen-15Hz, SO181 Profile 06.

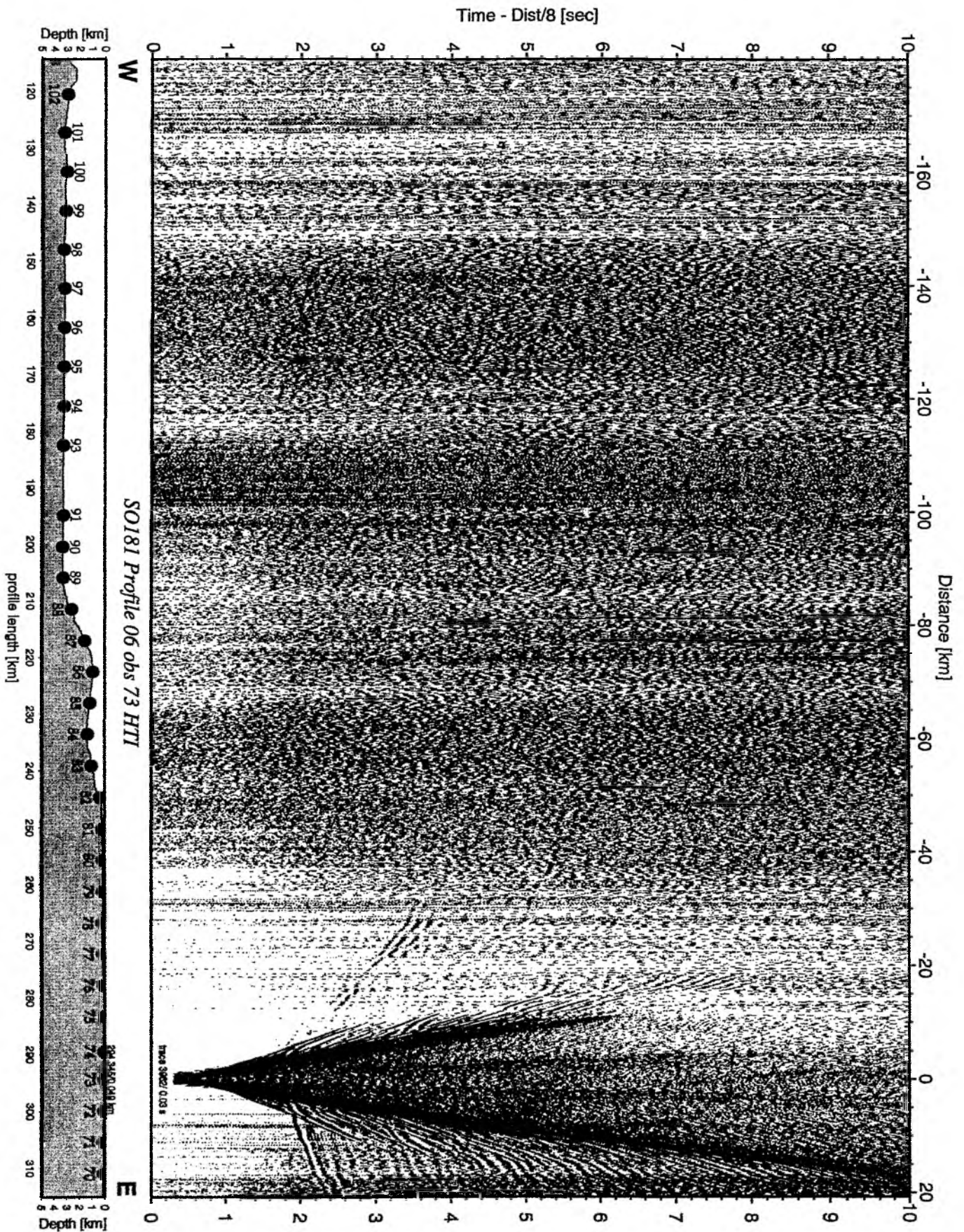


Figure 6.6.6.8: Record section from obs 73 HTI, Profile 06.

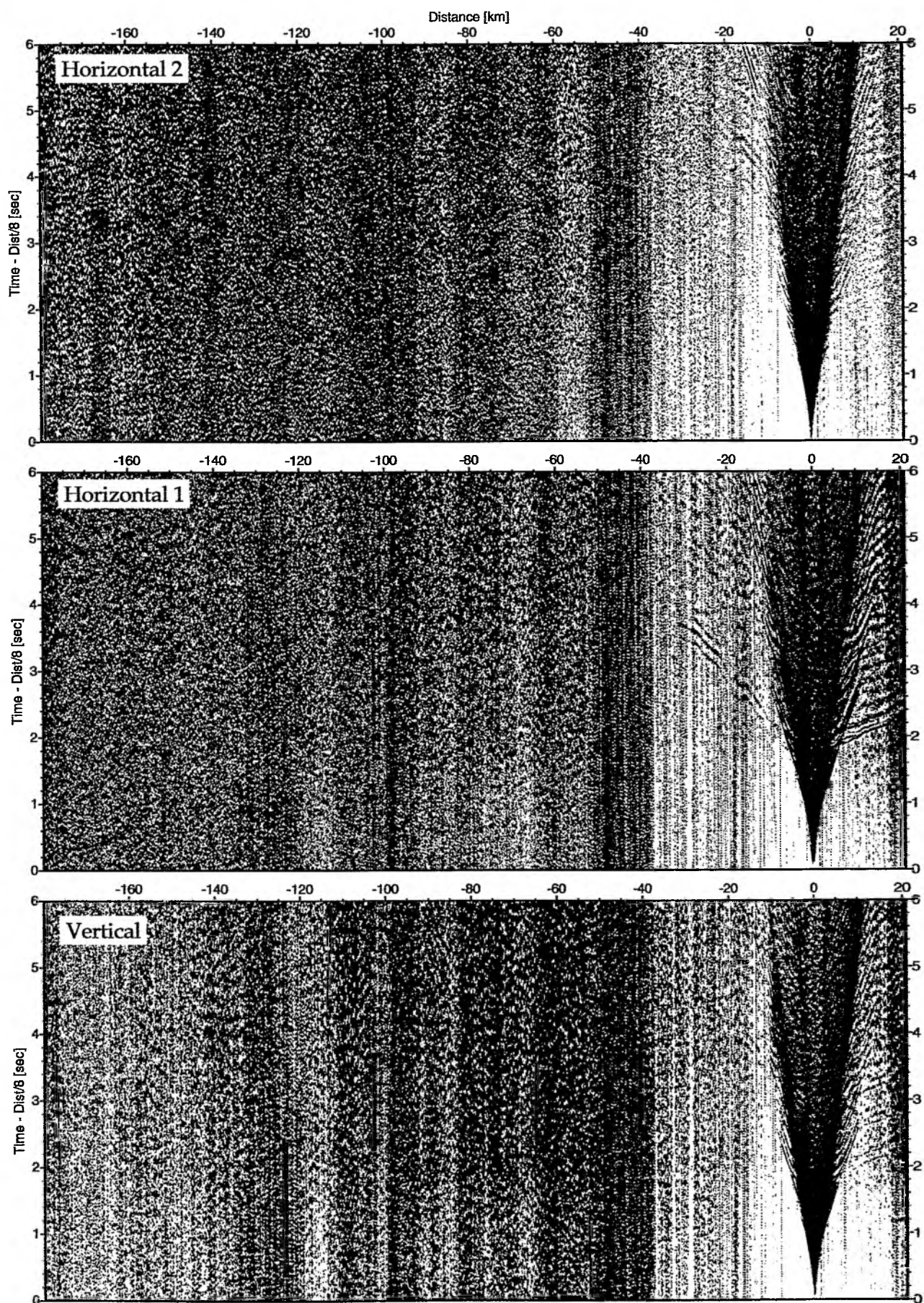


Figure 6.6.6.9: Record sections from obs 73 HTI/Owen-4.5Hz, SO181 Profile 06.

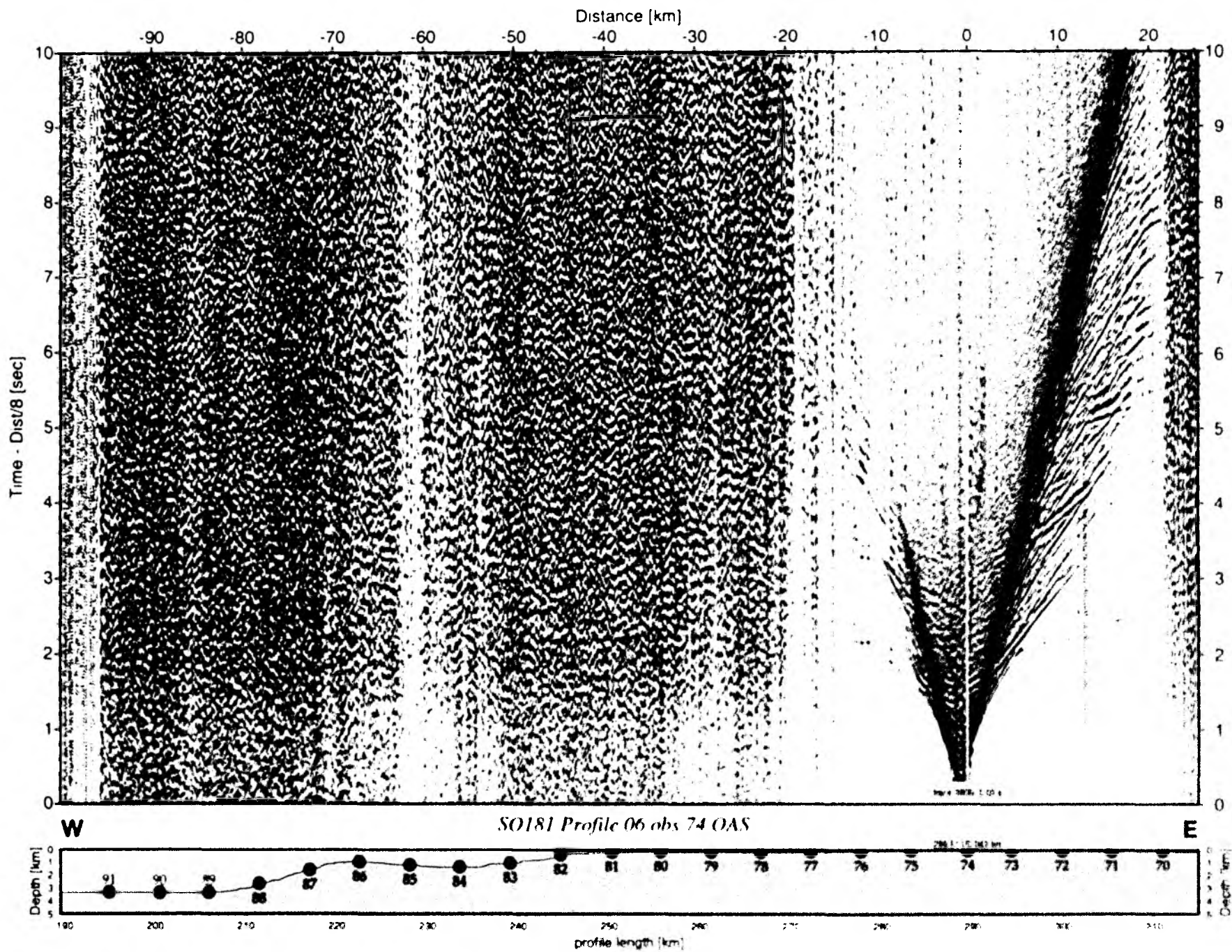


Figure 6.6.6.10: Record section from obs 74 OAS, Profile 06.

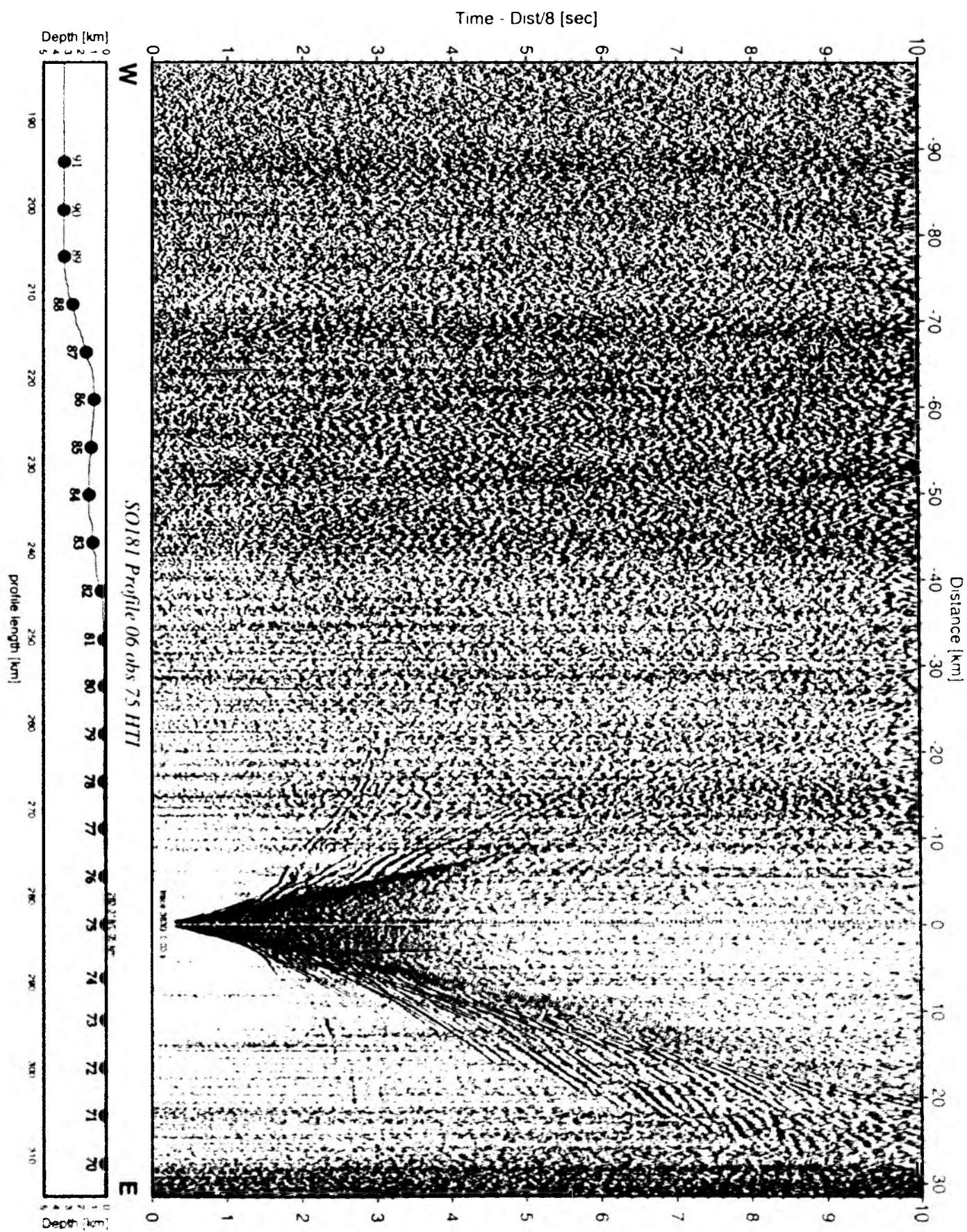


Figure 6.6.6.11: Record section from obs 75 HTI, Profile 06.

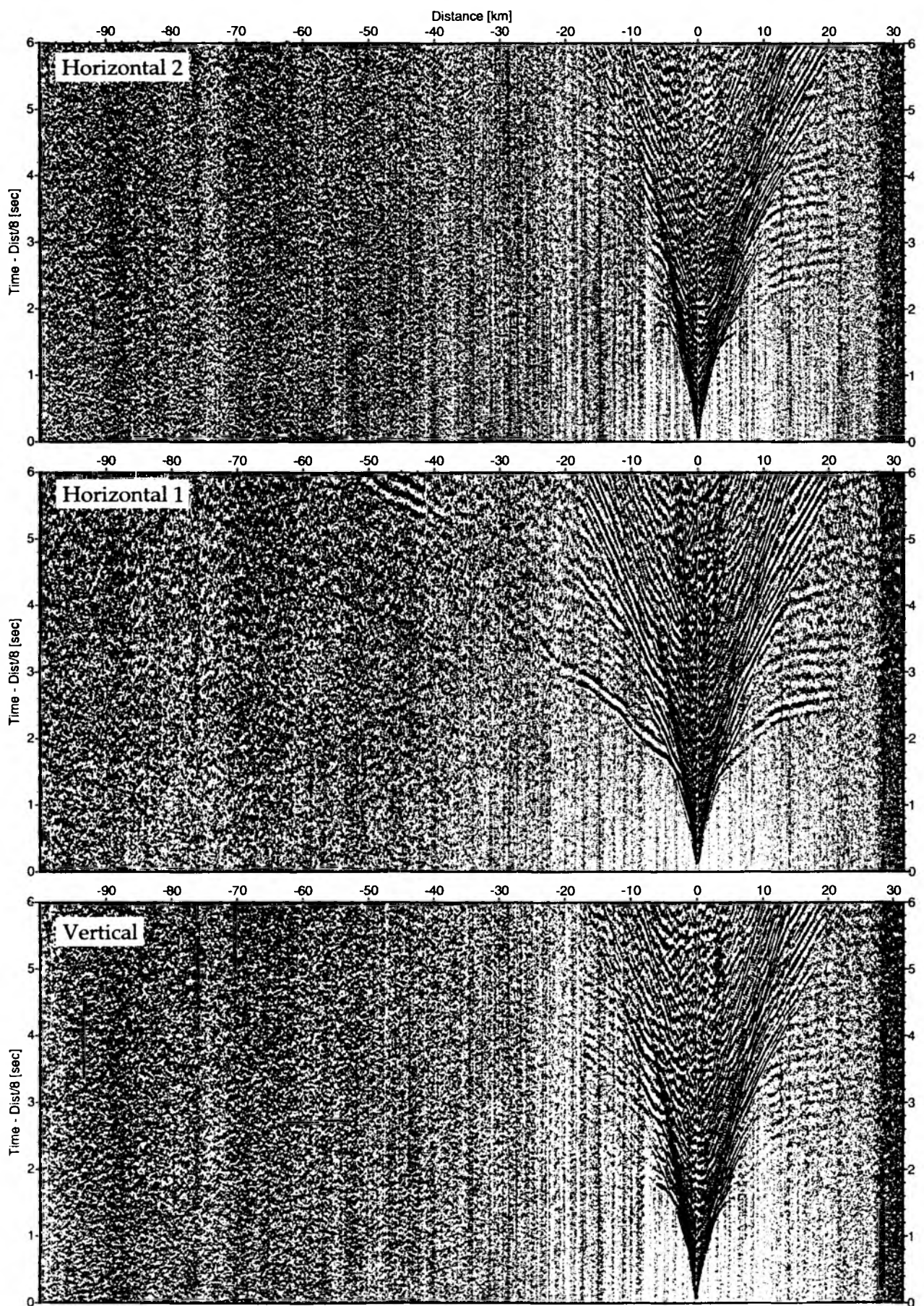


Figure 6.6.6.12: Record sections from obs 75 HTI/Owen-4.5Hz, SO181 Profile 06.

Time - Dist/8 [sec]

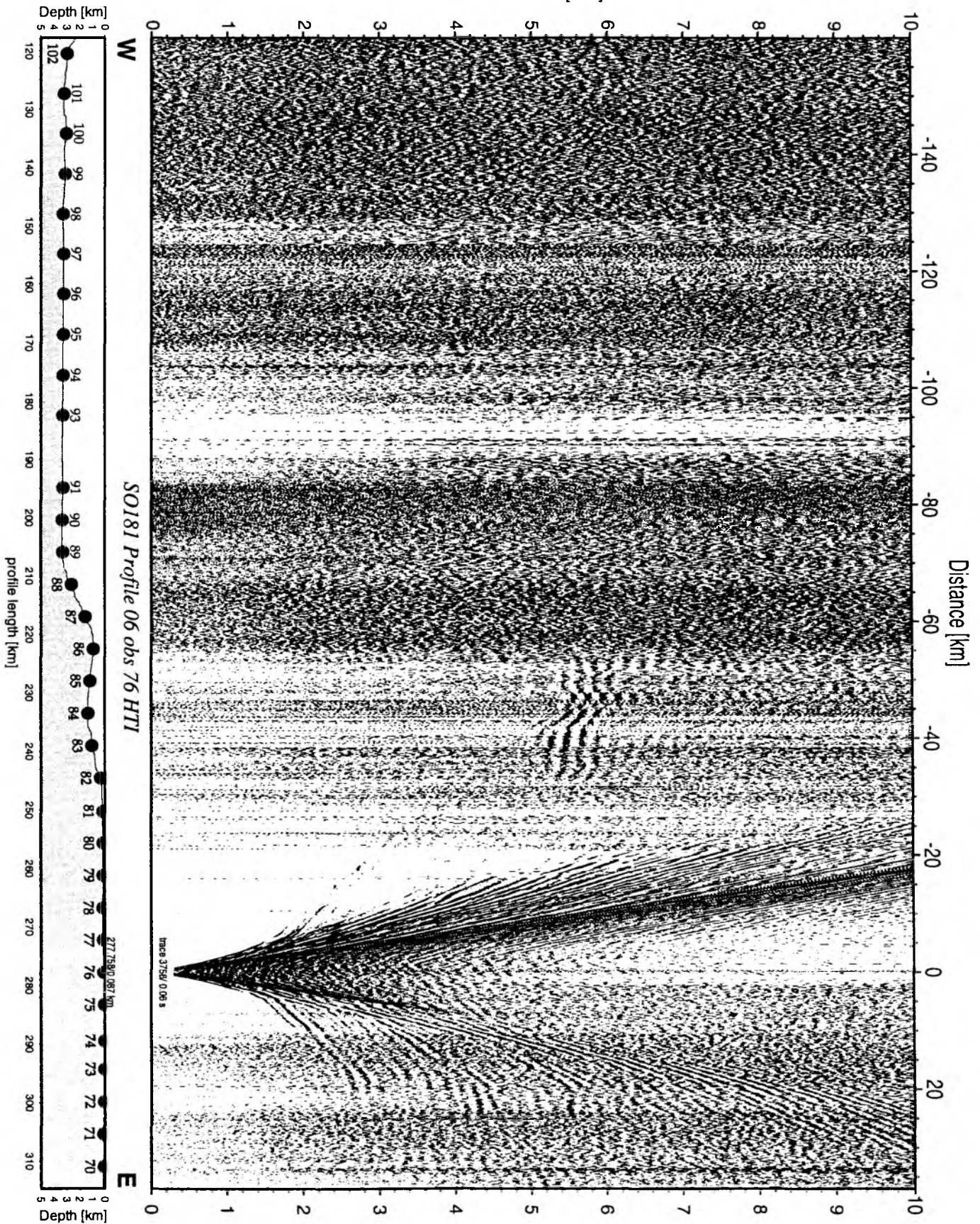


Figure 6.6.13: Record section from obs 76 HTI, Profile 06.

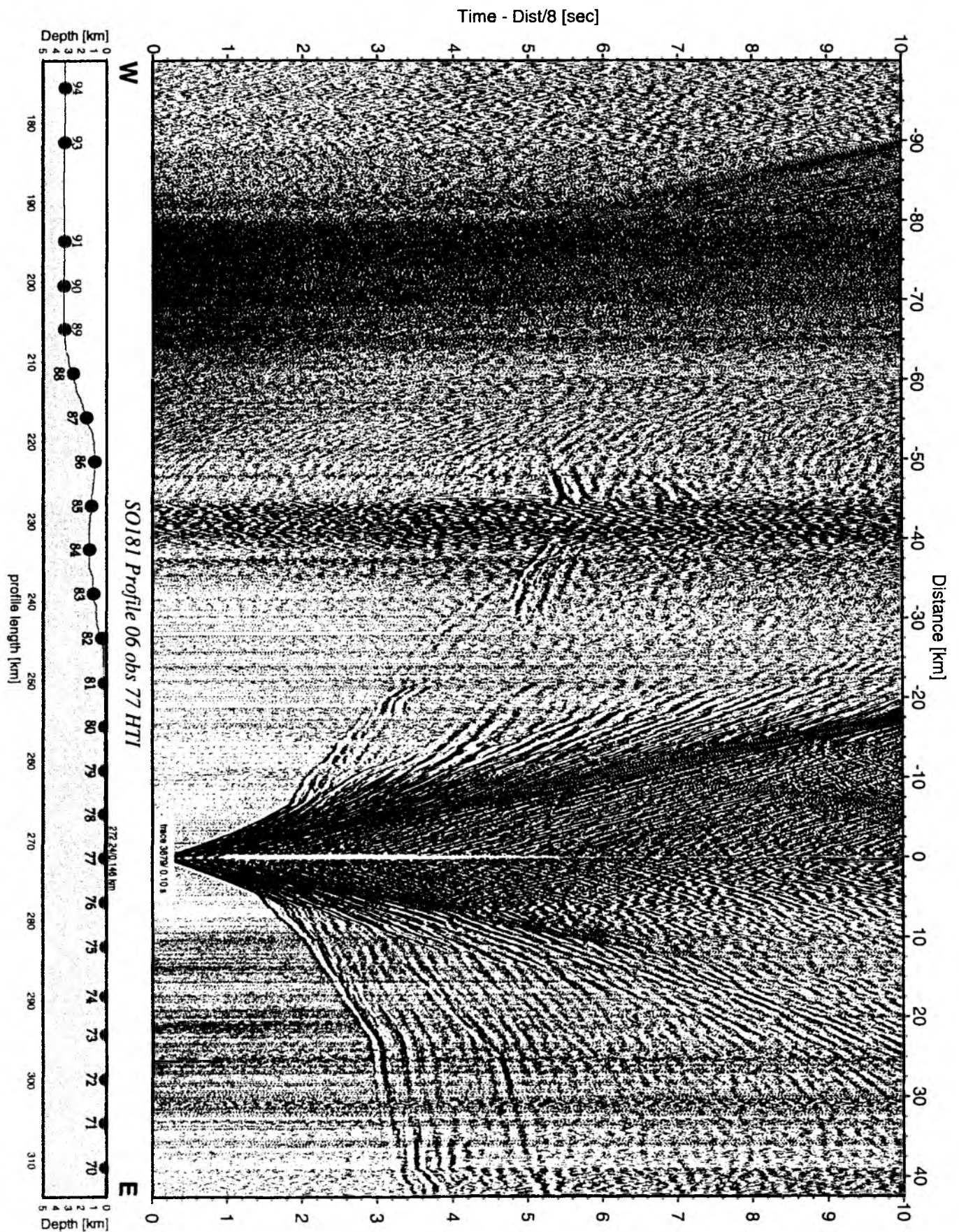


Figure 6.6.6.14: Record section from obs 77 HTI, Profile 06.

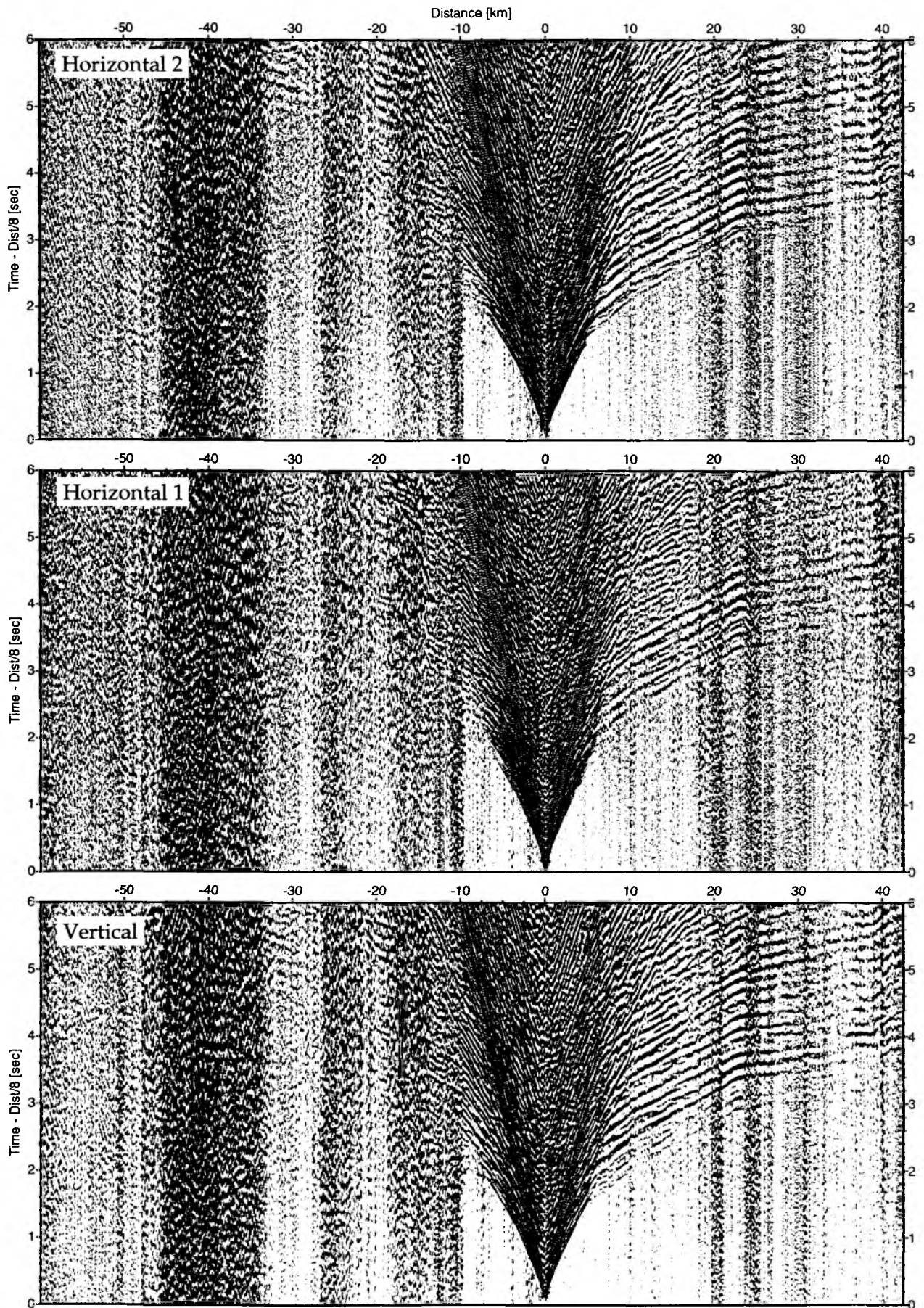


Figure 6.6.6.15: Record sections from obs 77 HTI/Owen-4.5Hz, SO181 Profile 06.

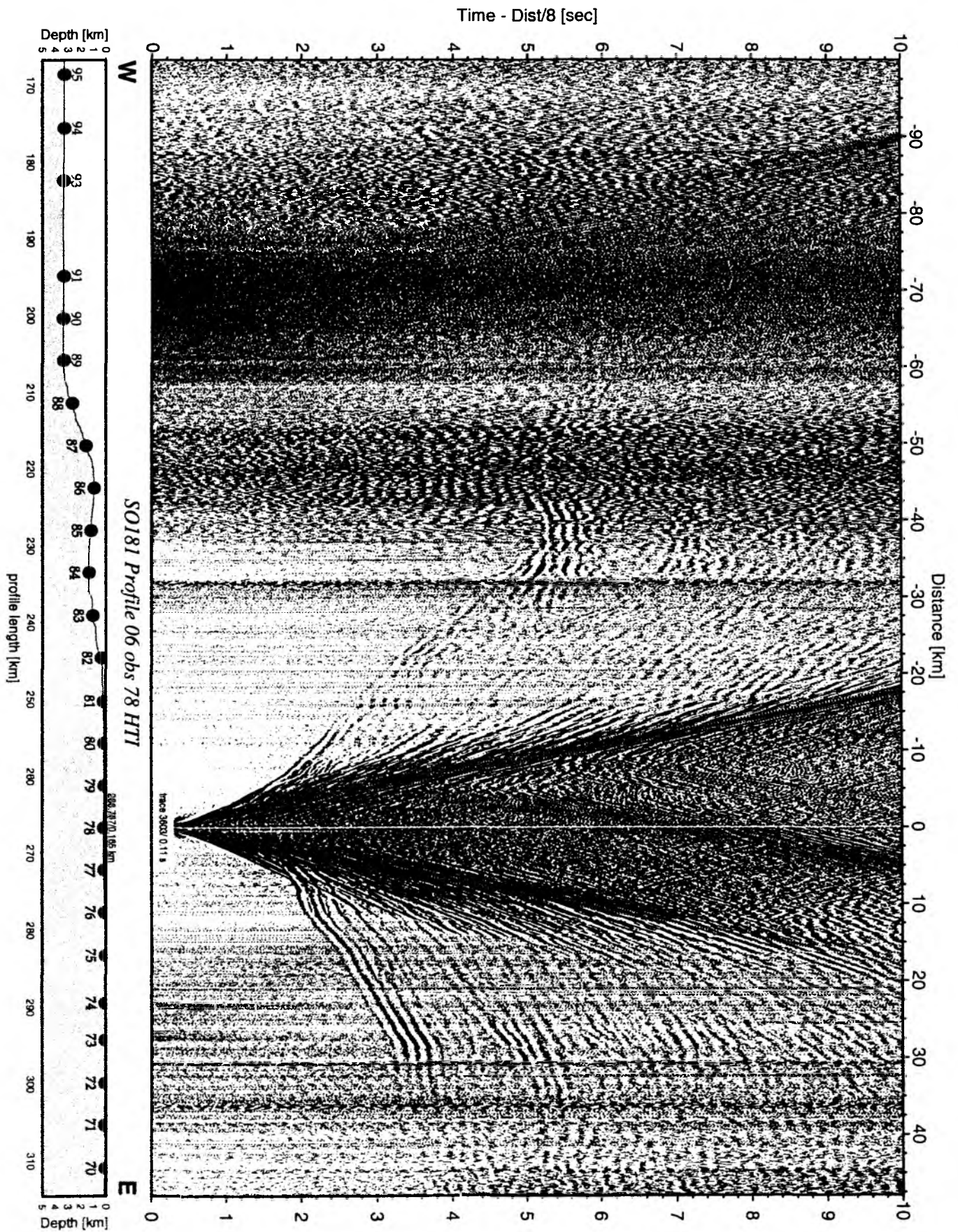


Figure 6.6.6.16: Record section from obs 78 HTI, Profile 06.

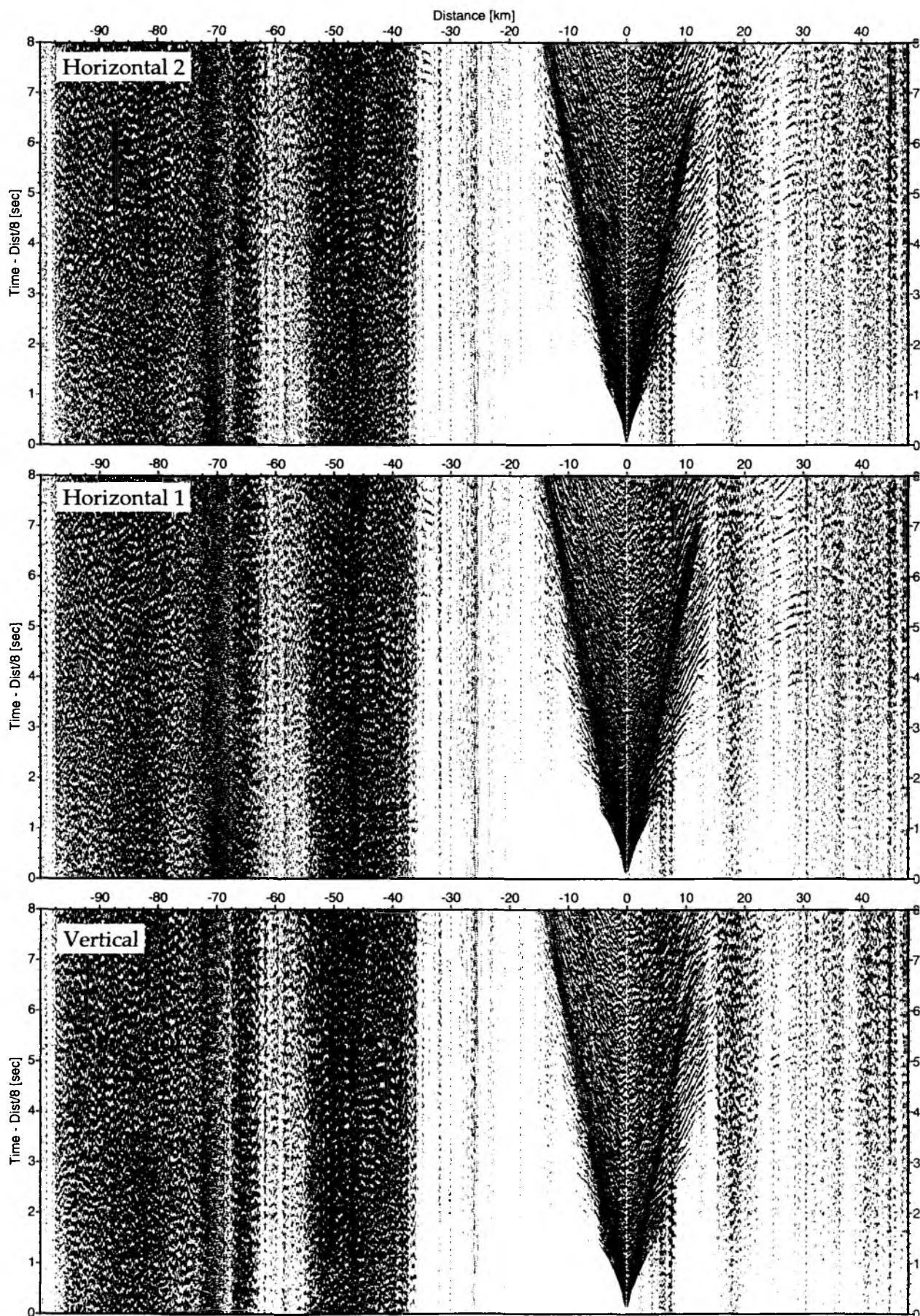


Figure 6.6.6.17: Record sections from obs 78 HTI/Owen-4.5Hz, SO181 Profile 06.

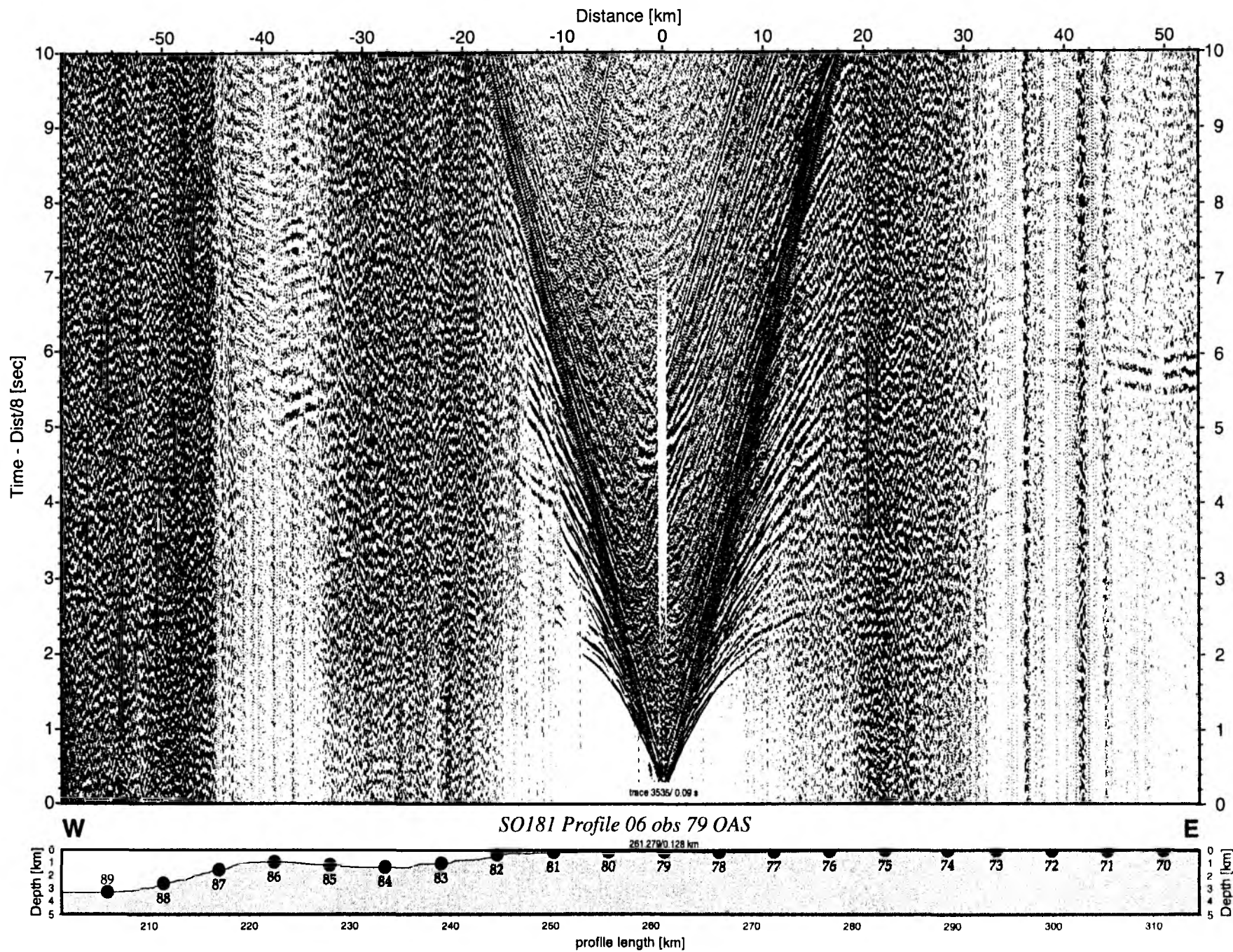


Figure 6.6.6.18: Record section from obs 79 OAS, Profile 06.

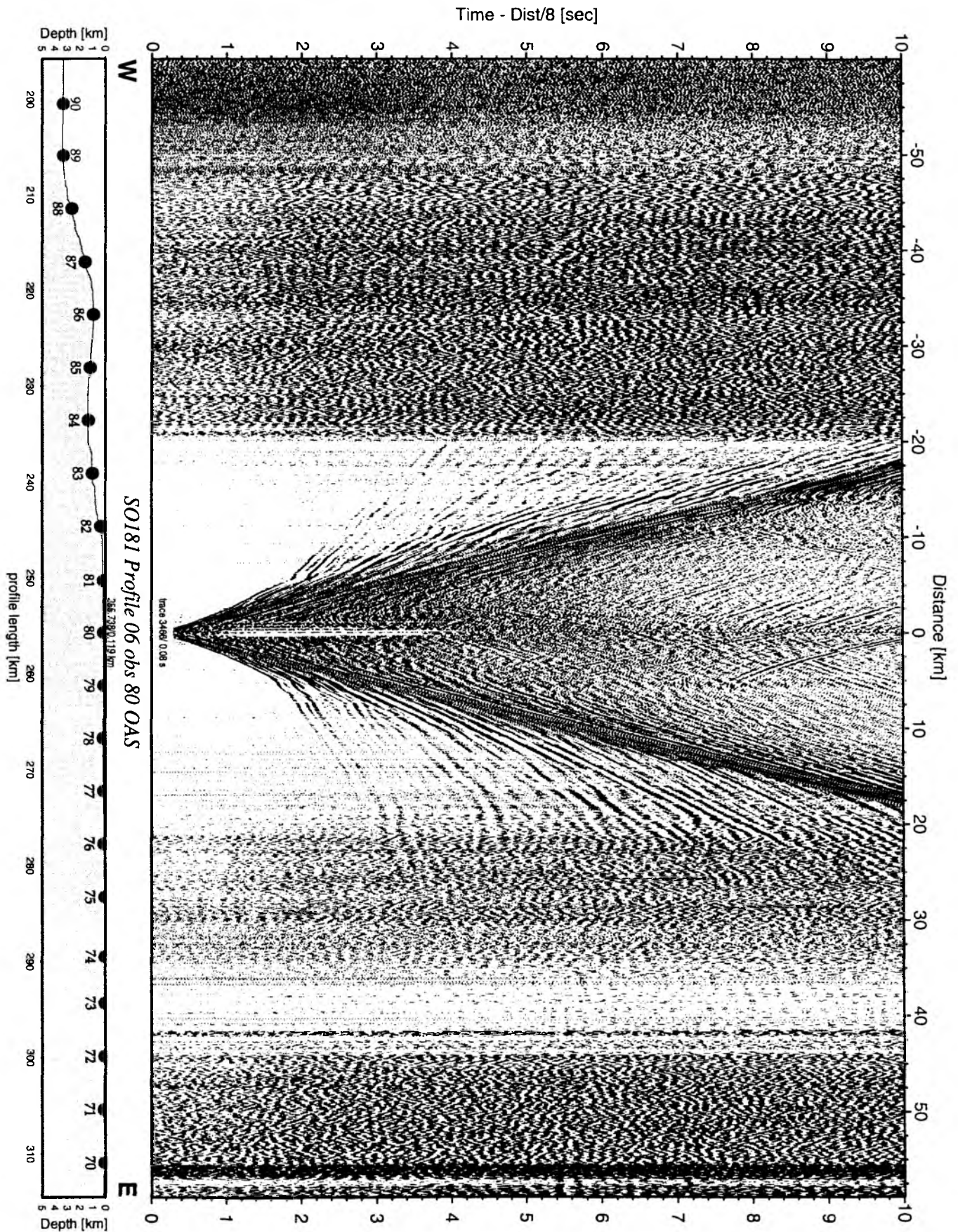


Figure 6.6.6.19: Record section from obs 80 OAS, Profile 06.

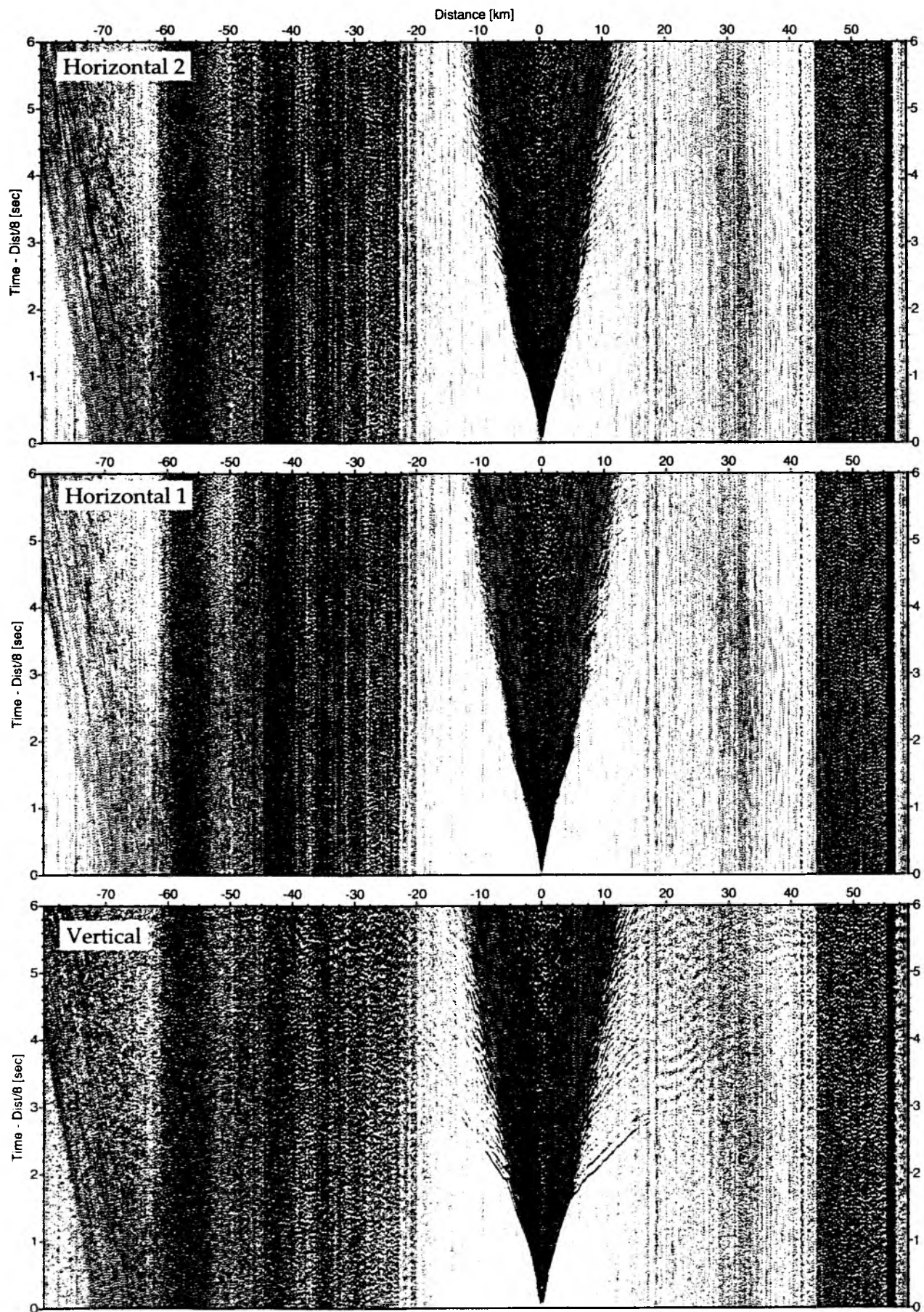


Figure 6.6.6.20: Record sections from obs 80 OAS/Owen-4.5Hz, SO181 Profile 06.

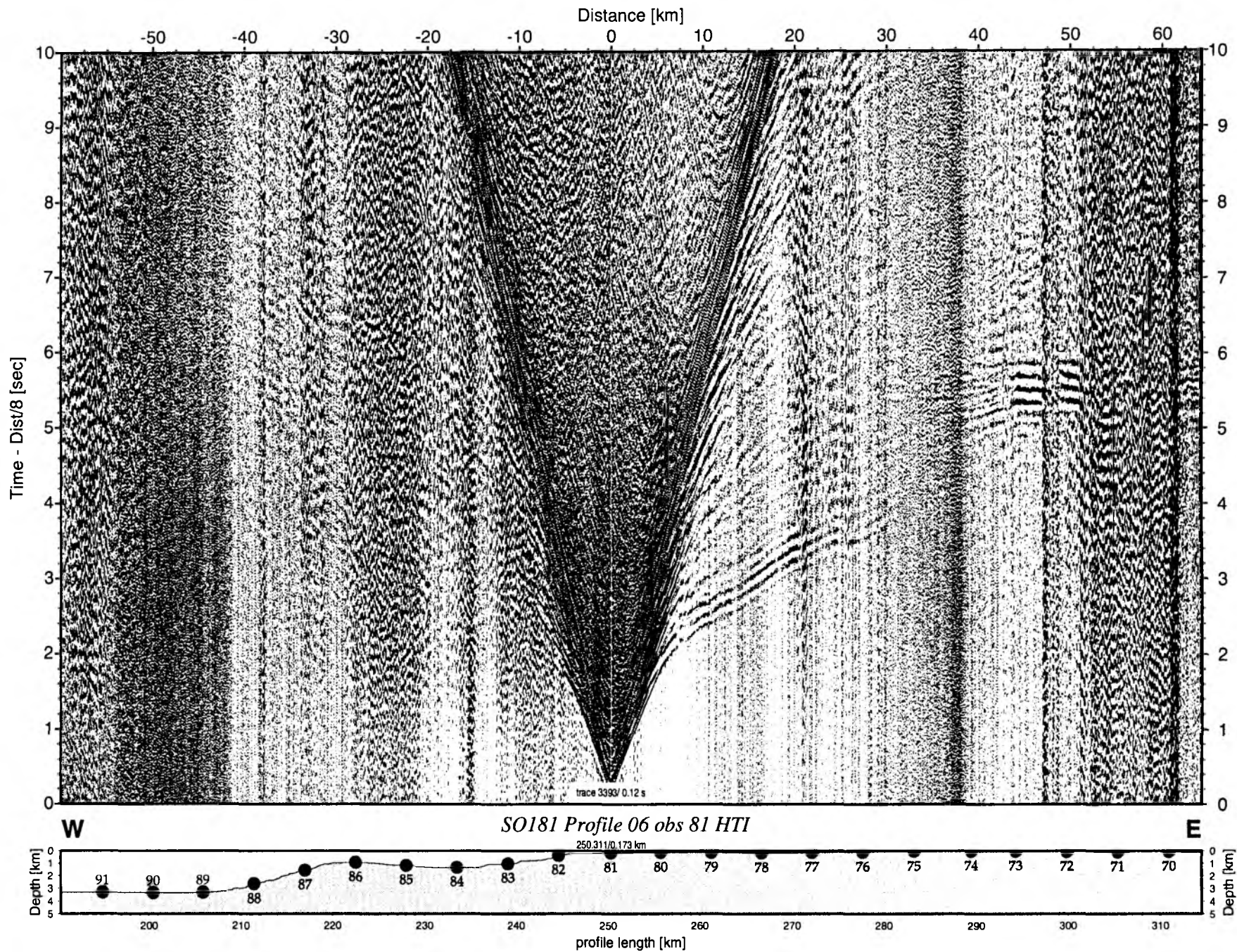


Figure 6.6.6.21: Record section from obs 81 HTI, Profile 06.

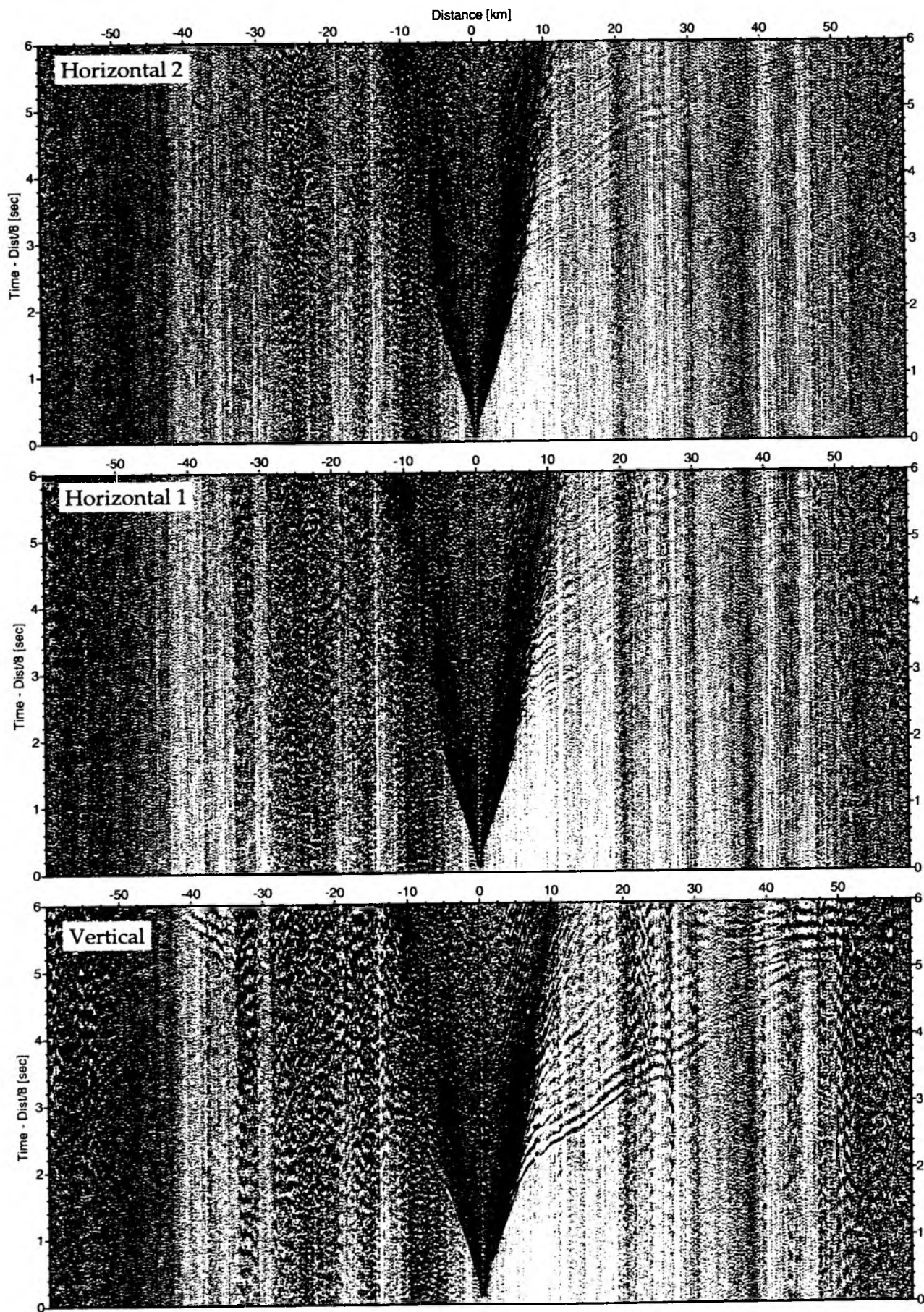


Figure 6.6.6.22: Record sections from obs 81 HTI/Owen-4.5Hz, SO181 Profile 06.

Time - Dist/8 [sec]

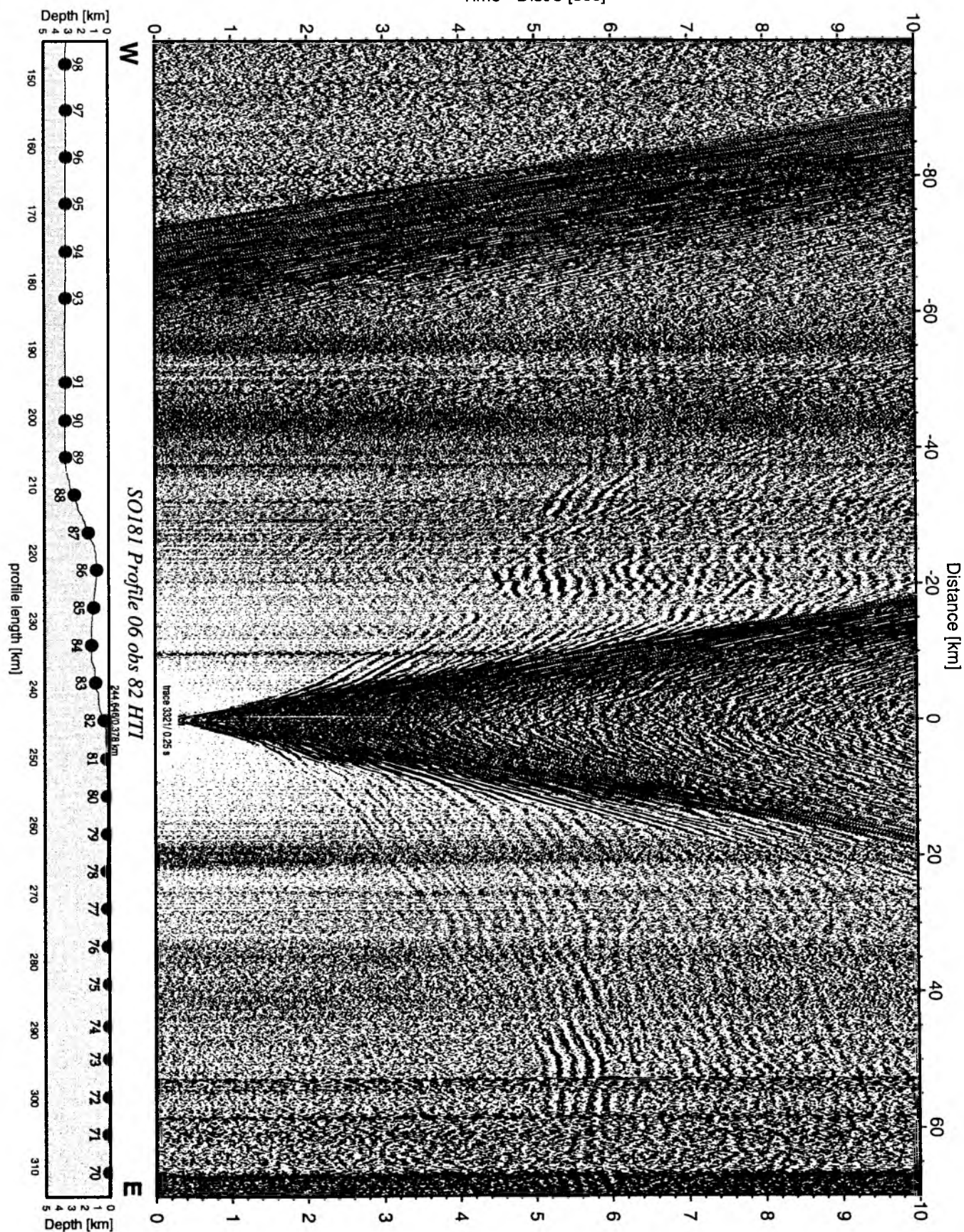


Figure 6.6.23: Record section from obs 82 HTI, Profile 06.

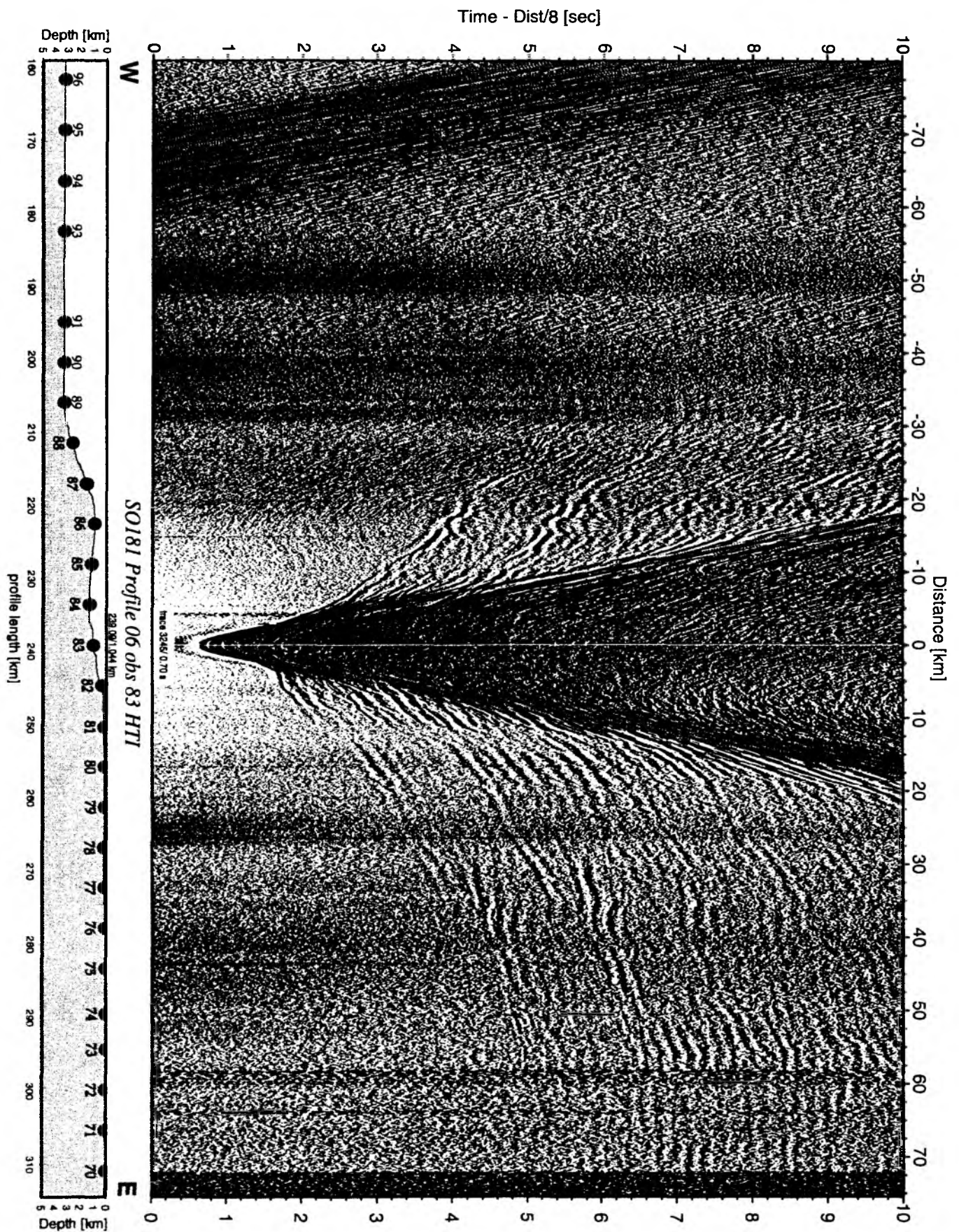


Figure 6.6.6.24: Record section from obs 83 HTI, Profile 06.

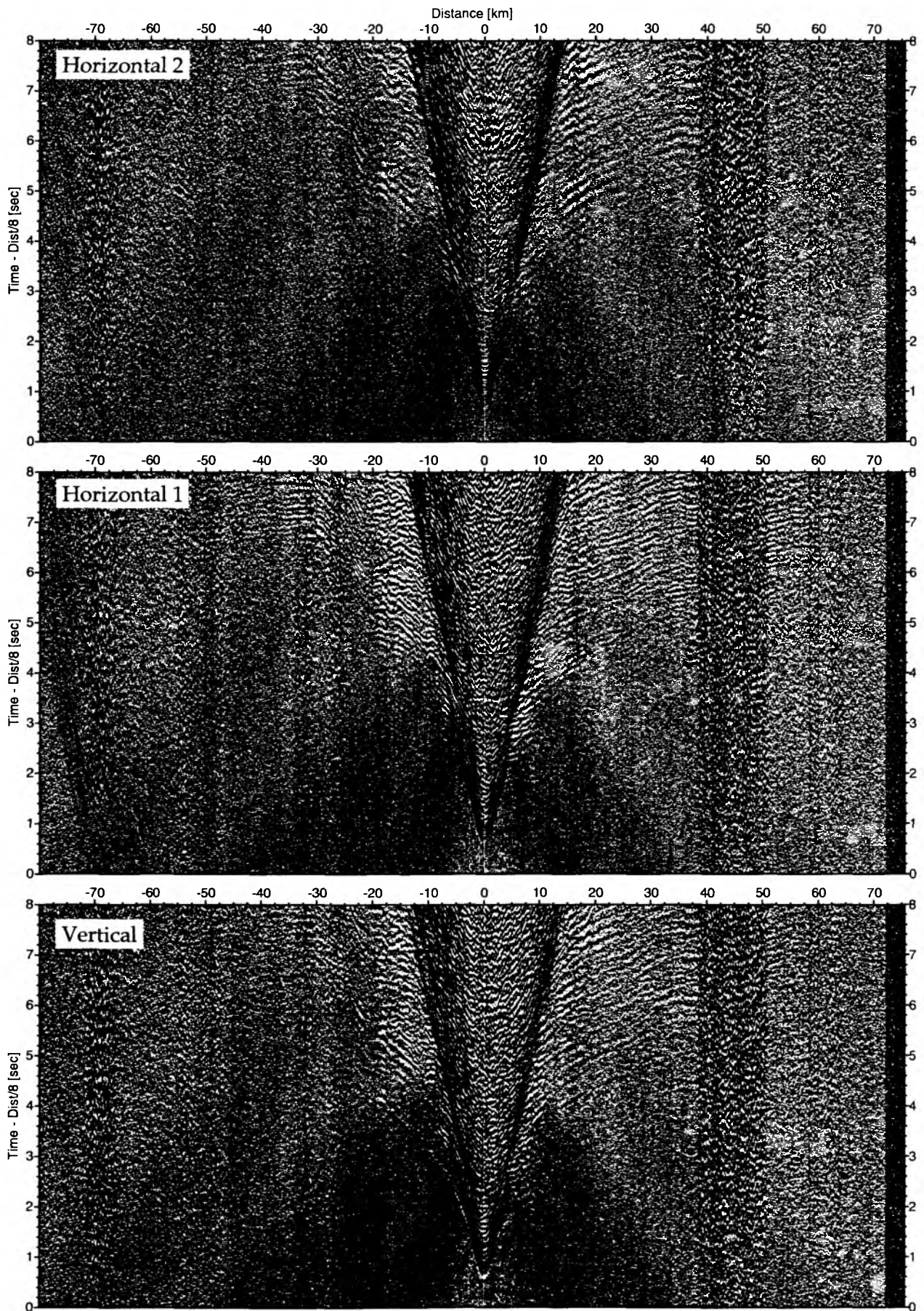


Figure 6.6.6.25: Record sections from obs 83 HTI/Owen-4.5Hz, SO181 Profile 06.

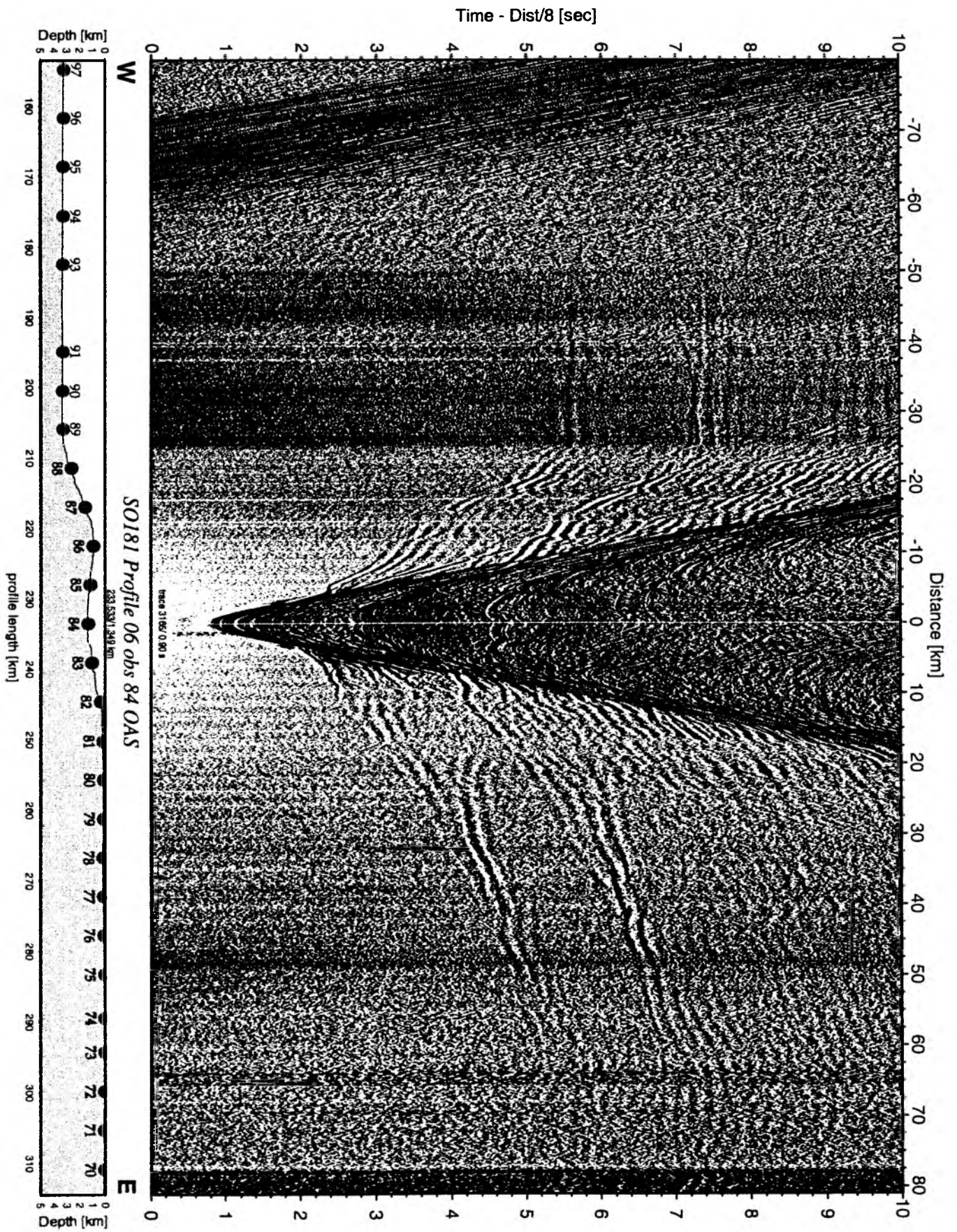


Figure 6.6.6.26: Record section from obs 84 OAS, Profile 06.

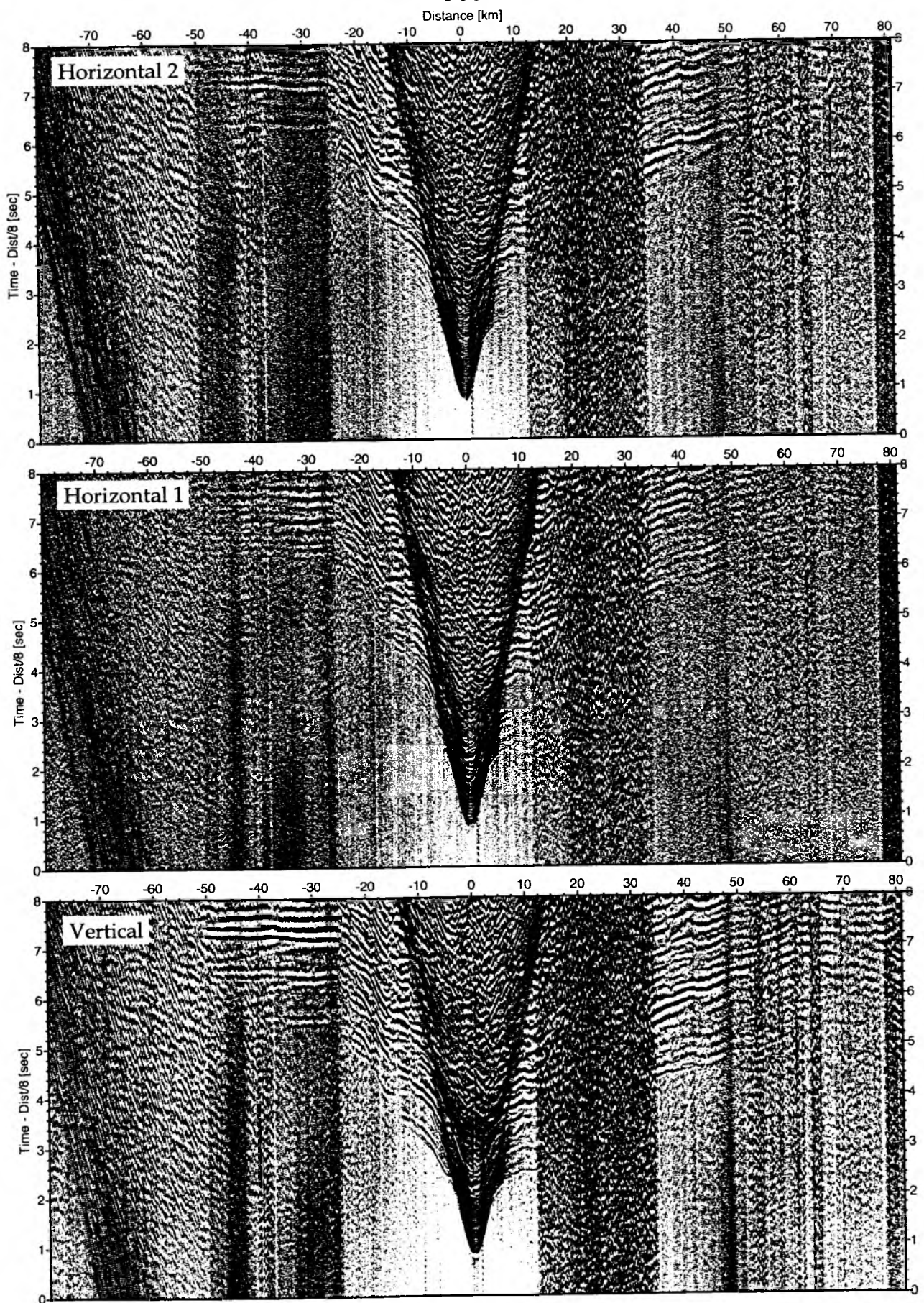


Figure 6.6.6.27: Record sections from obs 84 OAS/Owen-4.5Hz, SO181 Profile 06.

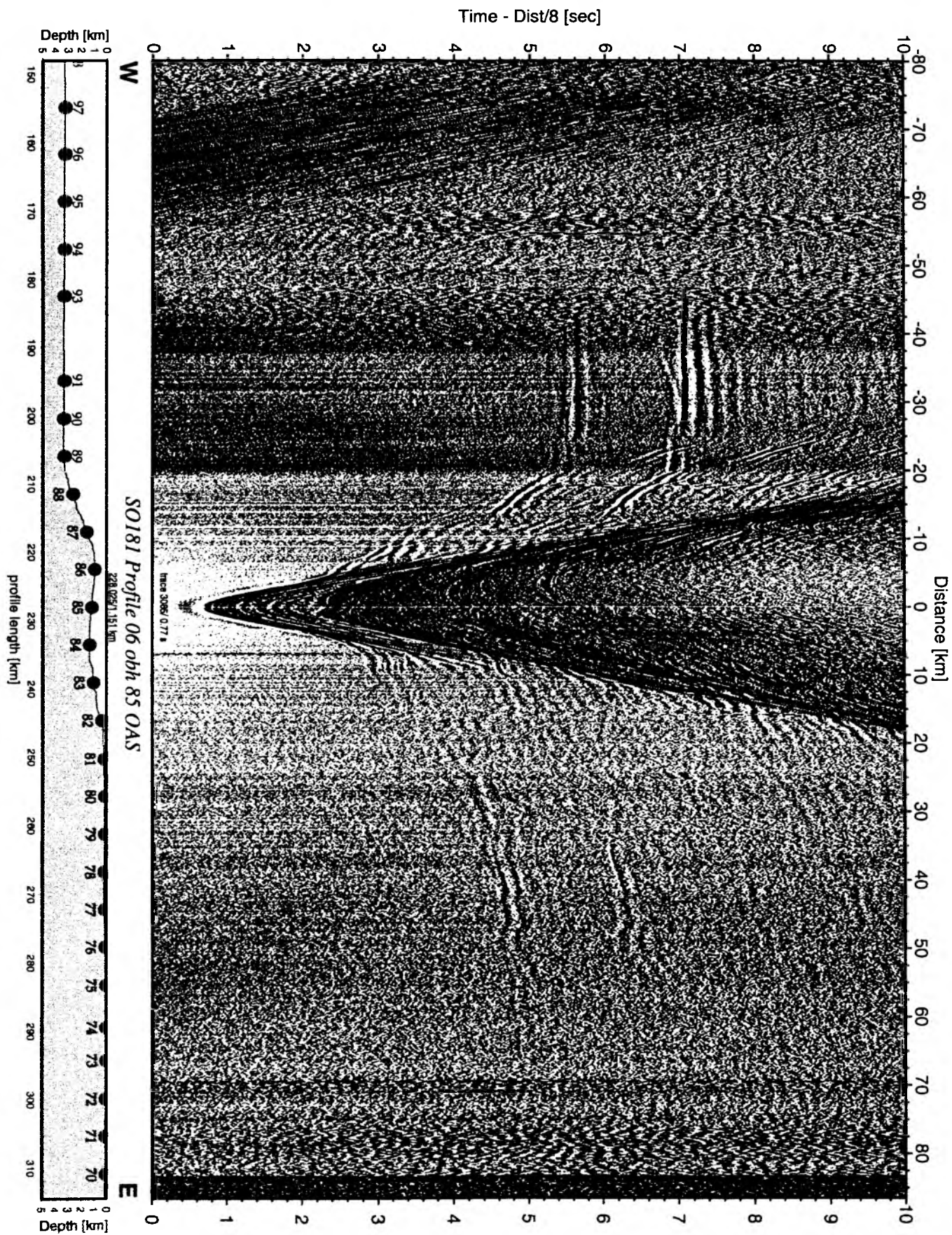


Figure 6.6.28: Record section from obh 85 OAS, Profile 06.

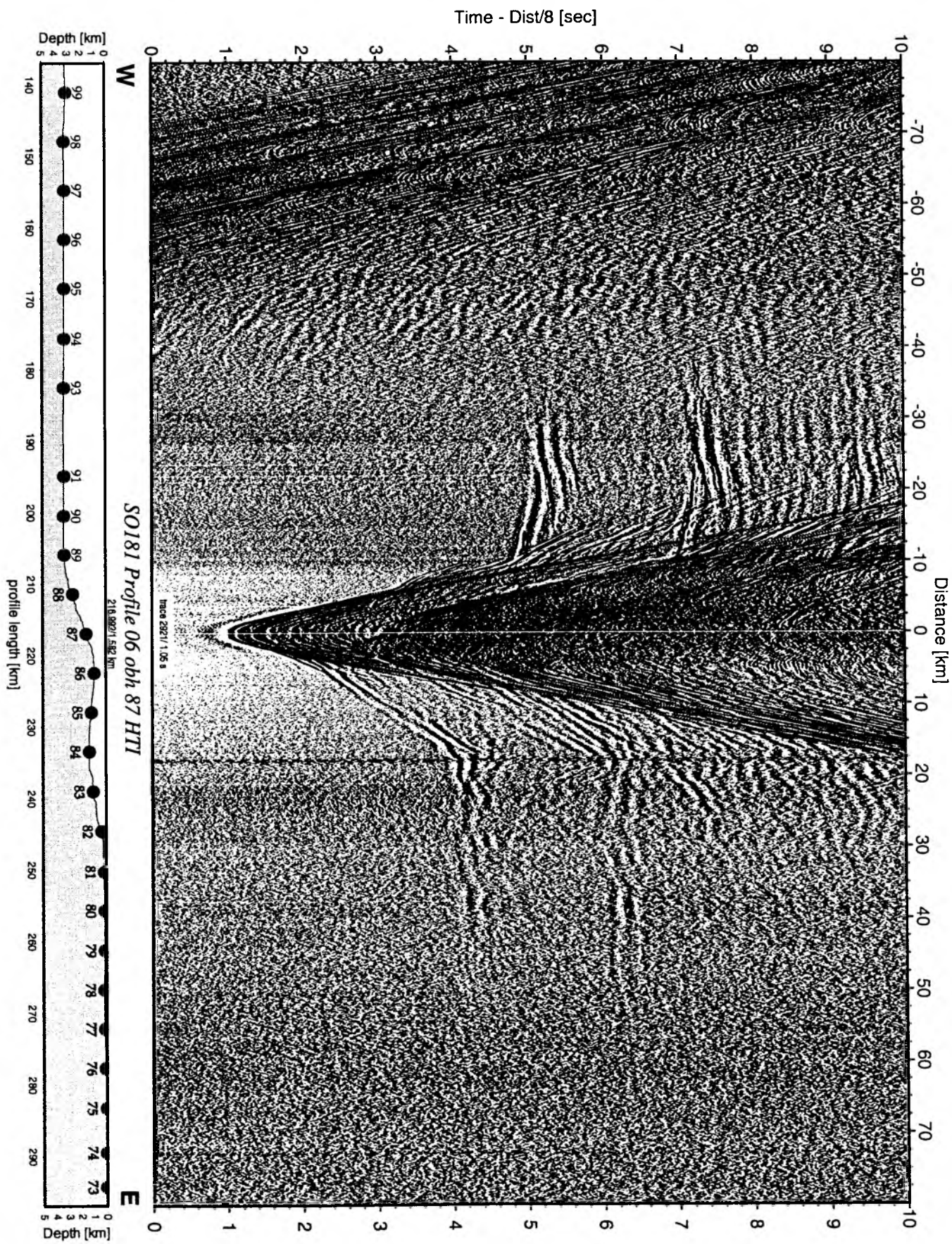


Figure 6.6.6.29: Record section from obh 87 HTI, Profile 06.

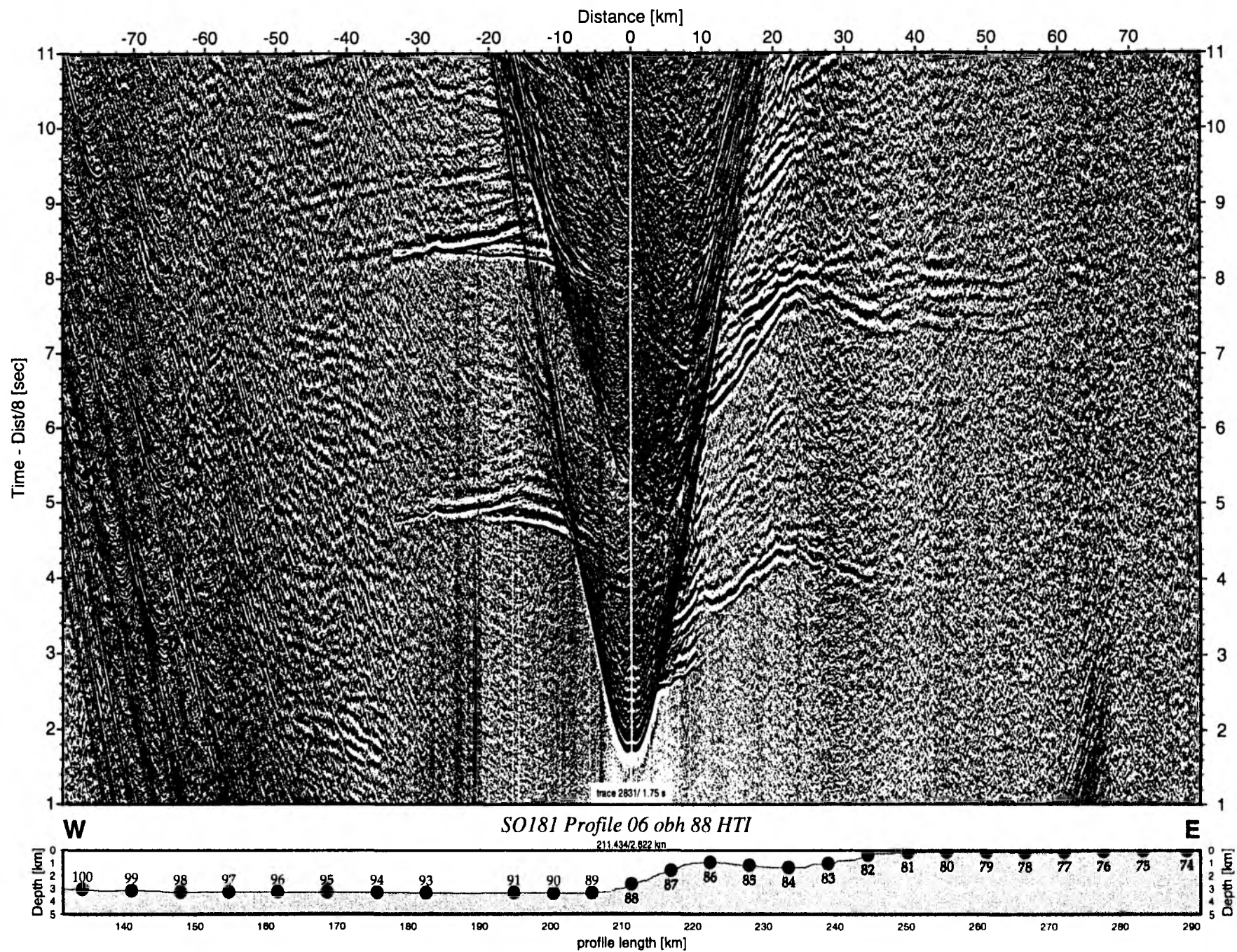


Figure 6.6.6.30: Record section from obh 88 HTI, Profile 06.

Time - Dist/8 [sec]

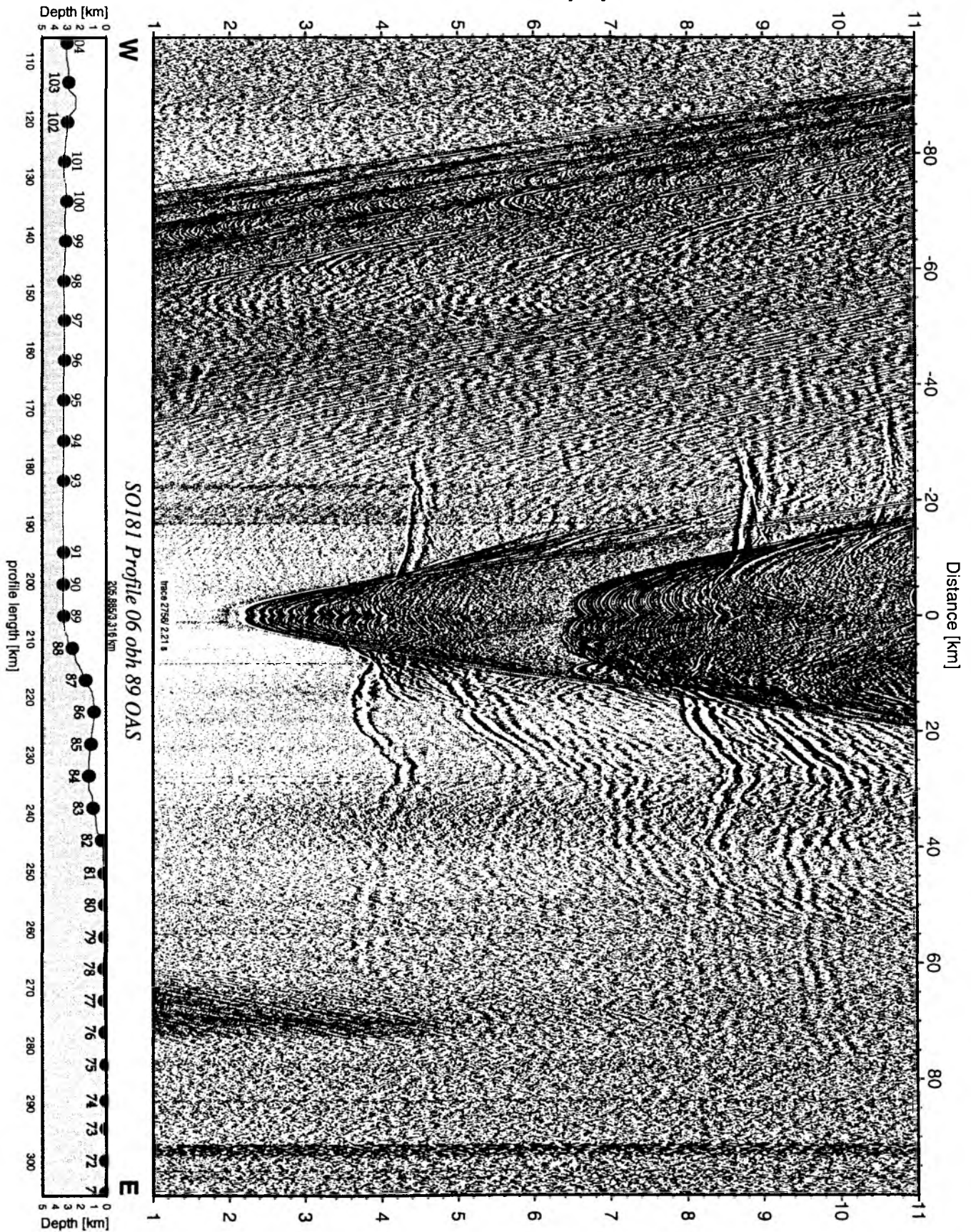


Figure 6.6.6.31: Record section from obh 89 OAS, Profile 06.

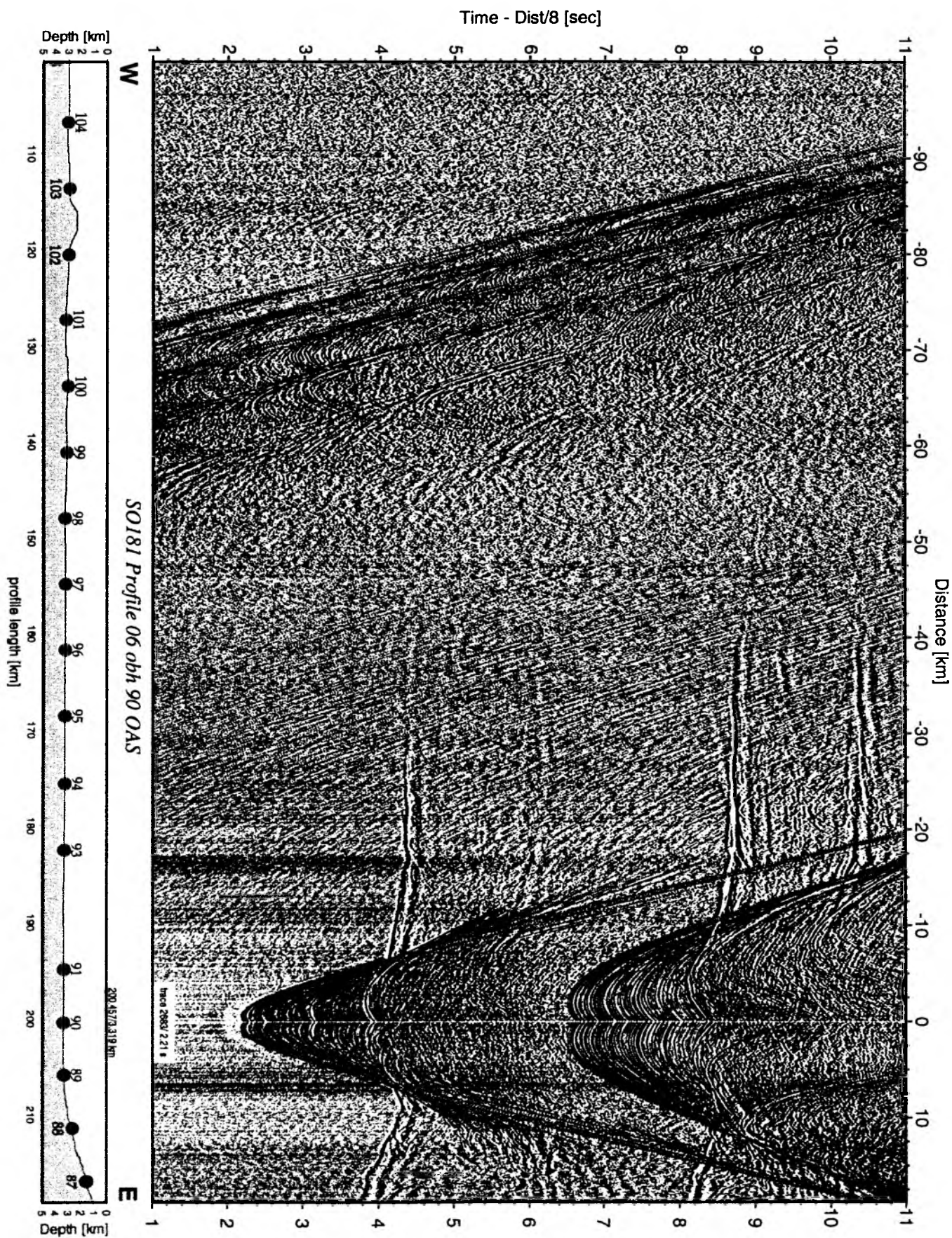


Figure 6.6.6.32: Record section from obh 90 OAS, Profile 06.

Time - Dist/8 [sec]

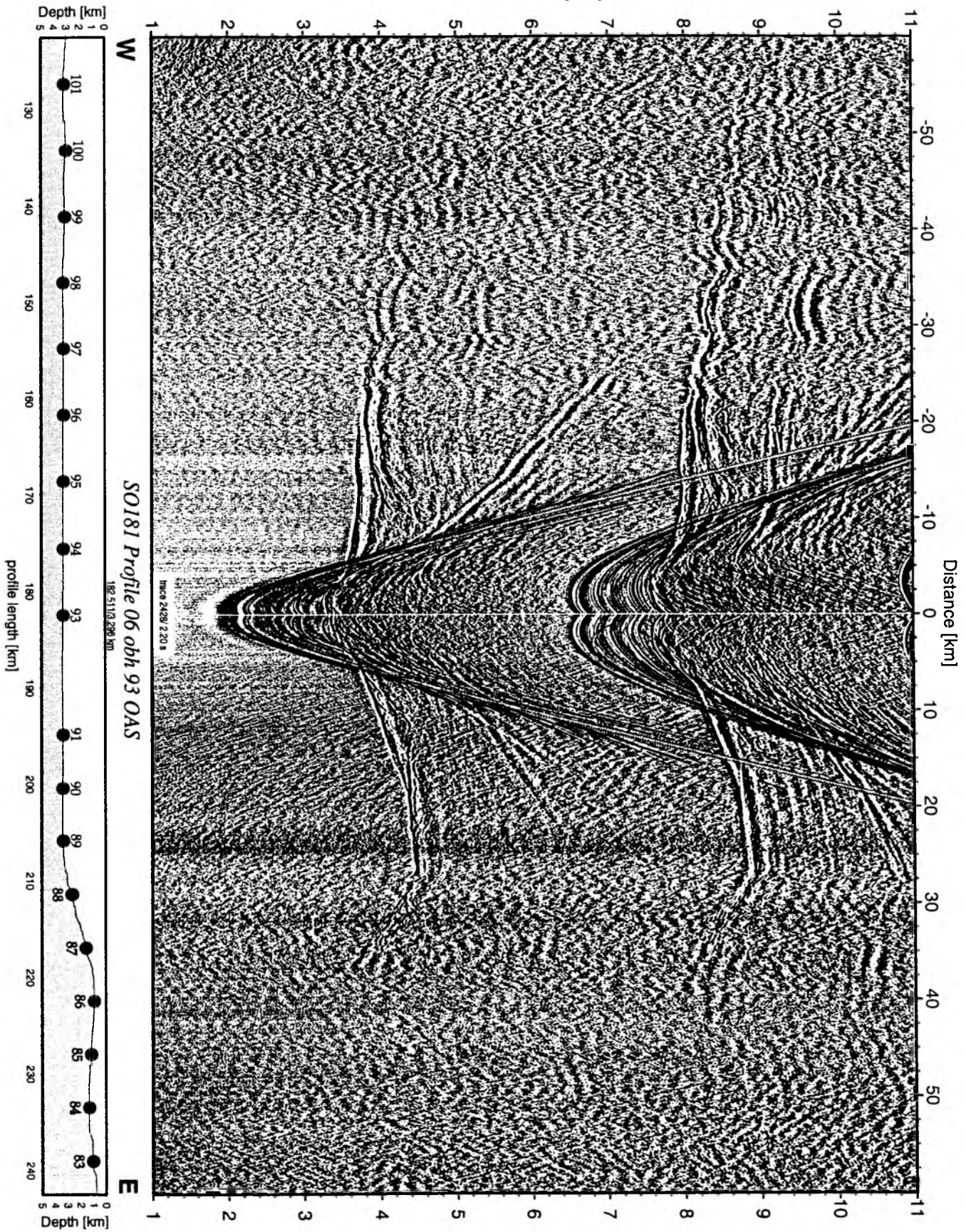


Figure 6.6.6.33: Record section from obh 93 OAS, Profile 06.

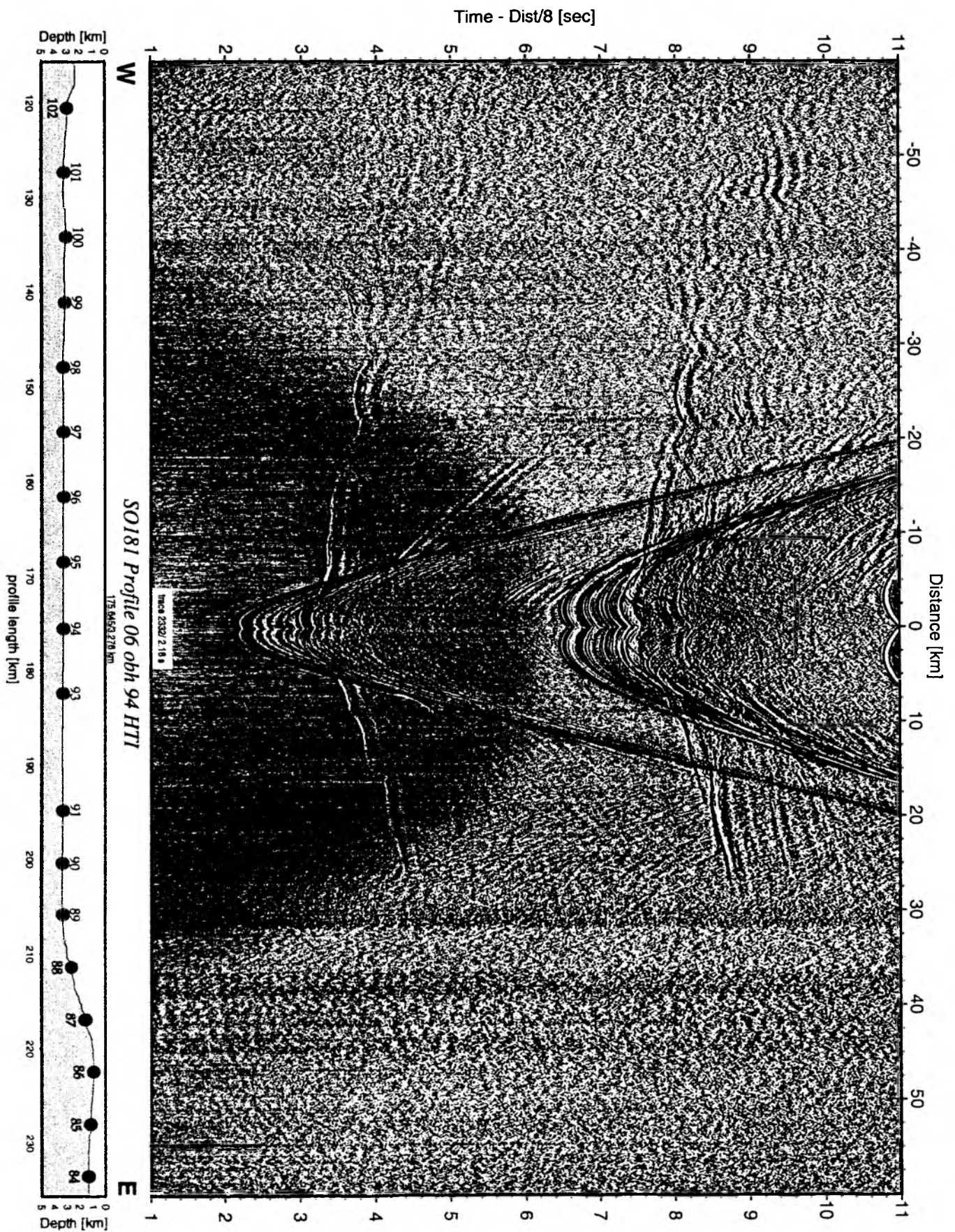


Figure 6.6.6.34: Record section from obh 94 HTI, Profile 06.

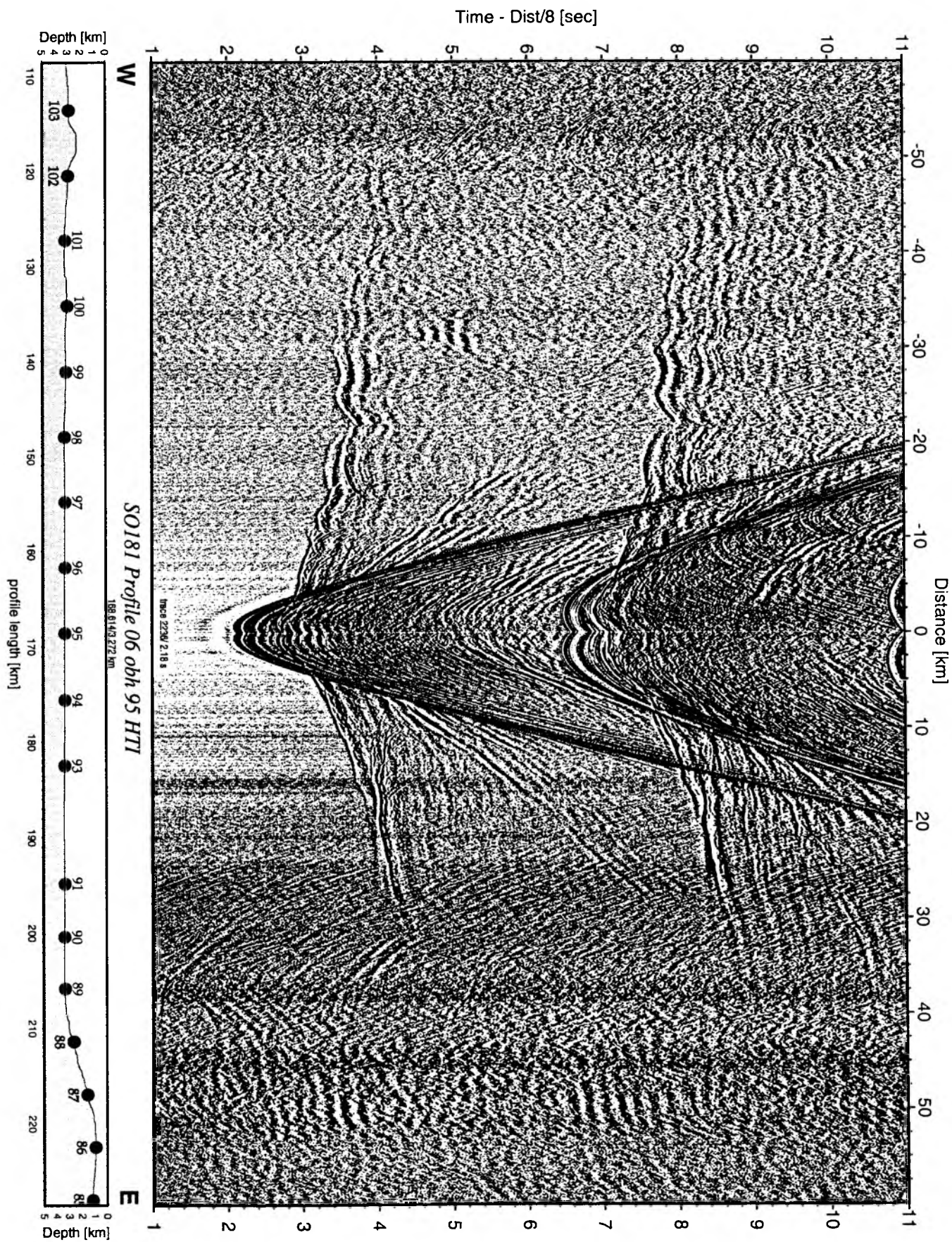


Figure 6.6.35: Record section from obh 95 HTI, Profile 06.

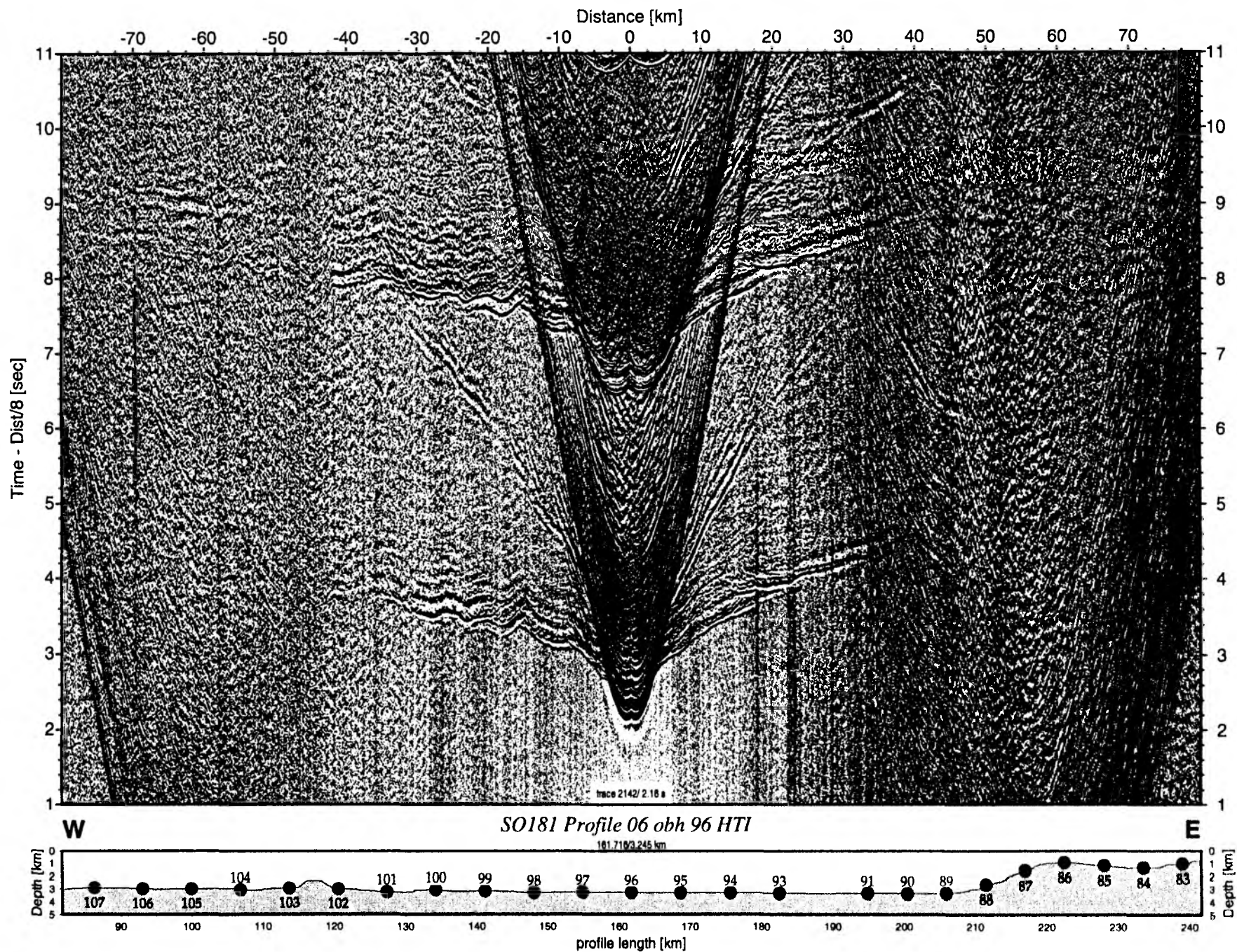


Figure 6.6.6.36: Record section from obh 96 HTI, Profile 06.

Time - Dist/8 [sec]

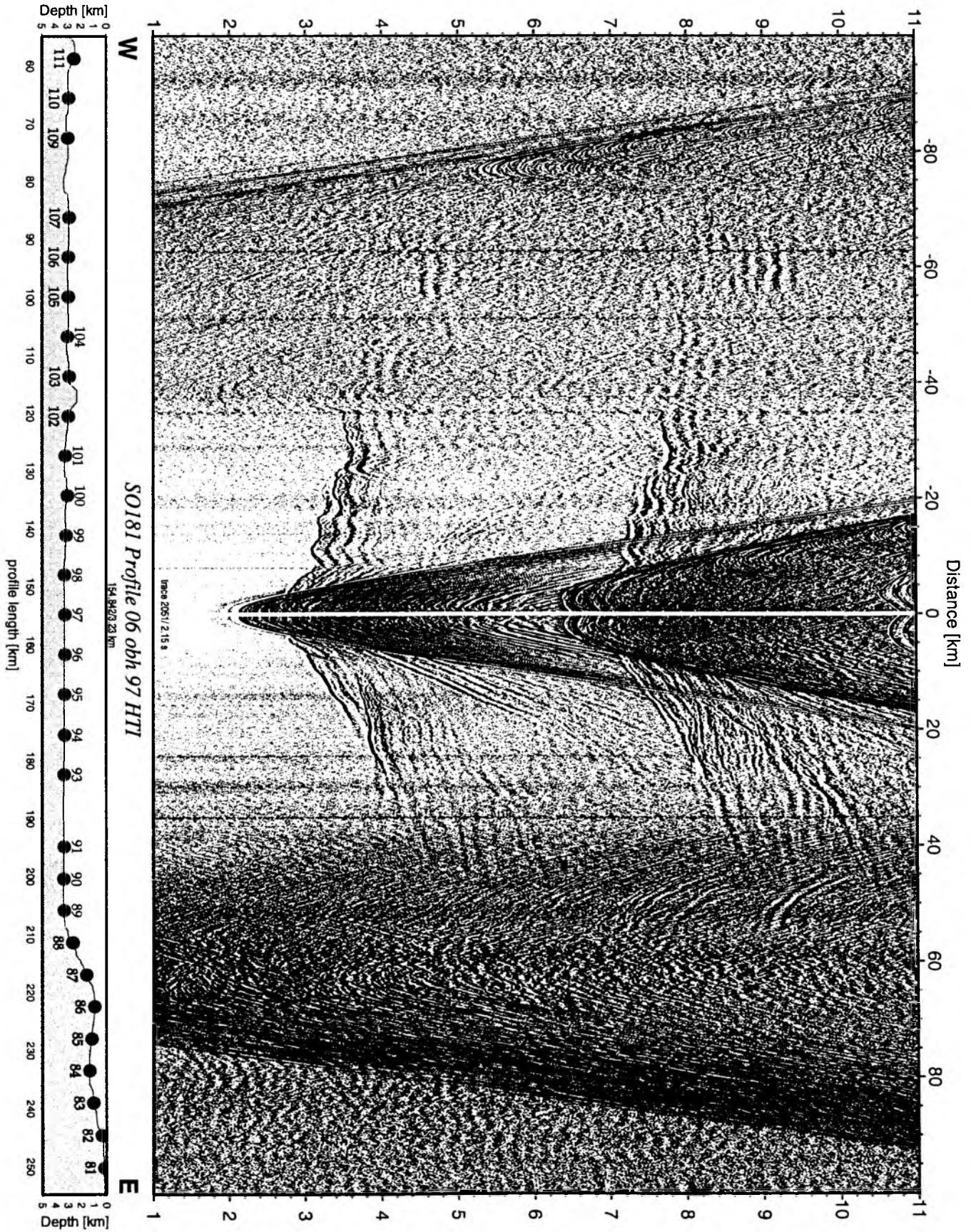


Figure 6.6.6.37: Record section from obh 97 HTI, Profile 06.

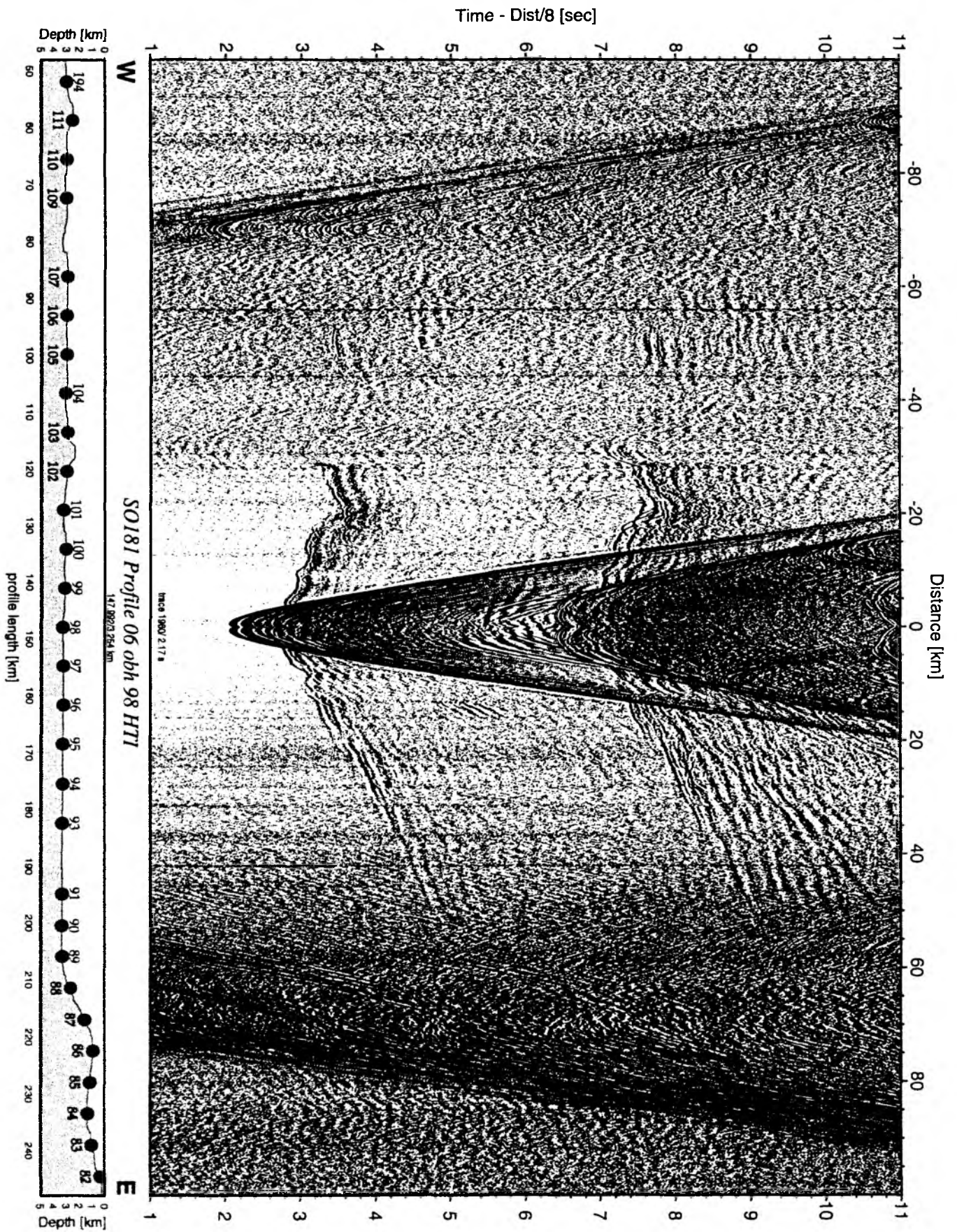


Figure 6.6.6.38: Record section from obh 98 HTI, Profile 06.

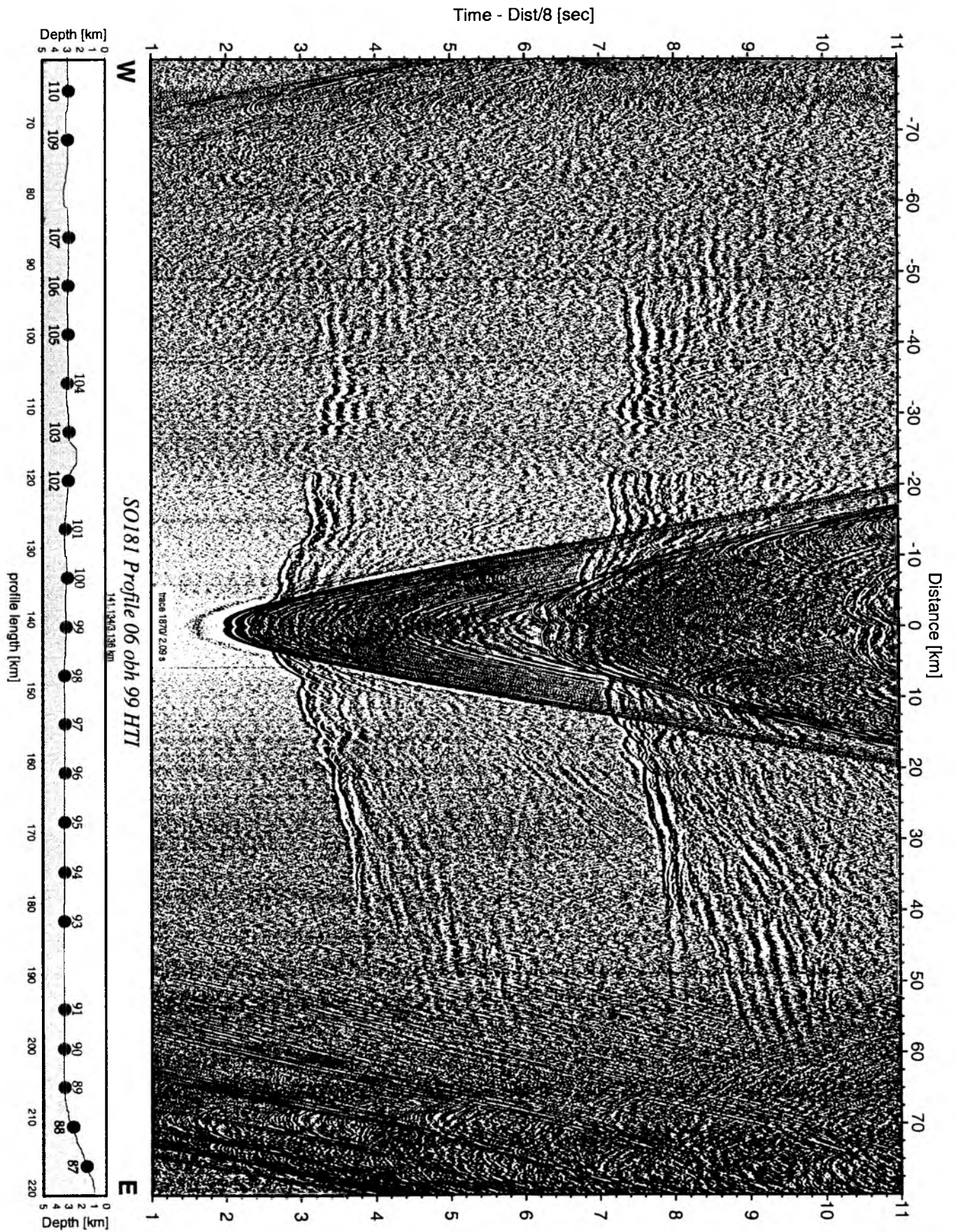


Figure 6.6.6.39: Record section from obh 99 HTI, Profile 06.

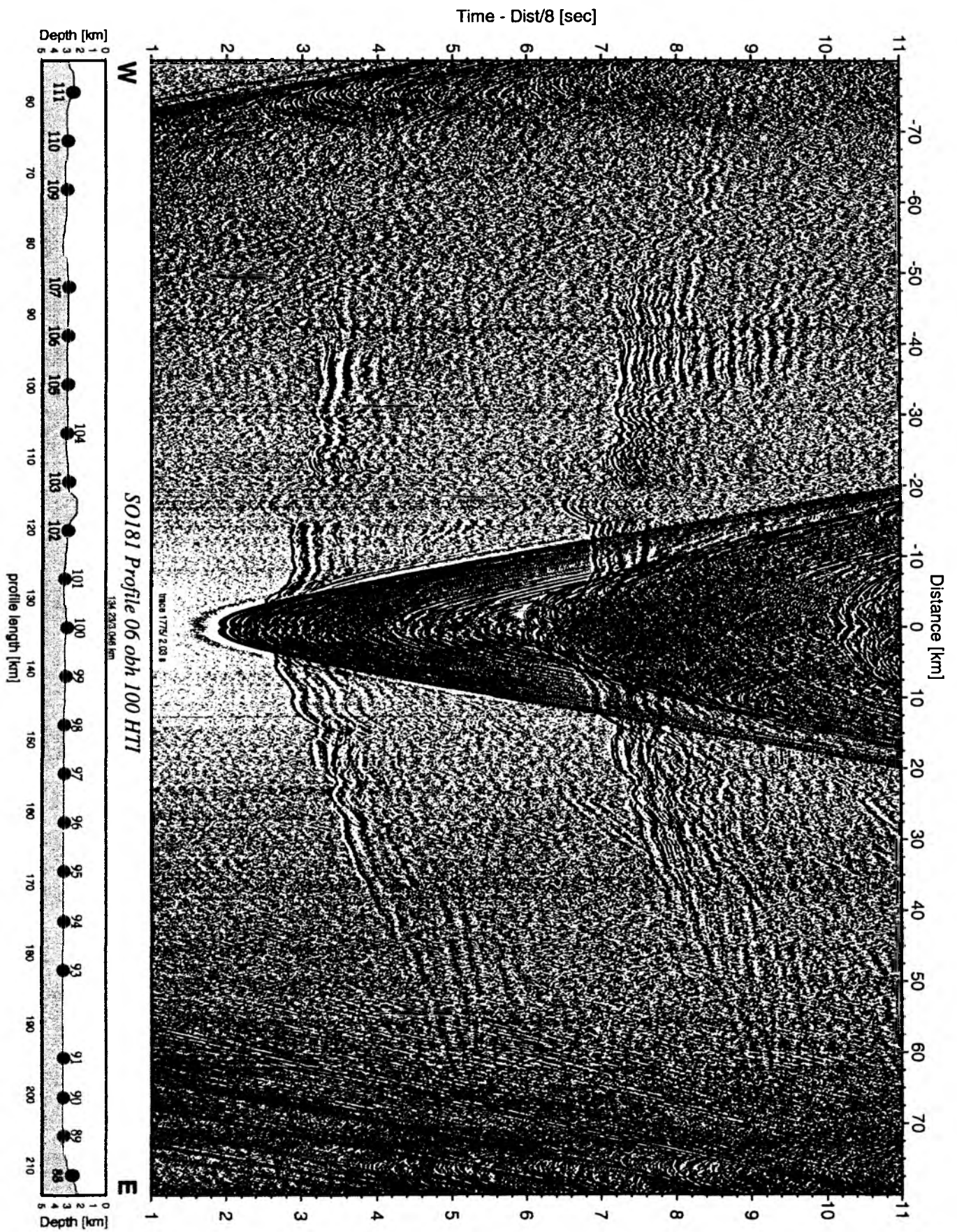


Figure 6.6.6.40: Record section from obh 100 HTI, Profile 06.

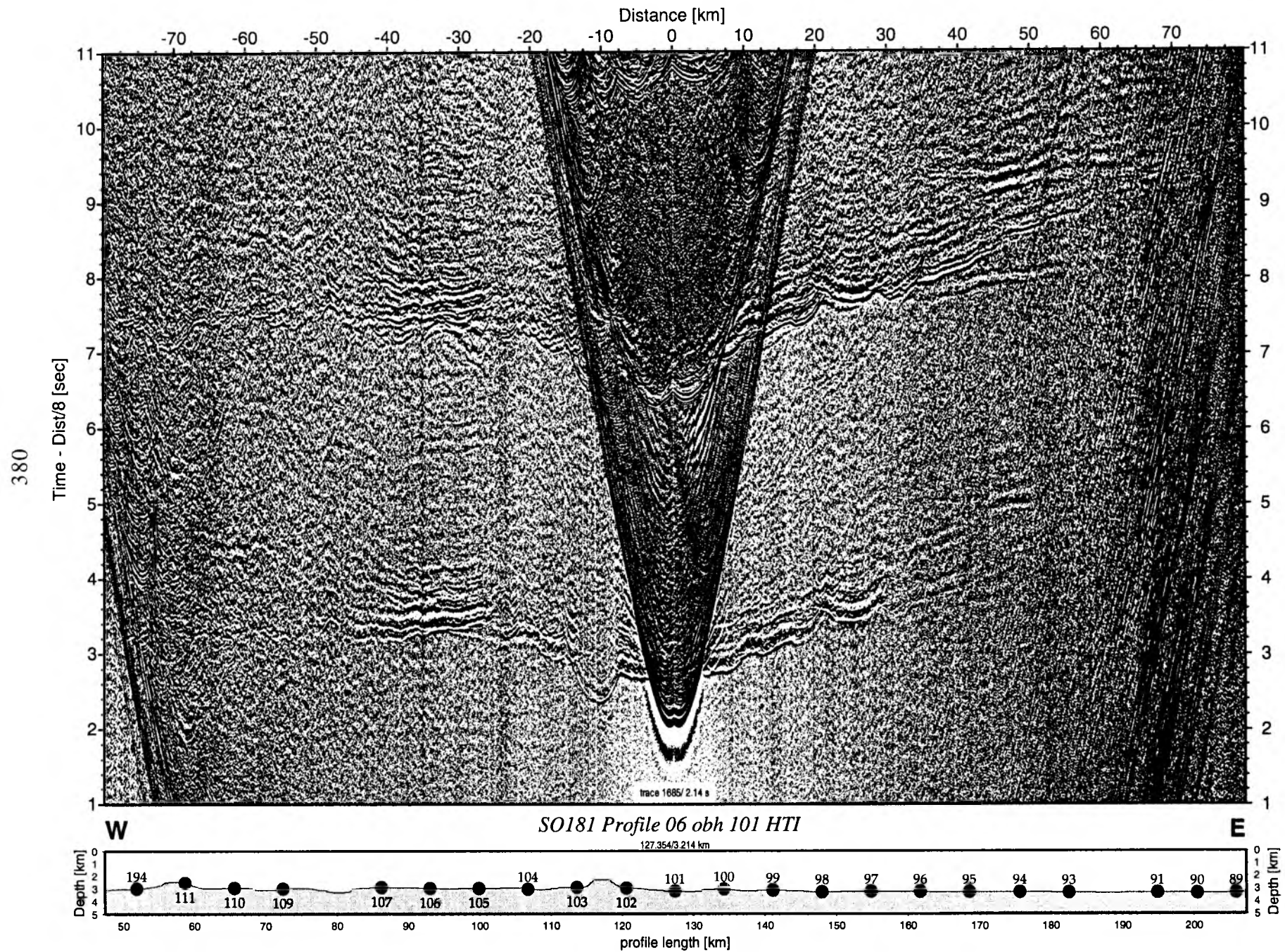


Figure 6.6.6.41: Record section from obh 101 HTI, Profile 06.

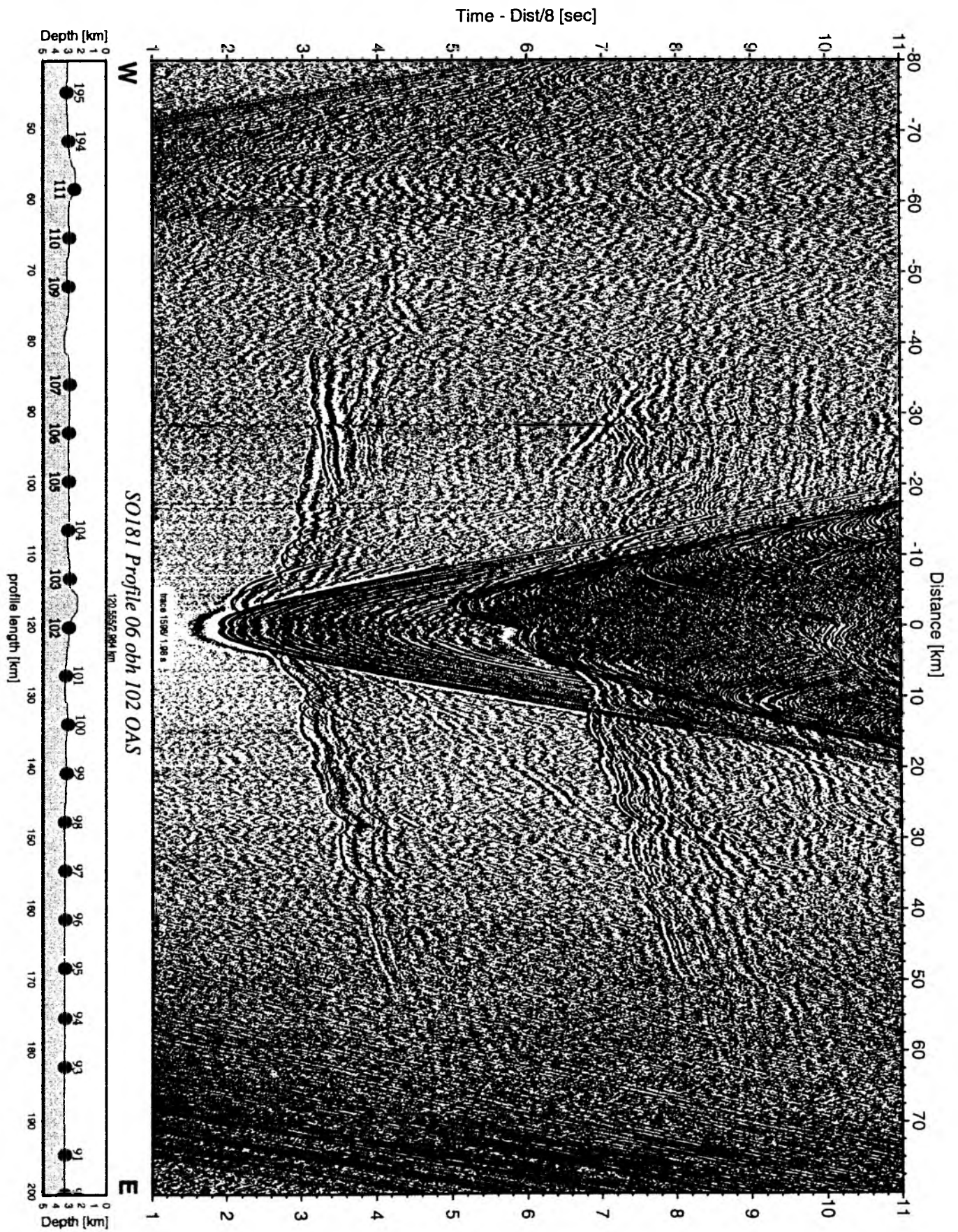


Figure 6.6.642: Record section from obh 102 OAS, Profile 06.

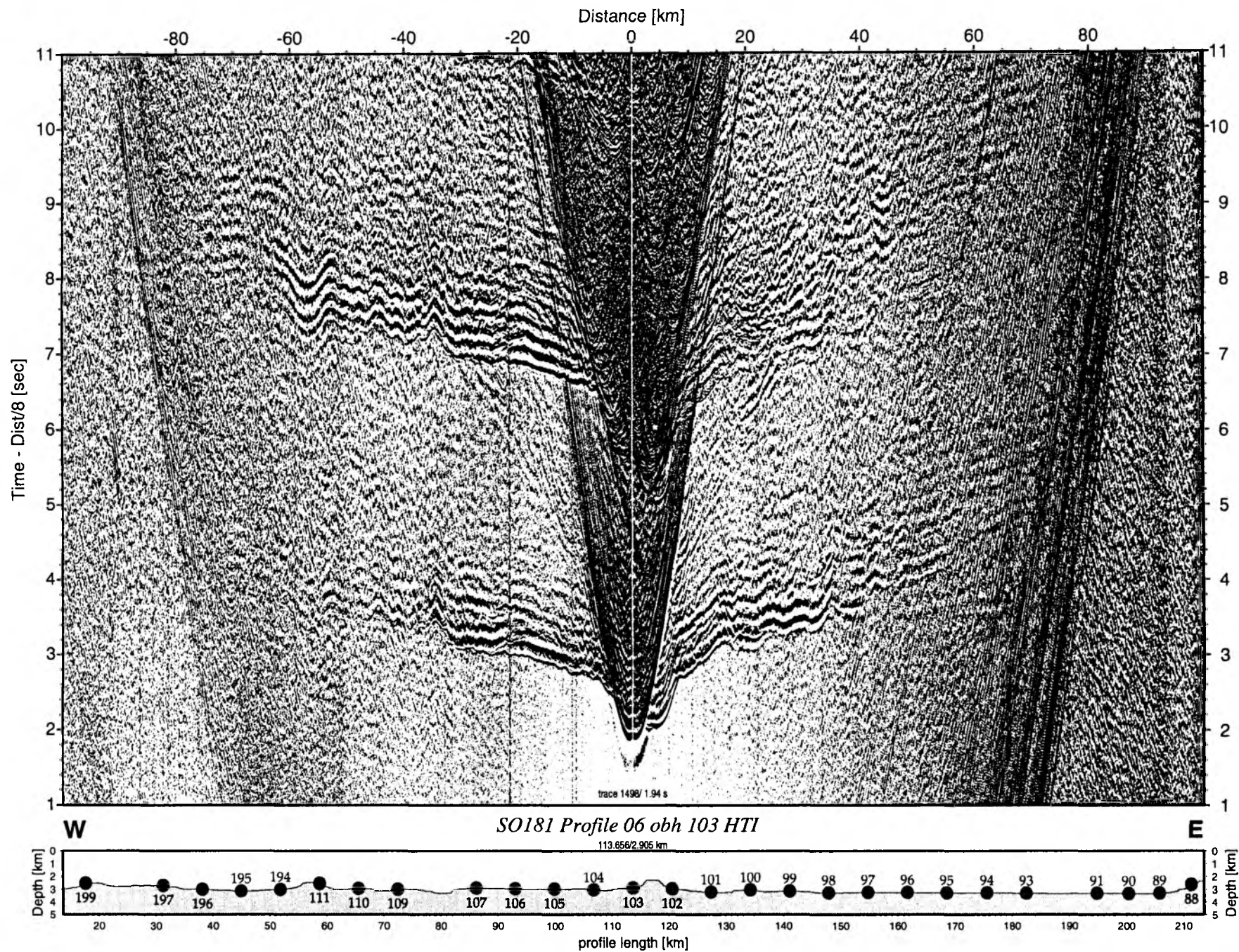


Figure 6.6.6.43: Record section from obh 103 HTI, Profile 06.

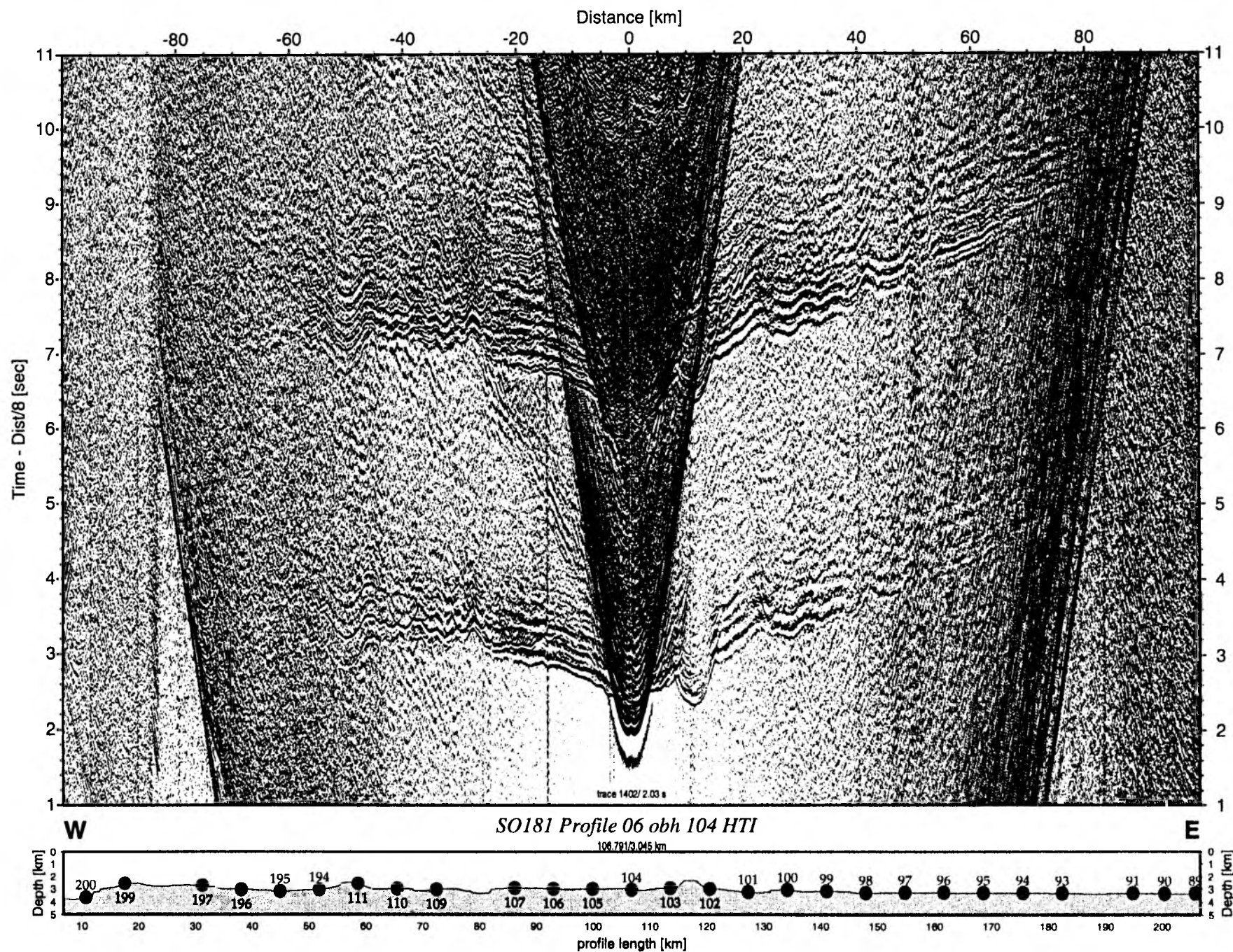


Figure 6.6.6.44: Record section from obh 104 HTI, Profile 06.

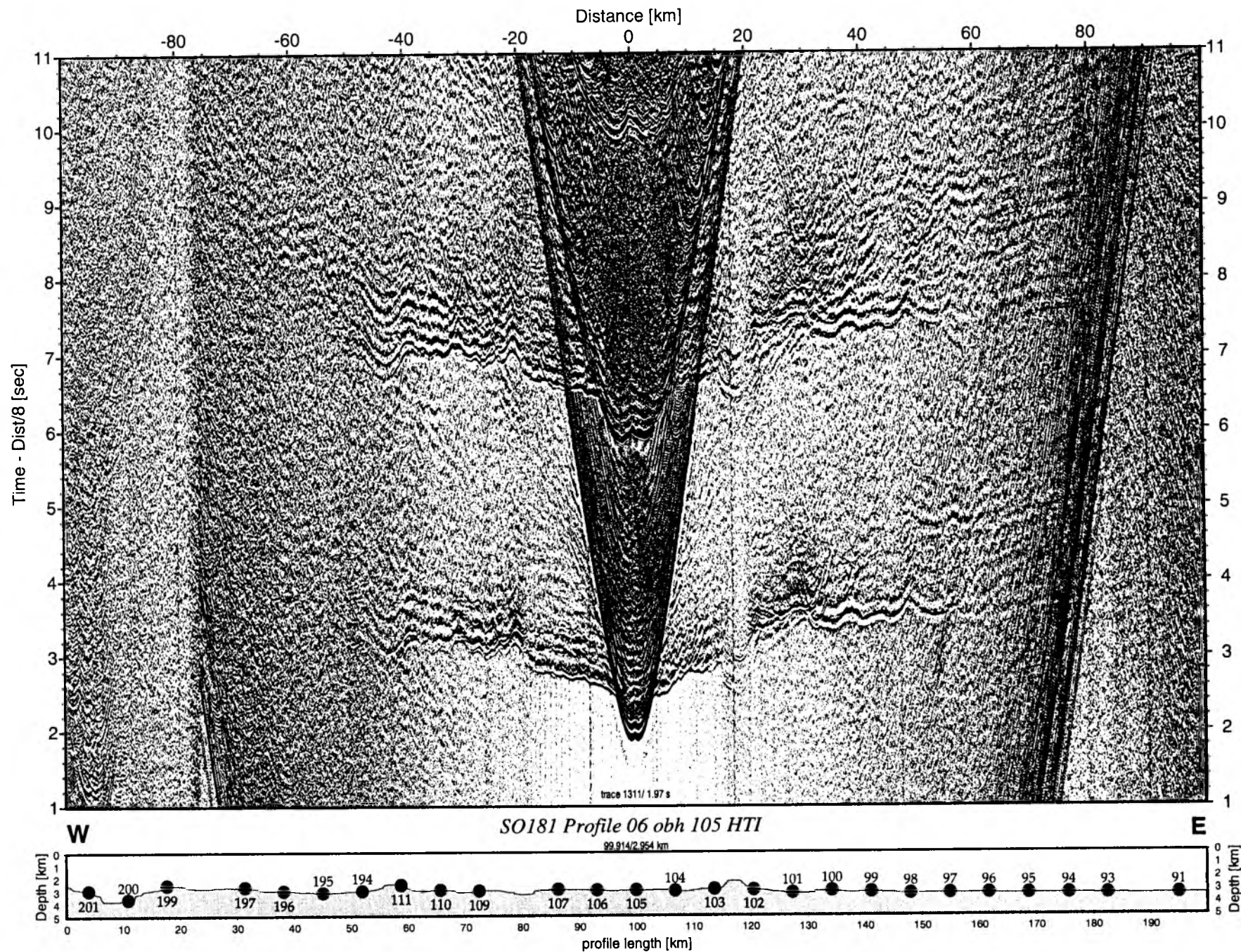


Figure 6.6.6.45: Record section from obh 105 HTI, Profile 06.

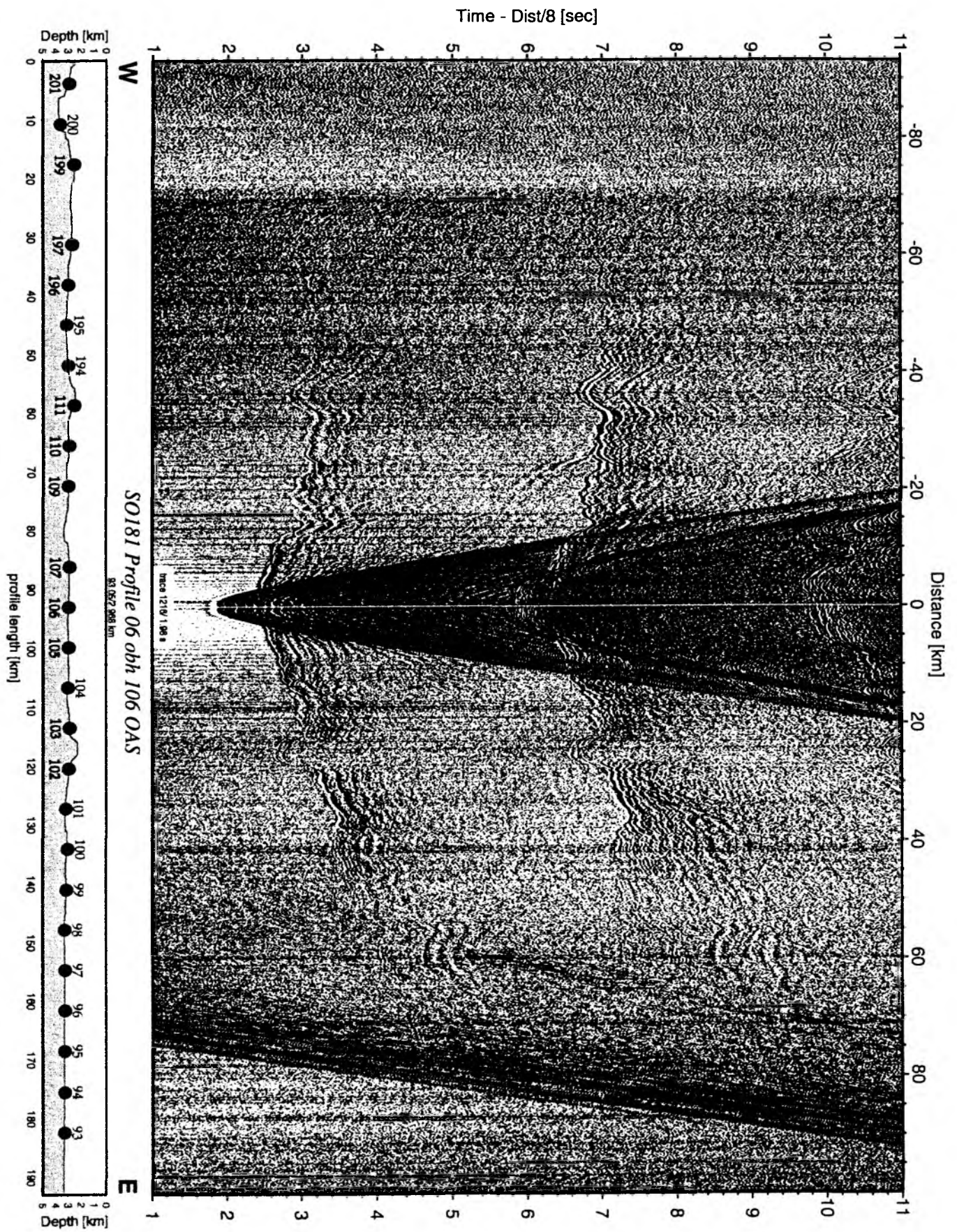


Figure 6.6.6.46: Record section from obh 106 OAS, Profile 06.

Time - Dist/8 [sec]

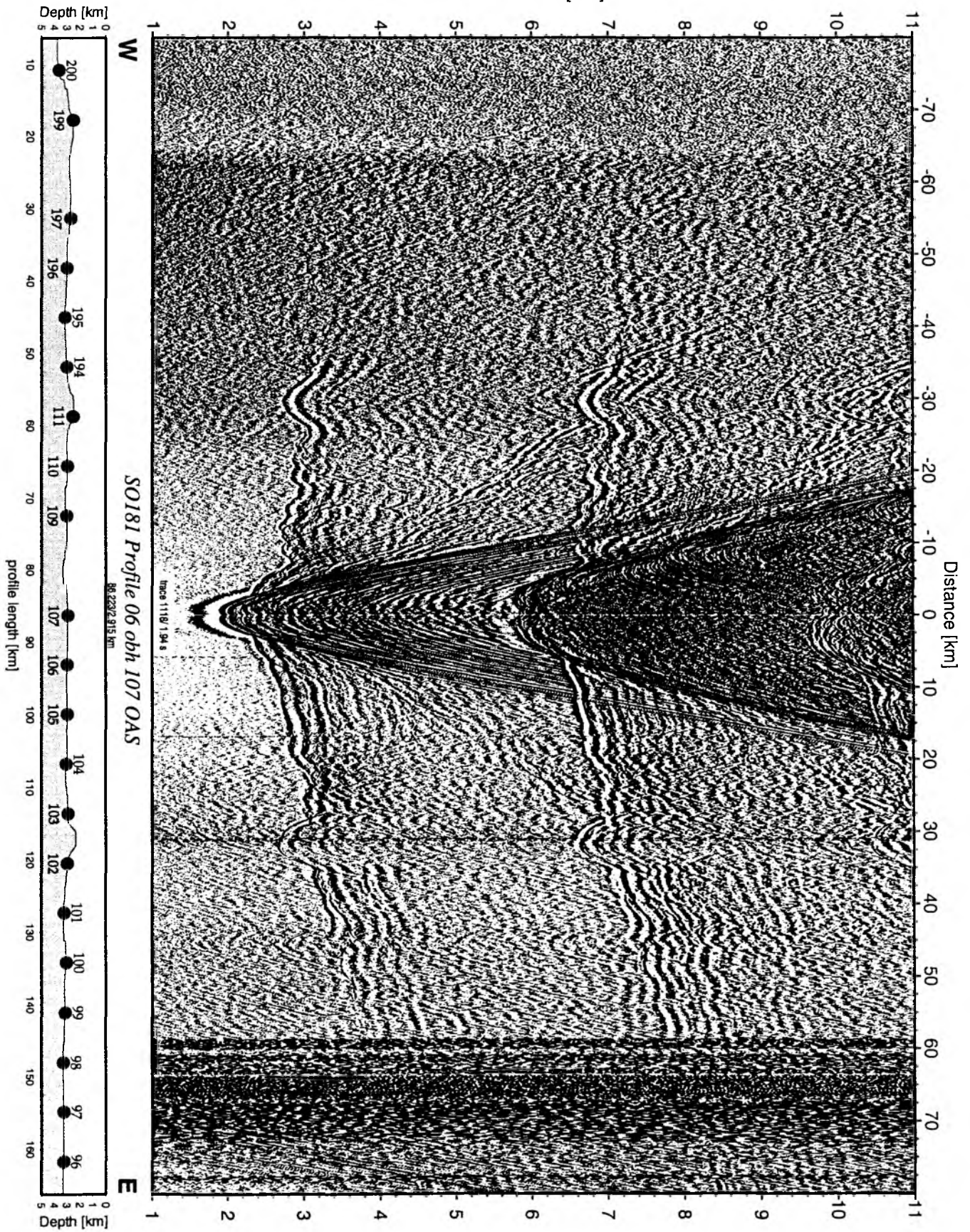


Figure 6.6.6.47: Record section from obh 107 OAS, Profile 06.

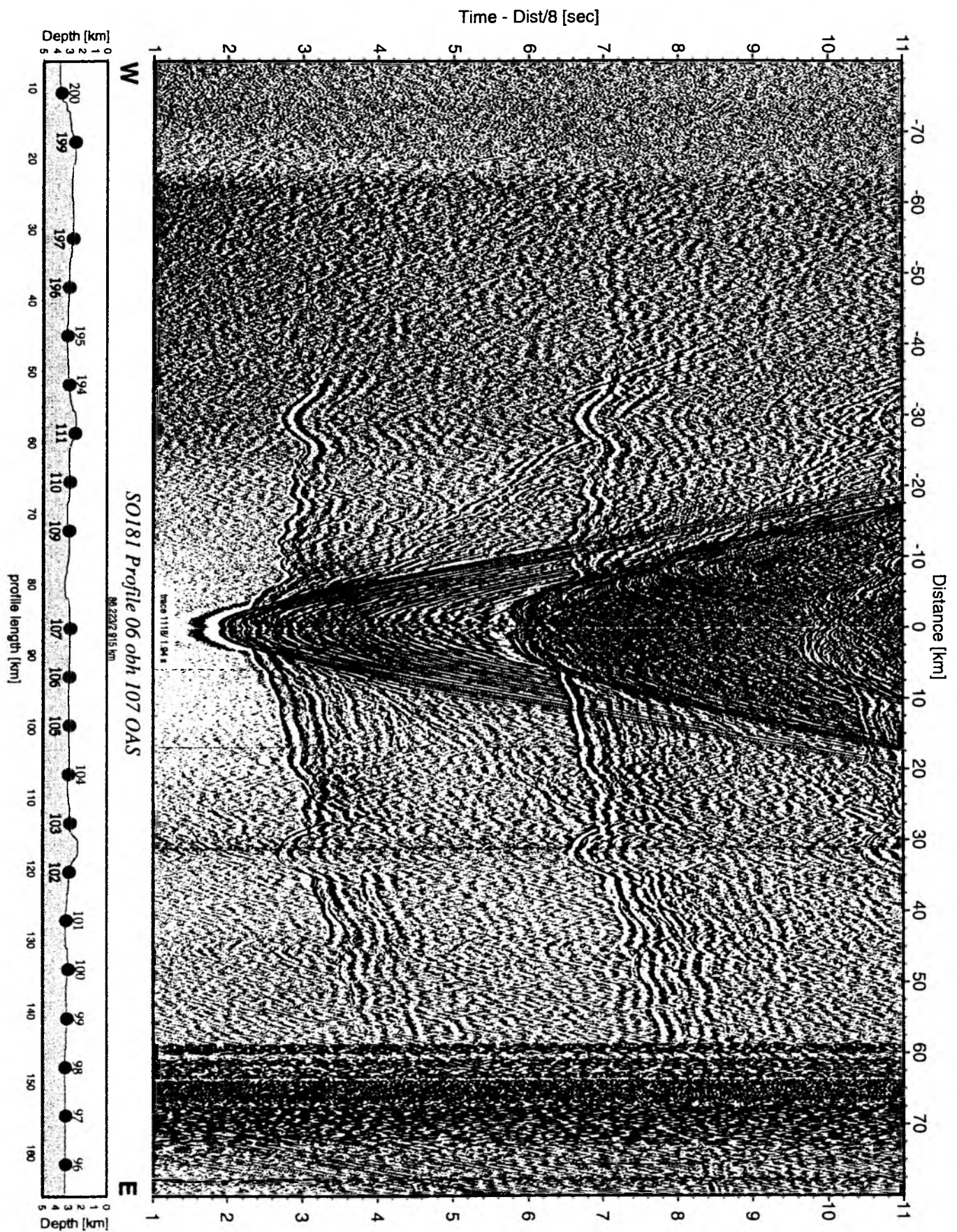


Figure 6.6.6.47: Record section from obh 107 OAS, Profile 06.

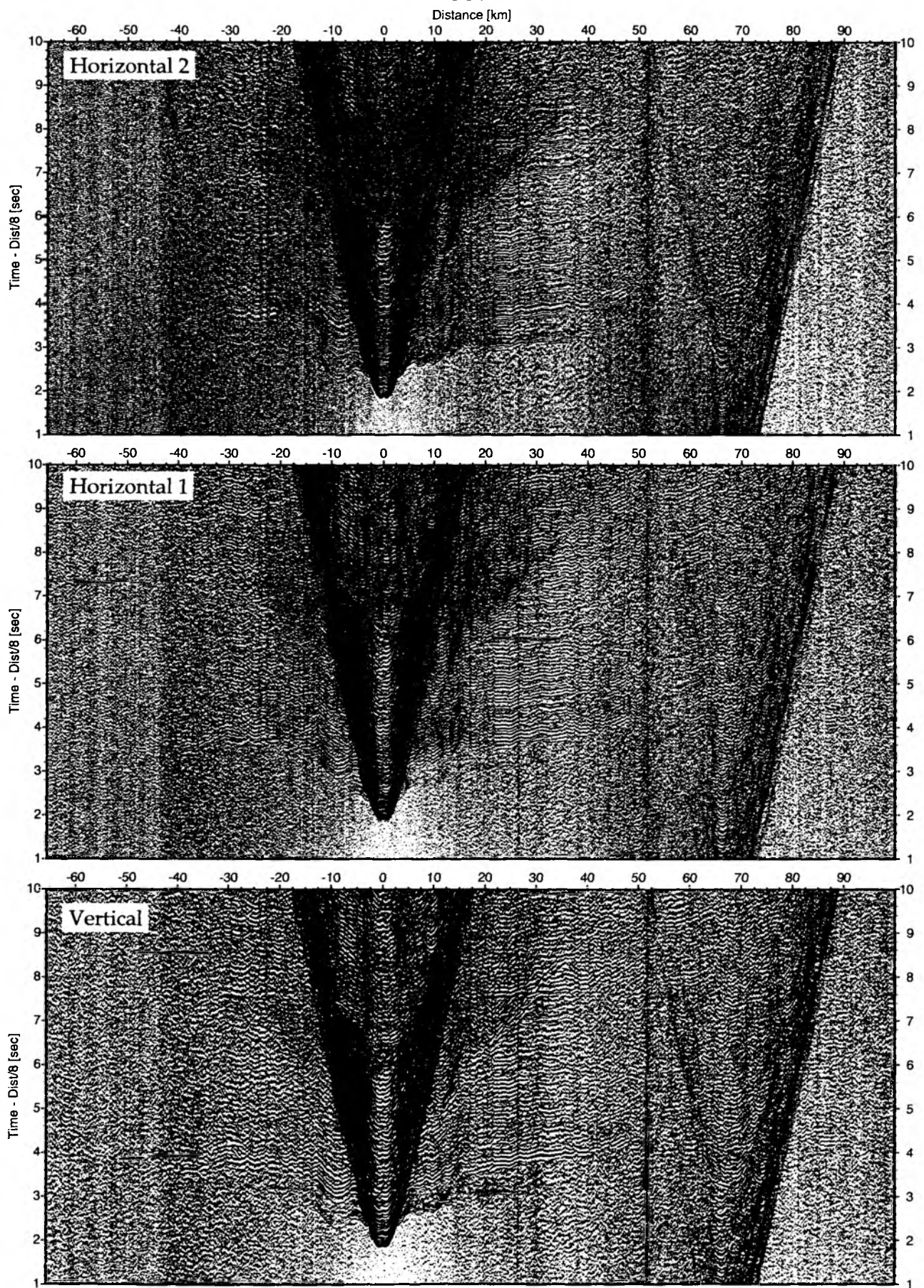


Figure 6.6.6.49: Record sections from obs 110 HTI/Owen-15Hz, SO181 Profile 06.

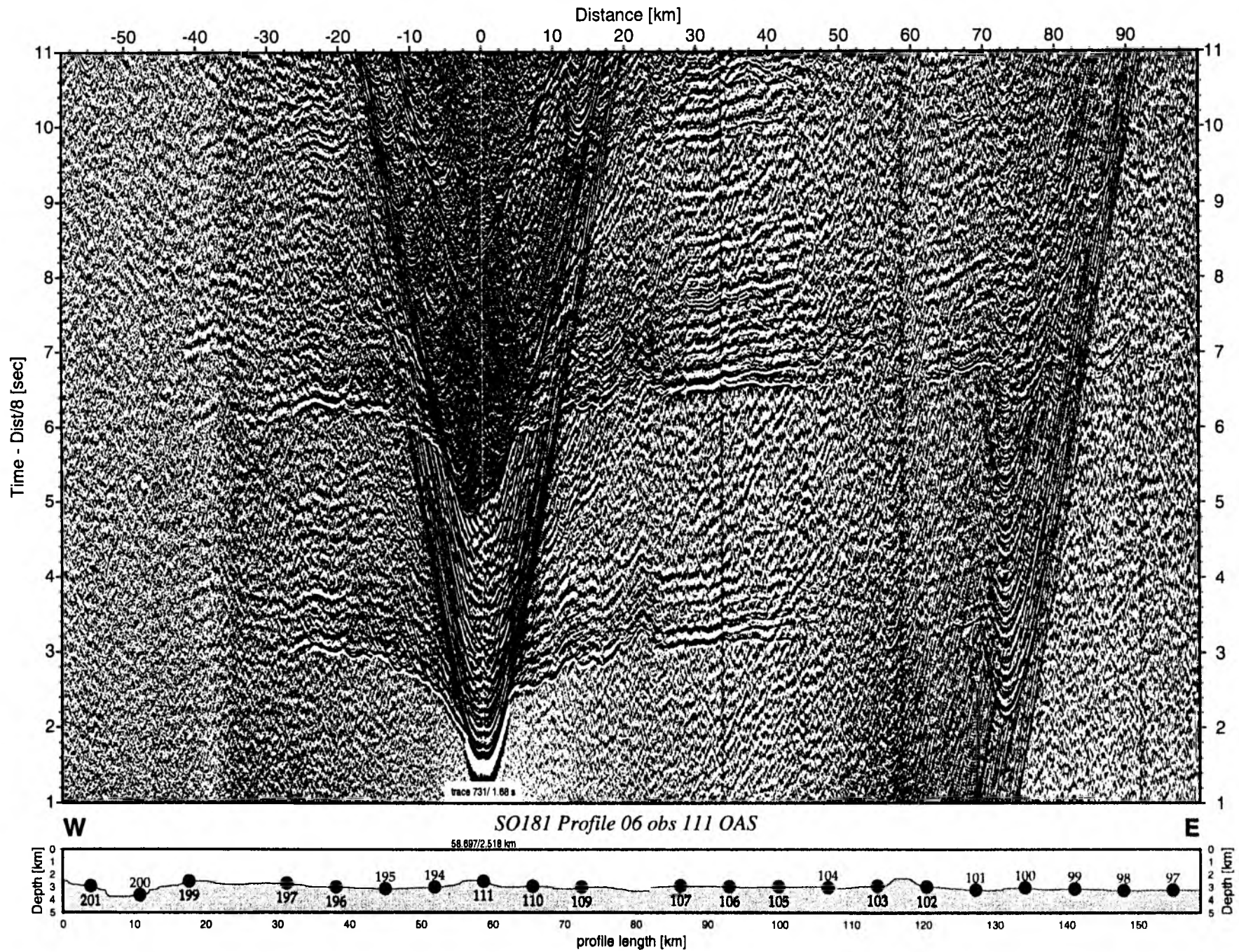


Figure 6.6.6.50: Record section from obs 111 OAS, Profile 06.

Time - Dist/8 [sec]

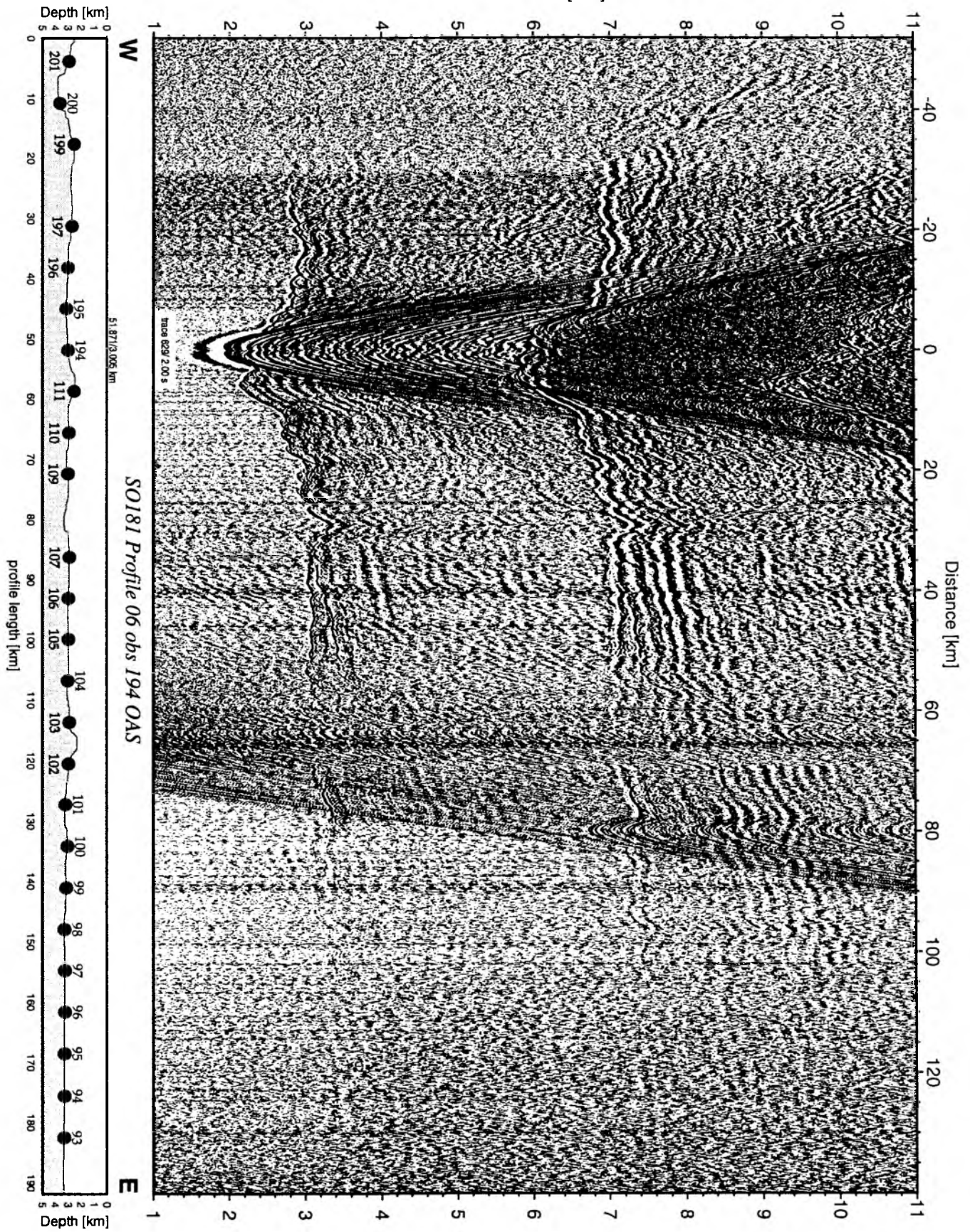


Figure 6.6.6.51: Record section from obs 194 OAS, Profile 06.

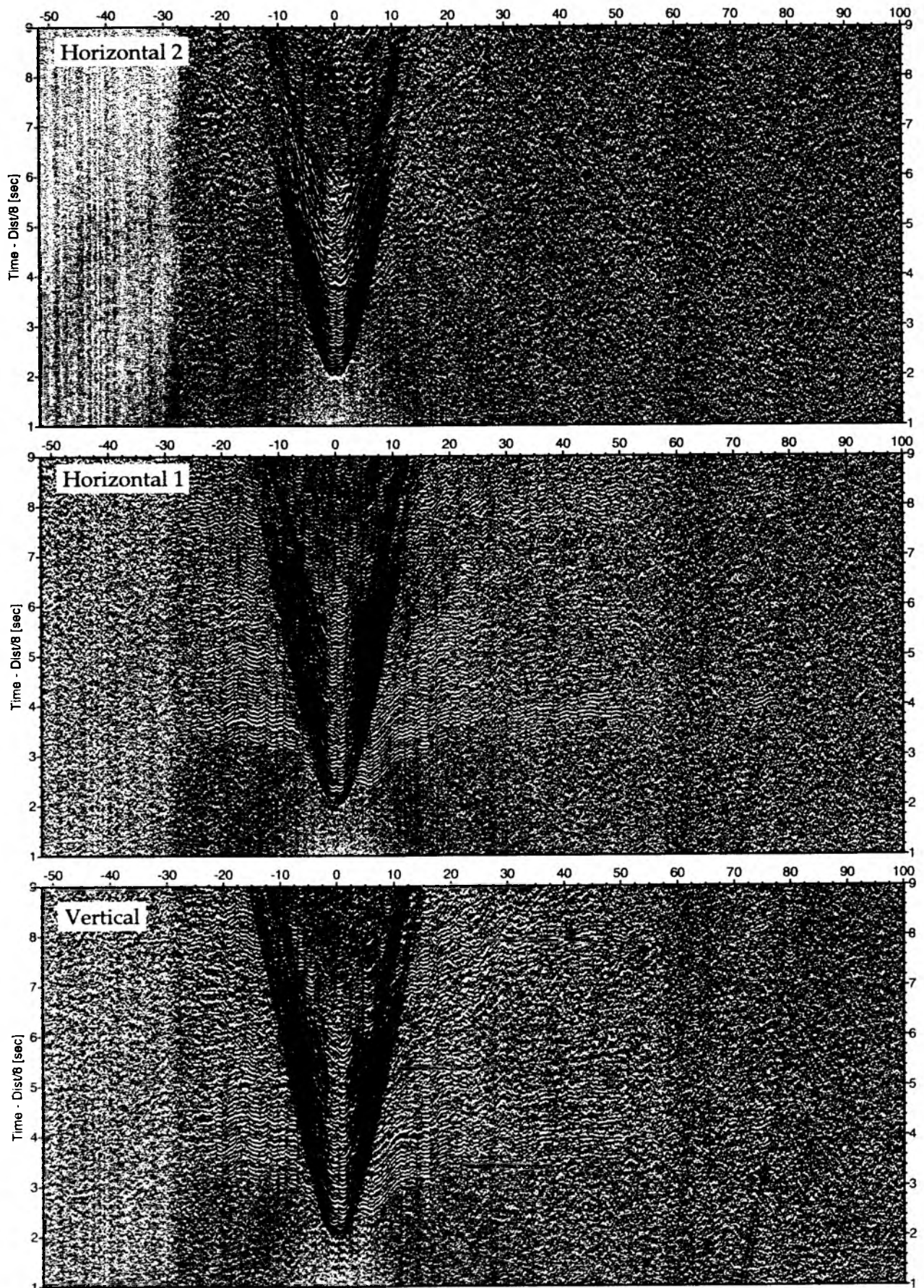


Figure 6.6.6.52: Record sections from obs 194 OAS/Seismo, SO181 Profile 06.

Time - Dist/8 [sec]

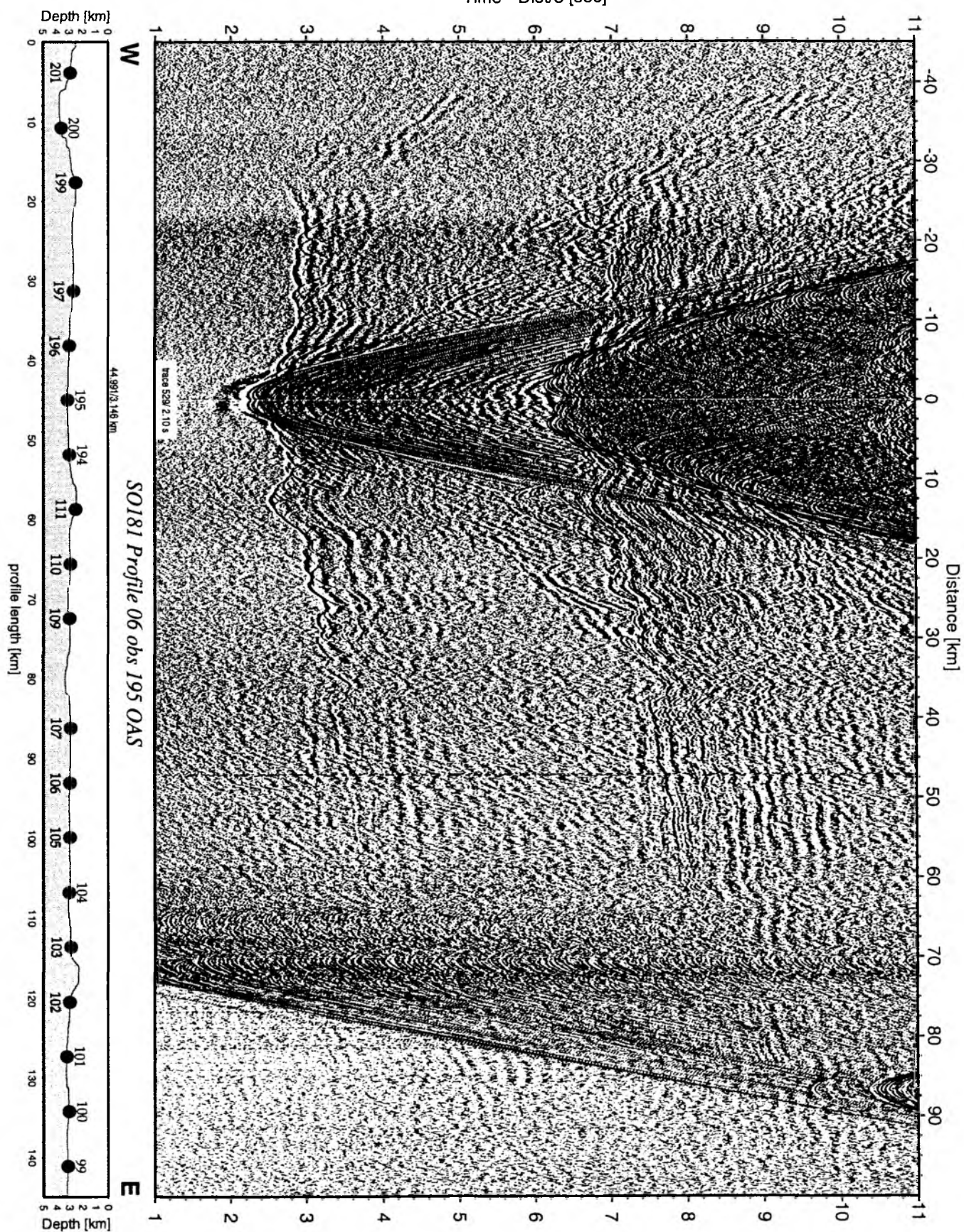


Figure 6.6.6.53: Record section from obs 195 OAS, Profile 06.

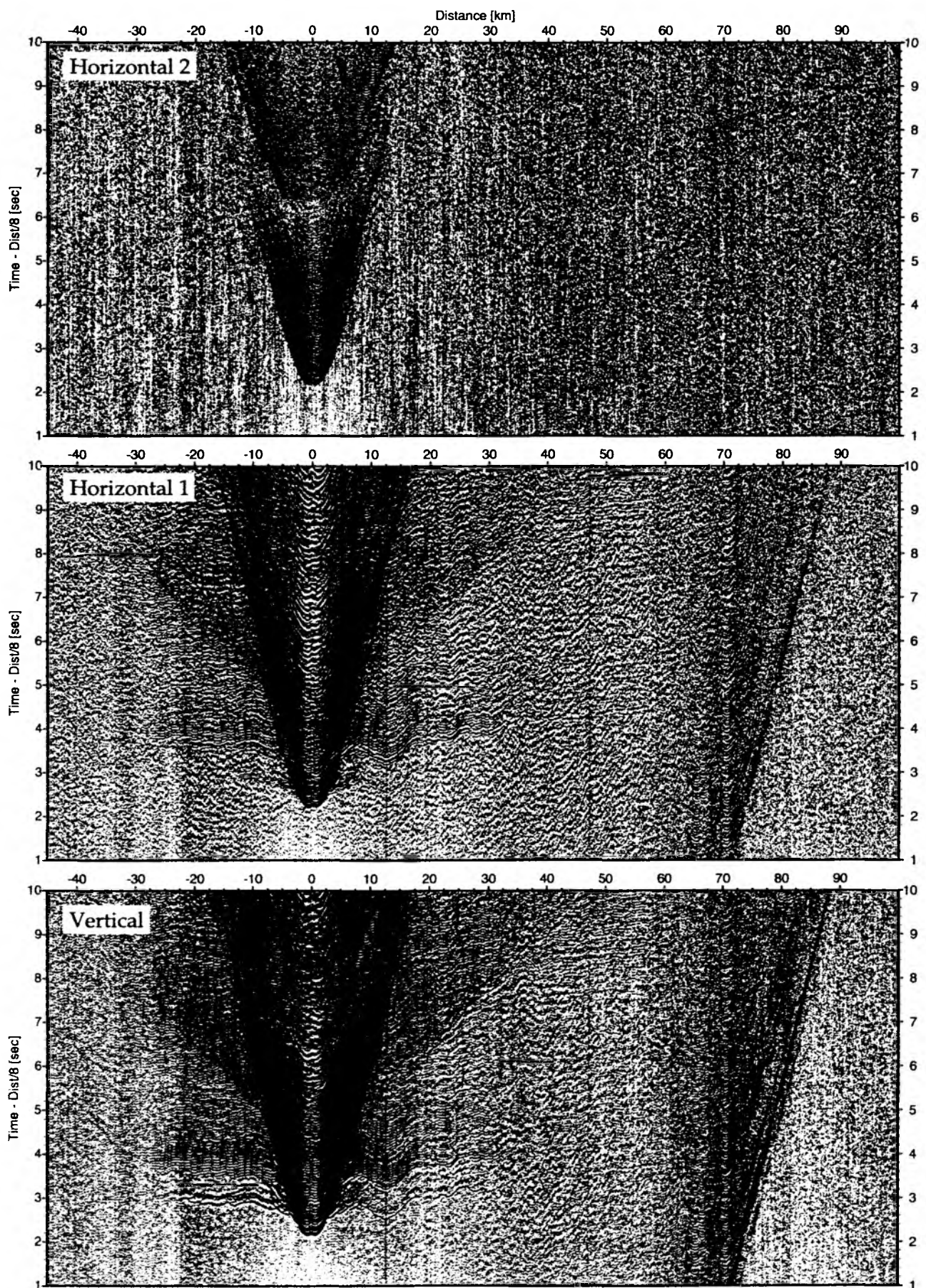


Figure 6.6.6.54: Record sections from obs 195 OAS/Owen-4.5Hz, SO181 Profile 06.

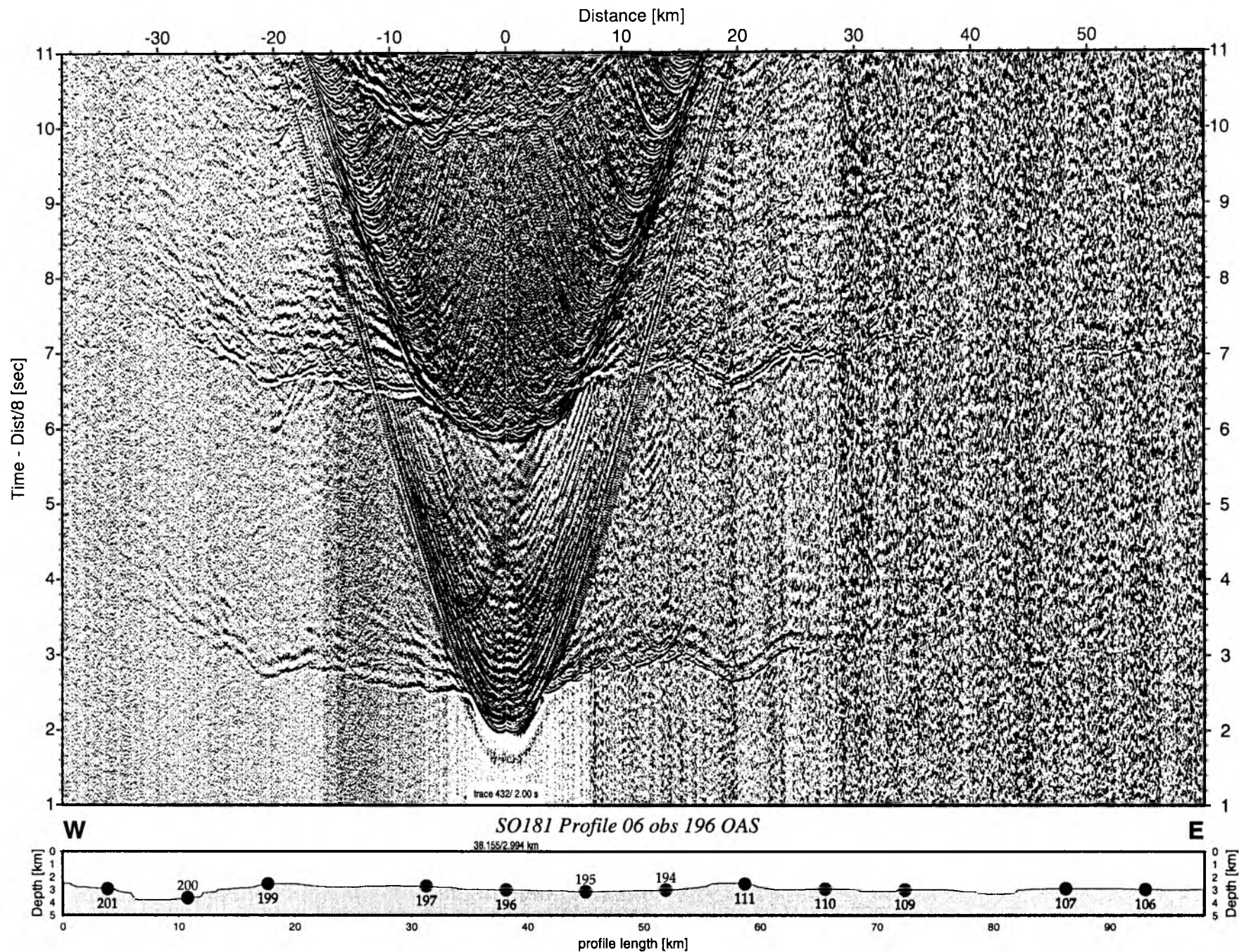


Figure 6.6.55: Record section from obs 196 OAS, Profile 06.

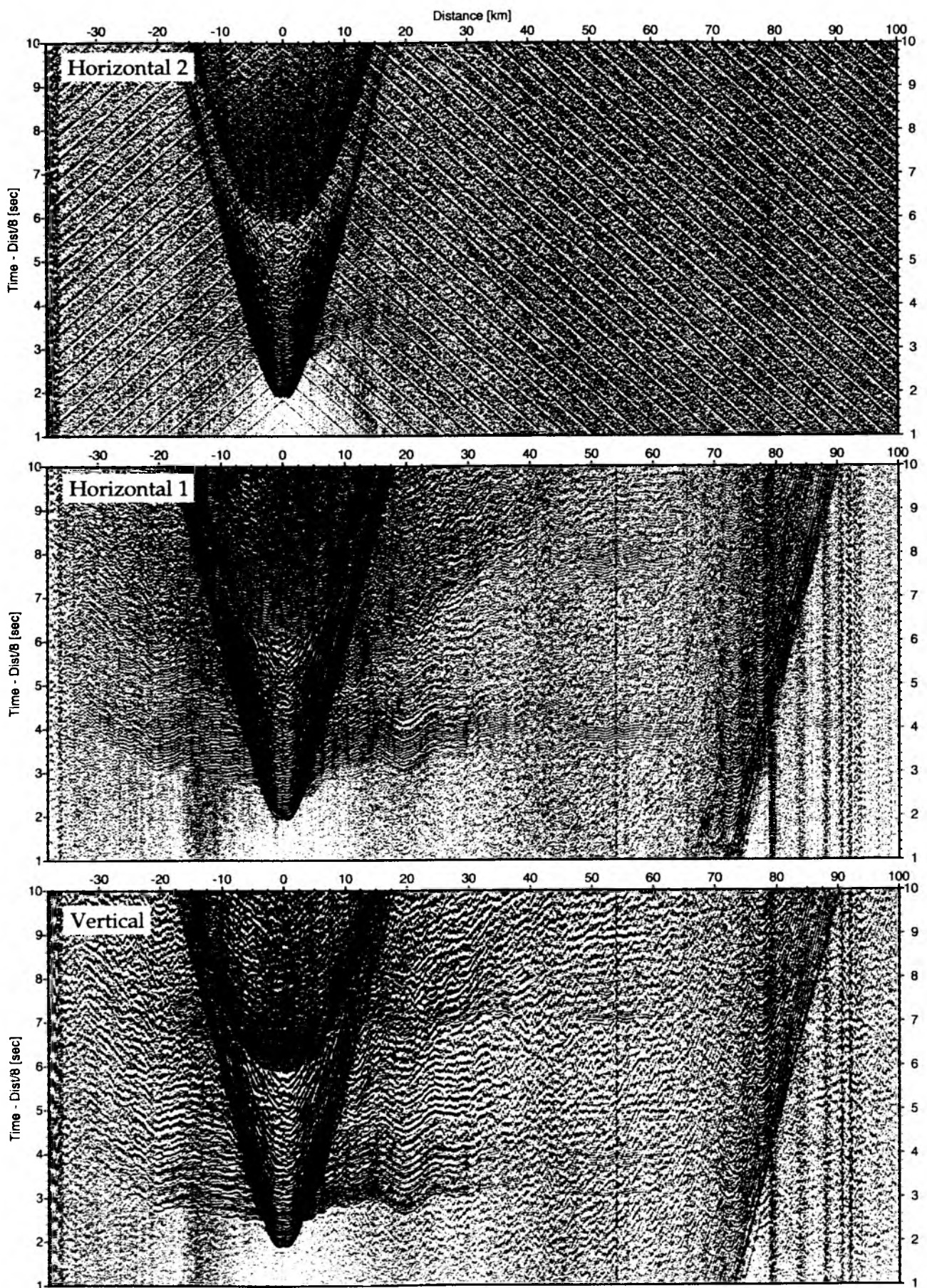


Figure 6.6.6.56: Record sections from obs 196 OAS/Owen-4.5Hz, SO181 Profile 06.

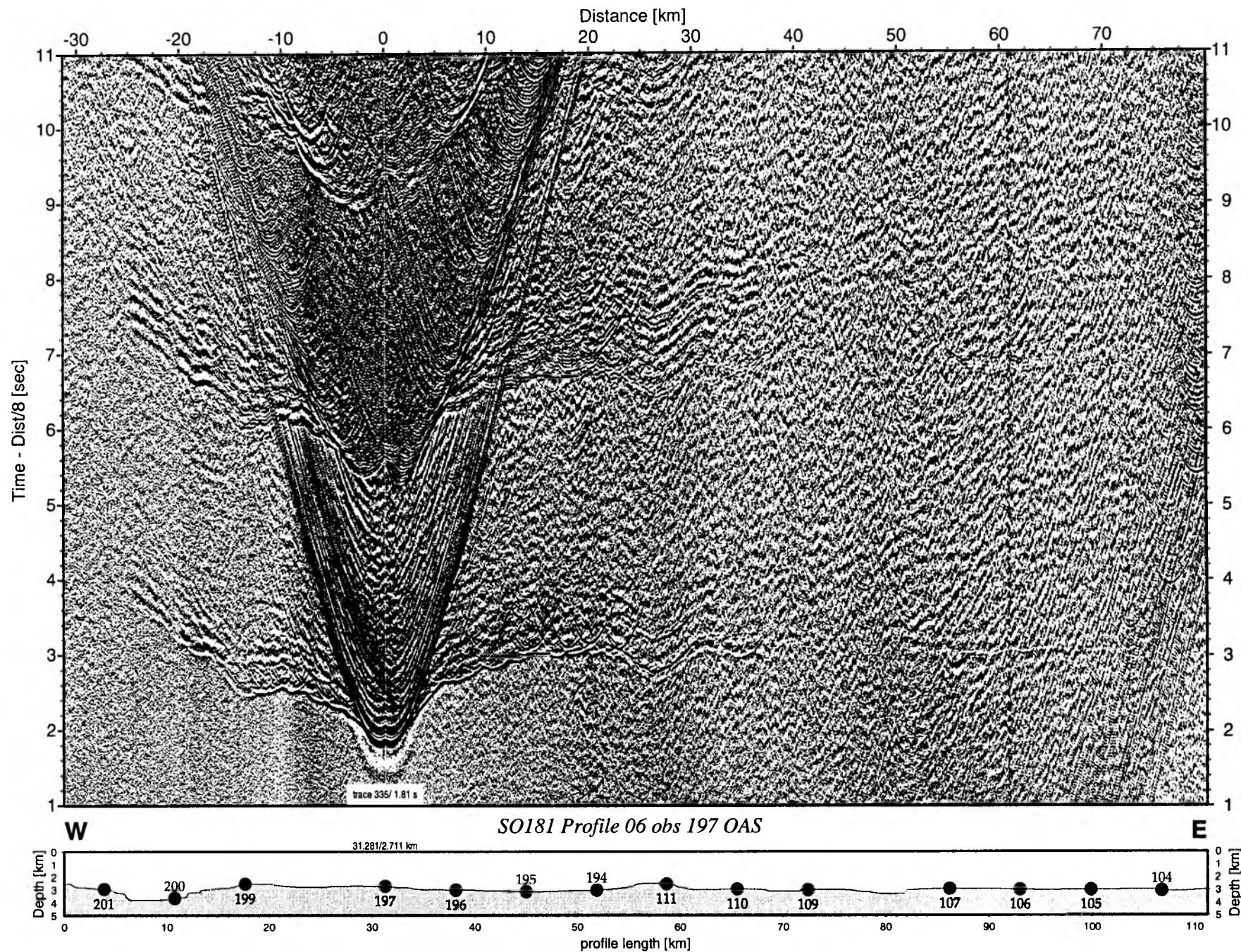


Figure 6.6.6.57: Record section from obs 197 OAS, Profile 06.

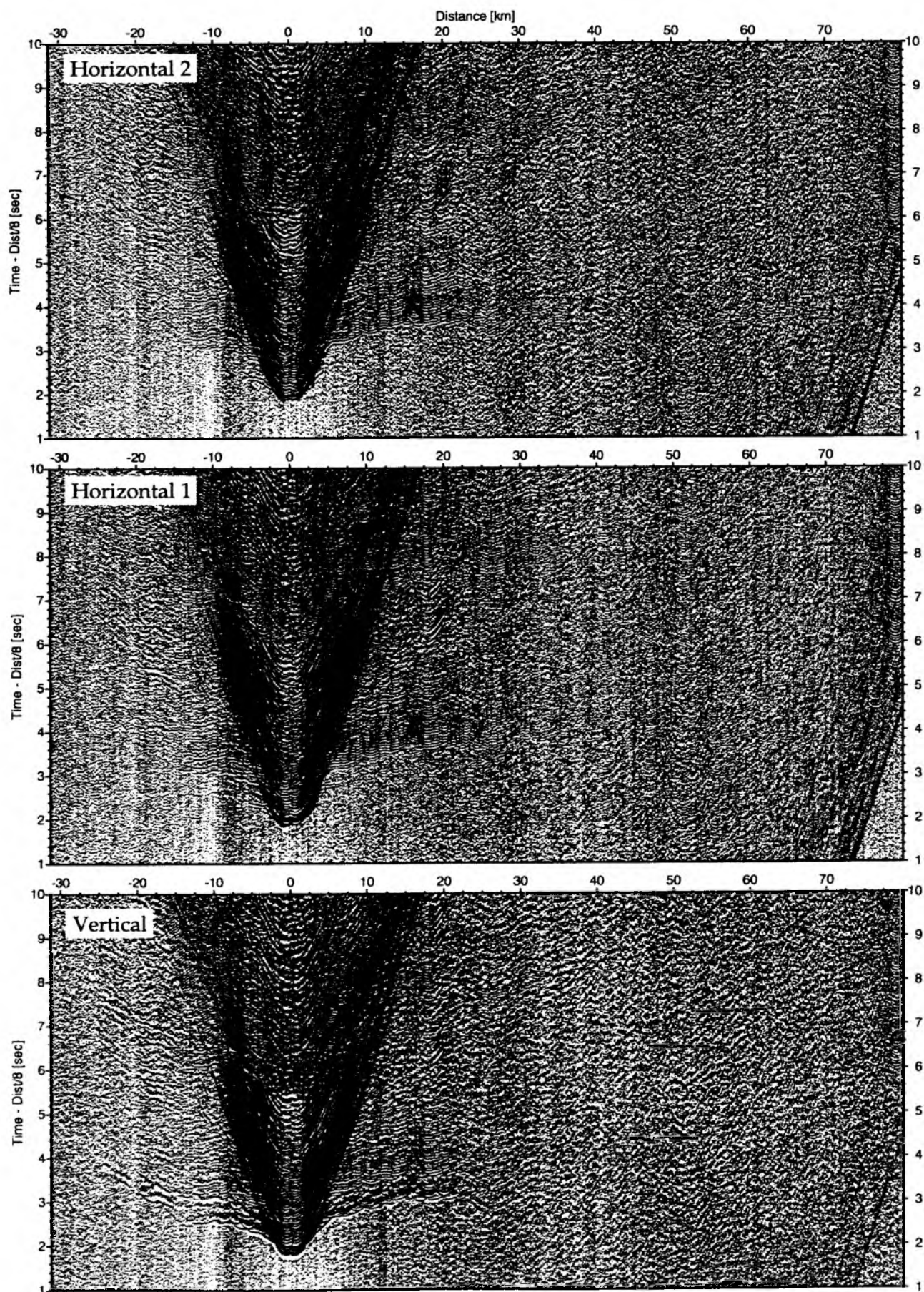


Figure 6.6.6.58: Record sections from obs 197 OAS/Owen-4.5Hz, SO181 Profile 06.

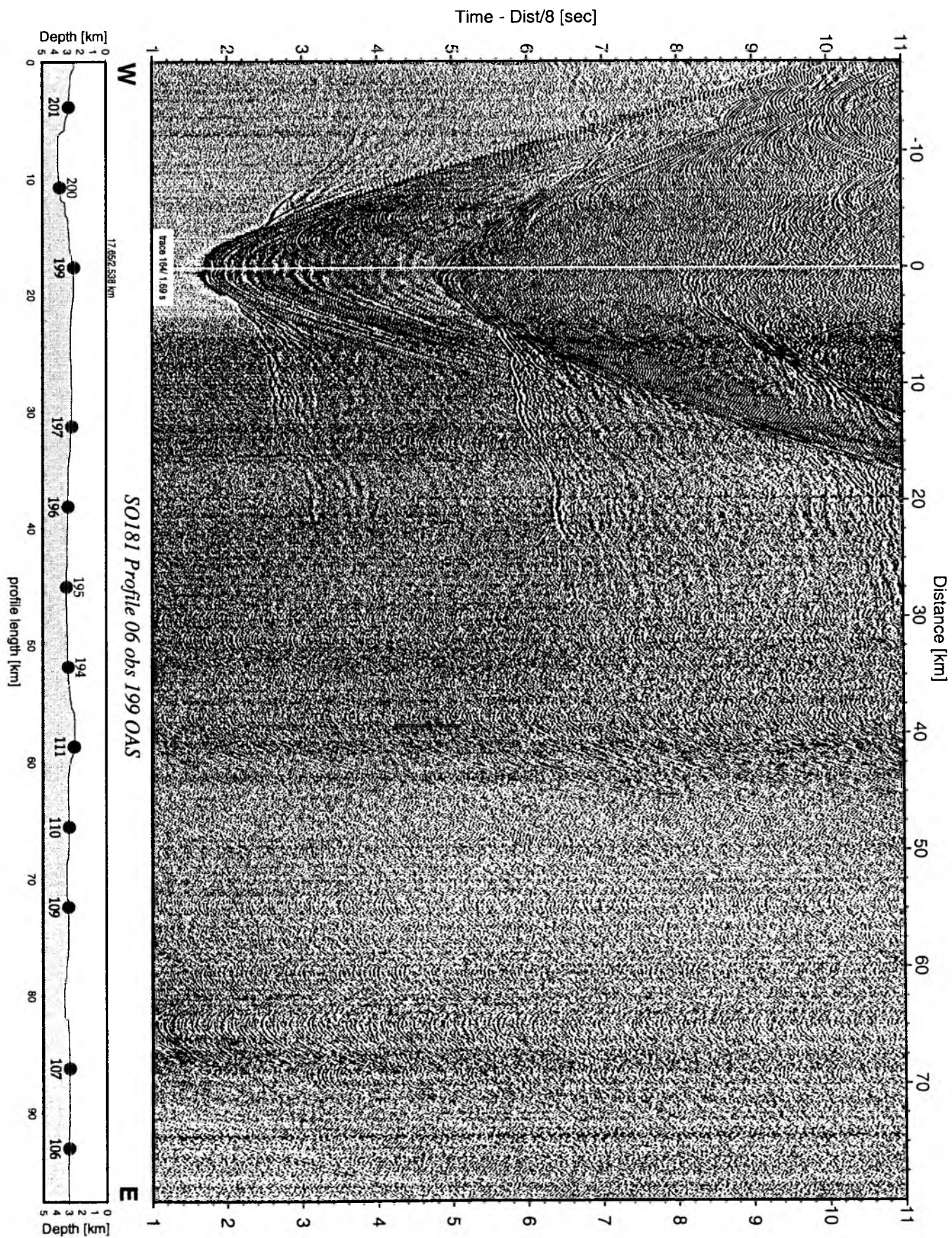


Figure 6.6.659: Record section from obs 199 OAS, Profile 06.

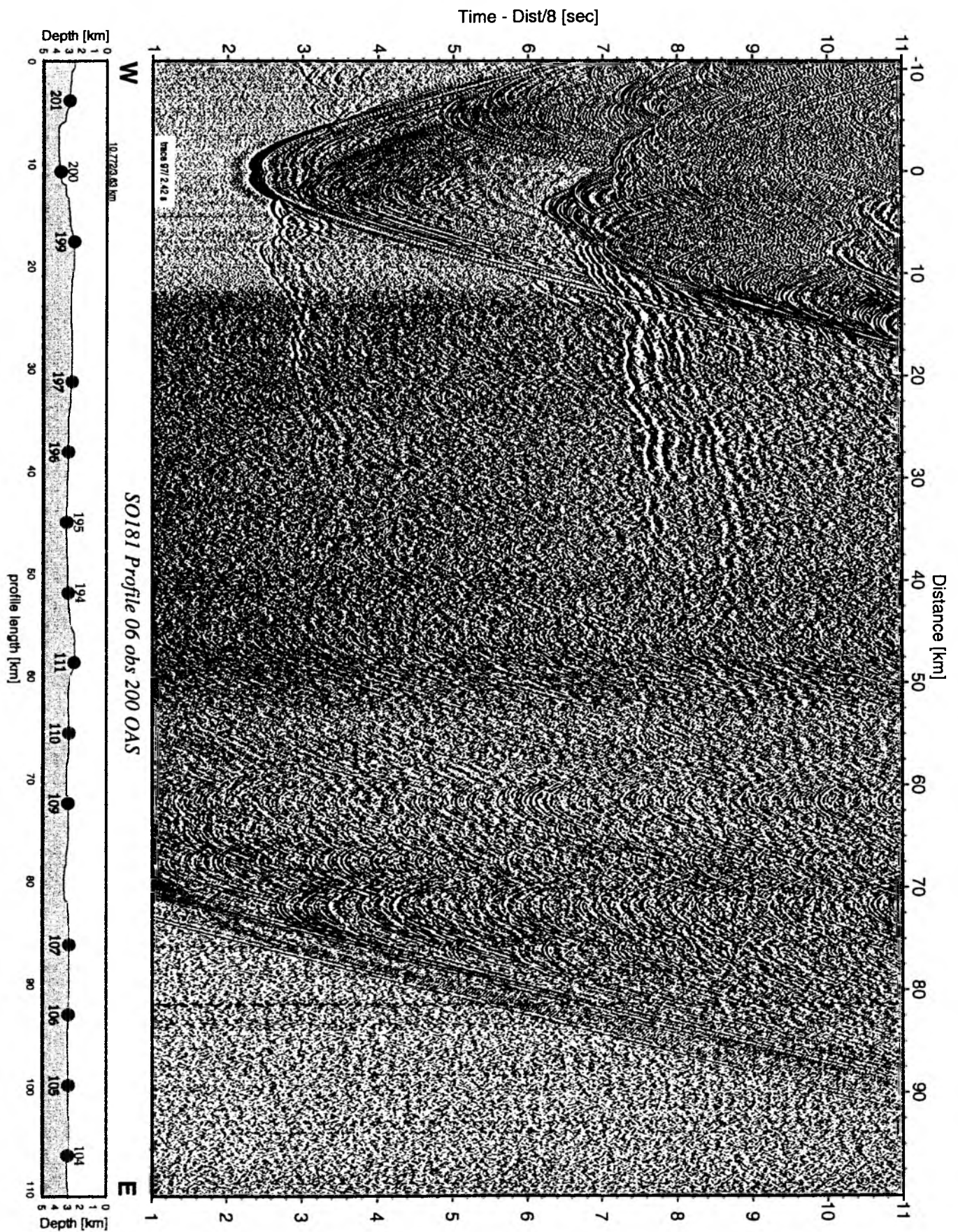


Figure 6.6.6.60: Record section from obs 200 OAS, Profile 06.

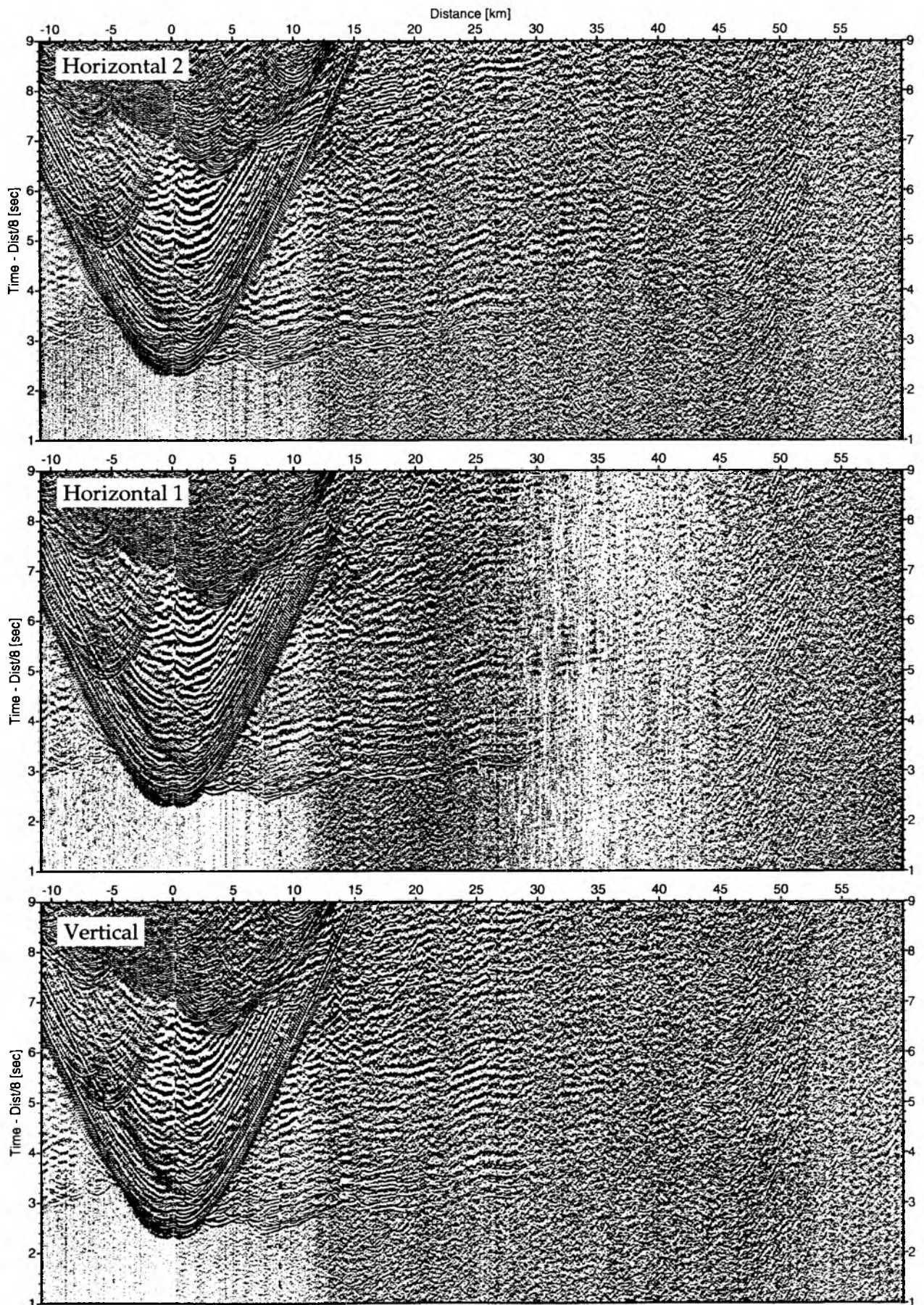


Figure 6.6.61: Record sections from obs 200 OAS/Owen-4.5Hz, SO181 Profile 06.

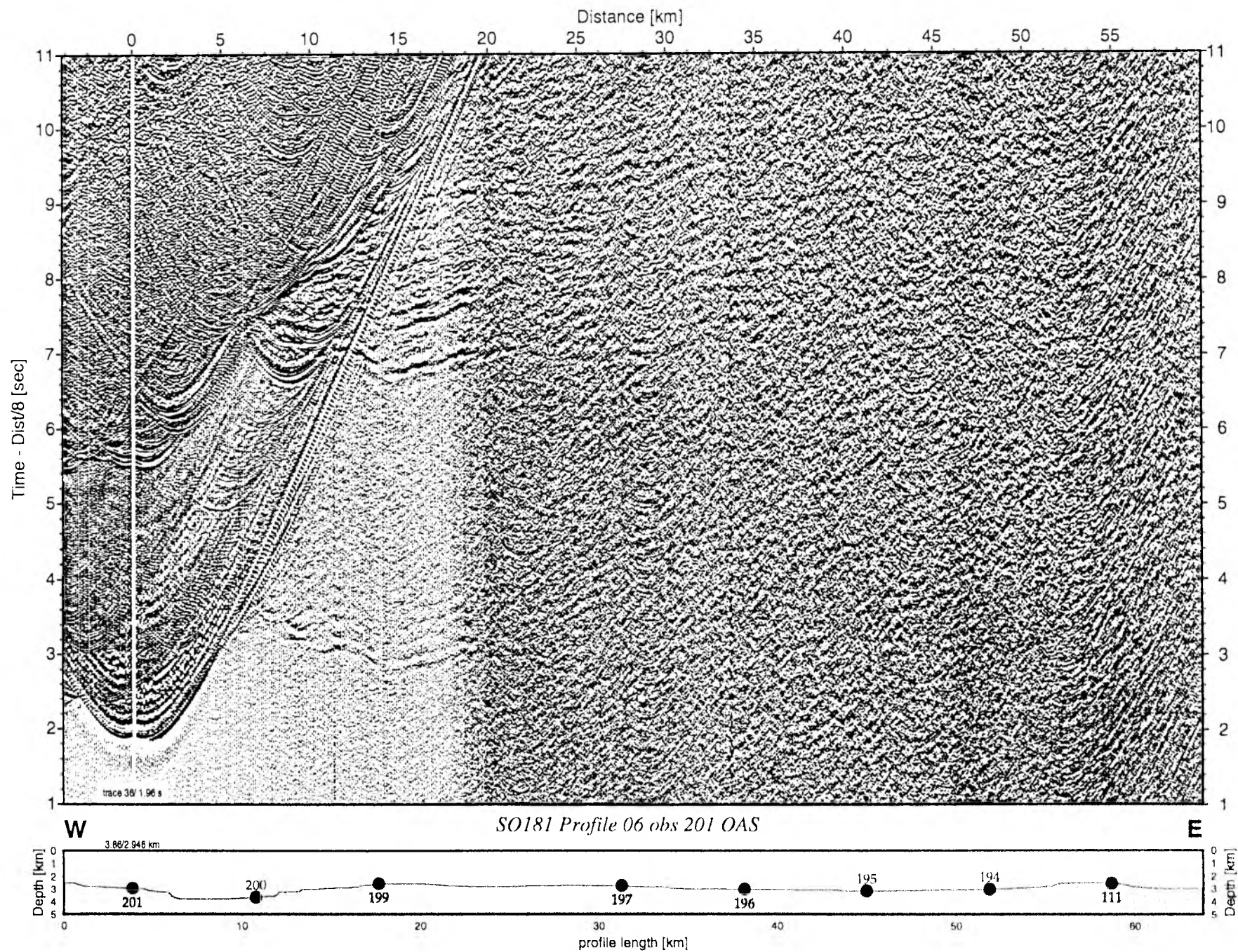


Figure 6.6.6.62: Record section from obs 201 OAS, Profile 06.

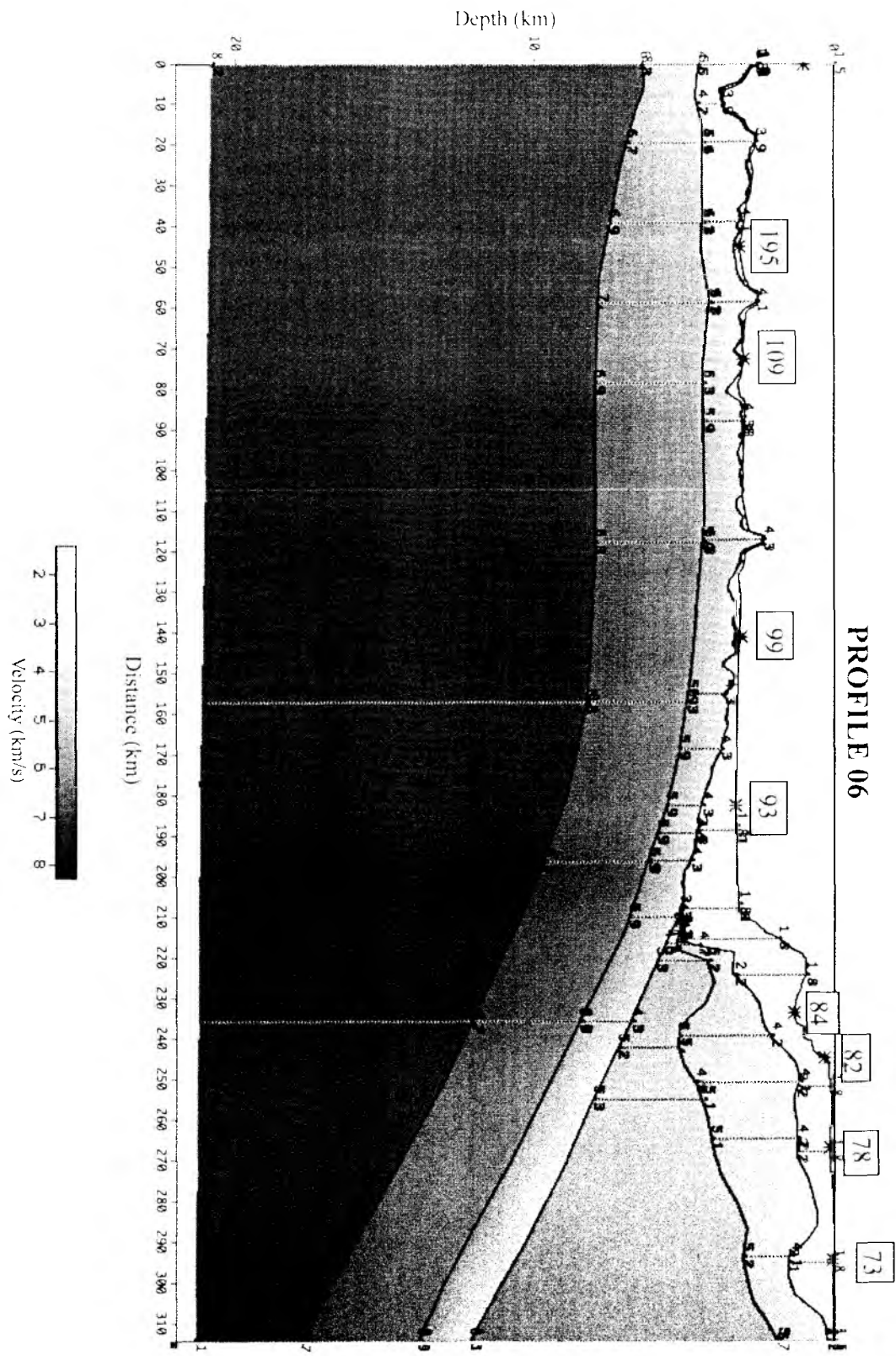


Fig 6.6.6.63 : Preliminary model of profile P07

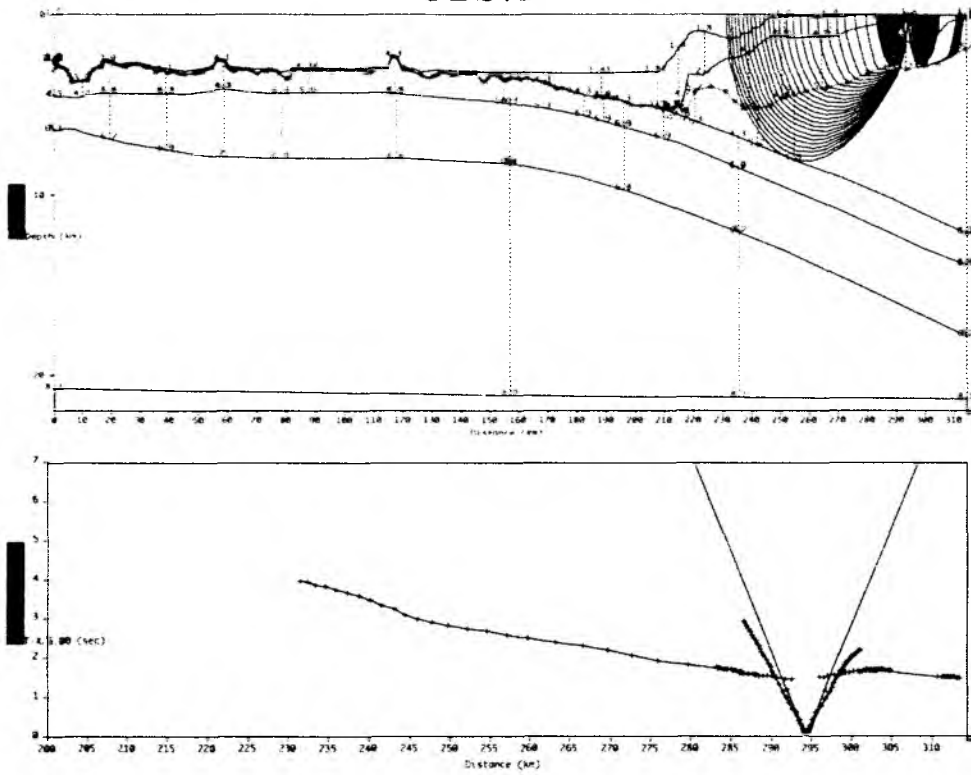
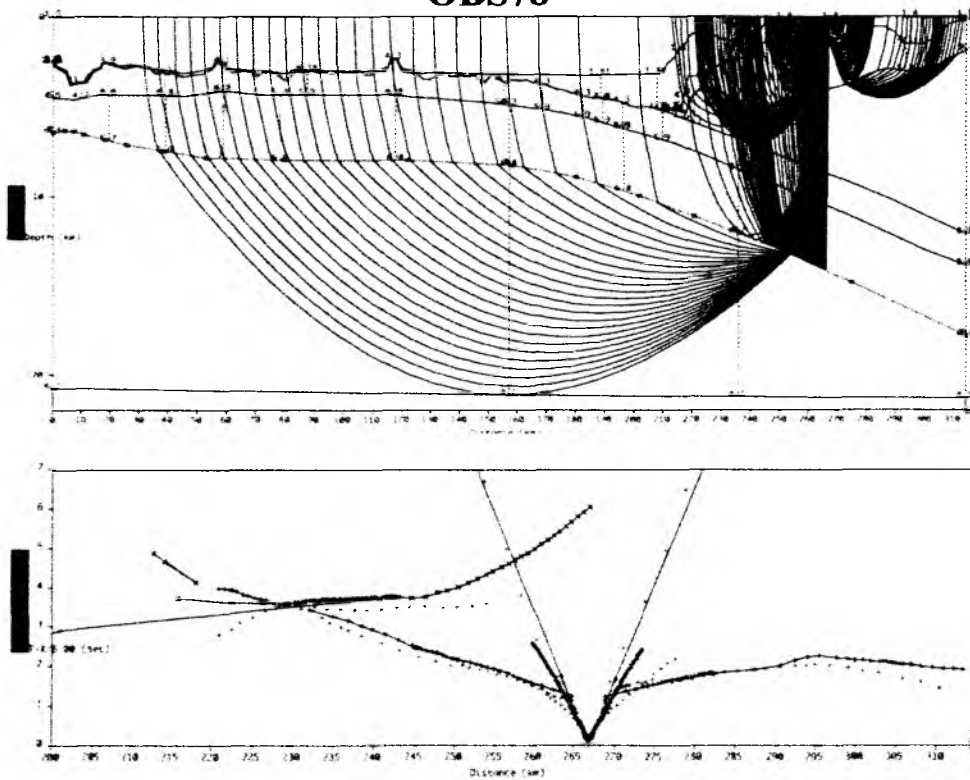
OBS73**OBS78**

Fig 6.6.6.64 : raypaths and traveltimes picks of OBS73 and OBS78

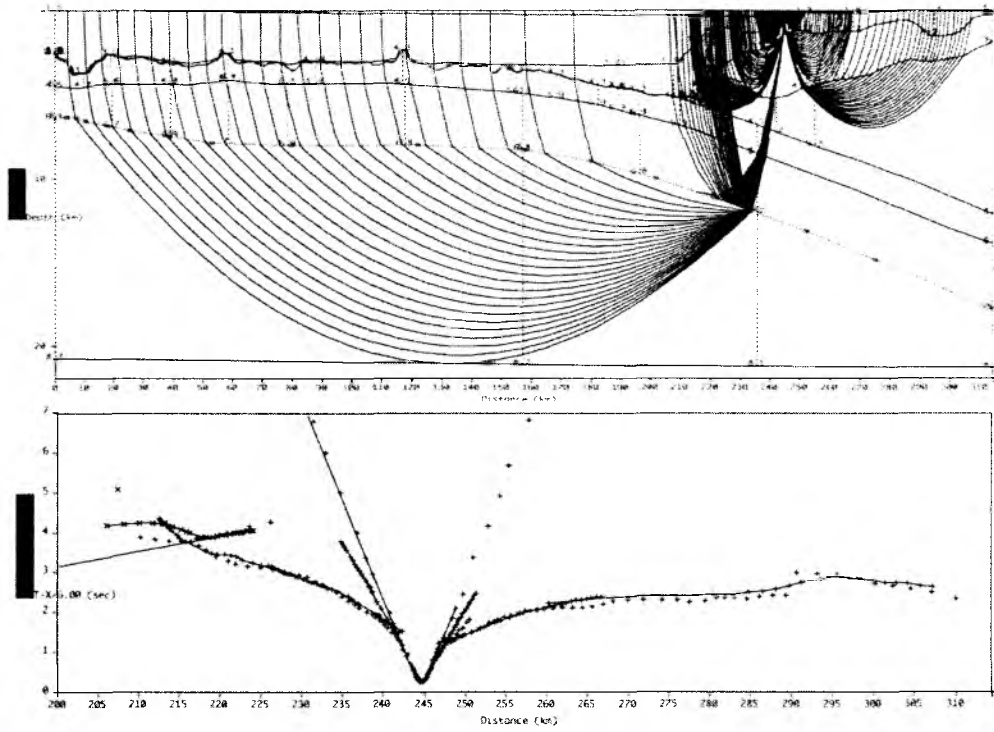
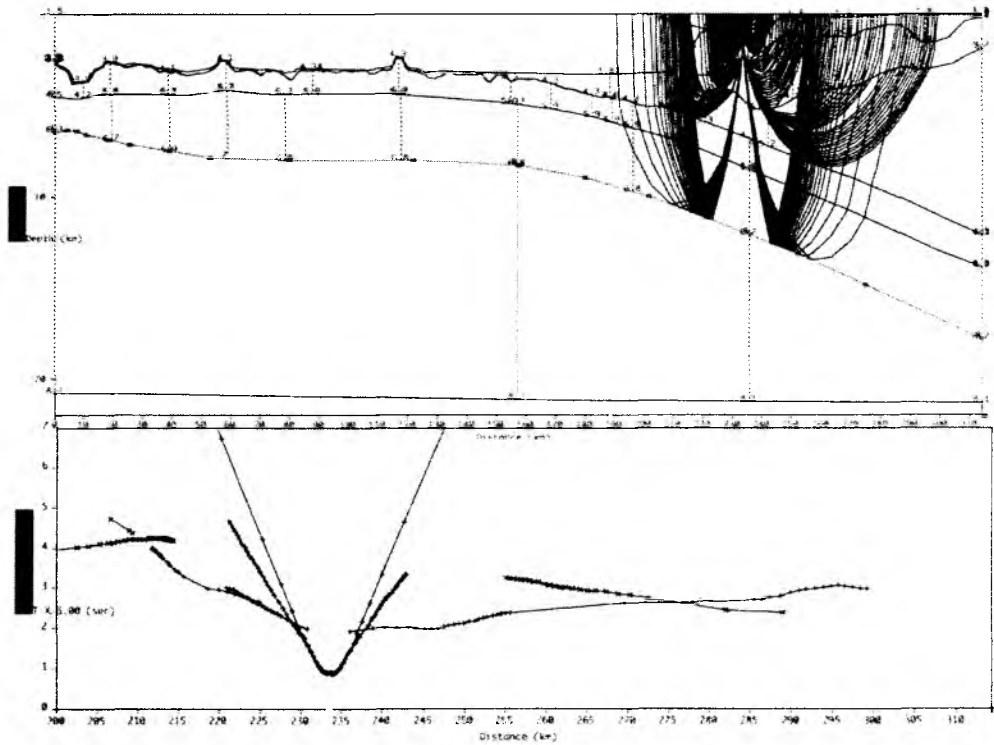
OBS82**OBS84**

Fig 6.6.6.65 : raypaths and traveltimes picks of OBS82 and OBS84

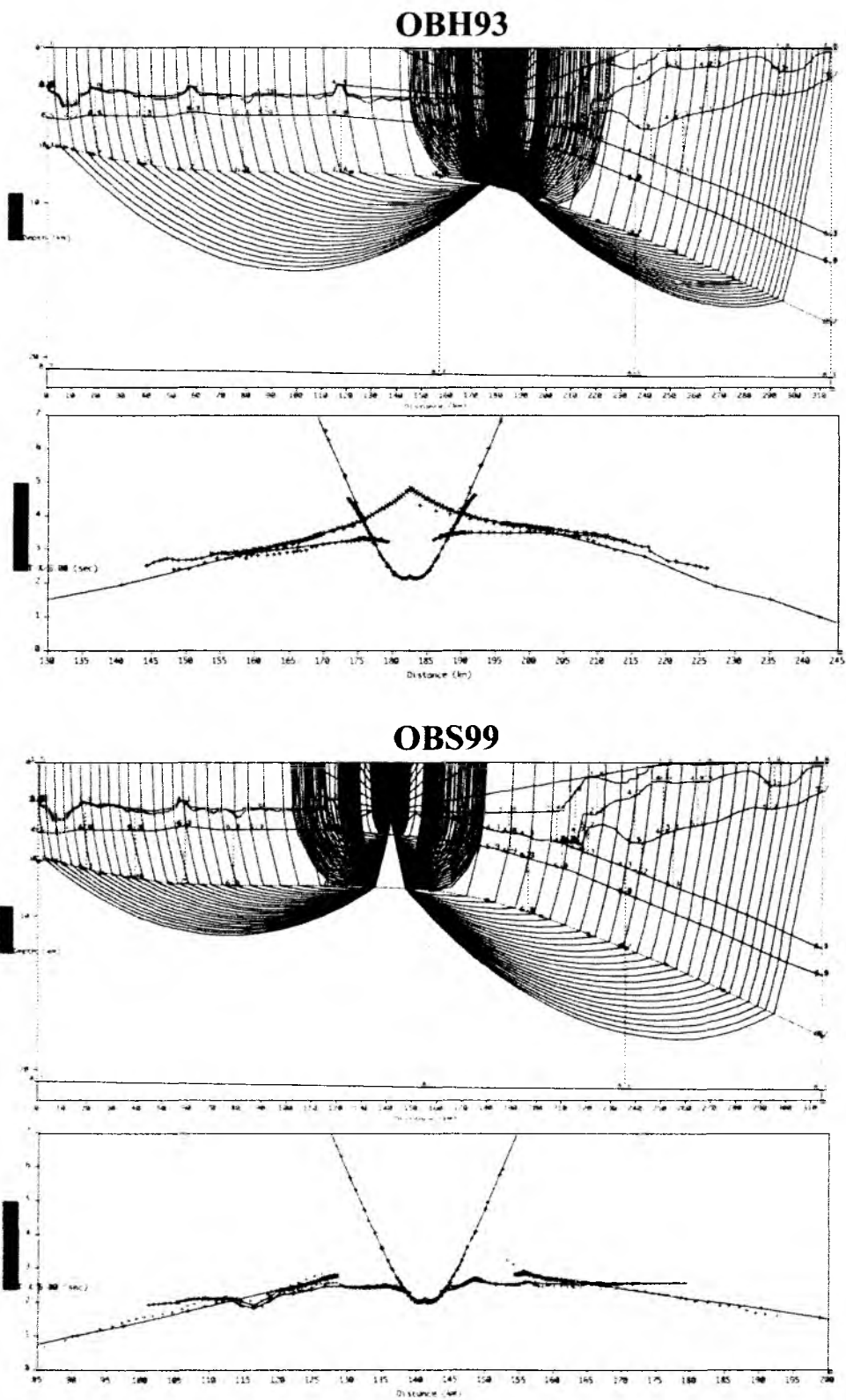


Fig 6.6.6.66 : raypaths and traveltimes picks of OBH93 and OBS99

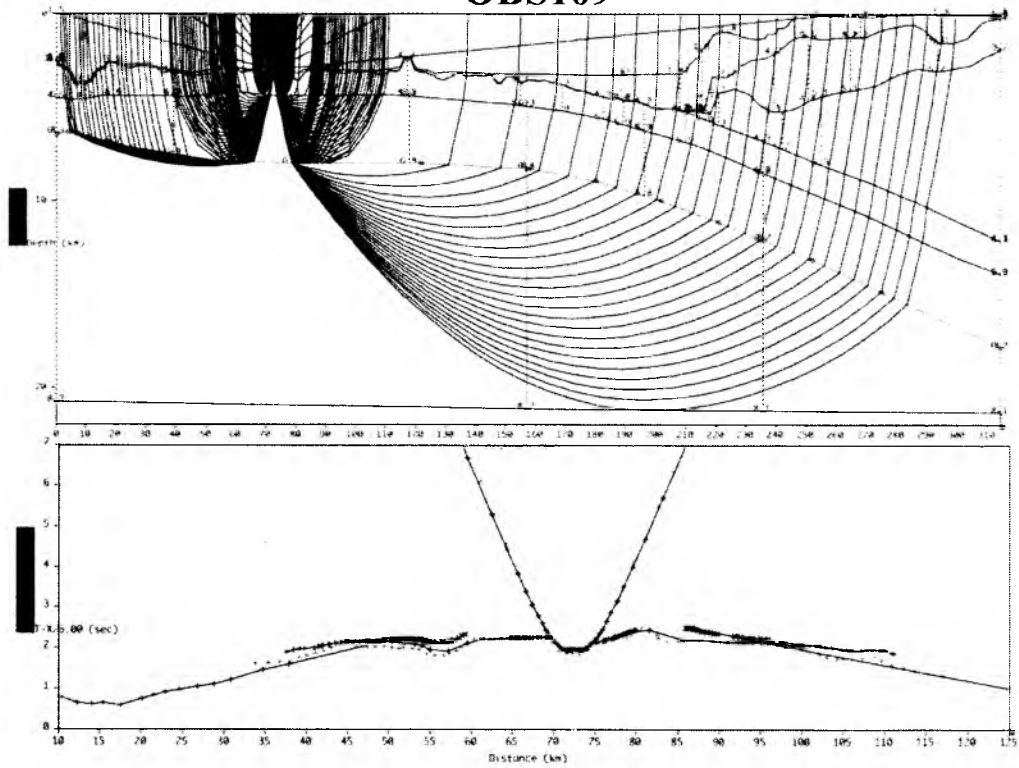
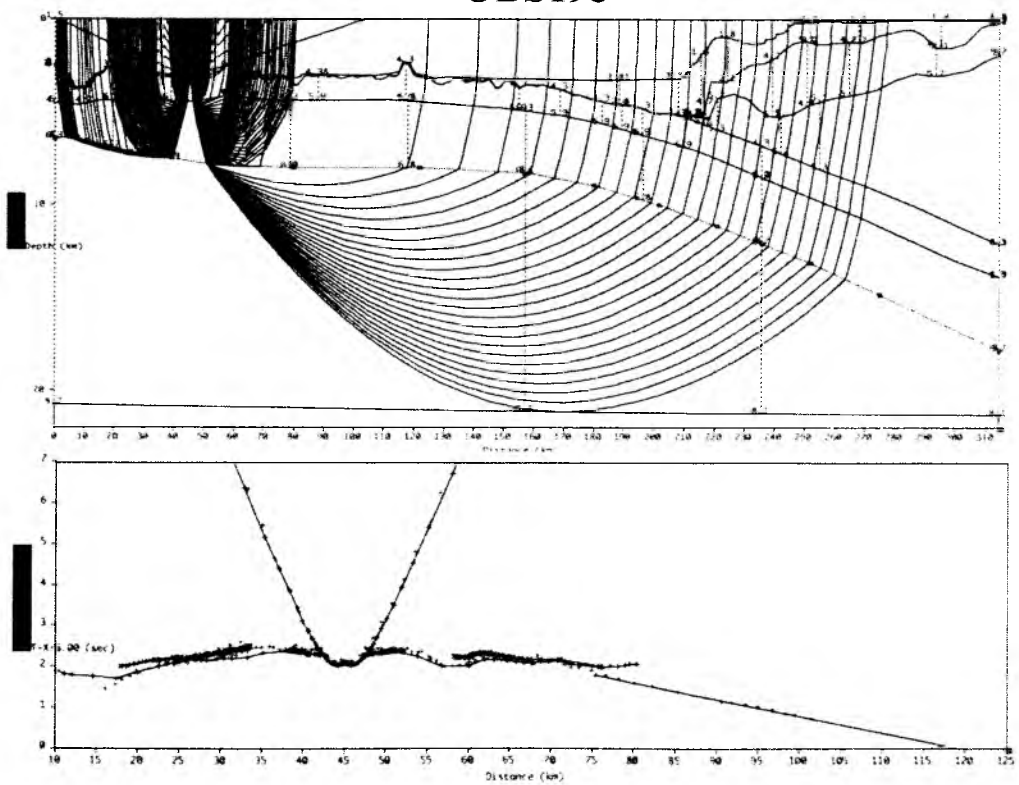
OBS109**OBS195**

Fig 6.6.6.67 : raypaths and traveltimes picks of OBS109 and OBS195

6.6.7 Profile P09

Along this profile a total of 29 instruments were deployed from the Chile Trench to the northwest on 15 Feb. Shooting was done in almost perfect conditions from 02:30 on 16 Feb to 18:00 on 17 Feb. Throughout the entire profile seven G-Guns were operating. The shooting interval was set to 50 sec. A four channel streamer was recording throughout the profile, augmenting existing MCS data for parts of the profile, collected during cruise SO161. Instruments were picked up once shooting was terminated, and they were all back onboard by 05:00 on 18 Feb.

Details of instruments and shots can be found in Appendices 9.2 and 9.3, most instruments recorded well. A location map is shown in Figure 6.6.7.1, and record sections are shown in Figures 6.6.7.2 to 6.6.7.40. In the hydrophone data, the multiples are usually stronger than the primary arrivals. We therefore chose a time window and a reduction velocity that, for far offsets, focuses on the multiple in the record sections. In the best record sections (OBH 239 and 240, Figures 6.6.7.28 and 6.6.7.29) Pn-arrivals can be seen out to distances of more than 130 km, which was rarely observed in the past. Also many record sections from the seismometers are of superb quality, and one can clearly distinguish between the different components. The data will have to be rotated into in-line and cross-line components for further analysis. The streamer data allow to define the sedimentary thickness exactly, which is almost zero in some places, and thus we expect to be able to model the P- and S-wave structure of the crust and upper mantle in hitherto unknown detail.

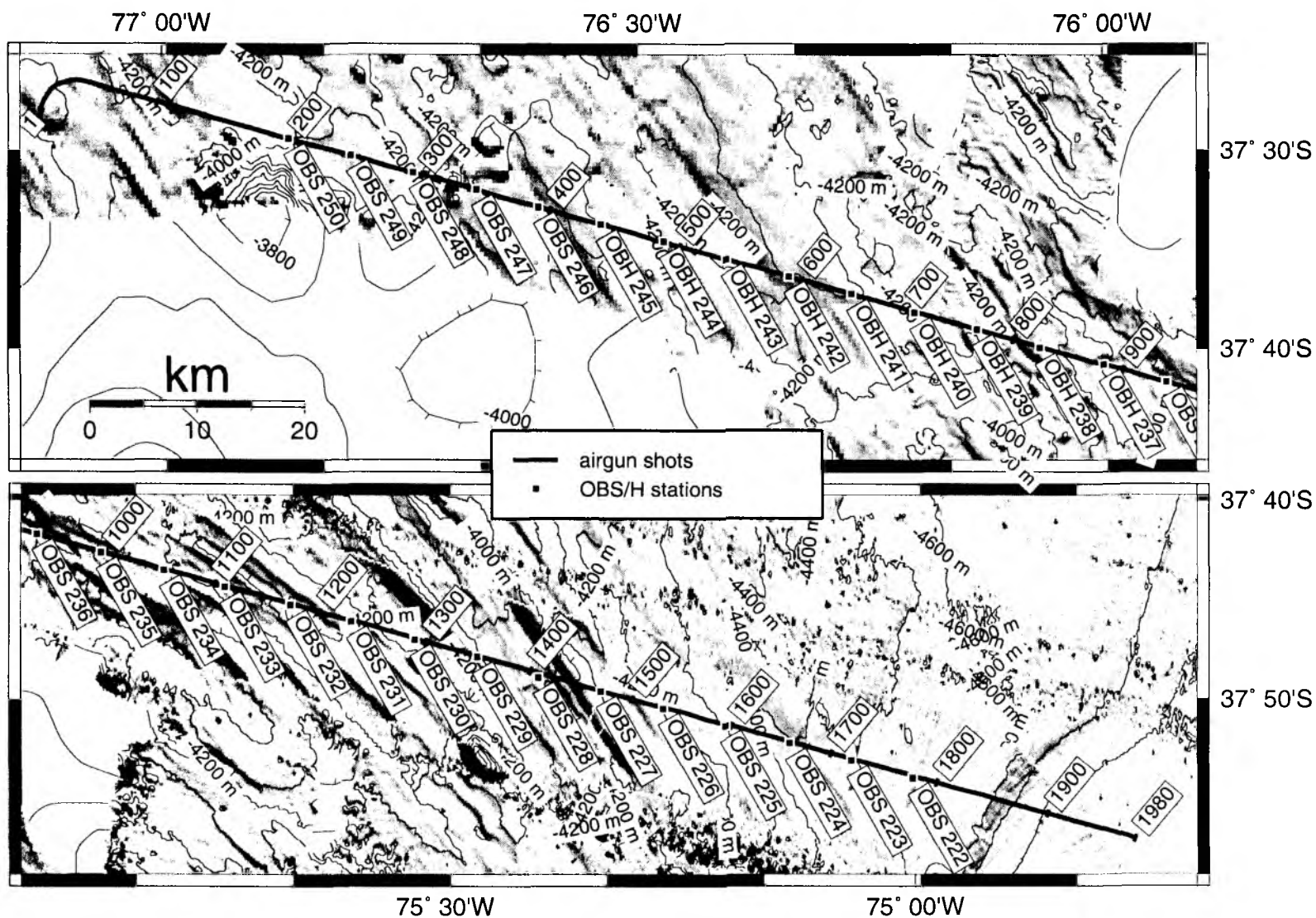


Figure 6.6.7.1: Basemap of P09; transect of ocean bottom seismometer and hydrophone stations and line of airgun shots. Bathymetry contours every 100m.

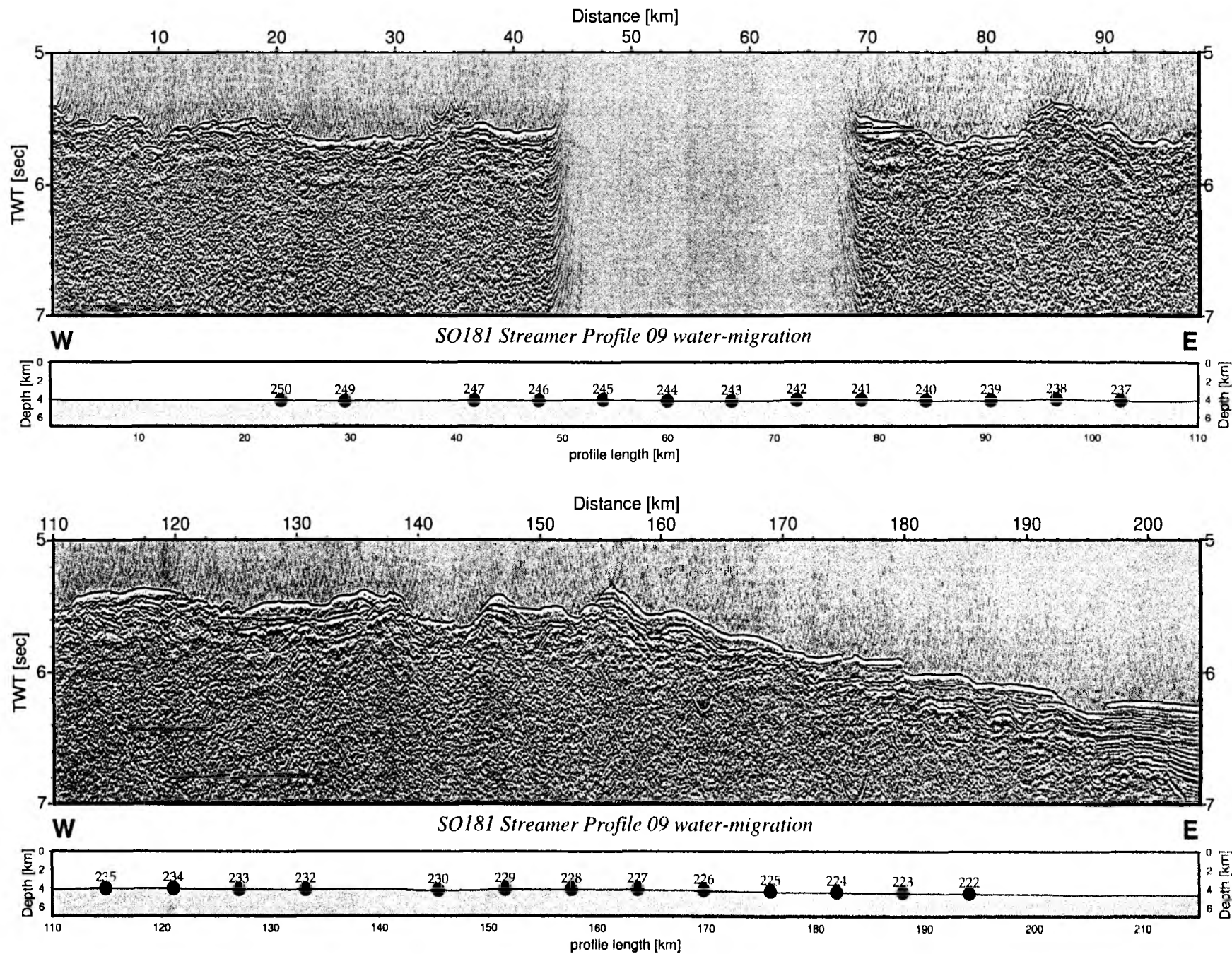


Figure 6.6.7.2: Record section from Streamer Profile 09 water-migration.

Time - Dist/6 [sec]

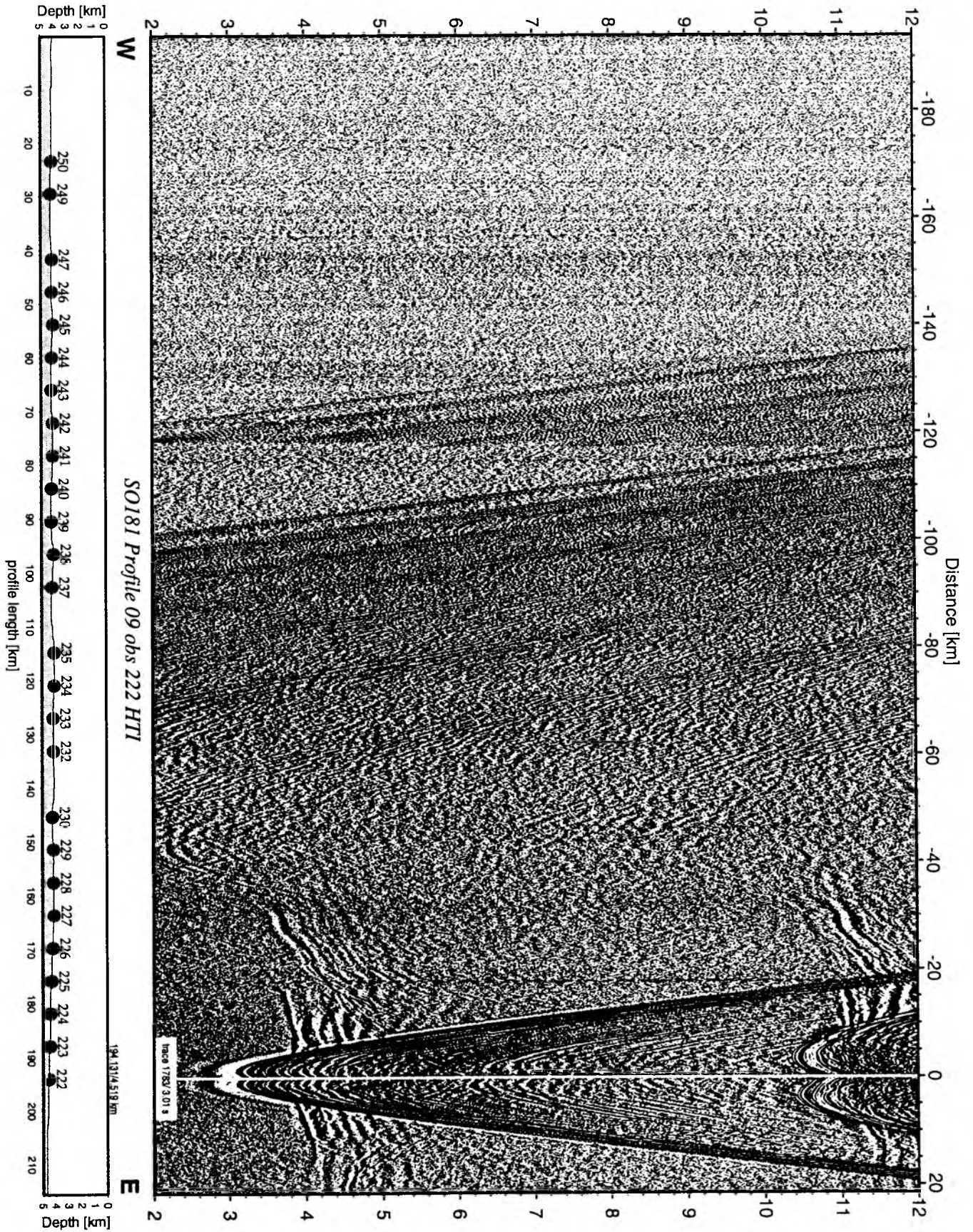


Figure 6.6.7.3: Record section from obs 222 HTI, Profile 09.

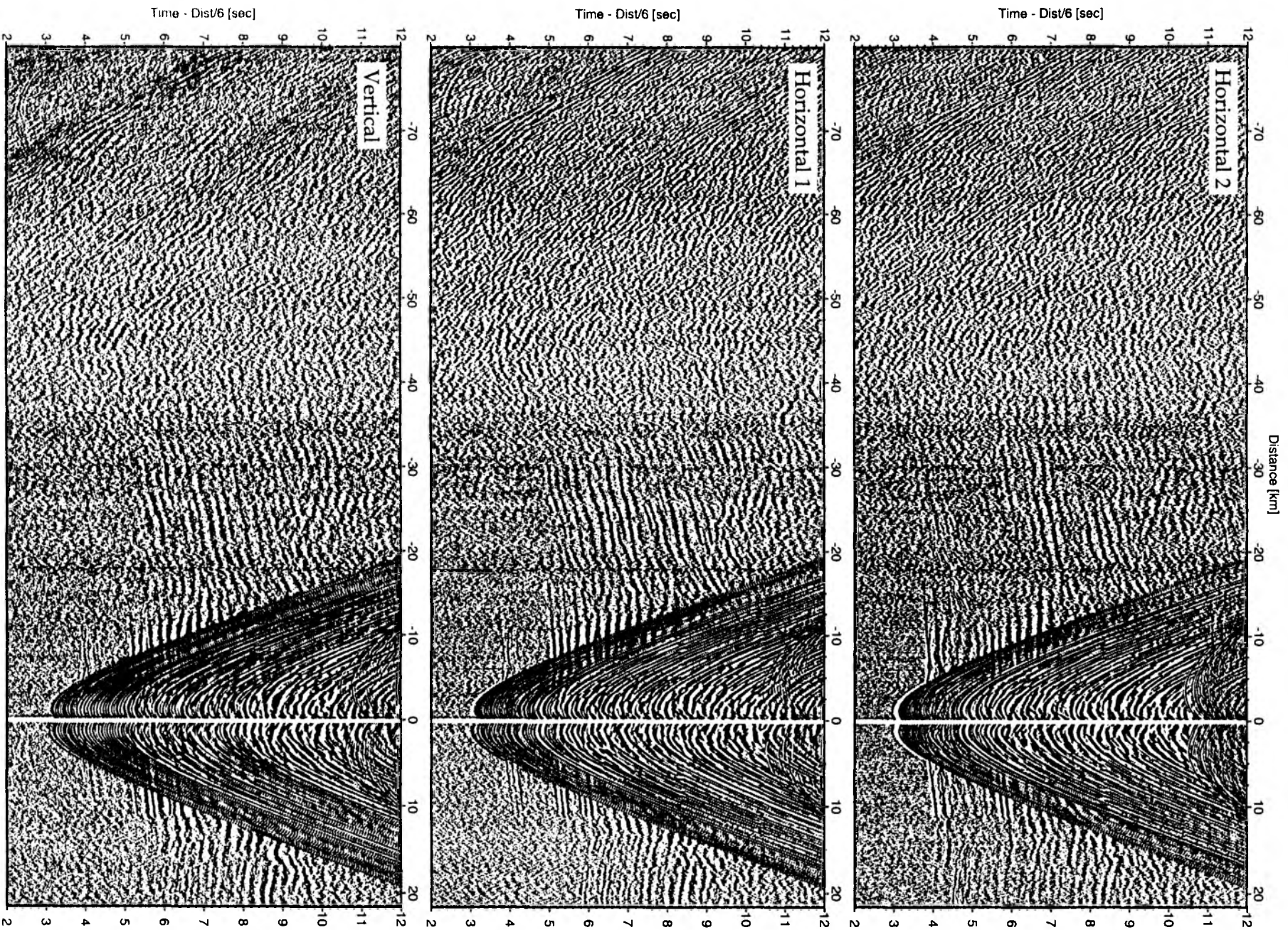


Figure 6.6.7.4:

Record sections from obs 222 HTI/Owen-4.5Hz, SO181 Profile 09.

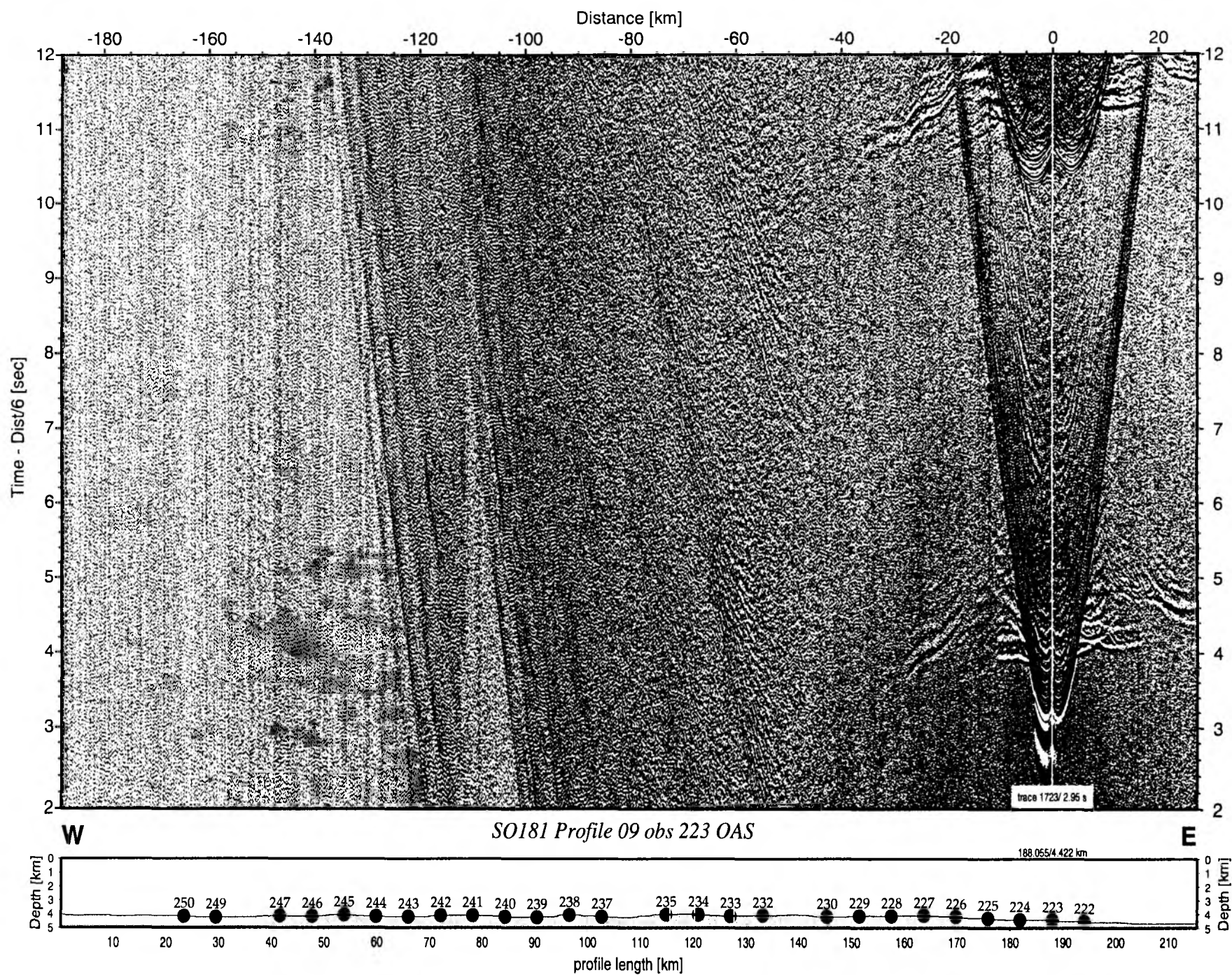


Figure 6.6.7.5: Record section from obs 223 OAS, Profile 09.

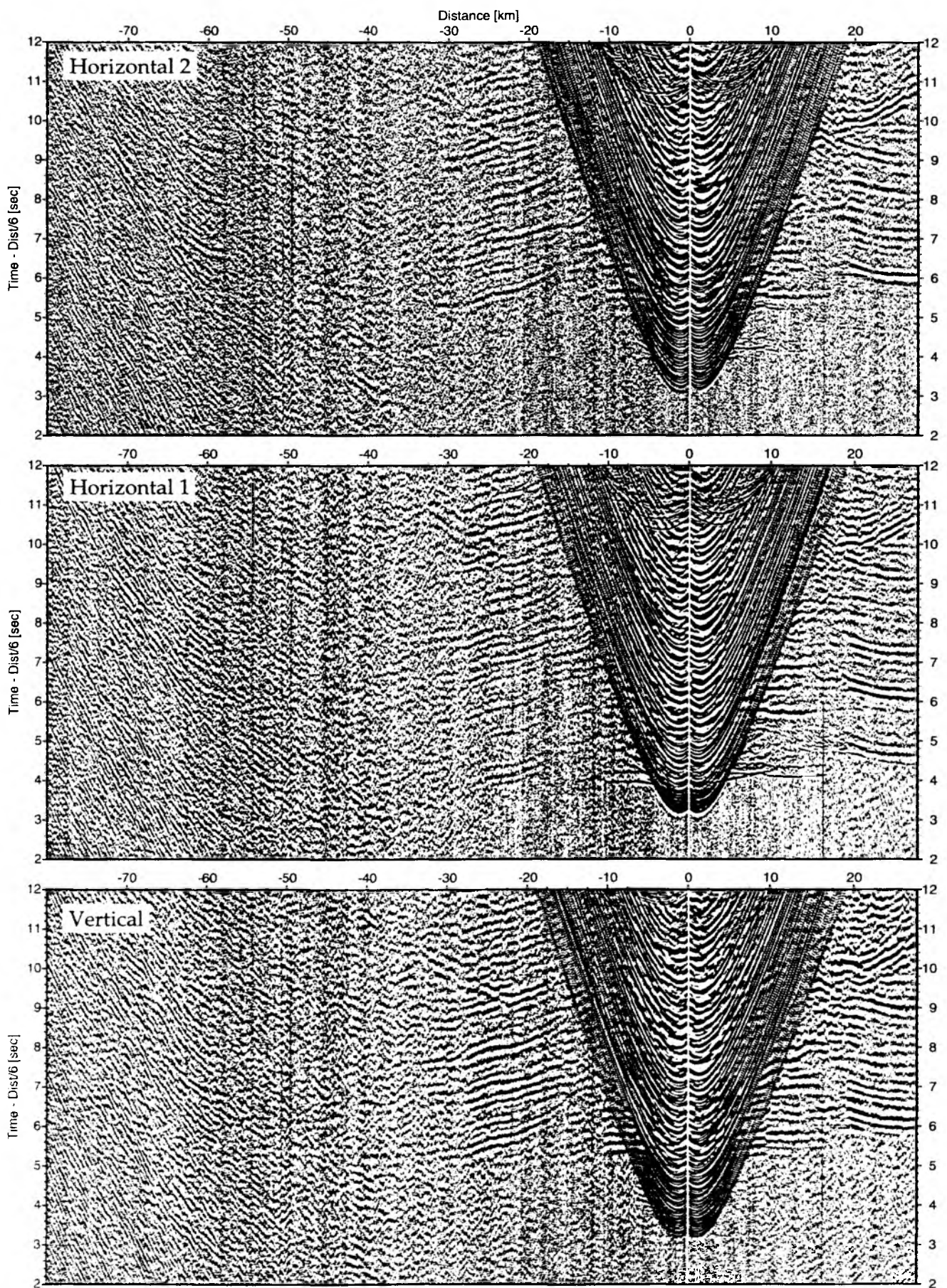


Figure 6.6.7.6: Record sections from obs 223 OAS/Owen, SO181 Profile 09.

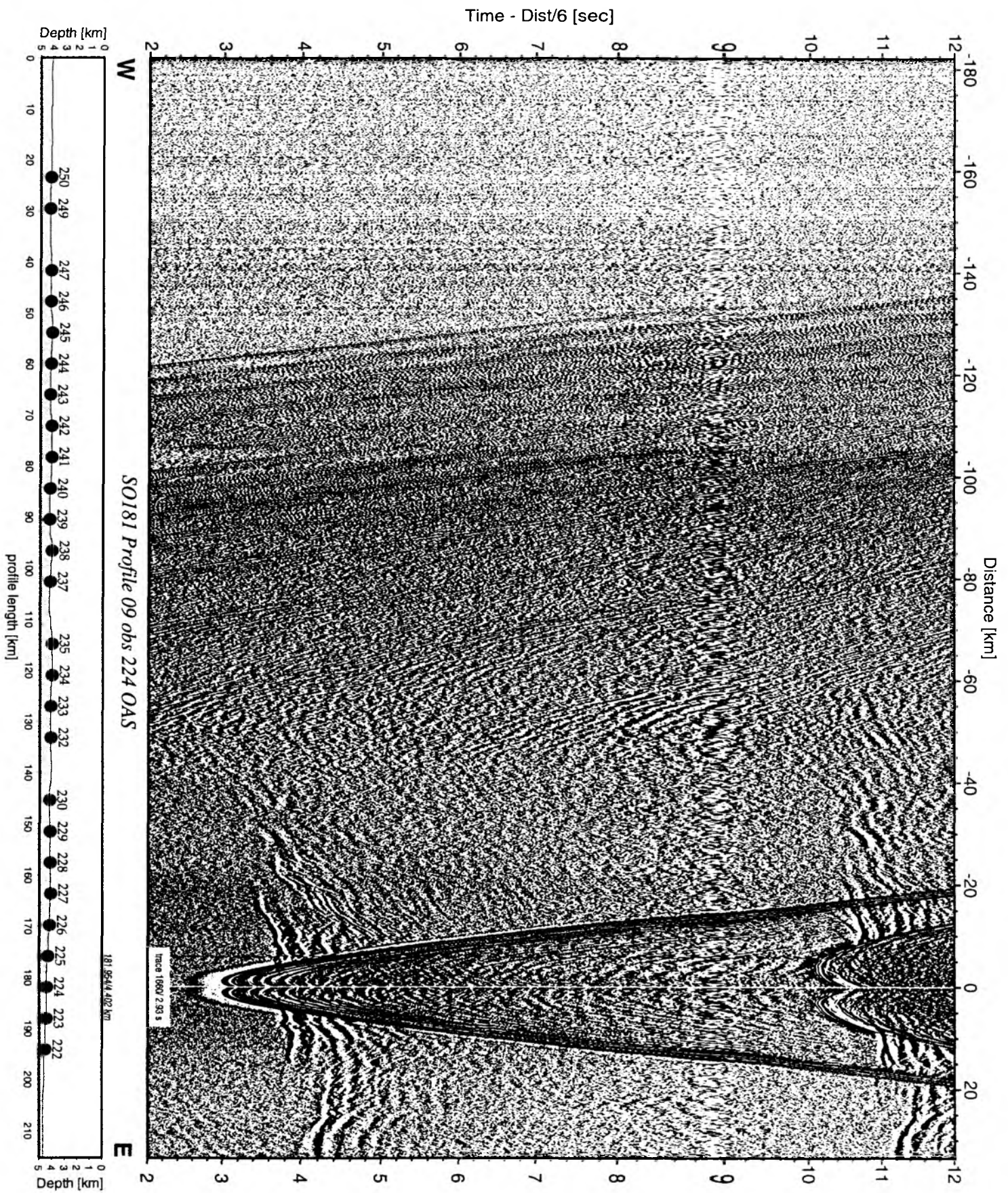


Figure 6.6.7.7: Record section from obs 224 OAS, Profile 09.

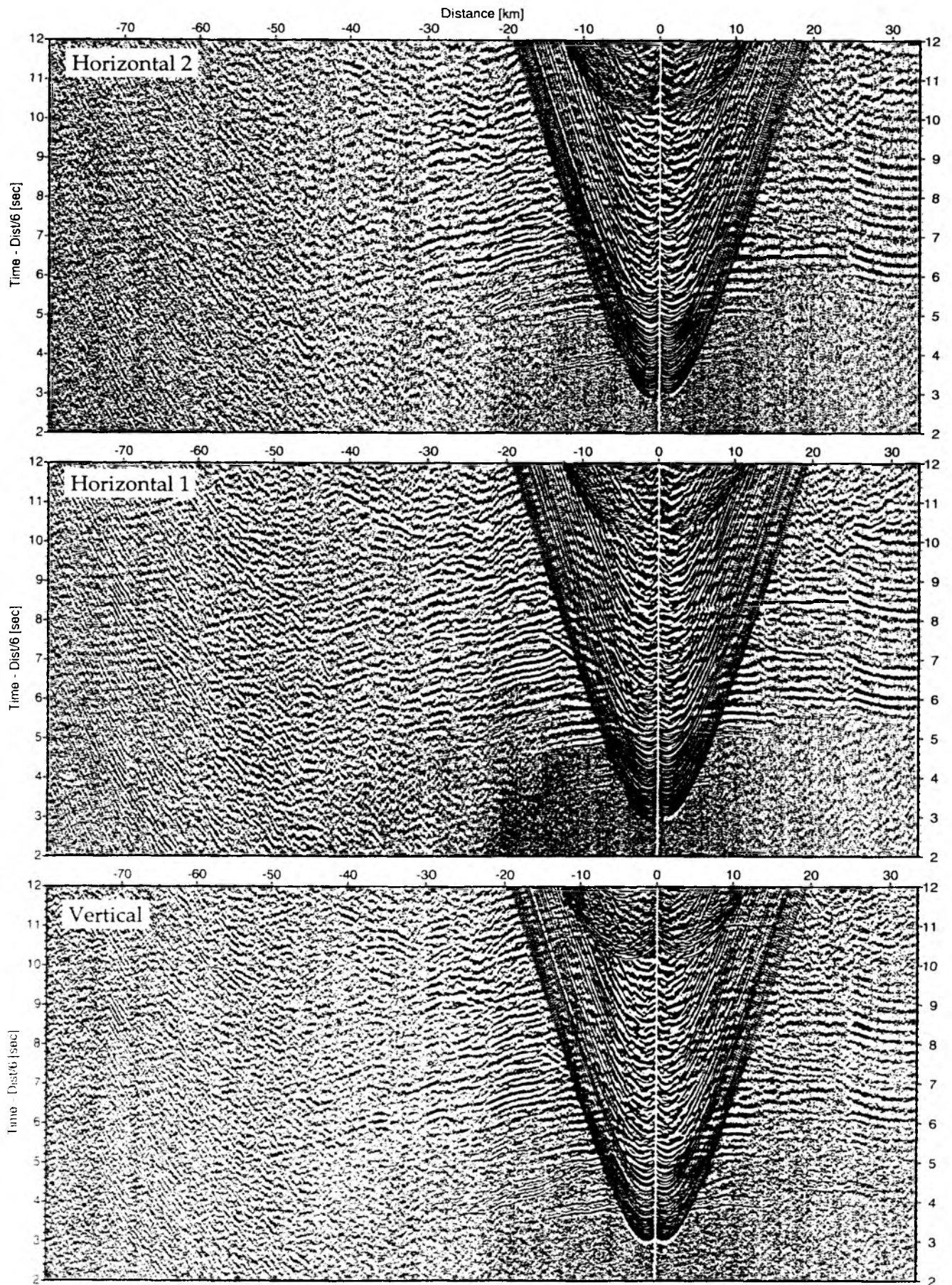


Figure 6.6.7.8: Record sections from obs 224 OAS/Owen, SO181 Profile 09.

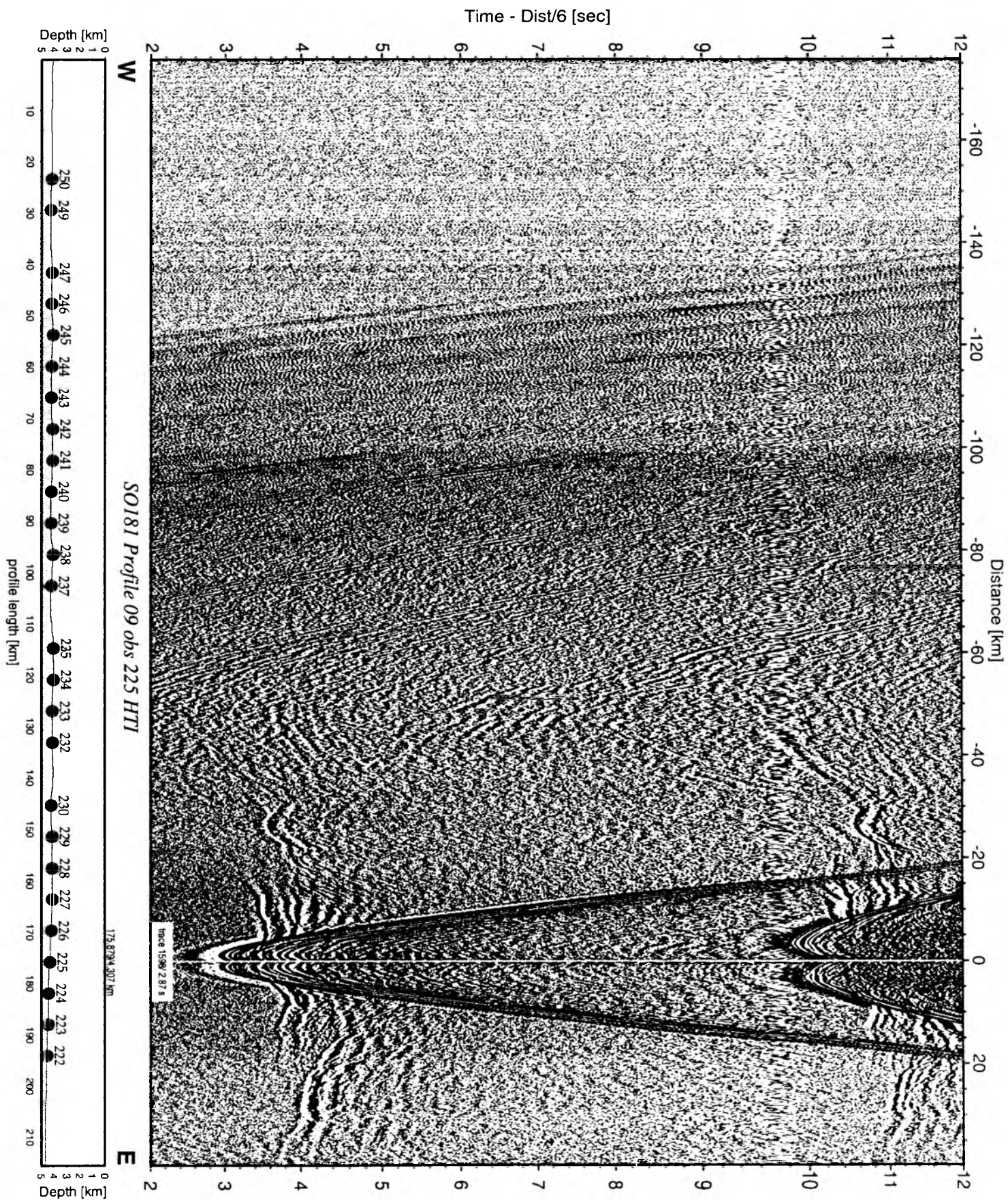


Figure 6.6.7.9: Record section from obs 225 HTI, Profile 09.

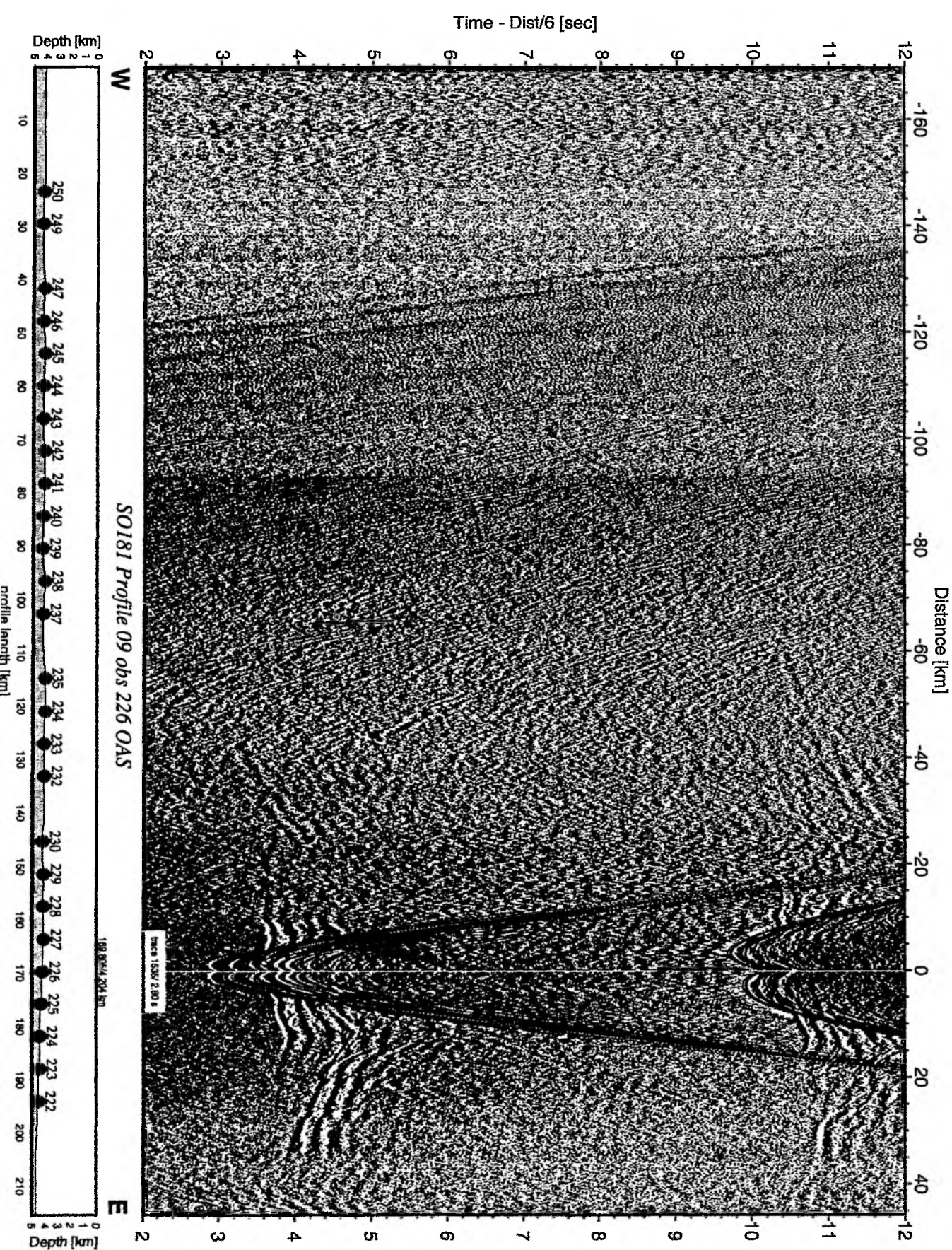


Figure 6.6.7.10: Record section from obs 226 OAS, Profile 09.

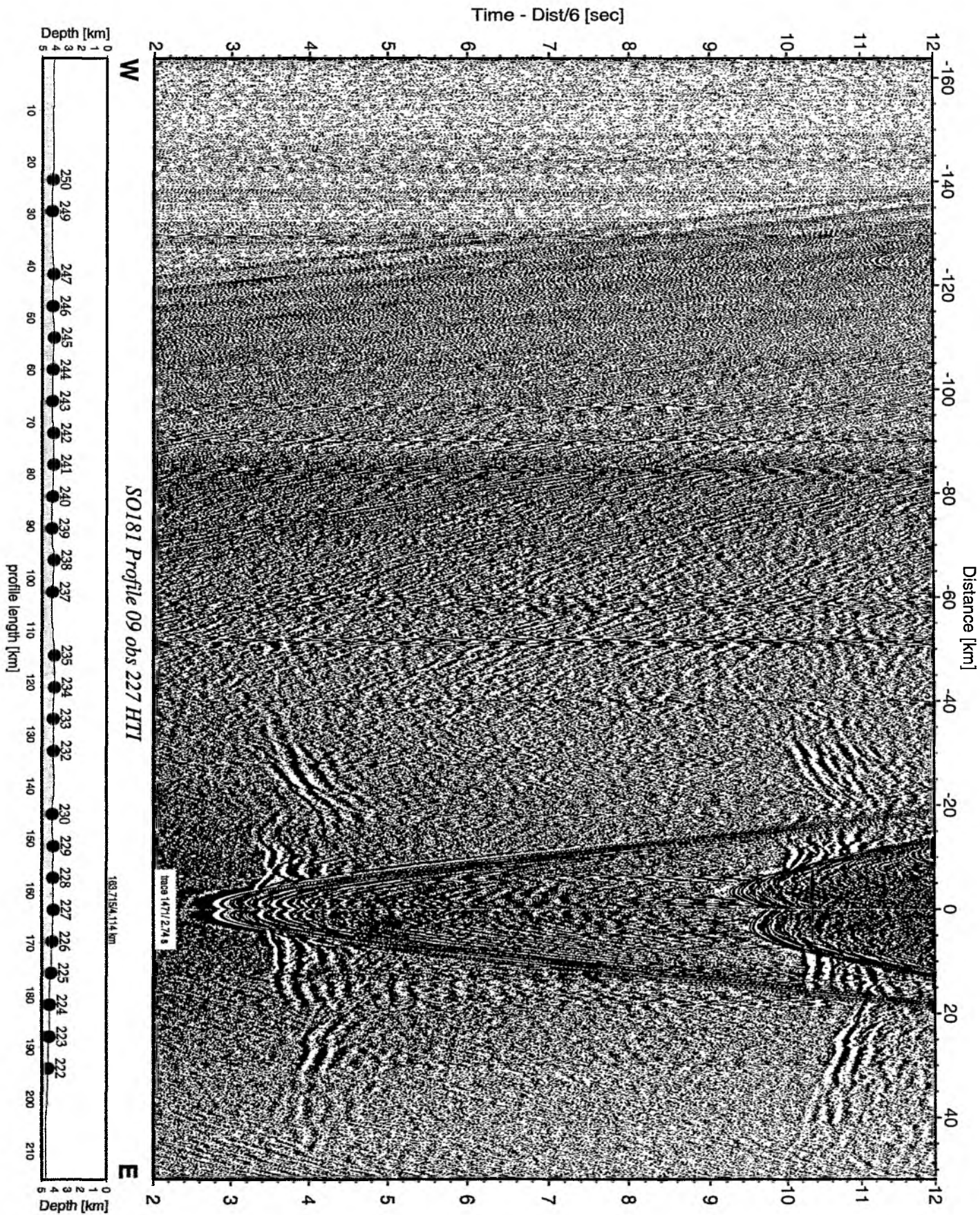


Figure 6.6.7.11: Record section from obs 227 HTI, Profile 09.

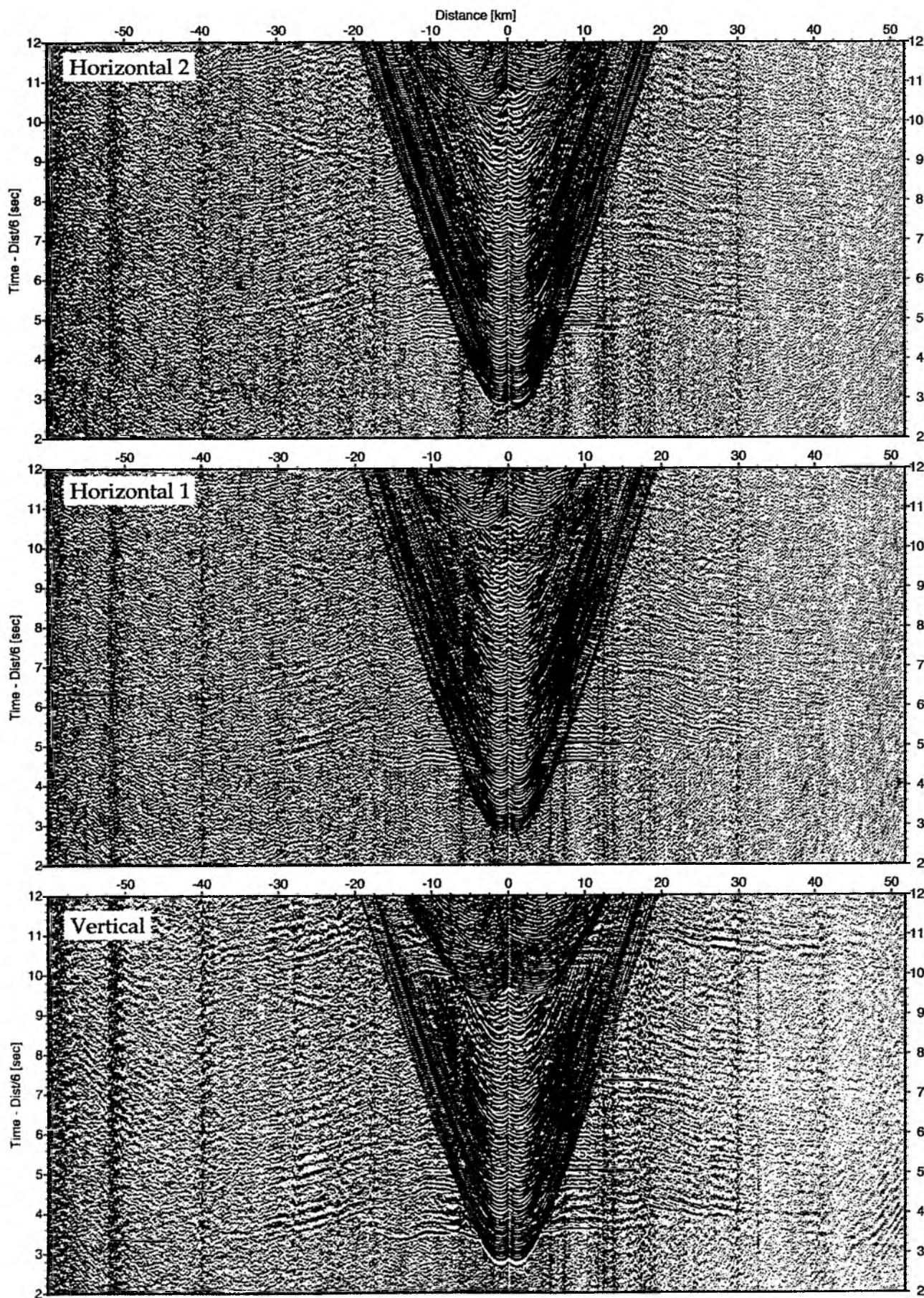


Figure 6.6.7.12: Record sections from obs 227 HTI/Owen-4.5Hz, SO181 Profile 09.

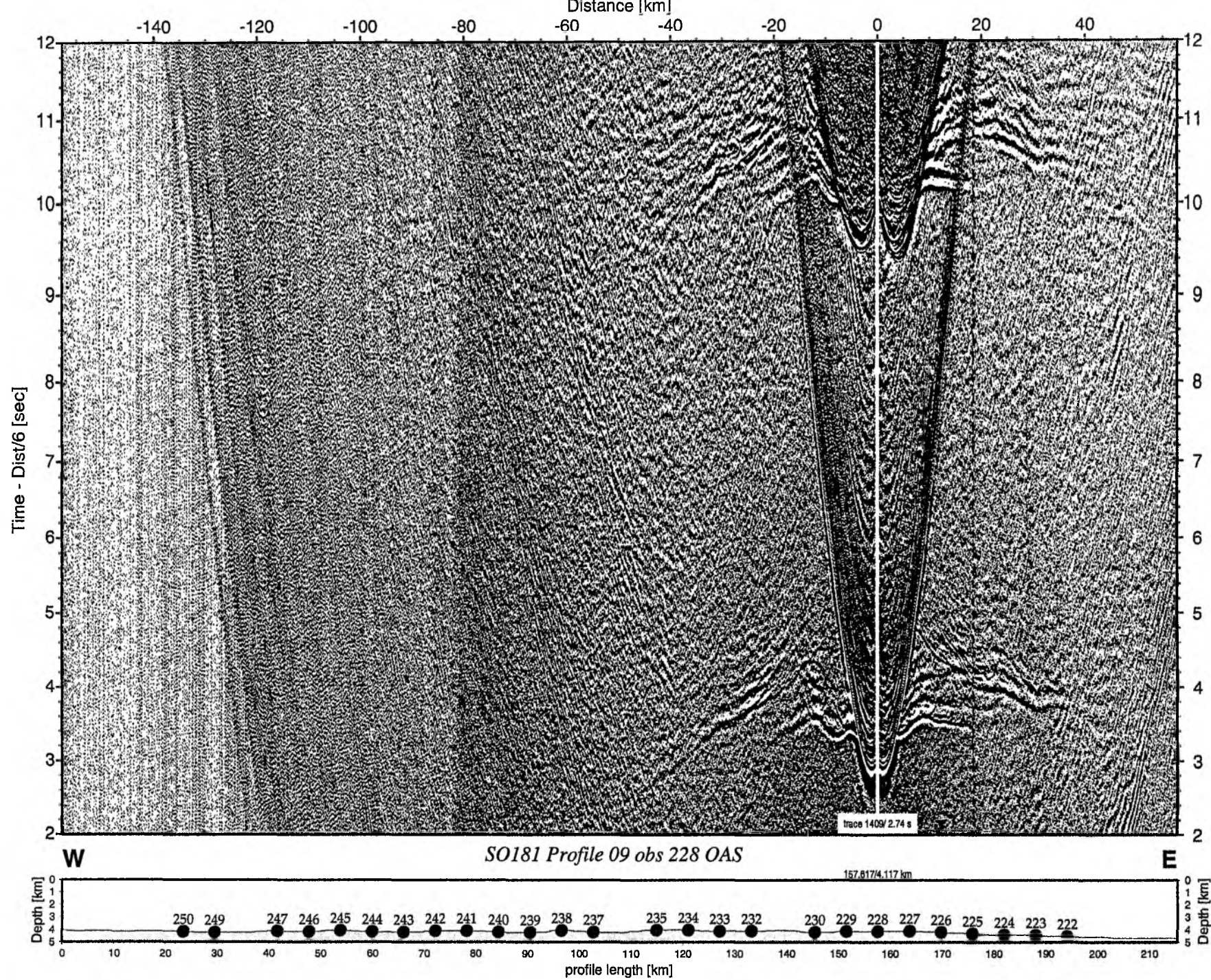


Figure 6.6.7.13: Record section from obs 228 OAS, Profile 09.

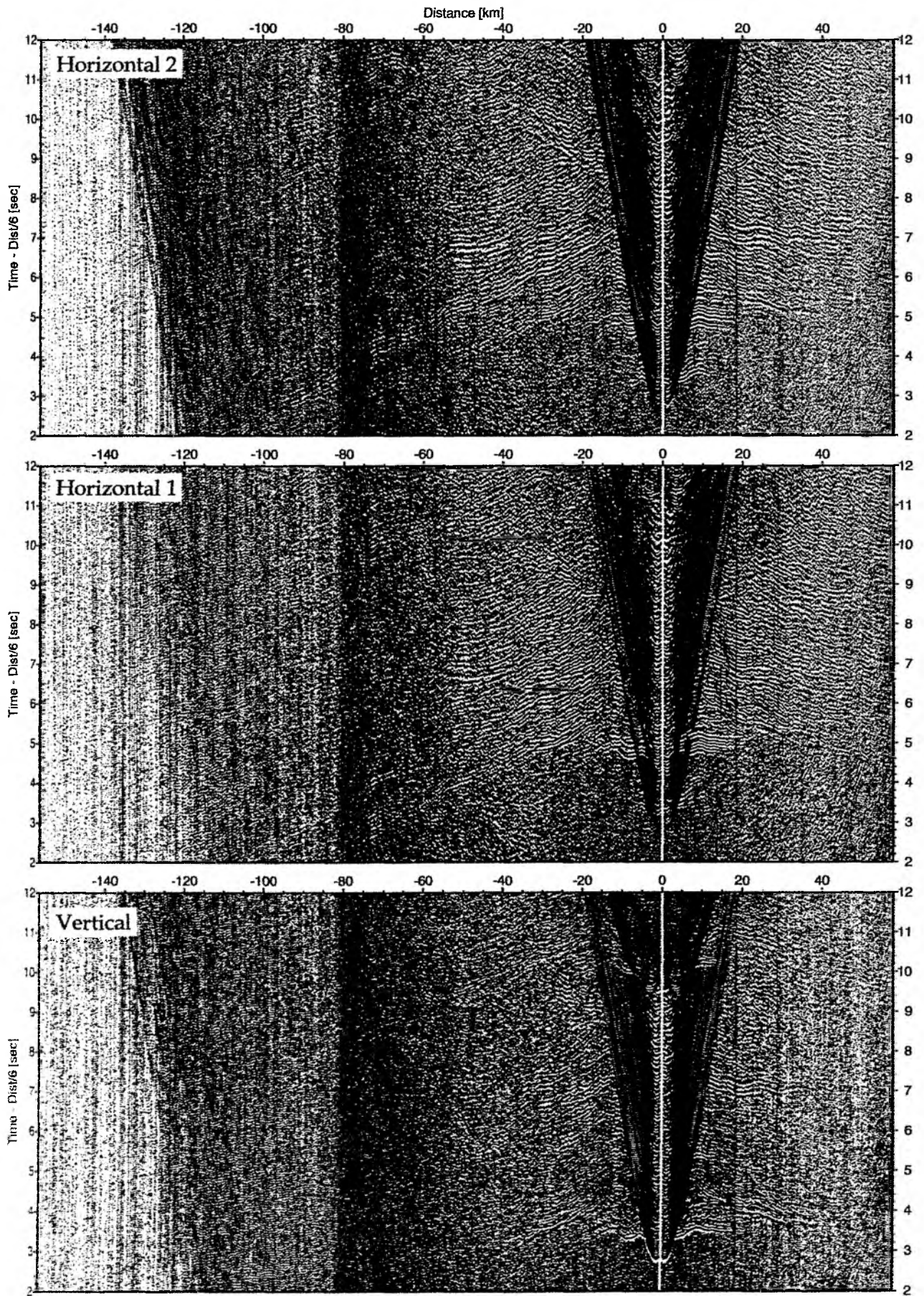


Figure 6.6.7.14: Record sections from obs 228 OAS/Owen-15Hz, SO181 Profile 09.

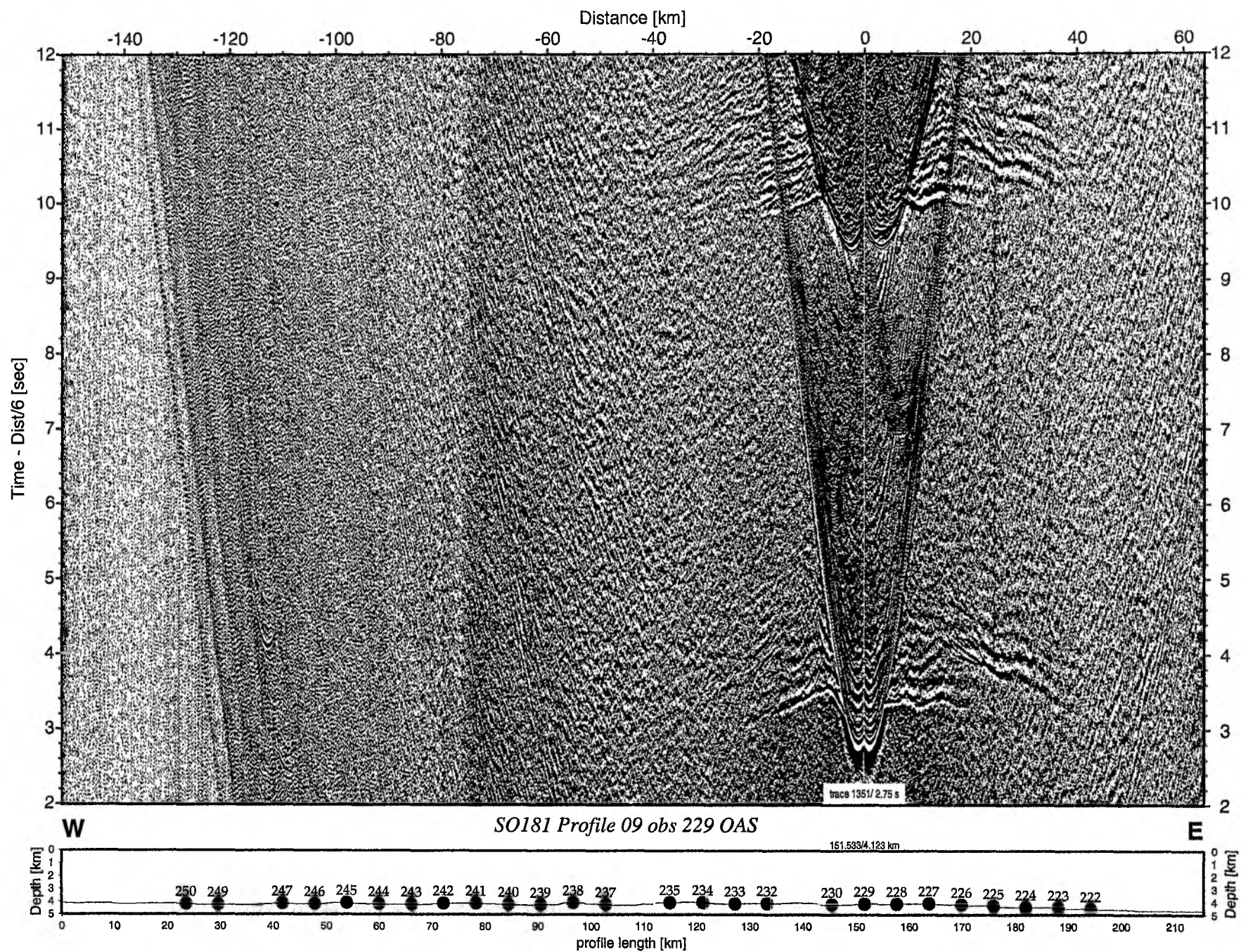


Figure 6.6.7.15: Record section from obs 229 OAS, Profile 09.

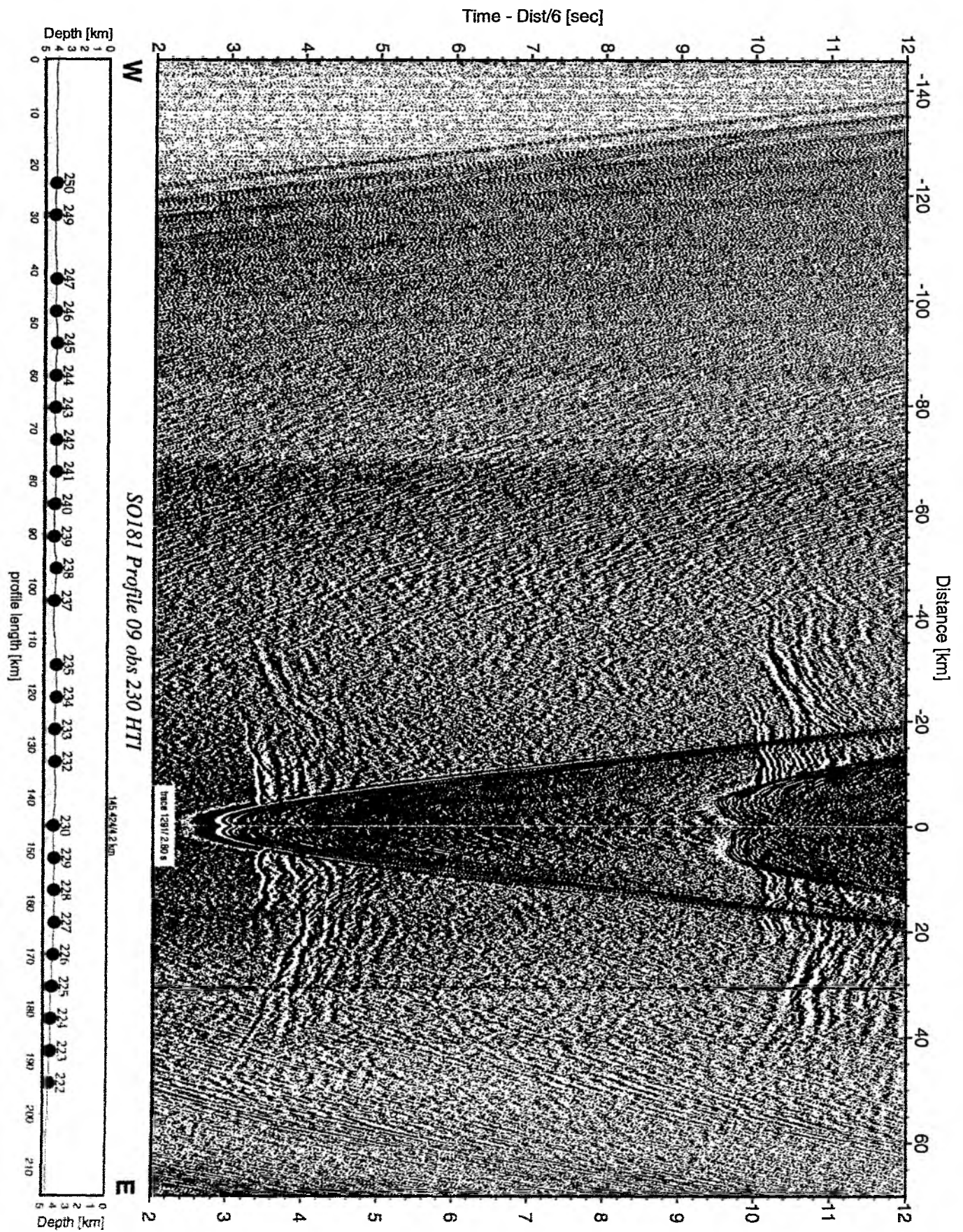


Figure 6.6.7.16: Record section from obs 230 HTI, Profile 09.

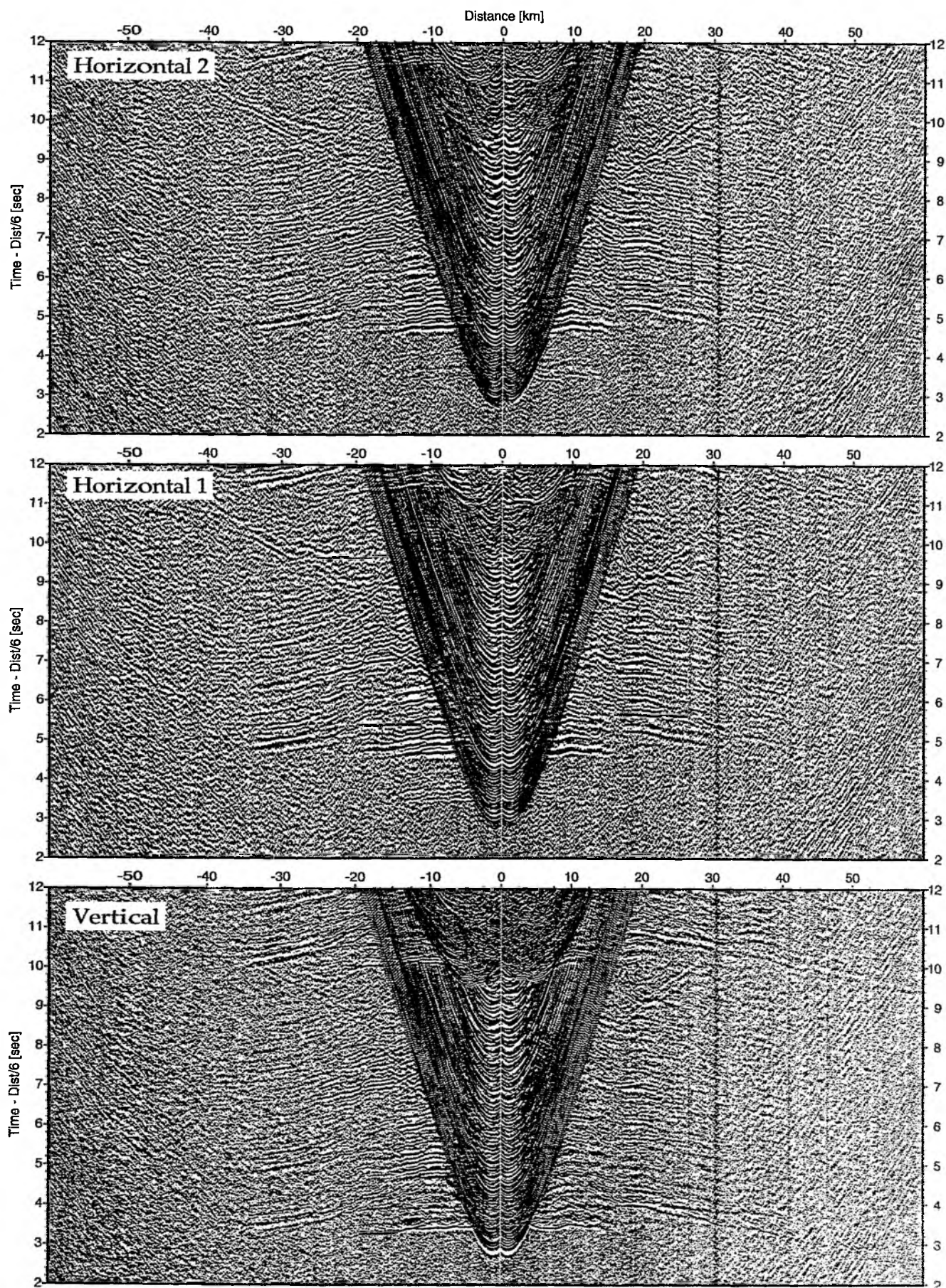


Figure 6.6.7.17: Record sections from obs 230 HTI/Owen-4.5Hz, SO181 Profile 09.

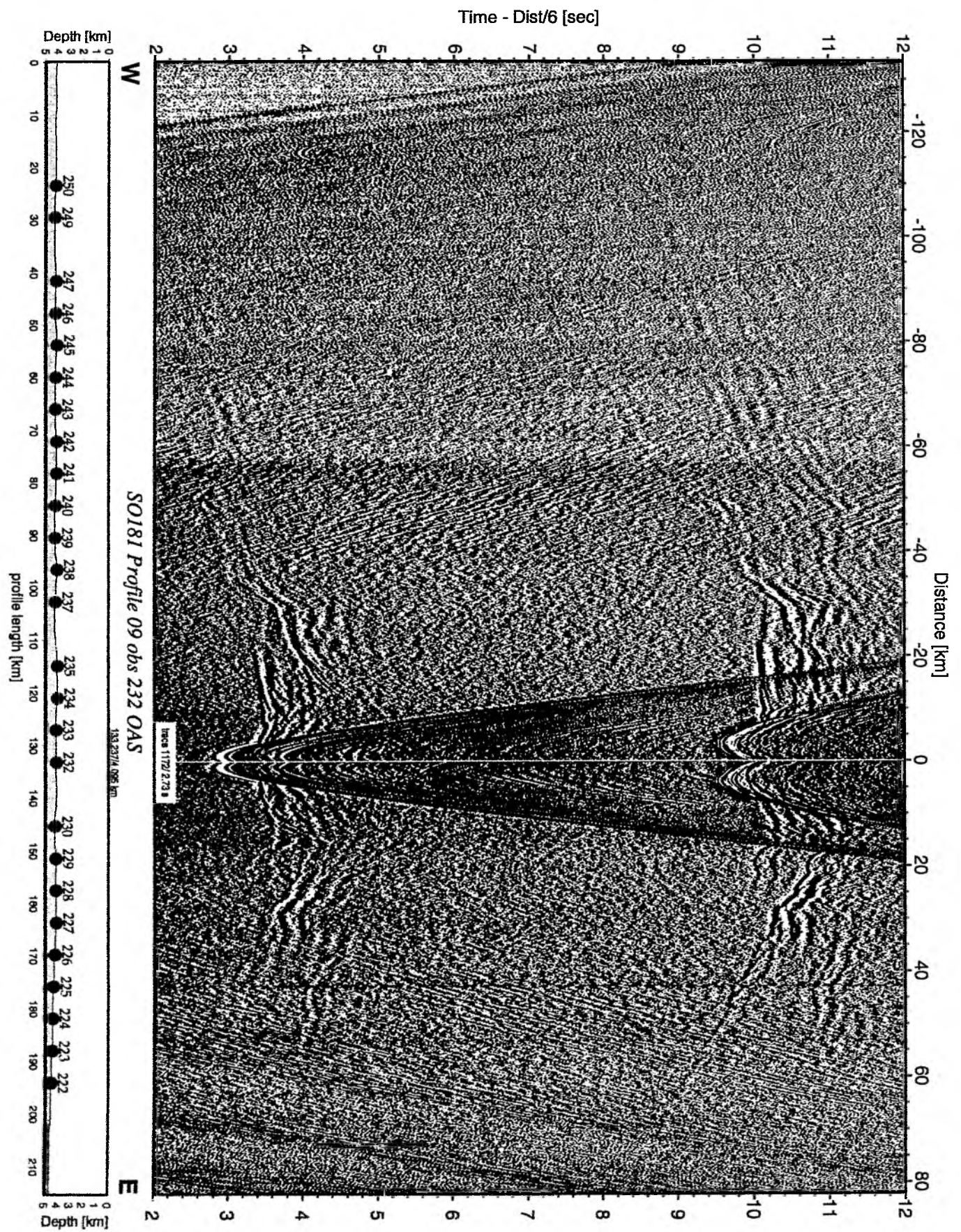


Figure 6.6.7.18: Record section from obs 232 OAS, Profile 09.

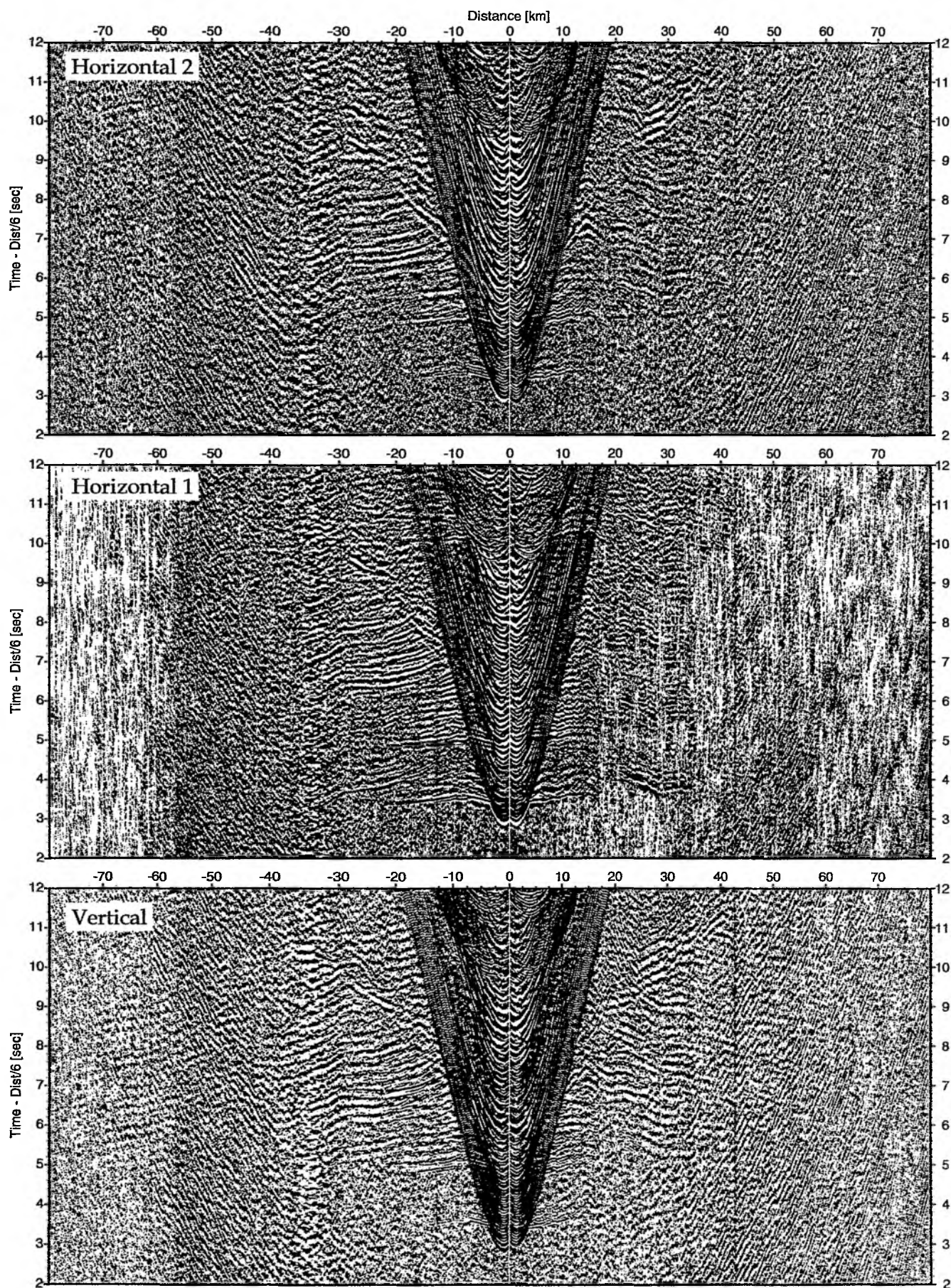


Figure 6.6.7.19: Record sections from obs 232 OAS/Owen-4.5Hz, SO181 Profile 09.

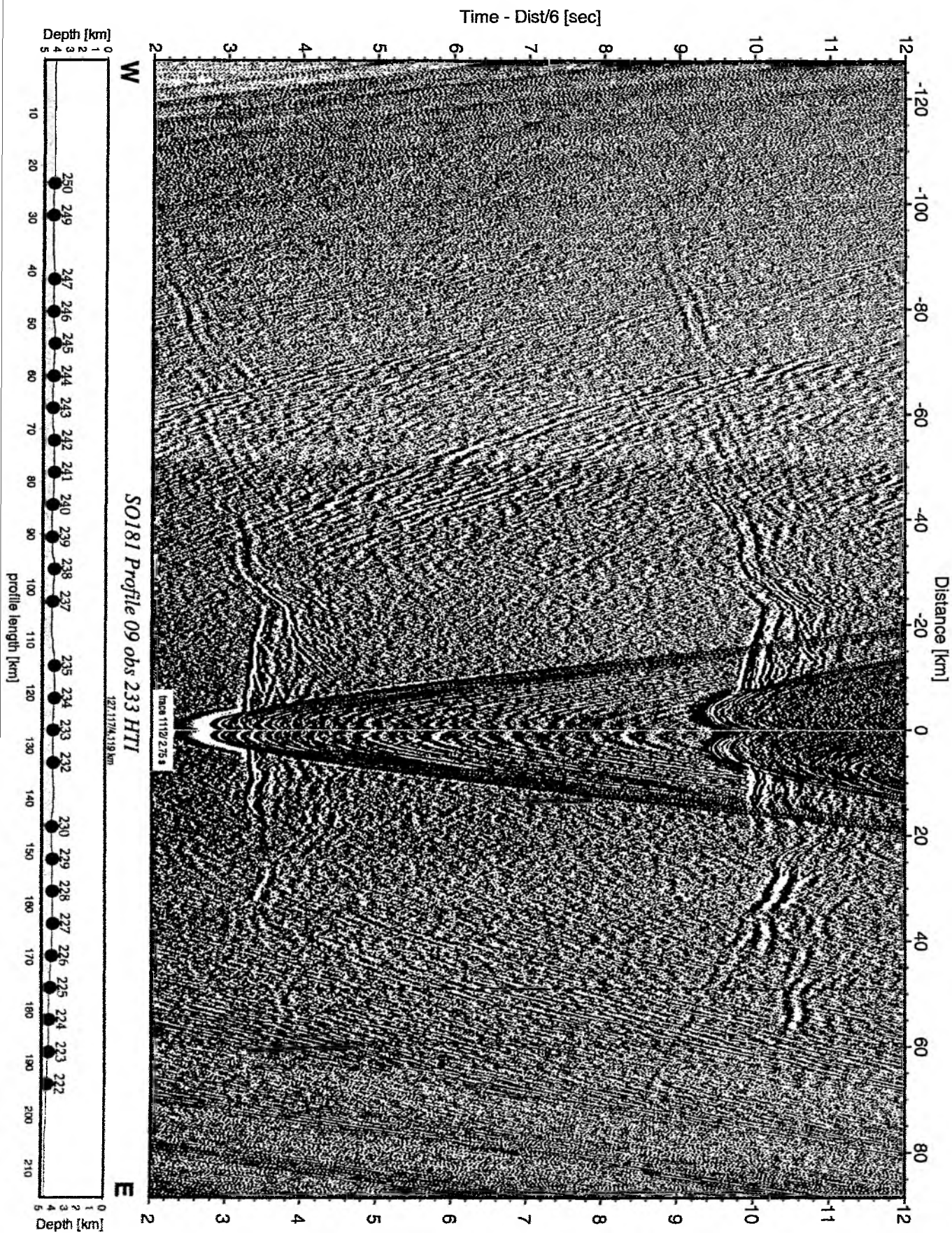


Figure 6.6.7.20: Record section from obs 233 HTI, Profile 09.

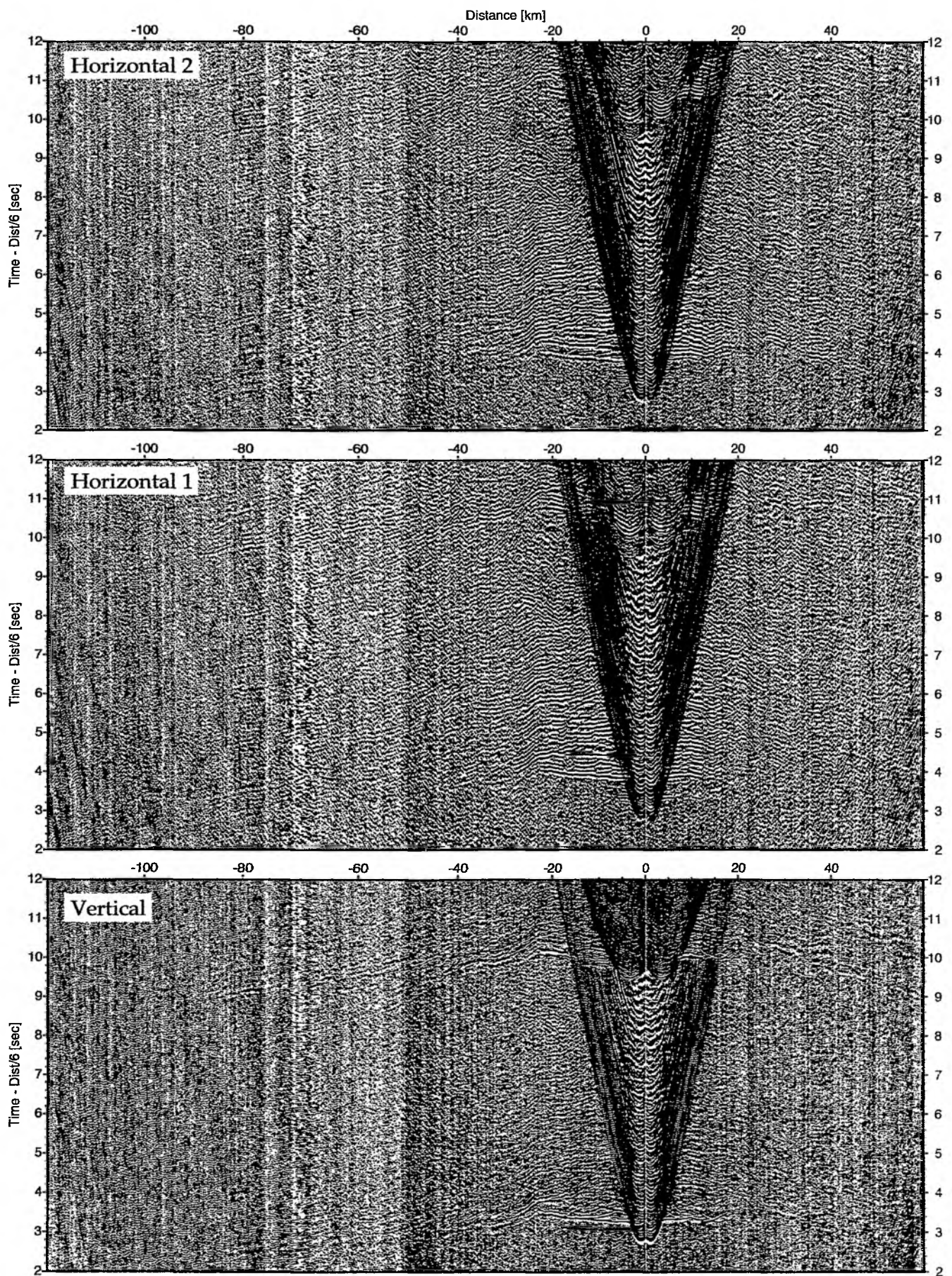


Figure 6.6.7.21: Record sections from obs 233 HTI/Owen-15Hz, SO181 Profile 09.

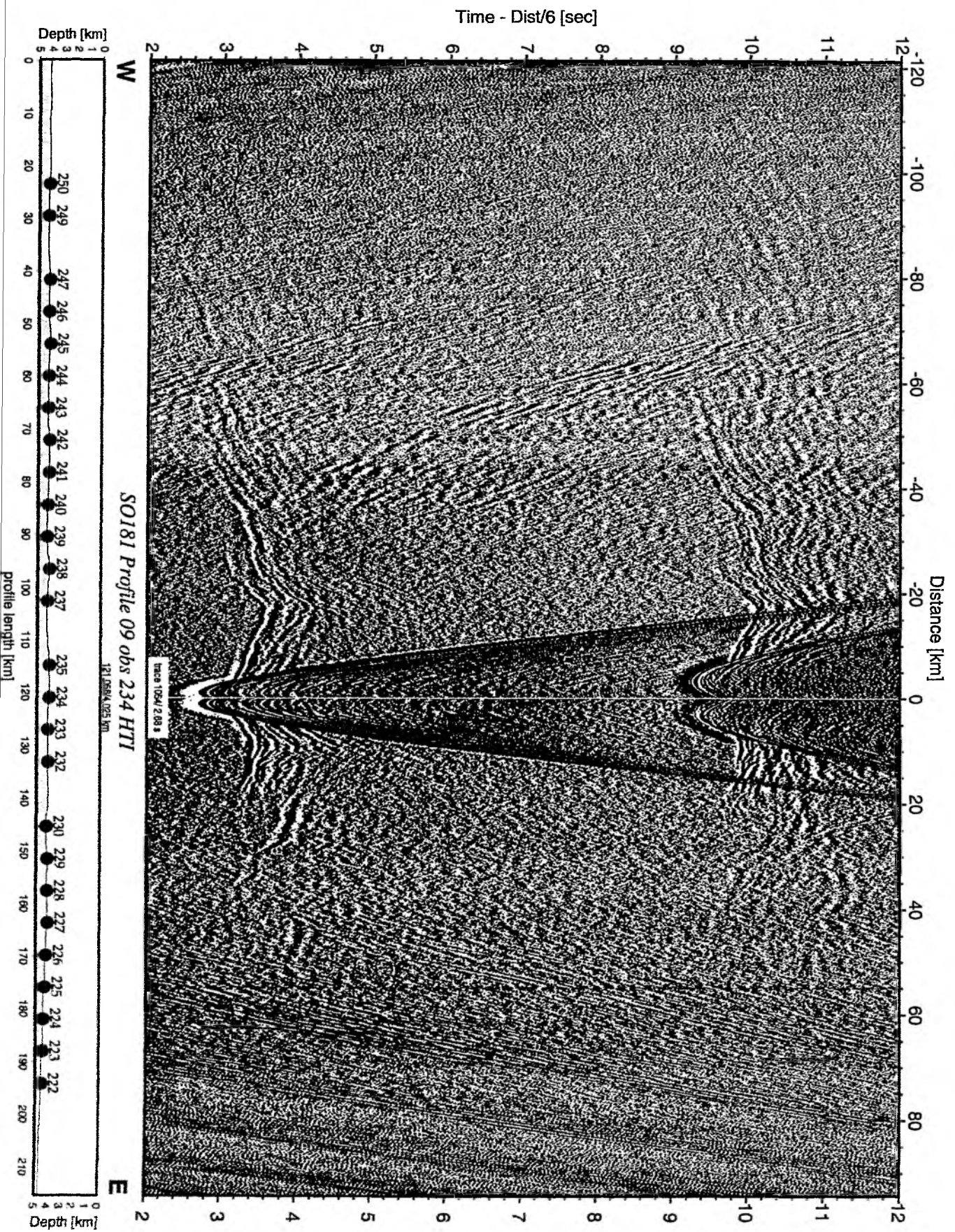


Figure 6.6.7.22: Record section from obs 234 HTI, Profile 09.

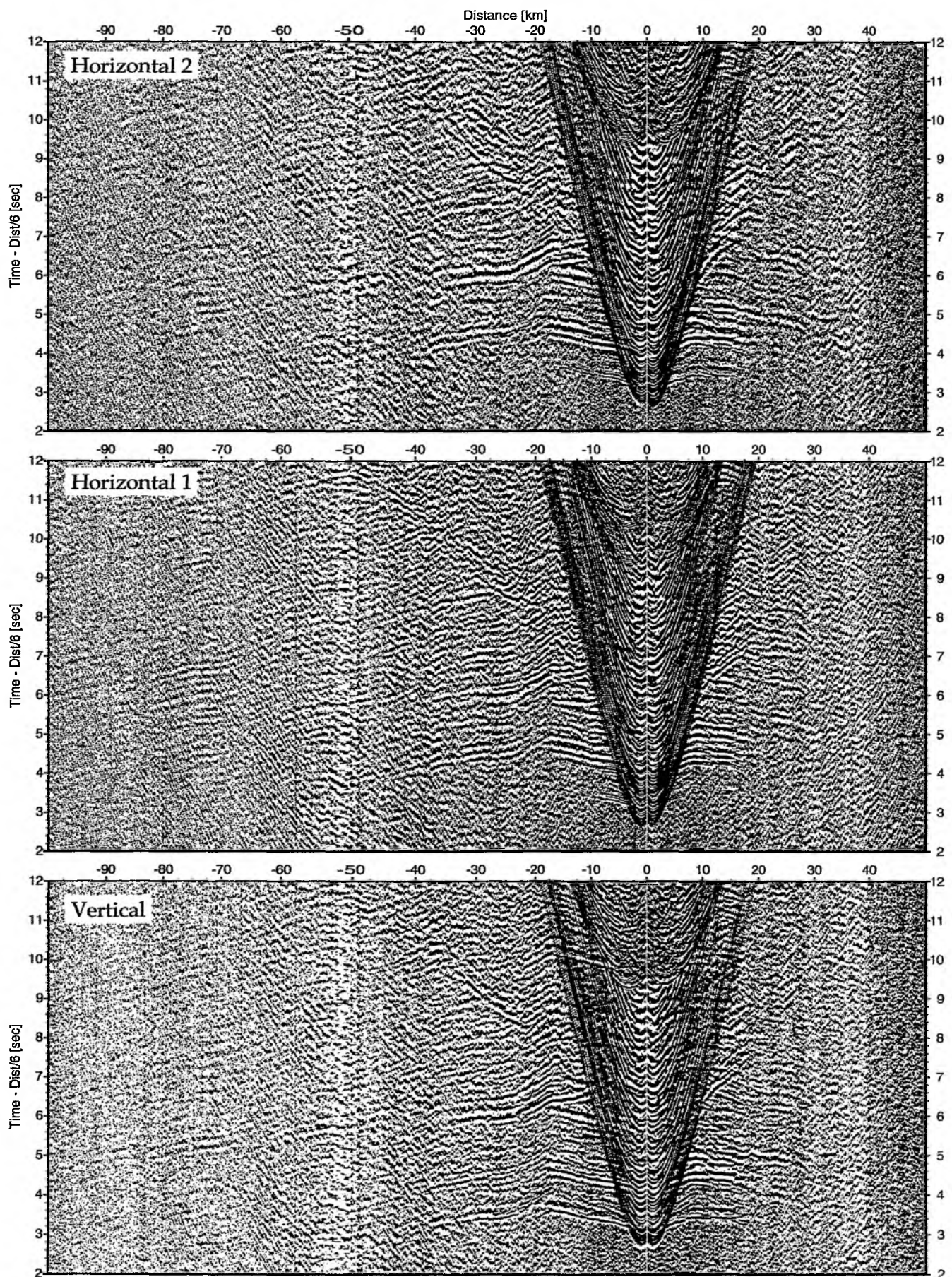


Figure 6.6.7.23: Record sections from obs 234 HTI/Owen-4.5Hz, SO181 Profile 09.

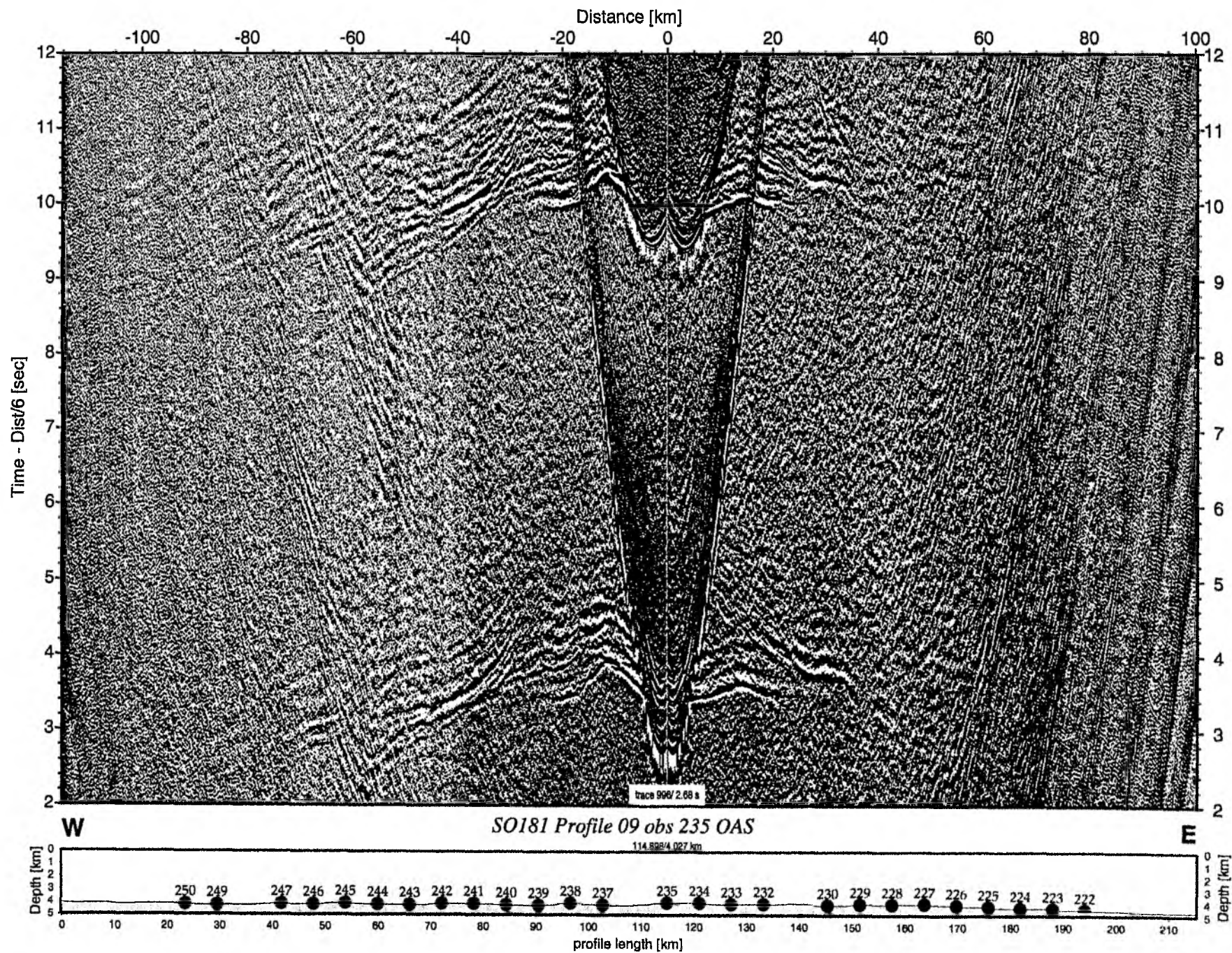


Figure 6.6.7.24: Record section from obs 235 OAS, Profile 09.

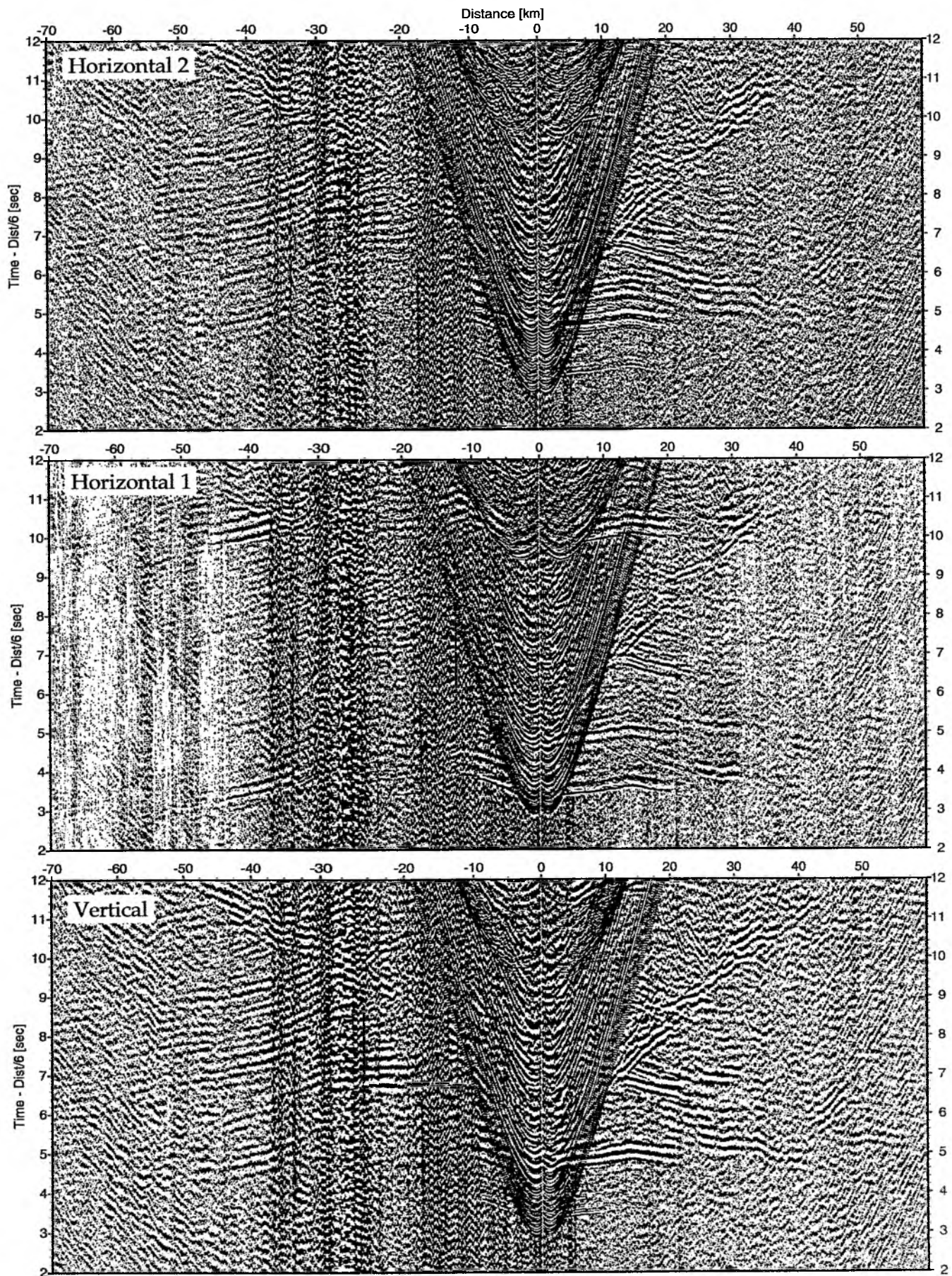


Figure 6.6.7.25: Record sections from obs 235 OAS/Owen-4.5Hz, SO181 Profile 09.

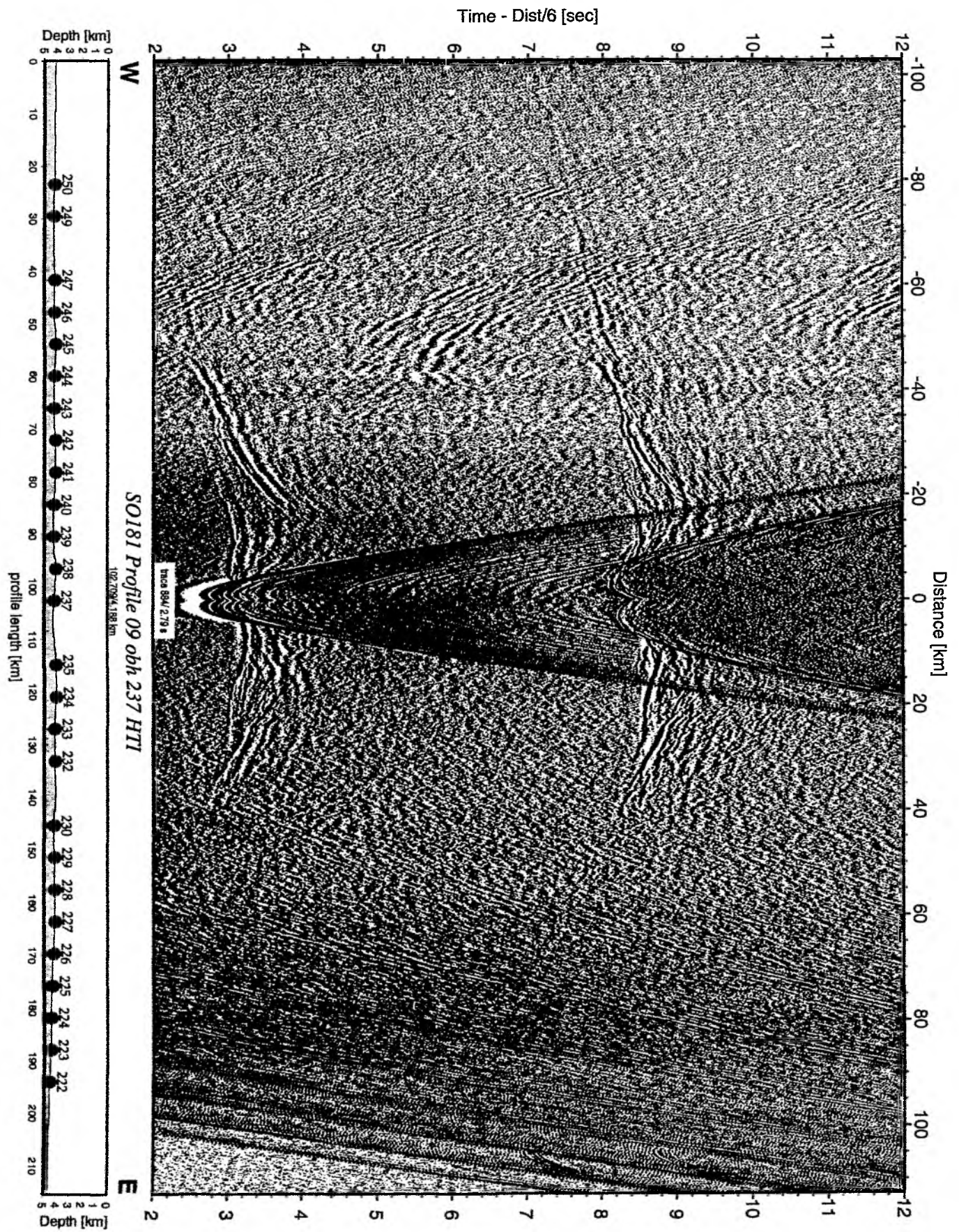


Figure 6.6.7.26: Record section from obh 237 HTI, Profile 09.

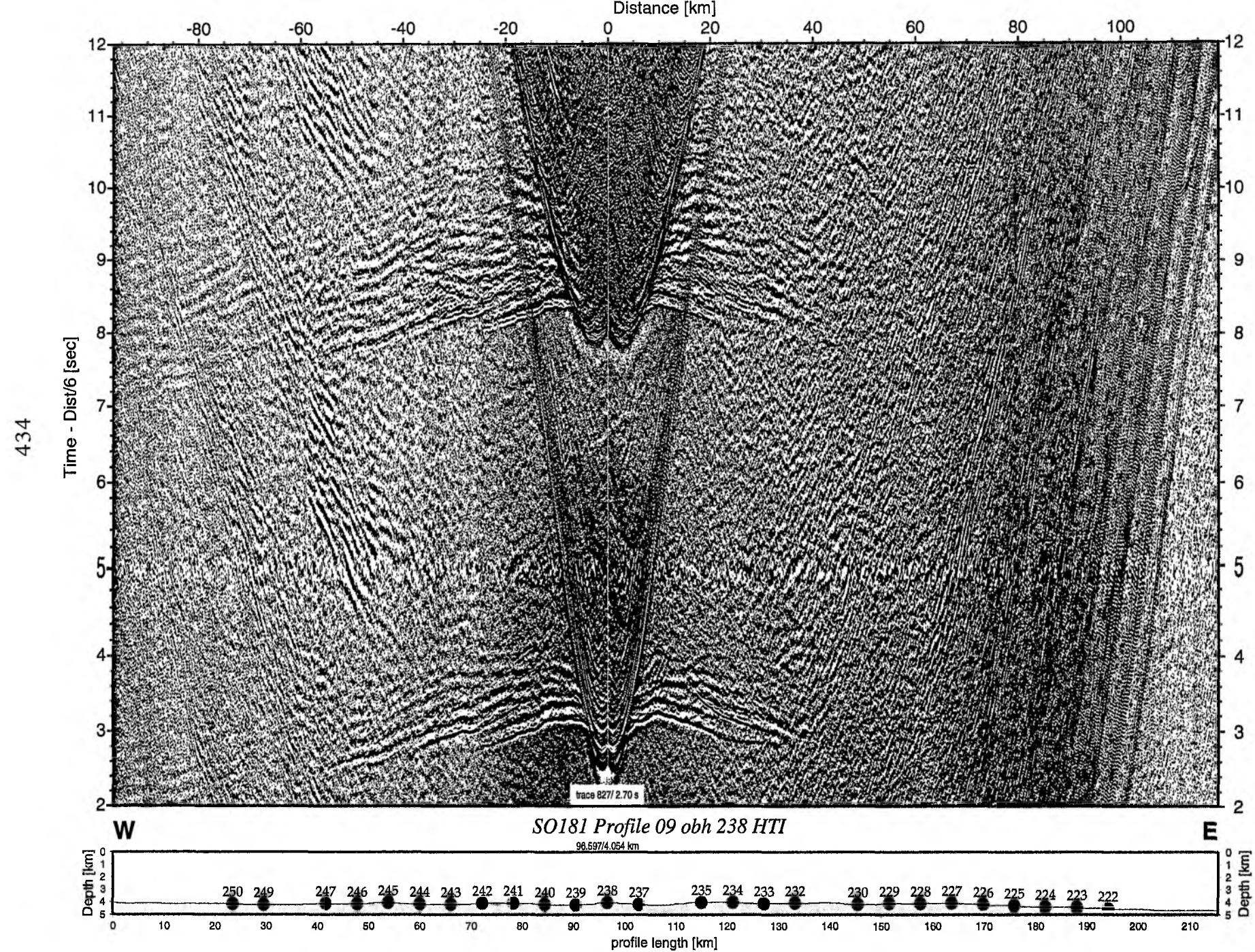


Figure 6.6.7.27: Record section from obh 238 HTI, Profile 09.

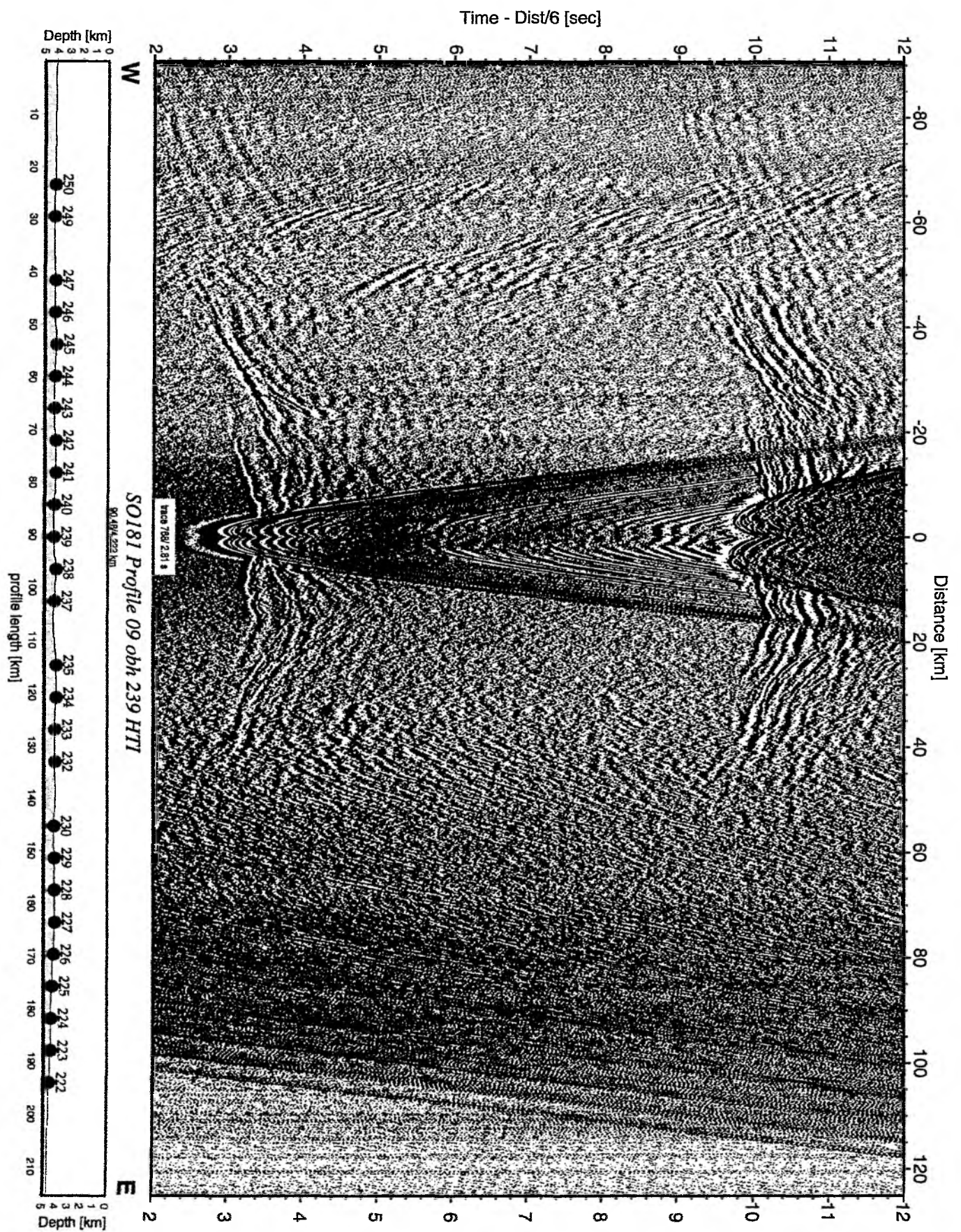


Figure 6.6.7.28: Record section from obh 239 HTI, Profile 09.

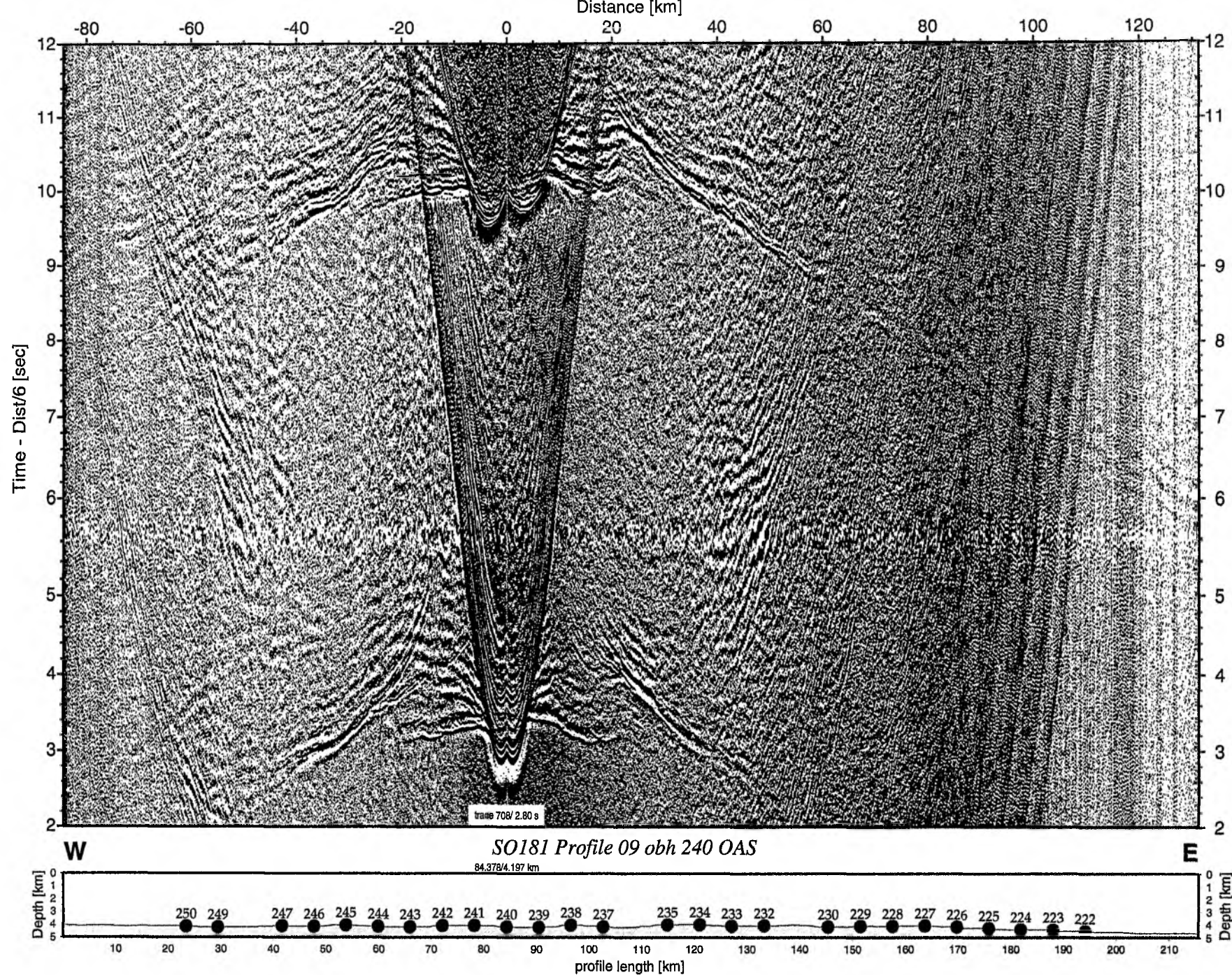


Figure 6.6.7.29: Record section from obh 240 OAS, Profile 09.

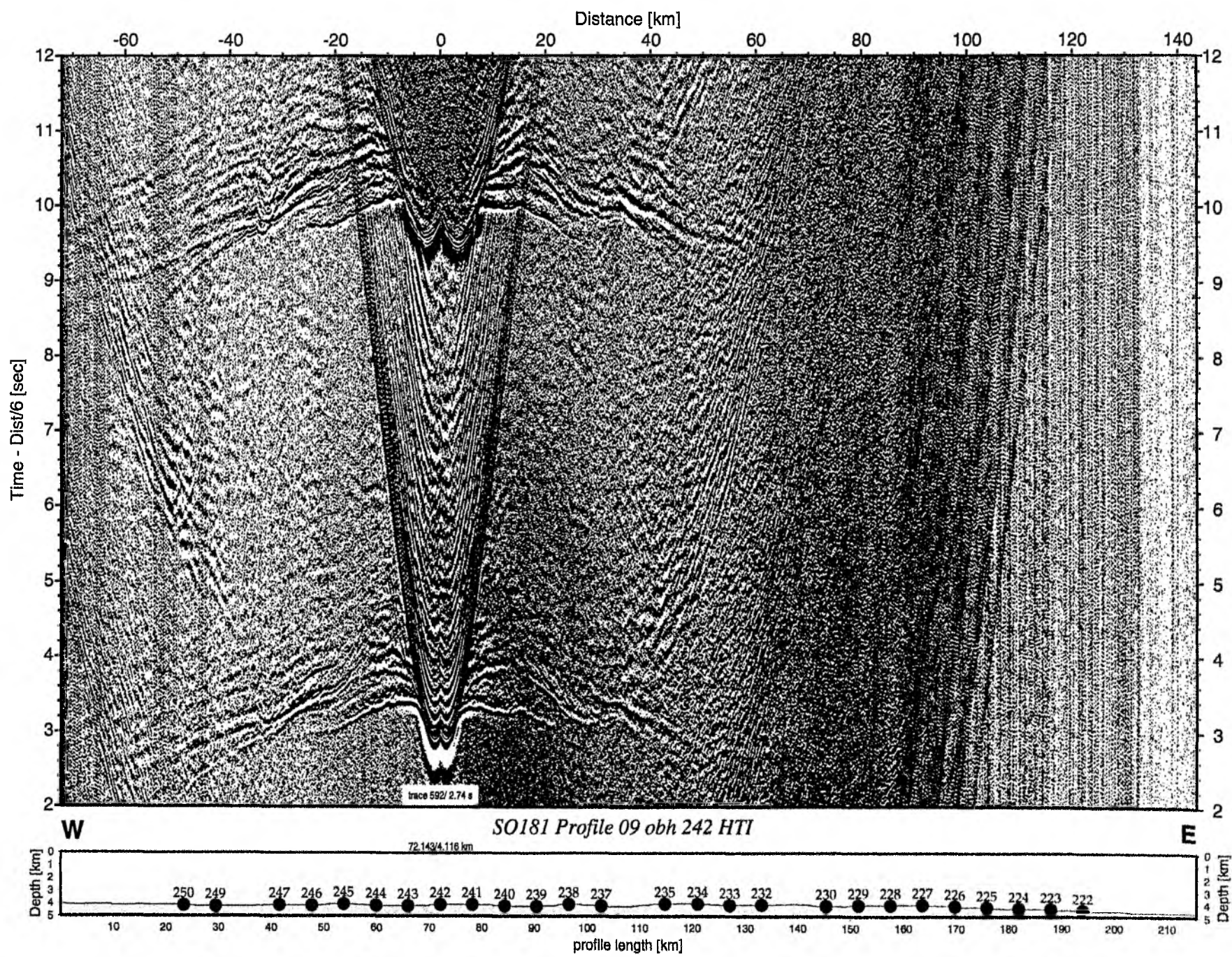


Figure 6.6.7.30: Record section from obh 242 HTI, Profile 09.

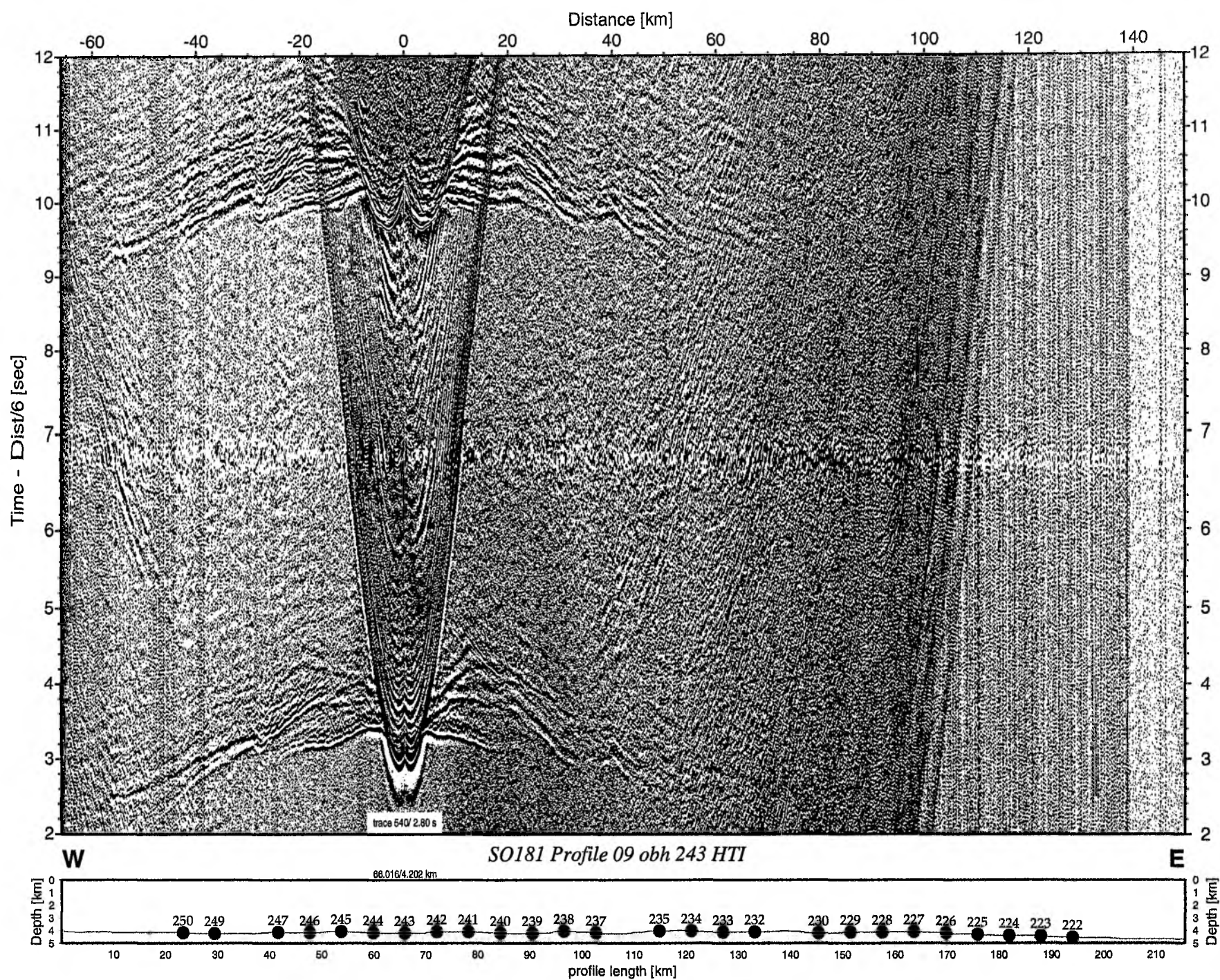


Figure 6.6.7.31: Record section from obh 243 HTI, Profile 09.

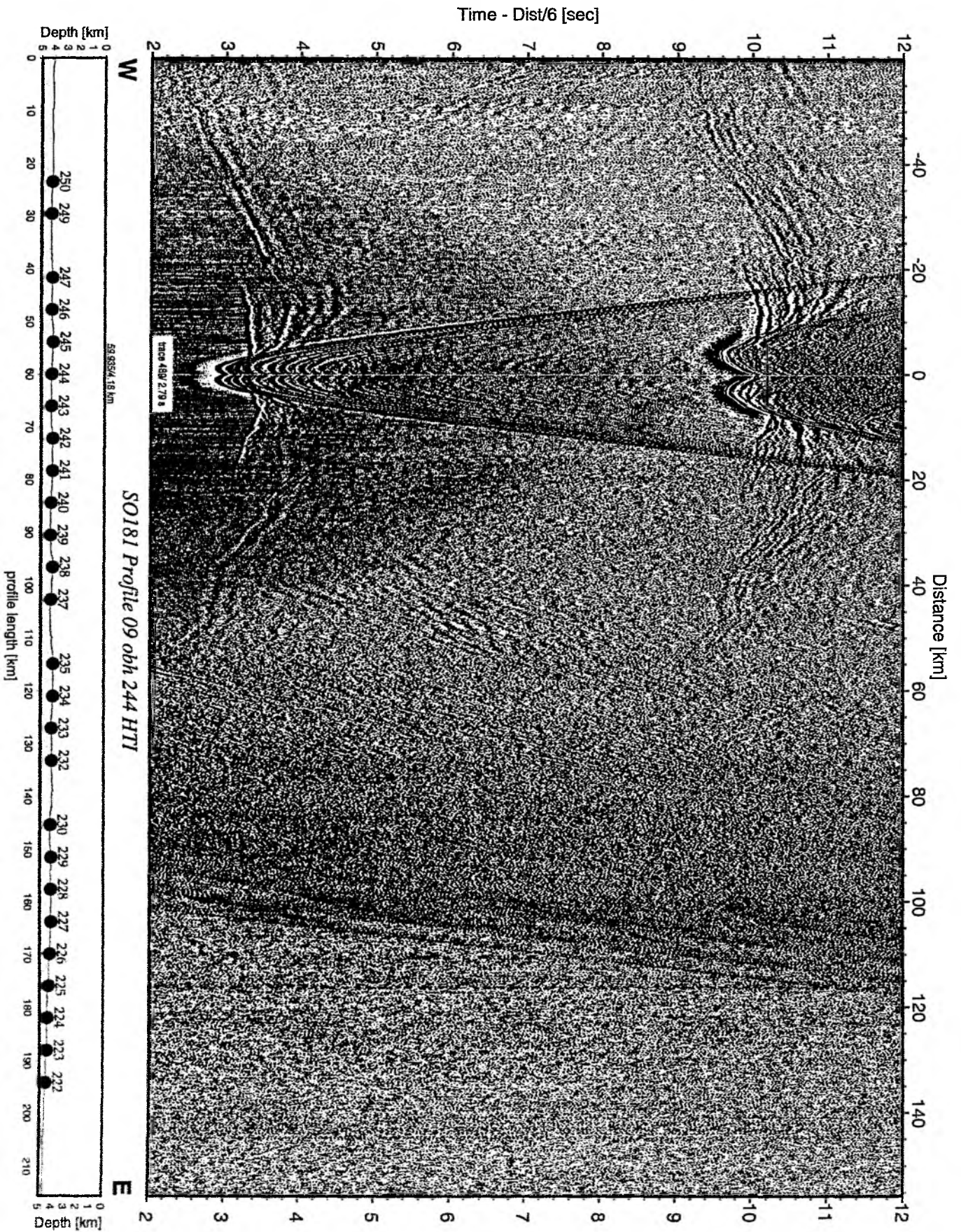


Figure 6.6.7.32: Record section from obh 244 HTI, Profile 09.

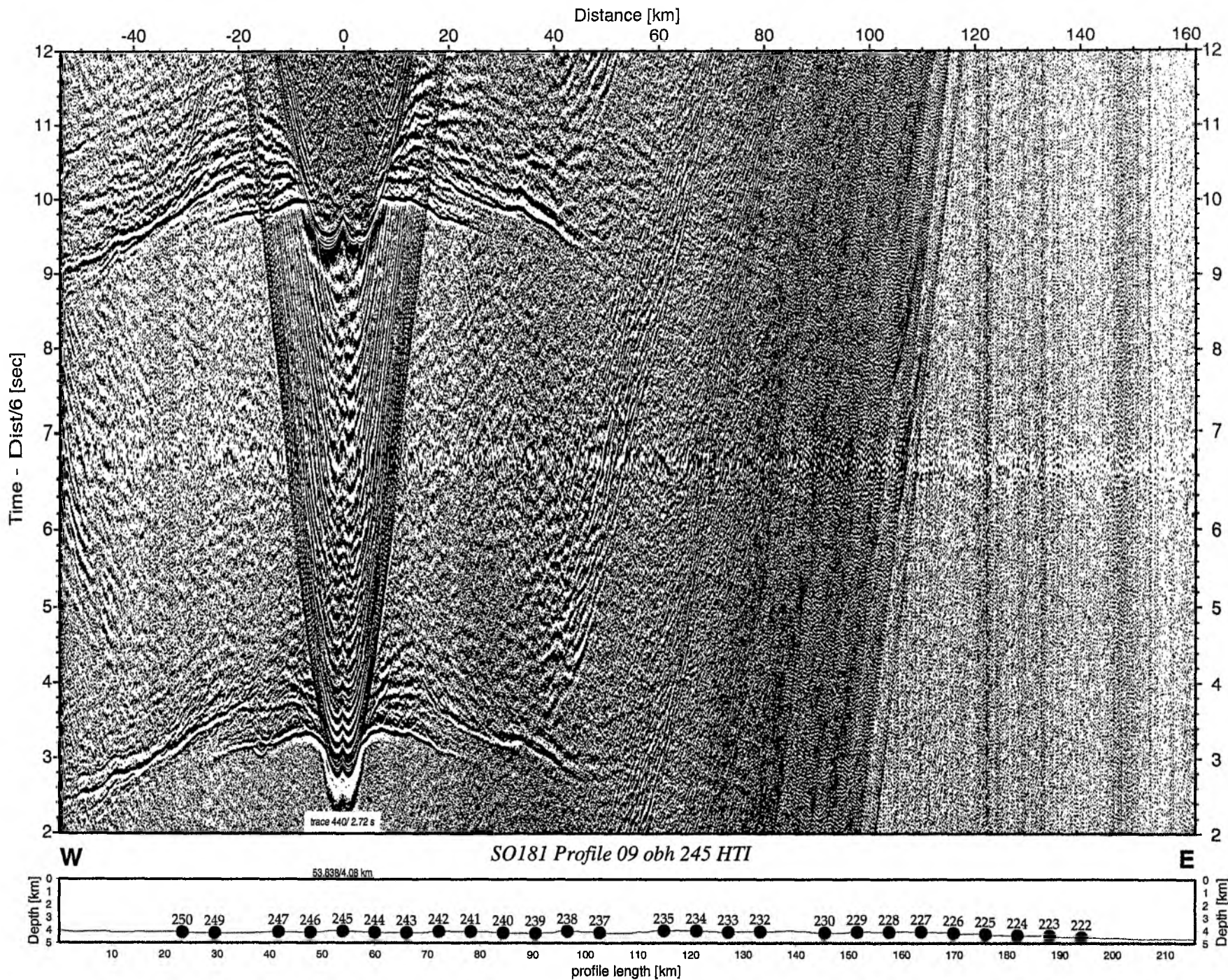


Figure 6.6.7.33: Record section from obh 245 HTI, Profile 09.

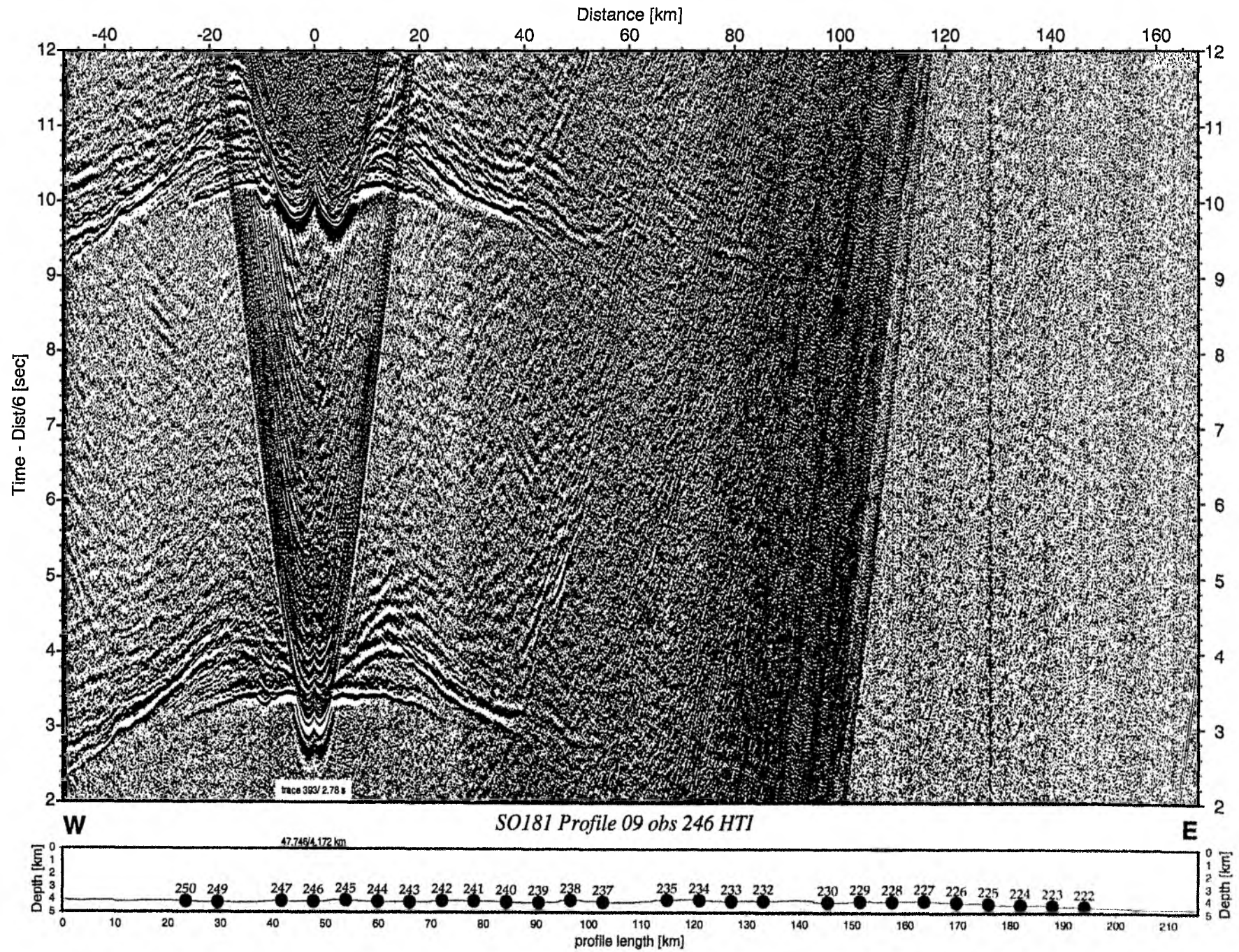


Figure 6.6.7.34: Record section from obs 246 HTI, Profile 09.

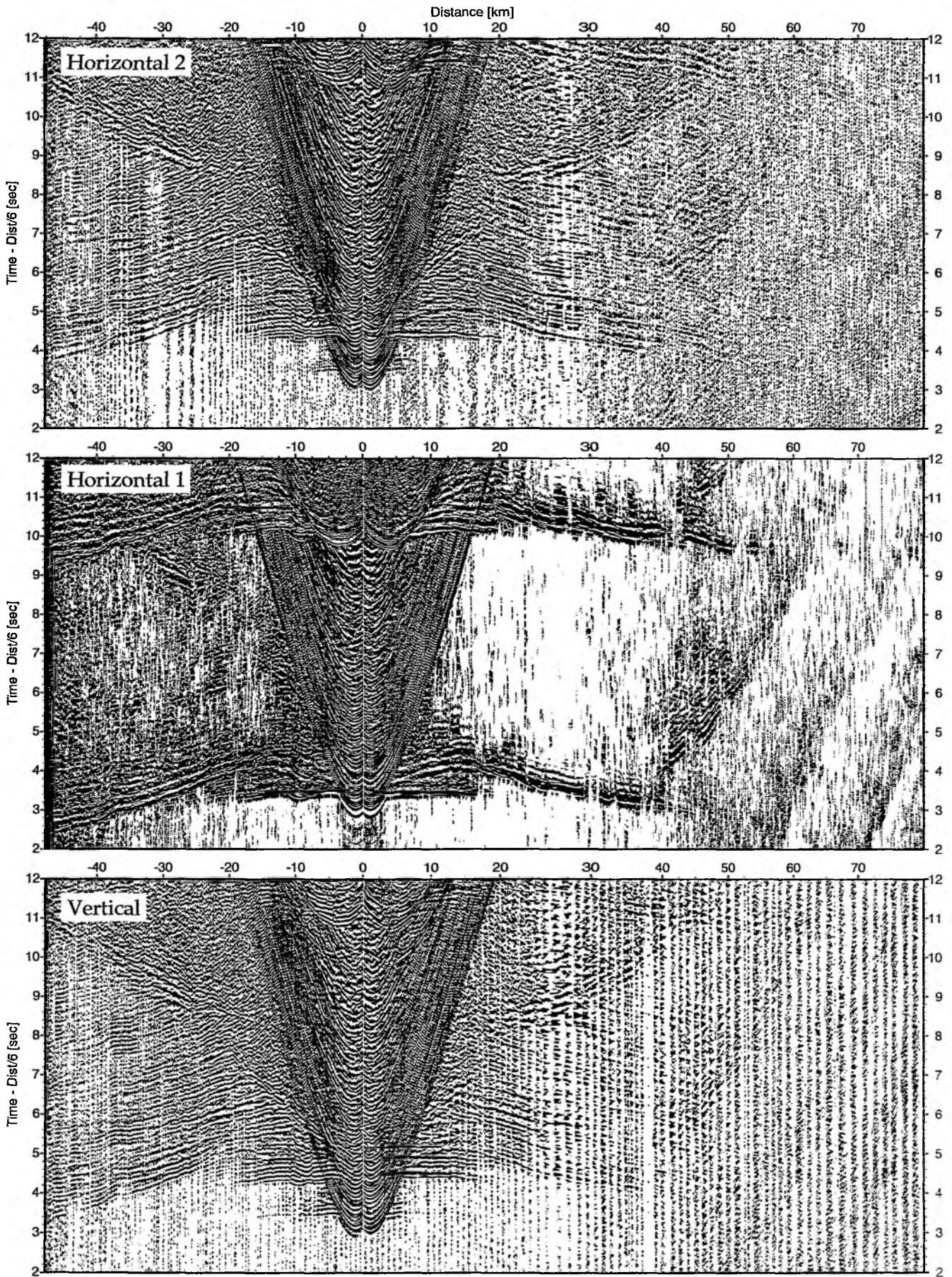


Figure 6.6.7.35: Record sections from obs 246 HTI/Owen-4.5Hz, SO181 Profile 09.

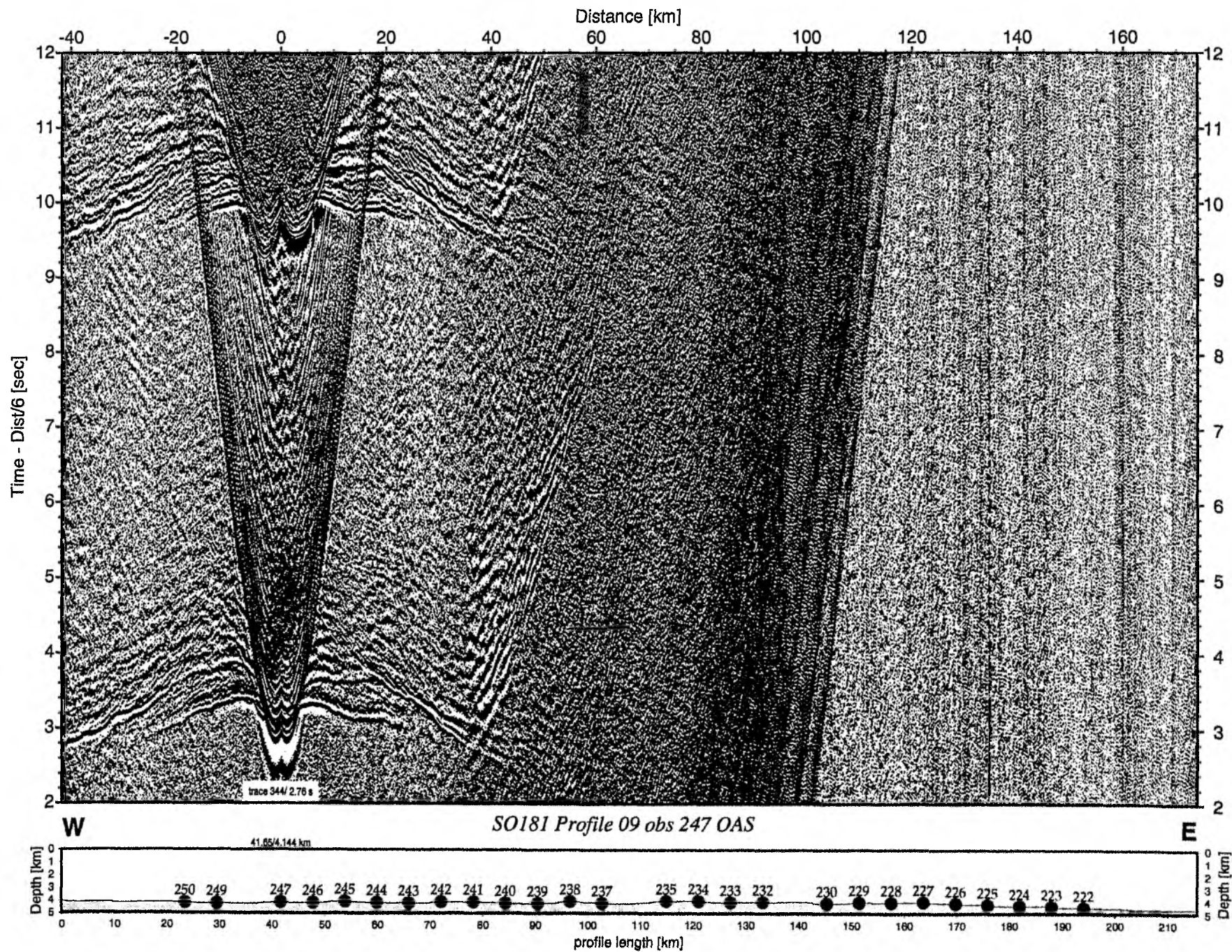


Figure 6.6.7.36: Record section from obs 247 OAS, Profile 09.

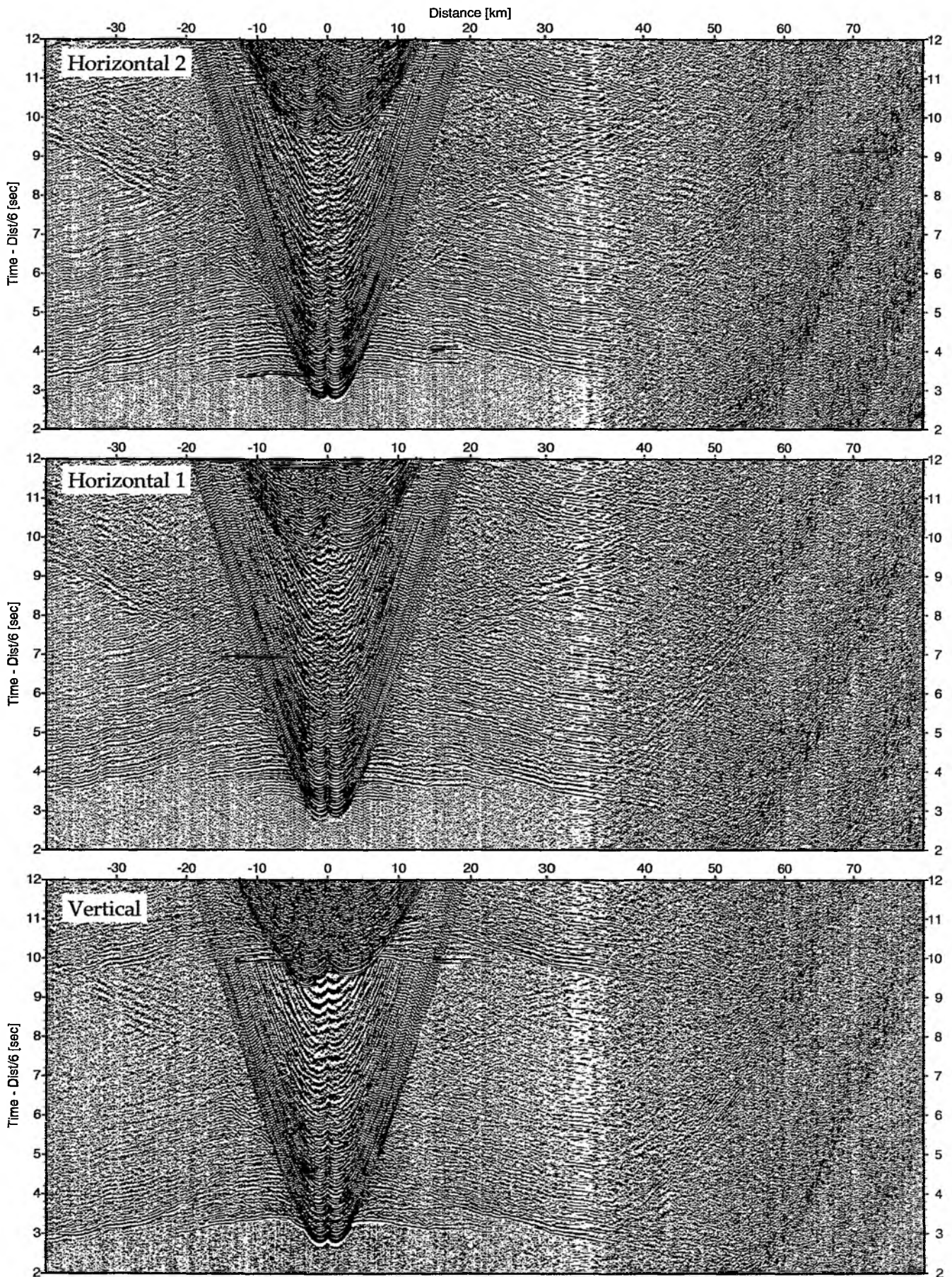


Figure 6.6.7.37: Record sections from obs 247 OAS/Owen-4.5Hz, SO181 Profile 09.

Time - Dist/6 [sec]

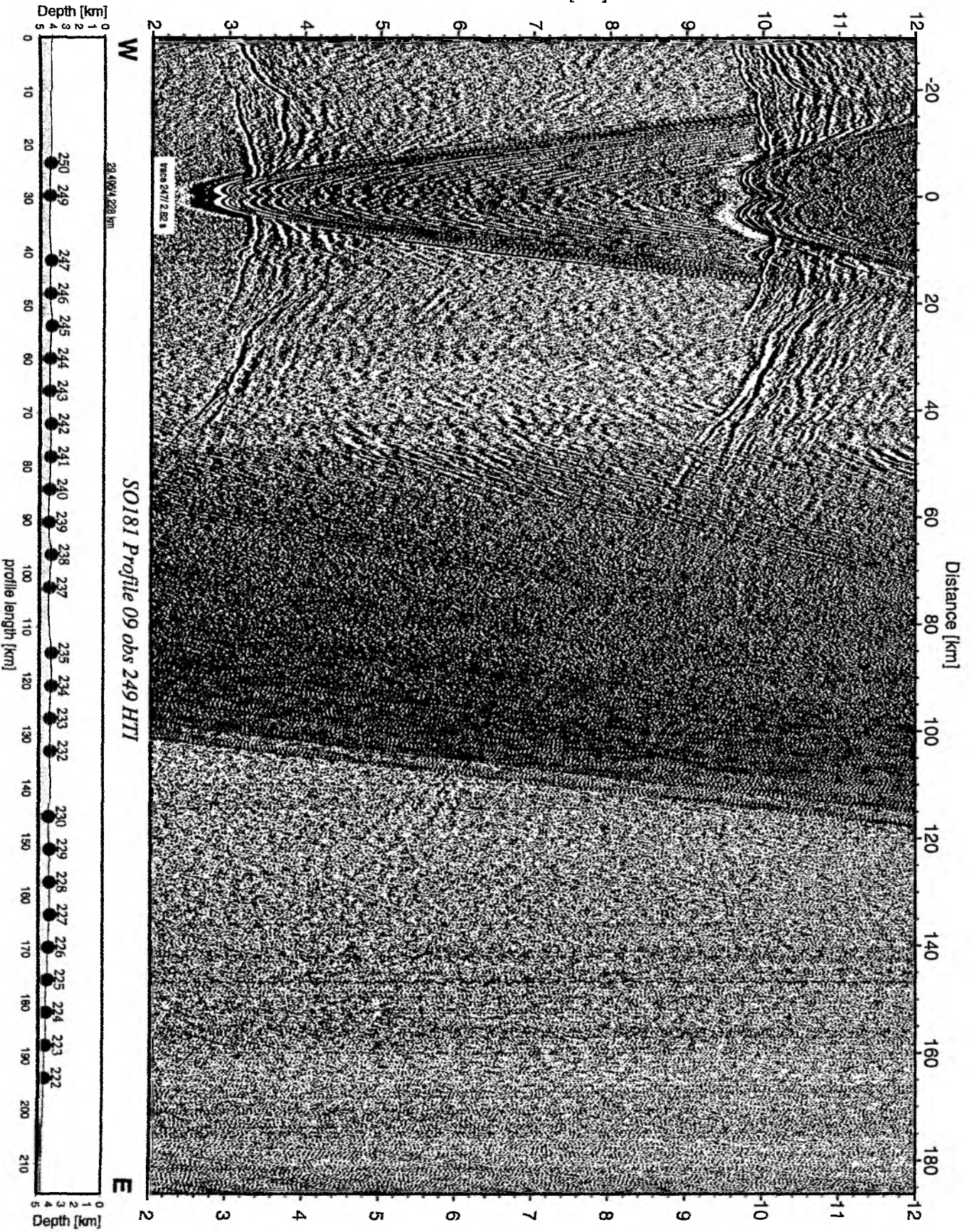


Figure 6.6.7.38: Record section from obs 249 HTI, Profile 09.

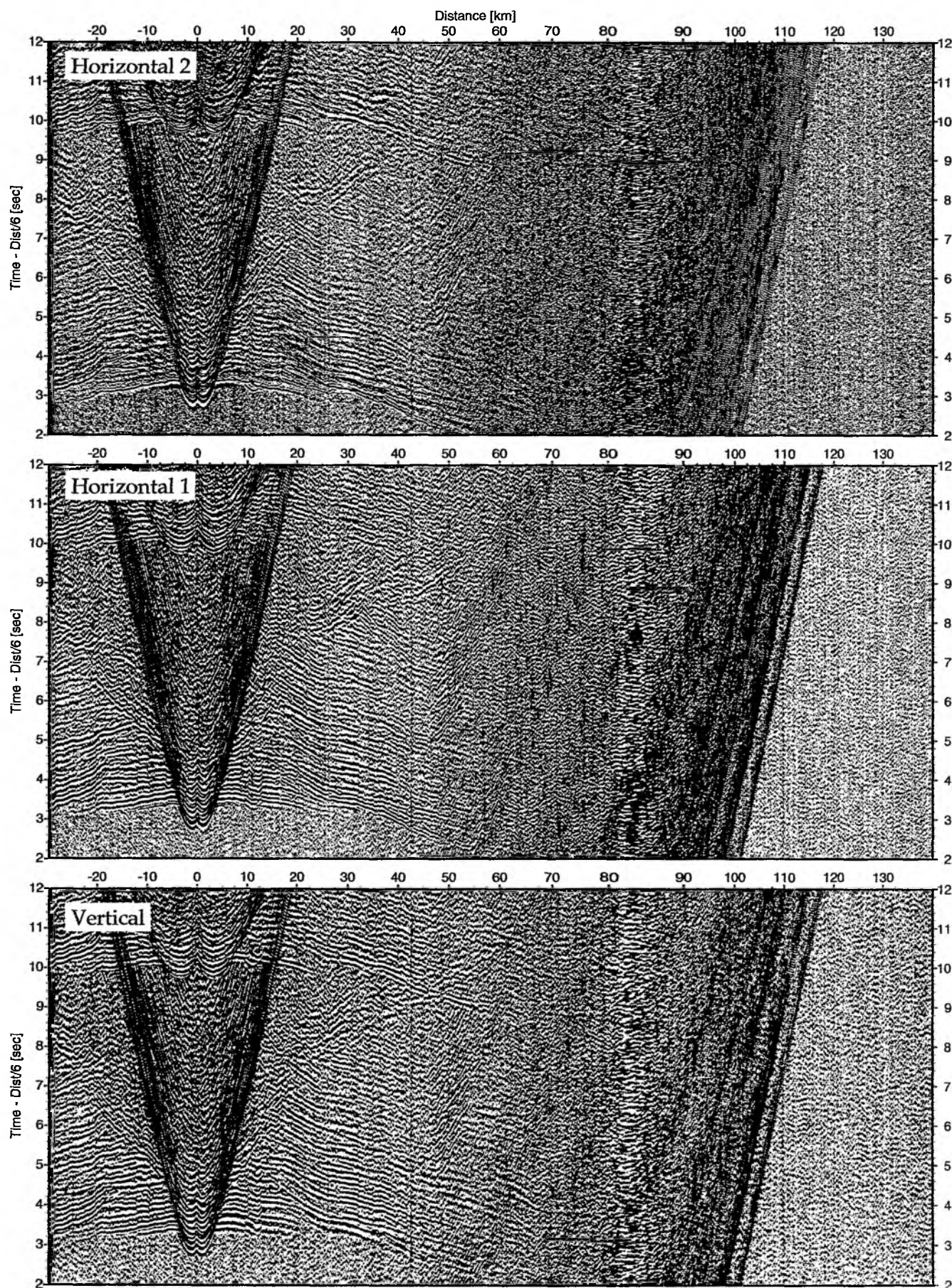


Figure 6.6.7.39: Record sections from obs 249 HTI/Owen-4.5Hz, SO181 Profile 09.

Time - Dist/6 [sec]

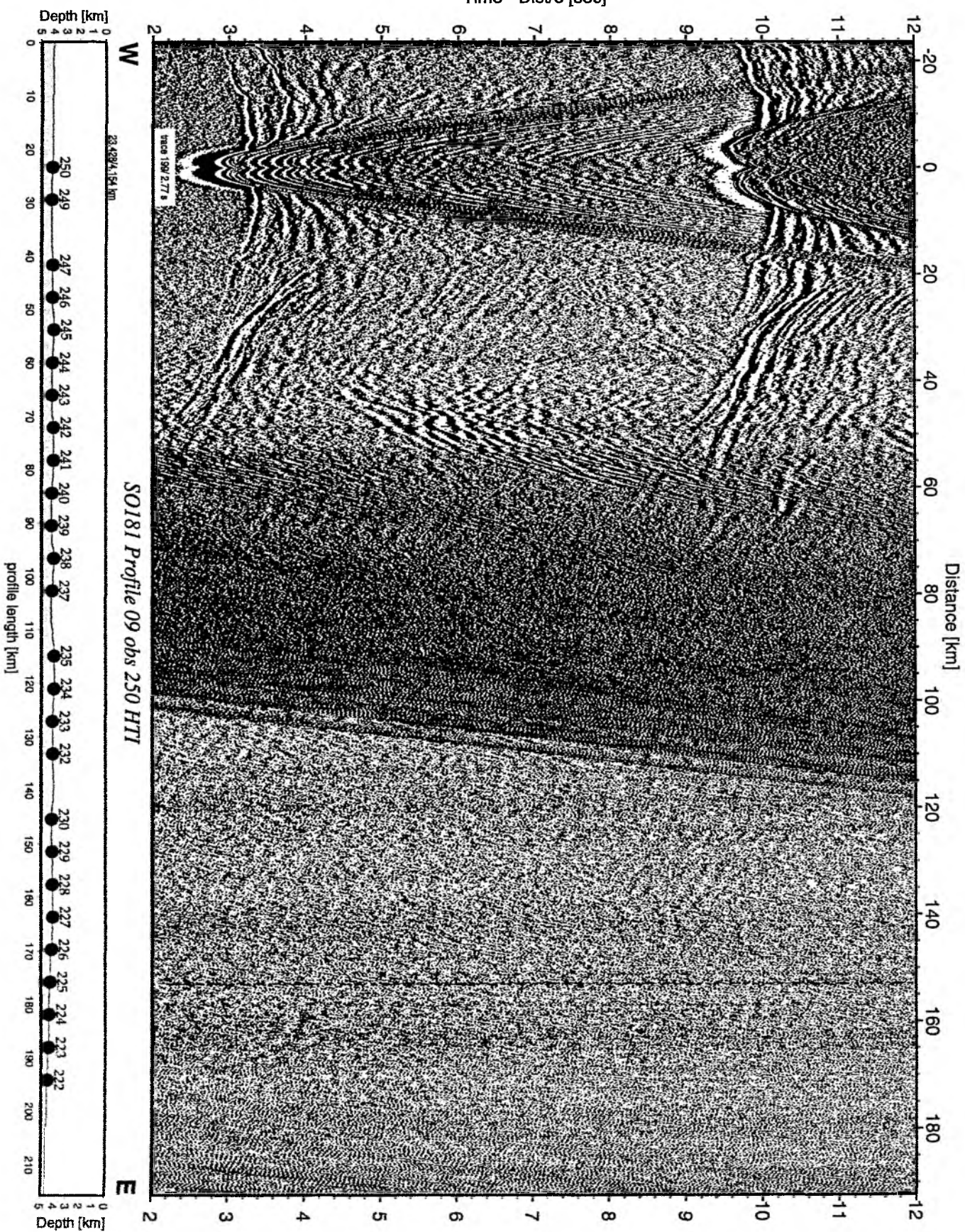


Figure 6.6.7.40: Record section from obs 250 HTI, Profile 09.

6.6.8 Test of the SEND prototype long period seismometer

A prototype seismometer manufactured by SEND GmbH, Hamburg, was tested during the deployment of profile 06 located off Chile at about 45° S (see chapter 6.6.6 for location maps and bathymetric information). This seismometer consists of three identical 4.5 Hz geophones in a tri-axial geometry, and a capacitive back coupling system to record a wide frequency range down to 1/30 Hz (see Section 5.3, Figures 5.3 and 5.7).

During the deployment of profile 06 several local earthquakes were recorded. We compare the recordings of these events on different instruments to investigate their performance. Unfortunately, no teleseismic event could be detected during the deployment, and thus only the high frequency spectrum can be investigated.

The main finding of this preliminary study is that the SEND seismometer is best adapted to record seismic waves with a frequency content below ~20 Hz, i.e. teleseismic and most regional earthquakes, but its frequency range is not sufficient to get proper seismograms of local (high frequency) events or active seismic profiling.

This can be clearly seen by comparing the seismogram quality of the first arrivals of local earthquakes, which is significantly lower on the prototype's recordings compared to Owen-type short period sensors (4.5 and 15 Hz). In the following subsection we take a closer look at an earthquake recorded on 11 Feb 2005 at 17:13 UTC, which was the strongest event that occurred during the deployment time (Figures 6.6.8.1 – 6.6.8.4).

In the second subsection we compare the spectra of the 17:13 UTC event of different sensor types. While the prototype's amplitude drops off sharply above its maximum at ~11 Hz reaching the noise level at ~20 Hz, the Owen 4.5 and 15 Hz sensors still record signal amplitudes up to 40-50 Hz (Figures 6.6.8.5 – 6.6.8.7).

In the third part we show other examples of local earthquakes to illustrate our findings (Figures 6.6.8.8 – 6.6.8.14).

In the last subsection we discuss the long period noise spectra of three seismometer types, including the prototype. Due to the lack of teleseismic earthquakes this was the only way to get some information about the long period behaviour of the new seismometer. It is obvious that the noise spectrum of the prototype is strongly enhanced for frequencies below 0.01 Hz (Figure 6.6.8.16). The maximum of its noise spectrum is at ~0.03 Hz which corresponds to a period of about 30 seconds.

Our findings may be rather negative, but since no teleseismic events were found this investigation may not be conclusive. However, it should be pointed out that the mechanical connection of the seismometer to the OBS was far from ideal.

On all figures in this section the eastern stations on the EW-oriented profile are placed at the top, western stations at the bottom. OBS 110 is an Owen 15 Hz geophone, OBS 194 is the SEND seismometer, OBS 111, 195, 196, 201 are Owen 4.5 Hz sensors. All seismometers are three-component instruments. Trace 4 of each instrument shows its vertical component, 2 and 3 the horizontals.

The 11 Feb 2005, 17:13 event

The 17:13 earthquake is the strongest and best recorded event during deployment.

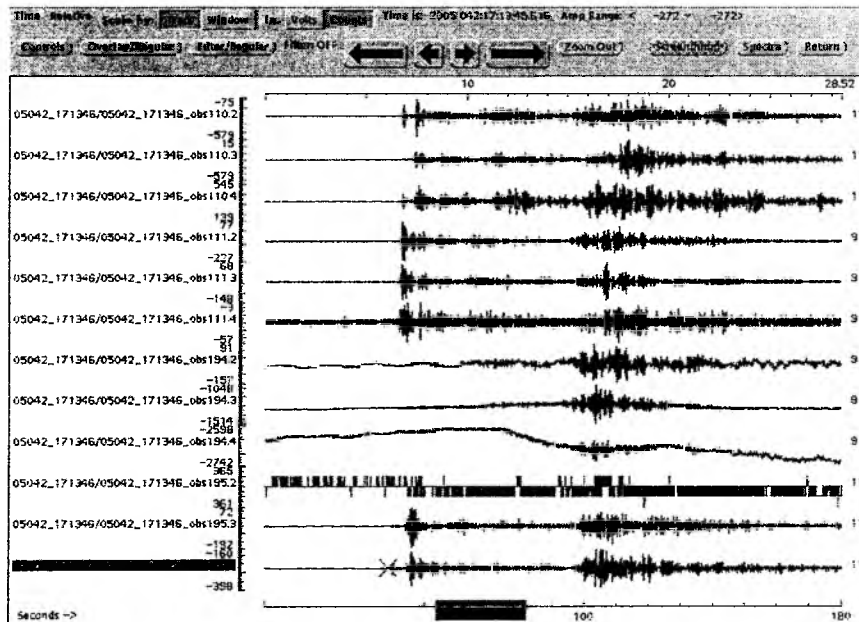


Figure 6.6.8.1: Raw plot of the local earthquake recorded on 11 Feb 2005, 17:13 UTC. The vertical component of OBS 111 has low gain. Channel 2 of OBS 195 is disturbed. Instruments are aligned along profile. The SEND prototype's signal (OBS 194) is dominated by long period noise. The earthquake wavefront crossed the profile from west to east (first arrival on lower traces).

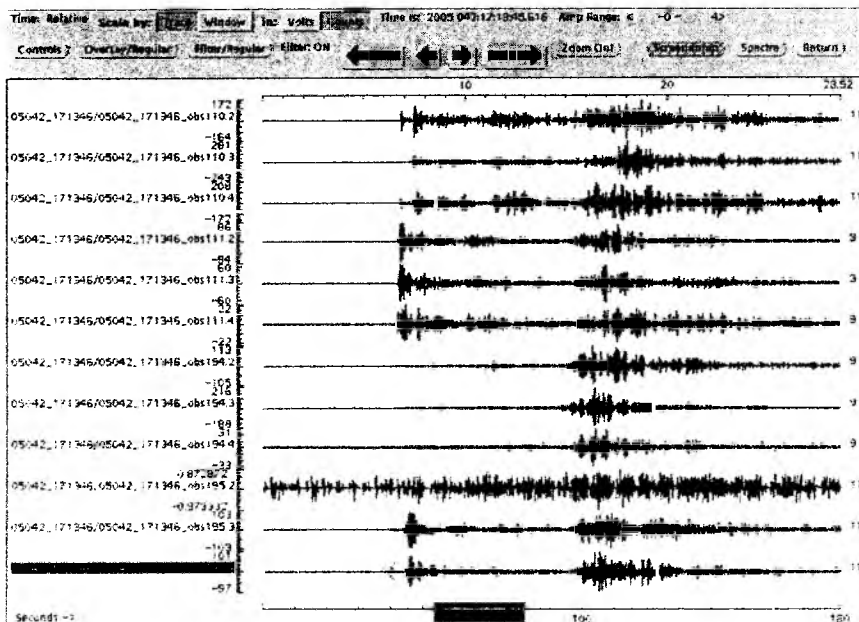


Figure 6.6.8.2: The same earthquake as in the previous figure, but 5-20 Hz bandpass filtered. Except the prototype, all OBS show clear first arrivals (see next figures).

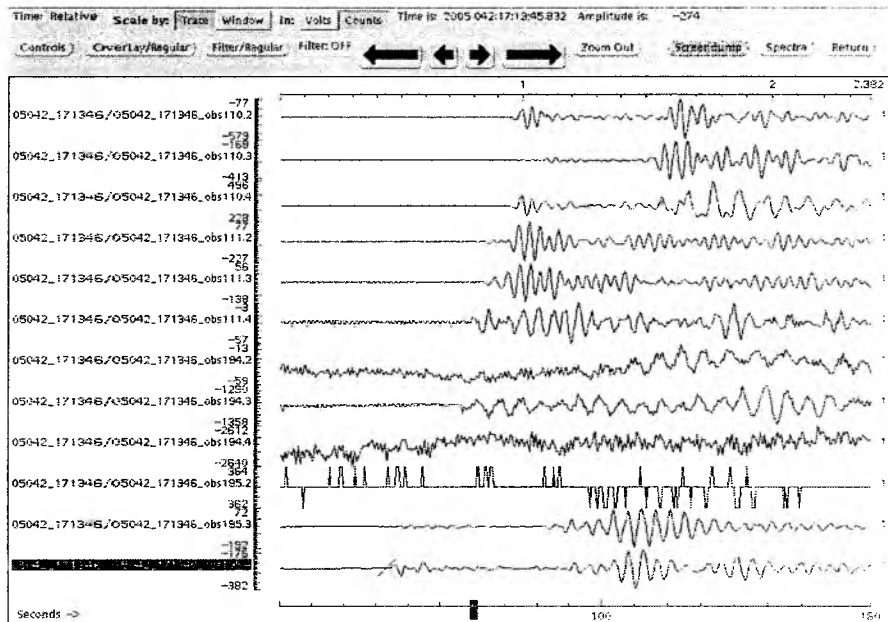


Fig 6.6.8.3: The P-wavelet of the earthquake shown in the previous figure. All Owen sensors show a clear first P-arrival on their verticals (4th traces), while it is poorly visible on the prototype recording. One horizontal (2) of OBS 195 is disturbed.

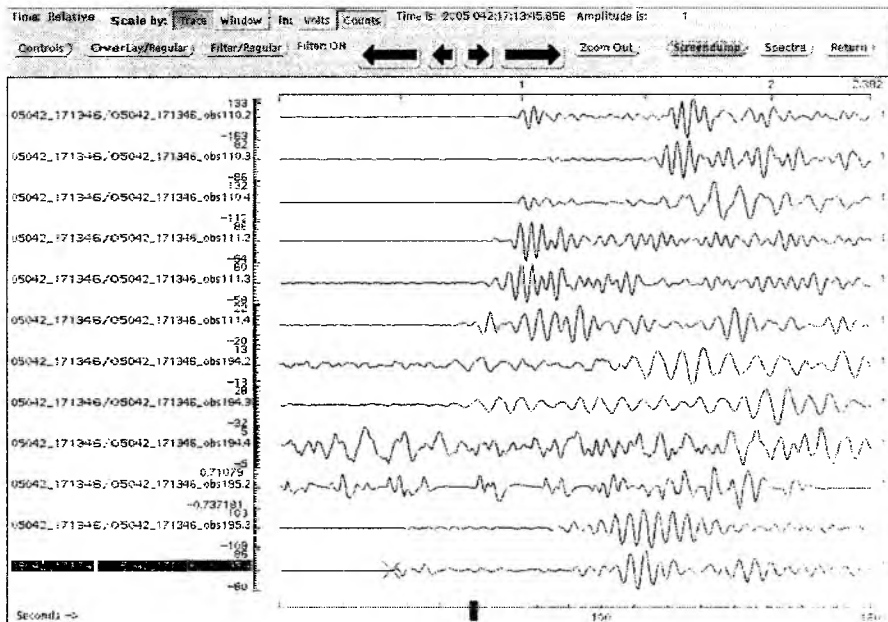


Figure 6.6.8.4: The P-wavelet of the earthquake shown in the previous figure, but 5-20 Hz bandpass filtered. No clear first arrivals can be seen on the prototype's channels, while on all other sensors they are clear.

The signal spectrum of the 17:13 earthquake

To understand why the prototype does not record the first arrivals of local earthquake in a similar quality than the Owen-type sensors, we study the signal spectrum of the 17:13 event recorded by these instruments.

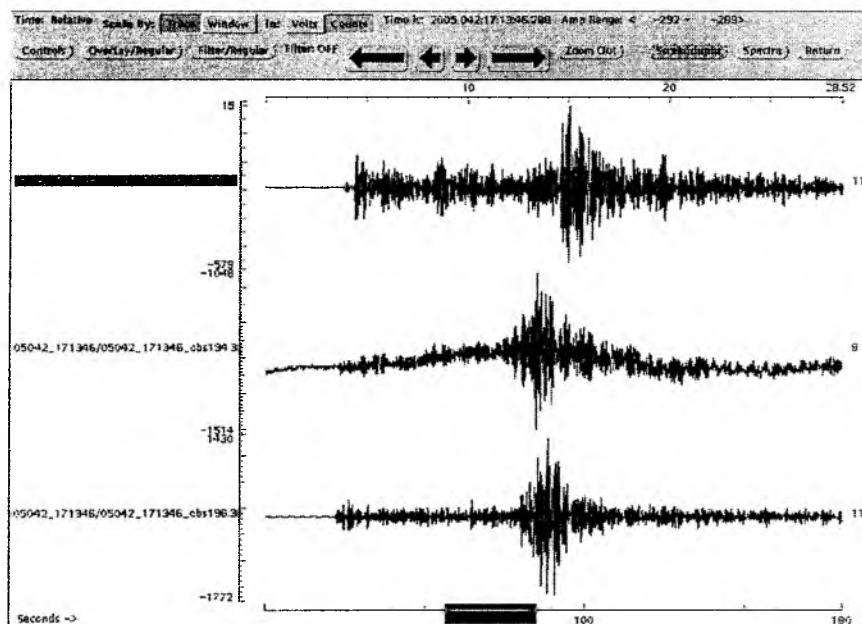


Figure 6.6.8.5: Recordings of the 17:13 event from the horizontals of OBS 110 (Owen 15 Hz), OBS 194 (SEND) and OBS 196 (Owen 4.5 Hz). We prefer the horizontals because the SEND vertical's signal-to-noise ratio is too low. The SEND sensor (centre) shows long period noise.

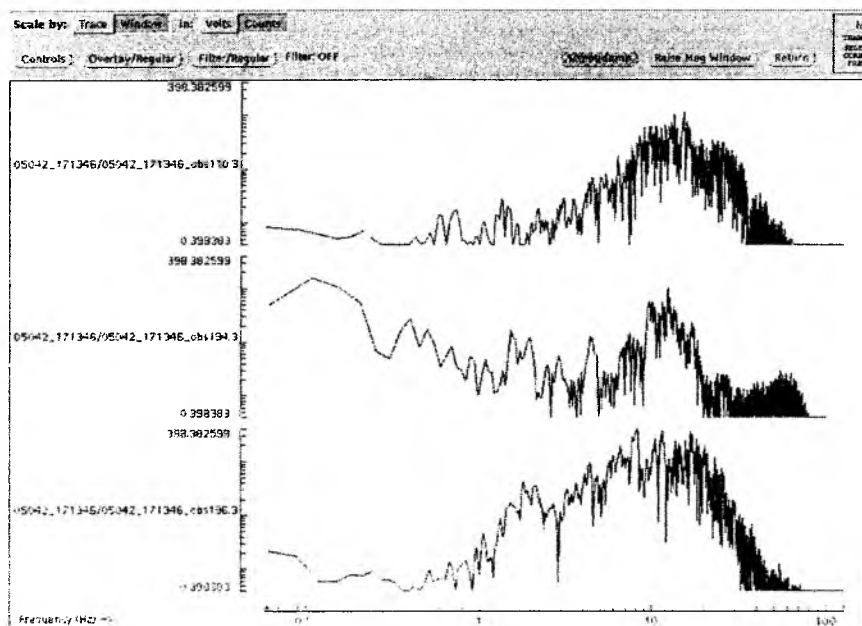


Figure 6.6.8.6: Signal spectra of the 17:13 earthquake of the horizontals of OBS 110, 194 and 196. The signal amplitude of OBS 194 (centre) drops off strongly down to noise level (see also next figure) beyond its maximum at ~11 Hz, while the Owen-type sensors record signal amplitudes up to 40-50 Hz. This results in clearer first arrivals on the seismograms.

To separate the signal from the noise content of the spectrum we plot the spectrum of the noise recordings before the earthquake (Figure 6.6.8.7).

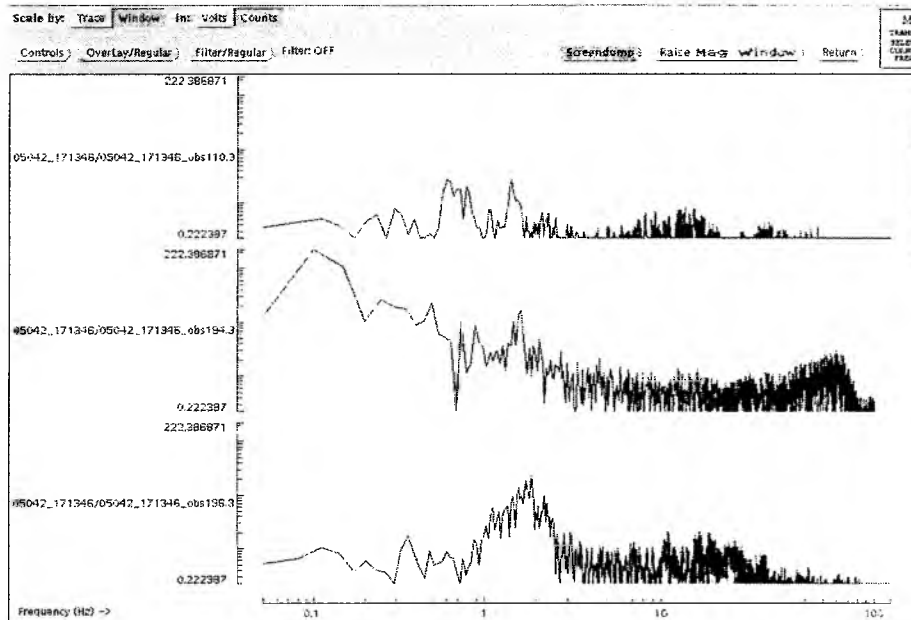


Figure 6.6.8.7: Noise spectra of the recordings of OBS 110, 194 and 196 of ~100 seconds before the 17:13 earthquake. Comparing the spectrum of the OBS 194 SEND seismometer (centre) with its signal spectrum (previous figure), it becomes obvious that the amplitude increase after the sharp drop off in the signal spectrum above 30 Hz is caused only by noise.

Other earthquake examples from testing the SEND prototype seismometer

Additional earthquakes were recorded during the deployment of the instruments on profile 06. Some of them are shown here to underline the previous results.

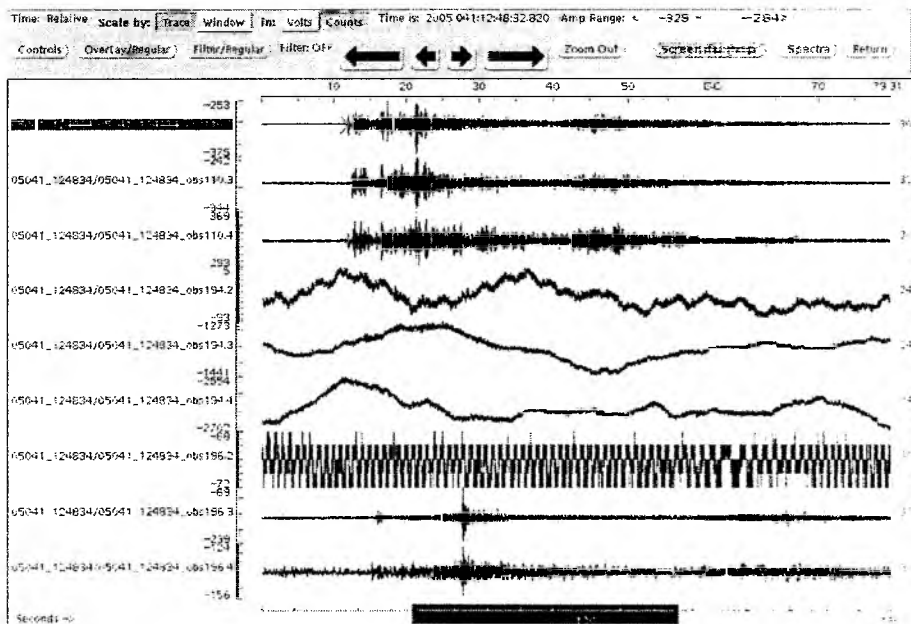


Figure 6.6.8.8: Raw plot of an earthquake recorded on 10 Feb 2005. 12:48 UTC. The sensor of OBS 110 (top traces) is an Owen 15 Hz geophone, OBS 194 (centre) the SEND prototype, OBS 196 (bottom) an Owen 4.5 Hz geophone. Horizontal (2) of OBS 196 failed.

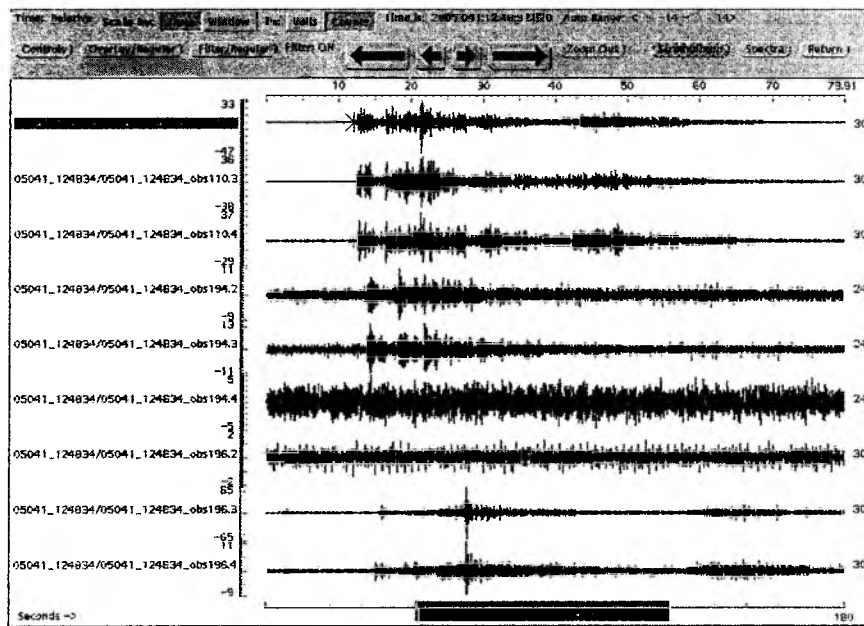


Figure 6.6.8.9: The same earthquake as in the previous figure, but 5-20 Hz bandpass filtered. The vertical component (4) of the prototype did not record any signal from the earthquake, while its records of the horizontals are poor compared to the Owen geophones.

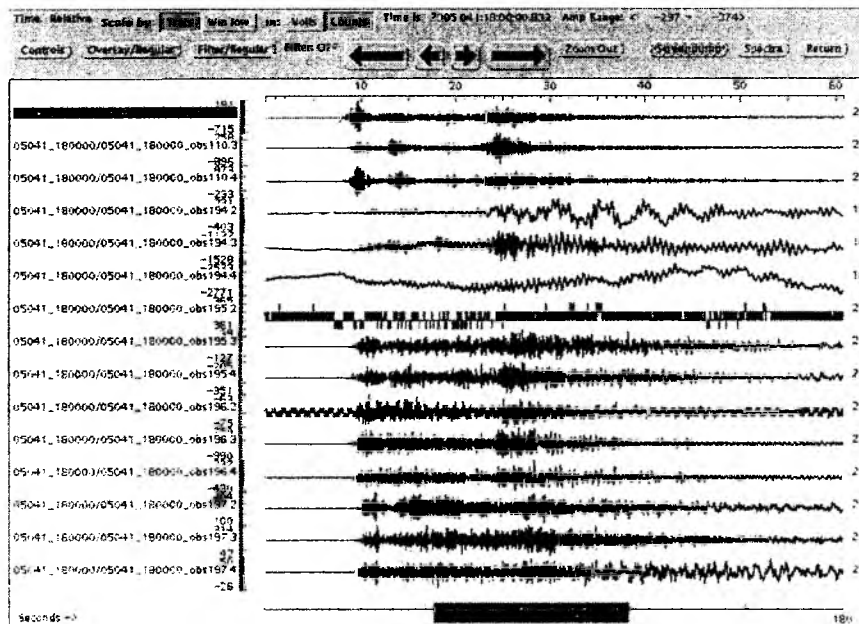


Figure 6.6.8.10: Raw plot of a local earthquake recorded on 10 Feb 2005, 18:00 UTC. Two additional Owen 4.5 Hz-type stations (OBS 195 and 197) are included. Channels 2 of OBS 195 and 196 are disturbed. The instruments are aligned along the profile. The SEND prototype (OBS 194) shows long period S-wave signals.

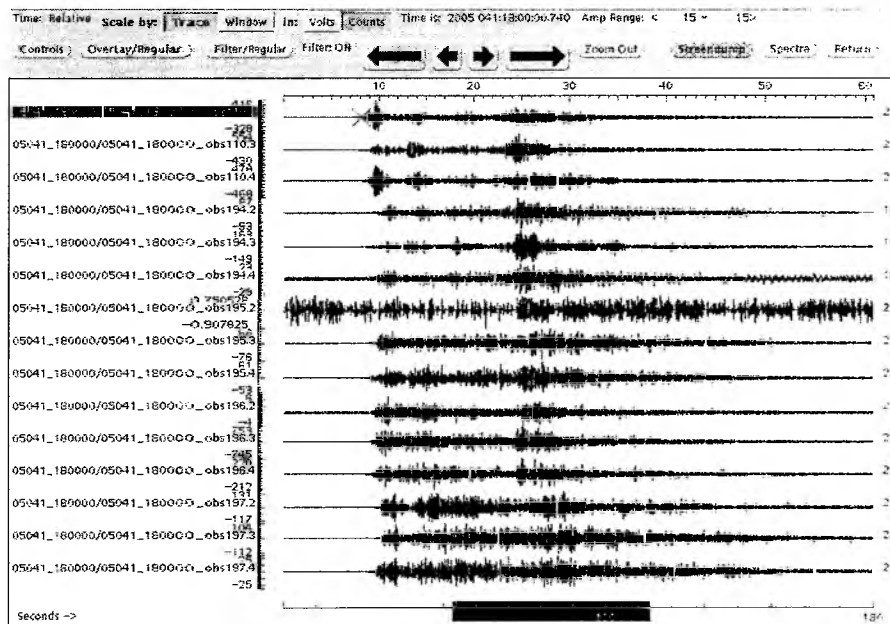


Figure 6.6.8.11: The same earthquake as in the previous figure, but 5-20 Hz bandpass filtered. The signal-to-noise ratio of the vertical component of the prototype is low compared to the other sensors, while the horizontals are fine.

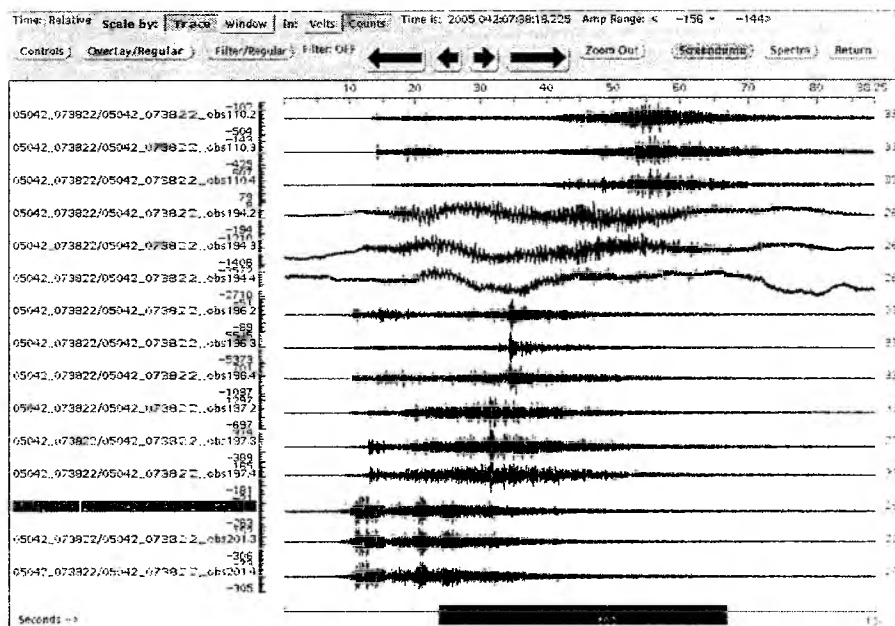


Figure 6.6.8.12: Local earthquake recorded 11 Feb 2005, 07:38 UTC. Including additional OBS 201 all stations below the prototype (OBS 194) are Owen 4.5 Hz instruments. The prototype's traces are dominated by long period noise.

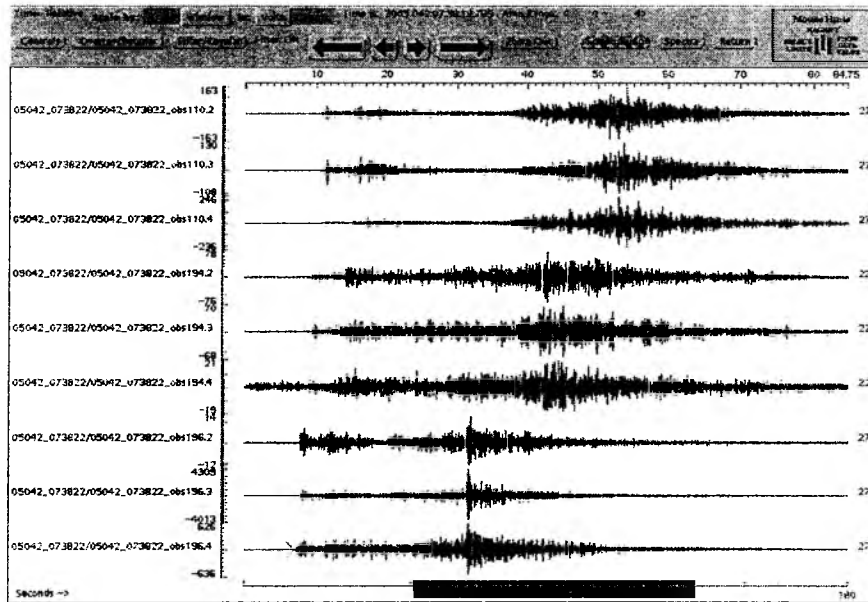


Figure 6.6.8.13: The same event as in the previous figure, but 5-20 Hz bandpass filtered. While the Owen sensors show clear first arrivals, the vertical component (4) of the prototype is very noisy, while its horizontals are comparable to the others instruments.

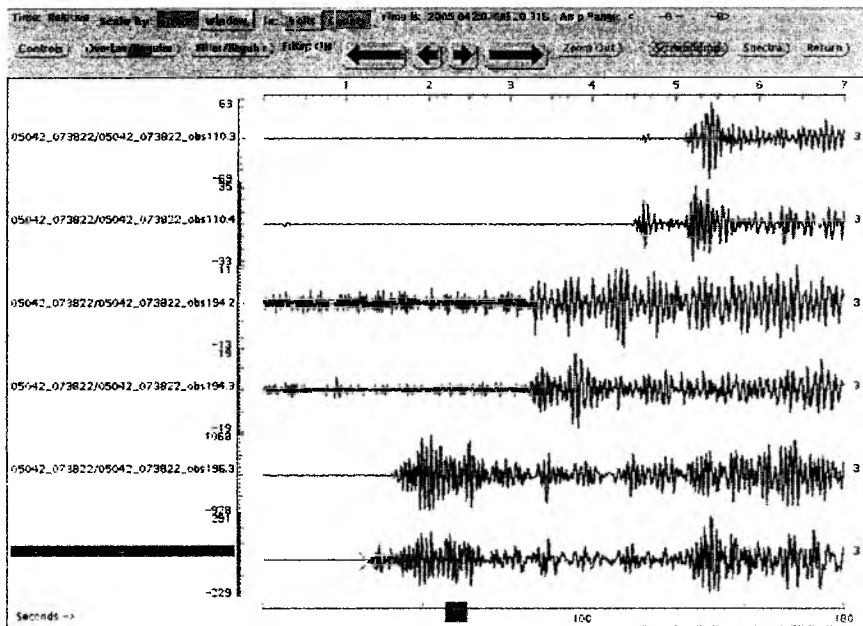


Figure 6.6.8.14: The first arrivals of the previous event 10-40 Hz bandpass filtered. We show the vertical and a horizontal of the Owen-type sensors of OBS 110 (top) and 196 (bottom), both horizontals of the SEND sensor of OBS 194 (centre). The Owen recordings still show clear first arrivals, while the SEND sensor has a highly increased noise content before the first arrival.

Long period noise characteristics of the SEND prototype seismometer

Because of the lack of good recordings of teleseismic earthquakes during the testing period we looked at the long period noise characteristics of the new seismometers and compared it to Owen-type sensors. See Figures 6.6.8.15 and 6.6.8.16 for details.

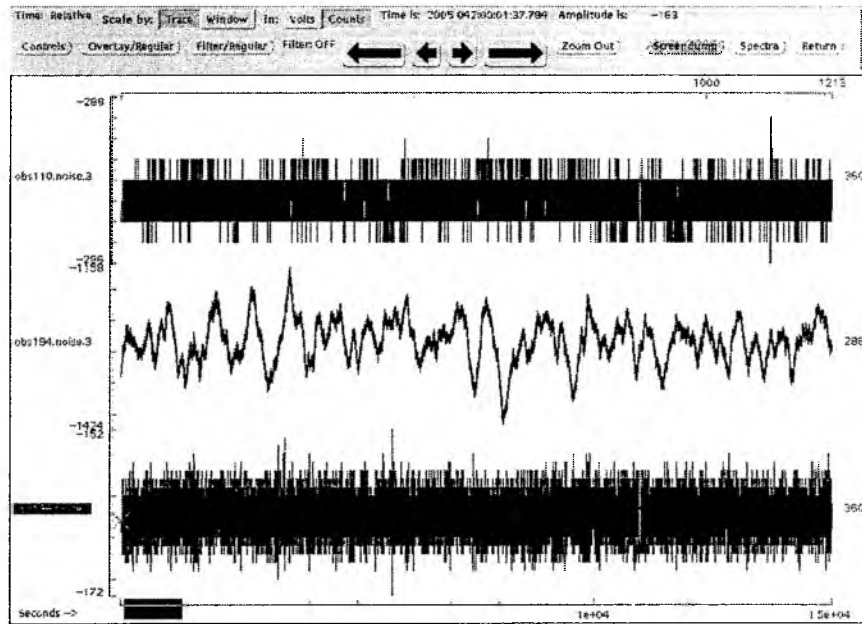


Figure 6.6.8.15: A twenty minutes noise sample from 11 Feb 2005, 00:01 UTC, recorded with an Owen 15 Hz sensor (top trace), the prototype seismometer (centre), and an Owen 4.5 Hz geophone. Unfortunately the gain of the 4.5 Hz instrument is very low. The prototype recording is dominated by long period noise.

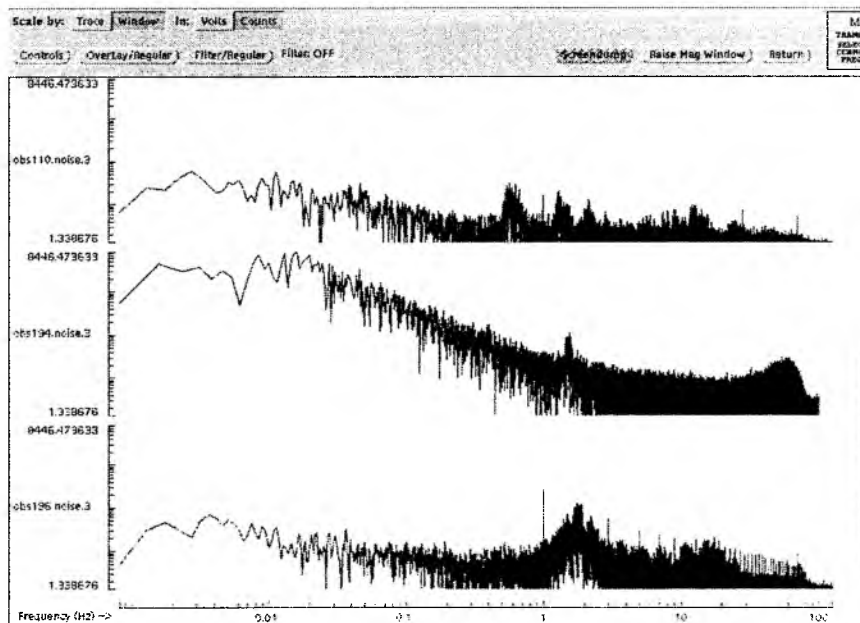


Figure 6.6.8.16: The noise spectrum of the previous traces. The prototype instrument (centre) shows a broad amplitude maximum around 100 seconds (0.01 Hz), which is more than 2 magnitudes higher than the short period instrument's spectra (upper and lower panel).

7. Acknowledgements

Cruises SO 181 1&2 were funded by the German Ministry of Education and Research (BMBF) under project No. 03G0163A to IFM-GEOMAR within the continued and generous most commendable support for marine sciences with an outstanding research vessel such as SONNE. This cruise is part of integrated research project TIPTEQ, carried out by nine German and seven Chilean institutions.

We warmly thank masters M. Kull and L. Mallon and their crews for their excellent support in all work done and for the splendid working atmosphere throughout the entire and the ambitious working program.

8. References

- Atwater, T., Implications of plate tectonics for the Cenozoic tectonic evolution of western North America, *Geol. Soc. Am. Bull.*, 81 3515-3536, 1970.
- Bangs, N. L., and C. Cande, Episodic development of a convergent margin inferred from structures and processes along the southern Chile margin, *Tectonics*, 16, 489-503, 1997.
- Bangs N. L., S. C. Cande, S. D. Lewis, and J. J. Miller, Structural framework of the Chile margin at the Chile Ridge collision zone, *Proc. Ocean Drill. Program, Initial Rep.*, 141, 11-21, 1992.
- Barazangi, M., and B. L. Isacks, Spatial distribution of earthquakes and subduction of the Nacza plate beneath South America, *Geology*, 4, 686-692, 1976.
- Barker, P. F., The Cenozoic subduction history of the Pacific margin of the Antarctic Peninsula: Ridge crest-trench interactions, *J. Geol. Soc.*, 139, 787-802, 1982.
- Behrmann, J.H. and A. Kopf, Balance of tectonically accreted and subducted sediment at the Chile Triple Junction, *Int. J. Earth Sciences*, 90, 753-768, 2001.
- Behrmann, J.H., S.D. Lewis, S. Cande and ODP Leg 141 Scientific Party, Tectonics and geology of spreading ridge subduction at the Chile Triple Junction; a synthesis of results from Leg 141 of the Ocean Drilling Program, *Geol. Rundschau*, 83, 832-852, 1994.
- Behrmann, J.H., S.D. Lewis, R. Musgrave, N. Bangs, P. Bodén, K. Brown, H. Collombat, A. Didenko, B.M. Didyk, P.N. Froelich, X. Golovchenko, R. Forsythe, V. Kurnosov, N. Lindsley-Griffin, K. Marsaglia, S. Osozawa, D. Prior, D. Sawyer, D. Scholl, D. Spiegler, K. Strand, K. Takahashi, M. Torres, M. Vega-Faundez, H. Vergara and A. Waseda, Chile Triple Junction, *Proc. ODP, Init. Repts. (Pt. A)*, 141, 1-708, 1992.
- Bialas J. and Flueh E.R., 1999, A new Ocean Bottom Seismometer (with a new type of data logger), *Sea Technology*, Vol. 40, 4
- Bialas, J. and Flueh, E.R., Phipps Morgan, J., Schleisiek, K. and Neuhaeusser, G., 2002, Ocean Bottom Seismology in the Third Millennium, in: Beranzoli, L., Favali, P., and Smiraglio, G. (eds.), *Science technology Synergy for Research in the Marine Environment: Challenges for the XXI Century*
- Blondel, P., and Murton, B.J., 1997, *Handbook of Seafloor Sonar Imagery*. John Wiley and Sons, Chichester, pp314.
- Bourgeois J., Guivel, C., Lagabrielle, Y., Calmus, T., Boulegue, J. and V. Daux, Glacial-interglacial trench supply variation, spreading-ridge subduction, and feedback controls on the Andean margin development at the Chile triple junction area (45-48 S), *J. Geophys. Res.*, 105, 8355-8386, 2000.
- Bourgeois, J., H. Martin, Y. Lagabrielle, J. Le Moigne, and J. Frutos Jara, Subduction erosion related to spreading-ridge subduction: Taitao peninsula (Chile margin triple junction area), *Geology*, 24 723-726, 1996.
- Bullard, E.C., 1954. The flow of heat through the floor of the Atlantic Ocean, *Proc. R. Soc. London, A*, 222, 408-425.
- Bullard, E.C., 1939. Heat flow in South Africa, *Proc. R. Soc. London, A*, 173, 474-502.

- Cande, S.C., and Leslie, R.B., 1986, Late Cenozoic tectonics of the Chile trench, *J. Geophys. Res.* 91, 471-496
- Chave, A.D., Constable, S.C. & Edwards, R.N. (1991): Electrical Exploration Methods for the Seafloor, in: *Electromagnetic Methods in Applied Geophysics*, Vol. 2 (ed. M.N. Nabighian). Society of Exploration Geophysicists, Tulsa, Oklahoma, 931-966.
- DeLong, S. E., W. M. Schwarz, and R. N. Anderson, Thermal effects of ridge subduction, *Earth Planet. Sci. Lett.*, 44, 239-246, 1979.
- Filloux, J.H. (1973): Techniques and instrumentation for study of natural electromagnetic induction at sea, *Phys. Earth Planet. Int.*, 7, 323-338.
- Filloux, J.H. (1974): Electric Field Recording on the Sea Floor with Short Span Instruments. *J. Geomag. Geoelectr.*, 26, 269-279.
- Flüh, E. R., Kukowski, N. and Reichert, C. (Ed.) 1997, FS SONNE, Fahrtbericht/Cruise Report SO123: MAMUT (MAKRAN MURRAY TRAVERSE - Geophysik Plattentektonischer Extremfälle). Maskat - Maskat, 07.09 - 03.10.1997, GEOMAR Report 62, 292 pp.
- Forsythe, R., and E. Nelson, Geological manifestations of ridge collision: evidence from the Golfo de Penas-Taitao Basin, southern Chile, *Tectonics*, 4, 477-495, 1985.
- Gonzalo, A. Y., Ranero, C. R., von Huene, R. and J. Diaz, Magnetic anomaly interpretation across the southern central Andes (32 -34 S): The role of the Juan Fernandez Ridge in the late Tertiary evolution of the margin, *J. Geophys. Res.*, 106, 6325-6345, 2001.
- Grevemeyer, I., and H. Villinger, Gas hydrate stability and the assessment of heat flow through continental margins, *Geophys. J. Int.*, 145,, 647-660, 2001.
- Grevemeyer, I., J.L. Diaz-Naveas, C.R. Ranero, H.W. Villinger and Ocean Drilling Program Leg 202 Scientific Party, Heat flow over the descending Nazca plate in Central Chile, 32°S to 41°S: evidence from ODP Leg 202 and the occurrence of natural gas hydrates, *Earth Planet. Sci. Lett.*, 213, 285-298, 2003.
- Grevemeyer, I., N. Kaul, and J.L. Dias-Naveas, Geothermal evidence for fluid flow through the gas hydrate stability field off Central Chile: transient flow related to large subduction zone earthquakes?, *Geophys. J. Int.*, revised, 2005.
- Grow, J. A., and T. Atwater, Mid-Tertiary tectonic transition in the Aleutian arc, *Geol. Soc. Am. Bull.*, 81, 3715-3722, 1970.
- Gutenberg, B. and C.F. Richter, *Seismicity of the earth and associated phenomena*, Princeton University Press, 310, 1954.
- Haeussler, P. J., D. Bradley, R. Goldfarb, L. Snee, and C. Taylor, Link between ridge subduction and gold mineralization in southern Alaska, *Geology*, 23, 995-998, 1995.
- Hartmann, A. and Villinger, H., 2002. Inversion of heat flow measurements by expansion of the temperature decay function. *Geophys. J. Int.* 148, 628–636
- Havskov, J. and L. Ottemöller (eds), *SEISAN: The earthquake analysis software for Windows, Solaris and LINUX*, version 7.2, Institute of Solid Earth Physics, University of Bergen, Norway, 2001.
- Hyndman, R.D., Davis, E.E. & Wright, J.A., 1979. The measurement of marine geothermal heat flow by a multipenetration probe with digital acoustic telemetry and in situ thermal conductivity, *Mar. Geophys. Res.*, 4, 181–205.
- Herron, E. M., and B. E. Tucholke, Sea-floor magnetic patterns and basement structure in the southeastern Pacific, *Initial Rep. Deep Sea Drill. Proj.*, 35, 263-278, 1976.
- Herron, E. M., S. C. Cande, and B. R. Hall, An active spreading center collides with a subduction zone: A geophysical survey of the Chile margin triple junction, *Mem. Geol. Soc. Am.*, 154, 683-701, 1981.
- Kilian, R. and J.H. Behrmann, Geochemical constraints on the sources of continent-related deep-sea sediments and their recycling in arc magmas of the Southern Andes, *J. Geol. Soc. Lond.*, 160, 57-70, 2003.

- Kopp, H., Flueh, E.R., Papenberg, C., Klaeschen, D., and SPOC Scientists, 2004, Seismic investigation of the O'Higgins Seamount Group and Juan Fernandez Ridge: Aseismic ridge emplacement and lithosphere hydration, *Tectonics* 2(23), TC2009, 10.1002/2003TC001590.
- Lagabriele, Y., Guivel, C., C. Maury, R., Bourgois, J., Fourcade, S. and H. Martin, Magmatic-tectonic effects of high thermal regime at the site of active ridge subduction: the Chile Triple Junction model, *Tectonophysics*, 326, 255-268, 2000.
- Lagabriele, Y., J. Le Moigne, R. Maury, J. Cotten, and J. Bourgois, Volcanic record of the subduction of an active spreading ridge, Taitao peninsula (southern Chile), *Geology*, 22, 515-518, 1994.
- Lay, W. and T.C. Wallace, *Modern Global Seismology*, Academic Press, 1995.
- Lee, W.H.K., R.E. Bennet and L. Meagher, A method for estimating magnitude of local earthquakes from signal duration, U.S.G.S. Open file report, 1972.
- Lewis, S.D., Behrmann, J.H., R. Musgrave, N. Bangs, P. Bodén, K. Brown, H. Collombat, A. Didenko, B.M. Didyk, P.N. Froelich, X. Golovchenko, R. Forsythe, V. Kurnosov, N. Lindsley-Griffin, K. Marsaglia, S. Osozawa, D. Prior, D. Sawyer, D. Scholl, D. Spiegler, K. Strand, K. Takahashi, M. Torres, M. Vega-Faundez, H. Vergara and A. Waseda, Chile Triple Junction, *Proc. ODP, Sci. Results*, 141, 1-499, 1995.
- Lienert, B.R. and J. Havskov, A computer program for locating earthquakes both locally and globally, *Seismological Res. Letters*, 66, 26-36, 1995.
- Lister, C.R.B., 1970. Measurement of in situ sediment conductivity by means of a Bullard-type probe, *Geophys. J. R. astr. Soc.*, 19, 521-532.
- Lister, C.R.B., 1979. The pulse-probe method of conductivity measurement, *Geophys. J. R. astr. Soc.*, 57, 451-461.
- Luegert, J.H., 1992, R1D One-Dimensional Seismic Travel Modeling: USGS Open File Report 43.
- Murdie, R., D. Prior, P. Styles, S. Flint, R. Pearce, and S. Agar, Seismic responses to ridge-transform subduction: Chile Triple junction, *Geology*, 21, 1095-1098, 1993.
- Ramos, V. A., and S. M. Kay, Southern Patagonian plateau basalts and deformation: backarc testimony of ridge collision, *Tectonophysics*, 205, 261-282, 1992.
- Seeber, G., 1996: Stand und Einsatzmöglichkeiten von GPS - ein Überblick, *Proc. 11th Annual Meeting of the German Hydrographic Society*, Glücksburg, 3.-5.6.
- Tebbens, S. F., S. C. Cande, L. Kovacs, J. C. Parra, J. L. LaBrecque, and H. Vergara, The Chile ridge: A tectonic framework, *J. Geophys. Res.*, 102, 12,035-12,059, 1997.
- Uyeda, S., and A. Miyashiro, Plate tectonics and the Japanese Islands: A synthesis, *Geol. Soc. Am. Bull.*, 85, 1159-1170, 1974.
- Villinger, H. & Davis, E.E., 1987. A new reduction algorithm for marine heat flow measurements, *J. geophys. Res.*, 92(B12), 12 846-12 856.

9. Appendices

Appendix 9.1 Magnetic profiles

Magnetic profiles of SO181-1

Profile No.	Date	Time	Latitude	Longitude	Action
SO181-1b-1	18.12.04	15:30	39° 50.02' S	73° 39.15' W	Begin Profile
SO181-1b-1	20.12.04	12:00	42° 37.75' S	74° 38.50' W	End Profile
SO181-1b-2	20.12.04	12:01	42° 37.80' S	74° 38.54' W	Begin Profile
SO181-1b-2	21.12.04	23:03	43° 11.40' S	78° 29.98' W	End Profile
SO181-1b-3	22.12.04	12:47	43° 10.63' S	78° 28.83' W	Begin Profile
SO181-1b-3	22.12.04	22:27	42° 57.41' S	76° 41.00' W	End Profile
SO181-1b-4	23.12.04	11:25	42° 58.60' S	76° 49.21' W	Begin Profile
SO181-1b-4	23.12.04	19:26	42° 42.48' S	75° 9.81' W	End Profile
SO181-1b-5	24.12.04	11:40	42° 35.29' S	75° 9.07' W	Begin Profile
SO181-1b-5	27.12.04	09:02	42° 59.49' S	75° 27.91' W	End Profile
SO181-1b-6	28.12.04	01:02	43° 39.78' S	75° 53.48' W	Begin Profile
SO181-1b-6	29.12.04	09:33	45° 2.29' S	76° 11.53' W	End Profile
SO181-1b-8	03.01.05	11:07	44° 21.97' S	75° 4.05' W	Begin Profile
SO181-1b-8	04.01.05	18:44	44° 31.92' S	76° 47.06' W	End Profile
SO181-1b-10	09.01.05	15:14	40° 36.66' S	74° 25.29' W	Begin Profile
SO181-1b-10	10.01.05	13:10	40° 51.23' S	76° 40.34' W	End Profile
SO181-1b-11	10.01.05	17:29	41° 26.51' S	76° 41.13' W	Begin Profile
SO181-1b-11	11.01.05	02:13	41° 14.17' S	74° 49.06' W	End Profile
SO181-1b-12	12.01.05	16:12	38° 15.03' S	76° 10.12' W	Begin Profile
SO181-1b-12	14.01.05	11:50	36° 0.80' S	75° 9.97' W	End Profile
SO181-1b-13	14.01.05	23:57	36° 2.13' S	75° 1.10' W	Begin Profile
SO181-1b-13	16.01.05	02:45	35° 55.30' S	73° 57.71' W	End Profile

Appendix 9.1 (continued)*Magnetic profiles of SO181-2*

Profile No.	Date	Time	Latitude	Longitude	Action
SO181-2-1	01.02.05	20:10	47° 35.53' S	77° 24.63' W	Begin Profile
SO181-2-1	02.02.05	06:07	47° 20.08' S	74° 53.74' W	End Profile
SO181-2-2	06.02.05	12:08	45° 52.24' S	76° 59.85' W	Begin Profile
SO181-2-2	06.02.05	15:21	45° 25.34' S	77° 28.72' W	End Profile
SO181-2-3	06.02.05	15:21	45° 24.95' S	77° 28.51' W	Begin Profile
SO181-2-3	06.02.05	19:21	45° 16.00' S	76° 30.26' W	End Profile
SO181-2-4	06.02.05	20:28	45° 3.25' S	76° 31.62' W	Begin Profile
SO181-2-4	07.02.05	04:01	45° 16.92' S	78° 19.27' W	End Profile
SO181-2-5	07.02.05	05:00	45° 7.85' S	78° 19.88' W	Begin Profile
SO181-2-5	07.02.05	17:58	44° 29.91' S	75° 14.67' W	End Profile
SO181-2-6	12.02.05	06:27	44° 59.71' S	78° 15.31' W	Begin Profile
SO181-2-6	12.02.05	16:49	44° 31.52' S	76° 6.37' W	End Profile
SO181-2-7	14.02.05	14:11	41° 55.32' S	76° 6.96' W	Begin Profile
SO181-2-7	15.02.05	09:15	38° 30.31' S	76° 18.99' W	End Profile
SO181-2-8	15.02.05	09:15	38° 29.89' S	76° 18.73' W	Begin Profile
SO181-2-8	15.02.05	15:32	37° 55.76' S	75° 3.82' W	End Profile
SO181-2-9	18.02.05	09:24	37° 20.02' S	76° 49.49' W	Begin Profile
SO181-2-9	18.02.05	12:13	37° 29.83' S	76° 15.84' W	End Profile
SO181-2-10	18.02.05	12:13	37° 30.16' S	76° 15.46' W	Begin Profile
SO181-2-10	18.02.05	18:19	38° 30.03' S	76° 19.94' W	End Profile
SO181-2-11	18.02.05	18:40	38° 32.27' S	76° 14.34' W	Begin Profile
SO181-2-11	19.02.05	03:16	39° 12.78' S	74° 33.10' W	End Profile
SO181-2-12	22.02.05	01:28	37° 33.62' S	75° 45.95' W	Begin Profile
SO181-2-12	22.02.05	06:21	36° 42.54' S	75° 31.13' W	End Profile
SO181-2-13	22.02.05	07:32	36° 35.18' S	75° 43.17' W	Begin Profile
SO181-2-13	22.02.05	13:47	37° 36.00' S	76° 7.04' W	End Profile
SO181-2-14	22.01.05	17:56	37° 39.97' S	76° 8.74' W	Begin-Profile
SO181-2-14	22.01.05	19:07	37° 46.85' S	76° 19.85' W	End-Profile
SO181-2-15	22.01.05	19:07	37° 46.89' S	76° 20.44' W	Begin-Profile
SO181-2-15	22.01.05	21:03	37° 42.19' S	76° 44.08' W	End-Profile
SO181-2-16	22.01.05	21:03	37° 42.27' S	76° 44.59' W	Begin-Profile
SO181-2-16	22.01.05	21:48	37° 49.63' S	76° 42.15' W	End-Profile
SO181-2-17	22.01.05	21:48	37° 49.99' S	76° 41.83' W	Begin-Profile
SO181-2-17	22.01.05	23:32	37° 56.00' S	76° 19.87' W	End-Profile
SO181-2-18	22.01.05	23:32	37° 55.96' S	76° 19.25' W	Begin-Profile
SO181-2-18	23.01.05	01:18	37° 39.66' S	76° 8.28' W	End-Profile
SO181-2-19	23.01.05	02:30	37° 33.53' S	76° 9.33' W	Begin-Profile
SO181-2-19	23.01.05	16:13	35° 10.15' S	75° 22.85' W	End-Profile
SO181-2-20	23.01.05	16:14	35° 10.01' S	75° 22.29' W	Begin-Profile
SO181-2-20	24.01.05	01:24	35° 10.97' S	73° 23.88' W	End-Profile

APPENDIX 9.2.1

TIPTEQ

SO181 - Outer Rise Seismology

INST.	LAT (S)	Lon (W)	DIST.	DEPTH	REL.	ANT.	REC.	SKEW	SENSORS	POSITION AFTER RELOBS	
	D:M	D:M	NEXT	(m)	CODE	CH.	NO.	(ms)		LAT (S) [D:M]	Lon (E) [D:M]
OBS 01	42° 41.491'	76° 39.690'	8.098	3543	0387+0355	D	990701	73	OAS 21, WEBB 2329	42° 41.536'	76° 39.681'
OBS 02	42° 49.576'	76° 38.285'	8.092	3526	03BD+0355	D	010402	-390	OAS 75	42° 49.555'	76° 38.339'
OBS 03	42° 57.538'	76° 36.713'	8.091	3537	03BC+0355	D	991238	n.d.	OAS 05, OWEN 63	42° 57.540'	76° 36.708'
OBS 04	43° 05.616'	76° 35.036'	8.109	3524	0386+0355	C	010409	6	DPG 87, WEBB 2352	43° 05.446'	76° 35.084'
OBS 05	43° 04.395'	76° 24.070'	8.098	3566	03B7+0355	C	00711	-89	Hydr. 2, OWEN 62	43° 04.389'	76° 24.151'
OBS 06	42° 56.400'	76° 25.700'	8.092	3559	6B34	B	020301	n.d.	Hydr.HH 5	42° 56.412'	76° 25.710'
OBS 07	42° 48.400'	76° 27.312'	8.099	3555	3609	C	991256	-78	OAS 30, OWEN 59	42° 48.312'	76° 27.338'
OBS 08	42° 40.385'	76° 29.013'	8.121	3553	3624	D	991247	61	OAS 44, OWEN 26	42° 40.380'	76° 29.022'
OBS 09	42° 39.112'	76° 18.039'	8.093	3590	03B8+0355	C	991242	0	DPG 75, WEBB 2353	42° 39.316'	76° 18.005'
OBS 10	42° 47.191'	76° 16.462'	8.092	3627	3614	D	030902	-24	OAS 06	42° 47.176'	76° 16.461'
OBS 11	42° 55.166'	76° 14.866'	8.092	3616	0206+0255	C	000704	n.d.	Hydr.HH 02	42° 55.170'	76° 14.808'
OBS 12	43° 03.152'	76° 13.164'	8.548	3590	3679	D	991259	-108	OAS 15, WEBB 1625	43° 03.323'	76° 13.158'
OBS 13	43° 10.010'	76° 06.000'	7.359	3613	0208+0255	B	000702	150	Hydr.HH 4	43° 10.004'	76° 05.966'
OBS 14	43° 11.033'	76° 16.479'	7.361	3559	0207+0255	C	000714	-40	Hydr.HH 7	43° 10.976'	76° 16.029'
OBS 15	43° 12.070'	76° 26.650'	7.357	3530	03B5+0355	C	00706	113	OAS 3, WEBB 2328	43° 12.000'	76° 25.980'
OBS 16	43° 13.006'	76° 35.991'	7.355	3511	03B6+0355	C	991249	174	OAS32	43° 12.991'	76° 35.923'
OBS 17	43° 14.000'	76° 45.950'		3504	3674	D	991251	-17	HTI 63	43° 13.997'	76° 45.956'
OBS 18	44° 36.475'	76° 56.946'	8.092	3074	133664	C	991235	88	HTI 61, OWEN 19		
OBS 19	44° 44.353'	76° 53.893'	8.091	2787	3629	B	991236	-67	OAS 07		
OBS 20	44° 52.052'	76° 50.732'	8.075	3025	133736	C	010403	7109	OAS 45, OWEN 27		
OBS 21	44° 59.829'	76° 47.588'	8.077	3106	133525	D	991246	-75	OAS 37, OWEN 24		
OBS 22	44° 57.609'	76° 36.657'	8.096	3262	250177	D	040804	15	OAS 35, OWEN 41	44°57.576'	76°36.678'
OBS 23	44° 49.868'	76° 39.707'	8.097	3237	134037	D	040806	11	OAS 29, OWEN 29	44°49.986'	76°39.654'
OBS 24	44° 42.030'	76° 42.777'	8.087	3221	131317	D	040805	27	OAS 17, OWEN 20	44°42.030'	76°42.780'
OBS 25	44° 34.326'	76° 45.926'	8.099	3029	133563	D	010405	4	HTI 28, OWEN 60	44°34.326'	76°45.924'
OBS 26	44° 32.086'	76° 35.073'	8.093	3017	133770	C	040101	n.d.	HTI 43, OWEN 40		
OBS 27	44° 39.923'	76° 31.789'	8.098	3240	134071	A	010401	-163	HTI 37, OWEN 10		
OBS 28	44° 47.647'	76° 28.630'	8.090	3255	0209+0255	B	030506	109	Hydr.HH 06		
OBS 29	44° 53.373'	76° 25.557'		3263	131415	D	040807	18	OAS 4, OWEN 57		

APPENDIX 9.2.2

TIPTEQ

SO181 - Profile P05

INST.	LAT (S)	LONG (W)	DIST.	DEPTH	REL.	ANT.	REC.	SKEW	SENSORS	POSITION AFTER RELOSS	
	D:M	D:M	NEXT	(m)	CODE	CH.	NO.	(mg)		LAT (N) (D:M)	LONG (W) (D:M)
OBH 30	42° 44.510'	74° 45.001'	2,976	130	0397+0355	A	980906	10	HTI 21	42° 44.510'	74° 45.001'
OBH 31	42° 44.573'	74° 49.028'	2,976	193	C454	D	971201	-17	HTI 39	42° 44.573'	74° 49.028'
OBH 32	42° 45.456'	74° 52.881'	2,976	456	3A06	C	991292	-10	HTI 29	42° 45.451'	74° 52.838'
OBH 33	42° 45.927'	74° 57.023'	2,975	769	6354	B	010708	-1	HTI 36	42° 45.922'	74° 56.981'
OBH 34	42° 46.405'	75° 01.020'	2,975	844	D634		020503	12	HTI 66	42° 46.405'	75° 01.020'
OBH 35	42° 46.880'	75° 04.987'	2,975	1107	B219	C	000661	-21	HTI 60	42° 46.874'	75° 04.934'
OBH 37	42° 47.405'	75° 09.002'	2,974	1133	3659	D	020507	59	HTI 54	42° 47.402'	75° 08.977'
OBH 38	42° 47.865'	75° 12.911'	2,974	1795	03BB+0355	A	980908	5	HTI 67	42° 47.843'	75° 12.886'
OBH 38	42° 48.362'	75° 17.021'	2,973	2200	03BA+0355	D	980907	-2	HTI 53	42° 48.320'	75° 16.996'
OBH 39	42° 48.810'	75° 20.914'	2,973	2373	A319	C	010703	-13	HTI 59	42° 48.789'	75° 20.907'
OBH 40	42° 49.257'	75° 24.953'	2,973	3191	6334	C	001005	17	HTI 27	42° 49.233'	75° 24.924'
OBH 41	42° 49.773'	75° 29.026'	2,972	3707	C444	C	980901	36	HTI 23	42° 49.728'	75° 28.997'
OBS 42	42° 50.253'	75° 33.027'	2,972	3741	9295	D	000610	-16	HTI 12, OWEN 64	42° 50.190'	75° 33.030'
OBS 43	42° 50.762'	75° 37.102'	2,972	3745	9256	D	980902	10	OAS 22, OWEN 25	42° 50.727'	75° 37.116'
OBS 44	42° 51.223'	75° 41.029'	2,971	3741	3619	B	990712	-12	OAS 25, OWEN 3	42° 51.187'	75° 41.067'
OBS 45	42° 51.693'	75° 45.081'	2,971	3738	03B1+0355	D	031002	n.d.	OAS 13, OWEN 56	42° 51.627'	75° 45.133'
OBS 46	42° 52.189'	75° 49.109'	2,970	3740	9252	C	020506	45	OAS 74, OWEN 54	42° 52.194'	75° 49.148'
OBS 47	42° 52.628'	75° 53.079'	2,970	3732	9285	D	030901	2	HTI 47, OWEN 39	42° 52.642'	75° 53.192'
OBS 48	42° 53.145'	75° 57.030'	2,970	3725	133477	D	031001	9	HTI 42, OWEN 5	42° 53.164'	75° 57.177'
OBS 49	42° 53.627'	76° 01.072'	2,969	3720	131245	C	000614	-27	HTI 41, OWEN 9	42° 53.664'	76° 01.391'
OBS 50	42° 54.100'	76° 04.998'	2,969	3684	131203	C	980901	-9	HTI 35, OWEN 37	42° 54.100'	76° 04.998'
OBS 51	42° 54.576'	76° 09.017'	2,969	3633	133622	D	010791	-45	HTI 25, OWEN 6	42° 54.603'	76° 09.246'
OBH 52	42° 55.042'	76° 13.005'	1,296	3620	6969	C	030904	-3	HTI 34	42° 54.961'	76° 13.153'
OBH 11	42° 55.166'	76° 14.866'	3,160	3616	0206+0255	C	000704	38	Hydr.HH 02	42° 55.045'	76° 14.917'
OBH 53	42° 55.793'	76° 19.012'	4,931	3598	3674	C	030903	1	HTI 63	42° 55.810'	76° 19.149'
OBH 06	42° 56.400'	76° 25.701'	2,496	3559	6b34	B	020301	1	Hydr.HH 5	42° 56.410'	76° 25.709'
OBH 54	42° 56.971'	76° 29.033'	2,967	3547	3614	D	001002	-157	OAS 06	42° 56.981'	76° 29.115'
OBS 55	42° 57.460'	76° 32.990'	2,639	3543	3609	C	010402	-35	OAS 30, OWEN 59	42° 57.460'	76° 32.990'
OBS 03	42° 57.538'	76° 36.713'	1,846	3537	03BC+0355	D	991238	-3.425	OAS 05, OWEN 63	42° 57.540'	76° 36.710'
OBS 56	42° 58.190'	76° 38.980'	4,449	3530	03BD+0355	D	000711	-9	OAS 75, OWEN 61	42° 58.201'	76° 39.069'
OBS 57	42° 58.933'	76° 48.025'	4,448	3526	3624	D	991256	-8	OAS 44, OWEN 26	42° 58.610'	76° 45.162'
OBS 58	42° 54.587'	76° 50.958'	4,447	3522	03B7+0355	C	991247	6	OAS 02, OWEN 52	42° 59.713'	76° 50.883'
OBH 59	43° 00.327'	76° 56.935'	4,446	3520	03B6+0355	D	991249	17	OAS 32	43° 00.329'	76° 56.450'
OBH 60	43° 01.064'	77° 02.984'	4,445	3524	AD654	C	991251	-2	OAS 68	43° 01.064'	77° 02.984'
OBH 61	43° 01.765'	77° 08.912'	4,444	3518	4A49	C	030902	-6	OAS 30	43° 01.772'	77° 08.969'
OBH 62	43° 02.476'	77° 14.947'	4,443	3540	B495	D	990701	-2.322	OAS 38	43° 02.486'	77° 15.033'
OBS 63	43° 03.207'	77° 20.979'	4,443	3553	0386+0355	C	000706	11	OAS 03, WEBB 2352	43° 03.135'	77° 20.428'
OBS 64	43° 03.937'	77° 27.030'	4,442	3556	03B5+0355	C	991242	-5	DPG 75, WEBB 2328	43° 03.943'	77° 27.077'
OBS 65	43° 04.646'	77° 32.996'	4,441	3554	3679	D	991259	-10	OAS 15, WEBB 1695	43° 04.651'	77° 33.038'
OBS 66	43° 05.382'	77° 39.005'	4,440	3563	03B8+0355	C	010409	1	DGP 86, WEBB 2353	43° 05.387'	77° 39.048'
OBH 67	43° 06.095'	77° 45.006'	4,439	3559	0208+0255	B	991293	-28	OAS HH 04	43° 06.095'	77° 45.006'
OBH 68	43° 06.823'	77° 51.025'	4,438	3527	0207+0255	C	000201	-8	OAS HH 07	43° 06.823'	77° 51.026'
OBH 69	43° 07.593'	77° 57.001'		3596	0387+0355	D	991243	3	OAS 28	43° 07.593'	77° 57.001'

APPENDIX 9.2.3

TIPTEQ

SO81 - Profile P07

INST.	LAT (S)	LON (E)	DIST.	DEPTH	REL.	ANT.	REC.	SKEW	SENSORS	POSITION AFTER RELOBS	
	D:M	D:M	N(E)T	(m)	CODE	CH.	NO.	(m)		LAT (S) [D:M]	LON (E) [D:M]
OBS 112	47° 17.600'	74° 31.041'	2.744	75	133563	D	031002	-5.5	HTI 28, Owen 60	47° 17.600'	74° 31.021'
OBS 113	47° 17.976'	74° 34.947'	2.744	114	131415	C	000614	-17	HTI 43, Owen 40	47° 17.975'	74° 34.919'
OBS 114	47° 18.403'	74° 38.983'	2.744	140	133525	D	030901	3	OAS 35, Owen 41	47° 18.405'	74° 38.901'
OBS 115	47° 18.812'	74° 43.001'	2.743	152	131203	D	990712	-3	HTI 04, Owen 37	47° 18.807'	74° 42.950'
OBS 116	47° 19.000'	74° 47.000'	2.742	160	133664	D	030904	-1,584	HTI 37, Owen 10	47° 19.263'	74° 46.995'
OBS 117	47° 19.600'	74° 51.000'	2.742	173	133770	D	001005	7	OAS 37, Owen 24	47° 19.637'	74° 50.948'
OBS 118	47° 20.070'	74° 54.970'	2.742	162	250177	D	030902	-6	OAS 17, Owen 20	47° 20.069'	74° 54.955'
OBS 119	47° 20.460'	74° 54.000'	2.741	108	134071	D	020506	30	OAS 29, Owen 29	47° 20.478'	74° 58.980'
OBS 120	47° 20.746'	75° 02.792'	2.741	102	134037	C	990901	-3	OAS 45, Owen 27	47° 20.877'	75° 02.971'
OBS 121	47° 21.300'	75° 07.000'	2.740	90	133622	C	030903	3,625	HTI 61, Owen 19	47° 21.296'	75° 06.958'
OBH 122	47° 21.723'	75° 11.021'	2.740	87	0208+0255	B	000201	-7	HH-blue	47° 21.723'	75° 11.020'
OBH 123	47° 22.084'	75° 15.081'	2.740	93	0207+0255	C	980401	-15	HH-yellow	47° 22.049'	75° 15.095'
OBH 124	47° 22.535'	75° 18.991'	2.739	97	0206+0255	B	000612	-9	HH-yellow	47° 22.543'	75° 19.061'
OBH 125	47° 22.919'	75° 23.041'	2.739	103	03B5+0355	A	001002	-10	HTI 45	47° 22.919'	75° 23.093'
OBH 126	47° 23.366'	75° 27.078'	2.739	122	B495	C	991243	2	HTI-38	47° 23.364'	75° 27.056'
OBH 127	47° 23.762'	75° 31.021'	2.738	153	4A49	D	991236	-5	HTI-30	47° 23.725'	75° 31.016'
OBH 128	47° 24.188'	75° 35.041'	2.738	897	3674	D	020503	9	HTI-68	47° 24.188'	75° 35.041'
OBH 129	47° 24.587'	75° 39.013'	2.738	1320	03B7+0355	C	991249	12	OAS-32	47° 24.587'	75° 39.013'
OBH 130	47° 25.003'	75° 43.124'	2.737	1759	03BC+0355	B	991251	-2	OAS-06	47° 25.000'	75° 43.095'
OBH 131	47° 25.394'	75° 46.941'	2.737	2038	3624	C	990701	4	HTI-63	47° 25.392'	75° 46.918'
OBH 132	47° 25.809'	75° 50.994'	2.737	2211	6969	C	020507	45	HTI-34	47° 25.805'	75° 50.958'
OBH 133	47° 26.265'	75° 55.026'	2.736	2308	C444	D	000611	-17	HTI-23	47° 26.265'	75° 54.985'
OBS 134	47° 26.642'	75° 59.031'	2.740	1607	131317	D	031001	3,4	HTI 25, Owen 06	47° 26.686'	75° 58.967'
OBS 135	47° 27.081'	76° 03.027'	2.736	2401	D654	C	010701	-31	OAS 30, Owen 59	47° 27.081'	76° 03.027'
OBS 136	47° 27.465'	76° 07.610'	2.735	2790	3609	C	991235	5	OAS 50, Owen 63	47° 27.461'	76° 07.024'
OBS 137	47° 27.925'	76° 11.014'	2.735	3143	133477	C	000610	-11	HTI 35, Owen 36	47° 27.924'	76° 11.004'
OBH 138	47° 28.325'	76° 15.040'	2.735	3306	6334	D	000711	-6	HTI	47° 28.321'	76° 14.996'
OBH 139	47° 28.730'	76° 18.981'	2.734	3470	A317	C	040806	2	HTI 59	47° 28.725'	76° 19.033'
OBH 140	47° 29.069'	76° 22.991'	2.734	3638	03BA+0355	D	040804	-1	HTI 53	47° 29.069'	76° 22.991'
OBH 141	47° 29.535'	76° 26.957'	2.734	3686	03BB+0355	C	010405	0	HIT 67	47° 29.535'	76° 26.957'
OBH 142	47° 29.950'	76° 30.999'	2.733	3672	3659	A	991247	n.d.	HTI 24	47° 29.950'	76° 30.999'
OBH 143	47° 30.332'	76° 34.973'	2.733	3731	B291	D	010403	7	HTI 60	47° 30.332'	76° 34.973'
OBH 144	47° 30.740'	76° 38.975'	2.732	3778	D634	D	040101	-800	HTI 66	47° 30.738'	76° 38.943'
OBS 145	47° 31.157'	76° 43.000'	2.732	3828	131245	D	010401	-10	HTI 42, Owen 17	47° 31.151'	76° 42.931'
OBS 146	47° 52.804'	76° 80.105'	2.733	3759	03B1+0355	C	040807	1	HTI 41, Owen 9	47° 31.538'	76° 46.965'
OBS 147	47° 31.992'	76° 50.974'	2.732	3758	03BD+0355	C	991238	-5	OAS 2, Owen 62	47° 31.990'	76° 50.957'
OBS 148	47° 32.409'	76° 54.962'	2.731	3615	03B6+0355	C	991246	-4	OAS 44, Owen 26	47° 32.409'	76° 54.955'
OBS 149	47° 32.816'	76° 59.041'	2.731	3600	03B6+0355	D	991256	-26	OAS 75, Owen 1461	47° 32.815'	76° 59.026'
OBS 150	47° 33.247'	77° 03.024'	2.730	3500	0397+0355	D	040805	1	OAS 12, Seismo001	47° 33.247'	77° 03.024'
OBS 151	47° 33.656'	77° 07.036'	2.730	3335	0387+0355	D	000613	-27	HTI 47, Owen 15	47° 33.656'	77° 07.036'
OBS 152	47° 34.047'	77° 10.990'	2.730	3572	03B8+0355	D	980902	7	OAS 13, Owen 56	47° 34.047'	77° 10.990'
OBS 153	47° 34.478'	77° 15.112'	2.729	3545	3629	C	010409	4	DPG 86, Webb 2353	47° 34.478'	77° 15.112'
OBS 154	47° 34.879'	77° 19.004'	2.729	3544	133736	C	991242	-3	DPG 75, Webb 2328	47° 34.878'	77° 18.997'
OBS 155	47° 35.273'	77° 22.982'	2.729	3521	3679	D	010703	-11	OAS 22, Owen 25	47° 35.273'	77° 22.982'
OBS 156	47° 35.707'	77° 27.047'		3571	3614	B	991259	-8	OAS 25, Owen 3	47° 35.707'	77° 27.047'

INST.	LAT (S) D-M	LONG (E) D-M	DIST. NEXT	DEPTH (m)	REL. CODE	ANT. CH.	REQ. NO.	SKW (mm)	SENSORS	POSITION AFTER RELEASE LAT (S) D-M LONG (E) D-M
OBH 157	45° 10.490'	74° 34.991'	3.064	74	133770	D	030903	-1917	OAS 37, Owen 24	45° 10.479' 74° 34.978'
OBH 158	45° 11.677'	74° 39.010'	3.063	85	250177	D	031002	-5.167	OAS 71	45° 11.673' 74° 38.995'
OBH 159	45° 12.862'	74° 43.021'	3.010	98	133664	D	030904	1.5	HTI 71, Owen 10	45° 12.840' 74° 43.021'
OBH 160	45° 14.071'	74° 47.061'	3.047	113	134037	C	030901	3.66	OAS 45, Owen 27	45° 14.064' 74° 47.041'
OBH 161	45° 15.253'	74° 51.004'	3.057	137	134071	D	030902	-3.209	OAS 29, Owen 29	45° 15.254' 74° 51.006'
OBH 162	45° 16.471'	74° 55.059'	3.060	270	131245	C	010701	-26	OAS 28, Owen 36	45° 16.466' 74° 55.042'
OBH 163	45° 17.649'	74° 59.021'	3.060	387	133477	C	020506	28	HTI 53, Owen 30	45° 17.639' 74° 58.988'
OBH 164	45° 18.857'	75° 03.035'	3.060	350	131351	D	990712	-3	HTI 04 Owen 57	45° 18.857' 75° 03.035'
OBH 165	45° 20.060'	75° 07.033'	3.050	137	131317	D	010703	-9	HTI 25, Owen 6	45° 20.051' 75° 07.002'
OBH 166	45° 21.237'	75° 11.030'	3.060	126	131203	D	001002	-10	OAS 04, Owen 37	45° 21.234' 75° 11.021'
OBH 167	45° 22.434'	75° 14.943'	3.060	130	133622	C	990901	-3	HTI 61, Owen 19	45° 22.432' 75° 14.934'
OBH 168	45° 23.630'	75° 18.992'	3.050	147	133563	D	000613	-24	HTI 28, Owen 1460	45° 23.629' 75° 18.988'
OBH 169	45° 24.799'	75° 22.980'	3.050	230	133525	D	980902	5	OAS 35, Owen 41	45° 24.806' 75° 23.003'
OBH 170	45° 25.989'	75° 26.994'	3.040	354	131415	C	000614	-16	HTI 43, Owen 40	45° 25.962' 75° 26.904'
OBH 171	45° 27.150'	75° 30.982'	3.050	614	D634	D	991259	-7	HTI 66	45° 27.145' 75° 30.964'
OBH 172	45° 28.384'	75° 35.000'	3.050	846	B219	D	991243	2	HTI 60	45° 28.377' 75° 34.975'
OBH 173	45° 29.567'	75° 38.980'	3.040	1032	0206+0255	B	000612 (HH)	-10	OAS 6 (HH)	45° 29.594' 75° 39.073'
OBH 174	45° 30.769'	75° 42.965'	3.050	1272	0207+0255	C	980401 (HH)	-13	OAS 11 (HH)	45° 30.761' 75° 42.939'
OBH 175	45° 31.893'	75° 46.956'	3.040	1923	03B7+0355	D	991256	-2	OAS 32	45° 31.887' 75° 46.936'
OBH 176	45° 33.105'	75° 50.986'	3.040	2590	3674	C	031001	-3.250	OAS 74	45° 33.086' 75° 50.921'
OBH 177	45° 34.275'	75° 54.986'	3.040	3049	4A49	D	010405	2	HTI 30	45° 34.262' 75° 54.892'
OBH 178	45° 35.478'	75° 59.032'	3.040	3317	B495	C	991246	-4	HTI 38	45° 35.478' 75° 59.032'
OBH 179	45° 36.643'	76° 03.018'	3.040	3310	03B5+0355	C	991238	-3	HTI 45	45° 36.617' 76° 02.932'
OBH 180	45° 37.848'	76° 07.026'	3.040	3290	6354	B	040806	2	OAS 36	45° 37.827' 76° 06.956'
OBH 181	45° 39.022'	76° 11.026'	3.040	3018	3A06	A	991235	3	HTI 29	45° 39.009' 76° 10.981'
OBH 182	45° 40.256'	76° 15.019'	3.040	2504	C454	C	990701	4	HTI 39	45° 40.240' 76° 14.964'
OBH 183	45° 41.438'	76° 19.023'	3.030	2978	03B1+0355	D	000711	n.d.	HTI 21	45° 41.426' 76° 18.979'
OBH 184	45° 42.604'	76° 22.991'	3.040	2622	3659	A	040804	1	HTI 24	45° 42.372' 76° 23.076'
OBH 185	45° 43.757'	76° 27.008'	3.020	2341	03BB+0355	D	010401	-8	OAS 67	45° 43.740' 76° 26.949'
OBH 186	45° 44.932'	76° 30.993'	3.040	2306	03BA+0355	D	040807	1	HTI 53	45° 44.912' 76° 30.930'
OBH 187	45° 46.133'	76° 35.034'	3.030	2678	A319	B	040101	1	HTI 59	45° 46.113' 76° 34.965'
OBH 188	45° 47.324'	76° 39.053'	3.030	2816	6334	D	040805	3	HTI 27	45° 47.324' 76° 39.053'
OBH 189	45° 48.516'	76° 43.026'	3.030	3411	C444	C	991251	-2	HTI 23	45° 48.516' 76° 43.009'
OBH 190	45° 49.689'	76° 46.998'	3.030	3755	6969	D	010403	6	HTI 34	45° 49.689' 76° 46.998'
OBH 191	45° 50.863'	76° 50.992'	3.030	2492	3624	D	010402	-25	HTI 63	45° 50.863' 76° 50.992'
OBH 192	45° 52.031'	76° 55.003'	3.020	2195	03BC+0355	D	991249	12	OAS 06	45° 52.036' 76° 55.019'
OBH 193	45° 53.211'	76° 59.063'		2481	03B7+0355	D	001005	11	HTI 47, Owen 15	45° 53.211' 76° 59.063'

INST.	LAT (S)	LONG (E)	DIST.	DEPTH	REL.	ANT.	REC.	SKEW	SENSORS	POSITION AFTER RELISS	
	D:M	D:M								NEXT	(m)
OBS 70	44 15.413'	74 32.023'	2.980	62	250177	D	031001	-0.375	OAS 17, Owen 20	44° 15.413'	74° 32.023'
OBS 71	44 16.246'	74 36.026'	2.979	86	134037	C	030901	5.166	OAS 45, Owen 27	44° 16.248'	74° 36.038'
OBS 72	44 17.087'	74 40.011'	2.976	58	133477	C	030903	0.833	HTI 35, Owen-15Hz 30	44° 17.087'	74° 40.011'
OBS 73	44 17.869'	74 44.038'	2.978	48	131351	D	031002	-4.417	HTI 42, Owen 17	44° 17.869'	74° 44.038'
OBS 74	44 18.687'	74 47.484'	2.974	45	133525	D	030904	-1.250	OAS 35, Owen 41	44° 18.687'	74° 47.484'
OBS 75	44 19.479'	74 52.010'	2.976	47	131317	D	030902	-2.750	HTI 25, Owen 6	44° 19.479'	74° 52.010'
OBS 76	44 20.305'	74 56.017'	2.973	86	133622	C	010703	-10	HTI 61, Owen 19	44° 20.306'	74° 56.025'
OBS 77	44 21.121'	75 00.021'	2.947	149	131203	D	990712	-3	HTI 04, Owen 57	44° 21.120'	75° 00.013'
OBS 78	44 21.910'	75 04.004'	2.973	167	133664	D	010701	-31	HTI 37, Owen 10	44° 21.904'	75° 03.979'
OBS 79	44 22.708'	75 07.983'	2.972	129	134071	D	020506	34	OAS 29, Owen 29	44° 22.702'	75° 07.952'
OBS 80	44 23.531'	75 11.964'	2.972	128	131245	C	000613	-27	OAS 28, Owen 36	44° 23.529'	75° 11.955'
OBS 81	44 24.337'	75 15.984'	2.971	181	133563	D	001005	8	HTI 128, Owen 60	44° 24.317'	75° 15.886'
OBS 82	44 25.182'	75 19.991'	2.971	381	131415	C	001002	-12	HTI 43, Owen 40	44° 25.178'	75° 19.974'
OBS 83	44 26.026'	75 24.007'	2.970	1079	133736	D	991237	-5	HTI 54, Owen 64	44° 26.015'	75° 23.987'
OBS 84	44 26.817'	75 28.024'	2.969	1353	133770	D	000614	-21	OAS 37, Owen 24	44° 26.807'	75° 28.021'
OBS 85	44 27.609'	75 32.013'	2.97	1163	03BC+0355	D	991246	-4	OAS 06	44° 27.609'	75° 32.013'
OBS 86	44 28.442'	75 36.013'	2.97	898	3624	C	991238	-5	HTI 63	44° 28.442'	75° 36.013'
OBS 87	44 29.271'	75 39.985'	2.96	1612	6969	B	010405	2	HTI 34	44° 29.272'	75° 39.989'
OBS 88	44 30.071'	75 44.017'	2.97	2626	C444	D	991259	n.d.	HTI 23	44° 30.014'	75° 44.048'
OBS 89	44 30.881'	75 47.984'	2.96	3316	0206+0255	B	000612	-15	OAS 6 (HH)	44° 30.893'	75° 48.044'
OBS 90	44 31.691'	75 51.979'	2.97	3323	0207+0255	C	980903	5	OAS 11 (HH)	44° 31.691'	75° 51.979'
OBS 91	44 32.532'	75 55.997'	2.97	3309	6B34	B	001006	-155	OAS 5 (HH)	44° 32.532'	75° 55.997'
OBS 92	44 33.356'	75 59.996'	2.97	3325	0208+0255	B	000201	n.d.	(HH)	44° 33.356'	75° 59.996'
OBS 93	44 34.404'	76 05.028'	3.71	3297	0209+0255	C	(Tsunami)	2	(HH)	44° 34.365'	76° 04.982'
OBS 94	44 35.407'	76 09.951'	3.703	3278	6334	A	020507	51	HTI 27	44° 35.407'	76° 09.951'
OBS 95	44 36.453'	76 14.998'	3.702	3237	A319	D	980908	5	HTI 59	44° 36.463'	76° 15.046'
OBS 96	44 37.449'	76 20.006'	3.701	3245	03BA+0355	C	000611	n.d.	HTI 53	44° 37.460'	76° 20.062'
OBS 97	44 38.466'	76 24.976'	3.7	3232	03BB+0355	D	980907	-2	HTI 67	44° 38.668'	76° 24.973'
OBS 98	44 39.460'	76 29.971'	3.698	3252	3659	C	990701	5	HTI 24	44° 39.473'	76° 30.034'
OBS 99	44 40.489'	76 34.995'	3.697	3130	03B1+0355	D	010403	7	HTI 21	44° 40.493'	76° 35.013'
OBS 100	44 41.511'	76 39.985'	3.696	3012	C454	B	010402	-30	HTI 39	44° 41.520'	76° 40.026'
OBS 101	44 42.526'	76 45.003'	3.695	3211	3A06	C	040804	1	HTI 29	44° 42.530'	76° 45.027'
OBS 102	44 43.540'	76 49.986'	3.694	2971	6354	C	010401	-11	OAS 36	44° 43.536'	76° 49.970'
OBS 103	44 44.544'	76 55.004'	3.693	2955	03B5+0355	D	000711	-7	HTI 45	44° 44.511'	76° 55.006'
OBS 104	44 45.546'	76 59.991'	3.695	3069	B495	C	040806	2	HTI 38	44° 45.546'	76° 59.991'
OBS 105	44 46.600'	77 04.993'	3.691	2961.5	4A49	D	991235	4	HTI 30	44° 46.629'	77° 04.968'
OBS 106	44 47.622'	77 09.997'	3.690	2929	3674	D	991243	3	OAS 74	44° 47.686'	77° 09.947'
OBS 107	44 48.606'	77 14.972'	3.689	2969	03B7+0355	D	991256	-4	OAS 32	44° 48.634'	77° 14.943'
OBS 108	44 49.638'	77 20.021'	3.689	3285	B219	A	040805	2	HTI 60	44° 49.638'	77° 20.021'
OBS 109	44 50.675'	77 25.007'	3.686	2933	D634	D	991249	14	HTI 66	44° 50.641'	77° 25.007'
OBS 110	44 51.670'	77 30.007'	3.686	2860	03B7+0355	A	980902	8	HTI 47, Owen-15Hz 39	44° 51.667'	77° 29.993'
OBS 111	44 52.678'	77 35.018'	3.684	2510	3679	C	040807	1	OAS 22, Owen 25	44° 52.676'	77° 35.009'
OBS 194	44 53.676'	77 40.008'	3.683	3060	3614	D	040101	1	OAS 25, Seismo	44° 53.667'	77° 39.993'
OBS 195	44 54.698'	77 45.022'	3.680	3194	03B8+0355	C	000610	n.d.	OAS 13, Owen 56	44° 54.695'	77° 45.007'
OBS 196	44 55.706'	77 50.014'	3.678	2973	D654	C	990901	-6	OAS 30, Owen 59	44° 55.687'	77° 50.001'
OBS 197	44 56.713'	77 55.039'	3.678	2974	3619	A	980906	8	OAS 50, Owen 54	44° 56.709'	77° 55.015'
OBS 198	44 57.715'	78 00.015'	3.677	2828	03B6+0355	C	991292	77	OAS 75, Owen 61	44° 57.715'	78° 00.015'
OBS 199	44 58.716'	78 05.001'	3.675	2499	03BD+0355	D	980901	27	OAS 2, Owen 62	44° 58.695'	78° 04.979'
OBS 200	44 59.721'	78 10.080'	3.677	3548	03B6+0355	C	030905	3.833	OAS 44, Owen 26	44° 59.715'	78° 10.001'
OBS 201	45 00.733'	78 15.053'		2782	3609	D	991236	-2	OAS 12, Owen 63	45° 00.733'	78° 15.053'

INST.	LAT (S)	LOX (E)	DIST.	DEPTH	REL.	ANT.	REC.	SKEW	SENSORS	POSITION AFTER RELOBS	
	D:M	D:M	NEXT	(m)	CODE	CH.	NO.	(ms)		LAT (S) D:M	LOX (E) D:M
OBS 222	37° 54.052'	75° 00.024'	3.277	4515	133622	C	980901	18	HTI 61, Owen 19	37°54.0215'	75°00.164'
OBS 223	37° 53.154'	75° 04.009'	3.278	4411	250177	D	031002	-9.375	OAS 17, Owen 20	37°53.1428'	75°04.060'
OBS 224	37° 52.282'	75° 08.018'	3.278	4399	134037	C	020506	23	OAS 43, Owen 27	37°52.289'	75°7.98167'
OBS 225	37° 51.410'	75° 12.008'	3.279	4298	133664	D	020501	3	HTI 37, Owen	37°51.393'	75°12.087'
OBS 226	37° 50.519'	75° 15.991'	3.279	4201	134071	D	030905	2.125	OAS 29, Owen 29	37°50.507'	75°16.045'
OBS 227	37° 49.635'	75° 19.987'	3.280	4112	133563	D	001002	-6	HTI 28, Owen 60	37°49.625'	75°20.028'
OBS 228	37° 48.768'	75° 23.992'	3.281	4173	131245	C	991292	-5	OAS 28, Owen 36	37°48.927'	75°24.027'
OBS 229	37° 47.882'	75° 27.982'	3.281	4052	133525	D	010701	-22	OAS 35, Owen 41	37°47.894'	75°27.929'
OBS 230	37° 47.017'	75° 31.994'	3.282	4199	131351	D	000613	-19	HTI 42, Owen 5	37°47.032'	75°31.924'
OBS 231	37° 46.136'	75° 35.993'	3.282	4034	131317	D	990901	n.d.	HTI 25, Owen 6	37°46.136'	75°35.993'
OBS 232	37° 45.255'	75° 39.986'	3.283	4090	131203	D	030902	-1	OAS 4, Owen 7	37°45.280'	75°39.866'
OBS 233	37° 44.399'	75° 44.007'	3.283	4140	133477	C	020509	7	HTI 35, Owen 37	37°44.384'	75°44.044'
OBS 234	37° 43.525'	75° 47.980'	3.284	4019	131415	C	010703	-6	HTI 43, Owen 40	37°43.547'	75°47.879'
OBS 235	37° 42.624'	75° 52.013'	3.285	4020	133770	D	031001	0.857	OAS 37, Owen 4	37°42.651'	75°51.887'
OBS 236	37° 41.750'	75° 55.970'	3.285	4222	133736	D	991237	-4	HTI 54, Owen 64	37°41.750'	75°55.970'
OBS 237	37° 40.847'	75° 59.996'	3.286	4185	C444	C	040807	1	HTI 60	37°40.858'	75°59.943'
OBS 238	37° 39.967'	76° 04.001'	3.287	4017	B219	C	991252	-2	HTI 30	37°40.006'	76°03.996'
OBS 239	37° 39.081'	76° 08.008'	3.287	4217	4A49	D	001006	-5	HTI 38	37°39.079'	76°08.0145'
OBS 240	37° 38.202'	76° 12.006'	3.288	4205	B495	C	98097	-1	OAS 36	37°38.232'	76°12.0387'
OBS 241	37° 37.316'	76° 16.017'	3.288	4097	6354	C	020503	7	HTI 29	37°37.310'	76°16.044'
OBS 242	37° 36.442'	76° 20.023'	3.289	4116	3A06	D	980908	3	HTI 39	37°36.436'	76°20.049'
OBS 243	37° 35.548'	76° 24.035'	3.290	4218	C454	C	00061	-12	HTI 27	37°35.544'	76°24.0548'
OBS 244	37° 34.635'	76° 28.010'	3.290	4210	6334	C	020507	32	HTI 23	37°34.635'	76°28.010'
OBS 245	37° 33.798'	76° 32.017'	3.291	4064	6969	D	01078	1	HTI 34	37°33.797'	76°32.022'
OBS 246	37° 32.917'	76° 36.025'	3.291	4170	3614	D	030901	1.625	OAS 25, Owen 26	37°32.919'	76°36.012'
OBS 247	37° 32.020'	76° 40.007'	3.292	4139	D654	C	980906	7	OAS 22, Owen 39	37°32.024'	76°39.989'
OBS 248	37° 31.170'	76° 41.000'	3.292	4206	9252	C	980902	4	OAS 44, Owen 59	37°31.170'	76°41.000'
OBS 249	37° 30.278'	76° 48.001'	3.294	4203	9295	D	00614	-13	HTI 47, Owen 1	37°30.286'	76°47.965'
OBS 250	37° 29.410'	76° 52.010'	3.294	4161	9285	D	990712	-6	HTI 68, Owen 0	37°29.422'	76°51.948'

APPENDIX 9.2.7

TIPTEQ

SO181 - Seismology Chiloe and Mocha

INST.	LAT (S)	LON (E)	DIST. TO	DEPTH	REL.	ANT.	REC.	SKEW	SENSORS	POSITION AFTER RELOBS	
	D:M	D:M	NEXT (nm)	(m)	CODE	CH.	NO.	(ms)		LAT (S) [D:M]	LON (E) [D:M]
OBH 202	43°07.965	75°04.964	12.82	1013	3609	C	990701		OAS 74		
OBH 203	42°56.950	74°56.023	13.09	163	3674	A	040804		HTI 45		
OBS 204	43°05.949	74°42.962	13.69	118	0397 + 0355	D	991256		DPG 74, Webb 1695		
OBH 205	42°54.012	74°33.967	13.36	129	03b5 + 0355	C	010401		HTI 21		
OBH 206	42°42.003	74°25.952	21.32	122	03b1 + 0355	A	040101		HTI 24		
OBS 207	42°21.000	74°30.998	13.18	176	3629	D	010409		DPG 86, Webb 2328		
OBH 208	42°24.995	74°48.007	9.940	272	3659	A	991243		HTI-67		
OBH 209	42°32.989	74°40.006	12.48	908	03bb + 0355	C	00711		HTI-53		
OBH 210	42°44.022	74°47.970	12.46	201	03ba + 0355	C	991259		HTI-59		
OBS 211	42°36.024	75°0.977	12.84	1080	a 319	C	010405		OAS-12 Owen-63		
OBH 212	42°46.993	75°10.002	14.92	1186	3624	D	040806		HTI-63		
OBS 213	43°0.026	75°19.999	11.23	2169	3679	D	991235		OAS-15 Owen-62		
OBS 214	43°9.995	75°26.999	13.79	2641	0386-0355	D	010402		OAS 2, Owen 25 (4.5 Hz)		
OBS 215	42°59.992	75°40.009	11.25	3740	0387 + 0355	D	991242		DPG 78, Webb 2329		
OBS 216	42°53.914	75°52.970	14.58	3730	03BD + 0355	B	991238		OAS 13, Owen 56 (4.5 Hz)		
OBS 217	42°41.090	75°44.048	12.59	3751	03B8 - 0355	C	010403		OAS 50, Owen 54 (4.5 Hz)		
OBS 218	42°49.995	75°31.998	12.83	3741	3619	D	991249		OAS 75, Owen 61 (4.5 Hz)		
OBH 219	42°39.009	75°22.980	14.27	2714	03B7 - 0355	B	991246		HTI 66		
OBH 220	42°26.009	75°14.960	11.47	2209	03BC - 0355	D	991236		OAS 06		
OBS 221	42°29.012	75°29.992		3734	03b6 + 0355	D	000706		DPG 91, Webb 2352		
OBS251	38 08.834	73 50.973	14.79	552	0206 + 0255	A	020301		PMD + OAS HH		
OBS252	38 00.010	74 06.020	11.46	1067	0209 + 0255	C	000704		PMD + OAS HH		
OBS253	37 50.940	73 57.040	21.52	610	6B34	B	000714		PMD + OAS HH		
OBS254	37 54.050	74 24.020	12.90	2957	0207 + 0255	C	030506		PMD + OAS HH		
OBH255	38°06:006	74°30:030	13.23	4125	3614	D	040807		OAS 36		
OBH256	38°11:993	74°15:007	12.23	749	6334 Mode B	D	00702		HTI 34		
OBH257	38°23.989	74°11.995	14.43	2259	b495 Mode A	D	030502		HTI 23		
OBH258	38°21.001	74°30.004	13.55	3335	6354 mode B	C	991237		HTI-39		
OBH259	38°09.014	74°38.030	15.00	4664	c454 mode A	C	991251		HTI-27		
OBH260	37°54.034	74°38.187		2957	0204 + 0255	B	040808		OAS HH		

PROFILE NO.	SHOT NO.	DATE UTC	TIME UTC	LAT (S) D:M	LON (W) D:M	PULSE INT.	GUN POSITION	REMARKS
SO181_1a-P01-3	1	12.12.2004	20:51	43°13,910	76°44,461	60 s	B,S	32 liters each
	440	13.12.2004	04:10	43°09,051	76°00,393	60 s		End P01, start turn
	485	13.12.2004	04:55	43°98,454	76°02,000	60 s		End Turn, Start P01b
	595	13.12.2004	06:46	43°04,518	76°12,818	60 s		Start P02
	949	13.12.2004	12:32	42°37,760	76°18,673	60 s		End P02, Start P02b
	1128	13.12.2004	15:31	42°39,167	76°38,938	60 s		Start P03
	1147	13.12.2004	15:49	42°40,164	76°40.010	60 s		lost Streamer
	1693	14.12.2004	00:55	43°20,409	76°29,858	60 s		end P03
SO181-P04	1	15.12.2004	01:26	45:00,0	76°36,000	60 s	S	first Shot
	373	15.12.2004	07:38	44°32,420	76°47,292	60 s		last Shot
SO181_b_SCS01	1	20.12.2004	13:36	42°44.215	74°43.086	10s	S	kurzer Stop Stop- delay-Änderung- 3000ms Profil- Ende
	634	20.12.2004	14:56			10s		
	1694	20.12.2004	18:52	42°48.619	75°18.943	10s		
	11219	21.12.2004	23:04	43°11.42	78°30.15	10s		
SO181_b_SCS02	1	03.01.2005	11:11	44°22.036	75°4.555	10s	S	Profil- Anfang
	1004	03.01.2005	13:32:30	44°25.1515	75°22.904	10s		Kompressor-Wartung
	1015	03.01.2005	14:14	44°26.1	75°24.775	10s		Start
	1949	03.01.2005	16:50	44°29.775	75°42.449	10s		Delay auf 3000 ms
	7371	04.01.2005	07:57	44°49.444	77°19.602	10s		Profil- Ende - Seegang
SO181_b_SCS03	1	09.01.2005	15:10	40°36.549	74°25.088	10s	S	Profil- Anfang
	80	09.01.2005	15:38	40°36.845	74°27.789	10s		Delay auf 40
	1238	09.01.2005	18:41	40°38.854	74°46.422	10s		Kanone defekt
	1253	09.01.2005	20:06	40°38.813	74°46.068	10s		nach Schleife wieder auf Profil
	7358	10.01.2005	13:07	40°51.217	76°40.187	10s		Profil- Ende

Appendix 9.3 AIRGUN SHOTS

PROFILE NO.	SHOT NO.	DATE UTC	TIME UTC	LAT (S) D:M	LON (W) D:M	PULSE INT.	GUN POSITION	REMARKS
SO181_b_SCS04	1	13.01.2005	20:27	36°13.724	73°36.05	10s	S	Profil Anfang
	840	13.01.2005	22:49			10s		Delay auf 3000 ms
	913	13.01.2005	23:02			10s		Delay auf 0 ms
	933	13.01.2005	23:04			10s		Delay auf 3000 ms
	1370	14.01.2005	00:19:12	36°10.593	73°59.525	10s		Delay auf 4000 ms
	1523	14.01.2005	00:44	36°10.24	74°18.102	10s		Delay auf 5000 ms
	5526	14.01.2005	11:51	36°0.772	75°10.170	10s		Profil- Ende
SO181-2-P05	1	23.01.2005	23:31	43°11,059	78°28,912	60s	S, B	Profil- Anfang, 8 guns
	357	24.01.2005	05:27	43°7,320	77°55,410	60s		Druckabfall, 7 guns
	1485	25.01.2005	00:15	42°54,589	76°08,644	60s		Druckabfall, 6 guns
	2668	25.01.2005	19:58	42°40,355	74°13,899	60s		change course
	2733	25.01.2005	21:03	42°36,080	74°16,116	60s		Profil- Ende
SO181-2-P07	1	29.01.2005	19:36	47°36,2	77°32,8	60s	S,B	Profil Anfang, 8 guns
	2433	31.01.2005	12:09	47°14,174	74°31,277	60s		Profil Ende
SO181-2-P08	1	03.02.2005	19:51	45°53,512	77°0,291	60	S,B	Start of line, 8 guns
	156	03.02.2005	22:26	45°50,711	76°50,673	60		sensor 5 broke
	169	03.02.2005	22:27			60		2 short shots in row
	170	03.02.2005	22:40			60		3 & 6 pressure low
	1215	04.02.2005	16:05	45°31,027	75°44,025	60		Stbd away off
	1230	04.02.2005	16:20	45°30,790	75°43,178	60		2 x G-gun array + 32l Bolt
	1287	04.02.2005	17:17	45°29,728	75°39,551	60		Bolt test shot
	1303	04.02.2005	17:32	45°29,438	75°38,558	60		1-5,7,8 & Bolt
	1393	04.02.2005	19:03	45°27,819	75°32,427	60		Stbd off, recover Bolt
	1406	04.02.2005	19:16	45°27,586	75°32,427	60		Both 9 gun arrays
	2414	05.02.2005	12:04	45°36,74	74°30,75	60		End of line

Appendix 9.3 AIRGUN SHOTS

Appendix 9.3 AIRGUN SHOTS

PROFILE NO.	SHOT NO.	DATE UTC	TIME UTC	LAT (S) D:M	LON (W) D:M	PULSE INT.	GUN POSITION	REMARKS
SO181-2-P06	1	08.02.2005	20:42	45°1.316	78°17.45	55	S, B	Start of line, 8 guns
	205	08.02.2005	23:49	44°58.11	78°1.84	50		change of shoting rate
	212	08.02.2005	23:55	44°58.024	78°1.408	45		change of shoting rate
	216	09.02.2005	00:06			40		change of shoting rate
	2011	10.02.2005	20:03	44°14.662	74°31.752	40		4 guns only
	2020	10.02.2005	20:09			40		all 8 guns shoting
	2080	10.02.2005	20:59	44°11.989	74°30.760	40		End of line
SO181-2-P09	1	16.02.2005	06:29	37°27.947	77°07.46	60	S, B	Start of line, 7 guns, gun 6 off
	622	16.02.2005	16:50			55		change of shoting rate
	630	16.02.2005	16:58			50		change of shoting rate
	1980	17.02.2005	11:43	37°57.044	74°45.955	50		End of line

Appendix 9.4.1 TIPTEQ SO181-1B

Station H0401

Pen	Longitude		Latitude		Water Depth	No of sensors used	Tilt	Mean Gradient	Mean thermal conductivity	Mean heatflow	Distance from Deformation Front	Crustal age	Shot point # SCS 01
	Degree	Minutes	Degree	Minutes	[m]		[°]	[K/km]	[W/m K]	[mW/m ²]	[km]	[Ma]	
1	-78	21,952	-43	10,451	-3544	10	0,7	136,2	0,87	119,9	234,7	14	10974
2	-78	22,693	-43	10,523	-3672	11	1,6	108,6	0,86	93,4	235,7	14	10994
3	-78	23,400	-43	10,620	-3595	11	3,7	229,8	0,86	200,6	236,6	14	11012
4	-78	24,142	-43	10,685	-3612	11	1,6	98,1	0,86	84,4	237,7	14	11031
5	-78	24,881	-43	10,760	-3573	10	6,3	146,6	0,86	127,5	238,7	14	11050
6	-78	25,581	-43	10,865	-3534	11	2,2	182,5	0,87	160,9	239,6	14	11067
7	-78	26,347	-43	10,964	-3567	11	1,9	146,5	0,86	126	240,7	14	11086
8	-78	27,082	-43	11,047	-3595	9	7,2	79,1	0,83	64,4	241,7	14	11105
9	-78	27,806	-43	11,149	-3574	10	9,1	147,7	0,86	126,9	242,7	14	11124
10	-78	28,518	-43	11,235	-3585	11	4,9	90,5	0,86	78,6	243,6	14	11142

Appendix 9.4.2 TIPTEQ SO181-1B

Station H0402

Pen	Longitude		Latitude		Water Depth	No of sensors used	Tilt	Mean Gradient	Mean thermal conductivity	Mean heatflow	Distance from Deformation Front	Crustal age	Shot point # SCS 01
	Degree	Minutes	Degree	Minutes	[m]		[°]	[K/km]	[W/m K]	[mW/m²]	[km]	[Ma]	
1	-76	41,731	-42	58,538	-3533	11	0,7	7	0,86	7	97,2	14	5623
2	-76	42,422	-42	58,561	-3530	11	5,5	9	0,87	9	98,1	14	5654
3	-76	43,192	-42	58,657	-3530	11	12,3	13	0,89	13	99,2	14	5689
4	-76	43,913	-42	58,720	-3528	11	5,0	19	0,93	19	100,2	14	5721
5	-76	44,630	-42	58,784	-3528	11	13,0	23	0,95	22	101,2	14	5755
6	-76	45,342	-42	58,909	-3530	11	6,6	50	0,94	45	102,2	14	5789
7	-76	46,087	-42	58,984	-3525	11	7,6	115	0,94	109	103,2	14	5822
8	-76	46,844	-42	59,088	-3526	11	6,7	166	0,94	156	104,2	14	5858
9	-76	47,552	-42	59,167	-3527	11	15,8	169	0,94	160	105,2	14	5891
10	-76	48,278	-42	59,256	-3522	11	8,3	118	0,89	99	106,2	14	5925

Appendix 9.4.3 TIPTEQ SO181-1B

Station H0403

Pen	Longitude		Latitude		Water Depth	No of sensors used	Tilt	Mean Gradient	Mean thermal conductivity	Mean heatflow	Distance from Deformation Front	Crustal age	Shot point # SCS01															
	Degree	Minutes	Degree	Minutes	[m]		[°]	[K/km]	[W/m K]	[mW/m²]	[km]	[Ma]																
1	-75	11,660	-42	47,710	-1583	no penetration due to stiff sediments					n/a	n/a	1358															
2	-75	10,930	-42	47,610	-1423						no penetration due to stiff sediments					n/a	n/a	1339										
3	-75	10,200	-42	47,500	-1236											no penetration due to stiff sediments					n/a	n/a	1320					
4	-75	9,480	-42	47,430	-1146	7	4,5	in situ temperatures disturbed due to bottom water temperature transients		n/a											n/a	1301						
5	-75	8,770	-42	47,350	-1121	3	4,7			n/a	n/a	1282																
6	-75	8,030	-42	47,300	-1123	3	5,5			n/a	n/a	1262																
7	-75	7,290	-42	47,210	-1121	no penetration due to stiff sediments					n/a	n/a	1242															
8	-75	6,530	-42	47,110	-1071						no penetration due to stiff sediments					n/a	n/a	1223										
9	-75	5,790	-42	47,000	-1076											no penetration due to stiff sediments					n/a	n/a	1204					
10	-75	5,060	-42	46,910	-1106																no penetration due to stiff sediments					n/a	n/a	1185
11	-75	4,400	-42	46,820	-1092																					no penetration due to stiff sediments		

Appendix 9.4.4 TIPTEQ SO181-1B

Station H0404

Pen	Longitude		Latitude		Water Depth	No of sensors used	Tilt	Mean Gradient	Mean thermal conductivity	Mean heatflow	Distance from Deformation Front	Crustal age	Shot point # SCS 01	Sediment Thickness TWT
	Degree	Minutes	Degree	Minutes	[m]		[°]	[K/km]	[W/m K]	[mW/m²]	[km]	[Ma]		[s]
1	-75	34,670	-42	50,449	-3743	17	0,7	84	0,86	72	5,00	16,0	2252	
2	-75	33,954	-42	50,369	-3742	17	2,2	80	0,84	68	4,00	16,0	2214	
3	-75	33,241	-42	50,280	-3744	17	3,6	75	0,81	62	3,00	16,0	2175	
4	-75	32,498	-42	50,191	-3736	17	1,9	71	0,84	60	2,00	16,0	2135	
5	-75	31,786	-42	50,118	-3736	17	1,1	68	0,87	59	1,00	16,0	2103	
6	-75	31,773	-42	50,108	-3736	17	1,0	66	0,88	59	1,00	16,0	2103	

Appendix 9.4.5 TIPTEQ SO181-1B

Station H0405

Pen	Latitude		Longitude		Water Depth	No of sensors used	Tilt	Mean Gradient	Mean thermal conductivity	Mean heatflow	Distance from Deformation Front	Crustal age	Shot point # CONRAD 743
	Degree	Minutes	Degree	Minutes	[m]		[°]	[K/km]	[W/m K]	[mW/m²]	[km]	[Ma]	
1	-75	52,343	-45	33,854	-2524	9	0,9	72,9	0,92	67,1	-6,4	n/a	
2	-75	53,044	-45	34,059	-2436	13	2,9	50,4	1,04	53,1	-5,4	n/a	
3	-75	53,757	-45	34,256	-2558	3	3,5	60,2	1,16	69,3	-4,4	n/a	
4	-75	54,434	-45	34,419	-2707	10	2	59,6	1,25	74,3	-3,5	n/a	
5	-75	55,192	-45	34,685	-3058	10	8,4	60,1	1,33	77,4	-2,4	n/a	
6	-75	55,781	-45	34,856	-3191	8	3,6	101,4	1,28	129,8	-1,6	n/a	
7	-75	56,527	-45	35,083	-3262	9	4,6	148,2	1,24	184,6	-0,5	n/a	
8	-75	57,365	-45	35,299	-3333	9	5,2	188,5	1,18	222,4	0,6	1,4	
9	-75	58,060	-45	35,527	-3317	8	4,2	196,2	1,13	218,6	1,6	1,4	

Appendix 9.4.6 TIPTEQ SO181-1B

Station H0406

Pen	Longitude		Latitude		Water Depth	No of sensors used	Tilt	Mean Gradient	Mean thermal conductivity	Mean heatflow	Distance from Deformation Front	Crustal age	Shot point # SCS02	Sediment Thickness TWT
	Degree	Minutes	Degree	Minutes	[m]		[°]	[K/km]	[W/m K]	[mW/m²]	[km]	[Ma]		[s]
1	-76	15,180	-44	36,370	-3275	9	1	223,1	1,06	234,3	36,4	n/a	3613	
2	-76	15,880	-44	36,510	-3281	9	3,8	342,6	1,04	356,3	37,3	n/a	3652	
3	-76	16,610	-44	36,680	-3281	8	15,7	395,7	0,98	387,4	38,3	n/a	3694	
4	-76	17,355	-44	36,830	-3332	9	6,5	385,6	0,97	374,0	39,3	n/a	3735	
5	-76	18,076	-44	36,968	-3333	8	14,4	434,5	0,96	420,6	40,3	n/a	3775	
6	-76	18,744	-44	37,074	-3321	8	6	457,1	0,96	438,8	41,2	n/a	3812	
7	-76	19,533	-44	37,281	-3259	no data due to malfunction of heat probe							3856	
8	-76	20,255	-44	37,423	-3247								3898	
9	-76	20,985	-44	37,567	-3238								3941	
10	-76	21,658	-44	37,636	-3231								3980	
11	-76	22,432	-44	37,872	-3235								4026	

Appendix 9.4.7 TIPTEQ SO181-1B

Station H0407

Pen	Longitude		Latitude		Water Depth	No of sensors used	Tilt	Mean Gradient	Mean thermal conductivity	Mean heatflow	Distance from Deformation Front	Crustal age	Shot point # SCS02
	Degree	Minutes	Degree	Minutes	[m]		[°]	[K/km]	[W/m K]	[mW/m ²]	[km]	[Ma]	
1	-75	42,605	-44	29,779	-2355	no penetration due to stiff sediments						n/a	1953
2	-75	43,300	-44	29,900	-2510							n/a	1987
3	-75	44,082	-44	30,043	-2637	9	5,8	63,3	1,05	66,7	-6,4	n/a	2026
4	-75	44,845	-44	30,265	-2957	4	2,3	83,1	1,05	87,3	-5,3	n/a	2064
5	-75	45,489	-44	30,345	-3044	no penetration due to stiff sediments						n/a	2096
6	-75	46,270	-44	30,480	-3218	8	10,3	73,5	1,15	85,0	-3,4	n/a	2134
7	-75	46,945	-44	30,665	-3242	12	2,6	78,1	1,2	93,7	-2,4	n/a	2168
8	-75	47,665	-44	30,799	-3333	10	4,2	90,3	1,18	105,4	-1,4	n/a	2204
9	-75	48,390	-44	30,953	-3317	no penetration due to stiff sediments						n/a	2239
10	-75	49,110	-44	31,092	-3319							n/a	2274

Appendix 9.4.8 TIPTEQ SO181-1B

Station H0408

Pen	Longitude		Latitude		Water Depth	No of sensors used	Tilt	Mean Gradient	Mean thermal conductivity	Mean heatflow	Distance from Deformation Front	Crustal age	Shot point # SCS01
	Degree	Minutes	Degree	Minutes	[m]		[°]	[K/km]	[W/m K]	[mW/m²]	[km]	[Ma]	
1	-76	23,201	-42	56,288	3582	10	0,3	129,5	0,89	118	71,7		4799
2	-76	22,466	-42	56,216	3588	10	3,7	126,2	1,05	133	70,7		4765
3	-76	21,737	-42	56,106	3592	9	3,9	94,4	1,01	95	69,7		4730

Appendix 9.4.9 TIPTEQ SO181-1B

Station H0409

Pen	Longitude		Latitude		Water Depth	No of sensors used	Tilt	Mean Gradient	Mean thermal conductivity	Mean heatflow	Distance from Deformation Front	Crustal age	Shot point # SCS01
	Degree	Minutes	Degree	Minutes	[m]		[°]	[K/km]	[W/m K]	[mW/m²]	[km]	[Ma]	
1	-75	11,643	-42	47,472	1558	no penetration due to stiff sediments						n/a	1356
2	-75	12,374	-42	47,555	1665	3	22,1	56,4	1,03	59	-25,8	n/a	1376
3	-75	13,109	-42	47,656	1799	no penetration due to stiff sediments						n/a	1396

Appendix 9.4.10 TIPTEQ SO181-1B

Station H0410

Pen	Longitude		Latitude		Water Depth	No of sensors used	Tilt	Mean Gradient	Mean thermal conductivity	Mean heatflow	Distance from Deformation Front	Crustal age	Shot point # SCS03
	Degree	Minutes	Degree	Minutes	[m]		[°]	[K/km]	[W/m K]	[mW/m²]	[km]	[Ma]	
1	-75	4,437	-40	40,811	3470	9	1,7	34,6	0,9	31	-5,6	n/a	2246
2	-75	3,742	-40	40,758	3342	9	4	36,7	0,91	33	-6,7	n/a	2209
3	-75	3,026	-40	40,691	3238	8	4	42,6	0,92	39	-7,6	n/a	2172
4	-75	2,3	-40	40,619	3206	11	4,8	37,5	0,91	27	-8,7	n/a	2132
5	-75	1,577	-40	40,517	3159	9	5	45,4	0,9	40	-9,7	n/a	2093
6	-75	0,9	-40	40,468	3076	6	4,5	51,3	0,91	47	-10,6	n/a	2056

Appendix 9.4.11 TIPTEQ SO181-1B

Station H0411

Pen	Longitude		Latitude		Water Depth	No of sensors used	Tilt	Mean Gradient	Mean thermal conductivity	Mean heatflow	Distance from Deformation Front	Crustal age	Shot point # SCS04
	Degree	Minutes	Degree	Minutes									
1	-75	6,701	-36	1,249	4342	7	1,4	9,6	0,82	8	n/a	n/a	5321
2	-75	6,051	-36	1,340	4331	5	1,6	24,2	0,8	19	n/a	n/a	5281
3	-75	5,364	-36	1,432	4297	5	3,9	73,7	0,83	61	n/a	n/a	5239
4	-75	4,754	-36	1,524	4267	8	1,4	29,1	0,8	23	n/a	n/a	5201
5	-75	4,084	-36	1,610	4231	7	5,6	32,2	0,83	27	n/a	n/a	5160
6	-75	3,454	-36	1,706	4263	8	2,8	23,8	0,8	19	n/a	n/a	5123

Appendix 9.5 Magnetotellurics

Position and recovery information:

Site #	Deployment		Position			Acoustic Release		Radio beacon		
	Date	Time	Lat	Lon	Depth	Serial #	Ping Code	Serial #	Freq 1	Freq 2
		(UTC)			(m)				(MHz)	
1	12/9/2004	10:55	38° 08,90' S	73° 49,53' W	512	53	4225	28	161.800	161.925
2	12/9/2004	12:53	38° 04,93' S	74° 09,48' W	685	73	8341	25	161.800	161.850
3	12/9/2004	15:15	38° 00,09' S	74° 32,68' W	4568	68	8315	46	161.900	161.925
4	12/9/2004	21:48	37° 54,95' S	74° 57,47' W	4565	82	8385	1	161.800	161.925
5	12/9/2004	23:32	37° 50,43' S	75° 18,92' W	4163	70	8325	35	161.825	161.950
6	12/10/2004	1:27	37° 45,42' S	75° 41,94' W	4150	57	4251	12	161.800	161.900
7	12/10/2004	3:30	37° 39,56' S	76° 08,10' W	4189	54	4231	16	161.800	161.950

Sensor and electronics information:

Site #	Pressure	Electronics			CF Card		Electrodes					Arm
	Tube	Mother-board	Compass	Clock	Serial #	Filename	X+	X-	Y+	Y-	Ref	Length (in)
1	6	2	6809	15	102	SO181C02	01-067	01-069	01-073	01-062	96-066	256
2	7	8	5498	9	109	SO181C09	01-064	01-065	96-054	96-028	01-063	259
3	12	3	5426	2	103	SO181C03	01-072	96-032	96-011	96-013	96-015	257
4	2	1	5557	6	101	SO181C01	96-092	96-051	96-077	96-090	96-027	256
5	9	4	5499	11	104	SO181C04	4-26	96-009	4-34	96-97	4-41	257.5
6	5	5	6819	1	105	SO181C05	01-070	4-47	96-029	96-098	96-044	256
7	3	6	6722	5	106	SO181C06	96-001	96-018	96-081	96-086	96-005	256

Table A.5.1: MT Instruments deployment summary, December 9th, 2004 – Dec 10th, 2004

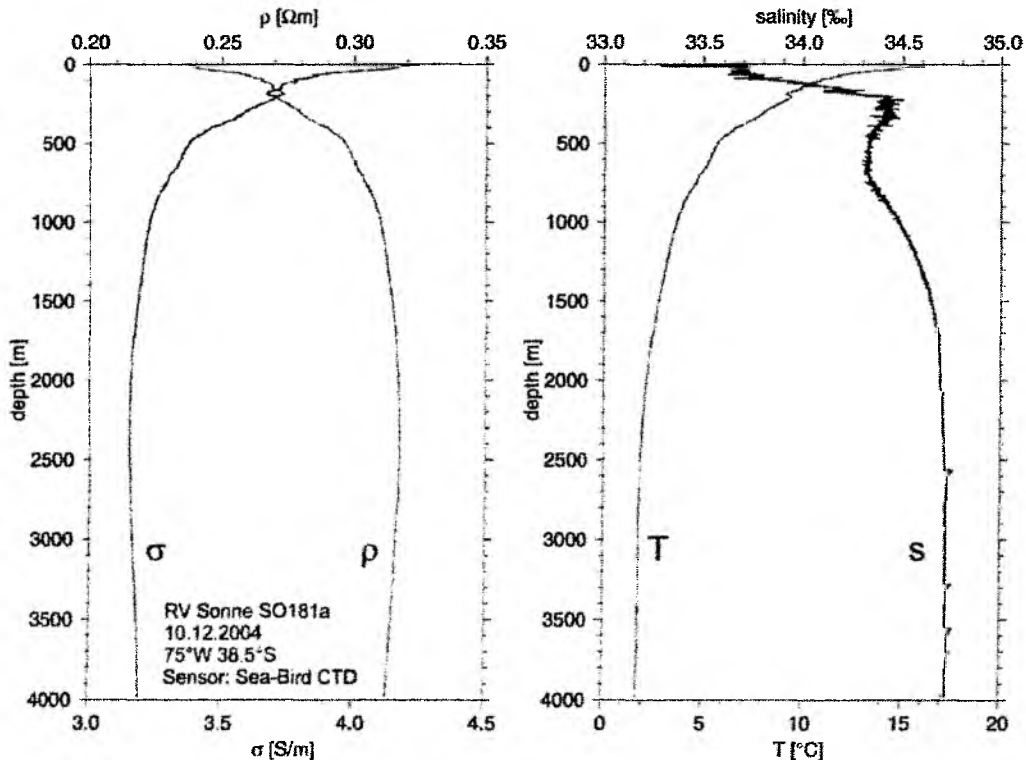


Fig. A.5.1: Logs of electrical conductivity, resistivity (left), temperature and salinity (right).

Appendix 9.6 SO181 - 1a & 1b TIPTEQ Gravity Core Stations

Abreveations:

RL	Rope Length	SP	Weight Section penetrated Sediment
RT	Rope Tension	RE	Recovery
TP	Twisted Pipe	NR	No Recovery

Station	Date	Time UTC	Position Lat	Position Long	Depth [m]	Action	Comment
SO181/001-2	08.12.04	12:41	35° 59,94' S	74° 25,00' W	4935	begin station	<i>SL-181-01</i>
SO181/001-2	08.12.04	12:43	35° 59,93' S	74° 24,98' W	4935	watercontact	
SO181/001-2	08.12.04	13:53	35° 59,99' S	74° 25,05' W	4939	impact	RL: 4934m, RT: 54,8kN, SP
SO181/001-2	08.12.04	15:31	36° 0,01' S	74° 25,04' W	4936	at deck	RE: 5,0m
SO181/001-2	08.12.04	15:33	36° 0,04' S	74° 25,05' W	4933	end station	
SO181/002-1	08.12.04	19:02	36° 35,00' S	74° 35,03' W	4832	begin station	<i>SL-181-02</i>
SO181/002-1	08.12.04	19:03	36° 35,00' S	74° 35,05' W	4831	watercontact	
SO181/002-1	08.12.04	20:26	36° 35,00' S	74° 35,00' W	4830	impact	RL: 4822m, RT: 52,4kN
SO181/002-1	08.12.04	20:27	36° 35,00' S	74° 35,00' W	4829	lift	RT: 77,9kN
SO181/002-1	08.12.04	21:54	36° 35,04' S	74° 35,03' W	4827	at deck	RE: 1,7m
SO181/002-1	08.12.04	21:55	36° 35,04' S	74° 35,04' W	4829	end station	
SO181/003-1	09.12.04	02:56	37° 30,00' S	74° 50,15' W	4687,4	begin station	<i>SL-181-03</i>
SO181/003-1	09.12.04	03:00	37° 30,00' S	74° 50,22' W	4684,6	watercontact	
SO181/003-1	09.12.04	04:08	37° 30,31' S	74° 50,35' W	4688,4	impact	RL: 4679 m, RT: 45,5kN
SO181/003-1	09.12.04	04:10	37° 30,31' S	74° 50,36' W	4683,4	lift	
SO181/003-1	09.12.04	05:26	37° 30,51' S	74° 50,41' W	4685,6	at deck	RE: 6,5m
SO181/003-1	09.12.04	05:28	37° 30,51' S	74° 50,40' W	4685,6	end station	
SO181/007-1	09.12.04	16:54	38° 15,02' S	74° 35,02' W	4610	begin station	<i>SL-181-04</i>
SO181/007-1	09.12.04	16:56	38° 15,01' S	74° 35,02' W	4611	watercontact	
SO181/007-1	09.12.04	18:00	38° 15,00' S	74° 35,49' W	4612	impact	RL: 4606m, RT: 48,8kN
SO181/007-1	09.12.04	18:01	38° 15,00' S	74° 35,50' W	4611	lift	RT: 50kN
SO181/007-1	09.12.04	19:23	38° 15,20' S	74° 35,91' W	4634	at deck	RE: 4,6m
SO181/007-1	09.12.04	19:23	38° 15,20' S	74° 35,91' W	4634	end station	

SO181/012-1	10.12.04	11:34	38° 45,01' S	74° 46,00' W	4526	begin station	SL-181-05/1
SO181/012-1	10.12.04	11:37	38° 45,00' S	74° 45,96' W	4527	watercontact	
SO181/012-1	10.12.04	12:41	38° 45,05' S	74° 46,14' W	4518	impact	RL: 4513m, RT: 47,9kN
SO181/012-1	10.12.04	14:01	38° 45,18' S	74° 46,13' W	4518	at deck	RE: 0,0m, slightly TP
SO181/012-3	10.12.04	17:53	38° 45,01' S	74° 46,03' W	4528	watercontact	SL-181-05/2
SO181/012-3	10.12.04	19:04	38° 45,02' S	74° 46,11' W	4520	impact	RL: 4513m, RT: 48,4kN
SO181/012-3	10.12.04	19:05	38° 45,02' S	74° 46,10' W	4524	lift	RT: 76kN
SO181/012-3	10.12.04	19:12	38° 45,03' S	74° 46,06' W	4522	impact	RL: 4513
SO181/012-3	10.12.04	19:13	38° 45,03' S	74° 46,06' W	4522	lift	RT: 75,5 kN
SO181/012-3	10.12.04	20:39	38° 45,20' S	74° 46,03' W	4520	at deck	RE: 2,4m, TP
SO181/012-3	10.12.04	20:40	38° 45,20' S	74° 46,04' W	4519	end station	

SO181/013-1	11.12.04	01:16	39° 35,01' S	74° 59,99' W	4302	begin station	SL-181-06
SO181/013-1	11.12.04	01:18	39° 35,01' S	74° 59,98' W	4308	watercontact	
SO181/013-1	11.12.04	02:22	39° 34,97' S	75° 00,00' W	4300	impact	RL: 4293m, RT: 46,9kN
SO181/013-1	11.12.04	02:23	39° 34,97' S	75° 00,00' W	4297	lift	RT: 76kN
SO181/013-1	11.12.04	03:31	39° 34,99' S	75° 00,08' W	4303	at deck	RE: 5,0m, SP
SO181/013-1	11.12.04	03:31	39° 34,99' S	75° 00,08' W	4303	end station	

SO181/014-1	11.12.04	05:04	39° 49,97' S	75° 00,02' W	4315	begin station	SL-181-07
SO181/014-1	11.12.04	05:06	39° 49,97' S	75° 00,02' W	4317	watercontact	
SO181/014-1	11.12.04	06:05	39° 50,07' S	75° 00,10' W	4309	impact	RL: 4300m, RT: 52,9kN
SO181/014-1	11.12.04	06:07	39° 50,08' S	75° 00,12' W	4313	lift	RT: 70kN
SO181/014-1	11.12.04	07:23	39° 50,05' S	75° 00,16' W	4311	at deck	RE: 7,0m
SO181/014-1	11.12.04	07:24	39° 50,06' S	75° 00,16' W	4316	end station	

SO181/015-1	11.12.04	14:22	41° 0,02' S	75° 10,97' W	3914	begin station	SL-181-08
SO181/015-1	11.12.04	14:25	41° 0,05' S	75° 10,97' W	3913	watercontact	
SO181/015-1	11.12.04	15:18	41° 0,00' S	75° 11,09' W	3912	impact	RL: 3905m, RT: 42,9kN
SO181/015-1	11.12.04	15:20	40° 59,98' S	75° 11,11' W	3914	lift	RT: 60kN
SO181/015-1	11.12.04	16:24	40° 59,94' S	75° 10,96' W	3912	at deck	RE: 5,85m
SO181/015-1	11.12.04	16:26	40° 59,95' S	75° 10,98' W	3912	end station	

SO181/018-1	14.12.04	01:17	43° 21,27' S	76° 29,62' W	3512	begin station	SL-181-09
SO181/018-1	14.12.04	01:19	43° 21,27' S	76° 29,62' W	3510	watercontact	
SO181/018-1	14.12.04	02:06	43° 21,26' S	76° 29,51' W	3512	impact	RL: 3522m, RT: 34,5kN

SO181/018-1	14.12.04	02:10	43° 21,26' S	76° 29,51' W	3512	lift	RT: 69,6kN
SO181/018-1	14.12.04	03:08	43° 21,31' S	76° 29,58' W	3513	at deck	RE: 2,75m
SO181/018-1	14.12.04	03:09	43° 21,31' S	76° 29,59' W	3512	end station	
SO181/020-1	14.12.04	18:57	44° 40,00' S	76° 29,91' W	3257	begin station	<i>SL-181-10</i>
SO181/020-1	14.12.04	18:58	44° 39,99' S	76° 29,90' W	3257	watercontact	
SO181/020-1	14.12.04	19:36	44° 40,05' S	76° 29,86' W	3255	impact	RL: 3260m, RT: 35,4kN
SO181/020-1	14.12.04	19:38	44° 40,05' S	76° 29,85' W	3254	lift	RT: 60,5kN
SO181/020-1	14.12.04	22:04	44° 40,16' S	76° 28,28' W	3256	at deck	RE: 5,6m
SO181/020-1	14.12.04	22:13	44° 40,16' S	76° 28,18' W	3259	end station	
SO181/023-1	15.12.04	11:24	44° 30,04' S	75° 49,98' W	3329	begin station	<i>SL-181-11</i>
SO181/023-1	15.12.04	11:27	44° 30,07' S	75° 49,97' W	3330	watercontact	
SO181/023-1	15.12.04	12:12	44° 30,03' S	75° 49,87' W	3328	impact	RL: 3334m, RT: 30,7kN
SO181/023-1	15.12.04	12:14	44° 30,03' S	75° 49,87' W	3328	lift	RT: 61kN
SO181/023-1	15.12.04	12:57	44° 29,96' S	75° 49,91' W	3330	at deck	RE: 2,75m, TP
SO181/023-1	15.12.04	13:03	44° 29,96' S	75° 49,91' W	3332	end station	
SO181/024-1	15.12.04	22:26	42° 49,94' S	75° 29,91' W	3703	begin station	<i>SL-181-12</i>
SO181/024-1	15.12.04	22:28	42° 49,94' S	75° 29,95' W	3700	watercontact	
SO181/024-1	15.12.04	23:20	42° 50,04' S	75° 30,00' W	3703	impact	RL: 3720m, RT: 38,5kN
SO181/024-1	15.12.04	23:22	42° 50,04' S	75° 30,00' W	3703	lift	RT: 69,4kN
SO181/024-1	16.12.04	00:17	42° 50,07' S	75° 30,09' W	3700	at deck	RE: 5,0m, TP
SO181/024-1	16.12.04	00:17	42° 50,07' S	75° 30,09' W	3700	end station	
SO181/038-1	29.12.04	14:15	45° 45,95' S	76° 35,03' W	2694	begin station	<i>SL181-1b-1</i>
SO181/038-1	29.12.04	14:31	45° 45,96' S	76° 34,99' W	2693	watercontact	
SO181/038-1	29.12.04	15:11	45° 45,99' S	76° 35,00' W	2692	impact	RL: 2722m, RT: 20,3kN
SO181/038-1	29.12.04	15:12	45° 45,99' S	76° 35,00' W	2690	lift	RT: 63kN
SO181/038-1	29.12.04	16:05	45° 46,03' S	76° 35,04' W	2687	at deck	RE: 5,0m
SO181/038-1	29.12.04	16:34	45° 46,06' S	76° 35,19' W	2678	end station	
SO181/040-1	29.12.04	19:03	45° 36,22' S	76° 0,01' W	3316	begin station	<i>SL181-1b-2</i>
SO181/040-1	29.12.04	19:12	45° 36,04' S	75° 59,98' W	3316	watercontact	
SO181/040-1	29.12.04	20:03	45° 36,00' S	76° 0,00' W	3316	impact	RL: 3350m, RT: 32,7kN

SO181/040-1	29.12.04	20:06	45° 36,00' S	76° 0,00' W	3316	lift	RT: 69kN
SO181/040-1	29.12.04	21:04	45° 36,04' S	76° 0,01' W	3316	at deck	RE: 4,0m
SO181/040-1	29.12.04	21:05	45° 36,05' S	76° 0,01' W	3316	end station	
SO181/043-1	30.12.04	16:07	46° 40,04' S	75° 55,02' W	3375	begin station	SL181-1b-3
SO181/043-1	30.12.04	16:09	46° 40,07' S	75° 55,03' W	3372	watercontact	
SO181/043-1	30.12.04	17:05	46° 40,16' S	75° 55,38' W	3386	impact	RL: 3412m, RT: 38,3kN
SO181/043-1	30.12.04	17:09	46° 40,21' S	75° 55,32' W	3392	lift	RT: 64kN
SO181/043-1	30.12.04	18:16	46° 40,55' S	75° 56,06' W	3412	at deck	RE: 2,35m
SO181/043-1	30.12.04	18:23	46° 40,59' S	75° 56,02' W	3416	end station	
SO181/045-1	30.12.04	21:31	46° 13,05' S	75° 41,01' W	1527	begin station	SL181-1b-4
SO181/045-1	30.12.04	21:33	46° 13,05' S	75° 41,01' W	1534	watercontact	
SO181/045-1	30.12.04	22:02	46° 13,02' S	75° 41,02' W	1515	impact	RL: 1535m, RT: 9,3kN
SO181/045-1	30.12.04	22:03	46° 13,02' S	75° 41,01' W	1519	lift	RT: 50kN
SO181/045-1	30.12.04	22:30	46° 13,14' S	75° 41,11' W	1599	at deck	RE: 2,7m
SO181/045-1	30.12.04	22:31	46° 13,15' S	75° 41,12' W	1623	end station	
SO181/046-1	30.12.04	22:42	46° 13,02' S	75° 41,49' W	1688	begin station	SL181-1b-5/1
SO181/046-1	30.12.04	22:54	46° 13,01' S	75° 41,51' W	1681	watercontact	
SO181/046-1	30.12.04	23:26	46° 13,00' S	75° 41,51' W	1664	impact	RL: 1718m ; RT: 42kN
SO181/046-1	30.12.04	23:56	46° 13,04' S	75° 41,59' W	1742	at deck	NR
SO181/046-2	31.12.04	00:12	46° 13,01' S	75° 41,52' W	1707	watercontact	SL181-1b-5/2
SO181/046-2	31.12.04	00:43	46° 13,00' S	75° 41,50' W	1690	impact	RL: 1705m, RT: 38kN
SO181/046-2	31.12.04	01:14	46° 13,01' S	75° 41,50' W	1679	at deck	NR
SO181/046-2	31.12.04	01:16	46° 13,01' S	75° 41,49' W	1687	end station	
SO181/047-1	31.12.04	01:26	46° 13,03' S	75° 42,03' W	1998	begin station	SL181-1b-6
SO181/047-1	31.12.04	01:30	46° 13,01' S	75° 42,01' W	1984	watercontact	
SO181/047-1	31.12.04	02:04	46° 13,00' S	75° 42,00' W	1968	impact	RL: 2011m
SO181/047-1	31.12.04	02:05	46° 13,00' S	75° 42,00' W	1968	lift	RT: 43kN
SO181/047-1	31.12.04	02:38	46° 12,99' S	75° 42,00' W	1969	at deck	NR
SO181/047-1	31.12.04	02:42	46° 13,00' S	75° 42,00' W	1975	end station	

Appendix 9.7.1

STATIONBOOK

SO 181-1a

Abkürzungen / Abbreviation

z.W	zu Wasser
a.D.	an Deck
SL (max.)	(maximale) Seillänge
LT	Lottiefe nach Hydrosweep
W x	eingesetzte Winde
SM	Simrad - Multibeam - Lot
PS	Parasound
rwk:	Rechtweisender Kurs
d:	Distanz
v:	Geschwindigkeit in Knoten

Eingesetzte Geräte

CTD/Ro	CTD- Rosettengestell für Releasertest
Airgun	Air-Gun (2 Airguns à 32 Ltr. Volumen)
Streamer	Streamer (50m Länge)
Magn.	Magnetometer
MT	Magnetotellurik-Geräte (nur Auslage)
OBH/OBS	Auslage der Geräte (nur Auslage)
Sonatrack	Einsatz für Magnetotellurik-Geräte MT 1-7
CTD+SVP	CTD- und Wasserschallschallsonde je 1x mit Auslösertest an W 6
GC 6m	Schwerelos 6m
EM/PS	Vermessungsprofile

Einsätze

2	
4 Profile	mit 114 sm Länge in 25,5 Std. Profilzeit
2 Profile	auf Profil P 02 d. Fleischbiß verloren
2 Profile	auf 2 Profilen mit 63sm Länge eingesetzt
7	
29	
7	
2	
13	
28	Datenaufzeichnung auf 1780 sm Profillänge mit 114 Std. Profilzeit

Geräteverluste:

50m-Streamer mit 80m Kabelvorlauf durch Fleischbiß am 13.12.04 verloren

Winde	D/M	Typ	RF-Nr	SO 181.1a Einsatz	Gesamt Einsatz	SO 181.1a S'länge	Gesamt S'länge	Zust.	SO 181.1a gefierte max. L	jemale gefierte max. Länge
W 1	18.01.00	LWL	812001	6 h	349 h	10554 m	199039 m	3-4	3720 m	8022 m
W 2	18.01.00	LWL	815286	0 h	0 h	0 m	0 m	1	0 m	0 m
W 4	11.01.00	NSW	818045	3 h	268 h	57333 m	220273 m	3	3400 m	8081 m
W 5	11.01.00	NSW	812106	0 h	0 h	0 m	0 m	1	0 m	0 m
W 6	18.01.00	DRAKO	818238	30,8	1124 h	51552 m	1061121 m	3-4	4962 m	7809 m

Station	Datum	UTC	PositionLat	PositionLon	Tiefe [m]	Windstärke [m/s]	Kurs [°]	v [kn]	Gerät	Geräte Kürzel	Aktion	Bemerkung
SO181/001-1	07.12.04		32° 57,00' S	71° 37,00' W	0	SSW 10	270	12	Vermessung	EM / PS	Beginn Profil	rwk: 270°, d: 13 nm
SO181/001-1	07.12.04	15:00	32° 57,19' S	71° 51,88' W	955	SSW 13	224	9,6	Vermessung	EM / PS	Kursänderung	rwk: 187°, d: 5 nm
SO181/001-1	07.12.04	15:27	33° 02,03' S	71° 52,86' W	718	S 15	195	10,5	Vermessung	EM / PS	Kursänderung	rwk: 214°, d: 71 nm
SO181/001-1	07.12.04	22:07	34° 00,00' S	72° 43,00' W	2870	SW 11	205	11,8	Vermessung	EM / PS	Kursänderung	rwk: 205°, d: 130 nm
SO181/001-1	08.12.04	09:59	35° 58,00' S	73° 49,00' W	0	SSW 10	266	10	Vermessung	EM / PS	Kursänderung	rwk: 266°, d: 29 nm
SO181/001-1	08.12.04	12:40	35° 59,95' S	74° 25,00' W	4934	SSW 11	182	0,9	Vermessung	EM / PS	Ende Profil	
SO181/001-2	08.12.04	12:41	35° 59,94' S	74° 25,00' W	4935	SSW 11	26	0,7	Gravity Corer 6 m	GC 6M	Beginn Station	SL-181-01
SO181/001-2	08.12.04	12:43	35° 59,93' S	74° 24,98' W	4935	SSW 10	66	0,7	Gravity Corer 6 m	GC 6M	zu Wasser	
SO181/001-2	08.12.04	13:53	35° 59,99' S	74° 25,05' W	4939	SW 8	349	1,2	Gravity Corer 6 m	GC 6M	Bodenkontakt	SL: 4962m, SZ:85,3 KN
SO181/001-2	08.12.04	15:31	36° 00,01' S	74° 25,04' W	4936	SSW 10	218	0,7	Gravity Corer 6 m	GC 6M	an Deck	
SO181/001-2	08.12.04	15:33	36° 00,04' S	74° 25,05' W	4933	SSW 10	193	1,1	Gravity Corer 6 m	GC 6M	Ende station	
SO181/001-3	08.12.04	15:34	36° 00,07' S	74° 25,08' W	4936	SSW 12	188	3,4	Vermessung	PROFIL	Kursänderung	
SO181/001-3	08.12.04	15:35	36° 00,12' S	74° 25,07' W	4931	SSW 12	190	3,7	Vermessung	PROFIL	Beginn Profil	(Fortsetzung Profil)
SO181/001-3	08.12.04	19:00	36° 34,97' S	74° 35,01' W	4830	SSW 11	201	3	Vermessung	PROFIL	Ende Profil	(Unterbrechung Profil) 36 sm
SO181/002-1	08.12.04	19:02	36° 35,00' S	74° 35,03' W	4832	SSW 9	260	1,1	Gravity Corer 6 m	GC 6M	Beginn Station	SL-181-02
SO181/002-1	08.12.04	19:03	36° 35,00' S	74° 35,05' W	4831	SSW 9	247	1,1	Gravity Corer 6 m	GC 6M	zu Wasser	
SO181/002-1	08.12.04	20:26	36° 35,00' S	74° 35,00' W	4830	SW 8	0	0	Gravity Corer 6 m	GC 6M	Bodenkontakt	SL: 4856 m

Appendix 9.7.1

STATIONBOOK

SO 181-1a

Station	Datum	UTC	PositionLat	PositionLon	Tiefe [m]	Windstärke [m/s]	Kurs [°]	v [kn]	Gerät	Gerätekurzel	Aktion	Bemerkung
SO181/002-1	08.12.04	20:27	36° 35,00' S	74° 35,00' W	4829	SSW 8	0	0	Gravity Corer 6 m	GC 6M	hieven	SZ: 77,9 kN
SO181/002-1	08.12.04	21:54	36° 35,04' S	74° 35,03' W	4827	SSW 9	0	0	Gravity Corer 6 m	GC 6M	an Deck	
SO181/002-1	08.12.04	21:55	36° 35,04' S	74° 35,04' W	4829	SW 10	0	0	Gravity Corer 6 m	GC 6M	Ende Station	
SO181/002-2	08.12.04	21:55	36° 35,04' S	74° 35,04' W	4829,3	SSW 8	0	0	Vermessung	EM / PS	Beginn Profil	rwk: 192°, d: 58 nm
SO181/002-1	08.12.04	21:55	36° 35,04' S	74° 35,04' W	4829,3	SSW 8	0	0	Gravity Corer 6 m	GC 6M	Ende station	EM/PS-Profilfortsetzung
SO181/002-2	09.12.04	02:53	37° 29,98' S	74° 50,07' W	4685,6	SSW 8	292	0,7	Vermessung	EM / PS	Profilende	D 56 sm
SO181/003-1	09.12.04	02:56	37° 30,00' S	74° 50,15' W	4687,4	S 7	231	1,3	GC 6 meter	GC 6M	Beginn Station	
SO181/003-1	09.12.04	03:00	37° 30,00' S	74° 50,22' W	4684,8	S 6	236	0,8	Gravity Corer 6 m	GC 6M	zu wasser	
SO181/003-1	09.12.04	04:06	37° 30,31' S	74° 50,35' W	4688,4	SSW 6	0	0	Gravity Corer 6 m	GC 6M	Bodenkontakt	Seillänge: 4676 m
SO181/003-1	09.12.04	04:10	37° 30,31' S	74° 50,36' W	4683,4	SSW 6	0	0	Gravity Corer 6 m	GC 6M	hieven	
SO181/003-1	09.12.04	05:26	37° 30,51' S	74° 50,41' W	4685,6	SSW 5	0	0	Gravity Corer 6 m	GC 6M	an deck	
SO181/003-1	09.12.04	05:28	37° 30,51' S	74° 50,40' W	4685,6	SSW 5	226	0,3	Gravity Corer 6 m	GC 6M	Ende station	ak
SO181/003-2	09.12.04	05:31	37° 30,53' S	74° 50,39' W	4683,4	SSW 5	188	1,1	Vermessung	EM / PS	Beginn Profil	rwk: 126°
SO181/003-2	09.12.04	09:40	37° 59,64' S	73° 57,57' W	226,5	SSW 5	122	13,6	Vermessung	EM / PS	Kursänderung	rwk: 147°, d: 11 nm
SO181/003-2	09.12.04	10:31	38° 08,43' S	73° 49,88' W	511,2	SSW 3	147	10,2	Vermessung	EM / PS	Ende Profil	D 52 sm
SO181/004-1	09.12.04	10:35	38° 08,79' S	73° 49,57' W	509,7	S 3	143	3,8	MT	MT	Beginn Station	MT 01
SO181/004-1	09.12.04	10:54	38° 08,90' S	73° 49,53' W	512,5	SSE 3	0	0	MT	MT	MT zu Wasser	Tranducer z.W. / Sonatrack
SO181/004-1	09.12.04	11:20	38° 08,92' S	73° 49,50' W	517,3	SSE 2	0	0	MT	MT	Ende Station	
SO181/004-2	09.12.04	11:21	38° 08,92' S	73° 49,50' W	516	SSE 1	0	0	Vermessung	EM / PS	Beginn Profil	rwk: 264
SO181/004-2	09.12.04	12:49	38° 04,90' S	74° 09,46' W	683	SSW 4	213	2,1	Vermessung	EM / PS	Ende Profil	d: 16 sm
SO181/005-1	09.12.04	12:50	38° 04,91' S	74° 09,47' W	684	SW 4	155	0,9	MT	MT	Beginn Station	MT 2
SO181/005-1	09.12.04	12:52	38° 04,93' S	74° 09,48' W	685	SW 3	197	0,7	MT	MT	MT zu Wasser	Tranducer z.W. / Sonatrack
SO181/005-1	09.12.04	13:07	38° 05,05' S	74° 09,55' W	678	WSW 3	0	0	MT	MT	Ende Station	
SO181/005-2	09.12.04	13:27	38° 05,23' S	74° 09,72' W	672	WSW 3	0	0	Vermessung	EM / PS	Beginn Profil	rwk: 286
SO181/005-2	09.12.04	15:10	38° 00,11' S	74° 32,68' W	4567	NE 3	0	0	Vermessung	EM / PS	Ende Profil	D 16 sm
SO181/006-1	09.12.04	15:15	38° 00,10' S	74° 32,68' W	4568	NNW 2	0	0	MT	MT	Beginn Station	MT 03
SO181/006-1	09.12.04	15:16	38° 00,09' S	74° 32,68' W	4568	NW 2	0	0	MT	MT	MT zu Wasser	Tranducer z.W. / Sonatrack
SO181/006-2	09.12.04	15:29	37° 59,97' S	74° 32,67' W	4566	NNW 3	281	1,2	Vermessung	EM / PS	Beginn Profil	rwk: 187°, d: 15 nm
SO181/006-2	09.12.04	16:53	38° 15,02' S	74° 35,02' W	4610	ESE 4	0	0	Vermessung	EM / PS	Ende Profil	
SO181/007-1	09.12.04	16:54	38° 15,02' S	74° 35,02' W	4610	NW 4	0	0	Gravity Corer 6 m	GC 6M	Beginn Station	
SO181/007-1	09.12.04	16:56	38° 15,01' S	74° 35,02' W	4611	NW 4	0	0	Gravity Corer 6 m	GC 6M	z.W.	
SO181/007-1	09.12.04	18:00	38° 15,00' S	74° 35,49' W	4612	NW 4	0	0	Gravity Corer 6 m	GC 6M	Bodenkontakt	SL: 4620 m
SO181/007-1	09.12.04	18:01	38° 15,00' S	74° 35,50' W	4611	NNW 4	280	0,9	Gravity Corer 6 m	GC 6M	hieven	SZ: 50 kN
SO181/007-1	09.12.04	18:23	38° 15,20' S	74° 35,91' W	4634	NNW 4	248	0,6	Gravity Corer 6 m	GC 6M	a.D.	
SO181/007-1	09.12.04	18:23	38° 15,20' S	74° 35,91' W	4634	NNW 4	248	0,6	Gravity Corer 6 m	GC 6M	Ende station	
SO181/007-2	09.12.04	19:23	38° 15,20' S	74° 35,91' W	4634	N 4	248	0,6	Vermessung	EM / PS	Beginn Profil	rwk: 319°

Appendix 9.7.1

STATIONBOOK

SO 181-1a

Station	Datum	UTC	PositionLat	PositionLon	Tiefe [m]	Windstärke [m/s]	Kurs [°]	v [kn]	Gerät	Gerätekürzel	Aktion	Bemerkung
SO181/007-2	09.12.04	21:44	37° 54,98' S	74° 57,43' W	4569	N 7	318	2,7	Vermessung	EM / PS	Ende Profil	D 27 sm
SO181/008-1	09.12.04	21:45	37° 54,96' S	74° 57,46' W	4573	NNW 7	326	1,1	MT	MT	Beginn Station	MT 04
SO181/008-1	09.12.04	21:47	37° 54,95' S	74° 57,47' W	4585	NNW 6	0	0	MT	MT	MT zu Wasser	
SO181/008-1	09.12.04	21:51	37° 54,95' S	74° 57,47' W	4571	NNE 6	0	0	MT	MT	Ende Station	
SO181/008-2	09.12.04	21:52	37° 54,95' S	74° 57,48' W	4567	NNW 6	0	0	Vermessung	EM / PS	Beginn Profil	rwk: 265°
SO181/008-2	09.12.04	23:21	37° 50,67' S	75° 17,87' W	4185	NW 12	288	11,2	Vermessung	EM / PS	Ende Profil	d:18 sm
SO181/009-1	09.12.04	23:30	37° 50,43' S	75° 18,93' W	4166	NW 6	0	0	MT	MT	Beginn Station	
SO181/009-1	09.12.04	23:31	37° 50,43' S	75° 18,92' W	4163	WNW 6	85	0,9	MT	MT	MT zu Wasser	MT 5
SO181/009-1	09.12.04	23:35	37° 50,44' S	75° 18,86' W	4156	WNW 6	72	0,7	MT	MT	Ende Station	
SO181/009-2	09.12.04	23:36	37° 50,44' S	75° 18,85' W	4159	NW 5	58	1,1	Vermessung	EM / PS	Beginn Profil	rwK: 285
SO181/009-2	10.12.04	01:22	37° 45,41' S	75° 41,94' W	4137	WSW 9	237	2,9	Vermessung	EM / PS	Ende Profil	d: 19 sm
SO181/010-1	10.12.04	01:24	37° 45,42' S	75° 41,95' W	4133	WSW 8	42	0,4	MT	MT	Beginn Station	
SO181/010-1	10.12.04	01:27	37° 45,42' S	75° 41,94' W	4150	WSW 8	0	0	MT	MT	MT zu Wasser	MT 6
SO181/010-1	10.12.04	01:28	37° 45,42' S	75° 41,93' W	4135	WSW 8	0	0	MT	MT	Ende Station	
SO181/010-2	10.12.04	01:29	37° 45,41' S	75° 41,93' W	4132	WSW 4	7	0,9	Vermessung	EM / PS	Beginn Profil	rwK: 286°
SO181/010-2	10.12.04	03:30	37° 39,64' S	76° 08,23' W	4177	WSW 4	299	0,6	Vermessung	EM / PS	Ende Profil	D 22 sm
SO181/011-1	10.12.04	03:33	37° 39,62' S	76° 08,22' W	4178	WSW 4	0	0	MT	MT	Beginn Station	
SO181/011-1	10.12.04	03:40	37° 39,56' S	76° 08,10' W	4189	WSW 4	47	1,5	MT	MT	MT zu Wasser	MT 7
SO181/011-1	10.12.04	03:40	37° 39,56' S	76° 08,10' W	4189	WSW 5	47	1,5	MT	MT	Ende Station	
SO181/011-2	10.12.04	03:41	37° 39,55' S	76° 08,07' W	4188	WSW 4	50	1,5	Vermessung	EM / PS	Beginn Profil	rwK: 162°
SO181/011-2	10.12.04	05:37	38° 0,08' S	75° 59,89' W	4075	WSW 8	132	11,3	Vermessung	EM / PS	Kursänderung	rwK: 126°
SO181/011-2	10.12.04	11:33	38° 45,00' S	74° 46,00' W	4525	WSW 7	235	0,9	Vermessung	EM / PS	Ende Profil	D 94 sm
SO181/012-1	10.12.04	11:34	38° 45,01' S	74° 46,00' W	4526	WSW 7	27	0,5	Gravity Corer 6 m	GC 6M	Beginn Station	
SO181/012-1	10.12.04	11:37	38° 45,00' S	74° 45,96' W	4527	WSW 5	126	0,6	Gravity Corer 6 m	GC 6M	zu wasser	
SO181/012-1	10.12.04	12:41	38° 45,05' S	74° 46,14' W	4518	SW 4	154	0,5	Gravity Corer 6 m	GC 6M	Bodenkontakt	SL: 4537 m, SZ: 79 kN
SO181/012-1	10.12.04	14:01	38° 45,18' S	74° 46,13' W	4518	SW 3	0	0	Gravity Corer 6 m	GC 6M	an deck	
SO181/012-2	10.12.04	14:18	38° 45,23' S	74° 46,20' W	4518	W 2	218	0,7	CTD/Rosette	CTD/Ro	z.W.mit Auslösertest	CTD SL15 m/SVP SL2000 m
SO181/012-2	10.12.04	15:32	38° 45,08' S	74° 46,01' W	4520	W 2	0	0	CTD/Rosette	CTD/Ro	auf Tiefe	SL: 4000 m, SZ: 45 kN
SO181/012-2	10.12.04	17:45	38° 45,04' S	74° 46,04' W	4522	SW 2	77	0,8	CTD/Rosette	CTD/Ro	a.D.	
SO181/012-3	10.12.04	17:53	38° 45,01' S	74° 46,03' W	4528	W 2	0	0	Gravity Corer 6 m	GC 6M	z.W.	SL-181-05.1
SO181/012-3	10.12.04	19:04	38° 45,02' S	74° 46,11' W	4520	WSW 2	0	0	Gravity Corer 6 m	GC 6M	Bodenkontakt	18:40-18:50 SchwimmtestOBH
SO181/012-3	10.12.04	19:05	38° 45,02' S	74° 46,10' W	4524	WSW 3	41	0,1	Gravity Corer 6 m	GC 6M	hieven	SL: 4535 m, SZ: 76 kN
SO181/012-3	10.12.04	19:12	38° 45,03' S	74° 46,06' W	4522	WSW 2	95	0,2	Gravity Corer 6 m	GC 6M	Bodenkontakt	
SO181/012-3	10.12.04	19:13	38° 45,03' S	74° 46,06' W	4522	WSW 3	0	0	Gravity Corer 6 m	GC 6M	hieven	SL: 4540 m, SZ: 75,5 kN
SO181/012-3	10.12.04	20:39	38° 45,20' S	74° 46,03' W	4520	WSW 5	0	0	Gravity Corer 6 m	GC 6M	a.D.	Banane !
SO181/012-3	10.12.04	20:40	38° 45,20' S	74° 46,04' W	4519	WSW 5	154	0,8	Gravity Corer 6 m	GC 6M	Ende station	

Appendix 9.7.1

STATIONBOOK

SO 181-1a

Station	Datum	UTC	PositionLat	PositionLon	Tiefe [m]	Windstärke [m/s]	Kurs [°]	v [kn]	Gerät	Geräte Kürzel	Aktion	Bemerkung
SO181/012-4	10.12.04	20:42	38° 45,21' S	74° 46,08' W	4519	WSW 5	237	2,6	Vermessung	EM / PS	Beginn Profil	rwk: 192°
SO181/012-4	11.12.04	01:14	39° 35,01' S	74° 59,98' W	4299	W 6	248	1,5	Vermessung	EM / PS	Ende Profil	D 51 sm
SO181/013-1	11.12.04	01:16	39° 35,01' S	74° 59,98' W	4302	WSW 4	133	0,3	Gravity Corer 6 m	GC 6M	Beginn Station	SL-181-08
SO181/013-1	11.12.04	01:18	39° 35,01' S	74° 59,98' W	4308	WSW 4	0	0	Gravity Corer 6 m	GC 6M	z.W.	
SO181/013-1	11.12.04	02:22	39° 34,97' S	75° 00,00' W	4300	WSW 4	151	0,9	Gravity Corer 6 m	GC 6M	BoKo	SL 4327 m
SO181/013-1	11.12.04	02:23	39° 34,97' S	75° 00,00' W	4297	WSW 4	0	0	Gravity Corer 6 m	GC 6M	hieven	SZ: 76 kN
SO181/013-1	11.12.04	03:31	39° 34,99' S	75° 00,08' W	4303	WSW 4	4	0,4	Gravity Corer 6 m	GC 6M	a.D.	
SO181/013-1	11.12.04	03:31	39° 34,99' S	75° 00,08' W	4303	WSW 4	4	0,4	Gravity Corer 6 m	GC 6M	Ende station	
SO181/013-2	11.12.04	03:33	39° 35,00' S	75° 00,09' W	4311	W 4	182	1	Vermessung	EM / PS	Beginn Profil	
SO181/013-2	11.12.04	05:03	39° 49,98' S	75° 00,03' W	4316	WSW 4	304	1,5	Vermessung	EM / PS	Ende Profil	D 15 nm
SO181/014-1	11.12.04	05:04	39° 49,97' S	75° 00,02' W	4315	WSW 4	113	1,4	Gravity Corer 6 m	GC 6M	Beginn Station	SL-181-07
SO181/014-1	11.12.04	05:06	39° 49,97' S	75° 00,02' W	4317	WSW 4	132	0,7	Gravity Corer 6 m	GC 6M	zu wasser	
SO181/014-1	11.12.04	06:05	39° 50,07' S	75° 00,10' W	4309	WNW 5	188	0,6	Gravity Corer 6 m	GC 6M	Bodenkontakt	SL: 4318 m
SO181/014-1	11.12.04	06:07	39° 50,08' S	75° 00,12' W	4313	W 5	324	0,7	Gravity Corer 6 m	GC 6M	hieven	SZ: 70 kN
SO181/014-1	11.12.04	07:23	39° 50,05' S	75° 00,18' W	4311	WSW 5	188	1,1	Gravity Corer 6 m	GC 6M	an deck	
SO181/014-1	11.12.04	07:24	39° 50,06' S	75° 00,16' W	4316	WSW 6	226	1,3	Gravity Corer 6 m	GC 6M	Ende station	
SO181/014-2	11.12.04	07:25	39° 50,07' S	75° 00,17' W	4313	WSW 6	275	1,3	Vermessung	EM / PS	Beginn Profil	rwk: 160° d: 22 nm
SO181/014-2	11.12.04	09:21	40° 10,82' S	74° 50,07' W	2684	WNW 6	147	12,5	Vermessung	EM / PS	Kursänderung	rwk: 189° d: 50 nm
SO181/014-2	11.12.04	13:28	40° 59,75' S	74° 59,92' W	2389	NNW 6	180	12,9	Vermessung	EM / PS	Kursänderung	rwk: 270° d: 08 nm
SO181/014-2	11.12.04	14:22	41° 00,02' S	75° 10,97' W	3914	NNW 12	141	1,5	Vermessung	EM / PS	Ende Profil	GesamtDistanz: 80 sm
SO181/015-1	11.12.04	14:22	41° 00,02' S	75° 10,97' W	3914	NNW 12	141	1,5	Gravity Corer 6 meter	GC 6M	Beginn Station	
SO181/015-1	11.12.04	14:25	41° 00,05' S	75° 10,97' W	3913	NNW 11	257	0,9	Gravity Corer 6 m	GC 6M	zu wasser	
SO181/015-1	11.12.04	15:18	41° 00,00' S	75° 11,09' W	3912	NW 9	318	1	Gravity Corer 6 m	GC 6M	Bodenkontakt	SL: 3920m
SO181/015-1	11.12.04	15:20	40° 59,98' S	75° 11,11' W	3914	NW 8	283	1,3	Gravity Corer 6 m	GC 6M	hieven	SZ: 60kN
SO181/015-1	11.12.04	16:24	40° 59,94' S	75° 10,96' W	3912	WNW 10	0	0	Gravity Corer 6 m	GC 6M	an deck	
SO181/015-1	11.12.04	16:26	40° 59,95' S	75° 10,98' W	3912	NNE 11	181	0,8	Gravity Corer 6 m	GC 6M	Ende station	
SO181/015-2	11.12.04	16:40	41° 0,34' S	75° 10,77' W	3789	NW 11	228	4,5	Vermessung	EM / PS	Beginn Profil	rwk: 228°
SO181/015-2	12.12.04	01:40	41° 59,95' S	76° 39,85' W	3504	WNW 14	230	9,6	Vermessung	EM / PS	Kursänderung	ä.K. rwk: 180° D 90 sm
SO181/015-2	12.12.04	05:24	42° 41,54' S	76° 39,70' W	3541	WNW 11	170	1,6	Vermessung	EM / PS	Profilwechsel	ä.K. Profil D 42 sm
SO181/016-1	12.12.04	05:25	42° 41,51' S	76° 39,69' W	3546	WNW 10	352	2,3	OBS/OBH	OBS/OBH	Beginn Station	
SO181/016-1	12.12.04	05:26	42° 41,50' S	76° 39,69' W	3546	WNW 10	280	0	OBS/OBH	OBS/OBH	OBS zu Wasser	OBS 01
SO181/016-1	12.12.04	06:43	42° 49,58' S	76° 38,28' W	3528	WNW 11	357	1,8	OBS/OBH	OBS/OBH	OBH zu Wasser	OBH 02 Profil 8 sm
SO181/016-1	12.12.04	07:47	42° 57,54' S	76° 36,71' W	3532	NW 11	16	1,6	OBS/OBH	OBS/OBH	OBH zu Wasser	OBH 03 Profil 8 sm
SO181/016-1	12.12.04	08:39	43° 5,62' S	76° 35,04' W	3521	NW 12	53	1,1	OBS/OBH	OBS/OBH	OBS zu Wasser	OBS 04 Profil 8 sm
SO181/016-1	12.12.04	09:28	43° 04,38' S	76° 24,07' W	3564	NW 10	179	1,5	OBS/OBH	OBS/OBH	OBS zu Wasser	OBS 05 Profil 8 sm
SO181/016-1	12.12.04	10:22	42° 58,41' S	76° 25,71' W	3568	WNW 10	287	2,3	OBS/OBH	OBS/OBH	OBH zu Wasser	OBH 06 Profil 8 sm

Appendix 9.7.1

STATIONBOOK

SO 181-1a

Station	Datum	UTC	PositionLat	PositionLon	Tiefe [m]	Windstärke [m/s]	Kurs [°]	v [kn]	Gerät	Gerätekürzel	Aktion	Bemerkung
SO181/016-1	12.12.04	11:18	42° 48,40' S	76° 27,32' W	3555	WNW 12	0	0	OBS/OBH	OBS/OBH	OBS zu Wasser	OBS 07 Profil 8 nm
SO181/016-1	12.12.04	12:14	42° 40,38' S	76° 29,02' W	3549	NW 10	0	0	OBS/OBH	OBS/OBH	OBS zu Wasser	OBS 08 rwK: 081 Profil 8 nm
SO181/016-1	12.12.04	13:08	42° 38,12' S	76° 18,05' W	3590	NW 9	0	0	OBS/OBH	OBS/OBH	OBS zu Wasser	OBS 09 (Walze) 171° 8 nm
SO181/016-1	12.12.04	14:01	42° 47,19' S	76° 16,46' W	3627	NW 9	0	0	OBS/OBH	OBS/OBH	OBH zu Wasser	OBH 10 Profil 8 nm
SO181/016-1	12.12.04	14:51	42° 55,17' S	76° 14,81' W	3615	NW 10	223	2,2	OBS/OBH	OBS/OBH	OBH zu Wasser	OBH 11 Profil 8 nm
SO181/016-1	12.12.04	15:49	43° 03,15' S	76° 13,13' W	3591	W 8	166	0,5	OBS/OBH	OBS/OBH	OBS zu Wasser	OBS 12, rwK: 143°, d: 8nm
SO181/016-1	12.12.04	16:43	43° 10,01' S	76° 6,00' W	3612	WNW 6	250	1,2	OBS/OBH	OBS/OBH	OBH zu Wasser	OBH 13, rwK: 262°, d: 7nm
SO181/016-1	12.12.04	17:35	43° 11,00' S	76° 16,00' W	3559	NW 8	253	1,6	OBS/OBH	OBS/OBH	OBH zu Wasser	OBH 14, d: 7nm
SO181/016-1	12.12.04	18:27	43° 12,00' S	76° 25,98' W	3537	NNW 8	262	0	OBS/OBH	OBS/OBH	OBS zu Wasser	OBS 15, d: 7nm
SO181/016-1	12.12.04	19:17	43° 13,00' S	76° 35,96' W	3512	WNW 10	281	2,3	OBS/OBH	OBS/OBH	OBH zu Wasser	OBH 16 d 7nm
SO181/016-1	12.12.04	20:05	43° 14,00' S	76° 45,95' W	3504	NW 11	268	2,6	OBS/OBH	OBS/OBH	OBH zu Wasser	OBH 17 d 7nm
SO181/016-1	12.12.04	20:06	43° 14,01' S	76° 45,99' W	3504	NW 11	266	0,7	OBS/OBH	OBS/OBH	Ende Station	Anfahrt Seismikprof. P01
SO181/017-1	12.12.04	20:08	43° 14,01' S	76° 46,05' W	3511	NW 10	77	2,9	Vermessung	EM / PS	Profilbeginn	
SO181/017-1	12.12.04	20:25	43° 14,10' S	76° 45,94' W	3505	WNW 8	77	2,6	Vermessungsende	EM / PS	Profilende / Airgun z.W.	D 4 nm
SO181/017-1	12.12.04	20:30	43° 14,08' S	76° 45,56' W	3508	NW 9	88	2	Beginn Prof. P01	P01	Bb Airgun z.W.	rwk: 082° 4,5 kn
SO181/017-1	12.12.04	20:45	43° 13,99' S	76° 44,83' W	3503	NW 9	64	2,6	Seismikprofilfahrt	P01	Streamer z.W.	50m + 100m Vorlaufkabel
SO181/017-1	12.12.04	20:50	43° 13,92' S	76° 44,51' W	3501	WNW 8	75	3,3	Seismikprofilfahrt	P01	Stb. Airgun z.W.	
SO181/017-1	13.12.04	04:13	43° 9,01' S	75° 59,97' W	3651	WSW 8	82	4,3	Profilende	PR	Ende Profil	Seismikprofil P01 34 nm
									Anfahrt Profil 02	EM / PS	Vermessung	EM-Profil 2,3 h 10 nm
SO181/017-2	13.12.04	06:29	43° 05,68' S	76° 12,23' W	3592	WNW 9	351	6,1	Profilbeginn P02	PR	Beginn Profil P 02	rwK: 351° P02
SO181/017-2	13.12.04	12:23	42° 38,05' S	76° 17,98' W	3607	NW 9	354	5,2	Profilende	PR	Ende Profil P 02	rwK 263° D: 28 nm
									Anfahrt Profil 03	EM / PS	Vermessung	EM-Profil 3,4 h 16 nm
SO181/017-3	13.12.04	15:46	42° 39,94' S	76° 40,14' W	3546	WNW 6	190	4,2	Profilbeginn P03	PR	Beginn Profil P 03	rwk: 170° P 03
SO181/017-3	13.12.04	16:00	42° 40,91' S	76° 39,77' W	3544	NW 9	170	3,7	Seismikprofilfahrt	PR	50m Streamer und	80m Vorlaufkabel verloren
SO181/017-3	13.12.04	16:38	42° 43,62' S	76° 39,06' W	3541	NNW 8	162	3,9	Seismikprofilfahrt	PR	Magnetometer z.W.	L: 300 m
SO181/017-3	13.12.04	18:55	42° 53,23' S	76° 36,64' W	3393	NW 9	182	2,4	Seismikprofilfahrt	PR	Bb airgun an Deck	
SO181/017-3	13.12.04	19:17	42° 54,03' S	76° 36,67' W	3419	NW 8	166	2,8	Seismikprofilfahrt	PR	Bb Airgun zu Wasser	
SO181/017-3	14.12.04	00:47	43° 19,94' S	76° 29,98' W	3512	NNW 6	180	4	Ende Profil P 03	PR	Ende Profil	D 41 sm
SO181/017-3	14.12.04	00:52	43° 20,27' S	76° 29,90' W	3512	NNW 7	180	3,9			Magnetometer a.D.	
SO181/017-3	14.12.04	01:02	43° 20,76' S	76° 29,75' W	3508	NNW 8	179	2			Bb airgun an Deck	
SO181/017-3	14.12.04	01:03	43° 20,80' S	76° 29,73' W	3511	NW 7	156	2,6			Stb Airgun an Deck	
SO181/017-3	14.12.04	01:10	43° 21,09' S	76° 29,61' W	3510	NW 6	163	3	Ende Seismikfahrt			Vorbereitungen für GC 6m
SO181/018-1	14.12.04	01:17	43° 21,27' S	76° 29,62' W	3512	NNW 12	55	0,7	Gravity Corer 6 m	GC 6M	Beginn Station	
SO181/018-1	14.12.04	01:19	43° 21,27' S	76° 29,62' W	3510	NNW 11	58	1,2	Gravity Corer 6 m	GC 6M	zu wasser	
SO181/018-1	14.12.04	02:06	43° 21,26' S	76° 29,51' W	3512	NNW 10	0	0	Gravity Corer 6 m	GC 6M	Bodenkontakt	SL: 3522 m; SZ: 69,6 kN
SO181/018-1	14.12.04	03:08	43° 21,31' S	76° 29,58' W	3513	NNW 12	0	0	Gravity Corer 6 m	GC 6M	an deck	

Appendix 9.7.1

STATIONBOOK

SO 181-1a

Station	Datum	UTC	PositionLat	PositionLon	Tiefe [m]	Windstärke [m/s]	Kurs [°]	v [kn]	Gerät	GeräteKürzel	Aktion	Bemerkung	
SO181/018-1	14.12.04	03:09	43° 21,31' S	76° 29,59' W	3512	NW 11	310	1,1	Gravity Corer 6 m	GC 6M	Ende station		
SO181/018-2	14.12.04	03:19	43° 21,20' S	76° 29,78' W	3511	NNW 12	194	1,9	Vermessung	EM / PS	Beginn Profil	rwk: 194°	
SO181/018-2	14.12.04	10:09	44° 35,98' S	76° 56,70' W	3074	SW 13	196	9,7	Vermessung	EM / PS	Ende Profil	D 79 nm	
SO181/019-1	14.12.04	10:15	44° 36,44' S	76° 56,91' W	3065	???	13	251	1,5	OBS/OBH	OBS/OBH	Beginn Station	OBS-Auslage
SO181/019-1	14.12.04	10:17	44° 38,47' S	76° 56,94' W	3060	SW 13	219	0,9	OBS/OBH	OBS/OBH	OBS zu Wasser	OBS 18	
SO181/019-1	14.12.04	11:11	44° 44,35' S	76° 53,89' W	2774	SW 14	220	1,3	OBS/OBH	OBS/OBH	OBH zu Wasser	OBH 19	
SO181/019-1	14.12.04	12:08	44° 52,05' S	76° 50,73' W	3025	WSW 13	248	1,4	OBS/OBH	OBS/OBH	OBS zu Wasser	OBS 20	
SO181/019-1	14.12.04	13:03	44° 59,83' S	76° 47,58' W	3094	SW 11	0	0	OBS/OBH	OBS/OBH	OBS zu Wasser	OBS 21; Anf OBS 22: rwk 074	
SO181/019-1	14.12.04	13:56	44° 57,59' S	76° 36,63' W	3253	WSW 10	200	1,7	OBS/OBH	OBS/OBH	OBS zu Wasser	OBS 22; andere rwk: 344	
SO181/019-1	14.12.04	14:48	44° 49,86' S	76° 39,70' W	3235	SW 12	0	0	OBS/OBH	OBS/OBH	OBS zu Wasser	OBS 23	
SO181/019-1	14.12.04	15:45	44° 42,03' S	76° 42,78' W	3223	WSW 12	201	2	OBS/OBH	OBS/OBH	OBS zu Wasser	OBS 24 z.W.	
SO181/019-1	14.12.04	16:45	44° 34,32' S	76° 45,93' W	3019	WSW 12	255	1,2	OBS/OBH	OBS/OBH	OBS zu Wasser	OBS 25 z.W. rwk: 074°	
SO181/019-1	14.12.04	17:38	44° 32,08' S	76° 35,08' W	3009	W 12	155	1,2	OBS/OBH	OBS/OBH	OBS zu Wasser	OBS 26 z.W.; KÄ: rwk: 164°	
SO181/019-1	14.12.04	18:34	44° 39,92' S	76° 31,79' W	3230	WSW 11	120	1,8	OBS/OBH	OBS/OBH	OBS zu Wasser	OBS 27 z.W., KÄ: rwk: 097°	
SO181/020-1	14.12.04	18:57	44° 40,00' S	76° 29,91' W	3257	WSW 10	83	0,3	Gravity Corer 6 m	GC 6M	Beginn Station	SL-181-10	
SO181/020-1	14.12.04	18:58	44° 39,99' S	76° 29,90' W	3257	W 11	88	0,9	Gravity Corer 6 m	GC 6M	z.W.		
SO181/020-1	14.12.04	19:36	44° 40,05' S	76° 29,86' W	3255	WSW 10	303	0,8	Gravity Corer 6 m	GC 6M	Bodenkontakt		
SO181/020-1	14.12.04	19:38	44° 40,05' S	76° 29,85' W	3254	WSW 11	55	0,7	Gravity Corer 6 m	GC 6M	hieven	SL: 3260 m, SZ: 60,5 kN	
SO181/020-1	14.12.04	22:04	44° 40,16' S	76° 28,28' W	3256	WSW 10	34	1,1	Gravity Corer 6 m	GC 6M	an deck	W 6 Ölverlust Sopzeit 1,3 Std	
SO181/020-1	14.12.04	22:13	44° 40,16' S	76° 28,18' W	3259	WSW 9	0	0	Gravity Corer 6 m	GC 6M	Ende station		
SO181/021-1	14.12.04	23:08	44° 47,63' S	76° 28,60' W	3255	WSW 10	303	0,2	Auslage OBS/OBH	OBS/OBH	Beginn Station		
SO181/021-1	14.12.04	23:09	44° 47,64' S	76° 28,62' W	3255	WSW 9	204	0,9	OBS/OBH	OBS/OBH	OBH zu Wasser	OBH 28	
SO181/021-1	15.12.04	00:06	44° 55,37' S	76° 25,55' W	3265	W 10	229	1,1	OBS/OBH	OBS/OBH	OBH zu Wasser	OBH 29 D 16sm	
SO181/021-1	15.12.04	00:06	44° 55,37' S	76° 25,55' W	3265	W 10	229	1,1	OBS/OBH	OBS/OBH	Anfahrt Seismik	Ende Ausl.OBH; Anf. rwk:244	
SO181/021-2	15.12.04	00:10	44° 55,42' S	76° 25,69' W	3235	W 9	243	2,9	Vermessung	EM / PS	Beginn Profil		
SO181/021-2	15.12.04	01:11	44° 59,91' S	76° 35,49' W	3250	WNW 12	327	3,2	Vermessung	EM / PS	Ende Profil	D 11 sm	
SO181/022-1	15.12.04	01:12	44° 59,86' S	76° 35,52' W	3251	W 10	326	2,5		PR	Stationsbeginn		
SO181/022-1	15.12.04	01:25	44° 59,40' S	76° 35,75' W	3249	W 11	328	3,5		PR	Stb Airgun z.W.		
SO181/022-1	15.12.04	01:32	44° 59,04' S	76° 36,05' W	3253	W 10	329	4,2	Seismikprofil P 04	PR	Beginn Profil	rwk: 343° P 04	
SO181/022-1	15.12.04	01:35	44° 58,84' S	76° 36,14' W	3252	W 11	329	4,4	Seismikprofil	PR	Magnetometer z.W.	L: 300 m	
SO181/022-1	15.12.04	07:37	44° 32,58' S	76° 47,23' W	3007	WNW 12	336	4,6	Seismikprofil	PR	Magnetometer a.D.		
SO181/022-1	15.12.04	07:38	44° 32,51' S	76° 47,26' W	3015	WNW 12	335	3,8	Seismikprofil P 04	PR	Ende Profil P 04	D 27 sm	
SO181/022-1	15.12.04	07:47	44° 32,18' S	76° 47,33' W	2997	W 14	351	2,2	Profil	PR	Stb Airgun an Deck		
SO181/022-1	15.12.04	07:47	44° 32,18' S	76° 47,33' W	2997	W 14	351	2,2	Profil	PR	Ende Profilfahrt		
SO181/022-2	15.12.04	07:48	44° 32,15' S	76° 47,33' W	2972	W 14	23	1,5	Vermessung	EM / PS	Beginn Profil	rwk: 86°	
SO181/022-2	15.12.04	11:23	44° 30,03' S	75° 49,98' W	3328	W 9	254	1,6	Vermessung	EM / PS	Ende Profil	D 41 nm	

Appendix 9.7.1

STATIONBOOK

SO 181-1a

Station	Datum	UTC	PositionLat	PositionLon	Tiefe [m]	Windstärke [m/s]	Kurs [°]	v [kn]	Gerät	Gerätekürzel	Aktion	Bemerkung
SO181/023-1	15.12.04	11:24	44° 30,04' S	75° 49,98' W	3329	W 10	0	0	Gravity Corer 6 m	GC 6M	Beginn Station	
SO181/023-1	15.12.04	11:27	44° 30,07' S	75° 49,97' W	3330	W 8	0	0	Gravity Corer 6 m	GC 6M	zu wasser	Winde 1
SO181/023-1	15.12.04	12:12	44° 30,03' S	75° 49,87' W	3328	WNW 10	331	1	Gravity Corer 6 m	GC 6M	Bodenkontakt	SL: 3334m; SZ:61 KN
SO181/023-1	15.12.04	12:57	44° 29,96' S	75° 49,91' W	3330	WNW 9	240	1	Gravity Corer 6 m	GC 6M	an deck	Banane
SO181/023-1	15.12.04	13:03	44° 29,96' S	75° 49,91' W	3332	W 9	304	0,7	Gravity Corer 6 m	GC 6M	Ende station	
SO181/023-2	15.12.04	13:04	44° 29,96' S	75° 49,91' W	3329	W 11	72	1,4	Vermessung	EM / PS	Beginn Profil	rwK: 002°
SO181/023-2	15.12.04	21:05	42° 59,97' S	75° 44,99' W	3729	WNW 14	33	11,2	Vermessung	EM / PS	Kursänderung	rwk: 048° D 90 nm
SO181/023-2	15.12.04	22:20	42° 49,92' S	75° 30,21' W	3695	W 8	43	6,9	Vermessung	EM / PS	Ende Profil	D 15 nm
SO181/024-1	15.12.04	22:26	42° 49,94' S	75° 29,91' W	3703	NW 10	257	1,1	Gravity Corer 6 m	GC 6M	Beginn Station	SL-181-12 Winde W 1
SO181/024-1	15.12.04	22:28	42° 49,94' S	75° 29,95' W	3700	WNW 10	237	1,1	Gravity Corer 6 m	GC 6M	z.W.	
SO181/024-1	15.12.04	23:20	42° 50,04' S	75° 30,00' W	3703	NW 11	295	0,7	Gravity Corer 6 m	GC 6M	Bodenkontakt	SL: 3720m; SZ:69,4KN
SO181/024-1	16.12.04	00:17	42° 50,07' S	75° 30,09' W	3700	WNW 10	0	0	Gravity Corer 6 m	GC 6M	a.D.	
SO181/024-1	16.12.04	00:17	42° 50,07' S	75° 30,09' W	3700	WNW 10	0	0	Gravity Corer 6 m	GC 6M	Ende station	
SO181/024-2	16.12.04	00:18	42° 50,07' S	75° 30,08' W	3700	NW 11	137	1	Vermessung	EM / PS	Beginn Profil	rwK: 090°, d: 51 nm
SO181/024-2	16.12.04	04:34	42° 49,92' S	74° 20,19' W	71	WNW 10	61	11,5	Vermessung	EM / PS	Kursänderung	rwK: 360°, d: 20 nm
SO181/024-2	16.12.04	06:20	42° 30,20' S	74° 20,04' W	122	NNW 9	342	10,8	Vermessung	EM / PS	Kursänderung	rwK: 283°, d: 45 nm
SO181/024-2	16.12.04	10:36	42° 20,00' S	75° 18,86' W	2682	NNW 12	311	8,8	Vermessung	EM / PS	Kursänderung	rwk: 071°, d: 31 nm
SO181/024-2	16.12.04	13:13	42° 10,13' S	74° 40,29' W	138	NW 10	75	11,8	Vermessung	EM / PS	Kursänderung	rwK:285; d:38sm
SO181/024-2	16.12.04	16:59	41° 59,99' S	75° 29,87' W	3875	NW 12	266	2,7	Vermessung	EM / PS	Ende Profil	
SO181/025-1	16.12.04	17:00	41° 59,99' S	75° 29,94' W	3680	NW 12	276	2,9	CTD	CTD	Beginn Station	
SO181/025-1	16.12.04	17:01	41° 59,99' S	75° 29,95' W	3679	NNE 14	359	1,2	CTD	CTD	zu Wasser	CTD Releasetest
SO181/025-1	16.12.04	18:02	42° 0,29' S	75° 30,33' W	0	NW 12	287	1,6	CTD	CTD	auf Tiefe	SL: 3500 m, Transducer in Betr. Und
SO181/025-1	16.12.04	19:45	42° 0,50' S	75° 30,68' W	3874	NW 12	133	0,3	CTD	CTD	an Deck	von 18.31 - 18:45 Hydrophon z.W.
SO181/025-1	16.12.04	20:05	42° 0,49' S	75° 30,77' W	3871	NW 11	207	1,1	CTD	CTD	Ende Station	Ende der Stationsarbeiten der Releas
SO181/025-2	16.12.04	20:08	42° 0,44' S	75° 30,78' W	3875	WNW 11	17	3,2	Vermessung	EM / PS	Beginn Profil	rwk: 024°, d: 68 nm
SO181/025-2	17.12.04	01:40	41° 0,11' S	74° 55,09' W	1810	WNW 12	29	12,1	Vermessung	EM / PS	Kursänderung	rwK: 008°, d: 56 nm
SO181/025-2	17.12.04	06:36	40° 5,19' S	74° 44,92' W	2357	WNW 10	81	9,7	Vermessung	EM / PS	Kursänderung	rwK: 090°, d: 11 nm
SO181/025-2	17.12.04	07:39	40° 5,01' S	74° 30,18' W	1602	WNW 12	88	10,8	Vermessung	EM / PS	Kursänderung	rwk: 090°, d: 15 nm
SO181/025-2	17.12.04	08:57	40° 5,02' S	74° 10,14' W	515	WNW 9	88	11,5	Vermessung	EM / PS	Kursänderung	rwk: 360°, d: 7 nm
SO181/025-2	17.12.04	09:36	39° 58,04' S	74° 9,97' W	626	NW 10	27	10,4	Vermessung	EM / PS	Kursänderung	rwk: 090°, d: 8 nm
SO181/025-2	17.12.04	10:14	39° 57,99' S	74° 0,07' W	759	WNW 12	59	12,2	Vermessung	EM / PS	Kursänderung	rwk: 360°, d: 28 nm
SO181/025-2	17.12.04	12:47	39° 29,99' S	73° 59,99' W	555	WNW 12	356	11,2	Vermessung	EM / PS	Ende Profil	Ende der Datenaufzeichnungen
												Anfahrt Corral-Reede D 33 sm

Abkürzungen / Abbreviation

z.W	zu Wasser
a.D.	an Deck
SL (max.)	(maximale) Seillänge
LT	Lottiefe nach Hydrosweep
W x	eingesetzte Winde
SM	Simrad - Multibeam - Lot
PS	Parasound
rwk:	Rechtweisender Kurs
d:	Distanz
v:	Geschwindigkeit in Knoten
SL:	Seillänge
KL:	Kabellänge

Eingesetzte Geräte

CTD/Ro	CTD- Rosettengestell für Releasertest
Airgun	1x GI-Gun 2,5 l
Streamer	Streamer {100m + 100m Vorlaufkabel}
Magn.	Magnetometer
Seismk	Seismikprofile mit Magnetometer
Vermess.	EM/PS-Vermessungsprofile mit / ohne Magnetometer
GHF	Wärmestromsonde 5m auf 7 Profilen
HF	Wärmestromsonde 3m auf 4 Profilen
GC (SL)	Schwerelos 5m

Geräteverluste: KEINE

Einsätze

0	
auf 4 Profilen	
auf 4 Profilen	
auf 13 Profilen	
4 Profile	Profilzeit: 99 Sld. Profillänge 484 nm
22 Profile	Profilzeit: 449 Sld. Profillänge 4570 nm
57	
34	
7	

Winde	D/M	Typ	RF-Nr	SO 181.1b Einsatz	Gesamt Einsatz	SO 181.1b S'länge	Gesamt S'länge	Zust.	SO 181.1b geferte max. L	Jemals geferte max. Länge
W 1	18.01.00	LWL	812001	114 h	483 h	36109	235148	3-4	4397 m	8022 m
W 2	18.01.00	LWL	815286	0 h	0 h	0 m	0 m	1	0 m	0 m
W 4	11.01.00	NSW	818045	0 h	268 h	0 m	220273 m	3	0 m	8081 m
W 5	11.01.00	NSW	812106	0 h	0 h	0 m	0 m	1	0 m	0 m
W 6	18.01.00	DRAKO	818238	11 h	1135 h	16453 m	1079674 m	3-4	3412 m	7609 m

Station	Datum	UTC	PositionLat	PositionLon	Tiefe [m]	Windstärke [m/s]	Kurs [°]	v [kn]	Gerät	Gerätekürzel	Aktion	Bemerkung
	18.12.04	13:48	Corral	Reede							Abfahrt Corral	Beginn der Reise SO 181.1b
SO181/026-1	18.12.04	15:00	39° 49.64' S	73° 36.65' W	70	W 10	269	8,6	Magnetometer	MAGN	Beginn Station	Survey 1b-1
SO181/026-1	18.12.04	15:01	39° 49.64' S	73° 36.56' W	70	WSW 9	271	7,3	Magnetometer	MAGN	Beginn Profil	rwk: 258°, d: 50 nm
SO181/026-1	18.12.04	15:30	39° 50.02' S	73° 39.15' W	76	SW 9	247	4	Magnetometer	MAGN	Magnetometer zu Wasser	SL = 200 m
SO181/026-1	18.12.04	20:25	39° 59.97' S	74° 40.84' W	1919	SW 8	241	11,6	Magnetometer	MAGN	Kursänderung	rwk: 188°, d: 64 nm
SO181/026-1	19.12.04	02:46	41° 2.75' S	74° 52.97' W	1727	SW 7	189	10,5	Magnetometer	MAGN	Kursänderung	rwk: 243°, d: 18 nm
SO181/026-1	19.12.04	04:36	41° 11.06' S	75° 13.76' W	3543	WSW 2	219	9	Magnetometer	MAGN	Kursänderung	rwk: 183°, d: 128 nm
SO181/026-1	19.12.04	17:07	43° 18.35' S	75° 23.37' W	2302	N 7	153	9,7	Magnetometer	MAGN	Kursänderung	rwk: 090°, d: 4 nm
SO181/026-1	19.12.04	17:30	43° 18.46' S	75° 18.28' W	1841	NE 4	62	9,6	Magnetometer	MAGN	Kursänderung	rwk: 003°, d: 98 nm
SO181/026-1	20.12.04	03:16	41° 40.61' S	75° 9.92' W	2533	NNW 5	28	10,2	Magnetometer	MAGN	Kursänderung	rwk: 083°, d: 4 nm
SO181/026-1	20.12.04	03:39	41° 40.13' S	75° 4.93' W	2183	WNW 6	115	9,6	Magnetometer	MAGN	Kursänderung	rwk: 184°, d: 55 nm
SO181/026-1	20.12.04	08:57	42° 34.95' S	75° 9.00' W	1351	NNW 6	158	10,5	Magnetometer	MAGN	Kursänderung	rwk: 083°, d: 25 nm
SO181/026-1	20.12.04	11:20	42° 32.04' S	74° 35.57' W	930	N 8	82	10,5	Magnetometer	MAGN	Kursänderung	rwk: 204; d: 65m
SO181/026-1	20.12.04	12:00	42° 37.75' S	74° 38.50' W	167	NNW 4	200	4,9	Magnetometer	MAGN	Ende Profil	Magnetometer bleibt z.W.
SO181/027-1	20.12.04	12:01	42° 37.80' S	74° 38.54' W	166	NNW 4	203	3,1	Profil	PR	Stationsbeginn	Magnetometer z.W. (Station 26)
SO181/027-1	20.12.04	12:06	42° 38.02' S	74° 38.64' W	166	NNW 5	184	2,7	Profil	PR	Streamer zu Wasser	Länge: 100 + 100m Vorlaufkabel
SO181/027-1	20.12.04	12:14	42° 38.34' S	74° 38.74' W	165	NNW 5	210	3,7	Profil	PR	Stb Airgun zu Wasser	
SO181/027-1	20.12.04	13:25	42° 43.69' S	74° 42.24' W	126	NNW 4	205	5,4	Profil	PR	Kursänderung	rwk: 261°
SO181/027-1	20.12.04	13:34	42° 44.18' S	74° 42.92' W	128	NNW 6	253	4,4	Seismikprofil SC501	PR	Beginn Profil SC501	rwk: 261°, d: 168 nm
SO181/027-1	21.12.04	23:03	43° 11.40' S	78° 29.98' W	3584,6	NNW 13	275	5,4	Seismikprofil SC502	PR	Ende Profil	
SO181/027-1	21.12.04	23:09	43° 11.42' S	78° 30.42' W	3544,1	NNW 13	247	2,2	Profil	PR	Magnetometer an Deck	
SO181/027-1	21.12.04	23:14	43° 11.41' S	78° 30.62' W	3542,5	NNW 13	300	2,1	Profil	PR	Stb Airgun an Deck	

Station	Datum	UTC	PositionLat	PositionLon	Tiefe [m]	Windstärke [m/s]	Kurs [°]	v [kn]	Gerät	Gerätekürzel	Aktion	Bemerkung
SO181/027-1	21.12.04	23:23	43° 11,35' S	78° 31,03' W	3512,8	NNW 15	289	2	Profil	PR	Streamer an Deck	
SO181/027-1	21.12.04	23:26	43° 11,33' S	78° 31,11' W	3577,1	NNW 14	292	2,8	Profil	PR	Stationsende	
SO181/028-1	22.12.04	00:11	43° 10,44' S	78° 22,00' W	3559,6	NNW 14	315	2	Wärmestromsonde 3 m	HF	Beginn Station HF 01	
SO181/028-1	22.12.04	00:28	43° 10,43' S	78° 21,99' W	3543,4	NNW 12	221	0,4	Wärmestromsonde 3 m	HF	z.W.	W 1 Pinger bei KL:50m
SO181/028-1	22.12.04	01:38	43° 10,45' S	78° 21,95' W	3545,4	NNW 13	160	0,3	Wärmestromsonde 3 m	HF	Boko	SL: 3578 m P 01
SO181/028-1	22.12.04	01:53	43° 10,45' S	78° 21,97' W	3545,8	NNW 13	177	0,9	Wärmestromsonde 3 m	HF	hieven	SZ:84,9kN; Winde stop SL:3400m
SO181/028-1	22.12.04	01:57	43° 10,46' S	78° 21,96' W	3548,9	NNW 13	182	1,1	Wärmestromsonde 3 m	HF	verholen	rwk: 262°, d: 0,54 nm
SO181/028-1	22.12.04	02:56	43° 10,54' S	78° 22,68' W	3668,3	NNW 12	44	0,3	Wärmestromsonde 3 m	HF	Boko	SL: 3638 m P 02
SO181/028-1	22.12.04	03:07	43° 10,53' S	78° 22,67' W	3663,7	N 13	16	0,9	Wärmestromsonde 3 m	HF	hieven	SZ: 49 kN, SL: 3539 m
SO181/028-1	22.12.04	03:08	43° 10,53' S	78° 22,68' W	3664,8	NNW 14	301	1,4	Wärmestromsonde 3 m	HF	verholen	rwk: 260°, d: 0,54 nm
SO181/028-1	22.12.04	03:59	43° 10,62' S	78° 23,42' W	3588,1	NNW 13	152	1,1	Wärmestromsonde 3 m	HF	Boko	SL: 3666 m P 03
SO181/028-1	22.12.04	04:12	43° 10,62' S	78° 23,42' W	3581,2	NNW 12	182	2,1	Wärmestromsonde 3 m	HF	hieven	SZ: 48 kN; Winde stop, SL: 3400 m
SO181/028-1	22.12.04	04:14	43° 10,63' S	78° 23,41' W	3582	NNW 13	78	0,8	Wärmestromsonde 3 m	HF	verholen	rwk: 261°, d: 0,54 nm
SO181/028-1	22.12.04	05:08	43° 10,70' S	78° 24,13' W	3603	NNW 13	61	3,1	Wärmestromsonde 3 m	HF	Boko	SL: 3641 m P 04
SO181/028-1	22.12.04	05:15	43° 10,70' S	78° 24,14' W	3599	NNW 14	4	1	Wärmestromsonde 3 m	HF	hieven	SZ: 49 kN, Winde stop, SL: 3400 m
SO181/028-1	22.12.04	05:17	43° 10,70' S	78° 24,14' W	3607	NNW 14	282	0,6	Wärmestromsonde 3 m	HF	verholen	rwk: 260°, d: 0,54 nm
SO181/028-1	22.12.04	06:06	43° 10,79' S	78° 24,86' W	3563	NNW 14	292	1,5	Wärmestromsonde 3 m	HF	Boko	SL: 3624 m P 05
SO181/028-1	22.12.04	06:19	43° 10,80' S	78° 24,88' W	3568	NNW 14	251	2,2	Wärmestromsonde 3 m	HF	hieven	SZ: 57 kN, Winde stop, SL: 3400 m
SO181/028-1	22.12.04	06:21	43° 10,78' S	78° 24,89' W	3561	NNW 14	85	1,2	Wärmestromsonde 3 m	HF	verholen	rwk: 260°, d: 0,54 nm
SO181/028-1	22.12.04	07:33	43° 10,86' S	78° 25,60' W	3538	NNW 13	0	0	Wärmestromsonde 3 m	HF	Boko	SL: 3585 m, P 06
SO181/028-1	22.12.04	07:45	43° 10,88' S	78° 25,59' W	3541	NNW 13	0	0	Wärmestromsonde 3 m	HF	hieven	
SO181/028-1	22.12.04	07:48	43° 10,88' S	78° 25,59' W	3535	NNW 14	303	0,2	Wärmestromsonde 3 m	HF	verholen	rwk: 262°, d: 0,54 nm
SO181/028-1	22.12.04	08:40	43° 10,98' S	78° 26,34' W	3568	NNW 13	254	0,9	Wärmestromsonde 3 m	HF	Boko	SL: 3672 m P 07
SO181/028-1	22.12.04	08:50	43° 10,96' S	78° 26,34' W	3567	NNW 12	87	0,5	Wärmestromsonde 3 m	HF	hieven	
SO181/028-1	22.12.04	08:52	43° 10,96' S	78° 26,34' W	3567	NNW 13	298	1,2	Wärmestromsonde 3 m	HF	verholen	rwk: 260°, d: 0,54 nm
SO181/028-1	22.12.04	09:34	43° 11,03' S	78° 27,06' W	3596	NNW 13	112	1,2	Wärmestromsonde 3 m	HF	Boko	SL: 3692 m P 08
SO181/028-1	22.12.04	09:46	43° 11,03' S	78° 27,06' W	3600	NNW 13	23	1,6	Wärmestromsonde 3 m	HF	hieven	
SO181/028-1	22.12.04	09:50	43° 11,02' S	78° 27,06' W	3595	NNW 14	188	0,5	Wärmestromsonde 3 m	HF	verholen	rwk: 259°, d: 0,54 nm
SO181/028-1	22.12.04	10:32	43° 11,14' S	78° 27,80' W	3569	NNW 14	221	0,2	Wärmestromsonde 3 m	HF	Boko	SL: 3685 m, P 09
SO181/028-1	22.12.04	10:43	43° 11,13' S	78° 27,80' W	3566	NNW 13	279	0,6	Wärmestromsonde 3 m	HF	hieven	
SO181/028-1	22.12.04	10:49	43° 11,13' S	78° 27,80' W	3573	NNE 14	182	0,5	Wärmestromsonde 3 m	HF	verholen	rwk: 260°, d: 0,54 nm
SO181/028-1	22.12.04	11:33	43° 11,24' S	78° 28,52' W	3588	NNW 13	0	0	Wärmestromsonde 3 m	HF	Boko	SL: 3674m P 10
SO181/028-1	22.12.04	11:38	43° 11,23' S	78° 28,53' W	3588	NNW 13	158	0,3	Wärmestromsonde 3 m	HF	hieven	SZ: 50,9 kN
SO181/028-1	22.12.04	12:32	43° 11,18' S	78° 28,55' W	3597	NNW 13	245	1,5	Wärmestromsonde 3 m	HF	a.D.	12:28 Pinger a.D.
SO181/028-1	22.12.04	12:38	43° 11,17' S	78° 28,56' W	3586	NNW 13	103	1,8	Wärmestromsonde 3 m	HF	Ende Station HF 01	
SO181/029-1	22.12.04	12:44	43° 10,83' S	78° 28,74' W	3576	NNW 16	333	6,8	Simrad + Magnetik Survey	MAGN	Beginn Station	
SO181/029-1	22.12.04	12:47	43° 10,63' S	78° 28,83' W	3570	NNW 15	327	4,3	Magnetometer	MAGN	Magnetometer z.W.	SL: 200m
SO181/029-1	22.12.04	12:50	43° 10,50' S	78° 28,88' W	3573	NNW 14	326	3,8	Simrad+Magnetik Survey	MAGN	Beginn Profil 1b-2	rwk: 349 ; d:5 sm Profil 1b-2
SO181/029-1	22.12.04	13:24	43° 6,03' S	78° 30,18' W	3625	NNW 17	71	8,5	Simrad+Magnetik Survey	MAGN	Kursänderung	rwk: 081°, d: 81 nm
SO181/029-1	22.12.04	22:01	42° 53,13' S	76° 41,09' W	3284	NW 16	107	9,9	Simrad+Magnetik Survey	MAGN	Kursänderung	rwk: 180°, d: 4 nm
SO181/029-1	22.12.04	22:27	42° 57,41' S	76° 41,00' W	3533	NW 15	178	6,6	Simrad+Magnetik Survey	MAGN	Ende Profil	

Station	Datum	UTC	PositionLat	PositionLon	Tiefe [m]	Windstärke [m/s]	Kurs [°]	v [kn]	Gerät	Gerätekürzel	Aktion	Bemerkung
SO181/029-1	22.12.04	22:31	42° 57,78' S	76° 40,99' W	3536	NNW 14	157	4,8	Simrad+Magnetik Survey	MAGN	Magnetometer a.D.	
SO181/029-1	22.12.04	22:31	42° 57,78' S	76° 40,99' W	3536	NNW 14	157	4,8	Simrad+Magnetik Survey	MAGN	Ende Station	D gesamt: 90 sm Zeit: 9,7 Std.
SO181/030-1	22.12.04	22:48	42° 58,52' S	76° 41,73' W	3535	NNW 15	305	1,2	Wärmestromsonde 3 m	HF	Beginn Station HF 02	HF 02
SO181/030-1	22.12.04	22:50	42° 58,53' S	76° 41,73' W	3533	NNW 14	74	0,9	Wärmestromsonde 3 m	HF	z.W.	Pinger SL 60 m
SO181/030-1	22.12.04	23:58	42° 58,47' S	76° 41,72' W	3535	NNW 14	155	1	Wärmestromsonde 3 m	HF	Boko	SL:3559m P 01
SO181/030-1	23.12.04	00:13	42° 58,48' S	76° 41,72' W	3535	NNW 14	60	1,1	Wärmestromsonde 3 m	HF	hieven	Winde stop: 3400m
SO181/030-1	23.12.04	00:15	42° 58,47' S	76° 41,72' W	3534	NNW 14	250	1,5	Wärmestromsonde 3 m	HF	verholen	rwk: 261°, d: 0,54 nm
SO181/030-1	23.12.04	01:07	42° 58,56' S	76° 42,43' W	3530	N 14	110	1,1	Wärmestromsonde 3 m	HF	Boko	SL:3576m P 02
SO181/030-1	23.12.04	01:13	42° 58,55' S	76° 42,44' W	3531	N 14	151	1,8	Wärmestromsonde 3 m	HF	hieven	Winde stop SL:3400m
SO181/030-1	23.12.04	01:16	42° 58,57' S	76° 42,45' W	3532	N 15	241	1,7	Wärmestromsonde 3 m	HF	verholen	rwk: 260°, d: 0,54 nm
SO181/030-1	23.12.04	02:16	42° 58,66' S	76° 43,19' W	3531	NNW 12	260	1,8	Wärmestromsonde 3 m	HF	Boko	SL: 3577m P 03
SO181/030-1	23.12.04	02:32	42° 58,65' S	76° 43,20' W	3531	NNW 10	0	0	Wärmestromsonde 3 m	HF	hieven	Winde stop SL:3400m
SO181/030-1	23.12.04	02:35	42° 58,63' S	76° 43,22' W	3532	NNW 10	223	0,6	Wärmestromsonde 3 m	HF	verholen	rwk: 261°, d: 0,62 nm
SO181/030-1	23.12.04	03:37	42° 58,73' S	76° 43,92' W	3528	NW 9	92	0,7	Wärmestromsonde 3 m	HF	Boko	SL: 3569 m P 04
SO181/030-1	23.12.04	03:42	42° 58,74' S	76° 43,90' W	3528	NW 8	261	1,4	Wärmestromsonde 3 m	HF	hieven	Winde stop, SL: 3400 m
SO181/030-1	23.12.04	03:46	42° 58,72' S	76° 43,91' W	3528	NW 7	341	1,4	Wärmestromsonde 3 m	HF	verholen	rwk: 260°, d: 0,52 nm
SO181/030-1	23.12.04	04:48	42° 58,78' S	76° 44,63' W	3527	WNW 6	238	0,5	Wärmestromsonde 3 m	HF	Boko	SL: 3566 m P 05
SO181/030-1	23.12.04	05:00	42° 58,84' S	76° 44,66' W	3527	WNW 4	4	1,4	Wärmestromsonde 3 m	HF	hieven	Winde stop, SL: 3400 m
SO181/030-1	23.12.04	05:03	42° 58,83' S	76° 44,67' W	3527	WNW 4	284	0,8	Wärmestromsonde 3 m	HF	verholen	rwk: 261°, d: 0,62 nm
SO181/030-1	23.12.04	05:59	42° 58,91' S	76° 45,34' W	3527	NNW 8	273	1,4	Wärmestromsonde 3 m	HF	Boko	SL: 3566 m P 06
SO181/030-1	23.12.04	06:03	42° 58,92' S	76° 45,36' W	3526	NNW 7	28	1,3	Wärmestromsonde 3 m	HF	hieven	Winde stop: SL: 3400 m
SO181/030-1	23.12.04	06:06	42° 58,91' S	76° 45,39' W	3530	NW 7	345	2	Wärmestromsonde 3 m	HF	verholen	rwk: 261°, d: 0,52 nm
SO181/030-1	23.12.04	06:59	42° 58,98' S	76° 46,10' W	3521	NNW 7	50	1,3	Wärmestromsonde 3 m	HF	Boko	SL: 3569 m P 07
SO181/030-1	23.12.04	07:14	42° 58,97' S	76° 46,12' W	3528	NNW 6	224	1	Wärmestromsonde 3 m	HF	hieven	
SO181/030-1	23.12.04	07:17	42° 58,98' S	76° 46,12' W	3524	NW 6	295	1,2	Wärmestromsonde 3 m	HF	verholen	rwk: 261°, d: 0,54 nm
SO181/030-1	23.12.04	08:05	42° 59,09' S	76° 46,84' W	3526	NNW 6	56	1	Wärmestromsonde 3 m	HF	Boko	SL: 3572 m P 08
SO181/030-1	23.12.04	08:11	42° 59,09' S	76° 46,85' W	3531	NNW 6	0	0	Wärmestromsonde 3 m	HF	hieven	
SO181/030-1	23.12.04	08:14	42° 59,09' S	76° 46,85' W	3526	NNW 6	301	1	Wärmestromsonde 3 m	HF	verholen	rwk: 261°, d: 0,54 nm
SO181/030-1	23.12.04	08:51	42° 59,17' S	76° 47,55' W	3526	NNW 5	31	0,8	Wärmestromsonde 3 m	HF	Boko	SL: 3593 m, P 09
SO181/030-1	23.12.04	09:05	42° 59,17' S	76° 47,55' W	3527	NNW 6	350	0,4	Wärmestromsonde 3 m	HF	hieven	
SO181/030-1	23.12.04	09:09	42° 59,17' S	76° 47,54' W	3524	NNW 5	35	1,6	Wärmestromsonde 3 m	HF	verholen	rwk: 261°, d: 0,54 nm
SO181/030-1	23.12.04	09:53	42° 59,26' S	76° 48,28' W	3522	NW 5	359	1,1	Wärmestromsonde 3 m	HF	Boko	SL: 3584 m, P 10
SO181/030-1	23.12.04	10:07	42° 59,25' S	76° 48,28' W	3523	NNW 4	0	0	Wärmestromsonde 3 m	HF	hieven	
SO181/030-1	23.12.04	11:15	42° 58,98' S	76° 49,00' W	3529	SW 14	285	1,4	Wärmestromsonde 3 m	HF	a.D.	09:11 Pinger a.D.
SO181/030-1	23.12.04	11:17	42° 58,95' S	76° 49,04' W	3533	S 16	297	1	Wärmestromsonde 3 m	HF	Ende Station	
SO181/031-1	23.12.04	11:20	42° 58,89' S	76° 49,13' W	3523	SSW 15	324	2,8	Magnetometer	MAGN	Beginn Station	
SO181/031-1	23.12.04	11:25	42° 58,60' S	76° 49,21' W	3525	S 6	352	2,9	Magnetometer	MAGN	Magnetometer z.W.	SL: 200m
SO181/031-1	23.12.04	11:27	42° 58,49' S	76° 49,16' W	3524	S 10	55	3,5	Simrad + Magnetik Survey	MAGN	Beginn Profil 1b-3	rwK: 048; d:8sm
SO181/031-1	23.12.04	12:17	42° 53,25' S	76° 41,80' W	3531	S 9	48	9,4	Simrad + Magnetik Survey	MAGN	Kursänderung	rwK: 081°, d: 67 nm
SO181/031-1	23.12.04	19:26	42° 42,48' S	75° 9,81' W	1416	S 13	79,2	5,2	Simrad + Magnetik Survey	MAGN	Ende Profil	
SO181/031-1	23.12.04	19:31	42° 42,40' S	75° 9,39' W	1443	SSW 13	77,4	2,6	Simrad + Magnetik Survey	MAGN	Magnetometer an Deck	

Station	Datum	UTC	PositionLat	PositionLon	Tiefe [m]	Windstärke [m/s]	Kurs [°]	v [kn]	Gerät	Gerätekürzel	Aktion	Bemerkung
SO181/031-1	23.12.04	19:31	42° 42,40' S	75° 9,39' W	1443	SSW 13	77,4	2,6	Simrad + Magnetik Survey	MAGN	Ende Station	
SO181/032-1	23.12.04	20:23	42° 47,68' S	75° 11,64' W	1562	NNE 13	156	1,6	Wärmestromsonde 6 m	GHF	Beginn Station	GHF 03 (W 1)
SO181/032-1	23.12.04	20:29	42° 47,69' S	75° 11,64' W	1580	SSW 13	293,4	0,8	Wärmestromsonde 6 m	GHF	z.W.	
SO181/032-1	23.12.04	21:09	42° 47,72' S	75° 11,65' W	1581	SSW 13	90,9	2,5	Wärmestromsonde 6 m	GHF	Boko	SL: 1597 m, P 1
SO181/032-1	23.12.04	21:10	42° 47,72' S	75° 11,66' W	1583	SSW 12	265,1	0,8	Wärmestromsonde 6 m	GHF	hieven	umgefallen
SO181/032-1	23.12.04	21:15	42° 47,71' S	75° 11,66' W	1583	NNE 12	342,3	1,4	Wärmestromsonde 6 m	GHF	Boko	SL: 1594 m, P 1 die Zweite
SO181/032-1	23.12.04	21:16	42° 47,72' S	75° 11,66' W	1579	NNE 12	24,1	0,8	Wärmestromsonde 6 m	GHF	hieven	umgefallen
SO181/032-1	23.12.04	21:22	42° 47,74' S	75° 11,67' W	1590	SW 12	114,4	1,8	Wärmestromsonde 6 m	GHF	verholen	rwk: 081°, d: 0,54 nm
SO181/032-1	23.12.04	22:07	42° 47,61' S	75° 10,93' W	1423	SSW 11	194,5	1,1	Wärmestromsonde 6 m	GHF	Boko	SL: 1427 m, P 2
SO181/032-1	23.12.04	22:08	42° 47,60' S	75° 10,94' W	1423	SSW 12	280,5	0,5	Wärmestromsonde 6 m	GHF	hieven	umgefallen
SO181/032-1	23.12.04	22:10	42° 47,59' S	75° 10,94' W	1423	SSW 12	357,3	1,3	Wärmestromsonde 6 m	GHF	verholen	rwk: 081°, d: 0,54 nm
SO181/032-1	23.12.04	22:49	42° 47,50' S	75° 10,20' W	1236	SW 11	59,6	1	Wärmestromsonde 6 m	GHF	Boko	SL: 1239 m, P 3
SO181/032-1	23.12.04	22:49	42° 47,50' S	75° 10,20' W	1236	SW 11	59,6	1	Wärmestromsonde 6 m	GHF	hieven	umgefallen
SO181/032-1	23.12.04	22:51	42° 47,50' S	75° 10,21' W	1237	S 14	183,7	1,1	Wärmestromsonde 6 m	GHF	verholen	rwk: 081°, d: 0,54 nm
SO181/032-1	23.12.04	23:45	42° 47,43' S	75° 9,48' W	1146	SW 10	341,4	0,3	Wärmestromsonde 6 m	GHF	Boko	SL: 1169m P 4
SO181/032-1	24.12.04	00:00	42° 47,45' S	75° 9,50' W	1150	SW 12	13,6	0,2	Wärmestromsonde 6 m	GHF	hieven	
SO181/032-1	24.12.04	00:03	42° 47,46' S	75° 9,52' W	1154	SW 13	244,9	0,8	Wärmestromsonde 6 m	GHF	verholen	rwk: 081°, d: 0,54 nm
SO181/032-1	24.12.04	00:53	42° 47,35' S	75° 8,77' W	1121	SSW 11	24,1	0,8	Wärmestromsonde 6 m	GHF	Boko	SL: 1143m P 5
SO181/032-1	24.12.04	01:07	42° 47,34' S	75° 8,79' W	1124	SSW 11	224	1	Wärmestromsonde 6 m	GHF	hieven	
SO181/032-1	24.12.04	01:11	42° 47,37' S	75° 8,79' W	1121	SW 12	168	0,7	Wärmestromsonde 6 m	GHF	verholen	rwk: 081°, d: 0,54 nm
SO181/032-1	24.12.04	01:55	42° 47,30' S	75° 8,03' W	1129	SSW 12	165,3	0,3	Wärmestromsonde 6 m	GHF	Boko	SL: 1144m P 6
SO181/032-1	24.12.04	02:09	42° 47,29' S	75° 8,04' W	1124	SSW 12	297,6	1,1	Wärmestromsonde 6 m	GHF	hieven	
SO181/032-1	24.12.04	02:11	42° 47,30' S	75° 8,04' W	1122	SSW 13	167,2	1,7	Wärmestromsonde 6 m	GHF	verholen	rwk: 081°, d: 0,54 nm
SO181/032-1	24.12.04	02:57	42° 47,21' S	75° 7,29' W	1121	SW 12	121,1	0,9	Wärmestromsonde 6 m	GHF	Boko	SL: 1144m P 7
SO181/032-1	24.12.04	03:07	42° 47,17' S	75° 7,32' W	1134	SW 13	176,8	0,5	Wärmestromsonde 6 m	GHF	hieven	
SO181/032-1	24.12.04	03:14	42° 47,19' S	75° 7,28' W	1117	SW 12	0	0	Wärmestromsonde 6 m	GHF	verholen	rwk: 081°, d: 0,54 nm
SO181/032-1	24.12.04	03:50	42° 47,11' S	75° 6,53' W	1071	SW 11	359	1,3	Wärmestromsonde 6 m	GHF	Boko	SL: 1114 m P 8
SO181/032-1	24.12.04	03:52	42° 47,10' S	75° 6,54' W	1071	SW 10	309,7	1,1	Wärmestromsonde 6 m	GHF	hieven	
SO181/032-1	24.12.04	03:54	42° 47,09' S	75° 6,55' W	1075	SSW 12	258,4	1,9	Wärmestromsonde 6 m	GHF	verholen	rwk: 081°, d: 0,54 nm
SO181/032-1	24.12.04	04:28	42° 47,00' S	75° 5,79' W	1076	N 8	139	1,4	Wärmestromsonde 6 m	GHF	Boko	SL: 1092 m P 9
SO181/032-1	24.12.04	04:34	42° 46,98' S	75° 5,84' W	1076	SSW 12	36,4	0,8	Wärmestromsonde 6 m	GHF	hieven	
SO181/032-1	24.12.04	04:41	42° 47,01' S	75° 5,84' W	1078	SW 11	105,1	1,5	Wärmestromsonde 6 m	GHF	verholen	rwk: 081°, d: 0,54 nm
SO181/032-1	24.12.04	05:18	42° 46,91' S	75° 5,06' W	1106	SSW 10	199,2	0,8	Wärmestromsonde 6 m	GHF	Boko	SL: 1114 m P 10
SO181/032-1	24.12.04	05:30	42° 46,88' S	75° 5,13' W	1107	SW 10	264,8	1,2	Wärmestromsonde 6 m	GHF	hieven	
SO181/032-1	24.12.04	05:34	42° 46,90' S	75° 5,12' W	1104	SSW 10	280,5	0,6	Wärmestromsonde 6 m	GHF	verholen	rwk: 081°, d: 0,54 nm
SO181/032-1	24.12.04	06:23	42° 46,82' S	75° 4,40' W	1092	S 9	134	3,1	Wärmestromsonde 6 m	GHF	Boko	SL: 1105 m P 11
SO181/032-1	24.12.04	06:24	42° 46,82' S	75° 4,40' W	1092	SSW 8	348,7	0,7	Wärmestromsonde 6 m	GHF	hieven	
SO181/032-1	24.12.04	06:27	42° 46,82' S	75° 4,36' W	1090	SW 9	146	2,2	Wärmestromsonde 6 m	GHF	verholen	rwk: 081°, d: 0,54 nm
SO181/032-1	24.12.04	07:21	42° 46,74' S	75° 3,67' W	1062	SW 7	316,6	0,2	Wärmestromsonde 6 m	GHF	Boko	SL: 1087 m, P 12
SO181/032-1	24.12.04	07:30	42° 46,72' S	75° 3,68' W	1061	SSW 8	10,9	1,4	Wärmestromsonde 6 m	GHF	hieven	
SO181/032-1	24.12.04	07:34	42° 46,72' S	75° 3,69' W	1059	SSW 8	143,6	0,9	Wärmestromsonde 6 m	GHF	verholen	rwk: 081°, d: 0,54 nm

Station	Datum	UTC	PositionLat	PositionLon	Tiefe [m]	Windstärke [m/s]	Kurs [°]	v [kn]	Gerät	Gerätekürzel	Aktion	Bemerkung
SO181/032-1	24.12.04	08:38	42° 46,64' S	75° 2,96' W	999	SW 6	290,9	0,2	Wärmestromsonde 6 m	GHF	Boko	SL: 1013 m P 13
SO181/032-1	24.12.04	08:38	42° 46,64' S	75° 2,96' W	999	WSW 6	290,9	0,2	Wärmestromsonde 6 m	GHF	hieven	umgefallen
SO181/032-1	24.12.04	08:39	42° 46,63' S	75° 2,96' W	995	SW 7	3,4	0,4	Wärmestromsonde 6 m	GHF	verholen	nwk: 081°, d: 0,54 nm
SO181/032-1	24.12.04	09:38	42° 46,57' S	75° 2,24' W	900	NE 6	291,9	1	Wärmestromsonde 6 m	GHF	Boko	SL: 912 m P 14
SO181/032-1	24.12.04	09:39	42° 46,58' S	75° 2,24' W	901	NE 7	80,1	1	Wärmestromsonde 6 m	GHF	hieven	umgefallen
SO181/032-1	24.12.04	10:06	42° 46,65' S	75° 2,36' W	925	WSW 7	247,1	0,4	Wärmestromsonde 6 m	GHF	a.D.	
SO181/032-1	24.12.04	10:20	42° 46,69' S	75° 2,48' W	938	WSW 8	177,1	0,6	Wärmestromsonde 6 m	GHF	Ende Station	
SO181/033-1	24.12.04	11:33	42° 34,92' S	75° 9,04' W	1349	SW 9	220,3	2,8	Magnetometer	MAGN	Beginn Station	
SO181/033-1	24.12.04	11:40	42° 35,29' S	75° 9,07' W	1327	SW 9	197,4	5,2	Magnetometer	MAGN	Magnetometer z.W.	KL: 200m
SO181/033-1	24.12.04	11:40	42° 35,29' S	75° 9,07' W	1327	SW 9	197,4	5,2	Simrad+Magnetik Survey	MAGN	Beginn Profil	nwk: 184°, d: 43 nm SIMRAD+Magn. 1b-4
SO181/033-1	24.12.04	15:54	43° 18,02' S	75° 13,04' W	211	WSW 6	178,6	9,3	Simrad+Magnetik Survey	MAGN	Kursänderung	nwk: 191°, d: 114 nm
SO181/033-1	25.12.04	02:55	45° 9,72' S	75° 42,48' W	1349	NW 5	194,6	10,9	Simrad+Magnetik Survey	MAGN	Kursänderung	nwk: 270°, d: 15 nm
SO181/033-1	25.12.04	04:34	45° 9,90' S	76° 3,13' W	3324	NW 5	308,6	9,8	Simrad+Magnetik Survey	MAGN	Kursänderung	nwk: 011°, d: 92 nm
SO181/033-1	25.12.04	13:45	43° 40,07' S	75° 40,08' W	3478	W 4	11,2	9,8	Simrad+Magnetik Survey	MAGN	Kursänderung	nwk: 360°, d: 210 nm
SO181/033-1	26.12.04	10:47	40° 10,08' S	75° 40,00' W	3966	S 8	334,7	9,9	Simrad+Magnetik Survey	MAGN	Kursänderung	nwk: 270°, d: 6 nm
SO181/033-1	26.12.04	11:24	40° 10,01' S	75° 48,06' W	3994	S 11	253,4	10,7	Simrad+Magnetik Survey	MAGN	Kursänderung	nwk: 180°, d: 145 nm
SO181/033-1	27.12.04	01:41	42° 34,71' S	75° 48,58' W	3768	S 13	179	10,7	Simrad+Magnetik Survey	MAGN	Kursänderung	nwk: 081°, d: 33 nm
SO181/033-1	27.12.04	04:56	42° 30,19' S	75° 4,22' W	1947	SSW 5	118	10,1	Simrad+Magnetik Survey	MAGN	Kursänderung	nwk: 185°, d: 27 nm
SO181/033-1	27.12.04	07:35	42° 56,89' S	75° 7,45' W	1082	SW 7	194	10,6	Simrad+Magnetik Survey	MAGN	Kursänderung	nwk: 261°, d: 15 nm
SO181/033-1	27.12.04	09:02	42° 59,49' S	75° 27,91' W	2992	SSW 8	263	9,7	Simrad+Magnetik Survey	MAGN	Ende Profil	Profilidistanz gesamt: 700 nm
SO181/033-1	27.12.04	09:10	42° 59,61' S	75° 28,98' W	3317	SW 6	268	4,1	Magnetometer	MAGN	Magnetometer a.D.	Profilzeit: 69,4 Std.
SO181/033-1	27.12.04	09:11	42° 59,62' S	75° 29,07' W	3310	SW 6	266	4,6	Magnetometer	MAGN	Ende Station	
SO181/034-1	27.12.04	10:10	42° 50,46' S	75° 34,80' W	3748	SW 7	299	0,4	Wärmestromsonde 6 m	GHF	Beginn Station	GHF 04
SO181/034-1	27.12.04	10:13	42° 50,47' S	75° 34,80' W	3744	NNE 7	277	0,6	Wärmestromsonde 6 m	GHF	z.W.	
SO181/034-1	27.12.04	11:22	42° 50,44' S	75° 34,67' W	3746	SSW 6	301	0,4	Wärmestromsonde 6 m	GHF	Boko	SL: 3765 m P 1
SO181/034-1	27.12.04	11:43	42° 50,43' S	75° 34,68' W	3744	SW 7	328	0,2	Wärmestromsonde 6 m	GHF	hieven	
SO181/034-1	27.12.04	11:47	42° 50,45' S	75° 34,68' W	3743	SSW 6	294	1,1	Wärmestromsonde 6 m	GHF	verholen	nwk: 081°, d: 0,55 nm
SO181/034-1	27.12.04	12:55	42° 50,37' S	75° 33,95' W	3742	SW 6	56	0,3	Wärmestromsonde 6 m	GHF	Boko	SL: 3794 m P 2
SO181/034-1	27.12.04	13:07	42° 50,37' S	75° 33,95' W	3743	SW 7	29	0,3	Wärmestromsonde 6 m	GHF	hieven	
SO181/034-1	27.12.04	13:09	42° 50,37' S	75° 33,95' W	3741	SW 7	20	0,3	Wärmestromsonde 6 m	GHF	verholen	nwk: 081°, d: 0,54 nm
SO181/034-1	27.12.04	14:18	42° 50,28' S	75° 33,23' W	3744	SW 4	238	0,4	Wärmestromsonde 6 m	GHF	Boko	SL: 3769 m P 3
SO181/034-1	27.12.04	14:40	42° 50,28' S	75° 33,23' W	3744	SW 4	95	0,3	Wärmestromsonde 6 m	GHF	hieven	
SO181/034-1	27.12.04	14:54	42° 50,27' S	75° 33,24' W	3741	SSW 5	177	0,3	Wärmestromsonde 6 m	GHF	verholen	nwk: 081°, d: 0,54 nm
SO181/034-1	27.12.04	16:15	42° 50,19' S	75° 32,50' W	3736	SW 3	7	0,4	Wärmestromsonde 6 m	GHF	Boko	SL: 3773 m P 4
SO181/034-1	27.12.04	16:23	42° 50,20' S	75° 32,50' W	3738	SSW 4	67	1,1	Wärmestromsonde 6 m	GHF	hieven	
SO181/034-1	27.12.04	16:27	42° 50,18' S	75° 32,50' W	3738	SSW 4	256	1,5	Wärmestromsonde 6 m	GHF	verholen	nwk: 081°, d: 0,54 nm
SO181/034-1	27.12.04	18:00	42° 50,12' S	75° 31,80' W	3735	ENE 4	309	0,5	Wärmestromsonde 6 m	GHF	Boko	SL: 3771 m P 5
SO181/034-1	27.12.04	18:19	42° 50,11' S	75° 31,78' W	3737	WSW 4	58	0,4	Wärmestromsonde 6 m	GHF	hieven	
SO181/034-1	27.12.04	18:25	42° 50,11' S	75° 31,79' W	3738	SW 4	103	2,5	Wärmestromsonde 6 m	GHF	verholen	nwk: 081°, d: 0,03 nm
SO181/034-1	27.12.04	18:32	42° 50,11' S	75° 31,77' W	3736	WSW 4	209	0,2	Wärmestromsonde 6 m	GHF	Boko	SL: 3768 m P 6
SO181/034-1	27.12.04	18:52	42° 50,09' S	75° 31,77' W	3739	SW 5	266	1,1	Wärmestromsonde 6 m	GHF	hieven	

Station	Datum	UTC	PositionLat	PositionLon	Tiefe [m]	Windstärke [m/s]	Kurs [°]	v [kn]	Gerät	Gerätekürzel	Aktion	Bemerkung
SO181/034-1	27.12.04	20:02	42° 50,15' S	75° 31,67' W	3738	W 6	282	1,3	Wärmestromsonde 6 m	GHF	a.D.	Meßprofil mit 6 Messungen D 2 nm > 081°
SO181/034-1	27.12.04	20:02	42° 50,15' S	75° 31,67' W	3738	W 6	282	1,3	Wärmestromsonde 6 m	GHF	Ende Station	
SO181/035-1	27.12.04	20:03	42° 50,15' S	75° 31,67' W	3738	W 5	25	0,4	SIMRAD Survey	EM/PS	Beginn Profil	rwk: 235°, d: 17 nm SIMRAD Survey 1b-5
SO181/035-1	27.12.04	21:38	42° 59,88' S	75° 50,84' W	3722	NNE 5	227	10,9	SIMRAD Survey	MAGN	Kursänderung	rwk: 183°, d: 40 nm
SO181/035-1	28.12.04	01:02	43° 39,78' S	75° 53,48' W	3605	NW 3	188	4,2	Simrad+Magnetik Survey	MAGN	Magnetometer z.W.	200m SIMRAD+Magnetik Survey 1b-5
SO181/035-1	28.12.04	01:04	43° 39,95' S	75° 53,48' W	3604	NNW 3	204	5,9	Simrad+Magnetik Survey	MAGN	Kursänderung	rwk: 186°, d: 48 nm
SO181/035-1	28.12.04	05:44	44° 27,43' S	76° 0,11' W	3323	NNW 7	211	10,8	Simrad+Magnetik Survey	MAGN	Kursänderung	rwk: 254°, d: 112 nm
SO181/035-1	28.12.04	16:59	44° 58,53' S	76° 31,73' W	2884	NW 14	209	9,6	Simrad+Magnetik Survey	MAGN	Kursänderung	rwk: 180°, d: 5,5 sm
SO181/035-1	28.12.04	17:17	45° 1,64' S	76° 31,99' W	3059	NNW 10	185	7,8	Simrad+Magnetik Survey	MAGN	Ende Station	Magnetometer bleibt z.W.
SO181/036-1	28.12.04	17:18	45° 1,76' S	76° 32,00' W	3072	NW 12	184	5,7	Seismikprofil SCS 02	PR	Stationsbeginn	Seismik SCS 02
SO181/036-1	28.12.04	17:27	45° 2,17' S	76° 32,04' W	3075	NW 11	180	3	Profil	PR	Streamer zu Wasser	SL: 200 m
SO181/036-1	28.12.04	17:32	45° 2,38' S	76° 31,92' W	3075	NW 11	181	2,6	Profil	PR	Stb Airgun zu Wasser	
SO181/036-1	28.12.04	17:50	45° 3,78' S	76° 31,78' W	3060	NW 12	124	5,5	Profil	PR	Kursänderung	rwk: 074°
SO181/036-1	28.12.04	19:44	45° 1,46' S	76° 19,44' W	2326	NW 12	62	3,4	Profil	PR	Stb Airgun an Deck	Reparatur GI-Gun
SO181/036-1	28.12.04	21:10	45° 0,22' S	76° 12,93' W	3913	NW 15	59	2,7	Profil	PR	Stb Airgun zu Wasser	
SO181/036-1	28.12.04	22:12	44° 58,73' S	76° 5,84' W	2846	NW 16	71	3,6	Profil	PR	Stb Airgun an Deck	Reparatur GI-Gun
SO181/036-1	28.12.04	22:26	44° 58,52' S	76° 4,82' W	2370	NW 14	61	3,3	Ende Seismikprofil SCS 02	PR	Ende Profil	Abbruch Seismikprofil SCS 02 D 20 sm
SO181/036-1	28.12.04	22:35	44° 58,39' S	76° 4,17' W	2419	NW 14	67	2,9	Simrad + Magnetik Survey	PR	Streamer an Deck	rwk 074° 10,0 kn
SO181/036-1	28.12.04	22:36	44° 58,37' S	76° 4,08' W	2418	NW 14	76	4,8	Profil 1b-6	PR	Fortsetzung Magn. 1b-6	rwk: 074°, d: 7 nm
SO181/037-1	28.12.04	22:37	44° 58,35' S	76° 3,95' W	2505	NW 15	92	5,2	Simrad + Magnetik Survey	MAGN	Simrad + Magnetik	
SO181/037-1	28.12.04	23:21	44° 56,47' S	77° 54,53' W	2839	NNW 13	73	10,4	Magnetometer	MAGN	Kursänderung	rwk: 118°, d: 8 nm
SO181/037-1	29.12.04	00:07	44° 59,94' S	77° 44,76' W	3110	NNW 14	114	10,5	Magnetometer	MAGN	Kursänderung	rwk: 075°, d: 73 nm
SO181/037-1	29.12.04	07:12	44° 40,51' S	76° 5,66' W	3280	NW 16	102	9,4	Magnetometer	MAGN	Kursänderung	rwk: 191°, d: 28 nm
SO181/037-1	29.12.04	09:33	45° 2,29' S	76° 11,53' W	3301	WNW 15	188	4,1	Magnetometer	MAGN	Magnetometer an Deck	defekt
SO181/037-1	29.12.04	10:06	45° 7,46' S	76° 12,99' W	3309	WNW 13	199	9,1	EM/PS	EM/PS	Kursänderung	rwk: 202°, d: 41 nm
SO181/037-1	29.12.04	14:14	45° 45,96' S	76° 35,02' W	2693	WNW 10	18	1,3	EM/PS	EM/PS	Ende Profil	
SO181/037-1	29.12.04	14:15	45° 45,95' S	76° 35,03' W	2694	WNW 9	277	1,6	EM/PS	EM/PS	Ende Station	
SO181/038-1	29.12.04	14:15	45° 45,95' S	76° 35,03' W	2694	NNW 9	277	1,6	Gravity Corer 6 meter	GC 6M	Beginn Station	SL-1b-1
SO181/038-1	29.12.04	14:31	45° 45,96' S	76° 34,99' W	2693	WNW 8	178	1,8	Gravity Corer 6 meter	GC 6M	zu wasser	W 6
SO181/038-1	29.12.04	15:11	45° 45,99' S	76° 35,00' W	2692	NNW 7	158	0,5	Gravity Corer 6 meter	GC 6M	Bodenkontakt	SL: 2722 m
SO181/038-1	29.12.04	15:12	45° 45,99' S	76° 35,00' W	2690	NNW 7	321	0,9	Gravity Corer 6 meter	GC 6M	hieven	
SO181/038-1	29.12.04	16:05	45° 46,03' S	76° 35,04' W	2687	NW 10	93	0,7	Gravity Corer 6 meter	GC 6M	an deck	
SO181/038-1	29.12.04	16:34	45° 46,06' S	76° 35,19' W	2678	NNW 10	256	0,7	Gravity Corer 6 meter	GC 6M	Ende station	
SO181/039-1	29.12.04	16:35	45° 46,06' S	76° 35,21' W	2677	NNW 10	59	1,7	Vermessung	EM / PS	Beginn Profil	rwk: 068°, d: 26 nm
SO181/039-1	29.12.04	19:00	45° 36,24' S	76° 0,49' W	3315	NNW 10	86	8,2	Vermessung	EM / PS	Ende Profil	
SO181/040-1	29.12.04	19:03	45° 36,22' S	76° 0,01' W	3316	NW 9	60	4,8	Gravity Corer 6 meter	GC 6M	Beginn Station	SL-1b-2
SO181/040-1	29.12.04	19:12	45° 36,04' S	75° 59,98' W	3316	NNW 7	62	1,8	Gravity Corer 6 meter	GC 6M	zu wasser	
SO181/040-1	29.12.04	20:03	45° 36,00' S	76° 0,00' W	3316	NNE 10	312	0,5	Gravity Corer 6 meter	GC 6M	Bodenkontakt	SL: 3350 m
SO181/040-1	29.12.04	20:06	45° 36,00' S	76° 0,00' W	3316	NNE 10	118	0,3	Gravity Corer 6 meter	GC 6M	hieven	SZ: 69 kN
SO181/040-1	29.12.04	21:04	45° 36,04' S	76° 0,01' W	3316	NW 14	12	1,4	Gravity Corer 6 meter	GC 6M	an deck	
SO181/040-1	29.12.04	21:05	45° 36,05' S	76° 0,01' W	3316	NW 14	256	0,4	Gravity Corer 6 meter	GC 6M	Ende station	

Station	Datum	UTC	Position Lat	Position Lon	Tiefe [m]	Windstärke [m/s]	Kurs [°]	v [kn]	Gerät	Gerätekurzal	Aktion	Bemerkung
SO181/041-1	29.12.04	21:51	45° 33,89' S	75° 52,35' W	2516	NW 14	341	0,7	Wärmestromsonde 6 m	GHF	Beginn Station	GHF 06 W 1
SO181/041-1	29.12.04	22:00	45° 33,87' S	75° 52,33' W	2516	NW 14	338	1,4	Wärmestromsonde 6 m	GHF	z.W.	
SO181/041-1	29.12.04	22:59	45° 33,86' S	75° 52,34' W	2520	NNE 14	258	1,2	Wärmestromsonde 6 m	GHF	Boko	SL: 2644 m P 01
SO181/041-1	29.12.04	23:24	45° 33,86' S	75° 52,32' W	2518	NW 14	291	1,3	Wärmestromsonde 6 m	GHF	hieven	
SO181/041-1	29.12.04	23:28	45° 33,86' S	75° 52,33' W	2519	NNW 15	30	0,2	Wärmestromsonde 6 m	GHF	verholen	rwk: 247°, d: 0,55 nm
SO181/041-1	30.12.04	00:36	45° 34,05' S	75° 53,05' W	2432	NNW 14	185	2,2	Wärmestromsonde 6 m	GHF	Boko	SL: 2463 m P 02
SO181/041-1	30.12.04	00:48	45° 34,05' S	75° 53,06' W	2439	NNW 16	187	1,8	Wärmestromsonde 6 m	GHF	hieven	
SO181/041-1	30.12.04	00:50	45° 34,06' S	75° 53,05' W	2433	NNW 14	227	0,8	Wärmestromsonde 6 m	GHF	verholen	rwk: 247°, d: 0,54 nm
SO181/041-1	30.12.04	01:54	45° 34,26' S	75° 53,75' W	2572	NNW 18	297	0,5	Wärmestromsonde 6 m	GHF	Boko	SL: 2579 m P 03
SO181/041-1	30.12.04	02:17	45° 34,27' S	75° 53,73' W	2557	NNW 16	62	0,6	Wärmestromsonde 6 m	GHF	hieven	
SO181/041-1	30.12.04	02:18	45° 34,26' S	75° 53,75' W	2560	NNW 16	347	1,7	Wärmestromsonde 6 m	GHF	verholen	rwk: 247°, d: 0,54 nm
SO181/041-1	30.12.04	03:19	45° 34,42' S	75° 54,43' W	2732	NNW 17	239	2,1	Wärmestromsonde 6 m	GHF	Boko	SL: 2708 m P 05
SO181/041-1	30.12.04	03:29	45° 34,45' S	75° 54,47' W	2712	N 16	281	1,2	Wärmestromsonde 6 m	GHF	hieven	
SO181/041-1	30.12.04	03:34	45° 34,40' S	75° 54,53' W	2732	NW 16	146	1,2	Wärmestromsonde 6 m	GHF	verholen	rwk: 247°, d: 0,54 nm
SO181/041-1	30.12.04	04:19	45° 34,71' S	75° 55,20' W	3052	NNW 16	135	1	Wärmestromsonde 6 m	GHF	Boko	SL: 2980 m P 06
SO181/041-1	30.12.04	04:37	45° 34,70' S	75° 55,20' W	3068	NNW 16	181	0,9	Wärmestromsonde 6 m	GHF	hieven	
SO181/041-1	30.12.04	04:42	45° 34,70' S	75° 55,18' W	3048	NW 16	133	1,4	Wärmestromsonde 6 m	GHF	verholen	rwk: 247°, d: 0,54 nm
SO181/041-1	30.12.04	05:17	45° 34,87' S	75° 55,81' W	3182	NNW 18	75	2,3	Wärmestromsonde 6 m	GHF	Boko	SL: 3231 m P 07
SO181/041-1	30.12.04	05:33	45° 34,88' S	75° 55,83' W	3197	NW 16	78	1,7	Wärmestromsonde 6 m	GHF	hieven	
SO181/041-1	30.12.04	05:37	45° 34,86' S	75° 55,84' W	3195	NNW 17	112	2,5	Wärmestromsonde 6 m	GHF	verholen	rwk: 247°, d: 0,54 nm
SO181/041-1	30.12.04	06:17	45° 35,07' S	75° 56,49' W	3271	NNW 15	130	2,4	Wärmestromsonde 6 m	GHF	Boko	SL: 3285 m P 08
SO181/041-1	30.12.04	06:36	45° 35,09' S	75° 56,52' W	3263	NNW 15	25	1,5	Wärmestromsonde 6 m	GHF	hieven	
SO181/041-1	30.12.04	06:39	45° 35,07' S	75° 56,54' W	3263	NW 18	40	1,8	Wärmestromsonde 6 m	GHF	verholen	rwk: 248°, d: 0,54 nm
SO181/041-1	30.12.04	07:30	45° 35,30' S	75° 57,38' W	3321	NW 17	34	1,9	Wärmestromsonde 6 m	GHF	Boko	SL: 3363 m P 09
SO181/041-1	30.12.04	07:40	45° 35,31' S	75° 57,35' W	3320	NW 16	86	1,7	Wärmestromsonde 6 m	GHF	hieven	
SO181/041-1	30.12.04	07:44	45° 35,30' S	75° 57,38' W	3317	NW 17	345	1,1	Wärmestromsonde 6 m	GHF	verholen	rwk: 247°, d: 0,54 nm
SO181/041-1	30.12.04	08:35	45° 35,53' S	75° 58,06' W	3318	NNW 15	46	1,4	Wärmestromsonde 6 m	GHF	Boko	SL: 3355 m P 10
SO181/041-1	30.12.04	08:56	45° 35,51' S	75° 58,07' W	3318	WNW 16	54	3	Wärmestromsonde 6 m	GHF	hieven	
SO181/041-1	30.12.04	09:59	45° 35,39' S	75° 58,25' W	3323	WNW 15	327	0,8	Wärmestromsonde 6 m	GHF	a.D.	
SO181/041-1	30.12.04	09:59	45° 35,39' S	75° 58,25' W	3323	NW 15	327	0,8	Wärmestromsonde 6 m	GHF	Ende Station GHF 05	
SO181/042-1	30.12.04	10:00	45° 35,39' S	75° 58,25' W	3281	WNW 13	180	12	Vermessung	EM / PS	Beginn Profil	rwk 177 ; d:66 sm
SO181/042-1	30.12.04	16:05	46° 40,02' S	75° 54,98' W	3369	NNE 10	314	0,9	Vermessung	EM / PS	Ende Profil	Ende Station #42
SO181/043-1	30.12.04	16:07	46° 40,04' S	75° 55,02' W	3375	WNW 7	121	0,5	Gravity Corer 6 meter	GC 6M	Beginn Station	SL-1b-3
SO181/043-1	30.12.04	16:09	46° 40,07' S	75° 55,03' W	3372	WNW 8	232	1,9	Gravity Corer 6 meter	GC 6M	zu wasser	
SO181/043-1	30.12.04	17:05	46° 40,16' S	75° 55,38' W	3396	WNW 9	228	1,4	Gravity Corer 6 meter	GC 6M	Bodenkontakt	SL: 3412 m
SO181/043-1	30.12.04	17:09	46° 40,21' S	75° 55,32' W	3392	WNW 9	199	3,6	Gravity Corer 6 meter	GC 6M	hieven	
SO181/043-1	30.12.04	18:16	46° 40,55' S	75° 56,06' W	3412	N 11	91	2,3	Gravity Corer 6 meter	GC 6M	an deck	
SO181/043-1	30.12.04	18:23	46° 40,59' S	75° 56,02' W	3416	NNW 8	283	2,5	Gravity Corer 6 meter	GC 6M	Ende station	
SO181/044-1	30.12.04	18:24	46° 40,58' S	75° 56,04' W	3422	NW 9	84	1,8	Vermessung	EM / PS	Beginn Profil	rwk: 020°, d: 30 nm Profil 1b-6
SO181/044-1	30.12.04	21:21	46° 13,69' S	75° 41,18' W	1742	WNW 9	26	10,6	Vermessung	EM / PS	Ende Profil	
SO181/045-1	30.12.04	21:31	46° 13,05' S	75° 41,01' W	1527	NW 9	271	2,3	Gravity Corer 6 meter	GC 6M	Beginn Station	SL-1b-6

Station	Datum	UTC	PositionLat	PositionLon	Tiefe [m]	Windstärke [m/s]	Kurs [°]	v [kn]	Gerät	Gerätekürzel	Aktion	Bemerkung
SO181/045-1	30.12.04	21:33	48° 13,05' S	75° 41,01' W	1534	NW 9	126	1,2	Gravity Corer 6 meter	GC 6M	zu wasser	
SO181/045-1	30.12.04	22:02	48° 13,02' S	75° 41,02' W	1515	WNW 8	108	0,7	Gravity Corer 6 meter	GC 6M	Bodenkontakt	SL-1b-4
SO181/045-1	30.12.04	22:03	48° 13,02' S	75° 41,01' W	1519	WNW 8	196	1,8	Gravity Corer 6 meter	GC 6M	hieven	SL: 1535 m, SZ: 50 kN
SO181/045-1	30.12.04	22:30	48° 13,14' S	75° 41,11' W	1599	NW 8	217	1,7	Gravity Corer 6 meter	GC 6M	an deck	
SO181/045-1	30.12.04	22:31	48° 13,15' S	75° 41,12' W	1623	NW 8	107	0,4	Gravity Corer 6 meter	GC 6M	Ende station	
SO181/046-1	30.12.04	22:42	48° 13,02' S	75° 41,49' W	1688	NW 8	253	1	Gravity Corer 6 meter	GC 6M	Beginn Station	SL-1b-5
SO181/046-1	30.12.04	22:54	48° 13,01' S	75° 41,51' W	1691	NW 8	141	0,7	Gravity Corer 6 meter	GC 6M	zu wasser	
SO181/046-1	30.12.04	23:26	48° 13,00' S	75° 41,51' W	1664	WNW 8	339	0,2	Gravity Corer 6 meter	GC 6M	Bodenkontakt	SL: 1718m ; SZ: 42 kN SL-1b-5
SO181/046-1	30.12.04	23:58	48° 13,04' S	75° 41,59' W	1742	NW 7	176	1,5	Gravity Corer 6 meter	GC 6M	an deck	SL leer
SO181/046-2	31.12.04	00:12	48° 13,01' S	75° 41,52' W	1707	NNW 6	354	1	Gravity Corer 6 meter	GC 6M	zu wasser	SL-1b-5-2 ; W 6
SO181/046-2	31.12.04	00:43	48° 13,00' S	75° 41,50' W	1690	NW 8	124	0,5	Gravity Corer 6 meter	GC 6M	Bodenkontakt	SL: 1705 m ; SZ: 38 kN SL-1b-5.2
SO181/046-2	31.12.04	01:14	48° 13,01' S	75° 41,50' W	1679	NNW 8	77	2,2	Gravity Corer 6 meter	GC 6M	an deck	SL leer
SO181/046-2	31.12.04	01:16	48° 13,01' S	75° 41,49' W	1687	NW 8	107	1,6	Gravity Corer 6 meter	GC 6M	Ende station	
SO181/047-1	31.12.04	01:26	48° 13,03' S	75° 42,03' W	1998	NNW 10	45	1,9	Gravity Corer 6 meter	GC 6M	Beginn Station	
SO181/047-1	31.12.04	01:30	48° 13,01' S	75° 42,01' W	1984	NNW 8	7	1,8	Gravity Corer 6 meter	GC 6M	zu wasser	
SO181/047-1	31.12.04	02:04	48° 13,00' S	75° 42,00' W	1968	N 8	226	0,6	Gravity Corer 6 meter	GC 6M	Bodenkontakt	SL: 2011m ; SZ: 43 kN SL-1b-6
SO181/047-1	31.12.04	02:38	48° 12,99' S	75° 42,00' W	1969	N 7	73	0,8	Gravity Corer 6 meter	GC 6M	an deck	SL leer
SO181/047-1	31.12.04	02:42	48° 13,00' S	75° 42,00' W	1975	N 7	234	1,4	Gravity Corer 6 meter	GC 6M	Ende station	Ende Kernstation, Beginn Profil 1b-7
SO181/047-1	31.12.04	02:42	48° 13,00' S	75° 42,00' W	1975	N 7	234	1,4	Gravity Corer 6 meter	GC 6M	Ende station	
SO181/048-1	31.12.04	02:49	48° 12,99' S	75° 41,99' W	1956	N 7	82	0,5	Vermessung	EM / PS	Beginn Profil	nwk: 357°, d: 66 nm
SO181/048-1	31.12.04	09:21	48° 7,12' S	75° 47,03' W	2026	N 8	11	11,1	Vermessung	EM / PS	Kursänderung	nwk: 011°, d: 48 nm
SO181/048-2	31.12.04	11:28	44° 44,85' S	75° 40,88' W	1605	NNW 10	359	3,5	Vermessung mit Test	EM / PS	Stb Airgun zu Wasser	Testlauf GI-Gun mit 5,0 kn
SO181/048-2	31.12.04	11:53	44° 43,07' S	75° 40,40' W	1680	NNW 10	15	3,7	Vermessung mit Test	EM / PS	Stb Airgun an Deck	Test erfolgreich
SO181/048-2	31.12.04	12:02	44° 42,59' S	75° 40,25' W	1638	NNW 9	14	4,1	Vermessung mit Test	EM / PS	Magnetometer zu Wasser	L: 200m ; Testlauf Magnetometer v 5,0 kn
SO181/048-2	31.12.04	12:40	44° 37,57' S	75° 38,97' W	1676	NNW 9	24	3,7	Vermessung mit Test	EM / PS	Magnetometer an Deck	Test nicht erfolgreich
SO181/048-1	31.12.04	14:28	44° 20,13' S	75° 34,28' W	1830	N 15	14	11,2	Vermessung	EM / PS	Kursänderung	nwk: 010°, d: 59 nm v 10,5 - 11,0 kn
SO181/048-1	31.12.04	19:50	43° 24,34' S	75° 20,12' W	1611	NW 10	2	10,1	Vermessung	EM / PS	Kursänderung	nwk: 307°, d: 65 nm
SO181/048-1	01.01.05	04:12	42° 44,87' S	76° 31,31' W	3727	N 11	309	9,6	Vermessung	EM / PS	Kursänderung	nwk: 360°, d: 155 nm
SO181/048-1	01.01.05	18:12	40° 10,25' S	76° 31,00' W	3846	NNW 6	333	10,8	Vermessung	EM / PS	Kursänderung	nwk: 270°, d: 7 nm
SO181/048-1	01.01.05	18:50	40° 10,06' S	76° 39,73' W	3508	NW 6	230	9	Vermessung	EM / PS	Kursänderung	nwk: 180°, d: 115 nm
SO181/048-1	02.01.05	05:00	42° 5,05' S	76° 39,56' W	3437	NNW 11	100	9,6	Vermessung	EM / PS	Kursänderung	nwk: 082°, d: 53 nm
SO181/048-1	02.01.05	09:36	41° 57,52' S	75° 30,24' W	3876	NNW 14	85	11,6	Vermessung	EM / PS	Kursänderung	nwk: 180°, d: 43 nm
SO181/048-1	02.01.05	13:30	42° 40,33' S	75° 30,01' W	3680	WNW 12	182	10,6	Vermessung	EM / PS	Kursänderung	nwk: 090°, d: 11 nm
SO181/048-1	02.01.05	14:31	42° 40,59' S	75° 15,19' W	1582	W 2	87	10,8	Vermessung	EM / PS	Kursänderung	nwk: 184°, d: 40 nm
SO181/048-1	02.01.05	18:20	43° 19,94' S	75° 18,99' W	1821	W 7	178	10,6	Vermessung	EM / PS	Kursänderung	nwk: 230°, d: 10 nm
SO181/048-1	02.01.05	19:22	43° 26,60' S	75° 29,97' W	3332	SW 8	207	9,5	Vermessung	EM / PS	Kursänderung	nwk: 180°, d: 39 nm
SO181/048-1	02.01.05	23:00	44° 4,90' S	75° 39,38' W	2056	SW 10	195	10,3	Vermessung	EM / PS	Kursänderung	nwk: 189°, d: 32 nm
SO181/048-1	03.01.05	02:05	44° 36,50' S	75° 46,03' W	3251	SW 13	187	11,7	Vermessung	EM / PS	Kursänderung	nwk: 191°, d: 30 nm
SO181/048-1	03.01.05	04:58	45° 5,48' S	75° 53,93' W	2622	SSW 6	125	8,8	Vermessung	EM / PS	Kursänderung	nwk: 090°, d: 3 nm
SO181/048-1	03.01.05	05:13	45° 5,48' S	75° 50,13' W	2527	SW 4	79	10,7	Vermessung	EM / PS	Kursänderung	nwk: 012°, d: 32 nm
SO181/048-1	03.01.05	08:11	44° 34,59' S	75° 41,02' W	2159	WNW 4	17	10,1	Vermessung	EM / PS	Kursänderung	nwk: 064°, d: 30 nm

Station	Datum	UTC	PositionLat	PositionLon	Tiefe [m]	Windstärke [m/s]	Kurs [°]	v [kn]	Gerät	Gerätekurzel	Aktion	Bemerkung
SO181/048-1	03.01.05	10:51	44° 21,71' S	75° 3,57' W	169	SW 2	61	8,2	Vermessung	EM / PS	Ende Profil	Vermessungsprofil ges. D 838 nm 80 Std.
SO181/049-1	03.01.05	10:56	44° 21,84' S	75° 3,31' W	169	W 5	259	2,7	Profil	PR	Streamer zu Wasser	
SO181/049-1	03.01.05	11:03	44° 21,93' S	75° 3,78' W	168	W 5	255	3,9	Profil	PR	Stb Aigun zu Wasser	
SO181/049-1	03.01.05	11:07	44° 21,97' S	75° 4,05' W	169	W 5	268	4,2	Profil	PR	Magnetometer zu Wasser	LMF2 gewechselt auf LMF1 0,2 Std.
SO181/049-1	03.01.05	11:11	44° 22,03' S	75° 4,51' W	166	W 5	254	4,5	Profil	PR	Beginn Profil	nwk: 254°, d: 115 nm 8CS02-2
SO181/049-1	04.01.05	10:56	44° 53,33' S	77° 38,28' W	2895	NNE 9	254	1,9	Profil	PR	Stb Aigun an Deck	GI-Gun ausgefallen, zur Rep. a.D.
SO181/049-1	04.01.05	11:09	44° 53,52' S	77° 39,18' W	2888	WNW 9	250	3,2	Profil	PR	Streamer an Deck	
SO181/049-1	04.01.05	11:10	44° 53,54' S	77° 39,23' W	2875	NW 10	255	3,4	Profil	PR	Ende/Beginn Profil	Ende SCS 02-2 / Beginn Survey 1b-7
SO181/050-1	04.01.05	12:26	44° 56,70' S	77° 54,50' W	2727	WNW 13	248	11	Magnetometer	MAGN	Kursänderung	nwk: 360°, d: 11 nm
SO181/050-1	04.01.05	13:32	44° 46,11' S	77° 55,02' W	2840	NW 14	355	10	Magnetometer	MAGN	Kursänderung	nwk: 074°, d: 50 nm
SO181/050-1	04.01.05	18:34	44° 32,25' S	76° 48,23' W	2889	WNW 12	68	8,3	Magnetometer	MAGN	Ende Profil	
SO181/050-1	04.01.05	18:44	44° 31,92' S	76° 47,06' W	3033	WNW 11	48	3,4	Magnetometer	MAGN	Magnetometer an Deck	
SO181/050-1	04.01.05	18:47	44° 31,83' S	76° 46,93' W	3036	WNW 10	69	4,1	Magnetometer	MAGN	Ende Station	survey 1b-7 gesamt 7,4 Std. 61 nm
SO181/051-1	04.01.05	18:48	44° 31,83' S	76° 46,85' W	3032	WNW 11	92	3,8	Vermessung	EM / PS	Beginn Profil	nwk: 101°, d: 23 nm Survey 1b-08
SO181/051-1	04.01.05	20:46	44° 36,22' S	76° 15,18' W	3269	NW 10	85	7,1	Vermessung	EM / PS	Ende Profil	survey 1b-8 gesamt 2,0 Std. 23 nm
SO181/052-1	04.01.05	20:54	44° 36,40' S	76° 15,13' W	3273	WNW 10	238	1,2	Wärmestromsonde 3 m	HF	z.W.	Pinger 50 m HF06
SO181/052-1	04.01.05	21:56	44° 36,37' S	76° 15,18' W	3273	NW 10	246	1,9	Wärmestromsonde 3 m	HF	Boko	SL: 3305 m, P 1
SO181/052-1	04.01.05	22:09	44° 36,37' S	76° 15,18' W	3274	NNW 10	233	0,3	Wärmestromsonde 3 m	HF	hieven	
SO181/052-1	04.01.05	22:12	44° 36,36' S	76° 15,18' W	3273	NW 9	59	1,1	Wärmestromsonde 3 m	HF	verholen	nwk: 254°, d: 0,54 nm
SO181/052-1	04.01.05	22:58	44° 36,51' S	76° 15,88' W	3282	W 9	59	0,8	Wärmestromsonde 3 m	HF	Boko	SL: 3323 m, P 2
SO181/052-1	04.01.05	23:05	44° 36,54' S	76° 15,91' W	3282	NW 12	63	1,2	Wärmestromsonde 3 m	HF	hieven	
SO181/052-1	04.01.05	23:07	44° 36,55' S	76° 15,91' W	3282	WNW 11	284	1,1	Wärmestromsonde 3 m	HF	verholen	nwk: 254°, d: 0,54 nm
SO181/052-1	04.01.05	23:53	44° 36,68' S	76° 16,61' W	3278	NW 10	236	0,3	Wärmestromsonde 3 m	HF	Boko	SL: 3336 m, P 3
SO181/052-1	05.01.05	00:05	44° 36,67' S	76° 16,62' W	3279	WNW 10	195	2	Wärmestromsonde 3 m	HF	hieven	
SO181/052-1	05.01.05	00:08	44° 36,67' S	76° 16,63' W	3276	NW 11	123	0,8	Wärmestromsonde 3 m	HF	verholen	nwk: 254°, d: 0,54 nm
SO181/052-1	05.01.05	01:01	44° 36,83' S	76° 17,35' W	3276	NW 10	356	1,6	Wärmestromsonde 3 m	HF	Boko	SL: 3332 m, P 4
SO181/052-1	05.01.05	01:07	44° 36,82' S	76° 17,34' W	3276	W 10	37	0,8	Wärmestromsonde 3 m	HF	hieven	
SO181/052-1	05.01.05	01:10	44° 36,83' S	76° 17,35' W	3278	NW 9	145	1,4	Wärmestromsonde 3 m	HF	verholen	nwk: 254°, d: 0,54 nm
SO181/052-1	05.01.05	01:58	44° 36,97' S	76° 18,07' W	3274	NW 10	35	2,1	Wärmestromsonde 3 m	HF	Boko	SL: 3333 m, P 5
SO181/052-1	05.01.05	02:12	44° 36,97' S	76° 18,07' W	3276	WNW 11	186	1,9	Wärmestromsonde 3 m	HF	hieven	
SO181/052-1	05.01.05	02:14	44° 36,98' S	76° 18,08' W	3272	NW 10	203	1,8	Wärmestromsonde 3 m	HF	verholen	nwk: 254°, d: 0,54 nm
SO181/052-1	05.01.05	03:01	44° 37,09' S	76° 18,77' W	3269	NW 14	26	1,5	Wärmestromsonde 3 m	HF	Boko	SL 3305 m, P 6
SO181/052-1	05.01.05	03:08	44° 37,07' S	76° 18,77' W	3268	WNW 15	217	1,6	Wärmestromsonde 3 m	HF	hieven	
SO181/052-1	05.01.05	03:12	44° 37,08' S	76° 18,80' W	3267	WNW 15	299	0,3	Wärmestromsonde 3 m	HF	verholen	nwk: 254°, d: 0,54 nm
SO181/052-1	05.01.05	04:02	44° 37,28' S	76° 19,52' W	3263	WNW 14	260	0,8	Wärmestromsonde 3 m	HF	Boko	SL: 3325 m, P 7
SO181/052-1	05.01.05	04:15	44° 37,26' S	76° 19,51' W	3258	W 12	209	0,4	Wärmestromsonde 3 m	HF	hieven	
SO181/052-1	05.01.05	04:19	44° 37,25' S	76° 19,50' W	3256	W 13	163	0,5	Wärmestromsonde 3 m	HF	verholen	nwk: 254°, d: 0,54 nm
SO181/052-1	05.01.05	05:05	44° 37,42' S	76° 20,26' W	3243	W 14	215	1,1	Wärmestromsonde 3 m	HF	Boko	SL: 3310 m, P 8
SO181/052-1	05.01.05	05:11	44° 37,41' S	76° 20,25' W	3246	WNW 15	354	0,8	Wärmestromsonde 3 m	HF	hieven	
SO181/052-1	05.01.05	05:16	44° 37,40' S	76° 20,27' W	3245	WNW 13	72	1,6	Wärmestromsonde 3 m	HF	verholen	nwk: 254°, d: 0,54 nm
SO181/052-1	05.01.05	06:00	44° 37,57' S	76° 21,00' W	3239	NNE 11	121	1,2	Wärmestromsonde 3 m	HF	Boko	SL: 3318 m, P 9

Station	Datum	UTC	PositionLat	PositionLon	Tiefe [m]	Windstärke [m/s]	Kurs [°]	v [kn]	Gerät	Gerätekürzel	Aktion	Bemerkung
SO181/052-1	05.01.05	06:12	44° 37,50' S	76° 21,01' W	3239	W 15	230	0,9	Wärmestromsonde 3 m	HF	hieven	
SO181/052-1	05.01.05	06:16	44° 37,53' S	76° 20,97' W	3239	W 13	321	0,6	Wärmestromsonde 3 m	HF	verholen	rwk: 254°, d: 0,54 nm
SO181/052-1	05.01.05	07:08	44° 37,71' S	76° 21,76' W	3235	WNW 13	207	1,8	Wärmestromsonde 3 m	HF	Boko	SL: 3258 m, P 10
SO181/052-1	05.01.05	07:09	44° 37,71' S	76° 21,77' W	3234	WNW 14	175	1	Wärmestromsonde 3 m	HF	hieven	
SO181/052-1	05.01.05	07:10	44° 37,71' S	76° 21,77' W	3234	WNW 14	206	2	Wärmestromsonde 3 m	HF	verholen	rwk: 254°, d: 0,54 nm
SO181/052-1	05.01.05	08:05	44° 37,87' S	76° 22,44' W	3235	WNW 12	269	0,7	Wärmestromsonde 3 m	HF	Boko	SL: 3280 m, P 11
SO181/052-1	05.01.05	08:19	44° 37,87' S	76° 22,44' W	3235	W 13	59	0,5	Wärmestromsonde 3 m	HF	hieven	
SO181/052-1	05.01.05	09:23	44° 37,92' S	76° 22,63' W	3237	WNW 14	25	2,8	Wärmestromsonde 3 m	HF	a.O.	
SO181/052-1	05.01.05	09:23	44° 37,92' S	76° 22,63' W	3237	WNW 14	25	2,8	Wärmestromsonde 3 m	HF	Ende Station	
SO181/052-2	05.01.05	09:24	44° 37,91' S	76° 22,63' W	3235	WNW 13	185	1,1	Vermessung	EM / PS	Beginn Profil	rwk: 098°, d: 16 nm
SO181/052-2	05.01.05	10:59	44° 40,04' S	76° 0,16' W	3295	S 4	91	10,5	Vermessung	EM / PS	Kursänderung	rwk: 051°, d: 16 nm
SO181/052-2	05.01.05	12:27	44° 29,75' S	75° 42,58' W	2360	W 13	232	0,8	Vermessung	EM / PS	Ende Profil	EM/PS-Survey gesamt 3,0 Std. 32 sm
SO181/053-1	05.01.05	12:28	44° 29,76' S	75° 42,59' W	2356	W 13	168	1,8	Wärmestromsonde 6 m	GHF	Beginn Station GHF 07	
SO181/053-1	05.01.05	12:45	44° 29,75' S	75° 42,59' W	2347	W 8	44	1,6	Wärmestromsonde 6 m	GHF	z.W.	
SO181/053-1	05.01.05	13:34	44° 29,77' S	75° 42,60' W	2355	NW 14	132	0,8	Wärmestromsonde 6 m	GHF	Boko	SL: 2380 m, P 1/1, umgefallen
SO181/053-1	05.01.05	13:35	44° 29,78' S	75° 42,60' W	2356	WNW 14	341	1,2	Wärmestromsonde 6 m	GHF	hieven	SL: 2300m; Fieren
SO181/053-1	05.01.05	13:39	44° 29,76' S	75° 42,62' W	2350	WNW 14	331	0,3	Wärmestromsonde 6 m	GHF	Boko	SL: 2384 m, P 1/2
SO181/053-1	05.01.05	13:48	44° 29,77' S	75° 42,61' W	2344	NW 13	71	0,4	Wärmestromsonde 6 m	GHF	hieven	
SO181/053-1	05.01.05	13:52	44° 29,77' S	75° 42,63' W	2358	WNW 15	171	1,6	Wärmestromsonde 6 m	GHF	verholen	rwk: 254°, d: 0,54 nm
SO181/053-1	05.01.05	14:33	44° 29,91' S	75° 43,32' W	2513	WNW 14	153	1	Wärmestromsonde 6 m	GHF	Boko	SL: 2489 m, P 2/1, umgefallen
SO181/053-1	05.01.05	14:34	44° 29,91' S	75° 43,32' W	2518	WNW 14	230	0,9	Wärmestromsonde 6 m	GHF	hieven	SL: 2420 m; Fieren
SO181/053-1	05.01.05	14:37	44° 29,91' S	75° 43,33' W	2516	WNW 14	300	1,4	Wärmestromsonde 6 m	GHF	Boko	SL: 2499 m, P 2/2, umgefallen
SO181/053-1	05.01.05	14:38	44° 29,92' S	75° 43,34' W	2534	WNW 13	230	2,2	Wärmestromsonde 6 m	GHF	hieven	
SO181/053-1	05.01.05	14:39	44° 29,92' S	75° 43,33' W	2512	WNW 13	252	1,4	Wärmestromsonde 6 m	GHF	verholen	rwk: 254°, d: 0,54 nm
SO181/053-1	05.01.05	15:21	44° 30,04' S	75° 44,05' W	2623	NW 14	233	0,3	Wärmestromsonde 6 m	GHF	Boko	SL: 2636 m, P 3
SO181/053-1	05.01.05	15:42	44° 30,09' S	75° 44,10' W	2652	N 14	2	0,3	Wärmestromsonde 6 m	GHF	hieven	
SO181/053-1	05.01.05	15:44	44° 30,08' S	75° 44,13' W	2659	WNW 13	152	1,1	Wärmestromsonde 6 m	GHF	verholen	rwk: 254°, d: 0,54 nm
SO181/053-1	05.01.05	16:32	44° 30,21' S	75° 44,78' W	2958	WNW 16	102	1	Wärmestromsonde 6 m	GHF	Boko	SL: 2926 m, P 4/1, umgefallen
SO181/053-1	05.01.05	16:34	44° 30,20' S	75° 44,75' W	2950	WNW 15	75	1,4	Wärmestromsonde 6 m	GHF	hieven	...und erneut fieren
SO181/053-1	05.01.05	16:37	44° 30,19' S	75° 44,75' W	2955	WNW 16	288	1,1	Wärmestromsonde 6 m	GHF	Boko	SL: 2957 m, P 4/2
SO181/053-1	05.01.05	16:47	44° 30,26' S	75° 44,81' W	2970	NW 15	148	0,5	Wärmestromsonde 6 m	GHF	hieven	
SO181/053-1	05.01.05	16:50	44° 30,24' S	75° 44,81' W	2963	WNW 1413	8	2,6	Wärmestromsonde 6 m	GHF	verholen	rwk: 254°, d: 0,5 nm
SO181/053-1	05.01.05	17:39	44° 30,38' S	75° 45,51' W	3040	WNW 15	138	1	Wärmestromsonde 6 m	GHF	Boko	SL: 3075 m, P 5/1
SO181/053-1	05.01.05	17:41	44° 30,36' S	75° 45,54' W	3115	WNW 15	35	1,1	Wärmestromsonde 6 m	GHF	hieven	...und erneut fieren
SO181/053-1	05.01.05	17:42	44° 30,37' S	75° 45,54' W	3109	W 15	181	2,7	Wärmestromsonde 6 m	GHF	Boko	SL: 3051 m, P 5/2
SO181/053-1	05.01.05	17:47	44° 30,36' S	75° 45,53' W	3070	W 16	64	1,4	Wärmestromsonde 6 m	GHF	hieven	
SO181/053-1	05.01.05	17:51	44° 30,35' S	75° 45,50' W	3057	W 15	115	2,1	Wärmestromsonde 6 m	GHF	verholen	rwk: 254°, d: 0,54 nm
SO181/053-1	05.01.05	18:23	44° 30,49' S	75° 46,20' W	3171	WNW 17	166	1,3	Wärmestromsonde 6 m	GHF	Boko	SL: 3218 m, P 6
SO181/053-1	05.01.05	18:45	44° 30,52' S	75° 46,23' W	3180	NW 15	26	0,9	Wärmestromsonde 6 m	GHF	hieven	
SO181/053-1	05.01.05	18:49	44° 30,48' S	75° 46,18' W	3173	W 15	242	0,4	Wärmestromsonde 6 m	GHF	verholen	rwk: 254°, d: 0,54 nm
SO181/053-1	05.01.05	19:33	44° 30,66' S	75° 46,94' W	3257	WNW 13	355	0,7	Wärmestromsonde 6 m	GHF	Boko	SL: 3266 nm, P 7

Station	Datum	UTC	PositionLat	PositionLon	Tiefe [m]	Windstärke [m/s]	Kurs [°]	v [kn]	Gerät	Gerätekürzel	Aktion	Bemerkung
SO181/053-1	05.01.05	19:40	44° 30,66' S	75° 46,94' W	3258	WNW 13	26	2,2	Wärmestromsonde 6 m	GHF	hieven	
SO181/053-1	05.01.05	19:42	44° 30,66' S	75° 46,95' W	3255	WNW 14	287	0,7	Wärmestromsonde 6 m	GHF	verholen	rwk: 254°, d: 0,54 nm
SO181/053-1	05.01.05	20:28	44° 30,80' S	75° 47,66' W	3299	W 14	298	1,1	Wärmestromsonde 6 m	GHF	Boko	SL: 3338 m P 8
SO181/053-1	05.01.05	20:47	44° 30,79' S	75° 47,64' W	3299	NW 13	69	0,2	Wärmestromsonde 6 m	GHF	hieven	
SO181/053-1	05.01.05	20:50	44° 30,79' S	75° 47,66' W	3302	WNW 13	205	1	Wärmestromsonde 6 m	GHF	verholen	rwk: 254°, d: 0,54 nm
SO181/053-1	05.01.05	21:43	44° 30,96' S	75° 48,40' W	3317	WNW 14	193	2,1	Wärmestromsonde 6 m	GHF	Boko	SL: 3360 m, P 9, umgefallen
SO181/053-1	05.01.05	21:44	44° 30,96' S	75° 48,40' W	3317	WNW 15	131	0,6	Wärmestromsonde 6 m	GHF	hieven	
SO181/053-1	05.01.06	21:48	44° 30,95' S	75° 48,38' W	3317	NNE 16	151	1,2	Wärmestromsonde 6 m	GHF	verholen	rwk: 254°, d: 0,54 nm
SO181/053-1	05.01.05	22:43	44° 31,10' S	75° 49,11' W	3320	WNW 14	206	0,7	Wärmestromsonde 6 m	GHF	Boko	SL: 3358 m, P 10, umgefallen
SO181/053-1	05.01.05	22:45	44° 31,10' S	75° 49,10' W	3319	WNW 13	69	2,1	Wärmestromsonde 6 m	GHF	hieven	
SO181/053-1	05.01.05	23:50	44° 30,90' S	75° 49,21' W	3321	WNW 16	254	0,8	Wärmestromsonde 6 m	GHF	a.D.	
SO181/053-1	06.01.05	00:00	44° 30,90' S	75° 49,37' W	3324	W 14	261	0,7	Wärmestromsonde 6 m	GHF	Ende Station GHF 07	
SO181/054-1	06.01.05	00:01	44° 30,90' S	75° 49,39' W	3324	W 14	2	0,8	Vermessung	EM / PS	Beginn Profil 1b-9	rwk: 137°, d: 12 nm
SO181/054-1	06.01.05	01:20	44° 39,36' S	75° 38,25' W	2058	W 8	140	8,3	Vermessung	EM / PS	Kursänderung	rwk: 011°, d: 20 nm
SO181/054-1	06.01.05	04:01	44° 19,99' S	75° 33,29' W	1654	WNW 14	275	3,5	Vermessung	EM / PS	Kursänderung	rwk: 270°, d: 4 nm
SO181/054-1	06.01.05	04:26	44° 19,93' S	75° 38,40' W	2444	WNW 16	319	10,5	Vermessung	EM / PS	Kursänderung	rwk: 010°, d: 56 nm
SO181/054-1	06.01.05	10:24	43° 25,10' S	75° 24,55' W	2226	NW 7	10	9,5	Vermessung	EM / PS	Kursänderung	rwk: 321°, d: 8 nm
SO181/054-1	06.01.05	11:03	43° 20,16' S	75° 29,83' W	3513	NNW 13	326	9,7	Vermessung	EM / PS	Kursänderung	rwk: 360 ; d: 20 sm
SO181/054-1	06.01.05	13:08	43° 0,26' S	75° 30,01' W	3343	NW 14	357	8,9	Vermessung	EM / PS	Kursänderung	rwk: 133 ; d: 16 sm
SO181/054-1	06.01.05	14:36	43° 10,86' S	75° 14,16' W	1511	NW 6	133	10,9	Vermessung	EM / PS	Kursänderung	rwk: 191 ; d: 40sm
SO181/054-1	06.01.05	18:35	43° 50,04' S	75° 24,75' W	1870	NNW 14	251	5,3	Vermessung	EM / PS	Kursänderung	rwk: 256°, d: 43 nm, Magn z.W., SL: 200 m
SO181/054-1	06.01.05	23:38	43° 59,87' S	76° 22,76' W	3428	WNW 12	285	5,2	Vermessung	EM / PS	Kursänderung	rwk: 360°, d: 230 nm; Magn. a. D.
SO181/054-1	07.01.05	19:53	40° 10,13' S	76° 22,03' W	4017	NNW 7	0	11,4	Vermessung	EM / PS	Kursänderung	rwk: 090°, d: 7 nm
SO181/054-1	07.01.05	20:27	40° 9,99' S	76° 13,05' W	3985	NW 7	104	12,2	Vermessung	EM / PS	Kursänderung	rwk: 180°, d: 157 nm
SO181/054-1	08.01.05	10:00	42° 46,39' S	76° 13,01' W	3640	WSW 13	189	10,9	Vermessung	EM / PS	Kursänderung	rwk: 217°, d: 12 nm
SO181/054-1	08.01.05	11:15	42° 56,30' S	76° 23,22' W	3582	SW 10	203	1,2	Vermessung	EM / PS	Ende Profil 1b-9	Survey 1b-9 gesamt 623 nm 59,2 Std.
SO181/055-1	08.01.05	11:16	42° 56,31' S	76° 23,23' W	3582	WSW 11	303	0,3	Wärmestromsonde 6 m	GHF	Beginn Station	GHF 08
SO181/055-1	08.01.05	11:20	42° 56,31' S	76° 23,23' W	3584	SW 11	1	1	Wärmestromsonde 6 m	GHF	z.W.	
SO181/055-1	08.01.05	12:28	42° 56,29' S	76° 23,20' W	3583	SW 10	172	1,4	Wärmestromsonde 6 m	GHF	Boko	SL: 3609 m P 01
SO181/055-1	08.01.05	12:59	42° 56,30' S	76° 23,19' W	3583	WSW 9	286	0,6	Wärmestromsonde 6 m	GHF	hieven	
SO181/055-1	08.01.05	13:02	42° 56,30' S	76° 23,19' W	3583	WSW 10	131	0,2	Wärmestromsonde 6 m	GHF	verholen	rwk: 080 ; d: 0,54 sm
SO181/055-1	08.01.05	14:09	42° 56,21' S	76° 22,47' W	3588	WSW 11	172	0,9	Wärmestromsonde 6 m	GHF	Boko	SL: 3655 m P 02
SO181/055-1	08.01.05	14:21	42° 56,21' S	76° 22,50' W	3588	SW 10	234	0,7	Wärmestromsonde 6 m	GHF	hieven	
SO181/055-1	08.01.05	14:26	42° 56,21' S	76° 22,52' W	3588	SW 9	103	0,4	Wärmestromsonde 6 m	GHF	verholen	rwk: 080 ; d: 0,54 sm
SO181/055-1	08.01.05	15:40	42° 56,12' S	76° 21,73' W	3592	WSW 9	124	0,4	Wärmestromsonde 6 m	GHF	Boko	SL: 3661 m P 03
SO181/055-1	08.01.05	16:04	42° 56,14' S	76° 21,70' W	3590	WSW 10	227	0,3	Wärmestromsonde 6 m	GHF	hieven	
SO181/055-1	08.01.05	17:18	42° 56,45' S	76° 21,67' W	3591	WSW 11	245	0,7	Wärmestromsonde 6 m	GHF	a.D.	
SO181/055-1	08.01.05	17:25	42° 56,46' S	76° 21,67' W	3591	WSW 12	188	2,2	Wärmestromsonde 6 m	GHF	Ende Station GHF 08	KÄ: rwk: 080°, d: 50 nm
SO181/055-2	08.01.05	17:26	42° 56,60' S	76° 21,75' W	3589	WNW 11	277	3,7	Vermessung	EM / PS	Beginn Profil / Transit	rwk: 080°, d: 52 nm
SO181/055-2	08.01.05	21:49	42° 47,36' S	75° 11,69' W	1554	WSW 8	72	7	Vermessung	EM / PS	Ende Profil / Transit	Profil / Transit gesamt 52 nm 4,4 Std.
SO181/056-1	08.01.05	21:50	42° 47,38' S	75° 11,67' W	1511	WSW 9	128	4,7	Wärmestromsonde 3 m	HF	Beginn Station	HF 09

Station	Datum	UTC	PositionLat	PositionLon	Tiefe [m]	Windstärke [m/s]	Kurs [°]	v [kn]	Gerät	Gerätekürzel	Aktion	Bemerkung
SO181/056-1	08.01.05	21:55	42° 47,48' S	75° 11,62' W	1522	WSW 10	39	1,2	Wärmestromsonde 3 m	HF	z.W.	
SO181/056-1	08.01.05	22:28	42° 47,47' S	75° 11,66' W	1556	WSW 8	1	0,6	Wärmestromsonde 3 m	HF	Boko	SL: 1559 m, P 1
SO181/056-1	08.01.05	22:30	42° 47,46' S	75° 11,67' W	1537	WSW 9	120	0,3	Wärmestromsonde 3 m	HF	hieven	umgefallen
SO181/056-1	08.01.05	22:31	42° 47,46' S	75° 11,66' W	1557	WSW 10	138	1,4	Wärmestromsonde 3 m	HF	verholen	rwk: 260°, d: 0,54 nm
SO181/056-1	08.01.05	23:18	42° 47,56' S	75° 12,38' W	1668	N 9	16	0,4	Wärmestromsonde 3 m	HF	Boko	SL: 1680 m ; P2
SO181/056-1	08.01.05	23:32	42° 47,57' S	75° 12,38' W	1665	WSW 7	236	0,7	Wärmestromsonde 3 m	HF	hieven	
SO181/056-1	08.01.05	23:35	42° 47,57' S	75° 12,39' W	1666	WSW 9	20	0,2	Wärmestromsonde 3 m	HF	verholen	rwk: 260 ; d: 0,53 sm
SO181/056-1	09.01.05	00:22	42° 47,65' S	75° 13,12' W	1798	WSW 9	162	0,2	Wärmestromsonde 3 m	HF	Boko	SL: 1834 m ; P3
SO181/056-1	09.01.05	00:24	42° 47,66' S	75° 13,11' W	1799	WSW 9	322	0,6	Wärmestromsonde 3 m	HF	hieven	HF umgefallen ; Fieren
SO181/056-1	09.01.05	00:31	42° 47,64' S	75° 13,10' W	1797	WSW 8	357	1	Wärmestromsonde 3 m	HF	Boko	SL: 1826 m
SO181/056-1	09.01.05	00:31	42° 47,64' S	75° 13,10' W	1797	WSW 8	357	1	Wärmestromsonde 3 m	HF	hieven	HF geht nicht in Grund
SO181/056-1	09.01.05	01:07	42° 47,66' S	75° 13,10' W	1797	WSW 9	111	0,5	Wärmestromsonde 3 m	HF	a.D.	Mess-Strecke unten abgerissen
SO181/056-1	09.01.05	01:09	42° 47,66' S	75° 13,10' W	1797	WSW 9	337	0,2	Wärmestromsonde 3 m	HF	Ende Station HF 09	
SO181/057-1	09.01.05	01:21	42° 47,64' S	75° 13,20' W	1802	WSW 10	268	0,9	Vermessung	EM / PS	Beginn Profil 1b-10	rwk: 288°, d: 2 nm
SO181/057-1	09.01.05	01:38	42° 47,10' S	75° 15,79' W	2188	NW 12	288	10,8	Vermessung	EM / PS	Kursänderung	rwk: 307°, d: 8 nm
SO181/057-1	09.01.05	02:22	42° 42,20' S	75° 24,64' W	2747	WSW 12	307	11,1	Vermessung	EM / PS	Kursänderung	rwk: 360°, d: 46 nm
SO181/057-1	09.01.05	06:09	41° 56,14' S	75° 24,97' W	3886	SSW 6	352	12,5	Vermessung	EM / PS	Kursänderung	rwk: 074°, d: 11 nm
SO181/057-1	09.01.05	07:03	41° 53,03' S	75° 11,50' W	2476	SW 6	68	12,5	Vermessung	EM / PS	Kursänderung	rwk: 002°, d: 14 nm
SO181/057-1	09.01.05	08:12	41° 39,13' S	75° 10,74' W	2758	SSW 6	358	11,9	Vermessung	EM / PS	Kursänderung	rwk: 022°, d: 32 nm
SO181/057-1	09.01.05	10:51	41° 9,09' S	74° 54,57' W	1684	S 6	23	12,1	Vermessung	EM / PS	Kursänderung	rwk: 054°, d: 6 nm
SO181/057-1	09.01.05	11:22	41° 5,41' S	74° 47,99' W	1681	S 5	52	11,7	Vermessung	EM / PS	Kursänderung	rwk: 009 ; d: 23 sm
SO181/057-1	09.01.05	13:17	40° 42,56' S	74° 43,06' W	1472	SSE 5	5	11,5	Vermessung	EM / PS	Kursänderung	rwk: 081 ; d: 15 sm
SO181/057-1	09.01.05	14:32	40° 40,03' S	74° 24,23' W	895	SSE 9	84	11,7	Vermessung	EM / PS	Kursänderung	rwk: 360 ; d: 4 sm
SO181/057-1	09.01.05	14:52	40° 36,29' S	74° 24,03' W	1002	SSE 3	348	11,1	Vermessung	EM / PS	Ende Profil 1b-10	Profilzeit: 13,5 Std., Profildistanz: 161 nm
SO181/058-1	09.01.05	14:56	40° 36,06' S	74° 24,28' W	1014	SSE 10	231	2,8	Profil	PR	Stationsbeginn	
SO181/058-1	09.01.05	15:03	40° 36,28' S	74° 24,65' W	1044	S 8	247	2,9	Profil	PR	Streamer zu Wasser	SL: 200 m
SO181/058-1	09.01.05	15:07	40° 36,37' S	74° 24,82' W	1059	S 9	236	3	Profilbeginn SCS03	PR	Stb Airgun zu Wasser	rwk 262° d 17 nm bis Unterbrechung
SO181/058-1	09.01.05	15:14	40° 36,66' S	74° 25,29' W	1087	SSE 11	240	3,7	Profil	PR	Magnetometer zu Wasser	SL: 200 m
SO181/058-1	09.01.05	18:39	40° 38,85' S	74° 46,34' W	1863	S 11	248	2	Profil	PR	Stb Airgun an Deck	Unterbrechen Profilmessung
SO181/058-1	09.01.05	19:13	40° 39,10' S	74° 48,59' W	2103	SSE 10	258	3,4	Profil	PR	Kursänderung	dreher ü. Bb, rwk: 082°
SO181/058-1	09.01.05	19:51	40° 39,13' S	74° 45,65' W	1823	S 10	90	4,9	Profil	PR	Kursänderung	dreher ü. Bb, d: 3 nm
SO181/058-1	09.01.05	20:00	40° 38,81' S	74° 45,46' W	1795	S 11	277	3,8	Profil	PR	Stb Airgun zu Wasser	rwk: 262°, d: 86 nm, ff. SCS03
	09.01.05	20:00	40° 38,81' S	74° 45,46' W	1795	S 12	277	5	Seismikprofil SCS03	PR	Fortsetzung Seismik	Fortsetzung Profillfahrt Seismik SCO3
SO181/058-1	10.01.05	13:05	40° 51,19' S	76° 39,97' W	3784	NW 7	270	4,3	Profil	PR	Ende Profil SCS03	gesamt: d 103 sm
SO181/058-1	10.01.05	13:10	40° 51,23' S	76° 40,34' W	3784	WNW 8	259	2,2	Profil	PR	Magnetometer an Deck	
SO181/058-1	10.01.05	13:13	40° 51,24' S	76° 40,47' W	3785	WNW 7	279	1,7	Profil	PR	Stb Airgun an Deck	
SO181/058-1	10.01.05	13:19	40° 51,24' S	76° 40,70' W	3783	WNW 7	278	1,4	Profil	PR	Streamer an Deck	
SO181/058-1	10.01.05	13:19	40° 51,24' S	76° 40,70' W	3783	WNW 7	278	1,4	Profil	PR	Stationsende	
SO181/059-1	10.01.05	13:22	40° 51,23' S	76° 40,83' W	3772	WNW 7	282	2,9	Vermessung	EM / PS	Beginn Profil 1b-11	rwk: 249°, d: 7 nm
SO181/059-1	10.01.05	14:02	40° 53,41' S	76° 48,69' W	3705	WSW 11	247	11,7	Vermessung	EM / PS	Kursänderung	rwk: 180°, d: 30 nm
SO181/059-1	10.01.05	16:45	41° 23,08' S	76° 48,78' W	3712	S 3	124	8,3	Vermessung	EM / PS	Kursänderung	rwk: 117°, d: 8 nm

Station	Datum	UTC	PositionLat	PositionLon	Tiefe [m]	Windstärke [m/s]	Kurs [°]	v [kn]	Gerät	Gerätekürzel	Aktion	Bemerkung
SO181/059-1	10.01.05	17:29	41° 26,51' S	76° 41,13' W	3809	NW 9	62	2,1	Vermessung	EM / PS	Magnetometer z.W.	SL: 200 m
SO181/059-1	10.01.05	17:31	41° 26,49' S	76° 41,00' W	3804	NW 10	99	4,6	Vermessung	EM / PS	Kursänderung	rwk: 082°, d: 84 nm
SO181/059-1	11.01.05	02:13	41° 14,17' S	74° 49,06' W	1420	WNW 7	84	3,2	Vermessung	EM / PS	Magnetometer a.D.	rwk: 081°, d: 14 nm
SO181/059-1	11.01.05	03:30	41° 12,03' S	74° 30,25' W	638	WNW 6	79	11,8	Vermessung	EM / PS	Kursänderung	rwk: 360°, d: 4 nm
SO181/059-1	11.01.05	03:50	41° 8,58' S	74° 30,05' W	741	WSW 9	339	10,4	Vermessung	EM / PS	Kursänderung	rwk: 262°, d: 30 nm
SO181/059-1	11.01.05	06:40	41° 12,68' S	75° 9,12' W	2652	SW 10	320	10,2	Vermessung	EM / PS	Kursänderung	rwk: 322°, d: 7 nm
SO181/059-1	11.01.05	07:18	41° 7,06' S	75° 14,96' W	3700	SW 11	331	11,4	Vermessung	EM / PS	Kursänderung	rwk: 070°, d: 16 nm
SO181/059-1	11.01.05	08:36	41° 1,56' S	74° 55,62' W	2043	SW 7	67	12,1	Vermessung	EM / PS	Kursänderung	rwk: 005°, d: 21 nm
SO181/059-1	11.01.05	10:19	40° 40,50' S	74° 53,00' W	2325	SW 9	1	12,3	Vermessung	EM / PS	Ende Profil 1b-11	
SO181/060-1	11.01.05	11:12	40° 40,82' S	75° 4,38' W	3465	WSW 7	78	0,2	Wärmestromsonde 6 m	GHF	Beginn Station	GHF 10
SO181/060-1	11.01.05	11:16	40° 40,85' S	75° 4,39' W	3459	W 8	182	0,4	Wärmestromsonde 6 m	GHF	z.W.	
SO181/060-1	11.01.05	12:17	40° 40,81' S	75° 4,43' W	3475	W 6	56	0,5	Wärmestromsonde 6 m	GHF	Boko	SL: 3502 m P 01
SO181/060-1	11.01.05	12:39	40° 40,80' S	75° 4,45' W	3477	NNE 6	164	0,2	Wärmestromsonde 6 m	GHF	hieven	
SO181/060-1	11.01.05	12:42	40° 40,81' S	75° 4,44' W	3472	WSW 7	357	0,7	Wärmestromsonde 6 m	GHF	verholen	rwk: 082°, d: 0,56 nm
SO181/060-1	11.01.05	13:40	40° 40,76' S	75° 3,74' W	3345	WSW 6	129	0,2	Wärmestromsonde 6 m	GHF	Boko	SL: 3427 m P 02
SO181/060-1	11.01.05	13:50	40° 40,75' S	75° 3,76' W	3348	NNW 7	335	0,4	Wärmestromsonde 6 m	GHF	hieven	
SO181/060-1	11.01.05	13:53	40° 40,74' S	75° 3,74' W	3354	SW 6	244	0,1	Wärmestromsonde 6 m	GHF	verholen	rwk: 082°, d: 0,54 nm
SO181/060-1	11.01.05	14:46	40° 40,68' S	75° 3,04' W	3238	WSW 5	82	0,6	Wärmestromsonde 6 m	GHF	Boko	SL: 3305 m P 03
SO181/060-1	11.01.05	15:06	40° 40,68' S	75° 3,03' W	3239	W 6	258	0,2	Wärmestromsonde 6 m	GHF	hieven	
SO181/060-1	11.01.05	15:09	40° 40,68' S	75° 3,03' W	3247	W 5	184	0,5	Wärmestromsonde 6 m	GHF	verholen	rwk: 082°, d: 0,54 nm
SO181/060-1	11.01.05	15:27	40° 40,72' S	75° 2,94' W	3227	W 4	201	0,6	Wärmestromsonde 6 m	GHF	Boko	SL: 3262 m P 04
SO181/060-1	11.01.05	16:36	40° 40,63' S	75° 2,26' W	3212	WSW 7	94	0,8	Wärmestromsonde 6 m	GHF	hieven	
SO181/060-1	11.01.05	16:44	40° 40,64' S	75° 2,20' W	3197	W 5	190	0,6	Wärmestromsonde 6 m	GHF	verholen	rwk: 082°, d: 0,54 nm
SO181/060-1	11.01.05	17:34	40° 40,52' S	75° 1,58' W	3179	N 6	17	0,7	Wärmestromsonde 6 m	GHF	Boko	SL: 3227 m P 05
SO181/060-1	11.01.05	17:53	40° 40,58' S	75° 1,57' W	3152	NW 6	273	0,8	Wärmestromsonde 6 m	GHF	hieven	
SO181/060-1	11.01.05	17:56	40° 40,56' S	75° 1,56' W	3149	WSW 7	43	1,4	Wärmestromsonde 6 m	GHF	verholen	rwk: 082°, d: 0,54 nm
SO181/060-1	11.01.05	18:54	40° 40,46' S	75° 0,91' W	3080	WSW 8	343	0,8	Wärmestromsonde 6 m	GHF	Boko	SL: 3148 m P 06
SO181/060-1	11.01.05	19:03	40° 40,48' S	75° 0,92' W	3078	NW 9	341	0,8	Wärmestromsonde 6 m	GHF	hieven	
SO181/060-1	11.01.05	20:04	40° 40,48' S	75° 1,02' W	3096	WSW 8	242	0,4	Wärmestromsonde 6 m	GHF	a.D.	
SO181/060-1	11.01.05	20:04	40° 40,49' S	75° 1,02' W	3096	WSW 8	242	0,4	Wärmestromsonde 6 m	GHF	Ende Station GHF 10	6 Messungen Zeit: 8,9 Std. D = 2,5 nm
SO181/061-1	11.01.05	20:32	40° 40,05' S	74° 56,87' W	2644	WSW 7	71	11,7	Vermessung	EM / PS	Beginn Profil 1b-12	rwk: 067°, d: 13 nm
SO181/061-1	11.01.05	21:35	40° 35,03' S	74° 41,54' W	1736	SW 10	54	11,1	Vermessung	EM / PS	Kursänderung	rwk: 010°, d: 22 nm
SO181/061-1	11.01.05	23:27	40° 13,32' S	74° 36,57' W	1775	WSW 5	13	12,2	Vermessung	EM / PS	Kursänderung	rwk: 270°, d: 71 nm
SO181/061-1	12.01.05	06:01	40° 12,96' S	76° 8,17' W	3566	NW 11	269	10,5	Vermessung	EM / PS	Kursänderung	rwk: 360°, d: 118 nm
SO181/061-1	12.01.05	16:06	38° 15,37' S	76° 10,07' W	4020	SSW 9	8	5,2	Vermessung	EM / PS	Kursänderung	rwk: 006°, d: 77 nm
SO181/061-1	12.01.05	16:12	38° 15,03' S	76° 10,12' W	4006	S 11	350	2,8	Vermessung	EM / PS	Magnetometer z.W.	SL: 200 m
SO181/061-1	13.01.05	00:26	36° 58,63' S	76° 0,04' W	3519	SSE 6	10	9,8	Vermessung	EM / PS	Kursänderung	rwk: 019°, d: 87 nm
SO181/061-1	13.01.05	09:24	35° 36,34' S	75° 25,06' W	4162	S 14	41	9,2	Vermessung	EM / PS	Kursänderung	rwk: 104°, d: 19 nm
SO181/061-1	13.01.05	11:27	35° 40,89' S	75° 2,45' W	4164	SSW 13	85	10,5	Vermessung	EM / PS	Kursänderung	rwk: 102°, d: 68 nm
SO181/061-1	13.01.05	18:09	35° 55,05' S	73° 40,16' W	1844	SW 14	125	10,3	Vermessung	EM / PS	Kursänderung	rwk: 166°, d: 20 nm
SO181/061-1	13.01.05	20:09	36° 13,85' S	73° 34,10' W	386	SW 11	181	8,1	Vermessung	EM / PS	Ende Profil 1b-12	Survey 1b-12 gesamt: 47,6 Std. D 495 nm

Station	Datum	UTC	PositionLat	PositionLon	Tiefe [m]	Windstärke [m/s]	Kurs [°]	v [kn]	Gerät	Gerätekürzel	Aktion	Bemerkung
SO181/062-1	13.01.05	20:11	36° 14,01' S	73° 34,28' W	422	SW 10	283	5,2	Profil	PR	Stationsbeginn	SCS 04, Magn. Stat. 61 z.W.
SO181/062-1	13.01.05	20:16	36° 13,84' S	73° 34,66' W	475	SSW 10	279	3	Profil	PR	Streamer zu Wasser	SL: 200 m
SO181/062-1	13.01.05	20:22	36° 13,83' S	73° 34,97' W	527	SSW 10	286	3,3	Profil	PR	Sib Alrgun zu Wasser	
SO181/062-1	13.01.05	20:24	36° 13,80' S	73° 35,08' W	549	SSW 11	264	3,2	Seismikprofil SCS04 + Mag.	PR	Beginn Profil SCS04	rwk: 280°, d: 78 nm mit Magnetometer
SO181/062-1	14.01.05	11:50	36° 0,80' S	75° 9,97' W	4277	S 9	279	4,5	Profil	PR	Ende Profil	
SO181/062-1	14.01.05	11:57	36° 0,70' S	75° 10,47' W	4297	S 11	279	2	Profil	PR	Magnetometer an Deck	
SO181/062-1	14.01.05	12:00	36° 0,66' S	75° 10,63' W	4298	S 9	260	2,7	Profil	PR	Sib Alrgun an Deck	
SO181/062-1	14.01.05	12:07	36° 0,56' S	75° 10,98' W	4285	S 12	274	2,6	Profil	PR	Streamer an Deck	
SO181/062-1	14.01.05	12:07	36° 0,56' S	75° 10,98' W	4285	S 12	274	2,6	Profil	PR	Ende Profil SCS04	Profilzeit: 16,3 Std. Profillänge: 78 nm
SO181/063-1	14.01.05	12:44	36° 1,26' S	75° 6,68' W	4343	S 10	34	0,6	Wärmestromsonde 6 m	GHF	Beginn Station HF 11	
SO181/063-1	14.01.05	12:50	36° 1,24' S	75° 6,72' W	4346	S 9	283	0,4	Wärmestromsonde 6 m	GHF	z.W.	W 1
SO181/063-1	14.01.05	14:07	36° 1,24' S	75° 6,73' W	4345	SSW 9	196	0,6	Wärmestromsonde 6 m	GHF	Boko	SL: 4374 m P 01
SO181/063-1	14.01.05	14:27	36° 1,24' S	75° 6,73' W	4350	SSW 8	127	0,7	Wärmestromsonde 6 m	GHF	hieven	
SO181/063-1	14.01.05	14:30	36° 1,24' S	75° 6,73' W	4341	SSW 8	182	0,9	Wärmestromsonde 6 m	GHF	verholen	rwk: 100°, d: 0,55 nm
SO181/063-1	14.01.05	15:24	36° 1,34' S	75° 6,05' W	4313	SW 8	18	0,7	Wärmestromsonde 6 m	GHF	Boko	SL: 4397 m P 02
SO181/063-1	14.01.05	15:33	36° 1,33' S	75° 6,08' W	4329	SSW 6	255	1,5	Wärmestromsonde 6 m	GHF	hieven	
SO181/063-1	14.01.05	15:39	36° 1,36' S	75° 6,14' W	4341	SW 8	248	0,7	Wärmestromsonde 6 m	GHF	verholen	rwk: 100°, d: 0,54 nm
SO181/063-1	14.01.05	16:32	36° 1,44' S	75° 5,39' W	4299	S 7	144	0,5	Wärmestromsonde 6 m	GHF	Boko	SL: 4379 m P 03
SO181/063-1	14.01.05	16:55	36° 1,44' S	75° 5,40' W	4302	S 8	328	1,4	Wärmestromsonde 6 m	GHF	hieven	
SO181/063-1	14.01.05	16:58	36° 1,42' S	75° 5,45' W	4306	SSW 8	339	0,6	Wärmestromsonde 6 m	GHF	verholen	rwk: 100°, d: 0,54 nm
SO181/063-1	14.01.05	17:53	36° 1,54' S	75° 4,75' W	4266	SSW 8	306	0,6	Wärmestromsonde 6 m	GHF	Boko	SL: 4353 m P 04
SO181/063-1	14.01.05	18:04	36° 1,52' S	75° 4,78' W	4287	SSW 9	304	1	Wärmestromsonde 6 m	GHF	hieven	
SO181/063-1	14.01.05	18:07	36° 1,52' S	75° 4,78' W	4269	SSW 8	61	1	Wärmestromsonde 6 m	GHF	verholen	rwk: 100°, d: 0,54 nm
SO181/063-1	14.01.05	18:48	36° 1,61' S	75° 4,09' W	4230	SW 9	115	1,2	Wärmestromsonde 6 m	GHF	Boko	SL: 4351 m P 05
SO181/063-1	14.01.05	19:10	36° 1,63' S	75° 4,08' W	4230	SSW 9	143	0,4	Wärmestromsonde 6 m	GHF	hieven	
SO181/063-1	14.01.05	19:13	36° 1,63' S	75° 4,09' W	4228	SSW 11	171	0,8	Wärmestromsonde 6 m	GHF	verholen	rwk: 100°, d: 0,53 nm
SO181/063-1	14.01.05	20:06	36° 1,71' S	75° 3,45' W	4266	SSW 9	355	0,2	Wärmestromsonde 6 m	GHF	Boko	SL: 4314 m P 06
SO181/063-1	14.01.05	20:16	36° 1,73' S	75° 3,44' W	4273	SSW 9	252	0,6	Wärmestromsonde 6 m	GHF	hieven	
SO181/063-1	14.01.05	20:18	36° 1,73' S	75° 3,45' W	4272	SSW 9	167	0,2	Wärmestromsonde 6 m	GHF	verholen	rwk: 099°, d: 0,54 nm
SO181/063-1	14.01.05	21:08	36° 1,80' S	75° 2,77' W	4274	SSW 9	123	0,5	Wärmestromsonde 6 m	GHF	Boko	SL: 4349 m P 07
SO181/063-1	14.01.05	21:27	36° 1,81' S	75° 2,77' W	4273	SSW 9	291	0,1	Wärmestromsonde 6 m	GHF	hieven	
SO181/063-1	14.01.05	21:29	36° 1,81' S	75° 2,78' W	4273	SSW 9	174	0,5	Wärmestromsonde 6 m	GHF	verholen	rwk: 100°, d: 0,54 nm
SO181/063-1	14.01.05	22:12	36° 1,88' S	75° 2,11' W	4252	SSW 10	11	0,8	Wärmestromsonde 6 m	GHF	Boko	SL: 4353 m P 08
SO181/063-1	14.01.05	22:22	36° 1,88' S	75° 2,13' W	4251	SSW 10	259	0,2	Wärmestromsonde 6 m	GHF	hieven	
SO181/063-1	14.01.05	23:42	36° 2,02' S	75° 1,68' W	4229	N 11	181	0,5	Wärmestromsonde 6 m	GHF	a.D.	
SO181/063-1	14.01.05	23:49	36° 2,03' S	75° 1,60' W	4217	S 12	100	2	Wärmestromsonde 6 m	GHF	Ende Station HF 11	
SO181/064-1	14.01.05	23:54	36° 2,13' S	75° 1,38' W	4207	SSW 12	117	4,6	Magnetometer	MAGN	Beginn Station	survey 1b-1
SO181/064-1	14.01.05	23:57	36° 2,13' S	75° 1,10' W	4203	SSW 10	82	3,7	Magnetometer	MAGN	Magnetometer zu Wasser	SL: 200m
SO181/064-1	15.01.05	00:07	36° 2,30' S	75° 0,16' W	4259	S 15	224	7,6	Magnetometer	MAGN	Beginn Profil 1b-13	rwk: 226°, d: 47 nm
SO181/064-1	15.01.05	04:50	36° 34,87' S	75° 41,22' W	4028	S 9	185	9,6	Magnetometer	MAGN	Kursänderung	rwk: 136°, d: 50 nm
SO181/064-1	15.01.05	09:48	37° 10,48' S	74° 58,57' W	4452	S 7	116	9,7	Magnetometer	MAGN	Kursänderung	rwk: 046°, d: 46 nm

Appendix 9.7.2

STATIONBOOK

SO 181-1b

[illegible]

Abkürzungen / Abbreviation

z.W.	zu Wasser
a.D.	an Deck
SL (max.)	(maximale) Seillänge
LT	Lottiefe nach Hydrosweep
W x	eingesetzte Winde
SM	Simrad - Multibeam - Lot
PS	Parasound
r.wk.	Rechtweisender Kurs
d:	Distanz
v:	Geschwindigkeit in Knoten
SL:	Seillänge
KL:	Kabellänge

Eingesetzte Geräte

CTD/Ro	CTD- Rosettagestell für Releasertest
Airgun	2 x je 4 G-Gun 6 Ltr an Traverse
Airgun	Bolt-Gun 32 ltr
Streamer	Streamer (100m + 100m Vorlaufkabel)
Streamer	Streamer 10m + 50m Vorlauf
Magn.	Magnetometer
Seamk	Seismikprofile mit Magnetometer
Vermess.	EM - Vermessungsprofile mit / ohne Magnetometer
MT	Magnetotelluric

Einsätze

1	
auf 5 Profilen	
0	
auf 5 Profilen	
1	
auf 8 Profilen	
5 Profile	Profilzeit: 210 Std. Profillänge 739 nm
11 Profile	Profilzeit: 436 Std. Profillänge 2986 nm
5	

Geräteverluste: 1 x OBH, 2 x MT müssen als verloren angesehen werden

Winde	D/M	Typ	RF-Hr	SO 181.2 Einsatz	Gesamt Einsatz	SO 181.2 S'länge	Gesamt S'länge	Zust.	SO 181.2 gefahrene max. L	jemals gefahrene max. Länge
W 1	18.01.00	LWL	812001	9 h	472 h	5347	240495	3-4	2962	8022 m
W 2	18.01.00	LWL	815286	0 h	0 h	0 m	0 m	1	0 m	0 m
W 4	11.01.00	NSW	818045	0 h	268 h	0 m	220273 m	3	0 m	8081 m
W 5	11.01.00	NSW	812106	0 h	0 h	0 m	0 m	1	0 m	0 m
W 6	18.01.00	DRAKO	818238	12 h	1147 h	13473	1093147	3-4	6668	7608 m

Station	Datum	UTC	PositionLat	PositionLon	Tiefe [m]	Windstärke [m/s]	Kurs [°]	v [kn]	Gerät	Gerätekürzel	Aktion	Bemerkung
Transit	19.01.05	11:00	38° 41,3' S	73° 18,8' W					Beginn Forschungsarbeiten		Anf. AG, div. Kurse zur Vermessung, d: 123 am	
SO181/065-1	20.01.05	12:13	38° 8,44' S	74° 33,62' W	4571	SSW 11	188	1,5	CTD	CTD	Beginn Station	Releasertest
SO181/065-1	20.01.05	12:19	38° 8,48' S	74° 33,61' W	4595	SSW 12	299	1,3	CTD	CTD	zu Wasser	
SO181/065-1	20.01.05	13:31	38° 8,62' S	74° 33,55' W	4601	SSW 11	164	0,8	CTD	CTD	auf Tiefe	SL = 4000 m
SO181/065-1	20.01.05	15:44	38° 8,95' S	74° 33,58' W	4604	S 10	204	0,4	CTD	CTD	an Deck	
SO181/065-1	20.01.05	18:34	38° 8,97' S	74° 33,49' W	4589	SSW 9	105	1,1	CTD	CTD	Ende Station	
Transit	20.01.05	18:34	38° 8,97' S	74° 33,49' W	4589	SSW 9	105	1,1	Anfahrt AG			rwk: 189°, d: 131 am
SO181/066-1	21.01.05	23:01	42° 44,50' S	74° 44,88' W	127	WSW 12	254	4,1	OBS/OBH	OBS/OBH	Beginn Station	
SO181/066-1	21.01.05	23:02	42° 44,51' S	74° 44,95' W	129	WSW 12	277	2,8	OBS/OBH	OBS/OBH	OBH zu Wasser	OBH 30
SO181/066-1	21.01.05	23:27	42° 44,97' S	74° 49,01' W	195	WSW 12	270	2,5	OBS/OBH	OBS/OBH	OBH zu Wasser	OBH 31
SO181/066-1	21.01.05	23:51	42° 45,43' S	74° 52,83' W	445	W 11	258	2,8	OBS/OBH	OBS/OBH	OBH zu Wasser	OBH 32
SO181/066-1	22.01.05	00:18	42° 45,92' S	74° 57,04' W	771	WSW 13	296	1,6	OBS/OBH	OBS/OBH	OBH zu Wasser	OBH 33
SO181/066-1	22.01.05	00:42	42° 46,41' S	75° 1,00' W	844	WSW 12	305	1,7	OBS/OBH	OBS/OBH	OBH zu Wasser	OBH 34
SO181/066-1	22.01.05	01:07	42° 46,88' S	75° 4,96' W	1107	WSW 13	271	3,3	OBS/OBH	OBS/OBH	OBH zu Wasser	OBH 35
SO181/066-1	22.01.05	01:32	42° 47,40' S	75° 9,00' W	1131	WSW 12	263	1,8	OBS/OBH	OBS/OBH	OBH zu Wasser	OBH 36
SO181/066-1	22.01.05	01:57	42° 47,87' S	75° 12,87' W	1789	WSW 12	265	2,9	OBS/OBH	OBS/OBH	OBH zu Wasser	OBH 37
SO181/066-1	22.01.05	02:24	42° 48,36' S	75° 17,01' W	2200	WSW 12	274	2,2	OBS/OBH	OBS/OBH	OBH zu Wasser	OBH 38
SO181/066-1	22.01.05	02:48	42° 48,81' S	75° 20,91' W	2371	WSW 12	185	0,4	OBS/OBH	OBS/OBH	OBH zu Wasser	OBH 39
SO181/066-1	22.01.05	03:18	42° 49,26' S	75° 24,93' W	3153	WSW 11	283	1,4	OBS/OBH	OBS/OBH	OBH zu Wasser	OBH 40
SO181/066-1	22.01.05	03:47	42° 49,76' S	75° 28,95' W	3707	WSW 11	246	2,7	OBS/OBH	OBS/OBH	OBH zu Wasser	OBH 41
SO181/066-1	22.01.05	04:13	42° 50,26' S	75° 32,97' W	3737	WSW 10	201	1,2	OBS/OBH	OBS/OBH	OBS zu Wasser	OBS 42
SO181/066-1	22.01.05	04:44	42° 50,75' S	75° 37,06' W	3745	W 10	230	1,7	OBS/OBH	OBS/OBH	OBS zu Wasser	OBS 43
SO181/066-1	22.01.05	05:11	42° 51,23' S	75° 41,02' W	3741	SW 10	309	1,5	OBS/OBH	OBS/OBH	OBS zu Wasser	OBS 44
SO181/066-1	22.01.05	05:40	42° 51,70' S	75° 45,08' W	3737	WSW 9	20	1	OBS/OBH	OBS/OBH	OBS zu Wasser	OBS 45

Station	Datum	UTC	PositionLat	PositionLon	Tiefe [m]	Windstärke [m/s]	Kurs [°]	v [kn]	Gerät	Gerätekürzel	Aktion	Bemerkung
SO181/066-1	22.01.05	06:07	42° 52,19' S	75° 49,07' W	3736	W 10	284	0,9	OBS/OBH	OBS/OBH	OBS zu Wasser	OBS 46
SO181/066-1	22.01.05	06:37	42° 52,64' S	75° 53,07' W	3732	WSW 11	317	1,1	OBS/OBH	OBS/OBH	OBS zu Wasser	OBS 47
SO181/066-1	22.01.05	07:07	42° 53,15' S	75° 57,02' W	3724	WSW 10	355	0,8	OBS/OBH	OBS/OBH	OBS zu Wasser	OBS 48
SO181/066-1	22.01.05	07:27	42° 53,47' S	75° 59,75' W	3728	WSW 12	286	5,8	OBS/OBH	OBS/OBH	OBS zu Wasser	OBS 49
SO181/066-1	22.01.05	07:32	42° 53,58' S	76° 0,57' W	3723	WSW 10	280	8,5	OBS/OBH	OBS/OBH	OBS an Deck	OBS 49 zurück; Ausleger bei z.W. abgeklappt
SO181/066-1	22.01.05	08:07	42° 53,63' S	76° 1,10' W	3718	W 11	294	0,8	OBS/OBH	OBS/OBH	OBS zu Wasser	OBS 49, 2.Versuch
SO181/066-1	22.01.05	08:12	42° 53,60' S	76° 1,11' W	3719	W 10	320	0,8	OBS/OBH	OBS/OBH	OBS an Deck	OBS 49 zurück; Mikrofon abgefallen bevor z.W.
SO181/066-1	22.01.05	08:22	42° 53,62' S	76° 1,07' W	3718	WSW 8	44	0,4	OBS/OBH	OBS/OBH	OBS zu Wasser	OBS 49; 3.Versuch
SO181/066-1	22.01.05	08:52	42° 54,10' S	76° 5,00' W	3683	WSW 9	294	1,2	OBS/OBH	OBS/OBH	OBS zu Wasser	OBS 50
SO181/066-1	22.01.05	09:21	42° 54,58' S	76° 6,89' W	3639	W 8	290	2,8	OBS/OBH	OBS/OBH	OBS zu Wasser	OBS 51
SO181/066-1	22.01.05	09:50	42° 55,05' S	76° 12,96' W	3619	WSW 11	286	1,6	OBS/OBH	OBS/OBH	OBS zu Wasser	OBS 52
SO181/066-1	22.01.05	09:50	42° 55,05' S	76° 12,96' W	3619	WSW 11	286	1,6	OBS/OBH	OBS/OBH	Ende Station	
SO181/067-1	22.01.05	10:18	42° 58,59' S	76° 13,05' W	3612	W 13	183	9,4	OBS/OBH	OBS/OBH	Beginn Station	
SO181/067-1	22.01.05	10:18	42° 58,59' S	76° 13,05' W	3612	W 13	183	9,4	OBS/OBH	OBS/OBH	OBS ausgelöst	Keine klare Antwort; Simrad aus
SO181/067-1	22.01.05	11:06	43° 3,05' S	76° 12,97' W	3587	WNW 10	224	1,5	OBS/OBH	OBS/OBH	OBS gesichtet	OBS 12
SO181/067-1	22.01.05	11:15	43° 3,21' S	76° 13,25' W	3587	WNW 10	358	2,2	OBS/OBH	OBS/OBH	OBS an Deck	OBS 12
SO181/067-2	22.01.05	11:45	43° 6,59' S	76° 9,54' W	3611	WNW 7	142	10,4	OBS/OBH	OBS/OBH	OBH ausgelöst	OBH 13
SO181/067-2	22.01.05	12:40	43° 9,91' S	76° 5,63' W	3616	WNW 10	246	1,4	OBS/OBH	OBS/OBH	OBH gesichtet	OBH 13
SO181/067-2	22.01.05	12:51	43° 9,88' S	76° 6,09' W	3613	WNW 8	229	1,1	OBS/OBH	OBS/OBH	OBH an Deck	OBH 13
SO181/067-3	22.01.05	13:16	43° 10,40' S	76° 9,96' W	3606	WNW 14	282	8,6	OBS/OBH	OBS/OBH	OBH ausgelöst	OBH 14
SO181/067-3	22.01.05	14:17	43° 10,99' S	76° 15,98' W	0	WNW 12	280	7,2	OBS/OBH	OBS/OBH	OBH gesichtet	OBH 14
SO181/067-3	22.01.05	14:24	43° 10,92' S	76° 16,14' W	0	WNW 10	65	2,7	OBS/OBH	OBS/OBH	OBH an Deck	OBH 14
SO181/067-4	22.01.05	14:52	43° 11,45' S	76° 20,05' W	0	NW 14	282	9	OBS/OBH	OBS/OBH	OBS ausgelöst	OBS 15
SO181/067-4	22.01.05	15:37	43° 11,91' S	76° 25,67' W	0	NW 11	261	1,3	OBS/OBH	OBS/OBH	OBS gesichtet	OBS 15
SO181/067-4	22.01.05	15:56	43° 12,06' S	76° 26,08' W	0	WNW 13	331	0,4	OBS/OBH	OBS/OBH	OBS an Deck	OBS 15
SO181/067-5	22.01.05	16:23	43° 12,43' S	76° 30,20' W	0	WNW 17	286	9,4	OBS/OBH	OBS/OBH	OBH ausgelöst	OBH 16
SO181/067-5	22.01.05	16:57	43° 13,17' S	76° 35,66' W	0	NW 14	238	2	OBS/OBH	OBS/OBH	OBH gesichtet	OBH 16
SO181/067-5	22.01.05	17:12	43° 13,05' S	76° 35,95' W	0	NW 13	206	1,5	OBS/OBH	OBS/OBH	OBH an Deck	OBH 16
SO181/067-6	22.01.05	17:29	43° 13,24' S	76° 38,20' W	0	WNW 14	286	7,9	OBS/OBH	OBS/OBH	OBH ausgelöst	OBH 17
SO181/067-6	22.01.05	18:22	43° 14,18' S	76° 45,64' W	0	WNW 12	25	2,2	OBS/OBH	OBS/OBH	OBH gesichtet	OBH 17
SO181/067-6	22.01.05	18:36	43° 14,00' S	76° 45,80' W	0	WNW 14	332	0,9	OBS/OBH	OBS/OBH	OBH an Deck	OBH 17
SO181/067-7	22.01.05	19:24	43° 8,90' S	76° 39,25' W	0	W 12	49	9,3	OBS/OBH	OBS/OBH	OBS ausgelöst	OBS 04
SO181/067-7	22.01.05	20:12	43° 5,63' S	76° 34,56' W	0	W 13	214	0,5	OBS/OBH	OBS/OBH	OBS gesichtet	OBS 04
SO181/067-7	22.01.05	20:23	43° 5,48' S	76° 35,05' W	0	W 13	178	1,3	OBS/OBH	OBS/OBH	OBS an Deck	OBS 04
SO181/067-8	22.01.05	20:47	43° 4,99' S	76° 30,17' W	0	W 11	81	12	OBS/OBH	OBS/OBH	OBS ausgelöst	OBS 05
SO181/067-8	22.01.05	21:27	43° 4,42' S	76° 23,45' W	0	WNW 13	332	1,2	OBS/OBH	OBS/OBH	OBS gesichtet	OBS 05
SO181/067-8	22.01.05	21:42	43° 4,27' S	76° 24,03' W	0	WNW 15	54	3	OBS/OBH	OBS/OBH	OBS an Deck	
SO181/067-8	22.01.05	21:43	43° 4,26' S	76° 24,00' W	0	WNW 13	64	2,1	OBS/OBH	OBS/OBH	Ende Station	
SO181/068-1	22.01.05	22:42	42° 55,80' S	76° 18,99' W	3602	W 14	328	2,8	OBS/OBH	OBS/OBH	Beginn Station	
SO181/068-1	22.01.05	22:43	42° 55,79' S	76° 19,01' W	3600	W 14	308	1,6	OBS/OBH	OBS/OBH	OBH zu Wasser	OBH 53
SO181/068-1	22.01.05	22:43	42° 55,79' S	76° 19,01' W	3600	W 14	308	1,6	OBS/OBH	OBS/OBH	Ende Station	
SO181/069-1	22.01.05	23:09	42° 52,18' S	76° 17,85' W	3614	W 16	358	10	OBS/OBH	OBS/OBH	OBH ausgelöst	OBH 10
SO181/069-1	22.01.05	23:51	42° 47,13' S	76° 16,07' W	0	W 12	172	1	OBS/OBH	OBS/OBH	OBH gesichtet	OBH 10

Station	Datum	UTC	PositionLat	PositionLon	Tiefe [m]	Windstärke [m/s]	Kurs [°]	v [kn]	Gerät	Gerätekürzel	Aktion	Bemerkung
SO181/069-1	23.01.05	00:02	42° 47,05' S	76° 16,28' W	0	NW 12	35	2,5	OBS/OBH	OBS/OBH	OBH an Deck	OBH 10
SO181/069-2	23.01.05	00:18	42° 44,98' S	76° 16,98' W	0	NW 16	358	9,9	OBS/OBH	OBS/OBH	OBS ausgelöst	OBS 9
SO181/069-2	23.01.05	01:07	42° 39,18' S	76° 17,74' W	0	NW 12	336	1,2	OBS/OBH	OBS/OBH	OBS gesichtet	OBS 9
SO181/069-2	23.01.05	01:21	42° 39,27' S	76° 17,71' W	0	NW 11	111	2,5	OBS/OBH	OBS/OBH	OBS an Deck	OBS 9
SO181/069-3	23.01.05	01:45	42° 39,53' S	76° 21,26' W	0	WNW 16	255	6,2	OBS/OBH	OBS/OBH	OBS ausgelöst	OBS 8
SO181/069-3	23.01.05	02:26	42° 40,43' S	76° 28,64' W	0	WNW 14	311	1,2	OBS/OBH	OBS/OBH	OBS gesichtet	OBS 8
SO181/069-3	23.01.05	02:35	42° 40,29' S	76° 28,92' W	0	WNW 12	350	2,9	OBS/OBH	OBS/OBH	OBS an Deck	OBS 8
SO181/069-4	23.01.05	03:15	42° 41,07' S	76° 34,95' W	0	WNW 12	263	8	OBS/OBH	OBS/OBH	OBS ausgelöst	OBS 1
SO181/069-4	23.01.05	04:01	42° 41,66' S	76° 39,67' W	0	WNW 13	198	1,5	OBS/OBH	OBS/OBH	OBH gesichtet	OBH 01
SO181/069-4	23.01.05	04:23	42° 41,39' S	76° 39,66' W	0	WNW 15	223	0,6	OBS/OBH	OBS/OBH	OBS an Deck	OBH 01, rWK: 172°, d: 8 sm
SO181/069-5	23.01.05	04:50	42° 44,30' S	76° 39,25' W	0	WNW 15	172	11	OBS/OBH	OBS/OBH	OBH ausgelöst	OBH 02
SO181/069-5	23.01.05	05:40	42° 49,81' S	76° 37,20' W	0	WNW 13	262	2,9	OBS/OBH	OBS/OBH	OBH gesichtet	OBH 02
SO181/069-5	23.01.05	06:00	42° 49,47' S	76° 38,26' W	0	W 12	274	1,7	OBS/OBH	OBS/OBH	OBH an Deck	OBH 02
SO181/069-6	23.01.05	06:40	42° 48,76' S	76° 30,48' W	0	W 4	103	11,3	OBS/OBH	OBS/OBH	OBS ausgelöst	OBS 07
SO181/069-6	23.01.05	07:12	42° 48,38' S	76° 26,83' W	0	W 12	205	0,1	OBS/OBH	OBS/OBH	OBS gesichtet	OBS 07
SO181/069-6	23.01.05	07:30	42° 48,13' S	76° 27,25' W	0	W 10	28	2,8	OBS/OBH	OBS/OBH	OBS an Deck	OBS 07
SO181/069-6	23.01.05	07:31	42° 48,12' S	76° 27,25' W	0	W 11	253	0,7	OBS/OBH	OBS/OBH	Ende Station	Anf. Fwk: xxx, d: xx sm
SO181/070-1	23.01.05	08:39	42° 56,97' S	76° 28,94' W	3549	WSW 14	242	1,8	OBS/OBH	OBS/OBH	Beginn Station	
SO181/070-1	23.01.05	08:42	42° 56,97' S	76° 29,03' W	3547	WSW 10	337	1,4	OBS/OBH	OBS/OBH	OBH zu Wasser	OBH 54
SO181/070-2	23.01.05	09:10	42° 57,48' S	76° 32,95' W	3544	WSW 14	244	3,2	OBS/OBH	OBS/OBH	OBS zu Wasser	OBS 55
SO181/070-3	23.01.05	09:47	42° 58,19' S	76° 38,98' W	3527	WSW 11	213	1,1	OBS/OBH	OBS/OBH	OBS zu Wasser	OBS 56
SO181/070-4	23.01.05	10:24	42° 58,94' S	76° 45,03' W	3529	WSW 11	215	1,2	OBS/OBH	OBS/OBH	OBS zu Wasser	OBS 57
SO181/070-5	23.01.05	11:00	42° 59,59' S	76° 50,90' W	3522	WSW 11	191	0,7	OBS/OBH	OBS/OBH	OBS zu Wasser	OBS 58
SO181/070-6	23.01.05	11:39	43° 0,33' S	76° 56,96' W	3520	WSW 11	292	1,3	OBS/OBH	OBS/OBH	OBH zu Wasser	OBH 58
SO181/070-7	23.01.05	12:20	43° 1,06' S	77° 2,96' W	3523	WSW 12	264	3,4	OBS/OBH	OBS/OBH	OBH zu Wasser	OBH 59
SO181/070-8	23.01.05	12:59	43° 1,78' S	77° 8,96' W	3539	WSW 11	248	1,6	OBS/OBH	OBS/OBH	OBH zu Wasser	OBH 60
SO181/070-9	23.01.05	13:41	43° 2,49' S	77° 14,99' W	3545	WSW 12	233	1,3	OBS/OBH	OBS/OBH	OBH zu Wasser	OBH 61
SO181/070-10	23.01.05	14:18	43° 3,21' S	77° 20,99' W	3549	SW 13	252	1,9	OBS/OBH	OBS/OBH	OBS zu Wasser	OBS 62
SO181/070-11	23.01.05	14:58	43° 3,94' S	77° 27,04' W	3552	SW 10	281	2,8	OBS/OBH	OBS/OBH	OBS zu Wasser	OBS 63
SO181/070-12	23.01.05	15:41	43° 4,85' S	77° 32,98' W	3555	SW 9	305	1	OBS/OBH	OBS/OBH	OBS zu Wasser	OBS 64
SO181/070-13	23.01.05	16:24	43° 5,38' S	77° 38,98' W	3559	WSW 10	244	1,9	OBS/OBH	OBS/OBH	OBS zu Wasser	OBS 66
SO181/070-14	23.01.05	17:05	43° 6,09' S	77° 45,04' W	3561	WSW 12	253	1,5	OBS/OBH	OBS/OBH	OBH zu Wasser	OBH 67
SO181/070-15	23.01.05	17:47	43° 6,82' S	77° 51,00' W	3569	WSW 13	282	3	OBS/OBH	OBS/OBH	OBH zu Wasser	OBH 68
SO181/070-16	23.01.05	18:30	43° 7,53' S	77° 56,99' W	3590	SW 10	231	1,5	OBS/OBH	OBS/OBH	OBH zu Wasser	OBH 69
SO181/070-16	23.01.05	18:31	43° 7,55' S	77° 57,02' W	3587	SW 10	210	2	OBS/OBH	OBS/OBH	Ende Station	
Transit	23.01.05	18:31	43° 7,55' S	77° 57,02' W	3587	SW 10	193	12	Anf. # 071			rWK: 193°, d: 42 sm
SO181/071-1	23.01.05	22:36	43° 11,51' S	78° 29,99' W	3588	W 10	51	3,3	Profil	PR	Stationsbeginn	rWK: 081
SO181/071-1	23.01.05	23:07	43° 11,23' S	78° 28,28' W	3586	SW 10	68	2,8	Profil	PR	Bb Airgun zu Wasser	
SO181/071-1	23.01.05	23:19	43° 11,16' S	78° 27,88' W	3583	SW 9	75	1,7	Profil	PR	Stb Airgun zu Wasser	
SO181/071-1	23.01.05	23:31	43° 11,06' S	78° 26,96' W	3548	SW 8	74	3,2	Profil	PR	Beginn Profil	Profil 05, rWK: 084°, d: 190 sm
SO181/071-1	24.01.05	00:25	43° 10,63' S	78° 22,62' W	3687	SW 9	81	3,5	Profil	PR	Streamer zu Wasser	
SO181/071-1	24.01.05	05:30	43° 7,35' S	77° 55,39' W	3566	SW 5	80	4,6	Profil	PR	Airgun abgeschaltet	Kanone 5 aus
SO181/071-1	25.01.05	00:23	42° 54,59' S	76° 8,72' W	3633	SSW 5	65	3,7	Profil	PR	Airgun abgeschaltet	Kanone 6 aus

Station	Datum	UTC	PositionLat	PositionLon	Tiefe [m]	Windstärke [m/s]	Kurs [°]	v [kn]	Gerät	Geräte Kürzel	Aktion	Bemerkung
SO181/071-1	25.01.05	19:50	42° 40,78' S	74° 14,22' W	52	S 8	84	4,8	Profil	PR	Kursänderung	nwk: 360°
SO181/071-1	25.01.05	20:30	42° 37,82' S	74° 13,85' W	53	S 13	334	4,4	Profil	PR	Streamer an Deck	
SO181/071-1	25.01.05	20:40	42° 37,27' S	74° 14,26' W	52	S 11	326	4,9	Profil	PR	Kursänderung	nwk: 315
SO181/071-1	25.01.05	21:02	42° 36,14' S	74° 16,00' W	84	S 12	297	5	Profil	PR	Ende Profil	
SO181/071-1	25.01.05	21:12	42° 36,04' S	74° 16,66' W	70	S 12	270	2,5	Profil	PR	Stb Airgun an Deck	
SO181/071-1	25.01.05	21:22	42° 36,06' S	74° 17,26' W	78	S 12	254	2,8	Profil	PR	Bb airgun an Deck	
SO181/071-1	25.01.05	21:22	42° 36,06' S	74° 17,26' W	78	S 12	254	2,8	Profil	PR	Ende Station	
Transit	25.01.05	21:22	42° 36,06' S	74° 17,26' W	78	S 12	div	12	Anf. # 072			div. Kurse, d: 28 am
SO181/072-1	26.01.05	00:12	42° 44,09' S	74° 44,79' W	122	S 14	209	6,1	OBS/OBH	OBS/OBH	Beginn Station	
SO181/072-1	26.01.05	00:13	42° 44,18' S	74° 44,83' W	127	S 12	197	4,8	OBS/OBH	OBS/OBH	OBH ausgelöst	OBH 30
SO181/072-1	26.01.05	00:15	42° 44,31' S	74° 44,89' W	129	S 12	197	3,5	OBS/OBH	OBS/OBH	OBH gesichtet	OBH 30
SO181/072-1	26.01.05	00:21	42° 44,44' S	74° 44,98' W	130	S 10	246	1	OBS/OBH	OBS/OBH	OBH an Deck	OBH 30
SO181/072-2	26.01.05	00:42	42° 44,79' S	74° 46,83' W	188	SSW 12	204	3,2	OBS/OBH	OBS/OBH	OBH ausgelöst	OBH 31
SO181/072-2	26.01.05	00:45	42° 44,86' S	74° 46,84' W	194	SSW 10	140	1,3	OBS/OBH	OBS/OBH	OBH gesichtet	OBH 31
SO181/072-2	26.01.05	00:52	42° 44,96' S	74° 46,99' W	194	SSW 9	299	1,8	OBS/OBH	OBS/OBH	OBH an Deck	OBH 31
SO181/072-3	26.01.05	01:09	42° 45,12' S	74° 52,10' W	437	SSW 12	275	11,2	OBS/OBH	OBS/OBH	OBH ausgelöst	OBH 32
SO181/072-3	26.01.05	01:12	42° 45,09' S	74° 52,74' W	458	SSW 12	247	6,1	OBS/OBH	OBS/OBH	OBH gesichtet	OBH 31
SO181/072-3	26.01.05	01:20	42° 45,34' S	74° 52,87' W	449	SSW 10	295	0,7	OBS/OBH	OBS/OBH	OBH an Deck	OBH 32
SO181/072-4	26.01.05	01:33	42° 45,65' S	74° 55,18' W	0	SSW 12	259	11,1	OBS/OBH	OBS/OBH	OBH ausgelöst	OBH 33
SO181/072-4	26.01.05	01:41	42° 45,63' S	74° 56,82' W	0	SSW 11	223	2,4	OBS/OBH	OBS/OBH	OBH gesichtet	OBH 33
SO181/072-4	26.01.05	01:51	42° 45,82' S	74° 57,07' W	0	SSW 10	305	1,3	OBS/OBH	OBS/OBH	OBH an Deck	OBH 33
SO181/072-5	26.01.05	02:07	42° 46,06' S	74° 59,99' W	0	SSW 12	272	11,2	OBS/OBH	OBS/OBH	OBH ausgelöst	OBH 34
SO181/072-5	26.01.05	02:16	42° 46,15' S	75° 0,87' W	0	SS 9	281	0,4	OBS/OBH	OBS/OBH	OBH gesichtet	OBH 34
SO181/072-5	26.01.05	02:23	42° 46,35' S	75° 1,01' W	0	SSW	221	1,1	OBS/OBH	OBS/OBH	OBH an Deck	OBH 34
SO181/072-6	26.01.05	02:36	42° 46,59' S	75° 3,28' W	0	SSW 13	267	11,5	OBS/OBH	OBS/OBH	OBH ausgelöst	OBH 35
SO181/072-6	26.01.05	02:45	42° 46,67' S	75° 4,90' W	0	SSW 10	190	1,8	OBS/OBH	OBS/OBH	OBH gesichtet	OBH 35
SO181/072-6	26.01.05	02:52	42° 46,85' S	75° 4,97' W	0	SSW 8	266	0,9	OBS/OBH	OBS/OBH	OBH an Deck	OBH 35
SO181/072-7	26.01.05	02:55	42° 46,82' S	75° 5,10' W	0	SW 10	261	3,1	OBS/OBH	OBS/OBH	OBH ausgelöst	OBH 37
SO181/072-7	26.01.05	03:06	42° 46,97' S	75° 7,15' W	0	WNW 12	264	1,1	OBS/OBH	OBS/OBH	OBH gesichtet	OBH 37
SO181/072-7	26.01.05	03:27	42° 47,30' S	75° 9,04' W	0	S 9	333	0,7	OBS/OBH	OBS/OBH	OBH an Deck	OBH 37
SO181/072-8	26.01.05	03:31	42° 47,33' S	75° 9,14' W	0	SSW 9	263	2,4	OBS/OBH	OBS/OBH	OBH ausgelöst	OBH 38
SO181/072-8	26.01.05	03:57	42° 47,77' S	75° 13,01' W	0	S 10	6	1,3	OBS/OBH	OBS/OBH	OBH gesichtet	OBH 38
SO181/072-8	26.01.05	04:14	42° 47,89' S	75° 12,94' W	0	S 9	163	0,4	OBS/OBH	OBS/OBH	OBH an Deck	OBH 38
SO181/072-9	26.01.05	04:28	42° 47,99' S	75° 15,21' W	0	S 12	267	11,5	OBS/OBH	OBS/OBH	OBH ausgelöst	OBH 36
SO181/072-9	26.01.05	04:48	42° 48,09' S	75° 16,66' W	0	S 8	184	0,7	OBS/OBH	OBS/OBH	OBH gesichtet	OBH 36
SO181/072-9	26.01.05	05:02	42° 48,46' S	75° 16,98' W	0	SSW 9	283	1,1	OBS/OBH	OBS/OBH	OBH an Deck	OBH 36
SO181/072-9	26.01.05	05:07	42° 48,43' S	75° 17,38' W	0	SSW 11	269	6,2	OBS/OBH	OBS/OBH	OBH ausgelöst	OBH 39
SO181/072-9	26.01.05	05:25	42° 48,50' S	75° 20,77' W	0	S 12	274	7,3	OBS/OBH	OBS/OBH	OBH ausgelöst	OBH 40
SO181/072-11	26.01.05	05:27	42° 48,53' S	75° 21,02' W	0	SSW 11	227	3,3	OBS/OBH	OBS/OBH	OBH ausgelöst	OBH 41
SO181/072-9	26.01.05	05:27	42° 48,53' S	75° 21,02' W	0	S 11	227	3,3	OBS/OBH	OBS/OBH	OBH gesichtet	OBH 39
SO181/072-9	26.01.05	05:39	42° 48,67' S	75° 20,87' W	0	S 9	262	1,1	OBS/OBH	OBS/OBH	OBH an Deck	OBH 39
SO181/072-10	26.01.05	05:58	42° 48,95' S	75° 24,17' W	0	S 12	283	10,3	OBS/OBH	OBS/OBH	OBH gesichtet	OBH 40
SO181/072-10	26.01.05	06:07	42° 49,24' S	75° 24,86' W	0	SSW 9	205	0,7	OBS/OBH	OBS/OBH	OBH an Deck	OBH 40

Station	Datum	UTC	PositionLat	PositionLon	Tiefe [m]	Windstärke [m/s]	Kurs [°]	v [kn]	Gerät	Gerätekurzel	Aktion	Bemerkung
SO181/072-11	26.01.05	06:27	42° 49,44' S	75° 28,85' W	0	SSW 12	263	11,1	OBS/OBH	OBS/OBH	OBH gesichtet	OBH 41
SO181/072-12	26.01.05	06:32	42° 49,87' S	75° 29,00' W	0	SSW 9	209	2,8	OBS/OBH	OBS/OBH	OBS ausgelöst	OBS 42
SO181/072-11	26.01.05	06:34	42° 49,72' S	75° 29,06' W	0	SSW 10	239	1,8	OBS/OBH	OBS/OBH	OBS an Deck	OBH 41
SO181/072-12	26.01.05	06:55	42° 49,83' S	75° 32,65' W	0	SSW 11	261	7,3	OBS/OBH	OBS/OBH	OBS ausgelöst	OBS 43
SO181/072-12	26.01.05	07:01	42° 50,04' S	75° 32,83' W	0	S 8	43	0,8	OBS/OBH	OBS/OBH	OBS gesichtet	OBS 42
SO181/072-12	26.01.05	07:11	42° 50,22' S	75° 33,10' W	0	S 8	319	1,5	OBS/OBH	OBS/OBH	OBS an Deck	OBS 42
SO181/072-13	26.01.05	07:33	42° 50,30' S	75° 36,48' W	0	S 10	224	2,2	OBS/OBH	OBS/OBH	OBS ausgelöst	OBS 44
SO181/072-13	26.01.05	07:36	42° 50,35' S	75° 36,52' W	0	S 9	226	1,2	OBS/OBH	OBS/OBH	OBS gesichtet	OBS 43
SO181/072-13	26.01.05	07:51	42° 50,66' S	75° 37,21' W	0	S 9	321	0,8	OBS/OBH	OBS/OBH	OBS an Deck	OBS 43
SO181/072-14	26.01.05	08:08	42° 50,61' S	75° 39,84' W	0	S 10	266	8,4	OBS/OBH	OBS/OBH	OBS ausgelöst	OBS 45
SO181/072-14	26.01.05	08:17	42° 50,77' S	75° 40,89' W	0	SSW 8	211	1	OBS/OBH	OBS/OBH	OBS gesichtet	OBS 44
SO181/072-14	26.01.05	08:34	42° 51,13' S	75° 41,17' W	0	SSW 8	321	0,5	OBS/OBH	OBS/OBH	OBS an Deck	OBS 44
SO181/072-15	26.01.05	08:52	42° 51,17' S	76° 44,34' W	0	S 9	256	6,9	OBS/OBH	OBS/OBH	OBS ausgelöst	OBS 46
SO181/072-15	26.01.05	08:55	42° 51,21' S	75° 44,75' W	0	S 8	225	3,6	OBS/OBH	OBS/OBH	OBS gesichtet	OBS 45
SO181/072-15	26.01.05	09:07	42° 51,67' S	75° 45,22' W	0	SSW 7	248	0,4	OBS/OBH	OBS/OBH	OBS an Deck	OBS 45
SO181/072-16	26.01.05	09:28	42° 51,72' S	75° 48,74' W	0	SSW 7	252	5	OBS/OBH	OBS/OBH	OBS ausgelöst	OBS 47
SO181/072-16	26.01.05	09:36	42° 51,84' S	75° 48,84' W	0	SSW 5	253	0,5	OBS/OBH	OBS/OBH	OBS gesichtet	OBS 46
SO181/072-16	26.01.05	09:53	42° 52,18' S	75° 49,25' W	0	SSW 7	310	1,1	OBS/OBH	OBS/OBH	OBS an Deck	OBS 46
SO181/072-17	26.01.05	10:11	42° 52,21' S	75° 52,41' W	0	SSW 9	265	8	OBS/OBH	OBS/OBH	OBS ausgelöst	OBS 48
SO181/072-17	26.01.05	10:15	42° 52,28' S	75° 52,87' W	0	S 8	213	3,5	OBS/OBH	OBS/OBH	OBS gesichtet	OBS 47
SO181/072-17	26.01.05	10:27	42° 52,72' S	75° 53,34' W	0	SSW 6	282	0,8	OBS/OBH	OBS/OBH	OBS an Deck	OBS 47
SO181/072-18	26.01.05	10:47	42° 52,71' S	75° 56,89' W	0	SSW 6	222	2,5	OBS/OBH	OBS/OBH	OBS ausgelöst	OBS 49
SO181/072-18	26.01.05	12:17	42° 53,39' S	76° 1,02' W	0	SW 6	48	0,4	OBS/OBH	OBS/OBH	OBH ausgelöst	OBS 48
SO181/072-18	26.01.05	12:47	42° 53,41' S	76° 0,97' W	0	WSW 5	309	0,6	OBS/OBH	OBS/OBH	OBS ausgelöst	OBS 48, 2 x ausgelöst
SO181/072-18	26.01.05	13:00	42° 53,36' S	76° 0,96' W	0	SW 6	131	0,2	OBS/OBH	OBS/OBH	OBS gesichtet	OBS 49
SO181/072-18	26.01.05	13:14	42° 53,71' S	76° 1,46' W	0	SW 6	254	0,9	OBS/OBH	OBS/OBH	OBS an Deck	OBS 49
SO181/072-18	26.01.05	14:30	42° 52,96' S	75° 56,69' W	0	W 6	221	0,1	OBS/OBH	OBS/OBH	OBS ausgelöst	OBS 50
SO181/072-18	26.01.05	14:35	42° 53,00' S	75° 56,71' W	0	W 6	205	0,3	OBS/OBH	OBS/OBH	OBS gesichtet	OBS 48
SO181/072-18	26.01.05	14:45	42° 53,27' S	75° 57,23' W	0	W 6	262	0,8	OBS/OBH	OBS/OBH	OBS an Deck	OBS 48
SO181/072-19	26.01.05	15:29	42° 53,76' S	76° 3,73' W	0	SSW 4	270	1,1	OBS/OBH	OBS/OBH	OBS ausgelöst	OBS 51
SO181/072-19	26.01.05	15:35	42° 53,80' S	76° 4,43' W	0	SW 7	286	6,8	OBS/OBH	OBS/OBH	OBS gesichtet	OBS 50
SO181/072-19	26.01.05	15:46	42° 54,08' S	76° 5,43' W	0	SSW 5	286	2	OBS/OBH	OBS/OBH	OBS an Deck	OBS 50
SO181/072-20	26.01.05	16:00	42° 54,20' S	76° 7,27' W	0	W 8	263	8,3	OBS/OBH	OBS/OBH	OBS ausgelöst	OBS 52
SO181/072-20	26.01.05	16:10	42° 54,34' S	76° 8,88' W	0	W 6	230	4,3	OBS/OBH	OBS/OBH	OBS gesichtet	OBS 51
SO181/072-20	26.01.05	16:23	42° 54,47' S	76° 9,45' W	0	SW 6	277	1,8	OBS/OBH	OBS/OBH	OBS an Deck	OBS 51
SO181/072-21	26.01.05	16:39	42° 54,72' S	76° 11,60' W	0	SW 8	261	8	OBS/OBH	OBS/OBH	OBH ausgelöst	OBH 11
SO181/072-21	26.01.05	16:49	42° 54,98' S	76° 12,98' W	0	WSW 7	214	2,3	OBS/OBH	OBS/OBH	OBH gesichtet	OBH 52
SO181/072-21	26.01.05	16:57	42° 54,90' S	76° 13,38' W	0	SSW 7	305	1,9	OBS/OBH	OBS/OBH	OBS an Deck	OBS 52
SO181/072-22	26.01.05	17:06	42° 54,95' S	76° 14,02' W	0	SSW 7	262	5,2	OBS/OBH	OBS/OBH	OBH ausgelöst	OBH 53
SO181/072-22	26.01.05	17:39	42° 55,10' S	76° 14,55' W	0	SW 5	249	1,4	OBS/OBH	OBS/OBH	OBH gesichtet	OBH 11
SO181/072-22	26.01.05	17:52	42° 55,20' S	76° 15,24' W	0	WSW 5	237	1,2	OBS/OBH	OBS/OBH	OBH an Deck	OBH 11
SO181/072-23	26.01.05	18:11	42° 55,52' S	76° 16,73' W	0	WSW 7	268	6,6	OBS/OBH	OBS/OBH	OBH gesichtet	OBH 53
SO181/072-23	26.01.05	18:12	42° 55,54' S	76° 18,85' W	0	WSW 7	258	5,5	OBS/OBH	OBS/OBH	OBH ausgelöst	OBH 06

Station	Datum	UTC	PositionLat	PositionLon	Tiefe [m]	Windstärke [m/s]	Kurs [°]	v [kn]	Gerät	Gerätekürzel	Aktion	Bemerkung
SO181/072-23	26.01.05	18:21	42° 55,62' S	76° 19,56' W	0	WSW 5	291	1,5	OBS/OBH	OBS/OBH	OBH an Deck	OBH 53
SO181/072-24	26.01.05	18:35	42° 55,92' S	76° 22,28' W	0	W 9	260	11,8	OBS/OBH	OBS/OBH	OBH ausgelöst	OBH 54
SO181/072-24	26.01.05	19:13	42° 56,20' S	76° 25,53' W	0	W 4	111	0,5	OBS/OBH	OBS/OBH	OBH gesichtet	OBH 06
SO181/072-24	26.01.05	19:22	42° 56,30' S	76° 26,02' W	0	W 4	268	0,7	OBS/OBH	OBS/OBH	OBH an Deck	OBH 06
SO181/072-25	26.01.05	19:29	42° 56,40' S	76° 26,72' W	0	W 8	253	8,6	OBS/OBH	OBS/OBH	OBH ausgelöst	OBH 55
SO181/072-25	26.01.05	19:36	42° 56,76' S	76° 28,25' W	0	WSW 8	250	7,8	OBS/OBH	OBS/OBH	OBH gesichtet	OBH 54
SO181/072-25	26.01.05	19:48	42° 56,77' S	76° 29,38' W	0	WSW 3	278	0,4	OBS/OBH	OBS/OBH	OBH an Deck	OBH 54
SO181/072-26	26.01.05	19:56	42° 56,90' S	76° 30,40' W	0	W 8	255	9,7	OBS/OBH	OBS/OBH	OBH ausgelöst	OBH 03
SO181/072-26	26.01.05	20:08	42° 57,30' S	76° 32,50' W	0	WNW 5	252	4	OBS/OBH	OBS/OBH	OBH gesichtet	OBH 55
SO181/072-26	26.01.05	20:09	42° 57,32' S	76° 32,60' W	0	NNE 5	265	4,1	OBS/OBH	OBS/OBH	OBH ausgelöst	OBH 56
SO181/072-26	26.01.05	20:17	42° 57,40' S	76° 33,22' W	0	WSW 4	252	1,1	OBS/OBH	OBS/OBH	OBH an Deck	OBH 55
SO181/072-27	26.01.05	20:41	42° 57,51' S	76° 36,51' W	0	W 5	247	2,9	OBS/OBH	OBS/OBH	OBH gesichtet	OBH 03
SO181/072-27	26.01.05	20:51	42° 57,36' S	76° 36,88' W	0	NNW 4	52	1,1	OBS/OBH	OBS/OBH	OBH an Deck	OBH 03
SO181/072-28	26.01.05	21:08	42° 57,69' S	76° 38,70' W	0	WSW 8	238	6,8	OBS/OBH	OBS/OBH	OBH ausgelöst	OBH 57
SO181/072-28	26.01.05	21:08	42° 57,69' S	76° 38,70' W	0	WSW 8	238	6,8	OBS/OBH	OBS/OBH	OBH gesichtet	OBH 56
SO181/072-28	26.01.05	21:19	42° 57,95' S	76° 39,04' W	0	WSW 5	27	0,4	OBS/OBH	OBS/OBH	OBH an Deck	OBH 56
SO181/072-29	26.01.05	21:40	42° 58,65' S	76° 42,45' W	0	W 10	255	9,3	OBS/OBH	OBS/OBH	OBH gesichtet	OBH 57
SO181/072-29	26.01.05	21:58	42° 58,90' S	76° 44,82' W	0	W 6	289	3,3	OBS/OBH	OBS/OBH	OBH ausgelöst	OBH 58
SO181/072-29	26.01.05	22:05	42° 58,78' S	76° 45,14' W	0	W 5	300	0,3	OBS/OBH	OBS/OBH	OBH an Deck	OBH 57
SO181/072-30	26.01.05	22:37	42° 59,67' S	76° 50,52' W	0	W 5	316	0,1	OBS/OBH	OBS/OBH	OBH gesichtet	OBH 58
SO181/072-30	26.01.05	22:39	42° 59,66' S	76° 50,51' W	0	W 5	298	0,5	OBS/OBH	OBS/OBH	OBH ausgelöst	OBH 59
SO181/072-30	26.01.05	22:47	42° 59,46' S	76° 51,00' W	0	W 6	284	1,7	OBS/OBH	OBS/OBH	OBH an Deck	OBH 58
SO181/072-31	26.01.05	23:15	43° 0,58' S	76° 56,74' W	0	NNE 9	281	3,8	OBS/OBH	OBS/OBH	OBH gesichtet	OBH 59
SO181/072-31	26.01.05	23:18	43° 0,48' S	76° 56,89' W	0	NNW 7	350	3,4	OBS/OBH	OBS/OBH	OBH ausgelöst	OBH 60
SO181/072-31	26.01.05	23:23	43° 0,25' S	76° 57,00' W	0	NW 7	11	0,6	OBS/OBH	OBS/OBH	OBH an Deck	OBH 59
SO181/072-32	27.01.05	00:00	43° 1,20' S	77° 2,98' W	0	NNE 6	154	0,6	OBS/OBH	OBS/OBH	OBH ausgelöst	OBH 61
SO181/072-32	27.01.05	00:05	43° 1,20' S	77° 2,91' W	0	NE 6	114	0,6	OBS/OBH	OBS/OBH	OBH gesichtet	OBH 60
SO181/072-32	27.01.05	00:14	43° 1,00' S	77° 3,00' W	0	NW 6	7	0,9	OBS/OBH	OBS/OBH	OBH an Deck	OBH 60
SO181/072-33	27.01.05	00:42	43° 1,99' S	77° 8,59' W	0	NNE 11	291	5,1	OBS/OBH	OBS/OBH	OBH gesichtet	OBH 61
SO181/072-33	27.01.05	00:49	43° 1,72' S	77° 8,86' W	0	NNW 8	337	0,9	OBS/OBH	OBS/OBH	OBH an Deck	OBH 61
SO181/072-34	27.01.05	00:52	43° 1,69' S	77° 8,87' W	0	NNW 7	346	1,2	OBS/OBH	OBS/OBH	OBH ausgelöst	OBH 62
SO181/072-34	27.01.05	01:23	43° 2,63' S	77° 14,88' W	0	NNE 9	306	2	OBS/OBH	OBS/OBH	OBH gesichtet	OBH 62
SO181/072-34	27.01.05	01:25	43° 2,61' S	77° 14,93' W	0	NNE 8	329	1,6	OBS/OBH	OBS/OBH	OBH ausgelöst	OBH 63
SO181/072-34	27.01.05	01:30	43° 2,50' S	77° 15,02' W	0	NNE 8	275	0,2	OBS/OBH	OBS/OBH	OBH an Deck	OBH 62
SO181/072-35	27.01.05	02:07	43° 3,35' S	77° 20,82' W	0	NE 6	85	0,5	OBS/OBH	OBS/OBH	OBH gesichtet	OBH 63
SO181/072-35	27.01.05	02:09	43° 3,35' S	77° 20,81' W	0	NE 6	317	0,8	OBS/OBH	OBS/OBH	OBH ausgelöst	OBH 64
SO181/072-35	27.01.05	02:20	43° 2,82' S	77° 20,45' W	0	WNW 8	57	1,4	OBS/OBH	OBS/OBH	OBH an Deck	OBH 63
SO181/072-36	27.01.05	02:52	43° 4,15' S	77° 26,61' W	0	NE 11	259	4,9	OBS/OBH	OBS/OBH	OBH ausgelöst	OBH 65
SO181/072-36	27.01.05	02:54	43° 4,14' S	77° 26,78' W	0	NE 10	294	3,5	OBS/OBH	OBS/OBH	OBH gesichtet	OBH 64
SO181/072-36	27.01.05	03:06	43° 3,94' S	77° 26,95' W	0	WNW 7	53	1,1	OBS/OBH	OBS/OBH	OBH an Deck	OBH 64
SO181/072-37	27.01.05	03:35	43° 4,83' S	77° 32,22' W	0	NW 12	260	9	OBS/OBH	OBS/OBH	OBH ausgelöst	OBH 66
SO181/072-37	27.01.05	03:36	43° 4,85' S	77° 32,39' W	0	NW 12	256	7,3	OBS/OBH	OBS/OBH	OBH gesichtet	OBH 65
SO181/072-37	27.01.05	03:50	43° 4,59' S	77° 32,96' W	0	NW 6	6	1,7	OBS/OBH	OBS/OBH	OBH an Deck	OBH 65

Station	Datum	UTC	PositionLat	PositionLon	Tiefe [m]	Windstärke [m/s]	Kurs [°]	v [km]	Gerät	Gerätekürzel	Aktion	Bemerkung
SO181/072-38	27.01.05	04:11	43° 5,25' S	77° 36,80' W	0	NW 12	258	11,2	OBS/OBH	OBS/OBH	OBH ausgelöst	OBH 67
SO181/072-38	27.01.05	04:23	43° 5,48' S	77° 38,75' W	0	NW 8	311	2,4	OBS/OBH	OBS/OBH	OBS gesichtet	OBS 66
SO181/072-38	27.01.05	04:40	43° 5,10' S	77° 38,98' W	0	NW 7	68	0,8	OBS/OBH	OBS/OBH	OBS an Deck	OBS 66
SO181/072-39	27.01.05	05:06	43° 6,17' S	77° 43,77' W	0	NW 12	254	12	OBS/OBH	OBS/OBH	OBH ausgelöst	OBH 68
SO181/072-39	27.01.05	05:10	43° 6,33' S	77° 44,82' W	0	NNW 11	257	6,4	OBS/OBH	OBS/OBH	OBH gesichtet	OBH 67
SO181/072-39	27.01.05	05:22	43° 6,11' S	77° 45,06' W	0	WNW 8	343	0,9	OBS/OBH	OBS/OBH	OBH an Deck	OBH 67
SO181/072-40	27.01.05	05:52	43° 7,03' S	77° 50,89' W	0	NW 9	289	4	OBS/OBH	OBS/OBH	OBH ausgelöst	OBH 69
SO181/072-40	27.01.05	05:55	43° 6,91' S	77° 50,82' W	0	NW 8	13	1,8	OBS/OBH	OBS/OBH	OBH gesichtet	OBH 68
SO181/072-40	27.01.05	06:11	43° 6,83' S	77° 51,01' W	0	WNW 8	345	0,8	OBS/OBH	OBS/OBH	OBH an Deck	OBH 68
SO181/072-41	27.01.05	06:50	43° 7,89' S	77° 56,77' W	3602	NNW 7	141	1,2	OBS/OBH	OBS/OBH	OBH gesichtet	OBH 69
SO181/072-41	27.01.05	07:03	43° 7,59' S	77° 58,94' W	3597	WNW 9	81	1	OBS/OBH	OBS/OBH	OBH an Deck	OBH 69
SO181/072-41	27.01.05	07:04	43° 7,59' S	77° 58,94' W	3597	NW 9	81	1,2	OBS/OBH	OBS/OBH	Ende Station	
Transit	27.01.05	07:04	43° 7,59' S	77° 58,94' W	3597	NW 9	154	12	Anf. # 073			d: 99 sm
SO181/073-1	27.01.05	15:47	44° 32,10' S	76° 59,94' W	3088,8	W 4	49	1,3	OBS/OBH	OBS/OBH	Beginn Station	
SO181/073-1	27.01.05	15:47	44° 32,10' S	76° 59,94' W	3089	W 4	49	1,3	OBS/OBH	OBS/OBH	OBS ausgelöst	OBS 18
SO181/073-1	27.01.05	16:28	44° 35,38' S	76° 57,50' W	0	W 5	89	1,5	OBS/OBH	OBS/OBH	OBS gesichtet	OBS 18
SO181/073-1	27.01.05	16:54	44° 36,24' S	76° 56,77' W	0	W 6	291	1,2	OBS/OBH	OBS/OBH	OBS an Deck	OBS 18, KÄ: 184°, d: 8 sm
SO181/073-2	27.01.05	17:20	44° 39,81' S	76° 55,62' W	0	W 7	180	10,5	OBS/OBH	OBS/OBH	OBS ausgelöst	OBH 19
SO181/073-2	27.01.05	18:04	44° 44,34' S	76° 53,47' W	0	W 4	93	0,9	OBS/OBH	OBS/OBH	OBS gesichtet	OBH 19
SO181/073-2	27.01.05	18:14	44° 44,21' S	76° 53,84' W	0	SW 5	290	0,8	OBS/OBH	OBS/OBH	OBH an Deck	OBH 19
SO181/073-3	27.01.05	18:51	44° 48,19' S	76° 52,24' W	0	WSW 4	128	1	OBS/OBH	OBS/OBH	OBS ausgelöst	OBS 20
SO181/073-3	27.01.05	19:24	44° 52,03' S	76° 50,36' W	0	WSW 4	335	0,5	OBS/OBH	OBS/OBH	OBS gesichtet	OBS 20
SO181/073-3	27.01.05	19:39	44° 51,84' S	76° 50,67' W	0	W 4	15	0,2	OBS/OBH	OBS/OBH	OBS an Deck	OBS 20
SO181/073-4	27.01.05	20:04	44° 55,47' S	76° 49,23' W	0	WSW 8	159	12	OBS/OBH	OBS/OBH	OBS ausgelöst	OBS 21
SO181/073-4	27.01.05	20:47	44° 59,64' S	76° 47,12' W	0	WNW 7	163	0,8	OBS/OBH	OBS/OBH	OBS gesichtet	OBS 21
SO181/073-4	27.01.05	20:57	44° 59,73' S	76° 47,51' W	0	WNW 6	116	0,1	OBS/OBH	OBS/OBH	OBS an Deck	OBS 21
SO181/073-5	27.01.05	21:22	44° 58,88' S	76° 42,90' W	0	W 4	75	11,7	OBS/OBH	OBS/OBH	OBS ausgelöst	OBS 22
SO181/073-5	27.01.05	22:15	44° 57,63' S	76° 38,11' W	0	WNW 6	339	1	OBS/OBH	OBS/OBH	OBS gesichtet	OBS 22
SO181/073-5	27.01.05	22:26	44° 57,56' S	76° 38,66' W	0	WNW 6	355	1,1	OBS/OBH	OBS/OBH	OBS an Deck	OBS 22
SO181/073-6	27.01.05	22:43	44° 55,07' S	76° 37,58' W	0	WNW 10	346	11	OBS/OBH	OBS/OBH	OBS ausgelöst	OBS 23 ?
SO181/073-6	27.01.05	23:30	44° 49,80' S	76° 39,38' W	0	NNW 6	53	0,4	OBS/OBH	OBS/OBH	OBS gesichtet	OBS 23
SO181/073-6	27.01.05	23:41	44° 49,84' S	76° 39,73' W	0	NW 7	347	1,4	OBS/OBH	OBS/OBH	OBS an Deck	OBS 23
SO181/073-7	28.01.05	00:02	44° 47,09' S	76° 40,87' W	0	WNW 10	343	11,2	OBS/OBH	OBS/OBH	OBS ausgelöst	OBS 24
SO181/073-7	28.01.05	00:51	44° 42,15' S	76° 42,62' W	0	NW 5	40	1,5	OBS/OBH	OBS/OBH	OBS gesichtet	OBS 24
SO181/073-7	28.01.05	00:57	44° 41,94' S	76° 42,62' W	0	NW 6	14	1,6	OBS/OBH	OBS/OBH	OBS an Deck	OBS 24
SO181/073-8	28.01.05	01:19	44° 39,76' S	76° 44,24' W	0	NNW 10	338	11,2	OBS/OBH	OBS/OBH	OBS ausgelöst	OBS 25
SO181/073-8	28.01.05	02:00	44° 34,43' S	76° 45,89' W	0	NNW 4	76	0,8	OBS/OBH	OBS/OBH	OBS gesichtet	OBS 25
SO181/073-8	28.01.05	02:09	44° 34,32' S	76° 45,80' W	0	NNW 5	353	0,8	OBS/OBH	OBS/OBH	OBS an Deck	OBS 25
SO181/073-9	28.01.05	02:32	44° 33,33' S	76° 41,28' W	0	NW 8	74	12,1	OBS/OBH	OBS/OBH	OBS ausgelöst	OBS 26
SO181/073-9	28.01.05	02:46	44° 32,66' S	76° 37,88' W	0	WNW 7	72	10,3	OBS/OBH	OBS/OBH	OBS gesichtet	OBS 26
SO181/073-9	28.01.05	03:14	44° 32,10' S	76° 35,12' W	0	NW 4	266	1,7	OBS/OBH	OBS/OBH	OBS an Deck	OBS 26
SO181/073-10	28.01.05	03:46	44° 36,89' S	76° 32,97' W	0	NNW 2	158	11,1	OBS/OBH	OBS/OBH	OBS ausgelöst	OBS 27
SO181/073-10	28.01.05	04:25	44° 39,91' S	76° 31,58' W	0	NW 2	119	1,8	OBS/OBH	OBS/OBH	OBS gesichtet	OBS 27

Station	Datum	UTC	PositionLat	PositionLon	Tiefe [m]	Windstärke (m/s)	Kurs [°]	v [kn]	Gerät	Gerätekürzel	Aktion	Bemerkung
SO181/073-10	28.01.05	04:40	44° 40,02' S	76° 31,80' W	0	NW 3	313	1	OBS/OBH	OBS/OBH	OBS an Deck	OBS 27
SO181/07-11	28.01.05	05:10	44° 44,02' S	76° 30,03' W	0	W 5	161	10,8	OBS/OBH	OBS/OBH	OBH ausgelöst	OBH 28
SO181/073-11	28.01.05	05:53	44° 47,70' S	76° 28,37' W	0	WNW 4	21	0,6	OBS/OBH	OBS/OBH	OBH geschaltet	OBH 28
SO181/073-11	28.01.05	06:03	44° 47,73' S	76° 28,49' W	0	WNW 4	34	1,1	OBS/OBH	OBS/OBH	OBH an Deck	OBH 28
SO181/073-12	28.01.05	06:29	44° 51,73' S	76° 27,06' W	0	NW 5	150	12,4	OBS/OBH	OBS/OBH	OBS ausgelöst	OBS 29
SO181/073-12	28.01.05	07:12	44° 55,43' S	76° 25,10' W	0	NW 4	315	0,6	OBS/OBH	OBS/OBH	OBS geschaltet	OBS 29
SO181/073-12	28.01.05	07:27	44° 55,47' S	76° 25,39' W	3272	NW 4	85	1,1	OBS/OBH	OBS/OBH	OBS an Deck	OBS 29
SO181/073-12	28.01.05	07:28	44° 55,47' S	76° 25,37' W	3268	NW 4	80	1	OBS/OBH	OBS/OBH	Ende Station	
Transit	28.01.05	07:28	44° 55,47' S	76° 25,37' W	3268	NW 4	165	12	Anf. # 74			d: 177 am
SO181/074-1	28.01.05	23:07	47° 17,57' S	74° 30,77' W	82	WSW 12	264	2,5	OBS/OBH	OBS/OBH	Beginn Station	
SO181/074-1	28.01.05	23:10	47° 17,59' S	74° 30,97' W	81	WSW 13	262	2,9	OBS/OBH	OBS/OBH	OBS zu Wasser	OBS 112
SO181/074-2	28.01.05	23:35	47° 17,98' S	74° 34,92' W	114	WSW 12	283	0,5	OBS/OBH	OBS/OBH	OBS zu Wasser	OBS 113
SO181/074-3	28.01.05	00:01	47° 18,43' S	74° 38,92' W	140	WSW 12	297	1,7	OBS/OBH	OBS/OBH	OBS zu Wasser	OBS 114
SO181/074-4	28.01.05	00:28	47° 18,81' S	74° 43,01' W	153	WSW 14	290	2,6	OBS/OBH	OBS/OBH	OBS zu Wasser	OBS 115
SO181/074-5	28.01.05	00:51	47° 19,26' S	74° 47,01' W	160	SW 12	266	2	OBS/OBH	OBS/OBH	OBS zu Wasser	OBS 116
SO181/074-6	28.01.05	01:16	47° 19,64' S	74° 50,98' W	173	SW 12	275	1,5	OBS/OBH	OBS/OBH	OBS zu Wasser	OBS 117
SO181/074-7	28.01.05	01:41	47° 20,07' S	74° 54,97' W	182	SW 12	278	1,8	OBS/OBH	OBS/OBH	OBS zu Wasser	OBS 118
SO181/074-8	28.01.05	02:06	47° 20,46' S	74° 58,99' W	108	SW 13	275	1,3	OBS/OBH	OBS/OBH	OBS zu Wasser	OBS 119
SO181/074-9	28.01.05	02:30	47° 20,88' S	75° 2,98' W	102	SW 13	277	2,4	OBS/OBH	OBS/OBH	OBS zu Wasser	OBS 120
SO181/074-10	28.01.05	02:55	47° 21,31' S	75° 6,98' W	90	SSW 11	273	1,9	OBS/OBH	OBS/OBH	OBS zu Wasser	OBS 121
SO181/074-11	28.01.05	03:20	47° 21,69' S	75° 10,80' W	87	SW 12	267	3,1	OBS/OBH	OBS/OBH	OBS zu Wasser	OBS 122
SO181/074-12	28.01.05	03:52	47° 22,10' S	75° 15,10' W	92	SSW 11	308	1	OBS/OBH	OBS/OBH	OBS zu Wasser	OBS 123
SO181/074-13	28.01.05	04:18	47° 22,54' S	75° 18,96' W	97	SSW 10	297	1,2	OBS/OBH	OBS/OBH	OBS zu Wasser	OBS 124
SO181/074-14	28.01.05	04:43	47° 22,93' S	75° 23,02' W	104	SSW 14	318	1,7	OBS/OBH	OBS/OBH	OBS zu Wasser	OBS 125
SO181/074-15	28.01.05	05:06	47° 23,37' S	75° 26,95' W	124	SSW 9	263	3,7	OBS/OBH	OBS/OBH	OBS zu Wasser	OBS 126
SO181/074-16	28.01.05	05:31	47° 23,77' S	75° 31,01' W	153	SW 10	285	1,1	OBS/OBH	OBS/OBH	OBS zu Wasser	OBS 127
SO181/074-17	28.01.05	05:57	47° 24,19' S	75° 35,02' W	895	SSW 11	292	2,8	OBS/OBH	OBS/OBH	OBS zu Wasser	OBS 128
SO181/074-18	28.01.05	06:23	47° 24,59' S	75° 39,03' W	1320	SSW 12	261	1,6	OBS/OBH	OBS/OBH	OBS zu Wasser	OBS 129
SO181/074-19	28.01.05	06:51	47° 25,00' S	75° 43,13' W	1760	SW 8	251	2,5	OBS/OBH	OBS/OBH	OBS zu Wasser	OBS 130
SO181/074-20	28.01.05	07:20	47° 25,39' S	75° 46,94' W	2036	SSW 11	242	2	OBS/OBH	OBS/OBH	OBS zu Wasser	OBS 131
SO181/074-21	28.01.05	07:46	47° 25,81' S	75° 50,99' W	2211	SSW 13	236	1	OBS/OBH	OBS/OBH	OBS zu Wasser	OBS 132
SO181/074-22	28.01.05	08:11	47° 26,26' S	75° 55,02' W	2305	SSW 10	279	1,5	OBS/OBH	OBS/OBH	OBS zu Wasser	OBS 133
SO181/074-23	28.01.05	08:34	47° 26,65' S	75° 59,02' W	1597	SSW 10	9	0,3	OBS/OBH	OBS/OBH	OBS zu Wasser	OBS 134
SO181/074-24	28.01.05	08:59	47° 27,08' S	76° 3,03' W	2405	SW 9	279	0,4	OBS/OBH	OBS/OBH	OBS zu Wasser	OBS 135
SO181/074-25	28.01.05	09:24	47° 27,48' S	76° 7,05' W	2792	S 12	348	1,1	OBS/OBH	OBS/OBH	OBS zu Wasser	OBS 136
SO181/074-26	28.01.05	09:50	47° 27,93' S	76° 11,01' W	3143	SSW 12	306	1,6	OBS/OBH	OBS/OBH	OBS zu Wasser	OBS 137
SO181/074-27	28.01.05	10:17	47° 28,33' S	76° 15,04' W	3305	S 11	255	1,3	OBS/OBH	OBS/OBH	OBS zu Wasser	OBS 138
SO181/074-28	28.01.05	10:42	47° 28,72' S	76° 18,97' W	3461	SSW 12	235	1,8	OBS/OBH	OBS/OBH	OBS zu Wasser	OBS 139
SO181/074-29	28.01.05	11:08	47° 29,07' S	76° 22,98' W	3635	S 15	242	2,1	OBS/OBH	OBS/OBH	OBS zu Wasser	OBS 140
SO181/074-30	28.01.05	11:33	47° 29,54' S	76° 26,97' W	3684	SSW 11	296	1,7	OBS/OBH	OBS/OBH	OBS zu Wasser	OBS 141
SO181/074-31	28.01.05	11:57	47° 29,95' S	76° 30,98' W	3669	S 12	264	2,5	OBS/OBH	OBS/OBH	OBS zu Wasser	OBS 142
SO181/074-32	28.01.05	12:22	47° 30,35' S	76° 35,00' W	3660	S 12	205	2,1	OBS/OBH	OBS/OBH	OBS zu Wasser	OBS 143
SO181/074-33	28.01.05	12:45	47° 30,74' S	76° 38,96' W	3808	SSW 12	241	2,4	OBS/OBH	OBS/OBH	OBS zu Wasser	OBS 144

Station	Datum	UTC	PositionLat	PositionLon	Tiefe [m]	Windstärke [m/s]	Kurs [°]	v [km]	Gerät	Gerätekürzel	Aktion	Bemerkung
SO181/074-34	29.01.05	13:12	47° 31,15' S	76° 42,99' W	3817	SW 13	236	1,2	OBS/OBH	OBS/OBH	OBS zu Wasser	OBS 145
SO181/074-35	29.01.05	13:38	47° 31,56' S	76° 48,99' W	3750	SSW 13	264	1,3	OBS/OBH	OBS/OBH	OBS zu Wasser	OBS 146
SO181/074-36	29.01.05	14:03	47° 31,99' S	76° 50,99' W	3757	SSW 12	232	1,6	OBS/OBH	OBS/OBH	OBS zu Wasser	OBS 147
SO181/074-37	29.01.05	14:27	47° 32,41' S	76° 54,95' W	3616	SSW 13	242	2,1	OBS/OBH	OBS/OBH	OBS zu Wasser	OBS 148
SO181/074-38	29.01.05	14:52	47° 32,82' S	76° 59,04' W	3600	SSW 12	276	1,8	OBS/OBH	OBS/OBH	OBS zu Wasser	OBS 149
SO181/074-39	29.01.05	15:17	47° 33,25' S	77° 3,00' W	3458	SSW 9	316	1,8	OBS/OBH	OBS/OBH	OBS zu Wasser	OBS 150
SO181/074-40	29.01.05	15:42	47° 33,66' S	77° 7,04' W	3333	WSW 10	57	1,3	OBS/OBH	OBS/OBH	OBS zu Wasser	OBS 151
SO181/074-41	29.01.05	16:07	47° 34,05' S	77° 10,98' W	3572	SSW 11	264	0,8	OBS/OBH	OBS/OBH	OBS zu Wasser	OBS 152
SO181/074-42	29.01.05	16:37	47° 34,47' S	77° 15,20' W	3538	SSW 10	269	1,7	OBS/OBH	OBS/OBH	OBS zu Wasser	OBS 153
SO181/074-42	29.01.05	17:05	47° 34,88' S	77° 19,02' W	3539	SW 10	272	1,4	OBS/OBH	OBS/OBH	OBS zu Wasser	OBS 153
SO181/074-43	29.01.05	17:36	47° 35,27' S	77° 22,98' W	3527	S 11	223	1,4	OBS/OBH	OBS/OBH	OBS zu Wasser	OBS 154
SO181/074-44	29.01.05	18:04	47° 35,70' S	77° 27,03' W	3575	S 10	264	1,4	OBS/OBH	OBS/OBH	OBS zu Wasser	OBS 156
SO181/074-45	29.01.05	18:05	47° 35,71' S	77° 27,06' W	3578	S 10	336	1,1	OBS/OBH	OBS/OBH	Ende Station	
SO181/075-1	29.01.05	18:40	47° 36,31' S	77° 33,54' W	3523	S 10	234	5,2	Profil	PR	Stationenbeginn	Pr # 07, d: 140 sm
SO181/075-1	29.01.05	18:47	47° 36,47' S	77° 33,66' W	3529	SSW 9	226	1,7	Profil	PR	Stb Alrgun zu Wasser	Traverse mit je 4 x 8tr. G-Gun
SO181/075-1	29.01.05	18:58	47° 36,70' S	77° 34,33' W	3522	SSW 10	215	2,7	Profil	PR	Bb Alrgun zu Wasser	Traverse mit je 4 x 8 tr G-Gun
SO181/075-1	29.01.05	18:19	47° 36,28' S	77° 34,13' W	3514	SSW 6	85	3,7	Profil	PR	Beginn Profil	1. Schuß
SO181/075-1	29.01.05	19:30	47° 36,22' S	77° 33,31' W	3512	SSW 8	108	2,3	Profil	PR	Streamer zu Wasser	Streamer 100m + 100 m Vorlauf an Bb
SO181/075-1	31.01.05	12:17	47° 14,22' S	74° 31,65' W	137	SSW 2	268	3	Profil	PR	Ende Profil	letzter Schuß
SO181/075-1	31.01.05	12:27	47° 14,25' S	74° 32,45' W	137	SSW 2	265	1,6	Profil	PR	Bb alrgun an Deck	Traverse mit 4 G-Gun
SO181/075-1	31.01.05	12:37	47° 14,26' S	74° 32,83' W	137	SSW 2	274	1,5	Profil	PR	Stb Alrgun an Deck	Traverse mit 4 G-Gun
SO181/075-1	31.01.05	12:37	47° 14,26' S	74° 32,83' W	137	SSW 2	274	1,5	Profil	PR	Stationsende	Anf. # 76, d: 4 sm
SO181/076-1	31.01.05	12:57	47° 16,16' S	74° 31,42' W	106	SW 6	152	10,2	OBS/OBH	OBS/OBH	Beginn Station	
SO181/076-1	31.01.05	12:58	47° 16,30' S	74° 31,29' W	104	SW 6	145	10,2	OBS/OBH	OBS/OBH	OBS ausgelöst	OBS 112
SO181/076-1	31.01.05	13:55	47° 17,51' S	74° 30,79' W	0	SW 3	9	0,4	OBS/OBH	OBS/OBH	OBS ausgelöst	OBS 112; 2. X ausgelöst; STEIGT NICHT
SO181/076-2	31.01.05	14:16	47° 17,85' S	74° 33,40' W	0	NNW 5	258	11,5	OBS/OBH	OBS/OBH	OBS ausgelöst	OBS 113
SO181/076-2	31.01.05	14:18	47° 17,92' S	74° 33,92' W	0	NNW 5	260	10,6	OBS/OBH	OBS/OBH	OBS gesichtet	OBS 113
SO181/076-2	31.01.05	14:25	47° 17,95' S	74° 34,87' W	0	NNW 2	271	1,2	OBS/OBH	OBS/OBH	OBS an Deck	OBS 113
SO181/076-3	31.01.05	14:39	47° 18,08' S	74° 36,39' W	0	NNW 2	258	9,8	OBS/OBH	OBS/OBH	OBS ausgelöst	OBS 114
SO181/076-3	31.01.05	14:42	47° 18,19' S	74° 37,14' W	0	NNW 2	257	10,1	OBS/OBH	OBS/OBH	OBS gesichtet	OBS 114
SO181/076-3	31.01.05	14:54	47° 18,40' S	74° 38,86' W	0	NNW 2	301	0,9	OBS/OBH	OBS/OBH	OBS an Deck	OBS 114
SO181/076-4	31.01.05	15:09	47° 18,61' S	74° 40,97' W	0	NNW 2	259	11,5	OBS/OBH	OBS/OBH	OBS ausgelöst	OBS 115
SO181/076-4	31.01.05	15:18	47° 18,78' S	74° 42,40' W	0	SW 2	269	2,8	OBS/OBH	OBS/OBH	OBS gesichtet	OBS 115
SO181/076-4	31.01.05	15:36	47° 18,81' S	74° 43,02' W	0	SW 2	300	1,3	OBS/OBH	OBS/OBH	OBS an Deck	OBS 115
SO181/076-5	31.01.05	15:48	47° 18,54' S	74° 41,47' W	0	SW 2	82	11,7	OBS/OBH	OBS/OBH	OBS ausgelöst	OBS 112, steigt nicht auf
SO181/076-5	31.01.05		Suchgeschirr mit W6, SL 1300 m						Dredgen nach OBS 112			700 m Seil abgerissen, dredgen erfolgreich
SO181/076-5	31.01.05	17:28	47° 17,20' S	74° 31,30' W	80	WSW 3	5	0,3	OBS/OBH	OBS/OBH	OBS gesichtet	OBS 112, nach dredgen aufgestiegen
SO181/076-5	31.01.05	18:02	47° 17,18' S	74° 30,72' W	80	WSW 3	342	0,8	OBS/OBH	OBS/OBH	OBS an Deck	OBS 112
SO181/076-6	31.01.05	19:05	47° 19,08' S	74° 45,22' W	159	W 8	260	10,7	OBS/OBH	OBS/OBH	OBS ausgelöst	OBS 116
SO181/076-6	31.01.05	19:09	47° 19,17' S	74° 46,02' W	158	W 7	258	6,3	OBS/OBH	OBS/OBH	OBS gesichtet	OBS 116
SO181/076-6	31.01.05	19:24	47° 19,32' S	74° 48,90' W	160	W 4	198	0,1	OBS/OBH	OBS/OBH	OBS an Deck	OBS 116
SO181/076-7	31.01.05	19:38	47° 19,47' S	74° 48,86' W	168	W 2	262	9,2	OBS/OBH	OBS/OBH	OBS ausgelöst	OBS 117
SO181/076-7	31.01.05	19:43	47° 19,58' S	74° 49,85' W	170	W 3	264	7,7	OBS/OBH	OBS/OBH	OBS gesichtet	OBS 117

Station	Datum	UTC	PositionLat	PositionLon	Tiefe [m]	Windstärke [m/s]	Kurs [°]	v [km]	Gerät	Gerätekurzel	Aktion	Bemerkung
SO181/076-7	31.01.05	19:57	47° 19,61' S	74° 50,79' W	172	W 3	73	0,9	OBS/OBH	OBS/OBH	OBS an Deck	OBS 117
SO181/076-8	31.01.05	20:15	47° 19,96' S	74° 53,67' W	176	W 3	259	7	OBS/OBH	OBS/OBH	OBS ausgelöst	OBS 118; NICHT aufgestiegen
SO181/076-9	31.01.05	20:47	47° 20,13' S	74° 55,53' W	110	W 3	265	7,4	OBS/OBH	OBS/OBH	OBS ausgelöst	OBS 119
SO181/076-9	31.01.05	21:00	47° 20,39' S	74° 58,22' W	110	W 3	281	4	OBS/OBH	OBS/OBH	OBS gesichtet	OBS 119
SO181/076-9	31.01.05	21:14	47° 20,38' S	74° 58,92' W	108	W 4	45	0,8	OBS/OBH	OBS/OBH	OBS an Deck	OBS 119
SO181/076-10	31.01.05	21:29	47° 20,72' S	75° 1,28' W	108	W 3	258	9,2	OBS/OBH	OBS/OBH	OBS ausgelöst	OBS 120
SO181/076-10	31.01.05	21:31	47° 20,79' S	75° 1,73' W	108	W 4	255	8,8	OBS/OBH	OBS/OBH	OBS gesichtet	OBS 120
SO181/076-10	31.01.05	21:58	47° 20,75' S	75° 2,79' W	104	W 8	143	1	OBS/OBH	OBS/OBH	OBS an Deck	OBS 120
SO181/076-11	31.01.05	22:12	47° 21,14' S	75° 4,92' W	89	W 4	254	10	OBS/OBH	OBS/OBH	OBS ausgelöst	OBS 121
SO181/076-11	31.01.05	22:17	47° 21,32' S	75° 6,00' W	94	W 4	262	6,2	OBS/OBH	OBS/OBH	OBS gesichtet	OBS 121
SO181/076-11	31.01.05	22:40	47° 21,15' S	75° 6,83' W	91	W 3	353	0,2	OBS/OBH	OBS/OBH	OBS an Deck	OBS 121
SO181/076-12	31.01.05	22:58	47° 21,52' S	75° 10,08' W	88	W 3	257	8	OBS/OBH	OBS/OBH	OBH ausgelöst	OBH 122
SO181/076-12	31.01.05	23:00	47° 21,57' S	75° 10,44' W	0	W 3	260	5,3	OBS/OBH	OBS/OBH	OBH gesichtet	
SO181/076-12	31.01.05	23:07	47° 21,70' S	75° 11,00' W	0	W 5	277	1,1	OBS/OBH	OBS/OBH	OBH an Deck	OBH 122
SO181/076-13	31.01.05	23:24	47° 22,06' S	75° 13,91' W	0	W 4	259	6,2	OBS/OBH	OBS/OBH	OBH ausgelöst	OBH 123
SO181/076-13	31.01.05	23:29	47° 22,13' S	75° 14,57' W	0	W 4	268	3,3	OBS/OBH	OBS/OBH	OBH gesichtet	OBH 123
SO181/076-13	31.01.05	23:37	47° 22,02' S	75° 15,05' W	0	W 4	289	0,8	OBS/OBH	OBS/OBH	OBH an Deck	OBH 123
SO181/076-14	31.01.05	23:55	47° 22,51' S	75° 18,10' W	0	W 4	250	5,9	OBS/OBH	OBS/OBH	OBH ausgelöst	OBH 124
SO181/076-14	31.01.05	23:56	47° 22,55' S	75° 18,23' W	0	W 4	249	5,4	OBS/OBH	OBS/OBH	OBH gesichtet	OBH 124
SO181/076-14	01.02.05	00:07	47° 22,43' S	75° 18,91' W	0	W 4	82	1,2	OBS/OBH	OBS/OBH	OBH an Deck	OBH 124
SO181/076-15	01.02.05	00:24	47° 22,93' S	75° 22,04' W	0	W 4	254	8	OBS/OBH	OBS/OBH	OBH ausgelöst	OBH 125
SO181/076-15	01.02.05	00:37	47° 22,97' S	75° 22,90' W	0	NW 3	1	0,4	OBS/OBH	OBS/OBH	OBH gesichtet	OBH 125
SO181/076-15	01.02.05	00:44	47° 22,84' S	75° 23,01' W	0	W 4	358	1,2	OBS/OBH	OBS/OBH	OBH an Deck	OBH 125
SO181/076-16	01.02.05	01:02	47° 23,34' S	75° 26,13' W	0	W 4	263	7,1	OBS/OBH	OBS/OBH	OBH ausgelöst	OBH 126
SO181/076-16	01.02.05	01:03	47° 23,35' S	75° 26,29' W	0	W 4	256	6,1	OBS/OBH	OBS/OBH	OBH gesichtet	OBH 126
SO181/076-16	01.02.05	01:16	47° 23,26' S	75° 27,07' W	0	WNW 4	311	1,4	OBS/OBH	OBS/OBH	OBH an Deck	OBH 126
SO181/076-17	01.02.05	01:37	47° 23,79' S	75° 30,50' W	0	WNW 4	270	4	OBS/OBH	OBS/OBH	OBH ausgelöst	OBH 127
SO181/076-17	01.02.05	01:39	47° 23,79' S	75° 30,67' W	0	WNW 4	271	2,5	OBS/OBH	OBS/OBH	OBH gesichtet	OBH 127
SO181/076-17	01.02.05	01:49	47° 23,58' S	75° 31,03' W	0	WNW 4	339	1	OBS/OBH	OBS/OBH	OBH an Deck	OBH 127
SO181/076-18	01.02.05	02:00	47° 23,80' S	75° 32,38' W	0	WNW 4	252	10,5	OBS/OBH	OBS/OBH	OBH ausgelöst	OBH 128
SO181/076-18	01.02.05	02:11	47° 24,22' S	75° 34,66' W	0	WNW 4	263	3,8	OBS/OBH	OBS/OBH	OBH gesichtet	OBH 128
SO181/076-18	01.02.05	02:18	47° 24,13' S	75° 35,05' W	0	WNW 4	285	1,2	OBS/OBH	OBS/OBH	OBH an Deck	OBH 128
SO181/076-19	01.02.05	02:29	47° 24,43' S	75° 36,69' W	0	NW 8	282	7,9	OBS/OBH	OBS/OBH	OBH ausgelöst	OBH 129
SO181/076-19	01.02.05	02:41	47° 24,82' S	75° 38,69' W	0	NW 8	262	4,3	OBS/OBH	OBS/OBH	OBH gesichtet	OBH 129
SO181/076-19	01.02.05	02:50	47° 24,47' S	75° 39,02' W	0	NW 4	17	0,6	OBS/OBH	OBS/OBH	OBH an Deck	OBH 129
SO181/076-20	01.02.05	02:59	47° 24,48' S	75° 39,74' W	0	NNW 7	252	7,3	OBS/OBH	OBS/OBH	OBH ausgelöst	OBH 130
SO181/076-20	01.02.05	03:15	47° 25,03' S	75° 42,45' W	0	NW 4	251	1,9	OBS/OBH	OBS/OBH	OBH gesichtet	OBH 130
SO181/076-20	01.02.05	03:27	47° 24,97' S	75° 43,05' W	0	NW 4	312	1,7	OBS/OBH	OBS/OBH	OBH an Deck	OBH 130
SO181/076-21	01.02.05	03:28	47° 24,96' S	75° 43,07' W	0	NW 4	280	1,1	OBS/OBH	OBS/OBH	OBS ausgelöst	OBH 131
SO181/076-21	01.02.05	03:41	47° 25,26' S	75° 45,08' W	0	NNW 6	256	9,7	OBS/OBH	OBS/OBH	OBS gesichtet	OBH 131
SO181/076-21	01.02.05	03:56	47° 25,46' S	75° 46,78' W	0	NW 3	197	0,6	OBS/OBH	OBS/OBH	OBH an Deck	OBH 131
SO181/076-22	01.02.05	03:58	47° 25,49' S	75° 46,83' W	0	NW 3	266	1,7	OBS/OBH	OBS/OBH	OBH ausgelöst	OBH 132
SO181/076-22	01.02.05	04:13	47° 25,79' S	75° 49,55' W	0	NW 8	265	8,8	OBS/OBH	OBS/OBH	OBH gesichtet	OBH 132

Station	Datum	UTG	Position Lat	Position Lon	Tide [m]	Winddir [m/s]	Kurs [°]	v [m/s]	Gerät	Geschwindigkeit	Aktion	Bemerkung
SO181076-22	01.02.05	04:35	47° 23.53' S	75° 51.00' W	0	NW 3	317	1.4	OBS/OBH	OBS/OBH	OBH an Deck	OBS 132
SO181076-23	01.02.05	04:36	47° 25.61' S	75° 51.01' W	0	NW 3	274	0.8	OBS/OBH	OBS/OBH	OBS ausgelöst	OBS 133
SO181076-23	01.02.05	04:51	47° 26.09' S	75° 53.54' W	0	NW 8	281	10	OBS/OBH	OBS/OBH	OBH gelöscht	OBS 133
SO181076-23	01.02.05	05:15	47° 26.10' S	75° 55.20' W	0	NW 5	17	0.4	OBS/OBH	OBS/OBH	OBH an Deck	OBS 133
SO181076-24	01.02.05	05:16	47° 26.09' S	75° 55.22' W	0	NW 3	300	2.1	OBS/OBH	OBS/OBH	OBS ausgelöst	OBS 134
SO181076-24	01.02.05	05:54	47° 26.55' S	75° 56.90' W	0	WNW 3	288	0.8	OBS/OBH	OBS/OBH	OBS gelöscht	OBS 134
SO181076-24	01.02.05	06:13	47° 26.61' S	75° 56.09' W	0	W 2	349	1.3	OBS/OBH	OBS/OBH	OBS an Deck	OBS 134
SO181076-24	01.02.05	06:15	47° 26.57' S	75° 56.11' W	0	NW 3	289	1.9	OBS/OBH	OBS/OBH	OBS ausgelöst	OBS 135
SO181076-24	01.02.05	06:42	47° 27.05' S	75° 56.58' W	0	W 3	263	2	OBS/OBH	OBS/OBH	OBS gelöscht	OBS 136
SO181076-24	01.02.05	06:49	47° 27.07' S	75° 56.78' W	0	W 2	253	0.9	OBS/OBH	OBS/OBH	OBS ausgelöst	OBS 136
SO181076-24	01.02.05	07:00	47° 27.12' S	75° 56.34' W	0	W 4	271	2	OBS/OBH	OBS/OBH	OBS an Deck	OBS 135
SO181076-25	01.02.05	07:17	47° 27.42' S	75° 56.43' W	0	W 5	268	4.3	OBS/OBH	OBS/OBH	OBS gelöscht	OBS 136
SO181076-25	01.02.05	07:28	47° 27.57' S	75° 56.72' W	0	W 3	223	1	OBS/OBH	OBS/OBH	OBS an Deck	OBS 136
SO181076-26	01.02.05	07:38	47° 27.67' S	75° 56.75' W	0	W 3	266	8.5	OBS/OBH	OBS/OBH	OBS ausgelöst	OBS 137
SO181076-26	01.02.05	08:00	47° 27.83' S	75° 56.53' W	0	W 3	269	1.6	OBS/OBH	OBS/OBH	OBS gelöscht	OBS 137
SO181076-26	01.02.05	08:00	47° 27.83' S	75° 56.53' W	0	W 3	269	1.6	OBS/OBH	OBS/OBH	OBS ausgelöst	OBS 138
SO181076-26	01.02.05	08:12	47° 27.86' S	75° 56.24' W	0	W 3	223	0.7	OBS/OBH	OBS/OBH	OBS an Deck	OBS 137
SO181076-27	01.02.05	08:15	47° 27.87' S	75° 56.40' W	0	W 4	256	5.5	OBS/OBH	OBS/OBH	OBS ausgelöst	OBS 138
SO181076-27	01.02.05	08:33	47° 28.28' S	75° 56.71' W	0	WSW 4	243	0.3	OBS/OBH	OBS/OBH	OBH gelöscht	OBS 138
SO181076-27	01.02.05	08:43	47° 28.25' S	75° 56.09' W	0	W 4	288	1.1	OBS/OBH	OBS/OBH	OBS an Deck	OBS 138
SO181076-28	01.02.05	08:52	47° 28.41' S	75° 56.14' W	0	W 4	261	9.6	OBS/OBH	OBS/OBH	OBS gelöscht	OBS 139
SO181076-28	01.02.05	09:04	47° 28.67' S	75° 56.45' W	0	W 4	269	4	OBS/OBH	OBS/OBH	OBS ausgelöst	OBS 140
SO181076-29	01.02.05	09:10	47° 28.64' S	75° 56.01' W	0	WSW 5	275	2.7	OBS/OBH	OBS/OBH	OBS ausgelöst	OBS 141
SO181076-29	01.02.05	09:13	47° 28.62' S	75° 56.10' W	0	WSW 4	334	0.2	OBS/OBH	OBS/OBH	OBS an Deck	OBS 139
SO181076-29	01.02.05	09:16	47° 28.61' S	75° 56.21' W	0	WSW 4	258	4.1	OBS/OBH	OBS/OBH	OBS gelöscht	OBS 140
SO181076-29	01.02.05	09:44	47° 28.96' S	75° 56.31' W	0	WSW 4	338	0.8	OBS/OBH	OBS/OBH	OBS an Deck	OBS 140
SO181076-30	01.02.05	09:56	47° 29.20' S	75° 55.07' W	0	WSW 4	255	8.8	OBS/OBH	OBS/OBH	OBS ausgelöst	OBS 142
SO181076-30	01.02.05	09:58	47° 29.32' S	75° 55.79' W	0	WSW 4	258	9.8	OBS/OBH	OBS/OBH	OBS gelöscht	OBS 141
SO181076-30	01.02.05	10:12	47° 29.50' S	75° 57.06' W	0	SW 4	22	0.4	OBS/OBH	OBS/OBH	OBS an Deck	OBS 141
SO181076-31	01.02.05	10:26	47° 29.82' S	75° 57.57' W	0	WSW 4	261	9	OBS/OBH	OBS/OBH	OBS ausgelöst	OBS 143
SO181076-31	01.02.05	10:30	47° 29.82' S	75° 56.43' W	0	WSW 5	262	7.5	OBS/OBH	OBS/OBH	OBS gelöscht	OBS 142
SO181076-31	01.02.05	10:41	47° 30.00' S	75° 56.14' W	0	SW 4	74	0.3	OBS/OBH	OBS/OBH	OBS an Deck	OBS 142
SO181076-32	01.02.05	11:08	47° 30.38' S	75° 56.81' W	0	SW 4	295	0.4	OBS/OBH	OBS/OBH	OBS gelöscht	OBS 143
SO181076-32	01.02.05	11:09	47° 30.38' S	75° 56.81' W	0	SW 4	121	0.1	OBS/OBH	OBS/OBH	OBS ausgelöst	OBS 144
SO181076-32	01.02.05	11:15	47° 30.31' S	75° 55.03' W	0	SW 5	324	1.3	OBS/OBH	OBS/OBH	OBS an Deck	OBS 143
SO181076-33	01.02.05	11:52	47° 30.82' S	75° 56.85' W	0	SW 5	214	1.1	OBS/OBH	OBS/OBH	OBS ausgelöst	OBS 145
SO181076-33	01.02.05	11:57	47° 30.81' S	75° 56.85' W	0	WNW 5	181	0.7	OBS/OBH	OBS/OBH	OBS gelöscht	OBS 144
SO181076-33	01.02.05	12:03	47° 30.69' S	75° 56.86' W	0	WNW 5	16	1.3	OBS/OBH	OBS/OBH	OBS an Deck	OBS 144
SO181076-34	01.02.05	12:27	47° 31.17' S	75° 56.77' W	0	WNW 5	280	1.4	OBS/OBH	OBS/OBH	OBS ausgelöst	OBS 146
SO181076-34	01.02.05	12:41	47° 31.21' S	75° 56.77' W	0	WSW 4	20	0.2	OBS/OBH	OBS/OBH	OBS gelöscht	OBS 145
SO181076-34	01.02.05	12:50	47° 31.12' S	75° 56.00' W	0	SW 5	262	0.5	OBS/OBH	OBS/OBH	OBS an Deck	OBS 145
SO181076-35	01.02.05	13:08	47° 31.37' S	75° 56.15' W	0	WSW 8	264	6.3	OBS/OBH	OBS/OBH	OBS ausgelöst	OBS 147
SO181076-35	01.02.05	13:26	47° 31.48' S	75° 56.74' W	0	WSW 4	221	2	OBS/OBH	OBS/OBH	OBS gelöscht	OBS 146

Station	Datum	UTC	PositionLat	PositionLon	Tiefe [m]	Windstärke [m/s]	Kurs [°]	v [kn]	Gerät	Gerätekurzel	Aktion	Bemerkung
SO181/076-35	01.02.05	13:35	47° 31,41' S	76° 46,98' W	0	WSW 5	345	0,5	OBS/OBH	OBS/OBH	OBH an Deck	OBH 148
SO181/076-36	01.02.05	13:52	47° 31,78' S	76° 50,04' W	0	WSW 5	257	6	OBS/OBH	OBS/OBH	OBS ausgelöst	OBS 148
SO181/076-36	01.02.05	13:56	47° 31,86' S	76° 50,55' W	0	WSW 5	236	3,2	OBS/OBH	OBS/OBH	OBS gesichtet	OBS 147
SO181/076-36	01.02.05	14:05	47° 31,85' S	76° 50,96' W	0	WSW 5	26	0,7	OBS/OBH	OBS/OBH	OBH an Deck	OBH 147
SO181/076-37	01.02.05	14:22	47° 32,31' S	76° 54,13' W	0	WSW 5	255	5,3	OBS/OBH	OBS/OBH	OBS ausgelöst	OBS 149
SO181/076-37	01.02.05	14:35	47° 32,37' S	76° 54,79' W	0	WSW 5	188	0,1	OBS/OBH	OBS/OBH	OBS gesichtet	OBS 148
SO181/076-37	01.02.05	14:43	47° 32,20' S	76° 54,90' W	0	WSW 5	352	1,3	OBS/OBH	OBS/OBH	OBS an Deck	OBS 148
SO181/076-38	01.02.05	15:04	47° 32,74' S	76° 58,31' W	0	WSW 6	242	3,6	OBS/OBH	OBS/OBH	OBS gesichtet	obs 149
SO181/076-38	01.02.05	15:05	47° 32,76' S	76° 58,39' W	0	WSW 5	251	3,3	OBS/OBH	OBS/OBH	OBS ausgelöst	OBS 150
SO181/076-38	01.02.05	15:17	47° 32,74' S	76° 58,94' W	0	SSW 4	307	1,1	OBS/OBH	OBS/OBH	OBS an Deck	OBS 149
SO181/076-39	01.02.05	15:53	47° 33,20' S	77° 2,53' W	0	SSW 4	241	1	OBS/OBH	OBS/OBH	OBS ausgelöst	OBS 151
SO181/076-39	01.02.05	16:07	47° 33,18' S	77° 2,78' W	0	W 4	297	0,4	OBS/OBH	OBS/OBH	OBS gesichtet	OBS 150
SO181/076-39	01.02.05	16:18	47° 33,20' S	77° 2,94' W	0	W 4	334	1,9	OBS/OBH	OBS/OBH	OBS an Deck	OBS 150
SO181/076-40	01.02.05	16:35	47° 33,58' S	77° 6,06' W	0	W 4	257	7,2	OBS/OBH	OBS/OBH	OBS gesichtet	OBS 151
SO181/076-40	01.02.05	16:36	47° 33,57' S	77° 6,22' W	0	W 4	276	6	OBS/OBH	OBS/OBH	OBS ausgelöst	OBS 152
SO181/076-40	01.02.05	16:46	47° 33,43' S	77° 6,88' W	0	WSW 4	290	1,2	OBS/OBH	OBS/OBH	OBS an Deck	OBS 151
SO181/076-41	01.02.05	16:51	47° 33,50' S	77° 7,32' W	0	WSW 4	253	5,7	OBS/OBH	OBS/OBH	OBS ausgelöst	OBS 153
SO181/076-41	01.02.05	17:21	0° 0,00' N	0° 0,00' E	0	W 4	0	0	OBS/OBH	OBS/OBH	OBS gesichtet	OBS 152
SO181/076-41	01.02.05	17:31	47° 33,93' S	77° 10,91' W	0	W 4	321	0,8	OBS/OBH	OBS/OBH	OBS an Deck	OBS 152
SO181/076-42	01.02.05	17:37	47° 34,03' S	77° 11,59' W	0	W 7	257	8,3	OBS/OBH	OBS/OBH	OBS ausgelöst	OBS 154
SO181/076-42	01.02.05	17:53	47° 34,48' S	77° 14,67' W	0	W 5	284	2,7	OBS/OBH	OBS/OBH	OBS gesichtet	OBS 153
SO181/076-42	01.02.05	18:02	47° 34,26' S	77° 15,05' W	0	W 5	345	2,2	OBS/OBH	OBS/OBH	OBS an Deck	OBS 153
SO181/076-43	01.02.05	18:21	47° 34,72' S	77° 18,21' W	0	W 5	257	3,5	OBS/OBH	OBS/OBH	OBS ausgelöst	OBS 155
SO181/076-43	01.02.05	18:31	47° 34,77' S	77° 19,70' W	0	W 5	253	0,9	OBS/OBH	OBS/OBH	OBS gesichtet	OBS 154
SO181/076-43	01.02.05	18:40	47° 34,80' S	77° 19,00' W	0	W 4	21	1	OBS/OBH	OBS/OBH	OBS an Deck	OBS 154
SO181/076-44	01.02.05	18:54	47° 35,01' S	77° 21,47' W	0	W 4	280	8,4	OBS/OBH	OBS/OBH	OBS ausgelöst	OBS 156
SO181/076-44	01.02.05	18:56	47° 35,06' S	77° 21,90' W	0	W 4	264	7,6	OBS/OBH	OBS/OBH	OBS gesichtet	OBS 155
SO181/076-44	01.02.05	19:08	47° 35,20' S	77° 22,80' W	0	W 4	34	1,2	OBS/OBH	OBS/OBH	OBS an Deck	OBS 155
SO181/076-45	01.02.05	19:36	47° 35,59' S	77° 26,79' W	0	WNW 4	59	0,8	OBS/OBH	OBS/OBH	OBS gesichtet	OBS 156
SO181/076-45	01.02.05	19:44	47° 35,65' S	77° 26,96' W	0	NW 5	1	0,9	OBS/OBH	OBS/OBH	OBS an Deck	OBS 156
SO181/076-45	01.02.05	19:46	47° 35,63' S	77° 26,97' W	0	NW 4	26	0,5	OBS/OBH	OBS/OBH	Ende Station	
SO181/077-1	01.02.05	19:51	47° 35,80' S	77° 26,94' W	3576	W 5	46	0,2	Magnetometer	MAGN	Beginn Station	rwk:083, d: 46 sm
SO181/077-1	01.02.05	20:07	47° 35,80' S	77° 25,56' W	3566	W 3	82	8,8	Magnetometer	MAGN	Magnetometer zu Wasser	
SO181/077-1	01.02.05	00:47	47° 30,00' S	76° 20,00' W	2576	W 3	83	10	Magnetometer	MAGN	Kursänderung	rwk: 074°, d: 35 sm
SO181/077-1	02.02.05	03:46	47° 20,01' S	75° 30,03' W	133	WSW 1	84	9	Magnetometer	MAGN	Kursänderung	KÄ: rwk: 080°, d: 28 sm
SO181/077-1	02.02.05	06:14	47° 20,08' S	74° 52,96' W	174	SW 4	89	2,8	Magnetometer	MAGN	Magnetometer an Deck	
SO181/077-1	02.02.05	06:15	47° 20,08' S	74° 52,90' W	173	ESE 4	89	2,5	Magnetometer	MAGN	Ende Station	
SO181/078-1	02.02.05	06:36	47° 19,98' S	74° 54,82' W	161	SSW 6	194	1,5	Ocean Floor Observation Sys	OFOS	Beginn Station	
SO181/078-1	02.02.05	06:55	47° 20,06' S	74° 54,90' W	60	SW 5	90	0,5	Ocean Floor Observation Sys	OFOS	Zu wasser	HH - OFOS
SO181/078-1	02.02.05	07:05	47° 20,08' S	74° 54,89' W	162	SW 4	180	0,9	Ocean Floor Observation Sys	OFOS	Bodensicht	sl: 159m
SO181/078-1	02.02.05	09:53	47° 20,07' S	74° 54,96' W	163	SW 6	180	0,5	Ocean Floor Observation Sys	OFOS	Beginn hieven	
SO181/078-1	02.02.05	10:01	47° 20,06' S	74° 54,91' W	164	SSW 6	75	0,9	Ocean Floor Observation Sys	OFOS	An deck	
SO181/078-2	02.02.05	10:14	47° 20,01' S	74° 54,84' W	165	SW 4	152	0,4	Suchgeschirr	Suchg	Zu wasser	Suchgeschirr, W 6

Station	Datum	UTC	PositionLat	PositionLon	Tiefe [m]	Windstärke [m/s]	Kurs [°]	v [kn]	Gerät	Gerätekürzel	Aktion	Bemerkung
SO181/078-2	02.02.05	10:20	47° 20,02' S	74° 54,84' W	165	SW 4	143	0,1	Suchgeschirr	Suchg	Boko	SL: 178 m
SO181/078-2	02.02.05	11:06	47° 19,98' S	74° 55,47' W	158	SSW 7	288	1,1	Suchgeschirr	Suchg	Beginn hieven	max. SL 1505 m
SO181/078-3	02.02.05	11:06	47° 19,98' S	74° 55,47' W	158	SSW 7	288	1,1	OBS/OBH	OBS/OBH	OBS gesichtet	OBS 118, nach dredgen aufgetaucht
SO181/078-3	02.02.05	11:59	47° 19,72' S	74° 54,48' W	173	WSW 6	188	0,6	OBS/OBH	OBS/OBH	OBS an Deck	OBS 118
SO181/078-3	02.02.05	12:00	47° 19,73' S	74° 54,48' W	173	SW 8	264	0,6	OBS/OBH	OBS/OBH	Ende Station	
Transit	02.02.05	12:00	47° 19,73' S	74° 54,48' W	173	SW 8	dlv	11,8	Anf., Pr OB			d: 170 sm
SO181/079-1	03.02.05	02:22	45° 10,16' S	74° 35,14' W	75	SSW 10	98	4,4	OBS/OBH	OBS/OBH	Beginn Station	
SO181/079-1	03.02.05	02:29	45° 10,48' S	74° 34,99' W	74	SSW 10	220	1,9	OBS/OBH	OBS/OBH	OBS zu Wasser	OBS 157
SO181/079-2	03.02.05	02:55	45° 11,88' S	74° 39,01' W	85	SSW 11	212	1,4	OBS/OBH	OBS/OBH	OBS zu Wasser	OBS 159
SO181/079-3	03.02.05	03:32	45° 11,75' S	74° 39,16' W	86	SW 13	241	3,4	OBS/OBH	OBS/OBH	OBS zu Wasser	OBS 159
SO181/079-4	03.02.05	04:02	45° 14,08' S	74° 47,04' W	113	SW 13	278	2,1	OBS/OBH	OBS/OBH	OBS zu Wasser	OBS 180
SO181/079-5	03.02.05	04:30	45° 15,25' S	74° 51,00' W	136	SW 13	243	1,5	OBS/OBH	OBS/OBH	OBS zu Wasser	obs 181
SO181/079-6	03.02.05	04:58	45° 16,47' S	74° 55,06' W	276	SW 15	297	1,5	OBS/OBH	OBS/OBH	OBS zu Wasser	OBS 182
SO181/079-7	03.02.05	05:27	45° 17,85' S	74° 59,01' W	391	SSW 14	266	1	OBS/OBH	OBS/OBH	OBS zu Wasser	OBS 183
SO181/079-8	03.02.05	05:55	45° 18,88' S	75° 3,02' W	351	SSW 14	262	1,2	OBS/OBH	OBS/OBH	OBS zu Wasser	OBS 184
SO181/079-9	03.02.05	06:23	45° 20,08' S	75° 7,04' W	137	SW 15	306	1	OBS/OBH	OBS/OBH	OBS zu Wasser	OBS 185
SO181/079-10	03.02.05	06:49	45° 21,24' S	75° 11,02' W	126	SSW 14	266	1,3	OBS/OBH	OBS/OBH	OBS zu Wasser	OBH 186
SO181/079-11	03.02.05	07:18	45° 22,43' S	75° 14,94' W	131	SSW 13	206	0,8	OBS/OBH	OBS/OBH	OBS zu Wasser	OBH 187
SO181/079-12	03.02.05	07:47	45° 23,63' S	75° 18,98' W	147	S 11	302	0,7	OBS/OBH	OBS/OBH	OBS zu Wasser	OBS 188
SO181/079-13	03.02.05	08:16	45° 24,80' S	75° 22,98' W	230	S 12	216	1	OBS/OBH	OBS/OBH	OBS zu Wasser	OBS 189
SO181/079-14	03.02.05	08:46	45° 25,99' S	75° 26,95' W	354	SSW 12	20	2,8	OBS/OBH	OBS/OBH	OBS zu Wasser	OBS 170
SO181/079-15	03.02.05	09:16	45° 27,15' S	75° 30,99' W	622	SSW 12	234	0,8	OBS/OBH	OBS/OBH	OBH zu Wasser	OBH 171
SO181/079-16	03.02.05	09:42	45° 28,38' S	75° 35,00' W	844	S 12	229	0,7	OBS/OBH	OBS/OBH	OBH zu Wasser	OBH 172
SO181/079-17	03.02.05	10:09	45° 29,57' S	75° 38,98' W	1035	SW 11	251	0,8	OBS/OBH	OBS/OBH	OBH zu Wasser	OBH 173
SO181/079-18	03.02.05	10:37	45° 30,77' S	75° 42,96' W	1274	S 10	3	0,8	OBS/OBH	OBS/OBH	OBH zu Wasser	OBH 174
SO181/079-19	03.02.05	11:04	45° 31,89' S	75° 46,96' W	1923	SSW 11	335	0,7	OBS/OBH	OBS/OBH	OBS zu Wasser	OBH 175
SO181/079-20	03.02.05	11:30	45° 33,11' S	75° 50,98' W	2590	S 10	289	1,9	OBS/OBH	OBS/OBH	OBH zu Wasser	OBH 176
SO181/079-21	03.02.05	11:55	45° 34,27' S	75° 54,97' W	3035	S 10	252	2,5	OBS/OBH	OBS/OBH	OBH zu Wasser	OBH 177
SO181/079-22	03.02.05	12:24	45° 35,50' S	75° 59,07' W	3318	SSW 12	236	2,5	OBS/OBH	OBS/OBH	OBH zu Wasser	OBH 178
SO181/079-23	03.02.05	12:51	45° 36,64' S	76° 3,02' W	3310	S 10	280	1,2	OBS/OBH	OBS/OBH	OBS zu Wasser	OBH 179
SO181/079-24	03.02.05	13:16	45° 37,84' S	76° 7,00' W	3291	SSW 10	263	2,3	OBS/OBH	OBS/OBH	OBS zu Wasser	OBH 180
SO181/079-25	03.02.05	13:43	45° 39,02' S	76° 11,02' W	3018	S 10	216	2,2	OBS/OBH	OBS/OBH	OBH zu Wasser	OBH 181
SO181/079-26	03.02.05	14:08	45° 40,28' S	76° 15,03' W	2517	SSW 10	268	2,3	OBS/OBH	OBS/OBH	OBH zu Wasser	OBH 183
SO181/079-27	03.02.05	14:32	45° 41,43' S	76° 19,01' W	2978	S 9	265	3	OBS/OBH	OBS/OBH	OBH zu Wasser	OBH 183
SO181/079-28	03.02.05	14:57	45° 42,60' S	76° 22,97' W	2697	SW 9	257	1,4	OBS/OBH	OBS/OBH	OBH zu Wasser	OBH 184
SO181/079-29	03.02.05	15:25	45° 43,78' S	76° 27,01' W	2348	SSW 8	225	1,5	OBS/OBH	OBS/OBH	OBS zu Wasser	OBH 185
SO181/079-30	03.02.05	15:54	45° 44,94' S	76° 31,00' W	2297	SSW 8	39	0,5	OBS/OBH	OBS/OBH	OBS zu Wasser	OBH 186
SO181/079-31	03.02.05	16:19	45° 46,12' S	76° 34,99' W	2678	SSW 9	241	2,4	OBS/OBH	OBS/OBH	OBS zu Wasser	OBH 187
SO181/079-32	03.02.05	16:45	45° 47,32' S	76° 39,04' W	2823	SSW 8	263	2,5	OBS/OBH	OBS/OBH	OBH zu Wasser	OBH 188
SO181/079-33	03.02.05	17:11	45° 48,52' S	76° 43,02' W	3480	SW 8	268	1,9	OBS/OBH	OBS/OBH	OBH zu Wasser	OBH 189
SO181/079-34	03.02.05	17:37	45° 49,69' S	76° 46,97' W	3734	SW 8	265	1	OBS/OBH	OBS/OBH	OBH zu Wasser	OBH 190
SO181/079-35	03.02.05	18:05	45° 50,88' S	76° 50,98' W	2482	SSW 6	253	2,4	OBS/OBH	OBS/OBH	OBH zu Wasser	OBH 191
SO181/079-36	03.02.05	18:33	45° 52,03' S	76° 54,98' W	2195	SW 8	262	1,2	OBS/OBH	OBS/OBH	OBH zu Wasser	OBH 192

Station	Datum	UTC	Position Lat	Position Lon	Tiefe [m]	Windstärke [m/s]	Kurs [°]	v [kn]	Gerät	Gerätekürzel	Aktion	Bemerkung
SO181/079-37	03.02.05	19:00	45° 53,21' S	76° 59,05' W	2575	SW 9	252	2,2	OBS/OBH	OBS/OBH	OBH zu Wasser	OBH 193
SO181/079-37	03.02.05	19:00	45° 53,21' S	76° 59,05' W	2575	SW 9	252	2,2	OBS/OBH	OBS/OBH	Ende Station	
SO181/080-1	03.02.05	19:10	45° 53,50' S	76° 59,66' W	2225	SW 9	233	4,7	Profil	PR	Stationsbeginn	
SO181/080-1	03.02.05	19:17	45° 53,71' S	76° 59,97' W	2323	WSW 7	237	2,5	Profil	PR	Stb Airgun zu Wasser	Traverse mit 4 x 8 ltr G-Gun
SO181/080-1	03.02.05	19:29	45° 54,00' S	77° 0,47' W	2214	WSW 7	219	1,2	Profil	PR	Bb Airgun zu Wasser	Traverse mit 4 x 8 ltr G-Gun
SO181/080-1	03.02.05	19:38	45° 53,96' S	77° 0,98' W	2417	SW 7	345	3,2	Profil	PR	Airgun eingeschaltet	1. Schuß
SO181/080-1	03.02.05	19:51	45° 53,52' S	77° 0,34' W	2281	WSW 4	78	2,7	Profil	PR	Beginn Profil	Pr # 08, nwk: 067, d: 119 sm
SO181/080-1	03.02.05	19:54	45° 53,47' S	77° 0,13' W	2231	SSW 6	79	2,8	Profil	PR	Streamer zu Wasser	Streamer 100m + 100m Vorlauf
SO181/080-1	04.02.05	18:18	45° 30,83' S	75° 43,40' W	1318	SW 5	85	2,6	Profil	PR	Stb Airgun zu Wasser	Boltgun 32 Liter, STB Baum 5
SO181/080-1	04.02.05	19:11	45° 27,68' S	75° 32,75' W	876	SW 4	59	2,5	Profil	PR	Stb Airgun an Deck	Bolt-Gun 32 ltr
SO181/080-1	05.02.05	09:49	45° 10,59' S	74° 35,14' W	75	S 5	73	3,4	Profil	PR	Kursänderung	nwk: 024,
SO181/080-1	05.02.05	12:09	45° 3,61' S	74° 30,70' W	71	SW 5	19	0,8	Profil	PR	Streamer an Deck	
SO181/080-1	05.02.05	12:09	45° 3,61' S	74° 30,70' W	71	SW 5	19	0,8	Profil	PR	Airgun abgeschaltet	
SO181/080-1	05.02.05	12:09	45° 3,61' S	74° 30,70' W	71	SW 5	19	0,8	Profil	PR	Ende Profil	
SO181/080-1	05.02.05	12:18	45° 3,50' S	74° 30,57' W	72	SW 5	82	1	Profil	PR	Bb airgun an Deck	Traverse mit 4 x 8 ltr. G-Gun
SO181/080-1	05.02.05	12:26	45° 3,39' S	74° 30,44' W	73	WSW 5	33	1,2	Profil	PR	Stb Airgun an Deck	Traverse mit 4 x 8 ltr. G-Gun
SO181/080-1	05.02.05	12:27	45° 3,37' S	74° 30,42' W	74	WSW 5	36	1	Profil	PR	Stationsende	
Transit											Anf. OBH 157	Anf. # 81, d: 8 sm
SO181/081-1	05.02.05	13:10	45° 9,70' S	74° 34,43' W	74	SW 10	203	10,7	OBS/OBH	OBS/OBH	Beginn Station	Aufnahme OBH/S
SO181/081-1	05.02.05	13:12	45° 10,01' S	74° 34,62' W	74	WSW 10	203	9,3	OBS/OBH	OBS/OBH	OBS ausgelöst	OBS 157
SO181/081-1	05.02.05	13:12	45° 10,01' S	74° 34,62' W	74	WSW 10	203	9,3	OBS/OBH	OBS/OBH	OBS gesichtet	OBS 157
SO181/081-1	05.02.05	13:21	45° 10,51' S	74° 35,05' W	74	WSW 5	252	1,3	OBS/OBH	OBS/OBH	OBS an Deck	OBS 157
SO181/081-2	05.02.05	13:38	45° 11,47' S	74° 38,32' W	0	SW 6	247	7,2	OBS/OBH	OBS/OBH	OBS ausgelöst	OBS 158
SO181/081-2	05.02.05	13:40	45° 11,56' S	74° 38,57' W	0	SW 5	240	5,1	OBS/OBH	OBS/OBH	OBS gesichtet	OBS 158
SO181/081-2	05.02.05	13:48	45° 11,66' S	74° 39,14' W	0	SW 2	311	1,6	OBS/OBH	OBS/OBH	OBS an Deck	OBS 158
SO181/081-3	05.02.05	14:05	45° 12,71' S	74° 42,33' W	0	WSW 6	244	6,5	OBS/OBH	OBS/OBH	OBS ausgelöst	OBS 159
SO181/081-3	05.02.05	14:07	45° 12,79' S	74° 42,59' W	0	SW 5	247	5,7	OBS/OBH	OBS/OBH	OBS gesichtet	OBS 159
SO181/081-3	05.02.05	14:14	45° 12,83' S	74° 43,14' W	0	WSW 4	276	1,9	OBS/OBH	OBS/OBH	OBS an Deck	OBS 159
SO181/081-4	05.02.05	14:32	45° 13,87' S	74° 46,27' W	0	SW 9	251	7,7	OBS/OBH	OBS/OBH	OBS ausgelöst	OBS 160
SO181/081-4	05.02.05	14:34	45° 13,94' S	74° 46,57' W	0	SW 7	252	5,3	OBS/OBH	OBS/OBH	OBS gesichtet	OBS 160
SO181/081-4	05.02.05	14:42	45° 13,99' S	74° 47,12' W	0	SW 4	320	1,3	OBS/OBH	OBS/OBH	OBS an Deck	OBS 160
SO181/081-5	05.02.05	14:59	45° 15,05' S	74° 50,12' W	0	SW 10	244	11,3	OBS/OBH	OBS/OBH	OBS ausgelöst	OBS 161
SO181/081-5	05.02.05	15:03	45° 15,19' S	74° 50,66' W	0	SW 6	248	2,7	OBS/OBH	OBS/OBH	OBS gesichtet	OBS 161
SO181/081-5	05.02.05	15:22	45° 15,15' S	74° 51,03' W	0	WSW 4	283	1,6	OBS/OBH	OBS/OBH	OBS an Deck	OBS 161
SO181/081-6	05.02.05	15:47	45° 16,34' S	74° 54,58' W	0	SW 4	254	2	OBS/OBH	OBS/OBH	OBS ausgelöst	OBS 162
SO181/081-6	05.02.05	15:51	45° 16,35' S	74° 54,70' W	0	SW 4	254	1,2	OBS/OBH	OBS/OBH	OBS gesichtet	OBS 162
SO181/081-6	05.02.05	16:01	45° 16,37' S	74° 54,99' W	0	WSW 3	267	1,2	OBS/OBH	OBS/OBH	OBS an Deck	OBS 162
SO181/081-7	05.02.05	16:21	45° 17,48' S	74° 58,40' W	0	WSW 8	248	5,6	OBS/OBH	OBS/OBH	OBS ausgelöst	OBS 163
SO181/081-7	05.02.05	16:25	45° 17,55' S	74° 58,71' W	0	WSW 5	255	1,3	OBS/OBH	OBS/OBH	OBS gesichtet	OBS 163
SO181/081-7	05.02.05	16:38	45° 17,54' S	74° 59,02' W	0	SW 4	231	1,3	OBS/OBH	OBS/OBH	OBS an Deck	OBS 163
SO181/081-8	05.02.05	16:59	45° 18,72' S	75° 2,57' W	0	SW 7	242	4,5	OBS/OBH	OBS/OBH	OBS ausgelöst	OBS 164
SO181/081-8	05.02.05	17:01	45° 18,75' S	75° 2,72' W	0	SW 6	251	3,1	OBS/OBH	OBS/OBH	OBS gesichtet	OBS 164
SO181/081-8	05.02.05	17:10	45° 18,78' S	75° 3,01' W	0	WSW 5	334	1,7	OBS/OBH	OBS/OBH	OBS an Deck	OBS 164

Station	Datum	UTC	PositionLat	PositionLon	Tiefe [m]	Windstärke [m/s]	Kurs [°]	v [kn]	Gerät	Gerätekurzel	Aktion	Bemerkung
SO181/081-9	05.02.05	17:30	45° 19,81' S	75° 6,17' W	0	WSW 10	246	10,4	OBS/OBH	OBS/OBH	OBH ausgelöst	OBS 165
SO181/081-9	05.02.05	17:33	45° 19,84' S	75° 6,67' W	0	WSW 8	247	4,2	OBS/OBH	OBS/OBH	OBS gesichtet	OBS 165
SO181/081-9	05.02.05	17:42	45° 20,00' S	75° 7,06' W	0	W 4	241	0,9	OBS/OBH	OBS/OBH	OBS an Deck	OBS 165
SO181/081-10	05.02.05	18:02	45° 21,09' S	75° 10,57' W	0	WSW 7	250	5,2	OBS/OBH	OBS/OBH	OBS ausgelöst	OBS 166
SO181/081-10	05.02.05	18:04	45° 21,12' S	75° 10,73' W	0	WSW 5	244	3,7	OBS/OBH	OBS/OBH	OBS gesichtet	OBS 166
SO181/081-10	05.02.05	18:11	45° 21,17' S	75° 11,08' W	0	W 5	261	1,1	OBS/OBH	OBS/OBH	OBS an Deck	OBS 166
SO181/081-11	05.02.05	18:31	45° 22,27' S	75° 14,49' W	0	W 6	240	3,2	OBS/OBH	OBS/OBH	OBS ausgelöst	OBS 167
SO181/081-11	05.02.05	18:32	45° 22,29' S	75° 14,58' W	0	W 6	255	3,7	OBS/OBH	OBS/OBH	OBS gesichtet	OBS 167
SO181/081-11	05.02.05	18:42	45° 22,35' S	75° 14,82' W	0	W 4	285	0,8	OBS/OBH	OBS/OBH	OBS an Deck	OBS 167
SO181/081-12	05.02.05	18:02	45° 23,43' S	75° 18,33' W	0	W 9	248	7	OBS/OBH	OBS/OBH	OBS ausgelöst	OBS 168
SO181/081-12	05.02.05	19:04	45° 23,50' S	75° 18,60' W	0	WSW 8	247	5	OBS/OBH	OBS/OBH	OBS gesichtet	OBS 168
SO181/081-12	05.02.05	19:10	45° 23,56' S	75° 19,03' W	0	W 6	299	0,5	OBS/OBH	OBS/OBH	OBS an Deck	OBS 168
SO181/081-13	05.02.05	19:30	45° 24,58' S	75° 22,29' W	0	W 8	252	5	OBS/OBH	OBS/OBH	OBS ausgelöst	OBS 169
SO181/081-13	05.02.05	19:33	45° 24,65' S	75° 22,60' W	0	WSW 7	231	4,5	OBS/OBH	OBS/OBH	OBS gesichtet	OBS 169
SO181/081-13	05.02.05	19:42	45° 24,85' S	75° 23,08' W	0	WSW 6	7	1,3	OBS/OBH	OBS/OBH	OBS an Deck	OBS 169
SO181/081-14	05.02.05	20:01	45° 25,80' S	75° 26,25' W	0	WSW 10	244	5,6	OBS/OBH	OBS/OBH	OBS ausgelöst	OBS 170
SO181/081-14	05.02.05	20:05	45° 25,90' S	75° 26,67' W	0	W 7	250	3,8	OBS/OBH	OBS/OBH	OBS gesichtet	OBS 170
SO181/081-14	05.02.05	20:12	45° 25,84' S	75° 26,98' W	0	WSW 6	271	0,2	OBS/OBH	OBS/OBH	OBS an Deck	OBS 170
SO181/081-15	05.02.05	20:29	45° 26,91' S	75° 29,92' W	0	W 11	250	11,2	OBS/OBH	OBS/OBH	OBH ausgelöst	OBH 171
SO181/081-15	05.02.05	20:36	45° 27,07' S	75° 30,77' W	0	WSW 7	250	0,9	OBS/OBH	OBS/OBH	OBH gesichtet	OBH 171
SO181/081-15	05.02.05	20:45	45° 27,05' S	75° 31,08' W	0	WSW 7	303	0,8	OBS/OBH	OBS/OBH	OBH an Deck	OBH 171
SO181/081-16	05.02.05	20:58	45° 27,86' S	75° 33,18' W	0	WSW 10	243	11,3	OBS/OBH	OBS/OBH	OBH ausgelöst	OBH 172
SO181/081-16	05.02.05	21:11	45° 28,34' S	75° 34,64' W	0	W 6	275	0,9	OBS/OBH	OBS/OBH	OBH gesichtet	OBH 172
SO181/081-16	05.02.05	21:18	45° 28,28' S	75° 35,01' W	0	W 6	310	0,5	OBS/OBH	OBS/OBH	OBH an Deck	OBH 172
SO181/081-17	05.02.05	21:35	45° 29,21' S	75° 37,61' W	0	W 11	245	9,6	OBS/OBH	OBS/OBH	OBH ausgelöst	OBH 173
SO181/081-17	05.02.05	21:52	45° 29,57' S	75° 38,75' W	0	W 7	72	0,3	OBS/OBH	OBS/OBH	OBH gesichtet	OBH 173
SO181/081-17	05.02.05	22:01	45° 29,41' S	75° 38,94' W	0	WSW 7	188	1,6	OBS/OBH	OBS/OBH	OBH an Deck	OBH 173
SO181/081-18	05.02.05	22:17	45° 30,31' S	75° 41,33' W	0	W 10	239	10,4	OBS/OBH	OBS/OBH	OBH ausgelöst	OBH 174
SO181/081-18	05.02.05	22:35	45° 30,72' S	75° 42,68' W	0	WSW 6	11	0,5	OBS/OBH	OBS/OBH	OBH gesichtet	OBH 174
SO181/081-18	05.02.05	22:44	45° 30,59' S	75° 42,91' W	0	WSW 6	18	0,7	OBS/OBH	OBS/OBH	OBH an Deck	OBH 174
SO181/081-18	05.02.05	22:58	45° 31,35' S	75° 44,90' W	0	W 10	243	11,7	OBS/OBH	OBS/OBH	OBH ausgelöst	OBH 175
SO181/081-19	05.02.05	23:15	45° 31,86' S	75° 46,68' W	0	W 6	294	0,8	OBS/OBH	OBS/OBH	OBH gesichtet	OBH 175
SO181/081-19	05.02.05	23:23	45° 31,76' S	75° 46,68' W	0	W 7	18	1,4	OBS/OBH	OBS/OBH	OBH an Deck	OBH 175
SO181/081-19	05.02.05	23:25	45° 31,73' S	75° 46,89' W	0	WSW 6	262	1,6	OBS/OBH	OBS/OBH	OBH ausgelöst	OBH 176
SO181/081-19	05.02.05	23:57	45° 33,05' S	75° 50,88' W	0	W 5	84	0,4	OBS/OBH	OBS/OBH	OBH gesichtet	OBH 176
SO181/081-19	06.02.05	00:00	45° 33,04' S	75° 50,82' W	0	W 5	6	0,5	OBS/OBH	OBS/OBH	OBH ausgelöst	OBH 177
SO181/081-19	06.02.05	00:08	45° 32,95' S	75° 50,74' W	0	WSW 6	49	1,7	OBS/OBH	OBS/OBH	OBH an Deck	OBH 176
SO181/081-20	06.02.05	00:47	45° 34,20' S	75° 54,65' W	0	W 4	11	1	OBS/OBH	OBS/OBH	OBH gesichtet	OBH 177
SO181/081-20	06.02.05	01:00	45° 34,21' S	75° 54,79' W	0	W 5	317	0,6	OBS/OBH	OBS/OBH	OBH ausgelöst	OBH 178
SO181/081-20	06.02.05	01:13	45° 34,20' S	75° 54,72' W	0	WNW 4	96	0,3	OBS/OBH	OBS/OBH	OBH an Deck	OBH 177
SO181/081-21	06.02.05	01:38	45° 35,41' S	75° 58,58' W	0	W 6	262	1,2	OBS/OBH	OBS/OBH	OBH gesichtet	OBH 178
SO181/081-21	06.02.05	01:40	45° 35,42' S	75° 58,65' W	0	W 6	275	1,3	OBS/OBH	OBS/OBH	OBH ausgelöst	OBH 179
SO181/081-21	06.02.05	01:46	45° 35,46' S	75° 58,95' W	0	WNW 6	287	0,8	OBS/OBH	OBS/OBH	OBH an Deck	OBH 178

Station	Datum	UTC	PositionLat	PositionLon	Tiefe [m]	Windstärke [m/s]	Kurs [°]	v [kn]	Gerät	Gerätekurzel	Aktion	Bemerkung
SO181/081-22	06.02.05	02:15	45° 36,62' S	76° 2,83' W	0	W 6	270	2	OBS/OBH	OBS/OBH	OBH ausgelöst	OBH 180
SO181/081-22	06.02.05	02:21	45° 36,61' S	76° 2,84' W	0	W 5	52	1,3	OBS/OBH	OBS/OBH	OBH gesichtet	OBH 179
SO181/081-22	06.02.05	02:32	45° 36,61' S	76° 2,80' W	0	W 6	192	0,8	OBS/OBH	OBS/OBH	OBH an Deck	OBH 179
SO181/081-23	06.02.05	02:50	45° 37,57' S	76° 5,78' W	0	W 9	248	10,3	OBS/OBH	OBS/OBH	OBH gesichtet	OBH 180
SO181/081-23	06.02.05	02:53	45° 37,71' S	76° 6,38' W	0	W 10	253	6	OBS/OBH	OBS/OBH	OBH ausgelöst	OBH 181
SO181/081-23	06.02.05	03:08	45° 37,66' S	76° 6,82' W	0	W 6	331	0,8	OBS/OBH	OBS/OBH	OBH an Deck	OBH 180
SO181/081-24	06.02.05	03:25	45° 38,53' S	76° 9,32' W	0	W 10	245	9,7	OBS/OBH	OBS/OBH	OBH gesichtet	OBH 181
SO181/081-24	06.02.05	03:45	45° 38,85' S	76° 10,73' W	0	W 5	347	1,4	OBS/OBH	OBS/OBH	OBH an Deck	OBH 181
SO181/081-25	06.02.05	04:14	45° 40,14' S	76° 14,73' W	0	WNW 6	50	0,3	OBS/OBH	OBS/OBH	OBH ausgelöst	OBH 183
SO181/081-25	06.02.05	04:18	45° 40,13' S	76° 14,68' W	0	W 6	56	0,7	OBS/OBH	OBS/OBH	OBH gesichtet	OBH 182
SO181/081-25	06.02.05	04:28	45° 40,20' S	76° 14,90' W	0	NW 6	221	2,8	OBS/OBH	OBS/OBH	OBH an Deck	OBH 182
SO181/081-26	06.02.05	04:46	45° 40,96' S	76° 17,42' W	0	WNW 9	248	8,8	OBS/OBH	OBS/OBH	OBH gesichtet	OBH 183
SO181/081-26	06.02.05	04:48	45° 41,08' S	76° 17,82' W	0	WNW 9	245	8	OBS/OBH	OBS/OBH	OBH ausgelöst	OBH 184
SO181/081-26	06.02.05	05:18	45° 41,34' S	76° 18,95' W	0	WSW 9	0	0,9	OBS/OBH	OBS/OBH	OBH an Deck	OBH 183
SO181/081-27	06.02.05	05:23	45° 41,38' S	76° 19,26' W	0	W 10	249	6,6	OBS/OBH	OBS/OBH	OBH gesichtet	OBH 184
SO181/081-27	06.02.05	05:33	45° 42,03' S	76° 21,14' W	0	W 10	241	8,9	OBS/OBH	OBS/OBH	OBH ausgelöst	OBH 185
SO181/081-27	06.02.05	05:45	45° 42,82' S	76° 22,85' W	0	W 7	342	1,1	OBS/OBH	OBS/OBH	OBH an Deck	OBH 184
SO181/081-28	06.02.05	06:01	45° 43,26' S	76° 25,18' W	0	WSW 12	245	11	OBS/OBH	OBS/OBH	OBH gesichtet	OBH 185
SO181/081-28	06.02.05	06:06	45° 43,57' S	76° 26,29' W	0	WSW 12	249	9	OBS/OBH	OBS/OBH	OBH ausgelöst	OBH 186
SO181/081-28	06.02.05	06:15	45° 43,70' S	76° 26,83' W	0	WSW 7	10	0,4	OBS/OBH	OBS/OBH	OBH an Deck	OBH 185
SO181/081-29	06.02.05	06:31	45° 44,42' S	76° 29,31' W	0	WSW 12	246	9,8	OBS/OBH	OBS/OBH	OBH gesichtet	OBH 186
SO181/081-29	06.02.05	07:15	45° 44,88' S	76° 30,87' W	0	SW 6	329	0,7	OBS/OBH	OBS/OBH	OBH an Deck	OBH 186
SO181/081-30	06.02.05	07:19	45° 44,96' S	76° 30,95' W	0	WSW 8	244	6	OBS/OBH	OBS/OBH	OBH ausgelöst	OBH 187
SO181/081-30	06.02.05	07:20	45° 45,00' S	76° 31,09' W	0	WSW 8	243	7,6	OBS/OBH	OBS/OBH	OBH gesichtet	OBH 187
SO181/081-30	06.02.05	07:21	45° 45,05' S	76° 31,28' W	0	WSW 9	239	8,1	OBS/OBH	OBS/OBH	OBH ausgelöst	OBH 188
SO181/081-30	06.02.05	07:45	45° 45,88' S	76° 34,83' W	0	WSW 5	357	2,1	OBS/OBH	OBS/OBH	OBH an Deck	OBH 187
SO181/081-31	06.02.05	08:17	45° 47,20' S	76° 38,51' W	0	SW 4	286	1,1	OBS/OBH	OBS/OBH	OBH gesichtet	OBH 188
SO181/081-31	06.02.05	08:30	45° 47,20' S	76° 39,04' W	0	WSW 5	316	1,8	OBS/OBH	OBS/OBH	OBH ausgelöst	OBH 189
SO181/081-31	06.02.05	08:32	45° 47,18' S	76° 39,07' W	0	SW 4	254	0,4	OBS/OBH	OBS/OBH	OBH an Deck	OBH 188
SO181/081-32	06.02.05	08:57	45° 48,46' S	76° 42,43' W	0	SW 3	295	0,4	OBS/OBH	OBS/OBH	OBH ausgelöst	OBH 190
SO181/081-32	06.02.05	09:17	45° 48,35' S	76° 42,49' W	0	WSW 4	247	1	OBS/OBH	OBS/OBH	OBH gesichtet	OBH 189 gehört; KEIN Blitzar
SO181/081-32	06.02.05	09:30	45° 48,48' S	76° 42,89' W	0	WSW 6	244	2,1	OBS/OBH	OBS/OBH	OBH gesichtet	OBH 189
SO181/081-32	06.02.05	09:44	45° 48,27' S	76° 43,27' W	0	SW 5	336	1,5	OBS/OBH	OBS/OBH	OBH an Deck	OBH 189
SO181/081-33	06.02.05	10:00	45° 49,17' S	76° 45,59' W	0	WSW 10	233	10,8	OBS/OBH	OBS/OBH	OBH gesichtet	OBH 190
SO181/081-33	06.02.05	10:02	45° 49,28' S	76° 45,97' W	0	W 9	259	7,8	OBS/OBH	OBS/OBH	OBH ausgelöst	OBH 191
SO181/081-33	06.02.05	10:13	45° 49,46' S	76° 47,23' W	0	WSW 5	281	1,6	OBS/OBH	OBS/OBH	OBH an Deck	OBH 190
SO181/081-34	06.02.05	10:36	45° 50,86' S	76° 50,57' W	0	WSW 4	250	2,7	OBS/OBH	OBS/OBH	OBH gesichtet	OBH 191
SO181/081-34	06.02.05	10:38	45° 50,85' S	76° 50,68' W	0	WSW 4	280	3,1	OBS/OBH	OBS/OBH	OBH ausgelöst	OBH 192
SO181/081-34	06.02.05	10:45	45° 50,76' S	76° 51,11' W	0	WSW 3	243	1,4	OBS/OBH	OBS/OBH	OBH an Deck	OBH 191
SO181/081-35	06.02.05	11:02	45° 51,67' S	76° 53,95' W	0	W 9	242	9,8	OBS/OBH	OBS/OBH	OBH gesichtet	OBH 192
SO181/081-35	06.02.05	11:06	45° 51,89' S	76° 54,64' W	0	W 7	244	5	OBS/OBH	OBS/OBH	OBS ausgelöst	OBS 193
SO181/081-35	06.02.05	11:15	45° 52,05' S	76° 55,21' W	0	WNW 3	341	1	OBS/OBH	OBS/OBH	OBH an Deck	OBH 192
SO181/081-36	06.02.05	11:32	45° 52,96' S	76° 58,07' W	0	W 7	247	7,5	OBS/OBH	OBS/OBH	OBS gesichtet	OBS 193

Station	Datum	UTC	PositionLat	PositionLon	Tiefe [m]	Windstärke [m/s]	Kurs [°]	v [kn]	Gerät	Geräte Kürzel	Aktion	Bemerkung
SO181/081-36	06.02.05	11:49	45° 53,39' S	78° 59,44' W	0	WNW 2	192	0,8	OBS/OBH	OBS/OBH	OBS an Deck	OBS 193
SO181/081-36	06.02.05	11:50	45° 53,40' S	78° 59,45' W	0	WNW 3	211	1,4	OBS/OBH	OBS/OBH	Ende Station	
SO181/082-1	06.02.05	11:56	45° 53,31' S	78° 59,43' W	0	WSW 2	10	2,9	Magnetometer	MAGN	Beginn Station	
SO181/082-1	06.02.05	12:03	45° 52,84' S	78° 59,28' W	2493	WSW 3	2	5,5	Magnetometer	MAGN	Magnetometer zu Wasser	300m
SO181/082-1	06.02.05	15:20	45° 25,24' S	77° 28,72' W	2649	NW 8	340	10,1	Magnetometer	MAGN	Kursänderung	rwk: 078°, d: 43 sm
SO181/082-1	06.02.05	19:20	45° 15,99' S	78° 30,15' W	3254	SW 1	59	10,4	Magnetometer	MAGN	Kursänderung	rwk: 360, d:13 sm
SO181/082-1	06.02.05	20:32	45° 3,50' S	78° 30,48' W	3258	SSW 5	315	10,2	Magnetometer	MAGN	Kursänderung	rwk: 280, d: 79 sm
SO181/082-1	07.02.05	04:07	45° 16,88' S	78° 19,91' W	2693	NNW 6	307	10,7	Magnetometer	MAGN	Kursänderung	rwk: 360°, d: 10 sm
SO181/082-1	07.02.05	05:00	45° 9,00' S	78° 19,95' W	2512	WNW 6	2	10,3	Magnetometer	MAGN	Kursänderung	rwk: 080°, d: 86 sm
SO181/082-1	07.02.05	13:11	44° 52,07' S	78° 20,10' W	3272	S 5	66	10,7	Magnetometer	MAGN	Kursänderung	rwk: 65, d: 85 sm
SO181/082-1	07.02.05	18:00	44° 29,71' S	75° 14,09' W	158	SW 7	56	5,9	Magnetometer	MAGN	Ende Profil	
SO181/082-1	07.02.05	18:03	44° 29,60' S	75° 13,78' W	157	SW 6	58	4,2	Magnetometer	MAGN	Magnetometer an Deck	
SO181/082-1	07.02.05	18:04	44° 29,57' S	75° 13,69' W	156	SW 6	60	5,1	Magnetometer	MAGN	Ende Station	
Transit							65	11	Anf. # 83			d: 33 sm
SO181/083-1	07.02.05	21:08	44° 15,39' S	74° 32,02' W	63	SW 14	154	2,2	OBS/OBH	OBS/OBH	Beginn Station	
SO181/083-1	07.02.05	21:09	44° 15,41' S	74° 32,02' W	64	SW 13	152	0,1	OBS/OBH	OBS/OBH	OBS zu Wasser	OBS 70
SO181/083-2	07.02.05	21:33	44° 16,24' S	74° 36,02' W	86	S 10	235	2	OBS/OBH	OBS/OBH	OBS zu Wasser	OBS 71
SO181/083-3	07.02.05	21:56	44° 17,08' S	74° 40,00' W	58	SSW 7	167	1,8	OBS/OBH	OBS/OBH	OBS zu Wasser	OBS 72
SO181/083-4	07.02.05	22:18	44° 17,86' S	74° 44,02' W	49	S 7	246	1,3	OBS/OBH	OBS/OBH	OBS zu Wasser	OBS 73
SO181/083-5	07.02.05	22:43	44° 18,68' S	74° 47,98' W	45	SSW 10	250	0,7	OBS/OBH	OBS/OBH	OBS zu Wasser	OBS 74
SO181/083-6	07.02.05	23:08	44° 19,48' S	74° 52,00' W	48	SW 10	242	2,2	OBS/OBH	OBS/OBH	OBS zu Wasser	OBS 75
SO181/083-7	07.02.05	23:31	44° 20,31' S	74° 56,03' W	86	SSW 8	236	1,9	OBS/OBH	OBS/OBH	OBS zu Wasser	OBS 76
SO181/083-8	07.02.05	23:52	44° 21,11' S	75° 0,01' W	149	S 8	239	2	OBS/OBH	OBS/OBH	OBS zu Wasser	OBS 77
SO181/083-9	08.02.05	00:16	44° 21,91' S	75° 4,01' W	188	S 7	260	1,8	OBS/OBH	OBS/OBH	OBS zu Wasser	OBS 78
SO181/083-10	08.02.05	00:39	44° 22,71' S	75° 7,96' W	129	SSW 10	283	1,9	OBS/OBH	OBS/OBH	OBS zu Wasser	OBS 79
SO181/083-11	08.02.05	01:04	44° 23,53' S	75° 11,96' W	127	SSW 9	275	1,1	OBS/OBH	OBS/OBH	OBS zu Wasser	OBS 80
SO181/083-12	08.02.05	01:27	44° 24,34' S	75° 15,96' W	179	S 10	261	2,2	OBS/OBH	OBS/OBH	OBS zu Wasser	OBS 81
SO181/083-13	08.02.05	01:51	44° 25,18' S	75° 19,98' W	377	S 10	269	2,2	OBS/OBH	OBS/OBH	OBS zu Wasser	OBS 82
SO181/083-14	08.02.05	02:15	44° 26,03' S	75° 24,02' W	1079	S 10	253	2,3	OBS/OBH	OBS/OBH	OBS zu Wasser	OBS 83
SO181/083-15	08.02.05	02:37	44° 26,82' S	75° 28,02' W	1350	S 11	275	2,2	OBS/OBH	OBS/OBH	OBS zu Wasser	OBS 84
SO181/083-16	08.02.05	03:03	44° 27,60' S	75° 32,00' W	1182	SSW 11	220	1,4	OBS/OBH	OBS/OBH	OBS zu Wasser	OBS 85
SO181/083-17	08.02.05	03:39	44° 28,44' S	75° 36,03' W	897	SSW 11	273	2	OBS/OBH	OBS/OBH	OBS zu Wasser	OBS 86
SO181/083-18	08.02.05	04:07	44° 29,27' S	75° 40,00' W	1615	SSW 12	256	2,1	OBS/OBH	OBS/OBH	OBS zu Wasser	OBS 87
SO181/083-19	08.02.05	04:33	44° 30,07' S	75° 43,99' W	2626	SSW 11	268	2,4	OBS/OBH	OBS/OBH	OBS zu Wasser	OBS 88
SO181/083-20	08.02.05	05:01	44° 30,87' S	75° 48,00' W	3316	SSW 9	312	2,1	OBS/OBH	OBS/OBH	OBS zu Wasser	OBS 89
SO181/083-21	08.02.05	05:27	44° 31,69' S	75° 51,99' W	3322	SSW 10	257	0,4	OBS/OBH	OBS/OBH	OBS zu Wasser	OBS 90
SO181/083-22	08.02.05	05:56	44° 32,53' S	75° 56,00' W	3309	SSW 11	280	1,2	OBS/OBH	OBS/OBH	OBS zu Wasser	OBS 91
SO181/083-23	08.02.05	06:25	44° 33,36' S	76° 0,00' W	3329	S 9	289	1,1	OBS/OBH	OBS/OBH	OBS zu Wasser	OBS 92
SO181/083-24	08.02.05	07:00	44° 34,41' S	76° 5,04' W	3296	SSE 8	282	1,1	OBS/OBH	OBS/OBH	OBS zu Wasser	OBS 93
SO181/083-25	08.02.05	07:29	44° 35,41' S	76° 9,95' W	3278	S 11	157	1,2	OBS/OBH	OBS/OBH	OBS zu Wasser	OBS 94
SO181/083-26	08.02.05	07:58	44° 36,45' S	76° 15,00' W	3274	SSE 10	149	0,3	OBS/OBH	OBS/OBH	OBS zu Wasser	OBS 95
SO181/083-27	08.02.05	08:28	44° 37,45' S	76° 20,01' W	3245	S 10	356	0,2	OBS/OBH	OBS/OBH	OBS zu Wasser	OBS 96
SO181/083-28	08.02.05	08:56	44° 38,46' S	76° 24,98' W	3233	S 10	270	1,5	OBS/OBH	OBS/OBH	OBS zu Wasser	OBS 97

Station	Datum	UTC	PositionLat	PositionLon	Tiefe [m]	Windstärke [m/s]	Kurs [°]	v [kn]	Gerät	Gerätekürzel	Aktion	Bemerkung
SO181/083-29	08.02.05	09:29	44° 39.46' S	76° 29.98' W	3251	S 8	273	0.4	OBS/OBH	OBS/OBH	OBH zu Wasser	OBH 98
SO181/083-30	08.02.05	09:59	44° 40.49' S	76° 34.99' W	3138	S 9	183	1	OBS/OBH	OBS/OBH	OBH zu Wasser	OBH 99
SO181/083-31	08.02.05	10:28	44° 41.51' S	76° 39.99' W	3026	S 10	212	1	OBS/OBH	OBS/OBH	OBH zu Wasser	OBH 100
SO181/083-32	08.02.05	10:58	44° 42.53' S	76° 45.01' W	3212	S 8	36	0.6	OBS/OBH	OBS/OBH	OBH zu Wasser	OBH 101
SO181/083-33	08.02.05	11:28	44° 43.54' S	76° 50.01' W	2983	S 7	264	2	OBS/OBH	OBS/OBH	OBH zu Wasser	OBH 102
SO181/083-34	08.02.05	11:55	44° 44.54' S	76° 55.01' W	2956	S 6	265	1.8	OBS/OBH	OBS/OBH	OBH zu Wasser	OBH 103
SO181/083-35	08.02.05	12:21	44° 45.56' S	77° 0.00' W	3069	SSE 7	213	1.5	OBS/OBH	OBS/OBH	OBH zu Wasser	OBH 104
SO181/083-36	08.02.05	12:48	44° 46.61' S	77° 4.99' W	2982	S 5	218	1.9	OBS/OBH	OBS/OBH	OBH zu Wasser	OBH 105
SO181/083-37	08.02.05	13:14	44° 47.62' S	77° 9.98' W	2916	SSW 5	217	2.9	OBS/OBH	OBS/OBH	OBH zu Wasser	OBH 106
SO181/083-38	08.02.05	13:42	44° 48.61' S	77° 14.98' W	2970	WSW 5	263	2.1	OBS/OBH	OBS/OBH	OBH zu Wasser	OBH 107
SO181/083-39	08.02.05	14:09	44° 49.64' S	77° 20.02' W	3290	SW 5	257	2.1	OBS/OBH	OBS/OBH	OBH zu Wasser	OBH 108
SO181/083-40	08.02.05	14:35	44° 50.68' S	77° 25.01' W	2933	WSW 5	242	2	OBS/OBH	OBS/OBH	OBH zu Wasser	OBH 109
SO181/083-41	08.02.05	15:02	44° 51.68' S	77° 29.93' W	2913	SW 6	267	2.6	OBS/OBH	OBS/OBH	OBH zu Wasser	OBH 110
SO181/083-42	08.02.05	15:34	44° 52.68' S	77° 35.00' W	2531	SW 6	277	1.4	OBS/OBH	OBS/OBH	OBH zu Wasser	OBH 111
SO181/083-43	08.02.05	16:02	44° 53.67' S	77° 39.93' W	3081	SSW 6	270	2.7	OBS/OBH	OBS/OBH	OBH zu Wasser	OBH 112
SO181/083-44	08.02.05	16:33	44° 54.69' S	77° 44.98' W	3214	SSW 7	261	3	OBS/OBH	OBS/OBH	OBH zu Wasser	OBH 195
SO181/083-45	08.02.05	17:06	44° 55.71' S	77° 50.01' W	2956	SW 7	262	2.1	OBS/OBH	OBS/OBH	OBH zu Wasser	OBH 196
SO181/083-46	08.02.05	17:36	44° 56.72' S	77° 55.08' W	2786	SSW 8	236	1.9	OBS/OBH	OBS/OBH	OBH zu Wasser	OBH 197
SO181/083-47	08.02.05	18:06	44° 57.71' S	78° 0.00' W	2628	SW 5	267	1.8	OBS/OBH	OBS/OBH	OBH zu Wasser	OBH 198
SO181/083-48	08.02.05	18:33	44° 58.71' S	78° 4.99' W	2520	SSW 5	250	1.6	OBS/OBH	OBS/OBH	OBH zu Wasser	OBH 199
SO181/083-49	08.02.05	19:00	44° 59.71' S	78° 9.99' W	3567	SW 6	255	2.4	OBS/OBH	OBS/OBH	OBH zu Wasser	OBH 200
SO181/083-50	08.02.05	19:29	45° 0.73' S	78° 15.01' W	2730	WSW 6	268	3	OBS/OBH	OBS/OBH	OBH zu Wasser	OBH 201
SO181/083-50	08.02.05	19:30	45° 0.73' S	78° 15.06' W	2783	WSW 5	254	1.4	OBS/OBH	OBS/OBH	Ende Station	Anf. # 84, d: 4 sm
SO181/084-1	08.02.05	19:57	45° 2.07' S	78° 20.58' W	2477	W 9	273	5.9	Profil	PR	Stationsbeginn	
SO181/084-1	08.02.05	20:05	45° 1.87' S	78° 20.31' W	2405	WSW 3	73	3.3	Profil	PR	Streamer zu Wasser	Streamer 100m+100 m Vorlauf
SO181/084-1	08.02.05	20:12	45° 1.76' S	78° 19.84' W	2312	WSW 3	70	2.9	Profil	PR	Stb Airgun zu Wasser	Traverse mit 4 x 8 ltr. G-Gun's
SO181/084-1	08.02.05	20:21	45° 1.84' S	78° 19.30' W	2296	WSW 3	73	2.5	Profil	PR	Bb Airgun zu Wasser	Traverse mit 4 x 8 ltr. G-Gun's
SO181/084-1	08.02.05	20:42	45° 1.33' S	78° 17.81' W	2483	WSW 3	68	2.8	Profil	PR	Beginn Profil	d: 167 sm
SO181/084-1	08.02.05	20:42	45° 1.33' S	78° 17.81' W	2483	WSW 3	68	2.8	Profil	PR	Airgun eingeschaltet	1. Schuß
SO181/084-1	10.02.05	19:51	44° 15.41' S	74° 32.12' W	64	SSW 11	60	4.6	Profil	PR	Kursänderung	rwk: 015, d: 5 sm
SO181/084-1	10.02.05	20:08	44° 14.48' S	74° 31.68' W	79	SSW 7	26	2.8	Profil	PR	Streamer an Deck	
SO181/084-1	10.02.05	21:00	44° 11.99' S	74° 30.78' W	82	SSW 9	18	2.7	Profil	PR	Airgun abgeschaltet	
SO181/084-1	10.02.05	21:00	44° 11.99' S	74° 30.78' W	82	SSW 9	18	2.7	Profil	PR	Ende Profil	
SO181/084-1	10.02.05	21:08	44° 11.65' S	74° 30.63' W	57	SSW 9	13	3.1	Profil	PR	Bb airgun an Deck	
SO181/084-1	10.02.05	21:17	44° 11.22' S	74° 30.46' W	57	SSW 9	18	2.7	Profil	PR	Stb Airgun an Deck	
SO181/084-1	10.02.05	21:18	44° 11.18' S	74° 30.44' W	57	SSW 9	22	3	Profil	PR	Stationsende	
SO181/085-1	10.02.05	21:58	44° 14.84' S	74° 31.84' W	0	SW 19	199	8.3	OBS/OBH	OBS/OBH	Beginn Station	
SO181/085-1	10.02.05	21:58	44° 14.88' S	74° 31.74' W	0	SW 17	195	5.9	OBS/OBH	OBS/OBH	OBS ausgelöst	OBH 70
SO181/085-1	10.02.05	21:58	44° 14.88' S	74° 31.74' W	0	SW 17	195	5.9	OBS/OBH	OBS/OBH	OBS gesichtet	OBH 70
SO181/085-1	10.02.05	22:13	44° 15.37' S	74° 32.24' W	0	SSW 14	329	1.3	OBS/OBH	OBS/OBH	OBS an Deck	OBH 70
SO181/085-2	10.02.05	22:31	44° 15.92' S	74° 35.58' W	0	S 14	252	8.2	OBS/OBH	OBS/OBH	OBS ausgelöst	OBH 71
SO181/085-2	10.02.05	22:31	44° 15.92' S	74° 35.58' W	0	S 14	252	8.2	OBS/OBH	OBS/OBH	OBS gesichtet	OBH 71
SO181/085-2	10.02.05	22:41	44° 16.17' S	74° 36.30' W	0	SW 12	295	1.1	OBS/OBH	OBS/OBH	OBS an Deck	OBH 71

Station	Datum	UTC	PositionLat	PositionLon	Tiefe [m]	Windstärke [m/s]	Kurs [°]	v [kn]	Gerät	Gerätekürzel	Aktion	Bemerkung
SO181/085-3	10.02.05	22:59	44° 16,76' S	74° 39,61' W	0	S 10	240	4,6	OBS/OBH	OBS/OBH	OBS ausgelöst	OBS 72
SO181/085-3	10.02.05	23:00	44° 16,79' S	74° 39,70' W	0	SSW 10	231	4,2	OBS/OBH	OBS/OBH	OBS gesichtet	OBS 72
SO181/085-3	10.02.05	23:09	44° 17,01' S	74° 40,37' W	0	SSW 9	269	1,8	OBS/OBH	OBS/OBH	OBS an Deck	OBS 72
SO181/085-4	10.02.05	23:26	44° 17,73' S	74° 43,64' W	0	S 12	254	5,5	OBS/OBH	OBS/OBH	OBS ausgelöst	OBS 73
SO181/085-4	10.02.05	23:27	44° 17,74' S	74° 43,75' W	0	S 12	265	4,1	OBS/OBH	OBS/OBH	OBS gesichtet	OBS 73
SO181/085-4	10.02.05	23:50	44° 17,70' S	74° 44,90' W	0	SSW 11	292	0,7	OBS/OBH	OBS/OBH	OBS an Deck	OBS 73
SO181/085-5	11.02.05	00:06	44° 18,56' S	74° 47,81' W	0	SSW 9	265	4,5	OBS/OBH	OBS/OBH	OBS ausgelöst	OBS 74
SO181/085-5	11.02.05	00:08	44° 18,58' S	74° 47,95' W	0	SSW 10	264	2,2	OBS/OBH	OBS/OBH	OBS gesichtet	OBS 74
SO181/085-5	11.02.05	00:14	44° 18,68' S	74° 48,18' W	0	SW 10	286	1,2	OBS/OBH	OBS/OBH	OBS an Deck	OBS 74
SO181/085-6	11.02.05	00:26	44° 19,29' S	74° 51,29' W	0	SSW 14	255	8,9	OBS/OBH	OBS/OBH	OBS ausgelöst	OBS 75
SO181/085-6	11.02.05	00:32	44° 19,44' S	74° 51,88' W	0	SSW 12	245	4,1	OBS/OBH	OBS/OBH	OBS gesichtet	OBS 75
SO181/085-6	11.02.05	00:39	44° 19,47' S	74° 52,30' W	0	SSW 10	274	2	OBS/OBH	OBS/OBH	OBS an Deck	OBS 75
SO181/085-7	11.02.05	00:53	44° 20,15' S	74° 55,29' W	0	SSW 12	251	8,8	OBS/OBH	OBS/OBH	OBS ausgelöst	OBS 76
SO181/085-7	11.02.05	00:55	44° 20,22' S	74° 55,59' W	0	SSW 11	258	6	OBS/OBH	OBS/OBH	OBS gesichtet	OBS 76
SO181/085-7	11.02.05	01:03	44° 20,37' S	74° 56,28' W	0	SSW 10	248	1,5	OBS/OBH	OBS/OBH	OBS an Deck	OBS 76
SO181/085-8	11.02.05	01:19	44° 21,00' S	74° 59,47' W	0	SSW 13	258	5,4	OBS/OBH	OBS/OBH	OBS ausgelöst	OBS 77
SO181/085-8	11.02.05	01:22	44° 21,05' S	74° 59,77' W	0	SSW 12	255	3,3	OBS/OBH	OBS/OBH	OBS gesichtet	OBS 77
SO181/085-8	11.02.05	01:29	44° 21,13' S	75° 0,12' W	0	SW 11	288	1,1	OBS/OBH	OBS/OBH	OBS an Deck	OBS 77
SO181/085-9	11.02.05	01:44	44° 21,76' S	75° 3,08' W	0	SSW 14	252	9,9	OBS/OBH	OBS/OBH	OBS ausgelöst	OBS 78
SO181/085-9	11.02.05	01:48	44° 21,83' S	75° 3,44' W	0	SSW 12	253	7,2	OBS/OBH	OBS/OBH	OBS gesichtet	OBS 78
SO181/085-9	11.02.05	01:55	44° 21,81' S	75° 4,07' W	0	SSW 11	290	1,2	OBS/OBH	OBS/OBH	OBS an Deck	OBS 78
SO181/085-10	11.02.05	02:12	44° 22,59' S	75° 7,28' W	0	SSW 15	251	6	OBS/OBH	OBS/OBH	OBS ausgelöst	OBS 79
SO181/085-10	11.02.05	02:14	44° 22,62' S	75° 7,47' W	0	SSW 12	278	3,5	OBS/OBH	OBS/OBH	OBS gesichtet	OBS 79
SO181/085-10	11.02.05	02:21	44° 22,51' S	75° 7,96' W	0	S 12	338	1,6	OBS/OBH	OBS/OBH	OBS an Deck	OBS 79
SO181/085-11	11.02.05	02:39	44° 23,30' S	75° 10,93' W	0	SSW 15	246	10,2	OBS/OBH	OBS/OBH	OBS ausgelöst	OBS 80
SO181/085-11	11.02.05	02:41	44° 23,41' S	75° 11,30' W	0	SSW 14	248	7,3	OBS/OBH	OBS/OBH	OBS gesichtet	OBS 80
SO181/085-11	11.02.05	02:49	44° 23,39' S	75° 12,02' W	0	S 13	293	1,5	OBS/OBH	OBS/OBH	OBS an Deck	OBS 80
SO181/085-12	11.02.05	03:11	44° 24,23' S	75° 15,42' W	0	SSW 11	259	3,9	OBS/OBH	OBS/OBH	OBS ausgelöst	OBS 81
SO181/085-12	11.02.05	03:18	44° 24,14' S	75° 15,84' W	0	S 11	3	1,6	OBS/OBH	OBS/OBH	OBS gesichtet	OBS 81
SO181/085-12	11.02.05	03:29	44° 23,89' S	75° 15,95' W	0	S 11	327	2,1	OBS/OBH	OBS/OBH	OBS an Deck	OBS 81
SO181/085-13	11.02.05	03:53	44° 25,04' S	75° 19,12' W	0	SSW 14	256	7,9	OBS/OBH	OBS/OBH	OBS ausgelöst	OBS 82
SO181/085-13	11.02.05	04:01	44° 25,11' S	75° 19,83' W	0	S 12	310	2,1	OBS/OBH	OBS/OBH	OBS gesichtet	OBS 82
SO181/085-13	11.02.05	04:08	44° 25,01' S	75° 19,92' W	0	S 11	197	1,4	OBS/OBH	OBS/OBH	OBS an Deck	OBS 82
SO181/085-14	11.02.05	04:23	44° 25,64' S	75° 22,22' W	0	SSW 13	256	10,3	OBS/OBH	OBS/OBH	OBS ausgelöst	OBS 83
SO181/085-14	11.02.05	04:36	44° 25,88' S	75° 23,54' W	0	SSW 11	190	1,6	OBS/OBH	OBS/OBH	OBS gesichtet	OBS 83
SO181/085-14	11.02.05	04:45	44° 25,95' S	75° 23,87' W	0	SSW 10	301	1,5	OBS/OBH	OBS/OBH	OBS an Deck	OBS 83
SO181/085-15	11.02.05	04:56	44° 26,02' S	75° 24,69' W	0	SSW 15	241	7,5	OBS/OBH	OBS/OBH	OBS ausgelöst	OBS 84
SO181/085-15	11.02.05	05:18	44° 26,68' S	75° 27,53' W	0	S 10	309	1,1	OBS/OBH	OBS/OBH	OBS gesichtet	OBS 84
SO181/085-15	11.02.05	05:28	44° 26,52' S	75° 27,94' W	0	SSW 11	344	2,2	OBS/OBH	OBS/OBH	OBS an Deck	OBS 84
SO181/085-16	11.02.05	05:37	44° 26,78' S	75° 28,72' W	0	S 12	235	7,4	OBS/OBH	OBS/OBH	OBH ausgelöst	OBH 85
SO181/085-16	11.02.05	06:11	44° 27,45' S	75° 31,59' W	0	SE 6	325	4,7	OBS/OBH	OBS/OBH	OBH gesichtet	OBH 85
SO181/085-16	11.02.05	06:22	44° 27,38' S	75° 31,99' W	0	S 9	350	1,3	OBS/OBH	OBS/OBH	OBH an Deck	OBH 85
SO181/085-17	11.02.05	06:32	44° 27,76' S	75° 33,02' W	0	S 13	245	7,8	OBS/OBH	OBS/OBH	OBH ausgelöst	OBH 86

Station	Datum	UTC	PositionLat	PositionLon	Tiefe [m]	Windstärke [m/s]	Kurs [°]	v [kn]	Gerät	Gerätekürzel	Aktion	Bemerkung
SO181/085-17	11.02.05	08:43	0° 0,00' N	0° 0,00' E	0	N 0	0	0	OBS/OBH	OBS/OBH	OBH gesichtet	OBH 86
SO181/085-17	11.02.05	08:57	44° 26,12' S	75° 35,82' W	0	S 11	3	2,6	OBS/OBH	OBS/OBH	OBH an Deck	OBH 86
SO181/085-18	11.02.05	07:10	44° 28,42' S	75° 37,80' W	0	S 12	252	7,3	OBS/OBH	OBS/OBH	OBH ausgelöst	OBH 87
SO181/085-18	11.02.05	07:33	44° 28,64' S	75° 39,65' W	0	S 8	308	1	OBS/OBH	OBS/OBH	OBH gesichtet	OBH 87
SO181/085-18	11.02.05	07:36	44° 28,63' S	75° 39,69' W	0	SSW 9	218	2,2	OBS/OBH	OBS/OBH	OBH ausgelöst	OBH 88
SO181/085-18	11.02.05	07:45	44° 28,90' S	75° 39,82' W	0	SSW 10	329	1,2	OBS/OBH	OBS/OBH	OBH an Deck	OBH 87
SO181/085-19	11.02.05	08:07	44° 29,57' S	75° 43,74' W	0	S 11	254	6	OBS/OBH	OBS/OBH	OBH gesichtet	OBH 88
SO181/085-19	11.02.05	08:10	44° 29,77' S	75° 43,95' W	0	S 12	198	2,7	OBS/OBH	OBS/OBH	OBH ausgelöst	OBH 88
SO181/085-19	11.02.05	08:14	44° 29,78' S	75° 43,99' W	0	S 10	344	1,2	OBS/OBH	OBS/OBH	OBH an Deck	OBH 88
SO181/085-20	11.02.05	08:36	44° 30,30' S	75° 47,55' W	0	SSW 10	229	1,8	OBS/OBH	OBS/OBH	OBH ausgelöst	OBH 89
SO181/085-20	11.02.05	08:57	44° 30,22' S	75° 47,72' W	0	SSW 10	340	0,5	OBS/OBH	OBS/OBH	OBH gesichtet	OBH 89
SO181/085-20	11.02.05	09:13	44° 30,52' S	75° 48,10' W	0	SSW 10	0	1,3	OBS/OBH	OBS/OBH	OBH an Deck	OBH 89
SO181/085-21	11.02.05	09:27	44° 30,82' S	75° 50,30' W	0	S 13	255	9,9	OBS/OBH	OBS/OBH	OBH gesichtet	OBH 90
SO181/085-21	11.02.05	09:30	44° 30,97' S	75° 50,98' W	0	S 13	280	9,2	OBS/OBH	OBS/OBH	OBH ausgelöst	OBH 91
SO181/085-21	11.02.05	09:53	44° 31,01' S	75° 52,00' W	0	S 10	331	2,1	OBS/OBH	OBS/OBH	OBH an Deck	OBH 90
SO181/085-22	11.02.05	10:20	44° 31,84' S	75° 55,48' W	0	SSW 11	357	1,8	OBS/OBH	OBS/OBH	OBH ausgelöst	OBH 92
SO181/085-22	11.02.05	10:37	44° 31,88' S	75° 55,63' W	0	SSW 13	226	2,3	OBS/OBH	OBS/OBH	OBH gesichtet	OBH 91
SO181/085-22	11.02.05	10:48	44° 32,06' S	75° 55,82' W	0	SSW 10	328	2,1	OBS/OBH	OBS/OBH	OBH an Deck	OBH 91
SO181/085-23	11.02.05	11:50	44° 33,28' S	76° 0,03' W	0	SSW 14	218	5,4	OBS/OBH	OBS/OBH	OBH ausgelöst	OBH 93
SO181/085-23	11.02.05	12:16	44° 33,99' S	76° 3,72' W	0	S 13	247	4	OBS/OBH	OBS/OBH	OBH ausgelöst	OBH 94
SO181/085-23	11.02.05	12:35	44° 34,14' S	76° 4,83' W	0	S 10	92	1,2	OBS/OBH	OBS/OBH	OBH gesichtet	OBH 93
SO181/085-23	11.02.05	12:43	44° 34,25' S	76° 4,89' W	0	SSW 9	300	0,4	OBS/OBH	OBS/OBH	OBH an Deck	OBH 93
SO181/085-24	11.02.05	13:08	44° 34,90' S	76° 8,80' W	0	S 13	254	9,1	OBS/OBH	OBS/OBH	OBH ausgelöst	OBH 95
SO181/085-24	11.02.05	13:08	44° 34,98' S	76° 9,20' W	0	S 13	251	9,9	OBS/OBH	OBS/OBH	OBH gesichtet	OBH 94
SO181/085-24	11.02.05	13:21	44° 35,41' S	76° 9,68' W	0	SW 11	186	0,6	OBS/OBH	OBS/OBH	OBH an Deck	OBH 94
SO181/085-25	11.02.05	13:47	44° 36,14' S	76° 14,34' W	0	SSW 13	248	7,9	OBS/OBH	OBS/OBH	OBH ausgelöst	OBH 96
SO181/085-25	11.02.05	13:50	44° 36,22' S	76° 14,67' W	0	S 12	243	3,8	OBS/OBH	OBS/OBH	OBH gesichtet	OBH 95
SO181/085-25	11.02.05	14:01	44° 36,51' S	76° 14,97' W	0	SW 11	221	1,2	OBS/OBH	OBS/OBH	OBH an Deck	OBH 95
SO181/085-26	11.02.05	14:24	44° 37,22' S	76° 18,83' W	0	SSW 14	255	6,2	OBS/OBH	OBS/OBH	OBH ausgelöst	OBH 97
SO181/085-26	11.02.05	14:25	44° 37,28' S	76° 19,02' W	0	SSW 14	250	8,8	OBS/OBH	OBS/OBH	OBH gesichtet	OBH 96
SO181/085-26	11.02.05	14:35	44° 37,52' S	76° 20,03' W	0	SSW 11	285	1	OBS/OBH	OBS/OBH	OBH an Deck	OBH 96
SO181/085-27	11.02.05	14:58	44° 38,31' S	76° 24,29' W	0	SSW 14	259	6,4	OBS/OBH	OBS/OBH	OBH ausgelöst	OBH 98
SO181/085-27	11.02.05	15:05	44° 38,35' S	76° 24,72' W	0	SW 11	17	1,9	OBS/OBH	OBS/OBH	OBH gesichtet	OBH 97
SO181/085-27	11.02.05	15:20	44° 38,47' S	76° 25,07' W	0	SW 12	50	2	OBS/OBH	OBS/OBH	OBH an Deck	OBH 97
SO181/085-28	11.02.05	15:45	44° 39,31' S	76° 29,05' W	0	SSW 15	256	8	OBS/OBH	OBS/OBH	OBH gesichtet	OBH 98
SO181/085-28	11.02.05	15:48	44° 39,35' S	76° 29,62' W	0	S 14	267	9	OBS/OBH	OBS/OBH	OBH ausgelöst	OBH 99
SO181/085-28	11.02.05	15:55	44° 39,38' S	76° 30,09' W	0	S 11	329	0,9	OBS/OBH	OBS/OBH	OBH an Deck	OBH 98
SO181/085-29	11.02.05	16:20	44° 40,28' S	76° 34,17' W	0	SSW 15	285	7,4	OBS/OBH	OBS/OBH	OBH gesichtet	OBH 99
SO181/085-29	11.02.05	16:24	44° 40,19' S	76° 34,75' W	0	SSW 14	285	5,4	OBS/OBH	OBS/OBH	OBH ausgelöst	OBH 100
SO181/085-29	11.02.05	16:32	44° 40,33' S	76° 35,05' W	0	SSW 12	318	0,9	OBS/OBH	OBS/OBH	OBH an Deck	OBH 99
SO181/085-30	11.02.05	17:00	44° 41,30' S	76° 39,51' W	0	SSW 13	263	4,4	OBS/OBH	OBS/OBH	OBH gesichtet	OBH 100
SO181/085-30	11.02.05	17:02	44° 41,27' S	76° 39,74' W	0	SSW 13	275	5,2	OBS/OBH	OBS/OBH	OBH ausgelöst	OBH 101
SO181/085-30	11.02.05	17:12	44° 41,34' S	76° 40,02' W	0	SSW 11	193	0,5	OBS/OBH	OBS/OBH	OBH an Deck	OBH 100

Station	Datum	UTC	PositionLat	PositionLon	Tiefe [m]	Windstärke [m/s]	Kurs [°]	v [kn]	Gerät	Gerätekürzel	Aktion	Bemerkung
SO181/085-31	11.02.05	17:38	44° 42,14' S	76° 43,74' W	0	SSW 14	258	9	OBS/OBH	OBS/OBH	OBH gesichtet	OBH 101
SO181/085-31	11.02.05	17:40	44° 42,18' S	76° 44,17' W	0	SSW 14	259	8	OBS/OBH	OBS/OBH	OBH ausgelöst	OBH 102
SO181/085-31	11.02.05	17:51	44° 42,27' S	76° 44,91' W	0	SSW 10	283	0,5	OBS/OBH	OBS/OBH	OBH an Deck	OBH 101
SO181/085-32	11.02.05	18:12	44° 43,08' S	76° 48,87' W	0	SSW 14	250	7,2	OBS/OBH	OBS/OBH	OBH gesichtet	OBH 102
SO181/085-32	11.02.05	18:14	44° 43,14' S	76° 49,06' W	0	SSW 14	261	8,1	OBS/OBH	OBS/OBH	OBH ausgelöst	OBH 103
SO181/085-32	11.02.05	18:25	44° 43,28' S	76° 49,98' W	0	SSW 11	344	0,7	OBS/OBH	OBS/OBH	OBH an Deck	OBH 102
SO181/085-33	11.02.05	18:48	44° 44,14' S	76° 54,21' W	0	SSW 13	258	8,2	OBS/OBH	OBS/OBH	OBH ausgelöst	OBH 104
SO181/085-33	11.02.05	18:48	44° 44,14' S	76° 54,21' W	0	SSW 13	258	8,2	OBS/OBH	OBS/OBH	OBH gesichtet	OBH 103
SO181/085-33	11.02.05	18:59	44° 43,28' S	76° 50,12' W	0	SSW 11	245	4	OBS/OBH	OBS/OBH	OBH an Deck	OBH 103
SO181/085-34	11.02.05	19:24	44° 45,28' S	76° 59,52' W	0	SSW 12	261	6	OBS/OBH	OBS/OBH	OBH gesichtet	OBH 104
SO181/085-34	11.02.05	19:24	44° 45,28' S	76° 59,52' W	0	SSW 12	261	6	OBS/OBH	OBS/OBH	OBH ausgelöst	OBH 105
SO181/085-34	11.02.05	19:38	44° 45,44' S	77° 0,08' W	0	SW 10	329	1,4	OBS/OBH	OBS/OBH	OBS an Deck	OBH 104
SO181/085-35	11.02.05	19:58	44° 46,09' S	77° 3,81' W	0	SSW 11	252	9,1	OBS/OBH	OBS/OBH	OBH gesichtet	OBH 105
SO181/085-35	11.02.05	19:59	44° 46,14' S	77° 3,83' W	0	SSW 12	249	11,4	OBS/OBH	OBS/OBH	OBH ausgelöst	OBH 106
SO181/085-35	11.02.05	20:08	44° 46,55' S	77° 4,98' W	0	SSW 10	275	0,5	OBS/OBH	OBS/OBH	OBH an Deck	OBH 105
SO181/085-36	11.02.05	20:35	44° 47,39' S	77° 9,88' W	0	S 10	252	3,3	OBS/OBH	OBS/OBH	OBH ausgelöst	OBH 107
SO181/085-36	11.02.05	20:49	44° 47,38' S	77° 9,98' W	0	SSW 8	8	0,4	OBS/OBH	OBS/OBH	OBH gesichtet	OBH 106
SO181/085-36	11.02.05	20:57	44° 47,60' S	77° 10,03' W	0	SSW 8	266	2	OBS/OBH	OBS/OBH	OBH an Deck	OBH 106
SO181/085-37	11.02.05	21:17	44° 47,95' S	77° 12,42' W	0	SSW 12	258	9,1	OBS/OBH	OBS/OBH	OBH ausgelöst	OBH 108
SO181/085-37	11.02.05	21:39	44° 48,36' S	77° 14,80' W	0	SSW 8	315	0,5	OBS/OBH	OBS/OBH	OBH gesichtet	OBH 107
SO181/085-37	11.02.05	21:47	44° 48,58' S	77° 15,00' W	0	SSW 9	210	1	OBS/OBH	OBS/OBH	OBH an Deck	OBH 107
SO181/085-38	11.02.05	22:11	44° 49,33' S	77° 18,40' W	0	SSW 11	254	5,4	OBS/OBH	OBS/OBH	OBH gesichtet	OBH 108
SO181/085-38	11.02.05	22:12	44° 49,34' S	77° 18,53' W	0	SSW 11	267	5,2	OBS/OBH	OBS/OBH	OBH ausgelöst	OBH 109
SO181/085-38	11.02.05	22:21	44° 49,41' S	77° 20,18' W	0	S 10	203	0,2	OBS/OBH	OBS/OBH	OBH an Deck	OBH 108
SO181/085-39	11.02.05	22:35	44° 49,85' S	77° 22,53' W	0	S 12	248	10,1	OBS/OBH	OBS/OBH	OBH ausgelöst	OBH 110
SO181/085-39	11.02.05	23:00	44° 50,13' S	77° 24,68' W	0	SSW 9	343	0,8	OBS/OBH	OBS/OBH	OBH gesichtet	OBH 109
SO181/085-39	11.02.05	23:11	44° 50,67' S	77° 24,96' W	0	SSW 10	230	1,3	OBS/OBH	OBS/OBH	OBH an Deck	OBH 108
SO181/085-40	11.02.05	23:30	44° 51,40' S	77° 28,58' W	0	S 10	258	11	OBS/OBH	OBS/OBH	OBS ausgelöst	OBS 111
SO181/085-40	11.02.05	23:37	44° 51,80' S	77° 29,67' W	0	S 10	271	2,9	OBS/OBH	OBS/OBH	OBS gesichtet	OBS 110
SO181/085-40	11.02.05	23:42	44° 51,51' S	77° 29,94' W	0	S 7	260	0,8	OBS/OBH	OBS/OBH	OBS an Deck	OBS 110
SO181/085-41	11.02.05	23:59	44° 52,26' S	77° 32,92' W	0	SSW 12	250	10,2	OBS/OBH	OBS/OBH	OBS ausgelöst	OBS 194
SO181/085-41	12.02.05	00:05	44° 52,54' S	77° 34,27' W	0	SSW 12	255	8,8	OBS/OBH	OBS/OBH	OBS gesichtet	OBS 111
SO181/085-41	12.02.05	00:12	44° 52,57' S	77° 35,00' W	0	SSW 9	319	0,1	OBS/OBH	OBS/OBH	OBS an Deck	OBS 111
SO181/085-42	12.02.05	00:30	44° 53,33' S	77° 38,24' W	0	SSW 12	253	10,5	OBS/OBH	OBS/OBH	OBS ausgelöst	OBS 195
SO181/085-42	12.02.05	00:53	44° 53,50' S	77° 39,86' W	0	S 8	118	1,4	OBS/OBH	OBS/OBH	OBS gesichtet	OBS 194
SO181/085-42	12.02.05	01:00	44° 53,61' S	77° 39,99' W	0	SW 9	322	0,6	OBS/OBH	OBS/OBH	OBS an Deck	OBS 194
SO181/085-43	12.02.05	01:17	44° 54,35' S	77° 43,23' W	0	SSW 12	258	10,9	OBS/OBH	OBS/OBH	OBS ausgelöst	OBS 196
SO181/085-43	12.02.05	01:18	44° 54,40' S	77° 43,48' W	0	SSW 13	245	10,5	OBS/OBH	OBS/OBH	OBS gesichtet	OBS 195
SO181/085-43	12.02.05	01:29	44° 54,53' S	77° 45,06' W	0	SSW 9	282	2,1	OBS/OBH	OBS/OBH	OBS an Deck	OBS 195
SO181/085-44	12.02.05	01:47	44° 55,41' S	77° 48,54' W	0	SSW 12	249	10,7	OBS/OBH	OBS/OBH	OBS ausgelöst	OBS 197
SO181/085-44	12.02.05	02:14	44° 55,44' S	77° 49,92' W	0	SSW 8	267	0,6	OBS/OBH	OBS/OBH	OBS gesichtet	OBS 196
SO181/085-44	12.02.05	02:22	44° 55,63' S	77° 49,99' W	0	SW 8	198	0,1	OBS/OBH	OBS/OBH	OBS an Deck	OBS 196
SO181/085-45	12.02.05	02:36	44° 56,20' S	77° 52,50' W	0	SSW 12	254	10,6	OBS/OBH	OBS/OBH	OBS ausgelöst	OBS 198

Station	Datum	UTC	PositionLat	PositionLon	Tiefe [m]	Windstärke [m/s]	Kurs [°]	v [kn]	Gerät	Gerätekürzel	Aktion	Bemerkung
SO181/085-45	12.02.05	02:37	44° 55,24' S	77° 52,74' W	0	SSW 11	255	9,8	OBS/OBH	OBS/OBH	OBS geschlöt	OBS 197
SO181/085-45	12.02.05	02:51	44° 56,43' S	77° 55,08' W	0	S 8	293	1,3	OBS/OBH	OBS/OBH	OBS an Deck	OBS 197
SO181/085-46	12.02.05	03:12	44° 57,28' S	77° 58,28' W	0	SSW 11	255	9,8	OBS/OBH	OBS/OBH	OBS geschlöt	OBS 198
SO181/085-46	12.02.05	03:20	44° 57,40' S	77° 59,51' W	0	SSW 7	285	2,3	OBS/OBH	OBS/OBH	OBS ausgelöt	OBS 198
SO181/085-46	12.02.05	03:31	44° 57,38' S	77° 59,98' W	0	S 6	227	0,4	OBS/OBH	OBS/OBH	OBS an Deck	OBS 198
SO181/085-47	12.02.05	03:58	44° 58,58' S	78° 4,02' W	0	SSW 9	257	7,2	OBS/OBH	OBS/OBH	OBS ausgelöt	OBS 200
SO181/085-47	12.02.05	04:20	44° 58,80' S	78° 4,63' W	0	SSW 5	23	0,8	OBS/OBH	OBS/OBH	OBS geschlöt	OBS 199
SO181/085-47	12.02.05	04:33	44° 58,81' S	78° 4,99' W	0	SSW 6	349	2	OBS/OBH	OBS/OBH	OBS an Deck	OBS 199
SO181/085-48	12.02.05	04:50	44° 59,11' S	78° 7,07' W	0	SW 10	251	9,7	OBS/OBH	OBS/OBH	OBS geschlöt	OBS 200
SO181/085-48	12.02.05	04:55	44° 59,33' S	78° 8,13' W	0	SSW 10	256	9,9	OBS/OBH	OBS/OBH	OBS ausgelöt	OBS 201
SO181/085-48	12.02.05	05:14	44° 59,57' S	78° 9,94' W	0	SSW 8	253	0,7	OBS/OBH	OBS/OBH	OBS an Deck	OBS 200
SO181/085-49	12.02.05	05:52	45° 0,60' S	78° 14,86' W	0	SSW 5	320	2,1	OBS/OBH	OBS/OBH	OBS geschlöt	OBS 201
SO181/085-49	12.02.05	06:07	45° 0,72' S	78° 15,12' W	2840	SW 5	248	0,7	OBS/OBH	OBS/OBH	OBS an Deck	OBS 201
SO181/085-49	12.02.05	06:08	45° 0,73' S	78° 15,14' W	2795	SW 5	212	0,9	OBS/OBH	OBS/OBH	Ende Station	
SO181/086-1	12.02.05	06:09	45° 0,73' S	78° 15,18' W	2873	WSW 5	284	1,1	Magnetometer	MAGN	Beginn Station	nwk: 349°, d: 8 sm
SO181/086-1	12.02.05	06:22	45° 0,27' S	78° 15,14' W	2766	SSW 8	331	4,1	Magnetometer	MAGN	Magnetometer zu Wasser	SL: 200 m
SO181/086-1	12.02.05	07:05	44° 53,92' S	78° 16,87' W	3248	SW 7	350	10,7	Magnetometer	MAGN	Kursänderung	nwk: 045 ; d: 20 sm
SO181/086-1	12.02.05	09:01	44° 38,93' S	77° 58,14' W	2834	WSW 2	38	10,7	Magnetometer	MAGN	Kursänderung	nwk: 076 ; d: 42 sm
SO181/086-1	12.02.05	13:02	44° 28,55' S	77° 0,26' W	3054	WSW 2	79	10,2	Magnetometer	MAGN	Kursänderung	nwk: 079° ; d: 73sm
SO181/086-1	12.02.05	15:05	44° 24,53' S	76° 29,64' W	3246	WSW 3	108	11,2	Magnetometer	MAGN	Kursänderung	nwk: 113° ; d: 23 sm
SO181/086-1	12.02.05	16:54	44° 31,81' S	76° 5,80' W	3292	W 5	144	2,9	Magnetometer	MAGN	Magnetometer an Deck	
SO181/086-1	12.02.05	16:55	44° 31,84' S	76° 5,79' W	3292	W 5	157	2	Magnetometer	MAGN	Ende Station	
SO181/087-1	12.02.05	17:51	44° 33,14' S	76° 0,20' W	3322	W 3	104	8,4	OBS/OBH	OBS/OBH	Beginn Station	Suche nach OBH 92
SO181/087-1	12.02.05	17:57	44° 33,45' S	75° 59,95' W	3321	W 6	228	4,7	Suchgeschlir an Draht W6	OBS/OBH	einmessen OBH 92	OBH 92, geortet, steht noch am Boden
SO181/087-1	12.02.05	18:39	44° 32,97' S	75° 59,88' W	3325	W 5	128	1,5	Suchgeschlir an Draht W6	OBS/OBH	Suchgeschlir z.W.	W 6, bestückt mit verschiedenen Suchankern
SO181/087-1	12.02.05	19:03	44° 33,09' S	75° 59,91' W	3320	WSW 6	114	0,9	Suchgeschlir an Draht W6	OBS/OBH	ausdampfen Draht	Ankerstein am Grund, SL: 3380m
SO181/087-1	12.02.05	20:06	44° 32,53' S	76° 0,45' W	3321	WNW 3	21	2,5	Suchgeschlir an Draht W6	OBS/OBH	ausdampfen Draht	SL max: 6601m
SO181/087-1	12.02.05	22:19	44° 30,18' S	75° 59,92' W	3328	WNW 4	255	0,4	Suchgeschlir an Draht W6	OBS/OBH	hieven	SL max: 6668 m, suche erfolglos
SO181/087-1	12.02.05	22:48	44° 30,24' S	75° 59,61' W	3329	W 5	4	0,6	Suchgeschlir an Draht W6	OBS/OBH	Ende Station	Draht mit Suchgeschlir abgerissen bei SL: 5584m
Transit												
SO181/088-1	13.02.05	08:05	43° 7,94' S	75° 4,96' W	1007	NNE 3	144	0,9	OBS/OBH	OBS/OBH	Beginn Station	
SO181/088-1	13.02.05	08:06	43° 7,96' S	75° 4,96' W	1014	N 2	231	1,4	OBS/OBH	OBS/OBH	OBH zu Wasser	OBH 202
SO181/088-2	13.02.05	09:22	42° 58,95' S	74° 56,02' W	162	N 6	24	1,5	OBS/OBH	OBS/OBH	OBH zu Wasser	OBH 203
SO181/088-3	13.02.05	10:41	43° 6,01' S	74° 42,94' W	118	N 7	159	1	OBS/OBH	OBS/OBH	OBS zu Wasser	OBS 204
SO181/088-4	13.02.05	12:02	42° 54,01' S	74° 33,97' W	129	N 7	94	1	OBS/OBH	OBS/OBH	OBH zu Wasser	OBH 205
SO181/088-5	13.02.05	13:21	42° 42,01' S	74° 25,95' W	122	NW 5	23	1,4	OBS/OBH	OBS/OBH	OBH zu Wasser	OBH 206
SO181/088-6	13.02.05	15:21	42° 21,01' S	74° 31,00' W	178	NNE 6	355	1,8	OBS/OBH	OBS/OBH	OBS zu Wasser	OBS 207, KÄ: 252°, d: 13 sm
SO181/088-7	13.02.05	16:50	42° 25,00' S	74° 48,00' W	273	N 4	297	0,7	OBS/OBH	OBS/OBH	OBH zu Wasser	OBH 208, KÄ: 144°, d: 10 sm
SO181/088-8	13.02.05	18:05	42° 33,00' S	74° 40,02' W	911	NNE 4	210	1,2	OBS/OBH	OBS/OBH	OBH zu Wasser	OBH 209, KÄ: 208°, d: 12 sm
SO181/088-9	13.02.05	19:19	42° 44,02' S	74° 47,96' W	198	NNE 5	301	1,1	OBS/OBH	OBS/OBH	OBH zu Wasser	OBH 210
SO181/088-10	13.02.05	20:33	42° 36,03' S	75° 0,97' W	1081	NE 9	295	1,3	OBS/OBH	OBS/OBH	OBS zu Wasser	OBS 211; KÄ: 211; D: 13 sm
SO181/088-11	13.02.05	21:53	42° 46,99' S	75° 10,00' W	1187	NNE 5	193	1	OBS/OBH	OBS/OBH	OBH zu Wasser	OBH 212; KÄ: 209 ; d: 15 sm
SO181/088-12	13.02.05	23:19	43° 0,02' S	75° 19,99' W	2159	NNE 5	211	2,8	OBS/OBH	OBS/OBH	OBS zu Wasser	OBS 213

Station	Datum	UTC	PositionLat	PositionLon	Tiefe [m]	Windstärke [m/s]	Kurs [°]	v [kn]	Gerät	Geräte Kürzel	Aktion	Bemerkung
SO181/088-13	14.02.05	00:25	43° 10,00' S	75° 27,00' W	2640	NNE 4	222	2,2	OBS/OBH	OBS/OBH	OBS zu Wasser	OBS 214
SO181/088-14	14.02.05	01:49	42° 59,97' S	75° 40,02' W	3739	NNW 7	1	1,8	OBS/OBH	OBS/OBH	OBS zu Wasser	OBS 215
SO181/088-15	14.02.05	02:58	42° 53,99' S	75° 52,97' W	3731	N 8	354	1,8	OBS/OBH	OBS/OBH	OBH zu Wasser	OBH 216
SO181/088-16	14.02.05	04:15	42° 41,44' S	75° 44,31' W	3751	N 12	35	11,8	OBS/OBH	OBS/OBH	OBH zu Wasser	OBH 217, KÄ: rwK, I&A*, 13 sm
SO181/088-17	14.02.05	06:02	42° 50,00' S	75° 32,00' W	3741	N 8	178	1,2	OBS/OBH	OBS/OBH	OBS zu Wasser	OBH 218, KÄ: 013*, 13 sm
SO181/088-18	14.02.05	07:21	42° 39,01' S	75° 22,98' W	2714	N 6	80	0,5	OBS/OBH	OBS/OBH	OBH zu Wasser	OBH 219; KÄ: 024; d: 14 sm
SO181/088-19	14.02.05	08:45	42° 28,01' S	75° 14,98' W	2209	NE 6	62	0,7	OBS/OBH	OBS/OBH	OBH zu Wasser	OBH 220; KÄ: 255; d: 11 sm
SO181/088-20	14.02.05	09:58	42° 29,01' S	75° 29,99' W	3731	NNE 7	207	0,4	OBS/OBH	OBS/OBH	OBS zu Wasser	OBS 221
SO181/088-20	14.02.05	09:58	42° 29,01' S	75° 29,99' W	3731	NNE 7	207	0,4	OBS/OBH	OBS/OBH	Ende Station	
SO181/089-1	14.02.05	10:01	42° 29,01' S	75° 30,07' W	3732	NNE 6	297	2,2	Magnetometer	MAGN	Beginn Station	
SO181/089-1	14.02.05	10:08	42° 28,68' S	75° 30,42' W	3738	NNE 9	322	5,1	Magnetometer	MAGN	Magnetometer zu Wasser	L: 200 m
SO181/089-1	14.02.05	10:09	42° 28,61' S	75° 30,48' W	3738	NNE 8	327	4,8	Magnetometer	MAGN	Beginn Profil	rwK: 320; d: 42 sm
SO181/089-1	14.02.05	14:08	41° 56,09' S	76° 6,82' W	3765	N 12	332	11	Magnetometer	MAGN	Kursänderung	rwK: 002*, d: 96sm
SO181/089-1	14.02.05	23:00	40° 19,98' S	76° 3,51' W	4049	NNW 11	3	11	Magnetometer	MAGN	Kursänderung	rwK: 329; d: 23 sm
SO181/089-1	15.02.05	01:08	40° 0,00' S	76° 18,93' W	4030	NW 11	345	11,4	Magnetometer	MAGN	Kursänderung	rwK: 000*, d: 90sm
SO181/089-1	15.02.05	09:14	38° 30,28' S	76° 18,98' W	3966	WSW 5	356	11,2	Magnetometer	MAGN	Kursänderung	rwK: 080; d: 72 sm
SO181/089-1	15.02.05	15:41	37° 55,53' S	75° 3,32' W	4480	SSW 2	68	2,2	Magnetometer	MAGN	Magnetometer an Deck	
SO181/089-1	15.02.05	15:42	37° 55,51' S	75° 3,28' W	4484	SSW 2	79	2,5	Magnetometer	MAGN	Ende Station	
SO181/090-1	15.02.05	16:12	37° 54,05' S	75° 0,04' W	4513	SSW 3	105	1,1	OBS/OBH	OBS/OBH	Beginn Station	
SO181/090-1	15.02.05	16:13	37° 54,05' S	75° 0,03' W	4518	SSW 3	97	0,4	OBS/OBH	OBS/OBH	OBS zu Wasser	OBS 222, KÄ: 286*
SO181/090-2	15.02.05	16:47	37° 53,16' S	75° 4,01' W	4412	WSW 4	246	1,1	OBS/OBH	OBS/OBH	OBS zu Wasser	OBS 223
SO181/090-3	15.02.05	17:19	37° 52,29' S	75° 8,02' W	4406	SW 5	232	0,9	OBS/OBH	OBS/OBH	OBS zu Wasser	OBS 224
SO181/090-4	15.02.05	17:50	37° 51,41' S	75° 12,01' W	4298	WSW 5	241	1,3	OBS/OBH	OBS/OBH	OBS zu Wasser	OBS 225
SO181/090-5	15.02.05	18:19	37° 50,52' S	75° 16,00' W	4211	WSW 4	26	0,6	OBS/OBH	OBS/OBH	OBS zu Wasser	OBS 226
SO181/090-6	15.02.05	18:45	37° 49,63' S	75° 20,00' W	4110	SW 4	288	1,3	OBS/OBH	OBS/OBH	OBS zu Wasser	OBS 227
SO181/090-7	15.02.05	19:09	37° 48,77' S	75° 23,98' W	4174	SW 4	307	1	OBS/OBH	OBS/OBH	OBS zu Wasser	OBS 228
SO181/090-8	15.02.05	19:35	37° 47,88' S	75° 28,00' W	4048	SW 5	307	0,4	OBS/OBH	OBS/OBH	OBS zu Wasser	OBS 229
SO181/090-9	15.02.05	20:01	37° 47,01' S	75° 32,00' W	4199	WSW 5	286	1	OBS/OBH	OBS/OBH	OBS zu Wasser	OBS 230
SO181/090-10	15.02.05	20:27	37° 46,14' S	75° 35,99' W	4035	SW 4	289	1,1	OBS/OBH	OBS/OBH	OBS zu Wasser	OBS 231
SO181/090-11	15.02.05	20:54	37° 45,25' S	75° 39,98' W	4091	SW 4	118	0,2	OBS/OBH	OBS/OBH	OBS zu Wasser	OBS 232
SO181/090-12	15.02.05	21:21	37° 44,40' S	75° 44,01' W	4142	SW 6	232	1	OBS/OBH	OBS/OBH	OBS zu Wasser	OBS 233
SO181/090-13	15.02.05	21:48	37° 43,62' S	75° 47,98' W	4019	SW 7	316	0,3	OBS/OBH	OBS/OBH	OBS zu Wasser	OBS 234
SO181/090-14	15.02.05	22:15	37° 42,62' S	75° 52,01' W	4020	SW 6	214	0,6	OBS/OBH	OBS/OBH	OBS zu Wasser	OBS 235
SO181/090-15	15.02.05	22:41	37° 41,74' S	75° 55,97' W	4220	SSW 7	230	0,5	OBS/OBH	OBS/OBH	OBS zu Wasser	OBS 236
SO181/090-16	15.02.05	23:06	37° 40,85' S	75° 59,99' W	4192	SSW 7	281	1,5	OBS/OBH	OBS/OBH	OBH zu Wasser	OBH 237
SO181/090-17	15.02.05	23:31	37° 39,97' S	76° 3,98' W	4018	SSW 5	288	2,5	OBS/OBH	OBS/OBH	OBH zu Wasser	OBH 238
SO181/090-18	15.02.05	23:55	37° 39,09' S	76° 7,99' W	4222	SSW 6	288	2,7	OBS/OBH	OBS/OBH	OBH zu Wasser	OBH 239
SO181/090-19	16.02.05	00:18	37° 38,21' S	76° 11,98' W	4195	SSW 6	282	3,1	OBS/OBH	OBS/OBH	OBH zu Wasser	OBH 240
SO181/090-20	16.02.05	00:42	37° 37,32' S	76° 16,02' W	4107	SSW 5	289	2	OBS/OBH	OBS/OBH	OBH zu Wasser	OBH 241
SO181/090-21	16.02.05	01:04	37° 36,45' S	76° 19,98' W	4107	SSW 5	283	2,3	OBS/OBH	OBS/OBH	OBH zu Wasser	OBH 242
SO181/090-22	16.02.05	01:28	37° 35,55' S	76° 24,03' W	4217	SW 6	283	2,3	OBS/OBH	OBS/OBH	OBH zu Wasser	OBH 243
SO181/090-23	16.02.05	01:51	37° 34,67' S	76° 28,02' W	4210	SSW 8	295	2	OBS/OBH	OBS/OBH	OBH zu Wasser	OBH 244
SO181/090-24	16.02.05	02:13	37° 33,81' S	76° 31,98' W	4078	SSW 6	293	2	OBS/OBH	OBS/OBH	OBH zu Wasser	OBH 245

Station	Datum	UTC	PositionLat	PositionLon	Tiefe [m]	Windstärke [m/s]	Kurs [°]	v [kn]	Gerät	Gerätekürzel	Aktion	Bemerkung
SO181/090-25	16.02.05	02:36	37° 32,93' S	76° 35,89' W	4178	S 7	288	2,2	OBS/OBH	OBS/OBH	OBH zu Wasser	OBH 246
SO181/090-26	16.02.05	03:00	37° 32,03' S	76° 40,00' W	4141	SSW 5	308	1,9	OBS/OBH	OBS/OBH	OBS zu Wasser	OBS 247
SO181/090-27	16.02.05	03:32	37° 31,17' S	76° 44,00' W	4207	SSW 4	19	1	OBS/OBH	OBS/OBH	OBS zu Wasser	OBS 248
SO181/090-28	16.02.05	04:04	37° 30,28' S	76° 48,00' W	4201	SSE 4	335	0,7	OBS/OBH	OBS/OBH	OBS zu Wasser	OBS 249
SO181/090-29	16.02.05	04:35	37° 29,41' S	76° 52,00' W	4157	S 6	277	1,3	OBS/OBH	OBS/OBH	OBS zu Wasser	OBS 250, rWK: 270°, d: 13 sm
SO181/090-29	16.02.05	04:36	37° 29,41' S	76° 52,02' W	4158	SSW 5	311	0,8	OBS/OBH	OBS/OBH	Ende Station	
SO181/091-1	16.02.05	05:58	37° 29,40' S	77° 7,84' W	4076	SW 7	307	5	Profil	PR	Stationsbeginn	KÄ: 360°, d: 3,5 sm
SO181/091-1	16.02.05	06:06	37° 28,95' S	77° 8,00' W	4119	SSW 4	356	3,9	Profil	PR	Streamer zu Wasser	SL: 200 m
SO181/091-1	16.02.05	06:15	37° 28,54' S	77° 8,01' W	4090	SW 4	0	1,5	Profil	PR	Stb Airgun zu Wasser	
SO181/091-1	16.02.05	06:23	37° 28,27' S	77° 7,88' W	4068	SSW 3	39	2,8	Profil	PR	Bb Airgun zu Wasser	
SO181/091-1	16.02.05	06:29	37° 28,04' S	77° 7,78' W	4028	SSW 3	30	2,8	Profil	PR	Beginn Profil	06:29 1. Schuß, rWK: 106°, d: 117 sm
SO181/091-1	17.02.05	11:43	37° 57,04' S	74° 46,00' W	4673	SSW 10	123	3,4	Profil	PR	Ende Profil	
SO181/091-1	17.02.05	11:49	37° 57,12' S	74° 45,75' W	4683	SSW 10	88	1,7	Profil	PR	Bb airgun an Deck	
SO181/091-1	17.02.05	11:57	37° 57,31' S	74° 45,57' W	4676	SSW 11	178	2,8	Profil	PR	Stb Airgun an Deck	
SO181/091-1	17.02.05	12:05	37° 57,55' S	74° 45,53' W	4674	SSW 10	141	1,4	Profil	PR	Streamer an Deck	
SO181/091-1	17.02.05	12:05	37° 57,55' S	74° 45,53' W	4674	SSW 10	141	1,4	Profil	PR	Stationsende	Anf. OBS 222, d: 10 sm
SO181/092-1	17.02.05	12:52	37° 55,89' S	74° 53,46' W	4710	S 11	294	11,3	OBS/OBH	OBS/OBH	Beginn Station	
SO181/092-1	17.02.05	12:54	37° 55,77' S	74° 53,87' W	4698	S 9	288	11	OBS/OBH	OBS/OBH	OBS ausgelöst	OBS 222
SO181/092-1	17.02.05	13:49	37° 53,67' S	75° 0,09' W	0	S 10	171	1,4	OBS/OBH	OBS/OBH	OBS gesichtet	OBS 222
SO181/092-1	17.02.05	13:50	37° 53,69' S	75° 0,08' W	0	S 9	224	2,3	OBS/OBH	OBS/OBH	OBS ausgelöst	OBS 223
SO181/092-1	17.02.05	13:58	37° 53,72' S	75° 0,37' W	0	SSE 8	314	2,2	OBS/OBH	OBS/OBH	OBS an Deck	OBS 222
SO181/092-2	17.02.05	14:20	37° 52,92' S	75° 3,47' W	0	S 8	304	3,9	OBS/OBH	OBS/OBH	OBS ausgelöst	OBS 224
SO181/092-2	17.02.05	14:44	37° 52,87' S	75° 4,05' W	0	S 9	181	0,5	OBS/OBH	OBS/OBH	OBS gesichtet	OBS 223
SO181/092-2	17.02.05	14:55	37° 52,82' S	75° 4,32' W	0	SSE 9	281	2,1	OBS/OBH	OBS/OBH	OBS an Deck	OBS 223
SO181/092-3	17.02.05	15:08	37° 52,66' S	75° 6,07' W	0	S 10	280	10,9	OBS/OBH	OBS/OBH	OBS ausgelöst	OBS 225
SO181/092-3	17.02.05	15:09	37° 52,62' S	75° 6,28' W	0	S 10	285	10,4	OBS/OBH	OBS/OBH	OBS gesichtet	OBS 224
SO181/092-3	17.02.05	15:32	37° 51,63' S	75° 8,43' W	0	S 8	321	2,7	OBS/OBH	OBS/OBH	OBS an Deck	OBS 224
SO181/092-4	17.02.05	15:51	37° 51,55' S	75° 11,26' W	0	S 10	283	6,4	OBS/OBH	OBS/OBH	OBS ausgelöst	OBS 226
SO181/092-4	17.02.05	15:58	37° 51,37' S	75° 11,73' W	0	SSE 9	339	2,4	OBS/OBH	OBS/OBH	OBS gesichtet	OBS 225
SO181/092-4	17.02.05	16:17	37° 50,95' S	75° 12,47' W	0	SSE 9	290	2,3	OBS/OBH	OBS/OBH	OBS an Deck	OBS 225
SO181/092-5	17.02.05	16:23	37° 50,94' S	75° 13,03' W	0	S 10	269	6,7	OBS/OBH	OBS/OBH	OBS ausgelöst	OBS 227
SO181/092-5	17.02.05	16:35	37° 50,75' S	75° 15,04' W	0	S 10	284	7,7	OBS/OBH	OBS/OBH	OBS gesichtet	OBS 226
SO181/092-5	17.02.05	16:52	37° 50,07' S	75° 16,37' W	0	SSE 8	275	1,7	OBS/OBH	OBS/OBH	OBS an Deck	OBS 226
SO181/092-6	17.02.05	17:08	37° 49,84' S	75° 19,10' W	0	S 10	284	9,4	OBS/OBH	OBS/OBH	OBS ausgelöst	OBS 228
SO181/092-6	17.02.05	17:35	37° 49,29' S	75° 19,80' W	0	SSE 9	270	4	OBS/OBH	OBS/OBH	OBS gesichtet	OBS 227
SO181/092-6	17.02.05	17:45	37° 49,26' S	75° 20,17' W	0	SSW 10	307	0,8	OBS/OBH	OBS/OBH	OBS an Deck	OBS 227
SO181/092-7	17.02.05	17:57	37° 49,26' S	75° 21,76' W	0	S 11	287	9,3	OBS/OBH	OBS/OBH	OBS ausgelöst	OBS 229
SO181/092-7	17.02.05	18:02	37° 49,03' S	75° 22,73' W	0	S 10	287	7,4	OBS/OBH	OBS/OBH	OBS gesichtet	OBS 228
SO181/092-7	17.02.05	18:21	37° 48,33' S	75° 24,12' W	0	SSE 10	34	1,5	OBS/OBH	OBS/OBH	OBS an Deck	OBS 228
SO181/092-8	17.02.05	18:29	37° 48,05' S	75° 24,75' W	0	SSE 9	280	9	OBS/OBH	OBS/OBH	OBS ausgelöst	OBS 230
SO181/092-8	17.02.05	18:49	37° 47,58' S	75° 27,82' W	0	SSE 10	281	1,3	OBS/OBH	OBS/OBH	OBS gesichtet	OBS 229
SO181/092-8	17.02.05	18:59	37° 47,74' S	75° 27,91' W	0	S 9	285	1	OBS/OBH	OBS/OBH	OBS an Deck	OBS 229
SO181/092-9	17.02.05	19:05	37° 47,64' S	75° 28,34' W	0	SSE 9	286	8,2	OBS/OBH	OBS/OBH	OBS ausgelöst	OBS 231

Station	Datum	UTC	PositionLat	PositionLon	Tiefe [m]	Windstärke [m/s]	Kurs [°]	v [kn]	Gerät	Gerätekürzel	Aktion	Bemerkung
SO181/092-9	17.02.05	19:23	37° 46,87' S	75° 31,74' W	0	SSE 9	267	5,1	OBS/OBH	OBS/OBH	OBS gesichtet	OBS 230
SO181/092-9	17.02.05	19:30	37° 46,94' S	75° 31,90' W	0	S 10	253	2,2	OBS/OBH	OBS/OBH	OBS an Deck	OBS 230
SO181/092-10	17.02.05	19:31	37° 48,93' S	75° 31,92' W	0	S 9	299	1,3	OBS/OBH	OBS/OBH	OBS ausgelöst	OBS 232
SO181/092-10	17.02.05	19:55	37° 46,04' S	75° 35,71' W	0	SSE 11	270	3,3	OBS/OBH	OBS/OBH	OBS gesichtet	OBS 231
SO181/092-11	17.02.05	19:57	37° 48,07' S	75° 35,81' W	0	ESE 10	188	1,3	OBS/OBH	OBS/OBH	OBS ausgelöst	OBS 233
SO181/092-10	17.02.05	20:07	37° 46,17' S	75° 35,80' W	0	S 10	338	1,8	OBS/OBH	OBS/OBH	OBS an Deck	OBS 231
SO181/092-11	17.02.05	20:30	37° 45,26' S	75° 39,66' W	0	SSE 8	263	4,5	OBS/OBH	OBS/OBH	OBS gesichtet	OBS 232
SO181/092-11	17.02.05	20:39	37° 45,35' S	75° 39,84' W	0	S 9	344	0,9	OBS/OBH	OBS/OBH	OBS an Deck	OBS 232
SO181/092-12	17.02.05	20:51	37° 44,93' S	75° 41,59' W	0	SSE 9	286	10,8	OBS/OBH	OBS/OBH	OBS ausgelöst	OBS 234
SO181/092-12	17.02.05	21:01	37° 44,50' S	75° 43,62' W	0	SSE 8	281	6,3	OBS/OBH	OBS/OBH	OBS gesichtet	OBS 233
SO181/092-12	17.02.05	21:10	37° 44,65' S	75° 44,13' W	0	S 11	345	1,7	OBS/OBH	OBS/OBH	OBS an Deck	OBS 233
SO181/092-13	17.02.05	21:23	37° 44,09' S	75° 46,14' W	0	SSE 7	288	10,4	OBS/OBH	OBS/OBH	OBS ausgelöst	OBS 235
SO181/092-13	17.02.05	21:43	37° 43,41' S	75° 47,78' W	0	SSE 10	295	0,7	OBS/OBH	OBS/OBH	OBS gesichtet	OBS 234
SO181/092-13	17.02.05	21:56	37° 43,84' S	75° 47,96' W	0	S 10	210	1,3	OBS/OBH	OBS/OBH	OBS an Deck	OBS 234
SO181/092-14	17.02.05	22:09	37° 43,25' S	75° 49,98' W	0	SSE 8	290	10,5	OBS/OBH	OBS/OBH	OBS ausgelöst	OBS 236
SO181/092-14	17.02.05	22:16	37° 42,79' S	75° 51,31' W	0	SSE 7	284	8,3	OBS/OBH	OBS/OBH	OBS gesichtet	OBS 235
SO181/092-14	17.02.05	22:25	37° 43,02' S	75° 51,96' W	0	SSE 10	278	0,7	OBS/OBH	OBS/OBH	OBS an Deck	OBS 235
SO181/092-15	17.02.05	22:48	37° 41,83' S	75° 55,62' W	0	SSE 8	264	4,8	OBS/OBH	OBS/OBH	OBS ausgelöst	OBS 237
SO181/092-15	17.02.05	23:05	37° 41,76' S	75° 55,82' W	0	SSE 10	283	1,4	OBS/OBH	OBS/OBH	OBS gesichtet	OBS 236
SO181/092-15	17.02.05	23:18	37° 42,15' S	75° 55,92' W	0	S 11	257	0,9	OBS/OBH	OBS/OBH	OBS an Deck	OBS 236
SO181/092-16	17.02.05	23:37	37° 41,20' S	75° 58,98' W	0	SSE 8	291	11,1	OBS/OBH	OBS/OBH	OBH ausgelöst	OBH 238
SO181/092-16	17.02.05	23:40	37° 41,01' S	75° 59,56' W	0	SSE 8	280	8,5	OBS/OBH	OBS/OBH	OBH gesichtet	OBH 237
SO181/092-16	17.02.05	23:48	37° 40,97' S	75° 59,96' W	0	S 9	343	0,8	OBS/OBH	OBS/OBH	OBH an Deck	OBH 237
SO181/092-17	18.02.05	00:04	37° 40,31' S	76° 2,43' W	0	SSE 9	291	11,3	OBS/OBH	OBS/OBH	OBH ausgelöst	OBH 239
SO181/092-17	18.02.05	00:15	37° 40,04' S	76° 3,68' W	0	SSE 8	260	0,7	OBS/OBH	OBS/OBH	OBH gesichtet	OBH 238
SO181/092-17	18.02.05	00:22	37° 40,09' S	76° 4,05' W	0	SSE 11	275	0,8	OBS/OBH	OBS/OBH	OBH an Deck	OBH 238
SO181/092-18	18.02.05	00:36	37° 39,48' S	76° 6,21' W	0	SSE 8	286	10,6	OBS/OBH	OBS/OBH	OBH ausgelöst	OBH 240
SO181/092-18	18.02.05	00:55	37° 38,96' S	76° 7,88' W	0	SSE 8	328	0,8	OBS/OBH	OBS/OBH	OBH gesichtet	OBH 239
SO181/092-18	18.02.05	01:05	37° 39,10' S	76° 8,19' W	0	S 9	258	1,4	OBS/OBH	OBS/OBH	OBH an Deck	OBH 239
SO181/092-19	18.02.05	01:17	37° 38,60' S	76° 10,09' W	0	SSE 10	292	11,4	OBS/OBH	OBS/OBH	OBH ausgelöst	OBH 241
SO181/092-19	18.02.05	01:22	37° 38,36' S	76° 11,15' W	0	SSE 8	286	8,3	OBS/OBH	OBS/OBH	OBH gesichtet	OBH 240
SO181/092-19	18.02.05	01:34	37° 38,12' S	76° 12,19' W	0	SSE 9	315	1,2	OBS/OBH	OBS/OBH	OBH an Deck	OBH 240
SO181/092-20	18.02.05	01:46	37° 37,63' S	76° 14,23' W	0	SSE 10	284	11,3	OBS/OBH	OBS/OBH	OBH ausgelöst	OBH 242
SO181/092-20	18.02.05	01:55	37° 37,35' S	76° 15,64' W	0	SSE 8	264	3,8	OBS/OBH	OBS/OBH	OBH gesichtet	OBH 241
SO181/092-20	18.02.05	02:02	37° 37,29' S	76° 16,18' W	0	SSE 9	287	1,3	OBS/OBH	OBS/OBH	OBH an Deck	OBH 241
SO181/092-21	18.02.05	02:13	37° 36,90' S	76° 17,86' W	0	SSE 10	291	10,3	OBS/OBH	OBS/OBH	OBH ausgelöst	OBH 243
SO181/092-21	18.02.05	02:28	37° 36,45' S	76° 19,81' W	0	SSE 8	277	0,9	OBS/OBH	OBS/OBH	OBH gesichtet	OBH 242
SO181/092-21	18.02.05	02:36	37° 36,44' S	76° 20,17' W	0	SSE 10	301	0,5	OBS/OBH	OBS/OBH	OBH an Deck	OBH 242
SO181/092-22	18.02.05	02:49	37° 36,02' S	76° 22,01' W	0	S 8	282	8,8	OBS/OBH	OBS/OBH	OBH ausgelöst	OBH 244
SO181/092-22	18.02.05	03:00	37° 35,67' S	76° 23,38' W	0	SSE 8	268	3,2	OBS/OBH	OBS/OBH	OBH gesichtet	OBH 243
SO181/092-22	18.02.05	03:16	37° 35,47' S	76° 24,19' W	0	SSE 10	292	1,5	OBS/OBH	OBS/OBH	OBH an Deck	OBH 243
SO181/092-23	18.02.05	03:29	37° 35,19' S	76° 25,77' W	0	SSE 7	294	8,9	OBS/OBH	OBS/OBH	OBH ausgelöst	OBH 245
SO181/092-23	18.02.05	03:31	37° 35,11' S	76° 26,11' W	0	SSE 8	286	7,9	OBS/OBH	OBS/OBH	OBH gesichtet	OBH 244

Station	Datum	UTC	PositionLat	PositionLon	Tiefe [m]	Windstärke [nva]	Kurs [°]	v [kn]	Gerät	Gerätekürzel	Aktion	Bemerkung
SO181/092-23	18.02.05	03:55	37° 34,38' S	76° 28,27' W	0	SSE 8	250	1,1	OBS/OBH	OBS/OBH	OBH an Deck	OBH 244
SO181/092-24	18.02.05	04:08	37° 34,34' S	76° 29,76' W	0	SSE 10	286	8,1	OBS/OBH	OBS/OBH	OBH ausgelöst	OBH 246
SO181/092-24	18.02.05	04:10	37° 34,26' S	76° 30,09' W	0	SSE 8	288	9,2	OBS/OBH	OBS/OBH	OBH gesichtet	OBH 245
SO181/092-24	18.02.05	04:56	37° 33,49' S	76° 32,14' W	0	S 10	81	0,9	OBS/OBH	OBS/OBH	OBH an Deck	OBH 245
SO181/092-25	18.02.05	05:08	37° 33,24' S	76° 33,16' W	0	SSE 9	286	9,9	OBS/OBH	OBS/OBH	OBH ausgelöst	OBH 247
SO181/092-25	18.02.05	05:09	37° 33,21' S	76° 33,36' W	0	SSE 9	283	9,5	OBS/OBH	OBS/OBH	OBH gesichtet	OBH 246
SO181/092-25	18.02.05	05:33	37° 32,68' S	76° 35,98' W	0	SSE 8	267	1,2	OBS/OBH	OBS/OBH	OBH an Deck	OBH 246
SO181/092-26	18.02.05	05:55	37° 32,17' S	76° 39,41' W	0	S 8	282	5,7	OBS/OBH	OBS/OBH	OBH gesichtet	OBH 247
SO181/092-26	18.02.05	05:56	37° 32,14' S	76° 39,50' W	0	S 7	289	4,2	OBS/OBH	OBS/OBH	OBH ausgelöst	OBH 248
SO181/092-26	18.02.05	06:08	37° 31,90' S	76° 40,00' W	0	S 8	225	1,2	OBS/OBH	OBS/OBH	OBH an Deck	OBH 247
SO181/092-27	18.02.05	06:31	37° 31,49' S	76° 42,55' W	0	S 10	290	9,9	OBS/OBH	OBS/OBH	OBH ausgelöst	OBH 249
SO181/092-27	18.02.05	06:42	37° 31,26' S	76° 43,51' W	0	SSE 9	325	1,8	OBS/OBH	OBS/OBH	OBH gesichtet	OBH 248
SO181/092-27	18.02.05	07:01	37° 31,06' S	76° 44,03' W	0	SSE 9	296	0,6	OBS/OBH	OBS/OBH	OBH an Deck	OBH 248
SO181/092-28	18.02.05	07:15	37° 30,67' S	76° 45,79' W	0	S 10	290	10,1	OBS/OBH	OBS/OBH	OBS gesichtet	OBS 249
SO181/092-28	18.02.05	07:16	37° 30,61' S	76° 45,98' W	0	S 10	292	9	OBS/OBH	OBS/OBH	OBH ausgelöst	OBH 250
SO181/092-28	18.02.05	07:34	37° 30,08' S	76° 47,97' W	0	S 8	198	0,6	OBS/OBH	OBS/OBH	OBS an Deck	OBS 249
SO181/092-29	18.02.05	07:55	37° 29,23' S	76° 51,27' W	0	S 11	284	3,6	OBS/OBH	OBS/OBH	OBH gesichtet	OBS 250
SO181/092-29	18.02.05	08:08	37° 29,28' S	76° 51,89' W	0	S 10	322	0,7	OBS/OBH	OBS/OBH	OBS an Deck	OBS 250
SO181/092-29	18.02.05	08:09	37° 29,27' S	76° 51,89' W	0	S 10	347	1	OBS/OBH	OBS/OBH	Ende Station	
SO181/093-1	18.02.05	08:26	37° 28,96' S	76° 51,93' W	0	SW 9	346	3,2	Magnetometer	MAGN	Beginn Station	
SO181/093-1	18.02.05	08:30	37° 28,68' S	76° 51,88' W	0	S 5	15	5	Magnetometer	MAGN	Magnetometer zu Wasser	
SO181/093-1	18.02.05	08:30	37° 28,68' S	76° 51,88' W	0	S 5	15	5	Magnetometer	MAGN	Beginn Profil	rwK: 009 ; d: 9 sm
SO181/093-1	18.02.05	09:21	37° 20,27' S	76° 50,08' W	4136	S 4	5	10,5	Magnetometer	MAGN	Kursänderung	rwK: 110 ; d: 30 sm
SO181/093-1	18.02.05	12:14	37° 30,14' S	76° 15,45' W	4173	SSW 13	156	8,9	Magnetometer	MAGN	Kursänderung	rwK: 184° ; d: 60 sm
SO181/093-1	18.02.05	18:13	38° 29,86' S	76° 19,98' W	3941	SSW 12	173	9,1	Magnetometer	MAGN	Kursänderung	rwK: 117° ; d: 105 sm
SO181/093-1	19.02.05	03:15	39° 12,80' S	74° 33,07' W	2065	SSW 13	176	3	Magnetometer	MAGN	Magnetometer an Deck	
SO181/093-1	19.02.05	03:16	39° 12,82' S	74° 33,03' W	2062	SSW 13	84	1,8	Magnetometer	MAGN	Ende Station	
SO181/094-1	19.02.05	03:17	39° 12,85' S	74° 32,98' W	2047	SSW 13	124	1,9	Vermessung	EM / PS	Beginn Profil	Simrad EM 120
SO181/094-1	19.02.05	04:30	39° 17,85' S	74° 19,68' W	1914	SSE 15	52	10,6	Vermessung	EM / PS	Kursänderung	rwK: 063° ; d: 17 sm
SO181/094-1	19.02.05	06:04	39° 10,15' S	74° 0,03' W	711	WSW 7	151	7,8	Vermessung	EM / PS	Kursänderung	rwK: 180° ; d: 4 sm
SO181/094-1	19.02.05	06:29	39° 14,06' S	74° 0,10' W	751	WSW 18	236	9,5	Vermessung	EM / PS	Kursänderung	rwK: 243° ; d: 13 sm
SO181/094-1	19.02.05	07:46	39° 19,73' S	74° 14,31' W	2003	S 14	235	9,1	Vermessung	EM / PS	Kursänderung	rwK: 090 ; d: 10
SO181/094-1	19.02.05	08:43	39° 19,99' S	74° 2,29' W	927	S 13	93	10,5	Vermessung	EM / PS	Kursänderung	rwK: 137 ; d: 41 sm
SO181/094-1	19.02.05	11:35	39° 40,99' S	73° 36,28' W	66	SSW 11	145	10,2	Vermessung	EM / PS	Ende Profil	
Transit	nach Bahia Corral zum Crewchange						div					
SO181/095-1	20.02.05	02:35	38° 8,74' S	73° 51,02' W	555	SW 7	97	2,4	Ocean Floor Observation Sys	OFOS	Beginn Station	
SO181/095-1	20.02.05	02:38	38° 8,76' S	73° 50,96' W	551	SW 10	10	0,5	Ocean Floor Observation Sys	OFOS	Zu wasser	
SO181/095-1	20.02.05	02:58	38° 8,83' S	73° 50,97' W	553	S 9	242	0,3	Ocean Floor Observation Sys	OFOS	Bodensicht	
SO181/095-1	20.02.05	03:00	38° 8,84' S	73° 50,97' W	552	S 9	216	0,6	Ocean Floor Observation Sys	OFOS	Beginn hieven	SL: 559m, Klabaufermann abgesetzt
SO181/095-1	20.02.05	03:15	38° 8,79' S	73° 50,83' W	549	SSW 9	64	0,5	Ocean Floor Observation Sys	OFOS	An deck	
SO181/095-1	20.02.05	03:16	38° 8,79' S	73° 50,84' W	549	SSW 10	333	0,7	Ocean Floor Observation Sys	OFOS	Ende Station	
SO181/096-1	20.02.05	03:22	38° 8,72' S	73° 50,58' W	543	SSW 7	76	6,3	MT	MT	Beginn Station	
SO181/096-1	20.02.05	03:35	38° 8,69' S	73° 49,51' W	503	SSW 9	208	3	MT	MT	MT ausgelöst	MT 01

Station	Datum	UTC	PositionLat	PositionLon	Tiefe [m]	Windstärke [m/s]	Kurs [°]	v [kn]	Gerät	Gerätekürzel	Aktion	Bemerkung
SO181/086-1	20.02.05	04:17	38° 8,73' S	73° 49,58' W	0	SSW 8	180	1,5	MT	MT	MT gesichtet	MT 01
SO181/086-1	20.02.05	04:32	38° 8,65' S	73° 49,60' W	0	S 8	351	0,4	MT	MT	MT an Deck	MT 01
SO181/086-1	20.02.05	04:33	38° 8,63' S	73° 49,60' W	0	S 8	22	0,8	MT	MT	Ende Station	rwK: 341°, d: 18 sm
SO181/087-1	20.02.05	06:21	37° 51,10' S	73° 56,74' W	577	S 3	10	7,6	Ocean Floor Observation Sys	OFOS	Beginn Station	Skorbut
SO181/087-1	20.02.05	06:35	37° 50,92' S	73° 57,07' W	615	SSW 8	167	0,5	Ocean Floor Observation Sys	OFOS	Zu wasser	
SO181/087-1	20.02.05	06:59	37° 50,94' S	73° 57,04' W	616	SSW 8	228	0,2	Ocean Floor Observation Sys	OFOS	Bodensicht	SL: 609 m, 07:03 Gerät ausgelöst
SO181/087-1	20.02.05	07:03	37° 50,94' S	73° 57,04' W	610	SSW 8	183	0,4	Ocean Floor Observation Sys	OFOS	Beginn hieven	
SO181/087-1	20.02.05	07:22	37° 50,94' S	73° 57,01' W	608	SSW 8	340	0,4	Ocean Floor Observation Sys	OFOS	An deck	
SO181/087-1	20.02.05	07:27	37° 50,97' S	73° 57,02' W	606	SSW 8	179	1	Ocean Floor Observation Sys	OFOS	Ende Station	
SO181/088-1	20.02.05	08:42	37° 58,94' S	74° 6,03' W	1058	SSW 10	312	0,1	Ocean Floor Observation Sys	OFOS	Beginn Station	
SO181/088-1	20.02.05	08:47	37° 59,97' S	74° 6,12' W	1071	S 10	197	0,7	Ocean Floor Observation Sys	OFOS	Zu wasser	
SO181/088-1	20.02.05	08:24	37° 59,98' S	74° 6,03' W	1063	S 8	270	0,6	Ocean Floor Observation Sys	OFOS	Bodensicht	SL: 1058m
SO181/088-1	20.02.05	08:30	38° 0,01' S	74° 6,02' W	1067	S 8	289	1,6	Ocean Floor Observation Sys	OFOS	Beginn hieven	OBS 252 PEST ausgelöst
SO181/088-1	20.02.05	08:58	38° 0,15' S	74° 5,99' W	0	S 7	222	0,3	Ocean Floor Observation Sys	OFOS	An deck	
SO181/088-1	20.02.05	08:59	38° 0,16' S	74° 5,99' W	0	S 7	219	1,2	Ocean Floor Observation Sys	OFOS	Ende Station	
SO181/089-1	20.02.05	10:27	38° 3,67' S	74° 8,70' W	0	S 12	209	11,8	MT	MT	Beginn Station	
SO181/089-1	20.02.05	10:36	38° 4,41' S	74° 8,24' W	0	S 8	236	2,1	MT	MT	MT ausgelöst	1. Auslöseversuch: Keine Antwort
SO181/089-1	20.02.05	12:16	38° 4,62' S	74° 9,45' W	0	SSW 5	90	4	MT	MT	Ende Station	MT 2 nicht aufgetaucht, Station abgebrochen
SO181/100-1	20.02.05	13:45	38° 1,10' S	74° 28,08' W	0	S 10	274	12,1	MT	MT	Beginn Station	
SO181/100-1	20.02.05	13:46	38° 1,05' S	74° 28,30' W	0	S 10	293	11	MT	MT	MT ausgelöst	MT 03
SO181/100-1	20.02.05	17:34	38° 0,09' S	74° 32,88' W	0	SSW 5	4	4,6	MT	MT	MT gesichtet	MT 03
SO181/100-1	20.02.05	17:49	37° 59,94' S	74° 32,92' W	0	S 8	288	0,9	MT	MT	MT an Deck	MT 03
SO181/100-1	20.02.05	17:50	37° 59,93' S	74° 32,93' W	0	S 9	359	1,2	MT	MT	Ende Station	MT 03
SO181/101-1	20.02.05	19:27	37° 55,02' S	74° 54,37' W	0	S 10	282	11,6	MT	MT	Beginn Station	
SO181/101-1	20.02.05	19:30	37° 54,90' S	74° 55,04' W	0	S 10	276	9,4	MT	MT	MT ausgelöst	MT 04
SO181/101-1	20.02.05	22:57	37° 55,23' S	74° 57,70' W	0	SSW 8	190	3,6	MT	MT	MT gesichtet	MT 04
SO181/101-1	20.02.05	23:15	37° 55,09' S	74° 57,64' W	0	S 8	345	1,3	MT	MT	MT an Deck	MT 04
SO181/101-1	20.02.05	23:17	37° 55,05' S	74° 57,66' W	0	SSW 8	321	1,1	MT	MT	Ende Station	
SO181/102-1	21.02.05	00:53	37° 54,02' S	74° 38,22' W	0	S 7	84	0,1	OBS/OBH	OBS/OBH	Beginn Station	
SO181/102-1	21.02.05	00:53	37° 54,02' S	74° 38,22' W	0	S 7	84	0,1	OBS/OBH	OBS/OBH	OBS zu Wasser	OBS 260
SO181/102-2	21.02.05	02:21	38° 8,98' S	74° 38,02' W	4672	SSW 8	207	2	OBS/OBH	OBS/OBH	OBH zu Wasser	OBH 259
SO181/102-3	21.02.05	03:46	38° 21,00' S	74° 30,00' W	3335	S 7	81	1,9	OBS/OBH	OBS/OBH	OBS zu Wasser	OBS 258
SO181/102-4	21.02.05	05:24	38° 23,99' S	74° 12,00' W	2265	S 6	57	1,6	OBS/OBH	OBS/OBH	OBH zu Wasser	OBH 257
SO181/102-5	21.02.05	06:43	38° 12,00' S	74° 15,01' W	751	S 6	105	0,6	OBS/OBH	OBS/OBH	OBH zu Wasser	OBH 256
SO181/102-6	21.02.05	08:02	38° 6,00' S	74° 30,03' W	4130	S 6	203	0,8	OBS/OBH	OBS/OBH	OBH zu Wasser	OBH 255
SO181/102-6	21.02.05	08:03	38° 6,01' S	74° 30,03' W	4125	S 6	164	0,4	OBS/OBH	OBS/OBH	Ende Station	
SO181/103-1	21.02.05	09:24	37° 53,96' S	74° 23,98' W	2942	SSW 8	268	0,4	Ocean Floor Observation Sys	OFOS	Beginn Station	
SO181/103-1	21.02.05	09:26	37° 53,97' S	74° 23,99' W	2950	S 8	200	0,4	Ocean Floor Observation Sys	OFOS	Zu wasser	
SO181/103-1	21.02.05	10:38	37° 54,05' S	74° 24,02' W	2958	S 5	233	0,2	Ocean Floor Observation Sys	OFOS	Bodensicht	SL: 2962 m
SO181/103-1	21.02.05	10:40	37° 54,05' S	74° 24,02' W	2957	S 4	350	0,8	Ocean Floor Observation Sys	OFOS	Beginn hieven	OBS 204 Krabowsky ausgelöst
SO181/103-1	21.02.05	11:44	37° 54,11' S	74° 23,92' W	2953	S 4	98	0,5	Ocean Floor Observation Sys	OFOS	An deck	
SO181/103-1	21.02.05	11:45	37° 54,11' S	74° 23,92' W	2963	S 4	234	0,4	Ocean Floor Observation Sys	OFOS	Ende Station	Anf. # 104, d: 40 sm
SO181/104-1	21.02.05	15:20	37° 50,78' S	75° 12,78' W	0	WNW 7	271	11	MT	MT	Beginn Station	MT 05

Station	Datum	UTC	PositionLat	PositionLon	Tiefe [m]	Windstärke [m/s]	Kurs [°]	v [kn]	Gerät	Gerätekürzel	Aktion	Bemerkung
SO181/104-1	21.02.05	15:21	37° 50,78' S	75° 13,02' W	0	NW 7	277	11,8	MT	MT	MT ausgelöst	MT 05
SO181/104-1	21.02.05	18:41	37° 49,87' S	75° 18,94' W	0	WNW 2	155	7,8	MT	MT	MT gesichtet	MT 05
SO181/104-1	21.02.05	19:00	37° 49,85' S	75° 18,60' W	0	WNW 3	37	1,3	MT	MT	MT an Deck	MT 05
SO181/104-1	21.02.05	19:00	37° 49,85' S	75° 18,60' W	0	WNW 3	37	1,3	MT	MT	Ende Station	Anf. # 105, d: 20 sm
SO181/105-1	21.02.05	20:05	37° 47,10' S	75° 32,71' W	0	WNW 11	279	11	MT	MT	Beginn Station	MT 6; 1. Auslöseversuch
SO181/105-1	21.02.05	20:47	37° 45,51' S	75° 41,38' W	0	WNW 7	292	2,1	MT	MT	MT ausgelöst	MT 6 hat geantwortet
SO181/105-1	22.02.05	00:00	37° 45,43' S	75° 41,52' W	0	W 3	92	2,7	MT	MT	MT gesichtet	MT 06
SO181/105-1	22.02.05	00:11	37° 45,42' S	75° 41,40' W	0	W 5	314	0,5	MT	MT	MT an Deck	MT 06
SO181/105-1	22.02.05	00:12	37° 45,42' S	75° 41,40' W	0	W 5	12	0,5	MT	MT	Ende Station	
SO181/106-1	22.02.05	00:17	37° 45,22' S	75° 41,51' W	0	WSW 6	330	4,5	Magnetometer	MAGN	Beginn Station	
SO181/106-1	22.02.05	00:20	37° 45,06' S	75° 41,80' W	4084	WSW 6	342	3	Magnetometer	MAGN	Magnetometer zu Wasser	
SO181/106-1	22.02.05	00:23	37° 44,91' S	75° 41,68' W	4075	WSW 6	330	3,7	Magnetometer	MAGN	Beginn Profil	Magnetometer 300m, rwk: 344°, 12 sm
SO181/106-1	22.02.05	01:27	37° 33,97' S	75° 46,00' W	4121	W 7	358	10,9	Magnetometer	MAGN	Kursänderung	rwk: 013°, d: 53 sm
SO181/106-1	22.02.05	06:22	36° 42,10' S	75° 31,09' W	3958	SW 5	345	10,1	Magnetometer	MAGN	Kursänderung	rwk: 306°, d: 12 sm
SO181/106-1	22.02.05	07:30	36° 35,20' S	75° 42,62' W	4058	SW 9	304	10,3	Magnetometer	MAGN	Kursänderung	rwk: 201°, d: 16 sm
SO181/106-1	22.02.05	08:09	36° 50,03' S	75° 50,00' W	4014	WSW 10	202	9,9	Magnetometer	MAGN	Kursänderung	rwk: 197°, d: 45 sm
SO181/106-1	22.02.05	13:27	37° 32,86' S	76° 5,96' W	4207	SSE 13	193	10,8	Magnetometer	MAGN	Kursänderung	rwk: 195°, d: 7 sm
SO181/106-1	22.02.05	13:45	37° 35,91' S	76° 7,01' W	4160	SSE 13	196	9,2	Magnetometer	MAGN	Ende Profil	
SO181/106-1	22.02.05	13:53	37° 36,40' S	76° 7,18' W	0	SSE 9	207	2,2	Magnetometer	MAGN	Magnetometer an Deck	
SO181/106-1	22.02.05	13:53	37° 36,40' S	76° 7,18' W	0	SSE 9	207	2,2	Magnetometer	MAGN	Ende Station	
SO181/107-1	22.02.05	13:40	37° 35,08' S	76° 6,74' W	4131	S 13	197	10,6	MT	MT	MT ausgelöst	MT 07
SO181/107-1	22.02.05	13:55	37° 36,49' S	76° 7,21' W	0	SSE 10	189	3	MT	MT	Beginn Station	
SO181/107-1	22.02.05	17:42	37° 38,98' S	76° 8,70' W	0	S 7	15	0,3	MT	MT	Ende Station	MT07 nicht aufgetaucht, Range bei 3313 m
SO181/108-1	22.02.05	17:46	37° 39,04' S	76° 8,89' W	0	SSE 8	157	4,2	Magnetometer	MAGN	Beginn Station	
SO181/108-1	22.02.05	17:51	37° 39,47' S	76° 8,48' W	0	SSW 10	173	6	Magnetometer	MAGN	Magnetometer zu Wasser	SL: 200 m, rwk: 232°, d: 12 sm
SO181/108-1	22.02.05	17:52	37° 39,56' S	76° 8,47' W	0	SSW 10	179	5,6	Magnetometer	MAGN	Beginn Profil	
SO181/108-1	22.02.05	18:03	37° 46,62' S	76° 19,42' W	4028	SSE 10	232	10,2	Magnetometer	MAGN	Kursänderung	rwk: 284°, d: 20 sm
SO181/108-1	22.02.05	21:01	37° 42,20' S	76° 44,04' W	4118	S 7	267	9,6	Magnetometer	MAGN	Kursänderung	rwk: 164°, d: 8 sm
SO181/108-1	22.02.05	21:47	37° 49,65' S	76° 42,15' W	4118	S 11	159	10,8	Magnetometer	MAGN	Kursänderung	rwk: 109°, d: 18 sm
SO181/108-1	22.02.05	23:30	37° 55,97' S	76° 20,03' W	4093	S 11	108	10,8	Magnetometer	MAGN	Kursänderung	rwk: 030°, d: 19 sm
SO181/108-1	23.02.05	01:17	37° 39,62' S	76° 8,25' W	0	S 3	26	9,8	Magnetometer	MAGN	Kursänderung	rwk: 351°, d: 20 sm
SO181/108-1	23.02.05	03:48	37° 20,00' S	76° 11,98' W	4133	SSE 2	351	10,1	Magnetometer	MAGN	Kursänderung	rwk: 004°, d: 25 sm
SO181/108-1	23.02.05	06:07	36° 55,11' S	76° 10,00' W	4043	SSE 1	8	10,5	Magnetometer	MAGN	Kursänderung	rwk: 020°, d: 112 sm
SO181/108-1	23.02.05	16:11	35° 10,24' S	75° 23,01' W	4163	SSW 3	43	11,6	Magnetometer	MAGN	Kursänderung	rwk: 090°, d: 110 sm
SO181/108-1	24.02.05	01:06	35° 10,04' S	73° 25,02' W	3019	SSW 13	99	10,1	Magnetometer	MAGN	Ende Profil	
SO181/108-1	24.02.05	01:26	35° 11,01' S	73° 23,86' W	2958	SSW 13	185	2,8	Magnetometer	MAGN	Magnetometer an Deck	
SO181/108-1	24.02.05	01:26	35° 11,01' S	73° 23,86' W	2958	SSW 13	185	2,8	Magnetometer	MAGN	Ende Station	
SO 181-2	24.02.05	08:45	36° 11,72' S	73° 04,33' W	120	SSW 12	175	11,5	Simrad EM 120	Simrad	Ende der Stationsarbeiten Reise SO 181-2	

Entre Concepción y Valdivia:

Barco alemán busca terremotos

Geólogos alemanes y chilenos analizarán los procesos que se originan en los choques de las placas tectónicas.

CONA, D. CRUZAT

VALPARAÍSO.— Con participación de científicos alemanes y chilenos, hoy se inicia el proyecto de investigación geocientífica que busca analizar las causas de los sismos en las fronteras de las placas oceánicas y continentales. En esta oportunidad se hace a bordo del barco alemán de investigación Sonne, que durante 80 días realizará un cruceo con 21 científicos a bordo en la zona comprendida entre Concepción y Valdivia.

Según lo explicado por el coordinador del proyecto TUPTEQ, Orno Oncken, y el director científico de la excursión marítima, Ernst Flüh, ahora investigarán los procesos que se producen entre las dos placas (placa oceánica Nazca y placa Continental), por cuanto muchas veces el choque de ambas produce terremotos y actividad volcánica.

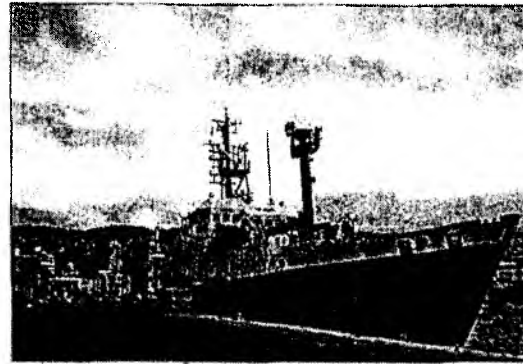
En esta aventura del descubrimiento participan numerosos científicos que realizan estudios tanto en tierra como en el mar.

El Sonne es un viejo conocido de las costas chilenas, porque ha participado en varios otros cruces científicos. Zarpó hoy desde Valparaíso, para terminar su tarea el 25 de febrero.

Contacto a fondo

Los científicos saben que su vida es medir para comprobar sus hipótesis. Depositaban diversos instrumentos en el fondo marino para registrar sismos y terremotos, tomaron muestras geológicas del fondo del mar para investigar la existencia de minerales. Aumentarán sus bases de datos.

También medirán la temperatura en tierra y harán perfiles sis-



LABORATORIO EN VALPARAÍSO.— El Sonne parte hoy a sondear la geología de nuestro mar.



ENCAMISA.— Uno de los 40 geólogos de 30 universidades alemanas que pasarán Navidad lejos de su invierno.

Lo costoso es la carga

A bordo el Sonne van científicos y 40 toneladas de sofisticados equipos de medición submarina. El barco está dotado de varios laboratorios donde se procesa la información obtenida en las mediciones de sismicidad a profundidades de hasta seis kilómetros. Los instrumentos se lanzan al fondo del mar y se dejan ahí por semanas o meses. Se recuperan mediante una señal de radio, con la cual se liberan los aparatos del ancla y suben a la superficie.

micos que llevan a comprender la estructura de la placa oceánica y de la continental.

En cruces científicos anteriores han obtenido diversos resultados de la placa tectónica y planos del relieve del fondo oceánico. Ya conocen dónde están las fallas y los lugares donde se han producido tsunamis. En este viaje —afirmó Flüh— esperan obtener más detalle, especialmente en lo relativo a los tsunamis.

En investigaciones de años anteriores se llegó a la parte austral y también a la zona norte.

Entonces determinaron que la placa de Nazca es más joven y con mayor temperatura en el sur, y más vieja y fría en el norte.

Tal descubrimiento —según Ernst Flüh— podría tener alguna influencia al producirse el choque entre la placa de Nazca y la Continental, especialmente a la altura del Golfo de Penas, en el Sur, porque —a una zona menos sísmica. Esta será una de las hipótesis que van a investigar.

La placa de Nazca es oceánica, tiene una corteza de alrededor de 40 kilómetros, en tanto que la

Continental es más vieja, formada por rocas continentales, con una corteza de 30 a 50 kilómetros, pero sus rocas son de menor intensidad.

Flüh dijo que cada día las lavas avanzan hacia el continente, producto de cómo la placa oceánica se introduce bajo la continental. Es un movimiento de alrededor de 10 centímetros al año. "Vamos a tener que esperar un poco para poder tener la idea de cómo aquí al lado", dijo sonriendo.

Predicción imposible

El científico dijo que no es posible predecir los terremotos, pero sí prever los riesgos.

"El proceso de los terremotos no está aún bien entendido. Sabemos algo, porque tienen un componente como el caos. No es un proceso lineal".

En los hitos estudiados está el terremoto de Valdivia en 1960.

que es el más grande y violento del mundo, desde que existe medición (9,5 grados). Vamos a estudiar la causa de tal magnitud del fenómeno.

Los científicos dijeron que no pueden medir la presión que se produce al introducirse una placa sobre la otra, causa de los temblores, porque no tienen los instrumentos para lograrlo, sólo pueden medir los temblores.

El trabajo se hace en forma conjunta con científicos del Servicio Hidrográfico y Oceanográfico de la Armada y de varias universidades chilenas. Además, utilizan los datos que entregan las estaciones sísmicas del país.

De paso, se ahorran el frío del invierno europeo.

EN INTERNET

El proyecto: www.geotecnologien.de/forschung/forsch2.de.html

BREVES



Diseño naval a prueba en Valdivia

EVENTOS

U. Austral inauguró su VII jornada científica

Ayer, en el Campus Isla Teja, partió la VII Jornada de Investigación Científica Universidad Austral de Chile, evento que reúne 190 trabajos en las más diversas áreas; también conferencias sobre energía nuclear, plantas medicinales y ecología de lobos finos.



A la izquierda, la lengua del glaciar vista desde la Estación Espacial

NASA:

Glaciares vistos desde el espacio

Los glaciares captan la atención de los expertos. Uno de los más importantes es el Perito Moreno, en el Parque Nacional Los Glaciares, sector argentino los Campos de Hielo Sur. Este congelado forma peridicame un dique de hielo entre la primera porción del lago Argentino noreste y una extensión menor llamada Brazo Rico.

EL MERCURIO

DE VALPARAISO

Domingo 12 de diciembre de 2004

Año 178 - Nro. 60981

Investigarán origen de terremotos

21 especialistas alemanes harán ambicioso estudio sobre los choques de las placas de Nazca y continental.

PABLO RAMOS

Analizar los procesos ocurridos entre la placa de Nazca y la placa continental sudamericana, que en muchas ocasiones terminan en terremotos, es el objetivo de un ambicioso proyecto de investigación sobre el origen de los sismos que llevan a cabo 21 científicos alemanes a bordo del buque "Sonne".

Según explicó Ernst Flüh, director científico del proyecto, la iniciativa que se llevará a cabo en el barco de investigación científica contará además con el apoyo de científicos y académicos de universidades chilenas.

Incluso, para el éxito del crucero, el Ministerio de Educación e Investigación de Alemania aportó con 4 millones de euros.

EN MAR Y EN TIERRA

Flüh precisó que el trabajo iniciado considera el apoyo de múltiples disciplinas. De hecho, profesionales aportarán con datos desde tierra hasta el final del crucero, previsto para el 25 de febrero.

Básicamente, los científicos colocarán instrumentos en el fondo del mar para registrar los temblores. También se tomarán muestras geológicas del fondo marino para investigar los minerales existentes. Y, junto con ello, el equipo de especialistas medirá la temperatura en la tierra, al tiempo que realizará perfiles sísmicos para entender la estructura de las placas oceánica y del margen continental.

El científico dijo que, en esta ocasión, las investigaciones van a estar localizadas al sur de Concepción. "Una de las cosas que vamos a estudiar el tamaño y las características del terremoto ocurrido en Valdivia en 1960, debido a que el resto de los terremotos en Chile es bastante más pequeño", expresó.

En esta ocasión, sostuvo, no tienen instrumentos para medir el choque de las placas de Nazca y continental, pero lo que sí harán será sacar una imagen del límite entre las dos placas, ya que el resultado de las fuerzas son los temblores.



INVESTIGACION.- Ernst Flüh encabeza la investigación, que cuenta con el apoyo de académicos de universidades chilenas. Monitoreos finalizarán en febrero.

Difícil predicción

"Es muy difícil predecir un terremoto porque uno debe saber el sitio exacto donde ocurrirá un sismo con una antelación necesaria para alcanzar a adoptar medidas", explicó el científico alemán Ernst Flüh.

"Lo que podemos hacer los sismólogos -añadió-, es un estudio del riesgo o la probabilidad que tiene un terremoto de ser grado 6, 7 u 8".

Según Flüh, el proceso de generación de los terremotos aún no está bien entendido, ya que no es un proceso lineal. "Ese es el motivo por el que no podemos hacer una predicción", aseguró.

IFM-GEOMAR Reports

- | No. | Title |
|------------|---|
| 1 | RV Sonne Fahrtbericht / Cruise Report SO 176 & 179 MERAMEX I & II (Merapi Amphibious Experiment) 18.05.-01.06.04 & 16.09.-07.10.04. Ed. by Heidrun Kopp & Ernst R. Flueh, 2004, 206 pp.
In English |
| 2 | RV Sonne Fahrtbericht / Cruise Report SO 181 TIPTEQ (from The Incoming Plate to mega Thrust EarthQuakes) 06.12.2004.-26.02.2005. Ed. by Ernst R. Flueh & Ingo Grevemeyer, 2005, 539 pp.
In English |